

**BIENNIAL RECEIVING WATERS MONITORING AND
ASSESSMENT REPORT FOR THE POINT LOMA
AND SOUTH BAY OCEAN OUTFALLS**

2022-2023



City of San Diego Ocean Monitoring Program
Environmental Monitoring and Technical Services Division

June 30, 2024

Mr. David W. Gibson, Executive Officer
California Regional Water Quality Control Board
San Diego Region
2375 Northside Drive, Suite 100
San Diego, CA 92108

Attention: POTW Compliance Unit

Dear Mr. Gibson:

Enclosed is the 2022-2023 Biennial Receiving Waters Monitoring and Assessment Report for the Point Loma and South Bay Ocean Outfalls, as per requirements set forth in the following Orders/Permits:

- (1) Order No. R9-2017-0007 (as amended by Order No. R9-2022-0078) for the City of San Diego's Point Loma Wastewater Treatment Plant (NPDES No. CA0107409).
- (2) Order No. R9-2021-0011 for the City's South Bay Water Reclamation Plant (NPDES No. CA0109045).
- (3) Order No. R9-2021-0001 for the United States Section of the International Boundary and Water Commission's South Bay International Wastewater Treatment Plant (NPDES No. CA0108928).

This combined report for the Point Loma and South Bay outfall regions contains data summaries, analyses, and assessments for all portions of the Ocean Monitoring Program conducted during 2022 and 2023. Additional data in support of this report will be submitted separately to either the Regional Water Quality Control Board or the California Environmental Data Exchange Network (CEDEN) in accordance with the aforementioned permits.

I certify under penalty of law that this document and all attachments were prepared under my direction or supervision in accordance with a system designed to assure that qualified personnel properly gather and evaluate the information submitted. Based on my inquiry of the person or persons who manage the system or those persons directly responsible for gathering the information, the information submitted is, to the best of my knowledge and belief, true, accurate, and complete. I am aware that there are significant penalties for submitting false information, including the possibility of fine and imprisonment for knowing violations.

If you have questions regarding this report, please call Dr. Ryan Kempster, the City's Senior Marine Biologist at (619) 758-2329.

Sincerely,



Peter S. Vroom, Ph.D.
Deputy Director, Public Utilities Department

PV/rk

cc: U.S. Environmental Protection Agency, Region 9
International Boundary and Water Commission, U.S. Section



BIENNIAL RECEIVING WATERS MONITORING AND ASSESSMENT REPORT FOR THE POINT LOMA AND SOUTH BAY OCEAN OUTFALLS

2022–2023

POINT LOMA WASTEWATER TREATMENT PLANT

(NPDES CA0107409; ORDER No. R9-2017-0007 AS AMENDED BY ORDER No. R9-2022-0078)

SOUTH BAY WATER RECLAMATION PLANT

(NPDES CA0109045; ORDER No. R9-2021-0011)

SOUTH BAY INTERNATIONAL WASTEWATER TREATMENT PLANT

(NPDES CA0108928; ORDER No. R9-2021-0001)

Prepared by:

City of San Diego Ocean Monitoring Program

Environmental Monitoring & Technical Services Division, Public Utilities Department

Ryan Kempster, Managing Editor

June 2024

Table of Contents

Production Credits and Acknowledgements	ii
Executive Summary	1
<i>R. Kempster</i>	
Chapter 1. General Introduction	7
<i>R. Kempster</i>	
Chapter 2. Coastal Oceanographic Conditions	17
<i>C. Lantz, S. Smith, W. Enright., Z. Scott, A. Webb, S. Jaeger</i>	
Chapter 3. Water Quality Compliance.....	57
<i>S. Smith</i>	
Chapter 4. Plume Dispersion	89
<i>S. Jaeger, W. Enright, S. Smith, C. Lantz, A. Webb, G. Rodriguez, A. Feit</i>	
Chapter 5. Sediment Quality	127
<i>A. Latker, W. Enright</i>	
Chapter 6. Macrobenthic Communities	162
<i>V. Rodriguez-Villanueva, W. Enright, R. Martinez-Lara, A. Webb</i>	
Chapter 7. San Diego Regional Benthic Conditions Assessment	187
<i>A. Webb, A. Latker, W. Enright, V. Rodriguez-Villanueva, L. Nanninga, R. Martinez-Lara</i>	
Chapter 8. Demersal Fishes and Megabenthic Invertebrates	222
<i>Z. Scott, M. Kasuya</i>	
Chapter 9. Contaminants in Marine Fishes	263
<i>L. Valentino, A. Latker</i>	

APPENDICES - ENHANCED MONITORING REPORTS

Appendix A: Evaluation of Anthropogenic Impacts on the San Diego Coastal Kelp Forest Ecosystem – Final Project Report, 2019 to 2024

*E. Parnell,
Scripps Institution of Oceanography, UC San Diego*

Appendix B: Satellite & Aerial Coastal Water Quality Monitoring in the San Diego/Tijuana Region, Annual Summary Report, 1 January 2022 – 31 December, 2023

*M. Hess,
Ocean Imaging, Littleton, CO*

Table of Contents

APPENDICES - SUPPLEMENTAL ANALYSES

- Appendix C: Coastal Oceanographic Conditions
- Appendix D: Water Quality Compliance
- Appendix E: Plume Dispersion
- Appendix F: Sediment Quality
- Appendix G: Macrobenthic Communities
- Appendix H: San Diego Regional Benthic Conditions Assessment
- Appendix I: Demersal Fishes and Megabenthic Invertebrates
- Appendix J: Contaminants in Marine Fishes

PRODUCTION CREDITS AND ACKNOWLEDGEMENTS

Managing Editor:

R. Kempster

GIS Graphics:

M. Kasuya, A. Webb

Production Editor:

Z. Scott

Production Team:

W. Enright, S. Smith, R. Kempster

Cover Photo:

Sunrise at Sea. Photo taken by C. Lantz.

Acknowledgments:

We are grateful to the personnel of the City's Marine Biology, Marine Microbiology, and Environmental Chemistry Services Laboratories for their assistance in the collection and/or processing of all samples, and for discussions of the results. The completion of this report would not have been possible without their continued efforts and contributions. Complete staff listings for the above labs and additional details concerning relevant QA/QC activities for the receiving waters monitoring data reported herein are available upon request.

How to cite this document:

City of San Diego. (2024). Biennial Receiving Waters Monitoring and Assessment Report for the Point Loma and South Bay Ocean Outfalls, 2022–2023. City of San Diego Ocean Monitoring Program, Public Utilities Department, Environmental Monitoring and Technical Services Division, San Diego, CA.

Executive Summary

Executive Summary

The City of San Diego (City) conducts an extensive Ocean Monitoring Program to evaluate potential environmental effects associated with the discharge of treated wastewater to the Pacific Ocean via the Point Loma and South Bay Ocean Outfalls (PLOO and SBOO, respectively). Data collected are used to determine compliance with receiving water quality requirements as specified in National Pollutant Discharge Elimination System (NPDES) permits, and associated orders; these permits and orders are issued by the San Diego Regional Water Quality Control Board (SDRWQCB) and the U.S. Environmental Protection Agency (USEPA) for the City's Point Loma Wastewater Treatment Plant (PLWTP), South Bay Water Reclamation Plant (SBWRP), and the South Bay International Wastewater Treatment Plant (SBIWTP), which is operated by the U.S. Section of the International Boundary and Water Commission (USIBWC). Treated effluent from both the SBWRP and SBIWTP commingle before being discharged to the ocean via the SBOO, thus a single monitoring and reporting program, approved by the SDRWQCB and USEPA, is conducted to comply with these two permits.

The principal objectives of the combined ocean monitoring efforts for both the PLOO and SBOO are to: (1) measure and document compliance with NPDES permit requirements and California Ocean Plan (Ocean Plan) water quality objectives and standards; (2) track movement and dispersion of the wastewater plumes discharged via the outfalls; (3) assess any impact of wastewater discharge on the local marine ecosystem, including effects on coastal water quality, seafloor sediments, and marine life.

Regular (core) monitoring is conducted on a weekly, quarterly, semiannual, and annual basis at a total of 142 discrete sites arranged in grids surrounding the PLOO and SBOO. The PLOO terminates at a discharge depth of around 100 m and is located approximately 7.2 km west of the PLWTP on the Point Loma peninsula. The SBOO terminates at a discharge depth of around 27 m and is located approximately 5.6 km offshore of southern San Diego, just north of the USA/Mexico border. Core monitoring in the PLOO region extends from Mission Beach southward to the tip of Point Loma along the shoreline, and from the nearshore to offshore waters from depths of around 9 to 116 m. Core monitoring of the SBOO region extends from Coronado, San Diego southward to Playa Blanca in northern Baja California, extending offshore from depths of around 9 to 55 m. In addition to monitoring at permanent core stations, an annual survey of benthic conditions (sediment quality, macrobenthic communities) is typically conducted each year at 40 randomly selected "regional" stations, which range from northern San Diego County southward to near the international border, extending offshore to depths of up to 500 m. These broader geographic surveys are useful for evaluating patterns over the entire San Diego coastal region and provide information important for distinguishing reference areas from those impacted by human activities. Additional information on background conditions for San Diego's coastal marine environment is also available from pre-discharge baseline studies conducted by the City for the PLOO region (1991–1993) and SBOO region (1995–1998).

Results of all receiving waters monitoring activities conducted for the PLOO and SBOO regions, between January 1, 2022 and December 31, 2023, are presented in this report (Chapters 2–9, Appendices A–B), and supplemental analyses are included in Appendices C–J. All raw data for the 2022–2023 sampling period have been submitted to either the SDRWQCB or the California Environmental Data Exchange Network (CEDEN) or may be made available upon request.

Chapter 1 represents a general introduction and overview of the combined Ocean Monitoring Program for the PLOO and SBOO regions, while chapters 2–9 include results of the main monitoring components conducted at the core and regional stations. In Chapter 2, data characterizing coastal oceanographic conditions and water mass transport for the region are evaluated. Chapter 3 presents the results of shoreline and offshore water quality compliance, including measurements of fecal indicator bacteria to assess compliance with water contact standards defined in the Ocean Plan. Chapter 4 presents the results of various plume tracking data collection efforts to assess the fate of discharged wastewater via the PLOO and SBOO. Assessments of regional benthic conditions, including benthic sediment quality (physical properties, sediment chemistry, and sediment toxicity), and the status of macrobenthic invertebrate communities are presented in Chapters 5, 6 and 7. Chapter 8 presents the results of trawling activities designed to monitor communities of bottom dwelling demersal fishes and megabenthic invertebrates. Finally, bioaccumulation assessments to measure contaminants in marine fishes are presented in Chapter 9.

In addition to the core monitoring activities described above, the City supports other projects relevant to assessing the status of receiving waters, including: (1) an ongoing long-term assessment of the health and status of San Diego’s kelp forest ecosystems conducted by the Scripps Institution of Oceanography (SIO) and funded by the City (see Appendix A); (2) satellite imaging of the San Diego/Tijuana coastal region to assess wastewater plume dispersion and coastal runoff (see Appendix B).

COASTAL OCEAN CONDITIONS

Oceanographic conditions, such as water temperatures, salinity, dissolved oxygen (DO) concentrations, pH, natural light levels (transmissivity or water clarity), and concentrations of chlorophyll *a* were generally within historical ranges and followed typical seasonal patterns reported for the PLOO and SBOO monitoring regions. As is characteristic for these waters, ocean conditions indicative of local coastal upwelling, such as relatively cold, dense waters with low DO and pH at subsurface depths, were most evident during the spring months of both years and winter months of 2023. These observations suggest that overall, the temporal and spatial variability observed in oceanographic conditions for coastal San Diego can be explained by a combination of local (e.g., coastal upwelling, rain-related runoff) and large-scale oceanographic-climatic processes, notably the transition from La Niña to El Niño conditions in late 2023, which allowed for the intrusion of warm water masses from offshore heatwave events once La Niña conditions broke down. Overall, ocean conditions during the past two years were consistent with well documented patterns for southern California and northern Baja California. As a result, proximity to either outfall is not considered a significant driver of the variations observed in oceanographic parameters discussed in this chapter.

WATER QUALITY COMPLIANCE

Overall water quality compliance during the 2022–2023 reporting period showed a general decline throughout San Diego coastal waters. Water quality was typically higher in the Point Loma region than the South Bay, and higher at offshore stations compared to shore stations region wide. Throughout the PLOO monitoring region, overall compliance with the 2015 Ocean Plan water contact standards was over 99%, while compliance with the 2019 Ocean Plan water contact standards in the PLOO region

was above the minimum threshold for all metrics throughout the report period. In contrast, all bacterial compliance metrics in the SBOO region, from the shoreline to offshore, indicate a decline in compliance when compared with the 2020–2021 reporting period. The SBOO nearshore stations continue to show the greatest water quality impacts, as has been reported in the past, with overall compliance below the minimum threshold for all fecal indicator bacteria (FIB) on at least 50% of days over the course of the report period. Stations with the highest occurrence of elevated FIB were those located closest to the mouth of the Tijuana River Estuary. Compliance at the SBOO kelp stations was better than the nearshore but still below the minimum threshold on one or more days throughout the report period. Compliance at the SBOO offshore stations was above the minimum threshold for both fecal coliforms and *Enterococcus* throughout the report period, while the standard for total coliforms was out of compliance at I16 on one or more days during the report period.

Precipitation, which is known to drive declines in water quality, especially at shore and kelp stations, was notably higher during the current report period compared to the previous report period (20.33 inches over 2022–2023 vs. 15.68 inches over 2020–2021). Additionally, since August 2022 the SBIWTP has increased flows to the SBOO (avg. 21 MGD to 31 MGD), and since March 2023 primary treatment has been limited, which has likely contributed to the observed decrease in water quality at offshore stations in the SBOO region. Nevertheless, the occurrence of samples with elevated bacterial levels near the outfall remain low compared to those taken before the initiation of secondary treatment, which began in January 2011 at the SBIWTP. By comparison, the majority of analyses showing elevated bacterial levels continue to be associated with stations near the mouth of the Tijuana River Estuary and they continue to be more prevalent in the wet season. However, even in the dry season, the South Bay region exhibits a much higher number of sample exceedances than those in the Point Loma region, which is likely driven by the shallow southern swell bringing surface currents northward along the coast in the summertime and thereby transporting transboundary flows of contaminated water into the South Bay. Thus, the primary source of contamination in San Diego coastal receiving waters is of known origin and likely associated with contaminated outflows from the Tijuana River and transboundary flows not related to wastewater discharge. The relatively low number of samples with elevated FIB near the outfalls, compared to the nearshore, highlight the minimal impact of treated wastewater discharge. As a result, we conclude that non-compliance with receiving water limitations for bacterial characteristics is primarily driven by known contaminated outflows from rivers, such as the Tijuana River Estuary, and other non-point source runoff and not a result of treated wastewater discharge.

PLUME DISPERSION

Observations of potential plume detections throughout the 2022–2023 reporting period demonstrated that the PLOO effluent plume generally remained offshore and below a depth of 34 m, while the SBOO plume was generally trapped below the pycnocline during seasonal periods of water column stratification. However, unlike the PLOO plume, the SBOO plume showed evidence of rising to the surface when waters became more mixed and stratification broke down, typically during the winter months. Despite differences in observed plume vertical rise heights between the outfalls, both effluent plumes generally remained offshore and were transported along the coast with no evidence of nearshore movement. Although variable over space and time, the general axes of subsurface current velocities in the PLOO and SBOO regions continued to follow a N:NW by S:SE trajectory regardless of season. In 2023, there were several eastward excursions of surface currents during stratified conditions; however, these depths were above the pycnocline and unlikely to impact plume dispersion. Thus, as effluent mixed

with ambient seawater, it generally travelled along the coast rather than being directed inshore toward the kelp beds, shoreline, or other recreational waters. As a result, there was no evidence that wastewater discharged to the ocean, via either the PLOO or SBOO, reached recreational waters along the shore or nearshore kelp beds. Similarly, results of water quality monitoring over the past 33 years off Point Loma, and 29 years in the South Bay, are consistent with observations from remote sensing studies (i.e., satellite imagery) over the last 20+ years, which show a lack of shoreward transport of wastewater plumes from either outfall. Within the shallower SBOO region, though bacteriological analyses from monitoring stations near the outfall do indicate a slight decrease in offshore water quality during the reporting period, the Tijuana River and Los Buenos Creek remain likely sources of contaminated water during or after storms or other periods of increased flows. The Tijuana River estuary often delivers less saline, dissolved organic matter and nutrient-rich water masses, resulting in a complex environment in the SBOO region. This is consistent with past studies, which indicate that other sources, such as terrestrial runoff or outflows from rivers and creeks were more likely to impact coastal water quality than wastewater discharge from the outfalls, especially during and immediately after significant rain events.

REGIONAL BENTHIC CONDITIONS

Benthic habitats, and associated biological communities, found on the continental shelf and upper slope off San Diego were found to be in excellent condition during the 2022–2023 reporting period. There was no evidence of fine particle loading related to wastewater discharge via the PLOO or SBOO, and no evidence of degraded benthic habitats, in terms of the chemical properties of the sediments, or spatial patterns in the distribution of the different types of contaminants. Instead, contaminant concentrations near the outfalls were generally within the range of variability observed throughout both outfall regions. Although, a number of indicators of organic loading, trace metals, pesticides, PCBs, PAHs, and PBDEs were detected in sediment samples throughout the San Diego region, almost all occurred at concentrations below available ERL (Effects Range Low) and ERM (Effects Range Median) thresholds, similar to that observed in previous years. This is further supported by results from sediment toxicity testing in offshore San Diego waters that revealed minimal toxicity at all regional stations tested.

Benthic macrofaunal communities off San Diego also appeared to be healthy, with most assemblages appearing to be similar to those observed in the region from 1991 through 2023, and throughout southern California and northern Baja California. Although communities varied across depth and sediment gradients, there was no evidence of disturbance or significant environmental degradation that could be attributed to anthropogenic factors, such as wastewater discharge. Instead, these communities segregated by habitat characteristics, such as depth and sediment particle size, often corresponding with the “patchy” habitats reported to occur naturally in southern California’s offshore coastal waters. Finally, the Benthic Response Index (BRI) further confirmed little evidence of disturbance off San Diego with 95% of all calculated BRI values being indicative of reference conditions, an improvement over previous reporting periods (2018–2019: 89%; 2020–2021: 94%). These results, when integrated with sediment chemistry and sediment toxicity results, demonstrated that the shelf off San Diego remains unimpacted by the PLOO or SBOO. Consequently, there is presently no evidence to suggest that wastewater discharge via the PLOO or SBOO is affecting the quality of benthic sediments off San Diego to the point that it may degrade resident marine biological communities.

DEMERSAL FISHES AND MEGABENTHIC INVERTEBRATES

Demersal fish and megabenthic invertebrate communities trawled off San Diego remain unaffected by wastewater discharge. Although highly variable, patterns in the abundance and distribution of individual species were similar regardless of proximity to either outfall and were representative of similar habitats throughout the Southern California Bight (SCB). Pacific Sanddabs dominated assemblages surrounding the PLOO (54% of fishes recorded in the region), and Speckled Sanddab dominated assemblages surrounding the SBOO (58% of fishes recorded in the region), as they have done since monitoring began in each region. Dover Sole, Halfbanded Rockfish and Longfin Sanddab were also prevalent in PLOO assemblages (24% of all fishes recorded), while Longfin Sanddab were also prevalent within the SBOO region during this period (12% of fishes recorded). More than 80% of the species collected in the PLOO and SBOO monitoring regions were < 30 cm in length. External examination of fish collected indicated that fish populations remained healthy off San Diego, with fewer than 0.4% of all fish having external parasites or showing any evidence of disease or other abnormalities. As abnormalities or parasites were present across the region, there does not appear to be a relationship between these anomalies and proximity to either outfall.

Trawl-caught invertebrate assemblages in the PLOO were dominated by the sea urchins *Lytechinus pictus* and *Strongylocentrotus fragilis* which accounted for 97% of the invertebrates recorded in the region. In contrast to the PLOO region, no single species dominated SBOO trawls over the reporting period. Rather, five species occurred in more than 50% of the hauls and accounted for between 2% to 30% of the total recorded invertebrates in the region, including the shrimps *Crangon nigromaculata* and *Sicyonia penicillata*, the sea stars *Astropecten californicus* and *Luidia armata*, and the snail *Philine auriformis*. No notable spatial patterns in megabenthic invertebrate community parameters were observed relative to the proximity of the PLOO or SBOO discharge sites and results were generally consistent with previous findings for the two regions and elsewhere in the SCB.

The abundance and distribution of fish and invertebrate species varied similarly at stations located near and far from the outfalls in both regions. The high degree of variability in these assemblages during this reporting period was similar to that observed in previous years, including before wastewater discharge began through either outfall. Furthermore, similar variability has been observed in comparable habitats elsewhere off the coast of southern California. Consequently, changes in local community structure of these fishes and invertebrates are more likely due to natural factors, such as changes in ocean temperatures associated with El Niño or other large-scale oceanographic events.

CONTAMINANTS IN MARINE FISHES

The accumulation of chemical contaminants in San Diego marine fishes varied across species and stations, but most values were within ranges reported previously for southern California fishes. Overall, there was no evidence of contaminant accumulation in PLOO or SBOO fishes that could be associated with wastewater discharge from either outfall, which is consistent with historical findings. Although several different trace metals, pesticides, PCB congeners, PBDEs and various PAHs were detected in both liver and muscle tissues, these contaminants occurred in fishes distributed throughout both regions, with no patterns that could be attributed to wastewater discharge via the outfalls. Consequently, the occurrence of these contaminants in some local fishes off San Diego is likely influenced by other factors, such as the widespread distribution of many contaminants in southern California sediments, differences

in the physiology and life history traits of various species of fish, different exposure pathways, and differences in the migration pathways of various species. For example, an individual fish may be exposed to contaminants at a polluted site, but then migrate to an area that is less contaminated. This is of particular concern for fishes collected in the vicinity of the PLOO and SBOO, as there are many other nearby potential point and non-point sources of contamination.

CONCLUSIONS

The findings and conclusions for the ocean monitoring efforts conducted for the PLOO and SBOO monitoring regions, during 2022 and 2023, were mostly consistent with previous years. The most notable change observed during this reporting period was a region wide decline in water quality largely attributed to heavier than normal rainfall resulting in increased terrestrial runoff and nearshore contamination. Otherwise, there were few changes to local receiving waters, benthic sediments, or marine invertebrate and fish communities that could be attributed to treated wastewater discharge. The spatial and temporal distribution of reduced water quality observations corroborate previous findings that terrestrial inputs, such as the Tijuana River, are the largest drivers of contamination in the region. Although an observed decrease in water quality at some offshore stations in the SBOO region may be attributed to an increase in flows and reduced primary treatment at the SBIWTP, there was no evidence that treated wastewater was a driver of nearshore contamination. Further still, there was no evidence that wastewater plumes from either of the two outfalls were transported shoreward into nearshore recreational waters. There were also no clear outfall related patterns in sediment contaminant distributions or differences between invertebrate and fish assemblages at the different monitoring sites. Additionally, benthic habitats surrounding both outfalls, and throughout the entire San Diego region, remained in good overall condition, similar to reference conditions for much of the SCB. Finally, the low level of contaminant accumulation, minimal sediment toxicity, and general lack of physical anomalies or other symptoms of disease or stress in local fishes was also indicative of a healthy marine environment off San Diego.

Chapter 1

General Introduction

Chapter 1. General Introduction

PROGRAM REQUIREMENTS & OBJECTIVES

Ocean monitoring within the Point Loma and South Bay outfall regions is conducted by the City of San Diego (City) in accordance with requirements set forth in National Pollution Discharge Elimination System (NPDES) permits and associated orders for the following: the Point Loma Wastewater Treatment Plant (PLWTP), the South Bay Water Reclamation Plant (SBWRP), and the South Bay International Wastewater Treatment Plant (SBIWTP), which is owned and operated by the U.S. Section of the International Boundary and Water Commission (USIBWC) (see Table 1.1). These documents specify the terms and conditions that allow treated effluent to be discharged to the Pacific Ocean via the Point Loma Ocean Outfall (PLOO) and South Bay Ocean Outfall (SBOO). In addition, the Monitoring and Reporting Program (MRP), included within each of these orders, defines the requirements for monitoring ocean (receiving) waters surrounding the two outfalls. These requirements include sampling design, frequency of sampling, field operations and equipment, regulatory compliance criteria, types of laboratory tests and analyses, data management and analysis, statistical methods and procedures, environmental assessment, and reporting guidelines.

The combined Ocean Monitoring Program for these regions is designed to assess the impact of wastewater discharged through the PLOO and SBOO on the coastal marine environment off San Diego. The main objectives of the program are to: (1) measure and document compliance with NPDES permit requirements and California Ocean Plan (Ocean Plan) water quality objectives and standards; (2) track movement and dispersion of the wastewater plumes discharged via the outfalls; (3) assess any impact of wastewater discharge on the local marine ecosystem, including effects on coastal water quality, seafloor sediments, and marine life.

BACKGROUND

Point Loma Ocean Outfall

The City began operation of the PLWTP and original PLOO off Point Loma in 1963, at which time treated effluent was discharged approximately 3.9 km west of the Point Loma peninsula at a depth of around 60 m. The PLWTP operated as a primary treatment facility from 1963 to 1985, after which it was upgraded to advanced primary treatment between mid-1985 and July 1986. This improvement involved the addition of chemical coagulation to the treatment process, which resulted in an increase in removal of total suspended solids (TSS) to about 75%. Since then, the treatment process has continued to be improved with the addition of more sedimentation basins, expanded aerated grit removal, and refinements in chemical treatment, which together further reduced mass emissions from the plant. For example, TSS removals are now consistently greater than the 80%, as required by the NPDES permit.

The structure of the PLOO was significantly modified in the early 1990s when it was extended about 3.3 km farther offshore in order to prevent intrusion of the waste field into nearshore waters and to increase compliance with Ocean Plan standards for water-contact sports areas. Discharge from the original 60-m

terminus was discontinued in November 1993 following completion of the outfall extension. Currently, the PLOO extends approximately 7.2 km west of the PLWTP to a depth of around 94 m, where the main outfall pipe splits into a Y-shaped (wye) multiport diffuser system. The two diffuser legs extend an additional 762 m to the north and south, each terminating at a depth of about 98 m. The average discharge of effluent through the PLOO in 2022–2023 was about 138.7–152.8 mgd (million gallons per day).

South Bay Ocean Outfall

The SBOO is located just north of the international border between the United States and Mexico where it terminates approximately 5.6 km offshore and west of Imperial Beach at a depth of around 27 m. Unlike other southern California ocean outfalls that lie on the surface of the seafloor, the SBOO pipeline begins as a tunnel on land that extends from the SBWRP and SBIWTP facilities to the coastline, after which it continues beneath the seabed 4.3 km offshore. The outfall pipe connects to a vertical riser assembly that conveys effluent to a pipeline buried just beneath the surface of the seafloor. This subsurface pipeline then splits into a Y-shaped (wye) multiport diffuser system with the two diffuser legs each extending an additional 0.6 km to the north or south. The SBOO was originally designed to discharge wastewater through 165 diffuser ports and risers, which included one riser at the center of the wye and 82 risers spaced along each diffuser leg. Since discharge began, however, low flow rates have required closure of all ports along the northern diffuser leg and many along the southern diffuser leg in order for the outfall to operate effectively. Consequently, wastewater discharge is restricted primarily to the distal end of the southern diffuser leg and to a few intermediate points at or near the center of the wye. The average discharge of effluent through the SBOO in 2022–2023 was about 29.1–30.9 mgd, including about 3.5–3.8 mgd of secondary and tertiary treated effluent from the SBWRP, and 25.6–27.1 mgd of secondary treated effluent from the SBIWTP.

RECEIVING WATERS MONITORING

The total area for the PLOO and SBOO monitoring program covers approximately 881 km² (~340 mi²) of coastal marine waters from Northern San Diego County into Northern Baja California. Core monitoring for the Point Loma region is conducted at 82 stations, located from the shore to a depth of around 116 m. Core monitoring for the South Bay region is conducted at a total of 53 stations, ranging from the shore to depths of around 61 m (Figure 1.1). Each of the core monitoring stations is sampled for specific parameters as stated in their respective MRPs. A summary of the results for all quality assurance procedures performed during 2022 and 2023, in support of these requirements, can be found in City of San Diego (2023, 2024a). Data collected during the 2022–2023 reporting period have been submitted to either the Regional Water Quality Control Board, the California Environmental Data Exchange Network (CEDEN) or the City’s Open Data Portal (2024b) and may be accessed upon request.

Prior to 1994, the City conducted an extensive ocean monitoring program off Point Loma surrounding the original 60-m discharge site. This program was subsequently expanded with the construction and operation of the deeper outfall, as discussed previously. Data from the last year of regular monitoring near the original PLOO discharge site are presented in City of San Diego (1995a), while the results of a 3-year “recovery study” are summarized in City of San Diego (1998). Additionally, a more detailed assessment of spatial and temporal patterns surrounding the original discharge site is available (Zmarzly et al. 1994). From 1991 through 1993, the City also conducted “pre-discharge” monitoring for the new PLOO discharge site in order to collect baseline data prior to wastewater discharge into these deeper waters (City of San Diego 1995a, b). All permit mandated ocean monitoring for the South Bay region

has also been performed by the City since wastewater discharge through the SBOO began in 1999; this included pre-discharge monitoring for 3½ years (July 1995–December 1998) in order to provide background information against which post-discharge conditions could be compared (City of San Diego, 2000). Results of NPDES mandated monitoring for the extended PLOO from 1994 to 2019, and the SBOO from 1999 to 2019, are available in previous annual receiving waters monitoring reports (e.g., City of San Diego 2020). Finally, additional detailed assessments of the PLOO region have been completed as part of past modified NPDES permit renewal applications for the PLWTP submitted by the City (e.g., City of San Diego 2022) and subsequent technical decisions issued by the USEPA (e.g., USEPA 2017).

The City has also conducted annual region-wide surveys off the coast of San Diego since 1994, either as part of regular outfall monitoring requirements (e.g., City of San Diego 1999), or as part of larger multi-agency surveys of the entire Southern California Bight (SCB) (e.g., Gillett et al. 2017). The latter include the 1994 Southern California Bight Pilot Project (SCCWRP 1998) and subsequent Bight programs from 1998 through 2018 (e.g., SCCWRP 2018). These large-scale surveys are useful for characterizing the ecological health of diverse coastal areas to distinguish reference sites from those impacted by wastewater or storm water discharges, urban runoff, or other sources of contamination. In addition to the above activities, the City participates as a member of the Region Nine Kelp Survey Consortium to fund aerial surveys of all the major kelp beds in San Diego and Orange Counties (e.g., MBC 2023).

SPECIAL STUDIES & ENHANCED MONITORING

The City has actively participated in, or supported, numerous important special projects, or enhanced ocean monitoring studies, over the past 10 years or more. Many of these projects to date were identified as part of a scientific review of the City’s Ocean Monitoring Program, conducted by the Scripps Institution of Oceanography (SIO) and other participating institutions (SIO 2004). This review evaluated the environmental monitoring needs of the region, and recommended special projects based on priorities identified. Examples of special projects currently underway, or being initiated include:

San Diego Kelp Forest Ecosystem Monitoring Project: This project represents continuation of a long-term commitment by the City to support important research conducted on local kelp forests by SIO. This work is essential to assessing the health of San Diego’s kelp forests and monitoring the effects of wastewater discharge on the local coastal ecosystem relative to other anthropogenic and natural influences (see Appendix A).

Real-Time Oceanographic Mooring Systems (RTOMS) for the Point Loma and South Bay Ocean Outfalls: This project addresses recommendations that the City should improve monitoring of the fate and behavior of wastewater discharged to the ocean via the SBOO (Terrill et al. 2009) and PLOO (Rogowski et al. 2012a, 2012b, 2013). The project involves the deployment of RTOMS at the terminal ends of the PLOO and SBOO to provide real time data on ocean conditions. The project began in late 2015 with initial deployment of the SBOO mooring in December 2016 and the PLOO mooring in March 2018. This project is being conducted in partnership with SIO, whom presently operate a similar mooring system off Del Mar. The project is expected to significantly enhance the City’s environmental monitoring capabilities in order to address current and emerging issues relevant to the health of San Diego’s coastal waters, including plume dispersion, subsurface current patterns, ocean

acidification, hypoxia, nutrient sources, and coastal upwelling. Additional details are available in the approved Plume Tracking Monitoring Plan for the project (City of San Diego 2018) and Chapter 4.

Sediment Toxicity Monitoring of the San Diego Ocean Outfall Regions: This project started with a 3-year pilot study implemented as a new joint regulatory requirement for the Point Loma and South Bay outfall regions in 2015. Findings for the 2016–2018 pilot study (City of San Diego 2015) were summarized in a final project report (City of San Diego 2019) that included recommendations for continued sampling through 2023. The findings are now being utilized as part of a Sediment Quality Triad Assessment alongside analyses of sediment chemistry and macrofaunal community data to provide a snapshot of the region’s sediment quality and benthic community structure (see Chapter 7).

Remote Sensing of the San Diego / Tijuana Coastal Region: This project represents a long-term effort, funded by the City and the USIBWC since 2002, to utilize satellite and aerial imagery to better understand regional water quality conditions off San Diego. The project is conducted by Ocean Imaging (Littleton, CO), and is focused on detecting and tracking the dispersion of wastewater plumes from local ocean outfalls and nearshore sediment plumes caused by stormwater runoff or outflows from local bays and rivers (see Appendix B and City of San Diego 2024c).

San Diego Regional Benthic Condition Assessment Project: This multi-phase study represents an ongoing, long-term project designed to assess the condition of continental shelf and slope habitats throughout the entire San Diego region.

REPORT COMPONENTS & ORGANIZATION

This report presents a comprehensive biennial assessment of the results of all receiving waters monitoring activities conducted during 2020 and 2021 for both the Point Loma and South Bay outfall regions. Included herein are results from all regular core stations that comprise the fixed-site monitoring grids surrounding the two outfalls (Figure 1.1), as well as results from the 2020–2021 summer benthic surveys of randomly selected sites that range from near the USA/Mexico border to northern San Diego County (Figure 1.2). The main components of the combined monitoring program are covered in the following sections or chapters: Executive Summary; General Introduction (Chapter 1); Coastal Oceanographic Conditions (Chapter 2); Water Quality Compliance (Chapter 3); Plume Dispersion (Chapter 4); Sediment Quality (Chapter 5); Macrobenthic Communities (Chapter 6); San Diego Regional Benthic Condition Assessment (Chapter 7); Demersal Fish and Megabenthic Invertebrate Communities (Chapter 8); Contaminants in Marine Fishes (Chapter 9). Supplemental analyses for Chapters 2–9 are included in Appendices C–J. All raw data for the 2020–2021 sampling period have been submitted to either the Regional Water Quality Control Board or the California Environmental Data Exchange Network (CEDEN) and will be provided upon request.

LITERATURE CITED

City of San Diego. (1995a). Receiving Waters Monitoring Report for the Point Loma Ocean Outfall, 1994. City of San Diego Ocean Monitoring Program, Metropolitan Wastewater Department, Environmental Monitoring and Technical Services Division, San Diego, CA.

- City of San Diego. (1995b). Outfall Extension Pre-Construction Monitoring Report (July 1991–October 1992). City of San Diego Ocean Monitoring Program, Metropolitan Wastewater Department, Environmental Monitoring and Technical Services Division, San Diego, CA.
- City of San Diego. (1998). Recovery Stations Monitoring Report for the Original Point Loma Ocean Outfall (1991–1996). City of San Diego Ocean Monitoring Program, Metropolitan Wastewater Department, Environmental Monitoring and Technical Services Division, San Diego, CA.
- City of San Diego. (1999). San Diego Regional Monitoring Report for 1994–1997. City of San Diego Ocean Monitoring Program, Metropolitan Wastewater Department, Environmental Monitoring and Technical Services Division, San Diego, CA.
- City of San Diego. (2000). Final Baseline Monitoring Report for the South Bay Ocean Outfall (1995–1998). City of San Diego Ocean Monitoring Program, Metropolitan Wastewater Department, Environmental Monitoring and Technical Services Division, San Diego, CA.
- City of San Diego. (2015). Sediment Toxicity Monitoring Plan for the South Bay Ocean Outfall and Point Loma Ocean Outfall Monitoring Regions, San Diego, California. Submitted by the City of San Diego Public Utilities Department to the San Diego Water Board and USEPA, Region IX, August 28, 2015 [approved 9/29/2015].
- City of San Diego. (2018). Plume Tracking Monitoring Plan for the Point Loma and South Bay Ocean Outfall Regions, San Diego, California. Submitted by the City of San Diego Public Utilities Department to the San Diego Water Board and USEPA, Region IX, March 28, 2018 [approved 4/25/2018].
- City of San Diego. (2019). Final Project Report for the Sediment Toxicity Pilot Study for the San Diego Ocean Outfall Monitoring Regions, 2016–2018. Submitted May 30, 2019 by the City of San Diego Public Utilities Department to the San Diego Regional Water Quality Control Board and U.S. Environmental Protection Agency, Region IX. 16 pp.
- City of San Diego. (2022). Application for Renewal of NPDES CA0107409 and 301(h) Modified Secondary Treatment Requirements for Biochemical Oxygen Demand and Total Suspended Solids, Point Loma Ocean Outfall and Point Loma Wastewater Treatment Plant. Volumes I–X, Appendices A–U. The City of San Diego, Public Utilities Department, San Diego, CA.
- City of San Diego. (2023). Annual Receiving Waters Monitoring & Toxicity Testing Quality Assurance Report, 2022. City of San Diego Ocean Monitoring Program, Public Utilities Department, Environmental Monitoring and Technical Services Division, San Diego, CA.
- City of San Diego. (2024a). Annual Receiving Waters Monitoring & Toxicity Testing Quality Assurance Report, 2023. City of San Diego Ocean Monitoring Program, Public Utilities Department, Environmental Monitoring and Technical Services Division, San Diego, CA.
- City of San Diego. (2024b). Open Data Portal. <https://data.sandiego.gov/datasets/>
- City of San Diego. (2024c). Ocean Monitoring Reports. <https://www.sandiego.gov/public-utilities/sustainability/ocean-monitoring/reports>

- Gillett, D.J., L.L. Lovell, and K.C. Schiff. (2017). Southern California Bight 2013 Regional Monitoring Program: Volume VI. Benthic Infauna. Technical Report 971. Southern California Coastal Water Research Project. Costa Mesa, CA.
- [MBC] MBC Aquatic Sciences. (2023). Status of the Kelp Beds 2021–2022, Kelp Bed Surveys: Orange, and San Diego Counties. Final Report, August 2023. MBC Aquatic Sciences, Costa Mesa CA.
- Rogowski, P., E. Terrill, M. Otero, L. Hazard, S.Y. Kim, P.E. Parnell, and P. Dayton. (2012a). Final Report: Point Loma Ocean Outfall Plume Behavior Study. Prepared for City of San Diego Public Utilities Department by Scripps Institution of Oceanography, University of California, San Diego, CA.
- Rogowski, P., E. Terrill, M. Otero, L. Hazard, and W. Middleton. (2012b). Mapping ocean outfall plumes and their mixing using Autonomous Underwater Vehicles. *Journal of Geophysical Research*, 117: C07016.
- Rogowski, P., E. Terrill, M. Otero, L. Hazard, and W. Middleton. (2013). Ocean outfall plume characterization using an Autonomous Underwater Vehicle. *Water Science & Technology*, 67(4): 925–933.
- [SCCWRP] Southern California Coastal Water Research Project. (1998). Southern California Bight 1994 Pilot Project: Volumes I–VI. Southern California Coastal Water Research Project, Westminster, CA .
- [SCCWRP] Southern California Coastal Water Research Project. (2018). Southern California Bight 2018 Regional Monitoring Program: Contaminant Impact Assessment Field Operations Manual. Southern California Coastal Water Research Project. Costa Mesa, CA.
- [SIO] Scripps Institution of Oceanography. (2004). Point Loma Outfall Project, Final Report, September 2004. Scripps Institution of Oceanography, University of California, La Jolla, CA.
- Terrill, E., K. Sung Yong, L. Hazard, and M. Otero. (2009). IBWC/Surfrider – Consent Decree Final Report. Coastal Observations and Monitoring in South Bay San Diego. Scripps Institution of Oceanography, University of California, San Diego, CA.
- [USEPA] United States Environmental Protection Agency. (2017). City of San Diego’s Point Loma Wastewater Treatment Plant Application for a Modified NPDES Permit under Sections 301(h) and (j)(5) of the Clean Water Act. Technical Decision Document. United States Environmental Protection Agency, Region IX, San Francisco, CA.
- Zmarzly, D.L., T.D. Stebbins, D. Pasko, R.M. Duggan, and K.L. Barwick. (1994). Spatial patterns and temporal succession in soft-bottom macroinvertebrate assemblages surrounding an ocean outfall on the southern San Diego shelf: relation to anthropogenic and natural events. *Marine Biology*, 118: 293–307.

CHAPTER 1

FIGURES & TABLES

Table 1.1

NPDES permits and associated orders issued by the San Diego Water Board for the Point Loma Wastewater Treatment Plant (PLWTP), South Bay Water Reclamation Plant (SBWRP), and South Bay International Wastewater Treatment Plant (SBIWTP) discharges to the Pacific Ocean via the PLOO and SBOO.

Facility	Outfall	NPDES Permit No.	Order No.	Effective Dates
PLWTP	PLOO	CA0107409	R9-2017-0007 ^a	October 1, 2017–September 30, 2022
SBWRP	SBOO	CA0109045	R9-2021-0011	July 1, 2021–June 30, 2026
SBIWTP	SBOO	CA0108928	R9-2021-0001	July 1, 2021–June 30, 2026

^a Order R9-2017-0007 amended by Order R9-2022-0078 (permit administratively extended)

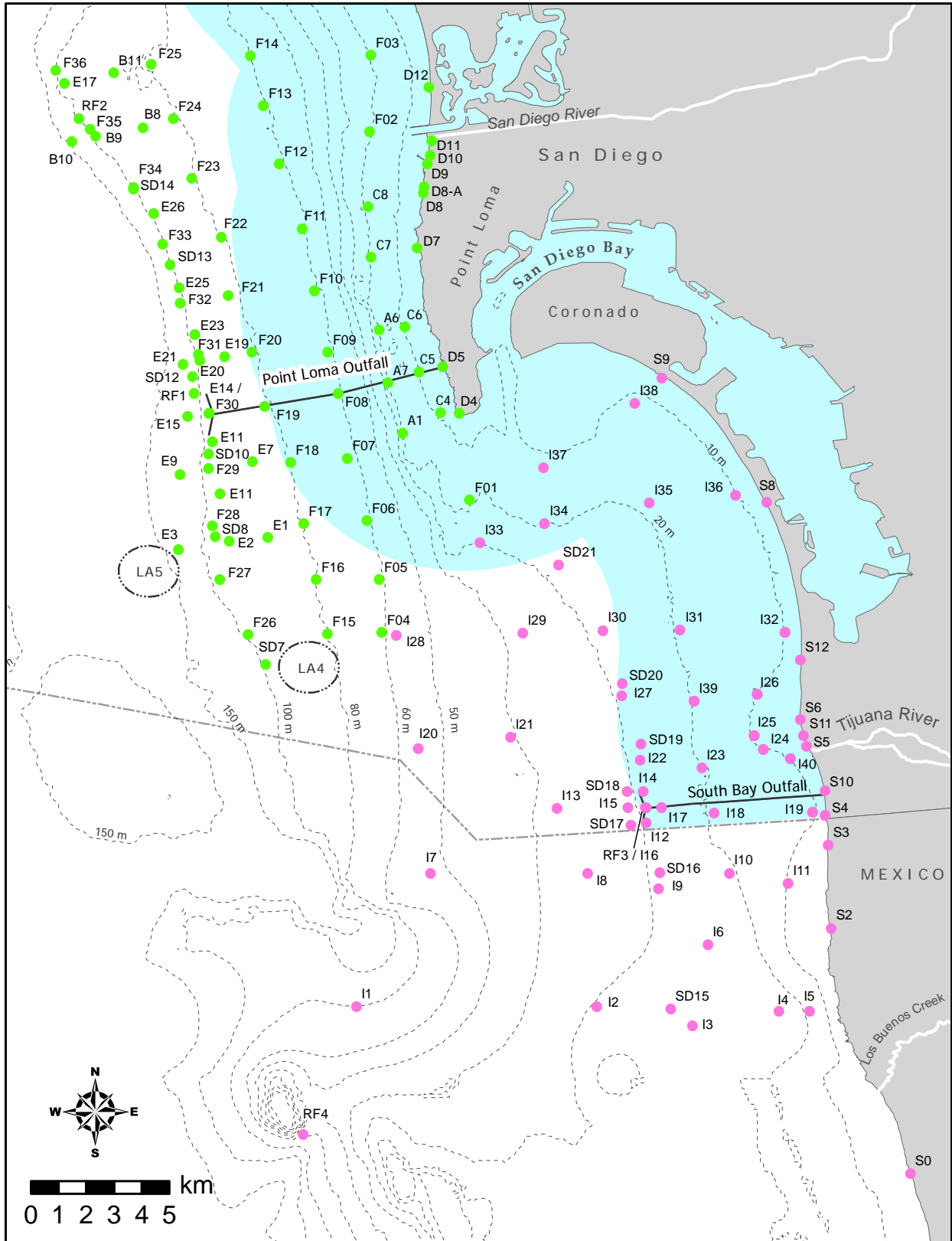


Figure 1.1

Core receiving waters monitoring stations for the PLOO (green) and SBOO (pink) as part of the City of San Diego's Ocean Monitoring Program. Light blue shading represents State of California jurisdictional waters.

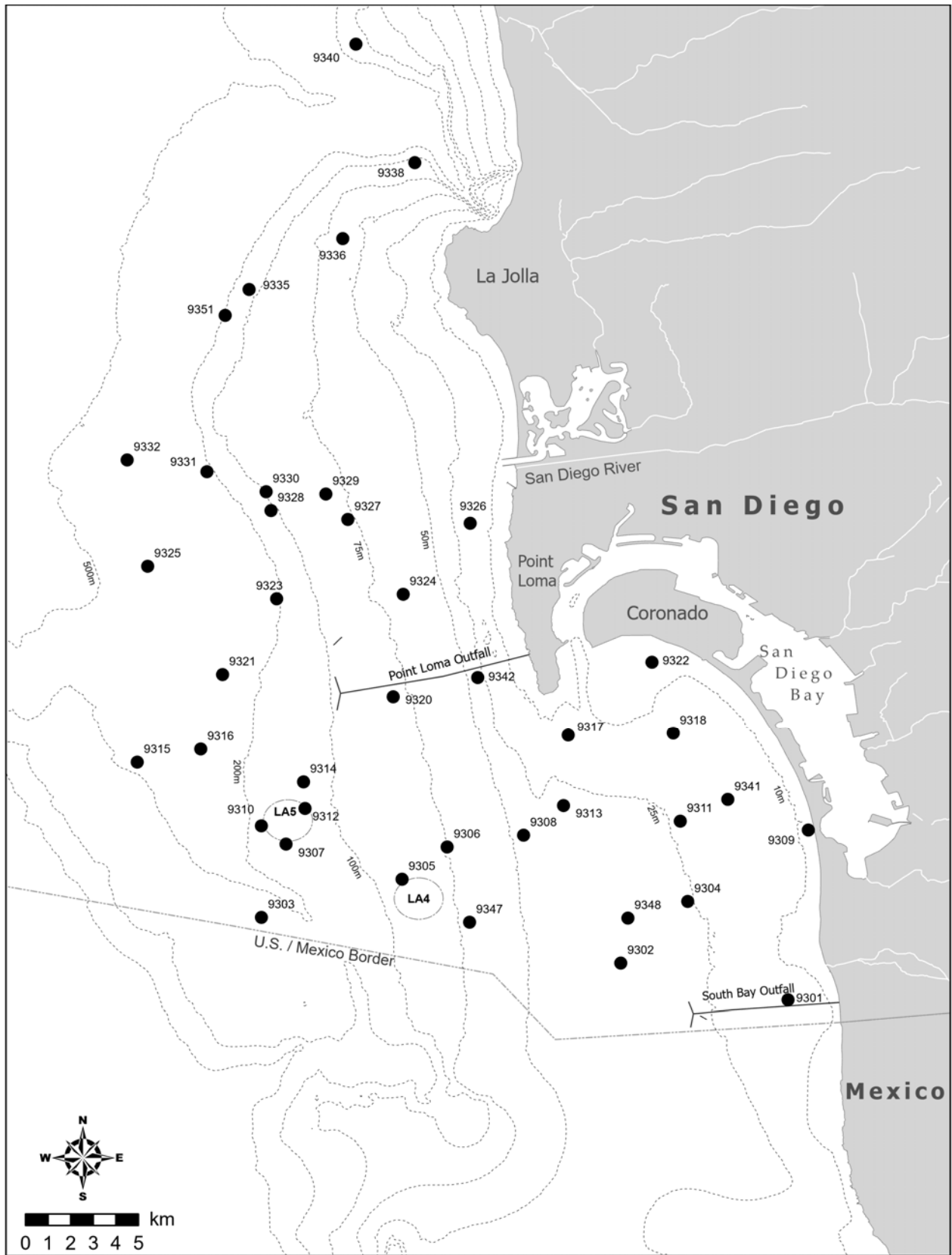


Figure 1.2
 Regional randomly selected benthic survey stations sampled during summer 2022 as part of the City of San Diego's Ocean Monitoring Program.

Chapter 2

Coastal Oceanographic Conditions

Chapter 2. Coastal Oceanographic Conditions

INTRODUCTION

The City of San Diego (City) collects a comprehensive suite of oceanographic data from coastal waters surrounding the Point Loma Ocean Outfall (PLOO) and South Bay Ocean Outfall (SBOO) to characterize regional conditions and to identify possible impacts of wastewater discharge and other factors on the marine environment. These data include measurements of ocean temperature, salinity, light transmittance (transmissivity), dissolved oxygen, pH, and chlorophyll *a* throughout the water column, all of which are considered important indicators of physical and biological processes that can impact marine life (Skirrow 1975, Mann 1982, Mann and Lazier 1991). As the fate of wastewater discharged into the ocean is determined by multiple factors (e.g., outfall geometry, rate of effluent discharge, water column mixing, ocean currents, tidal flows), evaluations of physical parameters that influence the mixing potential of the water column are important components of many ocean monitoring programs (Bowden 1975, Pickard and Emery 1990).

In the nearshore coastal waters of the Southern California Bight (SCB), including the PLOO and SBOO monitoring regions, ocean conditions are influenced by multiple factors. These include: (1) large-scale climatic processes, such as El Niño Southern Oscillations (ENSO), Pacific Decadal Oscillations (PDO), and North Pacific Gyre Oscillations (NPGO), which can affect long-term oceanographic trends (Peterson et al. 2006, McClatchie et al. 2008, 2009, Bjorkstedt et al. 2010, 2011, 2012, Wells et al. 2013, NOAA/NWS 2024); (2) the California Current System, coupled with local gyres that transport distinct water masses into and out of the SCB (Lynn and Simpson 1987, Leising et al. 2014); (3) seasonal changes in local weather patterns (Bowden 1975, Skirrow 1975, Pickard and Emery 1990), which are a primary driver of water column stratification typically observed off San Diego and in coastal waters throughout the rest of southern California (Terrill et al. 2009, Rogowski et al. 2012a,b, 2013). These seasonal patterns include typically warmer and more stratified waters in the dry season, from May through September, and cooler, weakly stratified and well-mixed waters, in the wet season, from October through April (e.g., City of San Diego 2022a, Hess 2019, 2020).

Understanding changes in oceanographic conditions due to natural processes, such as the seasonal patterns described above, is of utmost importance since they will likely affect the transport and distribution of wastewater, storm water, and other nearshore plumes. In the PLOO and SBOO monitoring regions, nearshore plumes include sediment or turbidity plumes associated with outflows from local bays, major rivers, lagoons and estuaries, discharges from storm drains or other point sources, surface runoff from local watersheds, seasonal upwelling, and variable ocean currents or eddies. Outflow plumes from the San Diego River, San Diego Bay, and the Tijuana River can contribute significantly to patterns of nearshore turbidity, sediment deposition, and bacterial contamination (see Largier et al. 2004, Terrill et al. 2009, Svejksky 2010, 2017, Hess 2018, 2019, 2020).

In order to assess conditions on a comprehensive spatial scale, quarterly water quality surveys have historically been conducted across the two outfall regions (beginning in 1991 at PLOO and 1995 at SBOO). Subsequent studies of the fate and behavior of wastewater discharged to the ocean via the

SBOO (Terrill et al. 2009) and the PLOO (Rogowski et al. 2012a,b, 2013) included recommendations to use real-time oceanographic mooring systems (RTOMS) and advanced sampling technologies to better understand nearshore coastal water quality and the impacts of local ocean currents and tidal fluxes on effluent plume dynamics. This higher temporal resolution data collection began in 2017 at SBOO and in 2018 at PLOO (City of San Diego 2018a, 2020). While quarterly surveys provide a snapshot of conditions across a large regional area, the RTOMS provide near-continuous information on how ocean conditions change over time near the two ocean outfalls. As such, some variations in ranges and seasonal comparisons between quarterly surveys and RTOMS data are expected, and differences between these sampling approaches are discussed in relevant sections.

This chapter presents analysis and interpretation of the oceanographic monitoring data collected during 2022 and 2023 for the coastal waters surrounding the PLOO and SBOO. The primary goals of this chapter are to: (1) summarize coastal oceanographic conditions in these regions to provide information on the state of local receiving waters; (2) determine if water clarity, pH or dissolved oxygen are significantly altered at any point outside of the Zone of Initial Dilution (ZID) as a result of the outfall discharge; (3) evaluate local ocean conditions off the coast of San Diego within the context of regional climatic processes. In addition, results of remote sensing observations (e.g., satellite imagery) are combined with measurements of physical oceanographic parameters to provide further insight on the horizontal transport of surface waters off San Diego. The results reported herein are also referred to in subsequent chapters to explain patterns of fecal indicator bacteria distributions and plume dispersion (see Chapters 3 and 4) as well as other changes in the local marine environment (see Chapters 5-9).

MATERIALS AND METHODS

Quarterly CTD surveys

Data Collection

A total of 69 offshore water quality monitoring stations were sampled quarterly to assess coastal oceanographic conditions in the two outfall regions (Figure 2.1). These include 36 stations surrounding the PLOO and 33 stations surrounding the SBOO. The PLOO stations are designated F1–F36 and are located along or adjacent to the 18, 60, 80, and 98-m depth contours. The SBOO stations are designated I1–I18, I20–I23, I27–I31, and I33–I38, and are located along the 9, 19, 28, 38 and 55-m depth contours, respectively. All 69 stations were monitored during winter (February), spring (May), summer (August), and fall (November) in 2022 and 2023, and were sampled over a four-day period during each survey (Appendix C.1). Sampling at an additional eight kelp bed stations off Point Loma (i.e., stations A1, A6, A7, C4–C8) and seven kelp/nearshore stations in the South Bay region (i.e., stations I19, I24–I26, I32, I39, I40) was conducted four to five times per month to meet bacterial monitoring requirements (see Chapter 3). However, only data collected at these 15 kelp bed stations that occurred within one week of the quarterly offshore stations are analyzed in this chapter (see Appendix C.1).

Oceanographic data were collected using a SeaBird SBE 25 Plus conductivity, temperature, and depth instrument (CTD). The CTD was lowered through the water column at each station to collect continuous measurements of water temperature, conductivity (used to calculate salinity), pressure (used to calculate depth), dissolved oxygen (DO), pH, transmissivity (a proxy for water clarity), chlorophyll *a* fluorescence (a proxy for phytoplankton), and colored dissolved organic material (CDOM). Vertical profiles of each parameter were constructed for each station per survey by averaging the data values recorded within

each 1-m depth bin. This level of data reduction ensures that physical measurements used in subsequent analyses will correspond to discrete sampling depths required for bacterial monitoring (see Chapter 3). Visual observations of weather and water conditions were recorded just prior to each CTD cast. These observations were previously reported in monthly receiving waters monitoring reports submitted to the San Diego Regional Water Quality Control Board (see City of San Diego 2022–2023a,b).

Data Analysis

Water column parameters were summarized as quarterly means pooled over all stations by the following depth layers: 1–20 m, 21–60 m, 61–80 m, 81–98 m (PLOO), and 1–9 m, 10–19 m, 20–28 m, 29–38 m, 39–55 m (SBOO). The top layer is herein referred to as surface water, while the subsurface layers account for mid and bottom waters. Unless otherwise noted, analyses were performed using R (R Core Team, 2024) and various functions within the reshape2, Rmisc, mixOmics, tidyverse, Hmisc, RODBC, and oce packages (Wickham 2007, Hope 2013, Rohart et al. 2017, Wickham et al. 2019, Harrell 2021, Ripley and Lapsley 2021, Kelley and Richards 2022).

Vertical density profiles were constructed from CTD data to depict the pycnocline (i.e., depth layer where the density gradient was greatest) for each survey and to illustrate seasonal changes in water column stratification. Data for these density profiles were limited to stations located along the 98-m depth contour in the PLOO region (i.e., stations F26–F36) and the 28-m depth contour in the SBOO region (i.e., stations I2, I3, I6, I9, I12, I14I17, I22, I27, I30, I33) to prevent masking trends that occur when data from multiple depth contours are combined. Buoyancy frequency (BF), a measure of the static stability of the water column, was used to quantify the magnitude of stratification for each station per survey and was calculated as follows:

$$BF = \sqrt{(g/\rho * (dp/dz))}$$

where g is the acceleration due to gravity, ρ is the seawater density, and dp/dz is the density gradient (Mann and Lazier 1991). The depth of maximum BF was used as a proxy for the depth at which stratification was the greatest.

Additionally, time series of anomalies for water temperature, salinity, and DO were calculated to evaluate regional oceanographic events within the context of large-scale climatic processes (i.e., ENSO events). These analyses were limited to data from the discharge depth stations for each outfall, with all water column depths combined. Anomalies were then calculated as the difference between the quarterly historical average and quarterly means for each year.

RTOMS

Data Collection

Two real-time oceanographic mooring systems were deployed at the terminal ends of the PLOO and SBOO (Figure 2.1), in partnership with Scripps Institution of Oceanography (SIO). The PLOO RTOMS was anchored at a depth of approximately 95 m, just east of the northern diffuser leg, and the SBOO RTOMS was anchored at a depth of approximately 31 m, just west of the southern diffuser leg terminus (Appendix C.2). Each mooring was deployed for a period of approximately one year. The PLOO RTOM completed three periods of deployment during the 2022-23 reporting period: November 3, 2021, to November 22, 2022; December 8, 2022, to October 26, 2023; and December 20, 2023, to present. The

SBOO RTOM completed two deployments during this period: November 3, 2021, to November 3, 2022; and from June 29, 2023, to present. Data presented here include only data collected in real-time from all deployments. Data are not available for the first half of 2023 at the SBOO due to the need to rebuild the entire SBOO mooring and replace instruments after it was lost to sea in November of 2022. For a summary of critical data loss issues for 2023, see Appendix C.3 and for 2022, see Addendum 2-1 in City of San Diego (2023b). For a more comprehensive list of all RTOMS issues for 2023, see Addendum 2-1 in City of San Diego (2024).

Each RTOMS was outfitted with a series of instruments/sensors at fixed depths (Table 2.1). Critical parameters that were measured on a real-time basis, by both systems, included temperature, conductivity (salinity), total pH, DO, dissolved carbon dioxide ($x\text{CO}_2$), nitrogen (nitrate + nitrite), chlorophyll *a*, CDOM, biological oxygen demand (BOD), and current direction and velocity. calibration and measurement method for seawater, while pH has been reported in National Bureau of Standards (NBS) scale from CTD casts; it is not recommended to convert between these scales (Marion et al. 2011). In general, pH_T ranges reported by RTOMS may be lower than those recorded by the CTD, and any pH comparisons should be interpreted with caution due to method differences. All parameters were recorded at 10-minute intervals, except for nitrate + nitrite, which was recorded at 1-hour intervals, and $x\text{CO}_2$, which was recorded at 10-hour intervals.

Temperature and ocean current data from static moorings were used to supplement data gaps between RTOMS deployments. These non-telemetered (static) upward-facing bottom-mounted acoustic doppler current profilers (ADCPs) (Teledyne RD Instruments 300 KHz Workhorse Monitor) and thermistor (Onset Tidbit temperature loggers) string arrays were moored near the RTOMS at the terminal end of the PLOO and SBOO (Figure 2.1, Appendix C.4), as part of the original Moored Observation System Pilot Study (Storms et al. 2006). Data from completed static mooring deployments are available throughout much of 2022 and 2023. These instrument packages are much smaller and less logistically challenging to retrieve and deploy compared to RTOMS. Data from ADCPs were collected every five minutes in 4-m depth bins, ranging from 9 to 93 m at the PLOO and from 6 to 30 m at the SBOO. Temperature data were collected from vertical series of thermistors every 10 minutes from duplicate arrays at the PLOO (100 m) and a single array at the SBOO (36 m). The thermistors were deployed on mooring lines at each site starting at 2 m above the seafloor and extending through the water column every 4 m to within 6 m of the surface.

Data Processing and Analysis

Prior to conducting analyses, RTOMS data were subject to a comprehensive suite of quality assurance/quality control (QA/QC) procedures following Quality Assurance of Real-Time Oceanographic Data (QARTOD) methodologies (US IOOS 2017, 2020). This collaborative effort was developed to address data quality issues of the U.S. Integrated Ocean Observing System (US IOOS) community and provides recommendations for applying automated data qualifier flags specific to each parameter Methodology for ADCP data differed slightly and is described separately. For all other RTOMS data, QARTOD tests were applied to all data prior to analysis (Appendices C.5–C.7, City of San Diego 2022a, 2023a). In addition to these automated tests, all data were reviewed manually and flagged to identify questionable data, which may result from biofouling, interference from bubbles, sensor drift, or other malfunctions. Major data and sensor problems are highlighted by parameter and location (Appendix C.3, City of San Diego 2022a), and a detailed log of data flagged manually by parameter, site, depth, and date range is available upon request. When possible, additional QA/QC procedures analyzing quarterly CTD casts to validate data from RTOMS sensors, and seawater samples to validate nitrate + nitrate results were

conducted. After review, all data that were flagged as suspect or bad were excluded from further analyses and are not presented in this report.

Analyses were performed in R (R Core Team 2024) using functions within various packages (i.e., zoo, reshape2, Rmisc, mixOmics, tidyverse, scales, pracma, data.table, gtools) (Zeileis and Grothendieck 2005, Wickham 2007, Hope 2013, Rohart et al. 2017, Wickham et al. 2019, Wickham and Seidel 2020, Borchers 2021, Dowle and Srinivasan 2021, Warnes et al. 2021). Annual time series of raw and daily averaged data were plotted at each depth and site for all parameters, except for ADCP data (described subsequently). Contour plots were generated in MATLAB (2016) using default settings, which display fixed isolines, and fill areas between isolines with constant colors. Density calculations and temperature-salinity plots were created using the SEAWATER toolbox library for MATLAB, version 3.3.1 (Morgan and Pender 2014). Vertical profiles were constructed for daily averages of temperature, salinity, and density, as these parameters had the most coverage through the water column. Density and thermal gradients were calculated by differences in daily-averaged values between sensors and dividing by the depth. In addition, summary statistics were completed at each depth and site with the following seasonal periods that align with quarterly water quality sampling: winter (January–March); spring (April–June); summer (July–September); fall (October–December). Large data gaps were identified as seasons with < 40% data recovery, based on expected number of samples for sensor-specific sampling intervals, and were excluded from summary analyses.

Ocean current data collected by ADCP were checked for quality by eliminating those measurements that did not meet echo intensity criteria (i.e., minimum correlation among the four beams of > 75%). Following this initial screening, tidal frequency data were removed using the PL33 filter (Alessi et al. 1984), compass direction was corrected to true north (+12.8 degrees), and data were hourly averaged. For all RTOMS and ADCP deployments in 2022, and all static ADCP deployments in 2022 and 2023, data were summarized as counts of observed velocities by season and select depth bins. The generalized axes of current direction and magnitude were determined by linear regression of 2022 RTOMS-based ADCP northern versus eastern velocities for select depth bins. Data not reported previously were summarized by season and depth bin.

Data collected during 2022 were reported previously (City of San Diego 2023a), and all applicable raw data for the 2022-2023 sampling period have been submitted to either the Regional Water Quality Control Board or the California Environmental Data Exchange Network (CEDEN) and may be accessed upon request.

RESULTS AND DISCUSSION

Oceanographic Conditions in 2022-2023

Water Temperature

Ocean temperatures recorded during the 2022–2023 quarterly CTD surveys followed expected seasonal patterns throughout the PLOO and SBOO regions, ranging from a minimum of 10.5 to a maximum of 15.8°C in winter, 9.6 to 18.0°C in spring, 10.2 to 23.8°C in summer, and 10.7 to 17.6°C in fall (Figures 2.2–2.5, City of San Diego 2023a). Regardless of the year or season, water temperature decreased throughout the water column with increasing depth. Surface waters during the summer were typically the warmest, and deeper waters during the spring were the coldest. Over the past two years, maximum

water temperatures were recorded in surface waters of both regions during summer 2022 (PLOO: 23.8°C; SBOO: 22.8°C, City of San Diego 2023a). Conversely, the coldest water temperatures were recorded in the deepest waters of both regions (PLOO: 81–98 m stations; SBOO: 39–55 m stations) during spring 2022 in the PLOO region (9.6°C), and spring of 2022 in the SBOO region (10.3°C) (City of San Diego 2023a).

Ocean temperatures observed by RTOMS and thermistor arrays showed similar seasonal patterns and comparable ranges to quarterly CTD surveys. Temperatures recorded during 2022–2023 from moorings near the PLOO and SBOO ranged from a minimum of 9.6 to a maximum of 17.3°C in winter, 9.4 to 23.3°C in spring, 9.6 to 24.8°C in summer, and 10.4 to 20.9°C in fall (Figures 2.6–2.7, Appendices C.8–C.12, City of San Diego 2023a). The warmest seasonal mean water temperatures were recorded at the surface in both regions during summer 2022 (PLOO: 24.7°C; SBOO: 24.8°C) (City of San Diego 2023a). Conversely, the coldest seasonal mean water temperatures were recorded in the deepest locations for both RTOMS (PLOO: 89 m; SBOO: 26 m) during spring 2022 (PLOO: 9.4°C; SBOO: 10.1°C), with minimums occurring in late April (PLOO: 9.3°C; SBOO: 10.6°C) (City of San Diego 2023a). Overall, cooler temperatures (< 9.8°C) occurred during the winter and spring of both years at deep depths (> 60 m), and warmer temperatures (> 22°C) occurred near the surface in the summer of both years. As a result of higher frequency sampling, maximum surface summer temperatures from moorings were up to 1.0°C higher than observations from any sites during quarterly surveys.

Salinity

Salinities recorded during the 2022–2023 quarterly surveys also followed expected seasonal patterns throughout the PLOO and SBOO regions, ranging from a minimum of 32.70 to a maximum of 34.12 ppt in winter, 33.56 to 34.18 ppt in spring, 33.30 to 33.95 ppt in summer, and 33.30 to 34.18 ppt in fall (Figures 2.2–2.5, City of San Diego 2023a). Within the PLOO region, the highest salinity values (> 34.0 ppt) were typically recorded at bottom depths (80 and 98-m stations) during spring 2022 and winter 2023. Similarly, high salinities in the SBOO region (> 33.8 ppt) were recorded at bottom depths (55-m stations) during spring 2022 and winter 2023. High salinity values, associated with deep waters during the spring in both the PLOO and SBOO regions, corresponded with the coldest temperatures, as described previously. Taken together, these results support the observation that local coastal upwelling appears to be strongest during the spring months (Jackson 1986). Unusual, elevated salinity appeared at near surface depths at some stations during spring 2022 (Figures 2.2, 2.4), likely influenced by excess organic matter from very high phytoplankton concentrations fouling the conductivity cell and is unlikely a true measure of elevated salinity.

Low salinity values in the PLOO (< 33.5 ppt) and SBOO (< 33.3 ppt) regions were limited to mostly surface waters in winter and fall in the PLOO region (Figures 2.2–2.5). Given the proximity of these SBOO locations to the mouth of the Tijuana River, the occurrence of the low salinity events may be correlated with winter rain events and the resultant influx of freshwater input into local receiving waters (Hess 2019, NOAA/NWS 2024).

Salinities observed from moorings near the PLOO and SBOO ranged from a minimum of 32.30 to a maximum of 34.01 PSU (Practical Salinity Unit) in winter, 32.79 to 34.09 PSU in spring, 32.06 to 33.79 PSU in summer, and 32.44 to 33.69 PSU during fall (Figures 2.8–2.9, Appendices C.10–C.12, City of San Diego 2023a). As described in Materials and Methods, salinity data from SBOO moorings is not available in fall 2022. High seasonal mean salinities (> 33.6 PSU) generally occurred at depth at both sites (PLOO: 75–89 m; SBOO: 26 m) and peaked during spring 2022 and winter 2023 when

upwelling and La Niña conditions were strongest. Relatively high seasonal mean salinity (SBOO: 34.09 PSU) was also recorded near the surface during spring 2022 (City of San Diego 2023a), likely due to evaporation caused by atmospheric warming (Jones et al. 2002) and corresponded to high mean summer temperatures.

Density and Ocean Stratification

Seasonal changes in thermal stratification over the past two years were mirrored by density stratification of the water column during each survey (Figures 2.2–2.5). These results align with regional studies showing that density in shallow coastal waters of southern California, and elsewhere, is primarily influenced by temperature differences, since salinity is relatively uniform (Bowden 1975, Jackson 1986, Pickard and Emery 1990). Additionally, maximum buoyancy frequency for both regions ranged from a minimum of 5.32 to a maximum of 8.03 cycles/min during the winter, 8.68 to 10.88 cycles/min during the spring, 12.56 to 16.93 cycles/min during the summer, and 3.89 to 8.99 cycles/min during the fall (Figure 2.10, Appendix C.13). As expected, the depth of the pycnocline also varied by season. Shallower pycnocline depths (≤ 11 m) occurred in spring and summer, which typically corresponded to greater stratification, although moderate stratification was observed during fall in the SBOO region in both 2022 and 2023.

Dissolved Oxygen and pH

Levels of DO and pH in the coastal waters off San Diego generally followed expected patterns in 2022 and 2023 that corresponded to seasonal fluctuations in water mass inputs. Additionally, changes in DO and pH tended to be closely linked, since both parameters reflect fluctuations in dissolved carbon dioxide, an indicator of biological activity in coastal waters (Skirrow 1975). Concentrations of DO across the PLOO and SBOO regions ranged from a minimum of 3.0 to a maximum of 9.7 mg/L in winter, 2.5 to 11.3 mg/L in spring, 3.4 to 9.4 mg/L in summer, and 3.6 to 11.7 mg/L in fall. The recorded pH ranged from a minimum of 7.7 to a maximum of 8.3 in winter, 7.6 to 8.3 in spring, 7.6 to 8.3 in summer, and 7.7 to 8.4 in fall (Figures 2.2–2.5, Appendices C.14–C.17, City of San Diego 2023a).

Maximum DO and pH were recorded in surface waters of PLOO during spring (PLOO: 10.1 mg/L and pH 8.3) and the surface waters of SBOO during winter (SBOO: 11.7 mg/L and pH 8.4) (Figures 2.2–2.5, Appendices C.14–C.17, City of San Diego 2023a). Conversely, minimum DO and pH were recorded in the bottom depths of nearshore stations (9 and 18-m stations) of both regions during spring 2022 (PLOO: 2.5 mg/L and pH 7.7; SBOO: 2.6 mg/L and pH 7.6) (City of San Diego 2023a), likely due to the upwelling of cold, saline, oxygen-poor water moving inshore like the pattern described previously for temperature and salinity.

Changes in DO and pH at the PLOO and SBOO RTOMS were also generally aligned and showed similar seasonal patterns to quarterly CTD surveys. Concentrations of DO ranged from a minimum of 1.6 to a maximum of 13.3 mg/L in winter, 1.4 to 15.4 mg/L in spring, 1.7 to 14.7 mg/L in summer, and from 3.4 to 10.9 mg/L in fall (Appendices C.10–C.12, City of San Diego 2023a). Similarly, pH_T (total scale) recorded ranged from a minimum of 7.7 to a maximum of 8.3 in winter, 7.6 to 8.4 in spring, 7.6 to 8.3 in summer, and during fall 2023 from 7.8 to 8.2 pH_T units (Appendices C.10–C.12, City of San Diego 2023a). As described in Materials and Methods, DO and pH_T data from SBOO moorings are not available in fall 2022, and generally RTOMS sensors report slightly lower pH values compared to quarterly CTD surveys due to difference in pH units (total scale and NBS units, respectively).

The highest DO and pH_T levels were observed during phytoplankton blooms at the SBOO RTOMS at the surface in spring 2022 (SBOO: 15.4 mg/L and pH_T 8.4) (City of San Diego 2023a). Conversely, the lowest DO and pH_T levels were observed at deep depths in late spring 2022 (SBOO: 1.4 mg/L and pH_T 7.6) (City of San Diego 2023a) and were likely due to the remineralization of the organic matter created during the blooms earlier that spring. At the PLOO, the lowest DO values (< 3 mg/L) at deep depths were closely associated with the coldest and highest salinity water masses (Figure 2.11). Similarly, low DO values at the bottom depth at the SBOO were generally recorded in coldest, saline waters, although some low DO values were also observed at moderate salinities and cool temperatures (Figure 2.12). These observations further support the role of upwelling in the spring as a significant driver of local conditions.

Dissolved CO_2

Surface seawater carbon dioxide levels (xCO_2) recorded from the RTOMS generally aligned with surface DO and pH_T levels. Concentrations of xCO_2 at the PLOO region ranged from a minimum of 364 to a maximum of 435 ppm in the winter and fall 2022, respectively (City of San Diego 2023a). Concentrations of xCO_2 at SBOO ranged from a minimum of 136 to a maximum of 593 ppm in the summer of 2022 for both values (Appendices C.10–C.12, City of San Diego 2023a). The lowest seasonal mean levels across both regions (136 ppm) were observed during early summer of 2022 in the SBOO region and were contrasted by the highest values roughly one week prior. (City of San Diego 2023a). Generally, biological productivity and surface water temperatures drive large seasonal amplitudes in xCO_2 (Sutton et al. 2019). The relatively large short-term variability (> 100 ppm change between days) observed during the spring and summer at the SBOO region was due to this biological productivity, as concentrations of xCO_2 followed trends in DO due to a phytoplankton bloom (and subsequent remineralization of organic matter). In contrast, winter generally shows more stable daily values (Appendix C.12) with similar seasonal variability and ranges to the closest near-coastal SIO carbon mooring (California Current Ecosystem mooring 2, NOAA/PMEL 2022). However, it is important to note that much of the 2023 PLOO xCO_2 data (February through October 2023) was not recorded due to a power failure with the solar panels, so trends in the PLOO region could not be described during this time.

Transmissivity

Although water clarity (transmissivity) ranged widely, from a minimum of 1 to a maximum of 94% throughout the PLOO and SBOO regions, values were generally quite high, exceeding 86% during most of 2022 and 2023 (Appendices C.14–C.17). During winter and spring, low transmissivity (< 75%) was most often observed at shallow monitoring stations in the SBOO region, located close to shore, where the influence of waves, currents, and land-based turbidity plumes was most acute. Low transmissivity during spring/winter surveys in both regions appeared to be associated with high concentrations of chlorophyll *a*, possibly indicative of dense accumulations of phytoplankton cells (see next section), most obvious during spring winter 2022. Finally, low transmissivity values were also occasionally observed in the midwater (~ 25 m) at stations located along deeper depth contours (< 60 m) in the PLOO region during summer 2022 and spring 2023, indicating a possible resuspension of soft sediments caused by the CTD approaching or hitting the seafloor. These low transmissivity values coincided with relatively high chlorophyll *a* concentration at the same midwater contour.

Chlorophyll *a*

Concentrations of chlorophyll *a* ranged from a minimum of 0.1 to a maximum of 68.2 $\mu\text{g/L}$ across the PLOO and SBOO regions in 2022 and 2023 (Appendices C.14–C.17, City of San Diego 2023a).

Elevated chlorophyll concentrations ($> 5 \mu\text{g/L}$) were recorded at depths from the surface to 40 m along all depth contours in the PLOO region during spring 2022, and to depths associated with (or just below) the mixed layer. Prolonged elevated concentrations ($> 50 \mu\text{g/L}$) were observed in the SBOO region during winter 2022 and spring 2023 and the maximum concentrations temporarily observed ($> 65 \mu\text{g/L}$) were in the SBOO region in summer 2022 and spring 2023 (Figure 2.13) (City of San Diego 2023a, Ocean Imaging 2024). Elevated concentrations were also recorded at depths from 25 to 60 m along deeper depth contours ($< 60 \text{ m}$) in the PLOO region during summer 2022 and spring 2023. Elevated chlorophyll *a* concentrations at these depths reflect the tendency for phytoplankton to accumulate along natural barriers such as isopycnals near the thermocline, where deeper water nutrients are available, and light is not yet limiting (Lalli and Parsons 1993).

Chlorophyll *a* observed at the PLOO and SBOO moorings ranged from a minimum of < 0.1 to a maximum of $> 13.4 \mu\text{g/L}$ through winter and spring 2022 (Appendices C.10–C.12, City of San Diego 2023a). Data are not available from fall 2022 through summer 2023 while RTOMS were not deployed, and multiple sensor failures occurred in the summer of 2022 (City of San Diego 2023a). Generally, the highest chlorophyll *a* concentration occurred at midwater depths (18 and 30 m) in spring and winter 2022 at PLOO and SBOO ($> 13.4 \mu\text{g/L}$). These elevated concentrations coincided with relatively high DO and pH_T levels at the surface and were indicative of localized phytoplankton blooms that were also captured by satellite imaging (Figure 2.13).

Nitrate (plus Nitrite)

Nitrate + nitrite concentrations observed at the RTOMS from winter through summer 2022 and fall 2023 at the PLOO ranged from < 0.01 to $31.6 \mu\text{M}$, and from < 0.01 to $21.5 \mu\text{M}$ at the SBOO (Appendices C.10–C.12, City of San Diego 2023a). Much of these data are not available from fall 2022 through summer 2023 while RTOMS were not deployed, and other data gaps occurred due to sensor failures (City of San Diego 2023a). The lowest seasonal mean levels were observed during the spring and summer of 2022 near the surface at both moorings ($< 2 \mu\text{M}$), likely due to uptake from phytoplankton. Generally, nitrate + nitrite concentrations increased with increasing depth and higher salinities, with the highest seasonal mean occurring in the winter of 2022 at PLOO ($31.6 \mu\text{M}$ at 75 m) (City of San Diego 2023a). These observations generally showed similar ranges to that of historical data (1969–2023) from nearby regional stations reported by the California Cooperative Oceanic Fisheries Investigations (CalCOFI) surveys, where the lowest nitrate levels occurred near the surface ($< 10 \text{ m}$: < 0.1 – $11.2 \mu\text{M}$) and higher levels occurred at depth, associated with higher salinities (70–130 m: < 0.1 – $33.4 \mu\text{M}$) (CalCOFI 2024, Weber et al. 2021)

Direction and Velocity of Subsurface Currents

Ocean currents surrounding the PLOO and SBOO varied by depth and season during the 2022–2023 reporting period. Seasonal mean current velocities (1-m depth bin for RTOM deployments) at the PLOO ranged from a minimum of 16 to a maximum of 165 mm/s during winter, 21 to 181 mm/s during spring, and 73 to 173 mm/s during summer, and 15 to 96 mm/s during fall (Appendix C.18). Seasonal mean current velocities (by 1-m depth bin for RTOM deployments) at the SBOO ranged from a minimum of 51 to a maximum of 116 mm/s during winter, 57 to 85 mm/s during spring, 61 to 106 mm/s during summer, and 58 to 93 mm/s in the fall (City of San Diego 2023a, Appendix C.19). The highest seasonal mean current velocities typically occurred in near-surface waters during the winter and spring at both the PLOO and SBOO. Generally, for all seasons, the highest mean current velocities occurred in the upper 20 m at the PLOO and the upper 10 m at the SBOO. Below these thresholds, velocities decreased with depth around both outfalls, with the lowest mean velocities roughly 15 m from the bottom at the PLOO and 5 m from the bottom at the SBOO.

Historically, currents predominantly flow along a north-northwest/south-southeast axis, regardless of season or outfall location, and this was true of most current data during this reporting period (Figures 2.14, 2.15). Additionally, linear regression of all current direction observations for select depth bins show that along-coast currents tend to dominate at the subsurface. Notably, surface currents appeared to differ from the along-coast trends observed in prior reporting periods (City of San Diego 2022a) and exhibited a more southeasterly flow at both PLOO and SBOO (Figure 2.16). However, given the relative shortened deployment time due to RTOMs issues in 2022-23, especially at SBOO (Appendix C.3), these flows do not represent a complete generalized flow across all seasons and are instead representative of the summertime southeasterly flows during which the RTOMs were predominantly deployed. Aside from these surface current anomalies, results are consistent with observations from the nearby bottom-mounted static ADCPs at both locations (Appendices C.20–C.23), and previous studies conducted in the region (Winant and Bratkovich 1981, Rogowski et al. 2012a).

Historical Assessment of Oceanographic Conditions

A review of temperature, salinity, and DO anomalies from all discharge depth stations sampled from 1991 through 2023 demonstrates how the PLOO and SBOO regions have responded to long-term climate-related changes in the SCB (Figure 2.17). Overall, these results are consistent with largescale temporal patterns in the California Current System (CCS) associated with ENSO, PDO and NPGO events (Peterson et al. 2006, McClatchie et al. 2008, 2009, Bjorkstedt et al. 2010, 2011, 2012, Wells et al. 2013, Leising et al. 2014, 2015, Thompson et al. 2018, 2019, Harvey et al. 2021, Weber et al. 2021, NOAA/NWS 2024). Several major events in the CCS have affected SCB coastal waters since 1997 (Table 2.2), notably transition periods between La Niña and El Niño conditions.

Temperature and salinity data for the entire San Diego region were overall consistent with the CCS events in Table 2.2, but there have been some notable deviations from these trends, where coastal waters may lag in response to transitions between El Niño/ La Niña conditions and temporarily differ from offshore, open ocean trends. For example, since the onset of marine heatwaves in 2012, the mean SST anomaly across the North Pacific Ocean has been steadily increasing, reaching a record high in 2022 (Thompson et al. 2024). However, surface temperature SBOO and PLOO regions were roughly 0.5 to 1.0°C below average in 2022 and early 2023, likely due to regional effects of a negative PDO and an ongoing La Niña trend, which acted to increase upwelling and decrease coastal California ocean temperatures (Harvey et al. 2023).

The overall heating of eastern Pacific Ocean temperatures has been evident in the SBOO and PLOO region since roughly 2013-14 (Figure 2.17), with a marine heatwave event recorded in the North Pacific Ocean every year since. Ocean temperatures were notably warmer than the long-term average during the majority of 2016 which corresponded to El Niño conditions that lasted until spring 2016 before switching to a La Niña that lasted from late 2016 through winter 2017. Deviations from the long-term average were minor, reflecting the ENSO neutral conditions that endured for most of 2017 (NOAA/NWS 2024). Ocean temperatures observed throughout the water column were warmer than the historical average during most of 2018, as confirmed by both CTD surveys and RTOMs (City of San Diego 2022a), and closer to average conditions during 2019 for the PLOO region.

In contrast, the CCS north of Monterey Bay showed surface water temperatures far above average in summer and fall 2019, consistent with a regionwide marine heat wave, as well as positive PDO and negative NPGO phases. With the switch to negative PDO and MEI phases in 2020, overall ocean

temperatures were roughly average, with surface temperatures above average in 2020. Despite the negative PDO and MEI phases, the 2020 heatwave affected the Southern California Bight region similarly to 2014, with surface temperatures above average in 2020 (Weber et al. 2021). Surface temperatures were 0.5 to 3.0°C above normal in 2020, except for fall in the PLOO region. 2021 was more typical, apart from a cooler than normal summer in the SBOO region. Above average salinity observed during 2018 through 2021 was consistent with conditions all along the west coast, shifting from relatively low salinities during the warm period of 2014–2016. These anomalous conditions were remotely observed moving towards the SCB prior to 2018, suggesting a shifting balance of water mass source waters being responsible for these temperature and salinity anomalies, which have remained through 2021 (Thompson et al. 2018, 2019, Harvey et al. 2021, Weber et al. 2021).

From 2019 to 2022, Pacific climate indices were generally negative (PDO, NPGO) indicating three consecutive years of La Niña conditions (Thompson et al. 2024). During La Niña events, upwelling tends to be prevalent region wide, and introduces deeper cold and saline water masses to coastal surface waters (Bond et al. 2008). This was evident by the negative temperature and positive salinity anomalies in both the SBOO and PLOO region from 2019 to 2022. La Niña conditions persisted into early 2023 when the PDO stopped decreasing and the NPGO began to trend positively, indicating the transition to an incoming El Niño phase by the fall of 2023 (Harvey et al. 2023). This transition weakened coastal upwelling along California and allowed the penetration of warmer, less saline offshore waters starting in late summer and fall of 2023 relative to 2022 (Figure 2.18), consistent with the same El Niño trends observed in the SCB region in 2016. Subsurface temperatures were average in 2023 along much of the California coastline, indicating that the 2023 heatwave did not penetrate relatively deep into the water column and effect DO trends along the coastline (e.g., HAB events; Leising et al. 2024)

Historical trends in local DO concentrations reflect several periods during which lower than normal DO has corresponded with low water temperatures and high salinity (Figure 2.17). The alignment of these anomalies is generally consistent with cold, saline, less oxygenated ocean waters, which coincided with relatively high salinities (e.g., 2002, 2005–2012, 2019–2021). The overall decrease observed in DO in the PLOO and SBOO regions through 2012 was also observed throughout the entire CCS and deep North Pacific and was thought to be linked to changing ocean climate and increased occurrence of El Niño events (Bjorkstedt et al. 2012). However, no significant long-term trend has been shown over the last 70 years in the North Pacific shelf depths (Schmidtke et al. 2017). These large negative anomalies have been absent since mid-2013 in the PLOO and SBOO regions but were present for some of 2022 and 2023 in the PLOO region.

SUMMARY

Oceanographic conditions in the PLOO and SBOO regions during 2022 and 2023 followed typical seasonal patterns for the coastal waters off San Diego. Maximum water column stratification occurred during spring and summer months, whereas waters were well mixed or weakly stratified in the winter. Ocean conditions indicative of local coastal upwelling, such as relatively cold, dense waters with low DO and pH at subsurface depths, were most evident during the spring months of both years and winter months of 2023. These were driven by a combination of localized processes (seasonal, wind-driven upwelling) and large-scale oceanographic trends in the Pacific Ocean (La Niña conditions that persisted from 2019 to 2022). Phytoplankton blooms, indicated by high concentrations of chlorophyll *a* (> 25 µg/L), were less severe than prior bloom events observed in 2021 (> 50 µg/L, City of San Diego 2022a)

and were most evident at subsurface depths and in satellite surface images during spring 2022 in the PLOO and SBOO regions. Ocean currents varied seasonally and generally trended along-coast. These results are similar to findings reported previously for the San Diego region (City of San Diego 2015a,b, 2016a,b, 2018b, 2020, 2022a,b, 2023a) and are generally consistent with conditions and long-term trends in the SCB (Peterson et al. 2006, McClatchie et al. 2008, 2009, Bjorkstedt et al. 2010, 2011, 2012, Wells et al. 2013, Leising et al. 2014, 2015, NOAA/NWS 2024), and northern Baja California waters (Peterson et al. 2006). These observations suggest that overall, the temporal and spatial variability observed in oceanographic conditions for coastal San Diego can be explained by a combination of local (e.g., coastal upwelling, rain-related runoff) and large-scale oceanographic-climatic processes, notably the transition from La Niña to El Niño conditions in late 2023 (i.e., shift from negative to positive PDO) which allowed for the intrusion of warm water masses from offshore heatwave events once La Niña conditions broke down (Harvey et al. 2024). As a result, proximity to either outfall is not considered a significant driver of the variations observed in oceanographic parameters discussed in this chapter.

LITERATURE CITED

- Alessi, C.A., R. Beardsley, R. Limeburner, and L.K. Rosenfeld. (1984). CODE-2: Moored Array and Large-Scale Data Report. Woods Hole Oceanographic Institution Technical Report. 85–35: 21.
- Bjorkstedt, E.P., R. Goericke, S. McClatchie, E. Weber, W. Watson, N. Lo, B. Peterson, B. Emmett, J. Peterson, R. Durazo, G. Gaxiola-Castro, F. Chavez, J.T. Pennington, C.A. Collins, J. Field, S. Ralston, K. Sakuma, S.J. Bograd, F.B. Schwing, Y. Xue, W.J. Sydeman, S.A. Thompson, J.A. Santora, J. Largier, C. Halle, S. Morgan, S.Y. Kim, K.B.P. Merkins, J.A. Hildebrand, and L.M. Munger. (2010). State of the California Current 2009–2010: Regional variation persists through transition from La Niña to El Niño (and back?). California Cooperative Oceanic Fisheries Investigations (CalCOFI) Reports, 51: 39–69.
- Bjorkstedt, E.P., R. Goericke, S. McClatchie, E. Weber, W. Watson, N. Lo, B. Peterson, B. Emmett, R. Brodeur, J. Peterson, M. Litz, J. Gómez-Valdés, G. Gaxiola-Castro, B. Lavaniegos, F. Chavez, C.A. Collins, J. Field, K. Sakuma, S.J. Bograd, F.B. Schwing, P. Warzybok, R. Bradley, J. Jahncke, G.S. Campbell, J.A. Hildebrand, W.J. Sydeman, S.A. Thompson, J.L. Largier, C. Halle, S.Y. Kim, and J. Abell. (2011). State of the California Current 2010–2011: Regionally variable responses to a strong (but fleeting?) La Niña. California Cooperative Oceanic Fisheries Investigations (CalCOFI) Reports, 52: 36–68.
- Bjorkstedt, E.P., R. Goericke, S. McClatchie, E. Weber, W. Watson, N. Lo, W.T. Peterson, R.D. Brodeur, T. Auth, J. Fisher, C. Morgan, J. Peterson, J. Largier, S.J. Bograd, R. Durazo, G. Gaxiola-Castro, B. Lavaniegos, F.P. Chavez, C.A. Collins, B. Hannah, J. Field, K. Sakuma, W. Satterthwaite, M. O’Farrell, S. Hayes, J. Harding, W.J. Sydeman, S.A. Thompson, P. Warzybok, R. Bradley, J. Jahncke, R.T. Golightly, S.R. Schneider, R.M. Suryan, A.J. Gladics, C.A. Horton, S.Y. Kim, S.R. Melin, R.L. DeLong, and J. Abell. (2012). State of the California Current 2011–2012: Ecosystems respond to local forcing as La Niña wavers and wanes. California Cooperative Oceanic Fisheries Investigations (CalCOFI) Reports, 53: 41–76.
- Bond, N. A., Batchelder, H. P., & Bograd, S. J. (2008). Forecasting northeastern Pacific ecosystem responses to La Nina. *Eos, Transactions American Geophysical Union*, 89(35), 321-322.

- Borchers, H.W. (2021). pracma: Practical Numerical Math Functions. R package version 2.3.6. <https://CRAN.R-project.org/package=pracma>.
- Bowden, K.F. (1975). Oceanic and Estuarine Mixing Processes. In: J.P. Riley and G. Skirrow (eds.). Chemical Oceanography, 2nd Ed., Vol.1. Academic Press, San Francisco, CA. p 1–41.
- [CalCOFI] California Cooperative Oceanic Fisheries Investigations (2024). Archive of nutrient bottle data, January 1969–January 2023. <https://calcofi.org/data/oceanographic-data/bottle-database/>.
- City of San Diego. (2015a). Point Loma Ocean Outfall Annual Receiving Waters Monitoring and Assessment Report, 2014. City of San Diego Ocean Monitoring Program, Public Utilities Department, Environmental Monitoring and Technical Services Division, San Diego, CA.
- City of San Diego. (2015b). South Bay Ocean Outfall Annual Receiving Waters Monitoring and Assessment Report, 2014. City of San Diego Ocean Monitoring Program, Public Utilities Department, Environmental Monitoring and Technical Services Division, San Diego, CA.
- City of San Diego. (2016a). Point Loma Ocean Outfall Annual Receiving Waters Monitoring and Assessment Report, 2015. City of San Diego Ocean Monitoring Program, Public Utilities Department, Environmental Monitoring and Technical Services Division, San Diego, CA.
- City of San Diego. (2016b). South Bay Ocean Outfall Annual Receiving Waters Monitoring and Assessment Report, 2015. City of San Diego Ocean Monitoring Program, Public Utilities Department, Environmental Monitoring and Technical Services Division, San Diego, CA.
- City of San Diego. (2018a). Plume Tracking Monitoring Plan for the Point Loma and South Bay Ocean Outfall Regions, San Diego, California. Submitted by the City of San Diego Public Utilities Department to the San Diego Water Board and USEPA, Region IX, March 28, 2018 (approved 4/25/2018).
- City of San Diego. (2018b). Biennial Receiving Waters Monitoring and Assessment Report for the Point Loma and South Bay Ocean Outfalls, 2016–2017. City of San Diego Ocean Monitoring Program, Public Utilities Department, Environmental Monitoring and Technical Services Division, San Diego, CA.
- City of San Diego. (2020). Biennial Receiving Waters Monitoring and Assessment Report for the Point Loma and South Bay Ocean Outfalls, 2018–2019. City of San Diego Ocean Monitoring Program, Public Utilities Department, Environmental Monitoring and Technical Services Division, San Diego, CA.
- City of San Diego. (2022a). Biennial Receiving Waters Monitoring and Assessment Report for the Point Loma and South Bay Ocean Outfalls, 2020–2021. City of San Diego Ocean Monitoring Program, Public Utilities Department, Environmental Monitoring and Technical Services Division, San Diego, CA.
- City of San Diego. (2022b). Appendix P. Oceanography. In: Application for Renewal of NPDES CA0107409 and 301(h) Modified Secondary Treatment Requirements, Point Loma Ocean Outfall.

Volume X, Appendices O thru U. Public Utilities Department, Environmental Monitoring and Technical Services Division, San Diego, CA.

City of San Diego. (2022c). Plume Tracking Monitoring Plan Progress Report for the Point Loma and South Bay Ocean Outfall Regions, San Diego, California; Report Period: January – December 2021. Submitted by the City of San Diego Public Utilities Department to the San Diego Water Board and USEPA, Region IX, March 3, 2023.

City of San Diego. (2023a). Interim Receiving Waters Monitoring Report for the Point Loma and South Bay Ocean Outfalls, 2022. City of San Diego Ocean Monitoring Program, Public Utilities Department, Environmental Monitoring and Technical Services Division, San Diego, CA.

City of San Diego. (2023b). Plume Tracking Monitoring Plan Progress Report for the Point Loma and South Bay Ocean Outfall Regions, San Diego, California; Report Period: January – December 2022. Submitted by the City of San Diego Public Utilities Department to the San Diego Water Board and USEPA, Region IX, March 1, 2023.

City of San Diego. (2024). Plume Tracking Monitoring Plan Progress Report for the Point Loma and South Bay Ocean Outfall Regions, San Diego, California; Report Period: January – December 2023. Submitted by the City of San Diego Public Utilities Department to the San Diego Water Board and USEPA, Region IX, March 1, 2024.

Dowle, M. and A. Srinivasan. (2021). data.table: Extension of `data.frame`. R package version 1.14.2. <https://CRAN.R-project.org/package=data.table>.

Harrell, F.E., Jr. (2021). Hmisc: Harrell Miscellaneous. R package version 4.6-0. <http://CRAN.R-project.org/package=Hmisc>.

Harvey, C.J., N. Garfield, G.D. Williams, and N. Tolimieri, editors. (2021). Ecosystem Status Report of the California Current for 2020–21: A Summary of Ecosystem Indicators Compiled by the California Current Integrated Ecosystem Assessment Team (CCIEA). U.S. Department of Commerce, NOAA Technical Memorandum NMFS-NWFSC-170.

Harvey, C.J., N. Garfield, G.D. Williams, and N. Tolimieri, editors. (2023). Ecosystem status report of the California Current for 2022-23: A summary of ecosystem indicators compiled by the California Current Integrated Ecosystem Assessment Team (CCIEA). U.S. Department of Commerce, National Oceanic and Atmospheric Administration, National Marine Fisheries Service, Northwest Fisheries Science Center.

Hess, M. (2018). Satellite & Aerial Coastal Water Quality Monitoring in the San Diego/Tijuana Region: Annual Summary Report 1 January 2017–31 December 2018. Littleton, CO.

Hess, M. (2019). Satellite & Aerial Coastal Water Quality Monitoring in the San Diego/Tijuana Region: Annual Summary Report 1 January 2018–31 December 2019. Littleton, CO.

Hess, M. (2020). Satellite & Aerial Coastal Water Quality Monitoring in the San Diego/Tijuana Region: Annual Summary Report 1 January 2019–31 June 2019. Littleton, CO.

- Hope, R.M. (2013). Rmisc: Ryan Miscellaneous. R package version 1.5. <http://CRAN.R-project.org/package=Rmisc>.
- Jackson, G.A. (1986). Physical Oceanography of the Southern California Bight. In: R. Eppley (ed.). Plankton Dynamics of the Southern California Bight. Springer Verlag, New York. p 13–52.
- Jones, B., M.A. Noble, and T.D. Dickey. (2002). Hydrographic and particle distributions over the Palos Verdes continental shelf: Spatial, seasonal and daily variability. *Continental Shelf Research*. 22: 945–965.
- Kelley, D. and C. Richards. (2022). oce: Analysis of Oceanographic Data. R package version 1.5.0. <http://CRAN.R-project.org/package=oce>.
- Lalli, C.M. and T.R. Parsons. (1993). *Biological Oceanography: an introduction*. Pergamon, New York.
- Largier, J., L. Rasmussen, M. Carter, and C. Searce. (2004). Consent Decree – Phase One Study Final Report. Evaluation of the South Bay International Wastewater Treatment Plant Receiving Water Quality Monitoring Program to Determine Its Ability to Identify Source(s) of Recorded Bacterial Exceedances. Scripps Institution of Oceanography, University of California, San Diego, CA.
- Leising, A.W., I.D. Schroeder, S.J. Bograd, E.P. Bjorkstedt, J. Field, K. Sakuma, J. Abell, R.R. Robertson, J. Tyburczy, W.T. Peterson, R. Brodeur, C. Barcelo, T.D. Auth, E.A. Daly, G.S. Campbell, J.A. Hildebrand, R.M. Suryan, A.J. Gladics, C.A. Horton, M. Kahru, M. Manzano-Sarabia, S. McClatchie, E.D. Weber, W. Watson, J.A. Santora, W.J. Sydeman, S.R. Melin, R.L. DeLong, J. Largier, S.Y. Kim, F.P. Chavez, R.T. Golightly, S.R. Schneider, P. Warzybok, R. Bradley, J. Jahncke, J. Fisher, and J. Peterson. (2014). State of the California Current 2013-2014: El Niño Looming. *California Cooperative Oceanic Fisheries Investigations (CalCOFI) Reports*, 55: 51–87.
- Leising, A.W., I.D. Schroeder, S.J. Bograd, J. Abell, R. Durazo, G. Gaxiola-Castro, E.P. Bjorkstedt, J. Field, K. Sakuma, R.R. Robertson, R. Goericke, W.T. Peterson, R.D. Brodeur, C. Barceló, T.D. Auth, E.A. Daly, R.M. Suryan, A.J. Gladics, J.M. Porquez, S. McClatchie, E.D. Weber, W. Watson, J.A. Santora, W.J. Sydeman, S.R. Melin, F.P. Chavez, R.T. Golightly, S.R. Schneider, J. Fisher, C. Morgan, R. Bradley, and P. Warybok. (2015). State of the California Current 2014-2015: Impacts of the Warm-Water “Blob”. *California Cooperative Oceanic Fisheries Investigations (CalCOFI) Reports*, 56: 31–69.
- Leising, A.W., M. Hunsicker, G.D. Williams, and N. Tolimieri, editors. (2024) State of the California Current 2023-24. A report of the NOAA California Current Integrated Ecosystem Assessment Team (CCIEA) to the Pacific Fishery Management Council.
- Lynn, R.J. and J.J. Simpson. (1987). The California Current System: The Seasonal Variability of its Physical Characteristics. *Journal of Geophysical Research*, 92(C12): 12947–12966.
- Mann, K.H. (1982). *Ecology of Coastal Waters, A Systems Approach*. University of California Press, Berkeley.

- Mann, K.H. and J.R.N. Lazier. (1991). *Dynamics of Marine Ecosystems, Biological–Physical Interactions in the Oceans*. Blackwell Scientific Publications, Boston.
- Marion, G.M, F.J. Millero, M.F. Camões, P. Spitzer, R. Feistel, and C.-T.A. Chen. (2011). pH of seawater. *Marine Chemistry*, 126: 89–96.
- MATLAB. (2016). Version R2016a. The MathWorks Inc., Natick, Massachusetts. URL <https://www.mathworks.com/products/matlab.html>.
- McClatchie, S., R. Goericke, J.A. Koslow, F.B. Schwing, S.J. Bograd, R. Charter, W. Watson, N. Lo, K. Hill, J. Gottschalck, M. l’Heureux, Y. Xue, W.T. Peterson, R. Emmett, C. Collins, G. Gaxiola-Castro, R. Durazo, M. Kahru, B.G. Mitchell, K.D. Hyrenbach, W.J. Sydeman, R.W. Bradley, P. Warzybok, and E. Bjorkstedt. (2008). The state of the California Current, 2007–2008: La Niña conditions and their effects on the ecosystem. *California Cooperative Oceanic Fisheries Investigations (CalCOFI) Reports*, 49: 39–76.
- McClatchie, S., R. Goericke, J.A. Koslow, F.B. Schwing, S.J. Bograd, R. Charter, W. Watson, N. Lo, K. Hill, J. Gottschalck, M. l’Heureux, Y. Xue, W.T. Peterson, R. Emmett, C. Collins, J. Gomez-Valdes, B.E. Lavaniegos, G. Gaxiola-Castro, B.G. Mitchell, M. Manzano-Sarabia, E. Bjorkstedt, S. Ralston, J. Field, L. Rogers-Bennet, L. Munger, G. Campbell, K. Merkens, D. Camacho, A. Havron, A. Douglas, and J. Hildebrand. (2009). The state of the California Current, Spring 2008–2009: Cold conditions drive regional differences in coastal production. *California Cooperative Oceanic Fisheries Investigations (CalCOFI) Reports*, 50: 43–68.
- Morgan, P. and L. Pender. (2014). SEAWATER library for calculating EOS-80 properties of seawater in MATLAB. CSIRO Marine Research, version 3.3.1. http://www.cmar.csiro.au/datacentre/ext_docs/seawater.html.
- [NOAA/NWS] National Oceanic and Atmospheric Administration/National Weather Service. (2024). Climate Weather Linkage Website. <http://www.cpc.ncep.noaa.gov/products/precip/CWlink/MJO/enso.shtml>.
- [NOAA/PMEL] National Oceanic and Atmospheric Administration/Pacific Marine Environmental Laboratory (2024). Carbon group data from California Current Ecosystem Mooring 2 (CCE2). <https://www.ncei.noaa.gov/access/ocean-carbon-acidification-data-system/oceans/Moorings/CCE2.html>.
- Ocean Imaging. (2024). Ocean Imaging Corporation archive of aerial and satellite-derived images. <http://www.oceani.com/SanDiegoWater/index.html>.
- Peterson, B., R. Emmett, R. Goericke, E. Venrick, A. Mantyla, S.J. Bograd, F.B. Schwing, R. Hewitt, N. Lo, W. Watson, J. Barlow, M. Lowry, S. Ralston, K.A. Forney, B.E. Lavaniegos, W.J. Sydeman, D. Hyrenbach, R.W. Bradley, P. Warzybok, F. Chavez, K. Hunter, S. Benson, M. Weise, J. Harvey, G. Gaxiola-Castro, and R. Durazo. (2006). The state of the California Current, 2005–2006: Warm in the north, cool in the south. *California Cooperative Oceanic Fisheries Investigations (CalCOFI) Reports*, 47: 30–74.

- Pickard, D.L. and W.J. Emery. (1990). *Descriptive Physical Oceanography*. 5th Ed. Pergamon Press, Oxford.
- R Core Team. (2024). *R: A language and environment for statistical computing*. R Foundation for Statistical Computing, Vienna, Austria. URL <https://www.R-project.org/>.
- Ripley, B. and M. Lapsley. (2021). RODBC: ODBC Database Access. R package version 1.3-19. <http://CRAN.R-project.org/package=RODBC>.
- Rogowski, P., E. Terrill, M. Otero, L. Hazard, S.Y. Kim, P.E. Parnell, and P. Dayton. (2012a). Final Report: Point Loma Ocean Outfall Plume Behavior Study. Prepared for City of San Diego Public Utilities Department by Scripps Institution of Oceanography, University of California, San Diego, CA.
- Rogowski, P., E. Terrill, M. Otero, L. Hazard, and W. Middleton. (2012b). Mapping ocean outfall plumes and their mixing using Autonomous Underwater Vehicles. *Journal of Geophysical Research*, 117: C07016.
- Rogowski, P., E. Terrill, M. Otero, L. Hazard, and W. Middleton. (2013). Ocean outfall plume characterization using an Autonomous Underwater Vehicle. *Water Science & Technology*, 67(4): 925–933.
- Rohart F., B. Gautier, A. Singh, and K-A Le Cao. (2017) mixOmics: An R package for 'omics feature selection and multiple data integration. *PLoS computational biology*, 13(11):e1005752.
- Schmidtko, S., L. Stramma, M. Visbeck. (2017). Decline in global oceanic oxygen content during the past five decades. *Nature*, 542(7641): 335-339.
- Skirrow, G. (1975). Chapter 9. The Dissolved Gases–Carbon Dioxide. In: *Chemical Oceanography*. J.P. Riley and G. Skirrow, eds. Academic Press, London. Vol. 2. p 1–181.
- Storms, W.E., T.D Stebbins, and P.E. Parnell. (2006). San Diego Moored Observation System Pilot Study Workplan for Pilot Study of Thermocline and Current Structure off Point Loma, San Diego, California. City of San Diego, Metropolitan Wastewater Department, Environmental Monitoring and Technical Services Division, and Scripps Institution of Oceanography, La Jolla, CA.
- Sutton, A. J., R. A. Feely, S. Maenner-Jones, S. Musielwicz, J. Osborne, C. Dietrich, N. Monacci, J. Cross, R. Bott, A. Kozyr, A. J. Andersson, N. R. Bates, W. Cai, M. F. Cronin, E. H. De Carlo, B. Hales, S. D. Howden, C. M. Lee, D. P. Manzello, M. J. McPhaden, M. Meléndez, J. B. Mickett, J. A. Newton, S. E. Noakes, J. H. Noh, S. R. Olafsdottir, J. E. Salisbury, U. Send, T. W. Trull, D. C. Vandemark, R. A. Weller. (2019). Autonomous seawater pCO₂ and pH time series from 40 surface buoys and the emergence of anthropogenic trends. *Earth System Science Data*, 11(1): 421–439.
- Svejkovsky, J. (2010). *Satellite and Aerial Coastal Water Quality Monitoring in the San Diego/Tijuana Region: Annual Summary Report for: 1 January 2009–31 December 2009*. Solana Beach, CA.
- Svejkovsky J. (2017). *Satellite and Aerial Coastal Water Quality Monitoring in the San Diego/Tijuana Region: Annual Summary Report for: 1 January 2016–31 December 2016*. Solana Beach, CA.

- Terrill, E., K. Sung Yong, L. Hazard, and M. Otero. (2009). IBWC/Surfrider – Consent Decree Final Report. Coastal Observations and Monitoring in South Bay San Diego. Scripps Institution of Oceanography, University of California, San Diego, CA.
- Thompson, A.R., I.D. Schroeder, S.J. Bograd, E.L. Hazen, M.G. Jacox, A. Leising, B.K. Wells, J. Largier, J. Fisher, E. Bjorkstedt, R.R. Robertson, F.P. Chavez, M. Kahru, R. Goericke, S. McClatchie, C.E. Peabody, T. Baumgartner, B.E. Lavaniegos, J. Gomez-Valdes, R.D. Brodeur, E.A. Daly, C.A. Morgan, T.D. Auth, B.J. Burke, J. Field, K. Sakuma, E.D. Weber, W. Watson, J. Coates, R. Schoenbaum, L. Rogers-Bennett, R.M. Suryan, J. Dolliver, S. Loreda, J. Zamon, S.R. Schneider, R.T. Golightly, P. Warzybok, J. Jahncke, J.A. Santora, S. A. Thompson, W. Sydeman, and S.R. Melin. (2018). State of the California Current 2017-2018: Still Not Quite Normal in the North and Getting Interesting in the South. California Cooperative Oceanic Fisheries Investigations (CalCOFI) Reports, 59: 1-66.
- Thompson, A.R., I.D. Schroeder, S.J. Bograd, E.L. Hazen, M.G. Jacox, A. Leising, B.K. Wells, J. Fisher, K. Jacobson, S. Zemen, E. Bjorkstedt, R.R. Robertson, M. Kahru, R. Goericke, C.E. Peabody, T. Baumgartner, B.E. Lavaniegos, L.E. Miranda, E. Gomez-Ocampo, J. Gomez-Valdez, T. Auth, E.A. Daly, C.A. Morgan, B.J. Burke, J.C. Field, K.M. Sakuma, E.D. Weber, W. Watson, J.M. Porquez, J. Dolliver, D. Lyons, R.A. Orben, J. Zamon, P. Warzybok, J. Jahncke, J.A. Santora, S. A. Thompson, B. Hoover, W. Sydeman, and S.R. Melin. (2019). State of the California Current 2018-2019: a Novel Anchovy Regime and a New Marine Heat Wave? California Cooperative Oceanic Fisheries Investigations (CalCOFI) Reports, 60: 1-65.
- Thompson, A. R., Swalethorp, R., Alksne, M., Santora, J. A., Hazen, E. L., Leising, A., ... & Wells, B. (2024). State of the California Current Ecosystem report in 2022: a tale of two La Niñas. *Frontiers in Marine Science*, 11, 1294011.
- [US IOOS] U.S. Integrated Ocean Observing System. (2017). Manual for the Use of Real-Time Oceanographic Data Quality Control Flags, Version 1.1. Silver Spring, MD, U.S. Department of Commerce, National Oceanic and Atmospheric Administration, National Ocean Service, Integrated Ocean Observing System, 43 pp.
- [US IOOS] U.S. Integrated Ocean Observing System (2020). Quality Assurance/Quality Control of Real Time Oceanographic Data. <https://ioos.noaa.gov/project/qartod/>.
- Warnes, G.R., B. Bolker, T. Lumley. (2021). gtools: Various R Programming Tools. R package version 3.9.2. <https://CRAN.R-project.org/package=gtools>.
- Weber, E.D., T.D. Auth, S. Baumann-Pickering, T.R. Baumgartner, E.P. Bjorkstedt, S.J. Bograd, B.J. Burke, J.L. Cadena-Ramirez, E.A. Daly, M. de la Cruz, H. Dewar, J.C. Field, J.L. Fisher, A. Giddings, R. Goericke, E. Gomez-Ocampo, J. Gomez-Valdes, E.L. Hazen, J. Hildebrand, C.A. Horton, K.C. Jacobson, M.G. Jacox, J. Jahncke, M. Kahru, R.M. Kudela, B.E. Lavaniegos, A. Leising, S.R. Melin, L.E. Miranda-Bojorquez, C.A. Morgan, C.F. Nickels, R.A. Orben, J.M. Porquez, E.J. Portner, R.R. Robertson, D.L. Rudnick, K.M. Sakuma, J.A. Santora, I.D. Schroeder, O.E. Snodgrass, W.J. Sydeman, A.R. Thompson, S.A. Thompson, J.S. Trickey, J. Villegas-Mendoza, P. Warzybok, W. Watson, and S.M. Zeman. (2021). State of the California Current 2019-2020: Back to the Future with Marine Heatwaves? *Frontiers in Marine Science*, 8: 1-23.

- Wells, B.K., I.D. Schroeder, J.A. Santora, E.L. Hazen, S.J. Bograd, E.P. Bjorkstedt, V.J. Loeb, S. McClatchie, E.D. Weber, W. Watson, A.R. Thompson, W.T. Peterson, R.D. Brodeur, J. Harding, J. Field, K. Sakuma, S. Hayes, N. Mantua, W.J. Sydeman, M. Losekoot, S.A. Thompson, J. Largier, S.Y. Kim, F.P. Chavez, C. Barcelo, P. Warzybok, R. Bradley, J. Jahncke, R. Goericke, G.S. Campbell, J.A. Hildebrand, S.R. Melin, R.L. DeLong, J. Gomez-Valdes, B. Lavaniegos, G. Gaxiola-Castro, R.T. Golightly, S.R. Schneider, N. Lo, R.M. Suryan, A.J. Gladics, C.A. Horton, J. Fisher, C. Morgan, J. Peterson, E.A. Daly, T.D. Auth, and J. Abell. (2013). State of the California Current 2012-2013: no such thing as an “average” year. California Cooperative Oceanic Fisheries Investigations (CalCOFI) Reports, 54: 37–71.
- Wickham, H. (2007). Reshaping Data with the reshape Package. *Journal of Statistical Software*, 21(12): 1–20. URL <http://www.jstatsoft.org/v21/i12/>.
- Wickham, H., M. Averick, J. Bryan, W. Chang, L. D’Agostino McGowan, R. François, G. Gromlund, A. Hayes, L. Henry, J. Hester, M. Kuhn, T. Lin Pedersen, E. Miller, S. Milton Bache, K. Müller, J. Ooms, D. Robinson, D. P. Seidel, V. Spinu, K. Takahashi, D. Vaughan, C. Wilke, K. Woo, H. Yutani. (2019). Welcome to the tidyverse. *Journal of Open Source Software*, 4(43), 1686, <https://doi.org/10.21105/joss.01686>.
- Wickham, H. and D. Seidel. (2020). scales: Scale Functions for Visualization. R package version 1.1.1. <https://CRAN.R-project.org/package=scales>.
- Winant, C. and A. Bratkovich. (1981). Temperature and currents on the southern California shelf: A description of the variability. *Journal of Physical Oceanography*, 11: 71–86.
- Zeileis, A. and G. Grothendieck. (2005). zoo: S3 Infrastructure for Regular and Irregular Time Series. *Journal of Statistical Software*, 14(6), 1-27. <https://doi.org/10.18637/jss.v014.i06>.

CHAPTER 2

FIGURES & TABLES

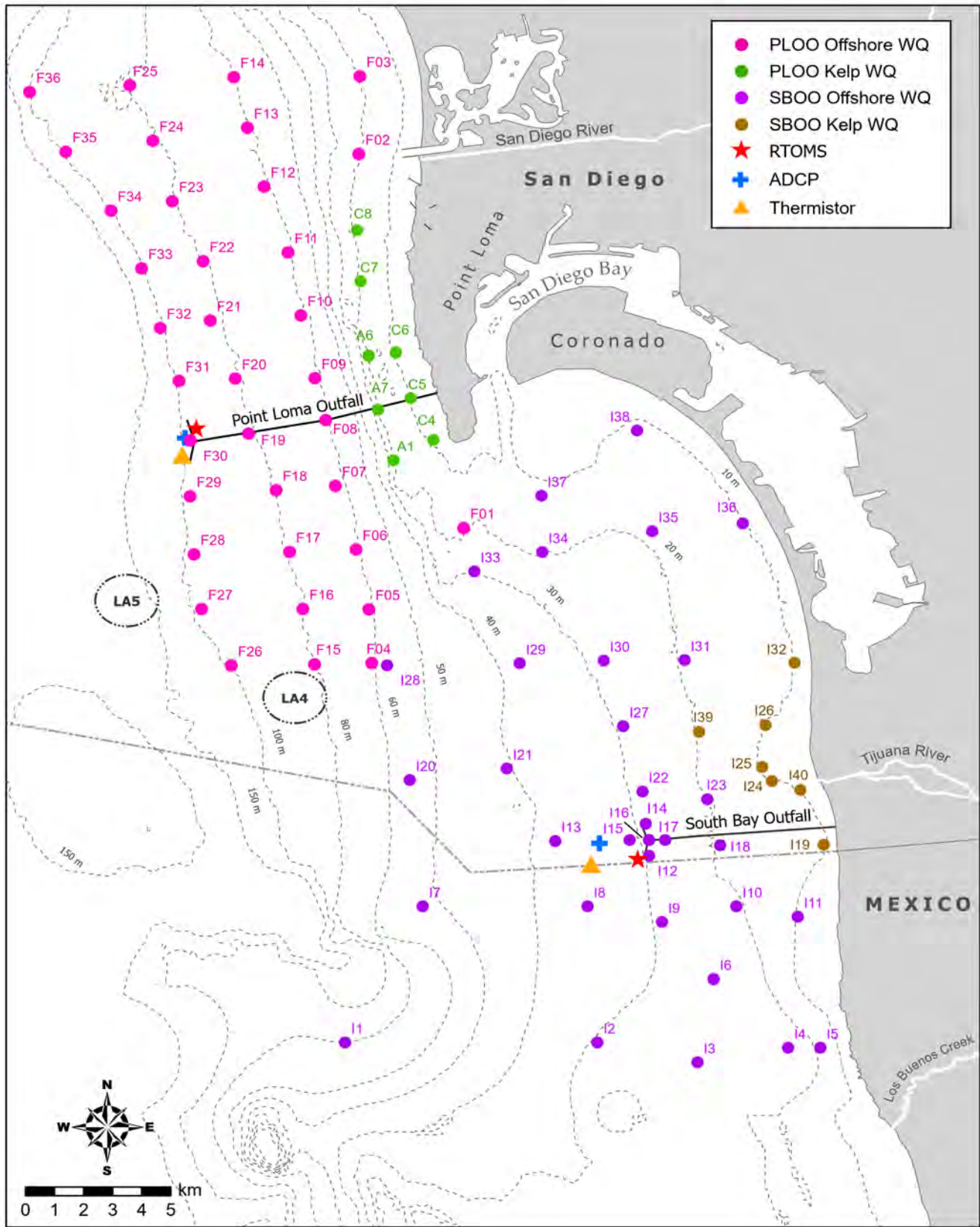


Figure 2.1

Locations of CTD water quality monitoring stations and mooring sites (RTOMS, ADCP, and thermistor arrays) sampled around the PLOO and SBOO as part of the City of San Diego's Ocean Monitoring Program.

Table 2.1

Sensor configuration and model type for RTOMS by site and depth during 2022 and much of 2023. In late December 2023, PLOO sensors on the bottom package (cage-2) were relocated to 89 m, and temperature, conductivity, and dissolved oxygen were retained at 75 m depth.

Sensor Depth		Parameters Measured (Sensor Types)
PLOO	SBOO	
1 m (surface)	1 m (surface)	Temperature, conductivity, pH (total), DO (Sea-Bird SeapHOx) Ocean currents (RDI 300kHz ADCP) Partial pressure of carbon dioxide (Pro-Oceanus pCO ₂ System) Chlorophyll a, CDOM, turbidity (Sea-Bird ECO triplet)
10 m	10 m	Temperature, conductivity (Sea-Bird MicroCAT)
	18 m	Temperature, conductivity, DO (Sea-Bird MicroCAT ODO) Chlorophyll a, CDOM, turbidity (Sea-Bird ECO triplet)
20 m		Temperature, conductivity (Sea-Bird MicroCAT)
	26 m (cage)	Temperature, conductivity, pH, DO (Sea-Bird SeapHOx) Chlorophyll a, CDOM, turbidity (Sea-Bird ECO triplet) Nitrate + nitrite (Sea-Bird SUNA V2) BOD (Chelsea UviLux)
30 m (cage-1)		Temperature, conductivity, pH, DO (Sea-Bird SeapHOx) Chlorophyll a, CDOM, turbidity (Sea-Bird ECO triplet) BOD (Chelsea UviLux) Nitrate + nitrite (Sea-Bird SUNA V2)
45 m		Temperature, conductivity (Sea-Bird MicroCAT)
60 m		Temperature, conductivity (Sea-Bird MicroCAT)
75 m (cage-2)		Temperature, conductivity, pH, DO (Sea-Bird Deep SeapHOx) Chlorophyll a, CDOM, turbidity (Sea-Bird ECO triplet) Nitrate + nitrite (Sea-Bird SUNA V2) BOD (Chelsea UviLux)
89m		Temperature, conductivity, DO (Sea-Bird MicroCAT ODO)

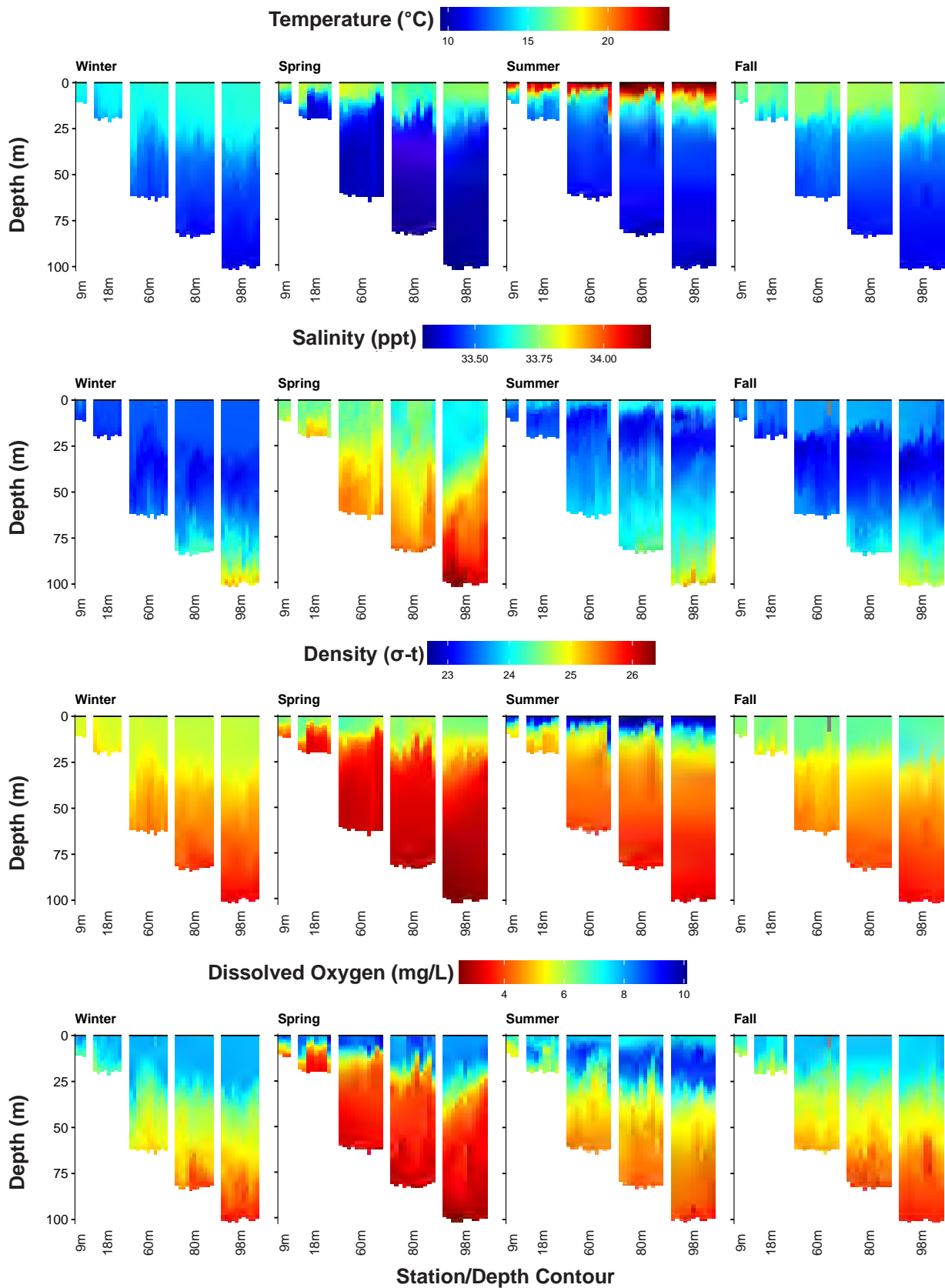


Figure 2.2

Temperature, density, salinity, and dissolved oxygen recorded in the PLOO region during 2022. Data are 1-m binned values per depth for each station and were collected over 4–5 days during each quarterly survey. Stations are depicted from north to south along each depth contour.

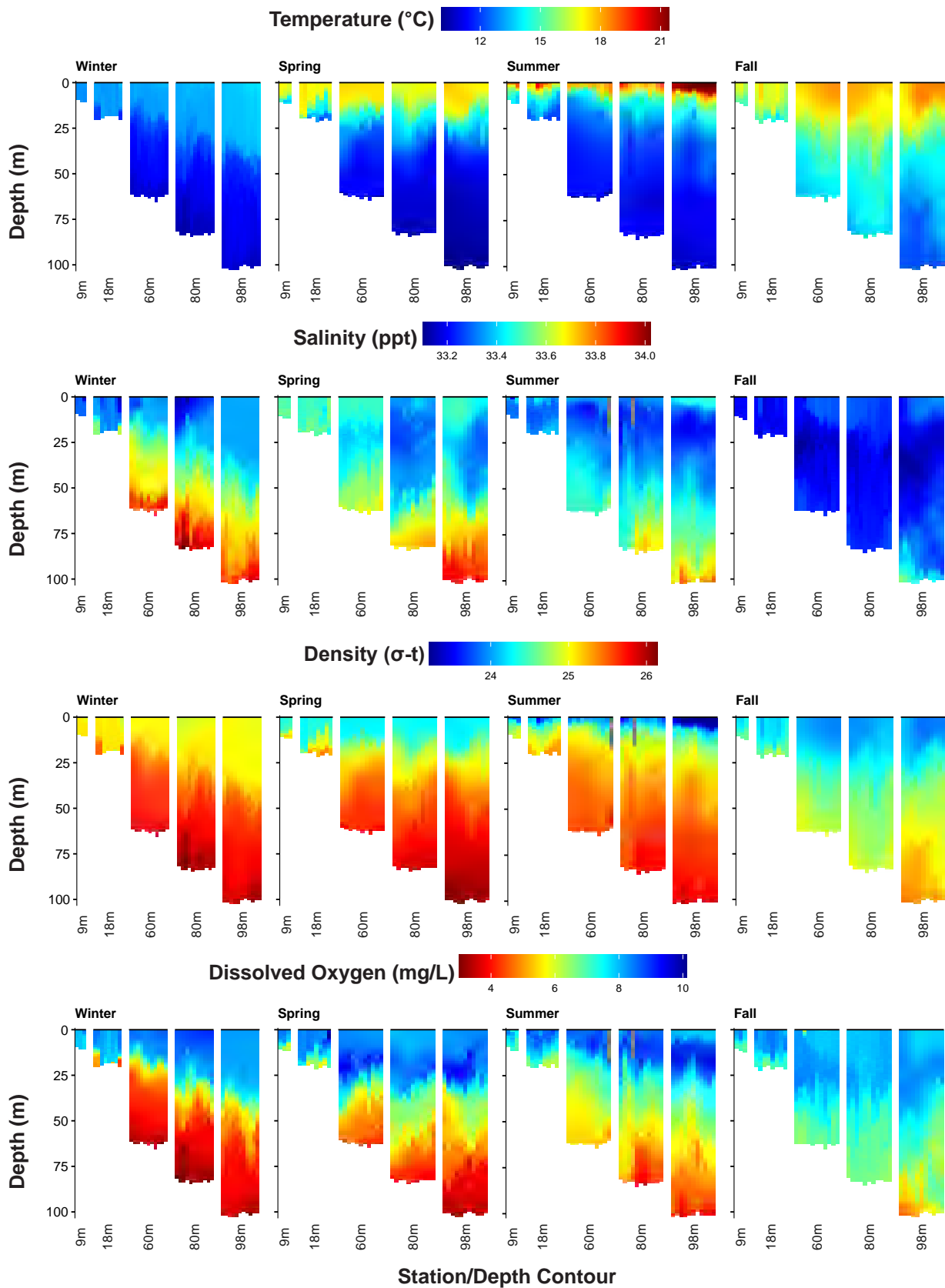


Figure 2.3

Temperature, density, salinity, and dissolved oxygen recorded in the PLOO region during 2023. Data are 1-m binned values per depth for each station and were collected over 4–5 days during each quarterly survey. Stations are depicted from north to south along each depth contour.

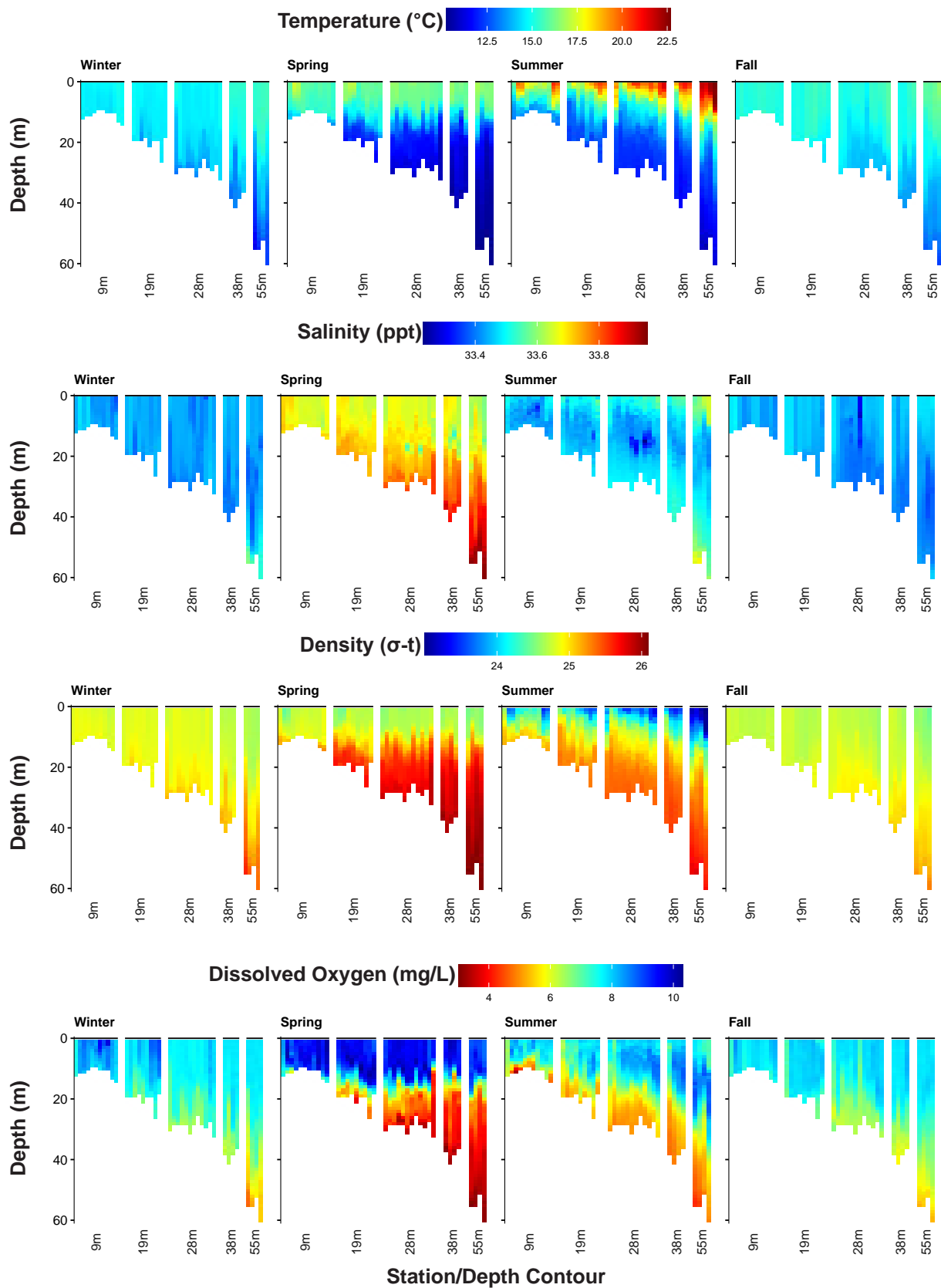


Figure 2.4

Temperature, density, salinity, and dissolved oxygen recorded in the SBOO region during 2022. Data are 1-m binned values per depth for each station and were collected over 4–5 days during each quarterly survey. Stations are depicted from north to south along each depth contour.

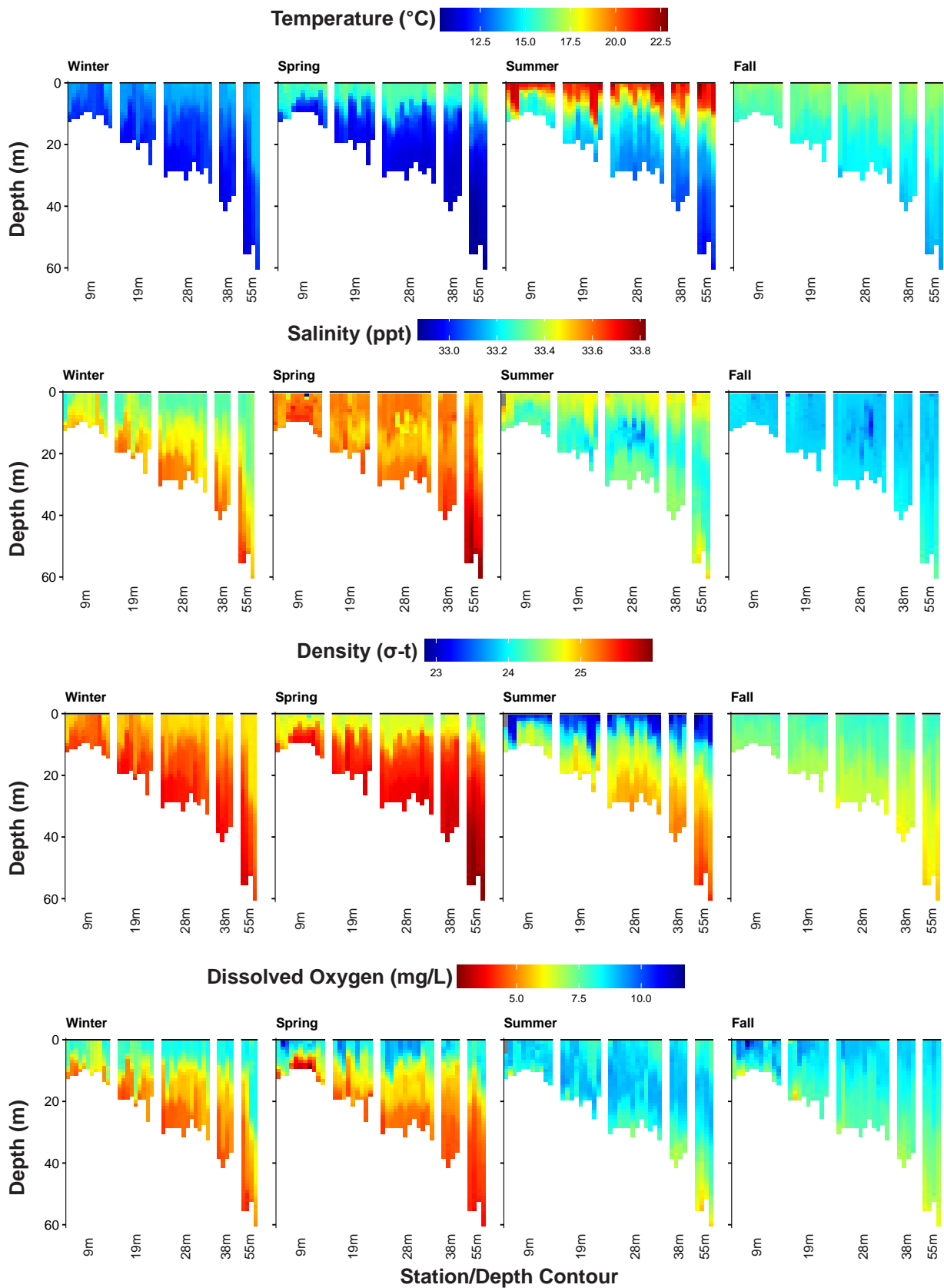


Figure 2.5

Temperature, density, salinity, and dissolved oxygen recorded in the SBOO region during 2023. Data are 1-m binned values per depth for each station and were collected over 4–5 days during each quarterly survey. Stations are depicted from north to south along each depth contour.

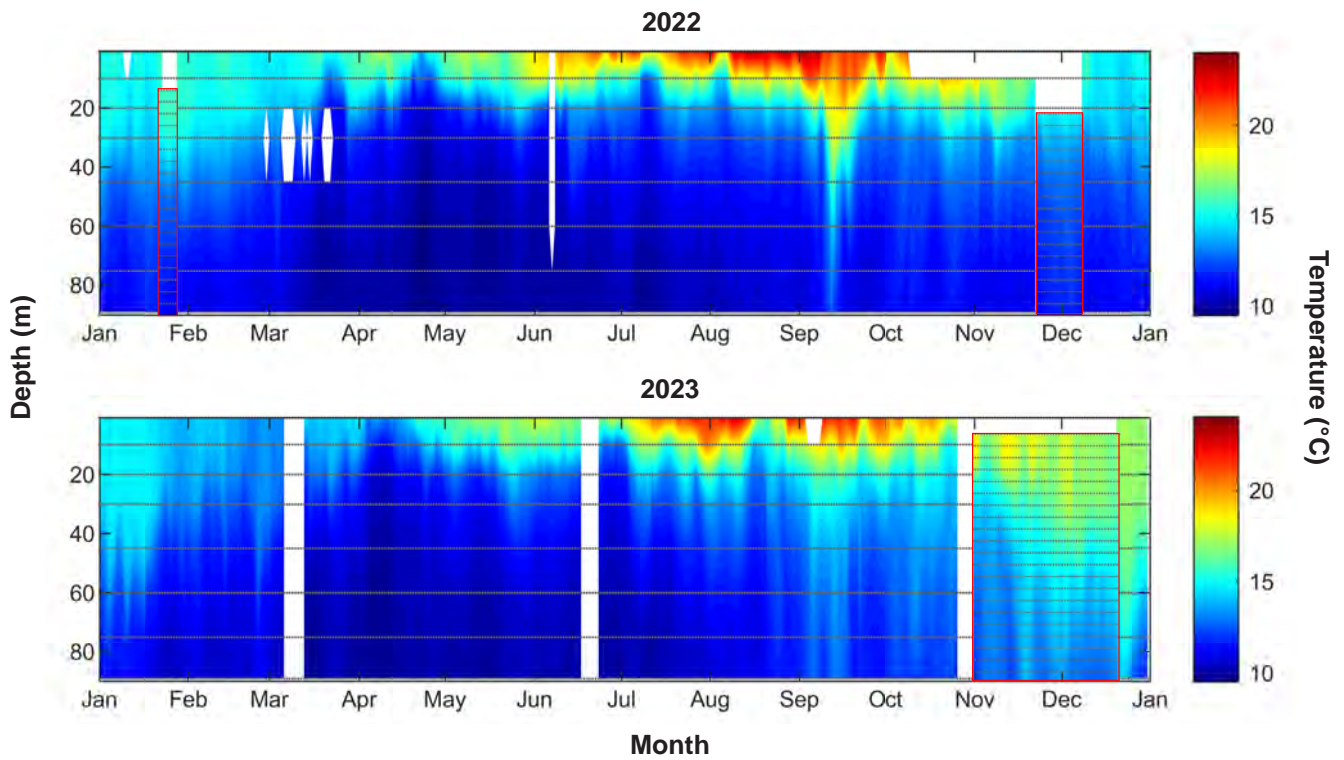


Figure 2.6

Daily averaged temperature recorded near the PLOO by the RTOMS during 2022 and 2023. Horizontal gray lines indicate depths at which sensors were located. Additional missing data shown as white spaces. Thermistor array data were used to replace missing RTOMS data (due to instrument failure) for all periods within a red border.

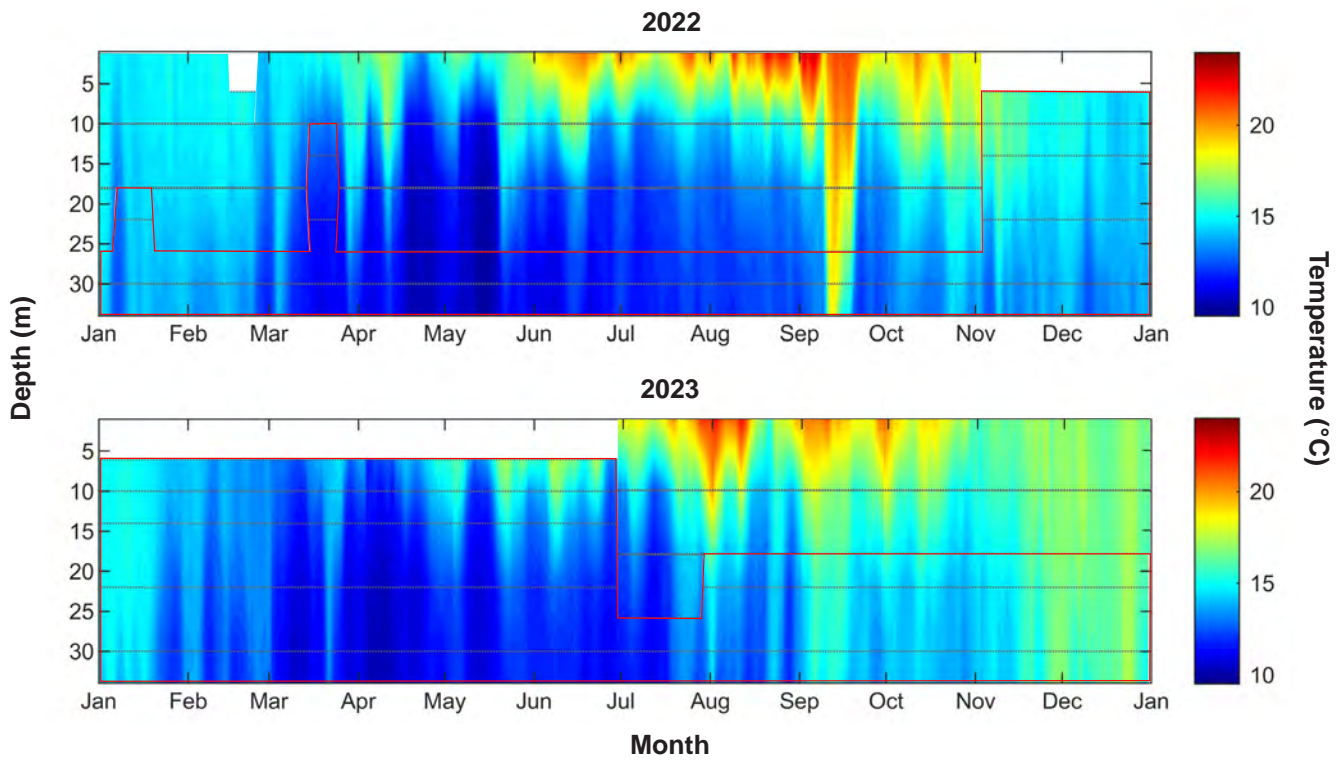


Figure 2.7

Daily averaged temperature recorded near the SBOO by the RTOMS or thermistor array during 2022 and 2023. Horizontal gray lines indicate depths at which sensors were located. Thermistor array data were used to replace missing RTOMS data (due to instrument failure) for all periods within a red border. Additional missing data shown as white spaces.

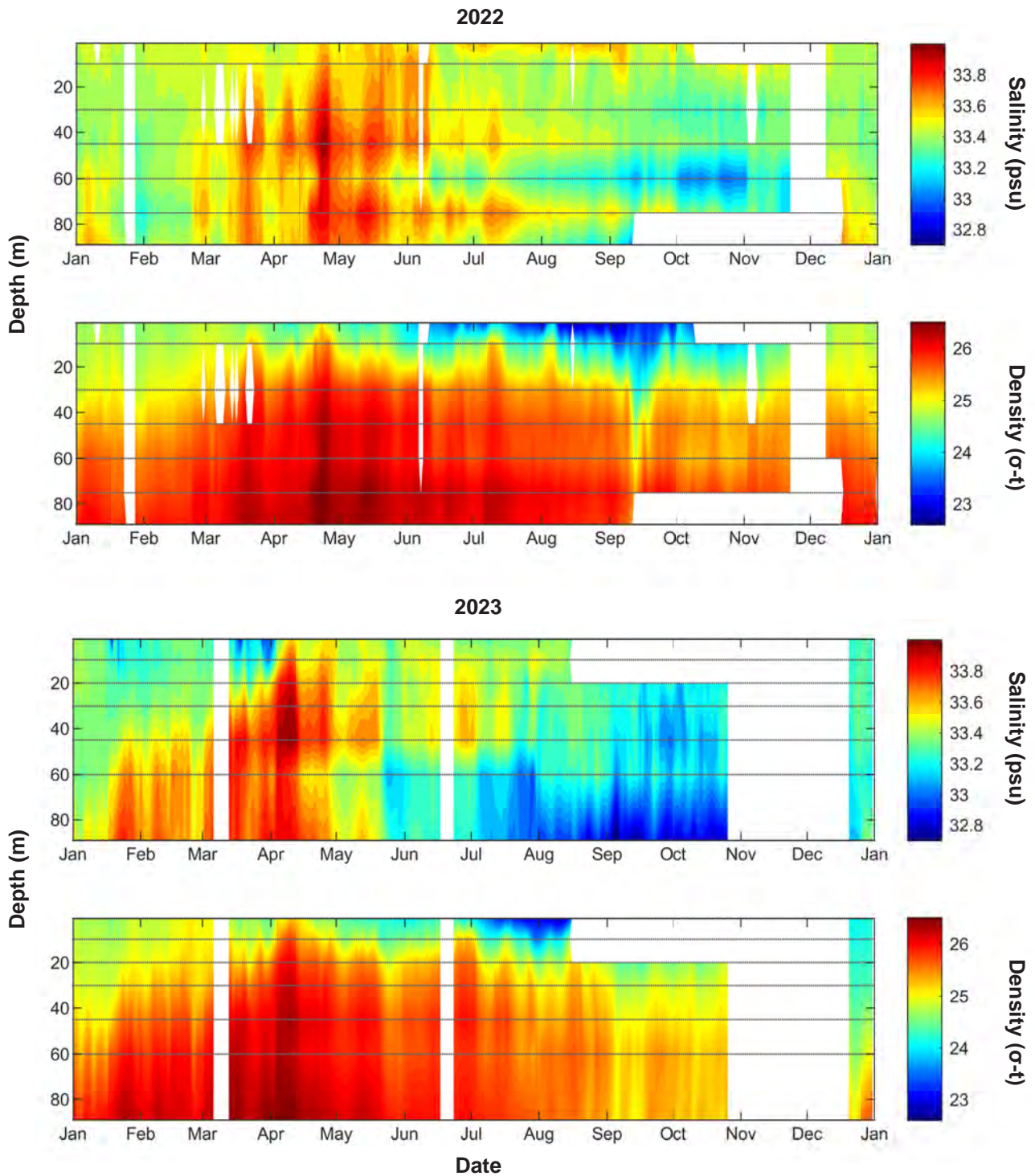


Figure 2.8

Daily averaged salinity and density recorded by the PLOO RTOMS during 2022 and 2023. Horizontal gray lines indicate depths at which sensors were located. Missing data due to instrument failure or loss shown as white spaces. Note that data from the 20 m depth in 2022 and 75 m depth in 2023 are omitted due to sensor failure.

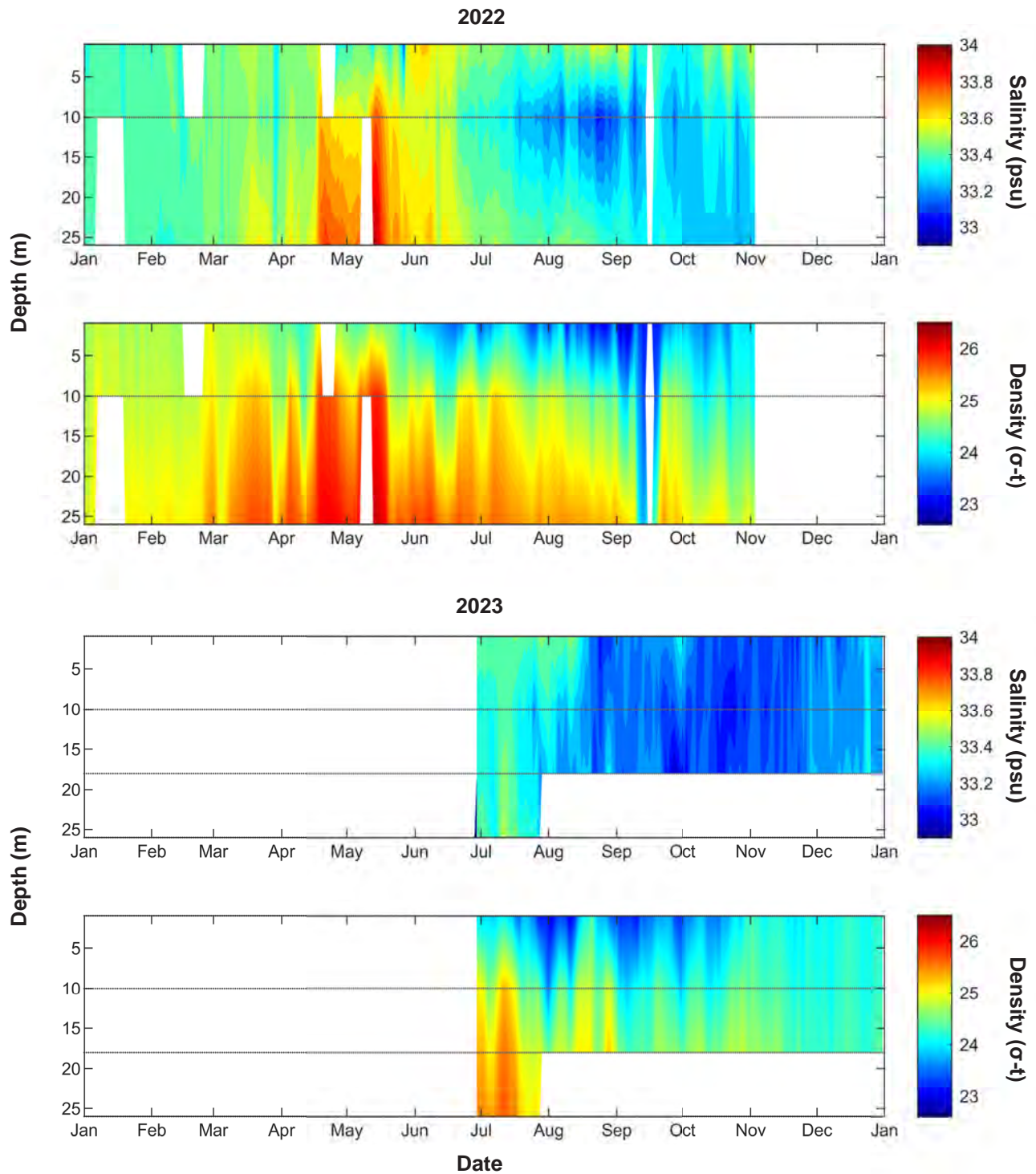


Figure 2.9

Daily averaged salinity and density recorded by the SBOO RTOMS during 2022 and 2023. Horizontal gray lines indicate depths at which sensors were located. Missing data due to instrument failure or loss shown as white spaces. Note that data from the 18 m depth in 2022 and 26 m depth in 2023 are omitted due to sensor failure.

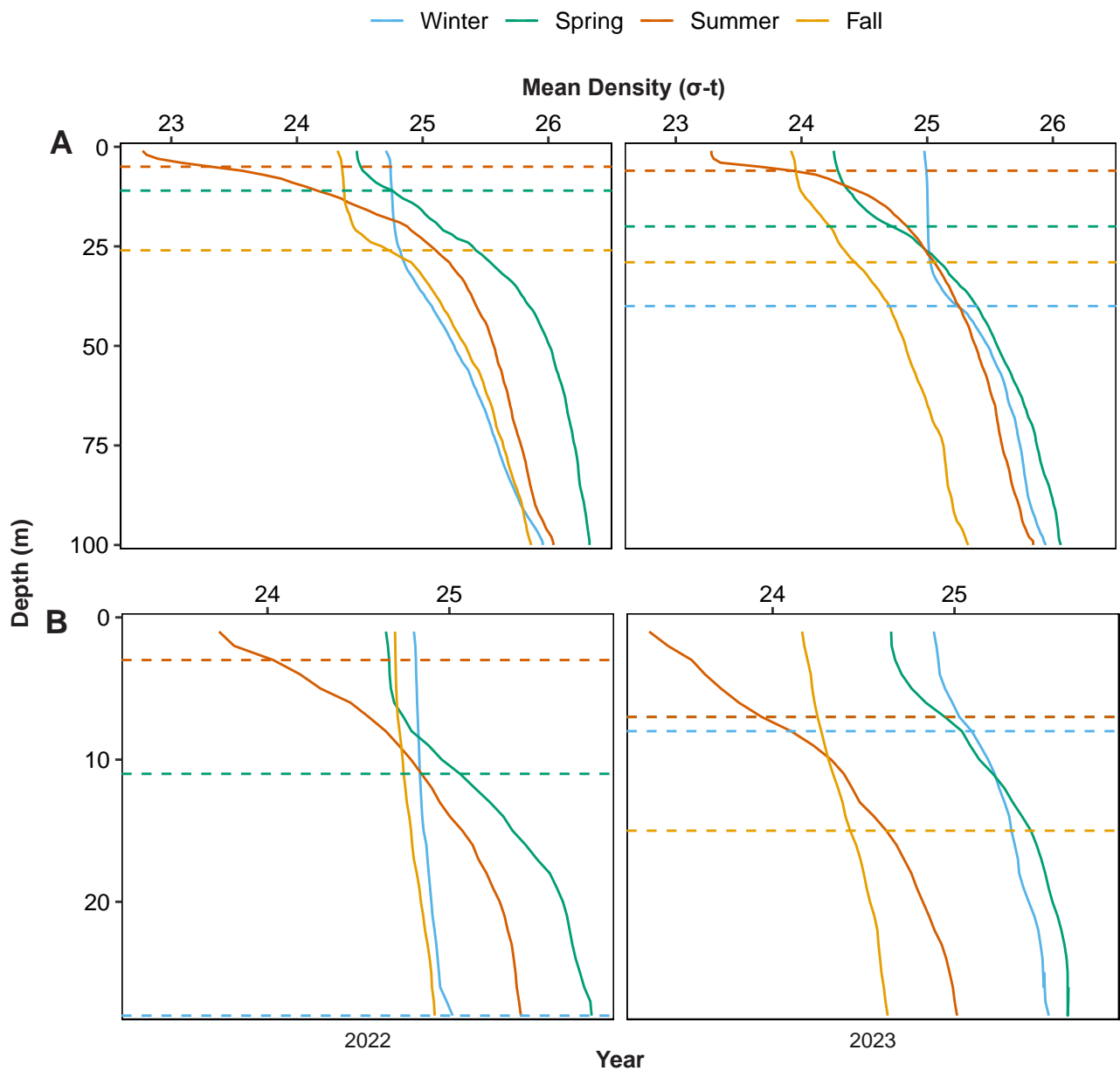


Figure 2.10

Mean density for each survey conducted during 2022 and 2023 at (A) PLOO discharge depth stations (n=11) and (B) SBOO discharge depth stations (n=13). Horizontal dashed lines indicate depth of maximum buoyancy frequency per respective season. Dashed line not shown for buoyancy frequencies less than 5.5 cycles/minute indicating a well mixed water column.

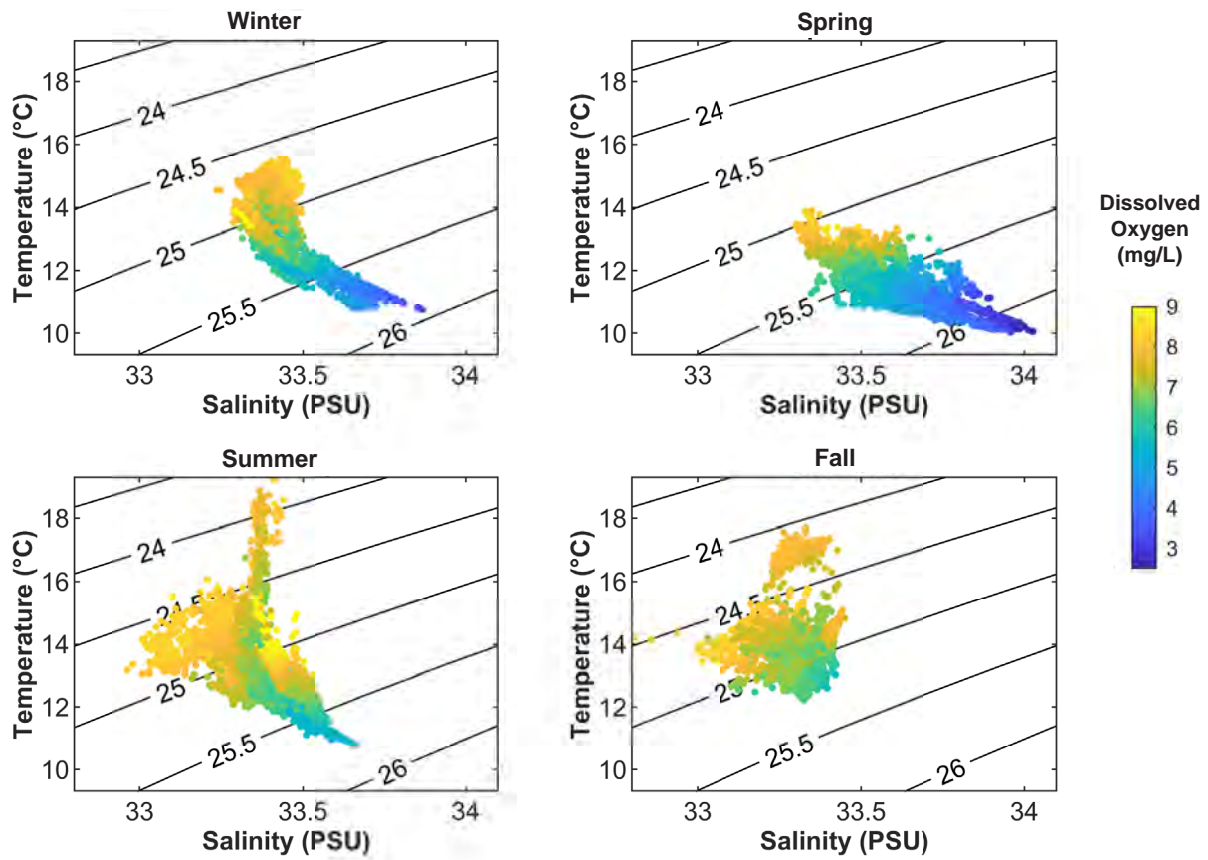


Figure 2.11

Hourly averaged DO by season shown on temperature versus salinity plots at 30 m for all available PLOO mooring data from 2022 to 2023. Isopycnals and corresponding σ -t values shown by black lines.

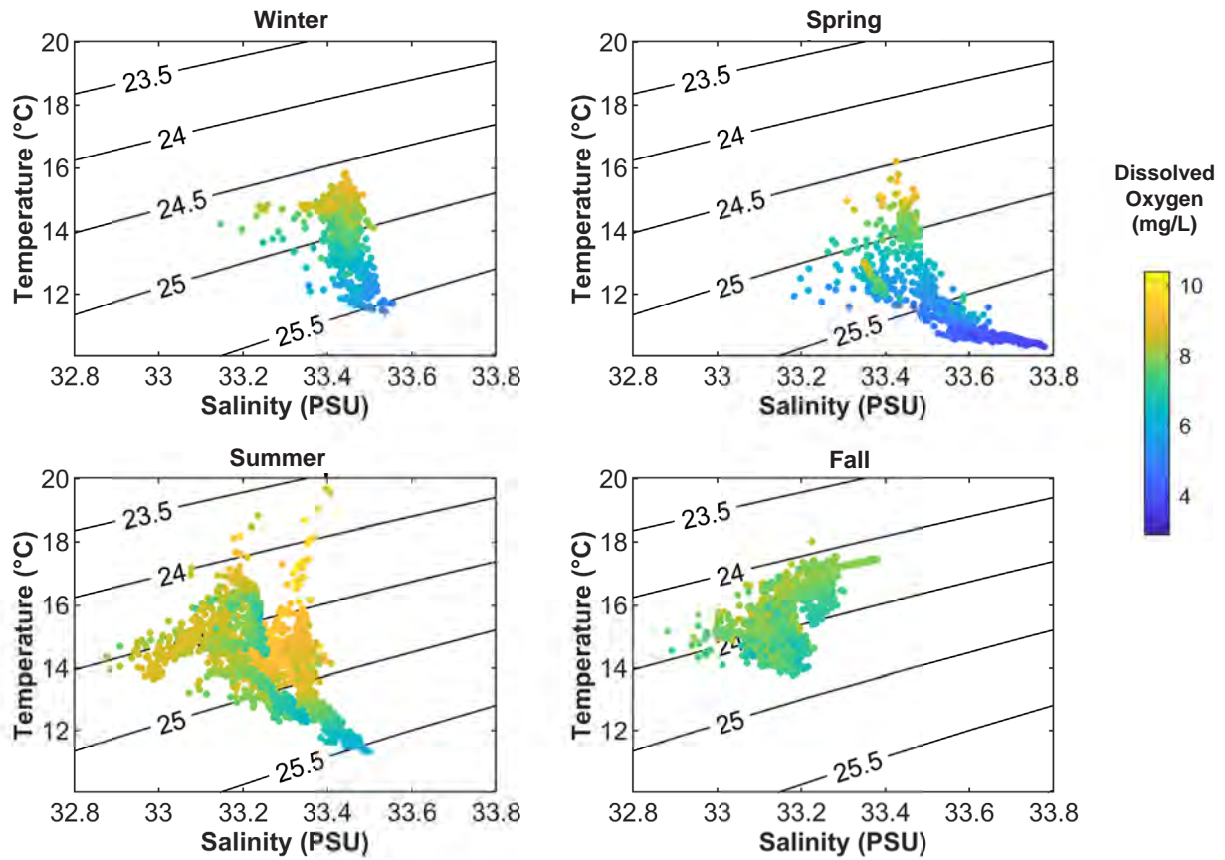


Figure 2.12

Hourly averaged DO by season shown on temperature versus salinity plots at 18 m for all available SBOO mooring data from 2022 to 2023. Isopycnals and corresponding σ -t values shown by black lines.

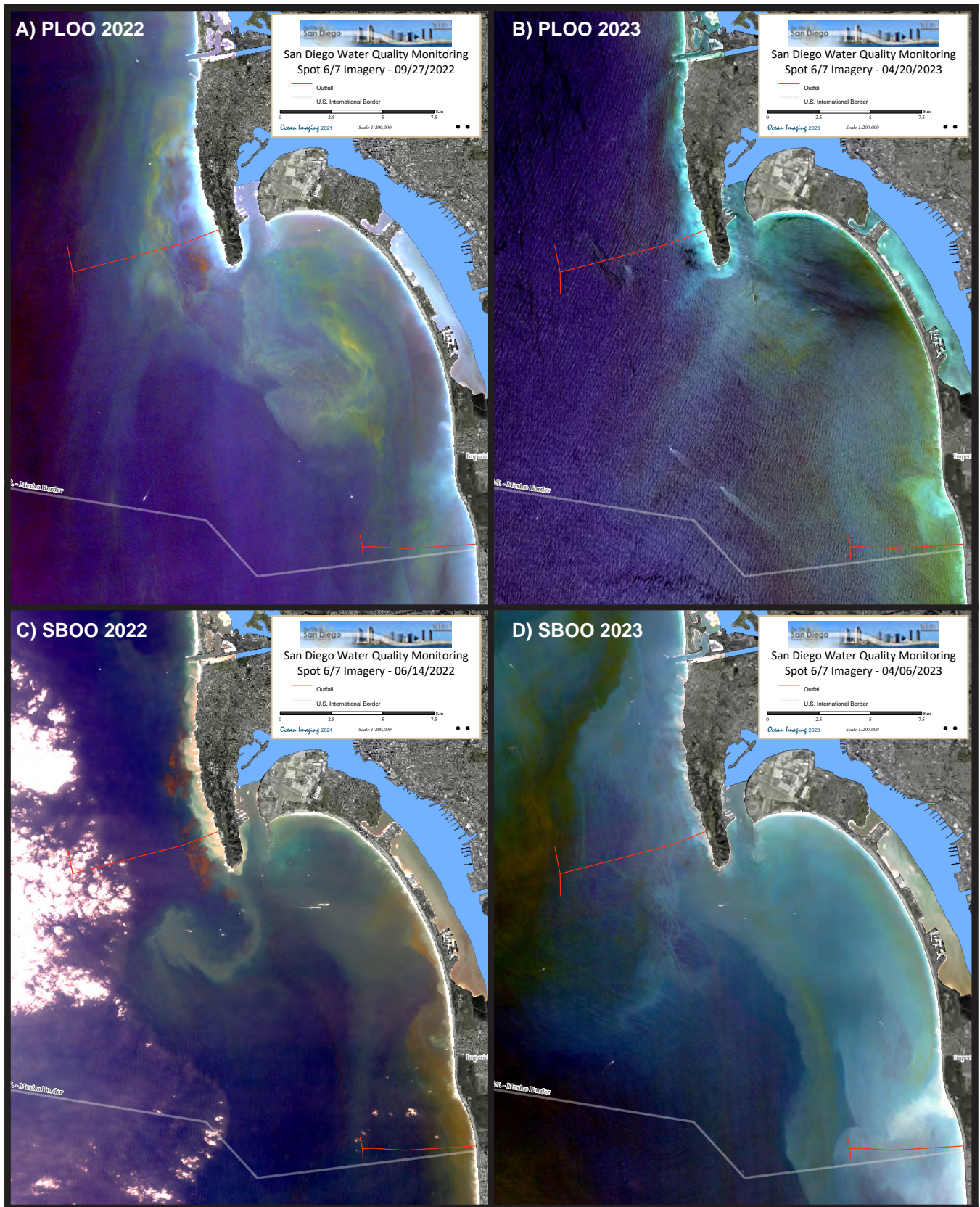


Figure 2.13

SPOT-6/7 satellite images of the San Diego region acquired nearest to the date of maximum chlorophyll a concentrations recorded for A) PLOO region in 2022 (October), B) PLOO region in 2023 (April), C) SBOO region in 2022 (June) and, D) SBOO region in 2023 (April) (Ocean Imaging 2024).

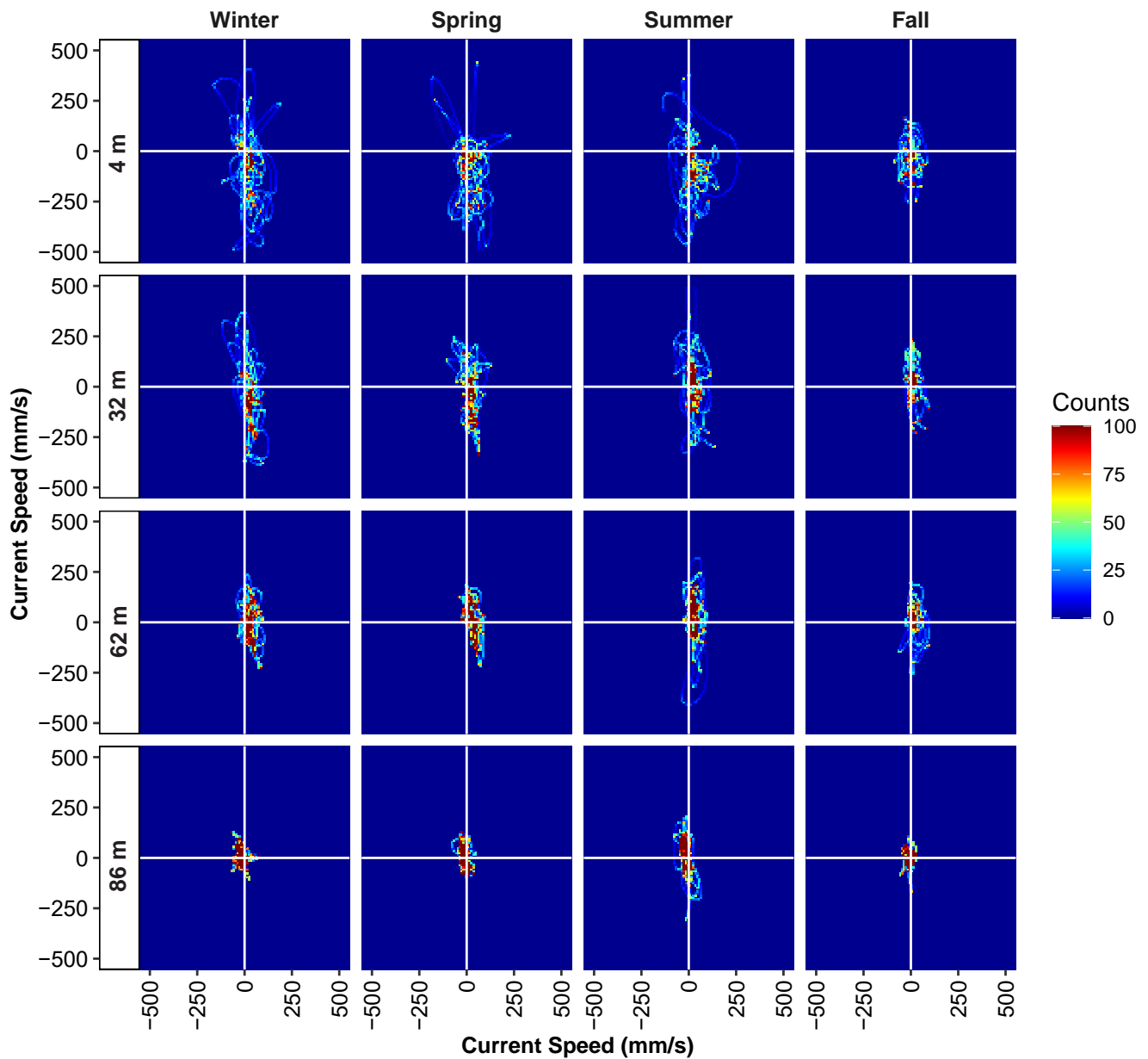


Figure 2.14

Frequency distribution (counts) by season of current speed (mm/s) and direction from 2022-2023 at the PLOO RTOMS ADCP location at representative depth bins. The deployment ended prior to the fall season 2023. On the x-axis, positive values indicate an eastward direction while negative values indicate a westward direction. On the y-axis, positive values indicate a northward direction while negative values indicate a southward direction.

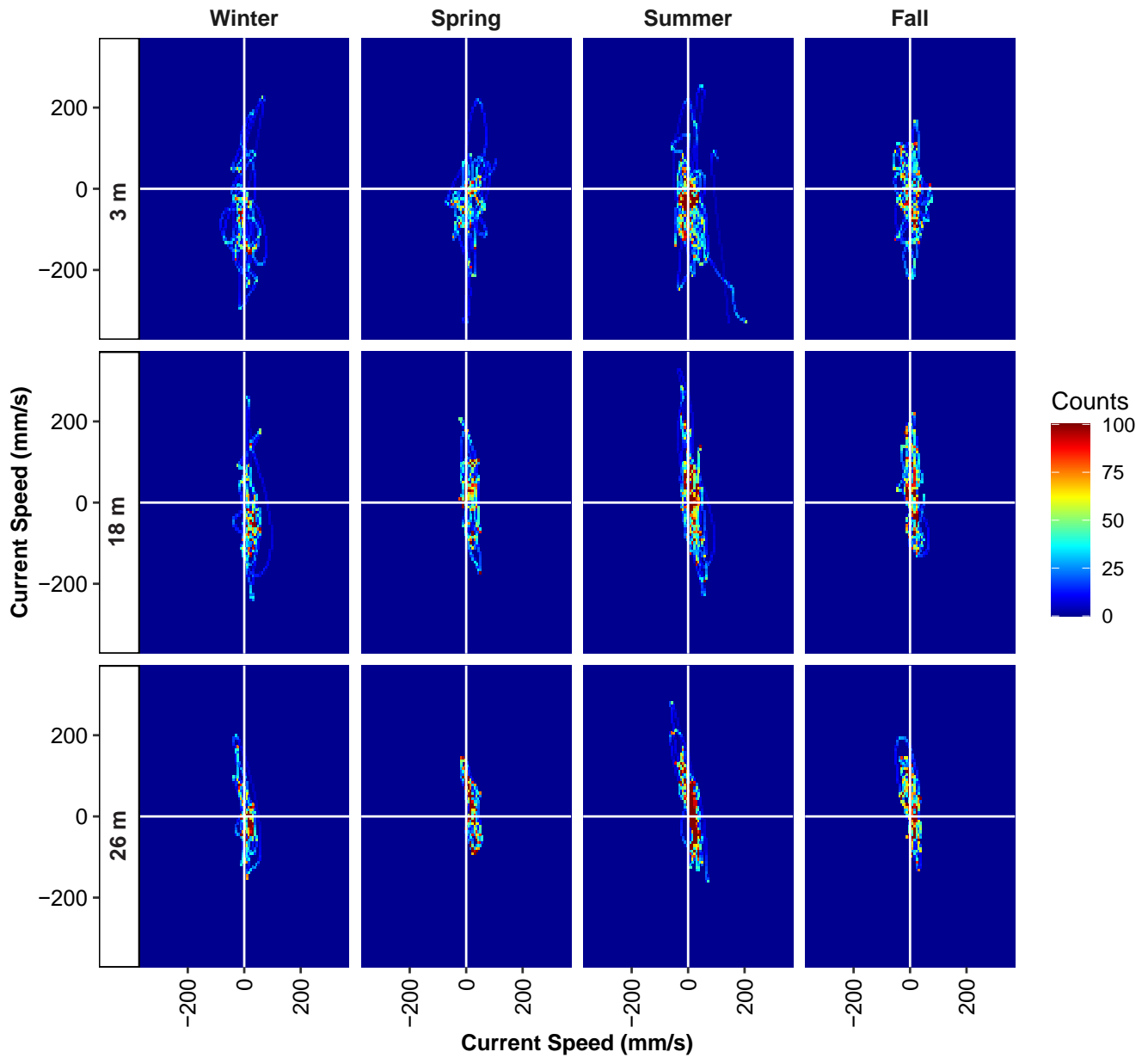


Figure 2.15

Frequency distribution (counts) by season of current speed (mm/s) and direction from 2022-2023 at the SBOO RTOMS ADCP location at representative depth bins. On the x-axis, positive values indicate an eastward direction while negative values indicate a westward direction. On the y-axis, positive values indicate a northward direction while negative values indicate a southward direction.

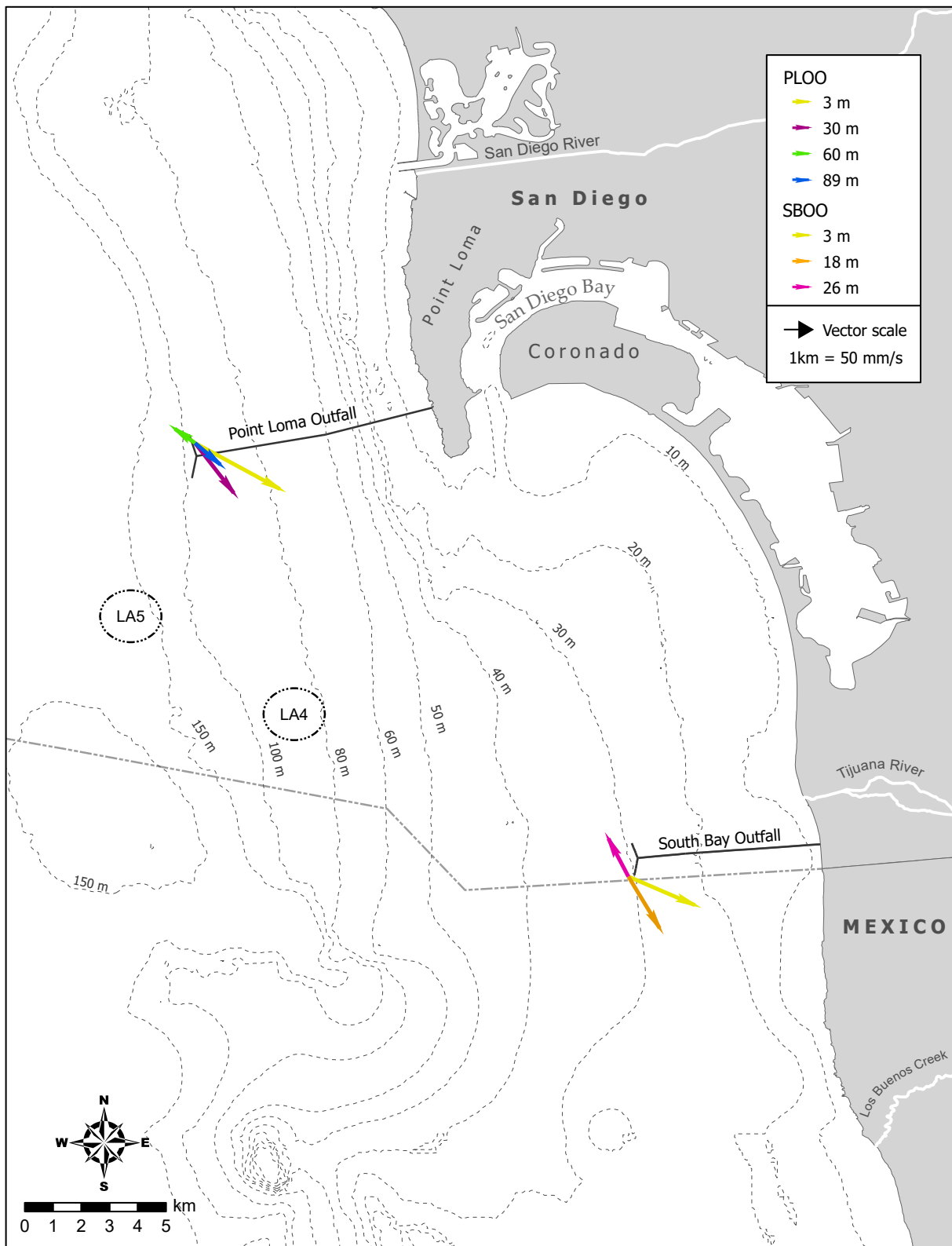


Figure 2.16

Generalized current speed and direction as determined by linear regression of all velocities for select depth bins at PLOO and SBOO RTOMS locations during the 2022-2023 deployment. Length of arrow reflects relative current speed or intensity. Due to the relative shortened deployment time of the RTOMS, flows do not represent a complete generalized flow across all seasons and are instead representative of the summertime southeasterly flows during which the RTOMS were predominantly deployed.

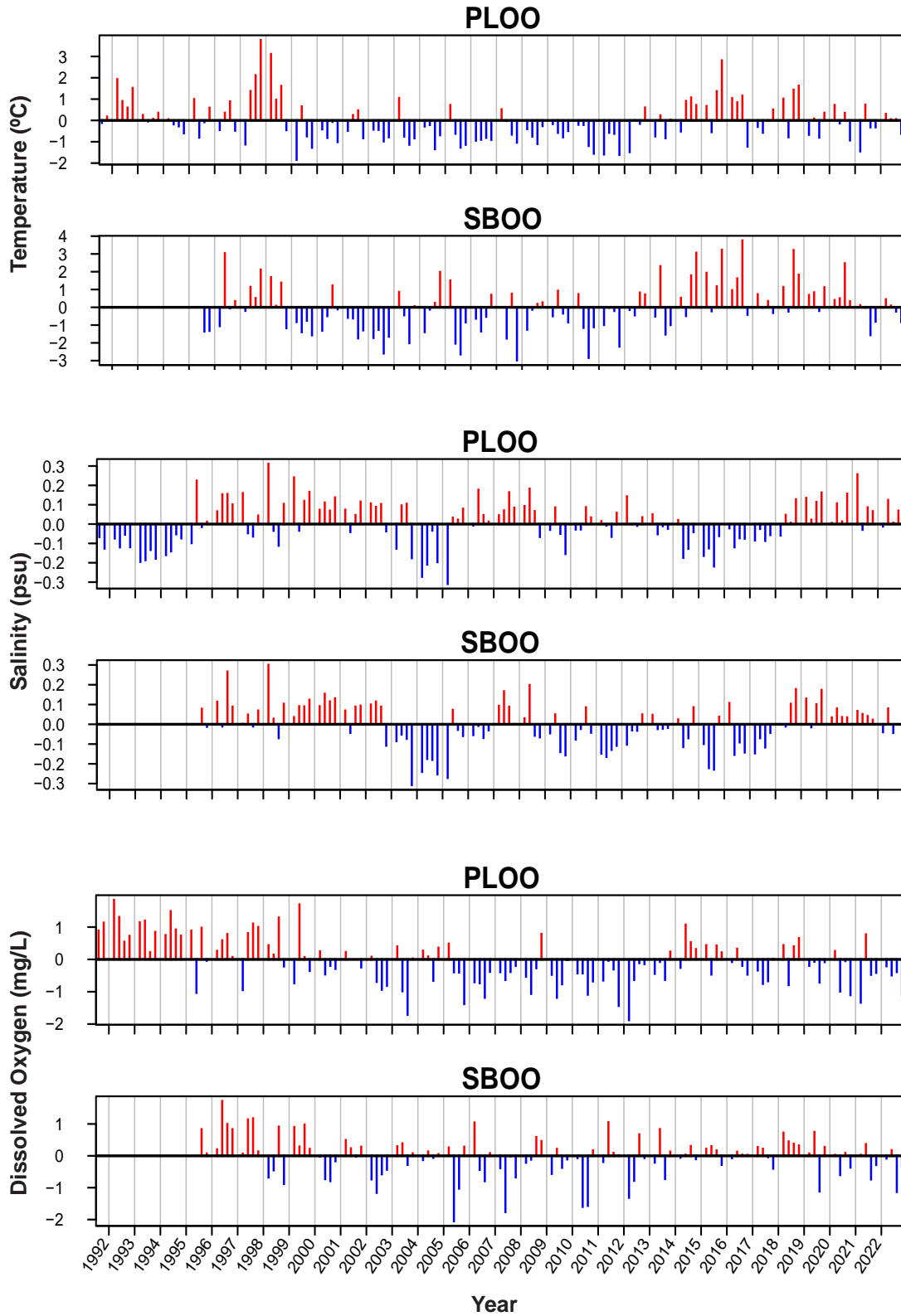


Figure 2.17

Time series of temperature, salinity, and dissolved oxygen (DO) anomalies from 1991 through 2023 at PLOO discharge depth stations (n=11) and SBOO discharge depth stations (n=13), all depths combined. Monitoring at the SBOO stations began in 1995.

Table 2.2

Long-term climate-related events in the Southern California Bight. El Niño Southern Oscillation (ENSO); Pacific Decadal Oscillation (PDO); California Current System (CCS); North Pacific Gyre Oscillation (NPGO); Multivariate ENSO Index (MEI)

Approximate Timespan	Large-Scale Climatic Event
1997-1998	Colossal El Niño
1998-2002	Phase change to (-) ENSO and (-) PDO indices to cold conditions
2002-2006	Return to warm ocean conditions in CCS
2002-2004	Intrusion of subarctic waters into CSS with lower than normal salinities
2007	Moderate to strong La Niña, negative PDO cooling event, positive NPGO indicating increased flow of cold, nutrient-rich water from the north
2010	Moderate to strong La Niña
2013-2014	Phase change to (+) PDO , (-) NPGO, and (+) MEI, resulting in region-wide warming
2014-2015	Largest marine heatwave (BLOB) in NE Pacific
2015	Colossal El Niño
2016-2018	Weak La Niña to Neutral ENSO conditions
2018-2019	Weak El Niño
2019	Marine heatwave in the CCS
2020	Marine heatwave offshore in the CCS (second largest to BLOB)
2021	Marine heatwave mostly offshore in the CCS
2020-2021	Phase change to (-) PDO and (-) MEI, with weak La Niña
2022-2023	Phase change from La Niña (2019-2022) to El Niño in late 2023

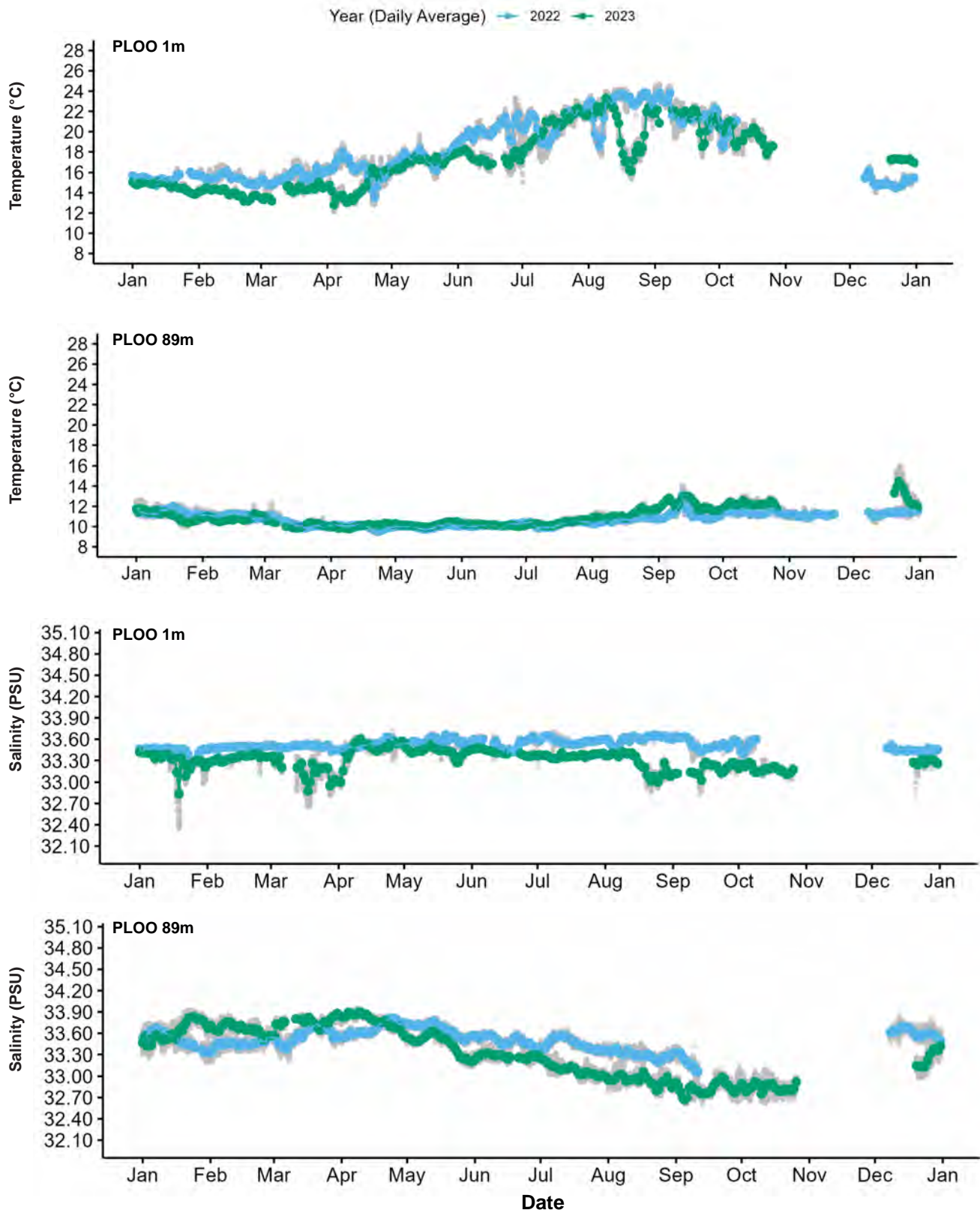


Figure 2.18

Surface and bottom (1 m and 89 m) temperature and salinity data recorded at the PLOO RTOMS during 2022–2023. Data presented as daily averages shown in color and raw values shown in gray.

Chapter 3

Water Quality Compliance

Chapter 3. Water Quality Compliance

INTRODUCTION

The City of San Diego (City) conducts extensive monitoring along the shoreline (beaches), nearshore (e.g., kelp forests), and other offshore coastal waters surrounding the Point Loma and South Bay Ocean Outfalls (PLOO and SBOO, respectively) to characterize regional water quality conditions and to identify possible impacts of wastewater discharge, or other contaminant sources, on the marine environment. Densities of fecal indicator bacteria (FIB), including total coliforms, fecal coliforms, and *Enterococcus*, are measured and evaluated to provide information about the dispersion of potentially contaminated water throughout the regions surrounding the two outfalls. Evaluation of these data may also help to identify the source of bacterial contamination throughout the region. In addition, the City's water quality monitoring efforts are designed to assess compliance with the bacterial water contact standards and other physical and chemical water quality objectives specified in the California Ocean Plan (Ocean Plan) that are intended to help protect the beneficial uses of State ocean waters (SWRCB, 2019).

Multiple sources of bacterial contamination exist in the Point Loma and South Bay monitoring regions and being able to separate any impact that may be associated with wastewater discharge from other point, or non-point, sources of contamination is often challenging. Examples include outflows from the San Diego River, San Diego Bay, the Tijuana River, and the San Antonio de Los Buenos Creek in northern Baja California (Largier et al., 2004, Nezlin et al., 2007, Gersberg et al., 2008, Terrill et al., 2009). Likewise, storm water discharges and terrestrial runoff from local watersheds during storms, or other wet weather events, can also flush sediments and contaminants into nearshore coastal waters (Noble et al., 2003, Reeves et al., 2004, Sercu et al., 2009, Griffith et al., 2010). Moreover, decaying kelp and seagrass (beach wrack), sediments and sludge accumulating in storm drains, and sandy beach sediments themselves can serve as reservoirs for bacteria until release into coastal waters by returning tides, rain events, or other disturbances (Gruber et al., 2005, Martin and Gruber, 2005, Noble et al., 2006, Yamahara et al. 2007, Phillips et al. 2011). Further, the presence of shore birds and their droppings has been associated with high bacterial counts that may impact nearshore water quality (Grant et al. 2001, Griffith et al. 2010).

This chapter presents an analysis and assessment of bacterial distribution patterns collected during 2022 and 2023, at more than 100 permanent water quality monitoring stations surrounding the PLOO and SBOO. The primary goals are to: (1) document bacteriological conditions off San Diego; (2) distinguish elevated bacteriological signals that may result from the PLOO and SBOO wastewater plumes versus other possible sources of contamination; (3) assess compliance with Ocean Plan water contact standards; (4) identify any unknown sources of fecal bacteria contamination and determine if human fecal waste is the cause. Results of remote sensing observations (i.e., satellite imagery) for the San Diego and Tijuana regions are also evaluated to provide insight into the transport and dispersal of wastewater and other types of surface water plumes during the study period. To better understand potential impacts of a wastewater plume on ocean conditions, Chapter 4 discusses natural chemical tracers that can be leveraged to detect and distinguish an outfall's effluent signal from other non-point sources.

MATERIALS AND METHODS

Field Sampling

Shore stations

Seawater samples were collected weekly at 19 shoreline stations to monitor concentrations of FIB in waters adjacent to public beaches (Figure 3.1). Sixteen of these stations are in California State waters and are therefore subject to Ocean Plan water contact standards (Box 3.1, SWRCB 2019). Eight PLOO stations (D4, D5, D7, D8-B, D9, D10, D11, D12) are located from Mission Beach southward to the tip of Point Loma. Eight SBOO stations (S4, S5, S6, S8, S9, S10, S11, S12) are located between the USA/Mexico border and Coronado, while the other three SBOO shoreline stations (S0, S2, S3) are located south of the border and are not subject to Ocean Plan standards.

Seawater samples were collected from the surf zone at each of the above stations in sterile 250 mL bottles, after which they were transported on blue ice to the City's Marine Microbiology Laboratory and analyzed to determine concentrations of three types of FIB (i.e., total coliform, fecal coliform, *Enterococcus* bacteria). In addition, weather conditions and visual observations of water color and clarity, surf height, and human or animal activity were recorded at the time of sample collection. Wind speed and direction were measured using a hand-held anemometer with a compass. These observations were previously reported in monthly receiving waters monitoring reports submitted to the SDRWQCB (see City of San Diego 2022–2024). These reports are available online (City of San Diego 2024a).

Kelp and offshore stations

Fifteen stations located in relatively shallow waters within or near the Point Loma or Imperial Beach kelp beds (i.e., referred to as “kelp” stations herein) were monitored weekly to assess water quality conditions and Ocean Plan compliance in nearshore areas used for recreational activities such as SCUBA diving, surfing, fishing, and kayaking (Figure 3.1). These included PLOO stations C4, C5 and C6 located along the 9-m depth contour near the inner edge of the Point Loma kelp forest; PLOO stations A1, A6, A7, C7 and C8 located along the 18-m depth contour near the outer edge of the Point Loma kelp forest; SBOO stations I25, I26 and I39 located at depths of 9–18 m contiguous to the Imperial Beach kelp bed; and SBOO stations I19, I24, I32 and I40 located in other nearshore waters along the 9-m depth contour.

An additional 69 offshore stations were sampled quarterly over consecutive days in winter (February or March), spring (May), summer (August), and fall (November) to monitor water quality conditions and to estimate dispersion of the PLOO and SBOO wastewater plumes (Figure 3.1). These included 36 stations surrounding the PLOO, and 33 stations surrounding the SBOO. The PLOO stations are designated F1–F36 and are located along or adjacent to the 18, 60, 80, and 98 m depth contours. Seawater samples for FIB were collected at all of these stations. The SBOO stations are designated I1–I18, I20–I23, I27–I31, and I33–I38 and are located along the 9, 19, 28, 38 and 55 m depth contours, respectively. Only a subset of SBOO sites ($n = 21$; I3, I5, I7, I8, I9, I10–I14, I16, I18, I20–I23, I30, I33, I36–I38), are sampled for FIB. Additionally, 15 of the PLOO stations (F01–F03, F06–F14, F18–F20) and 15 of the SBOO stations (I12, I14, I16–I18, I22–I23, I27, I31, I33–I38) are located within State jurisdictional waters (i.e., within 3 nautical miles of shore) and therefore subject to the Ocean Plan compliance standards.

Seawater samples for FIB analyses were collected from 3 to 5 discrete depths at the kelp and offshore stations as indicated in Table 3.1. These samples were typically collected using a rosette sampler fitted with Niskin bottles surrounding a central Conductivity, Temperature, and Depth (CTD) instrument,

although replacement samples due to misfires or other causes may have been collected from a separate follow-up cast using stand-alone Van Dorn bottles if necessary. All weekly kelp/nearshore samples and quarterly offshore SBOO samples were analyzed for all three types of FIB, while the quarterly offshore PLOO samples were only analyzed for *Enterococcus* per permit requirements. All samples were refrigerated at sea and then transported on blue ice to the City’s Marine Microbiology Laboratory for processing and analysis. Oceanographic data were collected simultaneously with the water samples at each station (see Chapter 2). Visual observations of weather, sea conditions, and human or animal activity were also recorded at the time of sampling. These latter observations were reported previously in monthly receiving waters monitoring reports submitted to the SDRWQCB (see City of San Diego 2022–2024).

Laboratory Analyses

The City Marine Microbiology Laboratory follows guidelines issued by the U.S. Environmental Protection Agency (USEPA) Water Quality Office, State Water Resources Control Board (SWRCB) including the 2019 Ocean Plan and Environmental Laboratory Accreditation Program (ELAP) with respect to sampling and analytical procedures (Bordner et al. 1978, APHA 2012, USEPA 2014). All bacterial analyses were initiated within eight hours of sample collection and conformed to standard membrane filtration techniques, for which the laboratory is certified (ELAP Field of Testing 126).

FIB densities were determined and validated in accordance with USEPA and APHA guidelines (Bordner et al. 1978, APHA 2012, USEPA 2014). Plates with FIB densities above or below the ideal counting range were given greater than (>), greater than or equal to (\geq), less than (<), or estimated (e) qualifiers. However, all qualifiers were dropped, and densities were treated as discrete values, when determining compliance with Ocean Plan standards.

Quality assurance tests were performed routinely on bacterial samples to ensure that analyses and sampling variability did not exceed acceptable limits. Laboratory and field duplicate bacteriological samples were processed according to method requirements to measure analyst precision and variability between samples, respectively. Results of these procedures were reported under separate cover (City of San Diego 2023a, 2024b).

Data Analyses

Bacteriology

Compliance with the running geometric mean standards for fecal coliforms and *Enterococcus* was assessed using running 30-day and 42-day windows, respectively. Compliance with the median standard for total coliforms was assessed over a running 30-day window. Compliance with the statistical threshold value (STV) metrics for total coliforms and *Enterococcus* was calculated at monthly intervals. Compliance calculations were limited to shore, kelp and offshore stations located within State waters, excluding resamples. In all instances, compliance was rounded to the nearest whole number (e.g. 99.5% equates to 100%). For the purpose of visualization, to assess temporal and spatial trends, and to assess compliance with the HF183 sampling standards (Box 3.2), elevated FIB was determined by the number of analyses in which FIB concentrations exceeded the threshold established by the 2019 Ocean Plan’s water quality bacterial objectives for single sample maximum (SSM) or STV benchmark levels (Box 3.1) (SWRCB 2019). Due to the nature of the STV metric, elevated FIB does not necessarily indicate out-of-compliance for individual analyses of *Enterococcus* and total coliform densities. Compliance

with the HF183 sampling metrics was calculated as the proportion of analyses showing elevated FIB within the rolling window specified in Box 3.2, assessed daily over the report period. To also comply with the 2015 Ocean Plan water quality bacterial objectives required by the National Pollutant Discharge Elimination System (NPDES) permit for the Point Loma Wastewater Treatment Plant (NPDES No. CA0107409; Order No. R9-2017-0007), additional analyses, and their associated methods, are presented in Appendix D.

Bacterial densities were compared to rainfall data from Lindbergh Field, San Diego, CA (NOAA 2024). For the purpose of analyses contained within this report, the San Diego dry season was defined as all days between May 1st and September 30th in any given year, while the wet season occurs October 1st through April 30th. Satellite images of the San Diego coastal region were provided by Ocean Imaging of Solana Beach, California and used to aid in the analysis and interpretation of water quality data (see Appendix B). All analyses were performed using R (R Core Team 2019) and various functions within the reshape2, tidyverse, Hmisc, flextable, gtools, psych, RODBC, ggpubr, quantreg, and openxlsx packages (Wickham 2007, 2017, Harrell et al. 2015, Gohel 2024, Warnes et al. 2015, Revelle 2015, Ripley and Lapsley 2017, Kassambara 2019, Koenker 2019, Schauburger and Walker 2019). Data collected during 2022 were reported previously (City of San Diego 2023b), and all raw data for the 2022–2023 sampling period have been submitted to either the Regional Water Quality Control Board or the California Environmental Data Exchange Network (CEDEN) and may be accessed upon request.

RESULTS AND DISCUSSION

Bacteriological Compliance and Distribution

Shore stations

Seawater samples collected from the eight PLOO shore stations were 100% compliant with the 30-day fecal coliform geometric mean standard, while the 42-day *Enterococcus* geometric mean standard and the total coliform median standard were in compliance 98% and 77% of the time over the report period, respectively (Figure 3.2A). Compliance with the fecal coliform SSM standard at these sites was 100% (Figure 3.2B). Compliance with the STV standards for *Enterococcus* and total coliforms ranged from 25–100% of stations each month (Figure 3.2B, Table 3.2). In contrast, compliance rates were more variable during these two years at the eight SBOO shore stations located in State waters. For example, compliance for the 30-day geometric mean of fecal coliforms was 70%, compliance with the 42-day geometric mean of *Enterococcus* was 52%, and compliance with the total coliform median standard was 40% (Figure 3.3A). Furthermore, compliance with the SSM for fecal coliforms was 71% (Figure 3.3B), and STV compliance for both total coliforms and *Enterococcus* ranged from 0–100% of stations in compliance each month (Figure 3.3B, Table 3.2). However, it is important to note that six of these eight stations (S4, S5, S6, S10, S11, S12) are located near or within areas listed as ‘impaired waters’ and are not anticipated to comply with State water contact standards (State of California 2010).

Of the 5895 analyses run on seawater samples collected at the PLOO and SBOO shore stations in 2022–2023 (not including resamples), about 25% (n = 1471) had elevated FIB (Table 3.3). In state waters, elevated FIB was detected in 19% of analyses (934 of 4992 total analyses). A majority (67%) of the shore samples with elevated FIB were collected during the wet seasons when rainfall totaled 17.65 inches over both years. This general relationship between rainfall and elevated bacterial levels at shore stations has been evident since water quality monitoring began in both regions (Figure 3.4). Further

analyses of data from PLOO and SBOO shore stations indicate that the occurrence of a sample with elevated FIB was significantly more likely during the wet season than during the dry season (13% versus 5%, respectively; $n = 75,030$, $\chi^2 = 1607$, $p < 0.0001$).

Regionally, elevated FIB densities occurred most often at SBOO shore stations S4, S5, S10 and S11 located near the mouth of the Tijuana River, as well as in northern Baja California waters at stations S0, S2 and S3 over the past two years (Table 3.3). Results from historical analyses also indicated that elevated FIB occurred more frequently at stations near the Tijuana River and south of the border near San Antonio de Los Buenos Creek, than at other PLOO or SBOO shore stations, especially during the wet seasons (Figure 3.4). Over the past several years, high FIB densities at these stations have consistently corresponded to outflows from the Tijuana River and San Antonio de Los Buenos Creek, typically following rain events (City of San Diego 2022). In addition, several sanitary sewer overflow events impacted the Tijuana River Valley during 2022 and 2023 (USIBWC 2022–2023).

Kelp bed stations

Seawater samples from the PLOO kelp stations were 100% compliant with the 30-day geometric mean standard for fecal coliforms and the six-week standard for *Enterococcus*, while compliance with the median standard for total coliforms was 99% (Figure 3.5A). Compliance with the SSM for fecal coliforms was also 100% (Figure 3.5B). STV compliance for total coliforms ranged from 50–100% of stations in compliance each month while compliance with the *Enterococcus* STV standard was 100% (Table 3.2). In the SBOO region, as was noted above for the shore stations, compliance rates were variable at the seven kelp bed, or nearshore, stations. For example, compliance in the SBOO kelp stations with the median standard for total coliforms was 60% over the report period, while compliance with the 30-day geometric mean for fecal coliforms was 89% and 79% for the six-week geometric mean standard for *Enterococcus* (Figure 3.6A). The SSM standard for fecal coliforms was met in 87% of samples (Figure 3.6B), and the STV standard for total coliforms and *Enterococcus* ranged from 0–100% (Table 3.2).

Of the 14,055 analyses run on samples collected at the PLOO and SBOO kelp stations in 2022–2023, approximately 9% ($n = 1275$) had elevated FIB, of which 83% occurred during the wet season (Table 3.4). However, analysis of water quality monitoring data collected at PLOO kelp stations over the course of the monitoring program (since 1991) shows that the difference in the occurrence of elevated FIB between wet and dry seasons is, though statistically significant, small in magnitude, indicating that rainfall has little impact on water quality in the PLOO region (2.8% in the dry season versus 3.6% in the wet season; $n = 171,966$, $\chi^2 = 90.2$, $p < 0.0001$). Instead, the likelihood of encountering elevated FIB at these stations was significantly higher before the PLOO was extended to its present discharge site in late 1993 (13% versus < 1%; $n = 171,966$, $\chi^2 = 15143$, $p < 0.0001$) (see Figure 3.7). The influence of rainfall on FIB is typically much more pronounced in the SBOO region, with elevated FIB significantly more likely to occur at these stations during the wet season than during the dry season (11% versus 2%, respectively, since the onset of monitoring; $n = 65783$, $\chi^2 = 1892.8$, $p < 0.0001$) (Figure 3.7). As at the shore stations, high FIB densities at the SBOO kelp stations have historically corresponded to outflows from the Tijuana River and San Antonio de Los Buenos Creek following rain events in the area (City of San Diego 2024a). Such rain-driven turbidity plumes have often been observed in satellite images of the region overlapping SBOO kelp stations with elevated FIB counts (e.g., Figure 3.8). The increasing incidence of elevated FIB at the SBOO kelp bed stations during the wet season since 2017, especially elevated in 2023, is likely related to a series of large sewage spills that originated in Tijuana before spreading through the Tijuana River Valley and eventually reaching ocean waters and moving offshore (see USIBWC 2017–2023).

Offshore stations

Of the 2640 analyses run on samples collected at offshore stations in the PLOO and SBOO over the past two years, only about 6% (n = 147) had elevated FIB, 59% of which occurred during the wet season (Table 3.5). The STV standard for *Enterococcus* at the 15 PLOO offshore stations located within State of California jurisdictional waters, where Ocean Plan water contact standards apply, ranged from 83–100% over the report period (Figure 3.9A, Table 3.2). Additionally, the 10 SBOO stations located within State of California jurisdictional waters were 97% compliant with the SSM standard for fecal coliforms (Figure 3.9B), and were 80–100% in compliance with the STV standard for *Enterococcus*, while compliance with the total coliforms STV standard ranged from 30–100% (Table 3.2).

In the PLOO region, all analyses showing elevated FIB were sampled at stations located along the 80 or 98-m depth contours and from depths of 60 m or deeper (Table 3.5). 35% of these were from stations F29, F30 and F31 located within 1000 m of the PLOO discharge site (i.e., nearfield stations). These results suggest that the PLOO wastewater plume continues to be restricted to relatively deep, offshore waters throughout the year. Additionally, there were no visual indications of wastewater at any of the 36 offshore PLOO stations based on visual observations of the surface. This conclusion is consistent with historical remote sensing observations that have provided no indication of the PLOO plume reaching surface waters (see Appendix B: Svejksky and Hess 2023, 2024).

The above findings are also consistent with historical ocean monitoring results, which revealed that < 4% of samples collected at depths of ≤ 25 m from the PLOO 98-m (i.e., discharge depth) stations had elevated levels of *Enterococcus* during the pre-chlorination years (1993–2008) (Figure 3.10). This percentage dropped to < 1% at these depths following the initiation of partial chlorination at the Point Loma Wastewater Treatment Plant (PLWTP) in 2008 (City of San Diego 2009) and was zero during the current reporting period. Overall, detection of elevated *Enterococcus* has been significantly more likely at the three nearfield stations (F29, F30, F31) than at any other 98-m site (14% versus 4%, respectively; n = 7345, $\chi^2 = 204.13$, $p < 0.0001$). The addition of chlorination significantly decreased the number of samples with elevated *Enterococcus* at these three stations (i.e., 16% before versus 10% after, n = 2371, $\chi^2 = 18.6$, $p < 0.0001$), and the other 98-m stations (6% before versus 3% after; n = 4899, $\chi^2 = 20.1$, $p < 0.0001$), though there has been an increase in elevated FIB detections at depths 60m or greater in recent years (Figure 3.10).

In the SBOO region, 6% analyses of offshore samples had elevated FIB during the two-year reporting period (Table 3.5). Historically, elevated bacterial levels were more likely at the three nearfield stations (i.e., I12, I14, I16) when compared to other SBOO 28-m (i.e., discharge depth) stations (10% versus 3%; n = 18,927, $\chi^2 = 477.25$, $p < 0.0001$) (Figure 3.11). Since the initiation of secondary treatment at the South Bay Wastewater Treatment Plant in January 2011, elevated FIB detections at nearfield station have remained low compared to such detections prior to initiation of secondary treatment (average 56 analyses showing elevated FIB per year prior to secondary versus average <4 after). However, analyses showing elevated FIB at nearfield stations have increased over the report period (2022–2023) compared to other years (2011–2021) since the onset of secondary treatment (average 9.5 analyses showing elevated FIB per year during the report period versus average 2.5 other years).

Receiving Water Bacterial Compliance

The 2022–2023 reporting period has highlighted a decline in water quality compliance throughout San Diego coastal waters in both the PLOO and SBOO regions. All bacterial compliance metrics in the SBOO region, from the shoreline to offshore, indicate a decline in compliance when compared with

the 2020–2021 reporting period. A number of factors may be influencing compliance. Precipitation, which is known to drive decreases in water quality especially at shore and kelp stations, was notably higher during the report period compared to the last report period (20.33 inches over 2022–2023 vs. 15.68 inches over 2020–2021, with 14.43 inches falling in 2023 alone). Also, since August 2022, the IBWC has increased flows from the SBIWTP to the SBOO in an effort to manage shoreline pollutants flowing from the Tijuana River which has increased SBOO flows from an average of 21 MGD to 31 MGD. Furthermore, since March 2023, primary treatment at the SBIWTP has been limited due to issues related to the function of the primary sedimentation tanks. All combined, these factors are likely driving the observed decrease in water quality at offshore stations in the SBOO region. Less dramatic declines in water quality at PLOO shore stations are likely attributable to higher precipitation during the report period. A steady decline in water quality at deep (60m or greater) depths at the stations nearest the PLOO (F29, F30, and F31) has also been observed—a gradual trend that has emerged over time since maximum compliance rates were achieved in 2013.

During the summer (i.e. dry season), there is a significant improvement in shoreline water quality compliance (Table 3.3 and 3.4), with less of a dramatic effect apparent at offshore stations (Table 3.5). Thus, rain events in the wet season are a significant driver of non-compliance region-wide, with the largest effect along the shore. However, despite this seasonal pattern, dry season non-compliance at SBOO region shore and nearshore stations occurs at rates an order of magnitude greater than dry season non-compliance in the PLOO region (Table 3.3). Therefore, although the impact of rain events on shoreline water quality is clear region wide, there remains an additional significant driver of dry weather non-compliance in the South Bay. This observation is likely explained by the northward transport of contaminated water, particularly from undertreated and untreated wastewater which discharges into the Pacific Ocean via San Antonio de los Buenos Creek, by the shallow southern swell, which is known to be strongest along the San Diego coast in the summertime (Fedderson et al. 2021, Bray et al. 1999).

Despite the factors highlighted above, compliance with receiving water limitations for bacterial characteristics (Box 3.2) in the PLOO region were above the minimum threshold for all metrics (for each parameter) throughout the report period (Table 3.6). Whereas the nearshore in the SBOO region continues to show water quality impacts, as has been reported in the past, with overall compliance below the minimum threshold (i.e. 90%) for fecal coliforms on 372 of the 730 days (51% days out of compliance) in the report period, 365 days (50%) for *Enterococcus*, and on all of the 730 days (100%) in the report period for total coliforms (Table 3.6). Stations with the highest occurrence of elevated FIB were shore and nearshore stations located close to the mouth of the Tijuana River Estuary. Furthermore, compliance with the kelp station metric was below the minimum threshold for fecal coliforms and *Enterococcus* at station I19, I24, and I40 on one or more days in the report period, and at I19, I24, I25, I26, I32, and I40 for total coliforms (Table 3.6). Compliance with the offshore station metric in the SBOO region was above the minimum threshold for both fecal coliforms and *Enterococcus* throughout the report period, while the standard for total coliforms was out of compliance at station I16 on one or more days in the report period (Table 3.6).

SUMMARY

Compliance with all standards for FIB was typically higher at the PLOO and SBOO kelp beds, and other offshore stations, compared to the shore stations, and tended to be higher at PLOO stations than at the SBOO stations. Reduced compliance at shore stations, in both regions, tended to occur during

the wet season. Historically, elevated FIB along the shore, or at the kelp bed stations, has typically been associated with storm activity (rain), heavy recreational use, the presence of seabirds, and decaying kelp or surfgrass (see City of San Diego 2024a). Exceptions to the above patterns have occurred over the years due to specific events. For example, elevated bacteria observed at the PLOO shore and kelp stations in 1992 followed a catastrophic rupture of the outfall that occurred within the Point Loma kelp forest (Tegner et al. 1995). A more frequent source of known contamination in the SBOO region has been cross-border transportation of sewage that originates from spills in Tijuana, Mexico such as the 25 billion gallon spill that occurred starting in December 2022 (USIBWC 2017–2023).

The spatial and temporal distribution of elevated FIB observed during the current report period corroborate the findings of previous City reports and other studies, which suggest that the Tijuana River and other terrestrial inputs are the largest drivers of contamination in the South Bay region (Svejkovsky and Jones 2001, Noble et al. 2003, Gersberg et al. 2004, 2006, 2008, Largier et al. 2004, Terrill et al. 2009, Svejkovsky and Hess 2022). For example, coastal runoff from rivers and creeks were more likely to impact coastal water quality than wastewater discharge from the outfall, especially during and immediately after significant rain events (Svejkovsky and Jones 2001, Terrill et al. 2009). Shore stations located near the mouths of the Tijuana River and in Mexican waters near San Antonio de Los Buenos Creek have historically had higher numbers of elevated FIB samples than stations located farther to the north. It is also well established that sewage-laden discharges from the Tijuana River and San Antonio de Los Buenos Creek are likely sources of bacteria during or after storms or other periods of increased flows (Svejkovsky and Jones 2001, Noble et al. 2003, Gersberg et al. 2004, 2006, 2008, Largier et al. 2004, Terrill et al. 2009, Svejkovsky and Hess 2024). Further, the general relationship between rainfall levels and elevated FIB densities in the SBOO region existed before wastewater discharge began in 1999 (City of San Diego 2000). The occurrence of samples with elevated FIB near the outfall remain low compared to that of samples taken before the initiation of secondary treatment, which began in January 2011 at the South Bay International Treatment Plant. A moderate increase in the occurrence of such samples during the report period coincides with measures adopted by the IBWC to mitigate the continued spilling of contaminated outflows to the Tijuana River Estuary by routing some flows through the South Bay ITP. The majority of analyses showing elevated FIB continue to be associated with stations near the mouth of the Tijuana River Estuary and they continue to be more prevalent in the wet season. As a result, we conclude that non-compliance with receiving water limitations for bacterial characteristics is primarily driven by known contaminated outflows from the Tijuana River Estuary and other non-point source runoff.

LITERATURE CITED

- [APHA] American Public Health Association. (2012). *Standard Methods for the Examination of Water and Wastewater*, 22nd edition. E.W. Rice, R. Baird, A. Eaton and L. Clesceri (eds.). American Public Health Association, American Water Works Association, and Water Pollution Control Federation.
- Bordner, R., J. Winter, and P. Scarpino, eds. (1978). *Microbiological Methods for Monitoring the Environment: Water and Wastes*, EPA Research and Development, EPA-600/8-78-017.
- Bray, N.A., A. Keyes, and W. M. L. Morawitz. (1999). The California Current system in the Southern California Bight and the Santa Barbara Channel. *Journal of Geophysical Research*, 104: 7695-7714.

- City of San Diego. (2000). International Wastewater Treatment Plant Final Baseline Ocean Monitoring Report for the South Bay Ocean Outfall (1995–1998). City of San Diego Ocean Monitoring Program, Metropolitan Wastewater Department, Environmental Monitoring and Technical Services Division, San Diego, CA.
- City of San Diego. (2022). Biennial Receiving Waters Monitoring and Assessment Report for the Point Loma and South Bay Ocean Outfalls, 2020–2021. City of San Diego Ocean Monitoring Program, Public Utilities Department, Environmental Monitoring and Technical Services Division, San Diego, CA.
- City of San Diego. (2022–2024). Monthly Receiving Waters Monitoring Reports for the South Bay Ocean Outfall (South Bay Water Reclamation Plant), January 2022–December 2023. City of San Diego Ocean Monitoring Program, Public Utilities Department, Environmental Monitoring and Technical Services Division, San Diego, CA.
- City of San Diego. (2023a). Annual Receiving Waters Monitoring and Toxicity Testing Quality Assurance Report, 2022. City of San Diego Ocean Monitoring Program, Public Utilities Department, Environmental Monitoring and Technical Services Division, San Diego, CA.
- City of San Diego. (2023b). Interim Receiving Waters Monitoring Report for the Point Loma Ocean Outfall and South Bay Ocean Outfalls, 2022. City of San Diego Ocean Monitoring Program, Public Utilities Department, Environmental Monitoring and Technical Services Division, San Diego, CA.
- City of San Diego. (2024a). Ocean Monitoring Reports. <https://www.sandiego.gov/public-utilities/sustainability/ocean-monitoring/reports>
- City of San Diego. (2024b). Annual Receiving Waters Monitoring and Toxicity Testing Quality Assurance Report, 2023. City of San Diego Ocean Monitoring Program, Public Utilities Department, Environmental Monitoring and Technical Services Division, San Diego, CA.
- Feddersen, F., Boehm, A. B., Giddings, S. N., Wu, X., & Liden, D. (2021). Modeling untreated wastewater evolution and swimmer illness for four wastewater infrastructure scenarios in the San Diego-Tijuana (US/MX) border region. *Geo Health*, 5, 1-20.
- Gersberg, R.M., D. Daft, and D. Yorkey. (2004). Temporal pattern of toxicity in runoff from the Tijuana River Watershed. *Water Research*, 38: 559–568.
- Gersberg, R.M., M.A. Rose, R. Robles-Sikisaka, and A.K. Dhar. (2006). Quantitative detection of hepatitis a virus and enteroviruses near the United States-Mexico Border and correlation with levels of fecal indicator bacteria. *Applied and Environmental Microbiology*, 72: 7438–7444.
- Gersberg, R., J. Tiedge, D. Gottstein, S. Altmann, K. Watanabe, and V. Luderitz. (2008). Effects of the South Bay Ocean Outfall (SBOO) on beach water quality near the USA-Mexico border. *International Journal of Environmental Health Research*, 18: 149–158.
- Gohel D, Skintzos P (2024). flextable: Functions for Tabular Reporting. R package version 0.9.5, <https://davidgohel.github.io/flextable/>, <https://ardata-fr.github.io/flextable-book/>.

- Grant, S.B., B.F. Sanders, A. Boehm, J. Redman, R. Kim, A. Chu, M. Gouldin, C. McGee, N. Gardiner, B. Jones, J. Svejksky, and G. Leipzig. (2001). Generation of enterococci bacteria in a coastal saltwater marsh and its impact on surf zone water quality. *Environmental Science Technology*, 35: 2407–2416.
- Griffith, J., K.C. Schiff, G. Lyon, and J. Fuhrman. (2010). Microbiological water quality at non-human influenced reference beaches in southern California during wet weather. *Marine Pollution Bulletin*, 60: 500–508.
- Gruber, S., L. Aumand, and A. Martin. (2005). Sediments as a reservoir of indicator bacteria in a coastal embayment: Mission Bay, California, Technical paper 0506. Weston Solutions, Inc. Presented at StormCon 2005. Orlando, FL, USA. July 2005.
- Harrell, F.E. Jr, C. Dupont et al. (2015). Hmisc: Harrell Miscellaneous. R package version 3.17-0. <http://CRAN.R-project.org/package=Hmisc>.
- Kassambara, A. (2019). ggpubr: 'ggplot2' Based Publication Ready Plots. R package version 0.2.4. <https://CRAN.R-project.org/package=ggpubr>.
- Koenker, R. (2019). quantreg: Quantile Regression. R package version 5.52. <https://CRAN.R-project.org/package=quantreg>.
- Largier, J., L. Rasmussen, M. Carter, and C. Scarce. (2004). Consent Decree – Phase One Study Final Report. Evaluation of the South Bay International Wastewater Treatment Plant Receiving Water Quality Monitoring Program to Determine Its Ability to Identify Source(s) of Recorded Bacterial Exceedances. Scripps Institution of Oceanography, University of California, San Diego, CA.
- Martin, A., and S. Gruber. (2005). Amplification of indicator bacteria in organic debris on southern California beaches. Technical Paper 0507. Weston Solutions, Inc. Presented at StormCon 2005. Orlando, FL, USA. July 2005.
- Nezlin, N.P., P.M. DiGiacomo, S.B. Weisberg, D.W. Diehl, J.A. Warrick, M.J. Mengel, B.H. Jones, K.M. Reifel, S.C. Johnson, J.C. Ohlmann, L. Washburn, and E.J. Terrill. (2007). Southern California Bight 2003 Regional Monitoring Program: V. Water Quality. Southern California Coastal Water Research Project. Costa Mesa, CA.
- [NOAA] National Oceanic and Atmospheric Administration. (2024). National Climatic Data Center. <https://www.ncdc.noaa.gov/cdo-web/datatools>
- Noble, R.T., D.F. Moore, M.K. Leecaster, C.D. McGee, and S.B. Weisberg. (2003). Comparison of total coliform, fecal coliform, and *Enterococcus* bacterial indicator response for ocean recreational water quality testing. *Water Research*, 37: 1637–1643.
- Noble, M.A., J.P. Xu, G.L. Robertson, and K.L. Rosenfeld. (2006). Distribution and sources of surfzone bacteria at Huntington Beach before and after disinfection of an ocean outfall—A frequency-domain analysis. *Marine Environmental Research*, 61: 494–510.

- Phillips, C.P., H.M. Solo-Gabriele, A.J. Reneiers, J.D. Wang, R.T. Kiger, and N. Abdel-Mottaleb. (2011). Pore water transport of enterococci out of beach sediments. *Marine Pollution Bulletin*, 62: 2293–2298.
- R Core Team. (2019). R: A language and environment for statistical computing. R Foundation for Statistical Computing, Vienna, Austria. URL <https://www.R-project.org/>.
- Reeves, R.L., S.B. Grant, R.D. Mrse, C.M. Copil Oancea, B.F. Sanders, and A.B. Boehm. (2004). Scaling and management of fecal indicator bacteria in runoff from a coastal urban watershed in southern California. *Environmental Science and Technology*, 38: 2637–2648.
- Revelle, W. (2015). psych: Procedures for Personality and Psychological Research, Northwestern University, Evanston, Illinois, USA, <http://CRAN.R-project.org/package=psych> version 1.5.8.
- Ripley, B. and M. Lapsley. (2017). RODBC: ODBC Database Access. R package version 1.3-12. <http://CRAN.R-project.org/package=RODBC>.
- Schauberger, P and A. Walker (2019). openxlsx: Read, Write and Edit xlsx Files. R package version 4.1.4. <https://CRAN.R-project.org/package=openxlsx>.
- Sercu, B., L.C. Van de Werfhorst, J. Murray, and P.A. Holden. (2009). Storm drains are sources of human fecal pollution during dry weather in three urban southern California watersheds. *Environmental Science and Technology*, 43: 293–298.
- State of California. (2010). Integrated Report (Clean Water Act Section 303(d) List/305(b) Report). http://www.waterboards.ca.gov/water_issues/programs/tmdl/integrated2010.shtml.
- Svejkovsky, J. and B. Jones. (2001). Detection of coastal urban storm water and sewage runoff with synthetic aperture radar satellite imagery. *Eos, Transactions, American Geophysical Union*, 82, 621–630.
- Svejkovsky, J. and Hess, M. (2023). Satellite & Aerial Coastal Water Quality Monitoring in the San Diego/Tijuana Region: Annual Summary Report: 1 January 2022 – 31 December 2022. Littleton, CO.
- Svejkovsky, J. and Hess, M. (2024). Satellite & Aerial Coastal Water Quality Monitoring in the San Diego/Tijuana Region: Annual Summary Report: 1 January 2023 – 31 December 2023. Littleton, CO.
- [SWRCB] California State Water Resources Control Board. (2019). California Ocean Plan, Water Quality Control Plan, Ocean Waters of California. California Environmental Protection Agency, Sacramento, CA.
- Tegner, M.J., P.K. Dayton, P.B. Edwards, K.L. Riser, D.B. Chadwick, T.A. Dean, and L. Deysher. (1995). Effects of a large sewage spill on a kelp forest community: Catastrophe or disturbance? *Marine Environmental Research*, 40: 181–224.

- Terrill, E., K. Sung Yong, L. Hazard, and M. Otero. (2009). IBWC/Surfrider – Consent Decree Final Report. Coastal Observations and Monitoring in South Bay San Diego. Scripps Institution of Oceanography, University of California, San Diego, CA.
- [USEPA] United States Environmental Protection Agency. (2014). Method 1600: Enterococci in Water by Membrane Filtration Using membrane-Enterococcus Indoxyl- β -D-Glucoside Agar (mEI). EPA Document EPA-821-R-14-011. Office of Water (4303T), Washington, DC.
- [USIBWC] United States International Boundary Water Commission (2022–2023). Executive Officer's Reports. https://www.waterboards.ca.gov/sandiego/publications_forms/publications/eoreports.html
- Warnes, G., B. Bolker, and T. Lumley. (2015). gtools: Various R Programming Tools. R package version 3.5.0. <http://CRAN.R-project.org/package=gtools>.
- Wickham, H. (2007). Reshaping Data with the reshape Package. *Journal of Statistical Software*, 21(12), 1-20. URL <http://www.jstatsoft.org/v21/i12/>.
- Wickham, H. (2017). tidyverse: Easily Install and Load the 'Tidyverse'. R package version 1.2.1. <https://CRAN.R-project.org/package=tidyverse>.
- Yamahara, K.M., B.A. Layton, A.E. Santoro, and A.B. Boehm. (2007). Beach sands along the California coast are diffuse sources of fecal bacteria to coastal waters. *Environmental Science and Technology*, 41: 4515–4521.

CHAPTER 3

FIGURES & TABLES

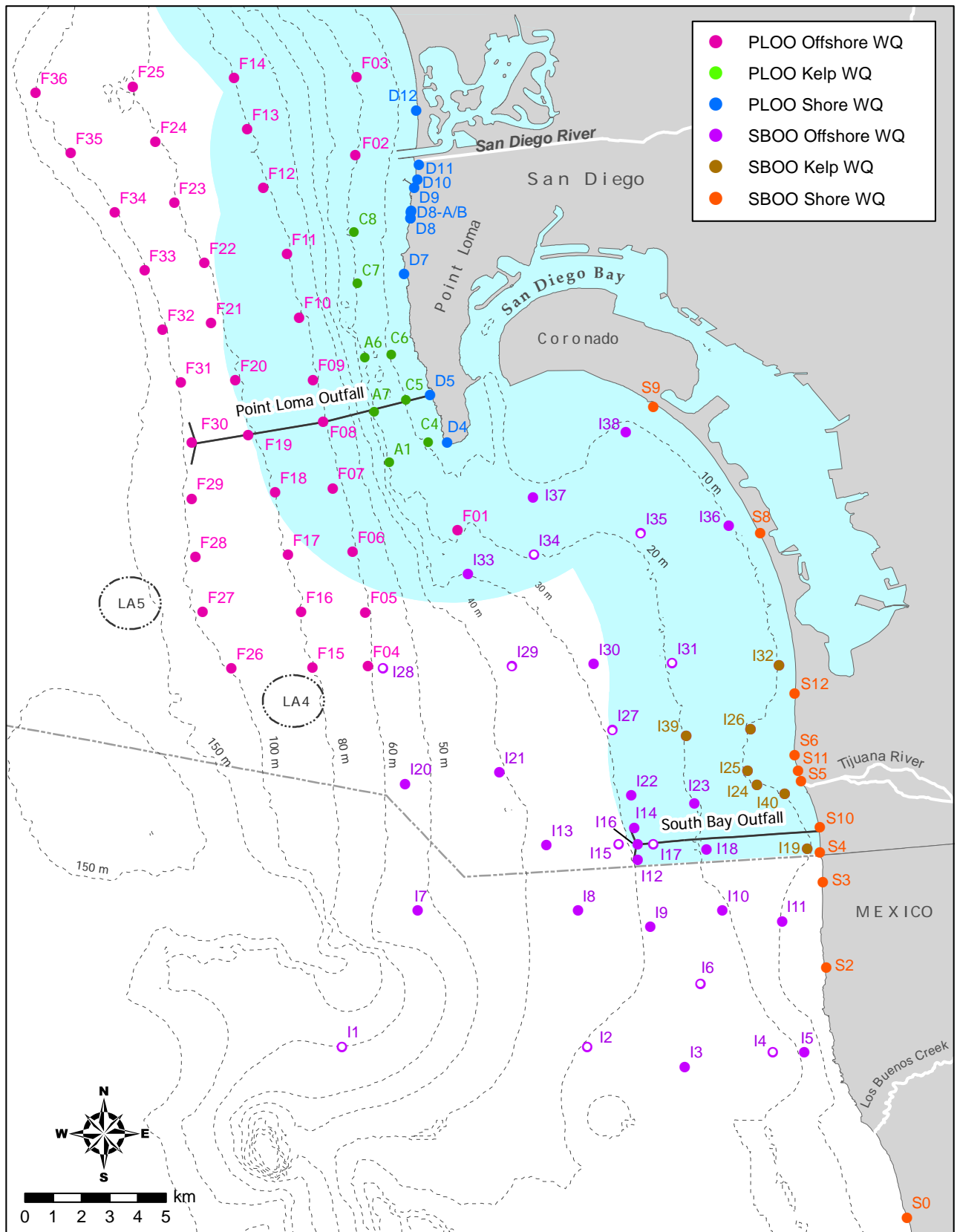


Figure 3.1

Water quality (WQ) monitoring station locations sampled around the PLOO and SBOO as part of the City of San Diego's Ocean Monitoring Program. Open circles are sampled by CTD only. Light blue shading represents State jurisdictional waters.

Box 3.1

Water quality objectives for water contact areas, California Ocean Plan (SWRCB 2019).

- A. Bacterial Characteristics – Water Contact Standards; CFU = colony forming units.
 - (a) *Fecal Coliforms*:
 - 1) A 30-day geometric mean of fecal coliform density shall not exceed 200 CFU/100 mL, calculated based on the five most recent samples from each site
 - 2) A single sample maximum of fecal coliform density shall not exceed 400 CFU/100 mL.
 - (b) *Enterococcus*:
 - 1) A 42-day geometric mean of *Enterococcus* density shall not exceed 30 CFU/100 mL, calculated weekly
 - 2) A statistical threshold value of *Enterococcus* density shall not exceed 110 CFU/100 mL in more than 10% of samples per calendar month.
 - (c) *Total Coliforms*:
 - 1) The median of total coliform density shall not exceed 70 CFU/100 mL*.
 - 2) A statistical threshold value of total coliform density shall not exceed 230 CFU/100 mL in more than 10% of samples.
- B. Physical Characteristics
 - (a) Floating particulates and oil and grease shall not be visible.
 - (b) The discharge of waste shall not cause aesthetically undesirable discoloration of the ocean surface.
 - (c) Natural light shall not be significantly reduced at any point outside of the initial dilution zone as the result of the discharge of waste.
- C. Chemical Characteristics
 - (a) The dissolved oxygen concentration shall not at any time be depressed more than 10% from what occurs naturally, as a result of the discharge of oxygen demanding waste materials.
 - (b) The pH shall not be changed at any time more than 0.2 units from that which occurs naturally.
- D. A time period is not specified for the total coliforms running median calculation. For the purposes of this report, the median was calculated over a 30-day running window,

Table 3.1

Depths from which seawater samples are collected for bacteriological analysis from kelp and offshore stations.

Station Contour	PLOO Sample Depth (m)									Station Contour	SBOO Sample Depth (m)							
	1	3	9	12	18	25	60	80	98		2	6	9/11	12	18	27	37	55
<i>Kelp Bed</i>										<i>Kelp Bed</i>								
9-m	x	x	x							9-m	x	x	x ^a					
18-m	x			x	x					18-m	x			x	x			
<i>Offshore</i>										<i>Offshore</i>								
18-m	x			x	x					9-m	x	x	x ^a					
60-m	x					x	x			18-m	x			x	x			
80-m	x					x	x	x		28-m	x			x	x			
98-m	x					x	x	x	x	38-m	x			x			x	
										55-m	x			x				x

^aStations I25, I26, I32, and I40 sampled at 9 m; stations I11, I19, I24, I36, I37, and I38 sampled at 11 m

Box 3.2

Receiving Water Bacterial Compliance (NPDES Permit No. CA0109045, Order No. R9-2021-0011; NPDES Permit No. CA0108928, Order No. R9-2021-0001).

Receiving water monitoring for human marker HF183 and effluent monitoring for fecal indicator bacteria may be required if any of the following conditions are true, and if the source of contamination is unknown.

- A. The overall compliance rate with the receiving water limitations for bacterial characteristics is below 90% within a rolling one-year period.
- B. A single monitoring location exceeds the bacteria receiving water limitations more than 50% of the time within a rolling one-year period for offshore monitoring locations.
- C. A single monitoring location exceeds the bacteria receiving water limitations more than 50% of the time within a rolling quarterly period for kelp/nearshore monitoring locations.

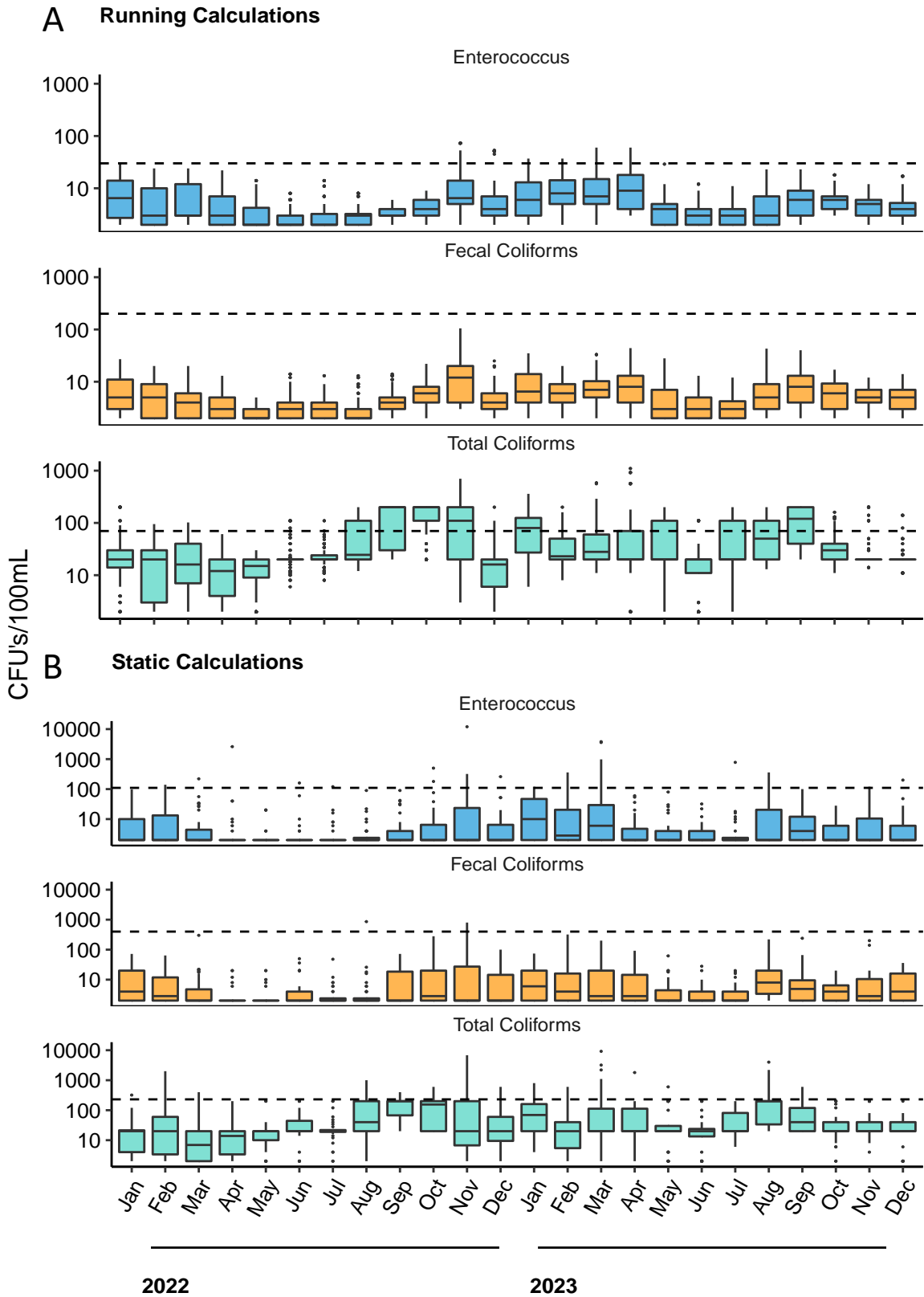


Figure 3.2

Distribution of values at PLOO shore stations during 2022 and 2023, binned monthly, for (A) running mean and median calculations and (B) single sample values. Dashed line represents the water contact standard compliance threshold*. Boxes=median, upper and lower quartiles; whiskers=1.5x interquartile range, dots=outliers. *STV compliance is calculated separately and shown in Table 3.2.

Table 3.2

Percent compliance with STV standards across all months in the reporting period, binned by year and region.

<i>Enterococcus</i>														
Year	Project		Jan	Feb	Mar	Apr	May	Jun	Jul	Aug	Sep	Oct	Nov	Dec
2022	PLOO	Shore	100	88	88	88	100	88	88	100	100	75	38	88
		Kelp	100	100	100	100	100	100	100	100	100	100	100	100
		Offshr	—	83	—	—	92	—	—	100	—	—	92	—
	SBOO	Shore	38	25	38	62	88	100	75	50	50	88	50	25
		Kelp	43	86	43	86	71	100	100	100	71	100	71	0
		Offshr	—	100	—	—	100	—	—	80	—	—	90	—
2023	PLOO	Shore	75	88	25	100	100	100	88	88	100	100	88	88
		Kelp	100	100	100	100	100	100	100	100	100	100	100	100
		Offshr	—	—	92	—	83	—	—	92	—	—	100	—
	SBOO	Shore	0	25	12	25	25	25	62	0	12	25	38	38
		Kelp	0	14	17	57	71	71	100	71	86	71	43	43
		Offshr	—	90	—	—	90	—	—	100	—	—	100	—
<i>Total Coliforms</i>														
Year	Project		Jan	Feb	Mar	Apr	May	Jun	Jul	Aug	Sep	Oct	Nov	Dec
2022	PLOO	Shore	88	88	88	100	100	100	100	88	88	75	25	62
		Kelp	100	100	100	100	100	100	100	100	100	100	100	88
		Offshr	—	100	—	—	90	—	—	80	—	—	90	—
	SBOO	Shore	25	25	25	38	38	100	50	50	38	38	38	25
		Kelp	0	0	14	57	14	57	83	43	14	0	43	14
		Offshr	—	100	—	—	90	—	—	80	—	—	90	—
2023	PLOO	Shore	62	75	25	88	88	100	100	50	88	100	100	100
		Kelp	100	100	88	50	100	100	100	50	100	100	100	100
	SBOO	Shore	0	12	0	12	0	25	38	0	0	25	25	25
		Kelp	0	0	0	0	57	57	100	0	71	29	14	43
		Offshr	—	30	—	—	80	—	—	80	—	—	90	—

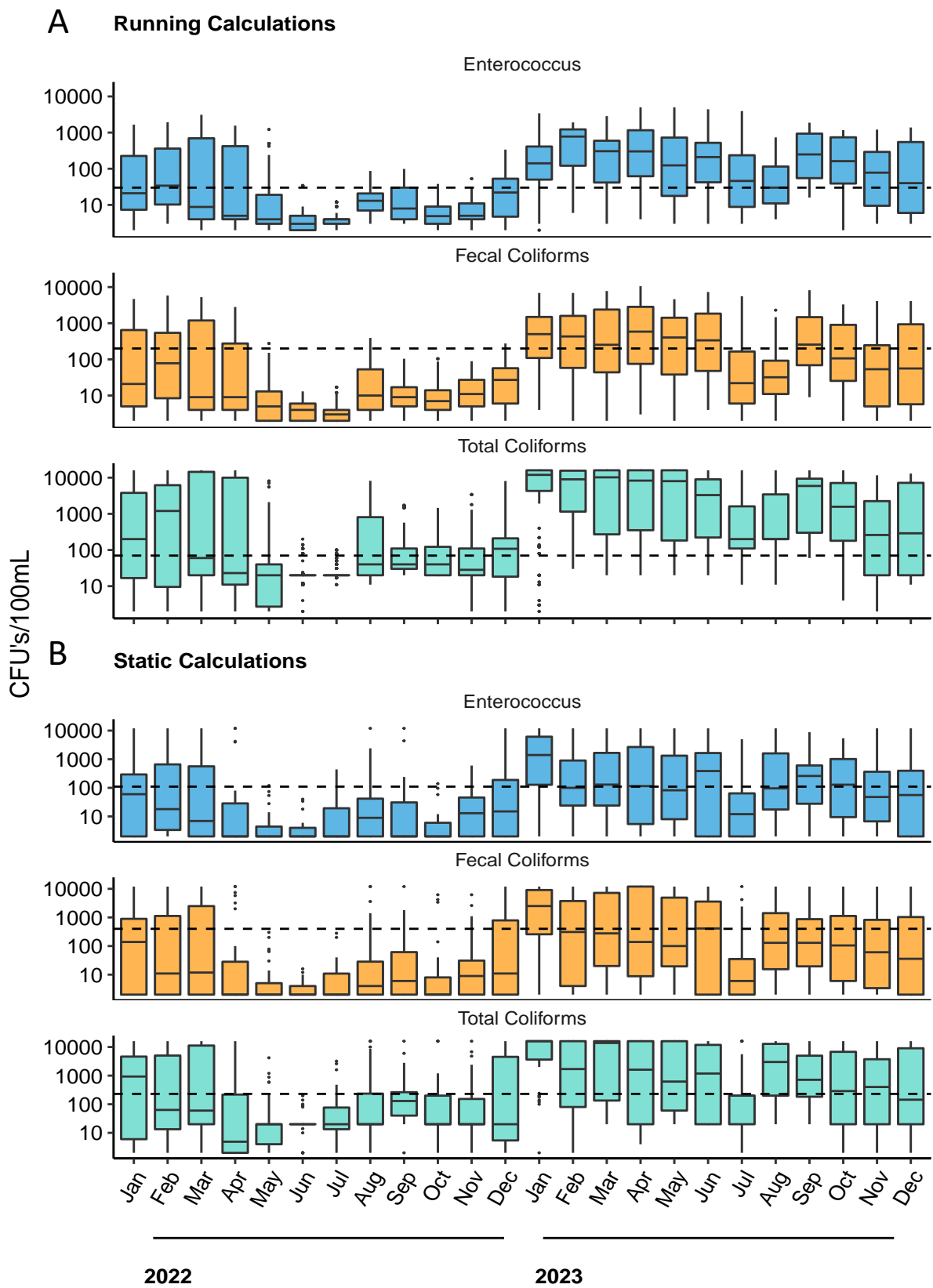


Figure 3.3

Distribution of values at SBOO shore stations during 2022 and 2023, binned monthly, for (A) running mean and median calculations and (B) single sample values. Dashed line represents the water contact standard compliance threshold*. Boxes=median, upper and lower quartiles; whiskers=1.5x interquartile range, dots=outliers. *STV compliance is calculated separately and shown in Table 3.2.

Table 3.3

Number of analyses showing elevated FIB (eFIB) collected from shore stations during wet and dry seasons, and percent occurring in the wet season (% wet) during 2022 and 2023. Stations are listed north to south from top to bottom. Stations not listed had no analyses showing elevated FIB during the report period.

	Seasons		% Wet
	Wet	Dry	
PLOO			
D12	2	0	100
D11	16	4	80
D10	7	2	78
D9	7	1	88
D8-B	14	4	78
D7	4	2	67
D5	5	0	100
Total eFIB	55	13	81
Total Analyses	1,440	1,056	58
SBOO			
S9	5	5	50
S8	16	10	62
S12	47	37	56
S6	74	49	60
S11	86	55	61
S5	127	72	64
S10	112	32	78
S4	108	31	78
S3	97	47	67
S2	92	40	70
S0	147	114	56
Total eFIB	911	492	65
Total Analyses	1,956	1,443	58

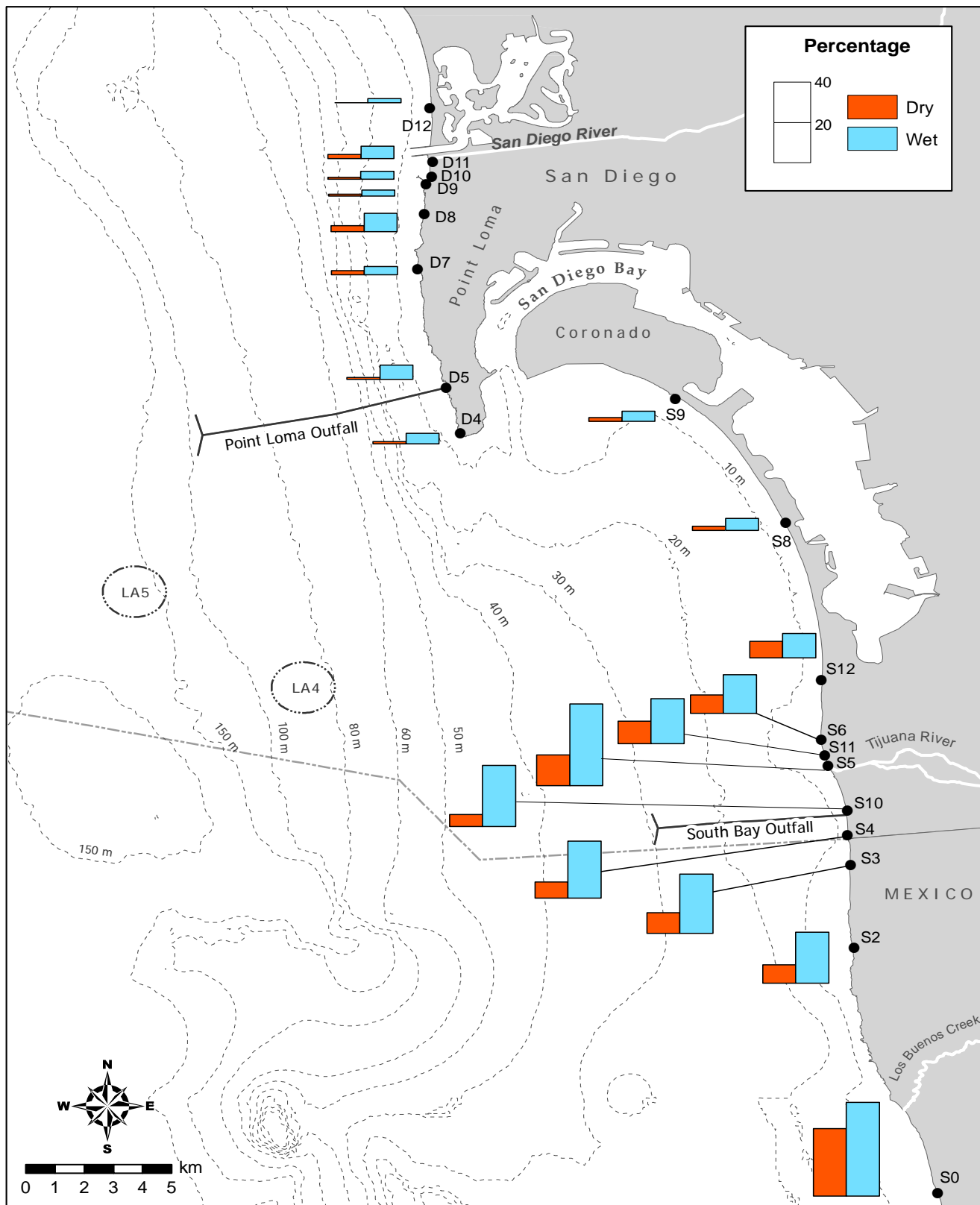


Figure 3.4

Percentage of samples with elevated FIB densities in wet versus dry seasons at shore stations from 1991 through 2023. Shore sampling in the SBOO region began in 1995.

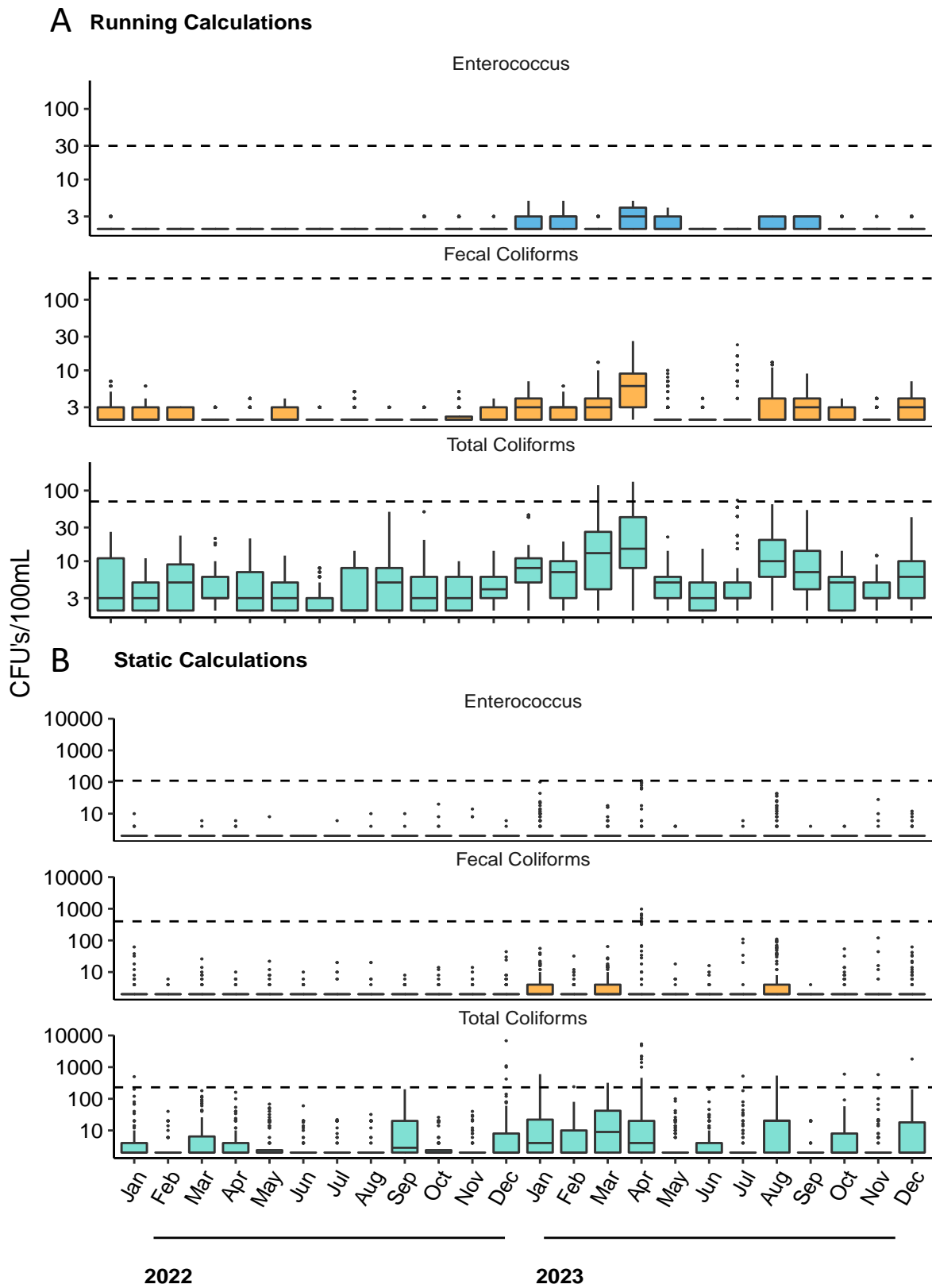


Figure 3.5

Distribution of values at PLOO kelp stations during 2022 and 2023, binned monthly, for (A) running mean and median calculations and (B) single sample values. Dashed line represents the water contact standard compliance threshold*. Boxes=median, upper and lower quantiles; whiskers=1.5x interquartile range, dots=outliers. *STV compliance is calculated separately and shown in Table 3.2.

A Running Calculations

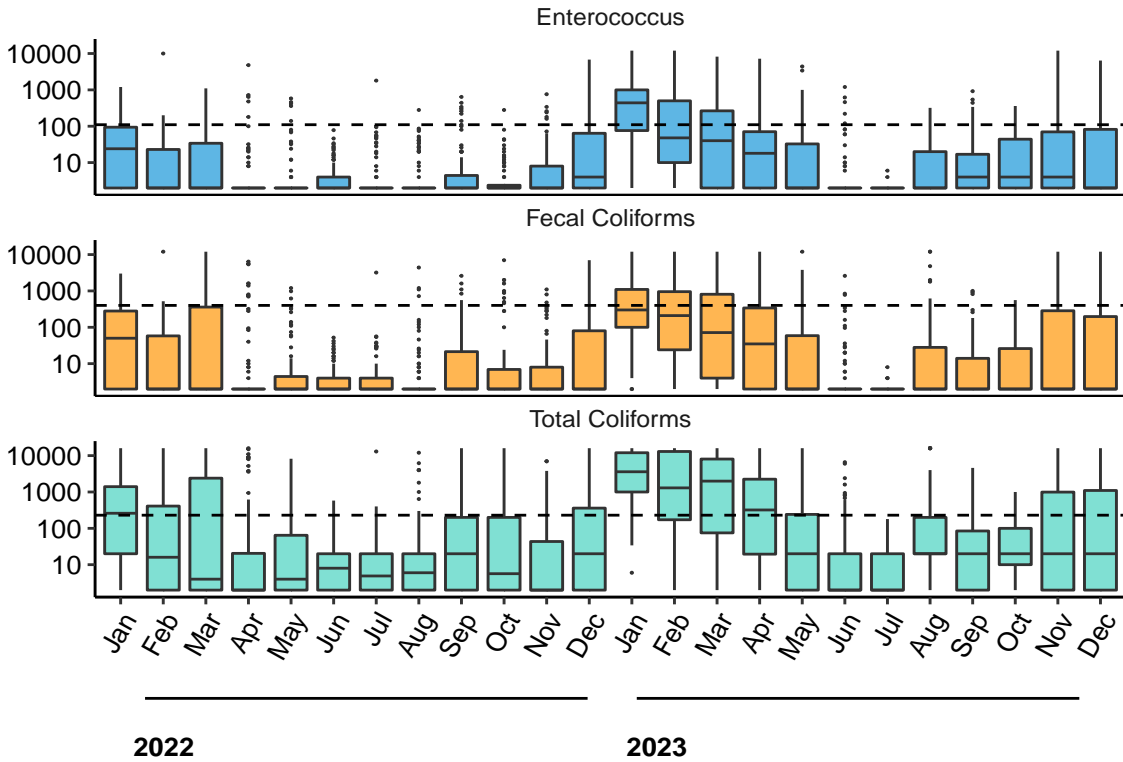
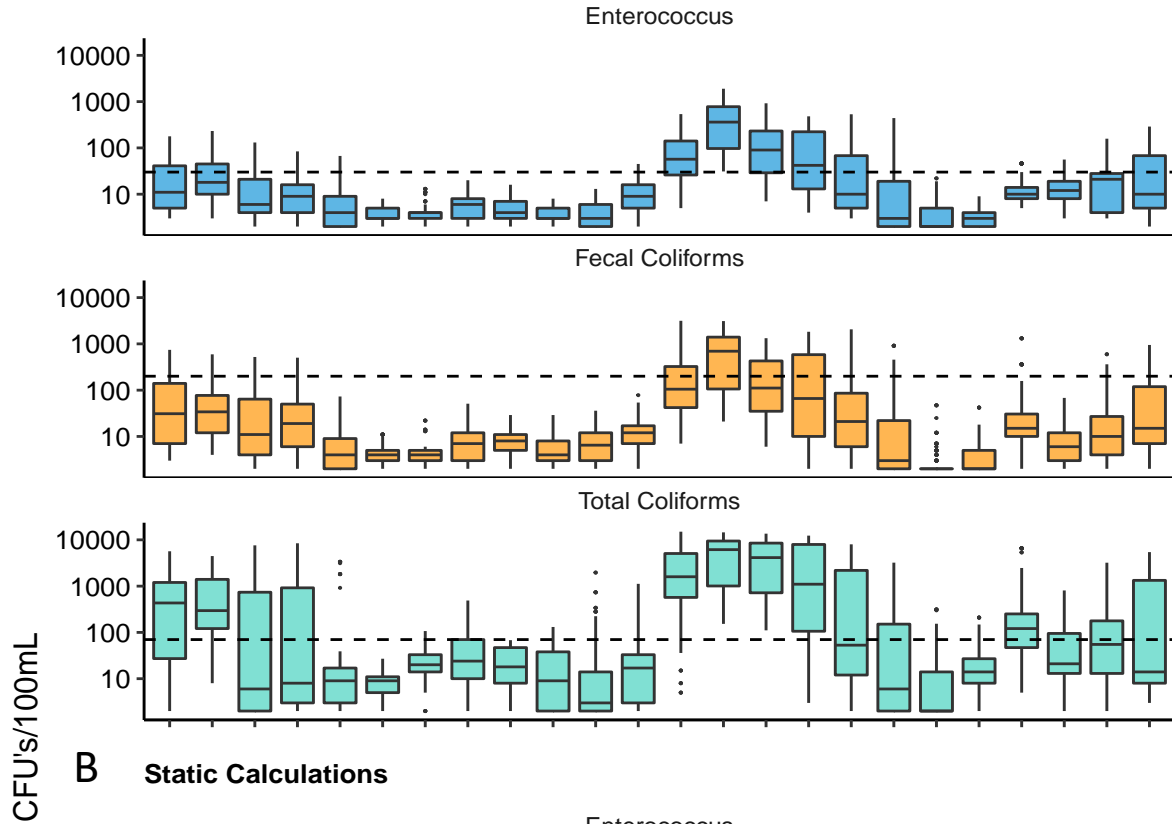


Figure 3.6

Distribution of values at SBOO kelp stations during 2022 and 2023, binned monthly, for (A) running mean and median calculations and (B) single sample values. Dashed line represents the water contact standard compliance threshold*. Boxes=median, upper and lower quartiles; whiskers=1.5x interquartile range, dots=outliers. *STV compliance is calculated separately and shown in Table 3.2.

Table 3.4

Number of analyses showing elevated FIB (eFIB) collected from kelp stations during wet and dry seasons, and percent occurring in the wet season (% wet) during 2022 and 2023. Within each contour stations are listed from north to south. Stations not listed had no analyses showing elevated FIB during the report period.

	Seasons		
	Wet	Dry	% Wet
PLOO			
<i>9-m Depth Contour</i>			
C6	1	0	100
C5	2	1	67
C4	3	0	100
<i>18-m Depth Contour</i>			
C8	3	2	60
C7	4	0	100
A6	1	3	25
A7	7	3	70
A1	11	3	79
Total eFIB	32	12	73
Total Analyses	4,320	3,168	58
SBOO			
<i>9-m Depth Contour</i>			
I32	78	46	63
I26	87	15	85
I25	143	19	88
I24	175	19	90
I40	263	53	83
I19	238	49	83
<i>18-m Depth Contour</i>			
I39	36	10	78
Total eFIB	1,020	211	83
Total Analyses	3,795	2,772	58

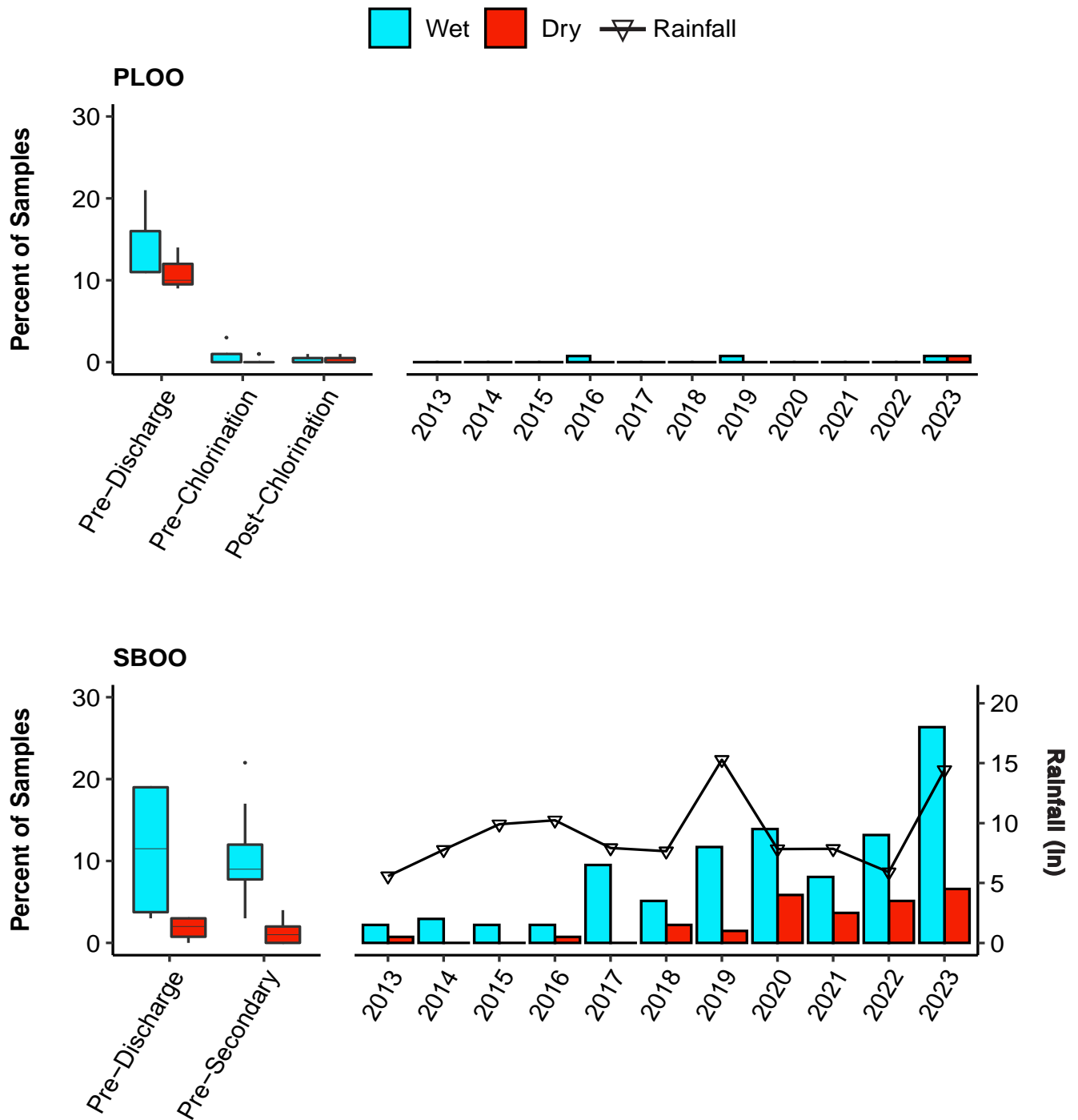


Figure 3.7

Comparison of annual rainfall with occurrence of elevated FIB densities in wet (blue bars) versus dry (red bars) seasons at PLOO and SBOO keep stations over the last decade. Boxed data show the distribution of % exceedances for each season over monitoring periods pre-dating the last decade. For PLOO, the Pre-Discharge period spanned from 1991 until the extension of the outfall to its current location in 1993. Chlorination of PLOO effluent began in 2008. For SBOO, Pre-Discharge data were collected in 1999, and secondary treatment began in 2011. Rain data are from Lindberg Field, San Diego, CA.

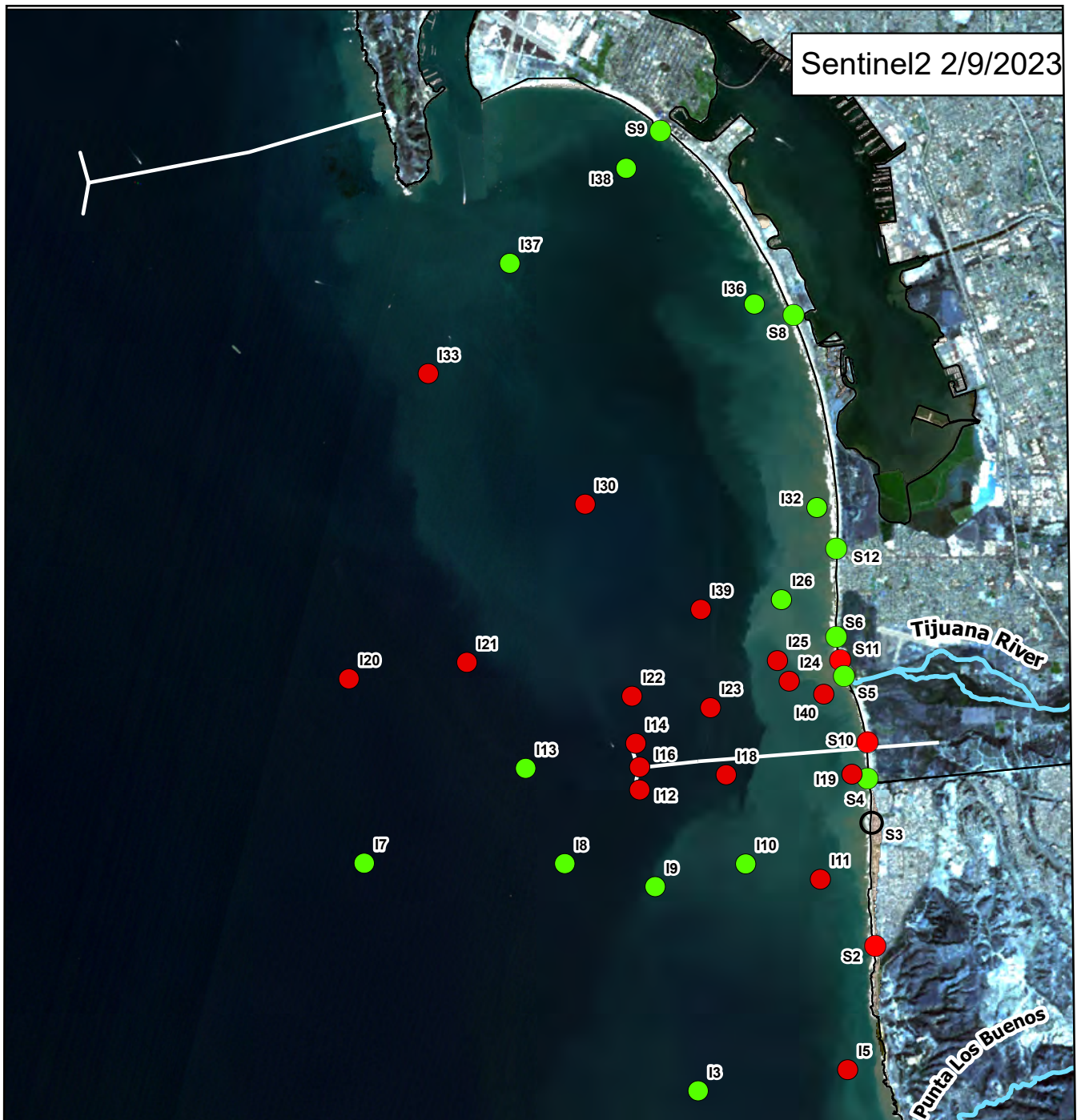


Figure 3.8

Sentinel 2 satellite image showing the SBOO regions on February 9th, 2023 (Ocean Imaging 2023) combined with bacteria levels sampled at shore, kelp, and offshore stations sampled between February 6th and 10th. Green circles indicate FIB met and red circles indicate at least one analysis with elevated FIB relative to 2019 OceanPlan thresholds. Station S0 is excluded as it lies outside the southern boundary of the image. The sample from station S3 during this time period was not analyzed due to contamination. Turbid waters follow heavy rains in mid January and a coincident >25 billion gallon transboundary flow from the Tijuana River main Channel that started on December 28th, 2022 and was ongoing at least through January 31st, 2023 (IBWC 2021).

Table 3.5

Number of analyses showing elevated FIB (eFIB) collected from offshore stations during wet and dry seasons, and percent occurring in the wet season (% wet) during 2022 and 2023. Within each contour stations are listed from north to south. Stations not listed had no analyses showing elevated FIB during the report period.

	Seasons		
	Wet	Dry	% Wet
PLOO			
<i>80-m Depth Contour</i>			
F25	0	1	0
F23	1	1	50
F22	1	2	33
F21	2	3	40
F20	1	3	25
F19	3	1	75
F17	0	1	0
<i>100-m Depth Contour</i>			
F36	1	0	100
F35	2	0	100
F34	1	0	100
F33	3	0	100
F32	4	1	80
F31	3	0	100
F30 *	5	8	38
F29 *	2	3	40
F28 *	2	1	67
F27	0	2	0
F26	1	1	50
Total eFIB	32	28	53
Total Analyses	564	564	50
SBOO			
<i>9-m Depth Contour</i>			
I38	0	4	0
I36	0	2	0
I11	14	2	88
I5	11	10	52
<i>18-m Depth Contour</i>			
I23	4	0	100
I18	7	0	100
I10	4	1	80
<i>28-m Depth Contour</i>			
I33	2	0	100
I30	1	0	100
I22	1	0	100
I14 *	1	0	100
I16 *	6	5	55
I12 *	1	6	14
<i>38-m Depth Contour</i>			
I21	1	0	100
<i>55-m Depth Contour</i>			
I20	2	1	67
I7	0	1	0
Total eFIB	55	32	63
Total Analyses	756	756	50

* Nearfield station

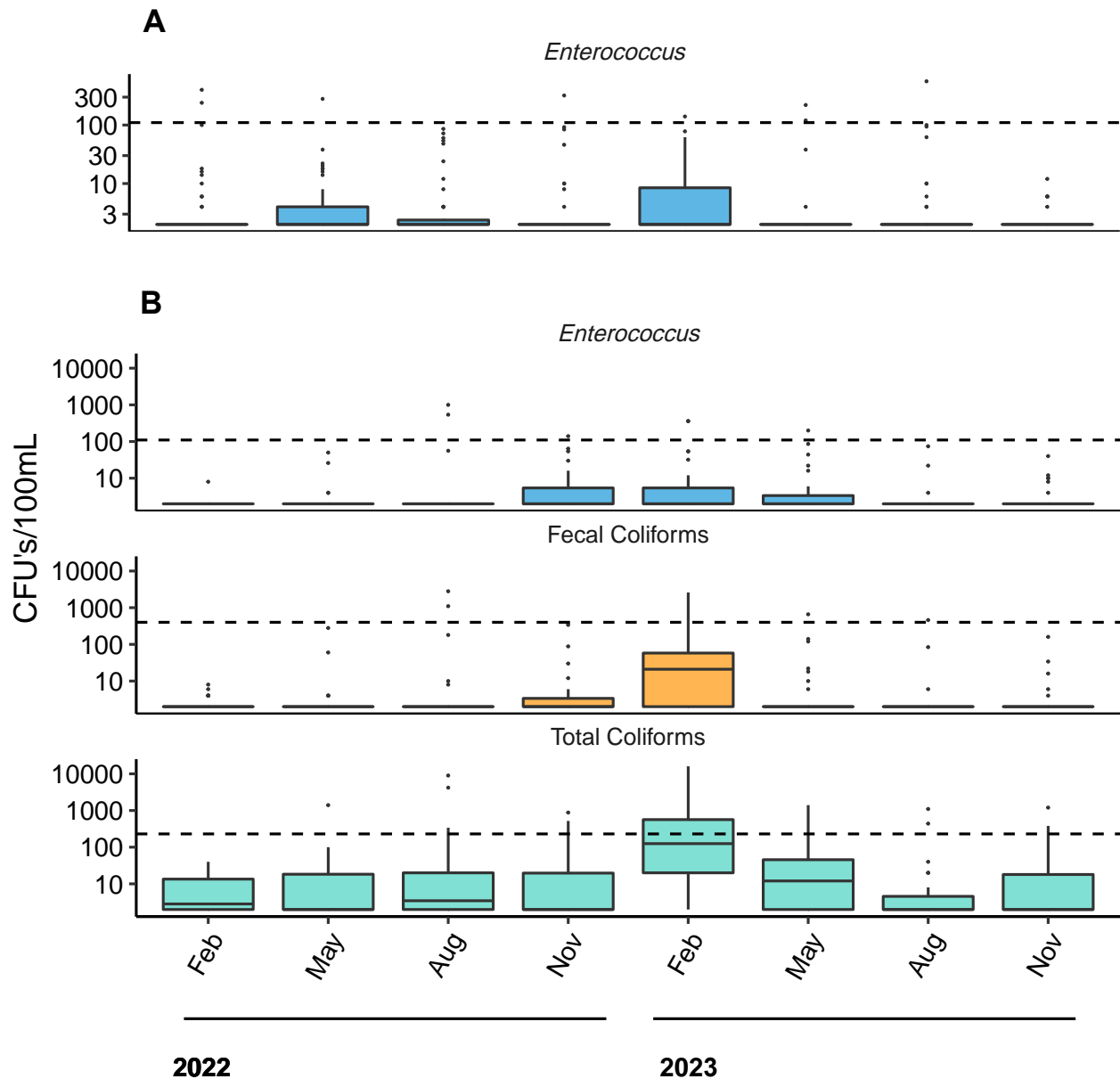


Figure 3.9

Distribution of values for PLOO (A) and SBOO (B) offshore stations during 2022 and 2023, binned monthly. Dashed line represents the water contact standard compliance threshold*. Boxes=median, upper and lower quantiles; whiskers=1.5x interquartile range, dots=outliers. *STV compliance is calculated separately and shown in Table 3.2. Only *Enterococcus* is measured at PLOO offshore stations.

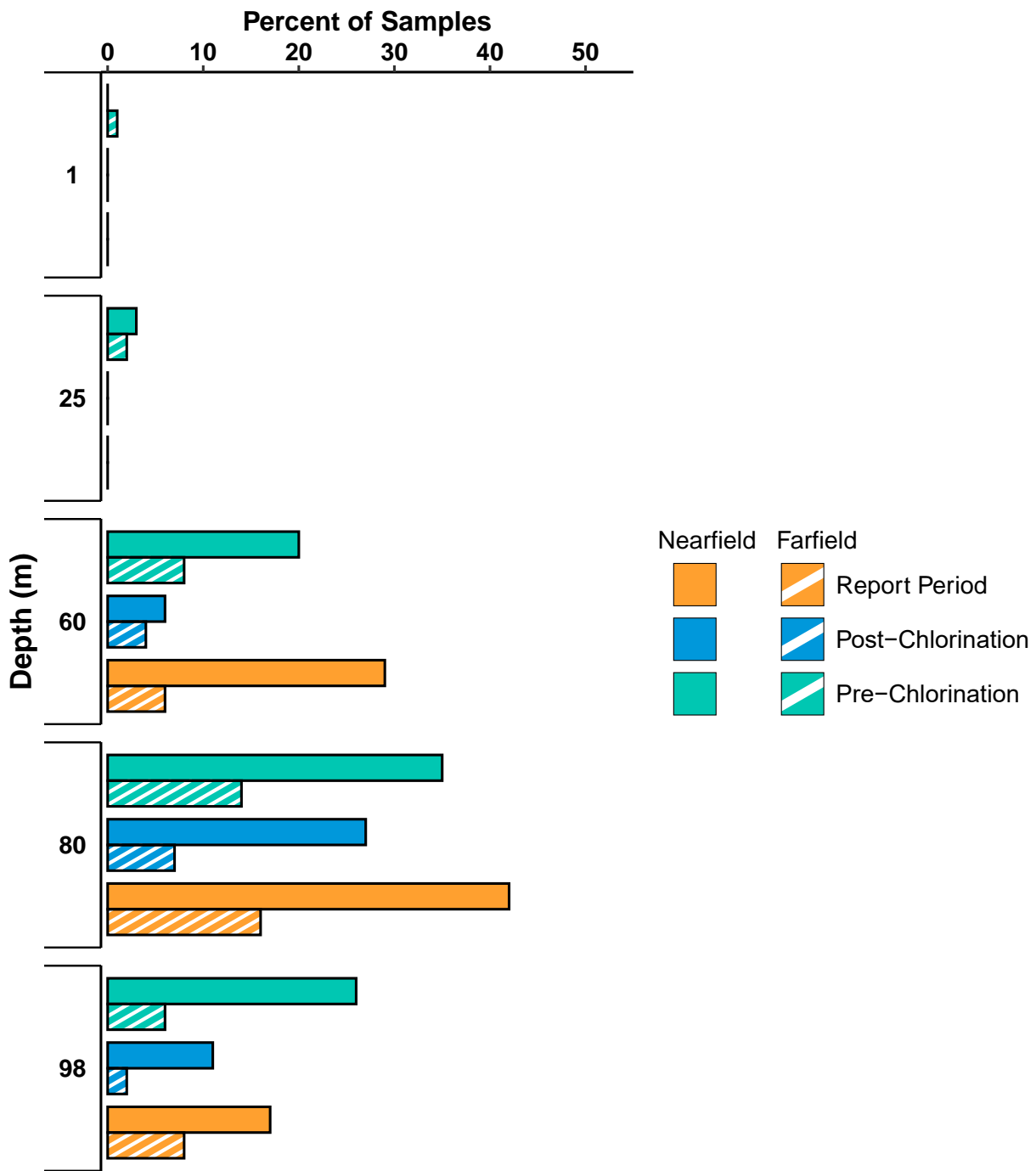


Figure 3.10

Percent of analyses of samples collected from PLOO 98-m offshore stations with elevated FIB. Samples from 2022 and 2023 are compared to those collected since the onset of discharge in 1993. Data for offshore stations in the PLOO region were only collected for seven months prior to discharge from the present location with no exceedances. Therefore, the Pre-Discharge group has been omitted.

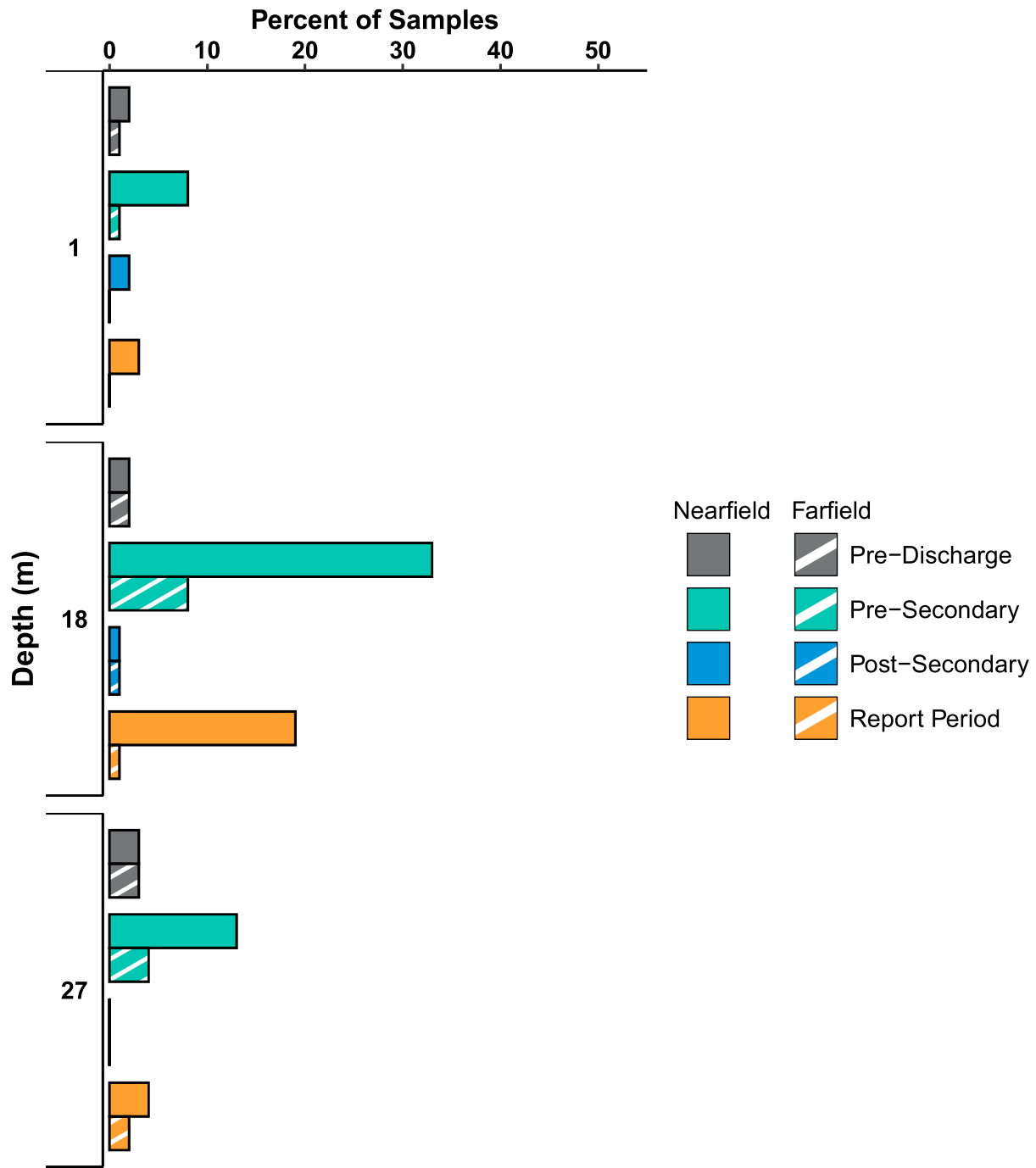


Figure 3.11

Percent of analyses of samples collected from SBOO 28-m offshore stations with elevated FIB. Samples from 2022 and 2023 are compared to those collected since the onset of monitoring in the South Bay in 1995.

Table 3.6

Percent compliance with the HF183 sampling standards, calculated as the proportion of rolling window calculations, taken daily over the report period, showing compliance rates above the threshold established for each metric (90% overall, 50% kelp, 50% offshore). In the case of kelp and offshore compliance metrics, any stations with compliance < 100% are listed individually.

		Fecal Coliforms	Total Coliforms	<i>Enterococcus</i>
PLOO				
Overall		100	100	100
Kelp		100	100	100
Offshore		—	—	100
SBOO				
Overall		49	0	50
Kelp	I19	86	62	85
	I24	97	79	93
	I25	100	82	100
	I26	100	93	100
	I32	100	90	100
	I40	86	57	83
Offshore	I16	100	98	100

Chapter 4

Plume Dispersion

Chapter 4. Plume Dispersion

INTRODUCTION

The City of San Diego (City) collects a comprehensive suite of oceanographic data in nearshore (e.g., kelp forests) and offshore coastal waters surrounding the Point Loma and South Bay Ocean Outfalls (PLOO and SBOO, respectively) to identify the presence of discharged treated wastewater effluent (‘plume’) and characterize regional water quality conditions. A range of specialized equipment are used to facilitate this data collection both temporally and spatially, including a conductivity, temperature, and depth (CTD) instrument package deployed weekly at nearshore stations, and quarterly at offshore stations; two real-time oceanographic mooring systems (RTOMS) anchored near the terminal ends of the PLOO and SBOO; and a remotely operated towed vehicle (ROTV) deployed quarterly in the PLOO and SBOO regions. The ability to monitor over a large spatial scale using a CTD and continuously in real-time using RTOMS, and to track potential wastewater discharge directly using an ROTV, ensures that the City has the most comprehensive suite of tools available to both assess plume dispersion and predict potential shoreward movement of wastewater plumes.

The specialized equipment utilized for plume tracking come equipped with auxiliary instruments that help to distinguish an outfall’s effluent signal from ambient ocean water. For example, colored dissolved organic material (CDOM) has proven useful in identifying wastewater plumes from the PLOO and SBOO in the San Diego region (Terrill et al. 2009, Rogowski et al. 2012a,b, 2013). The reliability of plume detection can be further improved by combining measurements of CDOM with additional parameters (e.g., low chlorophyll *a* concentrations), thus facilitating evaluation of possible wastewater impacts on coastal waters.

Historically, the City has assessed for the presence of effluent plumes via quarterly CTD surveys alone, which provide discrete measurements over a large spatial scale, but lack the temporal and spatial resolution that may be necessary to fully assess plume behavior and the ocean conditions that impact plume dispersion. Following an independent review of the City’s Ocean Monitoring Program (SIO 2004), the Scripps Institution of Oceanography (SIO) was contracted to develop and conduct enhanced monitoring intended to provide an improved understanding of physical circulation and current movement patterns in local coastal waters surrounding the PLOO. Initially, non-telemetered moored temperature loggers (thermistor arrays) and acoustic doppler current profilers (ADCPs) were utilized to characterize the thermocline structure and current regime in the area surrounding the PLOO (Storms et al. 2006). The use of these “static” moorings was later expanded to include both the PLOO and SBOO regions where the resultant data have been a valuable part of the City’s annual receiving waters reports (e.g., City of San Diego 2022a).

Subsequent studies of the fate and behavior of wastewater discharged to the ocean via the SBOO (Terrill et al. 2009) and the PLOO (Rogowski et al. 2012a,b, 2013) included recommendations to use RTOMS and advanced mobile sampling technologies (i.e., ROTVs or autonomous underwater vehicles) to better understand nearshore coastal water quality and the impacts of local ocean currents

and tidal fluxes on effluent plume dynamics. The ability to monitor in near real-time is an essential component of wastewater plume tracking, as it provides the City with the opportunity to predict potential shoreward movement of wastewater plumes, which may otherwise present a hazard to people utilizing recreational waters along the shoreline. Furthermore, real-time monitoring allows the City to quickly identify issues with mooring equipment to facilitate long-term maintenance. Used in conjunction with the RTOMS, optimized and adaptive sampling using ROTV surveys can improve evaluation of plume dispersion from outfalls. Based on these recommendations, the City, U.S. Section of the International Boundary and Water Commission (USIBWC), San Diego Regional Water Quality Control Board (SDRWQCB) and U.S. Environmental Protection Agency (USEPA) reached an agreement that real-time monitoring should be developed for the PLOO and SBOO regions. Therefore, between 2017 and 2021, the City developed and carried out the Plume Tracking Monitoring Plan (PTMP) for the Point Loma and South Bay Ocean Outfall Regions (City of San Diego 2018, 2020b, 2022a). As of July 1, 2021, the PTMP was included as a requirement in the National Pollutant Discharge Elimination System (NPDES) permit for the South Bay International Wastewater Treatment Plant (SBIWTP) and the South Bay Water Reclamation Plant (SBWRP).

This chapter presents the preliminary analysis and interpretation of available plume tracking data collected by CTD, RTOMS, and ROTV in 2022 and 2023 in the PLOO and SBOO regions. The primary goals of this chapter are to: (1) provide in-depth evaluations, interpretations, discussions, and conclusions concerning wastewater plume behavior in receiving waters; (2) determine if the wastewater plume is encroaching upon receiving water areas used for swimming, surfing, diving, and shellfish harvesting; (3) assess the fate of the discharged wastewater plume.

MATERIALS AND METHODS

CTD

Deployment and Configuration

Oceanographic data were collected using a Sea-Bird SBE 25 Plus CTD. The CTD was lowered through the water column at each station to collect continuous measurements of water temperature, conductivity (used to calculate salinity), pressure (used to calculate depth), dissolved oxygen (DO), pH, transmissivity (a proxy for water clarity), chlorophyll *a* fluorescence (a proxy for phytoplankton), and colored dissolved organic material (CDOM). Vertical profiles of each parameter were constructed for each station, per survey, by averaging the data values recorded within each 1-m depth bin (see Chapter 2).

Data Collection

Fifteen stations located in relatively shallow waters within or near the Point Loma or Imperial Beach kelp beds (i.e., referred to as “kelp” stations herein) were monitored weekly to assess water quality conditions and California Ocean Plan (Ocean Plan) (SWRCB 2019) compliance in nearshore areas used for recreational activities such as SCUBA diving, surfing, fishing, and kayaking (Figure 4.1). These included PLOO stations C4, C5, and C6, located along the 9m depth contour near the inner edge of the Point Loma kelp forest, PLOO stations A1, A6, A7, C7, and C8, located along the 18m depth contour near the outer edge of the Point Loma kelp forest, SBOO stations I25, I26, and I39, located at depths of 9–18 m contiguous to the Imperial Beach kelp bed, and SBOO stations I19, I24, I32, and I40 located in other nearshore waters along the 9m depth contour.

An additional 69 offshore stations were sampled quarterly over 3 to 4 days in winter (February), spring (May), summer (August), and fall (November) to monitor water quality conditions and to estimate dispersion of the PLOO and SBOO wastewater plumes (Figure 4.1). These included 36 stations surrounding the PLOO, and 33 stations surrounding the SBOO. The PLOO stations are designated F1–F36 and are located along or adjacent to the 18, 60, 80, and 98m depth contours. The SBOO stations are designated I1–I18, I20–I23, I27–I31, and I33–I38, and are located along the 9, 19, 28, 38 and 55m depth contours, respectively. Fifteen of the PLOO stations (F01–F03, F06–F14, F18–F20) and 15 of the SBOO stations (I12, I14, I16–I18, I22–I23, I27, I31, I33–I38) are located within State jurisdictional waters (i.e., within 3 nautical miles of shore) and therefore subject to the Ocean Plan compliance standards (see Chapter 3 for further details).

Data Analyses

Presence or absence of the wastewater plume at the PLOO and SBOO offshore stations was estimated by evaluating a combination of oceanographic parameters (i.e., detection criteria). All stations along the 9-m depth contour were excluded from these analyses, due to the potential for coastal runoff or sediment resuspension in shallow nearshore waters to confound any CDOM signal that could be associated with plume dispersion from the outfalls (see Hess 2024, Appendices E.1, E.2). Previous monitoring results have consistently shown that the PLOO plume remains trapped below the pycnocline with no evidence of surfacing throughout the year (City of San Diego 2020a, Rogowski et al. 2012a, b, 2013, Hess 2019, 2023, 2024). In contrast, the SBOO plume stays trapped below the pycnocline during seasonal periods of water column stratification but may rise to the surface when waters become more mixed and stratification breaks down. Water column stratification and pycnocline depth were quantified using buoyancy frequency (BF, cycles/min) calculations for each quarterly survey. This measure of the water column’s static stability was used to quantify the magnitude of stratification for each survey and was calculated as follows:

$$BF = \sqrt{g/\rho} * (dp/dz)$$

where g is the acceleration due to gravity, ρ is the seawater density, and dp/dz is the density gradient (Mann and Lazier 1991). The depth of maximum BF was used as a proxy for the depth at which stratification was the greatest. If the water column was determined to be stratified (i.e., maximum $BF > 5.5$ cycles/min), subsequent analyses were limited to depths below the pycnocline.

Identification of potential plume signal was determined for each quarterly survey at each monitoring station based on a combination of CDOM, chlorophyll a , and salinity levels, as well as a visual review of the overall water column profile. Detection thresholds for the PLOO and SBOO stations were set adaptively for each quarter according to the criteria described in City of San Diego (2016a, b). It should be noted that these thresholds are based on observations of ocean properties specific to the distinct PLOO and SBOO monitoring regions, and thus constrained to only those regions. Finally, water column profiles were visually interpreted to remove stations with spurious signals (e.g., CDOM signals near the seafloor that were likely caused by sediment resuspension). All analyses were performed using R (R Core Team 2023) and various functions within the `reshape2`, `Rmisc`, `RODBC`, `oce` and `tidyverse` packages (Wickham 2007, Hope 2013, Ripley and Lapsley 2017, Kelley and Richards 2019, Wickham et al. 2019). Further confirmation of these CTD-based parameters as being indicative of the effluent plume was determined by comparison of potential plume detections with fecal indicator bacteria (FIB) data at the same stations and similar depths (see Chapter 3).

The effect of any potential “plume detection” on local water quality, during each quarterly survey, was evaluated by comparing mean values of DO, pH, and transmissivity within the possible plume boundaries to thresholds calculated for the same depths from reference stations. For each quarter, stations with all CDOM values below the 85th percentile of that region’s values were considered “reference”. Individual non-reference stations were then determined to be out-of-range (OOR) compared to the reference stations if values exceeded narrative water quality standards defined in the Ocean Plan (see Box 3.1, Chapter 3). For example, the Ocean Plan defines OOR thresholds for DO as a 10% reduction from naturally-occurring concentrations, for pH as a 0.2 pH unit change, and for transmissivity as below the lower 95% confidence interval from the mean. For purposes of this report, “naturally” is defined for DO as the mean concentration minus one standard deviation (see Nezlin et al. 2016).

RTOMS

Deployment and Configuration

The RTOMS are anchored buoys suspended in the water column configured with a range of instruments, collecting near continuous oceanographic data and providing near real-time information of changing conditions. The RTOMS are outfitted with a series of instruments at various depths throughout the water column (see Chapter 2, Table 2.1). Critical parameters that were measured on a real-time basis included temperature, conductivity (salinity), total pH, DO, dissolved carbon dioxide ($x\text{CO}_2$), nitrate (nitrate + nitrite), chlorophyll *a*, CDOM, backscatter (turbidity), biological oxygen demand (BOD), and current direction and velocity. Parameters were recorded at 10-minute intervals, with the exception of nitrate + nitrite and $x\text{CO}_2$, which were recorded at 1-hour intervals.

Data Collection

Two RTOMS were anchored near the terminal ends of the PLOO and SBOO (nearfield), at a distance far enough from the diffuser ports to be outside the area of active plume rise. The PLOO RTOMS was anchored at a depth of approximately 95 m, just east of the northern diffuser leg, and the SBOO RTOMS was anchored at a depth of approximately 30 m, just west of the southern diffuser leg terminus (Figure 4.1). Each mooring was deployed for a period of approximately one year, with a gap in the SBOO deployment from November 2022 to June 2023 due to a loss of equipment after a mooring break (see Chapter 2).

In addition, temperature and ocean current data from static moorings were used to supplement data gaps between RTOMS deployments (from October 26, 2023 to December 19, 2023 at the PLOO; from November 3, 2022 to June 28, 2023 at the SBOO). These non-telemetered (static) upward-facing bottom-mounted ADCPs (Teledyne RD Instruments 300 KHz Workhorse Monitor) and thermistor (Onset Tidbit temperature loggers) string arrays were moored near the RTOMS at the terminal ends of the PLOO and SBOO (Figure 4.1; see Chapter 2 for details).

Data Processing and Analysis

Prior to conducting analyses, RTOMS data were subject to a comprehensive suite of quality assurance/quality control (QA/QC) procedures following Quality Assurance of Real-Time Oceanographic Data (QARTOD) methodologies (see Chapter 2). After review, all data that were flagged as suspect or bad were excluded from further analyses and are not presented in this report.

Ocean current data analyses were performed in R (R Core Team 2023) using functions within various packages (i.e., reshape2, Rmisc, mixOmics, tidyverse, scales, pracma, and gtools) (Wickham 2007,

Hope 2013, Le Cao et al. 2017, Wickham et al. 2019, Wickham and Seidel 2020, Borchers 2021, Warnes et al. 2021). Specifically, after data QA/QC, tidal frequency data were removed using the PL33 filter (Alessi et al. 1984) and then hourly averaged. Plots and analyses for all other RTOMS data were completed in MATLAB (2022). Contour plots were generated for parameters with sufficient vertical coverage in the water column using default settings, which display fixed isolines and fill areas between isolines with constant colors. Density calculations and temperature-salinity plots were created using the SEAWATER toolbox library for MATLAB, version 3.3.1 (Morgan and Pender 2014).

Temperature gradients were evaluated from RTOMS and thermistor data to illustrate daily and seasonal changes in thermal stratification. Vertical gradients were calculated by the daily average temperature difference between adjacent sensors in the water column (e.g., from 6 to 10 m at thermistor arrays) and then dividing by the depth between sensors. Depths of the maximum daily temperature gradients were used to evaluate stratification, with moderate stratification defined as greater than $0.2^{\circ}\text{C}/\text{m}$ gradients.

During time periods when the wastewater effluent plumes overlap with the fixed locations of the RTOMS, observations may be assessed for potential plume detections. In order to compare potential freshwater signals from effluent plumes to background ocean salinity levels, time series anomalies of RTOMS salinity were calculated and compared to historical salinity data from CTD surveys. Since there were no equivalent moorings deployed in similar ocean water masses to use as a farfield reference site on the same time scale, this approach provided a baseline comparison to typical salinity ranges by region and depth. The historical CTD salinity data included data from the last two decades (2001–2023) and excluded data from nearfield stations (F29, F30, F31 for PLOO; I12, I14, I15, I16 for SBOO). Historical CTD data averages and percentiles were calculated within a similar depth range for each mooring sensor (1–3 m for the surface bin for both RTOMS; other target depths spanned ± 3 m for PLOO and ± 1 m for SBOO). Salinity anomalies from RTOMS data were then calculated as the difference between the historical CTD average for each depth range and the daily means for each RTOMS sensor depth. Relatively low subsurface salinities (33.2–33.5 Practical Salinity Unit [PSU]) are frequently observed in the San Diego region (City of San Diego 2022a), likely influenced by seasonal evaporation at the surface and the incursion of the low salinity and low temperature Pacific Subarctic water mass within the California Current System (Lynn and Simpson 1987, Jones et al. 2002). Therefore, RTOMS salinity anomalies were compared to minimum CTD salinity observations at each depth range using the 99th percentile, in order to assess for high likelihood of potential influence from freshwater effluent plumes. In addition, average salinities across the region were lower than normal in the summer and fall in 2023 (see Chapter 2). Therefore, mean CTD salinity from farfield stations for each quarterly CTD survey in 2023 was calculated for comparison to 2023 RTOMS data.

While previous studies in the region used salinity signatures to estimate effluent dilution near outfalls (e.g., Washburn et al. 1992), more recent work has improved upon the impracticality of discerning effluent plumes using salinity signatures alone by examining additional identifying characteristics such as elevated CDOM (Rogowski et al. 2012a,b, 2013, City of San Diego 2016a, 2022a). Preliminary analyses of other parameters (i.e., CDOM, turbidity, nitrate + nitrite) that may aid in potential plume detections by the PLOO and SBOO RTOMS are presented, where an example is highlighted for each site along with challenges in deciphering plume signals. BOD levels have not been found to be a useful indicator of plume presence (City of San Diego 2022a) and this measurement was discontinued starting in 2023. Further work will be completed to evaluate potential wastewater plume detections by RTOMS to continue to refine and improve this monitoring approach.

ROTV

Deployment and Configuration

The ScanFish III is a wing-shaped ROTV that is towed behind the sampling vessel using a “live-wire” tow cable with ethernet communication capabilities to surface computing platforms aboard the sampling vessel. The surface computing platforms control the ROTV, and process, display, and record data as the data are collected. Using surface communication, the ROTV can be programmed to sample a variable depth range in the water column, moving in an undulating pattern from ocean surface to seabed, or moving in a fixed depth or terrain-following mode. Its large payload enables a variety of modular sensors to be outfitted to the vehicle frame. The City’s current package includes a Sea-Bird SBE 25 Plus CTD with a Sea-Bird pump, temperature, conductivity, DO, and CDOM sensors, and three Turner Designs Cyclops-7F fluorometers tuned for CDOM, Tryptophan and Optical Brightener (OB) measurements, and a Chelsea BOD sensor.

During all surveys, vessel speed while towing the ROTV was kept below 11 knots. The tow cable payout varied from 200 to 600 m depending on the depth of the transect and vessel speed. Data from the ROTV were continuously monitored in real-time to ensure instrument function. Fathometer readings from both the ROTV and the shipboard instruments were also closely monitored to ensure capture of the largest possible portion of the water column without damage to the ROTV. To prevent altimeter errors, the ROTV was typically flown no less than 10–15 m below the surface, especially after May 2020, when shallow depths were determined to be a cause of altimeter failure. To prevent collision with the seafloor, the ROTV was kept 5–15 m from the bottom.

Data Collection

City staff have been evaluating the use of the ROTV for plume tracking as part of an ongoing project (City of San Diego 2020b, 2022a,b). The initial goal of the project was to compare towed CTD measurements from the ROTV to traditional fixed grid vertical-profile CTD measurements during each quarterly water quality sampling period in 2020 and 2021. Surveys were initially conducted solely in the PLOO region to help develop ROTV survey methods. ROTV efforts in the first three quarters of 2020 were focused on cross-validation of ROTV data against CTD data collected during quarterly offshore surveys. Beginning in November 2020, ROTV surveys were conducted adaptively, so survey efforts were focused on areas and depths where there was evidence of the potential PLOO plume (typically where elevated CDOM and/or OB values were observed in real-time). In July 2021, the City’s primary monitoring vessel (M/V Oceanus) suffered catastrophic engine failure and was out of service until May 2022. Due to the loss of this sampling capability, ROTV surveys were only completed once in 2022, over the course of two days in September in 2022 (Figure 4.2). Three transects along the 90 to 100 m isobath were completed (one on September 14; two on September 15). In both instances, serial data communication failure resulted in sampling to end early. In 2023, ROTV operations were not possible due to the planned resource exchange which allowed the City to participate in the region wide Bight 2023 sampling. Additional issues continue to hamper the City’s ability to effectively utilize an ROTV for regular monitoring including staffing shortages, and delays caused by the unavailability of the City’s monitoring vessel due to unforeseen mechanical issues. However, during this time, progress was made toward resolving some technical concerns related to the ROTV’s operations, which were detailed in prior progress reports (see City of San Diego 2023b, 2024). For example, a new shell was installed on the ScanFish in February 2023 to address issues with flight likely caused by damage from previous crashes and entanglement with fishing gear. Additionally, new sensors, including a Sea-Bird SeaOwl (CDOM, chlorophyll *a*, turbidity), a transmissometer, and a pH sensor were purchased with installation planned for 2024.

The ROTV surveys in the SBOO region have proven to be significantly more problematic than the PLOO surveys due to the complicated hydrography, proximity of multiple sources of organic material (i.e., Tijuana River, San Diego Bay), shallower depths in comparison to the PLOO region survey area, and a high abundance of fishing gear and abandoned equipment in the area during all times of the year. During the SBOO fall survey in 2020, the ROTV became entangled in fishing gear, resulting in contact with the seafloor and significant damage to the ROTV structure. Issues such as these have prevented any successful ROTV surveys in the SBOO region during the reporting period and may completely rule out this form of monitoring in the future. The City continues to evaluate the viability of ROTV monitoring and will provide recommendations in the next plume tracking work plan.

Data Processing and Analysis

Data from the ROTV were processed and displayed in real-time via onboard computers, and were checked for anomalous sensor readings that may have indicated either possible plume detection or equipment malfunction during data collection. For analyses presented herein, data outside of climatological ranges established for RTOMS QA/QC were flagged as suspect and removed from analysis, as were data that appeared suspect upon initial manual review. For example, negative CDOM values (as low as -0.9 ppb in 2022) were removed from the dataset. Further QA/QC protocols for ROTV data are in development.

Data from the ROTV surveys were analyzed using the R programming language (R Core Team 2023), employing functions within various packages (i.e., tidyverse, marelac, fields) (Wickham et al. 2019, Soetaert et al. 2020, Nychka et al. 2021). In order to visualize the spatial extent of potential plume signals from data collected during ROTV surveys, color contour maps of the data from single transects (isobaths) were created by interpolating data between points using a locally estimated scatterplot smoothing (LOESS) regression using the R package “stats” (R Core Team 2023) and were overlaid with the ROTV track showing the actual location of the ROTV measurements in the water column. Data taken over consecutive days are considered part of the same mission and are visualized together in one plot for each parameter.

Within the array of data collected during the ROTV surveys, CDOM and OB were found to have the strongest correlation to potential plume signatures (Cao et al. 2009, Terrill et al. 2009, Rogowski et al. 2012a,b, 2013). In 2022, a chlorophyll *a* sensor was added to the ScanFish sensor package to aid in the interpretation of data for the purpose of plume tracking. Ongoing refinement of ROTV sensor technology integration and data analysis methodologies may lead to increasingly reliable plume detection.

RESULTS AND DISCUSSION

Potential Plume Signals Determined via CTD

PLOO Region

The dispersion of the treated wastewater plume from the PLOO and its effects on natural light (percent transmissivity), DO, and pH levels were assessed by evaluating the results of 328 CTD profile casts performed in 2022 and 2023. Based on the criteria described previously (City of San Diego 2016a,b), potential evidence of a plume signal was detected 53 times during the year from 26 different stations, while up to 32 stations were identified as reference sites during each quarterly survey (Table 4.1, Figure 4.3, Appendix E.3). About 21% of casts showing possible plume detections ($n = 11$) occurred at the

three stations located closest to the outfall (F29, F30, F31), equating to a detection rate of 46% at these nearfield sites over the past two years. Other possible detections occurred at stations along the 60, 80, or 98-m depth contours, located between 13 km to the north and 8 km to the south of the outfall. Overall, the variation in plume dispersion observed near Point Loma in 2022 and 2023 appeared similar to flow-mediated dispersal patterns reported previously for the region (Rogowski et al. 2012a,b, 2013).

The width and rise height of potential PLOO plume detections varied between stations throughout the year (Figure 4.4, Appendix E.3). Despite fluctuations in depth of the pycnocline, plume detections remained below 34 m even during periods of weak water column stratification. Additionally, detection depths were similar between nearfield and farfield stations. This finding aligns with historical satellite imagery observations that have not shown visual evidence of the plume surfacing (e.g., Svejksky 2010, Hess 2019, 2023, 2024). About 47% (n = 25) of the potential plume detections corresponded with elevated *Enterococcus* densities, all of which were collected at depths at or below 60 m (City of San Diego 2022–2024a).

Of the 53 potential plume signals that occurred during the reporting period, a total of 33 out-of-range (OOR) events were identified at various stations throughout the year, which consisted of 20 OOR events for natural light and 13 OOR events for DO (Table 4.1, Appendix E.3). Representative quarterly profiles from station F30 are shown in Appendices E.4–E.11. There were no OOR events for pH. Six of the natural light OOR events and eight of the OOR events for DO occurred at stations located within State jurisdictional waters where Ocean Plan compliance standards apply.

SBOO Region

The dispersion of the SBOO plume and its effects on natural light, DO and pH levels were assessed by evaluating the results of 232 CTD profile casts performed in 2022 and 2023. Potential evidence of a plume signal was detected 26 times during the reporting period from 12 different stations, while 11–21 stations were identified as reference sites during each quarterly survey (Table 4.1, Figure 4.3). About 54% of the possible detections (n = 14) occurred at nearfield stations (i.e., I12, I14, I15, I16). Three of these plume detections were associated with elevated FIB, each at 18 m (City of San Diego 2022–2024b). Other potential plume signals at farfield stations may be associated with their proximity to known sources of organic matter. For example, stations I23 and I27 are located within the possible influence of Tijuana River outflows.

The width and rise height of potential SBOO plume detections varied between stations throughout the reporting period (Figure 4.4, Appendix E.12). Unlike the observations at the PLOO, potential SBOO plume signals were detected throughout the water column, ranging from 7 to 20 m with a median depth of 14 m. However, as with the PLOO, potential plume detection depths in the SBOO region were similar between nearfield and farfield stations.

The effects of the SBOO wastewater plume on the three physical water quality indicators described above were calculated for each station and depth where a possible plume signal was detected (Table 4.1, Appendix E.12). Representative profiles from station I12 are shown in Appendices E.13–E.20. Of the 26 potential plume signals that occurred during the reporting period, a total of 17 OOR events were identified for transmissivity, while one OOR event occurred for DO. There were no OOR events for pH. Eleven of the 18 OOR events occurred at stations within State jurisdictional waters where Ocean Plan compliance standards apply, with nine of these events occurring at nearfield stations I12, I14, I15, or I16.

Receiving Waters Conditions and Potential Plume Signals Determined via RTOMS

Receiving Waters Conditions

Ocean conditions surrounding the PLOO and SBOO RTOMS that could potentially affect the dispersion of wastewater plumes, such as ocean currents and density structure of the water column, were generally within historical ranges and align with expected seasonality patterns for the region (see Chapter 2; Terrill et al. 2009, Rogowski et al. 2012a, City of San Diego 2022d).

Changes in ocean stratification are primarily influenced by water column temperature structure in the region, where larger differences in temperature between depths (thermal gradients) result in stronger stratification (see Chapter 2; Bowden 1975, Jackson 1986, Pickard and Emery 1990). The weakest thermal stratification ($<0.2^{\circ}\text{C}/\text{m}$) was observed during late fall and winter months (November through February) in 2022 and 2023, with daily maximum thermal gradients occurring more frequently at mid to deep depths (PLOO: 10–75m; SBOO: 10–34m) (Appendix E.21). Conversely, moderate ($>0.2^{\circ}\text{C}/\text{m}$) to strong ($>0.5^{\circ}\text{C}/\text{m}$) daily thermal stratification persisted from spring to fall (April through October) in 2022 and 2023 more frequently at shallower depths (PLOO: <10 to 20m; SBOO: <10 to 22m), with more variability in stratification occurring during transition months in the spring and fall (March and early November) of both years. As described in the CTD results in this chapter, previous monitoring results have consistently shown that the PLOO plume remains at depth even during periods of weak stratification, while the SBOO plume has a greater likelihood of reaching the surface during these periods when the water column is more mixed (Figure 4.4).

Ocean currents predominantly flowed along a north-northwest/south-southeast axis of variation near the PLOO and SBOO (Appendices E.22, E.23). Generally, along-coast currents tended to dominate, regardless of season although in 2023 there were several eastward excursions in shallow depths during stratified conditions (see Chapter 2, Appendix C). These periods were unlikely to impact the dispersion of the plume as these layers were generally above the pycnocline. Variability in currents occurred throughout 2022 to 2023, with distinct periods of predominantly N:NW and S:SE directed currents throughout the water column from days to weeks at a time (Appendices E.22, E.23). Transitions in current direction and speed often indicate a shift in local conditions that may also result in further mixing of the water column, especially when there is increased vertical shear (i.e., one section of the water column moving in a different direction than the other part of the water column) (see Pickard and Emery 1990). Additionally, ocean currents in the vicinity of the outfalls can influence the initial rise height and horizontal dispersion of the wastewater effluent plumes, as well as the rate of transport of effluent out of the discharge area on longer time scales (days to weeks) (City of San Diego 2022c).

PLOO Region

At the PLOO RTOMS, the lowest salinity values (daily average values <33.2 PSU) were observed from 60 to 89 m in the winter and fall in 2022 and in the summer and fall in 2023 (Figure 2.8, Chapter 2). Anomalously low salinity measurements from the PLOO RTOMS have occurred at these deep depths throughout prior deployments regardless of season and are lower than what has historically been reported from CTD data or the more recent ROTV surveys (Figure 4.5). In addition, these depths of lowest salinities overlapped with other observations of potential PLOO plume rise heights (Figure 4.4; Rogowski et al. 2012a). Given the proximity of the mooring to the PLOO, these low salinity values at deep depths (>45 m) may likely be attributable to the effluent plume. Additionally, the observations by the RTOMS of lower than normal salinities in deep waters in nearfield sites near the PLOO were likely due to the increased frequency of sampling that captured a larger range of variability, as well as a potential reduction in mixing

between the freshwater effluent plume and ocean water masses by the equipment itself. For example, the mooring instruments are suspended passively in the water column at a fixed location, while large towed or profiling packages such as the ROTV or CTD rosette may result in turbulence and additional mixing as moved through the water (e.g., Paver et al. 2020). Given these factors, it is expected that the potential presence of the plume may be better discerned using salinity at the RTOMS as a supplement to other methods. With an exception during the reporting period, during September through October 2023, salinity values at nearly all RTOMS depths approached or exceeded minimum CTD salinity observations (99th percentile) (Figure 4.5). Notably, in late 2023, salinity values across the region were lower than typical seasonal patterns due to a regionwide shift in ocean conditions (see Chapter 2), which was reflected in lower than normal mean CTD salinity (open red circles in Figure 4.5). Therefore, the anomalously low salinity observed by RTOMS in late 2023 at shallow and mid-depths aligned with regional ambient salinity at the time and is unlikely to be related to the effluent plume.

Auxiliary measurements from RTOMS, such as CDOM, were also assessed to assist with possible plume detection. Time periods with a strong potential for plume detection (e.g., low salinities at typical plume depths) and fewer confounding factors (such as during dry periods or low phytoplankton concentrations) may be targeted initially to identify other possible plume characteristics. As one example, near the PLOO in late February 2022, possible plume detections were evident from low salinity values at depths from 75 to 89 m (Figure 4.6). Beginning February 23, the plume appeared to be advected away from the sensors by a shift to a stronger south-easterly current. During the same period, slightly elevated CDOM and turbidity levels appear associated with lower salinity at 75 m, though the changes did not appear significant when compared to mid-depth (30 m) observations (Figure 4.6). Nitrate + nitrite measurements were relatively low for this time period of potential plume detections compared to other periods (Appendix C.12, City of San Diego 2022a), and values increased with the shift to higher salinity waters (Figure 4.6). This pattern aligns with the typical PLOO effluent's relatively low nitrate proportion of nitrogen (see City of San Diego 2022–2024c, CSWRCB 2024). This range falls within a similar range of ambient ocean nitrate levels (see Weber et al. 2021). Generally, higher nitrate levels were observed in cold, high salinity water masses during winter 2022 and 2023, while very slightly elevated CDOM levels tended to occur at warmer temperatures and lower salinities (Figure 4.7). This supports the role of upwelling in bringing cold, saline, nutrient-rich, oxygen-poor water masses into the region (see Chapter 2, Weber et al. 2021). During the PLOO RTOMS deployments in 2022–2023, as with prior deployments, BOD levels were not found to be a useful indicator of possible plume presence (see Appendix C.10, City of San Diego 2022a, 2023a). Overall, salinity observations, used in conjunction with CDOM, turbidity, and chlorophyll *a* levels may provide potential evidence of effluent plume signals at the PLOO RTOMS and further work will be completed to better evaluate these detections throughout the year.

SBOO Region

At the SBOO RTOMS, the detection of potential SBOO plume signals was often not discernable solely by examining salinity values alone. Low salinity anomalies were observed across depths from September through November in 2023 (Figure 4.5), which coincided with regionwide low salinities as described above. In order to target possible plume characteristics, time periods were examined in the same manner as the PLOO RTOMS data (e.g., during dry periods and low phytoplankton concentrations) where other auxiliary parameters were available. As one example, during early February 2022 near the SBOO, weak stratification and currents alternating between southeastern and weakly northwestern directions occurred on the same days as observations of slightly reduced salinity near the surface (1 m) (Figure 4.8). Additionally, these lower salinity periods coincided with slightly elevated CDOM and nitrate + nitrite levels at the surface, while these characteristics were not observed at the deepest sensor

depth (26 m) of the mooring (Figure 4.8). Taken together, these near surface signals may be attributed to effluent plume influence. In addition, high resolution satellite monitoring captured two days of surfacing events related to the SBOO wastewater plume during this same one-week period (Figure 4.9). Typically, the highest number of SBOO effluent surface plumes detected by satellite occur from November to January during periods of weak stratification. In 2022, there were 19 days in which the SBOO surface plume was evident by satellite while in 2023, there were 20 days (Hess 2023, 2024).

Overall, higher nitrate and CDOM levels were observed with slightly lower salinities at the surface during winter 2022 (Figure 4.10). In contrast to the PLOO, treated effluent from the SBWRP and SBIWTP discharged through the SBOO generally contained concentrations of nitrate higher than ambient ocean nitrate levels (for effluent levels, see City of San Diego 2022–2024d, CSWRCB 2024; for ocean levels, see Weber et al. 2021). Depending on the conditions and mixing regime, nitrate may be another potential indicator of SBOO plume presence. However, other confounding factors such as coastal runoff and influence from the Tijuana River estuary may also bring water masses into the region that are less saline, CDOM, and nutrient-rich, resulting in a complex environment in the SBOO region (Hess 2019, 2023, 2024). During the SBOO RTOMS deployments in 2022, as with prior deployments, BOD levels were relatively stable over time and did not appear to show possible plume influence (City of San Diego 2022a, 2023a). Further analyses with additional RTOMS data and other available data will be completed in the future to address these challenges with determining potential SBOO plume signals.

Potential Plume Signals Determined via ROTV

PLOO Region

ROTV surveys in September 2022 did not yield definitive plume detection as had been observed in prior years. The maximum value for CDOM detected (1.3 ppb) was less than plume detections during prior surveys that typically corresponded with higher CDOM values (>1.5 ppb). Similarly, optical brightener values did not exceed 32 ppb (Figure 4.11), where prior plume detections corresponded with higher OB values (>35 ppb). A weak midwater signal in both parameters does appear in the interpolated plots, which could be interpreted as an exceptionally diffuse plume signal. A notable chlorophyll *a* signature was observed in northern PLOO region surface waters, indicating the presence of a phytoplankton bloom during the survey. Ocean conditions during the fall 2022 ROTV survey showed moderate stratification at mid depths (30 m) (Figure 2.6; Figure 4.11). Just prior to the fall 2022 ROTV survey, ocean currents shifted from strong north-northwesterly to a moderate south-southeasterly direction (Appendix E.22), which may have resulted in enhanced mixing of the effluent plume through water column shear. As with RTOMS results described in the previous section, BOD and tryptophan levels measured during the 2022 ROTV surveys were not found to be reliable indicators of plume presence.

SUMMARY

Historically, the City has evaluated the fate and dispersal of treated wastewater effluent plumes through quarterly and weekly monitoring of a fixed grid of stations utilizing CTD instrumentation and bacteriological evidence (e.g., City of San Diego 2020a). Although this technique covers a large spatial area, the infrequent temporal sampling rate limits observations to just a few "snapshots" in time. This limited timeframe may not capture sporadic events, such as storm-driven transport or other oceanographic phenomena. To address this issue, the City installed non-telemetered ADCP and thermistor instrumentation to document hydrographic conditions in the immediate vicinity of the outfalls

over much finer timescales (Storms et al. 2006). Although variable over space and time, the general axes of current velocities were consistently observed to follow N:NW or S:SE trajectories. This has indicated that as effluent mixes with ambient seawater, it generally travels along the coast rather than being directed inshore toward the shoreline, kelp beds, or other recreational waters. The ADCP data have improved temporal coverage of conditions in the area; however, the 4-month recovery cycle for the data has rendered it useful only to understand events in retrospect and has not included auxiliary measurements for potential plume characterization.

More recently, real-time data have become available via the City's RTOMS, which include a variety of instrumentation at multiple depths providing near-continuous information from a single platform. These observations have enhanced the assessment of environmental conditions and the potential impacts of oceanographic and anthropogenic events in coastal waters. While not possible to understand the dispersion and spatial extent of plumes using RTOMS alone, these near-continuous data may show potential vertical spread of plumes as well as events that would otherwise be missed by fixed grid surveys. For example, they provided the ability to capture SBOO effluent plume surfacing events that aligned with observations from satellite monitoring (Figure 4.9, Hess 2023). In addition, these high frequency data at a single, fixed location provide context on the state and variability of the receiving waters into which the PLOO and SBOO discharge. For example, the rise height of the effluent plume is highly dependent on density structure and stratification of the water column, as well as ambient currents (Rogowski et al. 2012a,b, 2013, City of San Diego 2022b,c). Stronger currents may result in greater initial mixing while weaker currents may result in shallower rise heights depending on stratification. Other local ocean dynamics, such as internal waves, can result in further mixing and impact observed plume rise heights (Rogowski et al. 2012a). These data can be further used to validate predictive models that seek to characterize changes, which may cause environmental degradation. While initial RTOMS results presented show examples of potential indicators of effluent plume signals, one challenge remains: there is no equivalent farfield reference mooring station in similar water masses to use for comparison at the same time scales. Thus, it is difficult to confirm plume presence as well as any possible plume effects on DO, pH, or natural light water quality indicators (also note that moorings are located outside State jurisdictional waters where Ocean Plan compliance standards do not apply). To strengthen the ability to discern plume signals, further analyses are planned.

To complement the operations of the RTOMS, the ROTV may allow the City to develop a truly adaptive and dynamic sampling program that will be able to appropriately evaluate the extent of plume dispersion. Using real-time information on ocean stratification, currents, and potential plume detections from the RTOMS, targeted ROTV surveys may be completed for adaptive sampling and mapping of the plumes as needed. Furthermore, as ROTV data appeared to generally agree qualitatively with CTD data (City of San Diego 2022b), this potentially presents a more focused and higher resolution method for tracking plumes over a large spatial scale. While initial results from ROTV surveys in the PLOO region from prior surveys completed before 2022 showed strong potential for distinguishing PLOO plume signals, a similar evaluation of SBOO plume detections remains problematic. ROTV sampling has been more challenging in the SBOO region due to technical issues, logistical challenges, and environmental factors, which may hinder the usefulness of this technique for SBOO plume tracking purposes. Specifically, the frequent occurrence of obstacles and abandoned fishing gear caused significant damage to the ROTV and technical challenges such as altimeter issues in the shallower depths resulted in fewer successful surveys in the SBOO region. An assessment of the effectiveness of the ROTV is currently ongoing. Future work is planned to improve potential plume detections, including refinement of ROTV sensor technology integration and additional data analysis methodologies.

Despite the different spatial and temporal coverages of the CTD, RTOMS, and ROTV instrument packages utilized by the City, all observations from 2022–2023 demonstrated that the Point Loma effluent plume generally remained offshore below a depth of 34 m, and was transported along the coast. This finding concurs with prior plume tracking studies (Rogowski et al. 2012a,b, 2013), as well as historical satellite imagery observations that have not shown visual evidence of the plume surfacing (e.g., Svejksky 2010, Hess 2019, 2023, 2024). These observations support previous studies showing that there is no evidence that wastewater discharged to the ocean via the current configuration of the PLOO has ever reached the shoreline or had any significant impact on recreational waters (City of San Diego 2022b,c).

Within the shallower SBOO region, past studies have shown that other sources, such as coastal runoff from rivers and creeks, were more likely to impact coastal water quality than wastewater discharge from the outfall, especially during and immediately after significant rain events (Svejksky and Jones 2001, Terrill et al. 2009). Though bacteriological analyses from monitoring stations near the outfall do indicate a slight decrease in offshore water quality during the reporting period (see Chapter 3). The San Diego Bay and the Tijuana River estuary often deliver less saline, CDOM- and nutrient-rich water masses, resulting in a complex environment in the SBOO region. It is well established that sewage-laden discharges from the Tijuana River and Los Buenos Creek are likely sources of contaminated water during or after storms or other periods of increased flows (see Chapter 3). These factors confound efforts to decipher SBOO effluent plume signals from other coastal influences. While the SBOO plume generally stays trapped below the pycnocline during seasonal periods of water column stratification, it may rise to the surface when waters become more mixed and stratification breaks down (Terrill et al. 2009, Hess 2019, 2023, 2024, City of San Diego 2020a, 2022a). However, given predominant along-shore currents, it does not appear that wastewater discharged via the SBOO reaches the shoreline or impacts recreational waters, particularly compared to other coastal inputs (Largier et al. 2004, Terrill et al. 2009).

LITERATURE CITED

- Alessi, C.A., R. Beardsley, R. Limeburner, and L.K. Rosenfeld. (1984). CODE-2: Moored Array and Large-Scale Data Report. Woods Hole Oceanographic Institution Technical Report. 85–35: 21.
- Borchers, H.W. (2021). *pracma: Practical Numerical Math Functions*. R package version 2.3.3. <https://CRAN.R-project.org/package=pracma>.
- Bowden, K.F. (1975). Oceanic and Estuarine Mixing Processes. In: J.P. Riley and G. Skirrow (eds.). *Chemical Oceanography*, 2nd Ed., Vol.1. Academic Press, San Francisco, CA. p 1–41.
- Cao, Y., J.F. Griffith, and S.B. Weisberg. (2009). Evaluation of optical brightener photodecay characteristics for detection of human fecal contamination. *Water Research*, 43(8), 2273–2279.
- City of San Diego. (2016a). Point Loma Ocean Outfall Annual Receiving Waters Monitoring and Assessment Report, 2015. City of San Diego Ocean Monitoring Program, Public Utilities Department, Environmental Monitoring and Technical Services Division, San Diego, CA.
- City of San Diego. (2016b). South Bay Ocean Outfall Annual Receiving Waters Monitoring and Assessment Report, 2015. City of San Diego Ocean Monitoring Program, Public Utilities Department, Environmental Monitoring and Technical Services Division, San Diego, CA.

- City of San Diego. (2018). Plume Tracking Monitoring Plan for the Point Loma and South Bay Ocean Outfall Regions, San Diego, California. Submitted by the City of San Diego Public Utilities Department to the San Diego Water Board and USEPA, Region IX, March 28, 2018 (approved 4/25/2018).
- City of San Diego. (2020a). Biennial Receiving Waters Monitoring and Assessment Report for the Point Loma Ocean Outfall and South Bay Ocean Outfall, 2018-2019. City of San Diego Ocean Monitoring Program, Public Utilities Department, Environmental Monitoring and Technical Services Division, San Diego, CA.
- City of San Diego. (2020b). Plume Tracking Monitoring Plan Progress Report for the Point Loma and South Bay Ocean Outfall Regions, San Diego, California; Report Period: January – December 2019. Submitted by the City of San Diego Public Utilities Department to the San Diego Water Board and USEPA, Region IX, March 3, 2020.
- City of San Diego. (2022–2024a). Monthly Receiving Waters Monitoring Reports for the Point Loma Ocean Outfall (Point Loma Wastewater Treatment Plant), January 2022–December 2023. City of San Diego Ocean Monitoring Program, Public Utilities Department, Environmental Monitoring and Technical Services Division, San Diego, CA.
- City of San Diego. (2022–2024b). Monthly Receiving Waters Monitoring Reports for the South Bay Ocean Outfall (South Bay Water Reclamation Plant), January 2022–December 2023. City of San Diego Ocean Monitoring Program, Public Utilities Department, Environmental Monitoring and Technical Services Division, San Diego, CA.
- City of San Diego. (2022–2024c). Monthly Monitoring Reports for the Point Loma Wastewater Treatment Plant and Ocean Outfall, January 2022–December 2023. City of San Diego, Public Utilities Department, Environmental Monitoring and Technical Services Division, San Diego, CA.
- City of San Diego. (2022–2024d). Monthly Monitoring Reports for the South Bay Water Reclamation Plant and Ocean Outfall, January 2022–December 2023. City of San Diego, Public Utilities Department, Environmental Monitoring and Technical Services Division, San Diego, CA.
- City of San Diego. (2022a). Biennial Receiving Waters Monitoring and Assessment Report for the Point Loma and South Bay Ocean Outfalls, 2020–2021. City of San Diego Ocean Monitoring Program, Public Utilities Department, Environmental Monitoring and Technical Services Division, San Diego, CA.
- City of San Diego. (2022b). Plume Tracking Monitoring Plan Progress Report for the Point Loma and South Bay Ocean Outfall Regions, San Diego, California; Report Period: January – December 2021. Submitted by the City of San Diego Public Utilities Department to the San Diego Water Board and USEPA, Region IX, March 3, 2023.
- City of San Diego. (2022c). Appendix D. Plume Behavior and Tracking Summary. In: Report of Waste Discharge and Application for Renewal of NPDES CA 0107409 and 301(h) Modified Secondary Treatment Requirements. Volume VI, Appendices D–G. Public Utilities Department, San Diego, CA.

- City of San Diego. (2022d). Appendix P. Oceanography. Appendix Q. Initial Dilution Simulation Models. In: Report of Waste Discharge and Application for Renewal of NPDES CA 0107409 and 301(h) Modified Secondary Treatment Requirements. Volume X, Appendices O–U. Public Utilities Department, San Diego, CA.
- City of San Diego. (2023a). Interim Receiving Waters Monitoring Report for the Point Loma and South Bay Ocean Outfalls, 2022. City of San Diego Ocean Monitoring Program, Public Utilities Department, Environmental Monitoring and Technical Services Division, San Diego, CA.
- City of San Diego. (2023b). Plume Tracking Monitoring Plan Progress Report for the Point Loma and South Bay Ocean Outfall Regions, San Diego, California; Report Period: January – December 2022. Submitted by the City of San Diego Public Utilities Department to the San Diego Water Board and USEPA, Region IX, March 1, 2023.
- City of San Diego. (2024). Plume Tracking Monitoring Plan Progress Report for the Point Loma and South Bay Ocean Outfall Regions, San Diego, California; Report Period: January – December 2023. Submitted by the City of San Diego Public Utilities Department to the San Diego Water Board and USEPA, Region IX, March 1, 2024.
- [CSWRCB] California State Water Resources Control Board, Office of Information Management and Analysis (2024). California Integrated Water Quality System Project, Water Quality Effluent Electronic Self-Monitoring Report (eSMR) Data. <https://data.ca.gov/dataset/water-quality-effluent-electronic-self-monitoring-report-esmr-data>.
- Hess, M. (2019). Satellite & Aerial Coastal Water Quality Monitoring in the San Diego/Tijuana Region: Annual Summary Report 1 January 2018 – 31 December 2018. Littleton, CO.
- Hess, M. (2023). Satellite & Aerial Coastal Water Quality Monitoring in the San Diego/Tijuana Region: Annual Summary Report 1 January 2022 – 31 December 2022. Littleton, CO.
- Hess, M. (2024). Satellite & Aerial Coastal Water Quality Monitoring in the San Diego/Tijuana Region: Annual Summary Report 1 January 2023 – 31 December 2023. Littleton, CO.
- Hope, R.M. (2013). Rmisc: Ryan Miscellaneous. R package version 1.5. <http://CRAN.R-project.org/package=Rmisc>.
- Jackson, G.A. (1986). Physical Oceanography of the Southern California Bight. In: R. Eppley (ed.). Plankton Dynamics of the Southern California Bight. Springer Verlag, New York. p 13–52.
- Jones, B., M.A. Noble, and T.D. Dickey. (2002). Hydrographic and particle distributions over the Palos Verdes continental shelf: Spatial, seasonal and daily variability. *Continental Shelf Research*. 22: 945–965.
- Kelley, D. and C. Richards. (2019). oce: Analysis of Oceanographic Data. R package version 1.1-1. <http://CRAN.R-project.org/package=oce>.

- Largier, J., L. Rasmussen, M. Carter, and C. Scarce. (2004). Consent Decree – Phase One Study Final Report. Evaluation of the South Bay International Wastewater Treatment Plant Receiving Water Quality Monitoring Program to Determine Its Ability to Identify Source(s) of Recorded Bacterial Exceedances. Scripps Institution of Oceanography, University of California, San Diego, CA.
- Le Cao, K-A., F. Rohart, I. Gonzalez, S. Dejean, B. Gautier, F. Bartolo, P. Monget, J. Coquery, F. Yao, and B. Lique. (2017). mixOmics: Omics. R package version 6.8.0. <https://CRAN.R-project.org/package=mixOmics>.
- Lynn, R.J. and J.J. Simpson. (1987). The California Current System: The Seasonal Variability of its Physical Characteristics. *Journal of Geophysical Research*. 92(C12): 12947–12966.
- Mann, K.H. and J.R.N. Lazier. (1991). *Dynamics of Marine Ecosystems, Biological–Physical Interactions in the Oceans*. Blackwell Scientific Publications, Boston.
- MATLAB. (2022). Version R2022b. The MathWorks Inc., Natick, Massachusetts. URL <https://www.mathworks.com/products/matlab.html>.
- Morgan, P., and L. Pender. (2014). SEAWATER library for calculating EOS-80 properties of seawater in MATLAB. CSIRO Marine Research, version 3.3.1. http://www.cmar.csiro.au/datacentre/ext_docs/seawater.htm.
- Nezlin, N.P, J.A.T. Booth, C. Beegan, C.L. Cash, J.R. Gully, A. Latker, M.J. Mengel, G.L. Robertson, A. Steele, and S.B. Weisberg. (2016). Assessment of wastewater impact on dissolved oxygen around southern California’s submerged ocean outfalls. *Regional Studies in Marine Science*. In Press.
- Nychka, D., R. Furrer, J. Paige, S. Sain. (2021). “fields: Tools for spatial data.” R package version 13.3, <https://github.com/dnychka/fieldsRPackage>.
- Ocean Imaging. (2024). Ocean Imaging Corporation archive of aerial and satellite-derive images. <http://www.oceani.com/SanDiegoWater/index.html>.
- Paver, C.R., L.A. Codispoti, V.J. Coles, and L.W. Cooper. (2020). Sampling errors arising from carousel entrainment and insufficient flushing of oceanographic samples bottles. *Limnology & Oceanography: Methods*, 18: 311–326.
- Pickard, D.L. and W.J. Emery. (1990). *Descriptive Physical Oceanography*. 5th Ed. Pergamon Press, Oxford.
- R Core Team. (2023). R: A language and environment for statistical computing. R Foundation for Statistical Computing, Vienna, Austria. URL <https://www.R-project.org/>.
- Ripley, B. and M. Lapsley. (2017). RODBC: ODBC Database Access. R package version 1.3-12. <http://CRAN.R-project.org/package=RODBC>.
- Rogowski, P., E. Terrill, M. Otero, L. Hazard, S.Y. Kim, P.E. Parnell, and P. Dayton. (2012a). Final Report: Point Loma Ocean Outfall Plume Behavior Study. Prepared for City of San Diego Public Utilities Department by Scripps Institution of Oceanography, University of California, San Diego, CA.

- Rogowski, P., E. Terrill, M. Otero, L. Hazard, and W. Middleton. (2012b). Mapping ocean outfall plumes and their mixing using Autonomous Underwater Vehicles. *Journal of Geophysical Research*, 117: C07016.
- Rogowski, P., E. Terrill, M. Otero, L. Hazard, and W. Middleton. (2013). Ocean outfall plume characterization using an Autonomous Underwater Vehicle. *Water Science & Technology*, 67(4): 925–933.
- [SIO] Scripps Institution of Oceanography. (2004). Point Loma Outfall Project, Final Report, September 2004. Scripps Institution of Oceanography, University of California, La Jolla, CA.
- Soetaert, K., T. Petzoldt, F. Meysman, and L. Meire. (2020). “marelac: tools for aquatic sciences” R package version 2.1.10. <https://CRAN.R-project.org/package=marelac>.
- Storms, W.E., T.D Stebbins, and P.E. Parnell. (2006). San Diego Moored Observation System Pilot Study Workplan for Pilot Study of Thermocline and Current Structure off Point Loma, San Diego, California. City of San Diego, Metropolitan Wastewater Department, Environmental Monitoring and Technical Services Division, and Scripps Institution of Oceanography, La Jolla, CA.
- Svejkovsky, J. (2010). Satellite and Aerial Coastal Water Quality Monitoring in the San Diego/Tijuana Region: Annual Summary Report, 1 January 2009–31 December 2009. Ocean Imaging, Solana Beach, CA.
- Svejkovsky, J. and B. Jones. (2001). Detection of coastal urban storm water and sewage runoff with synthetic aperture radar satellite imagery. *Eos, Transactions, American Geophysical Union*, 82, 621–630.
- [SWRCB] California State Water Resources Control Board. (2019). California Ocean Plan, Water Quality Control Plan, Ocean Waters of California. California Environmental Protection Agency, Sacramento, CA.
- Terrill, E., K. Sung Yong, L. Hazard, and M. Otero. (2009). IBWC/Surfrider – Consent Decree Final Report. Coastal Observations and Monitoring in South Bay San Diego. Scripps Institution of Oceanography, University of California, San Diego, CA.
- Warnes, G., B. Bolker, and T. Lumley. (2021). gtools: Various R Programming Tools. R package version 3.5.0. <http://CRAN.R-project.org/package=gtools>.
- Washburn, L., B.H. Jones, A. Bratkovich, T.D. Dickey, and M.S. Chen. (1992). Mixing, dispersion, and resuspension in vicinity of ocean wastewater plume. *Journal of Hydraulic Engineering*, 118: 38–58.
- Weber, E.D., T.D. Auth, S. Baumann-Pickering, T.R. Baumgartner, E.P. Bjorkstedt, S.J. Bograd, B.J. Burke, J.L. Cadena-Ramirez, E.A. Daly, M. de la Cruz, H. Dewar, J.C. Field, J.L. Fisher, A. Giddings, R. Goericke, E. Gomez-Ocampo, J. Gomez-Valdes, E.L. Hazen, J. Hildebrand, C.A. Horton, K.C. Jacobson, M.G. Jacox, J. Jahncke, M. Kahru, R.M. Kudela, B.E. Lavaniegos, A. Leising, S.R. Melin, L.E. Miranda-Bojorquez, C.A. Morgan, C.F. Nickels, R.A. Orben, J.M. Porquez, E.J. Portner, R.R. Robertson, D.L. Rudnick, K.M. Sakuma, J.A. Santora, I.D. Schroeder,

O.E. Snodgrass, W.J. Sydeman, A.R. Thompson, S.A. Thompson, J.S. Trickey, J. Villegas-Mendoza, P. Warzybok, W. Watson, and S.M. Zeman. (2021). State of the California Current 2019-2020: Back to the Future with Marine Heatwaves? *Frontiers in Marine Science*, 8: 1-23.

Wickham, H. (2007). Reshaping Data with the reshape Package. *Journal of Statistical Software*, 21(12), 1-20, <http://www.jstatsoft.org/v21/i12/>.

Wickham, H., M. Averick, J. Bryan, W. Chang, L. D'Agostino McGowan, R. François, G. Grolemund, A. Hayes, L. Henry, J. Hester, M. Kuhn, T. Lin Pedersen, E. Miller, S. Milton Bache, K. Müller, J. Ooms, D. Robinson, D. P. Seidel, V. Spinu, K. Takahashi, D. Vaughan, C. Wilke, K. Woo, H. Yutani. (2019). Welcome to the tidyverse. *Journal of Open Source Software*, 4(43), 1686, <https://doi.org/10.21105/joss.01686>.

Wickham, H. and D. Seidel. (2020). scales: Scale Functions for Visualization. R package version 1.1.1. <https://CRAN.R-project.org/package=scales>.

CHAPTER 4

FIGURES & TABLES

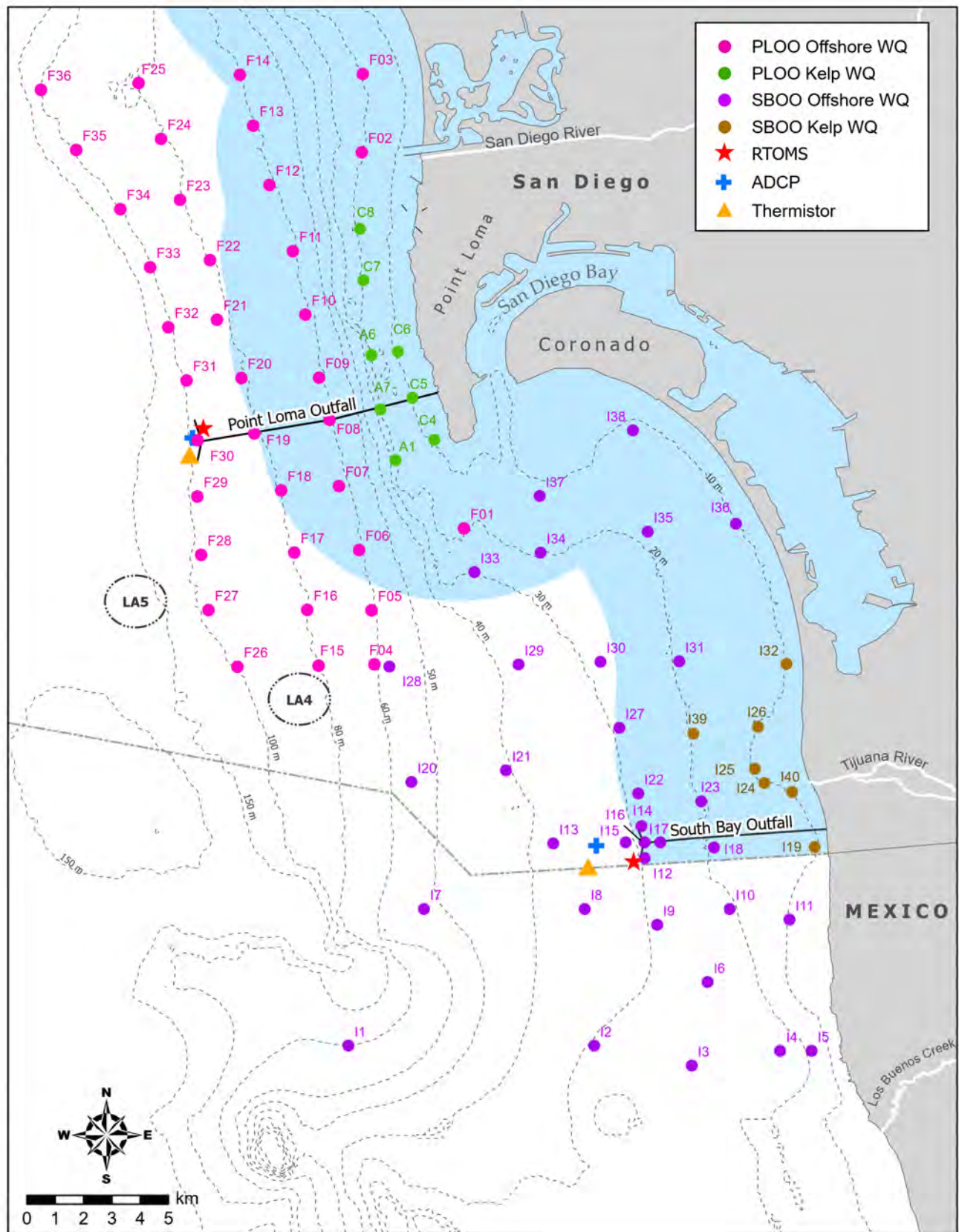


Figure 4.1

Oceanographic mooring and monitoring station locations around the PLOO and SBOO sampled as part of the City of San Diego's Ocean Monitoring Program. Light blue shading represents State jurisdictional waters.

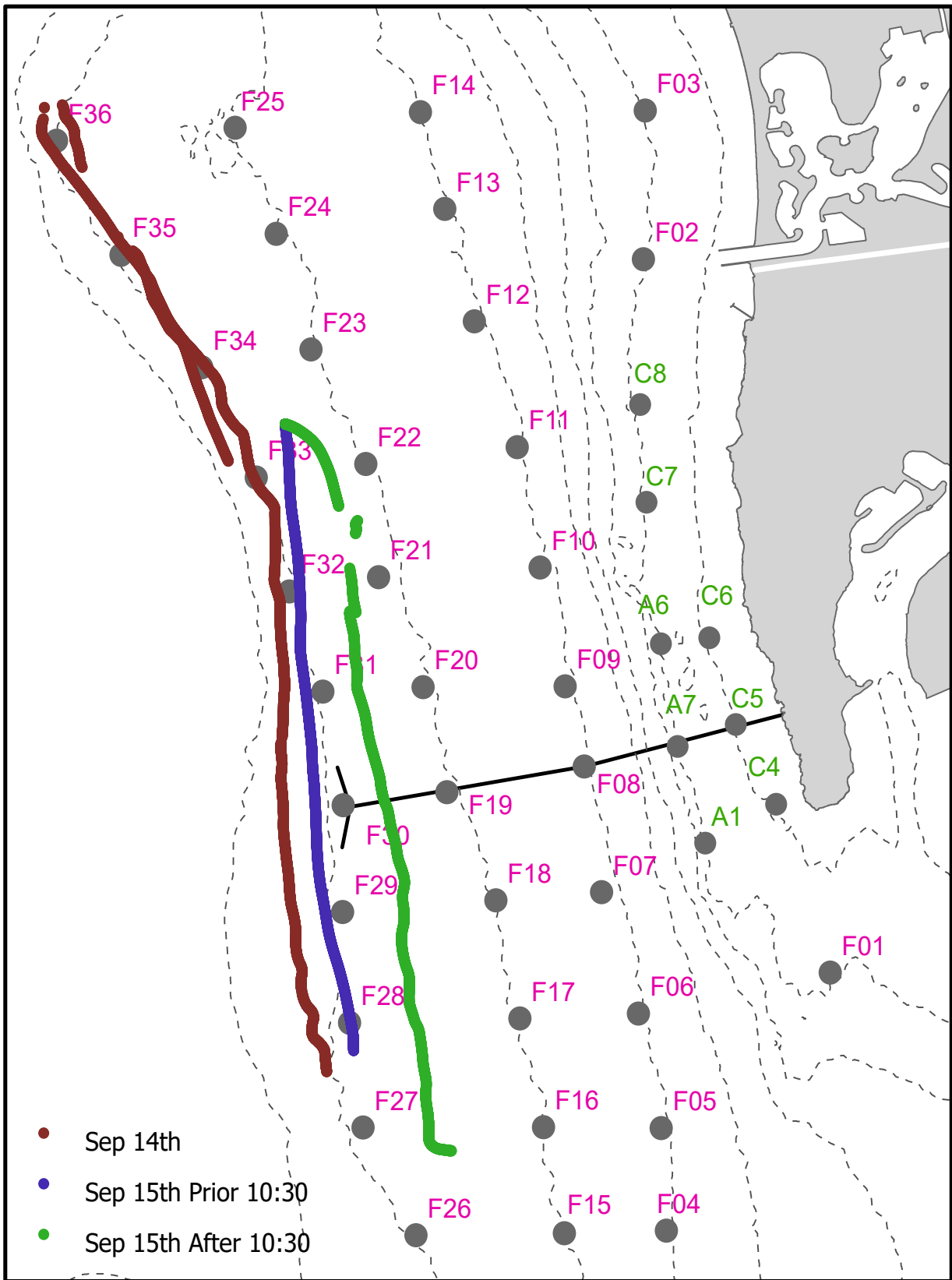


Figure 4.2

The ROTV tow path for the fall 2022 survey in the PLOO region. Sampling was conducted parallel to the regular offshore water quality stations. Colors indicate separate deployments.

Table 4.1

Summary of the numbers of reference stations, potential wastewater plume detections, and out-of-range values at offshore stations during 2022 and 2023. DO = dissolved oxygen; XMS = transmissivity.

			Reference Stations	Potential Plume Detections	Out of Range		
					DO	pH	XMS
PLOO	2022	Feb	18	10	3	0	2
		May	4	6	1	0	6
		Aug	14	6	0	0	1
		Nov	19	8	1	0	7
	2023	Feb	13	8	4	0	4
		May	10	6	0	0	0
		Aug	24	6	4	0	0
		Nov	32	3	0	0	0
	Detection Rate (%)			16	4	0	6
	Total Count			53	13	0	20
	Total Samples			328	328	328	328
	SBOO	2022	Feb	20	3	0	0
May			16	4	1	0	2
Aug			16	5	0	0	2
Nov			21	0	0	0	0
2023		Feb	11	2	0	0	2
		May	12	5	0	0	4
		Aug	18	4	0	0	2
		Nov	18	3	0	0	2
Detection Rate (%)			11	<1	0	7	
Total Count			26	1	0	17	
Total Samples			232	232	232	232	

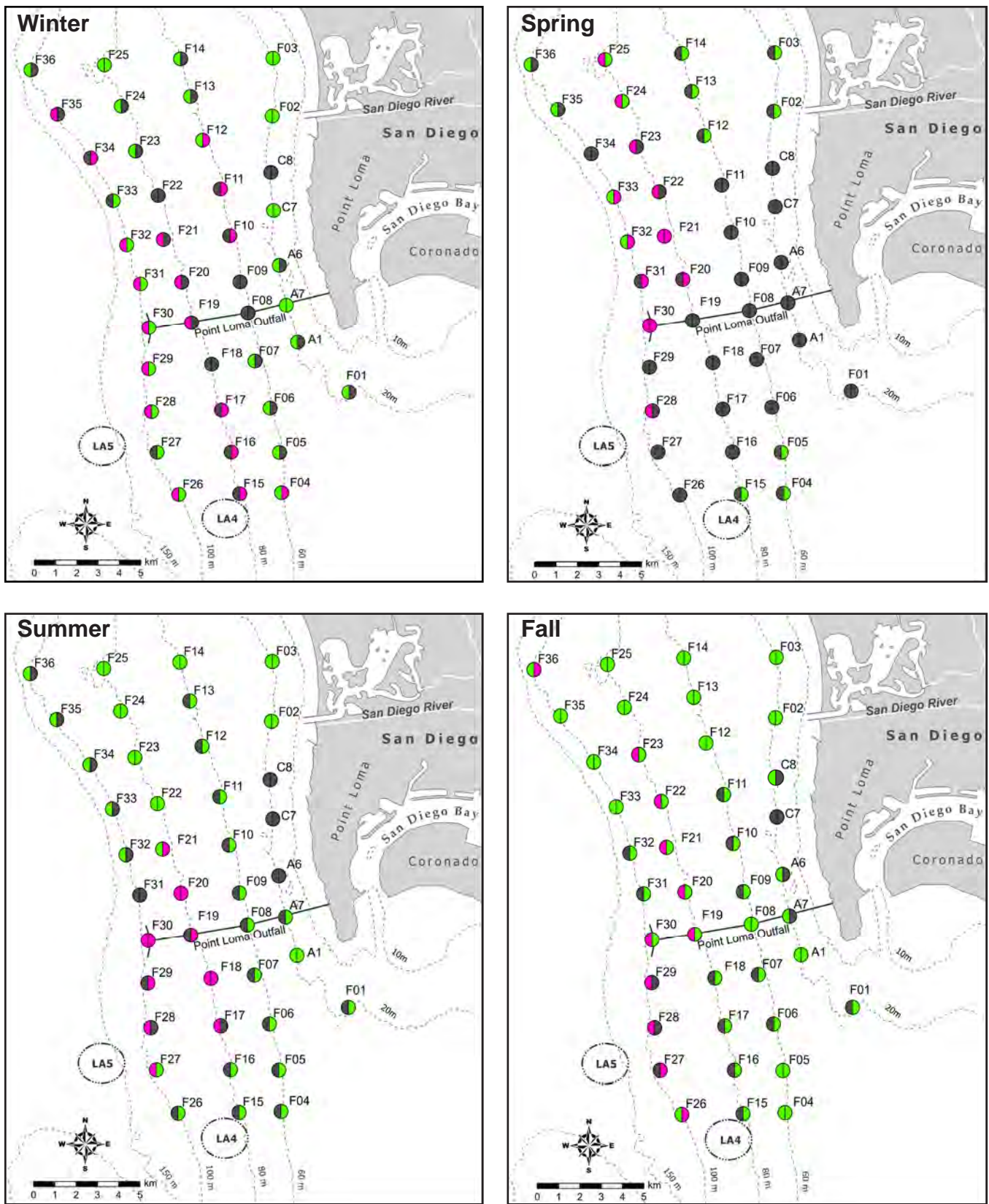


Figure 4.3
 Distribution of stations meeting potential plume criteria (pink), those used as reference stations (green), and stations meeting neither criteria (grey) near the PLOO (this page) and SBOO (facing page) during quarterly surveys in 2022 (left half of circle) and 2023 (right half).

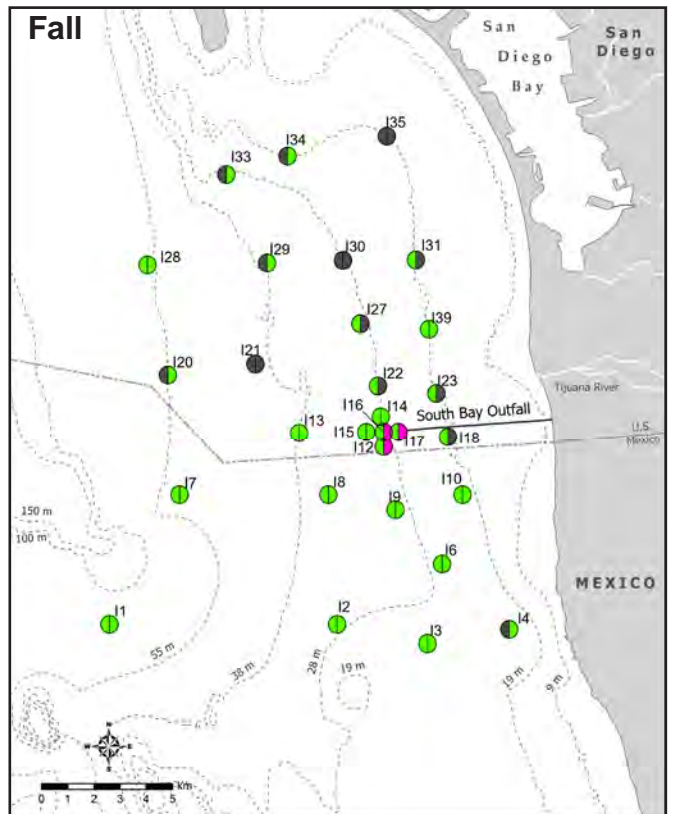
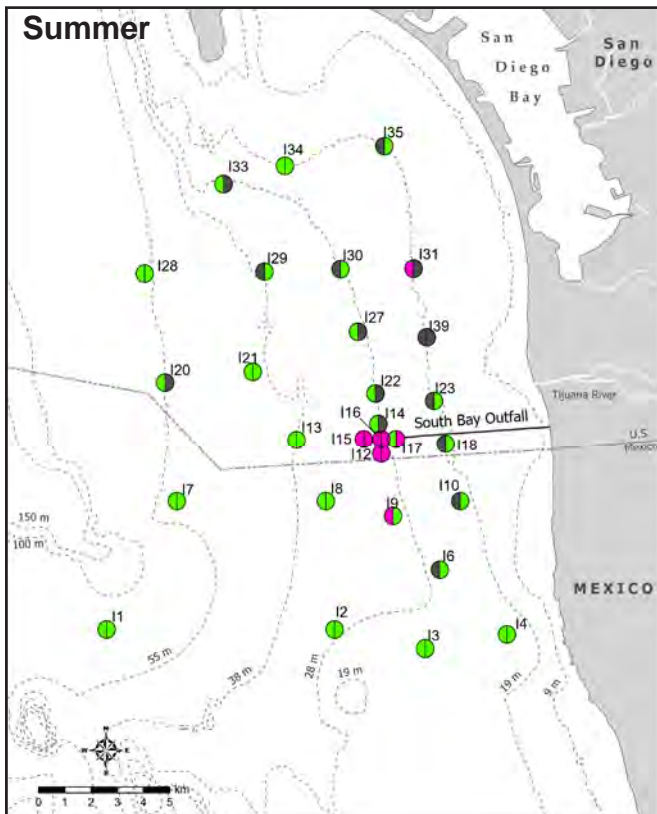
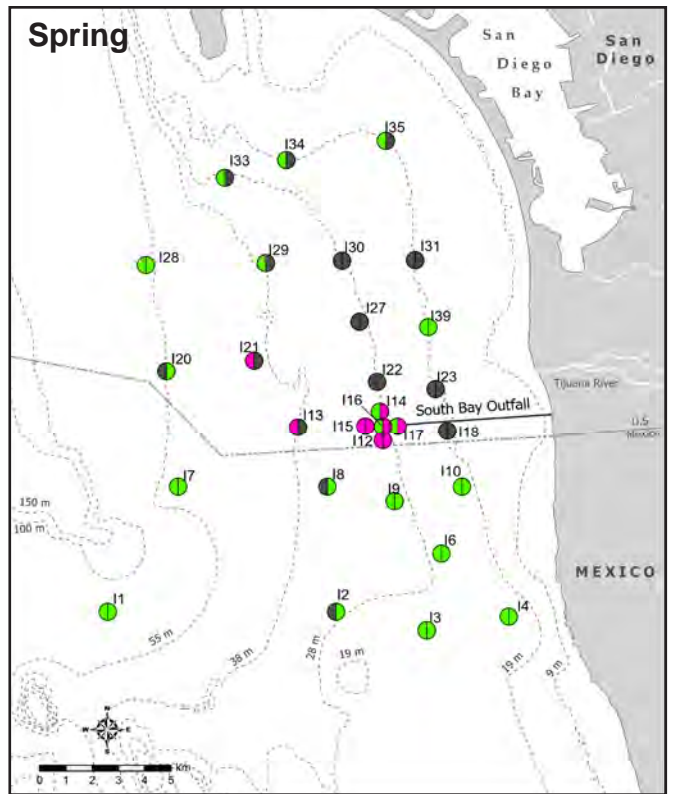
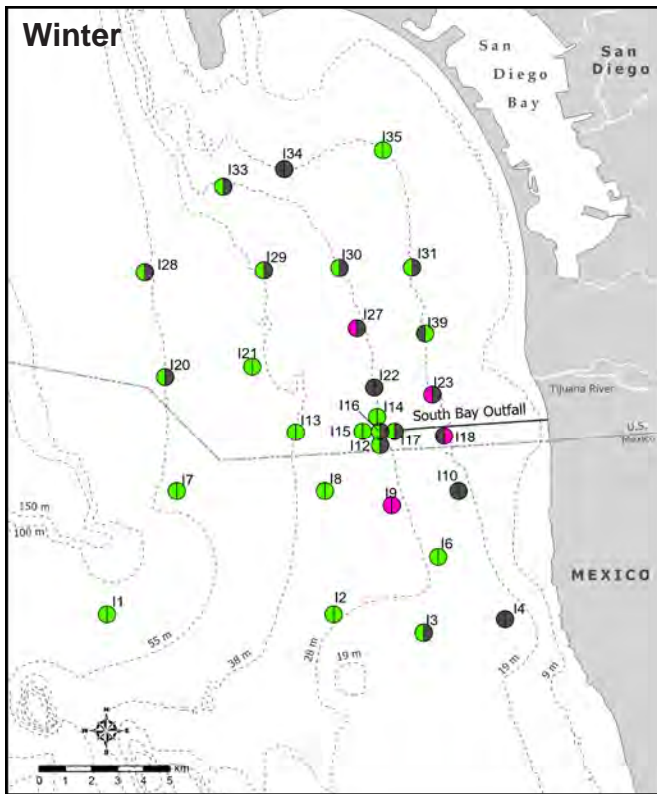


Figure 4.3 *continued*

PLOO

Farfield Nearfield

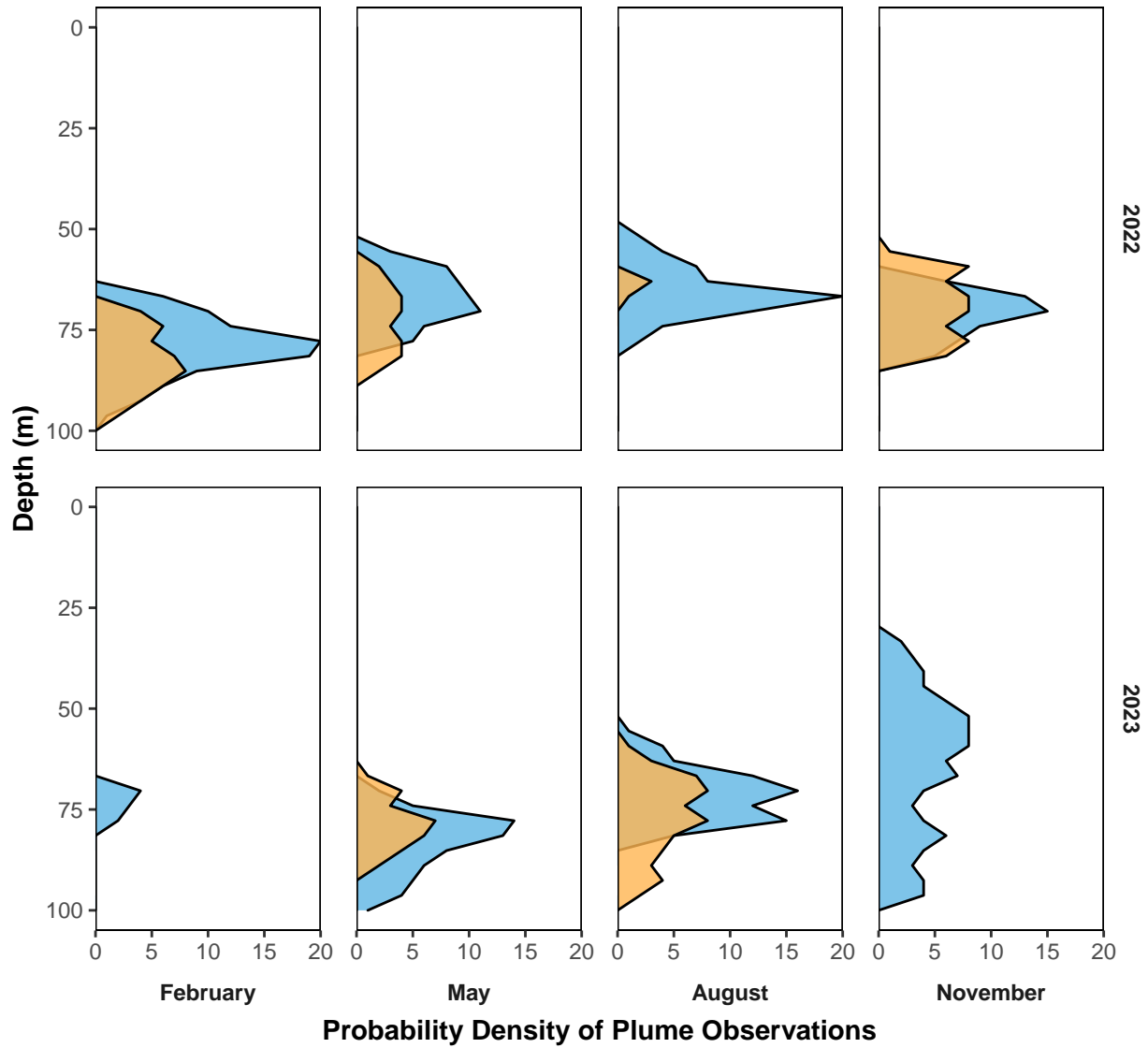


Figure 4.4

Depth profiles by season of the probability density of potential plume detections at PLOO and SBOO offshore stations during 2022 and 2023. Nearfield stations for PLOO are F29, F30, F31; nearfield stations for SBOO are I12, I14, I15, I16.

SBOO

Farfield Nearfield

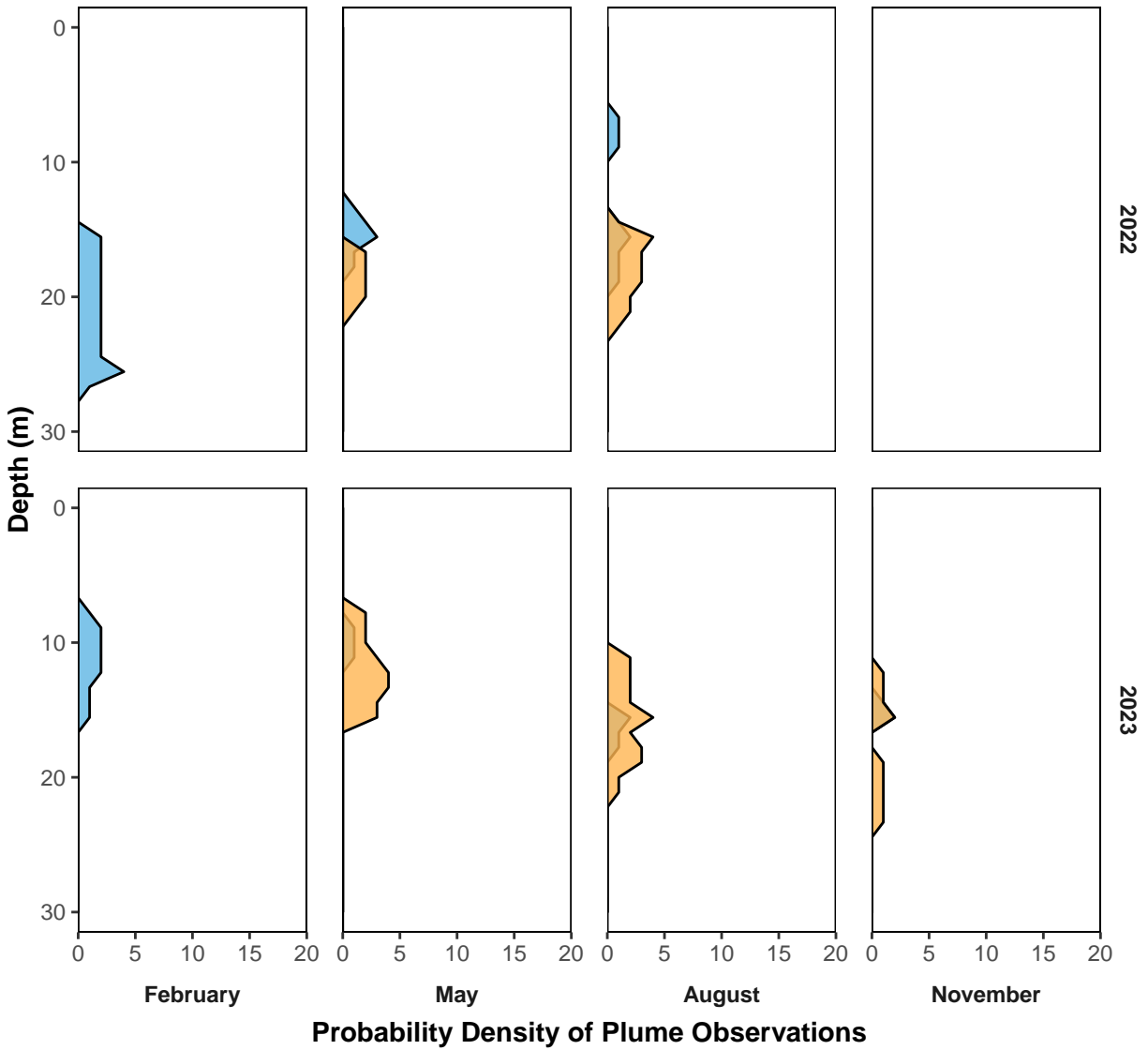


Figure 4.4 *continued*

PLOO

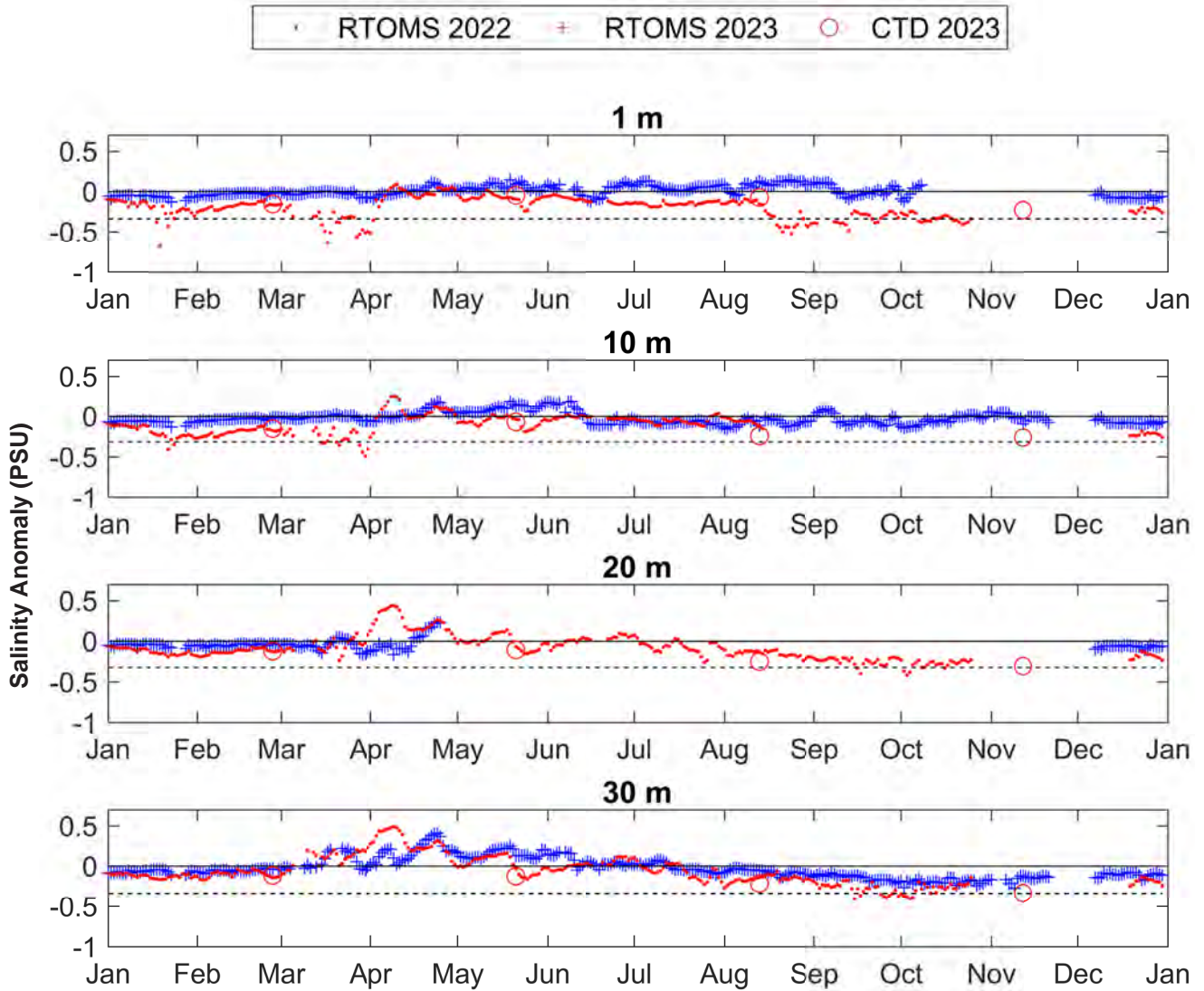


Figure 4.5

Daily averaged salinity anomalies from 2022 (blue) to 2023 (red) for each mooring sensor depth shown using available RTOMS data. Anomalies calculated from historical CTD survey data from 2001–2023 for each monitoring region and depth range, excluding nearfield stations (see text). Dashed line indicates 99th percentile minimum from CTD survey data. Due to low regional salinities in late 2023, mean salinity anomalies from each quarterly CTD survey from farfield stations are also shown for 2023 (open red circles; see text).

PLOO

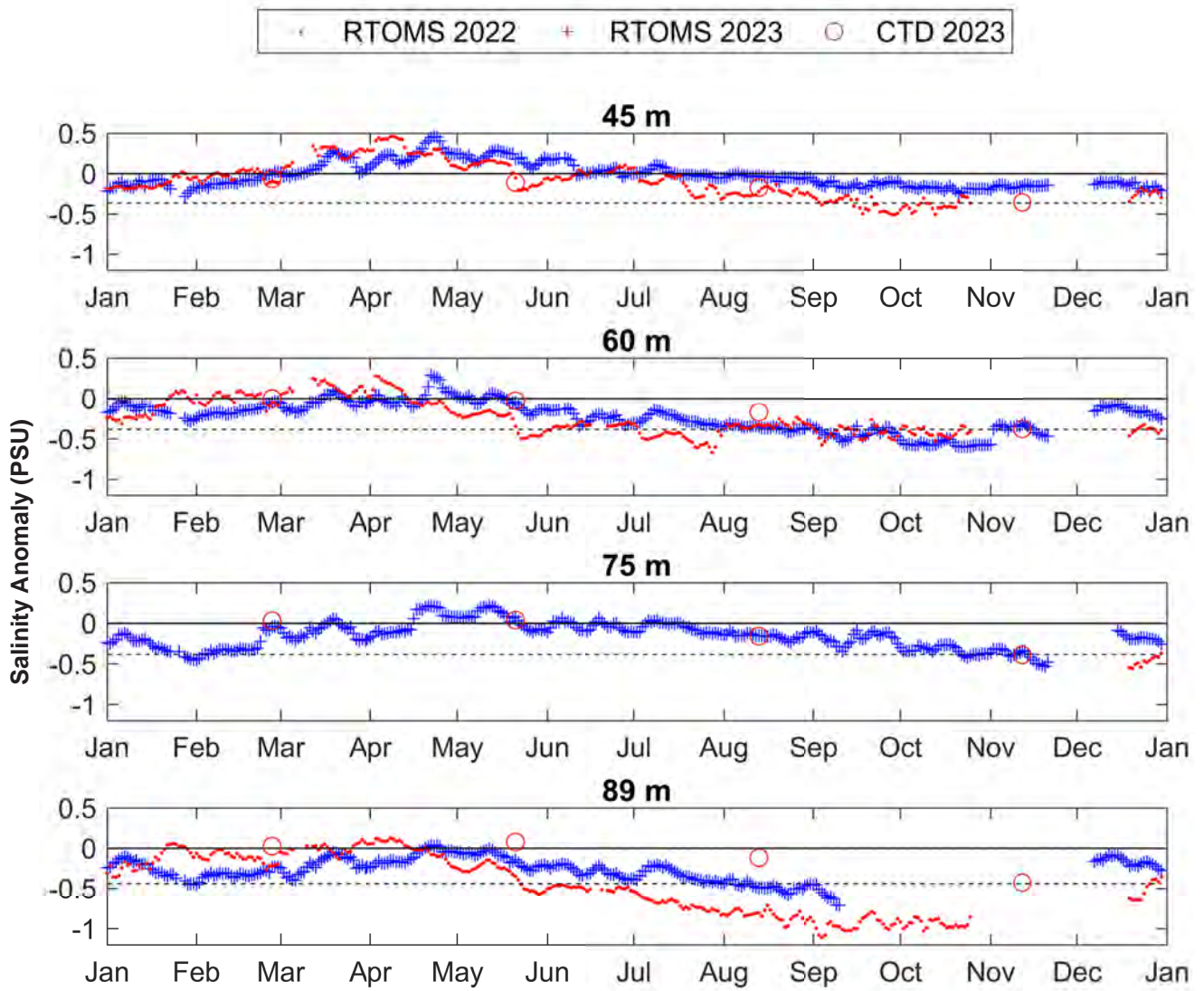


Figure 4.5 *continued*

SBOO

RTOMS 2022 RTOMS 2023 CTD 2023

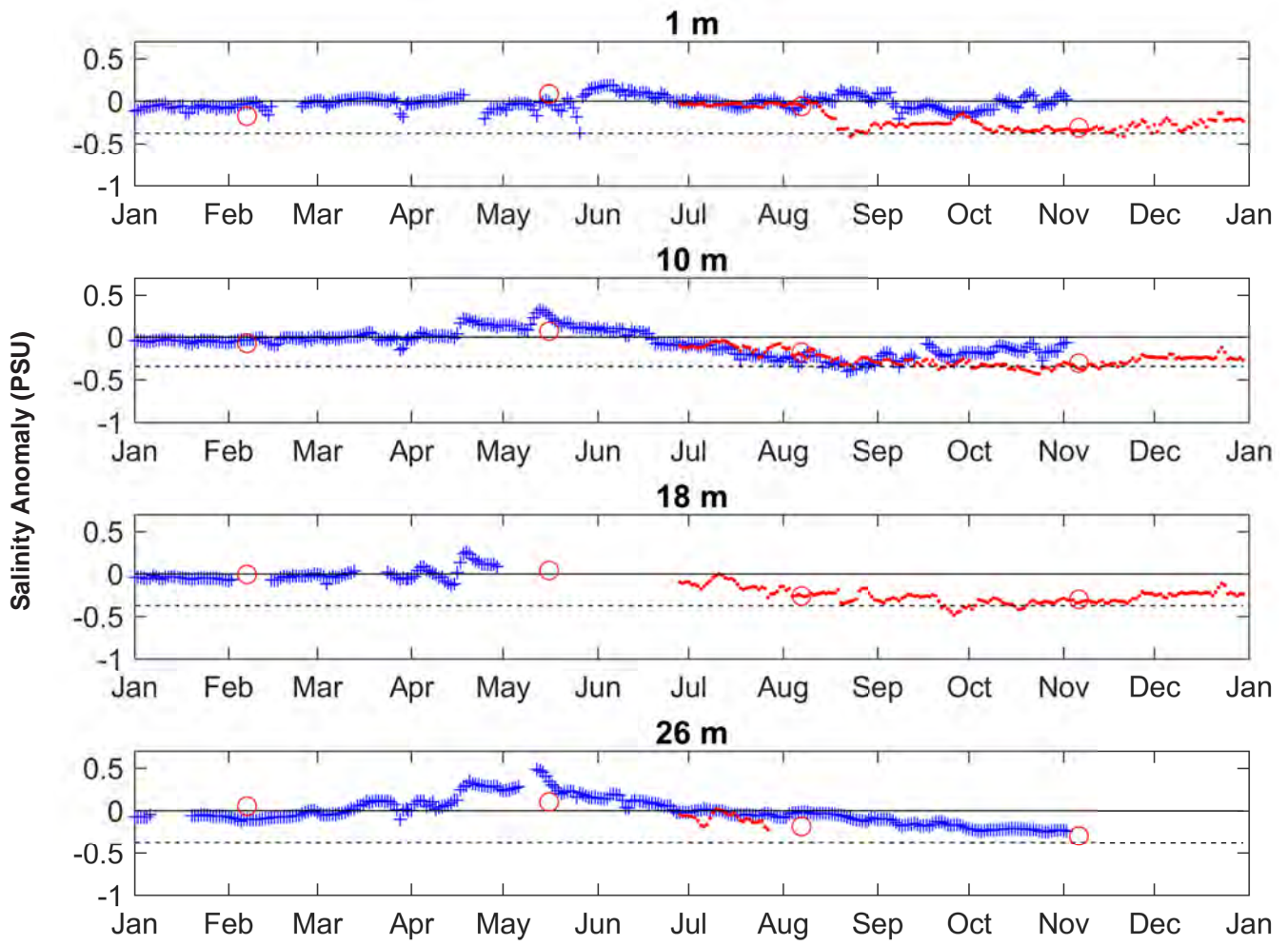


Figure 4.5 *continued*

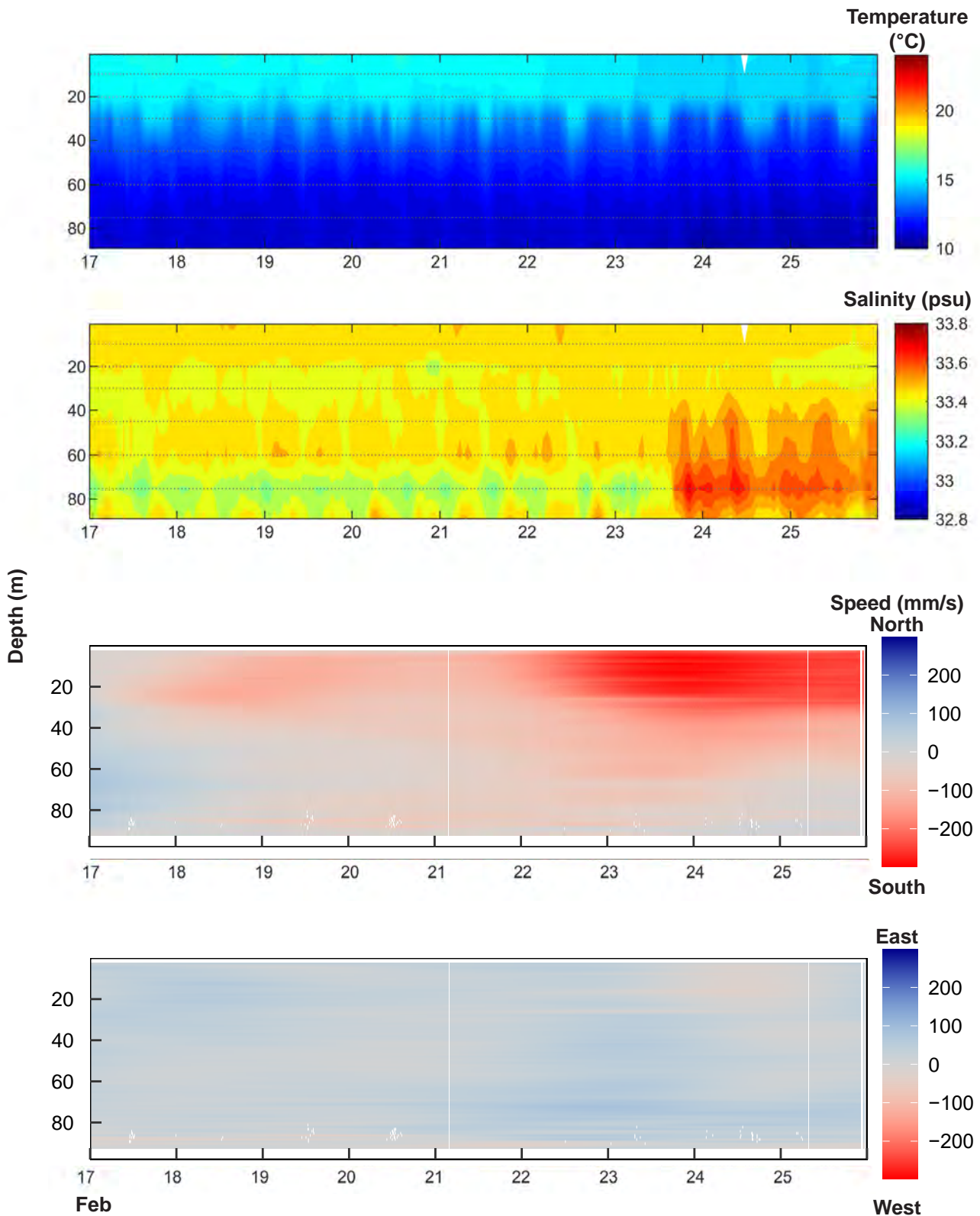


Figure 4.6

PLOO RTOMS hourly averaged ocean temperature, salinity, and current speeds (tides removed) interpolated for entire water column plus chlorophyll *a* (chl), CDOM, turbidity, and nitrate + nitrite for subsurface depths to show a change in conditions during the week of February 17–February 25, 2022. Gaps and white areas indicate loss of data due to instrumentation issues or failure to meet data quality criteria (see text).

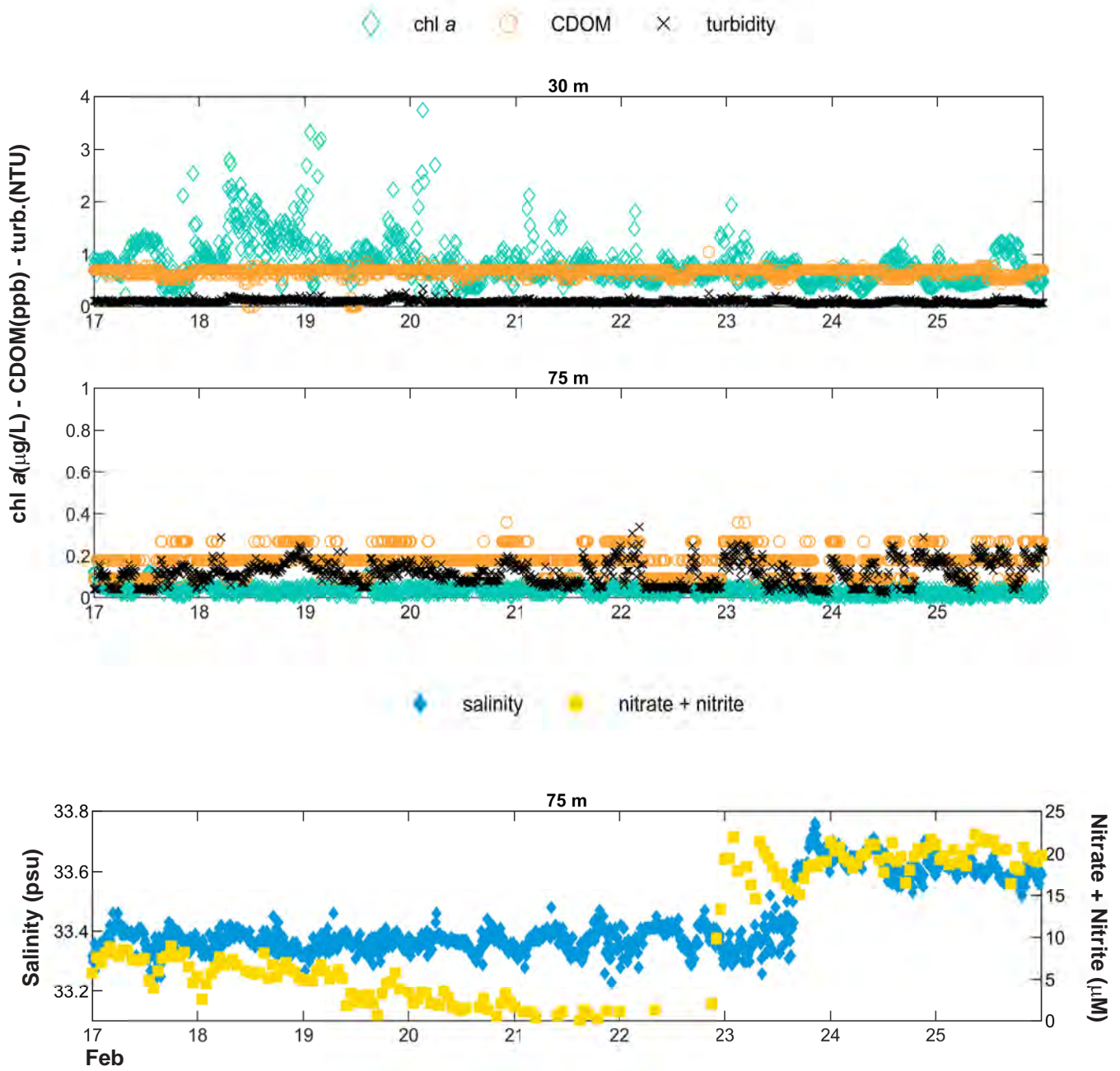


Figure 4.6 *continued*

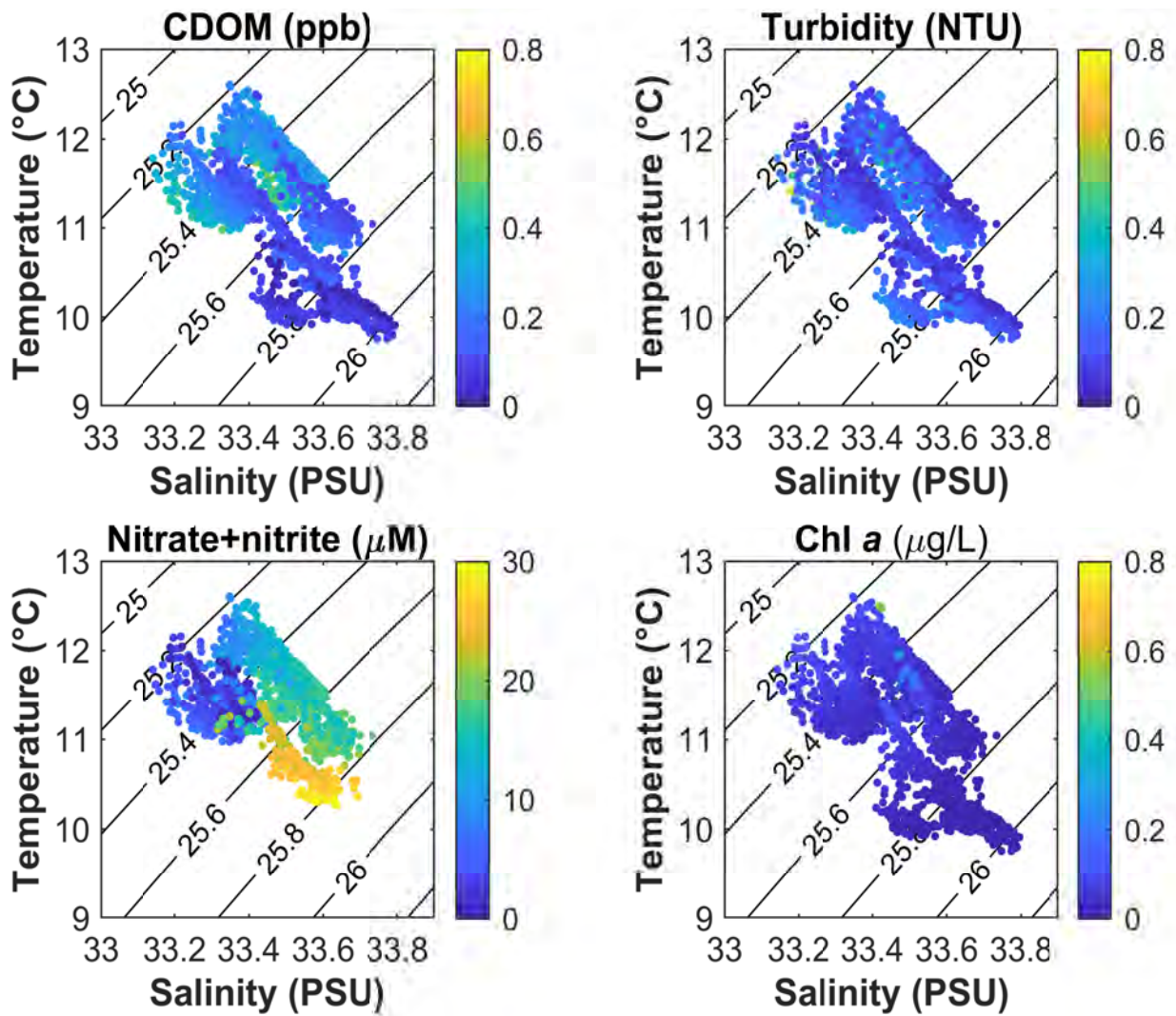


Figure 4.7

PLOO RTOMS hourly averaged CDOM, turbidity, nitrate + nitrite, and chlorophyll a shown on temperature versus salinity plots at 89 m for winter 2022 and 2023 (January–March). Isopycnals and corresponding σ -t values shown by black lines.

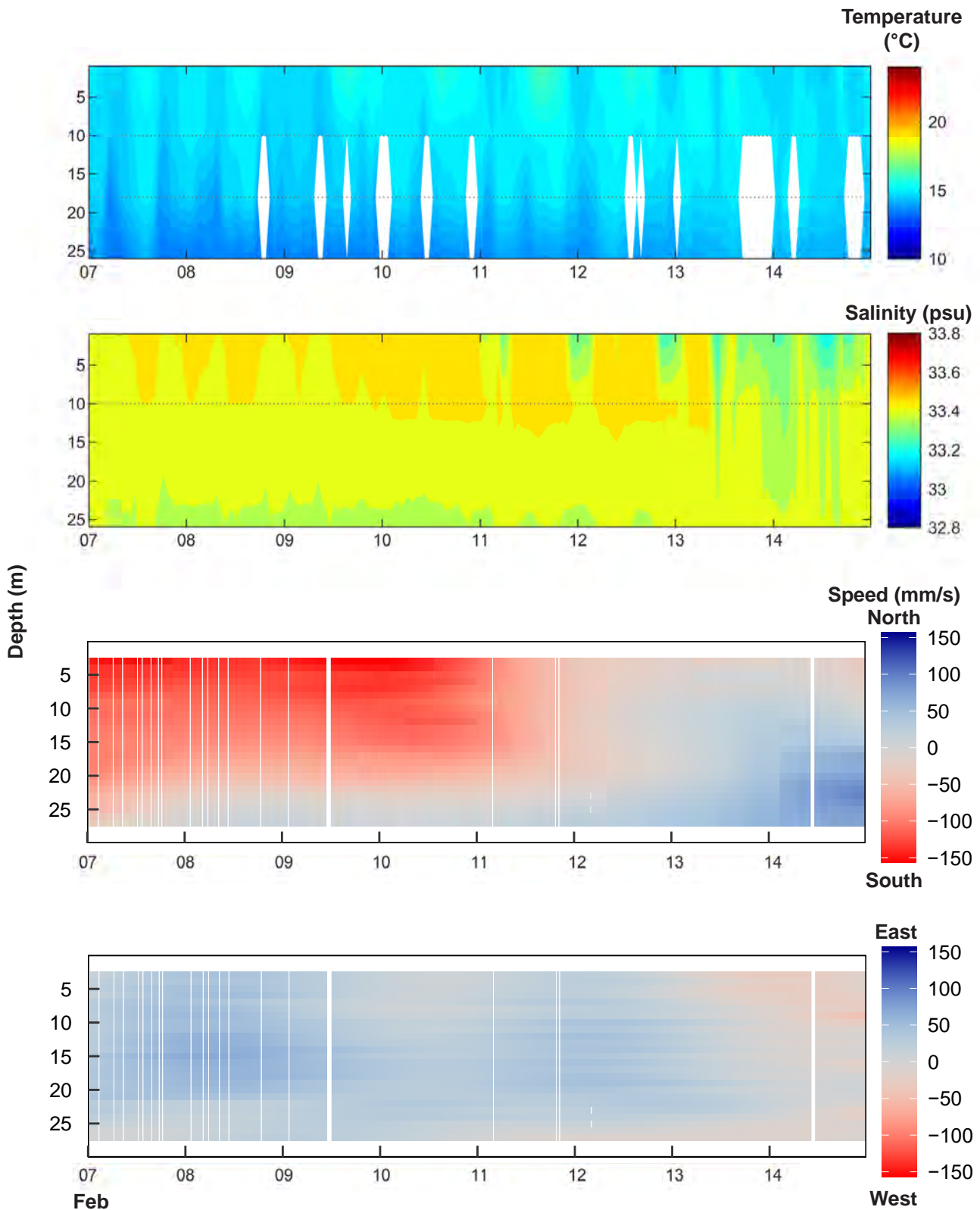


Figure 4.8

SBOO RTOMS hourly averaged ocean temperature, salinity, and current speeds (tides removed) interpolated for entire water column plus chlorophyll *a* (chl), CDOM, turbidity, and nitrate + nitrite for select depths during the week of February 7–14, 2022. Gaps and white areas indicate loss of data due to instrumentation issues or failure to meet data quality criteria (see text).

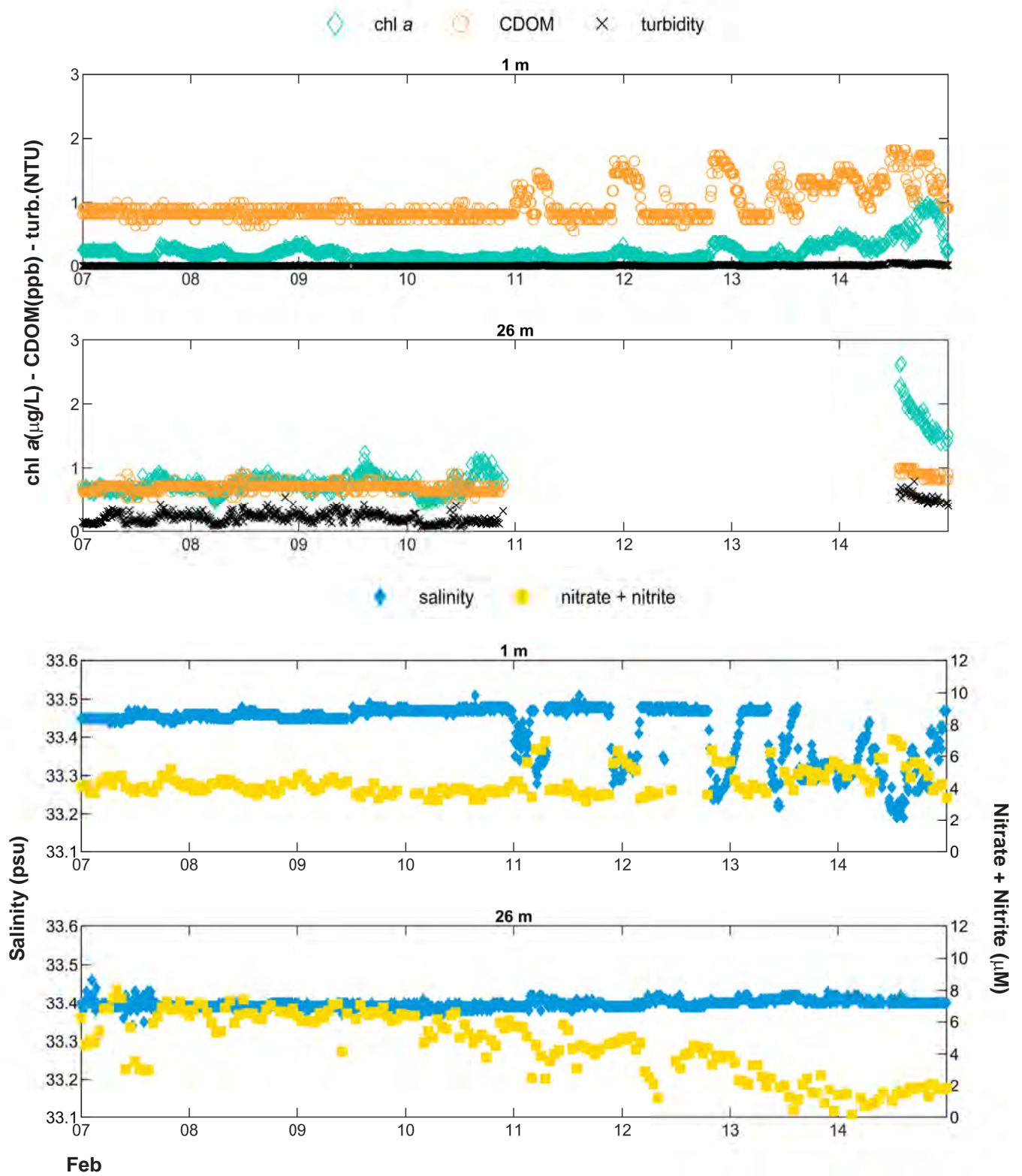


Figure 4.8 continued

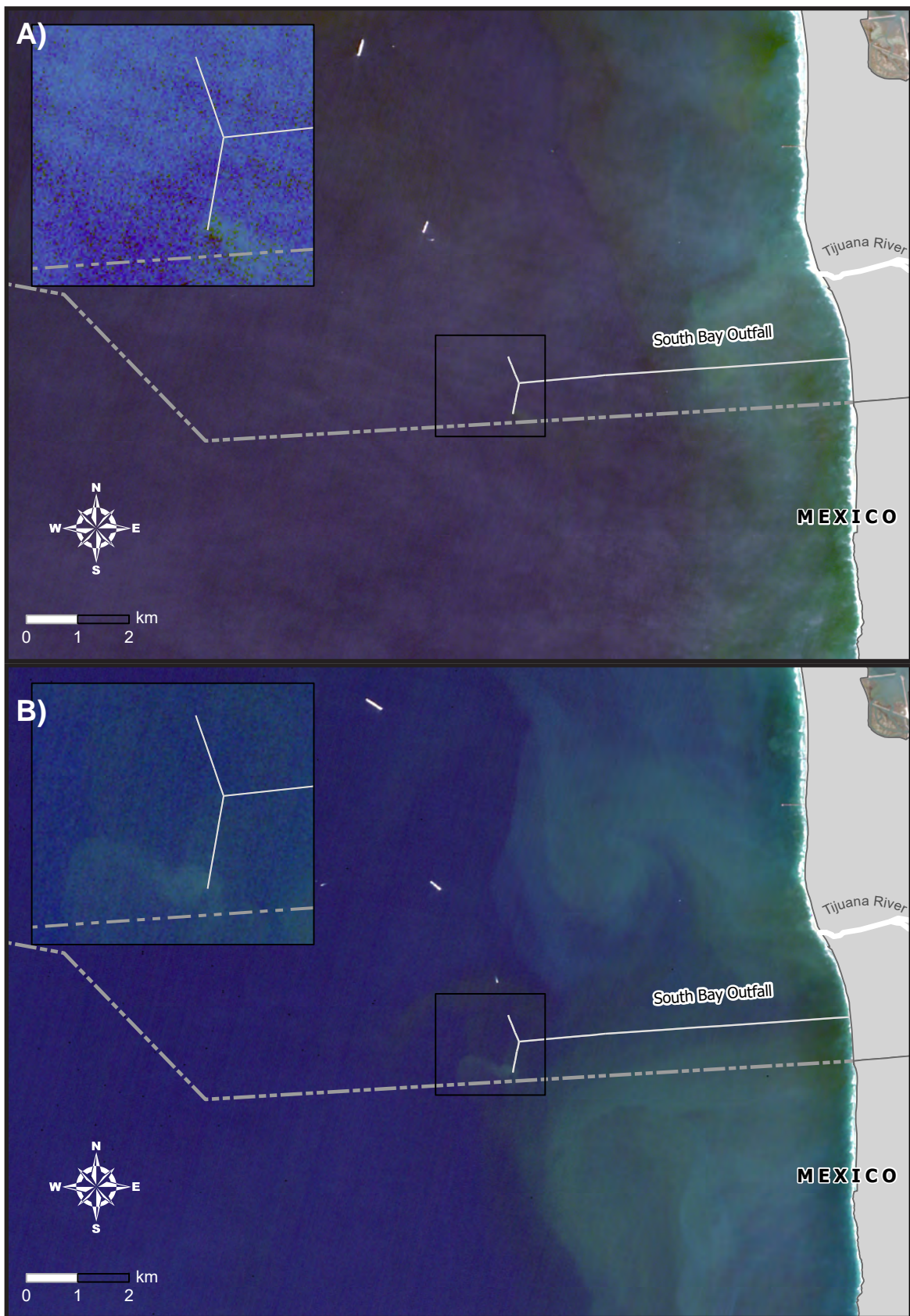


Figure 4.9

Sentinel 2A/2B high resolution satellite images of the South Bay region acquired that show SBOO-related wastewater plume at the surface on A) February 12, 2022 and B) February 14, 2022. (Ocean Imaging 2024).

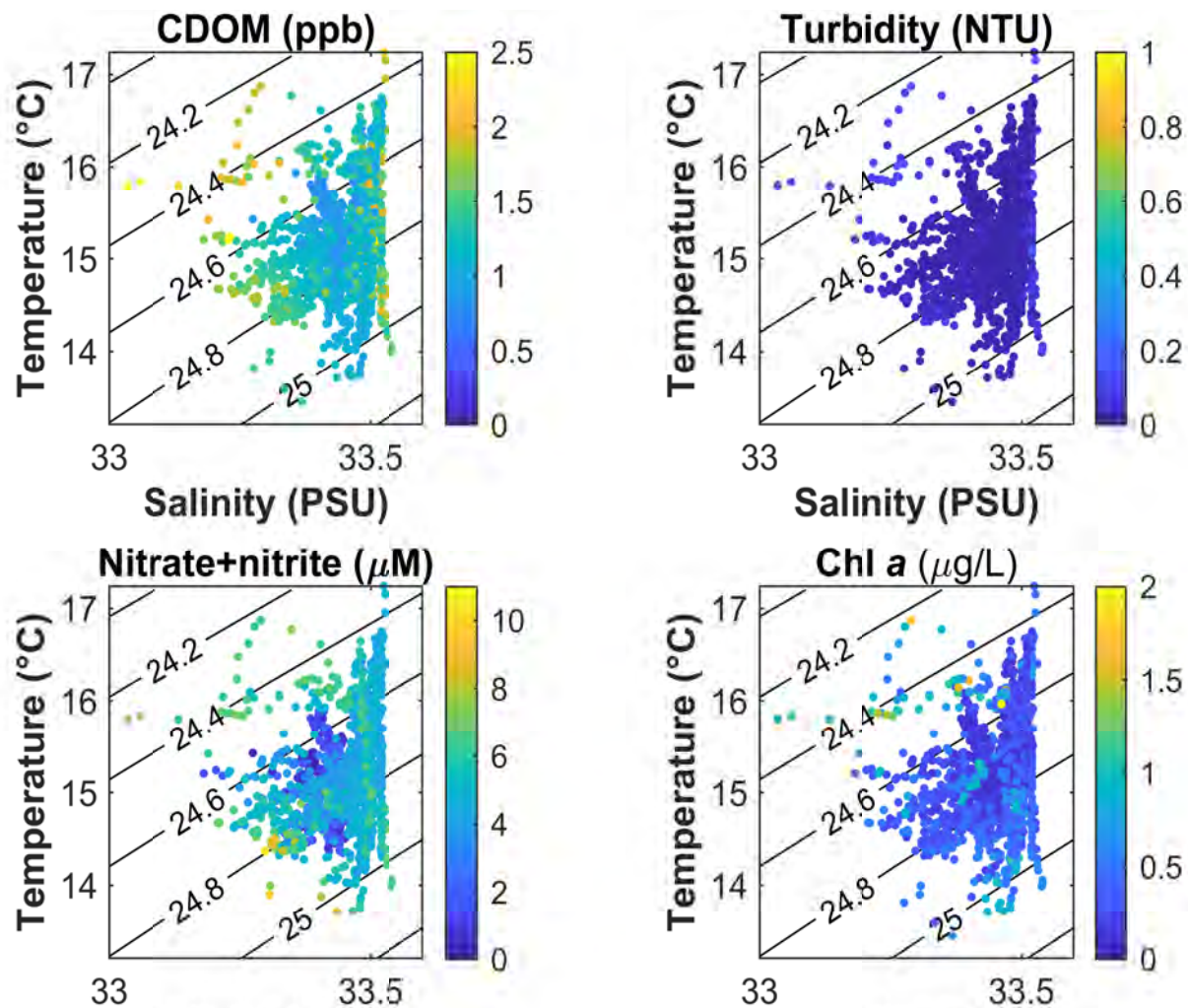


Figure 4.10

SBOO RTOMS hourly averaged CDOM, turbidity, nitrate + nitrite, and chlorophyll a shown on temperature versus salinity plots at 1 m for winter 2022 (January–March). Isopycnals and corresponding σ_t values shown by black lines. No SBOO RTOMS data are available during winter 2023 (see text).

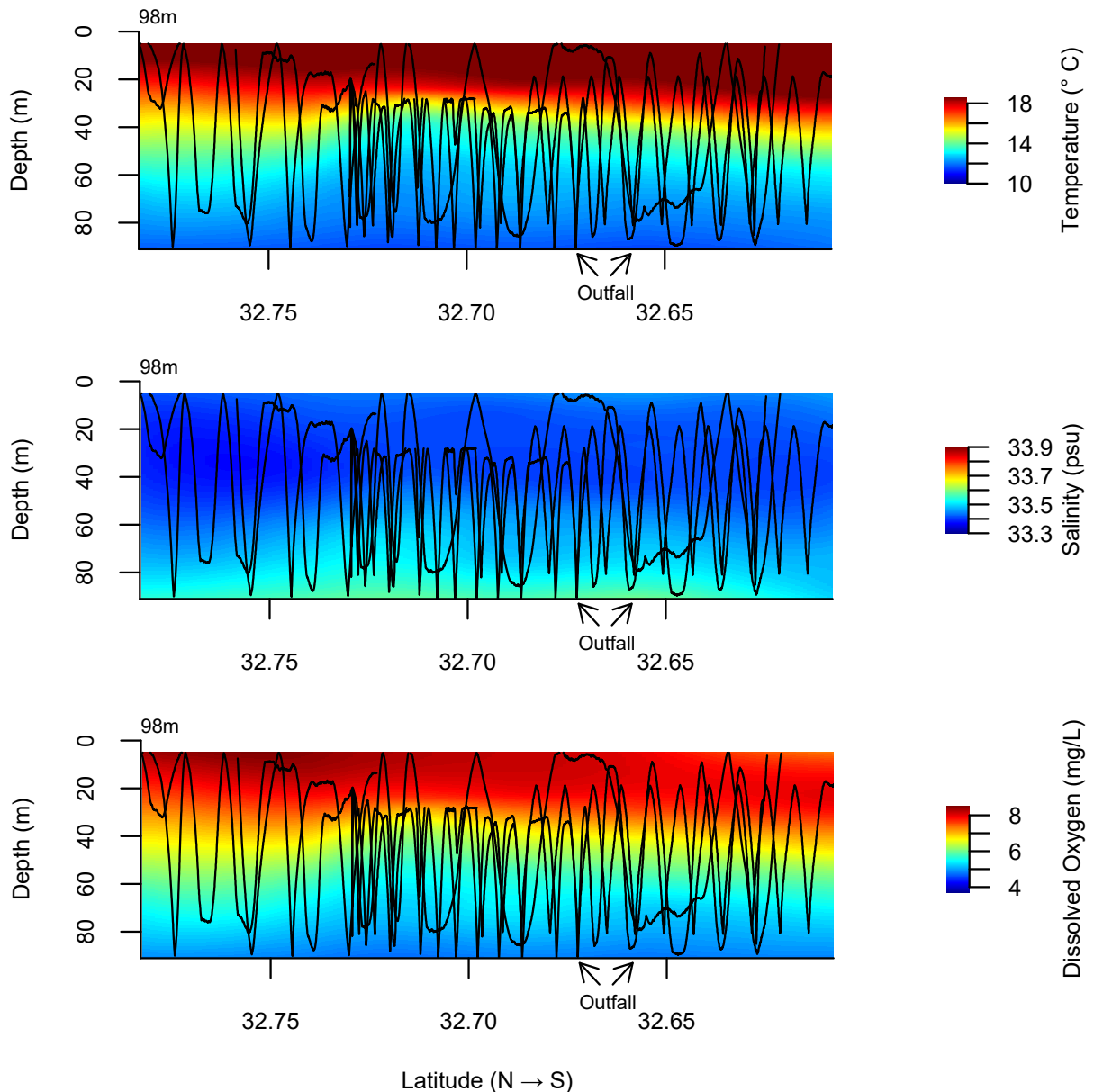


Figure 4.11

Select data from ROTV surveys of the PLOO region conducted September 14 and 15, 2022 along the 98m isobath. Data are interpolated over the water column using a LOESS regression. Black lines indicate the position of the ROTV in the water column. The two active ends of the outfall's wye are indicated by black arrows. Scales for each parameter are bounded by the 5th and 95th percentile of observed data for the region, using CTD-based observations from 2014-2020, with the exception of Optical Brightener, which uses the 5th and 95th percentile of observations made by previous ROTV surveys, and CDOM, which is scaled to highlight any potential plume signatures, typically observed as elevated CDOM (values exceeding roughly 1.6 ppb) positioned near the outfall wye. Anomalous color extremes occurring at plot edges and corners where ROTV position was not recorded are probable artifacts of the interpolation and to be interpreted with caution.

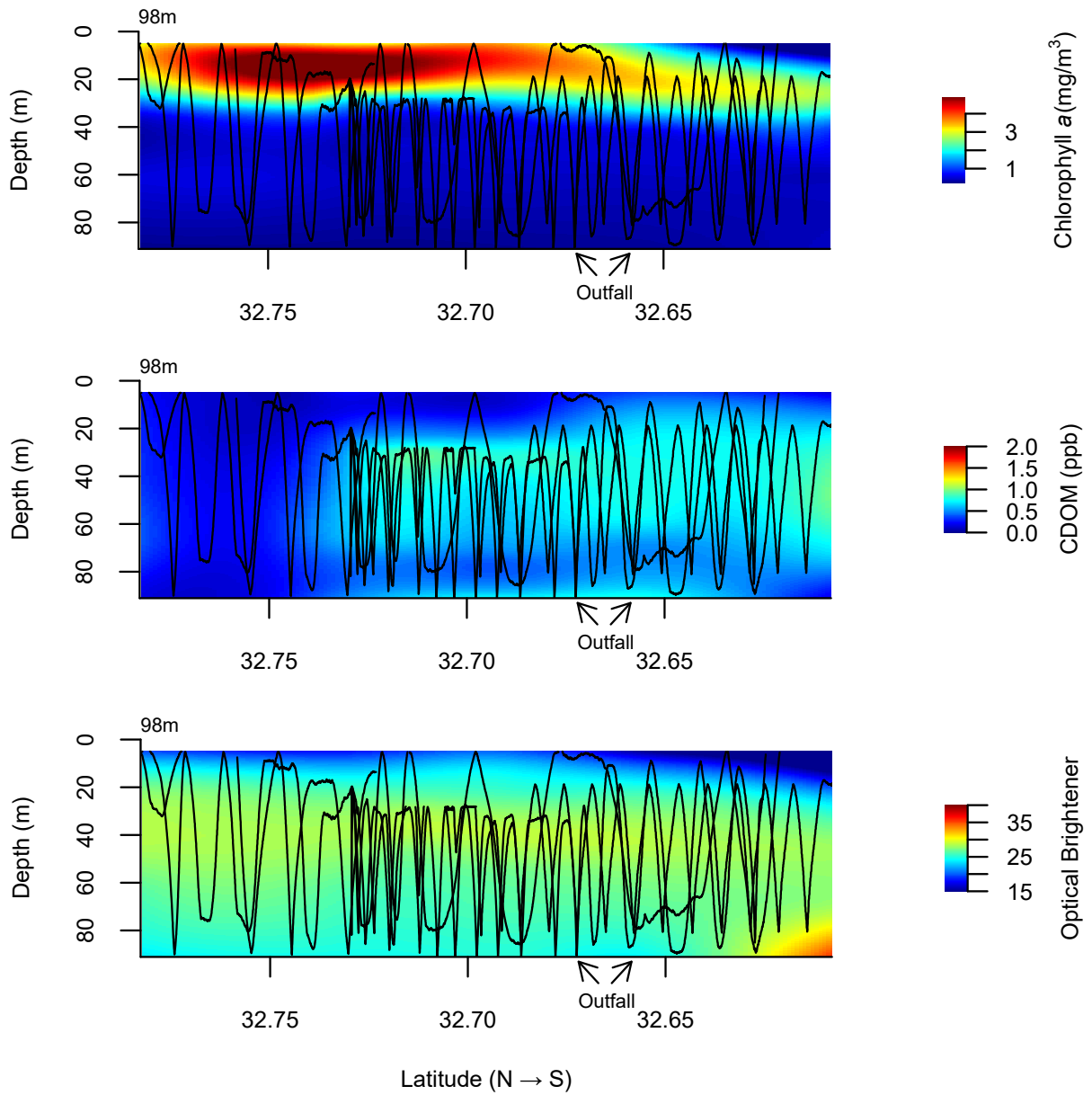


Figure 4.11 *continued*

Chapter 5

Sediment Quality

Chapter 5. Sediment Quality

INTRODUCTION

Ocean sediment samples are analyzed by the City of San Diego (City) as part of the Ocean Monitoring Program to examine the effects of wastewater discharge from the Point Loma Ocean Outfall (PLOO) and South Bay Ocean Outfall (SBOO), and other anthropogenic inputs, on the marine benthic environment. Analyses of various sediment contaminants are conducted as anthropogenic inputs to the marine ecosystem, including municipal wastewater, can lead to increased concentrations of pollutants within the local environment. The relative proportions of sand, silt, clay, and other particle size parameters are also examined as concentrations of some compounds are known to be directly linked to sediment composition (Emery 1960, Eganhouse and Venkatesan 1993). Physical and chemical sediment characteristics are also analyzed as they define the primary microhabitats for benthic macroinvertebrates (macrofauna) that live within or on the seafloor, and therefore influence the distribution and presence of various species. For example, differences in sediment composition and organic loading impact the burrowing, tube building, and feeding abilities of infaunal invertebrates, thus affecting benthic community structure (Gray 1981, Snelgrove and Butman 1994). Many demersal fish species are also associated with specific sediment types that reflect the habitats of their preferred invertebrate prey (Cross and Allen 1993). Thus, understanding changes in sediment condition and quality over time and space is crucial to assessing corresponding changes in benthic invertebrate and demersal fish populations (see Chapters 6 and 8, respectively).

Both natural and anthropogenic factors affect the composition, distribution, and stability of seafloor sediments on the continental shelf. Natural factors that affect sediment conditions include geologic history, strength and direction of bottom currents, exposure to wave action, seafloor topography, inputs from rivers and bays, beach erosion, runoff, bioturbation by fish and benthic invertebrates, and decomposition of calcareous organisms (Emery 1960). These processes affect the size and distribution of sediment particles, as well as the chemical composition of sediments. For example, erosion from coastal cliffs and shores, and flushing of terrestrial sediment and debris from bays, rivers, and streams strongly influence the overall organic content and particle size of coastal sediments (Emery 1960). These inputs can also contribute to the deposition and accumulation of trace metals, or other contaminants, on the sea floor. In addition, primary productivity by phytoplankton, and decomposition of marine and terrestrial organisms, are major sources of organic loading in coastal shelf sediments (Mann 1982, Parsons et al. 1990).

Municipal wastewater outfalls, such as the PLOO and SBOO off San Diego, are one of many anthropogenic sources which may influence sediment characteristics through the discharge of treated effluent and the subsequent deposition of a wide variety of organic and inorganic compounds. Some of the most commonly detected contaminants discharged via ocean outfalls are trace metals, pesticides, and various indicators of organic loading such as organic carbon, nitrogen, and sulfides (Anderson et al. 1993). In particular, organic enrichment due to wastewater discharge is of concern as it may impair habitat quality for resident marine organisms and, thus, disrupt ecological processes (Gray 1981). Lastly, the physical presence of a large outfall, and associated ballast materials (e.g., rock, sand) on the seafloor,

may alter the hydrodynamic regime in surrounding areas, thus affecting sediment movement and transport, as well as the structure of local fish and invertebrate communities.

This chapter presents analysis and interpretation of sediment particle size and chemistry data collected during 2022 and 2023, from core benthic monitoring stations throughout the PLOO and SBOO regions. The three primary goals of this chapter are to: (1) document sediment conditions at core monitoring stations; (2) identify if concentrations of pollutants in marine sediments are at levels that would degrade the benthic communities; (3) identify possible effects of wastewater discharge on sediment quality; (4) identify other potential natural or anthropogenic sources of sediment contamination. For additional information, a broader regional assessment of benthic conditions throughout the entire San Diego region is presented in Chapter 7.

MATERIALS AND METHODS

Field Sampling

Benthic samples analyzed in this chapter were collected at a total of 49 core monitoring stations, located at inner shelf (≤ 30 m) to middle shelf ($> 30 - 120$ m) depths, surrounding the PLOO and SBOO, during winter (January) and summer (July) of 2022 and 2023 (Figure 5.1). The PLOO sites include 12 primary core stations located along the 98-m discharge depth contour, and 10 secondary core stations located along or adjacent to the 88-m or 116-m depth contours. The SBOO sites include 12 primary core stations located along the 28-m discharge depth contour, and 15 secondary core stations located along or adjacent to the 19, 38, or 55-m depth contours. Stations located within 1000 m of the boundary of the zone of initial dilution (ZID), for either outfall, are considered to represent near-ZID conditions. These include PLOO stations E11, E14, E15 and E17, and SBOO stations I12, I14, I15 and I16. During the summer of 2023, only E15 and the primary core stations from the PLOO and SBOO regions were sampled, due to a resource exchange granted by the San Diego Regional Water Quality Control Board for participation in the 2023 Southern California Bight (SCB) Regional Monitoring Program (Bight'23).

Samples for benthic analyses were collected using a double 0.1-m² Van Veen grab, with one grab per cast used for sediment quality analyses, one grab per cast used for benthic community analysis, and subsequent grabs used for sediment toxicity testing where required (see Chapters 6 and 7). Visual observations of weather, sea conditions, and human/animal activity were also recorded at the time of sampling. Criteria established by the U.S. Environmental Protection Agency (USEPA) to ensure consistency of these types of samples were followed with regard to sample disturbance and depth of penetration (USEPA 1987). Sub-samples for particle size and sediment chemistry analyses were taken from the top 2 cm of the sediment surface and handled according to standard guidelines (USEPA 1987, SCCWRP 2018).

Laboratory Analyses

All sediment chemistry and particle size analyses were performed at the City's Environmental Chemistry Services Laboratory. Detailed analytical protocols are available upon request. Briefly, sediment sub-samples were analyzed on a dry weight basis to determine concentrations of various indicators of organic loading (biochemical oxygen demand, total organic carbon, total nitrogen, total sulfides, total volatile solids), 18 trace metals, nine chlorinated pesticides, 42 polychlorinated biphenyl compound congeners

(PCBs), 24 polycyclic aromatic hydrocarbons (PAHs), and 13 polybrominated ethers (PBDEs). Data were limited to values above the method detection limit (MDL) for each parameter (Appendix F.1). A variety of laboratory technical issues resulted in a number of non-reportable sediment chemistry data for the 2022 and 2023 benthic surveys, see Appendices F.2–F.13.

Particle size analysis was performed using either a Horiba LA-950V2 laser scattering particle analyzer or a set of nested sieves. The Horiba measures particles ranging in size from 0.5 to 2000 μm . Coarser sediments were removed and quantified prior to laser analysis by screening samples through a 2000 μm mesh sieve. These data were later combined with the Horiba results to obtain a complete distribution of particle sizes totaling 100%, and then classified into 11 sub-fractions and four main size fractions based on the Wentworth scale (Folk 1980) (see Appendix F.14). When a sample contained substantial amounts of coarse sand, gravel, shell hash or other large materials that could damage the Horiba analyzer, or where the general distribution of sediments would be poorly represented by laser analysis, a set of nested sieves was used with mesh sizes of 2000 μm , 1000 μm , 500 μm , 250 μm , 125 μm , 75 μm , and 63 μm to divide the samples into seven sub-fractions. See Appendix F.15 for visual observations for each PLOO and SBOO core station.

Data Analyses

Data for each parameter analyzed during 2022 were reported previously (City of San Diego 2023), and all raw data for the 2022–2023 sampling period have been submitted to either the Regional Water Quality Control Board or the California Environmental Data Exchange Network (CEDEN) and will be provided upon request.

Data summaries for the various sediment parameters included detection rate, minimum, maximum, and mean values for all samples combined by outfall region (i.e., PLOO, SBOO). Historical summaries were generated using data from current primary and secondary core stations but limited to samples collected during winter and summer surveys. For chemistry parameters, all means were calculated using detected values only, with no substitutions made for non-detects in the data (i.e., analyte concentrations < method detection limit [MDL]). Limiting analyses to detected values (i.e., excluding non-detects) is considered a conservative way of handling contaminant concentrations as it creates a strong upward bias in the data and respective summary statistics, and therefore may represent a worst-case scenario (e.g., see Helsel 2005a, b, 2006 for discussions of non-detect data). In contrast to previous reports (e.g., City of San Diego 2022c), estimated values that fell below method detection limits but were confirmed by mass-spectrometry were excluded from all data (1991–2023). Instead, estimated values were treated as non-detects for this report. Total chlordane, total DDT (tDDT), total hexachlorocyclohexane (tHCH), total PCB (tPCB), total PAH (tPAH), and total PBDE (tPBDE) were calculated for each sample as the sum of all individual constituents with reported values. When applicable, contaminant concentrations were compared to the Effects Range Low (ERL) and Effects Range Median (ERM) sediment quality guidelines of Long et al. (1995). The ERLs represent chemical concentrations below which adverse biological effects are rarely observed, while values above ERLs, but below ERMs, represent levels at which effects occasionally occur. Concentrations above the ERM indicate likely biological effects, although these may not always be validated by toxicity testing results (Schiff and Gossett 1998). Analyses were performed using R (R Core Team 2022) and various functions within the zoo, reshape2, plyr, stringr, Rmisc, ROBDC, tidyr, ggpubr, vegan, psych, tidyverse, ggplot2, and dplyr (Zeileis and Grothendieck 2005, Wickham 2007, 2011, 2019, Hope 2013, Ripley and Lapsley 2017, Wickham and Henry 2018, Kassambara 2019, Oksanen et al. 2019, Revell 2019, Wickham et al. 2019a,b, 2020).

RESULTS

Particle Size Distribution

Ocean sediments sampled at the core PLOO stations during 2022 and 2023 were composed primarily of fine silts and clays (fine particles, or percent fines), plus fine sands. Percent fines ranged from 21.1 to 71.2% per sample, while fine sands ranged from 21.2 to 60.5%, medium-coarse sands ranged from 0 to 28.2%, and coarse particles ranged from 0 to 20.8% (Table 5.1). Coarser particles often included shell hash, black sand, and/or gravel (Appendix F.15). Overall, there were no spatial patterns in sediment composition relative to proximity to the PLOO discharge site over the past two years (Figure 5.2). For example, most samples from the near-ZID stations (E11, E14, E15, and E17) had proportions of fine particles that fell within the range of the farfield stations (38.8-59.6% versus 21.1-71.2% per sample, respectively). One sample from station E11 had comparatively coarse sediments in winter 2023, with 53.2% fines, 33.3% fine sands, 8.3% medium-coarse sands, and 5.2% coarse particles. Sediments from farfield stations that also had larger proportions of medium-coarse sands ($\geq 9.3\%$ per sample) and/or coarse particles ($\geq 5.4\%$ per sample) included one sample from stations E1, E3, E5, and E9, two samples from stations B11 and E2, and three samples from station B12.

There was no evidence that fine sediments have been accumulating over time at any of the nearfield or farfield primary core PLOO stations since wastewater discharge began at the current discharge site in late 1993 (Figure 5.3). Instead, temporal variability of sediment composition at these sites has been primarily in the sand and coarse fractions (see City of San Diego 2014a, 2022a). This variability has corresponded to occasional patches of coarse sands (e.g., black sand) or larger particles (e.g., gravel, shell hash). For example, black sands have been observed at stations E9, E15, and E14 over the years (e.g., City of San Diego 2020, 2022c) possibly due in part to the presence of ballast or bedding material near the outfall (City of San Diego 2022a). In addition to the sporadic occurrence of coarser sediments at a few stations, a sudden, region-wide increase in fine particles was observed starting in winter 2019. This abrupt change remains unexplained.

In contrast to the PLOO region, seafloor sediments were much more diverse at the SBOO monitoring sites during 2022 and 2023. Percent fines ranged from 0 to 88.6% per sample at these stations, while fine sands ranged from 0 to 89.3%, medium-coarse sands ranged from 0.1 to 97.6%, and coarse particles ranged from 0 to 25.4% (Table 5.2). Coarser particles at the SBOO stations often comprised shell hash, red relict sands, black sand, or cobble (Appendix F.15). There were no spatial patterns in sediment composition relative to proximity to the SBOO discharge site over the past two years (Figure 5.2). Similar to the rest of the SBOO region, sediments from near-ZID stations (I12, I14, I15, and I16) were highly variable, with proportions of fine particles ranging from 0.3-47.9%, fine sands ranging from 5.1-79.1%, medium-coarse sands ranging from 0.9-87.8%, and coarse particles ranging from 0-11.2%. Stations with the highest proportions of medium-coarse sands ($\geq 27.0\%$ per sample) and/or coarse particles ($\geq 1.6\%$ per sample), including near-ZID stations I12, I15, and I16, tended to occur at, south and offshore of the outfall.

It is interesting to note that fine particles also appeared to increase starting in winter 2019 at some SBOO primary core stations (Figure 5.3). Previous analysis of particle size data revealed considerable temporal variability at some sites within the SBOO region and relative stability at others, with no clear patterns

evident relative to depth, proximity to the outfall, or other sources of nearshore sediment plumes, such as San Diego Bay and the Tijuana River (City of San Diego 2014b).

Indicators of Organic Loading

Detection rates and concentrations of the various indicators of organic loading in benthic sediments, surrounding the PLOO and SBOO, varied both within and between regions during 2022 and 2023 (Tables 5.1, 5.2). Only the parameter total volatile solids (TVS) was detected in all sediment samples from both regions. In contrast, total nitrogen (TN) and total organic carbon (TOC) were detected in 100% of the PLOO sediment samples, but only in 57% and 69% of the SBOO samples, respectively. Detection rates for sulfides were 66% in the PLOO region and 24% in the SBOO region. Although not a required parameter for any of the PLOO or SBOO permits, biochemical oxygen demand (BOD) has long been measured by the City at PLOO benthic stations; this parameter was detected in all PLOO primary core station sediment samples for which it was analyzed during 2022 and 2023. Detection rates for these parameters were similar to, or lower than, those recorded historically since monitoring began. Lower detection rates likely reflect changes in MDLs; for example, the MDL for sulfides went from 0.14 ppm in summer 2017 to 2.2 ppm for the current reporting period.

Sediments off Point Loma, in 2022 and 2023, had BOD concentrations ≤ 660 ppm per sample, while sulfides were ≤ 70.1 ppm, TN was $\leq 0.086\%$ weight, TOC was $\leq 3.12\%$ weight, and TVS was $\leq 3.4\%$ weight per sample (Table 5.1). The highest concentrations of TN, TOC, and TVS were consistently detected in sediments from the northern 'B' stations located at least 10 km north of the PLOO (Figure 5.4). In contrast, BOD and sulfide distributions were more variable over this period. The highest concentration of BOD occurred in one sample from near-ZID station E14. The highest concentrations of sulfides occurred in two samples for near-ZID station E14 and three samples from near-ZID station E17. In general, only sulfide and BOD have shown any changes in concentrations near the PLOO that appear consistent with possible organic enrichment (Figure 5.3) (see also City of San Diego 2022a,b).

Sediments surrounding the SBOO, in 2022 and 2023, had sulfide concentrations ≤ 39.5 ppm per sample, while TN concentrations were $\leq 0.074\%$ weight, TOC concentrations were $\leq 4.03\%$ weight, and TVS concentrations were $\leq 1.8\%$ weight per sample (Table 5.2). There was little evidence of any significant organic enrichment near the SBOO discharge site during these two years; the highest concentrations of the various organic loading indicators were widely distributed throughout the region (Figure 5.4). For TOC, TN and TVS, variable concentrations may be linked to regional differences in sediment particle composition since these parameters can co-vary with the amount of percent fines (see City of San Diego 2014b and Chapter 7). In contrast to the overall survey area, concentrations of these organic indicators have been less variable at the SBOO primary core stations, with no patterns indicative of organic enrichment being evident since wastewater discharge began in early 1999 (Figure 5.3). For both regions, all reported concentrations of TN and TOC over the past 27-31 years generally fell within ranges reported regionally off San Diego (e.g., Chapter 7; see also City of San Diego 2022b), and elsewhere in the SCB (e.g., Dodder et al. 2016, Du et al. 2020).

Trace Metals

Eight of the 18 trace metals analyzed were detected in all sediment samples collected at the PLOO and SBOO core benthic stations, in 2022 and 2023, including: aluminum, arsenic, barium, chromium, iron, lead, manganese, and zinc (Tables 5.1, 5.2). Antimony, beryllium, copper, mercury, nickel, and tin also

had high detection rates in both regions ($\geq 60\%$). Cadmium and selenium were found more often in the PLOO region (27% and 18%, respectively) than in the SBOO region (9% and 2%, respectively). Silver and thallium were not detected in any samples collected during the 2-year reporting period.

Of the nine metals with published ERLs and ERMs (Long et al. 1995), only arsenic was reported at levels above its threshold during 2022 or 2023 (Table 5.3). Arsenic exceeded its ERL in the two sediment samples collected from SBOO farfield station I21 collected during 2022. Neither of these exceeded the ERM for arsenic. In addition to low overall values, metal concentrations tended to vary in sediments throughout the two regions, with no discernible patterns relative to proximity to either outfall (Figure 5.5, Appendix F.16). Several of the highest concentrations of aluminum, antimony, arsenic, barium, beryllium, chromium, copper, iron, manganese, mercury, nickel, tin and zinc were found in sediments from one or more of the northern 'B' stations or southern 'E' stations within the PLOO region. As with TOC, TN and TVS, this pattern may be linked to regional differences in sediment particle composition since several of these metals can co-vary with the amount of percent fines (see City of San Diego 2014b and Chapter 7). Only cadmium tended to be highest near the PLOO, with the five highest values (≥ 0.101) recorded in sediments from near-ZID stations E14 and E17. Note, though, that the maximum value recorded at these sites (0.122 ppm) was an order of magnitude below the ERL of 1.2 ppm. Within the SBOO region, three stations had relatively high values of 10 or more metals. Farfield station I9 had relatively high values of aluminum, antimony, barium, beryllium, cadmium, chromium, copper, iron, manganese, nickel, selenium, tin, and zinc, while farfield station I29 had high values of aluminum, beryllium, chromium, copper, iron, lead, mercury, nickel, tin and zinc, and farfield station I35 had high values of aluminum, antimony, barium, chromium, copper, iron, lead, manganese, mercury, tin and zinc.

Historically, detection rates have been relatively high for several different metals at PLOO and SBOO stations. For example, aluminum, arsenic, barium, chromium, copper, iron, lead, manganese, nickel, and zinc have been detected in $\geq 67\%$ of the sediment samples collected in these areas since monitoring began (Tables 5.1, 5.2). Mercury and tin were also detected frequently ($\geq 67\%$) at PLOO stations, but less frequently at SBOO stations (29% and 53%, respectively). Concentrations of chromium and mercury have remained below their ERLs, while exceedances for arsenic, cadmium, copper, lead, nickel, silver, and zinc have also been rare (historical rates $\leq 7.1\%$ within each region; Table 5.3). Concentrations of the remaining metals have been extremely variable with most being detected within ranges reported regionally off San Diego (e.g., Chapter 7; see also City of San Diego 2022b), and elsewhere in the Southern California Bight (SCB) (e.g., Dodder et al. 2016, Du et al. 2020). While high metal concentrations have been occasionally recorded in sediments collected from both PLOO and SBOO near-ZID stations, no discernible long-term patterns have been identified that could be associated with proximity to either outfall or to the onset of wastewater discharge (Figure 5.6, Appendix F.17). It should be noted, however, that cadmium has been slightly higher at near-ZID station E14 versus other sites in several of the surveys over the past two decades. These values rarely exceeded the ERL of 1.2 ppm, never exceeded the ERM of 9.6 ppm, and there is no indication that cadmium is accumulating in the sediments around the outfall or within the region.

Pesticides, PCBs, PAHs, PBDEs

A total of five chlorinated pesticides were detected in benthic sediments off San Diego during 2022 and 2023, including chlordanes, DDT, hexachlorobenzene (HCB), and mirex (Tables 5.1, 5.2). The most common of these pesticides, DDT, was detected in 100% of the PLOO samples and 20% of the

SBOO samples, with total DDT concentrations ≤ 862 ppt and ≤ 1346 ppt per region, respectively. HCH was detected in 5% of PLOO samples, and 1% of SBOO samples, at concentrations ≤ 175 ppt for both regions. Chlordanes had a detection rate of 5% for PLOO samples with concentrations ≤ 650 ppt; this pesticide was not detected in sediments from the SBOO region. Mirex was detected in two SBOO samples, at concentrations ≤ 50 ppt, while HCB was detected in a single SBOO sample at a concentration of 196 ppt. These pesticides were not detected in sediments from the PLOO region. Aldrin, dieldrin, endosulfan (*alpha*, *beta*, endosulfan sulfate), endrin and endrin aldehyde were not detected in any PLOO or SBOO sediment samples during this reporting period. The spatial distribution of these pesticides varied in sediments from throughout the two regions over the past two years, with no discernible patterns relative to either outfall (e.g., Figure 5.7). For example, similar to many of the metals, the many of highest DDT values were found in sediments from the northern ‘B’ or southern ‘E’ PLOO stations. All PLOO and SBOO samples had DDT values below the ERL threshold of 1580 ppt.

During the 2022–2023 reporting period, PCBs were detected in 48% of sediment samples from the PLOO region at concentrations up to 50,682 ppt, and in 10% of samples from the SBOO region, at concentrations up to 558 ppt (Tables 5.1, 5.2). The highest value was found in sediments collected adjacent to the LA-5 dredge materials dumpsite, an area known for elevated PCBs (see City of San Diego 2022a and Parnell et al 2008). All other total PCB concentrations from the PLOO region were below 8,011 ppt. PAHs and PBDEs were also detected more frequently in the PLOO region (44% and 66%, respectively) versus the SBOO region (20% and 11%, respectively). Total PAH occurred at concentrations ≤ 402.9 ppb at all stations, well below the ERL threshold of 4022 ppb. Total PBDEs occurred at concentrations ≤ 623 ppt at all stations. Concentrations of total PCB and total PAH varied in sediments from throughout the two regions over the past two years, with no discernible patterns relative to either outfall. Instead, both contaminant types tended to be highest at the southern ‘E’ PLOO stations (Figure 5.7). In contrast, the highest values of total PBDE were found at near-ZID stations E14 and E17.

Historically, pesticide, PCB and PAH concentrations have been consistently low, with total DDT exceeding its ERL in just 8.7% of the samples collected in the PLOO region, and 2.2% of the samples in the SBOO region between 1991 or 1995 – 2021 (Table 5.3). Over this time period, total DDT exceeded its ERM in only 0.1% of PLOO sediment samples. Total PAH exceeded its ERL in 0.1% of the samples from PLOO stations, and never exceeded its ERM. These thresholds do not exist for PCBs measured as congeners, and historical comparisons cannot be made for PBDEs, since reporting of these only began in 2022. For both regions, all reported concentrations of total DDT, chlordanes, total PCB, and total PAHs were generally within values reported regionally off San Diego (e.g., Chapter 7; see also City of San Diego 2022b), and well below maximum values reported elsewhere in the SCB (e.g., Dodder et al. 2016, Du et al. 2020). Finally, changes in DDT, PCB and PAH demonstrated no discernible long-term patterns that can be associated with wastewater discharge via either outfall (Figure 5.8).

DISCUSSION

Particle size composition during the current reporting period (2022–2023) at PLOO and SBOO stations varied as expected by outfall region and depth stratum (e.g., Emery 1960, MBC 1988), and was generally consistent with results of previous surveys off San Diego (e.g., City of San Diego 2020, 2022a,b,c). Within the PLOO region, percent fines (silt and clay) and fine sands continued to comprise the largest proportion of sediments. Within the SBOO region, sands continued to comprise the largest proportion of sediments, with the relative amounts of coarser and finer particles varying among sites. No

spatial relationship was evident between sediment particle size composition and proximity to either the PLOO or SBOO discharge site. Further, there has not been any substantial accumulation of fine particles at any of the near-ZID stations or elsewhere since wastewater discharge began at the current PLOO discharge site in late 1993 or the SBOO discharge site in early 1999. Instead, a sudden increase in fine particles was observed across the entire PLOO region and part of the SBOO region starting in winter 2019 that has persisted through winter 2023. Further investigation is required to determine the origins of this dramatic change.

The diversity of sediment types in these areas reflect multiple geologic origins and complex patterns of transport and deposition. Variability in the composition of Point Loma sediments is likely affected by both anthropogenic and natural influences, including outfall construction or ballast materials, offshore disposal of dredged materials, and recent deposition of sediment and detrital materials (Emery 1960, Parnell et al. 2008, City of San Diego 2022a). For example, the PLOO lies within the Mission Bay littoral cell (Patsch and Griggs 2007), which has natural sources of sediments, such as outflows from Mission Bay, the San Diego River, and San Diego Bay. However, fine particles may also travel in suspension across littoral cell borders up and down the coast (e.g., Farnsworth and Warrick 2007, Svejkovsky 2013), thus widening the range of potential sediment sources to the region. Additionally, the presence of relict red sands at some stations in the SBOO region is indicative of minimal sediment deposition in recent years (Emery 1960). Several SBOO stations are also located within or near an accretion zone for sediments moving within the Silver Strand littoral cell (MBC-ES 1988, Patsch and Griggs 2007). Therefore, higher proportions of fine sands, silts, and clays at these sites are also likely associated with the transport of fine materials originating from the Tijuana River, the Silver Strand beach, and to a lesser extent from San Diego Bay (MBC-ES 1988).

Various organic loading indicators, trace metals, pesticides, PCBs, PAHs, and PBDEs were detected in sediment samples collected throughout the PLOO and SBOO regions in 2022 and 2023. However, concentrations of these parameters were below ERM thresholds, mostly below ERL thresholds, and typically within historical ranges at regional sites (e.g., City of San Diego 2020, 2022b,c). Additionally, values for most sediment parameters remained within ranges typical for other areas of the southern California continental shelf (see Schiff and Gossett 1998, City of San Diego 2022b, Noblet et al. 2002, Schiff et al. 2006, 2011, Maruya and Schiff 2009, Dodder et al. 2016, Du et al. 2020).

There have been few, if any, clear spatial patterns consistent with outfall discharge effects on sediment chemistry values over the past several years, with concentrations of most contaminants at near-ZID sites falling within the range of values observed at farfield stations. The only exceptions off San Diego have been slightly higher BOD, sulfide, cadmium, and PBDEs levels measured in sediments near the PLOO discharge site (see also City of San Diego 2022a). Instead, the highest concentrations of several organic indicators, trace metals, pesticides, PCBs, and PAHs have historically occurred in sediments from southern and/or northern farfield stations. The driver of elevated contaminants at the northern PLOO stations is unknown, while sediments from the southern PLOO stations are known to be impacted by the dumping of dredged materials destined originally for the LA-5 dredged disposal dumpsite (Anderson et al. 1993, Steinberger et al. 2003, Parnell et al. 2008). In the SBOO region, relatively high values of most parameters could be found distributed throughout the region, and several organic indicators and metals co-occurred in samples characterized by finer sediments. This association is expected due to the known correlation between particle size and concentrations of these chemical parameters (Eganhouse and Venkatesan 1993). For the four parameters found at slightly higher concentrations at PLOO near-ZID stations, there has been no indication of contaminant accumulation in the sediments.

The broad distribution of various contaminants in sediments throughout the PLOO and SBOO regions is likely derived from several sources. Mearns et al. (1991) described the distribution of contaminants, such as arsenic, mercury, DDT, and PCBs as being ubiquitous in the SCB. Additionally, Brown et al. (1986) concluded that there may be no coastal areas in southern California that are sufficiently free of chemical contaminants to be considered reference sites. This has been supported by more recent surveys of SCB continental shelf habitats (Schiff and Gossett 1998, Noblet et al. 2002, Schiff et al. 2006, 2011, Dodder et al. 2016, Du et al. 2020). The lack of contaminant-free reference areas clearly pertains to the PLOO and SBOO regions as demonstrated by the presence of many contaminants in sediments prior to wastewater discharge (see City of San Diego 2000, 2022a). In addition, historical assessments of benthic sediments off the coast of Los Angeles have shown that as wastewater treatment improved, sediment conditions were more likely affected by other factors (Stein and Cadien 2009). Such factors may include bioturbative re-exposure of buried legacy sediments (Niedoroda et al. 1996, Stull et al. 1996), large storms that assist redistribution of legacy contaminants (Sherwood et al. 2002), and stormwater discharges (Schiff et al. 2006, Nezlin et al. 2007). Possible non-outfall sources and pathways of contaminant dispersal off San Diego include transport of contaminated sediments from San Diego Bay via tidal exchange, offshore disposal of dredged sediments, nearshore turbidity plumes emanating from the Tijuana River, and surface runoff from local watersheds (Parnell et al. 2008).

In conclusion, there was no evidence of fine particle loading related to wastewater discharge via the PLOO or SBOO, during the current reporting period, or since the discharge originally began through either outfall in the 1990s. Likewise, contaminant concentrations at near-ZID stations were generally within the range of variability observed throughout both outfall regions and do not appear to reflect any significant organic enrichment. The only sustained effects have been restricted to a few sites located within 200 m of the PLOO (near-ZID stations E11, E14 and E17). These minor effects include sporadic occurrences of slightly higher values of BOD, sulfide, cadmium and PBDEs. Finally, the quality of PLOO and SBOO sediments in 2022 and 2023 was similar to previous years with overall contaminant concentrations remaining relatively low compared to available thresholds, or values found in other southern California coastal areas (Schiff and Gossett 1998, Noblet et al. 2002, Schiff et al. 2006, 2011, Maruya and Schiff 2009, Dodder et al. 2016, Du et al. 2020). Consequently, there is presently no evidence to suggest that wastewater discharge via the PLOO or SBOO is affecting the quality of benthic sediments off San Diego to the point that it may degrade resident marine biological communities (i.e., Chapters 6–8).

LITERATURE CITED

- Anderson, J.W., D.J. Reish, R.B. Spies, M.E. Brady, and E.W. Segelhorst. (1993). Human Impacts. In: M.D. Dailey, D.J. Reish, and J.W. Anderson (eds.). *Ecology of the Southern California Bight: A Synthesis and Interpretation*. University of California Press, Berkeley, CA. p 682–766.
- Brown, D.A., R.W. Gossett, G.P. Hershelman, C.G. Word, A.M. Westcott, and J.N. Cross. (1986). Municipal wastewater contamination in the Southern California Bight: Part I—metal and organic contaminants in sediments and organisms. *Marine Environmental Research*, 18: 291–310.
- City of San Diego. (2000). *International Wastewater Treatment Plant Final Baseline Ocean Monitoring Report for the South Bay Ocean Outfall (1995–1998)*. City of San Diego Ocean Monitoring Program, Metropolitan Wastewater Department, Environmental Monitoring and Technical Services Division, San Diego, CA.

- City of San Diego. (2014a). Point Loma Ocean Outfall Annual Receiving Waters Monitoring and Assessment Report, 2013. City of San Diego Ocean Monitoring Program, Public Utilities Department, Environmental Monitoring and Technical Services Division, San Diego, CA.
- City of San Diego. (2014b). South Bay Ocean Outfall Annual Receiving Waters Monitoring and Assessment Report, 2013. City of San Diego Ocean Monitoring Program, Public Utilities Department, Environmental Monitoring and Technical Services Division, San Diego, CA.
- City of San Diego. (2020). Biennial Receiving Waters Monitoring and Assessment Report for the Point Loma and South Bay Ocean Outfalls, 2018–2019. City of San Diego, Public Utilities Department, Environmental Monitoring and Technical Services Division, San Diego, CA.
- City of San Diego. (2022a). Appendix C.1 Benthic Sediments, Invertebrates and Fishes. In: Application for Renewal of NPDES CA0107409 and 301(h) Modified Secondary Treatment Requirements Point Loma Ocean Outfall. Volume V, Appendices C thru D. Public Utilities Department, Environmental Monitoring and Technical Services Division, San Diego, CA.
- City of San Diego. (2022b). Appendix C.2 San Diego Benthic Tolerance Intervals; 24-Year San Diego Regional Benthic Assessment and Reference Tolerance Intervals. In: Application for Renewal of NPDES CA0107409 and 301(h) Modified Secondary Treatment Requirements Point Loma Ocean Outfall. Volume V, Appendices C thru D. Public Utilities Department, Environmental Monitoring and Technical Services Division, San Diego, CA.
- City of San Diego. (2022c). Biennial Receiving Waters Monitoring and Assessment Report for the Point Loma and South Bay Ocean Outfalls, 2020–2021. City of San Diego, Public Utilities Department, Environmental Monitoring and Technical Services Division, San Diego, CA.
- City of San Diego. (2023). Interim Receiving Waters Monitoring Report for the Point Loma and South Bay Ocean Outfalls, 2022. City of San Diego, Public Utilities Department, Environmental Monitoring and Technical Services Division, San Diego, CA.
- Cross, J.N. and L.G. Allen. (1993). Fishes. In: M.D. Dailey, D.J. Reish, and J.W. Anderson (eds.). Ecology of the Southern California Bight: A Synthesis and Interpretation. University of California Press, Berkeley, CA. p 459–540.
- Dodder, N., K. Schiff, A. Latker, C-L Tang. (2016). Southern California Bight 2013 Regional Monitoring Program: IV. Sediment Chemistry. Southern California Coastal Water Research Project, Westminster, CA.
- Du, B., C.S. Wong, K. Mclaughlin, and K. Schiff. (2020). Southern California Bight 2018 Regional Monitoring Program: II. Sediment Chemistry. Southern California Coastal Water Research Project, Westminster, CA.
- Eganhouse, R.P. and M.I. Venkatesan. (1993). Chemical Oceanography and Geochemistry. In: M.D. Dailey, D.J. Reish, and J.W. Anderson (eds.). Ecology of the Southern California Bight: A Synthesis and Interpretation. University of California Press, Berkeley, CA. p 71–189.

- Emery, K.O. (1960). *The Sea off Southern California*. John Wiley, New York, NY.
- Farnsworth, K.L. and J.A. Warrick. (2007). Sources, dispersal, and fate of fine sediment supplied to coastal California. U.S. Geological Survey Scientific Investigations Report 2007–5254. Reston, VA.
- Folk, R.L. (1980). *Petrology of Sedimentary Rocks*. Hemphill, Austin, TX.
- Gray, J.S. (1981). *The Ecology of Marine Sediments: An Introduction to the Structure and Function of Benthic Communities*. Cambridge University Press, Cambridge, England.
- Helsel, D.R. (2005a). More than obvious: better methods for interpreting nondetect data. *Environmental Science & Technology* (October 15, 2005), 419A-423A.
- Helsel, D.R. (2005b). *Nondetects and Data Analysis: Statistics for Censored Environmental Data*. John Wiley, New York.
- Helsel, D.R. (2006). Fabrication data: how substituting values for nondetects can ruin results, and what can be done about it. *Chemosphere* 65: 2434–2439.
- Hope, R.M. (2013). Rmisc: Ryan Miscellaneous. R package version 1.5. <http://CRAN.R-project.org/package=Rmisc>.
- Kassambara, A. (2019). ggpubr: ‘ggplot2’ Based Publication Ready Plots. R package version 0.2.5. <https://CRAN.R-project.org/package=ggpubr>.
- Long, E.R., D.L. MacDonald, S.L. Smith, and F.D. Calder. (1995). Incidence of adverse biological effects within ranges of chemical concentration in marine and estuarine sediments. *Environmental Management*, 19: 81–97.
- [MBC] MBC Applied Environmental Sciences and Engineering-Science. (1988). Part F: Biological studies. In: Tijuana Oceanographic Engineering Study, Volume 1. Ocean Measurement Program. Prepared for the City of San Diego, CA.
- Mann, K.H. (1982). *The Ecology of Coastal Marine Waters: A Systems Approach*. University of California Press, Berkeley, CA.
- Maruya, K.A. and K. Schiff. (2009). The extent and magnitude of sediment contamination in the Southern California Bight. *Geological Society of America Special Paper*, 454: 399–412.
- Mearns, A.J., M. Matta, G. Shigenaka, D. MacDonald, M. Buchman, H. Harris, J. olas, and G. Lauenstein. (1991). *Contaminant Trends in the Southern California Bight: Inventory and Assessment*. NOAA Technical Memorandum NOS ORCA 62. Seattle, WA.
- Nezlin, N.P., P.M. DiGiacomo, S.B. Weisberg, D.W. Diehl, J.A. Warrick, M.J. Mengel, B.H. Jones, K.M. Reifel, S.C. Johnson, J.C. Ohlmann, L. Washburn, and E.J. Terrill. (2007). *Southern California Bight 2003 Regional Monitoring Program: V. Water Quality*. Southern California Coastal Water Research Project. Costa Mesa, CA.

- Niedoroda, A.W., D.J.P. Swift, C.W. Reed, and J.K. Stull. (1996). Contaminant dispersal on the Palos Verdes continental margin. *Science of the Total Environment*, 179: 109–133.
- Noblet, J.A., E.Y. Zeng, R. Baird, R.W. Gossett, R.J. Ozretich, and C.R. Phillips. (2002). Southern California Bight 1998 Regional Monitoring Program: VI. Sediment Chemistry. Southern California Coastal Water Research Project, Westminster, CA.
- Oksanen, J., F.G. Blanchet, R. Kindt, P. Legendre, P.R. Minchin, R.B. O’Hara, G.L. Simpson, P. Solymos, M.H.H. Stevens, and H. Wagner. (2019). *vegan: Community Ecology Package*. R package version 2.5-6. <http://CRAN.R-project.org/package=vegan>.
- Parnell, P.E., A.K. Groce, T.D. Stebbins, and P.K. Dayton. (2008). Discriminating sources of PCB contamination in fish on the coastal shelf off San Diego, California (USA). *Marine Pollution Bulletin*, 56: 1992–2002.
- Parsons, T.R., M. Takahashi, and B. Hargrave. (1990). *Biological Oceanographic Processes* 3rd Edition. Pergamon Press, Oxford.
- Patsch, K. and G. Griggs. (2007). *Development of Sand Budgets for California’s Major Littoral Cells*. Institute of Marine Sciences, University of California, Santa Cruz, CA.
- R Core Team. (2022). *R: A language and environment for statistical computing*. R Foundation for Statistical Computing, Vienna, Austria. URL <https://www.R-project.org/>.
- Revelle, W. (2019) *psych: Procedures for Personality and Psychological Research*, Northwestern University, Evanston, Illinois, USA, <https://CRAN.R-project.org/package=psych> Version = 1.9.12.31.
- Ripley, B. and M. Lapsley. (2017). *RODBC: ODBC Database Access*. R package version 1.3-12. <http://CRAN.R-project.org/package=RODBC>.
- [SCCWRP] Southern California Coastal Water Research Project. (2018). *Southern California Bight 2018 Regional Monitoring Program: Contaminant Impact Assessment Field Operations Manual*. Southern California Coastal Water Research Project. Costa Mesa, CA.
- Schiff, K.C. and R.W. Gossett. (1998). *Southern California Bight 1994 Pilot Project: III. Sediment Chemistry*. Southern California Coastal Water Research Project. Westminster, CA.
- Schiff, K., R. Gossett, K. Ritter, L. Tiefenthaler, N. Dodder, W. Lao, and K. Maruya. (2011). *Southern California Bight 2008 Regional Monitoring Program: III. Sediment Chemistry*. Southern California Coastal Water Research Project, Costa Mesa, CA.
- Schiff, K., K. Maruya, and K. Christenson. (2006). *Southern California Bight 2003 Regional Monitoring Program: II. Sediment Chemistry*. Southern California Coastal Water Research Project, Westminster, CA.

- Sherwood, C.R., D.E. Drake, P.L. Wiberg, and R.A. Wheatcroft. (2002). Prediction of the fate of p,p-DDE in sediment on the Palos Verdes shelf, California, USA. *Continental Shelf Research*, 32: 1025–1058.
- Snelgrove, P.V.R. and C.A. Butman. (1994). Animal-sediment relationships revisited: cause versus effect. *Oceanography and Marine Biology Annual Review*, 32: 111–177.
- Stein, E.D. and D.B. Cadien. (2009). Ecosystem response to regulatory and management actions: The Southern California experience in long-term monitoring. In: K. Schiff (ed.). *Southern California Coastal Water Research Project Annual Report 2009*. Southern California Coastal Water Research Project, Costa Mesa, CA.
- Steinberger, A., E. Stein, and K. Schiff. (2003). Characteristics of dredged material disposal to the Southern California Bight between 1991 and 1997. In: *Southern California Coastal Water Research Project Biennial Report 2001–2002*. Long Beach, CA. p 50–60.
- Stull, J.K., D.J.P. Swift, and A.W. Niedoroda. (1996). Contaminant dispersal on the Palos Verdes Continental margin. *Science of the Total Environment*, 179: 73–90.
- Svejkovsky, J. (2013). *Satellite and Aerial Coastal Water Quality Monitoring in the San Diego/Tijuana Region: Annual Summary Report, 1 January, 2012–31 December, 2012*. Ocean Imaging, Solana Beach, CA.
- [USEPA] United States Environmental Protection Agency. (1987). *Quality Assurance and Quality Control for 301(h) Monitoring Programs: Guidance on Field and Laboratory Methods*. EPA Document 430/9-86-004. Office of Marine and Estuary Protection, Washington, DC.
- Wickham, H. (2007). Reshaping Data with the reshape Package. *Journal of Statistical Software*, 21(12), 1–20. URL <http://www.jstatsoft.org/v21/i12/>.
- Wickham, H. (2011). The Split-Apply-Combine Strategy for Data Analysis. *Journal of Statistical Software*, 40(1), 1–29. URL <http://www.jstatsoft.org/v40/i01/>.
- Wickham, H. (2019). stringr: Simple, Consistent Wrappers for Common String Operations. R package version 1.4.0. <https://CRAN.R-project.org/package=stringr>.
- Wickham, H., R. Francois, L. Henry and K. Müller. (2020). dplyr: A Grammar of Data Manipulation. R package version 1.2.0. <https://CRAN.R-project.org/package=dplyr>.
- Wickham, H., M. Averick, J. Bryan, W. Chang, L. D’Agostino McGowan, R. François, G. Golemund, A. Hayes, L. Henry, J. Hester, M. Kuhn, T. Lin Pedersen, E. Miller, S. Milton Bache, K. Müller, J. Ooms, D. Robinson, D. P. Seidel, V. Spinu, K. Takahashi, D. Vaughan, C. Wilke, K. Woo, H. Yutani. (2019a). Welcome to the tidyverse. *Journal of Open Source Software*, 4(43), 1686, <https://doi.org/10.21105/joss.01686>.
- Wickham, H., W. Chang, L. Henry, T.L. Pedersen, K. Takahashi, C. Wilke, K. Woo, (2019b). Ggplot2: Create Elegant Data Visualizations Using the Grammar of Graphics. Version 3.2.0. Rstudio. URL <https://ggplot2.tidyverse.org/>.

Wickham H. and L. Henry. (2018). tidyr: Easily Tidy Data with ‘spread()’ and ‘gather()’ Functions. R package version 0.7.2. <https://CRAN.R-project.org/package=tidyr>.

Wickham, H., Francois, L. Henry and K. Müller (2020). dplyr: A Grammar of Data Manipulation. R package version 0.8.5. <https://CRAN.R-project.org/package=dplyr>.

Zeileis, A and G. Grothendieck. (2005). zoo: S3 Infrastructure for Regular and Irregular Time Series. Journal of Statistical Software, 14(6), 1-27. URL <http://www.jstatsoft.org/v14/i06/>

CHAPTER 5

FIGURES & TABLES

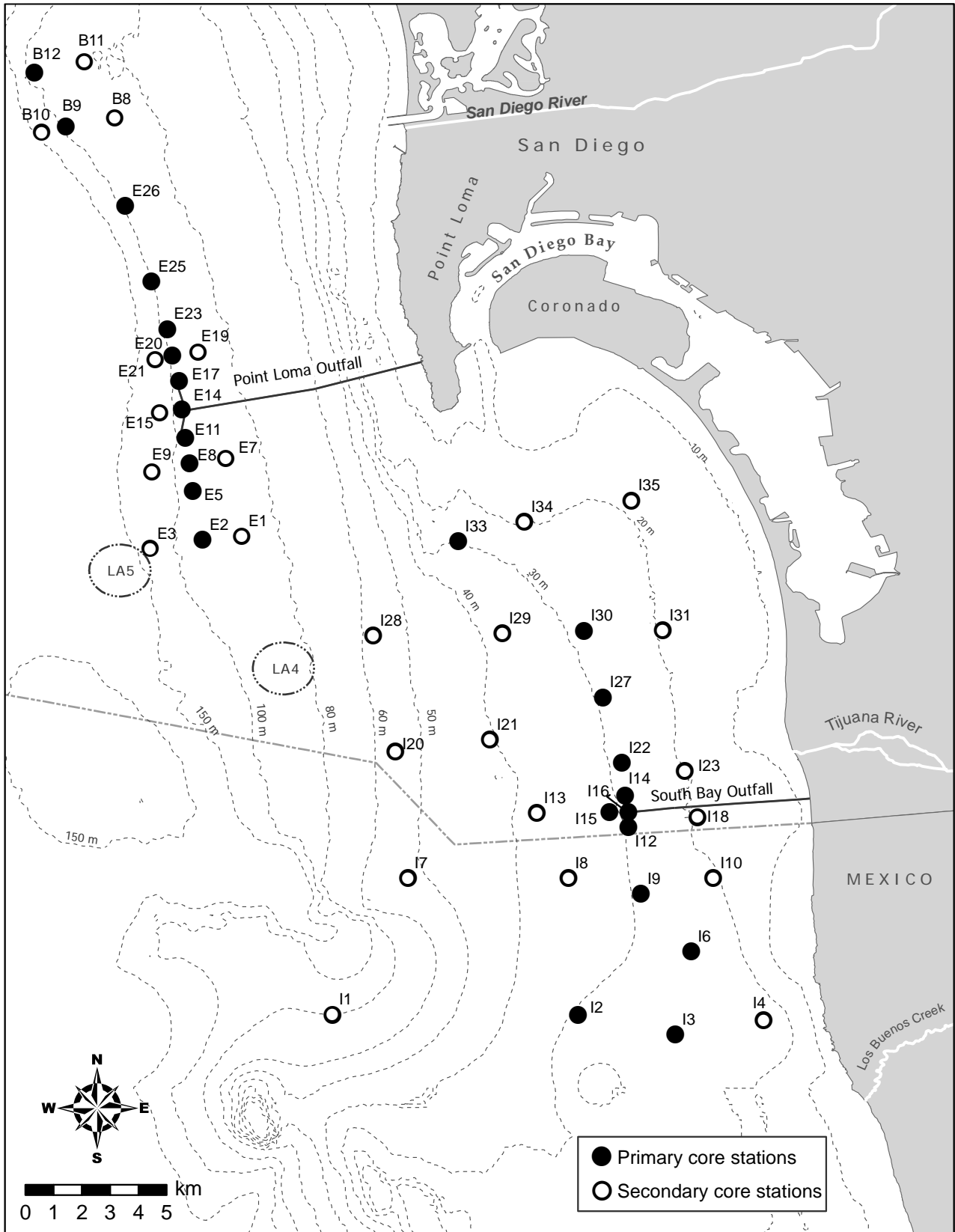


Figure 5.1

Benthic station locations sampled around the PLOO and SBOO as part of the City of San Diego's Ocean Monitoring Program.

Table 5.1

Summary of particle sizes and chemistry concentrations in sediments from PLOO benthic stations sampled historically (1991–2021) and during the current reporting period (2022–2023). Data include the total number of samples analyzed (n), detection rate (DR, %), minimum, maximum, and mean values for the entire survey area during each time period. For chemistry parameters, minimum and maximum values were calculated based on all samples, whereas means were calculated on detected values only; nd=not detected.

Parameter	Historical (1991–2021)					Current (2022–2023)				
	n	DR	Min	Max	Mean	n	DR	Min	Max	Mean
Particle Size (%)										
Coarse Particles	1241	27	0	64.2	1.4	79	16	0	20.8	1.4
Med-Coarse Sands	1241	95	0	66.5	3.7	79	99	0	28.2	2.9
Fine Sands	1241	100	0	85.6	52.1	79	100	21.2	60.5	40.8
Fine Particles	1241	100	0	80.9	42.7	79	100	21.2	71.2	54.9
Organic Indicators										
BOD (ppm)	1062	99	nd	980	303	36	100	186	660	319
Sulfides (ppm)	1260	94	nd	108	5.1	79	66	nd	70.1	13.2
TN (% weight)	1195	99	nd	0.192	0.052	79	100	0.028	0.086	0.048
TOC (% weight)	1196	100	0.13	4.85	0.69	79	100	0.29	3.12	0.72
TVS (% weight)	1248	100	0.2	5.4	2.4	66	100	1.4	3.4	2.1
Metals (ppm)										
Aluminum	1153	100	3130	31,800	9299	79	100	4220	10,900	6729
Antimony	1245	51	nd	13.90	1.68	79	75	nd	2.13	0.88
Arsenic	1263	100	0.75	8.82	3.02	79	100	1.81	5.84	2.70
Barium	757	100	10.3	155	36.15	79	100	15.8	46.6	28.7
Beryllium	1263	47	nd	6.76	0.43	79	100	0.102	0.362	0.166
Cadmium	1263	48	nd	6.27	0.58	79	27	nd	0.122	0.087
Chromium	1263	100	nd	40.6	17.25	79	100	9.4	27.1	14.9
Copper	1263	100	nd	82.4	8.05	79	100	4.2	18.8	6.9
Iron	1197	100	4840	31,900	12,882	79	100	6410	22,500	10,735
Lead	1263	69	nd	326.0	5.7	79	100	1.9	5.4	3.1
Manganese	1064	100	32	319	100	79	100	52	149	78
Mercury	1246	68	nd	0.140	0.030	79	100	0.009	0.057	0.023
Nickel	1263	97	nd	29.0	7.2	79	100	2.9	8.2	5.1
Selenium	1263	47	nd	0.90	0.28	79	18	nd	0.54	0.40
Silver	1263	12	nd	67.4	1.64	79	0	—	—	—
Thallium	1263	8	nd	113.0	11.1	66	0	—	—	—
Tin	1064	67	nd	42.00	1.31	79	100	0.27	1.23	0.62
Zinc	1263	100	nd	176.0	30.0	79	100	16.9	38.0	25.4
Pesticides (ppt)										
Total DDT	1238	54	nd	63,580	1237	66	100	101	862	301
Total Chlordane	1238	2	nd	2000	314	66	5	nd	650	247
Total HCH	1238	1	nd	980	231	66	5	nd	175	133
HCB	1031	5	nd	3300	704	66	0	—	—	—
Endrin aldehyde	1238	0.1	nd	970	970	66	0	—	—	—
Mirex	1238	0.1	nd	66	66	66	0	—	—	—
Total PCB (ppt)	928	22	nd	60,730	2337	66	48	nd	50,682	2674
Total PAH (ppb)	1243	24	nd	9751.3	119.7	79	44	nd	402.9	42.1
Total PBDE (ppt)	0	—	—	—	—	79	66	nd	623	166

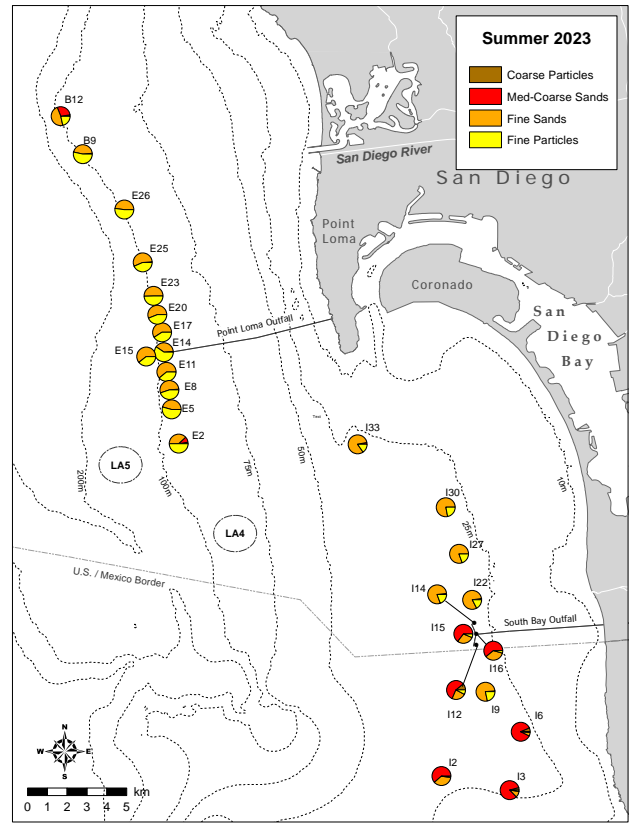
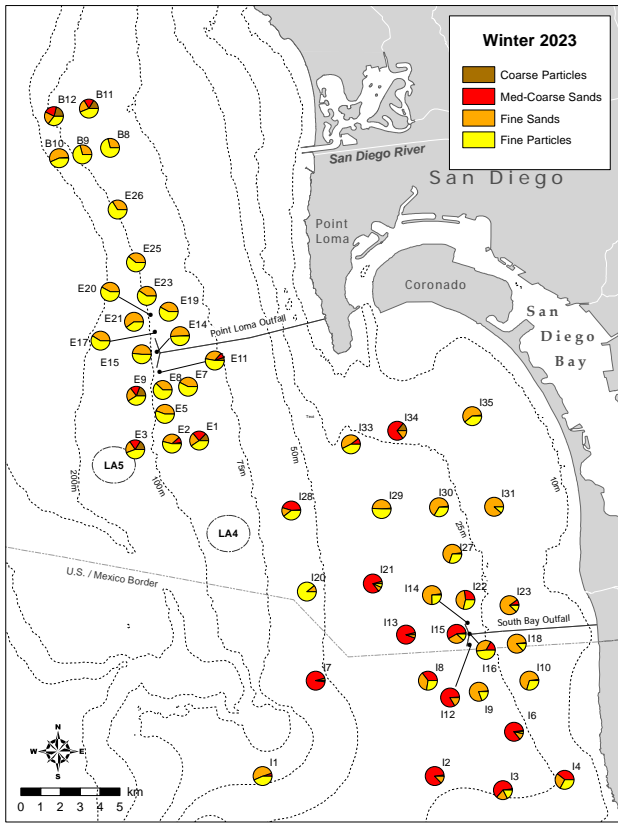
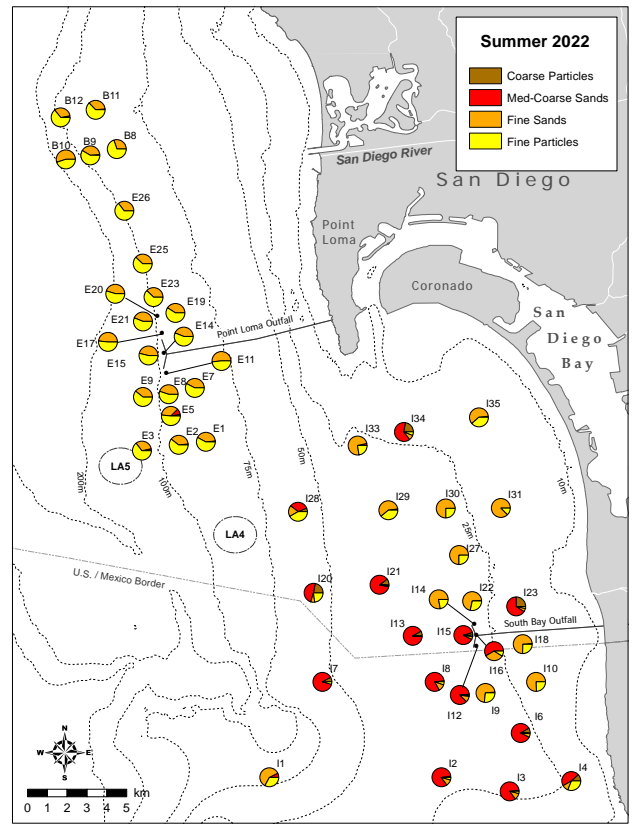
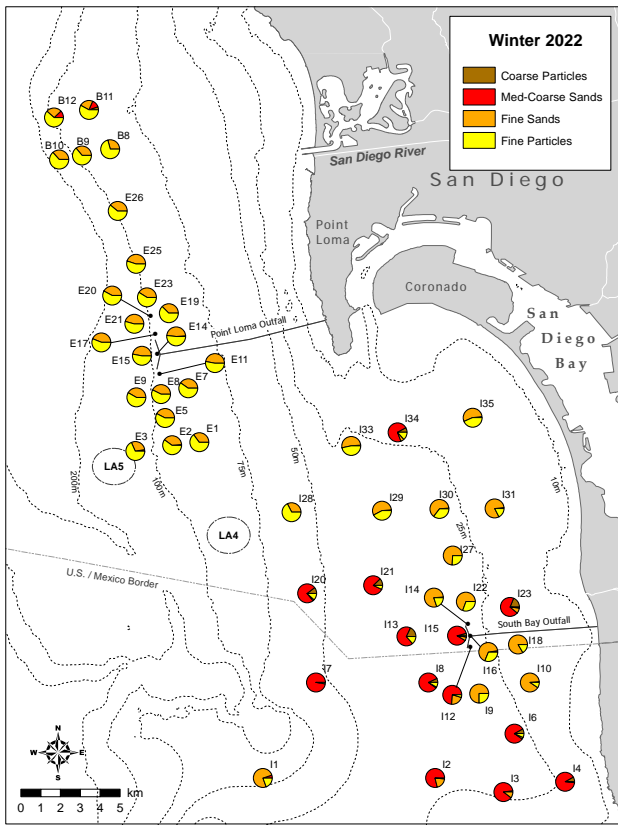


Figure 5.2

Sediment composition at PLOO and SBOO benthic stations during winter and summer surveys of 2022 and 2023.

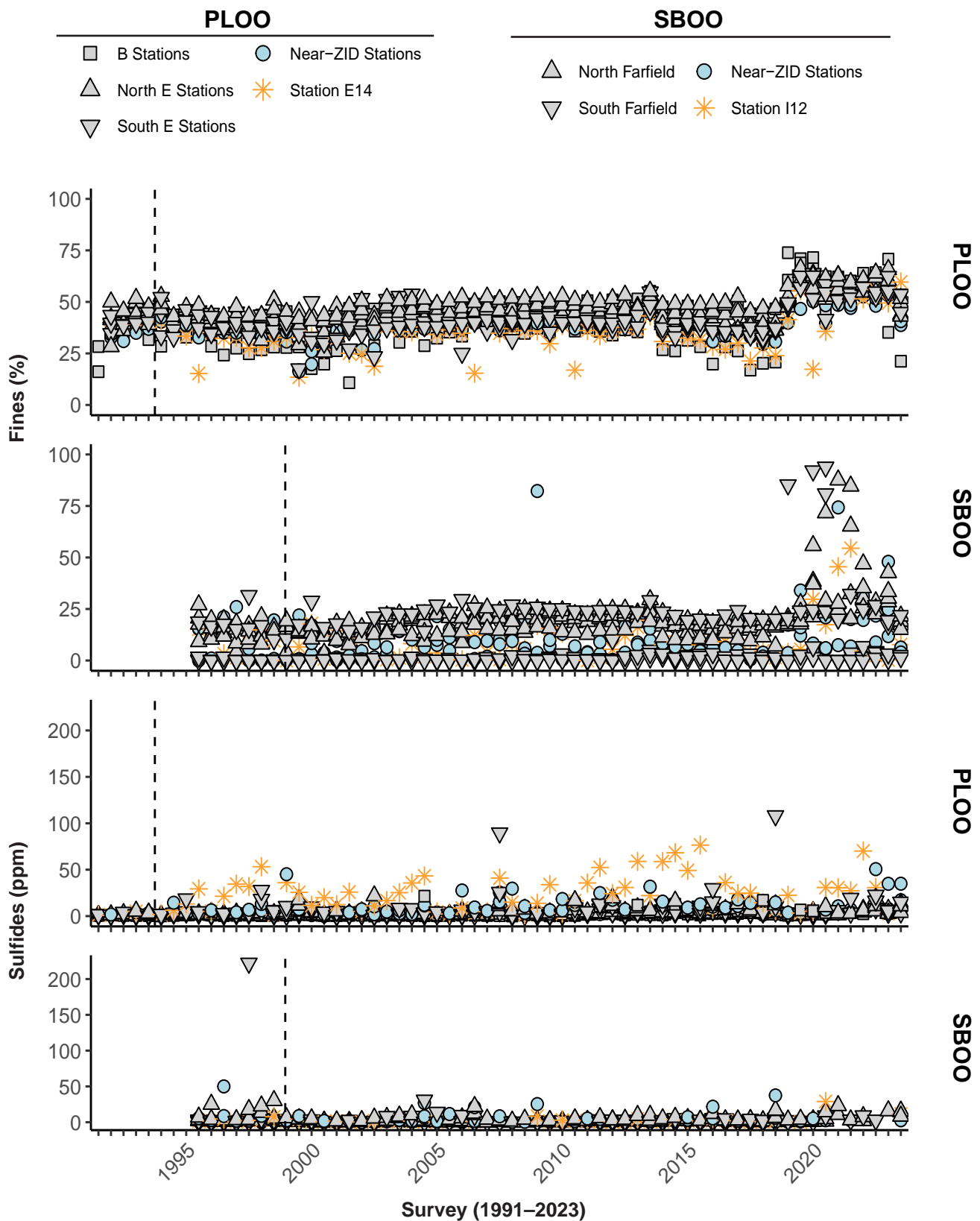


Figure 5.3
 Percent fines and concentrations of organic indicators in sediments sampled during winter and summer surveys at PLOO primary core stations from 1991 through 2023 and at SBOO primary core stations from 1995 through 2023. Data represent detected values from each station, $n \leq 12$ samples per survey. Dashed lines indicate onset of discharge from the PLOO or SBOO. Biochemical Oxygen Demand (BOD) only measured at PLOO stations.

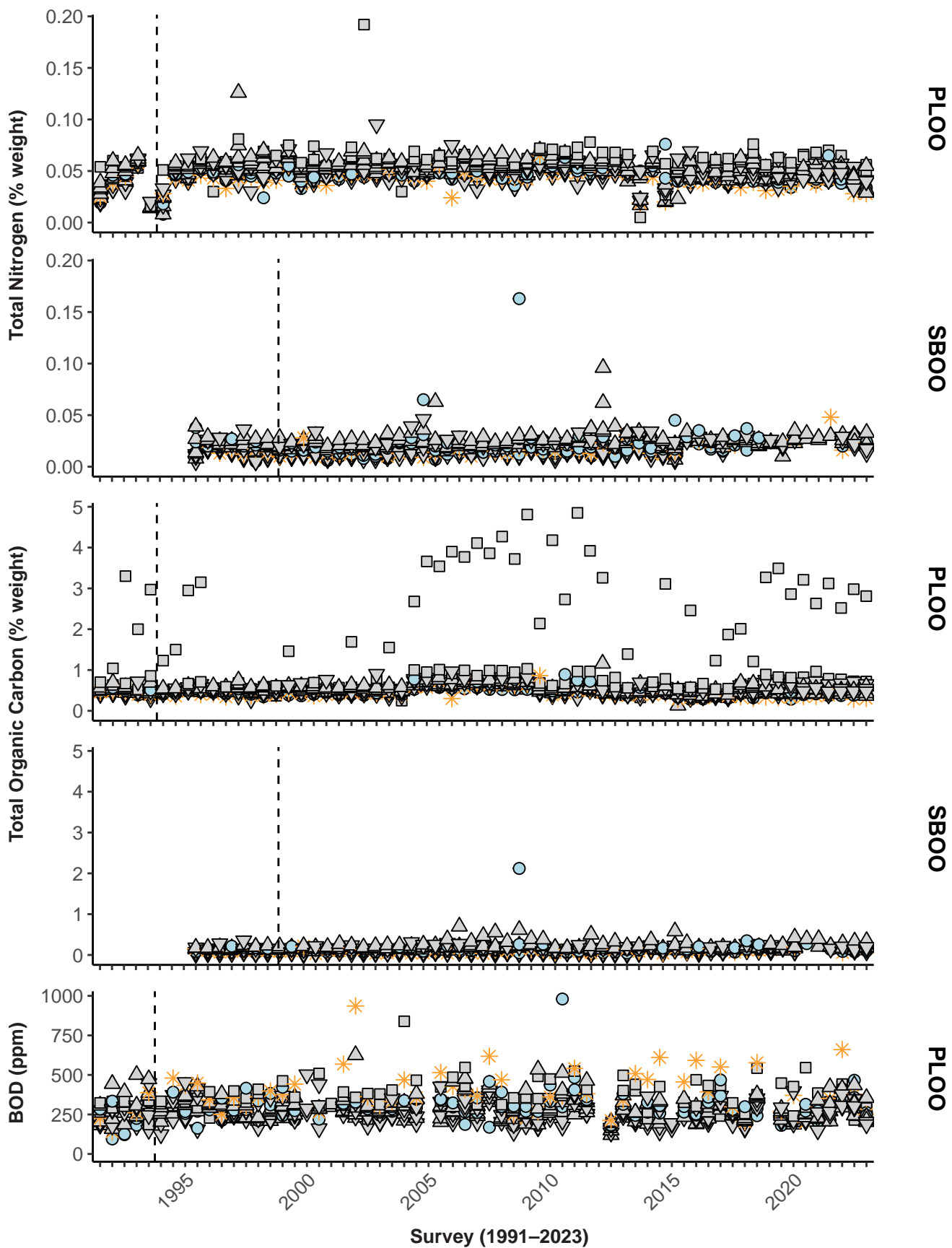


Figure 5.3 *continued*

Table 5.2

Summary of particle sizes and chemistry concentrations in sediments from SBOO benthic stations sampled historically (1995–2021) and during the current reporting period (2022–2023). Data include the total number of samples analyzed (n), detection rate (DR, %), minimum, maximum, and mean values for the entire survey area during each time period. For chemistry parameters, minimum and maximum values were calculated based on all samples, whereas means were calculated on detected values only; nd=not detected.

Parameter	Historical (1995–2021)					Current (2022–2023)				
	n	DR	Min	Max	Mean	n	DR	Min	Max	Mean
Particle Size (%)										
Coarse Particles	1410	44	0	56.8	2.8	93	52	0	25.4	3.2
Med-Coarse Sands	1410	99	0	99.8	34.7	93	100	0.1	97.6	37.6
Fine Sands	1410	100	0	97.4	49.6	93	98	0	89.3	40.3
Fine Particles	1410	88	0	100	12.9	93	96	0	88.6	18.9
Organic Indicators										
Sulfides (ppm)	1414	79	nd	222.0	3.1	76	24	nd	39.5	10.0
TN (% weight)	1415	84	nd	0.163	0.022	93	57	nd	0.074	0.029
TOC (% weight)	1415	93	nd	6.85	0.19	93	69	nd	4.03	0.29
TVS (% weight)	1355	100	0.2	39.8	0.9	81	100	0.2	1.8	0.8
Metals (ppm)										
Aluminum	1415	100	495	30,100	4530	93	100	628	7510	3151
Antimony	1415	36	nd	6.40	0.69	93	60	nd	1.23	0.60
Arsenic	1415	99	nd	11.90	2.43	93	100	0.47	9.81	2.25
Barium	1011	100	nd	177.0	19.4	93	100	1.4	46.2	15.1
Beryllium	1415	40	nd	3.09	0.19	93	88	nd	0.155	0.069
Cadmium	1415	28	nd	2.00	0.13	93	9	nd	0.088	0.042
Chromium	1415	100	nd	39.0	9.7	93	100	3.4	13.3	8.2
Copper	1415	74	nd	99.2	3.4	93	62	nd	4.8	2.7
Iron	1415	100	559	29,300	6172	93	100	1140	8670	4798
Lead	1415	67	nd	20.0	2.2	93	100	0.8	2.9	1.6
Manganese	1388	100	5	621	63	93	100	6	91	41
Mercury	1386	29	nd	0.135	0.011	68	66	nd	0.022	0.007
Nickel	1415	77	nd	22.8	2.9	93	96	nd	4.9	1.7
Selenium	1415	14	nd	0.62	0.22	93	2	nd	0.25	0.24
Silver	1415	12	nd	11.20	0.98	93	0	—	—	—
Thallium	1415	6	nd	18.0	2.5	81	0	—	—	—
Tin	1388	53	nd	4.50	0.80	93	80	nd	0.64	0.29
Zinc	1415	95	nd	136.0	13.4	93	100	1.8	24.0	10.1

Table 5.2 *continued*

Parameter	Historical (1995–2021)					Current (2022–2023)				
	n	DR	Min	Max	Mean	n	DR	Min	Max	Mean
<i>Pesticides (ppt)</i>										
Total DDT	1372	17	nd	23,380	938	81	20	nd	1346	352
Total Chlordane	1372	0	nd	600	221	81	0	—	—	—
Total HCH	1372	1	nd	3550	581	81	1	nd	32	32
HCB	1004	7	nd	6200	702	81	1	nd	196	196
Dieldrin	1372	0.1	nd	60	60	81	0	—	—	—
Endrin	1372	0.1	nd	133	133	81	0	—	—	—
Beta-Endosulfan	1372	0.1	nd	820	820	81	0	—	—	—
Mirex	1372	0	—	—	—	81	2	nd	50	41
<i>Total PCB (ppt)</i>	1217	4	nd	106,390	2991	81	10	nd	558	314
<i>Total PAH (ppb)</i>	1391	13	nd	1819.5	81.3	93	20	nd	44.3	11.6
<i>Total PBDE (ppt)</i>	0	—	—	—	—	93	11	nd	142	73

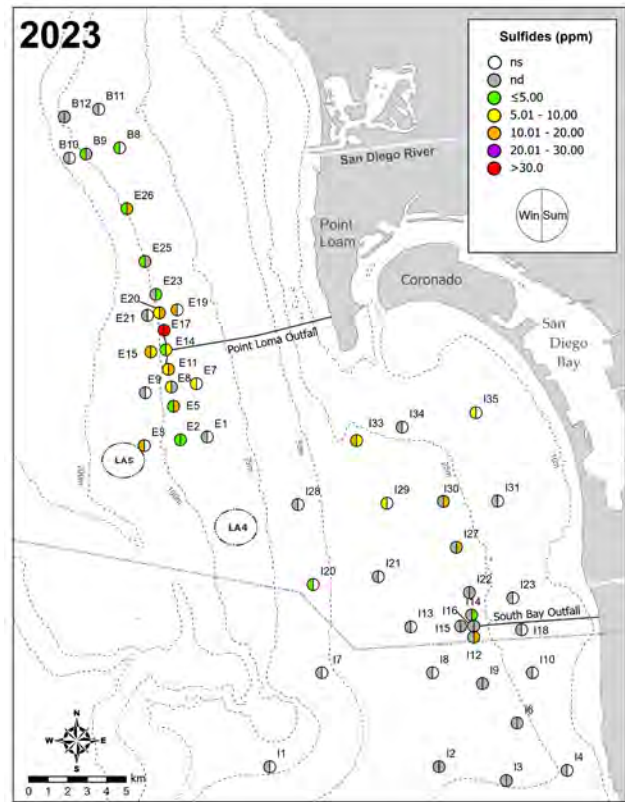
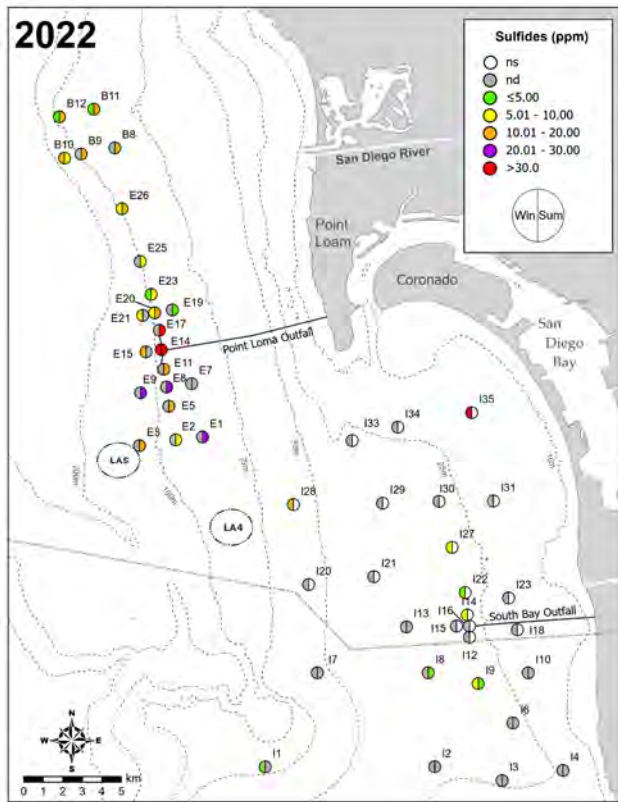
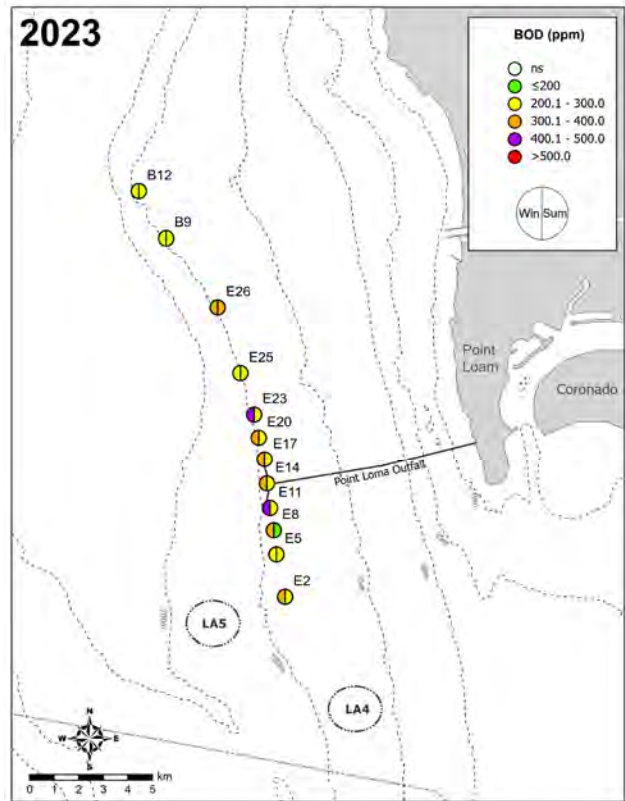
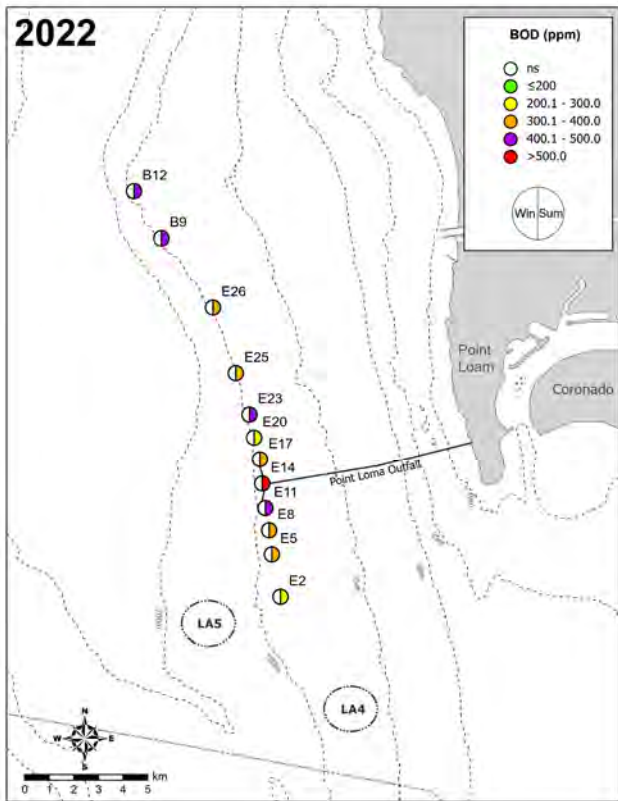


Figure 5.4

Distribution of select organic loading indicators in sediments from the PLOO and SBOO regions during winter and summer surveys of 2022 and 2023. BOD is only measured at PLOO primary core stations during summer surveys; ns = not sampled (or not reportable, see text); nd=not detected.

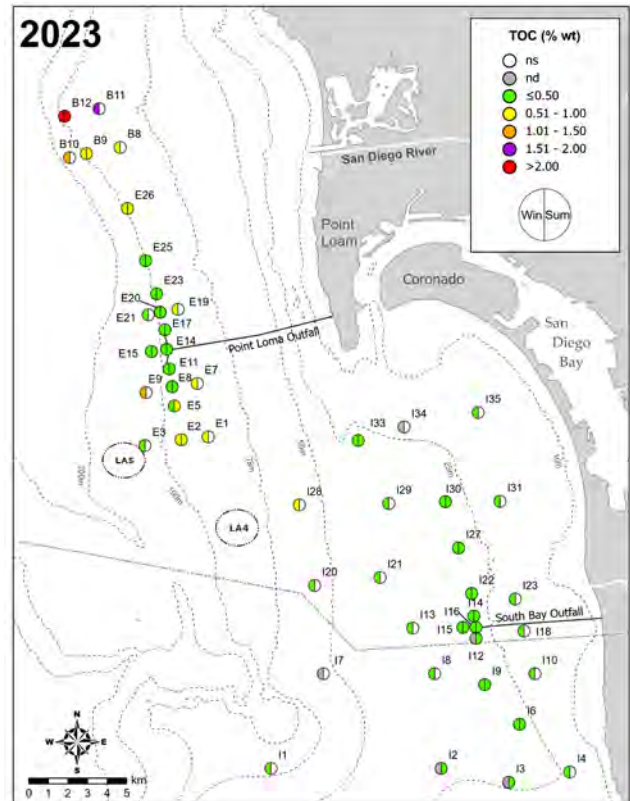
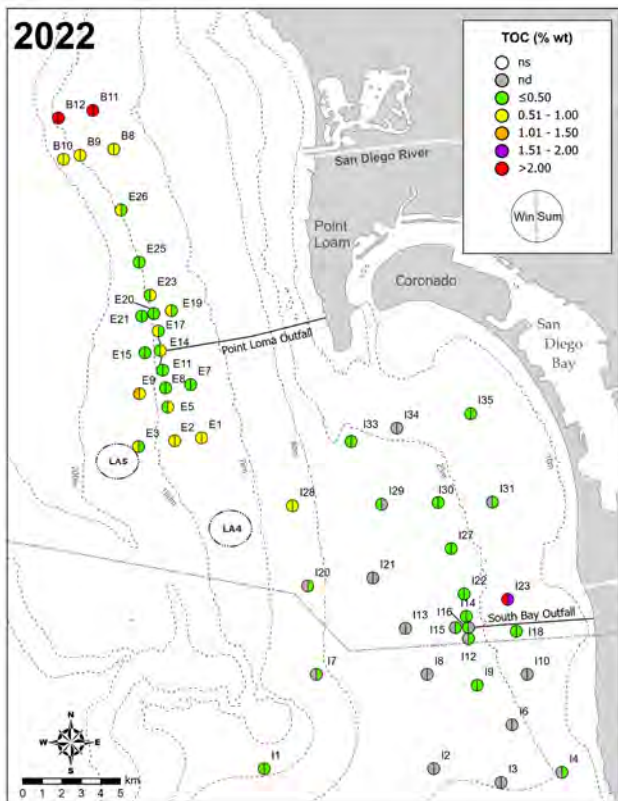
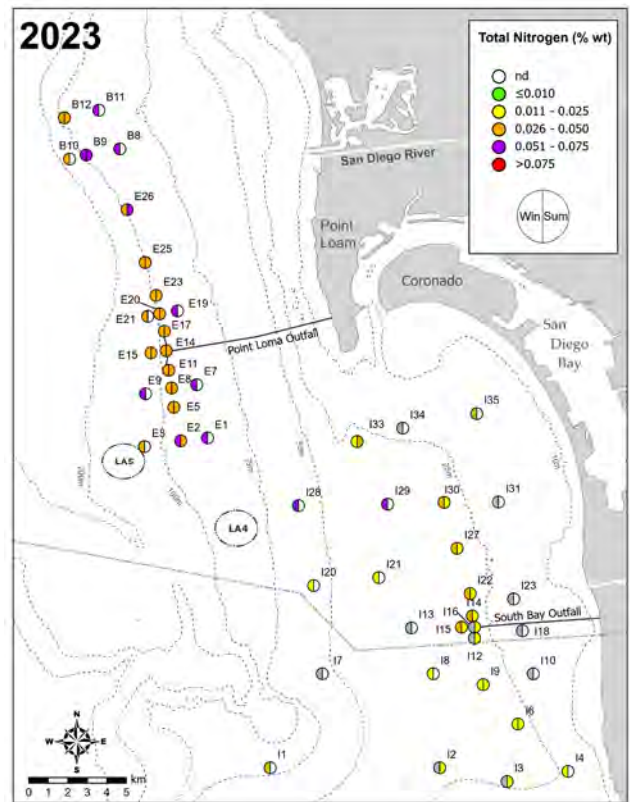
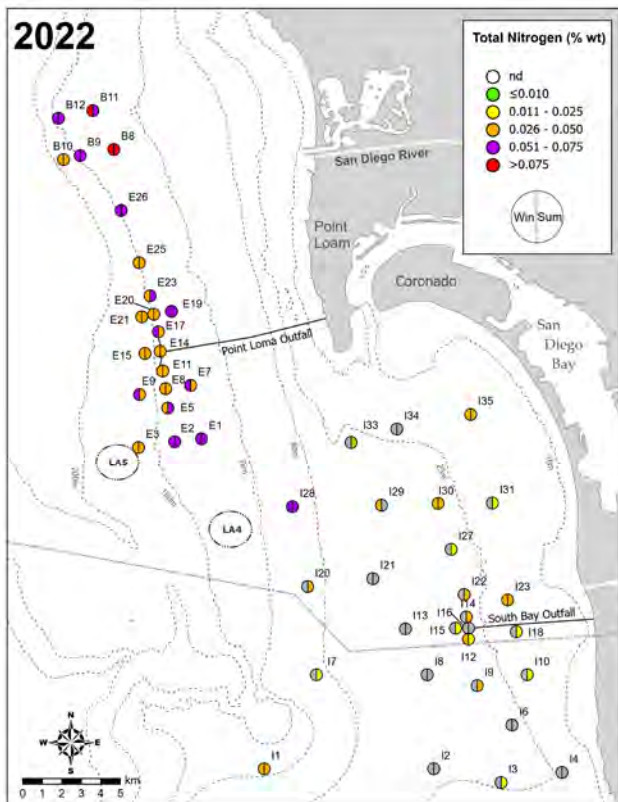


Figure 5.4 continued

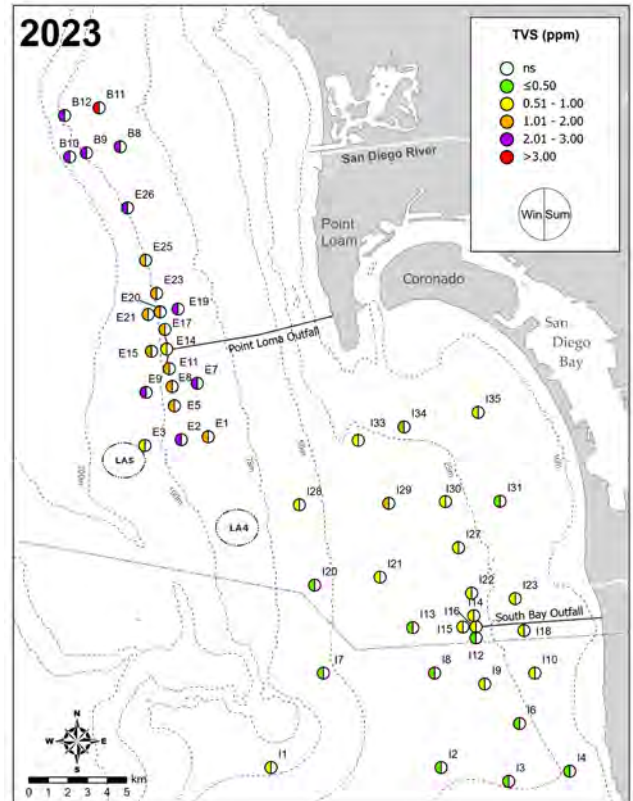
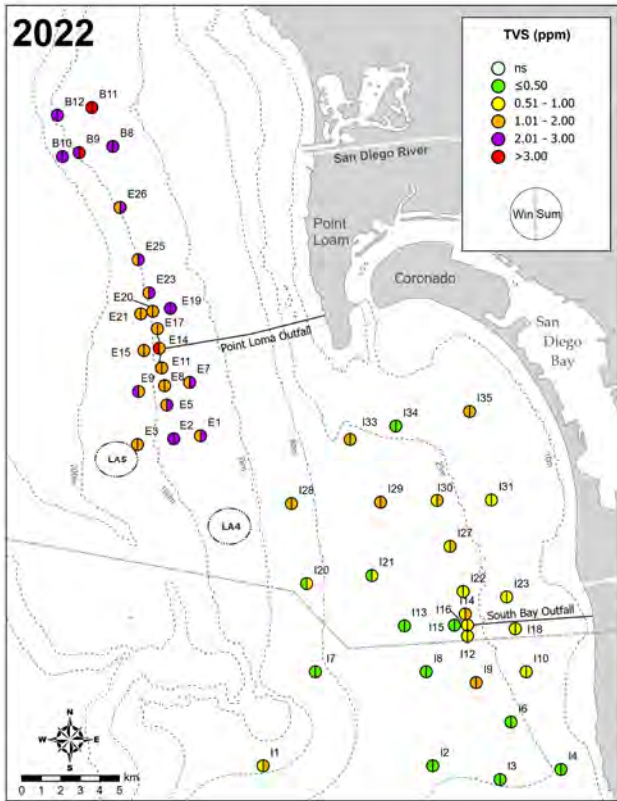


Figure 5.4 continued

Table 5.3

Summary of samples with chemistry concentrations that exceeded Effects Range Low (ERL) and Effects Range Median (ERM) thresholds (see Long et al 1995) in sediments from PLOO and SBOO benthic stations sampled historically (1991–2021) and during the current reporting period (2022–2023). Data include the percent of samples that exceeded the ERL (%ERL) and ERM (%ERM) thresholds during each time period. See Tables 5.1 and 5.2 for total number of samples analyzed.

Parameter	Thresholds		PLOO				SBOO			
	ERL	ERM	1991–2021		2022–2023		1995–2021		2022–2023	
			%ERL	%ERM	%ERL	%ERM	%ERL	%ERM	%ERL	%ERM
<i>Metals (ppm)</i>										
Arsenic	8.2	70.0	0.2	0	0	0	2.6	0	2.2	0
Cadmium	1.2	9.6	7.1	0	0	0	0.2	0	0	0
Chromium	81	370	0	0	0	0	0	0	0	0
Copper	34	270	0.3	0	0	0	0.1	0	0	0
Lead	46.7	218.0	0.2	0.1	0	0	0	0	0	0
Mercury	0.15	0.71	0	0	0	0	0	0	0	0
Nickel	20.9	51.6	0.1	0	0	0	0.1	0	0	0
Silver	1.0	3.7	5.5	0.6	0	0	3.5	1.0	0	0
Zinc	150	410	0.1	0	0	0	0	0	0	0
<i>tDDT (ppt)</i>	1580	461,000	8.7	0.1	0	0	2.2	0	0	0
<i>tPAH (ppb)</i>	4022	44,792	0.1	0	0	0	0	0	0	0

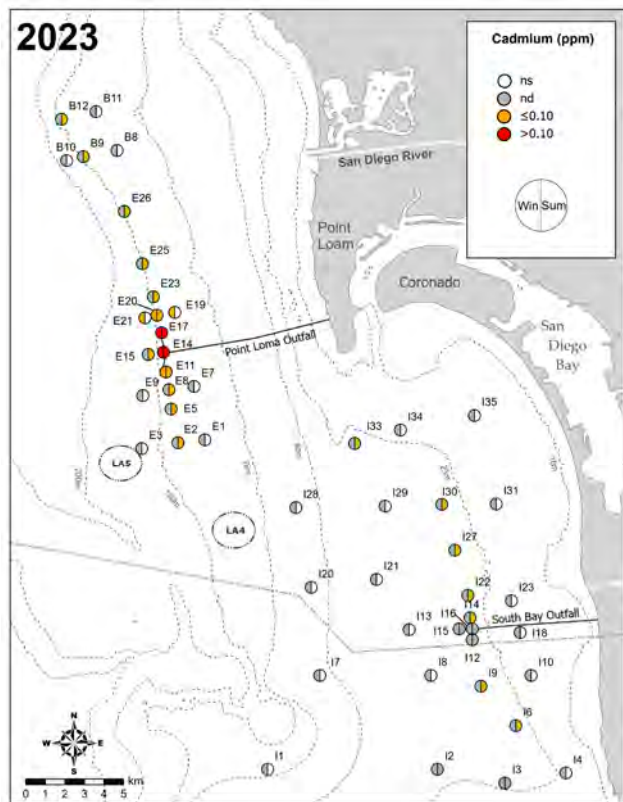
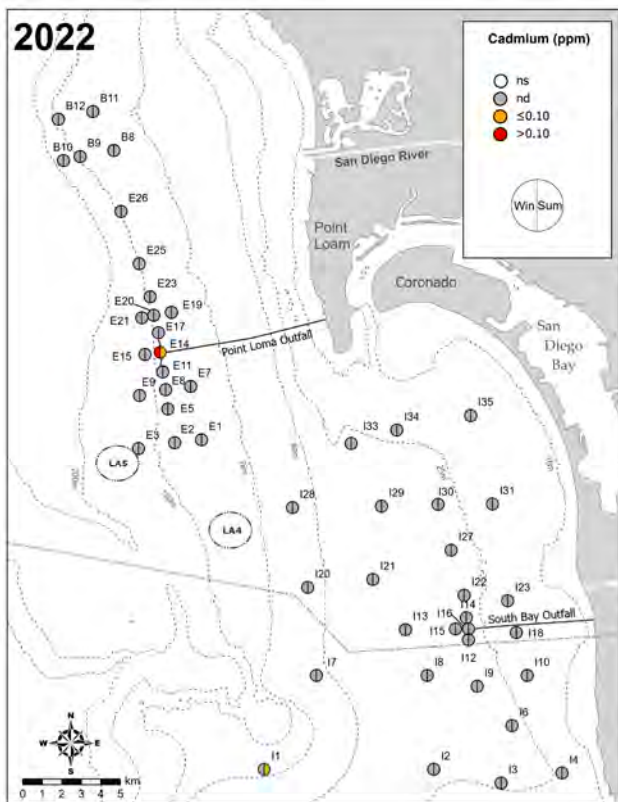
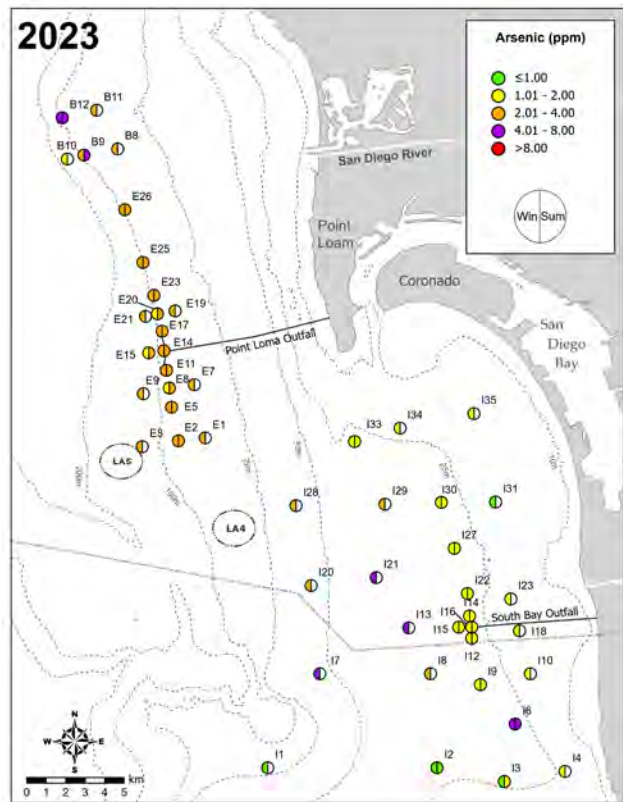
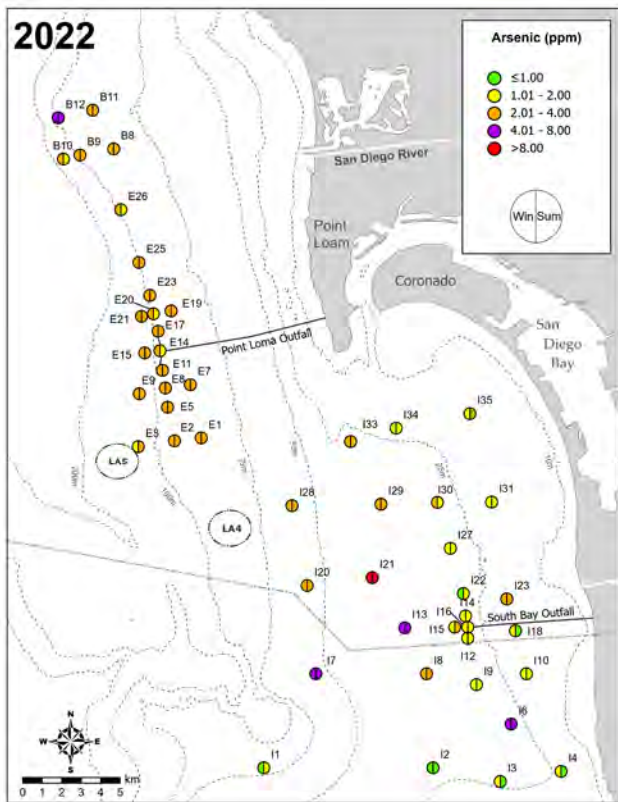


Figure 5.5
 Distribution of select metals (ppm) in sediments from the PLOO and SBOO regions during winter and summer surveys of 2022 and 2023; ns = not sampled (or not reportable, see text); nd=not detected.

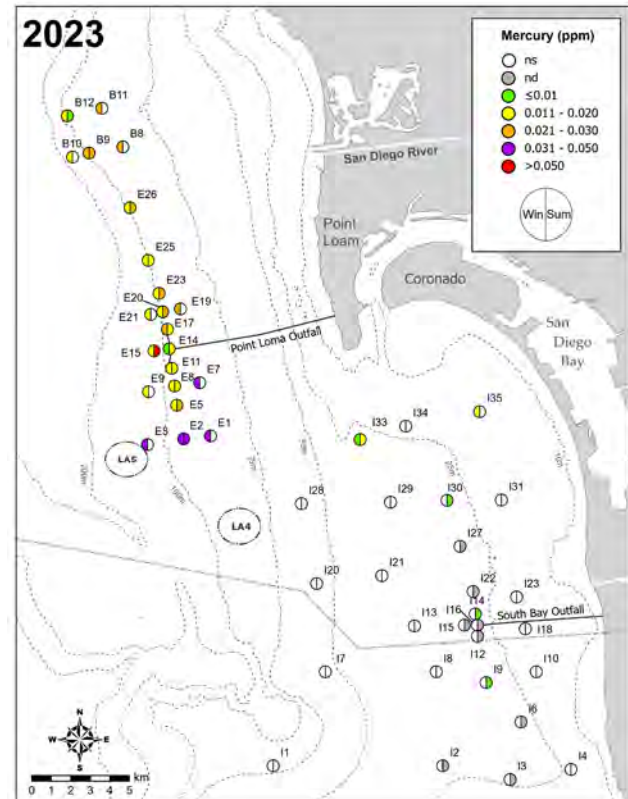
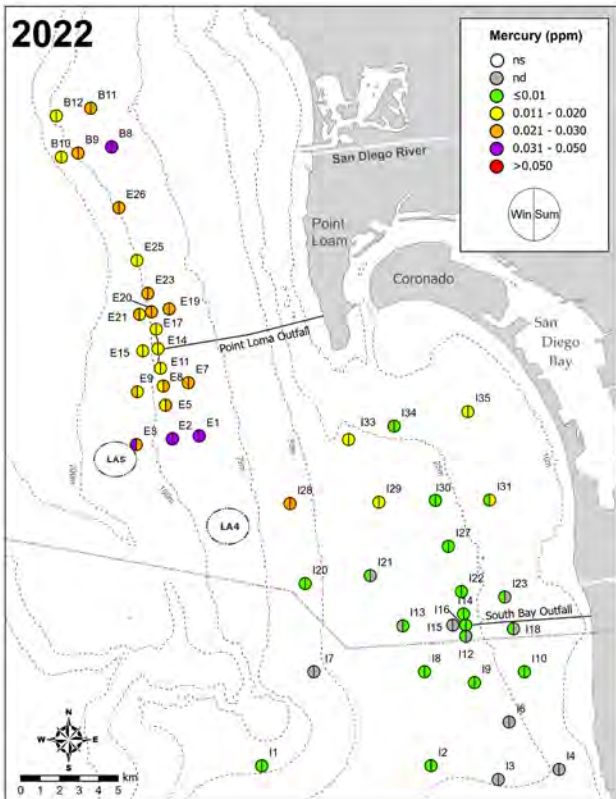
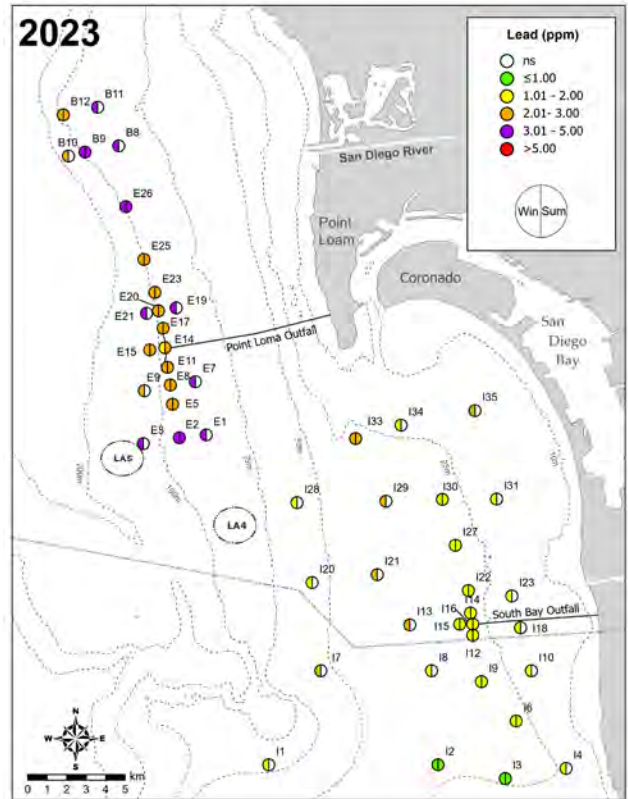
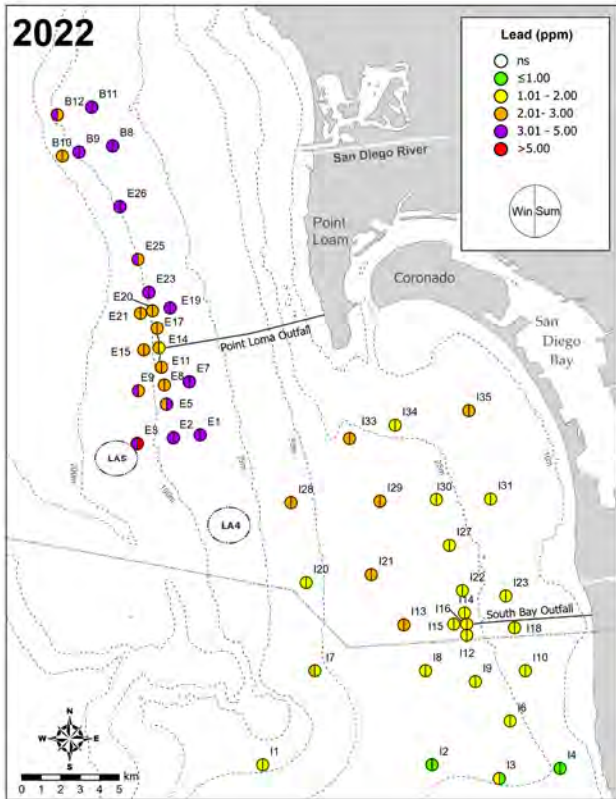


Figure 5.5 continued

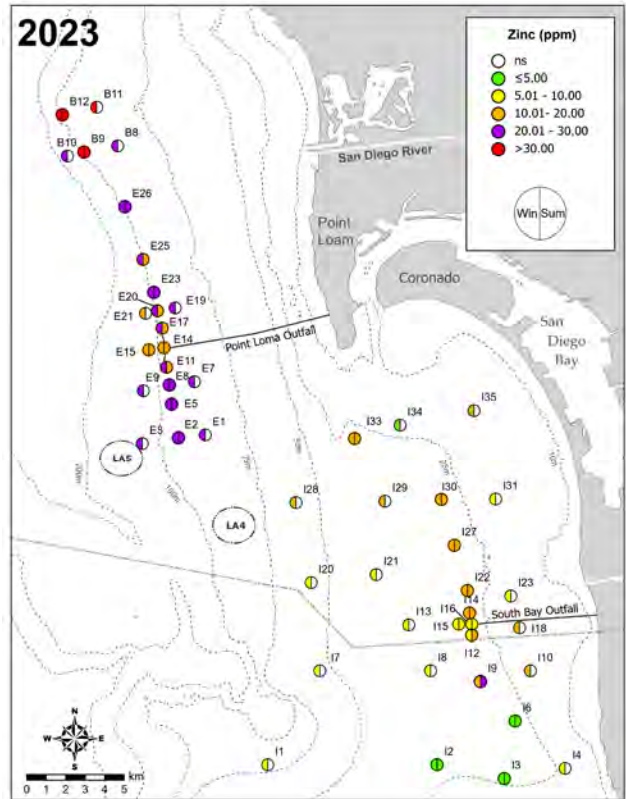
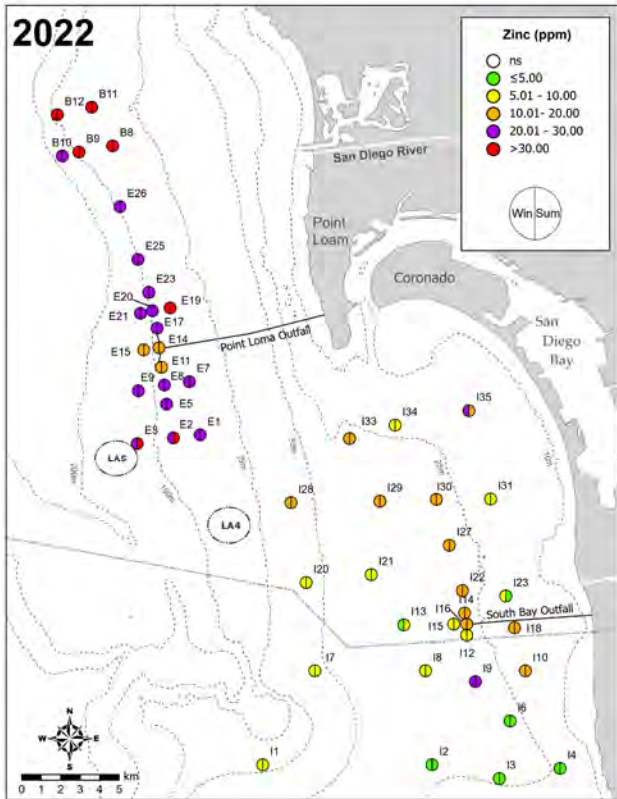


Figure 5.5 continued

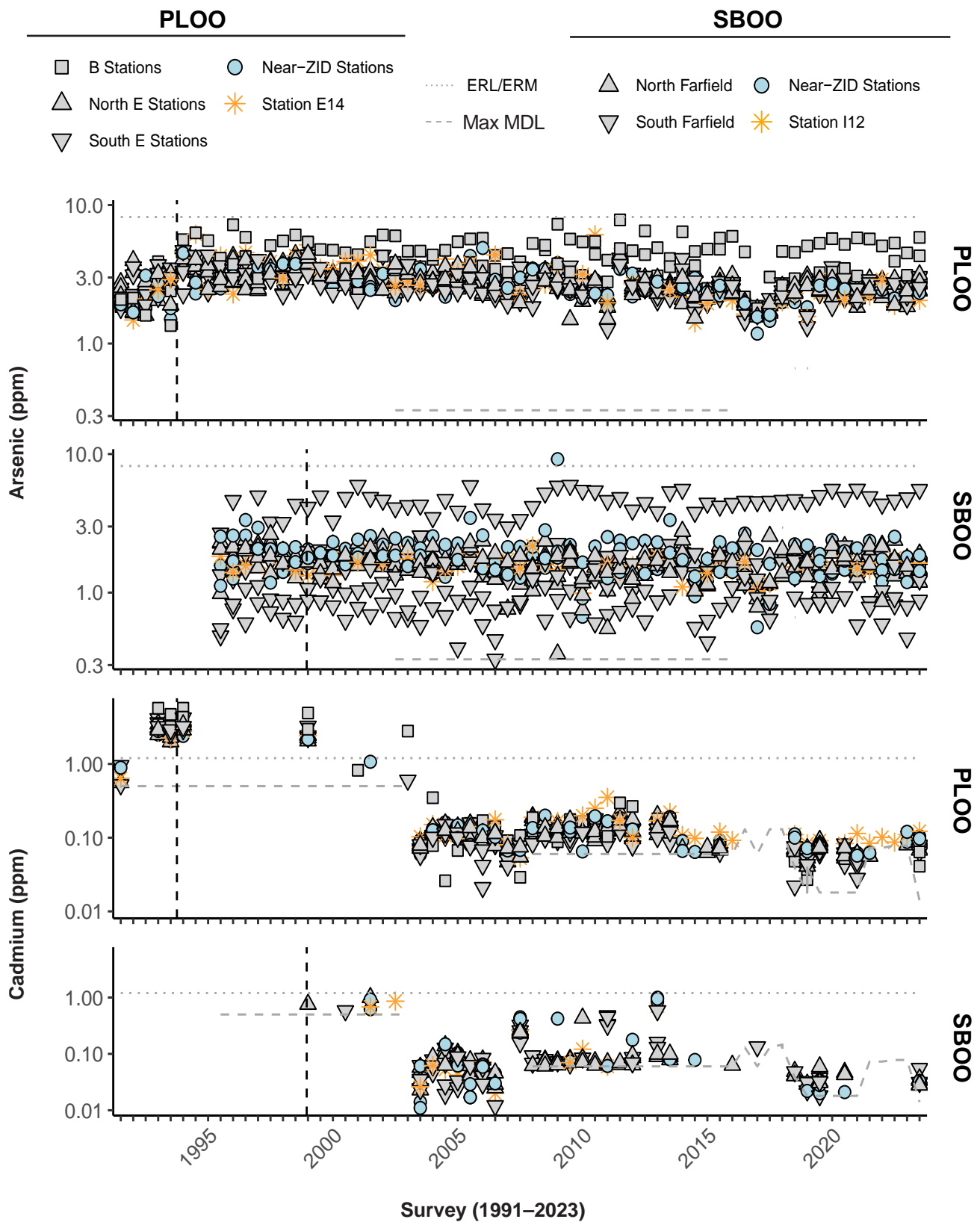


Figure 5.6

Concentrations of select metals in sediments sampled during winter and summer surveys at PLOO primary core stations from 1991 through 2023 and at SBOO primary core stations from 1995 through 2023. Data represent detected values from each station, $n \leq 12$ samples per survey. Dashed lines indicate onset of discharge from the PLOO or SBOO. Thresholds included (ERLs, ERMs) when relevant (see Table 5.3), along with the maximum MDL per survey.

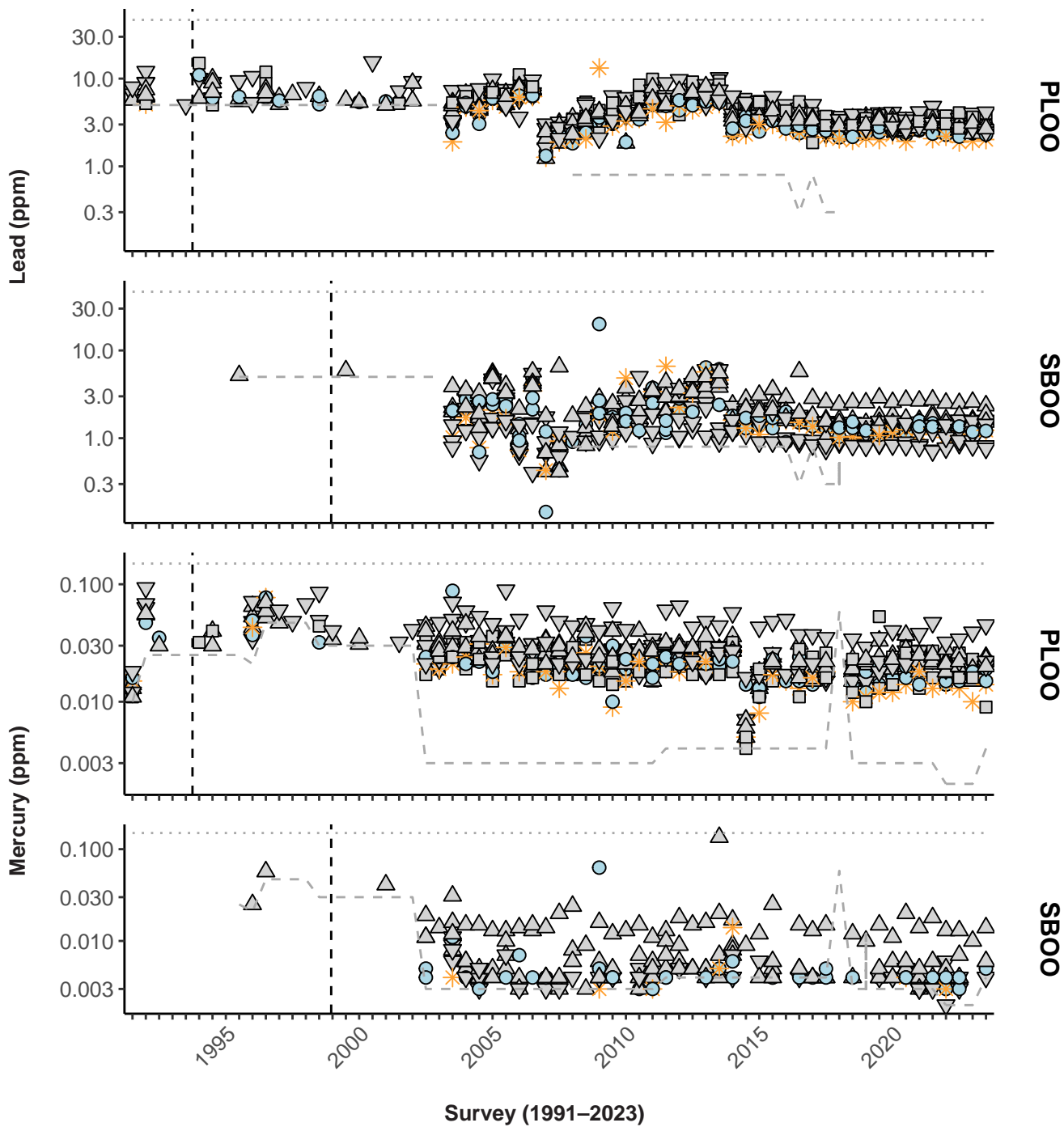


Figure 5.6 *continued*

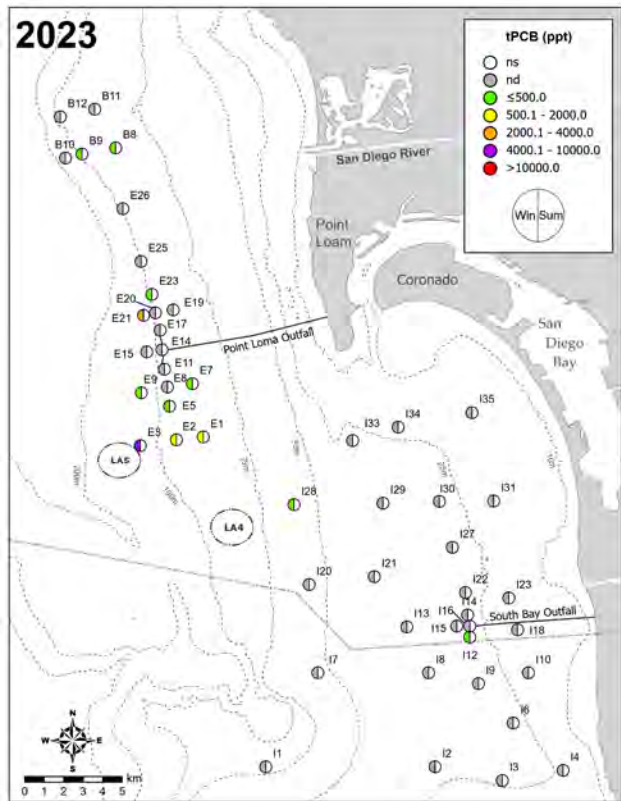
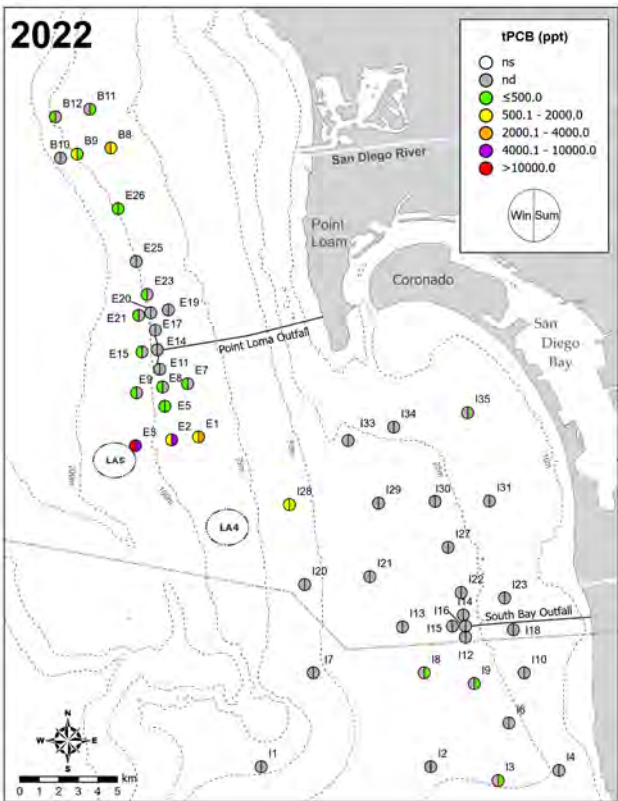
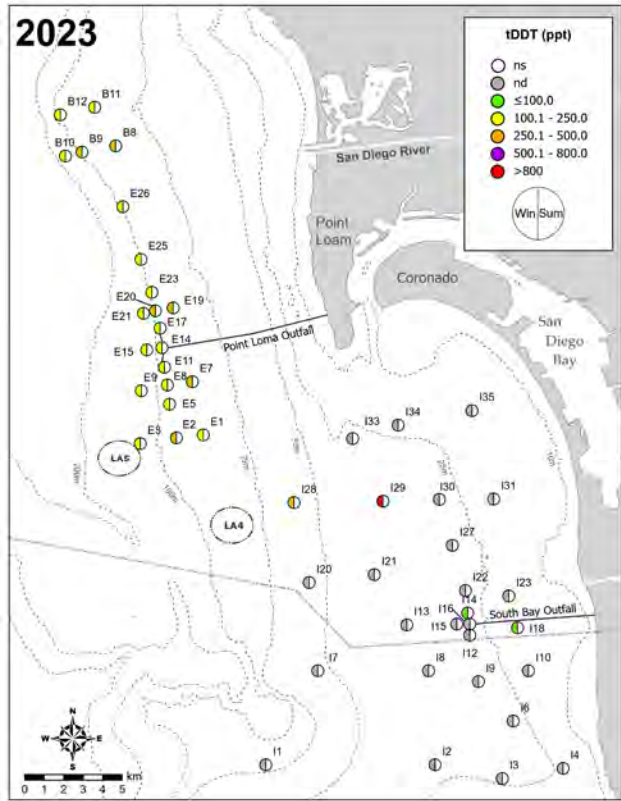
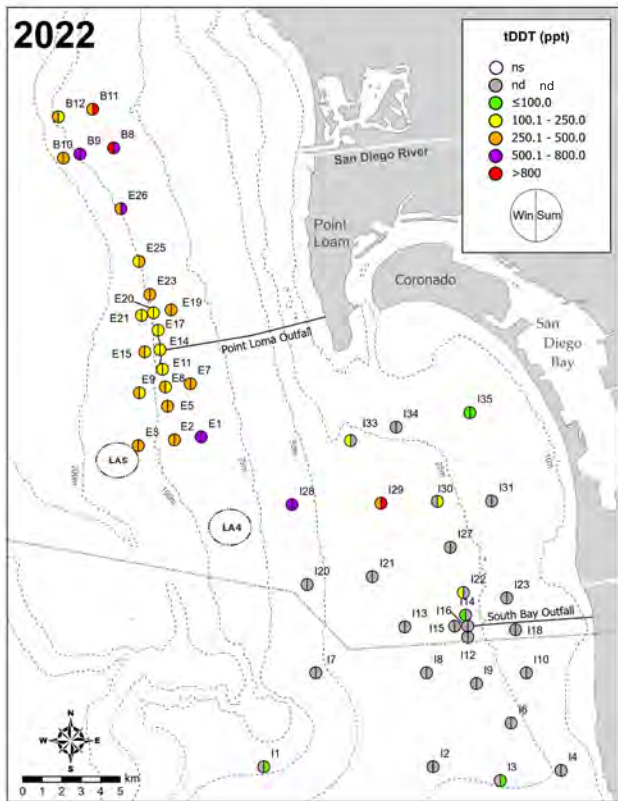


Figure 5.7 Distribution of total DDT, total PCB and total PAH in sediments from the PLOO and SBOO regions during winter and summer surveys of 2022 and 2023; ns = not sampled (or not reportable, see text); nd = not detected.

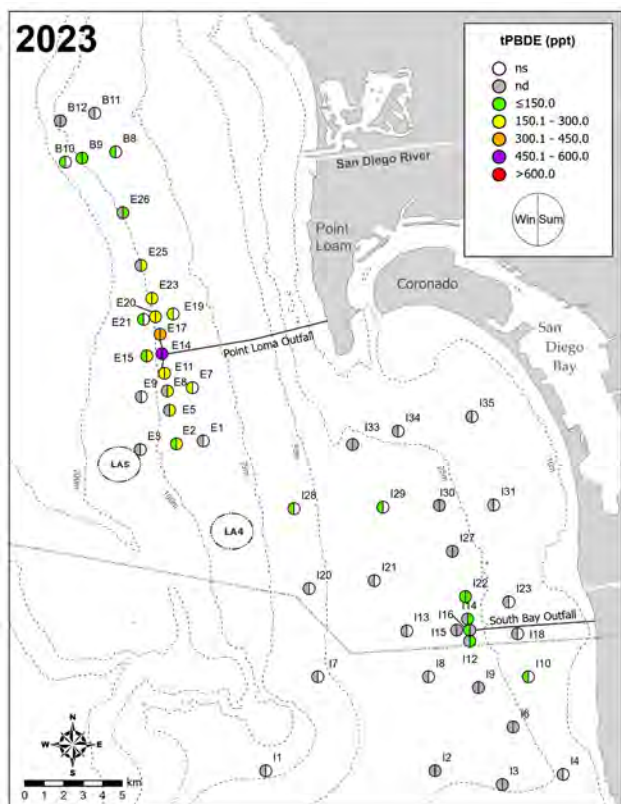
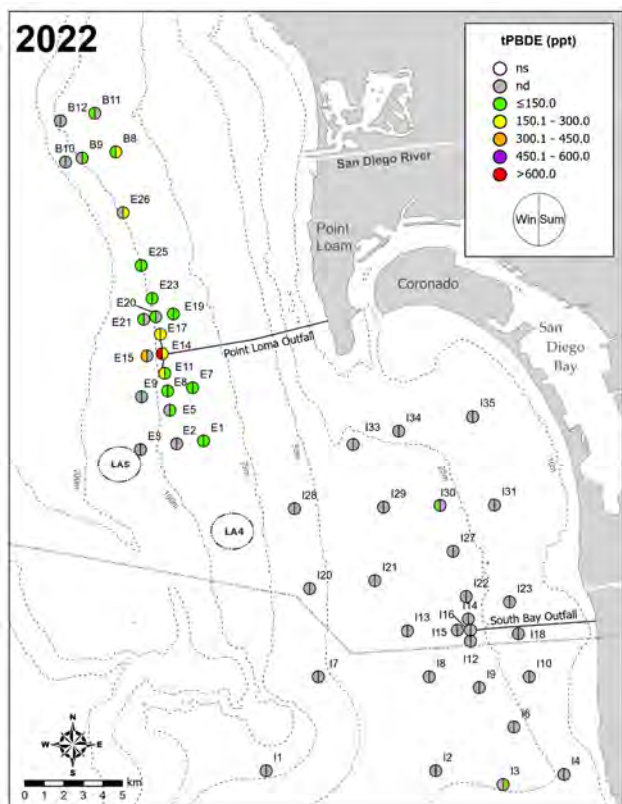
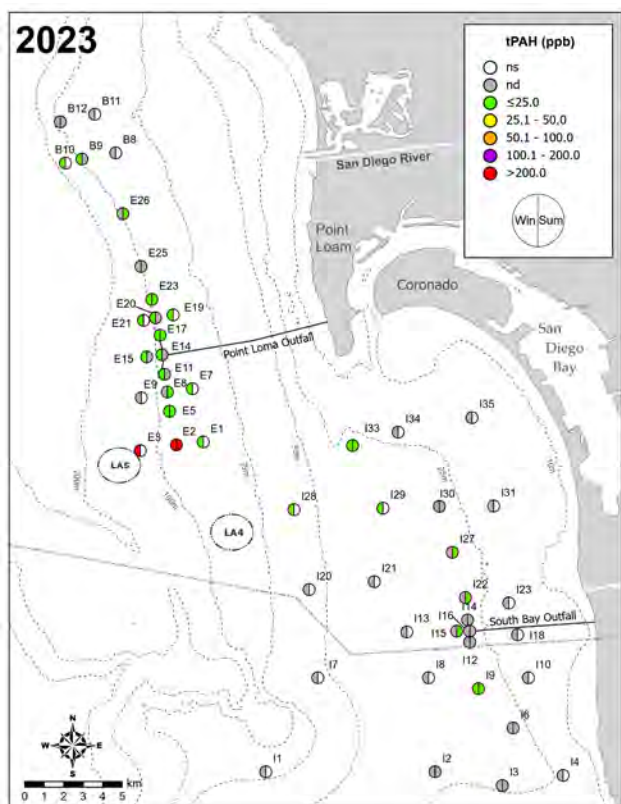
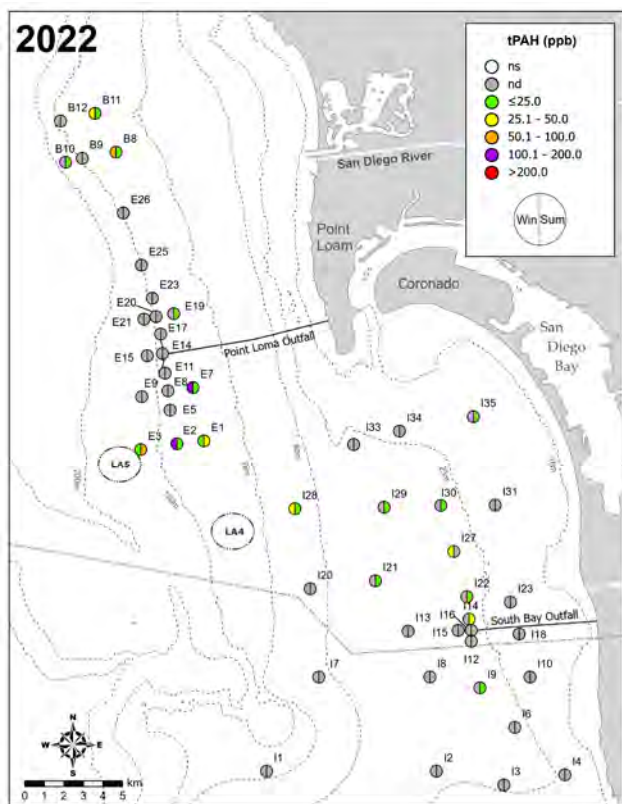


Figure 5.7 continued

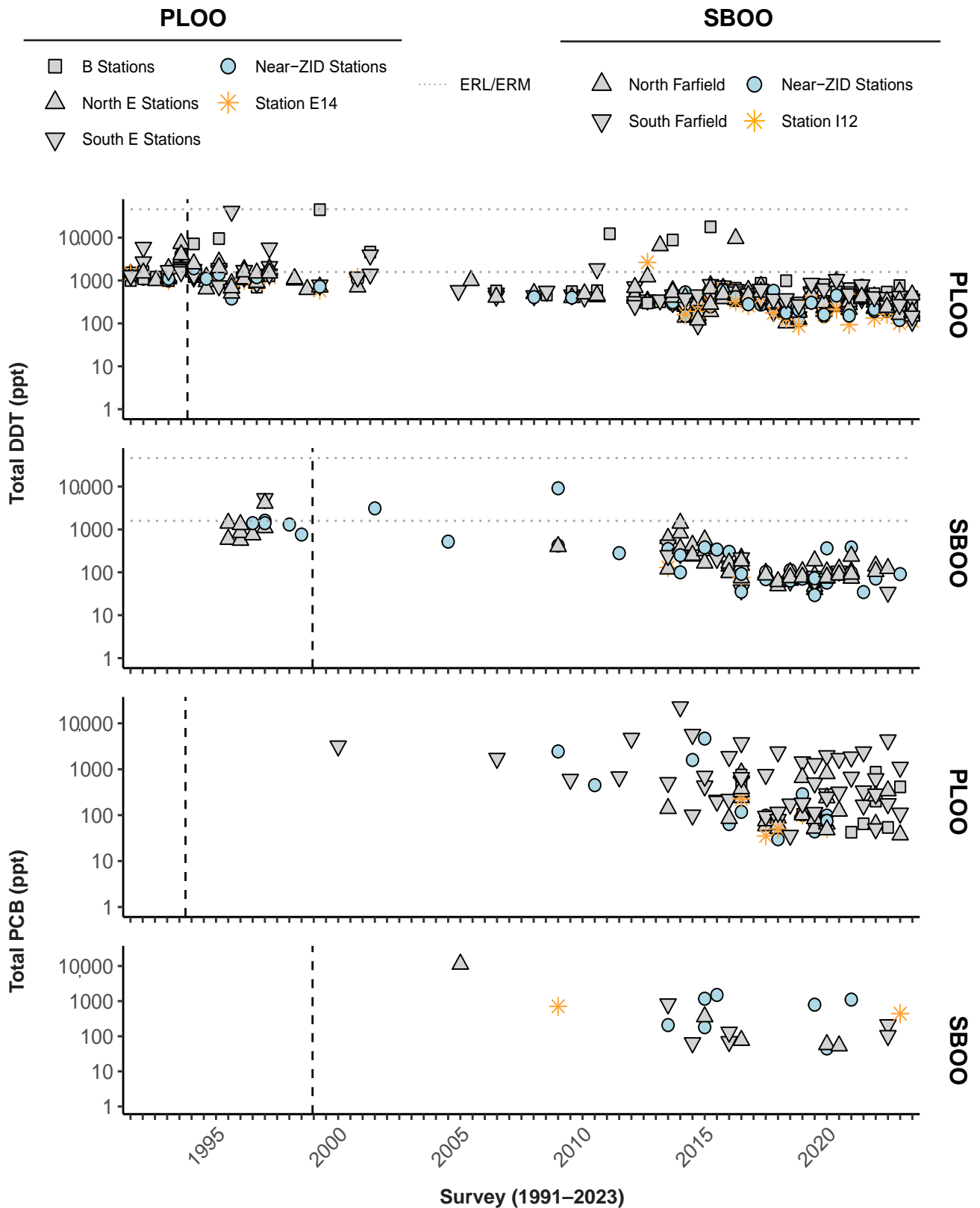


Figure 5.8

Concentrations of total DDT, total PCB, and total PAH in sediments sampled during winter and summer surveys at PLOO primary core stations from 1991 through 2023 and at SBOO primary core stations from 1995 through 2023. Data represent detected values from each station, $n \leq 12$ samples per survey. Dashed lines indicate onset of discharge from the PLOO or SBOO. Thresholds included (ERLs, ERM) when relevant (see Table 5.3).

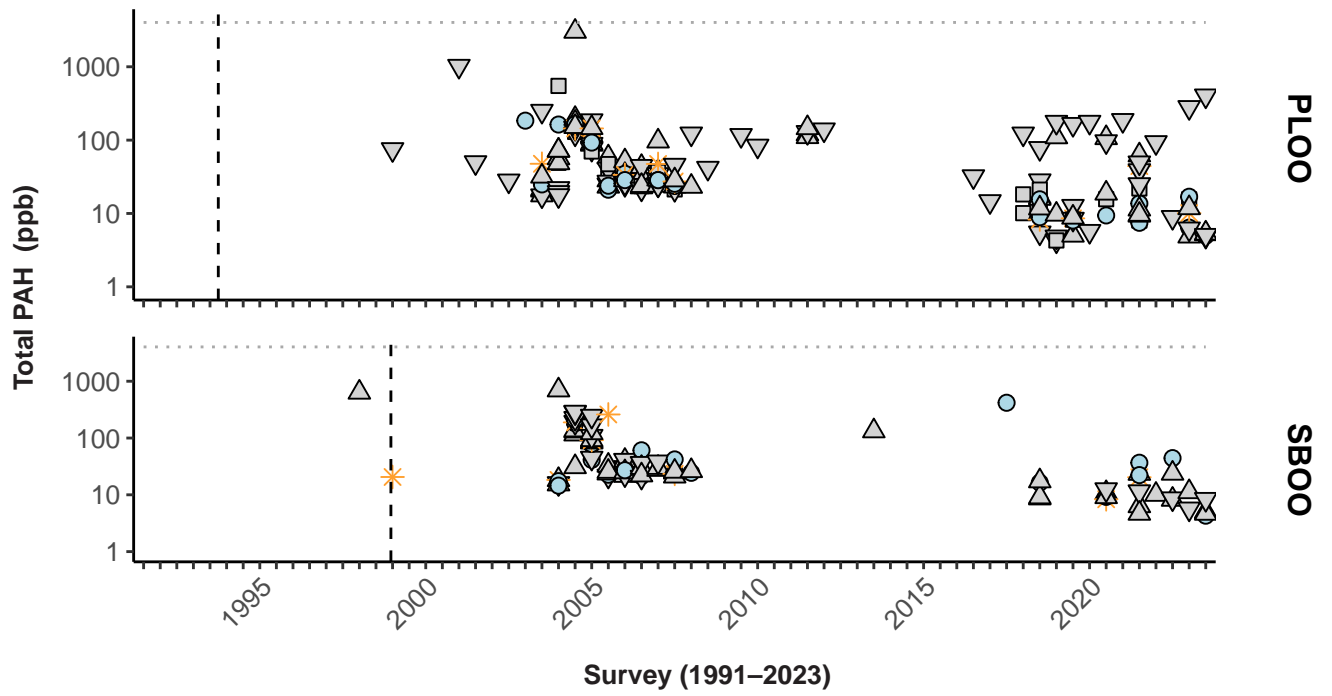


Figure 5.8 *Continued*

Chapter 6

Macrobenthic Communities

Chapter 6. *Macrobenthic Communities*

INTRODUCTION

The City of San Diego (City) conducts extensive monitoring of soft-bottom marine macrobenthic communities at permanent (core) monitoring sites surrounding the Point Loma Ocean Outfall (PLOO) and South Bay Ocean Outfall (SBOO). Additionally, a number of randomly selected (regional) stations, distributed throughout the broader San Diego coastal region are sampled in order to characterize the status of the local marine ecosystem and to identify any possible effects of wastewater discharge or other anthropogenic or natural influences. Benthic macrofauna (e.g., worms, crabs, clams, brittle stars, other small invertebrates) are targeted when monitoring seafloor habitats, because such organisms play important ecological roles in coastal marine ecosystems off southern California, and throughout the world (e.g., Fauchald and Jones 1979, Thompson et al. 1993a, Snelgrove et al. 1997). As many macrobenthic species live relatively long and stationary lives, their populations may exhibit the effects of pollution, or other disturbances over time (Hartley 1982, Bilyard 1987). The response of many of these species to environmental stressors is also well documented, and thus monitoring changes in discrete populations, or more complex communities, can help identify areas impacted by anthropogenic inputs (Pearson and Rosenberg 1978, Bilyard 1987, Warwick 1993, Smith et al. 2001). For example, pollution-tolerant species are often opportunistic, successfully colonizing impacted areas, and can therefore displace more sensitive species. In contrast, populations of pollution-sensitive species will typically decrease in response to contamination, oxygen depletion, nutrient loading, or other forms of environmental degradation (Gray 1979). For these reasons, the assessment of benthic community structure has become a major component of many ocean monitoring programs (e.g., Gillett et al. 2017).

The City relies on a suite of ecological indices to evaluate potential changes in local marine macrobenthic communities. Biological indices, such as the Benthic Response Index (BRI), Shannon Diversity Index (H'), and Swartz Dominance Index (Dom) are used as important metrics of community structure (e.g., Smith et al. 2001). The use of multiple measures of community health also provides better resolution than the evaluation of single parameters, some of which include established benchmarks for determining environmental impacts caused by anthropogenic influences. Collectively, these data are used to evaluate whether macrobenthic assemblages from habitats with comparable depth and sediment particle size are similar, or whether impacts from local ocean outfalls, or other sources, may be occurring. For example, minor organic enrichment due to wastewater discharge should be evident through increases in species richness and abundance in macrofaunal assemblages. Additionally, more severe impacts should result in decreases in the overall number of species, coupled with increases in dominance by a few pollution-tolerant species (Pearson and Rosenberg 1978).

This chapter presents analysis and interpretation of macrofaunal data collected at core benthic monitoring stations throughout the PLOO and SBOO regions, during 2022 and 2023. Included are descriptions of the different macrobenthic communities present in these two regions, along with comparisons of spatial patterns and long-term changes over time. The three primary goals of the chapter are to: (1) characterize and document the benthic assemblages present during the reporting period; (2) assess whether benthic communities are degraded as a result of wastewater discharge; (3) identify other potential natural or anthropogenic sources of variability in the San Diego coastal marine ecosystem.

A broader regional assessment of benthic conditions throughout the entire San Diego region, based on a subset of data reported in this chapter combined with a suite of randomly selected stations sampled during the summers of 2022 and 2023 is presented in Chapter 7.

MATERIALS AND METHODS

Field Sampling

Benthic samples analyzed in this chapter were collected at a total of 49 core monitoring stations located at inner shelf (≤ 30 m) to middle shelf (> 30 –120 m) depths, surrounding the PLOO and SBOO, during winter (January) and summer (July) of 2022 and 2023 (Figure 6.1). The PLOO sites include 12 primary core stations located along the 98m discharge depth contour, and 10 secondary core stations located along or adjacent to the 88m or 116m depth contours. The SBOO sites include 12 primary core stations located along the 28m discharge depth contour, and 15 secondary core stations located along or adjacent to the 19, 38, or 55m depth contours. Stations located within 1000 m of the boundary of the Zone of Initial Dilution (ZID) for either outfall are considered to represent near-ZID conditions. These include PLOO stations E11, E14, E15, and E17, and SBOO stations I12, I14, I15, and I16. All other stations are considered farfield. During the summer of 2023, only E15 and the primary core stations from the PLOO and SBOO regions were sampled, due to a resource exchange granted by the San Diego Regional Water Quality Control Board while participating in the region-wide Bight'23 sampling project.

Samples for benthic analyses were collected using a double 0.1m² Van Veen grab, with one grab per cast used for sediment quality analysis (see Chapters 5 and 7) and one grab per cast used for benthic community analysis. Criteria established by the U.S. Environmental Protection Agency (USEPA) to ensure consistency of these types of samples were followed with regard to sample disturbance and depth of penetration (USEPA 1987). Samples for infauna analysis were transferred to a wash table aboard ship, rinsed with seawater, and then sieved through a 1.0mm mesh screen in order to remove as much sediment as possible. The macroinvertebrates (macrofauna or infauna) retained on the screen were transferred to sample jars, relaxed for 30 minutes in a magnesium sulfate solution, and then fixed with buffered formalin. The preserved samples were then transferred back to the City's Marine Biology Laboratory. After a minimum of 72 hours, but no more than 10 days in formalin, each sample was thoroughly rinsed with fresh water and transferred to 70% ethanol for final preservation. All organisms were separated from the raw material (e.g., sediment grunge, shell hash, debris) and sorted into the following six taxonomic groups by an external contract lab: Annelids (e.g., polychaete and oligochaete worms), Arthropods (e.g., crustaceans, pycnogonids), Molluscs (e.g., bivalves, gastropods, scaphopods), non-ophiuroid Echinoderms (e.g., sea urchins, sea stars, sea cucumbers), Ophiuroids (i.e., brittle stars), and other phyla (e.g., Platyhelminthes, Nemertea, Cnidaria). The sorted macrofaunal samples were then returned to the City's Marine Biology Laboratory where all animals were identified to species or to the lowest taxon possible by staff marine biologists. All identifications during this reporting period followed nomenclatural standards established by the Southern California Association of Marine Invertebrate Taxonomists (SCAMIT 2021).

Data Analyses

Macrofaunal community parameter data for each PLOO and SBOO core station sampled in 2023 are listed in Appendices G.1 and G.2 while taxonomic listings of all specimens identified are listed

in Appendices G.3 and G.4. The following community metrics were determined for each station and expressed per 0.1-m² grab: species richness (number of species or distinct taxa), abundance (number of individuals), Shannon Diversity Index (H'), Pielou's Evenness Index (J'), Swartz Dominance Index (Dom) (see Swartz et al. 1986, Ferraro et al. 1994), and Benthic Response Index (BRI) (see Smith et al. 2001). Outfall contour stations are analyzed by three station groups: (1) north farfield stations (i.e., PLOO stations B9, B12, E20, E23, E25, E26 and SBOO stations I22, I27, I30, I33); (2) near-ZID stations (i.e., PLOO stations E11, E14, E17 and SBOO stations I12, I14, I15, I16); (3) south farfield stations (i.e., PLOO stations E2, E5, E8 and SBOO stations I2, I3, I6, I9). Unless otherwise noted, the above analyses were performed using the computational software package R (R Core Team 2021) and various functions within the ggpubr, reshape2, Rmisc, RODBC, scales, tidyverse, and vegan packages (Kassambara 2019, Wickham 2007, 2017, 2018, Hope 2013, Oksanen et al. 2017, Ripley and Lapsley 2017). Data collected during 2022 were reported previously (City of San Diego 2023), and all raw data for the 2022-2023 sampling period have been submitted to either the Regional Water Quality Control Board, the California Environmental Data Exchange Network (CEDEN) or the City's Open Data Portal (2024) and may be accessed upon request.

RESULTS AND DISCUSSION

Community Parameters

Species richness

A total of 882 different taxa were identified from 172 grabs collected at 22 core PLOO stations and 27 core SBOO stations during 2022 and 2023 (Appendices G.1, G.2, City of San Diego 2024). Approximately 90% (n = 790) of these taxa were fully identified to species, while the remainder could only be identified to genus or higher taxonomic levels. From the relatively deeper (88–116 m) mid-shelf waters off Point Loma, 559 taxa were identified during this period, of which at least 501 (90%) were distinct species. In contrast, 752 taxa were identified from the shallower (19–55 m) inner to mid-shelf stations in the SBOO region. Of these, 672 (89%) were distinct species. Most taxa occurred at multiple stations, although 18% (n = 159) of the PLOO taxa and 23% (n = 199) of the SBOO taxa were recorded only once. Six new taxa were reported that had not previously been recorded by the City's Ocean Monitoring Program, including three polychaetes, two arthropods and one Platyhelminthes.

During 2022 and 2023, species richness ranged from a mean of 74 to 112 taxa per grab at the PLOO stations, and 24 to 161 taxa per grab at the SBOO stations (Tables 6.1 and 6.2, respectively). The greatest number of taxa (n = 127), collected from a single grab, in the PLOO region was identified at station E9 during winter of 2023, while the fewest taxa (n = 49) were identified during winter of 2023 at near-ZID station E15 (Appendix G.1). In the SBOO region, the summer sample from 2022 at northern station I28 had the greatest number of taxa (n = 189), while southern farfield station I4 from winter of 2023 had the fewest taxa identified (n = 16) (Appendix G.2, City of San Diego 2024). These values were similar to the historical range of 19–198 taxa per grab for mid-shelf stations reported from 1994 through 2020 at regional stations (City of San Diego 2022). Comparisons of these parameters among near-ZID stations, versus northern and southern farfield stations, sampled during pre-discharge, historical post-discharge, and current discharge periods did not reveal any clear spatial patterns that could be attributed to wastewater discharge (Figure 6.2).

Macrofaunal abundance

A total of 48,921 macrofaunal animals were recorded for all core PLOO and SBOO stations sampled during 2022 and 2023. Mean abundance ranged from 121 to 481 animals in the PLOO region and from 74 to 833 animals in the SBOO region (Tables 6.1, 6.2, respectively). As shown for species richness, there were no clear patterns in abundance relative to their proximity to either outfall (see Figure 6.2). The highest abundance, per grab, in the PLOO region occurred during summer of 2022 at near-ZID station E14 ($n = 481$), while the lowest abundance occurred at near-ZID station E15 in winter of 2023 ($n = 121$) (Appendix G.1, City of San Diego 2024). In the SBOO region, the highest abundance occurred in summer 2022 at northern station I28 ($n = 833$), while the lowest abundance was observed at station I23 ($n = 74$) in winter of 2023 (Appendix G.2, City of San Diego 2024). These values were similar to the range of 47–1467 organisms per grab reported at mid-shelf stations from 1994 to 2020 (City of San Diego 2022).

Species diversity, evenness, and dominance

Shannon Diversity Index (H') values ranged from a mean of 3.3 to 4.5 at the PLOO stations, and 1.2 to 4.6 at the SBOO stations, during 2022 and 2023 (Tables 6.1, 6.2, respectively). In the PLOO region, the highest diversity per grab sample occurred at station E9 in winter 2023 ($H' = 4.5$) (Appendix G.1), and the lowest diversity was observed at near-ZID station E14 in the summer of 2022 ($H' = 3.3$) (City of San Diego 2024). In the SBOO region, the highest diversity per grab sample occurred at northern farfield station I28 in summer 2022 ($H' = 4.6$) (City of San Diego 2024), and the lowest diversity was observed at southern farfield station I4 in winter of 2023 ($H' = 1.2$) (Appendix G.2).

Pielou's Evenness Index (J') values ranged from a mean of 0.74 to 0.93 in the PLOO region, and 0.43 to 0.93 in the SBOO region (Tables 6.1, 6.2, respectively). In the PLOO region, the highest evenness values per grab sample occurred at southern farfield station E3 in summer 2022 ($J' = 0.93$) (City of San Diego 2024), and the lowest evenness values occurred at near-ZID station E14 in summer of 2022 ($J' = 0.74$) (City of San Diego 2024). In the SBOO region, the highest evenness occurred at station I10 in winter of 2023 ($J' = 0.93$), and the lowest value occurred at southern farfield station I4 in winter of 2023 ($J' = 0.43$) (Appendix G.2).

Swartz Dominance Index values ranged from a mean of 18 to 52 taxa at PLOO stations, and 2 to 59 taxa at SBOO stations (Table 6.1, 6.2, respectively). In the PLOO region, the highest dominance (i.e., lowest index value) per grab sample occurred at near-ZID station E14 in summer 2022 (18) (City of San Diego 2024), and the lowest dominance (i.e., highest index value) occurred at station E9 in winter of 2023 (52) (Appendix G.1). In the SBOO region, the highest dominance occurred at southern farfield station I4 in winter of 2023 (2) (Appendix G.2), and the lowest dominance occurred at northern station I28 in summer of 2022 (59) (City of San Diego 2024).

Overall, these results indicate that the PLOO and SBOO benthic communities remain characterized by relatively diverse assemblages of evenly distributed species. Values for all three of the above parameters in 2022 and 2023 (Appendices G.1, G.2, City of San Diego 2024), were within historical ranges (see City of San Diego 2022), and there remain no patterns that appear related to wastewater discharge in either region (see Figure 6.2).

Benthic response index

The BRI is an important tool for evaluating anthropogenic impacts on coastal seafloor habitats off southern California: BRI values less than 25 are considered indicative of reference conditions (i.e., not

impacted by natural and/or anthropogenic disturbance), values between 25 and 34 represent possible minor deviation from reference conditions, and values greater than 34 represent increasing levels of degradation (Smith et al. 2001). Overall, 95% (n = 163) of all individual benthic samples collected in the combined PLOO and SBOO regions during 2022 and 2023 were characteristic of reference conditions (Appendices G.1, G.2, City of San Diego 2024). No stations had BRI values considered indicative of degradation (i.e., all stations had a BRI \leq 34).

Almost all the individual samples (99%) in the PLOO region had BRI values indicative of reference conditions. Only the summer 2022 sample from near-ZID station E14, with individual BRI score of 26, appeared to show evidence of slight deviation from reference conditions (Appendix G.1, City of San Diego 2024). Station E14 was distinguished from the other primary core “E” stations, located along the 98-m PLOO discharge depth contour, as it had a higher proportion of coarse sediment particles and lower proportion of very fine particles (see Chapter 5). This difference in habitat may contribute to the slightly elevated BRI scores at station E14, as it may decrease the presence of certain pollution-sensitive species (e.g., the brittle star *Amphiodia urtica*) that are known to prefer finer sediments (Bergen 1995). No other spatial patterns relative to depth or sediments were observed (see Figures 5.2, 6.3, Tables 6.1, 6.2).

In the SBOO region, BRI values ranged from -7 at southern farfield station I4 to 27 at southern station I9 during winter and summer 2023, with about 91% of these being indicative of reference conditions (Appendix G.2, City of San Diego 2024). No SBOO samples had BRI values > 34 that would indicate environmental degradation. Individual sample BRI values corresponding to possible minor deviation from reference conditions (\geq 25) occurred at five stations (I9, I27, I30, I33, I35) (Appendix G.2, City of San Diego 2024). The slightly higher BRI values at these stations are not unexpected, due to naturally higher levels of organic matter that often occur at depths < 30 m due to proximity to terrestrial inputs (Smith et al. 2001). Historically, BRI values at the near-ZID SBOO stations have been similar to values observed for northern farfield SBOO stations, while BRI has been consistently lower at the southern farfield SBOO stations (Figure 6.3). Although these southern stations are also located along the 28-m depth contour, their sediments favor the presence of aggregations of the sand dollar, *Dendraster terminalis*, a pollution sensitive species that yields low BRI values.

Species of Interest

Dominant taxa

Annelid polychaete worms were the dominant taxonomic group found in both the PLOO and SBOO regions during 2022–2023, accounting for 48% and 47% of all taxa collected, respectively (Table 6.3). Crustaceans accounted for 22% of the taxa in both regions, molluscs for 11% and echinoderms 4% in both regions, and all other taxa combined equated to 14 and 16% respectively. Polychaetes were also the most abundant organisms encountered, accounting for 64% and 63% of all macrofauna in both the PLOO and SBOO regions, respectively. Crustaceans, molluscs, echinoderms, and “other phyla” each contributed to \leq 19% of the total abundance in each region. Overall, the percentage of taxa that occurred within each of the above major taxa groups, and their relative abundances, have shown little change since monitoring began (City of San Diego 2022) and are similar to the rest of the Southern California Bight (SCB) (see Ranasinghe et al. 2012, Gillet et al. 2017).

The 10 most abundant taxa in the PLOO region during 2022–2023 included eight species of polychaetes, one species of echinoderm, and one species of arthropod (Table 6.4). Together, these species accounted

for about 34% of all invertebrates identified during this period. The numerically dominant polychaetes included the spionids *Spiophanes duplex*, *Spiophanes kimbali*, *Prionospio jubata* and *Prionospio dubia*, capitellids in the genus *Mediomastus*, the maldanid Euclymeninae sp A, the orbiniid *Scoloplos armiger* Cmplx, and the onuphid *Paradiopatra parva*. The dominant ostracoda was *Euphilomedes producta*, while the brittle star *Amphiodia urtica* was the dominant ophiuroid. *Amphiodia urtica* populations have been declining across the region since monitoring at the current stations began in 1991, and especially since the warm water period of 2015–2017 (see Chapter 2, Figure 2.17). However, they are still a dominant taxon, accounting for approximately 5% of all invertebrates collected in the region and occurring in 96% of grabs with a mean abundance of approximately 15 individuals per grab. Historically, *Amphiodia urtica* and *Spiophanes duplex* (Figure 6.4), as well as *Proclea* sp A (Figure 6.5) have also been numerically dominant. However, another historically dominant species, the oweniid *Myriochele striolata*, and the terebellid, *Phisidia sanctaemariae* were not as abundant during the most recent reporting period (Appendix G.5). *Proclea* sp A and *M. striolata* have not been abundant in the region since 2005, while *P. sanctaemariae* has been largely absent since 2000.

The 10 most abundant taxa in the SBOO region during 2022–2023, included seven polychaetes, one tanaid, one ostracod, and members of the phylum Nematoda (Table 6.5). The dominant polychaetes included the spionids *Spiophanes norrisi* and *S. duplex*, the terebellid *Pista wui*, the cirratullid *Kirkegaardia siblina*, the sabellid *Jasmineira* sp B, the goniadid *Glycinde armiger*, and the ampharetid *Ampharete manriquei*. The dominant tanaid was represented by the species complex *Chondrochelia dubia*, while the other most abundant taxa were Nematoda and the ostracod *Euphilomedes carcharodonta*. The polychaete worm *Spiophanes norrisi* was the most abundant of all these species during the past two years, accounting for 15% of invertebrates collected in the SBOO area and occurring in 98% of all grabs. Although not as numerous as in previous surveys, *S. norrisi* has remained the most abundant species recorded in the SBOO region since 2007 (Figure 6.6), with up to 3009 individuals found in a single grab from station I6 during the summer of 2010 (City of San Diego 2011). Aside from *S. duplex*, all other taxa collected during the current reporting period averaged five individuals or fewer per grab (Table 6.5). Three other numerically dominant species occurred in $\geq 71\%$ of the samples, including *Glycinde armigera*, *Chondrochelia dubia* Cmplx, and *Euphilomedes carcharodonta* (Table 6.5). The remaining five of the top 10 taxa occurred in 18–58% of the samples with average abundances per grab of 4–5 animals. Historically, the polychaetes *S. norrisi*, *S. duplex*, and *Pista wui* (Figure 6.6), along with the cirratullid *Kirkegaardia siblina* and the tanaid *Chondrochelia dubia* cplx were the most numerically dominant taxa (Appendix G.6).

Indicator species

Several species known to be useful indicators of environmental change that occur in the PLOO and SBOO regions include the capitellid polychaete *Capitella teleta*, amphipods in the genera *Ampelisca* and *Rhepoxynius*, the terebellid polychaete *Proclea* sp A, the bivalve *Petrasma pervernicosa*, and the brittle star *Amphiodia urtica*. For example, increased abundances of pollution-tolerant species such as *C. teleta* and *P. pervernicosa* and decreased abundances of pollution-sensitive taxa such as *A. urtica*, are often indicative of organic enrichment and may indicate habitats impacted by human activity (Barnard and Ziesenhenné 1961, Anderson et al. 1998, Linton and Taghon 2000, Smith et al. 2001, Kennedy et al. 2009, McLeod and Wing 2009). During 2022 and 2023, a total of 149 individuals of *C. teleta* were found in samples collected across the entire region distributed among 15 different sites (stations E1, E5, E7, E11, E14, E15, E17, E19, E21, E23, E26, I8, I20, I28, I29), while a total of 56 individuals of *P. pervernicosa* were identified in samples from nine different sites (stations B10, E8, E11, E14, I14, I22, I27, I28, I29). Despite occasionally exceeding regional tolerance intervals of 0 to 1 animal per grab

(see City of San Diego 2022), abundances of *C. teleta* and *P. pervernicosa* remained characteristic of relatively undisturbed habitats (Figures 6.5, 6.7). For example, *C. teleta* commonly reaches densities as high as 600 individuals per 0.1m² grab in polluted sediments (Reish 1957, Swartz et al. 1986). Changes in abundance of *Ampelisca* and *Rhepoxynius* amphipod species varied at all PLOO primary core stations regardless of proximity to the outfall, which may have been influenced by the presence of large populations of pelagic red crabs from 2016 to 2019 (see City of San Diego 2020).

SUMMARY

Analyses of macrofaunal data for the 2022–2023 reporting period demonstrate that wastewater discharged through the Point Loma and South Bay outfalls has not negatively impacted macrobenthic communities in the coastal waters off San Diego. Values for most community parameters are similar at stations located both near to and far from the discharge areas. Major community metrics, such as species richness, abundance, diversity, evenness, and dominance were within historical ranges reported for the San Diego region (City of San Diego 2022), and were representative of those characteristic of similar SCB benthic habitats (Barnard and Ziesenhenné 1961, Jones 1969, Fauchald and Jones 1979, Thompson et al. 1987, 1993b, Zmarzly et al. 1994, Diener and Fuller 1995, Bergen et al. 1998, 2000, 2001, Ranasinghe et al. 2003, 2007, 2010, 2012, Mikel et al. 2007, Gillett et al. 2017). BRI values for 99% of the PLOO sites and 91% of the SBOO sites were considered characteristic of undisturbed habitats, while the remaining stations had values suggesting only a possible minor deviation from reference conditions. Additionally, BRI values at the shallower (i.e., less than 28 m) stations in the SBOO region have typically been higher than BRI values for deeper water stations since monitoring began. However, this pattern is not unexpected, since naturally higher levels of organic matter often occur closer to shore and particle sizes tend to be coarser (see Chapter 5). A similar phenomenon has been reported across the SCB where Smith et al. (2001) found a pattern of lower BRI values at mid-depth stations (25–130 m) versus shallower (10–35 m) or deeper (110–324 m) sites.

Changes in populations of pollution-sensitive and pollution-tolerant species, or other indicators of benthic condition, provide little or no evidence of habitat degradation in either outfall region. For example, the brittle star *Amphiodia urtica* is a well-known dominant species of the mid-shelf in fine sediment habitats in the SCB, which is known to be sensitive to environmental changes near wastewater outfalls (Swartz et al. 1986). However, abundances of *A. urtica* off Point Loma remained within the range of natural variation in SCB populations (Gillett et al. 2017). Additionally, populations of opportunistic species, such as the polychaete *Capitella teleta* and the bivalve *Petrasma pervernicosa*, remained low during 2022 and 2023, while populations of pollution-sensitive amphipods in the genera *Ampelisca* and *Rhepoxynius* have generally varied similarly between near-ZID and farfield stations. Furthermore, although spionid polychaetes are often abundant in other coastal areas of the world that possess high levels of organic matter (Díaz-Jaramillo et al. 2008), in the SCB these worms are known to be a stable, dominant component of many healthy environments with normal levels of organic inputs (Rodríguez-Villanueva et al. 2003). Thus, the presence of large populations of *Spiophanes norrisi* observed at many SBOO stations since 2007 is not considered to be indicative of habitat degradation related to wastewater discharge. Instead, population fluctuations of this spionid, in recent years, may correspond to natural changes in large-scale oceanographic conditions. Further support for this hypothesis is shown by the continued relatively low abundances of *S. norrisi* at all station groups during 2022 and 2023, compared to what would be expected at negatively impacted areas.

In conclusion, benthic macrofaunal communities appear to be in good condition overall throughout the PLOO and SBOO regions. Communities remain largely similar to those observed prior to outfall operations and are representative of natural communities from similar habitats on the southern California continental shelf. Overall, 95% of all benthic sites surveyed for the combined region, in 2022 and 2023, were classified as being in reference condition, based on assessments using the BRI. The few, slightly elevated, BRI values found at near-ZID stations, or along and shallower than the outfall discharge depth contour, generally fit historical patterns that have existed since before operation of either outfall began. More moderate indicators of disturbance at PLOO near-ZID station E14 remain highly localized and below the threshold of community degradation. These BRI values have also been trending downward over the last several years. Thus, no significant effects of wastewater discharge on the local macrobenthic communities off San Diego could be identified during this past 2-year reporting period.

LITERATURE CITED

- Anderson, B.S., J.W. Hunt, B.M. Philips, S. Tudor, R. Fairey, J. Newman, H.M. Puckett, M. Stephenson, E.R. Long, and R.S. Tjeerdema. (1998). Comparison of marine sediment toxicity test protocols for the amphipod *Rhepoxynius abronius* and the polychaete worm *Nereis (Neanthes) arenaceodentata*. *Environmental Toxicology and Chemistry*, 17(5): 859–866.
- Barnard, J.L. and F.C. Ziesenhenn. (1961). Ophiuroidea communities of southern Californian coastal bottoms. *Pacific Naturalist*, 2: 131–152.
- Bergen, M. (1995). Distribution of Brittlestar Amphiodia (Amphispina) spp. in the Southern California Bight in 1956 to 1959. *Bulletin of the Southern California Academy of Sciences*, 94(3): 190–203.
- Bergen, M., S.B. Weisberg, D. Cadien, A. Dalkey, D. Montagne, R.W. Smith, J.K. Stull, and R.G. Velarde. (1998). Southern California Bight 1994 Pilot Project: IV. Benthic Infauna. Southern California Coastal Water Research Project, Westminster, CA.
- Bergen, M., D.B. Cadien, A. Dalkey, D.E. Montagne, R.W. Smith, J.K. Stull, R.G. Velarde, and S.B. Weisberg. (2000). Assessment of benthic infaunal condition on the mainland shelf of southern California. *Environmental Monitoring Assessment*, 64: 421–434.
- Bergen, M., S.B. Weisberg, R.W. Smith, D.B. Cadien, A. Dalkey, D.E. Montagne, J.K. Stull, R.G. Velarde, and J.A. Ranasinghe. (2001). Relationship between depth, sediment, latitude, and the structure of benthic infaunal assemblages on the mainland shelf of southern California. *Marine Biology*, 138: 637–647.
- Bilyard, G.R. (1987). The value of benthic infauna in marine pollution monitoring studies. *Marine Pollution Bulletin*, 18(11): 581–585.
- City of San Diego. (2011). Annual Receiving Waters Monitoring Report for the South Bay Ocean Outfall (South Bay Water Reclamation Plant), 2010. City of San Diego Ocean Monitoring Program, Public Utilities Department, Environmental Monitoring and Technical Services Division, San Diego, CA.

- City of San Diego. (2020). Biennial Receiving Waters Monitoring and Assessment Report for the Point Loma and South Bay Ocean Outfalls, 2018-2019. City of San Diego Ocean Monitoring Program, Public Utilities Department, Environmental Monitoring and Technical Services Division, San Diego, CA.
- City of San Diego. (2022). Appendix C2: San Diego Benthic Tolerance Intervals. In: Report of Waste Discharge and Application for Renewal of NPDES CA 0107409 and 301(h) Modified Secondary Treatment Requirements. Volume V: Appendix C. City of San Diego Public Utilities Department, San Diego, CA.
- City of San Diego. (2023). Interim Receiving Waters Monitoring Report for the Point Loma and South Bay Ocean Outfalls, 2022. City of San Diego Ocean Monitoring Program, Public Utilities Department, Environmental Monitoring and Technical Services Division, San Diego, CA.
- City of San Diego. (2024). Open Data Portal – benthic invertebrates. <https://data.sandiego.gov/datasets/monitoring-ocean-benthic-invertebrates/>
- Díaz-Jaramillo, M., P. Muñoz, V. Delgado-Blas, and C. Bertrán. (2008). Spatio-temporal distribution of spionids (Polychaeta-Spionidae) in an estuarine system in south-central Chile. *Revista Chilena de Historia Natural*, 81: 501–514.
- Diener, D.R. and S.C. Fuller. (1995). Infaunal patterns in the vicinity of a small coastal wastewater outfall and the lack of infaunal community response to secondary treatment. *Bulletin of the Southern California Academy of Science*, 94: 5–20.
- Fauchald, K. and G.F. Jones. (1979). Variation in community structures on shelf, slope, and basin macrofaunal communities of the Southern California Bight. Report 19, Series 2. In: *Southern California Outer Continental Shelf Environmental Baseline Study, 1976/1977 (Second Year) Benthic Program. Principal Investigators Reports, Vol. II. Science Applications, Inc. La Jolla, CA.*
- Ferraro, S.P., R.C. Swartz, F.A. Cole, and W.A. Deben. (1994). Optimum macrobenthic sampling protocol for detecting pollution impacts in the Southern California Bight. *Environmental Monitoring and Assessment*, 29: 127–153.
- Gillett, D.J., L.L. Lovell and K.C. Schiff. (2017). Southern California Bight 2013 Regional Monitoring Program: Volume VI. Benthic Infauna. Technical Report 971. Southern California Coastal Water Research Project. Costa Mesa, CA.
- Gray, J.S. (1979). Pollution-induced changes in populations. *Philosophical Transactions of the Royal Society of London (Series B)*, 286: 545–561.
- Hartley, J.P. (1982). Methods for monitoring offshore macrobenthos. *Marine Pollution Bulletin*, 12: 150–154.
- Hope, R.M. (2013). Rmisc: Ryan Miscellaneous. R package version 1.5. <http://CRAN.R-project.org/package=Rmisc>.

- Jones, G.F. (1969). The benthic macrofauna of the mainland shelf of southern California. Allan Hancock Monographs of Marine Biology, 4: 1–219.
- Kassambara, A. (2019). ggpubr: ‘ggplot2’ Based Publication Ready Plots. R package version 0.2.2. <https://CRAN.R-project.org/package=ggpubr>.
- Kennedy, A.J., J.A. Stevens, G.R. Lotufo, J.D. Farrar, M.R. Reiss, R.K. Kropp, J. Doi, and T.S. Bridges. (2009). A comparison of acute and chronic toxicity methods for marine sediments. Marine Environmental Research, 68: 118–127.
- Linton, D.L. and G.L. Taghon. (2000). Feeding, growth, and fecundity of *Capitella* sp. I in relation to sediment organic concentration. Marine Ecology Progress Series, 205: 229–240.
- McLeod, R.J. and S.R. Wing. (2009). Strong pathways for incorporation of terrestrially derived organic matter into benthic communities. Estuarine, Coastal and Shelf Science, 82: 645–653.
- Mikel T.K., J.A. Ranasinghe, and D.E. Montagne. (2007). Characteristics of benthic macrofauna of the Southern California Bight. Appendix F. Southern California Bight 2003 Regional Monitoring Program, SCCWRP, Costa Mesa, CA.
- Oksanen, J., F. G. Blanchet, R. Kindt, P. Legendre, P. R. Minchin, R. B. O’Hara, G. L. Simpson, P. Solymos, M. H. H. Stevens and H. Wagner (2017). vegan: Community Ecology Package. R package version 2.3-1. <http://CRAN.R-project.org/package=vegan>.
- Pearson, T.H. and R. Rosenberg. (1978). Macrobenthic succession in relation to organic enrichment and pollution of the marine environment. Oceanography and Marine Biology Annual Review, 16: 229–311.
- R Core Team (2021). R: A language and environment for statistical computing. R Foundation for Statistical Computing, Vienna, Austria. URL <https://www.R-project.org/>.
- Ranasinghe, J.A., D.E. Montagne, R.W. Smith, T.K. Mikel, S.B. Weisberg, D. Cadien, R. Velarde, and A. Dalkey. (2003). Southern California Bight 1998 Regional Monitoring Program: VII. Benthic Macrofauna. Southern California Coastal Water Research Project, Westminster, CA.
- Ranasinghe, J.A., A.M. Barnett, K. Schiff, D.E. Montagne, C. Brantley, C. Beegan, D.B. Cadien, C. Cash, G.B. Deets, D.R. Diener, T.K. Mikel, R.W. Smith, R.G. Velarde, S.D. Watts, and S.B. Weisberg. (2007). Southern California Bight 2003 Regional Monitoring Program: III. Benthic Macrofauna. Southern California Coastal Water Research Project, Costa Mesa, CA.
- Ranasinghe, J.A., K.C. Schiff, D.E. Montagne, T.K. Mikel, D.B. Cadien, R.G. Velarde, and C.A. Brantley. (2010). Benthic macrofaunal community condition in the Southern California Bight, 1994–2003. Marine Pollution Bulletin, 60: 827–833.
- Ranasinghe, J.A., K.C. Schiff, C.A. Brantley, L.L. Lovell, D.B. Cadien, T.K. Mikel, R.G. Velarde, S. Holt, and S.C. Johnson. (2012). Southern California Bight 2008 Regional Monitoring Program:

VI. Benthic Macrofauna. Technical Report No. 665, Southern California Coastal Water Research Project, Costa Mesa, CA.

Reish, D. J. (1957). The relationship of the polychaetous annelid *Capitella capitata* (Fabricius) to waste discharges of biological origin. In: C.M. Tarzwell (ed.). Biological Problems in Water Pollution. U.S. Public Health Service, Washington, DC. p 195–200.

Ripley, B. and M. Lapsley. (2017). RODBC: ODBC Database Access. R package version 1.3-15. <http://CRAN.R-project.org/package=RODBC>.

Rodríguez-Villanueva, V., R. Martínez-Lara, and V. Macías Zamora. (2003). Polychaete community structure of the northwestern coast of Mexico: patterns of abundance and distribution. *Hydrobiologia*, 496: 385–399.

[SCAMIT] Southern California Association of Marine Invertebrate Taxonomists. (2021). A taxonomic listing of benthic macro- and megainvertebrates from infaunal and epibenthic monitoring programs in the Southern California Bight, Edition 13. Southern California Association of Marine Invertebrate Taxonomists, Natural History Museum of Los Angeles County Research and Collections, Los Angeles, CA.

Smith, R.W., M. Bergen, S.B. Weisberg, D. Cadien, A. Dalkey, D. Montagne, J.K. Stull, and R.G. Velarde. (2001). Benthic response index for assessing infaunal communities on the southern California mainland shelf. *Ecological Applications*, 11(4): 1073–1087.

Snelgrove, P.V.R., T.H. Blackburn, P.A. Hutchings, D.M. Alongi, J.F. Grassle, H. Hummel, G. King, I. Koike, P.J.D. Lamshead, N.B. Ramsing, and V. Solis-Weiss. (1997). The importance of marine sediment biodiversity in ecosystem processes. *Ambio*, 26: 578–583.

Swartz, R.C., F.A. Cole, and W.A. Deben. (1986). Ecological changes in the Southern California Bight near a large sewage outfall: benthic conditions in 1980 and 1983. *Marine Ecology Progress Series*, 31: 1–13.

Thompson, B.E., J.D. Laughlin, and D.T. Tsukada. (1987). 1985 reference site survey. Technical Report No. 221, Southern California Coastal Water Research Project, Long Beach, CA.

Thompson, B., J. Dixon, S. Schroeter, and D.J. Reish. (1993a). Chapter 8. Benthic invertebrates. In: M.D. Dailey, D.J. Reish, and J.W. Anderson (eds.). *Ecology of the Southern California Bight: A Synthesis and Interpretation*. University of California Press, Berkeley, CA.

Thompson, B.E., D. Tsukada, and D. O’Donohue. (1993b). 1990 reference site survey. Technical Report No. 269, Southern California Coastal Water Research Project, Long Beach, CA.

[USEPA] United States Environmental Protection Agency. (1987). Quality Assurance and Quality Control (QA/QC) for 301(h) Monitoring Programs: Guidance on Field and Laboratory Methods. EPA Document 430/9-86-004. Office of Marine and Estuarine Protection.

Warwick, R.M. (1993). Environmental impact studies on marine communities: pragmatical considerations. *Australian Journal of Ecology*, 18: 63–80.

- Wickham, H. (2007). Reshaping Data with the reshape Package. *Journal of Statistical Software*, 21(12), 1-20. URL <http://www.jstatsoft.org/v21/i12/>.
- Wickham, H. (2017). tidyverse: Easily Install and Load the ‘Tidyverse’. R package version 1.2.1. <https://CRAN.R-project.org/package=tidyverse>.
- Wickham, H. (2018). scales: Scale Functions for Visualization. R package version 1.0.0. <https://CRAN.R-project.org/package=scales>
- Zmarzly, D.L., T.D. Stebbins, D. Pasko, R.M. Duggan, and K.L. Barwick. (1994). Spatial patterns and temporal succession in soft-bottom macroinvertebrate assemblages surrounding an ocean outfall on the southern San Diego shelf: Relation to anthropogenic and natural events. *Marine Biology*, 118: 293–307.

CHAPTER 6

FIGURES & TABLES

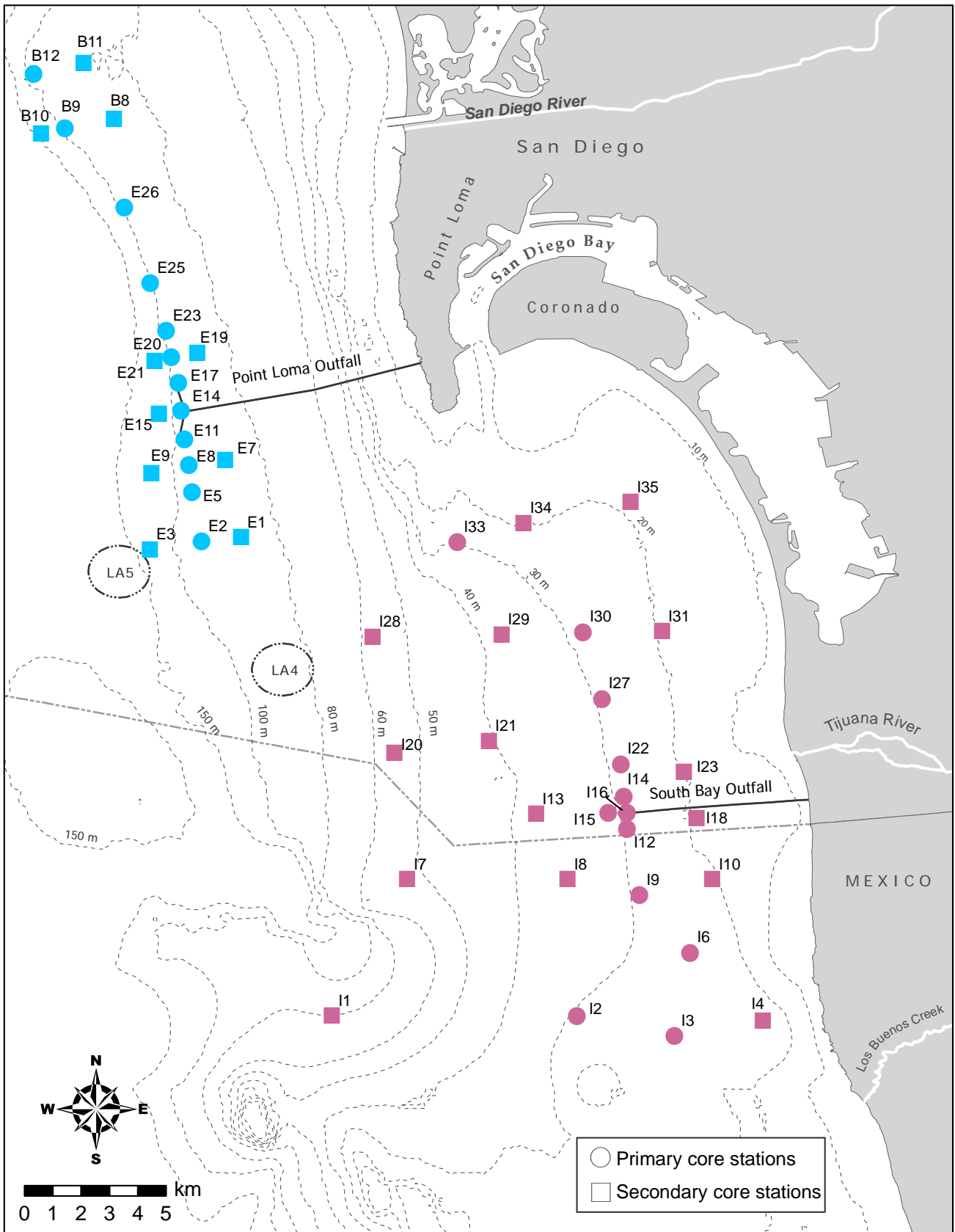


Figure 6.1

Benthic station locations sampled around the PLOO (blue) and SBOO (magenta) as part of the City of San Diego's Ocean Monitoring Program.

Table 6.1

Summary of macrofaunal community parameters for PLOO benthic stations sampled during 2022 and 2023. Data for each station are expressed as biennial means ($n \leq 4$). SR=species richness; Abun=abundance; H'=Shannon diversity index; J'=Pielou's evenness; Dom=Swartz dominance; BRI=Benthic Response Index; CI=confidence interval. Stations are listed north to south from top to bottom for each depth contour.

	Station	SR	Abun	H'	J'	Dom	BRI
<i>88-m Depth Contour</i>	B11	111	310	4.2	0.89	44	9
	B8	80	256	3.8	0.88	30	9
	E19	92	383	4.0	0.88	30	8
	E7	88	303	3.9	0.88	30	11
	E1	96	319	4.0	0.88	36	6
<i>98-m Depth Contour</i>	B12	96	242	4.1	0.90	40	12
	B9	85	255	4.0	0.90	33	11
	E26	99	347	4.0	0.88	34	9
	E25	98	352	4.1	0.89	36	8
	E23	97	381	4.0	0.88	32	9
	E20	82	298	3.9	0.89	30	10
	E17 ^a	89	318	3.9	0.86	28	16
	E14 ^a	78	357	3.5	0.81	22	24
	E11 ^a	85	316	3.9	0.88	29	16
	E8	82	279	4.0	0.89	32	10
	E5	91	313	4.0	0.90	34	10
	E2	100	276	4.2	0.91	40	10
<i>116-m Depth Contour</i>	B10	86	229	4.0	0.90	35	14
	E21	91	316	4.0	0.89	33	8
	E15 ^a	74	278	3.8	0.89	27	10
	E9	112	338	4.2	0.89	43	11
	E3	93	242	4.2	0.91	40	9
All Grabs	Mean	91	305	4.0	0.88	33	11
	95% CI	3	17	0.0	0.01	2	1
	Minimum	49	121	3.3	0.74	18	4
	Maximum	127	481	4.4	0.93	52	26

^aNear-ZID station

Table 6.2

Summary of macrofaunal community parameters for SBOO benthic stations sampled during 2022 and 2023. Data for each station are expressed as biennial means ($n \leq 4$). SR=species richness; Abun=abundance; H'=Shannon diversity index; J'=Pielou's evenness; Dom=Swartz dominance; BRI=Benthic Response Index; CI=confidence interval. Stations are listed north to south from top to bottom for each depth contour.

	Station	SR	Abun	H'	J'	Dom	BRI
<i>19-m Depth Contour</i>	I35	71	287	3.5	0.81	23	24
	I34	34	151	2.7	0.78	9	8
	I31	56	195	3.2	0.81	20	18
	I23	52	254	3.2	0.81	17	15
	I18	62	209	3.4	0.84	22	17
	I10	55	171	3.4	0.86	22	14
	I4	24	123	2.2	0.69	7	1
	<i>28-m Depth Contour</i>	I33	98	352	3.9	0.87	34
I30		76	248	3.6	0.84	25	24
I27		67	218	3.5	0.84	24	22
I22		64	198	3.6	0.86	24	23
I14 ^a		67	224	3.6	0.85	24	20
I16 ^a		55	346	2.8	0.69	12	18
I15 ^a		51	267	2.7	0.68	13	16
I12 ^a		46	245	2.6	0.70	12	19
I9		74	248	3.7	0.87	26	25
I6		42	224	2.6	0.69	10	10
I2		40	196	2.6	0.71	10	14
I3		32	217	2.3	0.66	6	10
<i>38-m Depth Contour</i>		I29	135	625	4.2	0.86	39
	I21	51	155	3.3	0.86	19	10
	I13	60	244	3.4	0.82	19	9
	I8	53	218	3.2	0.81	16	18
<i>55-m Depth Contour</i>	I28	161	678	4.4	0.86	50	14
	I20	84	338	3.4	0.77	25	8
	I7	61	222	3.2	0.79	18	6
	I1	109	417	4.0	0.86	36	11
All Grabs	Mean	65	267	3.2	0.79	21	16
	95% CI	7	34	0.1	0.02	2	1
	Minimum	16	74	1.2	0.43	2	-7
	Maximum	189	833	4.6	0.93	59	27

^aNear-ZID station

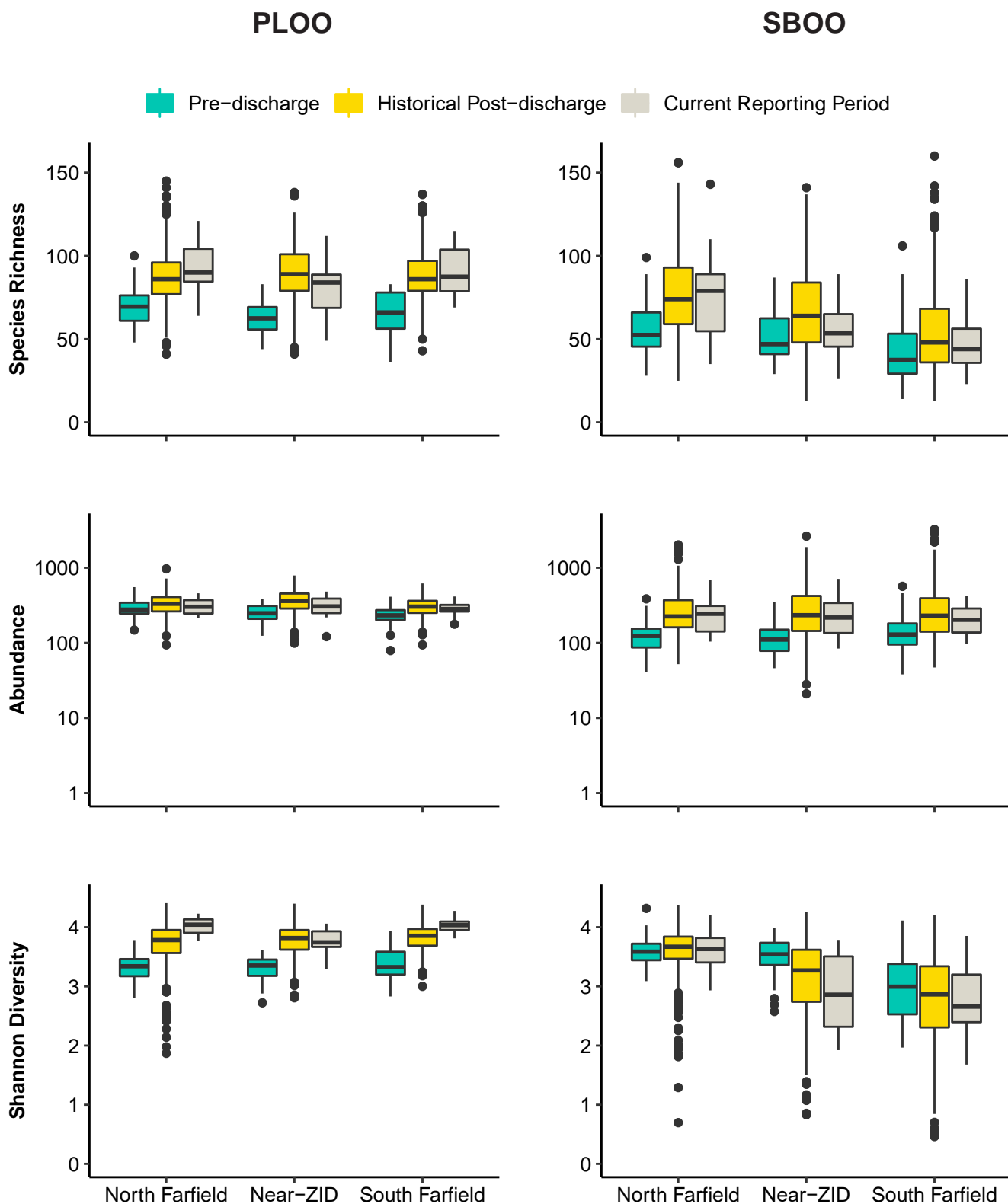


Figure 6.2

Species richness, abundance, and diversity (H') of benthic infauna collected from PLOO and SBOO north farfield, near-ZID, and south farfield primary core stations during pre-discharge, historical post-discharge, and current reporting period; Boxes=median, upper, and lower quantiles; whiskers=1.5x interquartile range; circles=outliers; see Chapter 1 for description of pre- versus post-discharge time periods for the two outfalls.

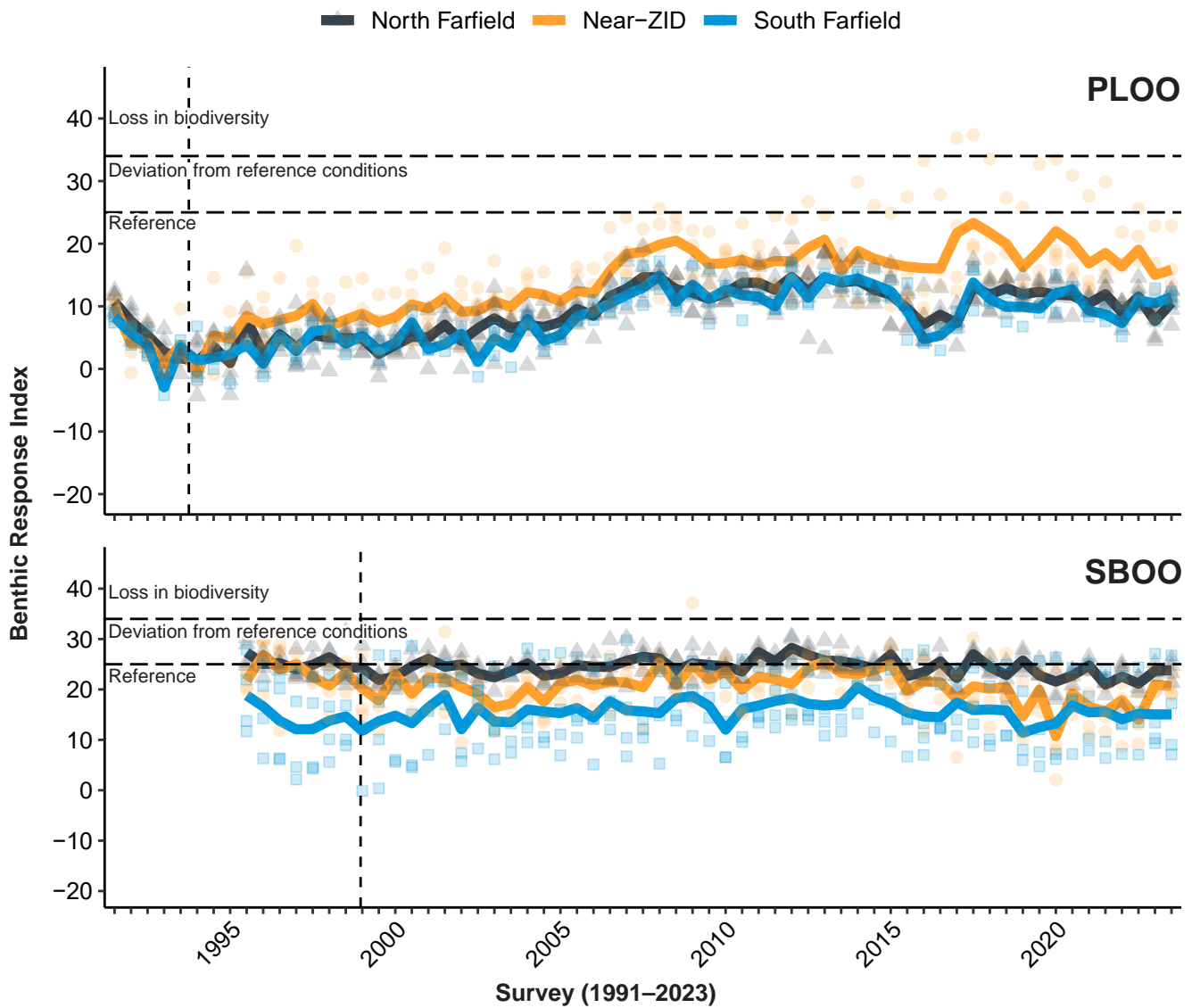


Figure 6.3

Benthic Response Index at PLOO and SBOO north farfield, near-ZID, and south farfield primary core stations sampled in the PLOO region from 1991 through 2023 and in the SBOO region from 1995 through 2023. For each station group, mean BRI per survey is shown by the solid line ($n \leq 8$) while BRI per station is shown by the symbols. Vertical dashed lines indicate onset of wastewater discharge at each outfall's current location.

Table 6.3

Percent composition and abundance of major taxonomic groups in PLOO and SBOO benthic grabs sampled during 2022 and 2023. Percentages may not add up to 100 due to rounding artifacts.

Phyla	PLOO		SBOO	
	Species (%)	Abundance (%)	Species (%)	Abundance (%)
Annelida (Polychaeta)	48	64	47	63
Arthropoda (Crustacea)	22	15	22	18
Echinodermata	4	10	4	3
Mollusca	11	4	11	8
Other Phyla	14	6	16	8

Table 6.4

The 10 most abundant macroinvertebrate taxa collected from PLOO benthic stations during 2022 and 2023. Data are expressed as percent abundance (number of individuals per species/total abundance of all species), frequency of occurrence (percentage of grabs in which a species occurred), and abundance per grab (mean number of individuals per grab, n=79).

Taxon	Taxonomic Classification	Percent Abundance	Frequency of Occurrence	Abundance per Grab
<i>Mediomastus</i> sp	Polychaeta: Capitellidae	6	99	19
<i>Amphiodia urtica</i>	Echinodermata: Ophiuroidea	5	96	15
<i>Scoloplos armiger</i> Cmplx	Polychaeta: Orbiniidae	4	94	12
<i>Spiophanes duplex</i>	Polychaeta: Spionidae	3	96	11
<i>Prionospio jubata</i>	Polychaeta: Spionidae	3	100	10
Euclymeninae sp A	Polychaeta: Maldanidae	3	97	9
<i>Paradiopatra parva</i>	Polychaeta: Onuphidae	3	100	9
<i>Prionospio dubia</i>	Polychaeta: Spionidae	3	99	8
<i>Euphilomedes producta</i>	Arthropoda: Ostracoda	2	86	7
<i>Spiophanes kimballi</i>	Polychaeta: Spionidae	2	90	7

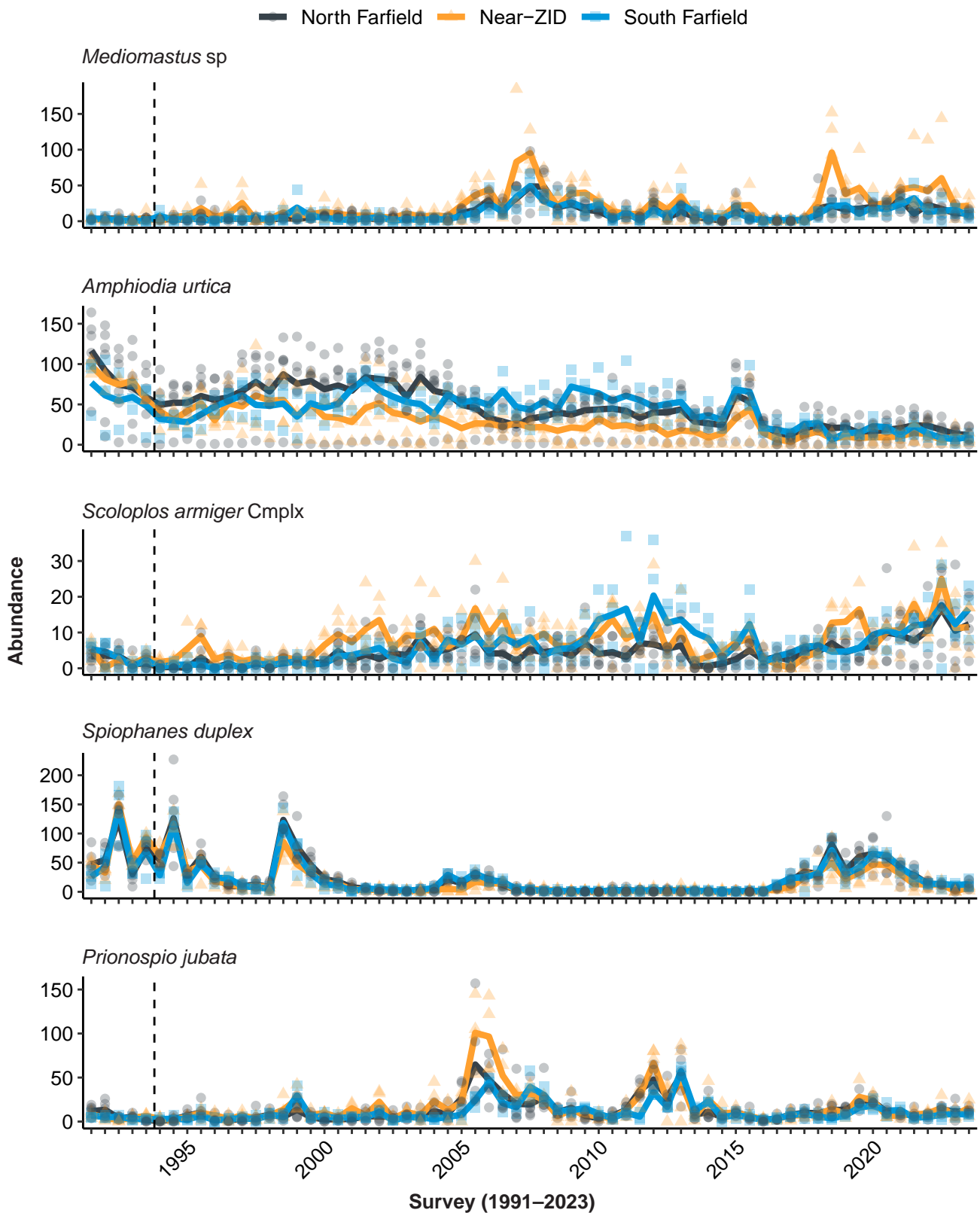


Figure 6.4

Abundances of the five most numerically dominant species recorded during 2022 and 2023 (presented in order) at PLOO north farfield, near-ZID, and south farfield primary core stations from 1991 through 2023. For each station group, mean abundance per survey is shown by the solid line ($n \leq 8$) while abundance per station is shown by the symbols. Dashed lines indicate onset of wastewater discharge at its current location.

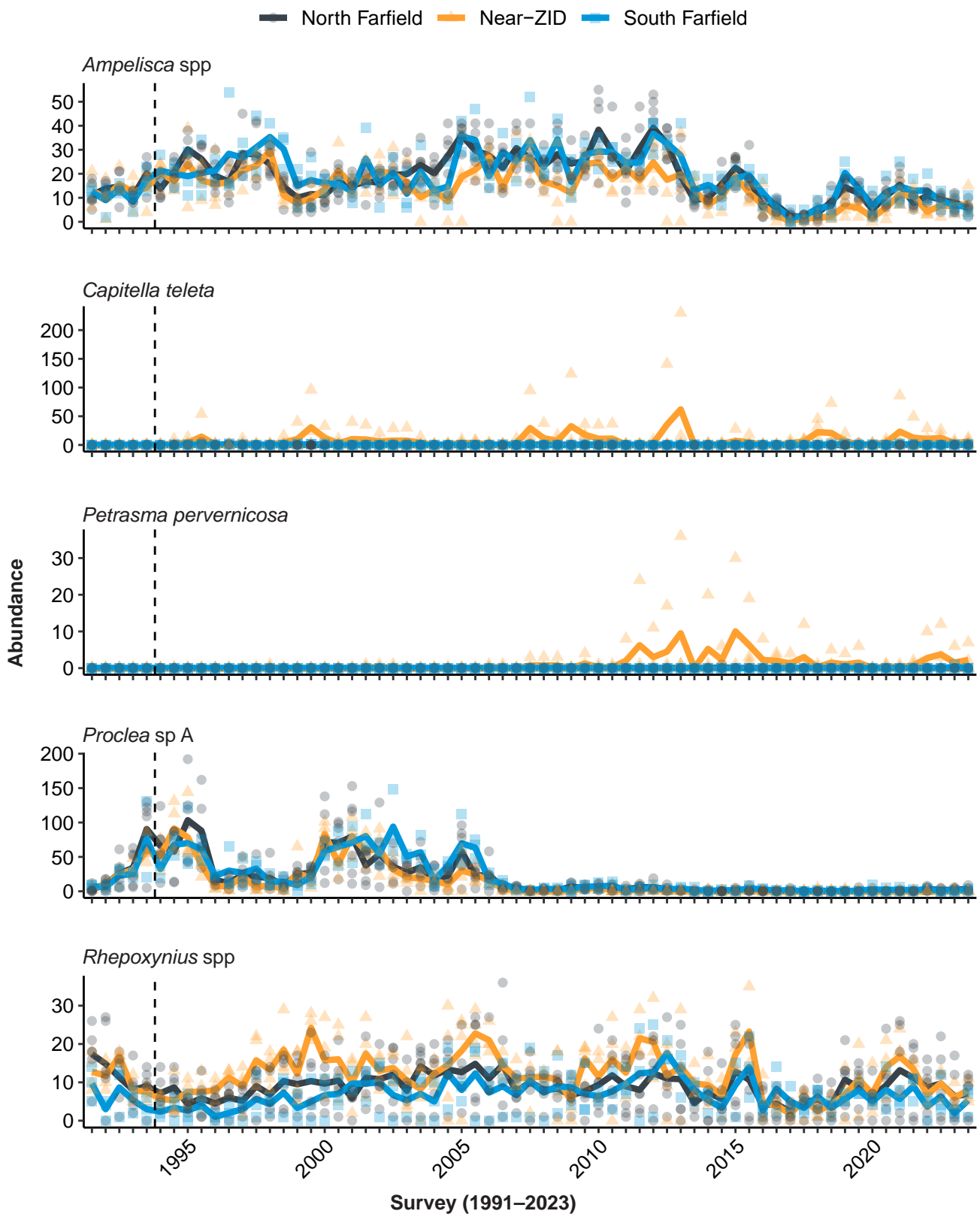


Figure 6.5

Abundances of representative ecologically important indicator taxa collected at PLOO north farfield, near-ZID, and south farfield primary core stations from 1991 through 2023. For each station group, mean abundance per survey is shown by the solid line ($n \leq 8$) while abundance per station is shown by the symbols. Dashed lines indicate onset of wastewater discharge at its current location.

Table 6.5

The 10 most abundant macroinvertebrate taxa collected from SBOO benthic stations during 2022 and 2023. Data are expressed as percent abundance (number of individuals per species/total abundance of all species), frequency of occurrence (percentage of grabs in which a species occurred), and abundance per grab (mean number of individuals per grab, n=93).

Taxon	Taxonomic Classification	Percent Abundance	Frequency of Occurrence	Abundance per Grab
<i>Spiophanes norrisi</i>	Polychaeta: Spionidae	15	98	41
<i>Spiophanes duplex</i>	Polychaeta: Spionidae	5	80	14
<i>Pista wui</i>	Polychaeta: Terebellidae	2	26	5
<i>Kirkegaardia siblina</i>	Polychaeta: Cirratulidae	2	47	5
<i>Chondrochelia dubia</i> Cmplx	Arthropoda: Tanaidacea	2	70	5
<i>Jasmineira</i> sp B	Polychaeta: Sabellidae	2	18	4
Nematoda		2	58	4
<i>Glycinde armigera</i>	Polychaeta: Goniadidae	1	71	4
<i>Ampharete manriquei</i>	Polychaeta: Ampharetidae	1	26	4
<i>Euphilomedes carcharodonta</i>	Arthropoda: Ostracoda	1	53	4

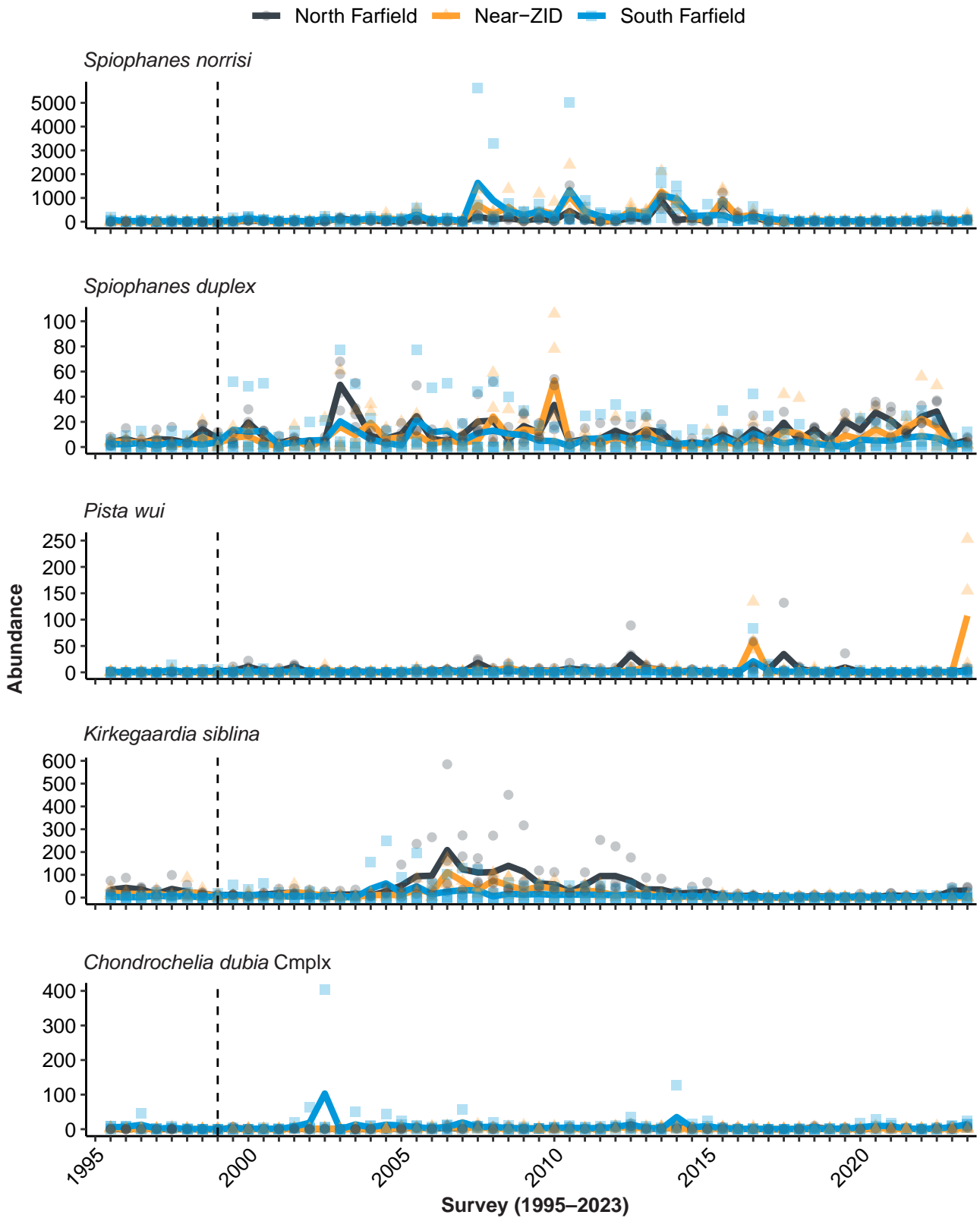


Figure 6.6

Abundances of the five most numerically dominant species (presented in order) recorded during 2022 and 2023 at SBOO north farfield, near-ZID, and south farfield primary core stations from 1995 through 2023. For each station group, mean abundance per survey is shown by the solid line ($n \leq 8$) while abundance per station is shown by the symbols. Dashed lines indicate onset of wastewater discharge.

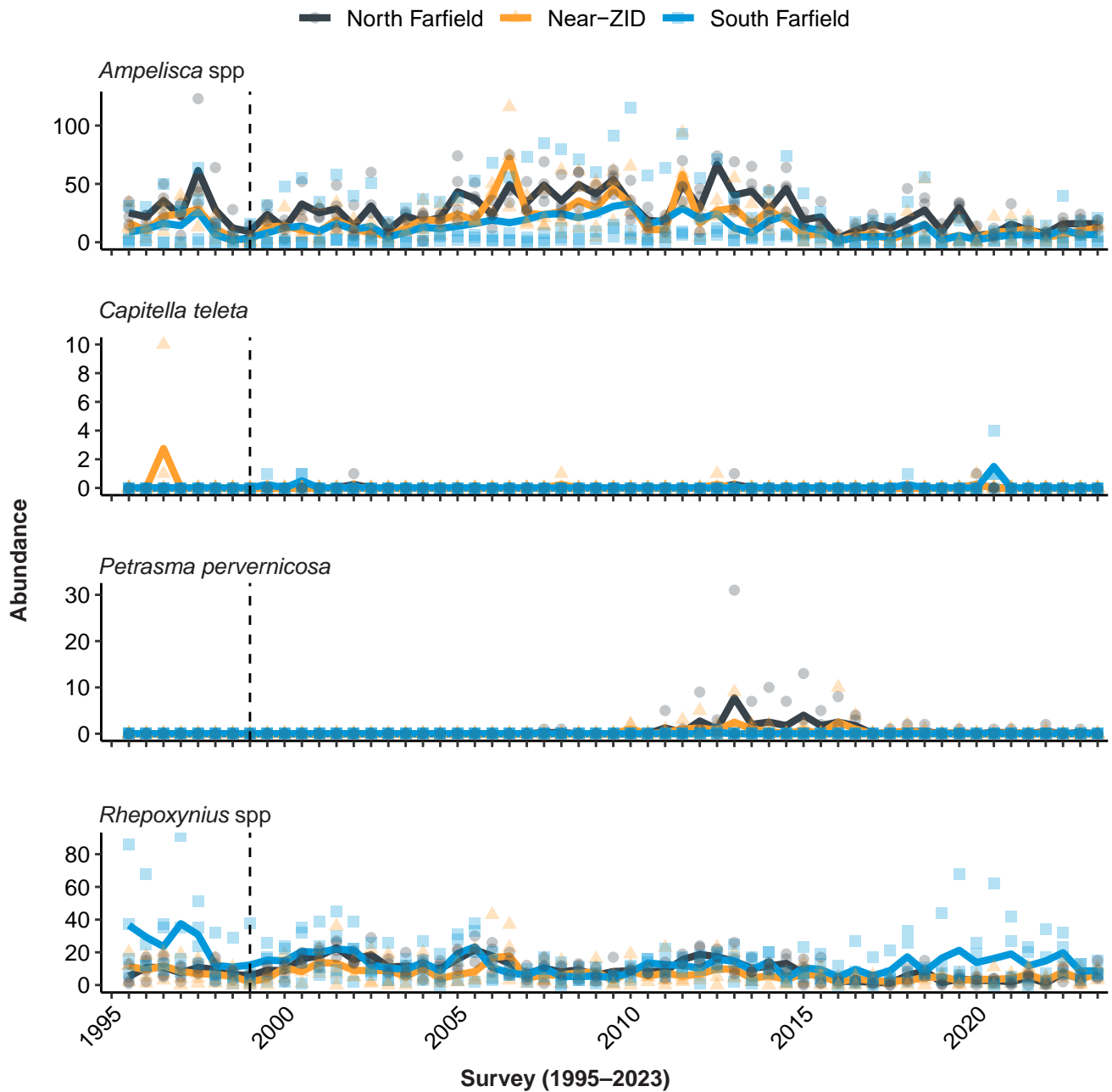


Figure 6.7

Abundances of representative ecologically important indicator taxa collected at SBOO north farfield, near-ZID, and south farfield primary core stations from 1995 through 2023. For each station group, mean abundance per survey is shown by the solid line ($n \leq 8$) while abundance per station is shown by the symbols. Dashed lines indicate onset of wastewater discharge.

Chapter 7
San Diego Regional
Benthic Condition Assessment

Chapter 7. San Diego Regional Benthic Condition Assessment

INTRODUCTION

The City of San Diego (City) has conducted annual surveys of randomly selected (regional) benthic stations off the coast of San Diego since 1994 (see Chapter 1). The location of these regional surveys typically range from offshore of Del Mar in northern San Diego County southward to the USA/Mexico border. An array of 40 stations are selected each year using a probability-based, random stratified sampling design as described in Bergen (1996), Stevens (1997), and Stevens and Olsen (2004). During 1995–1997, 1999–2002, and 2005–2007, the surveys off San Diego were restricted to continental shelf depths < 200 m. However, beginning in 2009, the survey area was expanded to include deeper habitats along the upper continental slope (200–500 m). No separate San Diego regional survey was conducted in 2004 due to sampling for a special sediment mapping project (Stebbins et al. 2004), while the 1994, 1998, 2003, 2008, 2013, and 2018 regional surveys were conducted as part of the larger Southern California Bight (SCB) Regional Monitoring Program (Bergen et al. 1998, 2001, Schiff and Gossett 1998, Noblet et al. 2002, Schiff et al. 2006, 2011, Maruya and Schiff 2009, Ranasinghe et al. 2003, 2007, 2010, 2012, Dodder et al. 2016, Gillett et al. 2017, SCCWRP 2018, Du et al. 2020). In total more than 1000 samples from 951 different regional stations have been sampled off San Diego over the past 29 years (1994–2022).

This chapter presents an overall assessment of regional benthic conditions on the continental shelf and upper slope off San Diego during 2022–2023. Included are analyses of sediment particle size, sediment chemistry, sediment toxicity, and macrofaunal community data collected from a total of 40 regional benthic stations sampled during summer 2022, and 49 core benthic stations sampled during summer 2022 and 2023. These data provide a snapshot of the region’s sediment quality and benthic community structure across the major depth strata defined by the SCB regional monitoring programs (e.g., SCCWRP 2018). Data from the 2023 SCB Regional Monitoring Program (Bight’23) are not yet available, and are, therefore, not included herein. Additional analysis of spatial patterns, winter vs. summer differences, and long-term changes over time at the core Point Loma Ocean Outfall (PLOO) and South Bay Ocean Outfall (SBOO) stations are presented in Chapters 5 and 6.

In an effort to provide a more comprehensive assessment of sediment quality in this region, sediment toxicity results have been integrated with other lines of evidence (LOEs), including sediment chemistry and benthic community structure. These LOEs were integrated using a framework adopted by the State of California to assess sediment quality within enclosed bays and estuaries (SWRCB 2009; Bay et al. 2013), but with the same modifications used for the coastal shelf as part of Southern California Bight (SCB) Regional Monitoring Program surveys (i.e., Bight regional surveys; see B13CIA 2017). These modifications included applying the results from the 10-day amphipod sediment toxicity test prescribed by the Sediment Toxicity Monitoring Plan (versus the two sediment toxicity tests available for embayments) (City of San Diego 2015a) and the benthic response index (BRI) that was developed specifically for evaluation of benthic macrofaunal (e.g., worms, crabs, clams, brittle stars, other small invertebrates) communities in offshore waters (Bergen et al. 2000, Smith et al. 2001). The same two sediment chemistry assessment indices developed for embayments were used, even though these indices have not been calibrated or validated for continental shelf sediments, as these are the best

tools currently available (B13CIA 2017). The integration of each line of evidence using the State of California's sediment quality assessment framework resulted in the classification of each site into one of five potential categories: (1) unimpacted; (2) likely unimpacted; (3) possibly impacted; (4) likely impacted; (5) clearly impacted. The State Water Board considers the first two categories as healthy, or representative of conditions undisturbed by pollutants in sediment (SWRCB 2009, B13CIA 2017).

The primary objectives of this chapter are to: (1) describe the overall condition and quality of the diverse benthic habitats that occur in the offshore coastal waters off San Diego; (2) characterize sediment quality, sediment toxicity, and the health of the soft-bottom marine benthos in the region; (3) gain a better understanding of regional variation in order to distinguish between the effects of anthropogenic and natural factors; (4) put into context the results of more frequent sampling at permanent (core) monitoring sites surrounding the PLOO and SBOO.

MATERIALS AND METHODS

Collection and Processing of Samples

Benthic samples analyzed in this chapter were collected during the summer of 2022 and 2023 at 89 stations that ranged from Del Mar southward to below the USA/Mexico border (Figure 7.1). A total of 40 of these stations, sampled in 2022, were selected using a probability-based random stratified sampling design as described in Bergen (1996), Stevens (1997), and Stevens and Olsen (2004). These "regional" stations were sampled at depths ranging from 8 to 453 m spanning four distinct depth strata off southern California. These included 10 regional stations along the inner shelf (8–30 m), 15 regional stations along the mid-shelf (30–120 m), 9 regional stations along the outer shelf (120–200 m), and 6 regional stations on the upper slope (200–453 m). In addition to the above, the results of 2022 summer sampling at the 49 primary and secondary core PLOO and SBOO monitoring stations located at inner to mid-shelf depths as described in Chapters 5 and 6 are also analyzed in this chapter. During summer 2023, sampling was limited to PLOO and SBOO primary core stations due to a resource exchange granted by the San Diego Regional Water Quality Control Board while participating in Bight'23. Stations located within 1000 m of the boundary of the zone of initial dilution (ZID) for either outfall are considered to represent near-ZID conditions. These include PLOO stations E11, E14, E15, E17, and SBOO stations I12, I14, I15, I16.

Samples for benthic analyses were collected using a double 0.1-m² Van Veen grab, with one grab per cast used for sediment quality analysis (see Chapter 5), one grab per cast used for benthic community analysis (see Chapter 6), and subsequent grabs used for sediment toxicity testing where required. Visual observations of weather, sea conditions, and human/animal activity were also recorded at the time of sampling. Criteria established by the U.S. Environmental Protection Agency (USEPA) to ensure consistency of these types of samples were followed with regard to sample disturbance and depth of penetration (USEPA 1987).

Sub-samples for particle size and sediment chemistry analyses were taken from the top 2 cm of the sediment surface and handled according to standard guidelines (USEPA 1987, SCCWRP 2018). For infauna analysis, sediment from an entire grab was transferred to a wash table aboard ship, rinsed with seawater, and then sieved through a 1.0-mm mesh screen in order to remove as much sediment as possible. The macroinvertebrates retained on the screen were transferred to sample jars, relaxed for 30 minutes in a magnesium sulfate solution, and then fixed with buffered formalin. The preserved samples

were then transferred back to the City's Marine Biology Laboratory. After a minimum of 72 hours, but no more than 10 days, in formalin, each sample was thoroughly rinsed with fresh water and transferred to 70% ethanol for final preservation.

For sediment toxicity samples, a plastic (high-density polyethylene [HDPE], polycarbonate, or Teflon) or stainless-steel scoop was used to collect sediment from the top 2 cm of the undisturbed surface material in the grab. Contact with sediment within 1 cm of the sides of the grab was avoided in order to minimize cross-contamination. In most cases, multiple grabs were required to obtain enough sediment for toxicity testing (i.e., up to 6 L of sediment). If more than one grab was required, sediment from each grab was added to a Teflon bag and homogenized thoroughly using either a clean Teflon or plastic spoon, or by kneading the sample within the bag. Once collected, the toxicity samples were stored in the dark at 4°C in the laboratory for no longer than four weeks prior to testing.

Laboratory Analyses

Sediment Particle Size

All sediment chemistry and particle size analyses were performed at the City's Environmental Chemistry Services Laboratory. Particle size analysis was performed using either a Horiba LA-950V2 laser scattering particle analyzer or a set of nested sieves. The Horiba measures particles ranging in size from 0.5 to 2000 µm. Coarser sediments were removed and quantified prior to laser analysis by screening samples through a 2000 µm mesh sieve. These data were later combined with the Horiba results to obtain a complete distribution of particle sizes totaling 100%, and then classified into 11 sub-fractions and four main size fractions based on the Wentworth scale (Folk 1980) (see Appendix F.2). When a sample contained substantial amounts of coarse sand, gravel, shell hash or other large materials that could damage the Horiba analyzer or where the general distribution of sediments would be poorly represented by laser analysis, a set of nested sieves with mesh sizes of 2000 µm, 1000 µm, 500 µm, 250 µm, 125 µm, 75 µm and 63 µm was used to divide the samples into seven sub-fractions. See Appendix H.1 for visual observations for each regional station; see Appendix F.3 for visual observations for each PLOO and SBOO core station.

Sediment Chemistry

A detailed description of the analytical protocols is available upon request. Briefly, sediment sub-samples were analyzed on a dry weight basis to determine concentrations of various indicators of organic loading (i.e., biochemical oxygen demand, total organic carbon, total nitrogen, total sulfides, total volatile solids), 18 trace metals, 9 chlorinated pesticides, 42 polychlorinated biphenyl compound congeners (PCBs), and 24 polycyclic aromatic hydrocarbons (PAHs), and 13 polybrominated ethers (PBDEs) (see Appendix F.1). A variety of laboratory technical issues resulted in a number of non-reportable sediment chemistry data for the 2022 and 2023 benthic surveys, see Appendices F.2–F.13 and Appendices H.2–H.7.

Sediment Toxicity Testing

A detailed description of the sediment toxicity testing protocols can be found in City of San Diego (2024). Briefly, all sediment toxicity testing was conducted by the City of San Diego Toxicology Laboratory (CSDTL) using the marine amphipod *Eohaustorius estuarius*. The 10-day amphipod tests were conducted in accordance with EPA 600/R-94/0925 (USEPA 1994) and the procedures approved for Southern California Bight 2018 Regional Monitoring Program (Bight'18 Toxicology Committee 2018). Juvenile *E. estuarius* were exposed for 10 days to both test and control sediments. Response

criteria included amphipod mortality, emergence from sediment during exposure, and, if considered a measurement of interest, the ability of amphipods to reburry in clean sediment at the end of the bioassay. In addition, a reference toxicant test (using seawater only) was conducted concurrently and under identical environmental conditions as the sediment toxicity tests to determine test organism sensitivity.

Macrobenthic Assemblages

All organisms were separated from the raw material (e.g., sediment grunge, shell hash, debris) and sorted into the following six taxonomic groups by an external contract lab: Annelids (e.g., polychaete and oligochaete worms), Arthropods (e.g., crustaceans and pycnogonids), Molluscs (e.g., clams, snails, and scaphopods), non-ophiuroid Echinoderms (e.g., sea urchins, sea stars, and sea cucumbers), Ophiuroids (i.e., brittle stars), and other phyla (e.g., flatworms, nemerteans, and cnidarians). The sorted macrofaunal samples were then returned to the City’s Marine Biology Laboratory where all animals were identified to species, or to the lowest taxon possible, by City Marine Biologists. All identifications followed nomenclatural standards established by the Southern California Association of Marine Invertebrate Taxonomists (SCAMIT 2021; see Appendix H.8).

Data Analyses

Data for each parameter analyzed during 2022 were reported previously (City of San Diego 2023), and all raw data for the 2022–2023 sampling period have been submitted to either the Regional Water Quality Control Board or the California Environmental Data Exchange Network (CEDEN) and will be submitted to the City’s Open Data Portal or provided upon request.

Sediment Chemistry

Data summaries for the various sediment parameters included detection rate, minimum, maximum, and mean values. For chemistry parameters, all means were calculated using detected values only, with no substitutions made for non-detects in the data (analyte concentrations < method detection limit [MDL]). Limiting analyses to detected values (i.e., excluding non-detects) is considered a conservative way of handling contaminant concentrations as it creates a strong upward bias in the data and respective summary statistics, and therefore may represent a worst-case scenario (e.g., see Helsel 2005a,b, 2006 for discussions of non-detect data). For continuity, and in contrast to previous reports (e.g., City of San Diego 2020), estimated values that fell below method detection limits but were confirmed by mass-spectrometry were excluded from all data (1991–2023). Estimated values were treated as non-detects for this report. Total chlordane, total DDT (tDDT), total hexachlorocyclohexane (tHCH), total PCB (tPCB), total PAH (tPAH), and total PBDE (tPBDE) were calculated for each sample as the sum of all individual constituents with reported values. When applicable, contaminant concentrations were compared to the Effects Range Low (ERL) and Effects Range Median (ERM) sediment quality guidelines (Long et al. 1995). The ERLs represent chemical concentrations below which adverse biological effects are rarely observed, while values above the ERL but below the ERM represent levels at which effects occasionally occur. Concentrations above the ERM indicate likely biological effects, although these are not always validated by toxicity testing (Schiff and Gossett 1998). Unless stated otherwise, analyses were performed using R (R Core Team 2023) and various functions within the zoo, reshape2, plyr, ggplot2, tidyverse, Rmisc, vegan, RODBC, stringr, ggpubr, psych, tidyr, and dplyr packages (Zeileis and Grothendieck 2005, Wickham 2007, 2011, 2016, Wickham et al. 2019, Hope 2022, Oksanen et al. 2022, Ripley and Lapsley 2022, Wickham 2022, Kassambara 2023, Revelle 2023, Wickham et al. 2023a, 2023b).

Spearman rank correlations were calculated to assess if values for the various parameters co-varied in the sediments. This non-parametric analysis accounts for non-detects in the data without the use of value substitutions (Helsel 2005b). However, depending on the data distribution, the instability in rank-based analyses may intensify with increased censoring (Conover 1980). Therefore, a criterion of <50% non-detects was used to screen eligible constituents for this analysis.

Sediment Toxicity Testing

All data were analyzed in accordance with procedures outlined in Sections 12 and 13 of EPA 600/R-94/0925 using the acceptability criterion of $\geq 90\%$ mean control survival at test termination. Additional information and the standard operation procedures for sediment toxicity testing are provided in Appendix B of the CSDTL's Quality Assurance Manual (City of San Diego 2024).

Macrobenthic Assemblages

The following community metrics were determined for each station and expressed per 0.1-m² grab: species richness (number of species or distinct taxa), abundance (number of individuals), Shannon Diversity Index (H'), Pielou's Evenness Index (J'), Swartz dominance index (see Swartz et al. 1986, Ferraro et al. 1994), and BRI (see Smith et al. 2001). Due to limitations in the validation dataset, BRI values were not calculated for samples collected at depths <10 m or >200 m (Smith et al. 2001). Unless otherwise noted, analyses were performed using the computational software package R (R Core Team 2023) and various functions within the zoo, reshape2, tidyverse, Rmisc, vegan, RODBC, scales, ggpubr, tidyr, and dplyr (Zeileis and Grothendieck 2005, Wickham 2007, Wickham et al. 2019, Hope 2022, Oksanen et al. 2022, Ripley and Lapsley 2022, Wickham and Seidel 2022, Kassambara 2023, Wickham et al. 2023a, 2023b).

Sediment Quality Triad Assessment

Following instructions provided in Bay et al. (2013), benthic macrofauna and sediment chemistry results were combined with sediment toxicity results from the 8 stations where sediment toxicity was conducted during 2022 to determine relevant condition categories. The benthic community LOE was determined by assigning condition categories to each sample collected at acceptable depths as follows: BRI values <25 = reference conditions, 25–33 = minor deviation from reference conditions, 34–43 = moderate disturbance, 44–71 = high disturbance (defined as loss in community function in Smith et al. 2001), and >72 = defaunation. The sediment toxicity LOE was determined by assigning scores to samples using the following thresholds: percent control $\geq 90\%$ = nontoxic, $\geq 82\%$ = low toxicity, $\geq 59\%$ = moderate toxicity, and <59% = high toxicity. The sediment chemistry LOE was determined by using the California Logistic Regression Model Index (LRM) and the Chemical Score Index (CSI) to calculate scores for each sample with sufficient parameters analyzed, calculating the mean score as (LRM + CSI)/2, and assigning the overall integrated chemistry category LOE as follows: mean score ≤ 1.0 = minimal exposure, 1.1–2.0 = low exposure, 2.1–3.0 = moderate exposure, and 3.1–4.0 = high exposure.

After the scores were converted to LOE categories, they were combined using the integration framework defined in Bay et al (2013). This framework is based on a conceptual approach that addresses two key elements: (1) is there biological degradation at the site, and (2) is chemical exposure at the site high enough to potentially result in a biological response? (see SWRCB 2009, Bay and Weisberg 2012). Station assessment (site condition) categories were assigned using benthic community condition as determined by the BRI (reference, or low, moderate, high disturbance), sediment toxicity (non-toxic, or low, moderate, high toxicity), and sediment chemistry exposure (minimal, low, moderate, high) according to Table 6.1 in Bay et al (2013). For example, if a sample had a benthic community in

reference condition, the sediments were found to be nontoxic, and the sediment chemistry exposure was minimal, then the station assessment (site condition) was deemed unimpacted. There is a total of 64 combinations resulting in the five categories: (1) unimpacted; (2) likely unimpacted; (3) possibly impacted; (4) likely impacted; (5) clearly impacted. The station assessment could also be inconclusive (e.g., reference benthic conditions plus moderate sediment toxicity exposure plus high sediment chemistry exposure).

Multivariate Analyses

Multivariate analyses were performed using PRIMER v7 software to examine spatial and temporal patterns in macrofaunal data collected at the 40 regional stations sampled during summer 2022 and 49 core stations sampled during summer 2022 and 2023 (total samples = 114) (Clarke et al. 2008, Clarke et al. 2014). These included ordination and hierarchical agglomerative clustering (cluster analysis) with group-average linking and similarity profile analysis (SIMPROF) to confirm the non-random structure of the resultant cluster dendrograms. Prior to these analyses, macrofaunal abundance data were square-root transformed to lessen the influence of overly abundant species and increase the importance (or presence) of rare species. Measures of similarity used as the basis for clustering included the Bray-Curtis measure of similarity for macrofaunal data. Major ecologically-relevant clusters receiving SIMPROF support were retained, and similarity percentages analysis (SIMPER) was used to determine which species were responsible for the greatest contributions to within-group similarity (characteristic species) and between-group dissimilarity for retained clusters. BEST tests, using the BVSTEP procedure, were conducted to determine which subset of species best described patterns within the dendrogram resulting from the cluster analyses. Additional BEST tests, using the BIO-ENV procedure, were conducted to determine which subsets of sediment sub-fractions were the best explanatory variables for similarity between the particle size and macrofaunal resemblance matrices.

RESULTS

Regional Sediment Quality

Particle Size Composition

Ocean sediment composition was diverse across the 114 benthic stations sampled during the 2022 and 2023 summer surveys. The proportion of fine silt and clay particles (combined as ‘fine particles’ or ‘percent fines’) ranged from a minimum of 0 to a maximum of 85.6% per sample, while fine sands ranged from 0.9 to 87.0%, medium-coarse sands ranged from 0.1 to 90.6%, and coarse particles ranged from 0 to 35.5% (Table 7.1). Overall, and as expected, sediment composition varied by depth and region (Table 7.1, Figure 7.2, Figure 7.3). For example, the amount of percent fines at regional stations increased with depth, with a mean of 24.3% per sample along the inner shelf, 57.5% along the mid-shelf, 55.1% along the outer shelf, and 80.4% along the upper slope (Table 7.1). Percent fines were also higher at PLOO core stations located at mid-shelf depths of 88–116 m (mean = 54.9%) versus SBOO core stations located at inner shelf depths of 19–28 m (mean = 17.1%) and at mid-shelf depths of 38–55 m (mean = 24%). Furthermore, correlation analysis confirmed that percent fines tended to increase with depth throughout the San Diego area ($r_s = 0.71$; Figure 7.2, Appendix H.9). Several exceptions to this overall pattern were observed during the current reporting period, where percent fines were higher or lower than expected by depth. Exceptions were found at PLOO core stations B12, E11, and E15, SBOO core stations I1, I7, and I20, and several inner and mid-shelf regional stations, including station 9335 located offshore of Point La Jolla at a depth of 123 m, station 9303 located on the Coronado Bank at

a depth of 129 m, station 9322 located southeast of the entrance to San Diego Bay at a depth of 8 m, stations 9348 and 9302 located offshore of the Tijuana River at depths of 36 and 35 m, respectively (Figure 7.3).

Sediment Chemistry

As with sediment particle size composition, regional patterns of sediment contamination during summer 2022 and 2023 were similar to patterns seen in previous years (e.g., City of San Diego 2018, 2020, 2022a). There was no evidence of degraded sediment quality in the general San Diego region. While various indicators of organic loading (Figure 7.4), trace metals (Figure 7.5), chlorinated pesticides, PCBs, PAHs and PBDEs were detected at variable concentrations in sediment samples collected throughout the region, no gradients were observed with proximity to either outfall and almost all contaminants occurred at levels below both ERL and ERM thresholds, within tolerance intervals calculated for the PLOO region, and within historical ranges (Table 7.1; see also Chapter 5 and City of San Diego 2022a). Of the 114 samples collected during these summer surveys, only 6% (n = 7) had elevated concentrations of a parameter with available thresholds. Arsenic exceeded its ERL in a single sample from SBOO farfield stations I21 (Figure 7.5). Total DDT exceeded its ERL in a total of 6 sediment samples from three regional stations located along the mid-shelf (stations 9302, 9305, 9306) and three samples from regional stations located along the upper slope (stations 9321, 9325, 9332) (Figure 7.6).

As in previous surveys (e.g., City of San Diego 2018, 2020, 2022a), concentrations of most metals increased with increasing proportions of fine particles ($r_s \geq 0.70$), including aluminum, barium, beryllium, chromium, copper, iron, lead, manganese, mercury, nickel, selenium, and zinc (Appendix H.9). Because of the relationship between fines and depth, several of these also increased across depth strata (aluminum, barium, beryllium, chromium, nickel, zinc) (Table 7.1, Figure 7.4, Figure 7.5, Appendix H.9, Appendix H.10). The organic loading indicators total nitrogen and total volatile solids also increased across depth strata.

Sediment Toxicity

During summer 2022, sediments were collected and tested for toxicity at eight regional stations that ranged in depth from 16 to 137 m (Figure 7.1, Appendix H.11). Mean survival rates for these regional stations ranged from 95 to 99%, indicating all sites were categorized as non-toxic.

Regional Macrobenthic Communities

A total of 37,261 macrobenthic invertebrates were identified from the 114 grabs collected during summer 2022 and 2023 surveys at depths ranging from 8 to 453 m off San Diego. Of the 850 taxa recorded, 82% (n = 694) were identified to the level of species, while the rest could only be identified to higher taxonomic levels. Macrofaunal community structure varied across both the continental shelf and slope: with species richness ranging from 11 to 189 taxa per grab; macrofaunal abundance ranging from 41 to 892 individuals per grab; Shannon Diversity Index (H') ranging from 1.1 to 4.6 per grab; Pielou's Evenness Index (J') ranging from 0.44 to 0.94 per grab; and Swartz Dominance Index ranging from 2 to 60 per grab (Table 7.2). Reported values for each parameter, and the variation observed between strata, generally correspond to findings reported previously for the San Diego region (e.g., City of San Diego 2020, 2022b). For example, species richness and abundance values were lowest at upper slope stations. As has also been reported previously, BRI values off San Diego have generally been indicative of reference, or non-impacted, conditions ($BRI < 25$) (Smith et al. 2001). This remained true for the 2022 and 2023 summer surveys with 93% of samples (n = 103), collected from BRI-validated depths,

having BRI values indicative of reference condition (Appendix H.12). A total of three samples (~3%) had slightly elevated BRI values between 25–34, which may indicate a minor deviation from reference condition; these samples were collected at near-ZID PLOO station E14, and SBOO farfield stations I9 and I35, with BRI values of 26, 27, and 26, respectively. None of the stations sampled in summer 2022 and 2023 had BRI values >34, which would indicate increasing levels of disturbance or environmental degradation.

Cluster and ordination analyses of the macrofaunal data, described above, resulted in 7 ecologically-relevant SIMPROF-supported cluster groups (groups A–G) (Figures 7.7, 7.8). These macrofauna cluster groups included from 1 to 82 grabs. The composition of each cluster group varied in terms of the specific taxa present and their relative abundance, as well as depth and sediment composition. For example, the macrofaunal assemblages represented by cluster groups A, B, and C occurred along the inner and mid-shelf at depths of 8–55 m, with all but seven samples located within the SBOO monitoring region. Macrofaunal assemblages associated with cluster group E, the largest group (n = 82), spanned a significant portion of the inner and middle shelf, as well as a smaller portion of the outer shelf and upper slope, off San Diego. Assemblages associated with cluster groups D, F, and G represented a total of five samples that occurred along the upper slope at depths of 236–453 m.

The sediment sub-fractions that were most highly correlated with the macrofaunal communities included fine sand, and fine particles (BEST/BIOENV $\rho = 0.676$, $p < 0.01$, number of permutations = 999). Of these sub-fractions, fine particles accounted for most of the variation (corr. = 0.645). According to BEST/BVSTEP ($\rho = 0.95$, $p < 0.01$, number of permutations = 999), a total of 15 species best described the overall pattern (gradient) of the cluster dendrogram, including the ophiuroids in the family Amphiuridae, the polychaetes *Prionospio jubata*, *Prionospio dubia*, *Spiophanes kimballi*, *Euclymeninae* sp A, *Spiophanes duplex*, *Phyllodoce hartmanae*, *Eclysippe trilobata*, *Paradiopatra parva*, *Mediomastus* sp, *Jasmineira* sp B, and *Spiophanes norrisi*, the amphipods *Ampelisca brevisimulata* and *Rhepoxynius menziesi*, and the sand dollar *Dendraster terminalis*. The main characteristics and distribution of each cluster group are described below.

Macrofauna cluster groups A and B represented small groups (2 grabs per cluster) of assemblages found on the inner shelf during summer 2022 and 2023, each associated with varying sediment composition (Figures 7.7, 7.8). For example, Group A comprised two grabs collected at a depth of 8 m from regional stations 9309 and 9322 located nearshore proximal to Coronado Beach and Silver Strand Beach. Compared to all other cluster groups, sediments from groups A and B sites had the largest proportions of fine sand (mean = 32.4% and 33.5% per grab), relatively large proportions of medium sand (mean = 16.5% and 8.9% per grab) and large proportions of fine particles (mean = 33.9% and 23.4% per grab) (Appendix H.13). According to SIMPER, group A assemblages were characterized by moderate numbers of the polychaete *Prionospio pygmaeus* (mean = 24 per grab), the sand dollar *Dendraster terminalis* (mean = 8 per grab), the amphipod *Rhepoxynius menziesi* (mean = 8 per grab), and Nemertean *Carinoma mutabilis* (mean = 6 per grab) and Lineidae (mean = 4 per grab) (Appendix H.14). Group B comprised two regional sites (9301, 9318), with assemblages that were characterized by high numbers of the polychaete *Spiophanes duplex* (mean = 45 per grab), with smaller numbers of the polychaetes *Polydora cirrosa* (mean = 23 per grab), *Prionospio pygmaeus* (mean = 15 per grab), *Goniada littorea* (mean = 8 per grab), and *Ampharete labrops* (mean = 7 per grab). Regional station 9301 was located near the US/Mexico border at a depth of 16 m, while regional station 9318 was located south of Coronado at a depth of 17 m.

Macrofauna cluster group C (n = 23) was the second largest group, representing assemblages from 19% of all grabs, at depths from 18 to 55 m and was primarily located on the inner shelf. Group C comprised grabs from SBOO near-ZID stations I12, I15, and I16, SBOO farfield stations I2, I3, I4, I6, I7, I8, I13, I20, I21, I23, and I34, and three regional stations near Point Loma at depths from 18 to 30 m. Sediments from these grabs had the largest proportions of medium sand (mean = 35.5% per grab), coarse sand (mean = 32.4% per grab), very coarse sand (mean = 8.2% per grab), and granules (mean = 2.4% per grab), with relatively small proportions of fine particles (mean = 11.1% per grab), very fine sand (mean = 4.0% per grab), and fine sand (mean = 11.0% per grab) (Appendix H.13). Assemblages represented by group C were characterized by the highest number of the polychaete *Spiophanes norrisi* (mean = 104 per grab), along with relatively high numbers of the polychaetes *Pista wui* (mean = 19 per grab), and *Jasmineira* sp B (mean = 8 per grab) (Appendix H.14).

Macrofauna cluster group E was the largest group (n = 82), representing assemblages from 72% of all grabs, and 85% of grabs collected on the mid-shelf during summer 2022 and 2023, including 100% of grabs from PLOO near-ZID and farfield stations, and most of the north farfield SBOO stations (Figures 7.7, 7.8). Overall, depths of group E sites ranged from 18 to 237 m. Sediments associated with this cluster group were largely a mix of fine particles (mean = 47.5% per grab), very fine sand (mean = 34.9% per grab) and fine sand (mean = 13.0% per grab), with relatively small amounts of medium sand (mean = 2.0% per grab), coarse sand (mean = 2.1% per grab), very coarse sand (mean = 1.3% per grab), with trace amounts (<1% per grab) of granules (Appendix H.13). Group E averaged 95 taxa and 357 individuals per grab. The five most characteristic taxa for cluster group E were *Spiophanes duplex* (mean = 19 per grab), *Mediomastus* sp (mean = 14 per grab), *S. norrisi* (mean = 11 per grab), *Amphiodia urtica* (mean = 10 per grab), and *Paradiopatra parva* (mean = 10 per grab) (Appendix H.14).

Macrofauna cluster groups D, F and G represented small groups (1–2 grabs per cluster) of assemblages found on the upper slope during summer 2022 (Figures 7.7, 7.8). Group D represented a unique assemblage present at regional station 9315 located on the inner edge of the Coronado Bank at a depth of 321 m. Sediments from this site, along with cluster group F, had the highest proportions of fine particles (n = 85.2%) (Appendix H.13), and characteristic (abundant) species included the highest numbers of the brittle stars *Amphiodia digitata* (mean = 22 per grab) and Amphiuridae (mean = 6 per grab), amphipod *Ampelisca unsocalae* (mean = 6 per grab), and polychaetes *Fauveliopsis magna* (mean = 5 per grab) and *Eclysippe trilobata* (mean = 4 per grab) (Appendix H.14). Group G represented a small assemblage present at regional stations 9316 and 9321 located east of the Coronado Bank at depths of 236 and 249 m. These two stations had a high proportion of fine particles (mean = 77.2% per grab), and compared to groups D and F, had higher proportions of very fine sand (mean = 17.8) and fine sand (mean = 4.7% per grab), and abundant species included the polychaetes *Phyllochaetopterus limicolus* (mean = 32 per grab), *Spiochaetopterus costarum* Complex (mean = 29 per grab), *Paraprionospio alata* (mean = 21 per grab), and *Spiophanes kimballi* (mean = 6 per grab). Group F represented the deepest assemblage sampled during summer 2022. This group included a total of two grabs collected from regional stations 9325, and 9332 at depths between from 422 to 453 m. Sediments from these sites, along with cluster group D, had the largest proportion of fine particles (mean = 85.2% per grab) compared to all other groups. According to SIMPER, the three most characteristic species for cluster group F were the polychaetes *Maldani sarsi* (mean = 8 per grab), *Prionospio ehlersi* (mean = 5 per grab), and *Paraprionospio alata* (mean = 2 per grab) (Appendix H.14). Relative to other groups, these were the highest numbers of *M. sarsi* and *P. ehlersi*.

Integrated Benthic Conditions Assessment

Overall, benthic community conditions were excellent off San Diego during summer 2022. Sediment toxicity was absent (percent control $\geq 97\%$, condition $\geq 90\%$ = non-toxic) at each of the eight samples tested (Table 7.3). All of these samples had combined sediment chemistry concentrations indicative of minimal exposure, which is the lowest level of exposure measured by the California Logistic Regression Model Index (LRM) and the Chemical Score Index (CSI). BRI scores at the eight sample locations ranged from -0.5 to 21.1, all of which were indicative of reference stations (i.e., <25). Thus, all BRI scores, when integrated with SQOs and sediment toxicity scores, resulted in 100% of the stations assessed in summer 2022 deemed as unimpacted.

DISCUSSION

Benthic habitats and associated macrofaunal communities found on the continental shelf and upper slope off San Diego remained in good condition during the 2022–2023 reporting period. Overall, this regional assessment is consistent with the findings from the more extensive sampling of the core PLOO and SBOO stations reported in Chapter 5 for sediment quality and Chapter 6 for macrofaunal communities.

The physical composition of the sediments at the regional and core benthic stations, sampled during the summer 2022 and 2023, was typical for this portion of the southern California coast (Emery 1960), and is consistent with results of previous surveys off San Diego (e.g., City of San Diego 2018, 2020, 2022a,b). Overall, particle size composition varied as expected by outfall region and depth stratum. For example, stations sampled along the inner and mid-shelf within the SBOO monitoring area tended to be composed of medium and coarse sands, whereas stations sampled along the middle and outer shelf within the PLOO region were typically characterized by much finer sediments (see also Chapter 5). Much of the variability in particle size distributions off San Diego is likely related to the complexities of local seafloor geology, topography, and current patterns all of which can significantly affect sediment transport and deposition (Emery 1960, Patsch and Griggs 2007).

Sediment quality was excellent throughout the entire San Diego region in summer 2022–2023. There was no evidence of degraded benthic habitats, in terms of the chemical properties of the sediments, or spatial patterns in the distribution of the different types of contaminants, which may accumulate over time (e.g., organic indicators, trace metals). In addition, results of sediment toxicity testing in offshore San Diego waters revealed minimal toxicity at all regional stations tested, and these results, when integrated with benthic infauna and sediment chemistry results, demonstrated that the shelf off San Diego remains unimpacted by the PLOO or SBOO.

Sediment contamination patterns during the current reporting period were also similar to those seen in previous years. Although, a number of indicators of organic loading, trace metals, pesticides, PCBs, PAHs, and PBDEs were detected in sediment samples throughout the San Diego region, almost all occurred at concentrations below critical ERL and ERM thresholds, similar to that observed in previous years (e.g., City of San Diego 2018, 2020, 2022a,b). Furthermore, examination of spatial patterns revealed no evidence of sediment contamination that could be attributed to local wastewater discharges via the PLOO or SBOO. Instead, concentrations of several trace metals were found to increase with increasing percent fines, and to a lesser degree, with increasing depth. Total nitrogen and total volatile solids also increased with increasing depth. This association is expected, due to the known correlation

between sediment size and concentrations of organics and trace metals (Eganhouse and Venkatesan 1993). Finally, concentrations of these contaminants in San Diego waters remained relatively low compared to other coastal areas located off southern California (Schiff and Gossett 1998, Noblet et al. 2002, Schiff et al. 2006, 2011, Maruya and Schiff 2009, Dodder et al. 2016, Du et al 2020).

Macrofaunal communities in the San Diego region also appeared healthy in summer 2022–2023, with assemblages consistent with those observed during previous regional surveys conducted from 1994 to 2021 (City of San Diego 2010–2013, 2015b, 2016, 2018, 2020, 2022a,b). BRI results revealed little evidence of disturbance off San Diego, with 97% of all calculated BRI values being indicative of reference condition and another 3% being characteristic of only a possible minor deviation. These results reflect assemblages characterized by expected abundances of pollution sensitive species, such as the amphipods *Ampelisca* spp and *Rhepoxynius* spp., and expected abundances of pollution tolerant species, such as the polychaete *Capitella teleta* and the bivalve *Petrasma vernicosa* (see also Chapter 6). Comparison of the results for other major benthic community metrics (e.g. species richness, macrofaunal abundance, diversity, evenness, and dominance) also showed no evidence of wastewater impact or significant habitat degradation during the 2022 and 2023 surveys. Furthermore, values for each of these community structure metrics remain within, or near, the range of tolerance intervals calculated for their specific habitats (see City of San Diego 2022a).

Most of the macrofaunal assemblages identified in summer 2022–2023 segregated by habitat characteristics such as depth and sediment particle size, often corresponding with the “patchy” habitats reported to occur naturally across the SCB (Fauchald and Jones 1979, Jones 1969, Bergen et al. 2000, Mikel et al. 2007). Several of the inner to mid-shelf assemblages described in this chapter were similar to those previously described in other shallow habitats across southern California (Barnard 1963, Jones 1969, Thompson et al. 1987, 1993a,b, MBC 1988, Mikel et al. 2007). These assemblages occurred in sandy sediments and were characterized by several species of polychaetes, including the spionids *Spiophanes norrisi* and *Spiophanes duplex*, and the capitellid *Mediomastus* sp. However, differences between these groups were probably driven by minor variations in sediment type (e.g., shell hash, relict red sand) or depth that differentially affected populations of the resident species. The middle to outer shelf strata off San Diego were dominated by macrofauna cluster group E, which represented assemblages from 87% of the samples analyzed at these depths during the current reporting period. These assemblages occurred in sediments with close to 50% fines and large proportions of very fine and fine sand. Benthic communities dominated by polychaete worms such as *S. duplex* have long been common off Point Loma, and in similar seafloor habitats in other areas of southern California (Jones 1969, Fauchald and Jones 1979, Thompson et al. 1987, 1993a,b, Zmarzly et al. 1994, Diener and Fuller 1995, Bergen et al. 1998, 2000, 2001, Mikel et al. 2007, City of San Diego 2022a). The even finer sediments of upper slope stations sampled off San Diego in summer 2022–2023 were characterized by macrofaunal assemblages with much lower total abundances and fewer species than at most shelf stations. This pattern is similar to results reported previously for the region since regular monitoring of these deeper slope habitats began (e.g., City of San Diego 2010–2013, 2015b, 2016, 2018, 2020, 2022a,b).

Although benthic habitats and their associated macrofaunal communities continue to vary across depth and sediment gradients throughout the San Diego region, there was no evidence of disturbance or environmental degradation in 2022–2023, which may be attributed to anthropogenic factors, such as wastewater discharge via the PLOO or SBOO, or other point sources. Macrobenthic communities appeared to be in good condition overall, with none of the sites surveyed showing evidence consistent with environmental disturbance. This result is similar to findings in Gillett et al. (2017) who reported that at least 98% of the entire SCB mainland shelf is in good condition, based on BRI data from bight-wide regional monitoring program.

LITERATURE CITED

- Barnard, J.L. (1963). Relationship of benthic Amphipoda to invertebrate communities of inshore sublittoral sands of southern California. *Pacific Naturalist*, 3: 439–467.
- Bay, S.M., D.J. Greenstein, J.A. Ranasinghe, D.W. Diehl, and A.E. Fetscher. (2013). Sediment Quality Assessment Technical Support Manual. Technical Report 777. Southern California Coastal Water Research Project. Costa Mesa, CA.
- Bay S.M. and S.B. Weisberg. (2012). Framework for interpreting sediment quality triad data. *Integrated Environ Assess Manag* 8:589-596.
- Bergen, M. (1996). The Southern California Bight Pilot Project: Sampling Design. In: M.J. Allen, C. Francisco, D. Hallock (Eds.). Southern California Coastal Water Research Project: Annual Report 1994–1995. Southern California Coastal Water Research Project, Westminster, CA.
- Bergen, M., D.B. Cadien, A. Dalkey, D.E. Montagne, R.W. Smith, J.K. Stull, R.G. Velarde, and S.B. Weisberg. (2000). Assessment of benthic infaunal condition on the mainland shelf of southern California. *Environmental Monitoring Assessment*, 64: 421–434.
- Bergen, M., S.B. Weisberg, D. Cadien, A. Dalkey, D. Montagne, R.W. Smith, J.K. Stull, and R.G. Velarde. (1998). Southern California Bight 1994 Pilot Project: IV. Benthic Infauna. Southern California Coastal Water Research Project, Westminster, CA.
- Bergen, M., S.B. Weisberg, R.W. Smith, D.B. Cadien, A. Dalkey, D.E. Montagne, J.K. Stull, R.G. Velarde, and J.A. Ranasinghe. (2001). Relationship between depth, sediment, latitude, and the structure of benthic infaunal assemblages on the mainland shelf of southern California. *Marine Biology*, 138: 637–647.
- [B13CIA] Bight '13 Contaminant Impact Assessment Planning Committee. (2017). Southern California Bight 2013 Regional Monitoring Program: Volume VIII. Contaminant Impact Assessment Synthesis Report. Technical Report 973. Southern California Coastal Water Research Project. Costa Mesa, CA.
- Bight'18 Toxicology Committee. (2018). Bight'18 Toxicology Laboratory Manual. Southern California Bight 2018 Regional Monitoring Program. Southern California Coastal Water Research Project. Costa Mesa, CA.
- City of San Diego. (2010–2013). Annual Receiving Waters Monitoring Report for the South Bay Ocean Outfall (South Bay Water Reclamation Plant), 2009-2012. City of San Diego Ocean Monitoring Program, Public Utilities Department, Environmental Monitoring and Technical Services Division, San Diego, CA.
- City of San Diego. (2015a). Sediment Toxicity Monitoring Plan for the South Bay Ocean Outfall and Point Loma Ocean Outfall Monitoring Regions, San Diego, California. Submitted by the City of San Diego Public Utilities Department to the San Diego Water Board and USEPA, Region IX, August 28, 2015 [approved 9/29/2015].

- City of San Diego. (2015b). South Bay Ocean Outfall Annual Receiving Waters Monitoring and Assessment Report, 2014. City of San Diego Ocean Monitoring Program, Public Utilities Department, Environmental Monitoring and Technical Services Division, San Diego, CA.
- City of San Diego. (2016). South Bay Ocean Outfall Annual Receiving Waters Monitoring and Assessment Report, 2015. City of San Diego Ocean Monitoring Program, Public Utilities Department, Environmental Monitoring and Technical Services Division, San Diego, CA.
- City of San Diego. (2018). Biennial Receiving Waters Monitoring and Assessment Report for the Point Loma and South Bay Ocean Outfalls, 2016–2017. City of San Diego, Public Utilities Department, Environmental Monitoring and Technical Services Division, San Diego, CA.
- City of San Diego. (2020). Biennial Receiving Waters Monitoring and Assessment Report for the Point Loma and South Bay Ocean Outfalls, 2018–2019. City of San Diego, Public Utilities Department, Environmental Monitoring and Technical Services Division, San Diego, CA.
- City of San Diego. (2022a). Appendix C. Ocean Benthic Conditions. In: Application for Renewal of NPDES CA0107409 and 301(h) Modified Secondary Treatment Requirements, Point Loma Ocean Outfall. Volume V, Appendix C. Public Utilities Department, Environmental Monitoring and Technical Services Division, San Diego, CA.
- City of San Diego. (2022b). Biennial Receiving Waters Monitoring and Assessment Report for the Point Loma and South Bay Ocean Outfalls, 2020–2021. City of San Diego, Public Utilities Department, Environmental Monitoring and Technical Services Division, San Diego, CA.
- City of San Diego. (2023). Interim Receiving Waters Monitoring Report for the Point Loma and South Bay Ocean Outfalls, 2022. City of San Diego, Public Utilities Department, Environmental Monitoring and Technical Services Division, San Diego, CA.
- City of San Diego. (2024). Quality Assurance Manual for Toxicity Testing. City of San Diego Toxicology Laboratory, Environmental Monitoring and Technical Services Division, Public Utilities Department, San Diego, CA.
- Clarke, K.R., R.N. Gorley, P.J. Somerfield, and R.M. Warwick. (2014). Change in marine communities: an approach to statistical analysis and interpretation, 3rd edition. PRIMER-E, Plymouth, England.
- Clarke, K.R., P.J. Somerfield, and R.N. Gorley. (2008). Testing of null hypotheses in exploratory community analyses: similarity profiles and biota-environment linkage. *Journal of Experimental Marine Biology and Ecology*, 366: 56–69.
- Conover, W.J. (1980). *Practical Nonparametric Statistics*, 2nd ed. John Wiley & Sons, Inc., New York, NY.
- Diener, D.R. and S.C. Fuller. (1995). Infaunal patterns in the vicinity of a small coastal wastewater outfall and the lack of infaunal community response to secondary treatment. *Bulletin of the Southern California Academy of Science*, 94: 5–20.

- Dodder, N., K. Schiff, A. Latker, and C-L Tang. (2016). Southern California Bight 2013 Regional Monitoring Program: IV. Sediment Chemistry. Southern California Coastal Water Research Project, Westminster, CA.
- Du, B., C.S. Wong, K. Mclaughlin, and K. Schiff. (2020). Southern California Bight 2018 Regional Monitoring Program: II. Sediment Chemistry. Southern California Coastal Water Research Project, Westminster, CA.
- Eganhouse, R.P. and M.I. Venkatesan. (1993). Chemical Oceanography and Geochemistry. In: M.D. Dailey, D.J. Reish, and J.W. Anderson (eds.). Ecology of the Southern California Bight: A Synthesis and Interpretation. University of California Press, Berkeley, CA. p 71–189.
- Emery, K. O. (1960). The Sea Off Southern California. John Wiley, New York, NY.
- Fauchald, K. and G.F. Jones. (1979). Variation in community structures on shelf, slope, and basin macrofaunal communities of the Southern California Bight. Report 19, Series 2. In: Southern California Outer Continental Shelf Environmental Baseline Study, 1976/1977 (Second Year) Benthic Program. Principal Investigators Reports, Vol. II. Science Applications, Inc. La Jolla, CA.
- Ferraro, S.P., R.C. Swartz, F.A. Cole, and W.A. Deben. (1994). Optimum macrobenthic sampling protocol for detecting pollution impacts in the Southern California Bight. Environmental Monitoring and Assessment, 29: 127–153.
- Folk, R.L. (1980). Petrology of Sedimentary Rocks. Hemphill, Austin, TX.
- Gillett, D.J., L.L. Lovell, and K.C. Schiff. (2017). Southern California Bight 2013 Regional Monitoring Program: Volume VI. Benthic Infauna. Technical Report 971. Southern California Coastal Water Research Project. Costa Mesa, CA.
- Helsel, D.R. (2005a). More than obvious: better methods for interpreting nondetect data. Environmental Science & Technology (October 15, 2005), 419A-423A.
- Helsel, D.R. (2005b). Nondetects and Data Analysis: Statistics for Censored Environmental Data. John Wiley, New York.
- Helsel, D.R. (2006). Fabrication data: how substituting values for nondetects can ruin results, and what can be done about it. Chemosphere 65: 2434-2439.
- Hope, R.M. (2022). Rmisc: Ryan Miscellaneous. R package version 1.5.1. <http://CRAN.R-project.org/package=Rmisc>.
- Jones, G.F. (1969). The benthic macrofauna of the mainland shelf of southern California. Allan Hancock Monographs of Marine Biology, 4: 1–219.
- Kassambara, A. (2023). ggpubr: Based Publication Ready Plots R package version 0.6.0. <http://www.sthda.com/english/rpkgs/ggpubr>.

- Long, E.R., D.L. MacDonald, S.L. Smith, and F.D. Calder. (1995). Incidence of adverse biological effects within ranges of chemical concentration in marine and estuarine sediments. *Environmental Management*, 19(1): 81–97.
- Maruya, K.A. and K. Schiff. (2009). The extent and magnitude of sediment contamination in the Southern California Bight. *Geological Society of America Special Paper*, 454: 399–412.
- [MBC] MBC Applied Environmental Sciences and Engineering-Science. (1988). Part F: Biological studies. In: Tijuana Oceanographic Engineering Study, Volume 1. Ocean Measurement Program. Prepared for the City of San Diego, CA.
- Mikel T.K., J.A. Ranasinghe, and D.E. Montagne. (2007). Characteristics of benthic macrofauna of the Southern California Bight. Appendix F. Southern California Bight 2003 Regional Monitoring Program, SCCWRP, Costa Mesa, CA.
- Noblet, J.A., E.Y. Zeng, R. Baird, R.W. Gossett, R.J. Ozretich, and C.R. Phillips. (2002). Southern California Bight 1998 Regional Monitoring Program: VI. Sediment Chemistry. Southern California Coastal Water Research Project, Westminster, CA.
- Oksanen, J., F.G. Blanchet, R. Kindt, P. Legendre, P.R. Minchin, R.B. O'Hara, G.L. Simpson, P. Solymos, M.H.H. Stevens, and H. Wagner. (2022). *vegan: Community Ecology Package*. R package version 2.6-4. <http://CRAN.R-project.org/package=vegan>.
- Patsch, K. and G. Griggs. (2007). Development of Sand Budgets for California's Major Littoral Cells. Institute of Marine Sciences, University of California, Santa Cruz, CA.
- R Core Team. (2023). R: A language and environment for statistical computing. R Foundation for Statistical Computing, Vienna, Austria. URL <https://www.R-project.org/>.
- Ranasinghe, J.A., A.M. Barnett, K. Schiff, D.E. Montagne, C. Brantley, C. Beegan, D.B. Cadien, C. Cash, G.B. Deets, D.R. Diener, T.K. Mikel, R.W. Smith, R.G. Velarde, S.D. Watts, and S.B. Weisberg. (2007). Southern California Bight 2003 Regional Monitoring Program: III. Benthic Macrofauna. Southern California Coastal Water Research Project. Costa Mesa, CA.
- Ranasinghe, J.A., D. Montagne, R.W. Smith, T.K. Mikel, S.B. Weisberg, D. Cadien, R. Velarde, and A. Dalkey. (2003). Southern California Bight 1998 Regional Monitoring Program: VII. Benthic Macrofauna. Southern California Coastal Water Research Project. Westminster, CA.
- Ranasinghe, J.A., K.C. Schiff, C.A. Brantley, L.L. Lovell, D.B. Cadien, T.K. Mikel, R.G. Velarde, S. Holt, and S.C. Johnson. (2012). Southern California Bight 2008 Regional Monitoring Program: VI. Benthic Macrofauna. Technical Report No. 665, Southern California Coastal Water Research Project, Costa Mesa, CA.
- Ranasinghe, J.A., K.C. Schiff, D.E. Montagne, T.K. Mikel, D.B. Cadien, R.G. Velarde, and C.A. Brantley. (2010). Benthic macrofaunal community condition in the Southern California Bight, 1994–2003. *Marine Pollution Bulletin*, 60: 827–833.

- Revelle, W. (2023) psych: Procedures for Personality and Psychological Research, Northwestern University, Evanston, Illinois, USA, <https://CRAN.R-project.org/package=psych> Version = 2.3.6.
- Ripley, B. and M. Lapsley. (2022). RODBC: ODBC Database Access. R package version 1.3-20. <http://CRAN.R-project.org/package=RODBC>.
- [SCAMIT] Southern California Association of Marine Invertebrate Taxonomists. (2021). A taxonomic listing of benthic macro- and megainvertebrates from infaunal and epibenthic monitoring programs in the Southern California Bight, edition 13. Southern California Association of Marine Invertebrate Taxonomists, Natural History Museum of Los Angeles County Research and Collections, Los Angeles, CA.
- [SCCWPR] Southern California Coastal Water Research Project. (2018). Southern California Bight 2018 Regional Monitoring Program: Contaminant Impact Assessment Field Operations Manual. Southern California Coastal Water Research Project. Costa Mesa, CA.
- Schiff, K.C. and R.W. Gossett. (1998). Southern California Bight 1994 Pilot Project: III. Sediment Chemistry. Southern California Coastal Water Research Project. Westminster, CA.
- Schiff, K., R. Gossett, K. Ritter, L. Tiefenthaler, N. Dodder, W. Lao, and K. Maruya. (2011). Southern California Bight 2008 Regional Monitoring Program: III. Sediment Chemistry. Southern California Coastal Water Research Project, Costa Mesa, CA.
- Schiff, K., K. Maruya, and K. Christenson. (2006). Southern California Bight 2003 Regional Monitoring Program: II. Sediment Chemistry. Southern California Coastal Water Research Project, Westminster, CA.
- Smith, R.W., M. Bergen, S.B. Weisberg, D. Cadien, A. Dalkey, D. Montagne, J.K. Stull, and R.G. Velarde. (2001). Benthic response index for assessing infaunal communities on the southern California mainland shelf. *Ecological Applications*, 11(4): 1073–1087.
- [SWRCB] State Water Resource Control Board. (2009). Water Quality Control Plan for Enclosed Bays and Estuaries – Part 1 Sediment Quality. Resolution Number 2008-0070, State Water Resources Control Board, Sacramento, CA.
- Stebbins, T.D., K.C. Schiff, and K. Ritter. (2004). San Diego Sediment Mapping Study: Workplan for Generating Scientifically Defensible Maps of Sediment Conditions in the San Diego Region. City of San Diego, Metropolitan Wastewater Department, Environmental Monitoring and Technical Services Division, and Southern California Coastal Water Research Project, Westminster, CA.
- Stevens Jr., D.L. (1997). Variable density grid-based sampling designs for continuous spatial populations. *Environmetrics*, 8: 167–195.
- Stevens Jr., D.L. and A.R. Olsen. (2004). Spatially-balanced sampling of natural resources in the presence of frame imperfections. *Journal of the American Statistical Association*, 99: 262–278.

- Swartz, R.C., F.A. Cole, and W.A. Deben. (1986). Ecological changes in the Southern California Bight near a large sewage outfall: benthic conditions in 1980 and 1983. *Marine Ecology Progress Series*, 31: 1–13.
- Thompson, B.E., J.D. Laughlin, and D.T. Tsukada. (1987). 1985 reference site survey. Technical Report No. 221, Southern California Coastal Water Research Project, Long Beach, CA.
- Thompson, B., J. Dixon, S. Schroeter, and D.J. Reish. (1993a). Chapter 8. Benthic invertebrates. In: M.D. Dailey, D.J. Reish, and J.W. Anderson (eds.). *Ecology of the Southern California Bight: A Synthesis and Interpretation*. University of California Press, Berkeley, CA.
- Thompson, B.E., D. Tsukada, and D. O’Donohue. (1993b). 1990 reference site survey. Technical Report No. 269, Southern California Coastal Water Research Project, Long Beach, CA.
- [USEPA] United States Environmental Protection Agency. (1987). Quality Assurance and Quality Control (QA/QC) for 301(h) Monitoring Programs: Guidance on Field and Laboratory Methods. EPA Document 430/9-86-004. Office of Marine and Estuarine Protection.
- [USEPA] United States Environmental Protection Agency. (1994). Methods for assessing the toxicity of sediment-associated contaminants with estuarine and marine amphipods. EPA/600/R-94/025. Office of Research and Development, UEPA. Narragansett, RI.
- Wickham, H. (2007). Reshaping Data with the reshape Package. *Journal of Statistical Software*, 21(12), 1-20. URL <http://www.jstatsoft.org/v21/i12/>.
- Wickham, H. (2011). The Split-Apply-Combine Strategy for Data Analysis. *Journal of Statistical Software*, 40(1), 1-29. URL <http://www.jstatsoft.org/v40/i01/>.
- Wickham, H. (2016). *Ggplot2: Elegant Graphics for Data Analysis*. Springer-Verlag, New York.
- Wickham, H., M. Averick, J. Bryan, W. Chang, L. D’Agostino McGowan, R. François, G. Grolemond, A. Hayes, L. Henry, J. Hester, M. Kuhn, T. Lin Pedersen, E. Miller, S. Milton Bache, K. Müller, J. Ooms, D. Robinson, D. P. Seidel, V. Spinu, K. Takahashi, D. Vaughan, C. Wilke, K. Woo, H. Yutani. (2019). Welcome to the tidyverse. *Journal of Open Source Software*, 4(43), 1686, <https://doi.org/10.21105/joss.01686>.
- Wickham, H. (2022). stringr: Simple, Consistent Wrappers for Common String Operations. R package version 1.5.0. <https://CRAN.R-project.org/package=stringr>.
- Wickham, H. and D. Seidel. (2022). Scales: Scale Functions for Visualization Rstudio. R package version 1.2.1. <https://scales.r-lib.org/>.
- Wickham, H. D. Vaughan, and M. Girlich. (2023a). tidyr: Easily Tidy Data with 'spread()' and 'gather()' Functions. R package version 1.3.0. <https://CRAN.R-project.org/package=tidyr>.
- Wickham, H., R. Francois, L. Henry, K. Müller, and D. Vaughan. (2023b). dplyr: A Grammar of Data Manipulation. R package version 1.1.2. <https://CRAN.R-project.org/package=dplyr>.

Zeileis, A and G. Grothendieck. (2005). zoo: S3 Infrastructure for Regular and Irregular Time Series. *Journal of Statistical Software*, 14(6), 1-27. URL <http://www.jstatsoft.org/v14/i06/>.

Zmarzly, D.L., T.D. Stebbins, D. Pasko, R.M. Duggan, and K.L. Barwick. (1994). Spatial patterns and temporal succession in soft-bottom macroinvertebrate assemblages surrounding an ocean outfall on the southern San Diego shelf: Relation to anthropogenic and natural events. *Marine Biology*, 118: 293–307.

CHAPTER 7

FIGURES & TABLES

Table 7.1

Summary of particle sizes and chemistry concentrations in sediments from San Diego regional (Reg) and core benthic stations sampled during summer 2022 and 2023. Data include detection rate (DR; %), minimum, maximum, and mean values for the entire survey area, as well as mean value by depth stratum. For chemistry parameters, minimum and maximum values were calculated using all samples, whereas means were calculated with detected values only; n=number of samples; nd=not detected.

Parameter	Depth Strata											
	2022–2023 Survey Area				Inner Shelf		Middle Shelf			Outer Shelf	Upper Slope	
	DR	Min	Max	Mean	SBOO n=17	Reg n=10	PLOO n=22	SBOO n=10	Reg n=15	Reg n=9	Reg n=6	
Particle Size (%)												
Coarse particles	29	0	35.5	2.9	2.6	10.0	1.4	4.9	0.5	6.3	0.0	
Med-coarse sands	100	0.1	90.6	16.7	33.3	18.9	2.9	50.0	2.0	9.5	0.2	
Fine sands	100	0.9	87.0	40.5	47.0	46.9	40.8	21.1	40.0	29.1	19.3	
Fine particles	99	0	85.6	39.9	17.1	24.3	54.9	24.0	57.5	55.1	80.4	
Organic Indicators												
Sulfides (ppm)	63	nd	50.6	12.7	11.3	4.5	13.2	6.6	7.1	3.7	21.1	
TN (% weight)	90	nd	0.22	0.05	0.03	0.02	0.05	0.03	0.05	0.05	0.15	
TOC (% weight)	91	nd	6.17	0.67	0.29	0.19	0.72	0.29	0.58	1.54	2.35	
TVS (% weight)	100	0.2	8.1	2.0	0.8	0.9	2.1	0.7	2.2	3.5	5.5	
Trace Metals (ppm)												
Aluminum	100	665	17,500	6117	3682	3766	6729	2138	8491	8933	14,425	
Antimony	89	nd	2.61	0.83	0.63	0.87	0.88	0.56	1.19	0.94	1.76	
Arsenic	100	0.81	9.81	2.63	1.71	1.93	2.70	3.26	2.91	3.04	3.54	
Barium	100	1.4	105.0	27.7	18.9	18.4	28.7	7.7	37.7	41.2	71.0	
Beryllium	100	0.016	0.381	0.139	0.071	0.064	0.166	0.066	0.170	0.210	0.324	
Cadmium	29	nd	0.409	0.107	0.035	—	0.087	0.088	0.088	0.174	0.255	
Chromium	100	2.8	37.0	13.2	8.2	7.3	14.9	8.1	15.4	18.2	30.6	
Copper	89	nd	30.3	7.4	2.7	5.4	6.9	2.6	10.1	15.4	16.9	
Iron	100	1140	22,500	8737	4766	4870	10,735	4859	10,483	13,754	16,950	
Lead	100	0.6	7.7	2.7	1.4	1.6	3.1	1.8	3.9	4.1	4.8	
Manganese	100	6	159	68	48	60	78	26	94	92	124	
Mercury	84	nd	0.113	0.023	0.006	0.005	0.023	0.007	0.030	0.043	0.055	
Nickel	99	nd	19.2	4.4	1.8	1.6	5.1	1.5	5.7	6.6	14.4	
Selenium	16	nd	0.63	0.40	0.24	—	0.40	—	—	0.45	0.59	
Silver	0	—	—	—	—	—	—	—	—	—	—	
Thallium	1	nd	0.341	0.341	—	0.341	—	—	—	—	—	
Tin	97	nd	1.47	0.55	0.31	0.29	0.62	0.24	0.78	0.78	1.13	
Zinc	100	1.9	61.4	21.4	11.4	11.9	25.4	7.7	28.1	34.1	47.7	

Table 7.1 *Continued*

Parameter	2022–2023 Survey Area				Depth Strata						
					Inner Shelf		Middle Shelf			Outer Shelf	Upper Slope
	DR	Min	Max	Mean	SBOO n=17	Reg n=10	PLOO n=22	SBOO n=10	Reg n=15	Reg n=9	Reg n=6
<i>Pesticides (ppt)</i>											
Total DDT	65	nd	9936	864	89	70	301	690	1807	561	1705
Total HCH	1	nd	54	54	32	—	133	—	—	—	—
Total Chlordane	2	nd	650	410	—	—	247	—	—	170	—
Hexachlorobenzene	1	nd	173	173	196	—	—	—	173	—	—
Mirex	2	nd	169	100	41	—	—	—	169	—	—
<i>Total PCB (ppt)</i>	38	nd	12,021	2143	223	—	2674	405	2069	6401	712
<i>Total PAH (ppb)</i>	40	nd	996.3	66.0	12.8	14.8	42.1	9.6	162.0	150.0	22.0
<i>Total PBDE (ppt)</i>	32	nd	529.3	160.7	63.1	—	165.9	111.7	196.7	—	—

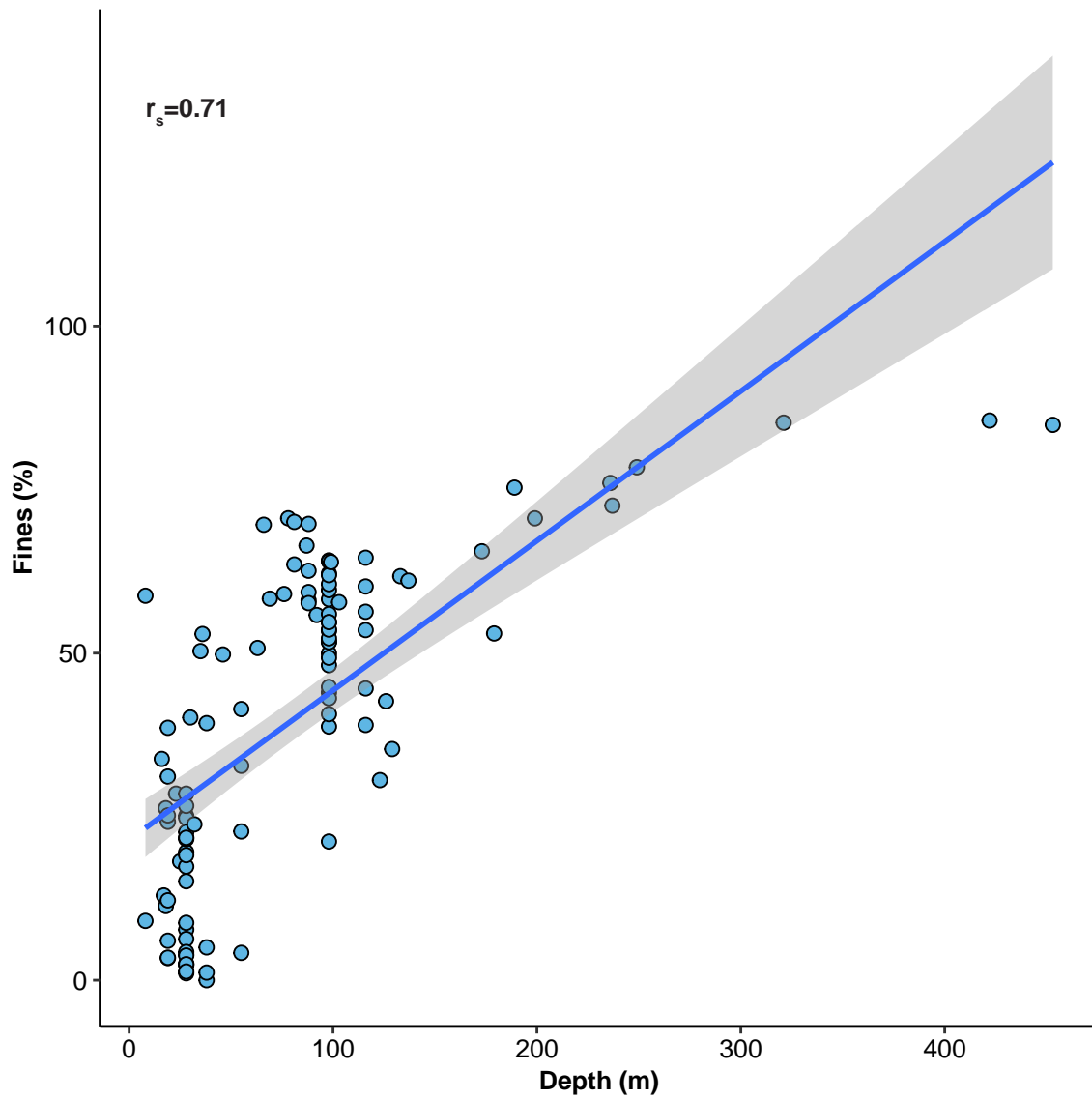


Figure 7.2

Scatterplot of concentrations of fine particles (Fines) versus depth for sediments collected from San Diego regional and core benthic stations during summer 2022 and 2023. Shaded area indicates 95% confidence interval.

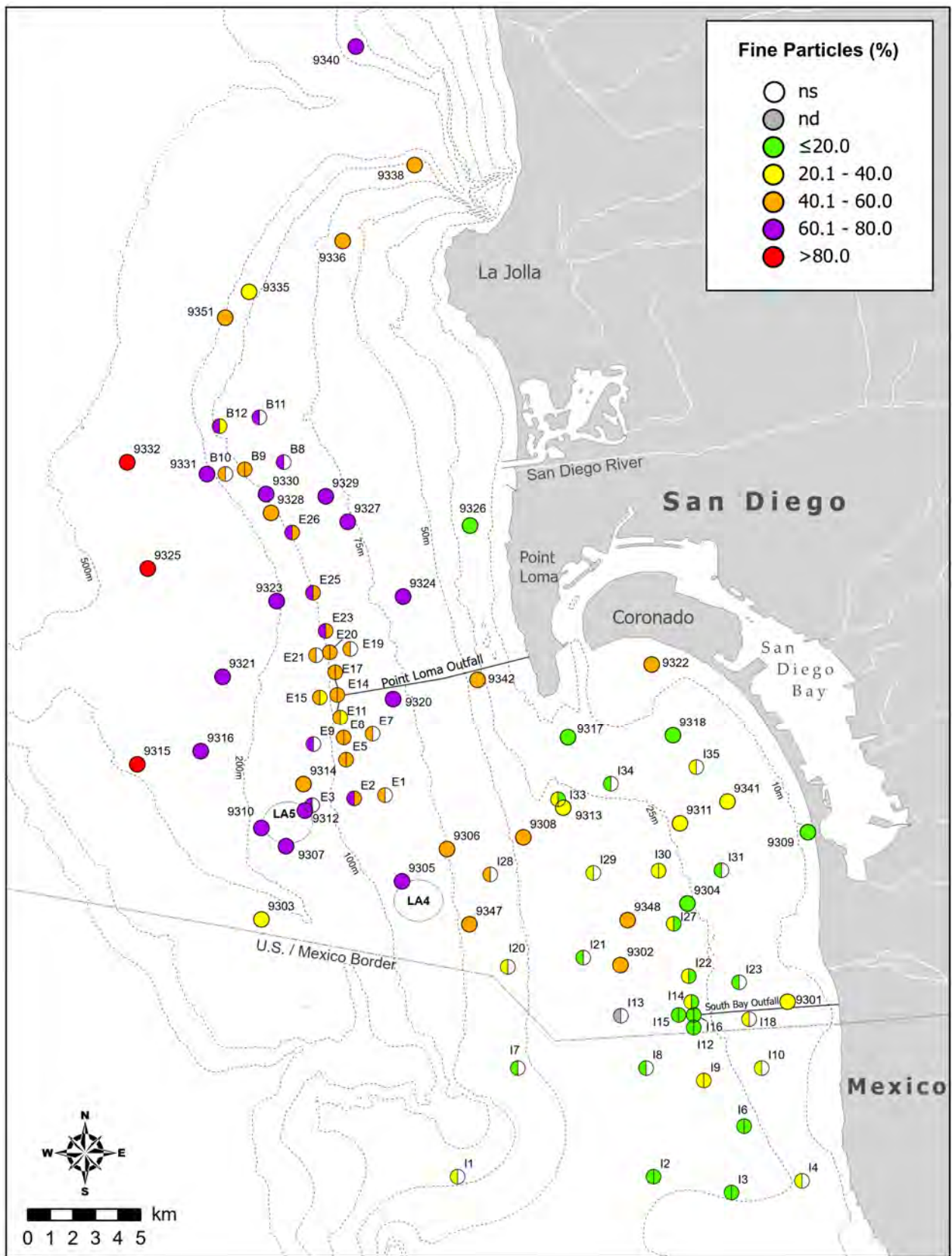


Figure 7.3
 Distribution of fine particles in sediments from San Diego regional and core benthic stations sampled during summer 2022 and 2023; ns = not sampled.

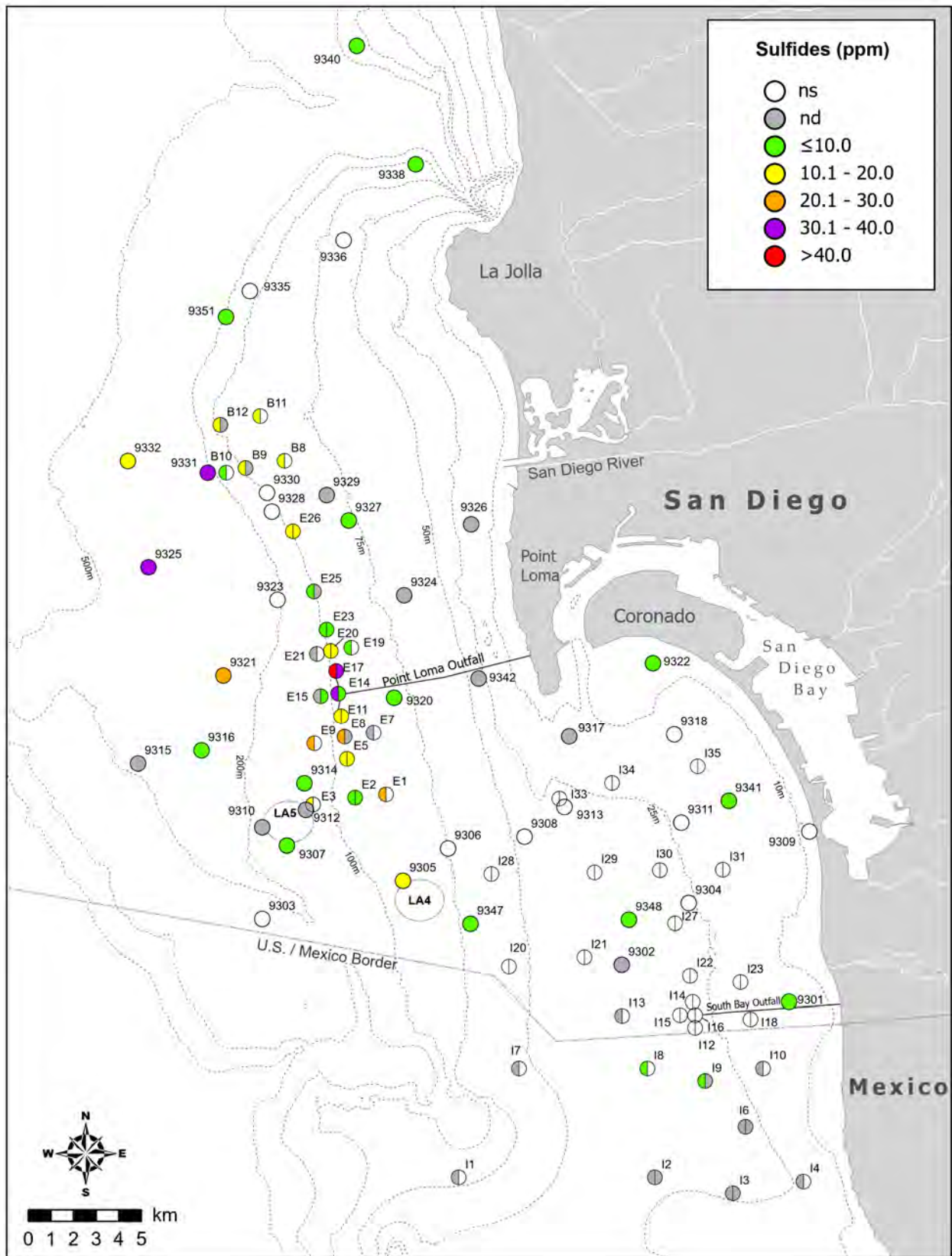


Figure 7.4
 Distribution of organic loading indicators in sediments from San Diego regional and core benthic stations sampled during summer 2022 and 2023; ns = not sampled (or not reportable, see text); nd= not detected.

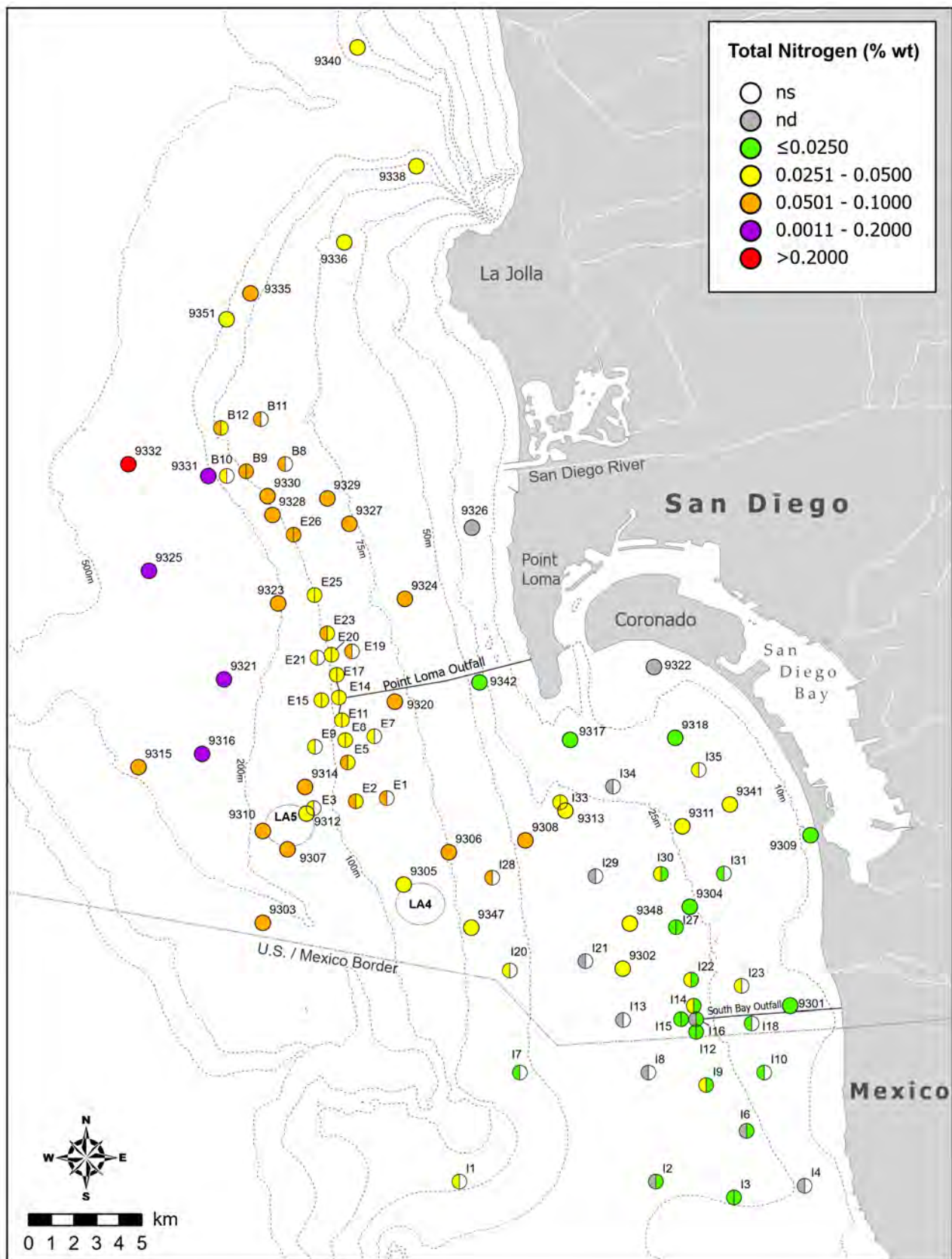


Figure 7.4 continued

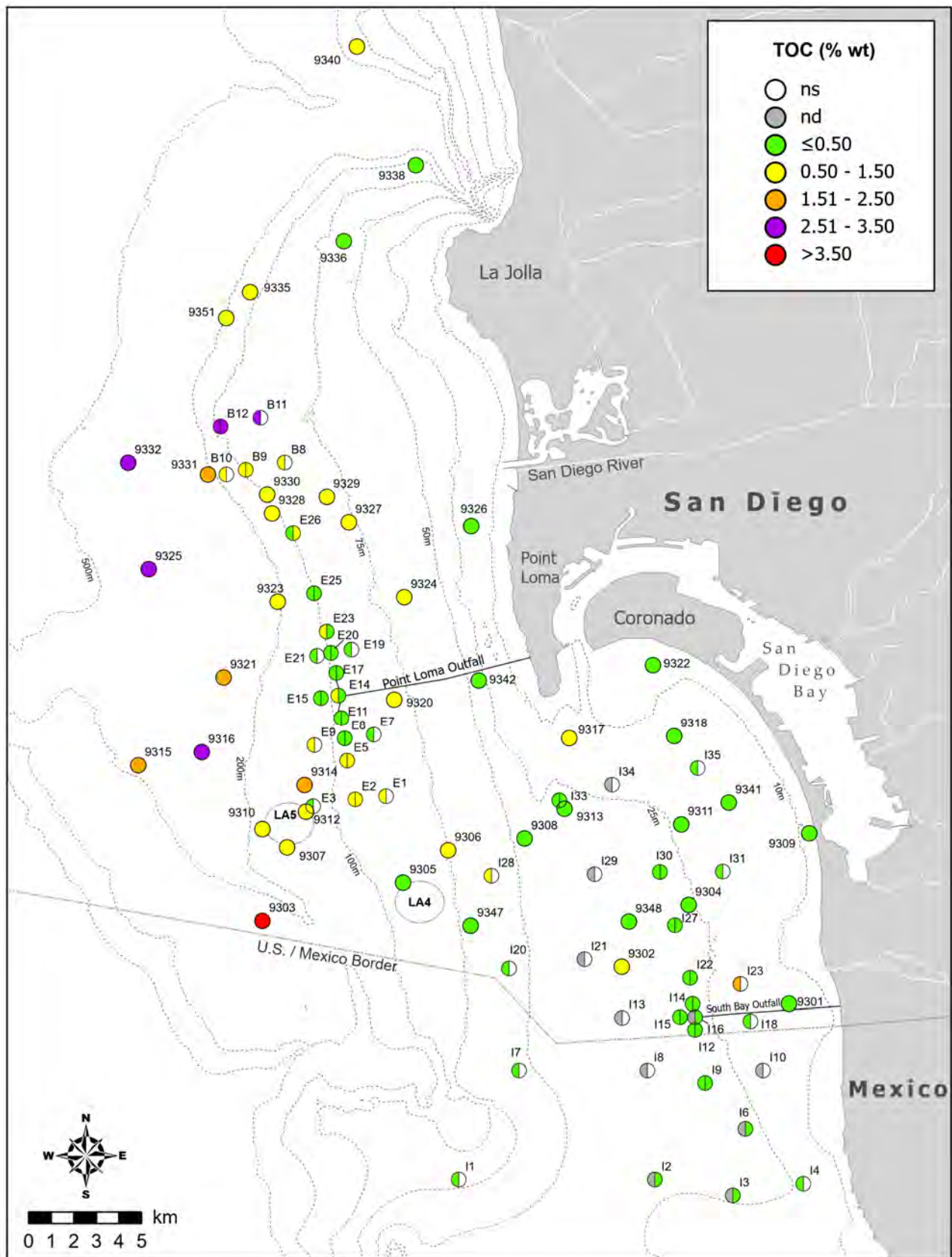


Figure 7.4 continued

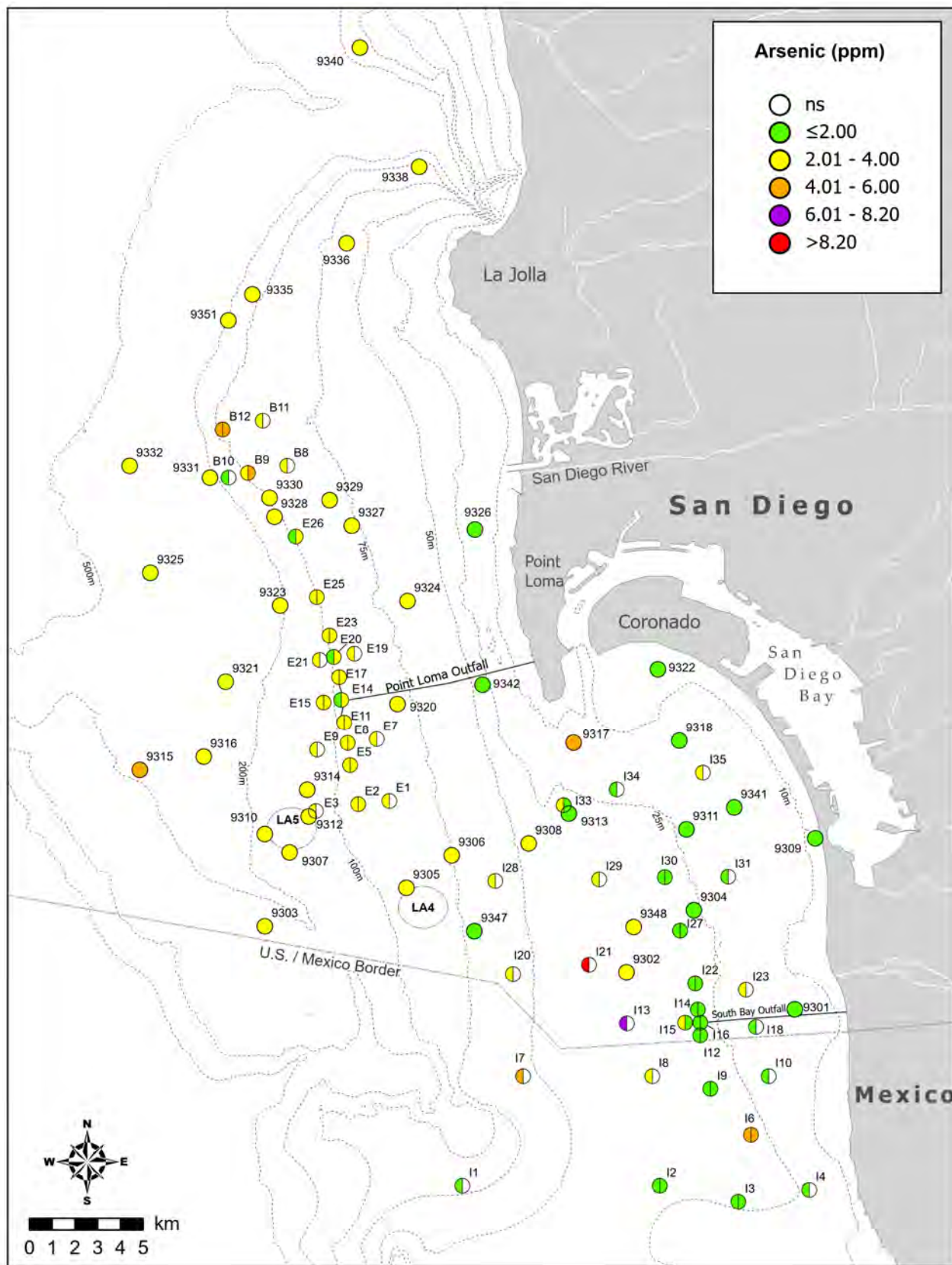


Figure 7.5

Distribution of select metals in sediments from San Diego regional and core benthic stations sampled during summer 2022 and 2023; ns = not sampled (or not reportable, see text); nd = not detected.

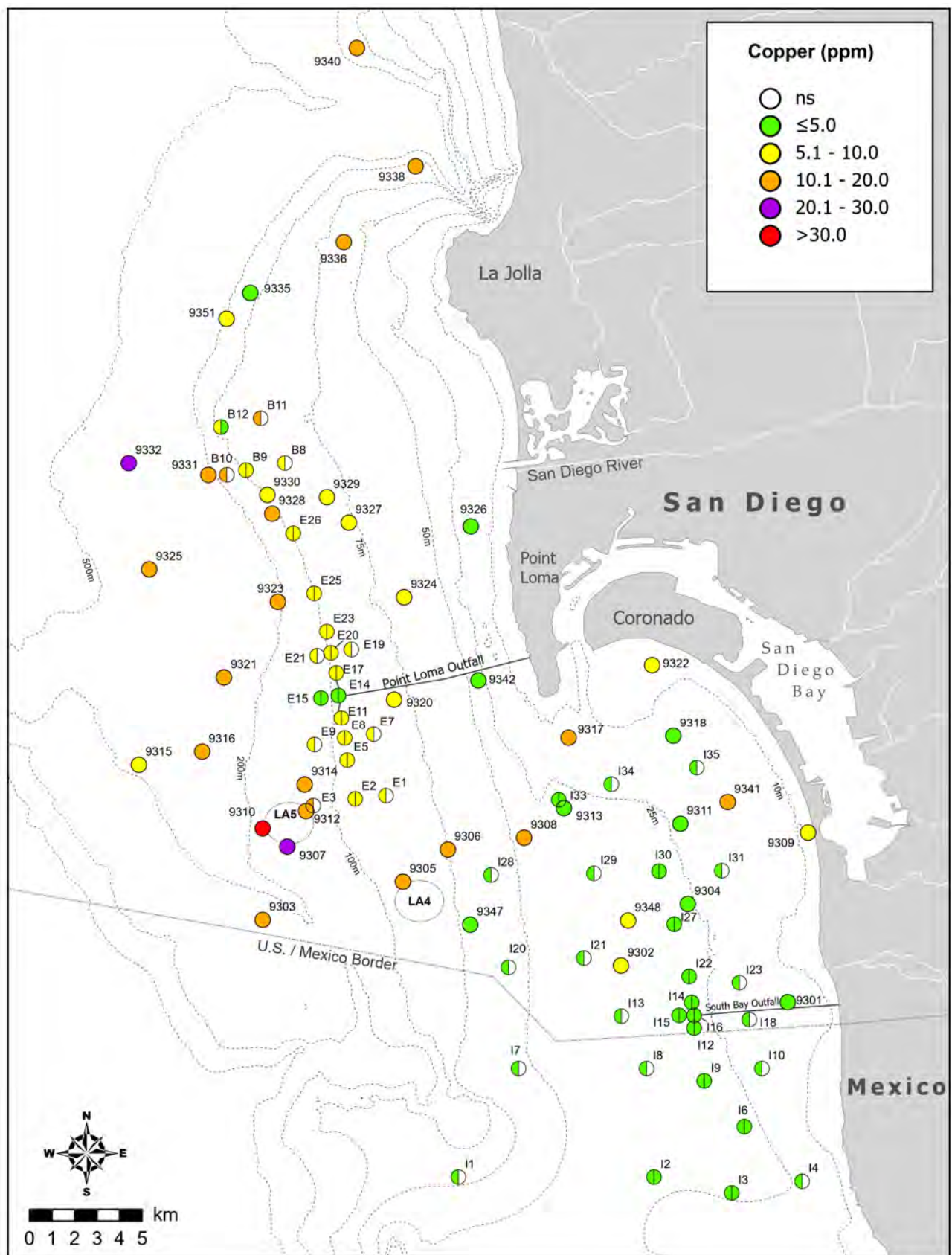


Figure 7.5 continued

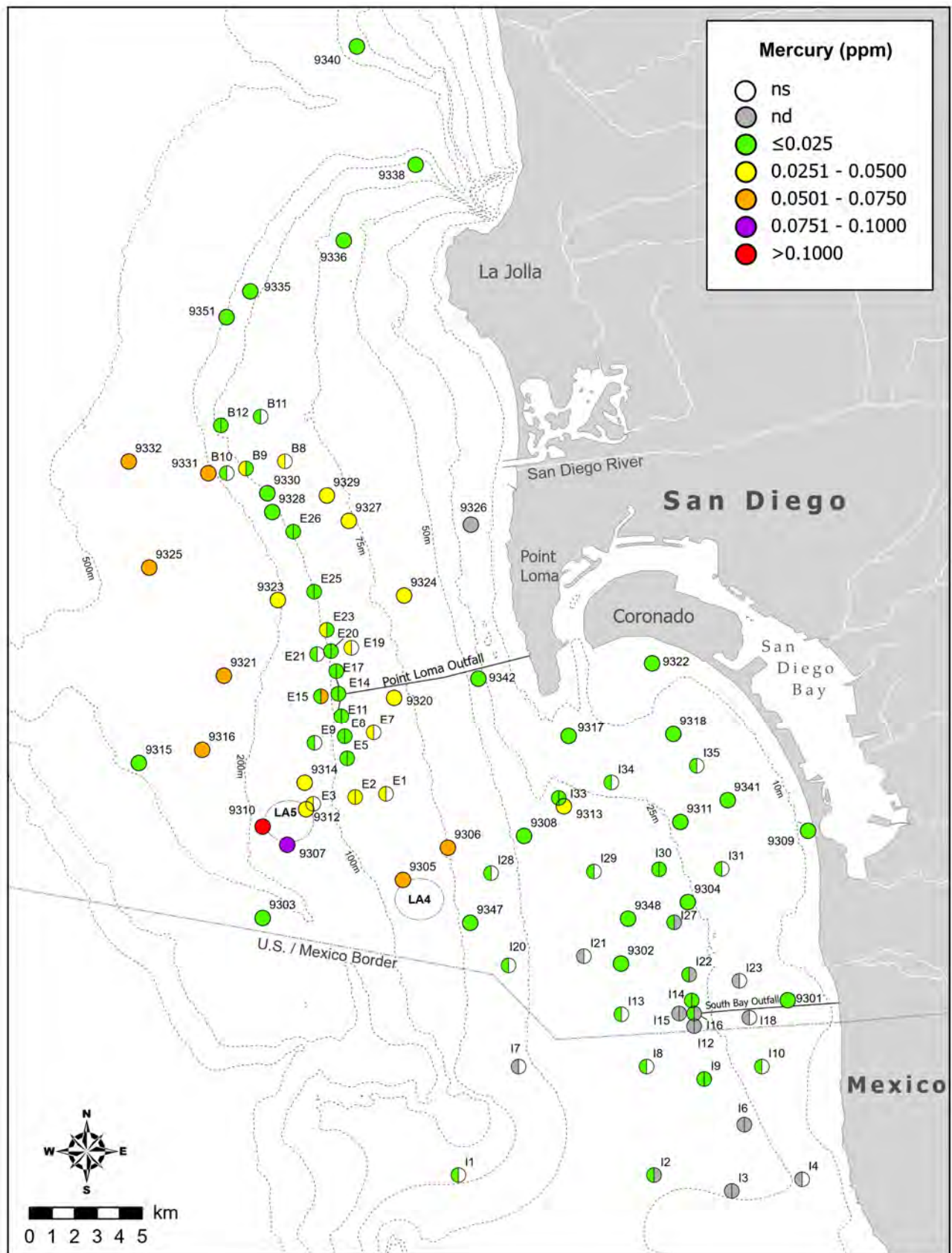


Figure 7.5 continued

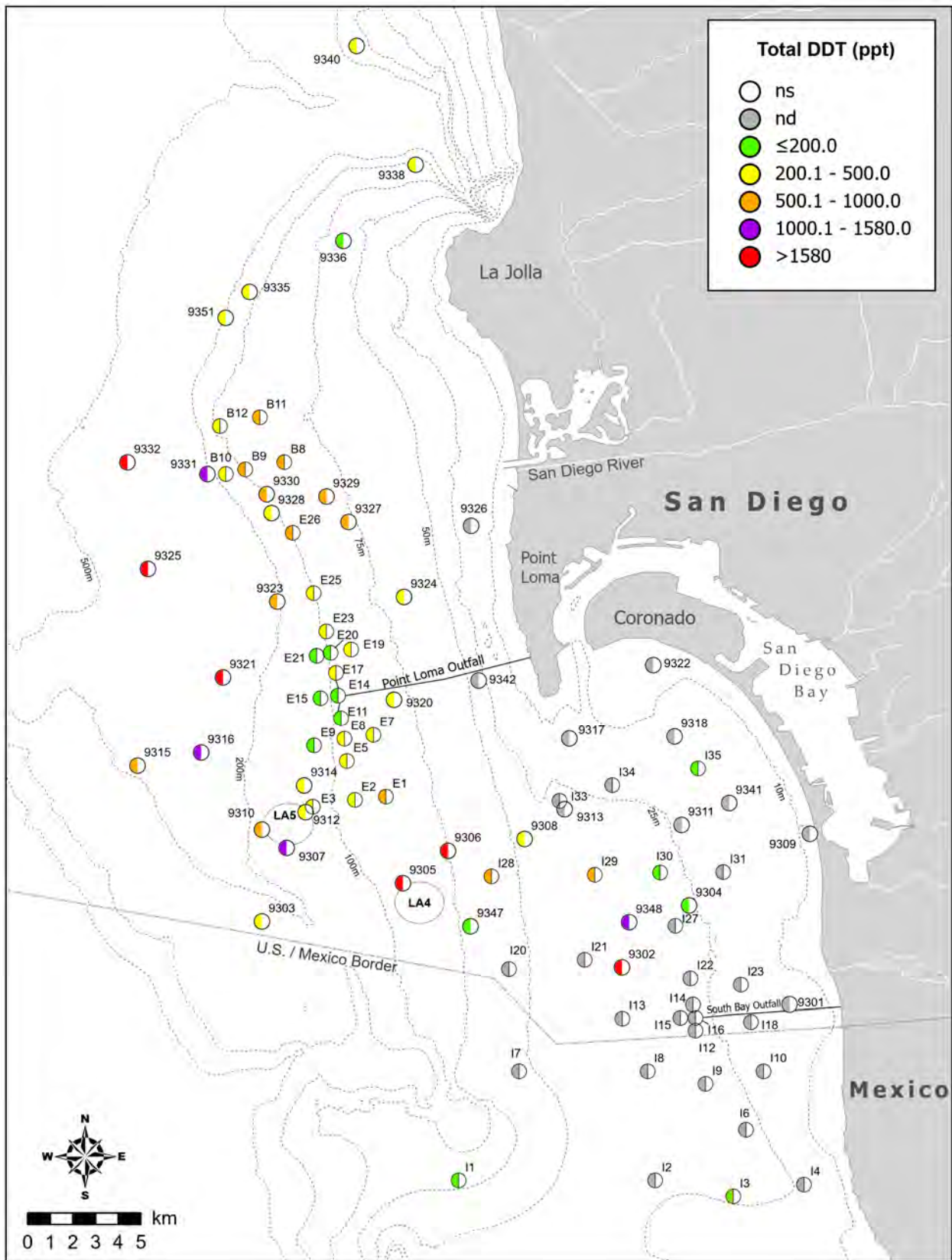


Figure 7.6
 Distribution of total DDT in sediments from San Diego regional and core benthic stations sampled during summer 2022 and 2023; ns = not sampled (or not reportable, see text); nd = not detected.

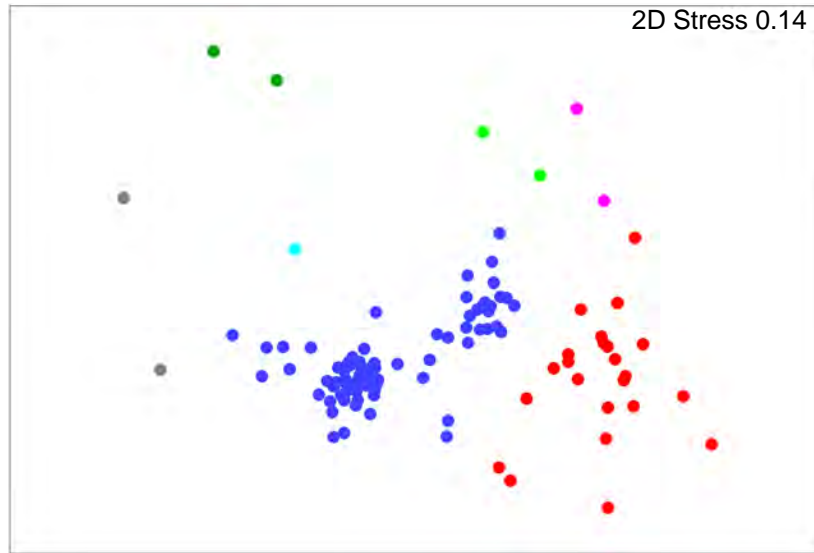
Table 7.2

Macrofaunal community summary statistics calculated for San Diego regional and core benthic stations sampled during summer 2022 and 2023. Data are presented as means (ranges) by stratum; n=number of grabs; SR=species richness; Abun=abundance; H'=Shannon diversity index; J'=Pielou's evenness; Dom=Swartz dominance; BRI=benthic response index.

Stratum		n	SR	Abun	H'	J'	Dom	BRI^a
<i>Inner Shelf</i>	SBOO	27	69 (33-143)	330 (96-710)	3.1 (1.7-4.2)	0.75 (0.44-0.89)	19 (3-41)	18 (7-27)
	Regional	10	50 (19-89)	231 (55-475)	3.0 (2.2-3.9)	0.78 (0.57-0.88)	15 (6-30)	16 (0-24)
	All Inner Shelf	37	64 (19-143)	303 (55-710)	3.1 (1.7-4.2)	0.76 (0.44-0.89)	18 (3-41)	17 (0-27)
<i>Middle Shelf</i>	PLOO	35	97 (69-121)	339 (177-481)	4.0 (3.3-4.3)	0.88 (0.74-0.93)	35 (18-47)	13 (7-26)
	SBOO	12	86 (46-189)	401 (200-833)	3.3 (1.9-4.6)	0.74 (0.50-0.87)	23 (5-59)	13 (5-19)
	Regional	15	106 (77-184)	402 (162-892)	4.0 (3.5-4.5)	0.86 (0.81-0.94)	36 (19-60)	14 (7-22)
	All Middle Shelf	62	97 (46-189)	366 (162-892)	3.9 (1.9-4.6)	0.85 (0.50-0.94)	33 (5-60)	13 (5-26)
<i>Outer Shelf</i>	Regional	9	75 (32-119)	290 (204-395)	3.5 (2.0-4.2)	0.81 (0.57-0.92)	25 (5-43)	14 (8-22)
<i>Upper Slope</i>	Regional	6	36 (11-77)	121 (41-294)	2.6 (1.1-3.6)	0.76 (0.44-0.93)	14 (2-27)	—
	All Stations	114	81 (11-189)	327 (41-892)	3.5 (1.1-4.6)	0.81 (0.44-0.94)	26 (2-60)	14 (0-27)

^aBRI statistic not calculated for stations located at depths < 10 m or > 200 m

A



B

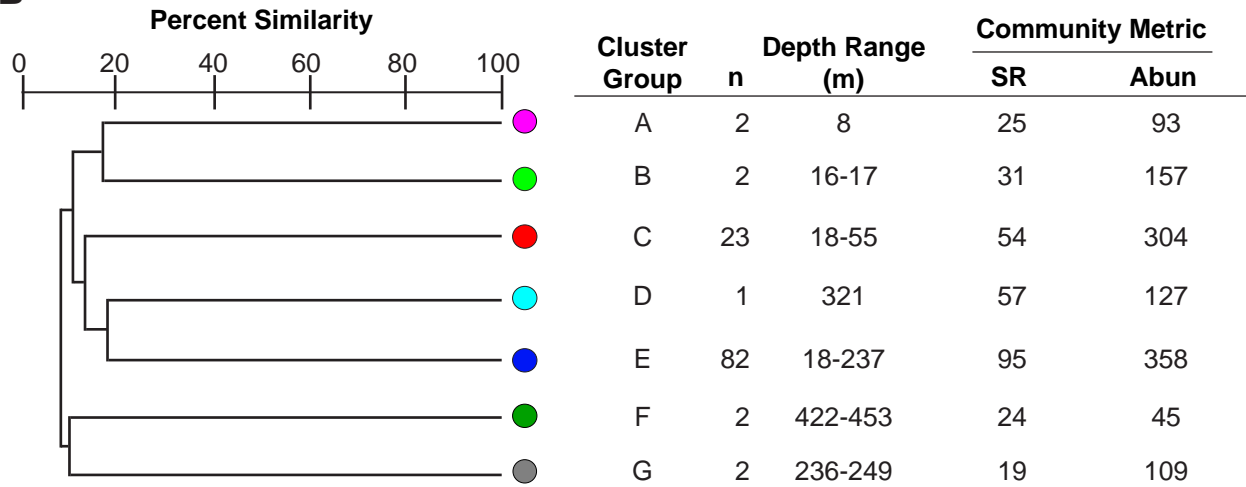


Figure 7.7

Results of ordination and cluster analysis of macrofauna data from San Diego regional and core benthic stations sampled during summer 2022 and 2023. Results are presented as (A) nMDS ordination and (B) a dendrogram of main cluster groups. Data are mean values over all stations in each group (n); SR = species richness; Abun = abundance.

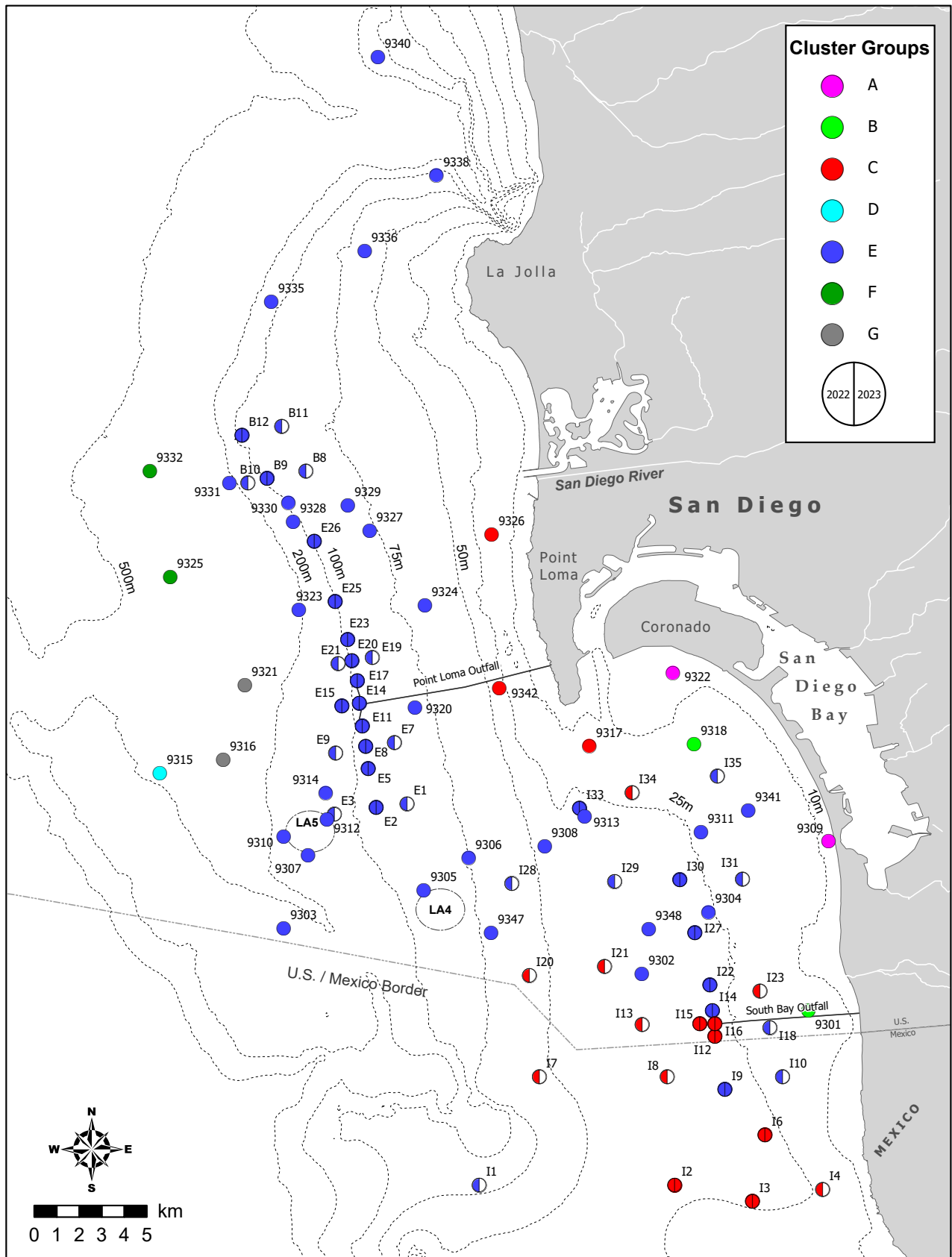


Figure 7.8

Spatial distribution of macrofaunal cluster groups A–G defined in Figure 7.7.

Table 7.3

Results for the benthic response index (BRI), sediment toxicity, and sediment quality objective (SQO) lines of evidence for San Diego regional benthic stations sampled during summer 2022 at which sediment toxicity testing was conducted. Cond=condition; TR=test result; TC=test control; %C=percent control; LRM=logistic regression model; CSI=chemical score index; Ref=reference; MD=minor deviation from reference conditions; NT=non-toxic; ME=minimal exposure; LE=low exposure; NA = not available (see text).

Survey	Station	Depth Fines		BRI		Sediment Toxicity				SQOs			Site
		(m)	(%)	Value	Cond	TR	TC	%C	Cond	LRM	CSI	Cond	Condition
2022	9301	16	34	21.1	Ref	95	98	97	NT	0.10	1.00	ME	Unimpacted
	9317	19	3	-0.5	Ref	96	98	98	NT	0.06	1.00	ME	Unimpacted
	9302	36	53	20.5	Ref	97	98	99	NT	0.18	1.23	ME	Unimpacted
	9327	78	71	7.3	Ref	96	98	98	NT	0.20	1.06	ME	Unimpacted
	9320	81	64	13.3	Ref	97	98	99	NT	0.21	1.00	ME	Unimpacted
	9305	87	67	10.0	Ref	98	98	100	NT	0.20	1.15	ME	Unimpacted
	9340	133	62	14.3	Ref	96	98	98	NT	0.15	1.00	ME	Unimpacted
	9312	137	61	10.1	Ref	99	98	101	NT	0.16	1.00	ME	Unimpacted

Chapter 8
Demersal Fishes
and Megabenthic Invertebrates

Chapter 8. Demersal Fishes and Megabenthic Invertebrates

INTRODUCTION

The City of San Diego (City) collects bottom dwelling (demersal) fishes, and relatively large (megabenthic) surface dwelling invertebrates, by otter trawl to examine the potential effects of wastewater discharge, or other natural and/or anthropogenic disturbances, on the marine environment around the Point Loma and South Bay Ocean Outfalls (PLOO and SBOO, respectively). These fish and invertebrate communities are targeted for monitoring as they are known to play critical ecological roles on the southern California coastal shelf (e.g., Allen et al. 2006, Thompson et al. 1993a,b). Trawled species typically live on or near the seafloor, and are therefore exposed to sediment conditions, which may be affected by both point and non-point sources such as discharges from ocean outfalls, runoff from watersheds, outflows from rivers and bays, or the disposal of dredged sediments (see Chapter 5: Sediment Quality). For these reasons, assessment of bottom dwelling fish and invertebrate communities has become an important focus of ocean monitoring programs throughout the world, but especially in the Southern California Bight (SCB) where they have been sampled extensively on the mainland shelf for the past four decades (e.g., Stein and Cadien 2009).

In healthy coastal marine ecosystems, demersal fish and megabenthic invertebrate communities vary widely and are influenced by many natural factors. For example, prey availability, seafloor topography, sediment composition, and changes in water temperatures associated with large scale oceanographic events, such as El Niño, may affect migration patterns or the recruitment of certain fish species (Cross et al. 1985, Helvey and Smith 1985, Karinen et al. 1985, Murawski 1993, Stein and Cadien 2009). Population fluctuations may also be due to the mobile nature of many species (e.g., fish schools, urchin aggregations). Therefore, an understanding of natural background conditions is essential to determine whether observed differences, or changes in community structure, may be related to anthropogenic activity. Pre-discharge and regional monitoring efforts by the City and others since 1991 provide baseline information on the variability of demersal fish and megabenthic invertebrate communities in the San Diego region critical for such comparative analyses (e.g., Allen et al. 1998, 2002, 2007, 2011, City of San Diego 1995, 1998, 2000, Walther et al. 2017).

The City relies on a suite of scientifically accepted indices and statistical analyses to evaluate changes in local fish and invertebrate communities. These include univariate measures of community structure, such as species richness, abundance, and diversity, while multivariate analyses are used to detect spatiotemporal differences among communities (e.g., Warwick 1993). The use of multiple types of analyses allows for more robust inference than relying on single parameters for determining anthropogenic environmental impacts. In addition, the examination of trawl-caught fishes for evidence of physical abnormalities or diseases is informative as they can be indicators of degraded habitats (e.g., Cross and Allen 1993, Stein and Cadien 2009). Collectively, these data are used to determine whether demersal fish and megabenthic invertebrate assemblages from habitats with comparable depth and sediment characteristics are similar, or if observable impacts from wastewater discharge or other sources have occurred.

This chapter presents analysis and interpretation of demersal fish and megabenthic invertebrate data collected at designated monitoring stations throughout the PLOO and SBOO regions during 2022 and 2023. Included are descriptions of the different fish and invertebrate communities present in these two regions during the reporting period, along with comparisons of spatial patterns and long-term changes over time. The four primary goals of this chapter are to: (1) characterize and document the demersal fish and megabenthic invertebrate assemblages present during the current reporting period; (2) determine the presence or absence of impacts on these assemblages that may be associated with wastewater discharge from the PLOO and SBOO; (3) identify other potential natural or anthropogenic sources of variability in the San Diego coastal marine ecosystem; (4) determine if the populations of selected species of fish and invertebrates are changing over time.

MATERIALS AND METHODS

Field Sampling

Trawls were conducted at 13 stations throughout the PLOO and SBOO regions to monitor demersal fishes and megabenthic invertebrates during the winters and summers of 2022 and 2023 (Figure 8.1). These included six PLOO stations located along the 100-m depth contour (discharge depth), ranging from 9 km south to 8 km north of the outfall, and seven SBOO stations located along the 28-m depth contour (discharge depth), ranging from 7 km south to 8.5 km north of the outfall. The two PLOO stations (SD10, SD12) and two SBOO stations (SD17, SD18) located within 1 km of the outfall structures are considered to represent nearfield conditions. Trawl sampling was not conducted in either region during the summer of 2023 due to a resource exchange granted by the San Diego Regional Water Quality Control Board (SDRWQCB) for participation in the region-wide Bight'23 sampling project.

A single trawl was performed at each station during each survey using a 7.6-m Marinovich otter trawl fitted with a 1.3-cm cod-end mesh net. Standard sampling procedures required towing the net for a total of at least 10 minutes bottom time per trawl, at a speed of around 2 knots, along a predetermined heading that follows the isobath at each station. A pressure-temperature sensor was attached to one of the trawl doors to measure water temperature, depth, and time of the individual trawls; these data were used to confirm acceptability of the trawl. The catch from each successful trawl was sorted, recorded, and immediately returned to the water to minimize mortality whenever possible. All individual fish and invertebrates captured were identified to species, or to the lowest taxon possible, based on accepted taxonomic protocols for the region (Eschmeyer and Herald 1998, Page et al. 2013, SCAMIT 2021, Miller 2020). If an animal could not be accurately identified to species in the field, it was returned to the laboratory for further identification where possible. The total number of individuals and total biomass (kg, wet weight) were recorded for each species of fish. Additionally, each fish was inspected for the presence of physical abnormalities (e.g., tumors, lesions, fin erosion, discoloration) or external parasites (e.g., copepods, cymothoid isopods, leeches). The length of each individual fish was measured to the nearest centimeter to determine size class; total length (TL) was measured for cartilaginous fishes while standard length (SL) was measured for bony fishes (SCCWRP 2018, 2023). For invertebrates, the total number of individuals was recorded for each species. In contrast to previous years, parasitic invertebrates no longer attached to their hosts, including the cymothoid isopod *Elthusa vulgaris* and leeches in the subclass Hirudinea, were recorded as present/absent rather than being counted individually, and are therefore no longer included in the analyses presented herein. This change aligns with Southern California Bight Regional Marine Monitoring Program methods (SCCWRP 2018, 2023). Visual observations of weather, sea conditions, and human and animal activity were also recorded at the time of sampling.

Data Analyses

Population characteristics of fish and invertebrate species among sites and between regions were summarized as percent abundance (PA; number of individuals per species/total abundance of all species), frequency of occurrence (FO; percentage of stations at which a species was collected), mean abundance per haul (MAH; number of individuals per species/total number of sites sampled), and mean abundance per occurrence (MAO; number of individuals per species/number of sites at which the species was collected). Additionally, the following community structure parameters were calculated per station for fishes and invertebrates separately: species richness (number of species), total abundance (number of individuals per species), and the Shannon Diversity Index (H'). For fishes, total biomass was also calculated per station. These analyses were performed using R (R Core Team 2021) and various functions within the reshape2, lubridate, tidyverse, glue, Rmisc, magrittr, vegan, RODBC, devtools, webshot, officer, flextable, ggpubr, and patchwork packages (Wickham 2007, Grolemund and Wickham 2011, Bolker et al. 2022, Hester and Bryan 2022, Hope 2022, Milton Bache and Wickham 2022, Oksanen et al. 2022, Ripley and Lapsley 2022, Wickham et al. 2022, Chang 2023, David Gohel 2023, Gohel and Skintzos 2023, Kassambara 2023, Lin Pedersen 2023).

To determine if the populations of fish and invertebrates are changing over time, multivariate analyses were performed in PRIMER v7 software using fish and invertebrate abundance data collected from 10-minute trawls conducted in the PLOO and SBOO regions from 1991 through 2023 (see Clarke 1993, Warwick 1993, Clarke et al. 2014). Prior to these analyses, all data were limited to summer surveys to reduce variability from natural seasonal variations. Additionally, data were transformed as appropriate to characterize the natural variability in species abundance more accurately. Additional multivariate analyses included Bray-Curtis measure of dissimilarity to serve as the basis for ordination (non-metric multidimensional scaling; nMDS) and hierarchical agglomerative clustering (cluster analysis) with group-average linking. Similarity profile analysis (SIMPROF) was used to confirm the non-random structure of the resultant cluster dendrogram (Clarke et al. 2008), with major ecologically-relevant clusters receiving SIMPROF support retained as cluster groups. A BEST test using the BVSTEP procedure was conducted to determine which subset of species best described patterns within the resulting cluster dendrograms. Similarity percentages analysis (SIMPER) was used to determine which species were responsible for > 70% of the contributions to within-group similarity (characteristic species) by cluster group to support cluster group selection.

Data collected during 2022 were reported previously (City of San Diego 2023), and all raw data for the 2022 and 2023 sampling period have been submitted to either the SDRWQCB or the California Environmental Data Exchange Network (CEDEN) and may be accessed upon request.

RESULTS AND DISCUSSION

Demersal Fish Populations in 2022 and 2023

A total of 15,961 fishes were captured from the 39 trawls conducted within the PLOO and SBOO monitoring regions during 2022 and 2023, representing at least 42 different species from 19 families in the PLOO, and 37 species from 23 families in SBOO (Appendices I.1, I.2). Pacific Sanddabs continued to dominate PLOO demersal fish assemblages over the past two years, occurring in every haul and

accounting for 54% of the fishes collected across trawls in that region (Table 8.1). Other species that were present in all PLOO assemblages during this period included Dover Sole, Halfbanded Rockfish and Longfin Sanddab, which accounted for 9%, 8%, and 7% of fishes collected, respectively. Other species of fish that were collected in at least 85% of the trawls, but in relatively low mean abundance (≤ 15 /haul), included English Sole, Yellowchin Sculpin, and Bigmouth Sole. Fish assemblages in the SBOO region were dominated by Speckled Sanddabs, which occurred in all trawls and accounted for 58% of the fishes collected, and by Longfin Sanddab, which occurred in 67% of the hauls and accounted for 12% of the fishes collected (Table 8.2). Though California Lizardfish occurred in 90% of trawls, they only accounted for 5% of the fishes collected. Other species that were collected in at least 50% of the trawls, but in relatively low numbers (≤ 8 /haul), included California Tonguefish, Hornyhead Turbot, Roughback Sculpin, and California Halibut. Rare species in both regions that are not included in Tables 8.1 and 8.2 can be found in Appendices I.1 and I.2.

More than 80% of the species collected in the PLOO and SBOO monitoring regions were < 30 cm in length. The only species collected from PLOO stations with individuals measuring ≥ 30 cm were California Skate, Longnose Skate, and California Halibut (Appendix I.1). Within the SBOO region, species with individuals measuring ≥ 30 cm included Shovelnose Guitarfish, California Skate, Longnose Skate, Round Stingray, Specklefin Midshipman, Bigmouth Sole, California Halibut, and English Sole (Appendix I.2).

The four most abundant fishes in the PLOO region showed some spatiotemporal variation in lengths (Appendix I.3). Pacific Sanddab, which are the most dominant species in PLOO, showed the greatest variation in lengths, ranging from 4–26 cm in length across the 5,253 individuals collected. Longfin Sanddab also showed considerable variation in lengths, ranging from 5–21 cm in length across the 683 individuals collected. On the contrary, Halfbanded Rockfish showed little variation in length across surveys, apart from at station SD7 in winter 2023 where individuals ranged from 7–15 cm in length. Like Pacific Sanddab, Dover Sole showed moderate variation in length across surveys, with larger individuals generally being collected during summer surveys. Overall, fish lengths varied across species and stations, with no notable patterns in relation to proximity to the PLOO discharge site.

Similarly, the four most abundant fishes in the SBOO region also exhibited spatiotemporal variation in lengths, though not to the same degree as in the PLOO region (Appendix I.4). Speckled Sanddab showed little variation in length, ranging from 3–14 cm across the 2,579 individuals collected. California Lizardfish, however, showed substantial variation in length across seasons, with the majority of the largest individuals (20–26 cm) being collected in summer of 2022. Though White Croaker were only collected in the winters of 2022 and 2023, 341 individuals were collected at sizes ranging from 10–19 cm, with no apparent pattern across stations. Longfin Sanddab, most of which were collected during summer of 2022, showed moderate variation in lengths, measuring between 4–17 cm. As in the PLOO region, overall, there were no notable patterns in lengths of fishes observed relative to their proximity to the SBOO discharge site.

Demersal Fish Community Structure Parameters

No prominent spatial patterns in the community parameters of demersal fishes were observed relative to the proximity of the PLOO or SBOO discharge sites during 2022 and 2023 (Table 8.3). Results were generally consistent with previous findings for the two regions, and elsewhere in the SCB (e.g., Allen et al. 1998, 2002, 2007, 2011, City of San Diego 1995, 1998, Walther et al. 2017, Wisenbaker

et al. 2021); mean species richness and diversity were consistently low ($SR \leq 17$ species, $H' \leq 1.6$, respectively); and fish abundance and biomass remained variable among both nearfield and farfield stations and between surveys over the past two years, with values ranging from 36–1,084 fishes/haul and 0.5–29.1 kg/haul, respectively.

Within the PLOO region, the largest 10% of hauls occurred at station SD10 in winter 2023 (Table 8.3). This haul included substantial numbers of Pacific Sanddab (436) and Pink Seaperch (230). The heaviest 10% of hauls occurred during winter 2023 at station SD10 (20.4 kg) largely due to the collection of 7.1 kg of Pacific Sanddab. The smallest 10% of hauls occurred in the winter 2022 at station SD10 (Table 8.3). This haul included relatively few Pacific Sanddabs ($n = 137$), Dover Sole ($n = 32$), and low numbers of all other species (≤ 26 individuals per species). The lightest 10% of trawls were collected from station SD13 in winter 2022 (6.8 kg), which comprised 4.2 kg of Pacific Sanddab and ≤ 0.7 kg of all other species.

Within the SBOO region, the largest haul occurred during summer 2022 at station SD16 (Table 8.3). The haul during these trawls comprised 414 Speckled Sanddab, and fewer than 50 individuals of all other species. The smallest haul occurred at winter 2022 at station SD15, co-occurring with some of the lowest species richness and biomass values recorded over the past two years (City of San Diego 2023). Biomass at SBOO trawl stations ranged from 0.6 kg during winter 2022 at station SD15 to 11.9 kg during winter 2023 at station SD18, and tended to reflect the total number of individuals collected (Table 8.3), with two exceptions; the trawls from station SD18 during winters of 2022 and 2023 weighed 11.1 and 11.9 kg and included 4.7 and 4.4 kg of White Croaker (141 and 90 individuals, respectively).

Historical comparisons indicate no noteworthy spatial patterns in demersal fishes community parameters relative to their proximity to the nearfield sites, but varying degrees of stability relative to the onset of wastewater discharge that began in in the PLOO and SBOO regions in 1994 and 1999, respectively (Figure 8.2). Since the initiation of discharge, mean species richness and diversity values for demersal fishes collected from PLOO and SBOO stations have remained low ($SR \leq 17$ species; $H' \leq 1.6$, respectively). However, there has been considerably greater variability in abundance, with post-discharge hauls generally having a greater abundances of fishes. The latter was largely due to population fluctuations of a few numerically dominant species in each region (Figures 8.3, 8.4). For example, differences in overall trawl catch abundances tend to track changes in Pacific Sanddab populations at the PLOO stations, and Speckled Sanddab populations at the SBOO stations, since these two species have been numerically dominant in these regions since monitoring began. In addition, occasional spikes in abundances within the PLOO region have been due to population fluctuations of other common species, such as Yellowchin Sculpin, Halfbanded Rockfish, Longspine Combfish, Dover Sole, Plainfin Midshipman, Stripetail Rockfish, California Lizardfish, Longfin Sanddab, and Pink Seaperch (Figure 8.3). In contrast, periodic spikes within the SBOO region have been due to population dynamics of California Lizardfish, Longfin Sanddab, White Croaker, Yellowchin Sculpin, Roughback Sculpin, Hornyhead Turbot, California Tonguefish, English Sole, and Northern Anchovy (Figure 8.4). Population dynamics of these species and communities over time do not appear to be associated with proximity to wastewater discharge from either outfall.

Physical Abnormalities and Parasitism in Demersal Fishes

Demersal fishes populations appeared healthy in the PLOO and SBOO regions in 2022 and 2023, with parasites and abnormalities reported for just 0.4% of fishes collected. Generally, eye parasites appear

to occur more frequently in the PLOO region, whereas gill and external parasites appear to occur more frequently in the SBOO region (Figure 8.5). As abnormalities or parasites were present across nearly all sites between regions, there does not appear to be a relationship between these anomalies and proximity to either outfall. There were no incidences of fin rot on any fishes sampled during the last two years, while other recorded abnormalities were limited to: (1) two instances of tumors: both found in winter 2023 on individuals of Dover Sole collected from stations SD12 and SD13; (2) a lesion, found in winter 2022 at station SD10 on a Dover Sole; (3) one leech, found in summer 2022 at station SD16 on a Hornyhead Turbot (Appendix I.5).

Incidences of parasites included: (1) the copepod eye parasite *Phrixecephalus cincinnatus*, which was present on 63 PLOO and 1 SBOO fishes including Pacific Sanddab, Longfin Sanddab, and Speckled Sanddab; (2) the cymothoid isopod *Elthusa vulgaris* (a gill parasite of fishes), which was present either externally or in the gills of 3 fishes including Speckled Sanddab and Hornyhead Turbot in the SBOO region (Appendix I.5). Several additional *E. vulgaris* specimens were noted as being present during each survey. Since *E. vulgaris* often become detached from their hosts during retrieval and sorting of the trawl catch, it is unknown which fishes were parasitized by these isopods. However, *E. vulgaris* is known to be especially common on Pacific and Speckled Sanddab, and California Lizardfish in southern California waters where it may reach infestation rates of 3% and 80%, respectively (see Brusca 1978, 1981).

Classification of Demersal Fishes Assemblages

PLOO Region

Cluster and ordination analyses of a total of 172 trawls resulted in seven ecologically-relevant SIMPROF-supported groups, or types of assemblages, in the PLOO region since the initiation monitoring in 1991 (cluster groups A–G; Figure 8.6, Appendix I.6). These assemblages represented from 1 to 138 hauls each and varied in both species richness and abundance per haul. A BEST/BVSTEP test implicated Bay Goby, California Lizardfish, Dover Sole, English Sole, Halfbanded Rockfish, Longfin Sanddab, Longspine Combfish, Pacific Sanddab, Pink Seaperch, Plainfin Midshipman, Shortspine Combfish, Slender Sole, Spotfin Sculpin, Stripetail Rockfish, and Yellowchin Sculpin as being influential to the overall pattern (gradient) of the cluster dendrogram ($\rho = 0.952$, $p \leq 0.001$, number of permutations = 999). Overall, the data show that when sites are compared over time, the outfall sites are not different from the farfield sites (Figure 8.6). Instead, assemblages appeared to be influenced by the distribution of the more abundant species or unique characteristics of specific station locations (e.g., habitat differences). For example, assemblages from stations SD7 and SD8 located south of the outfall often grouped apart from the remaining stations between 1992 and 2002, and station SD7 remained unique in 2007 and 2020 (see group G). The species composition and main descriptive characteristics of each of the cluster groups are included below.

Cluster group A represented a unique assemblage sampled at nearfield trawl station SD10 in 1997 (Figure 8.6, Appendix I.6). The assemblage represented by cluster group A was characterized by the lowest species richness (SR = 7) and total abundance (44/haul), and lowest mean abundance of Pacific Sanddabs of any cluster group (23/haul). Halfbanded Rockfish (16/haul), Longfin Sanddab, Gulf Sanddab, and Greenspotted Rockfish (1/haul each) also contributed to the dissimilarity between this and other cluster groups (Appendix I.6).

Cluster group B represented a unique assemblage sampled at nearfield trawl station SD12 in 1998 (Figure 8.6). The assemblage represented by cluster group B was characterized by 261 individuals comprising 16 species, and 75 Pacific Sanddabs per haul. Plainfin Midshipman (116/haul), Dover Sole (36/haul), Longspine Combfish (7/haul), and Gulf Sanddab (5/haul) also contributed to the dissimilarity between this and other cluster groups (Appendix I.6).

Cluster group C represented a unique assemblage sampled at nearfield trawl station SD12 in 1997 (Figure 8.6). The assemblage represented by cluster group C was characterized by 231 individuals comprising 19 species, and 110 Pacific Sanddabs per haul. Halfbanded Rockfish (60/haul), Squarespot Rockfish (23/haul), Greenblotched Rockfish (8/haul), and Vermillion Rockfish (6/haul) also contributed to the dissimilarity between this and other cluster groups (Appendix I.6).

Cluster group D represented nine assemblages sampled across stations in 2009, 2011, and 2014 (Figure 8.6). These assemblages included moderately sized hauls, averaging 13 species and 270 individuals per haul, and had the second highest mean Pacific Sanddab abundance ($\bar{x} = 89/\text{haul}$). Along with Pacific Sanddab, California Lizardfish ($\bar{x} = 126/\text{haul}$), Dover Sole ($\bar{x} = 8/\text{haul}$), and Longspine Combfish ($\bar{x} = 8/\text{haul}$) were the other most characteristic species of these assemblages (Appendix I.6).

Cluster group E was the largest group, representing assemblages from a total of 138 hauls that were conducted across the entire monitoring period (Figure 8.6). Approximately 60% ($n = 29$) of the trawls conducted from 1991 through 1998 were in this cluster group, including mostly nearfield and north farfield station assemblages. Beginning in 1999, this was the dominant cluster group across all stations, apart from three assemblages in cluster group D at stations SD8, SD10, and SD13 in 2009, and all stations apart from SD10 in 2014. Assemblages in cluster group E averaged 15 species of fish, 366 individuals per haul, and 220 Pacific Sanddab per haul—the highest average abundance among cluster groups (Figure 8.6, Appendix I.6). Along with Pacific Sanddabs, Halfbanded Rockfish ($\bar{x} = 26/\text{haul}$), Dover Sole ($\bar{x} = 28/\text{haul}$), Longspine Combfish ($\bar{x} = 18/\text{haul}$), and Shortspine Combfish ($\bar{x} = 7/\text{haul}$) were the other most characteristic species of these assemblages (Appendix I.6).

Cluster group F represented two unique assemblages sampled at south farfield station SD8 in 1994 and north farfield station SD14 in 1998 (Figure 8.6). These assemblages included the second smallest hauls, averaging just 10 species and 74 individuals per haul, and had the second lowest average Pacific Sanddab abundance ($\bar{x} = 48/\text{haul}$). Along with Pacific Sanddabs, Dover Sole ($\bar{x} = 6/\text{haul}$), Greenblotched Rockfish ($\bar{x} = 2/\text{haul}$), and Greenstriped Rockfish ($\bar{x} = 1/\text{haul}$) were the other most characteristic species of these assemblages (Appendix I.6).

Cluster group G was the second largest cluster group, representing assemblages from a total of 20 hauls that included 33% ($n = 14$) of the trawls conducted from 1992 through 1998 (Figure 8.6). Trawls at station SD7 in 2001, 2002, 2007, and 2020 were also included in this cluster group. These assemblages averaged 14 species and 116 individuals per haul. The most characteristic species of cluster group G were Pacific Sanddab ($\bar{x} = 71/\text{haul}$), Dover Sole ($\bar{x} = 9/\text{haul}$), Longfin Sanddab ($\bar{x} = 6/\text{haul}$), and California Tonguefish ($\bar{x} = 3/\text{haul}$) (Appendix I.6).

SBOO Region

Cluster and ordination analyses of a total of 187 trawls resulted in six ecologically-relevant SIMPROF-supported groups, or types of assemblages in the South Bay outfall region since the initiation

monitoring in 1995 (cluster groups A–F; Figure 8.7, Appendix I.7). These assemblages represented from 1 to 77 hauls each and represented a wide range of mean species richness (5–11 species/haul) and mean abundances (19–470/haul). A BEST/BVSTEP test implicated California Lizardfish, California Tonguefish, English Sole, Hornyhead Turbot, Longfin Sanddab, Roughback Sculpin, Speckled Sanddab, White Croaker, and Yellowchin Sculpin as being influential to the overall pattern (gradient) of the cluster dendrogram ($\rho = 0.957$, $p \leq 0.001$, number of permutations = 999). Overall, there were no discernable patterns associated with proximity to the SBOO discharge site. Instead, as observed in the PLOO region, SBOO fishes assemblages appear to be influenced by the distribution of the more abundant species or the unique characteristics of a specific station location. For example, cluster group F was distinguished by comparatively low abundances of Speckled Sanddab that generally coincided with or followed warm water El Niño events in 1994–1995, 1997–1998 and 2014–2016 (NOAA/NWS 2022). Additionally, station SD15, located farthest south of the SBOO in northern Baja California waters, often grouped apart from the remaining stations (see cluster group B), possibly due to habitat differences such as sandier sediments (see Chapter 5: Sediment Quality). The species composition and main descriptive characteristics of each of the six cluster groups are included below.

Cluster group A represented a unique assemblage sampled at nearfield trawl station SD17 in 2020 (Figure 8.7). The assemblage represented by cluster group A was characterized by 19 individuals comprising 5 species, and 7 Speckled Sanddabs per haul. Longfin Sanddab (5/haul), Pacific Sanddab (4/haul), California Tonguefish (2/haul), and California Lizardfish (1/haul) also contributed to the dissimilarity between this and other cluster groups (Appendix I.6).

Cluster group B comprised 53 hauls, including 36% ($n = 19$) of the trawls from south farfield station SD15 and 17% ($n = 9$) of the trawls from south farfield station SD16 over the past 29 years (Figure 8.7). This cluster group also included 48% ($n = 24$) of the trawls conducted at stations SD17–SD20 from 1997 through 2004. The remaining hauls from group B occurred at south farfield station SD16 in 2011 and 2015, at station SD20 in 2020. This type of assemblage never occurred at station SD21. The assemblages represented by cluster group B averaged 6 species and 88 fishes per haul. These assemblages averaged 74 Speckled Sanddab per haul and were also characterized by Hornyhead Turbot ($\bar{x} = 3$ /haul) (Appendix I.7).

Cluster group C represented assemblages from 9 trawls that included trawls conducted across stations from 2003 through 2011, and stations SD15–SD19 in 2022 (Figure 8.7). This cluster group averaged 10 species and 329 fishes per haul, the second highest mean abundance across all cluster groups. The most characteristic species for this group were Speckled Sanddab ($\bar{x} = 260$ /haul)—the highest average abundance among cluster groups—and Pacific Sanddab ($\bar{x} = 17$ /haul) (Appendix I.7).

Cluster group D was the second largest cluster group, comprising 30 trawls conducted across stations between 2006 through 2021 (Figure 8.7). Assemblages represented by cluster group D had the highest mean richness and abundance (SR = 11, $\bar{x} = 470$ /haul), and averaged 225 Speckled Sanddab per haul (Figure 8.7, Appendix I.7). In addition to Speckled Sanddab, California Lizardfish ($\bar{x} = 188$ /haul) characterized assemblages in this cluster group (Appendix I.7).

Cluster group E was the largest cluster group comprising 77 hauls spanning the entire monitoring period. This cluster group represented 10% ($n = 6$) of the hauls at nearfield and north farfield stations from 1995 through 2002, and 54% ($n = 71$) of all hauls conducted from 2003 through 2021 (Figure 8.7). Assemblages represented by cluster group E averaged 10 species and 247 individuals per haul. This

cluster group had the third highest mean abundance of Speckled Sanddab ($\bar{x} = 130/\text{haul}$) (Appendix I.7). In addition to Speckled Sanddab, the most characteristic species for this group were California Lizardfish ($\bar{x} = 36/\text{haul}$), Longfin Sanddab ($\bar{x} = 32/\text{haul}$), and Yellowchin Sculpin ($\bar{x} = 22/\text{haul}$) (Appendix I.7).

Cluster group F comprised 17 hauls, including 46% ($n = 13$) of trawls between 1995 through 1998, and assemblages at north farfield station SD21 in 2011, north farfield stations SD19 and SD20 in 2015, and south farfield station SD16 in 2019 (Figure 8.7). During summer 1996, all but two stations (SD15 and SD20) belonged to this cluster group, and their similar community compositions may be related to the warm water El Niño events in 1994–1995 (NOAA/NWS 2018). Likewise, the similarity of almost all station assemblages in 1998 into cluster group F could be related to the El Niño events in 1997–1998 (NOAA/NWS 2022). Assemblages in this cluster group averaged 11 species and 93 individuals per haul and had the lowest mean abundance of Speckled Sanddab ($\bar{x} = 32/\text{haul}$). Low numbers of California Lizardfish ($\bar{x} = 19/\text{haul}$), Longfin Sanddab ($\bar{x} = 13/\text{haul}$), and Hornyhead Turbot ($\bar{x} = 4/\text{haul}$) were also characteristic of these trawls (Appendix I.7).

Megabenthic Invertebrate Populations in 2022 and 2023

A total of 17,779 invertebrates were captured from the 39 trawls conducted within the PLOO and SBOO monitoring regions in 2022 and 2023, representing 77 taxa from five phyla (Arthropoda, Echinodermata, Mollusca, Cnidaria, Silicea) (Appendices I.8, I.9). The sea urchins *Lytechinus pictus* and *Strongylocentrotus fragilis* dominated PLOO trawls-caught invertebrates and accounted for 71% and 26%, respectively, of total abundance across trawls in that region (Table 8.4). Other species that were collected in at least 50% of the trawls, but in low numbers ($\leq 8/\text{haul}$), included the shrimp *Sicyonia ingentis*, the sea stars *Luidia asthenosoma*, *Luidia foliolata* and *Astropecten californicus*, and the cephalopod *Octopus rubescens* (Table 8.4). In contrast to the PLOO region, no single species dominated SBOO trawls over the past two years. Rather, five species occurred in more than 50% of the hauls and accounted for 2% to 30% of the total catch, including the shrimps *Crangon nigromaculata* and *Sicyonia penicillata*, the sea stars *A. californicus* and *Luidia armata*, and the snail *Philine auriformis* (Table 8.5). Rare species in both regions that are not included in Tables 8.4 and 8.5 can be found in Appendices I.8 and I.9.

Megabenthic Invertebrate Community Structure Parameters

No notable spatial patterns in megabenthic invertebrate community parameters were observed relative to the proximity of the PLOO or SBOO discharge sites during 2022 and 2023. Results were generally consistent with previous findings for the two regions and elsewhere in the SCB (e.g., Allen et al. 1998, 2002, 2007, 2011, City of San Diego 1995, 1998, Walther et al. 2017, Wisenbaker et al. 2021). For example, species richness and diversity were consistently low ($SR \leq 16$ species, $H' \leq 2.2$, respectively), whereas abundance remained highly variable among both nearfield and farfield stations and between surveys over the past two years, with values ranging from 5 to 4,196 individuals per haul (Table 8.6).

Within the PLOO region, species richness and diversity varied both over time and across nearfield and farfield stations. Much of this variation may be correlated with the population dynamics of the urchins *Lytechinus pictus* and *Strongylocentrotus fragilis*. When abundance of one or a combination of these species significantly increases, diversity tends to decline. For instance, some of the lowest diversity in the region ($H' \leq 0.02\text{--}0.1$) was observed at station SD8 between 2022 and 2023 (Table 8.6). *L. pictus*

was collected in large abundances at station SD8 in 2022, including 2,280 individuals in the winter and 2,600 individuals in the summer. In the winter of 2023, *S. fragilis* replaced *L. pictus* and had the highest recorded abundance (4,186/haul) collected in a single haul at station SD8. The highest diversity was recorded at station SD13 in winter 2023 ($H' = 2.1$) and no dominant species were observed in this trawl. Species richness does not seem to follow the same trend as diversity, as the second highest species richness values were recorded at south farfield stations SD7 and SD8 ($SR = 13$) in the summer of 2022 when relatively high number of *L. pictus* at both stations (335/haul, 2,600/haul, respectively) were recorded (Table 8.6).

Within the SBOO region, overall species richness and diversity were higher than seen in the PLOO region, due to a lack of one or two species dominating the community. For instance, the three most abundant species in the SBOO region, the sea star *Astropecten californicus*, the shrimp *Crangon nigromaculata*, and the snail *Philine auriformis* only accounted for 66% of the total abundance (Table 8.5). The highest diversity ($H' = 2.2$) was recorded at both station SD17 in the winter of 2022 and at station SD16 in the summer of 2022 (Table 8.6). Station SD18 had the highest species richness ($SR = 16$) in the summer of 2022, and had a lower total abundance (48/haul) relative to other stations. Conversely, the lowest species richness ($SR = 5$) and diversity ($H' = 0.9$) were seen at stations SD20 and SD21 in the winter of 2022, corresponding with trawl assemblages dominated by *A. californicus* (71/haul, 3/haul, respectively) and the shrimp *Sicyonia penicillata* (43/haul, 17/haul, respectively).

Historical comparisons indicate no notable spatial patterns in megabenthic invertebrate community parameters relative to the proximity of the PLOO or SBOO discharge sites, or to the onset of wastewater discharge that began in 1994 or 1999, respectively (Figure 8.8). Since the initiation of discharge, mean species richness and diversity for megabenthic invertebrates collected from the PLOO and SBOO regions have remained low ($SR \leq 12$ species; $H' \leq 1.3$, respectively). However, there has been considerably greater variability in total abundance (1–46,255/haul). The latter was largely due to population fluctuations of a few numerically dominant species in each region, rather than station proximity to either outfall (Figures 8.9, 8.10). For example, differences in overall megabenthic invertebrate abundances at the PLOO stations tended to track population changes of the pelagic red crab *Pleuroncodes planipes*, the sea urchins *L. pictus* and *S. fragilis*, the brittle star *Ophiura luetkenii*, the sea stars *Luidia foliolata* and *A. californicus*, the sea pen *Acanthoptilum* sp, the sea cucumber *Apostichopus californicus*, the shrimp *Sicyonia ingentis* and the crab *Platymera gaudichaudii* (Figure 8.9). Large hauls of *P. planipes* from PLOO trawl stations SD12 and SD13 in 2018 and 2020 were followed by decreased species richness and diversity ($SR = 4-7$, $H' = 0.03-0.8$), but species richness has slowly recovered to pre-2016 levels following their population decline in 2021 (City of San Diego 2019, 2020, 2021). Since 2021, *P. planipes* has been succeeded by *L. pictus*, and though species richness has improved at stations SD12 and SD13 ($SR = 3-11$), diversity has only shown marked improvement at station SD12 ($H' = 0.9-2.1$) (Table 8.6). Similarly, *S. fragilis* were typically caught in large numbers at north farfield stations SD13 and SD14 before *P. planipes* became the dominant species at these stations between 2016 and 2020. *S. fragilis* likely migrated to the southern PLOO region and established its population after *P. planipes* replaced them in the north farfield area (Figure 8.9).

Differences in overall abundances at SBOO stations also tended to track population changes of *P. planipes* and *L. pictus* but these two species were not as dominant as in the PLOO region. Other species with strong influence in the SBOO region were the sea star *A. californicus*, the shrimps *C. nigromaculata* and *S. penicillata*, crab *Latulambrus occidentalis*, the snail *P. auriformis*, the sand dollar *Dendraster terminalis*, the brittle star *Ophiothrix spiculata*, the swimming crab *Portunus xantusii*,

and the rock crab *Metacarcinus gracilis* (Figure 8.10). An ecologically interesting note is the recently consistent presence of *S. penicillata* in the SBOO region. *S. penicillata* has a documented range of Puntarenas, Costa Rica in the south to Punta Canoas, Mexico in the north, with noted incursions into the SCB only during El Niño events (Jensen 2014). However, since the 2014–2016 El Niño, *S. penicillata* appears to have established a resident population and has been seen with increased frequency and abundance in SBOO trawls (Figure 8.10). None of the observed trends in either region appear to be associated with proximity to wastewater discharge from either outfall.

Classification Analysis of Invertebrate Assemblages

PLOO Region

Cluster and ordination analyses of a total of 172 trawls resulted in seven ecologically-relevant SIMPROF-supported groups or types of megabenthic invertebrate assemblages in the PLOO region since the initiation monitoring in 1991 (cluster groups A–G). These assemblages represented from 1 to 97 hauls each, and varied in terms of species present, as well as the relative abundances per haul. A BEST/BVSTEP test implicated the sea pen *Acanthoptilum* sp, the sea urchins *Lytechinus pictus* and *Strongylocentrotus fragilis*, and the pelagic red crab *Pleuroncodes planipes*, as being influential to the overall pattern (gradient) of the cluster dendrogram ($\rho = 0.966$ $p \leq 0.001$, number of permutations = 999). Overall, there were no discernible patterns associated with proximity to the PLOO discharge site. Instead, assemblages appear influenced by the distribution of more abundant species or the unique characteristics of specific station locations. For example, stations SD13 and SD14 located north of the PLOO often grouped apart from the remaining stations (cluster group G) (Figure 8.11). The species composition and main descriptive characteristics of each of the six cluster groups are included below.

Cluster group A occurred between 2017 and 2021 and consisted of assemblages from five trawls (Figure 8.11). These assemblages had the lowest average species richness (SR = 5) and second lowest average abundance ($\bar{x} = 114$ /haul), and were primarily characterized by the shrimp *Sicyonia ingentis* ($\bar{x} = 53$ /haul) and the sea urchin, *Strongylocentrotus fragilis* ($\bar{x} = 51$ /haul) (Appendix I.10).

Cluster group B consisted of assemblages from seven trawls and was primarily dominated by *P. planipes* ($\bar{x} = 7,514$ /haul) (Figure 8.11). Assemblages in this cluster group were sampled between 2016 and 2020 during the period when *P. planipes* migrated to the PLOO region and its abundance peaked. These assemblages had the lowest average species richness of 5 species per haul and the highest average abundance of 7,791 individuals per haul (Appendix I.10).

Cluster group C was the second smallest group and included two trawls from stations SD7 in 2020 and SD13 in 2021. This cluster group had the lowest mean abundance ($\bar{x} = 21$ /haul) and was primarily characterized by *L. pictus* ($\bar{x} = 12$ /haul) (Figure 8.11, Appendix I.10). Species richness was also low (SR = 6) and two other characteristic species, *Sicyonia ingentis* and *Luidia foliolata* had average abundances of <1/haul and 3/haul, respectively.

Cluster group D comprised four trawl assemblages and had average abundance of 171 individuals per haul and the second highest mean species richness (SR = 13) (Figure 8.11). This cluster group was primarily characterized by the relatively high abundance of the sea pen *Acanthoptilum* sp ($\bar{x} = 121$ /haul) (Appendix I.10). Other characteristic species included *Ophiura luetkenii* ($\bar{x} = 2$ /haul) and *S. ingentis* ($\bar{x} = 6$ /haul).

Cluster group E comprised one trawl at the north farfield station SD14 in 2012. It had the second highest abundance (3,204/haul) and was heavily influenced by a large haul of the brittle star *O. luetkenii* (2,640/haul) (Figure 8.11, Appendix I.10). Other species characteristic of this assemblage included *L. pictus* (102/haul), *S. fragilis* (442/haul), *L. foliolata* (11/haul), and *Astropecten ornatissimus* (5/haul).

Cluster group F was the largest group, representing assemblages from a total of 97 trawls. The majority of these hauls occurred at the south farfield stations SD7 and SD8, and nearfield station SD10 (Figure 8.11). These assemblages had the highest average species richness (SR = 14) and the second highest mean abundance (\bar{x} = 2286/haul). This cluster group was characterized by the highest average number of *L. pictus* (\bar{x} = 2,151/haul), and assemblages included abundances from 197 to 8,000 individuals, which appear to differentiate these assemblages from those in cluster group G (Appendix I.10).

Cluster group G was the second largest group, representing assemblages from a total of 56 hauls. Most of these hauls occurred at the north farfield stations SD13 and SD14. Assemblages in this cluster group averaged 11 species per haul and 423 individuals per haul (Figure 8.11). The two most characteristic species of group G were *L. pictus* (\bar{x} = 228/haul) and *S. fragilis* (\bar{x} = 120/haul) (Appendix I.10). The shared higher abundance of these two species in these assemblages likely contributes to the similarity of assemblages within the cluster group, and demonstrates that communities with higher abundances of *L. pictus* ($n \leq 840$ /haul) or *S. fragilis* ($n \leq 472$ /haul) respond similarly.

SBOO Region

Cluster and ordination analyses of a total of 187 trawls resulted in five ecologically-relevant SIMPROF-supported groups or types of megabenthic invertebrate assemblages in the SBOO region since the initiation monitoring in 1995 (cluster groups A–E; Figure 8.12, Appendix I.11). These assemblages represented from 1 to 164 hauls each, and varied in terms of species present, as well as the relative abundances of individual species. A BEST/BVSTEP test implicated the sea stars *Astropecten californicus*, *Pisaster brevispinus*, and *Luidia armata*, the shrimps *Crangon nigromaculata* and *Sicyonia penicillata*, the sand dollar *Dendraster terminalis*, the snails *Kelletia kelletii*, *Crossata ventricosa*, and *Philine auriformis*, the dorid *Acanthodoris brunnea*, the cephalopod *Octopus rubescens*, the crabs *Latulambrus occidentalis*, *Metacarcinus gracilis*, *Pyromaia tuberculata*, and *Platymera gaudichaudii*, the urchin *Lytechinus pictus*, and the brittle star *Ophiothrix spiculata*, as being influential to the overall pattern (gradient) of the cluster dendrogram ($\rho = 0.952$, $p \leq 0.001$, number of permutations = 999). Overall, there were no discernible patterns associated with proximity to the SBOO discharge site (Figure 8.12). Instead, assemblages appear influenced by the distribution of the more abundant species during specific time periods (groups B and E) versus background conditions (group D). The species composition and main descriptive characteristics of each of the four cluster groups are included below.

Cluster group A was one of the smallest clusters, containing a single haul from station SD15 in 2009 (Figure 8.12). The brittle star *Ophiura luetkenii* was the dominant species (72/haul) and other species characteristic of this assemblage include *O. spiculata* (3/haul), *D. terminalis* (3/haul), *Crangon alba* (2/haul), and *P. tuberculata* (1 individual) (Appendix I.11).

Cluster group B represented assemblages from a total of 14 hauls collected in 2009, 2016, 2017, and 2019. In 2016, the cluster was found at all SBOO stations. Average species richness of hauls in this cluster was 7 species and the average abundance was 31 individuals per haul (Figure

8.12). *A. californicus* (\bar{x} = 2/haul), *S. penicillata* (\bar{x} = 8/haul), and *O. rubescens* (\bar{x} = 2/haul) were representative species of this group (Appendix I.11).

Cluster group C comprised a unique assemblage collected at nearfield station SD17 in 1995 (Figure 8.12). This cluster was represented by heavily dominant *L. pictus* (951/haul), which was the highest recorded abundance of *L. pictus* in the SBOO region. *A. californicus* (6/haul), *O. spiculata* (4/haul), *P. tuberculata* (4/haul), and *P. brevispinus* (2/haul) also characterized this cluster group (Appendix I.11). This unique cluster had the highest species richness (SR = 12) and abundance (975/haul).

Cluster group D was the largest cluster group, comprising 164 hauls found across all stations between 1995 and 2022, likely reflecting background conditions within the region (Figure 8.12). Assemblages represented by cluster group D averaged 8 species per haul and 60 individuals per haul, but over time there was variability in both parameters with species richness ranging from 1–25 species per haul and abundance ranging from 4 to 581 individuals per haul. This cluster group was primarily characterized by *A. californicus* (\bar{x} = 30/haul) and *P. brevispinus* (\bar{x} = 1/haul) (Appendix I.11).

Cluster group E represented assemblages from a total of seven hauls collected in 2000, 2017, and 2019 across all stations apart from north farfield station SD19 (Figure 8.12). Average species richness of hauls in this cluster was 6 species per haul and average abundance was 10 individuals per haul (Figure 8.12). The most characteristic species for cluster group E assemblages were *L. pictus* (\bar{x} = 2/haul), *C. ventricosa* (\bar{x} = 1/haul), *C. nigromaculata* (\bar{x} = <1/haul) (Appendix I.11).

SUMMARY

Demersal fishes and megabenthic invertebrate populations monitored in 2022 and 2023 do not show evidence of negative impacts associated with proximity to wastewater discharge from the PLOO and SBOO. Community parameters are similar at stations located both near and far from the outfall discharge sites in both regions. Major community metrics, such as species richness, abundance, and diversity were generally within historical ranges reported for the San Diego region (City of San Diego 1995, 1998, 2000, 2022), and were representative of those characteristic of similar habitats throughout the SCB (e.g., Allen et al. 1998, 2002, 2007, 2011, Walther et al. 2017).

Over the past two years, Pacific Sanddab dominated assemblages surrounding the PLOO, and Speckled Sanddab dominated assemblages surrounding the SBOO, as they have done so since monitoring began in each region. Halfbanded Rockfish were also prevalent in PLOO assemblages during 2022 and 2023, while California Lizardfish were also prevalent within the SBOO region during this period, as they have also done so in eleven of the past thirteen years. Other commonly captured, but less abundant fishes, collected from the PLOO and SBOO regions included California Tonguefish, Dover Sole, English Sole, Longfin Sanddab, Northern Anchovy, Longspine Combfish, Shortspine Combfish, and White Croaker.

Of the 17,779 megabenthic invertebrates encountered during 2022 and 2023, 88% were the sea urchins *Lytechinus pictus* (64%) and *Strongylocentrotus fragilis* (24%), collected mostly at PLOO trawl stations. *Lytechinus pictus* started to become the dominant species at PLOO stations after the population of pelagic red crab *Pleuroncodes planipes* crashed in 2021 and its abundance continued to increase in 2022 and 2023. Species richness, diversity, and cluster analysis all indicate that the PLOO region is returning to background conditions typically observed prior to the most recent *P. planipes* migration.

In contrast to the PLOO region, no single species of invertebrate dominated SBOO trawls over the past two years. Other commonly captured, but less abundant, trawl-caught invertebrates collected from the PLOO and SBOO regions included the shrimps *Sicyonia ingentis*, *Sicyonia penicillata*, and *Crangon nigromaculata*, and the sea star *Astropecten californicus*. However, consistent occurrences of historically more southerly located species, such as *Octopus veligero* and *S. penicillata*, are potential indicators of large-scale climate driven effects of species distribution and occurrence, which will likely only increase in the future (Lilly 2004).

The abundance and distribution of species varied similarly at stations located near and far from the outfalls in both regions. The high degree of variability in these assemblages during this reporting period was similar to that observed in previous years, including before wastewater discharge began through either outfall (City of San Diego 1995, 1998, 2000, 2022). Furthermore, this sort of variability has been observed in similar habitats elsewhere off the coast of southern California (Allen et al. 1998, 2002, 2007, 2011, Walther et al. 2017). Consequently, changes in local community structure of these fishes and invertebrates are more likely due to natural factors, such as changes in ocean temperatures associated with El Niño or other large-scale oceanographic events. Finally, the rarity of disease indicators, or other physical abnormalities, in local fishes suggests that populations in the Point Loma and South Bay outfall regions continue to be unimpacted by wastewater discharge.

LITERATURE CITED

- Allen, L.G., D.J. Pondella II, and M.H. Horn. (2006). *The Ecology of Marine Fishes: California and Adjacent Waters*. University of California Press, Berkeley, CA.
- Allen, M.J., S.L. Moore, K.C. Schiff, D. Diener, S.B. Weisburg, J.K. Stull, A. Groce, E. Zeng, J. Mubarak, C.L. Tang, R. Gartman, and C.I. Haydock. (1998). *Assessment of demersal fish and megabenthic invertebrate assemblages on the mainland shelf of Southern California in 1994*. Southern California Coastal Water Research Project, Westminster, CA.
- Allen, M.J., A.K. Groce, D. Diener, J. Brown, S.A. Steinert, G. Deets, J.A. Noblet, S.L. Moore, D. Diehl, E.T. Jarvis, V. Raco-Rands, C. Thomas, Y. Ralph, R. Gartman, D. Cadien, S.B. Weisberg, and T. Mikel. (2002). *Southern California Bight 1998 Regional Monitoring Program: V. Demersal Fishes and Megabenthic Invertebrates*. Southern California Coastal Water Research Project, Westminster, CA.
- Allen, M.J., T. Mikel, D.B. Cadien, J.E. Kalman, E.T. Jarvis, K.C. Schiff, D.W. Diehl, S.L. Moore, S. Walther, G. Deets, C. Cash, S. Watts, D.J. Pondella II, V. Raco-Rands, C. Thomas, R. Gartman, L. Sabin, W. Power, A.K. Groce, and J.L. Armstrong. (2007). *Southern California Bight 2003 Regional Monitoring Program: IV. Demersal Fishes and Megabenthic Invertebrates*. Southern California Coastal Water Research Project. Costa Mesa, CA.
- Allen, M.J., D.B. Cadien, E. Miller, D.W. Diehl, K. Ritter, S.L. Moore, C. Cash, D.J. Pondella, V. Raco-Rands, C. Thomas, R. Gartman, W. Power, A.K. Latker, J. Williams, J.L. Armstrong, and K. Schiff. (2011). *Southern California Bight 2008 Regional Monitoring Program: Volume IV. Demersal Fishes and Megabenthic Invertebrates*. Southern California Coastal Water Research Project, Costa Mesa, CA.

- Bolker, B., G.R. Warnes and T. Lumley (2022). *gtools: Various R Programming Tools*. R package version 3.9.4. <https://CRAN.R-project.org/package=gtools>
- Brusca, R.C. (1978). Studies on the cymothoid fish symbionts of the eastern Pacific (Crustacea: Cymothoidae). II. Systematics and biology of *Livoneca vulgaris* Stimpson 1857. *Occasional Papers of the Allan Hancock Foundation. (New Series)*, 2: 1–19.
- Brusca, R.C. (1981). A monograph on the Isopoda Cymothoidae (Crustacea) of the eastern Pacific. *Zoological Journal of the Linnean Society*, 73: 117–199.
- Chang, W. (2023). *webshot: Take Screenshots of Web Pages*. R package version 0.5.5. <https://CRAN.R-project.org/package=webshot>
- City of San Diego. (1995). *Outfall Extension Pre-Construction Monitoring Report (July 1991–October 1992)*. City of San Diego Ocean Monitoring Program, Metropolitan Wastewater Department, Environmental Monitoring and Technical Services Division, San Diego, CA.
- City of San Diego. (1998). *San Diego Regional Monitoring Report for 1994–1997*. City of San Diego Ocean Monitoring Program, Metropolitan Wastewater Department, Environmental Monitoring and Technical Services Division, San Diego, CA.
- City of San Diego. (2000). *International Wastewater Treatment Plant Final Baseline Ocean Monitoring Report for the South Bay Ocean Outfall (1995–1998)*. City of San Diego Ocean Monitoring Program, Metropolitan Wastewater Department, Environmental Monitoring and Technical Services Division, San Diego, CA.
- City of San Diego. (2019). *Interim Receiving Waters Monitoring Report for the Point Loma Ocean Outfall and South Bay Ocean Outfalls, 2018*. City of San Diego Ocean Monitoring Program, Public Utilities Department, Environmental Monitoring and Technical Services Division, San Diego, CA.
- City of San Diego. (2020). *Biennial Receiving Waters Monitoring and Assessment Report for the Point Loma and South Bay Ocean Outfalls, 2018–2019*. City of San Diego Ocean Monitoring Program, Public Utilities Department, Environmental Monitoring and Technical Services Division, San Diego, CA.
- City of San Diego. (2021). *Interim Receiving Waters Monitoring Report for the Point Loma Ocean Outfall and South Bay Ocean Outfalls, 2020*. City of San Diego Ocean Monitoring Program, Public Utilities Department, Environmental Monitoring and Technical Services Division, San Diego, CA.
- City of San Diego. (2022). *Appendix C.1 Benthic Sediments, Invertebrates, and Fishes*. In: *Application for Renewal of NPDES CA0107409 and 301(h) Modified Secondary Treatment Requirements Point Loma Ocean Outfall. Volume V, Appendix C*. Public Utilities Department, Environmental Monitoring and Technical Services Division, San Diego, CA.
- City of San Diego. (2023). *Interim Receiving Waters Monitoring Report for the Point Loma Ocean Outfall and South Bay Ocean Outfalls, 2022*. City of San Diego Ocean Monitoring Program, Public Utilities Department, Environmental Monitoring and Technical Services Division, San Diego, CA.

- Clarke, K.R. (1993). Non-parametric multivariate analyses of changes in community structure. *Australian Journal of Ecology*, 18: 117–143.
- Clarke, K.R., R.N. Gorley, P.J. Somerfield, and R.M. Warwick. (2014). *Change in marine communities: an approach to statistical analysis and interpretation*, 3rd edition. PRIMER-E, Plymouth, England.
- Clarke, K.R., P.J. Somerfield, and R.N. Gorley. (2008). Testing of null hypotheses in exploratory community analyses: similarity profiles and biota-environment linkage. *Journal of Experimental Marine Biology and Ecology*, 366: 56–69.
- Cross, J.N. and L.G. Allen. (1993). Chapter 9. Fishes. In: M.D. Dailey, D.J. Reish, and J.W. Anderson (eds.). *Ecology of the Southern California Bight: A Synthesis and Interpretation*. University of California Press, Berkeley, CA. 459–540.
- Cross, J.N., J.N. Roney, and G.S. Kleppel. (1985). Fish food habits along a pollution gradient. *California Fish and Game*, 71: 28–39.
- Eschmeyer, W.N. and E.S. Herald. (1998). *A Field Guide to Pacific Coast Fishes of North America*. Houghton and Mifflin Company, New York.
- Gohel, D. (2023). officer: Manipulation of Microsoft Word and PowerPoint Documents. R package version 0.6.2. <https://CRAN.R-project.org/package=officer>.
- Gohel, D. and P. Skintzos (2023). flextable: Functions for Tabular Reporting. R package version 0.9.3. <https://CRAN.R-project.org/package=flextable>
- Grolemund, G. and H. Wickham (2011). Dates and Times Made Easy with lubridate. *Journal of Statistical Software*, 40(3), 1-25. URL <https://www.jstatsoft.org/v40/i03/>.
- Helvey, M. and R.W. Smith. (1985). Influence of habitat structure on the fish assemblages associated with two cooling-water intake structures in southern California. *Bulletin of Marine Science*, 37: 189–199.
- Hester, J. and J. Bryan (2022). glue: Interpreted String Literals. R package version 1.6.2. <https://CRAN.R-project.org/package=glue>
- Hope, R.M. (2013). Rmisc: Ryan Miscellaneous. R package version 1.5. <http://CRAN.R-project.org/package=Rmisc>.
- Jensen, G.C. (2014). *Crabs and Shrimps of the Pacific Coast. A Guide to Shallow Water Decapods from Southeastern Alaska to the Mexican Border*. MolaMarine Publication. WA. 240 pp.
- Karinen, J.B., B.L. Wing, and R.R. Straty. (1985). Records and sightings of fish and invertebrates in the eastern Gulf of Alaska and oceanic phenomena related to the 1983 El Niño event. In: W.S. Wooster and D.L. Fluharty (eds.). *El Niño North: El Niño Effects in the Eastern Subarctic Pacific Ocean*. Washington Sea Grant Program, Seattle, WA. 253–267.

- Kassambara, A. (2018). ggpubr: Based Publication Ready Plots R package version 0.2. <http://www.sthda.com/english/rpkgs/ggpubr>.
- Lilly, M. (2004). *Octopus veligero*: Permanent Resident or Fair-Weather Friend? The Festivus. Vol XXXVI(1): pp 3-8.
- Lin Pedersen, T. (2023). patchwork: The Composer of Plots. R package version 1.1.3. <https://CRAN.R-project.org/package=patchwork>
- Miller, D. J. (2020). Miller and Lea's Guide to the Coastal Marine Fishes of California. United States: University of California Agriculture and Natural Resources.
- Milton Bache, S. and H. Wickham (2022). magrittr: A Forward-Pipe Operator for R. R package version 2.0.3. <https://CRAN.R-project.org/package=magrittr>
- Murawski, S.A. (1993). Climate change and marine fish distribution: forecasting from historical analogy. Transactions of the American Fisheries Society, 122: 647–658.
- [NOAA/NWS] National Oceanic and Atmospheric Administration/National Weather Service. (2022). Climate Prediction Center Website. https://origin.cpc.ncep.noaa.gov/products/analysis_monitoring/ensostuff/ONI_v5.php
- Oksanen, J., F.G. Blanchet, R. Kindt, P. Legendre, P.R. Minchin, R.B. O'Hara, G.L. Simpson, P. Solymos, M. Henry, H. Stevens and H. Wagner. (2015). vegan: Community Ecology Package. R package version 2.3-0. <http://CRAN.R-project.org/package=vegan>.
- Page, L., M., H. Espinosa-Pérez, L. T. Findley, C. R. Gilbert, R. N. Lea, N. E. Mandrak, R. L. Mayden, and J. S. Nelson. (2013). Common and Scientific names of fishes from the United States, Canada and Mexico. Special Publication 34. The American Fisheries Society, Bethesda, Maryland.
- R Core Team. (2021). R: A language and environment for statistical computing. R Foundation for Statistical Computing, Vienna, Austria. URL <https://www.R-project.org/>.
- Ripley, B. and M. Lapsley. (2015). RODBC: ODBC Database Access. R package version 1.3-12. <http://CRAN.R-project.org/package=RODBC>.
- [SCAMIT] Southern California Association of Marine Invertebrate Taxonomists. (2021). A taxonomic listing of benthic macro- and megainvertebrates from infaunal and epibenthic monitoring programs in the Southern California Bight, edition 13. Southern California Associations of Marine Invertebrate Taxonomists, Natural History Museum of Los Angeles County, Research and Collections, Los Angeles, CA.
- [SCCWRP] Southern California Coastal Water Research Project. (2018). Southern California Bight 2018 Regional Monitoring Program: Contaminant Impact Assessment Field Operations Manual. Southern California Coastal Water Research Project. Costa Mesa, CA.

- [SCCWRP] Southern California Coastal Water Research Project. (2023). Southern California Bight 2023 Regional Monitoring Program: Sediment Quality Assessment Workplan. Southern California Coastal Water Research Project. Costa Mesa, CA.
- Stein, E.D. and D.B. Cadien. (2009). Ecosystem response to regulatory and management actions: The southern California experience in long-term monitoring. *Marine Pollution Bulletin*, 59: 91–100.
- Thompson, B., J. Dixon, S. Schroeter, and D.J. Reish. (1993a). Chapter 8. Benthic invertebrates. In: M.D. Dailey, D.J. Reish, and J.W. Anderson (eds.). *Ecology of the Southern California Bight: A Synthesis and Interpretation*. University of California Press, Berkeley, CA. 369–458.
- Thompson, B., D. Tsukada, and J. Laughlin. (1993b). Megabenthic assemblages of coastal shelves, slopes, and basins off Southern California. *Bulletin of the Southern California Academy of Sciences*, 92: 25–42.
- Walther, S.M., J.P. Williams, A. Latker, D.B. Cadien, D.W. Diehl, K. Wisenbaker, E. Miller, R. Gartman, C. Stransky and K. Schiff. (2017). Southern California Bight 2013 Regional Monitoring Program: Volume VII. Demersal Fishes and Megabenthic Invertebrates. Southern California Coastal Water Research Project. Costa Mesa, CA.
- Warwick, R.M. (1993). Environmental impact studies on marine communities: pragmatical considerations. *Australian Journal of Ecology*, 18: 63–80.
- Wickham, H. (2007). Reshaping Data with the reshape Package. *Journal of Statistical Software*, 21(12), 1-20. URL <http://www.jstatsoft.org/v21/i12/>.
- Wickham, H., J. Hester, W. Chang and J. Bryan (2022). devtools: Tools to Make Developing R Packages Easier. R package version 2.4.5. <https://CRAN.R-project.org/package=devtools>
- Wisenbaker, K., K. McLaughlin, D. Diehl, A. Latker, K. Stolzenbach, R. Gartman, K. Schiff. (2021). Southern California Bight 2018 Regional Monitoring Program: Volume IV. Demersal Fishes and Megabenthic Invertebrates. Technical Report #1183. Southern California Coastal Water Research Project. Costa Mesa, CA.

CHAPTER 8

FIGURES & TABLES

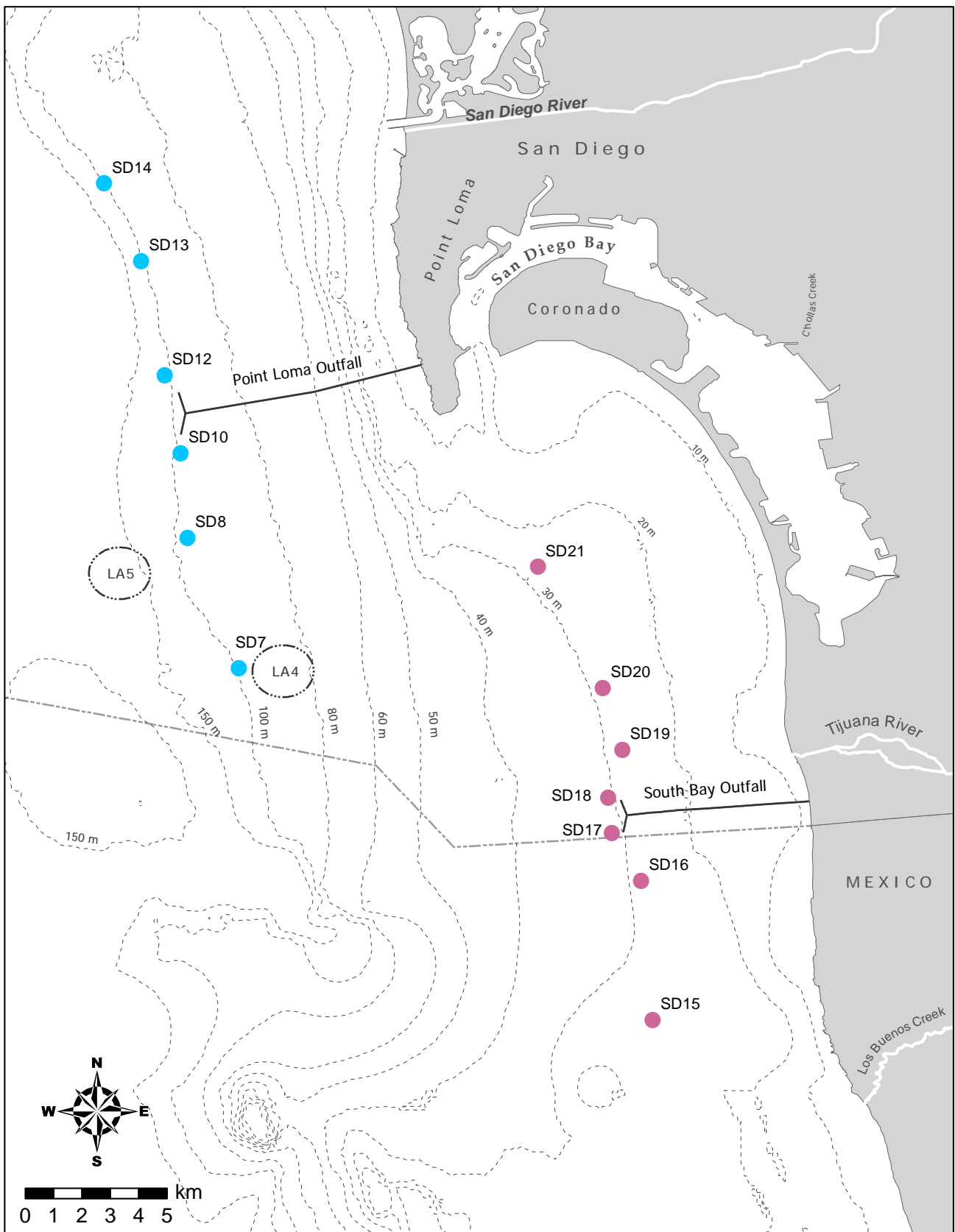


Figure 8.1

Trawl station locations sampled around the Point Loma and South Bay Ocean Outfalls as part of the City of San Diego's Ocean Monitoring Program.

Table 8.1

Top 30 most abundant demersal fish species collected from 18 trawls conducted in the PLOO region during 2022 and 2023. PA=percent abundance; FO=frequency of occurrence; MAH=mean abundance per haul; MAO=mean abundance per occurrence.

Species	PA	FO	MAH	MAO
Pacific Sanddab	54	100	307	307
Dover Sole	9	100	49	49
Halfbanded Rockfish	8	100	44	44
Longfin Sanddab	7	100	39	39
Longspine Combfish	4	100	20	20
Pink Seaperch	4	89	23	26
Stripetail Rockfish	4	94	21	23
Shortspine Combfish	3	94	19	20
English Sole	2	94	12	12
Yellowchin Sculpin	2	44	12	26
Bigmouth Sole	1	89	5	6
California Tonguefish	1	89	5	5
Blackbelly Eelpout	<1	28	1	2
Blacktip Poacher	<1	6	<1	2
Brown Rockfish	<1	6	<1	3
California Halibut	<1	6	<1	1
California Lizardfish	<1	33	<1	2
California Scorpionfish	<1	39	2	5
California Skate	<1	33	<1	1
Chilipepper	<1	17	<1	3
Cowcod	<1	6	<1	1
Flag Rockfish	<1	11	<1	2
Greenblotched Rockfish	<1	22	<1	1
Greenstriped Rockfish	<1	33	1	2
Hornyhead Turbot	<1	72	2	3
Longnose Skate	<1	6	<1	1
Northern Anchovy	<1	6	<1	9
Pacific Argentine	<1	39	1	2
Pacific Hake	<1	44	1	2
Pink Rockfish	<1	11	<1	2

Table 8.2

Top 30 most abundant demersal fish species collected from 21 trawls conducted in the SBOO region during 2022 and 2023. PA=percent abundance; FO=frequency of occurrence; MAH=mean abundance per haul; MAO=mean abundance per occurrence.

Species	PA	FO	MAH	MAO
Speckled Sanddab	58	100	155	155
Longfin Sanddab	12	67	31	47
White Croaker	6	29	16	57
California Lizardfish	5	90	12	13
Northern Anchovy	4	29	11	38
California Tonguefish	3	86	8	9
Pacific Sanddab	3	29	7	24
Yellowchin Sculpin	2	24	4	18
English Sole	1	48	3	5
Hornyhead Turbot	1	86	3	4
Pacific Pomfret	1	14	3	19
Roughback Sculpin	1	86	4	4
Shiner Perch	1	5	2	35
Barcheek Pipefish	<1	29	1	3
Bigmouth Sole	<1	19	<1	1
California Halibut	<1	71	1	2
California Scorpionfish	<1	19	<1	1
California Skate	<1	10	<1	2
Curlfin Sole	<1	5	<1	1
Fantail Sole	<1	29	1	2
Giant Kelpfish	<1	5	<1	1
Kelp Pipefish	<1	14	<1	2
Longnose Skate	<1	10	<1	1
Longspine Combfish	<1	38	1	4
Ocean Whitefish	<1	19	<1	1
Pacific Pompano	<1	5	1	19
Pacific Sardine	<1	5	<1	5
Pipefish Unidentified	<1	24	1	3
Plainfin Midshipman	<1	29	<1	1
Pygmy Poacher	<1	10	<1	1

Table 8.3

Summary of demersal fish community parameters for PLOO and SBOO trawl stations sampled during 2022 and 2023. Data are included for species richness, abundance, diversity (H'), and biomass (kg, wet weight).

Station	2022			2023		2022			2023		
	Winter	Summer	Fall	Winter	Summer ^a	Winter	Summer	Fall	Winter	Summer ^a	
	<i>Species Richness</i>					<i>Abundance</i>					
PLOO	SD7	17	17	—	19	ns	338	554	—	600	ns
	SD8	19	16	—	19	ns	483	642	—	509	ns
	SD10	17	—	16	20	ns	290	—	498	1084	ns
	SD12	16	14	—	19	ns	374	543	—	600	ns
	SD13	16	15	—	17	ns	430	661	—	770	ns
	SD14	16	18	—	20	ns	417	724	—	792	ns
SBOO	SD15	6	8	—	9	ns	36	307	—	80	ns
	SD16	10	12	—	15	ns	102	548	—	321	ns
	SD17	17	12	—	14	ns	108	274	—	169	ns
	SD18	17	11	—	17	ns	343	284	—	325	ns
	SD19	11	13	—	8	ns	201	516	—	158	ns
	SD20	9	—	14	11	ns	215	—	589	181	ns
SD21	10	—	11	9	ns	192	—	574	129	ns	
	<i>Diversity</i>					<i>Biomass</i>					
PLOO	SD7	1.8	1.3	—	2.0	ns	7.2	9.9	—	12.7	ns
	SD8	1.8	1.5	—	1.8	ns	14.3	13.5	—	14.6	ns
	SD10	1.9	—	1.5	1.9	ns	8.1	—	9.1	20.4	ns
	SD12	2.0	1.6	—	1.6	ns	9.7	14.8	—	20.1	ns
	SD13	1.4	1.0	—	1.7	ns	6.8	10.5	—	13.4	ns
	SD14	1.6	1.2	—	1.6	ns	7.8	16.8	—	15.6	ns
SBOO	SD15	1.2	0.2	—	1.1	ns	0.6	2.8	—	1.8	ns
	SD16	1.4	1.0	—	1.6	ns	2.1	7.6	—	7.3	ns
	SD17	2.0	1.2	—	1.9	ns	2.6	3.5	—	6.0	ns
	SD18	1.7	0.9	—	1.8	ns	11.1	6.7	—	11.9	ns
	SD19	1.4	1.2	—	1.0	ns	2.3	7.2	—	3.1	ns
	SD20	1.1	—	1.0	0.5	ns	4.3	—	9.1	4.7	ns
SD21	1.6	—	1.2	1.4	ns	3.2	—	9.0	3.0	ns	

^a No trawls conducted during the summer of 2023 due to Bight'23 resource exchange (see text)

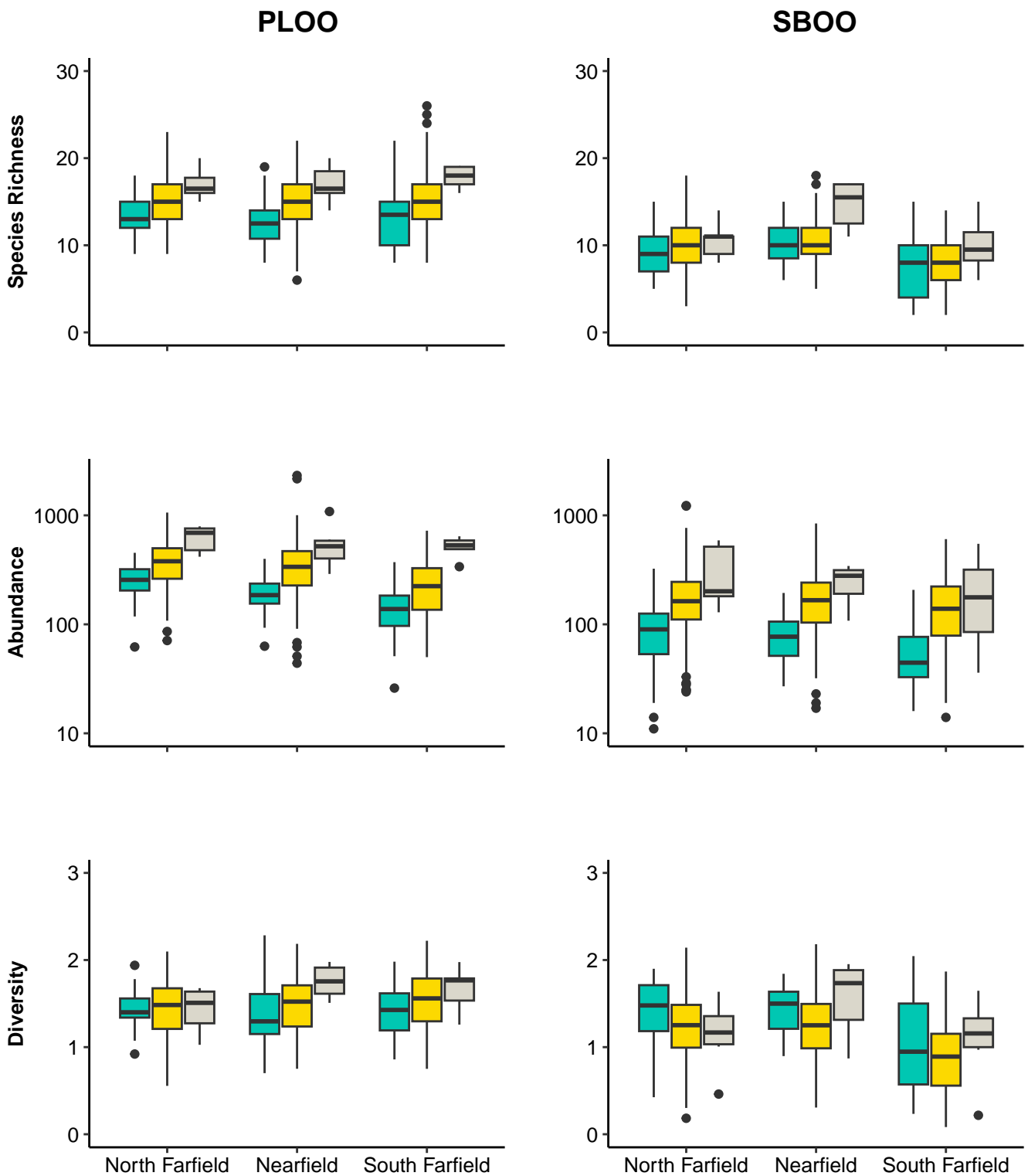


Figure 8.2

Species richness, abundance, and diversity (H') of demersal fishes collected from PLOO and SBOO north farfield, nearfield, and south farfield during pre-discharge (green), historical post-discharge (yellow), and current post-discharge (grey) periods. Data limited to 10-minute trawls. Boxes=median, upper, and lower quartiles; whiskers = 1.5x interquartile range; circles=outliers; see text for description of pre- versus post-discharge periods for the two outfalls.

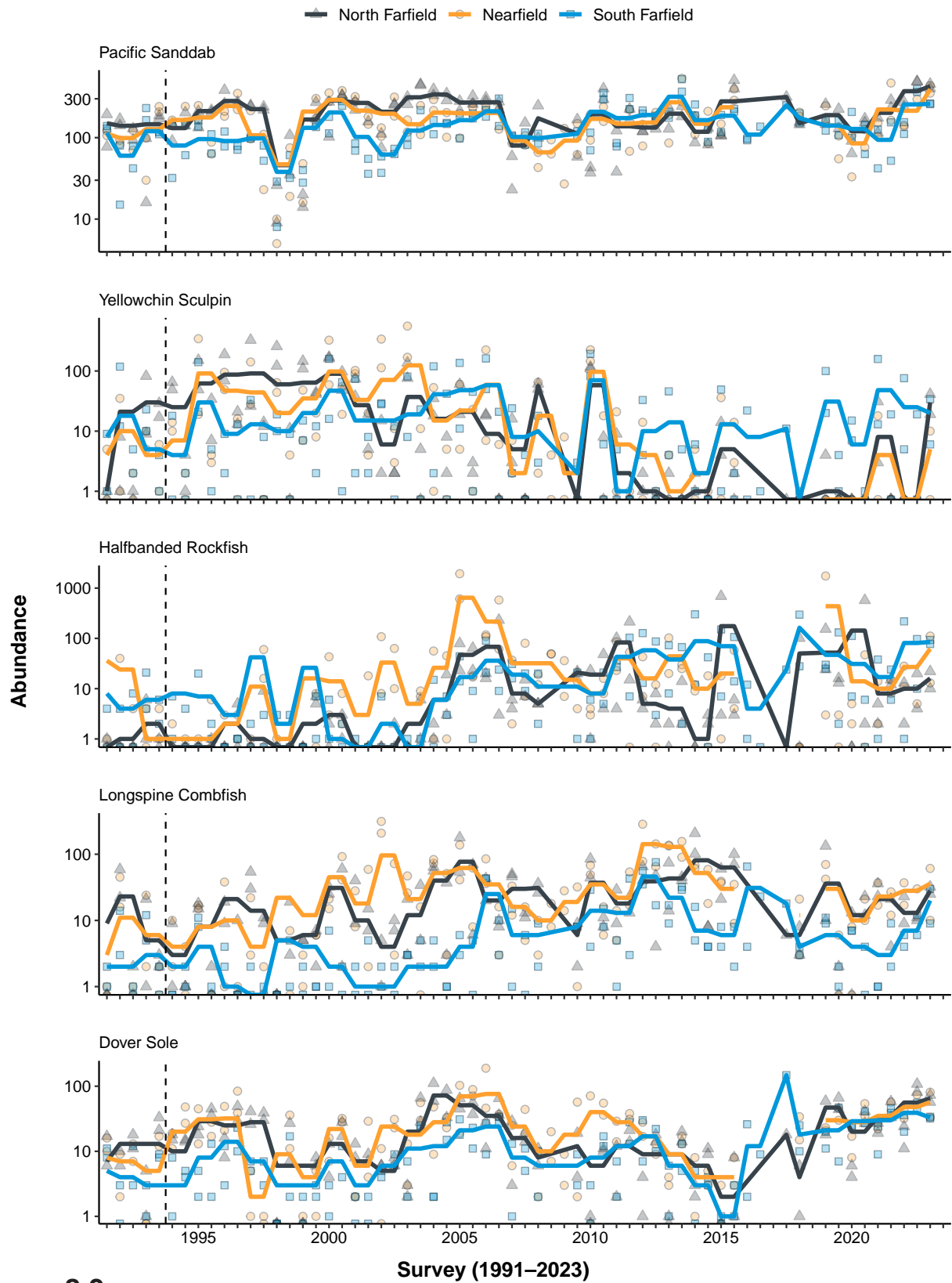


Figure 8.3

The ten most abundant demersal fish species (presented in order) collected from PLOO trawl stations sampled from 1991 through 2023. Data are limited to 10-minute trawls and are presented as quarterly means (lines) and total values per haul for north farfield (triangles), nearfield (circles), and south farfield (squares) stations. Dashed lines indicate onset of wastewater discharge.

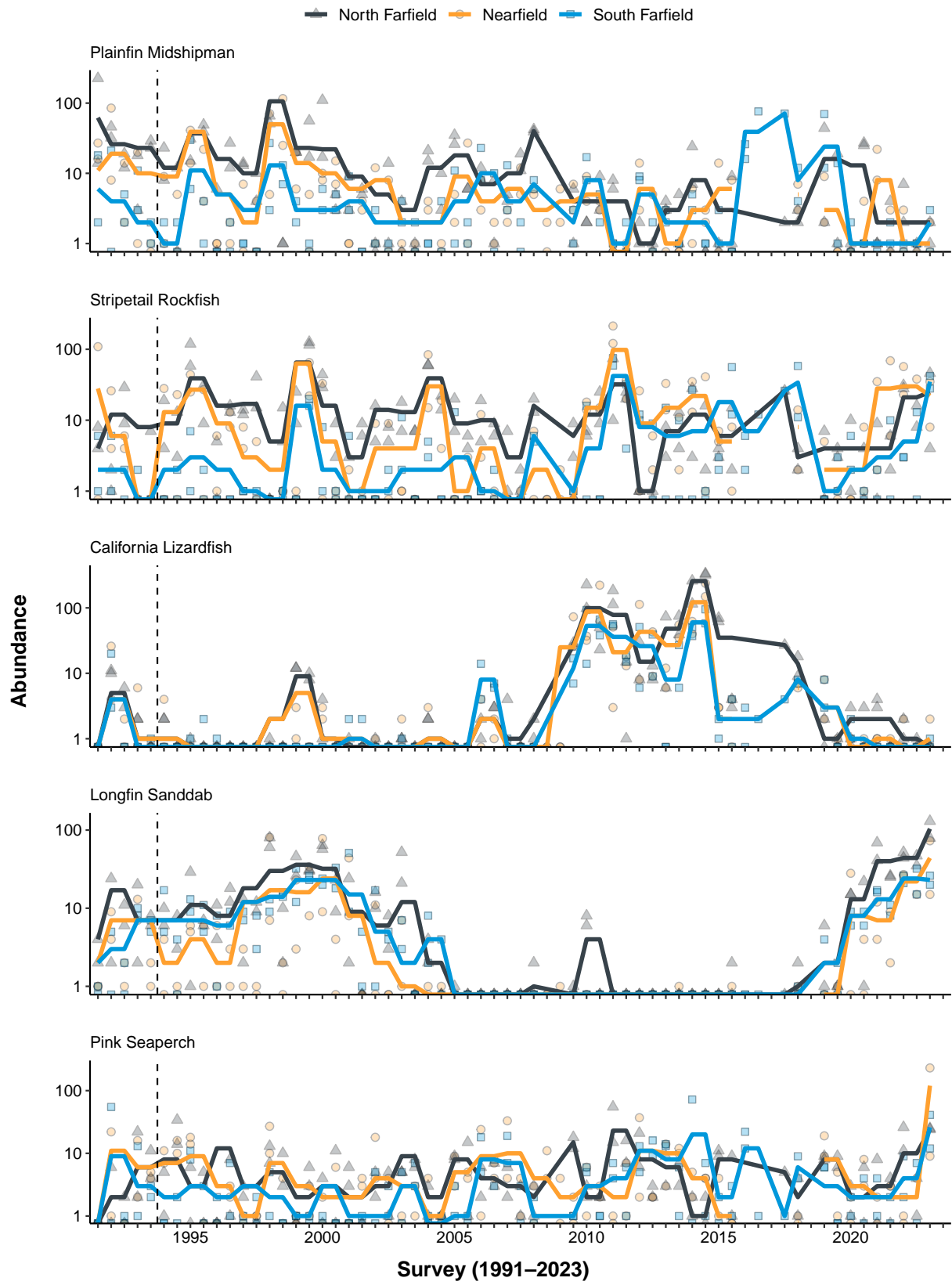


Figure 8.3 *continued*

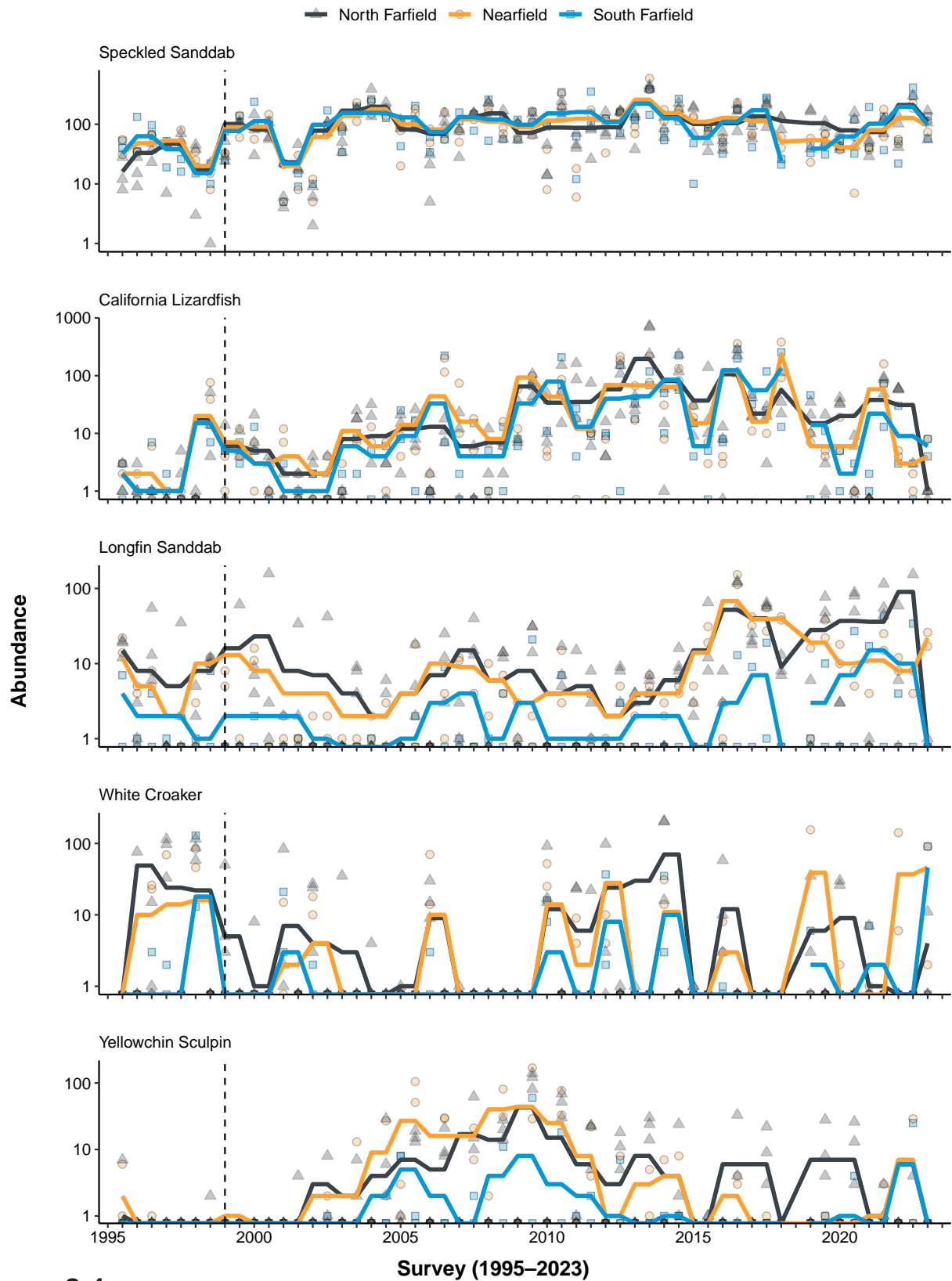


Figure 8.4

The ten most abundant demersal fish species (presented in order) collected from SBOO trawl stations sampled from 1995 through 2023. Data are limited to 10-minute trawls and are presented as quarterly means (lines) and total values per haul for north farfield (triangles), nearfield (circles), and south farfield (squares) stations. Dashed lines indicate onset of wastewater discharge.

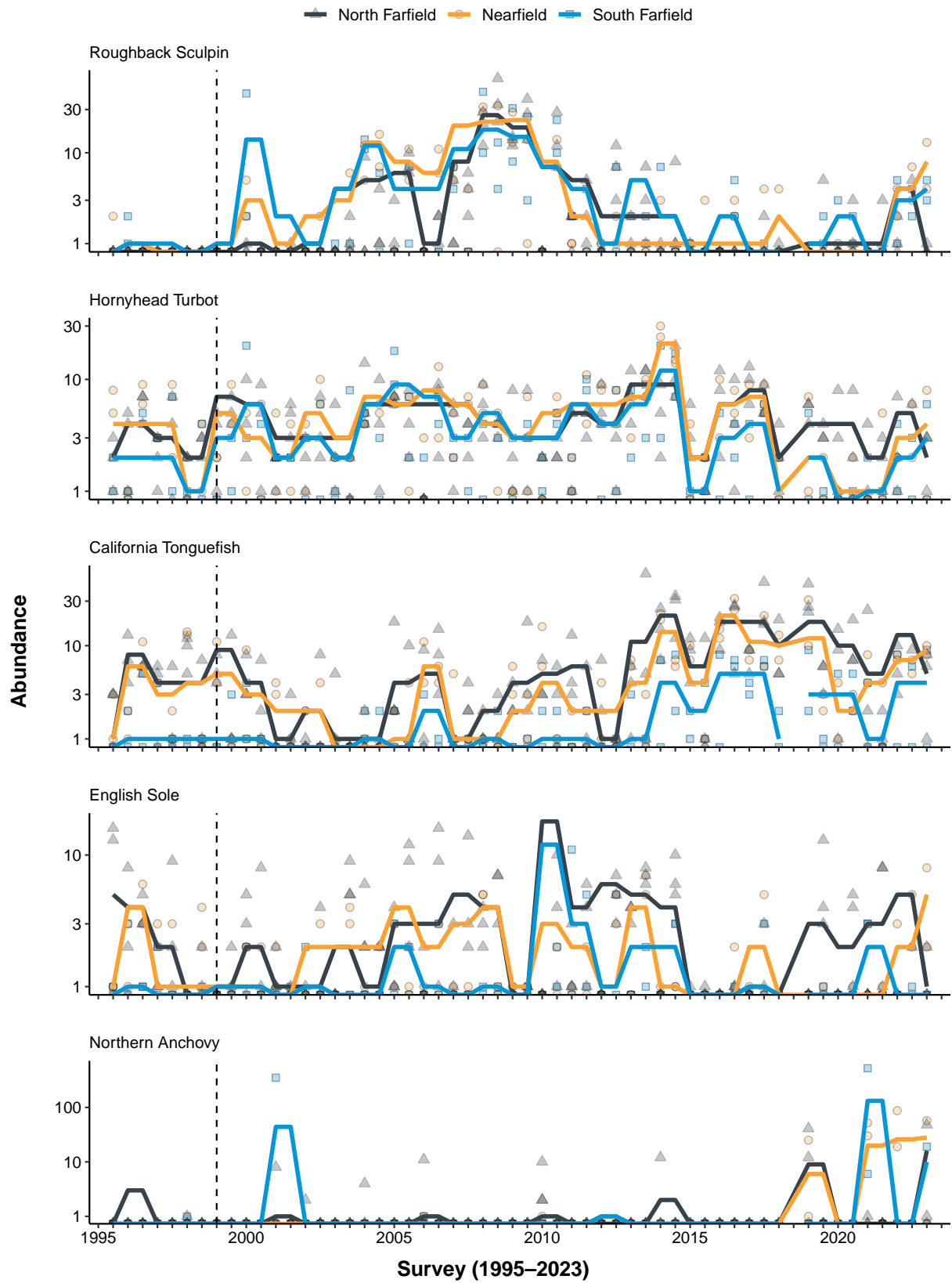


Figure 8.4 *continued*

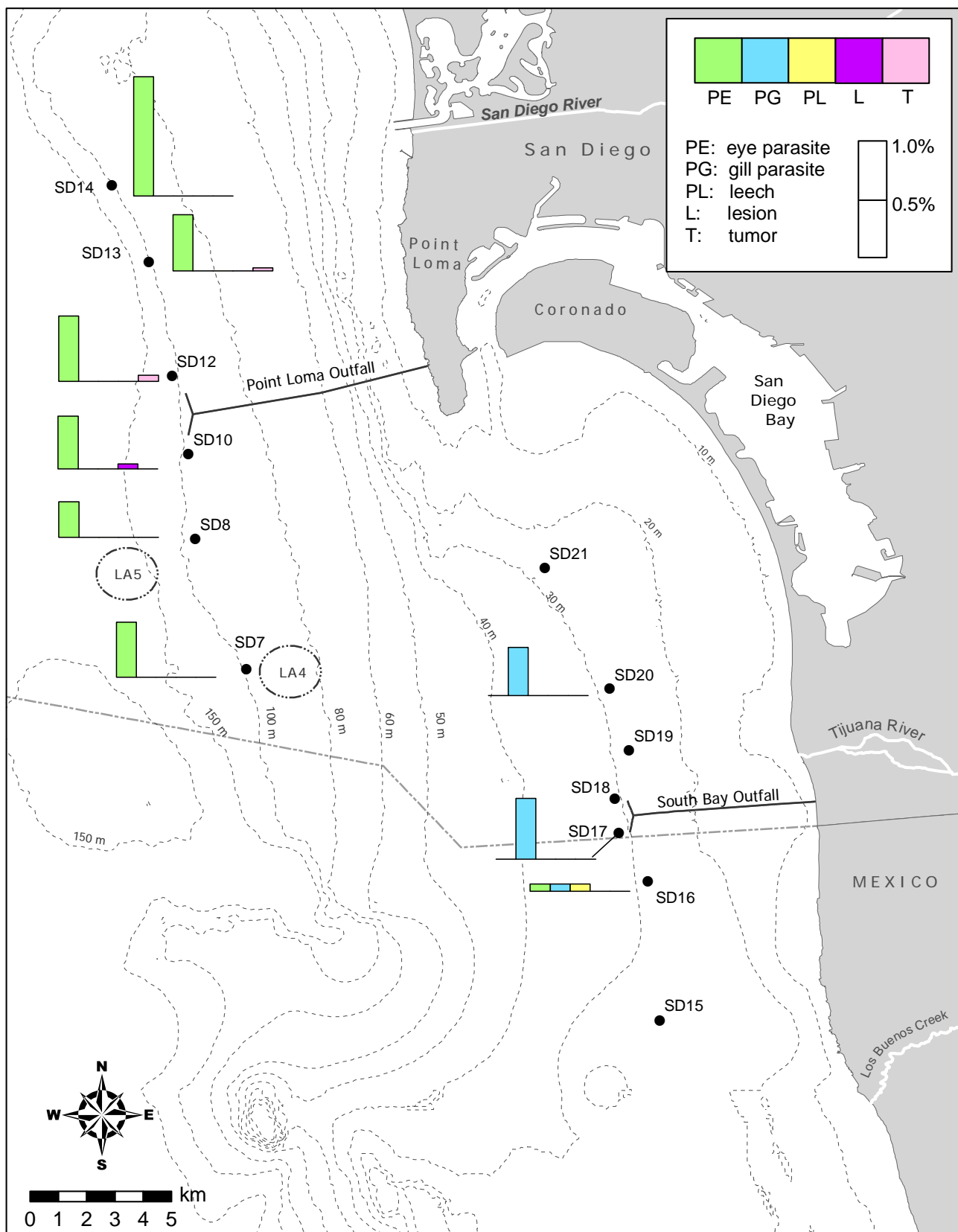


Figure 8.5

Percentages of fishes collected at stations with anomalies present during 2022 and 2023. PE = eye parasite; PG = gill parasite; PX = external parasite; L = leech; T = tumor; D = deformation; O = others.

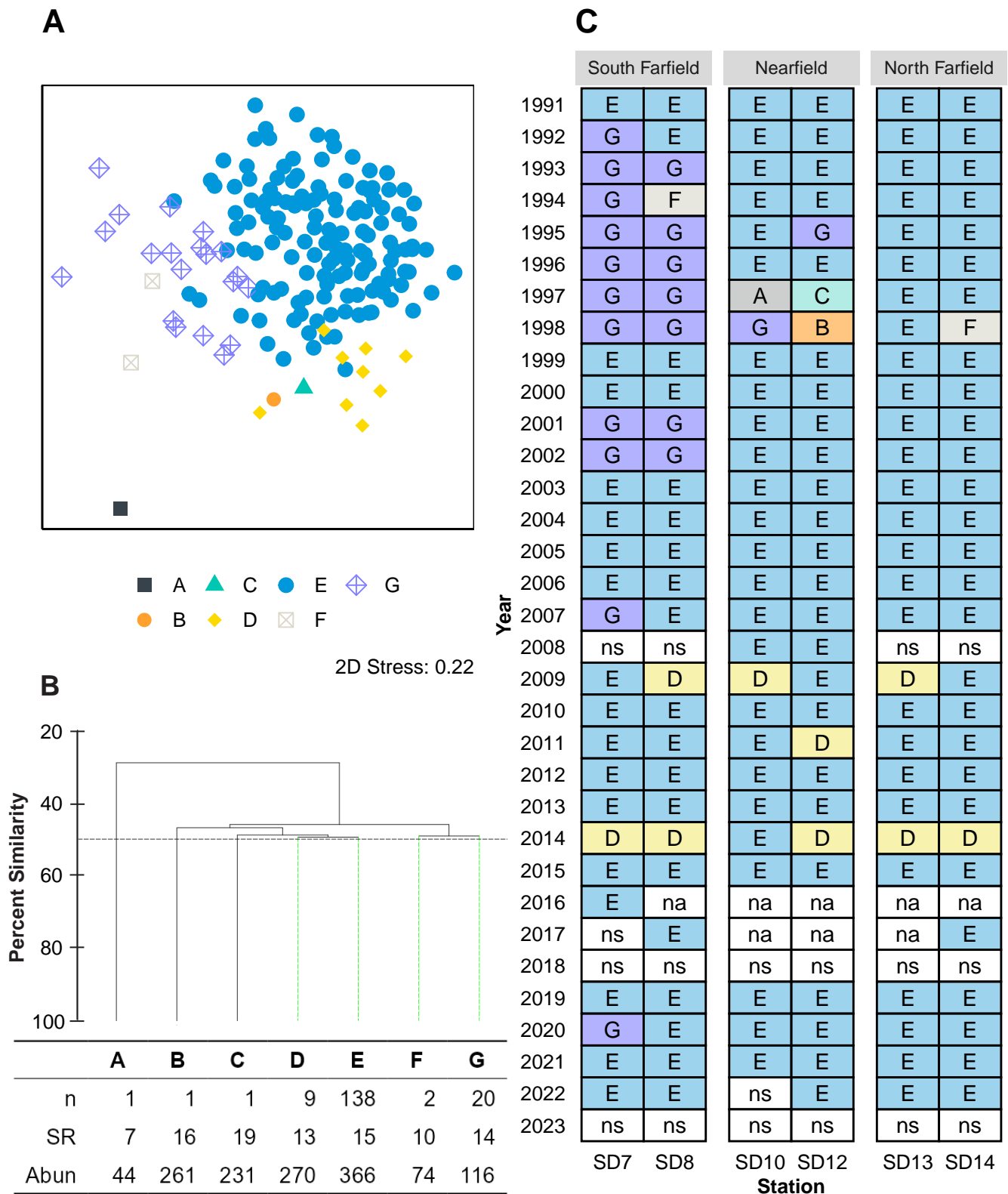


Figure 8.6

Results of ordination and cluster analysis of demersal fish assemblages from PLOO trawl stations sampled from 1991 through 2023. Data are limited to 10-minute trawls from summer surveys and presented as (A) nMDS ordination; (B) a dendrogram of main cluster groups; (C) a matrix showing distribution of cluster groups over time; n=number of hauls; SR=mean species richness; Abun=mean abundance; na=not analyzed; ns=not sampled.

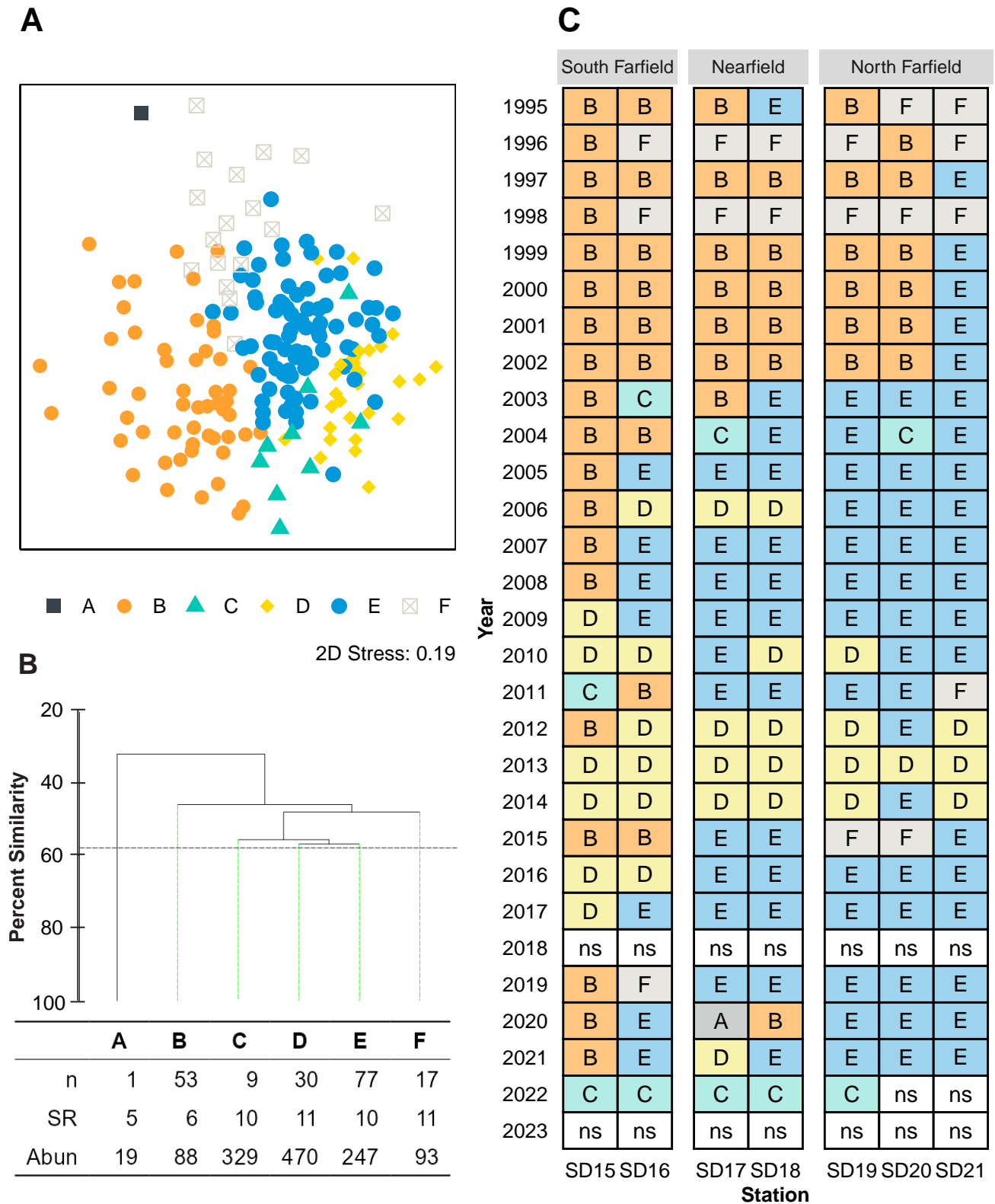


Figure 8.7

Results of ordination and cluster analysis of demersal fish assemblages from SBOO trawl stations sampled from 1995 through 2023. Data are limited to 10-minute trawls from summer surveys and presented as (A) nMDS ordination; (B) a dendrogram of main cluster groups; (C) a matrix showing distribution of cluster groups over time; n=number of hauls; SR=mean species richness; Abun=mean abundance; ns=not sampled.

Table 8.4

Top 30 most abundant megabenthic invertebrate species collected from 18 trawls conducted in the PLOO region during 2022 and 2023. PA=percent abundance; FO=frequency of occurrence; MAH=mean abundance per haul; MAO=mean abundance per occurrence.

Species	PA	FO	MAH	MAO
<i>Lytechinus pictus</i>	71	78	631	812
<i>Strongylocentrotus fragilis</i>	26	17	233	1,397
<i>Sicyonia ingentis</i>	1	61	8	13
<i>Acanthoptilum</i> sp	<1	22	<1	1
<i>Antiplanes catalinae</i>	<1	11	<1	1
<i>Aphorme horrida</i>	<1	11	<1	1
<i>Apostichopus californicus</i>	<1	39	1	2
<i>Astropecten californicus</i>	<1	83	4	5
<i>Calliostoma turbinum</i>	<1	11	<1	1
<i>Cancellaria cooperii</i>	<1	6	<1	1
<i>Cancellaria crawfordiana</i>	<1	6	<1	1
<i>Florometra serratissima</i>	<1	6	<1	1
<i>Loxorhynchus crispatus</i>	<1	6	<1	1
<i>Luidia asthenosoma</i>	<1	67	2	2
<i>Luidia foliolata</i>	<1	94	4	4
<i>Megasurcula carpenteriana</i>	<1	11	<1	1
<i>Metridium farcimen</i>	<1	11	<1	1
Naticidae	<1	6	<1	1
<i>Neocrangon zacaе</i>	<1	11	<1	1
<i>Octopus rubescens</i>	<1	50	2	3
<i>Octopus veligero</i>	<1	22	<1	1
<i>Ophiopholis bakeri</i>	<1	6	<1	1
<i>Ophiothrix spiculata</i>	<1	17	<1	1
<i>Ophiura luetkenii</i>	<1	44	1	3
<i>Paguristes bakeri</i>	<1	11	<1	2
<i>Paguristes turgidus</i>	<1	11	<1	1
<i>Pandalus danae</i>	<1	6	<1	1
<i>Philine auriformis</i>	<1	17	<1	1
<i>Platydoris macfarlandi</i>	<1	6	<1	1
<i>Platymera gaudichaudii</i>	<1	44	1	1

Table 8.5

Top 30 most abundant megabenthic invertebrate species collected from 21 trawls conducted in the SBOO region during 2022 and 2023. PA=percent abundance; FO=frequency of occurrence; MAH=mean abundance per haul; MAO=mean abundance per occurrence.

Species	PA	FO	MAH	MAO
<i>Astropecten californicus</i>	30	95	25	26
<i>Crangon nigromaculata</i>	20	86	17	20
<i>Philine auriformis</i>	16	67	13	20
<i>Sicyonia penicillata</i>	7	71	6	8
<i>Dendroaster terminalis</i>	5	19	4	22
<i>Lytechinus pictus</i>	3	43	2	5
<i>Ophiothrix spiculata</i>	3	29	2	8
<i>Lovenia cordiformis</i>	2	19	2	8
<i>Luidia armata</i>	2	62	2	2
<i>Crangon alba</i>	1	19	1	6
<i>Hemisquilla californiensis</i>	1	33	1	2
<i>Heptacarpus stimpsoni</i>	1	19	<1	2
<i>Metacarcinus gracilis</i>	1	29	<1	2
<i>Pagurus spilocarpus</i>	1	43	1	1
<i>Pleurobranchaea californica</i>	1	14	<1	3
<i>Portunus xantusii</i>	1	33	1	4
<i>Pyromaia tuberculata</i>	1	38	1	3
<i>Acanthodoris brunnea</i>	<1	14	<1	1
<i>Acanthodoris rhodoceras</i>	<1	10	<1	1
<i>Acanthoptilum</i> sp	<1	5	<1	1
<i>Burchia semiinflata</i>	<1	19	<1	2
<i>Calliostoma gloriosum</i>	<1	5	<1	1
Cancriidae	<1	5	<1	1
<i>Crossata ventricosa</i>	<1	14	<1	1
<i>Epitonium bellastriatum</i>	<1	5	<1	1
<i>Ericerodes hemphillii</i>	<1	24	<1	2
<i>Eualus subtilis</i>	<1	5	<1	4
<i>Farfantepenaeus californiensis</i>	<1	5	<1	2
<i>Flabellinopsis iodinea</i>	<1	5	<1	1
<i>Glossaulax reclusiana</i>	<1	10	<1	1

Table 8.6

Summary of megabenthic invertebrate community parameters for PLOO and SBOO trawl stations sampled during 2022 and 2023. Data are included for species richness, abundance, diversity (H').

Station	2022			2023		2022			2023		
	Winter	Summer	Fall	Winter	Summer ^a	Winter	Summer	Fall	Winter	Summer ^a	
	<i>Species Richness</i>					<i>Abundance</i>					
PLOO	SD7	9	13	—	14	ns	61	362	—	578	ns
	SD8	12	13	—	7	ns	2300	2626	—	4196	ns
	SD10	2	—	11	9	ns	5	—	198	107	ns
	SD12	5	11	—	9	ns	253	672	—	3203	ns
	SD13	3	10	—	11	ns	12	159	—	23	ns
	SD14	4	9	—	8	ns	292	119	—	855	ns
SBOO	SD15	8	9	—	8	ns	110	48	—	47	ns
	SD16	10	13	—	12	ns	33	42	—	89	ns
	SD17	12	12	—	9	ns	23	36	—	28	ns
	SD18	12	16	—	12	ns	64	48	—	63	ns
	SD19	10	12	—	8	ns	145	237	—	41	ns
	SD20	5	—	8	11	ns	120	—	58	105	ns
SD21	5	—	15	13	ns	23	—	261	137	ns	
	<i>Diversity</i>										
PLOO	SD7	1.2	0.4	—	0.5	ns					
	SD8	0.1	0.1	—	0.02	ns					
	SD10	0.5	—	0.6	1	ns					
	SD12	0.1	0.2	—	0.03	ns					
	SD13	0.9	1.1	—	2.1	ns					
	SD14	0.2	1	—	0.1	ns					
SBOO	SD15	1.1	1.7	—	1.7	ns					
	SD16	1.6	2.2	—	1.2	ns					
	SD17	2.2	2	—	2	ns					
	SD18	1.8	2.1	—	1.5	ns					
	SD19	1.1	0.9	—	1.2	ns					
	SD20	0.9	—	1.2	1.6	ns					
SD21	0.9	—	1.1	1.4	ns						

^aNo trawls conducted during the summer of 2023 due to Bight'23 resource exchange (see text)

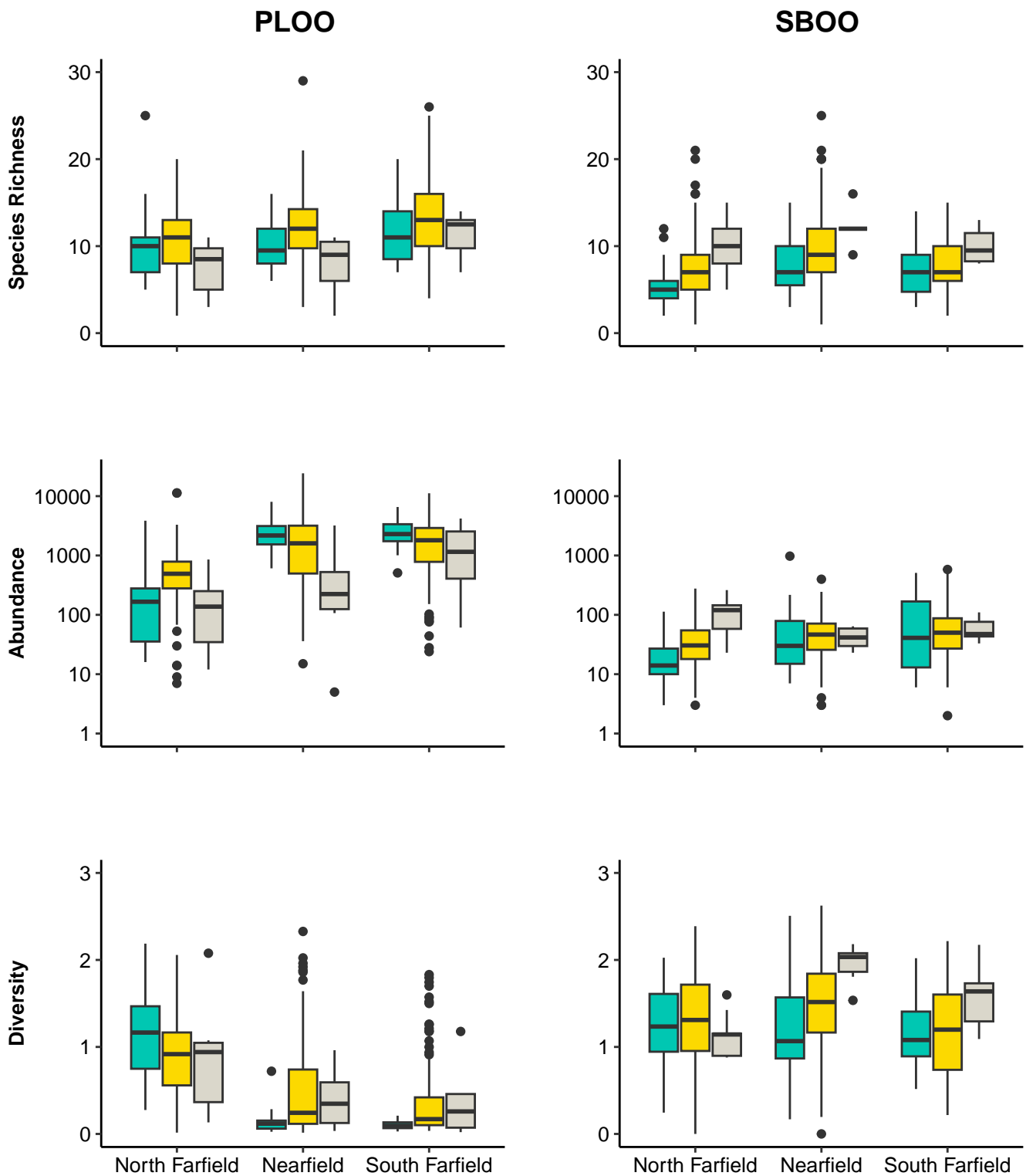


Figure 8.8

Species richness, abundance, and diversity (H') of megabenthic invertebrates collected from PLOO and SBOO north farfield, nearfield, and south farfield trawl stations during pre-discharge (green), historical post-discharge (yellow), and current post-discharge (grey) periods. Data are limited to 10-minute trawls. Boxes=median, upper, and lower quartiles; whiskers=1.5x interquartile range; circles=outliers; see text for description of pre- versus post-discharge periods for the two outfalls.

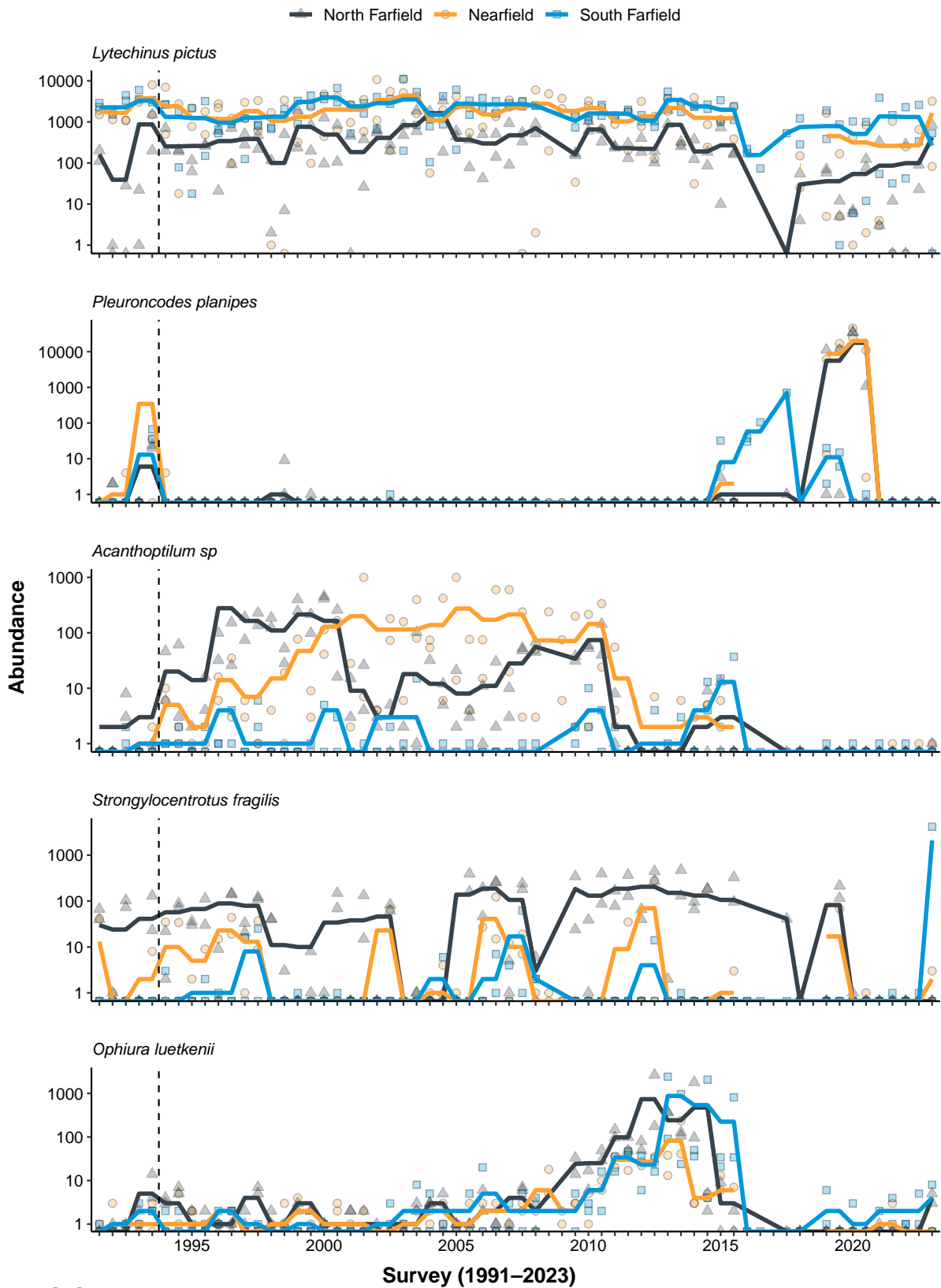


Figure 8.9

The ten most abundant megabenthic invertebrate species (presented in order) collected from PLOO trawl stations sampled from 1991 through 2023. Data are limited to 10-minute trawls and are presented as quarterly means (lines) and total values per haul for north farfield (triangles), nearfield (circles), and south farfield (squares) stations. Dashed lines indicate onset of wastewater discharge.

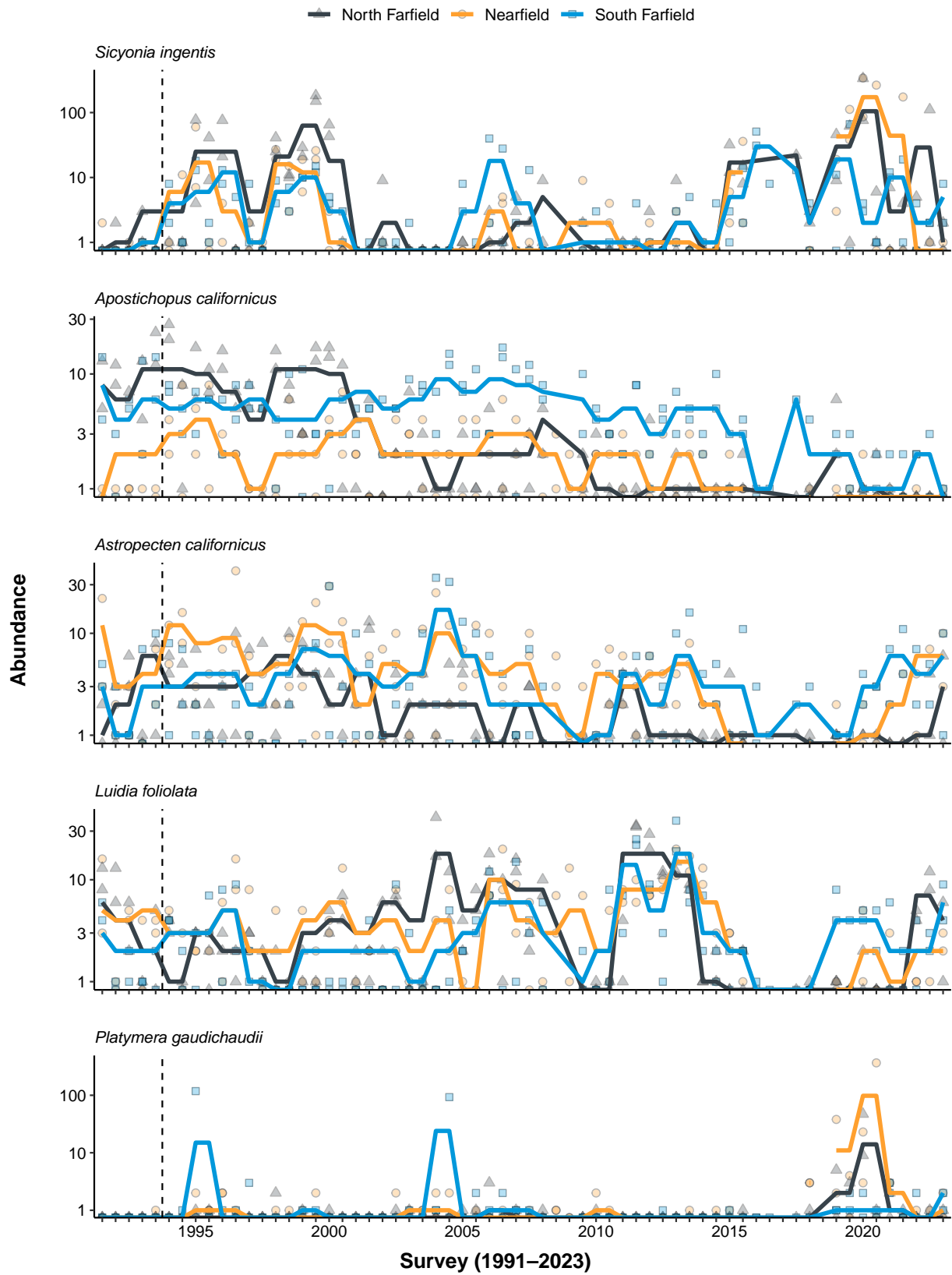


Figure 8.9 continued

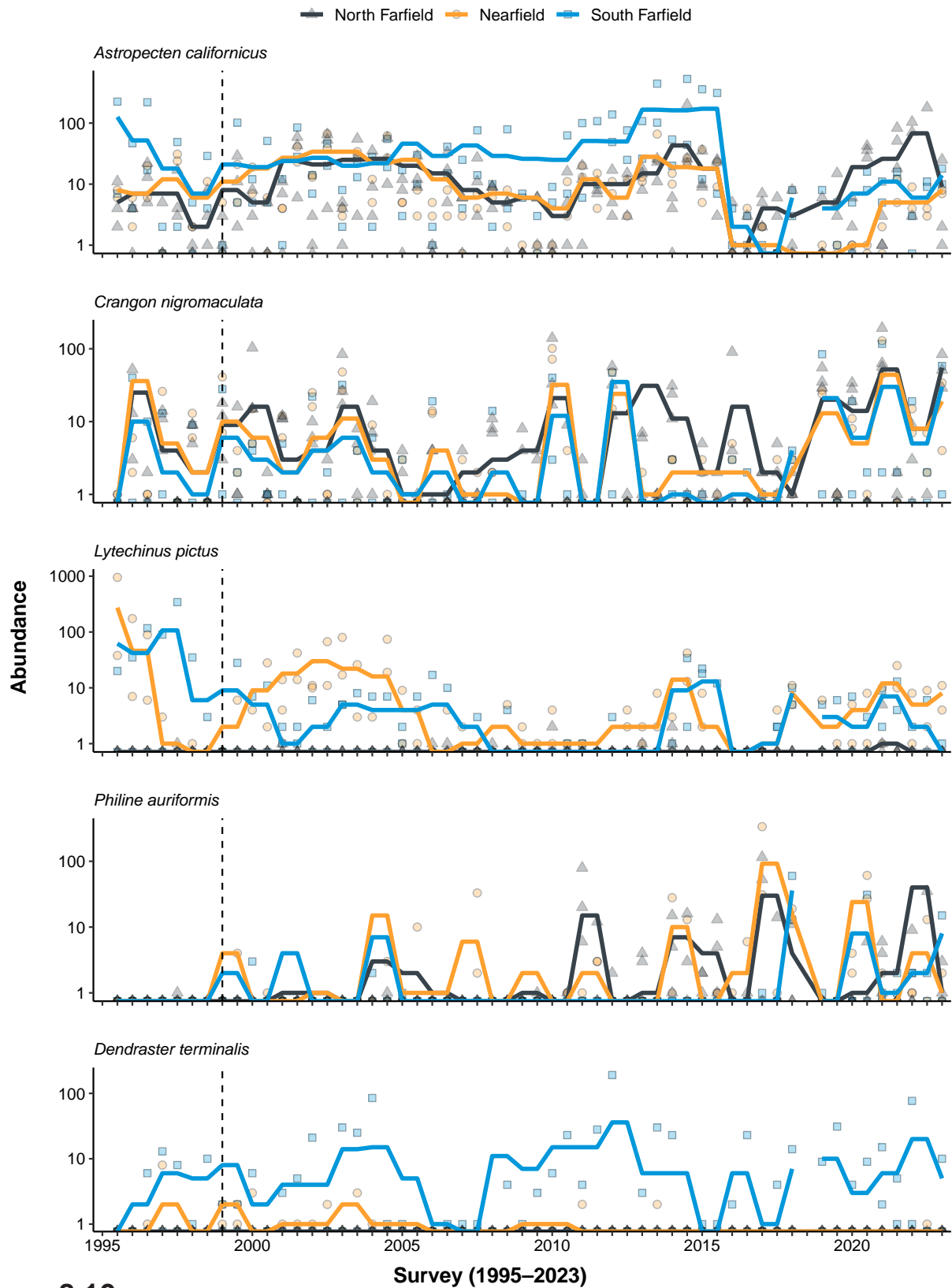


Figure 8.10

The ten most abundant megabenthic invertebrate species (presented in order) collected from SBOO trawl stations sampled from 1995 through 2023. Data are limited to 10-minute trawls and are presented as quarterly means (lines) and total values per haul for north farfield (triangles), nearfield (circles), and south farfield (squares) stations. Dashed lines indicate onset of wastewater discharge.

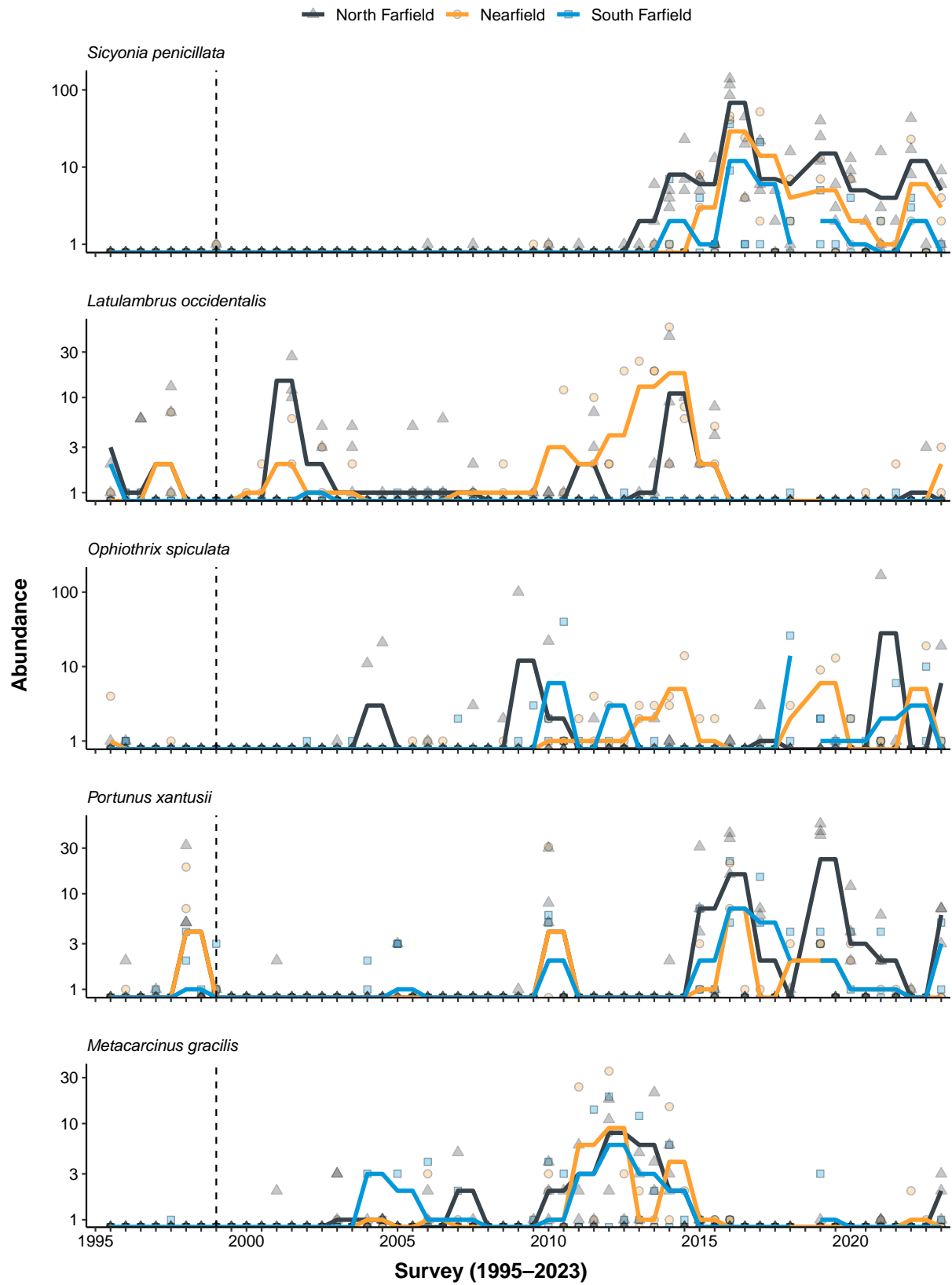


Figure 8.10 continued

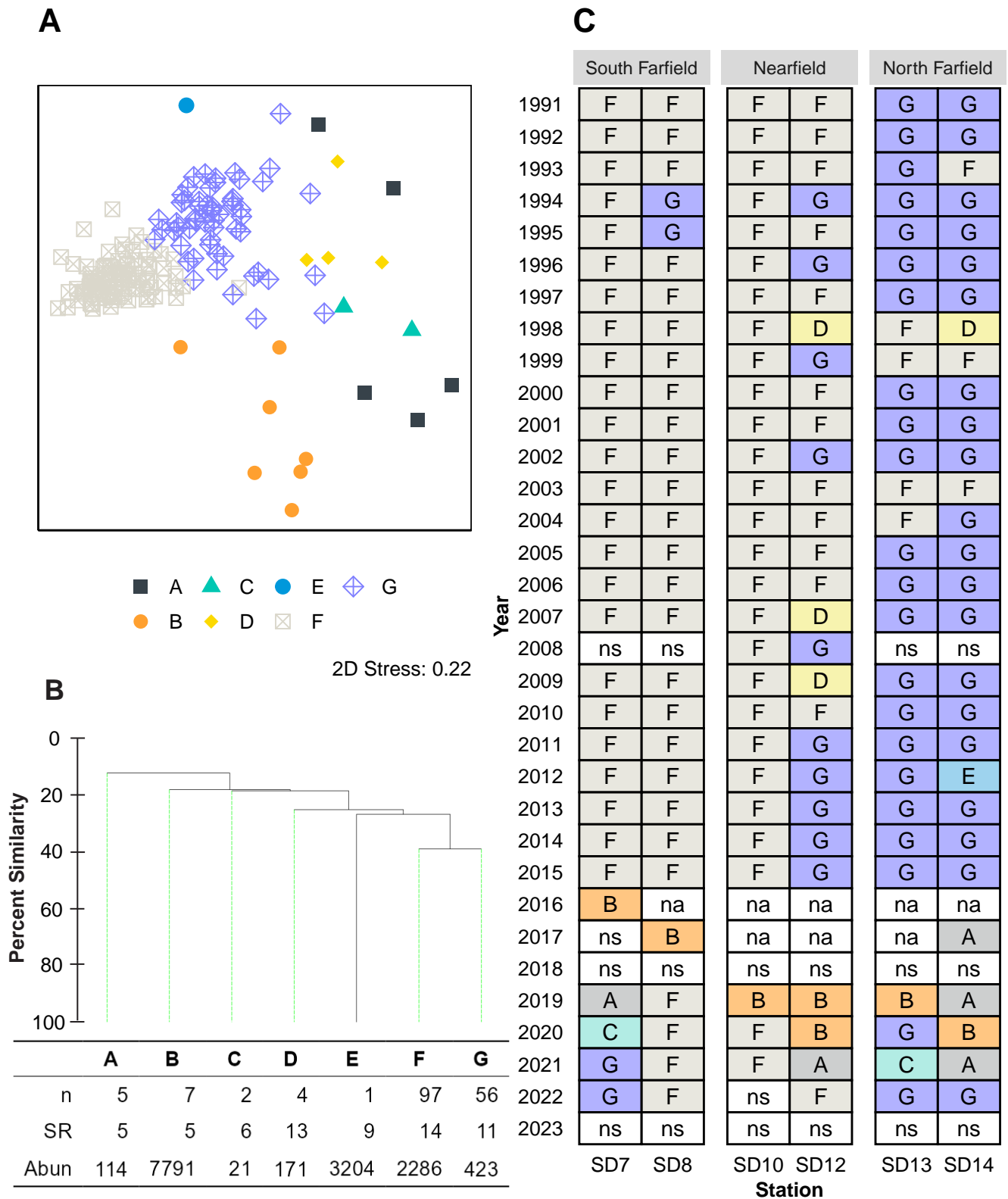
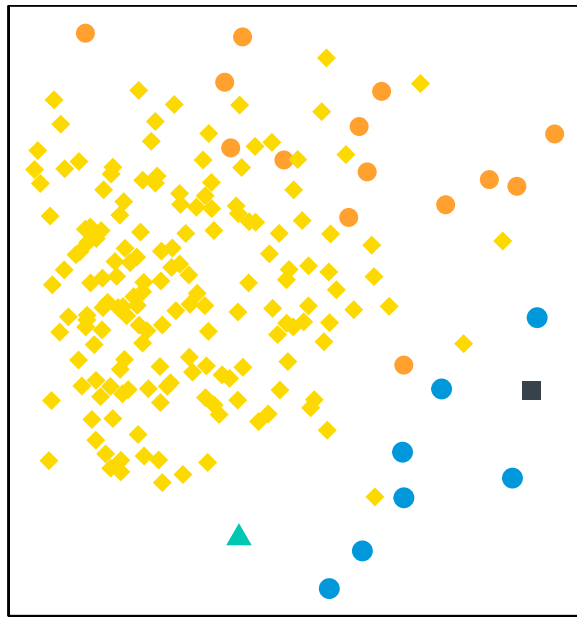


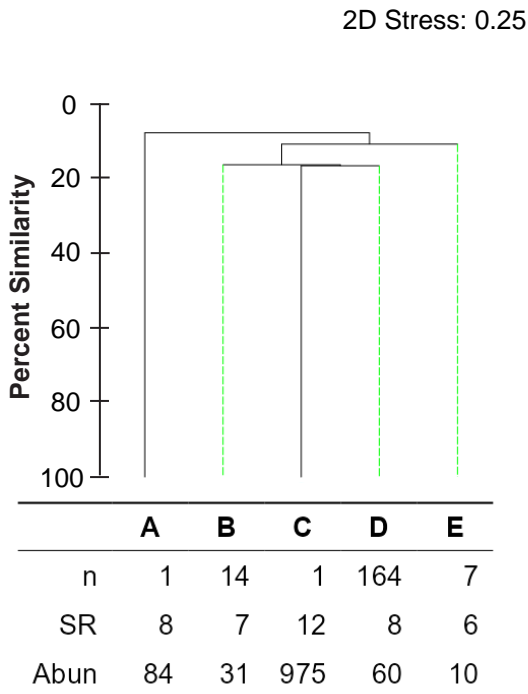
Figure 8.11

Results of ordination and cluster analysis of megabenthic invertebrate assemblages from PLOO trawl stations sampled from 1991 through 2023. Data are limited to 10-minute trawls from summer surveys and presented as (A) nMDS ordination; (B) a dendrogram of main cluster groups; (C) a matrix showing distribution of cluster groups over time; n=number of hauls; SR=mean species richness; Abun=mean abundance; na=not analyzed; ns=not sampled.

A



B



C

Year	South Farfield		Nearfield		North Farfield		
	SD15	SD16	SD17	SD18	SD19	SD20	SD21
1995	D	D	C	D	D	D	D
1996	D	D	D	D	D	D	D
1997	D	D	D	D	D	D	D
1998	D	D	D	D	D	D	D
1999	D	D	D	D	D	D	D
2000	D	D	E	D	D	E	E
2001	D	D	D	D	D	D	D
2002	D	D	D	D	D	D	D
2003	D	D	D	D	D	D	D
2004	D	D	D	D	D	D	D
2005	D	D	D	D	D	D	D
2006	D	D	D	D	D	D	D
2007	D	D	D	D	D	D	D
2008	D	D	D	D	D	D	D
2009	A	D	D	B	D	B	D
2010	D	D	D	D	D	D	D
2011	D	D	D	D	D	D	D
2012	D	D	D	D	D	D	D
2013	D	D	D	D	D	D	D
2014	D	D	D	D	D	D	D
2015	D	D	D	D	D	D	D
2016	B	B	B	B	B	B	B
2017	E	E	E	D	D	B	B
2018	ns	ns	ns	ns	ns	ns	ns
2019	D	B	D	E	D	B	B
2020	D	D	D	D	D	D	D
2021	D	D	D	D	D	D	D
2022	D	D	D	D	D	ns	ns
2023	ns	ns	ns	ns	ns	ns	ns

Figure 8.12

Results of ordination and cluster analysis of megabenthic invertebrate assemblages from SBOO trawl stations sampled from 1995 through 2023. Data are limited to 10-minute trawls from summer surveys and presented as (A) nMDS ordination; (B) a dendrogram of main cluster groups; (C) a matrix showing distribution of cluster groups over time; n=number of hauls; SR=mean species richness; Abun=mean abundance; ns=not sampled.

Chapter 9

Contaminants in Marine Fishes

Chapter 9. Contaminants in Marine Fishes

INTRODUCTION

Bottom dwelling (demersal) fishes are collected by the City of San Diego (City) as part of the Ocean Monitoring Program to evaluate the presence of contaminants in their tissues, which may result from the discharge of wastewater through the Point Loma Ocean Outfall (PLOO) and South Bay Ocean Outfall (SBOO). Anthropogenic inputs to coastal waters can result in increased concentrations of pollutants within the local marine environment, which may subsequently accumulate in the tissues of fishes and their prey. Such accumulation occurs through the biological uptake and retention of chemicals derived via various exposure pathways, including the absorption of dissolved chemicals directly from seawater, and the ingestion/assimilation of pollutants contained in different food sources (Connell 1988, Cardwell 1991, Rand 1995, USEPA 2000). In addition, demersal fishes may accumulate contaminants through the ingestion of suspended particulates or sediments because of their proximity to the seafloor. For this reason, contaminant levels in the tissues of these bottom dwelling fishes throughout the Southern California Bight (SCB) are often linked to those found in the surrounding environment (Schiff and Allen 1997), thus making these types of assessments useful in biomonitoring programs.

This portion of the City's Ocean Monitoring Program consists of two components: (1) analyzing liver tissues from mostly trawl-caught fishes; (2) analyzing muscle tissues from fishes collected by hook and line (rig fishing). Species targeted by trawling activities (see Chapter 8) are considered representative of the general demersal fish community off San Diego. The chemical analysis of liver tissues in target species of these fishes is important for assessing population effects because this is the organ where contaminants typically bioaccumulate. In contrast, species targeted for capture by rig fishing represent fish that are more characteristic of a typical sport fisher's catch and are therefore considered to be of recreational and commercial importance, and thus directly relevant to human health concerns. Consequently, muscle samples are analyzed from these fishes as this is the tissue most often consumed by humans. All liver and muscle tissue samples collected were analyzed for contaminants specified in the National Pollutant Discharge Elimination System (NPDES) discharge permits that govern monitoring requirements for the PLOO and SBOO regions (see Chapter 1).

This chapter presents analysis and interpretation of all chemical analyses performed on the tissues of fishes collected in the PLOO and SBOO regions during 2022. No fish tissue samples were collected during 2023 due to a resource exchange granted by the San Diego Regional Water Quality Control Board for participation in the region-wide 2023 SCB sampling project (Bight'23). The primary goals of this chapter are to: (1) document levels of contaminant loading in local demersal fishes to establish if concentrations accumulate to levels that may degrade marine communities and/or be harmful to human health; (2) identify whether any contaminant bioaccumulation detected in local fishes is changing over time and if the health of fish is changing as a result; (3) identify potential natural and anthropogenic sources of pollutants to the San Diego coastal marine environment that may play a role in contaminant bioaccumulation.

MATERIALS AND METHODS

Fishes were collected in fall (October) 2022 from a total of nine trawl zones (TZ1–TZ9) and four rig fishing zones (RF1–RF4) that span the PLOO and SBOO monitoring regions (Figure 9.1). Each trawl zone represents an area centered on (within a 1-km radius of) one or two trawl stations as specified in Chapter 8. Trawl Zone 1 includes the “nearfield” area of PLOO stations SD10 and SD12, which are located just south and north of the outfall discharge site, respectively. Trawl Zone 2 includes the area surrounding northern “farfield” PLOO stations SD13 and SD14. Trawl Zone 3 represents the area surrounding “farfield” PLOO station SD8, which is located south of the outfall near the LA-5 dredged material disposal site. Trawl Zone 4 is the area surrounding “farfield” PLOO station SD7 located several kilometers south of the outfall. Trawl Zone 5 includes the area surrounding SBOO stations SD17 and SD18, which are located just south and north of the outfall discharge site, respectively. Trawl Zone 6 includes the area surrounding northern SBOO stations SD19 and SD20, while Trawl Zone 7 includes the area surrounding northern SBOO station SD21. Trawl Zone 8 represents the area surrounding southern SBOO station SD16, while Trawl Zone 9 represents the area surrounding southern SBOO station SD15. Rig Fishing Zones 1–4 represent the areas within a 1-km radius of the nominal coordinates for stations RF1, RF2, RF3, and RF4. Stations RF1 and RF3 are located within 1 km of the PLOO and SBOO discharge sites, respectively, and are considered the “nearfield” rig fishing sites. In contrast, station RF2 is located about 11 km northwest of the PLOO, while station RF4 is located about 13.2 km southeast of the SBOO. These two sites are considered “farfield” or reference stations for the analyses herein. Efforts to collect target species by trawl were limited to five 10-minute (bottom time) trawls per site, while rig fishing effort was limited to 5 hours at each station. Occasionally, insufficient numbers of target species are obtained despite this effort; during 2022, this resulted in inadequate amounts of tissue at Trawl Zone 9 to complete three full composite samples.

A total of 14 species of fish were collected for analysis of liver and muscle tissues during the 2022 survey (Table 9.1). Five different species of flatfish were collected from the nine trawl zones for analysis of liver tissues, including Pacific Sanddab (*Citharichthys sordidus*), Longfin Sanddab (*Citharichthys xanhostigma*), Hornyhead Turbot (*Pleuronichthys verticalis*), Fantail Sole (*Xytreurys liolepis*), and Spotted Turbot (*Pleuronichthys ritteri*). These flatfish were collected from regular trawls at the SBOO stations, and by alternative hook and line methods at the PLOO stations. California Scorpionfish (*Scorpaena guttata*) were also collected. An additional nine species of fish were collected for analysis of muscle tissues at the rig fishing stations using standard hook and line fishing techniques. These species included Vermilion Rockfish (*Sebastes miniatus*), Squarespot Rockfish (*Sebastes hopkinsi*), Starry Rockfish (*Sebastes constellatus*), Brown Rockfish (*Sebastes auriculatus*), California Scorpionfish (*Scorpaena guttata*), Gopher Rockfish (*Sebastes carnatus*), Copper Rockfish (*Sebastes caurinus*), Flag Rockfish (*Sebastes rubrivinctus*), and Treefish (*Sebastes serriceps*).

Only fishes with standard lengths ≥ 12 cm were retained to ensure the collection of sufficient tissue for analysis while minimizing total catch necessary. These fishes were sorted into three composite samples per station, with a minimum of three individuals in each composite. All fishes were wrapped in aluminum foil, labeled, sealed in re-sealable plastic bags, placed on dry ice, and then transported to the City’s Marine Biology Laboratory where they were stored at -20°C prior to dissection and tissue processing.

Tissue Processing and Chemical Analyses

All dissections were performed according to standard techniques for tissue analysis. A brief summary follows, but detailed methods are available in City of San Diego (2023). Prior to dissection, each fish was partially defrosted, cleaned with a paper towel to remove loose scales and excess mucus, and the standard length (cm) and weight (g) were recorded (Appendices J.1, J.2). Dissections were carried out on Teflon® pads that were cleaned between samples. The liver or muscle tissues from each fish were removed and placed in separate glass jars for each composite sample, sealed, labeled, and stored in a freezer at -20°C prior to chemical analyses.

All tissue analyses were performed at the City's Environmental Chemistry Laboratory. Detailed analytical protocols are available upon request. Briefly, all fish tissue samples were analyzed on a wet weight basis to determine the concentrations of 18 different trace metals, nine chlorinated pesticides and their constituents, 42 polychlorinated biphenyl compound congeners (PCBs), 13 polybrominated diphenyl ethers (PBDEs) and 24 polycyclic aromatic hydrocarbons (PAHs). Data were limited to values above the method detection limit (MDL) for each parameter (Appendix J.3). A variety of laboratory technical issues resulted in a number of non-reportable tissue chemistry data for the 2022 survey, see Appendices J.4–J.13.

Data Analyses

Data summaries for each parameter include detection rate, minimum, maximum, and mean values for all samples combined by species for each outfall region. All means were calculated using detected values only, with no substitutions made for non-detects (analyte concentrations < method detection limit (MDL)). Limiting analyses to detected values (i.e., excluding non-detects) is considered a conservative way of handling contaminant concentrations as it creates a strong upward bias in the data and respective summary statistics, and therefore may represent a worst-case scenario (e.g., see Helsel 2005a, b, 2006 for discussions of non-detect data). Results recorded with a qualifier of Detected, But Not Quantified (DNQ) were treated as detected values. Total chlordane, total DDT (tDDT), total hexachlorocyclohexane (tHCH), total PCB (tPCB), total polybrominated diphenyl ethers (tPBDE) and total PAH (tPAH) were calculated for each sample as the sum of all constituents with reported values for individual constituents.

For comparative historical analyses, data were limited as follows: (1) fall (October) surveys only; (2) data collected after 1994; (3) specific species feeding guilds (e.g., mixed sanddabs, mixed rockfish) (see Allen et al. 2002) or the most frequently collected species (City of San Diego 2020). Data collected from the PLOO region prior to 1995 were excluded due to incompatible methods used by the external contract lab at the time (see City of San Diego 2015). Barred Sand Bass were also included in the historical analyses because it was the only species collected at SBOO station RF3 in 1995. Missing data from 2018 and 2023 are due to resource exchange agreements with the San Diego Regional Water Quality Control Board for participation in the region-wide Bight'18 and Bight'23 sampling projects. Data analyses were performed using R (R Core Team 2022) using various functions within the zoo, reshape2, plyr, scales, tidyverse, vegan, psych, and ggpubr packages (Zeileis and Grothendieck 2005, Wickham 2007, 2011, 2019, Oksanen et al. 2019, Revelle 2019, Wickham et al. 2019, Kassambara 2020).

Contaminant levels in muscle tissue samples were compared to state, national, and international limits and standards to address seafood safety and public health issues. These included: (1) fish contaminant

goals for chlordane, DDT, methylmercury, selenium, and PCBs developed by the California Office of Environmental Health Hazard Assessment (OEHHA) (Klasing and Brodberg 2008); (2) action limits on the amount of mercury, DDT, and chlordane in seafood that can be sold for human consumption, which are set by the U.S. Food and Drug Administration (USFDA) (Mearns et al. 1991); (3) international standards for acceptable concentrations of various metals and DDT (Mearns et al. 1991).

All raw data for 2022 have been submitted to either the Regional Water Quality Control Board or the California Environmental Data Exchange Network (CEDEN) and will be provided upon request.

RESULTS

Contaminants in Fish Liver Tissues

Trace Metals

Ten of the 18 trace metals analyzed were detected in fish liver tissue samples from PLOO and SBOO trawl zones in 2022, including: arsenic, cadmium, chromium, copper, iron, manganese, mercury, selenium, thallium, and zinc (Table 9.2). Arsenic, cadmium, copper, iron, manganese, mercury, selenium, and zinc were detected in all fish liver samples at concentrations ≤ 120 ppm. Detection rates for chromium and thallium were slightly less at 7–36% per region at concentrations ≤ 2.11 ppm. Lead and silver were detected in 7% of liver samples from the SBOO region at concentrations ≤ 0.439 ppm but were not detected in samples from the PLOO region. Aluminum, antimony, barium, beryllium, nickel and tin were not detected in any fish liver tissue samples from either region during 2022.

Detection rates have been relatively high for several different metals in liver tissues of fishes collected at trawl zones since 1995 (Table 9.3). Cadmium, copper, iron, manganese, mercury, selenium, and zinc were detected in $\geq 88\%$ of all Sanddab, Scorpionfish, and Hornyhead Turbot liver samples analyzed from the PLOO and SBOO trawl zones over the past 28 years. Detection rates for other metals varied by species. For example, arsenic was detected in $\geq 87\%$ of all Sanddab and Hornyhead Turbot liver samples, but only 45% of Scorpionfish samples. Aluminum and barium were detected in 87% and 93% of all California Scorpionfish, respectively, and 42–60% of Sanddab and Hornyhead Turbot samples. Chromium, silver, and tin were detected in 74%, 74%, and 57% of Hornyhead Turbot samples, respectively, and 23–57% of California Scorpionfish and Sanddab samples. Antimony, beryllium, lead, nickel, and thallium were detected in $\leq 30\%$ of all samples from both regions.

Metal concentrations have also been highly variable over these past 28 years, with most being detected within ranges reported elsewhere in the SCB (e.g., Mearns et al. 1991, CLA 2023, OCS 2024, McLaughlin et al 2020). While relatively high values of various metals have been occasionally recorded in liver tissues from fishes collected from nearfield zones, when compared to farfield zones, there were no discernable intra-species patterns that could be associated with proximity to either outfall (Figure 9.2, Appendix J.14).

Pesticides

Five chlorinated pesticides were detected in fish liver tissue samples from PLOO or SBOO trawl zones in 2022 (Table 9.4). Total DDT was detected in all samples in both regions, at concentrations ≤ 230.8 ppb. Total chlordane, hexachlorobenzene (HCB) and total HCH were detected in 100% of the PLOO samples and 60% of the SBOO samples, at concentrations ≤ 8.8 ppb. Dieldrin was only detected in 8%

of the Sanddab tissues from the PLOO region, at concentrations ≤ 6.9 ppb. The pesticides (or pesticide constituents) mirex, aldrin, *alpha*-endosulfan, *beta*-endosulfan, endosulfan sulfate, endrin, and endrin aldehyde were analyzed but not detected in any liver samples from fishes collected from either region.

DDT was the most frequently detected pesticide in liver tissues from trawl-zone fishes since 1995 with rates between 98–99% per species (or species group) (Table 9.5). In contrast, long-term detection rates were 6–39% for HCB, 1–34% for total chlordane, 0–9% for total HCH, $\leq 1\%$ for mirex and $\leq 2\%$ for aldrin, dieldrin, and endrin. In contrast, endrin aldehyde, *alpha*-endosulfan, *beta*-endosulfan, endosulfan sulfate, and toxaphene have been analyzed but never detected in any liver tissue samples from PLOO or SBOO trawl zones. As with metals, pesticide concentrations have been highly variable over time, with most being detected at levels within ranges reported elsewhere in the SCB (e.g., Allen et al. 1998, 2002, Mearns et al. 1991, LACSD 2022, McLaughlin et al 2020). While relatively high values of various pesticides have been occasionally recorded in liver tissues from nearfield zones, when compared to farfield zones, there were no discernable intra-species patterns that could be associated with proximity to either outfall (Figure 9.3, Appendix J.15).

PCBs

PCBs were detected in all fish liver tissue samples from PLOO and SBOO trawl zones in 2022, at concentrations ≤ 258.1 ppb (Table 9.4). Since 1995, PCBs have been detected in 93–99% of the liver samples from Sanddabs and Scorpionfish, and in 47% of the liver samples from Hornyhead Turbot (Table 9.5), with total PCB concentrations generally within ranges reported elsewhere in the SCB (e.g., Allen et al. 1998, Mearns et al. 1991, LACSD 2022, McLaughlin et al 2020). There were no discernable intra-species patterns that could be associated with proximity to either outfall over the past 28 years (Figure 9.3).

PBDEs

PBDEs were detected in all fish liver tissue samples from PLOO and 87% of fish liver tissue samples from SBOO trawl zones in 2022, at concentrations ≤ 112.2 ppb (Table 9.4). Since this is the first year reporting on PBDEs, no temporal evaluation could be completed. Recorded values for individual PBDE congeners were generally within ranges reported elsewhere in the SCB (Maruya et al 2012). For example, mean concentrations of BDE-47 were 17.7 ppb in Hornyhead Turbot livers from SBOO trawl stations in 2022, versus 156.0 ppm in Hornyhead Turbot livers collected from across the SCB in 2012.

PAHs

PAHs were detected in just 17% of liver tissue samples from PLOO trawl zones, and were not detected in liver tissues from SBOO trawl zones, during 2022 (Table 9.4). Concentrations of total PAH were ≤ 96 ppb. Historically, PAHs have been detected in $\leq 13\%$ of the liver tissue samples from Sanddabs, Scorpionfish, and Hornyhead Turbot analyzed since 1995 (Table 9.5), with total PAH concentrations generally within ranges reported elsewhere in the SCB (e.g., Allen et al. 1998, Mearns et al. 1991, LACSD 2022). There were no discernable intra-species patterns that could be associated with proximity to either outfall during the years that PAH was analyzed (Appendix J.15).

Contaminants in Fish Muscle Tissues

Trace Metals

Eleven of the 18 trace metals analyzed were detected in fish muscle tissue samples from PLOO and SBOO rig fishing zones in 2022, including: arsenic, cadmium, chromium, copper, iron, manganese,

mercury, selenium, thallium, and zinc (Table 9.6). Arsenic, cadmium, chromium, copper, mercury, selenium, and zinc were detected in all muscle samples. Detection rates for iron, manganese, nickel, and thallium were 17–100% per region. Tin was found in 17% of the muscle tissue samples from the SBOO region but was not detected in muscle tissue samples from the PLOO region. Aluminum, antimony, barium, beryllium, lead, and silver were analyzed but not detected in any muscle tissue samples from either region during 2022.

Detection rates have been relatively high for several different metals in muscle tissues of fishes captured at rig fishing zones since 1995 (Table 9.7). For example, arsenic, copper, iron, mercury, selenium, and zinc were detected in $\geq 63\%$ of all California Scorpionfish and rockfish muscle samples analyzed from the PLOO and SBOO rig fishing over the past 28 years. Aluminum, barium, cadmium, chromium, manganese, and tin were detected in 24–78% of all California Scorpionfish and rockfish muscle samples from both regions, while antimony, beryllium, lead, nickel, silver, and thallium were detected in $\leq 29\%$ of muscle samples from these species. In contrast to California Scorpionfish and mixed rockfish, iron, mercury, selenium, and zinc were the only metals detected in Barred Sand Bass muscle samples during the limited period this species was targeted. Metal concentrations in muscle tissues of San Diego fishes have been highly variable, but consistently lower than in liver tissues and within ranges reported elsewhere in the SCB (Mearns et al. 1991, CLA 2023, LACSD 2022, OCSD 2024, McLaughlin et al 2020). While relatively high values of various metals have been occasionally recorded in muscle tissues of fishes collected off San Diego, there were no discernable patterns at the rig fishing zones, which could be associated with proximity to either the PLOO or the SBOO (Figure 9.4, Appendix J.16).

Of the 12 rockfish muscle tissue samples collected from PLOO and SBOO rig fishing zones in 2022, 75% exceeded the median international standard for arsenic (67–100% per zone) and 100% exceeded this standard for selenium (Table 9.8). The OEHHA limit for mercury was exceeded in 33% of the samples from PLOO and SBOO farfield zones (RF2 and RF4, respectively), but all samples were below the USFDA mercury action limit. The OEHHA limit for total PCB was exceeded in 100% of samples from PLOO nearfield station RF1. All samples were below the OEHHA limit for total chlordane, total DDT, and selenium. Since 1995, median international standards were exceeded for arsenic (49–74% per zone), chromium ($\leq 4\%$ per zone), mercury (1–6% per zone), and selenium (29–76% per zone). Cadmium, copper, lead, tin, and zinc were never found at concentrations above their median international standards. Over this period, the OEHHA fish contaminant goals were exceeded for mercury (9–22% per zone), but not for selenium. The USFDA action limit for mercury was exceeded for just 1% of the samples from SBOO farfield zone RF4.

Pesticides

Four chlorinated pesticides were detected in fish muscle tissue samples from PLOO or SBOO rig fishing zones in 2022 (Table 9.9). Total DDT was detected in all PLOO and SBOO muscle tissue samples, at concentrations ≤ 6.4 ppb. For PLOO samples, total HCH was detected at a rate of 33% at concentrations ≤ 0.05 ppb, while HCB was detected at a rate of 100% at concentrations ≤ 0.20 ppb, and total chlordane was detected at a rate of 17% at concentrations ≤ 0.17 ppb. The latter three pesticides were not detected in any muscle tissue samples from SBOO rig fishing zones. Additionally, the pesticides (or pesticide constituents) aldrin, *alpha*-endosulfan, *beta*-endosulfan, dieldrin, endosulfan sulfate, endrin aldehyde, and mirex were not detected in any muscle samples from fishes collected from either region. None of the detected pesticide values from the past two years exceeded median international standards, OEHHA fish contaminant goal, or the USFDA action limits (Table 9.8).

Historically, only six pesticides have been found in muscle tissues from Barred Sand Bass, California Scorpionfish, and mixed rockfish samples from the PLOO or SBOO rig fishing zones (Table 9.10). Longterm detection rates were 50–93% per species (or species group) for DDT, $\leq 12\%$ for HCB, $\leq 3\%$ for total chlordane, and $\leq 2\%$ for total HCH, dieldrin and endrin. Other pesticides such as aldrin, *alpha*-endosulfan, *beta*endosulfan, , endrin aldehyde, endosulfan sulfate, mirex, and toxaphene have never been detected in muscle tissue samples from these species collected from the PLOO or SBOO regions over the past 28 years. As with metals, pesticides also typically occurred in lower concentrations in muscle tissues compared to liver tissue, and most were detected at levels within ranges reported elsewhere in the SCB (e.g., Allen et al. 1998, 2002, Mearns et al. 1991, CLA 2023, McLaughlin et al 2020). While relatively high values of various pesticides have been occasionally recorded in muscle tissues of fishes collected off San Diego, there were no discernable patterns at the rig fishing zones, which could be associated with proximity to either the PLOO or the SBOO (Figure 9.5, Appendix J.17).

Among the various detected pesticides, the rate of threshold exceedances for the current reporting period were similar to those observed previously (1995–2021) (Table 9.8). Since 1995, median international standards for total chlordane, total DDT, and hexachlorobenze, the OEHHA fish contaminant goal for total chlordane, and the USFDA action limits for total DDT and hexachlorobenze were never exceeded, while the OEHHA fish contaminant goal for total DDT was exceeded in $\leq 18\%$ of samples per zone.

PCBs

During 2022, PCBs were detected in all muscle tissue samples from PLOO and SBOO rig fishing zones, at concentrations ≤ 5.8 ppb (Table 9.9). All samples from PLOO zone RF1 had total PCB levels in exceedance of the OEHHA threshold of 3.6 ppb (Table 9.8). Historically, PCB detection rates were 21–75% per species (or species group) in muscle tissue samples, with highly variable concentrations falling within ranges reported elsewhere in the SCB (e.g., Allen et al. 2002, Mearns et al. 1991, LACSD 2022, OCSD 2024, McLaughlin et al 2020) and with no discernable patterns that could be associated with proximity to either outfall (Table 9.10, Figure 9.5). From 1995 through 2021, the OEHHA fish contaminant goal was exceeded in 4–27% of samples collected per zone (Table 9.8).

PBDEs

PBDEs were detected in all fish muscle tissue samples from PLOO and 83% of fish liver tissue samples from SBOO trawl zones in 2022, at concentrations ≤ 3.1 ppb (Table 9.4). Since this is the first year reporting on PBDEs, no temporal evaluation could be completed. Recorded values for individual PBDE congeners were generally within ranges reported elsewhere on the California coast (Brown et al. 2006).

PAHs

During 2022, PAHs were detected in 17% of the muscle tissue samples from PLOO, at concentrations ≤ 96.5 ppb (Table 9.9). PAHs were not detected in muscle tissues from fishes collected at SBOO rig fishing zones in 2022. Historically, PAH detection rates were 0–8% per species (or species group) in muscle tissue samples, with highly variable concentrations falling within ranges reported elsewhere in the SCB (e.g., Allen et al. 2002, Mearns et al. 1991, LACSD 2022, OCSD 2024) and with no discernable patterns that could be associated with proximity to either outfall (Table 9.10, Appendix J.17).

DISCUSSION

Several trace metals, pesticides, PCBs, PBDEs and PAHs were detected in liver tissues from various fish species collected in the Point Loma and South Bay monitoring regions in 2022. Many of the same metals, pesticides, PCBs, and PAHs were detected during this reporting period, as have been documented historically in California Scorpionfish and rockfish muscle tissues, albeit generally less frequently and/or in lower concentrations. Although tissue contaminant concentrations varied among different species of fish and across stations, most values were within ranges reported previously for southern California fishes (e.g., Mearns et al. 1991, Allen et al. 1998, 2002, CLA 2023, LACSD 2022, OCSD 2024, McLaughlin et al 2020). During 2022, arsenic and selenium were found to exceed their median international standards for human consumption in all of the muscle tissue samples from sport fish collected from PLOO and SBOO rig fishing zones. In contrast, all muscle tissue samples had concentrations of mercury, total chlordane, and total DDT below USFDA action limits. Historically, elevated levels of such contaminants have remained uncommon in sport fish collected from both survey areas.

The frequent occurrence of different trace metals and chlorinated hydrocarbons in the tissues of fish collected from the PLOO and SBOO regions is likely influenced by multiple factors. For example, many metals occur naturally in the environment, although little information is available on background levels in fish tissues. Brown et al. (1986) determined that there may be no area in the SCB sufficiently free of chemical contaminants to be considered a reference site, while Mearns et al. (1991) described the distribution of several contaminants, such as arsenic, mercury, DDT, and PCBs as being ubiquitous. The wide-spread distribution of contaminants in SCB fishes has been supported by more recent work regarding PCBs and DDT (e.g., Allen et al. 1998, 2002).

Other factors that affect contaminant loading in fish tissues include the physiology and life history of different species (see Groce 2002). Exposure to contaminants can also vary greatly between different species and among individuals of the same species depending on migration pathways (Otway 1991). Fishes may be exposed to contaminants in a highly polluted area and then move into areas free of contamination. For example, California Scorpionfish tagged in Santa Monica Bay have been recaptured as far south as the Coronado Islands (Hartmann 1987, Love et al. 1987). This is of particular concern for fishes collected in the vicinity of the PLOO and the SBOO, as there are many point and non-point sources that may contribute to local contamination in the region, including the San Diego River, San Diego Bay, Tijuana River, and offshore dredged material disposal sites (see Chapters 2–7 and Parnell et al. 2008). However, assessments of contaminant loading in San Diego offshore sediments have revealed no evidence to indicate that the PLOO or SBOO are major sources of pollutants in the region (see Chapters 5, 7, and Parnell et al. 2008).

Overall, there was no evidence of contaminant accumulation in PLOO or SBOO fishes during 2022 that could be associated with wastewater discharge from either outfall, which is consistent with historical findings. Concentrations of most contaminants were generally similar across trawl or rig fishing zones, and no relationships with the PLOO or SBOO were evident. These results are consistent with findings of other assessments of bioaccumulation in fishes off San Diego (Parnell et al. 2008, City of San Diego 2022). Finally, there were no other indications of poor fish health in the region, such as the presence of fin rot or other indicators of disease (see Chapter 8).

LITERATURE CITED

- Allen, M.J., S.L. Moore, K.C. Schiff, D. Diener, S.B. Weisberg, J.K. Stull, A. Groce, E. Zeng, J. Mubarak, C.L. Tang, R. Gartman, and C.I. Haydock. (1998). Assessment of demersal fish and megabenthic invertebrate assemblages on the mainland shelf of Southern California in 1994. Southern California Coastal Water Research Project, Westminster, CA.
- Allen, M.J., A.K. Groce, D. Diener, J. Brown, S.A. Steinert, G. Deets, J.A. Noblet, S.L. Moore, D. Diehl, E.T. Jarvis, V. Raco-Rands, C. Thomas, Y. Ralph, R. Gartman, D. Cadien, S.B. Weisberg, and T. Mikel. (2002). Southern California Bight 1998 Regional Monitoring Program: V. Demersal Fishes and Megabenthic Invertebrates. Southern California Coastal Water Research Project, Westminster, CA.
- Brown, D.A., R.W. Gossett, G.P. Hershelman, C.G. Word, A.M. Westcott, and J.N. Cross. (1986). Municipal wastewater contamination in the Southern California Bight: Part I — Metal and Organic Contaminations in Sediments and Organisms. *Marine Environmental Research*, 18:291–310
- Brown, F.R., J. Winkler, P. Visita, J. Dhaliwal, and M. Petreas. (2006). Levels of PBDEs, PCDDs, PCDFs, and coplanar PCBs in edible fish from California coastal waters. *Chemosphere Vol 4*, 2:276–286.
- Cardwell, R. D. (1991). Methods for evaluating risks to aquatic life and human health from exposure to marine discharges of municipal wastewaters. Pages 253–252 in A. G. Miskiewicz (ed.). *Proceedings of a Bioaccumulation Workshop: Assessment of the Distribution, Impacts, and Bioaccumulation of Contaminants in Aquatic Environments*. Australian Marine Science Association, Inc./WaterBoard.
- [CLA] City of Los Angeles, Environmental Monitoring Division. (2023). *Marine Monitoring in Santa Monica Bay: Biennial Assessment Report for the Period January 2021 through December 2022*. Report submitted to USEPA and RWQCB (Los Angeles). Department of Public Works, LA Sanitation, Hyperion Treatment Plant, Playa del Rey, California, pp. 1–220 + appendices.
- City of San Diego. (2015). *Point Loma Ocean Outfall Annual Receiving Waters Monitoring and Assessment Report, 2014*. City of San Diego Ocean Monitoring Program, Public Utilities Department, Environmental Monitoring and Technical Services Division, San Diego, CA.
- City of San Diego. (2020). *Biennial Receiving Waters Monitoring and Assessment Report for the Point Loma and South Bay Ocean Outfalls, 2018–2019*. City of San Diego, Public Utilities Department, Environmental Monitoring and Technical Services Division, San Diego, CA.
- City of San Diego. (2022). Appendix C5. Bioaccumulation Assessment. In: *Application for Renewal of NPDES CA0107409 and 301(h) Modified Secondary Treatment Requirements Point Loma Ocean Outfall. Volume V, Appendix C*. Public Utilities Department, Environmental Monitoring and Technical Services Division, San Diego, CA.

- City of San Diego. (2023). Quality Assurance Project Plan for Coastal Receiving Waters Monitoring. City of San Diego Ocean Monitoring Program, Public Utilities Department, Environmental Monitoring and Technical Services Division, San Diego, CA.
- Connell, D. W. (1988). Bioaccumulation behavior of persistent organic chemicals with aquatic organisms. *Review of Environmental Contamination and Toxicology*, 101:117–154.
- Groce, A.K. (2002). Influence of life history and lipids on the bioaccumulation of organo-chlorines in demersal fishes. Master's thesis. San Diego State University. San Diego, CA.
- Hartmann, A.R. (1987). Movement of scorpionfishes (Scorpaenidae: Sebastes and Scorpaena) in the Southern California Bight. *California Fish and Game*, 73: 68–79.
- Helsel, D.R. (2005a). More than obvious: better methods for interpreting nondetect data. *Environmental Science & Technology* (October 15, 2005), 419A–423A.
- Helsel, D.R. (2005b). *Nondetects and Data Analysis: Statistics for Censored Environmental Data*. John Wiley, New York.
- Helsel, D.R. (2006). Fabrication data: how substituting values for nondetects can ruin results, and what can be done about it. *Chemosphere* 65: 2434–2439.
- Kassambara, A. (2020). ggpubr: 'ggplot2' Based Publication Ready Plots. R package version 0.2.5 [https://CRAN.R-project.org/package = ggpubr](https://CRAN.R-project.org/package=ggpubr).
- Klasing, S. and R. Brodberg. (2008). Development of Fish Contaminant Goals and Advisory Tissue Levels for Common Contaminants in California Sport Fish: Chlordane, DDTs, Dieldrin, Methylmercury, PCBs, Selenium, and Toxaphene. California Environmental Protection Agency, Office of Environmental Health Hazard Assessment, Sacramento, CA.
- [LACSD] Los Angeles County Sanitation District. (2022). Joint Water Pollution Control Plant Biennial Receiving Water Monitoring Report 2020–2021. Los Angeles, CA.
- Love, M.S., B. Axell, P. Morris, R. Collins, and A. Brooks. (1987). Life history and fishery of the California scorpionfish, *Scorpaena guttata*, within the Southern California Bight. *Fisheries Bulletin*, 85: 99–116.
- Maruya, K.A, D.E Vidal-Dorsch, S.M. Bay, J.W. Kwon, K. Xia, and K.L. Armbrust. (2012). Organic contaminants of emerging concern in Southern California coastal waters. *Environ, Toxicol. Chem* 2012; 31:2683–2688.
- McLaughlin, K., K. Schiff, B. Du, J. Davis, A. Bonnema, G. Ichikawa, B. Jakl, and W. Heim. (2020). Southern California Bight 2018 Regional Monitoring Program: Volume V. Contaminant Bioaccumulation in Edible Sport Fish Tissue. Technical Report 1155. Southern California Coastal Water Research Project. Costa Mesa, CA.

- Mearns, A.J., M. Matta, G. Shigenaka, D. MacDonald, M. Buchman, H. Harris, J. Golas, and G. Lauenstein. (1991). Contaminant Trends in the Southern California Bight: Inventory and Assessment. NOAA Technical Memorandum NOS ORCA 62. Seattle, WA.
- Oksanen, J., F.G. Blanchet, R. Kindt, P. Legendre, P.R. Minchin, R.B. O'Hara, G.L. Simpson, P. Solymos, M.H.H. Stevens, and H. Wagner. (2019). *vegan*: Community Ecology Package. R package version 2.5–6. <http://CRAN.R-project.org/package=vegan>.
- [OCSD] Orange County Sanitation District. (2024). Marine Monitoring Annual Report, Program Year 2022 – 2023. Fountain Valley, CA.
- Otway, N. (1991). Bioaccumulation studies on fish: choice of species, sampling designs, problems and implications for environmental management. In: A.G. Miskiewicz (ed.). *Proceedings of a Bioaccumulation Workshop: Assessment of the Distribution, Impacts, and Bioaccumulation of Contaminants in Aquatic Environments*. Australian Marine Science Association, Inc./Water Board.
- Parnell, P.E., A.K. Groce, T.D. Stebbins, and P.K. Dayton. (2008). Discriminating sources of PCB contamination in fish on the coastal shelf off San Diego, California (USA). *Marine Pollution Bulletin*, 56: 1992–2002.
- R Core Team. (2022). *R: A language and environment for statistical computing*. R Foundation for Statistical Computing, Vienna, Austria. URL <https://www.R-project.org/>
- Rand, G.M., ed. (1995). *Fundamentals of Aquatic Toxicology: Effects, Environmental Fate, and Risk Assessment*. 2nd ed. Taylor and Francis, Washington, D.C.
- Revelle, W. (2019). *psych: Procedures for Personality and Psychological Research*, Northwestern University, Evanston, Illinois, USA, <https://CRAN.R-project.org/package=psych> Version = 1.9.12.31.
- Schiff, K. and M.J. Allen. (1997). Bioaccumulation of chlorinated hydrocarbons in livers of flatfishes from the Southern California Bight. In: S.B. Weisberg, C. Francisco, and D. Hallock (eds.). *Southern California Coastal Water Research Project Annual Report 1995–1996*. Southern California Coastal Water Research Project, Westminster, CA.
- [USEPA] United States Environmental Protection Agency. (2000). *Bioaccumulation Testing and Interpretation for the Purpose of Sediment Quality Assessment. Status and Needs*. EPA-823-R-00-001. U.S. Environmental Protection Agency. February 2000.
- Wickham, H. (2007). Reshaping Data with the reshape Package. *Journal of Statistical Software*, 21(12), 1–20. URL <http://www.jstatsoft.org/v21/i12/>.
- Wickham, H. (2011). The Split-Apply-Combine Strategy for Data Analysis. *Journal of Statistical Software*, 40(1), 1–29. URL <http://www.jstatsoft.org/v40/i01/>.
- Wickham, H. (2019). *Scales: Scale Functions for Visualization* Rstudio. R package version 1.1.0. <https://scales.r-lib.org/>.

Wickham, H., M. Averick, J. Bryan, W. Chang, L. D'Agostino McGowan, R. François, G. Golemund, A. Hayes, L. Henry, J. Hester, M. Kuhn, T. Lin Pedersen, E. Miller, S. Milton Bache, K. Müller, J. Ooms, D. Robinson, D. P. Seidel, V. Spinu, K. Takahashi, D. Vaughan, C. Wilke, K. Woo, H. Yutani. (2019). Welcome to the tidyverse. *Journal of Open Source Software*, 4(43), 1686, <https://doi.org/10.21105/joss.01686>.

Zeileis, A and G. Grothendieck. (2005). zoo: S3 Infrastructure for Regular and Irregular Time Series. *Journal of Statistical Software*, 14(6), 1–27. URL <http://www.jstatsoft.org/v14/i06/>.

CHAPTER 9

FIGURES & TABLES

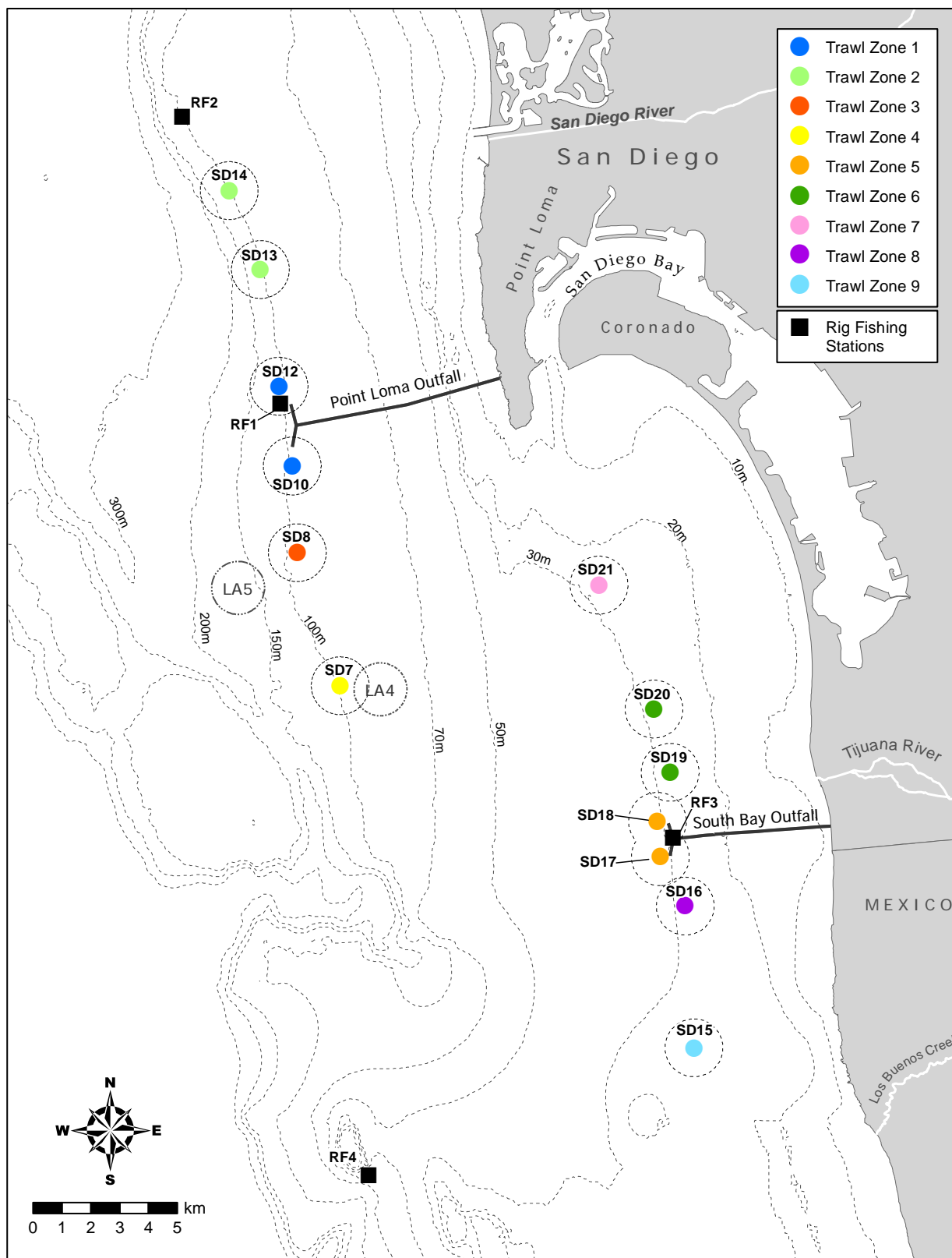


Figure 9.1

Trawl and rig fishing zone locations sampled around the PLOO and SBOO as part of the City of San Diego's Ocean Monitoring Program.

Table 9.1

Species of fish collected from each PLOO and SBOO trawl and rig fishing zone during 2022.

	Zone	Composite 1	Composite 2	Composite 3
PLOO	Rig Fishing Zone 1 (RF1)	Vermilion Rockfish	Vermilion Rockfish	Vermilion Rockfish
	Rig Fishing Zone 2 (RF2)	Squarespot Rockfish	Starry Rockfish	Mixed Rockfish ^a
	Trawl Zone 1 (TZ1)	Pacific Sanddab	Pacific Sanddab	Pacific Sanddab
	Trawl Zone 2 (TZ2)	Pacific Sanddab	Pacific Sanddab	Pacific Sanddab
	Trawl Zone 3 (TZ3)	Pacific Sanddab	Pacific Sanddab	Pacific Sanddab
	Trawl Zone 4 (TZ4)	Pacific Sanddab	Pacific Sanddab	Pacific Sanddab
SBOO	Rig Fishing Zone 3 (RF3)	Brown Rockfish	California Scorpionfish	Mixed Rockfish ^b
	Rig Fishing Zone 4 (RF4)	California Scorpionfish	Gopher Rockfish	Mixed Rockfish ^c
	Trawl Zone 5 (TZ5)	Longfin Sanddab	Longfin Sanddab	Hornyhead Turbot
	Trawl Zone 6 (TZ6)	Longfin Sanddab	Longfin Sanddab	Longfin Sanddab
	Trawl Zone 7 (TZ7)	Longfin Sanddab	Longfin Sanddab	Hornyhead Turbot
	Trawl Zone 8 (TZ8)	Longfin Sanddab	California Scorpionfish	Hornyhead Turbot
	Trawl Zone 9 (TZ9)	Hornyhead Turbot	Spotted Turbot	Fantail Sole ^d

^aincludes starry, flag, and copper rockfish; ^bincludes vermilion and gopher rockfish; ^cincludes treefish and gopher rockfish; ^dno metals or lipids were analyzed for this sample due to the collection of insufficient tissue

Table 9.2

Summary of metals (ppm) in liver tissues of fishes collected from PLOO and SBOO trawl zones during 2022. Data include the number of detected values (n), minimum, maximum, and mean detected concentrations for each species, and the total number of samples, detection rate, and maximum value for all species within each region. Minimum and maximum values were calculated based on all samples, whereas means were calculated from detected values only; nd = not detected.

	Al	Sb	As	Ba	Be	Cd	Cr	Cu	Fe	Pb	Mn	Hg	Ni	Se	Ag	Tl	Sn	Zn	
PLOO																			
Pacific Sanddab																			
n	0	0	12	0	0	12	1	12	12	0	12	12	0	12	0	3	0	12	
min	—	—	2.06	—	—	1.98	nd	3.17	74.0	—	0.52	0.080	—	1.26	—	nd	—	17.8	
max	—	—	3.82	—	—	5.11	0.199	5.17	111.0	—	1.33	0.199	—	1.76	—	1.35	—	26.9	
mean	—	—	3.04	—	—	3.32	0.199	4.55	92.3	—	0.96	0.112	—	1.47	—	1.24	—	23.2	
Total Samples	12	12	12	12	12	12	12	12	12	12	12	12	12	12	12	12	12	12	
Detection Rate (%)	0	0	100	0	0	100	8	100	100	0	100	100	0	100	0	25	0	100	
Max	nd	nd	3.82	nd	nd	5.11	0.199	5.17	111.0	nd	1.33	0.199	nd	1.76	nd	1.35	nd	26.9	
SBOO																			
CA Scorpionfish																			
n	0	0	1	0	0	1	0	1	1	0	1	1	0	1	0	0	0	1	
value	—	—	1.26	—	—	4.29	—	12.80	66.8	—	0.57	0.208	—	1.22	—	—	—	83.8	
Hornyhead Turbot																			
n	0	0	4	0	0	4	1	4	4	0	4	4	0	4	1	0	0	4	
min	—	—	4.63	—	—	3.70	nd	8.03	43.7	—	0.90	0.059	—	1.14	nd	—	—	52.2	
max	—	—	6.91	—	—	5.31	0.439	16.30	64.3	—	1.21	0.101	—	1.44	0.235	—	—	73.3	
mean	—	—	5.54	—	—	4.43	0.439	10.81	51.2	—	0.98	0.082	—	1.30	0.235	—	—	61.9	
Longfin Sanddab																			
n	0	0	8	0	0	8	0	8	8	0	8	8	0	8	0	5	0	8	
min	—	—	4.16	—	—	1.03	—	5.67	83.5	—	0.54	0.028	—	1.40	—	nd	—	18.4	
max	—	—	7.55	—	—	2.05	—	9.01	116.0	—	0.75	0.057	—	1.91	—	2.11	—	24.9	
mean	—	—	5.45	—	—	1.57	—	6.64	99.5	—	0.65	0.041	—	1.68	—	1.66	—	21.0	
Spotted Turbot																			
n	0	0	1	0	0	1	0	1	1	1	1	1	0	1	0	0	0	1	
value	—	—	8.20	—	—	0.58	—	8.85	120.0	0.49	1.25	0.040	—	1.96	—	—	—	46.2	
Total Samples	14	14	14	14	14	14	14	14	14	14	14	14	14	14	14	14	14	14	
Detection Rate (%)	0	0	100	0	0	100	7	100	100	7	100	100	0	100	7	36	0	100	
Max	nd	nd	8.20	nd	nd	5.31	0.439	16.30	120.0	0.49	1.25	0.208	nd	1.96	0.235	2.11	nd	83.8	

^aThis table has been updated from the 2022 Interim Report to reflect that metals were not analyzed for Fantail Sole (versus not detected)

Table 9.3

Summary of metals (ppm) in liver tissues of fishes collected from PLOO and SBOO trawl zones from 1995 through 2022. Data include the total number of samples (n), detection rate (DR%), minimum, maximum, and mean^a detected concentrations for each guild or species; nd = not detected.

	Al	Sb	As	Ba	Be	Cd	Cr	Cu	Fe	Pb	Mn	Hg	Ni	Se	Ag	Tl	Sn	Zn	
Mixed Sanddabs																			
PLOO	n	343	343	222	343	343	343	335	343	343	343	345	343	344	343	319	343	343	343
	DR%	57	15	91	55	94	57	100	100	17	98	90	17	98	23	25	50	100	100
	min	nd	nd	nd	nd	nd	nd	0.9	27	nd	nd	nd	nd	nd	nd	nd	nd	nd	8.61
	max	44.6	9.73	123	15.2	0.18	19.2	22.8	28.7	233	8.8	5.47	0.58	18.9	4.37	2.2	6.35	277	74.2
	mean	12.02	1.43	5.11	0.26	0.02	4.1	0.64	5.29	96.89	0.87	0.84	0.1	0.68	1.19	0.23	1.62	3.98	24.2
California Scorpionfish																			
n	105	105	105	43	105	105	105	105	105	105	105	107	105	107	105	105	105	105	105
DR%	87	11	45	93	10	94	54	100	100	14	88	94	25	99	41	14	26	100	100
min	nd	nd	nd	nd	nd	nd	nd	4.06	29.6	nd	nd	nd	nd	nd	nd	nd	nd	20.5	20.5
max	59.8	1.68	8.06	0.58	0.06	6.92	5.34	81.1	481	8.1	2.52	0.7	2.67	2.82	1.16	5.34	3.44	207	207
mean	13.55	0.85	2.25	0.09	0.01	2.66	0.92	22.85	177.84	1.41	0.58	0.18	0.42	0.89	0.31	4.16	1.29	97.24	97.24
Hornyhead Turbot																			
n	141	141	141	121	141	141	141	141	141	141	141	141	141	142	141	133	141	141	141
DR%	60	8	91	51	4	99	74	100	100	15	99	98	16	98	74	19	57	100	100
min	nd	nd	nd	nd	nd	nd	nd	2.30	19.40	nd	nd	nd	nd	nd	nd	nd	nd	23	23
max	27.8	1.77	25	0.29	0.02	12	7.67	41.7	263	3.30	3.21	0.41	4.61	3.38	1.32	3.84	88.2	233	233
mean	6.99	1.07	4.31	0.06	0.01	3.96	0.40	8.00	56.1	0.64	1.11	0.11	0.5	0.87	0.21	1.73	2.11	62.13	62.13
Longfin Sanddab																			
n	182	182	182	135	182	182	182	182	182	182	182	182	182	183	182	165	182	182	182
DR%	54	14	87	42	6	92	57	100	100	12	97	88	18	96	38	30	54	100	100
min	nd	nd	nd	nd	nd	nd	nd	1.38	33	nd	nd	nd	nd	nd	nd	nd	nd	10.30	10.30
max	49	2.38	12.1	0.6	0.04	9.31	3.56	23.2	449	14.3	2.01	0.44	1.59	2.3	1.63	2.74	4.61	109	109
mean	12.55	0.88	5.46	0.15	0.02	1.85	0.43	6.26	77.92	1.12	0.97	0.08	0.44	0.96	0.21	1.01	1.46	23.25	23.25

^a Minimum and maximum values were calculated based on all samples, whereas means were calculated from detected values only

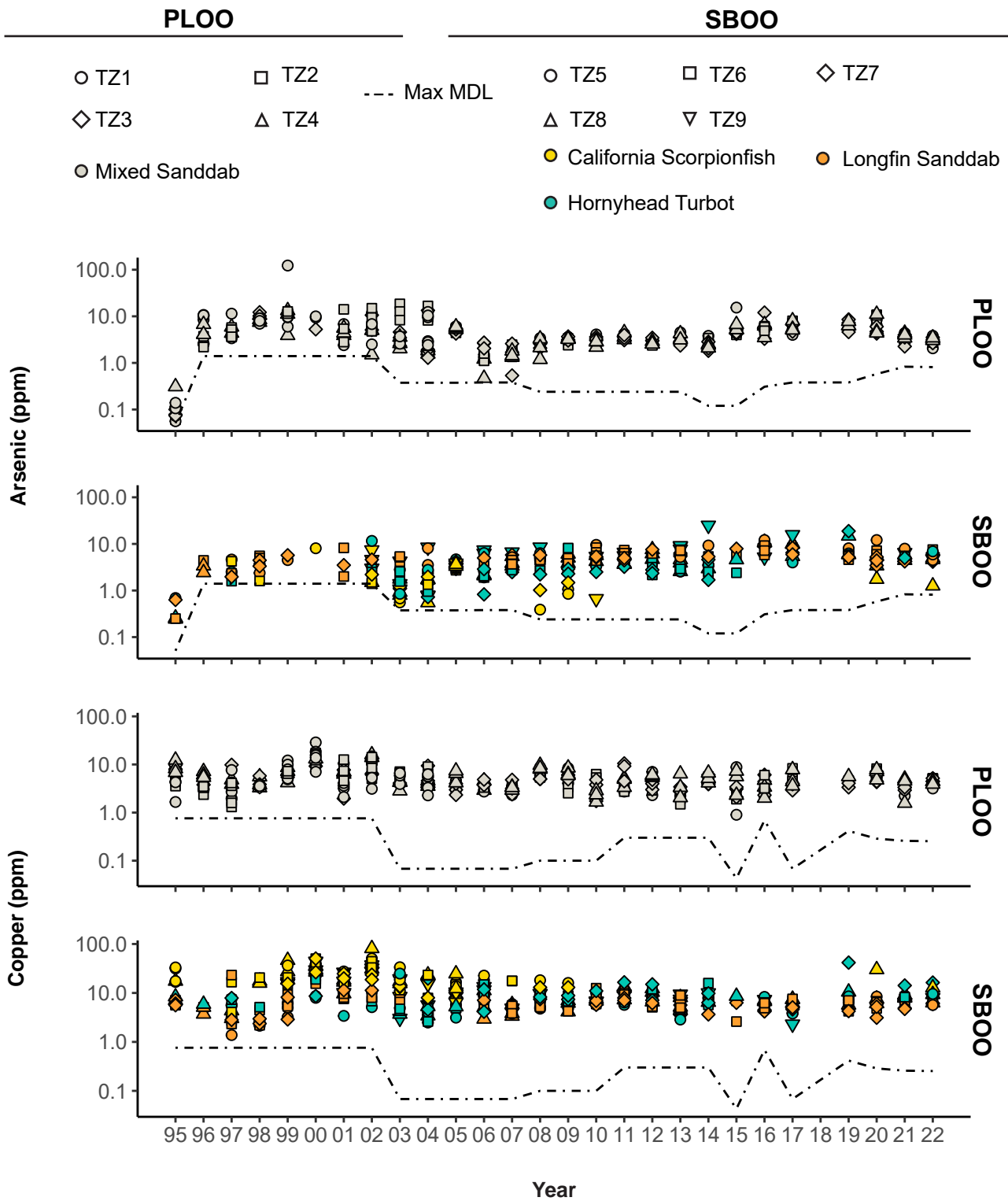


Figure 9.2
 Concentrations of select metals in liver tissues of fishes collected from PLOO and SBOO trawl zones from 1995 through 2022. Zones TZ1 and TZ5 are considered nearfield. No samples were collected in 2018 or 2023 as described in text.

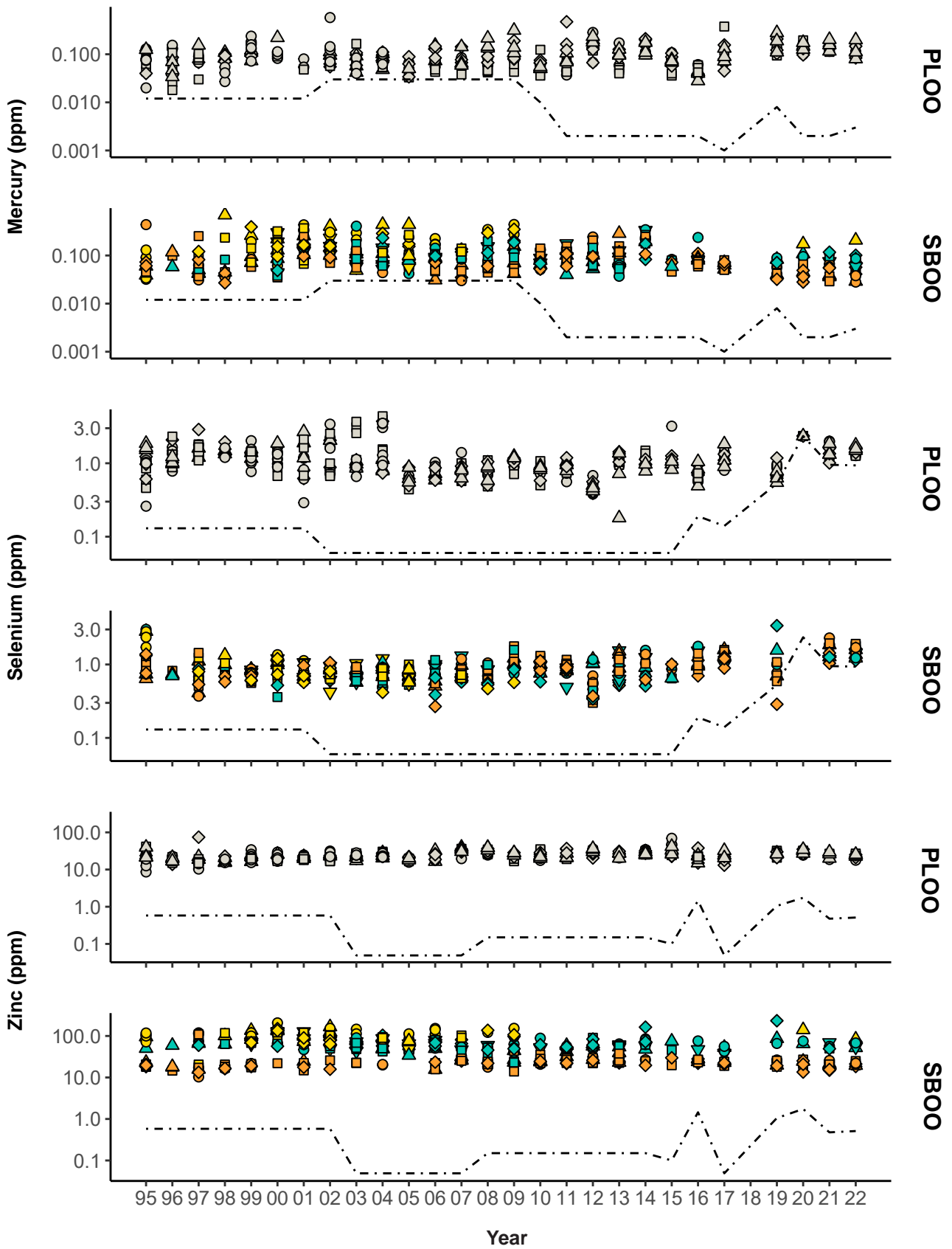


Figure 9.2 continued

Table 9.4

Summary of pesticides (ppb), total PCB (ppb), total PAH (ppb), total PBDE (ppb), and lipids (% weight) in liver tissues of fishes collected from PLOO and SBOO trawl zones during 2022. Data include the number of detected values (n), minimum, maximum, and mean detected concentrations for each species, and the total number of samples, detection rate and maximum value for all species within each region. Minimum and maximum values were based on all samples, whereas means were calculated from detected values only; nd=not detected; nr=not reportable, na=not analyzed.

	Pesticides					tPCB	tPAH	tPBDE	Lipids ^a
	tChlor	tDDT	HCB	tHCH	Dieldrin				
PLOO									
Pacific Sanddab									
n	12	12	12	12	1	12	1	12	12
min	1.65	71.2	2.93	1.33	nd	58.9	nd	14.29	25.4
max	8.80	150.0	5.43	2.51	6.9	258.1	96	51.77	47.4
mean	4.47	96.3	4.19	1.85	6.9	161.0	96	29.80	35.7
Total Samples	12	12	12	12	12	12	6	12	12
Detection Rate (%)	100	100	100	100	8	100	17	100	100
Max	8.80	150.0	5.43	2.51	6.9	258.1	96	51.77	47.4
SBOO									
CA Scorpionfish									
n	1	1	1	1	0	1	nr	1	1
value	3.32	183.3	0.86	0.67	—	115.6	—	84.10	17.7
Fantail Sole									
n	0	1	0	0	0	1	nr	0	na
value	—	6.2	—	—	—	1.3	—	—	—
Hornyhead Turbot									
n	0	4	0	0	0	4	0	4	4
min	—	12.4	—	—	—	3.6	—	20.59	5.8
max	—	19.7	—	—	—	21.3	—	52.94	8.6
mean	—	15.8	—	—	—	10.1	—	41.66	7.3
Longfin Sanddab									
n	8	8	8	8	0	8	0	8	8
min	1.36	95.9	1.68	1.40	—	53.7	—	36.92	38
max	5.72	230.9	2.82	1.62	—	173.1	—	112.60	47.2
mean	3.19	174.5	2.19	1.55	—	126.0	—	70.24	44.5
Spotted Turbot									
n	0	1	0	0	0	1	nr	0	1
value	—	3.9	—	—	—	25.5	—	—	2.2
Total Samples	15	15	15	15	15	15	8	15	14
Detection Rate (%)	60	100	60	60	0	100	0	87	100
Max	5.72	230.9	2.82	1.62	nd	173.1	nd	112.60	47.2

^aThis column has been updated from the 2022 Interim Report to reflect that lipids were not analyzed for Fantail Sole (versus not detected)

Table 9.5

Summary of pesticides (ppb), total PCB (ppb), total PAH (ppb), and lipids (% weight) in liver tissues of fishes collected from PLOO and SBOO trawl zones from 1995 through 2022. Data include total number of samples (n), detection rate (DR%), minimum, maximum, and mean^a detected concentrations per guild or species; nd=not detected; *tPBDE data only for 2022.

	Pesticides											tPAH	tPCB	tPBDE*	Lipids	
	Aldrin	tChlor	tDDT	Dieldrin	Endrin	HCB	tHCH	Mirex	tPCB	tPAH	tPBDE*					
Mixed Sanddab																
n	341	352	352	329	329	332	352	352	353	166	12	349				
DR%	0	34	98	2	0	29	9	0	99	13	100	100				
min	—	nd	nd	—	—	nd	nd	nd	nd	nd	14.29	6.9				
max	—	94	3800	15.8	—	120	22	48	3179.49	1353	51.77	69.6				
mean	—	15.34	675.61	6.31	—	7.37	3.63	48	422.06	206.68	29.8	37.41				
California Scorpionfish																
n	95	95	95	95	95	94	95	95	109	72	1	107				
DR%	2	14	98	2	2	6	4	0	93	0	100	100				
min	nd	nd	nd	nd	nd	nd	nd	—	nd	—	84.1	6.35				
max	19	122	15503	63	66	37.3	278	—	2187.9	—	84.10	45.4				
mean	12.05	32.54	1231.65	38.5	55	10.3	102.92	—	296.52	—	84.10	19.58				
Hornyhead Turbot																
n	144	147	147	142	142	141	147	147	149	128	4	146				
DR%	0	1	99	0	0	10	0	0	47	5	100	100				
min	—	nd	nd	—	—	nd	—	—	nd	nd	20.59	0.098				
max	—	32.04	2802	—	—	41	—	—	828.4	330.5	52.94	32.2				
mean	—	26.17	122.46	—	—	9.71	—	—	48.38	133.72	41.66	9.71				
Longfin Sanddab																
n	176	179	179	167	167	160	179	179	183	145	8	182				
DR%	0	23	99	0	0	39	6	1	99	3	100	100				
min	—	nd	nd	—	—	nd	nd	nd	nd	nd	36.92	6.15				
max	—	120	3600	—	—	51.3	3.2	2	6781.9	43167	112.6	62.4				
mean	—	9.14	598.94	—	—	4.11	1.81	1.75	508.59	8678.3	70.24	35.87				

^a Minimum and maximum values were based on all samples, whereas means were calculated from detected values only

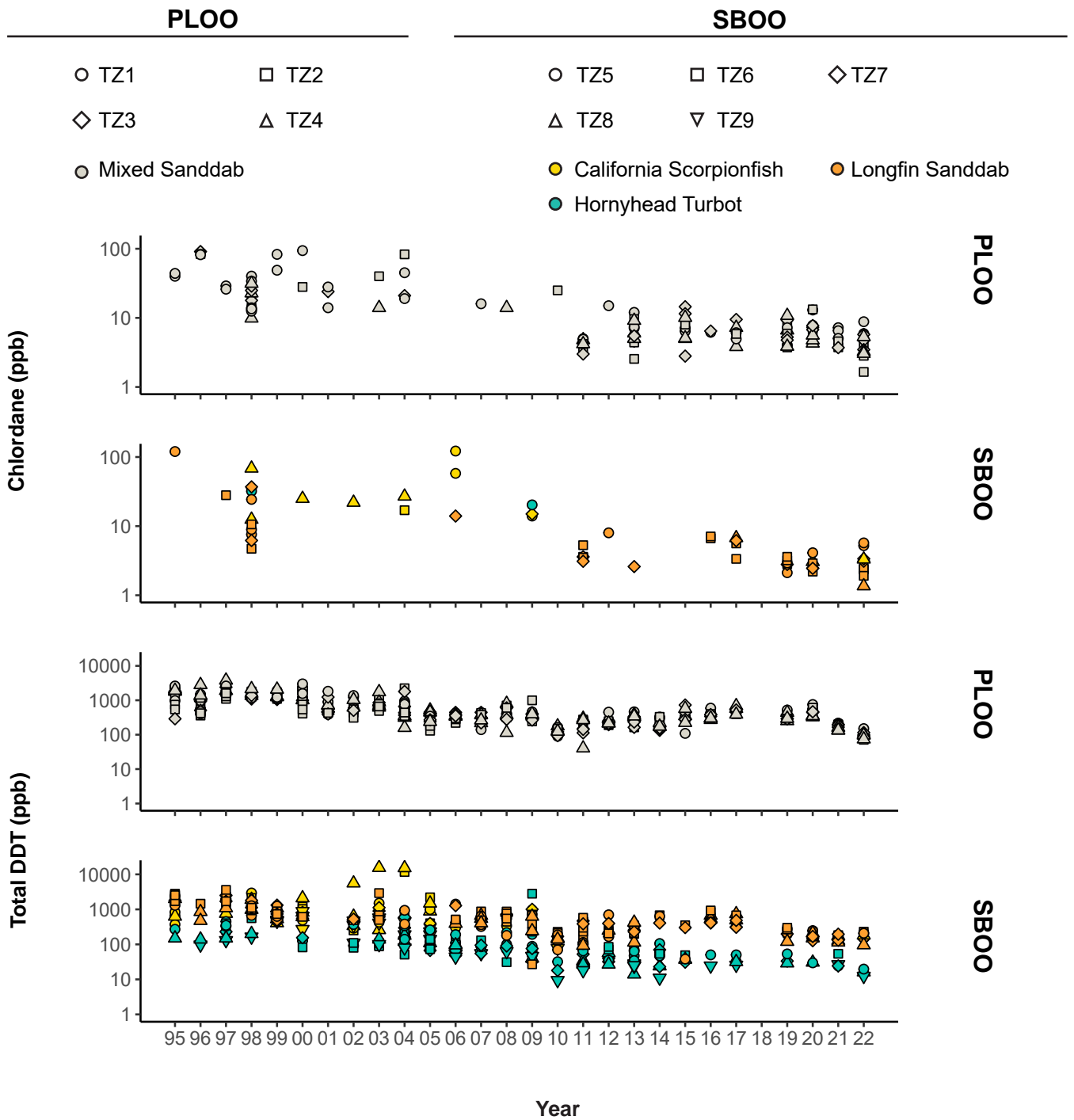


Figure 9.3

Concentrations of pesticides and total PCB in liver tissues of fishes collected from PLOO and SBOO trawl zones from 1995 through 2022. Zones TZ1 and TZ5 are considered nearfield. No samples were collected in 2018 and 2023 as described in text.

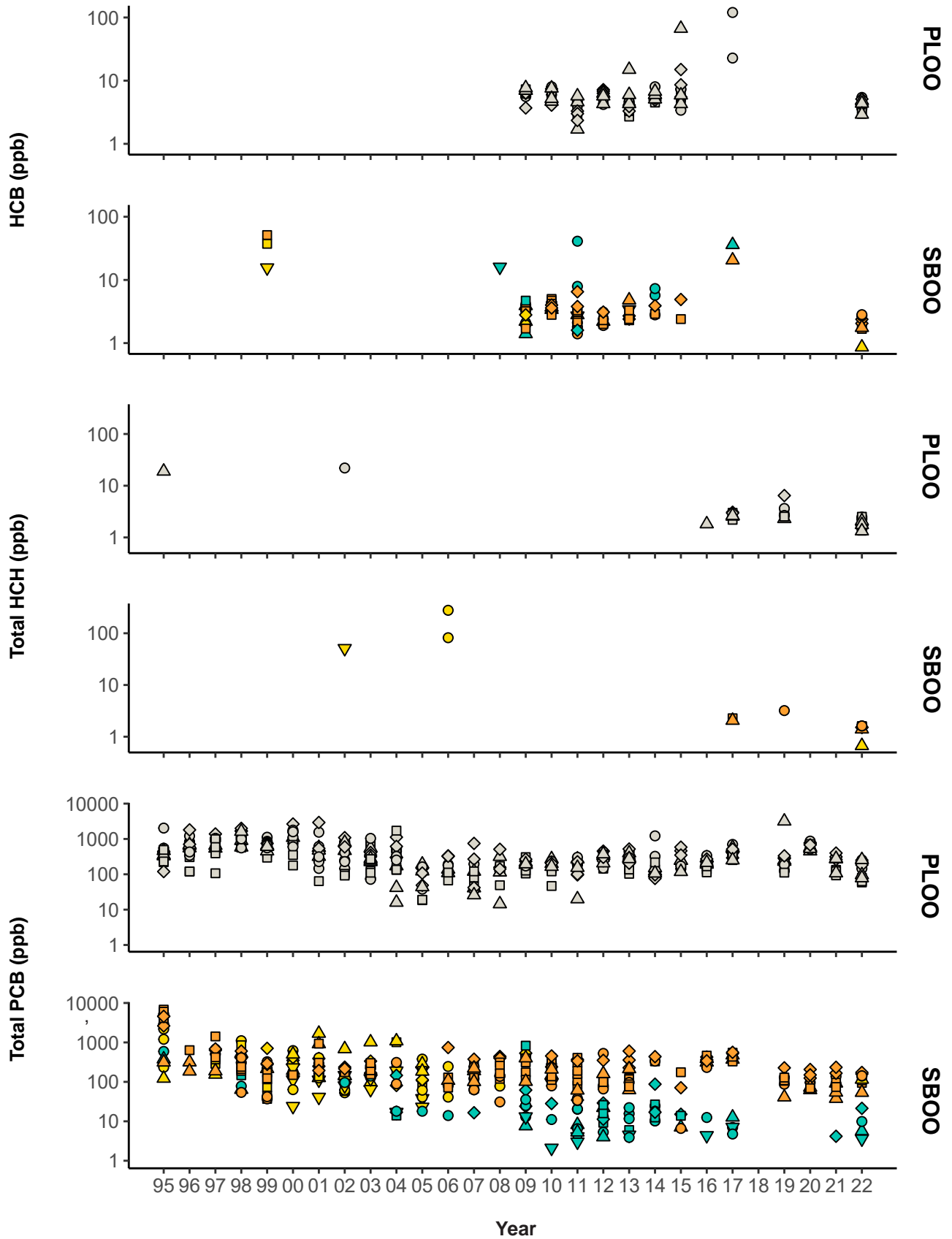


Figure 9.3 continued

Table 9.6

Summary of metals (ppm) in muscle tissues of fishes collected from PLOO and SBOO rig fishing zones during 2022. Data include the number of detected values (n), minimum, maximum, and mean detected concentrations per species and the total number of samples, detection rate, and maximum value for all species within each region. Minimum and maximum values based on all samples, whereas means were calculated from detected values only; nd=not detected.

	Al	Sb	As	Ba	Be	Cd	Cr	Cu	Fe	Pb	Mn	Hg	Ni	Se	Ag	Tl	Sn	Zn	
Mixed Rockfish																			
n	0	0	1	0	0	1	1	1	1	0	0	1	0	1	0	0	0	1	
value	—	—	1.99	—	—	0.029	0.089	0.374	1.14	—	—	0.149	—	0.674	—	—	—	3.61	
Squarespot Rockfish																			
n	0	0	1	0	0	1	1	1	1	0	0	1	1	1	0	1	0	1	
value	—	—	1.36	—	—	0.028	0.386	0.327	3.32	—	—	0.111	0.259	0.753	—	0.368	—	3.32	
Starry Rockfish																			
n	0	0	1	0	0	1	1	1	0	0	0	1	1	1	0	1	0	1	
value	—	—	1.57	—	—	0.023	0.119	0.263	—	—	—	0.224	0.038	0.689	—	0.358	—	3.14	
PLOO Vermilion Rockfish																			
n	0	0	3	0	0	3	3	3	2	0	1	2	1	3	0	1	0	3	
min	—	—	1.60	—	—	0.022	0.102	0.314	nd	—	nd	0.052	nd	0.463	—	nd	—	3.64	
max	—	—	3.44	—	—	0.044	0.158	0.433	6.11	—	0.135	0.093	0.056	0.799	—	0.386	—	4.32	
mean	—	—	2.65	—	—	0.033	0.130	0.392	3.84	—	0.135	0.073	0.056	0.640	—	0.386	—	4.09	
Total Samples	6	6	6	6	6	6	6	6	6	6	6	5	6	6	6	6	6	6	
Detection Rate (%)	0	0	100	0	0	100	100	100	67	0	17	100	50	100	0	50	0	100	
Max	nd	nd	3.44	nd	nd	0.044	0.386	0.433	6.11	nd	0.135	0.224	0.259	0.799	nd	0.386	nd	4.32	

Table 9.6 *continued*

	Al	Sb	As	Ba	Be	Cd	Cr	Cu	Fe	Pb	Mn	Hg	Ni	Se	Ag	Tl	Sn	Zn
Brown Rockfish																		
n	0	0	1	0	0	1	1	1	1	0	1	1	0	1	0	1	0	1
value	—	—	1.19	—	—	0.024	0.100	0.329	4.48	—	0.119	0.073	—	0.683	—	0.385	—	3.75
CA Scorpionfish																		
n	0	0	2	0	0	2	2	2	2	0	0	2	0	2	0	2	0	2
min	—	—	2.03	—	—	0.034	0.114	0.338	2.81	—	—	0.104	—	0.500	—	0.351	—	3.69
max	—	—	2.39	—	—	0.037	0.121	0.368	5.12	—	—	0.113	—	0.587	—	0.367	—	4.68
mean	—	—	2.21	—	—	0.036	0.118	0.353	3.97	—	—	0.109	—	0.544	—	0.359	—	4.19
Gopher Rockfish																		
n	0	0	1	0	0	1	1	1	1	0	0	1	0	1	0	1	0	1
value	—	—	2.73	—	—	0.043	0.114	0.258	3.71	—	—	0.205	—	0.721	—	0.340	—	3.68
Mixed Rockfish																		
n	0	0	2	0	0	2	2	2	2	0	1	2	1	2	0	2	1	2
min	—	—	1.40	—	—	0.025	0.159	0.249	7.52	—	nd	0.084	nd	0.667	—	0.375	nd	4.19
max	—	—	3.88	—	—	0.060	0.195	0.305	20.80	—	0.127	0.230	0.098	1.220	—	0.522	1.31	4.54
mean	—	—	2.64	—	—	0.043	0.177	0.277	14.16	—	0.127	0.157	0.098	0.944	—	0.449	1.31	4.37
Total Samples	6	6	6	6	6	6	6	6	6	6	6	6	6	6	6	6	6	6
Detection Rate (%)	0	0	100	0	0	100	100	100	100	0	33	100	17	100	0	100	17	100
Max	nd	nd	3.88	nd	nd	0.06	0.195	0.368	20.80	nd	0.127	0.230	0.098	1.220	nd	0.522	1.31	4.68

Table 9.7

Summary of metals (ppm) in muscle tissues of fishes collected from PLOO and SBOO rig fishing zones from 1995 through 2022. Data include the total number of samples (n), detection rate (DR%), minimum, maximum, and mean^a detected concentrations for each guild or species; nd = not detected.

	Al	Sb	As	Ba	Be	Cd	Cr	Cu	Fe	Pb	Mn	Hg	Ni	Se	Ag	Tl	Sn	Zn
Mixed Rockfish																		
n	148	148	148	104	148	148	148	148	148	148	148	145	148	148	148	136	148	148
DR%	33	8	86	42	3	29	57	63	78	3	36	97	12	97	5	15	36	99
min	nd	nd	nd	nd	nd	nd	nd	nd	nd	nd	nd	nd	nd	nd	nd	nd	nd	nd
max	22.1	1.11	13.5	0.19	0.04	0.18	1.78	8.96	257	0.42	5.3	0.79	0.38	0.88	0.5	2.93	2.12	5.9
mean	6.4	0.62	2.64	0.06	0.01	0.06	0.23	0.89	6.9	0.29	0.55	0.16	0.14	0.42	1.14	1.14	0.96	3.67
Barred Sand Bass																		
n	4	4	4	—	4	4	4	4	4	4	4	4	4	4	4	4	4	4
DR%	0	0	0	0	0	0	0	0	100	0	0	100	0	75	0	0	0	75
min	—	—	—	—	—	—	—	—	3.2	—	—	0.23	—	nd	—	—	—	0
max	—	—	—	—	—	—	—	—	6.65	—	—	0.36	—	0.71	—	—	—	5.01
mean	—	—	—	—	—	—	—	—	4.64	—	—	0.29	—	0.66	—	—	—	4.41
California Scorpionfish																		
n	84	84	84	51	84	84	84	84	84	84	84	84	84	84	84	78	84	84
DR%	37	1	74	33	5	24	48	70	81	5	25	96	8	87	4	21	29	100
min	nd	nd	nd	nd	nd	nd	nd	nd	nd	nd	nd	nd	nd	nd	nd	nd	nd	1.92
max	19.4	0.23	5.35	0.15	0.03	0.08	2.21	5.11	21.2	0.38	1.85	1.54	0.22	0.63	0.11	2.74	1.96	6.77
mean	6.49	0.23	2.39	0.06	0.01	0.04	0.27	1.01	5.17	0.28	0.18	0.19	0.1	0.27	0.09	0.97	0.84	3.93
Mixed Rockfish																		
n	67	67	67	58	67	67	67	67	67	67	67	67	67	67	67	62	67	67
DR%	31	13	93	45	0	30	78	76	75	3	49	96	16	96	3	29	48	100
min	nd	nd	nd	nd	—	nd	nd	nd	nd	nd	nd	nd	nd	nd	nd	nd	nd	1.42
max	16.1	1.57	11.2	0.2	—	0.2	0.81	3.8	20.8	0.44	2.6	0.33	0.73	1.22	0.07	2.87	2.43	6.16
mean	5.47	0.77	2.29	0.06	—	0.08	0.24	0.59	3.85	0.38	0.19	0.1	0.19	0.34	0.07	0.97	0.96	3.82

^aMinimum and maximum values were based on all samples, whereas means were calculated from detected values only

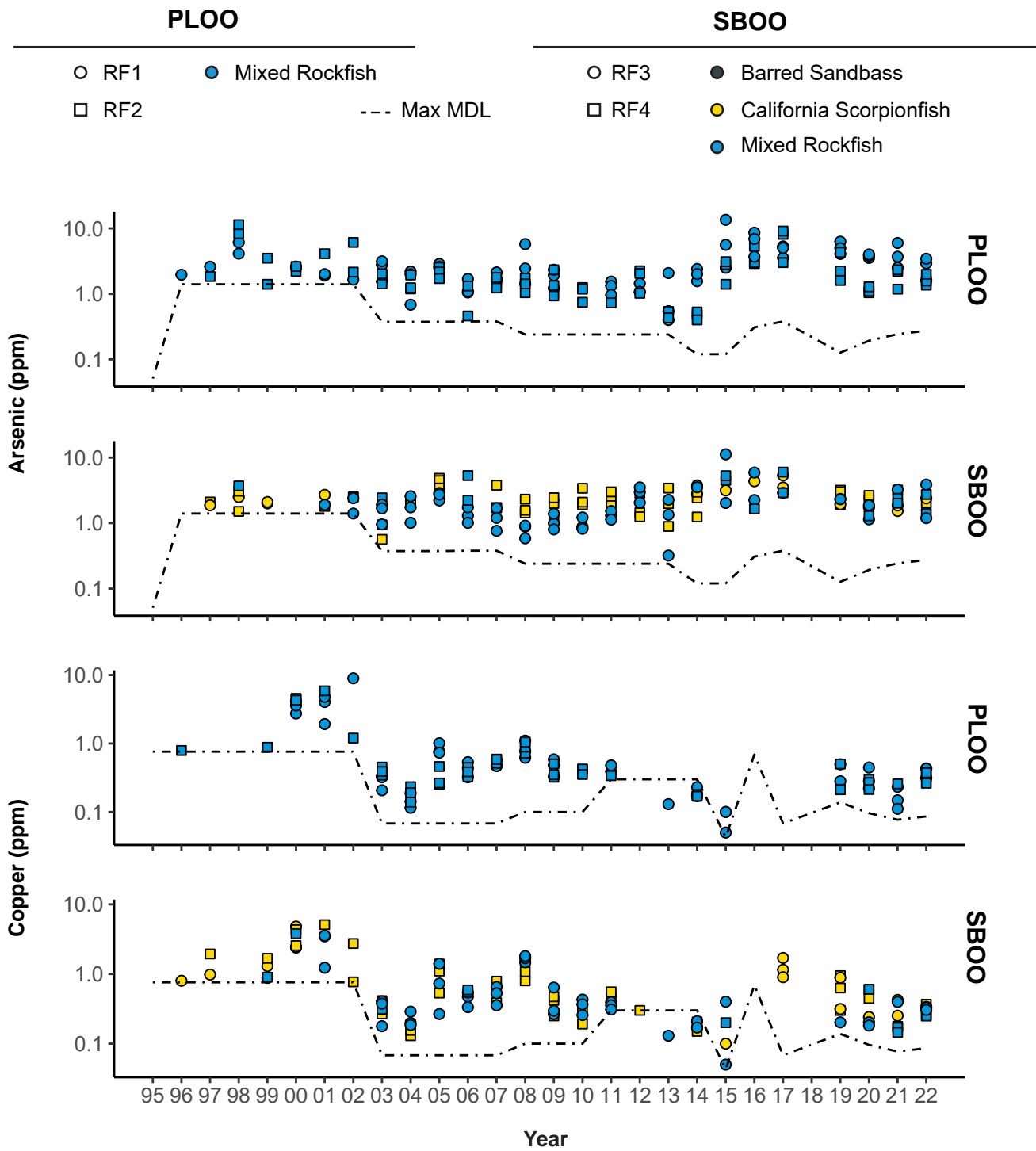


Figure 9.4

Concentrations of select metals detected in muscle tissues of fishes collected from PLOO and SBOO rig fishing zones from 1995 through 2022. Zones RF1 and RF3 are considered nearfield. No samples were collected in 2018 and 2023 as described in text.

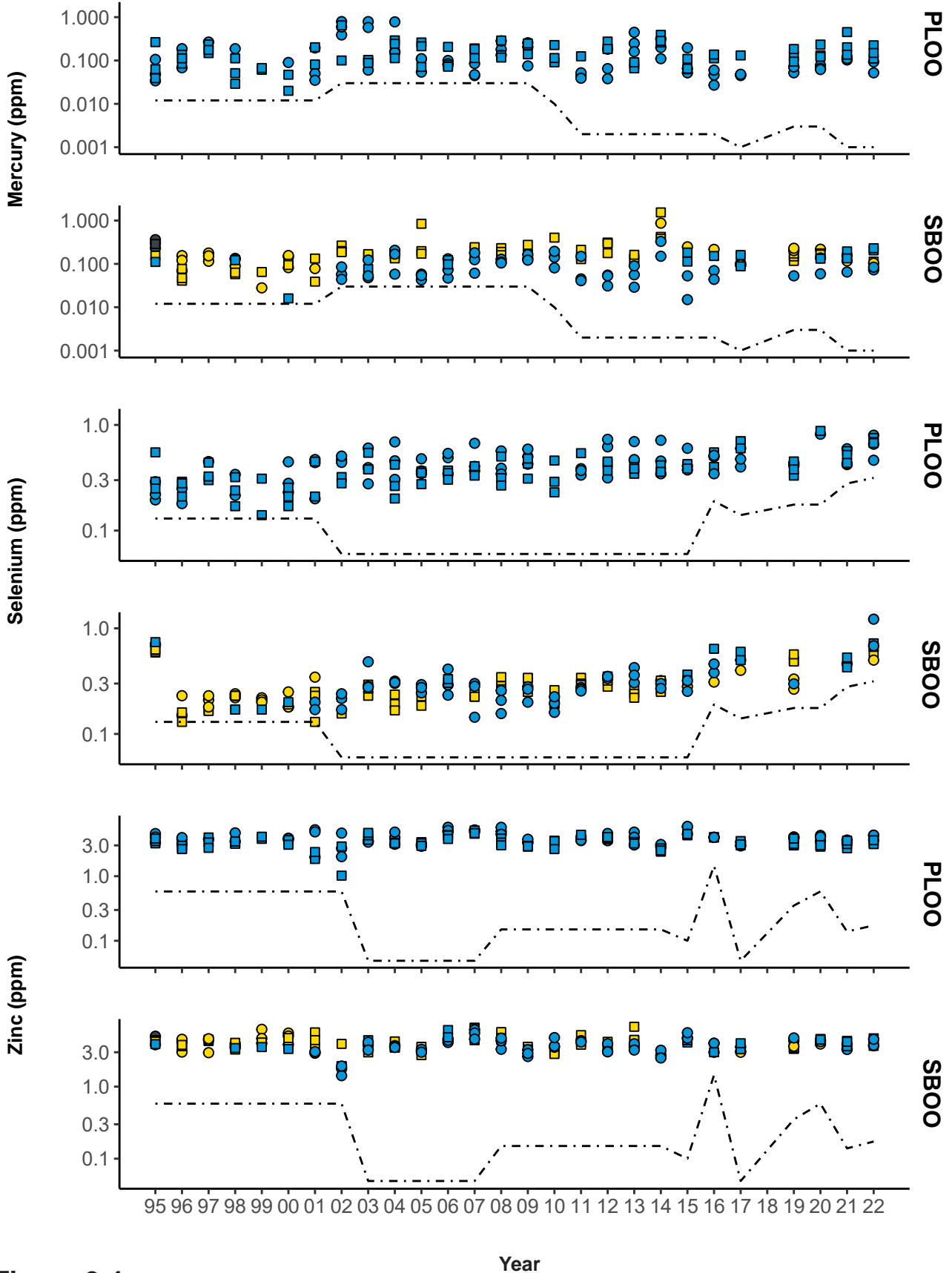


Figure 9.4 continued

Table 9.8

Summary of metals (ppm), pesticides (ppb), and total PCB (ppb) in fish muscle samples with chemistry concentrations that exceeded available thresholds (see Mearns et al 1991) from PLOO and SBOO rig fishing zones sampled historically (1995–2021) and during the current reporting period (2022). Data include the percent of samples that exceeded thresholds during each time period. See Tables 9.2–9.7, 9.9–9.10 for total number of samples analyzed.

Threshold	PLOO				SBOO				
	1995–2021		2022		1995–2021		2022		
	RF1	RF2	RF1	RF2	RF3	RF4	RF3	RF4	
Median International Standard^a									
Arsenic	1	74	49	100	67	53	68	67	67
Cadmium	1	0	0	0	0	0	0	0	0
Chromium	1	1	1	0	0	4	0	0	0
Copper	20	0	0	0	0	0	0	0	0
Lead	2	0	0	0	0	0	0	0	0
Mercury	1	6	1	0	0	1	3	0	0
Selenium	0.30	76	70	100	100	29	35	100	100
Tin	175	0	0	0	0	0	0	0	0
Zinc	70	0	0	0	0	0	0	0	0
Total Chlordane	100	0	0	0	0	0	0	0	0
Total DDT	5000	0	0	0	0	0	0	0	0
Hexachlorobenzene	100	0	0	0	0	0	0	0	0
OEHHA^b									
Mercury	0.22	18	22	0	33	9	17	0	33
Selenium	7.40	0	0	0	0	0	0	0	0
Total DDT	21	18	9	0	0	12	7	0	0
Total Chlordane	6	0	0	0	0	0	0	0	0
Total PCB	4	27	14	100	0	15	4	0	0
USFDA^a									
Mercury	1	0	0	0	0	0	1	0	0
Total DDT	5000	0	0	0	0	0	0	0	0
Hexachlorobenzene	300	0	0	0	0	0	0	0	0

^aFrom Mearns et al. 1991. USFDA action limits for mercury and all international standards are for shellfish, but are often applied to fish

^bFrom the California OEHHA (Klasing and Brodberg 2008)

Table 9.9

Summary of pesticides (ppb), total PCB (ppb), total PAH (ppb), total PBDE (ppb), and lipids (% weight) in muscle tissues of fishes collected from PLOO and SBOO rig fishing stations during 2022. Data include the number of detected values (n), minimum, maximum, and mean detected concentrations for each species, and the total number of samples, detection rate and maximum value for all species within region. Minimum and maximum values were based on all samples, whereas means were calculated from detected values only; nd = not detected; nr = not reportable.

	Pesticides				tPCB	tPAH	tPBDE	Lipids
	tChlor	tDDT	HCB	tHCH				
PLOO	Mixed Rockfish							
	n	0	1	1	0	1	0	1
	value	—	2.59	0.149	—	1.037	—	0.835
	Squarespot Rockfish							
	n	0	1	1	0	1	0	1
	value	—	2.08	0.187	—	0.443	—	0.472
	Starry Rockfish							
	n	0	1	1	0	1	0	1
	value	—	5.14	0.205	—	2.717	—	1.320
	Vermilion Rockfish							
	n	1	3	nr	2	3	1	3
	min	nd	4.86	—	nd	5.092	nd	1.512
	max	0.167	6.43	—	0.054	5.820	96.5	2.293
	mean	0.167	5.68	—	0.051	5.394	96.5	1.773
Total Samples	6	6	3	6	6	6	6	
Detection Rate (%)	17	100	100	33	100	17	100	
Max	0.167	6.43	0.205	0.054	5.820	96.5	2.293	
SBOO	Brown Rockfish							
	n	0	1	nr	0	1	0	1
	value	—	1.58	—	—	0.814	—	2.087
	CA Scorpionfish							
	n	0	2	0	0	2	0	2
	min	—	1.55	—	—	0.943	—	0.377
	max	—	4.37	—	—	3.262	—	3.120
	mean	—	2.96	—	—	2.103	—	1.749
	Gopher Rockfish							
	n	0	1	0	0	1	nr	1
	value	—	0.92	—	—	0.518	—	0.311
	Mixed Rockfish							
	n	0	2	0	0	2	0	1
	min	—	0.49	—	—	0.104	—	nd
max	—	0.56	—	—	0.442	—	1.632	
mean	—	0.52	—	—	0.273	—	1.632	
Total Samples	6	6	4	6	6	3	6	
Detection Rate (%)	0	100	0	0	100	0	83	
Max	nd	4.37	nd	nd	3.262	nd	3.120	

Table 9.10

Summary of pesticides (ppb), total PCB (ppb), total PAH (ppb), and lipids (% weight) in muscle tissues of fishes collected from PLOO and SBOO rig fishing zones from 1995 through 2022. Data include total number of samples (n), detection rate (DR%), minimum, maximum, and mean^a detected concentrations per species; nd=not detected.;*tPBDE data only for 2022.

	Pesticides							tPCB	tPAH	tPBDE*	Lipids
	tChlor	tDDT	Dieldrin	Endrin	HCB	tHCH					
PLOO											
Mixed Rockfish											
n	148	148	136	136	135	148	148	75	6	148	
DR (%)	3	92	0	0	12	2	43	8	100	98	
min	nd	nd	—	—	nd	nd	nd	nd	0.5	nd	
max	2.4	217.3	—	—	15.0	13.4	69.0	360.1	2.3	4.4	
mean	1.1	12.9	—	—	1.3	4.5	8.6	166.6	1.3	0.9	
Barred Sand Bass											
n	4	4	4	4	4	4	4	4	—	4	
DR (%)	0	50	0	0	0	0	75	0	—	100	
min	—	nd	—	—	—	—	nd	—	—	0.7	
max	—	13.0	—	—	—	—	32.0	—	—	1.4	
mean	—	9.6	—	—	—	—	20.0	—	—	1.0	
SBOO											
CA Scorpionfish											
n	80	80	78	78	74	80	84	62	2	84	
DR (%)	0	93	0	0	0	0	40	3	100	100	
min	—	nd	—	—	—	—	nd	nd	0.4	0.1	
max	—	195.7	—	—	—	—	49.3	22.7	3.1	2.6	
mean	—	16.9	—	—	—	—	5.2	18.4	1.7	0.6	
Mixed Rockfish											
n	65	65	58	58	60	65	67	61	4	67	
DR (%)	0	75	2	2	7	0	21	5	75	99	
min	—	nd	nd	nd	nd	—	nd	nd	nd	nd	
max	—	15.1	0.3	0.7	7.2	—	5.6	227.0	2.1	3.0	
mean	—	3.2	0.3	0.7	2.0	—	1.4	92.4	1.3	0.6	

^aMinimum and maximum values were based on all samples, whereas means were calculated from detected values only

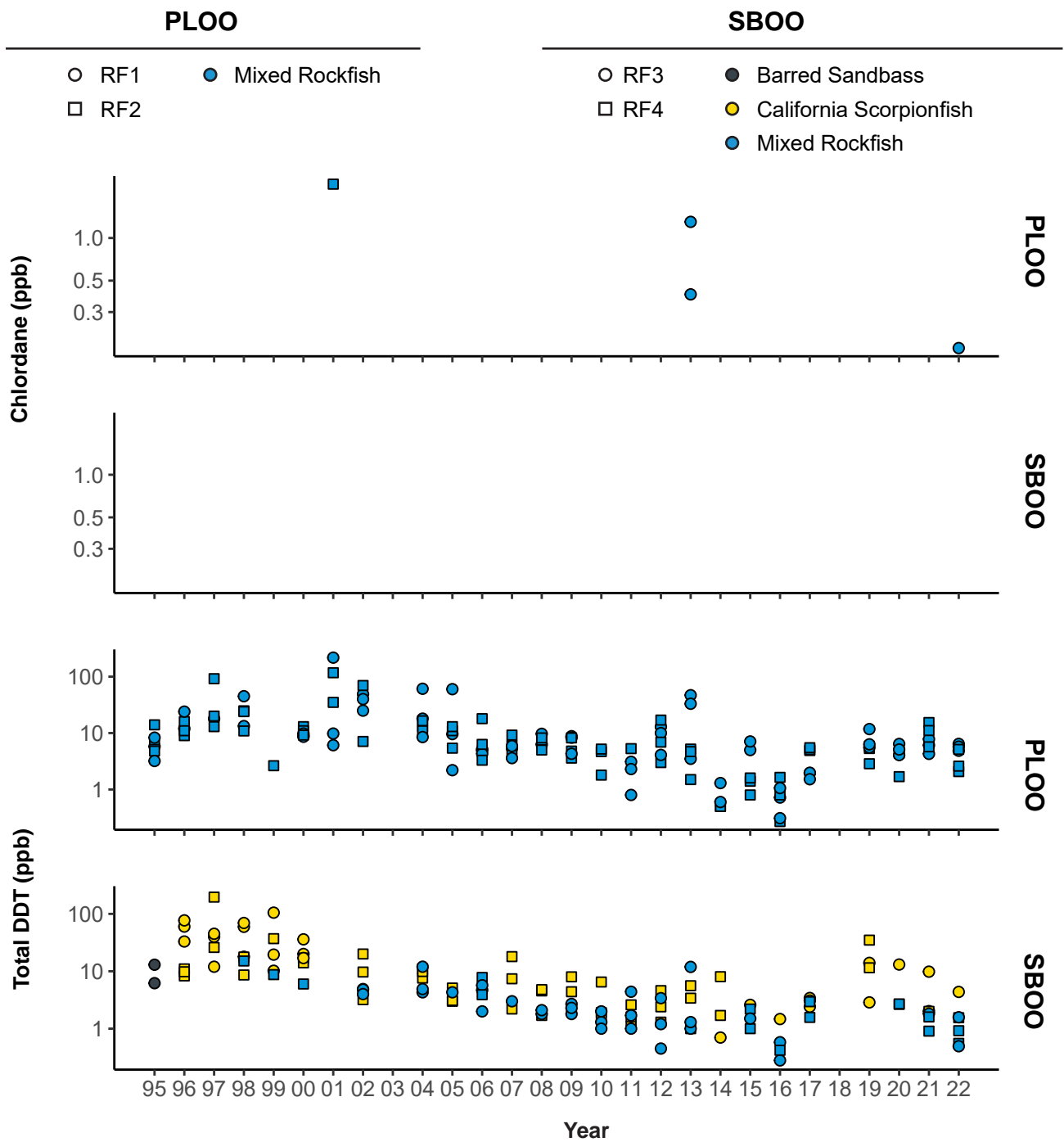


Figure 9.5 Concentrations of pesticides and total PCB in muscle tissues of fishes collected from PLOO and SBOO rig fishing zones from 1995 through 2022. Zones RF1 and RF3 are considered nearfield. No samples were collected in 2018 and 2023 as described in text.

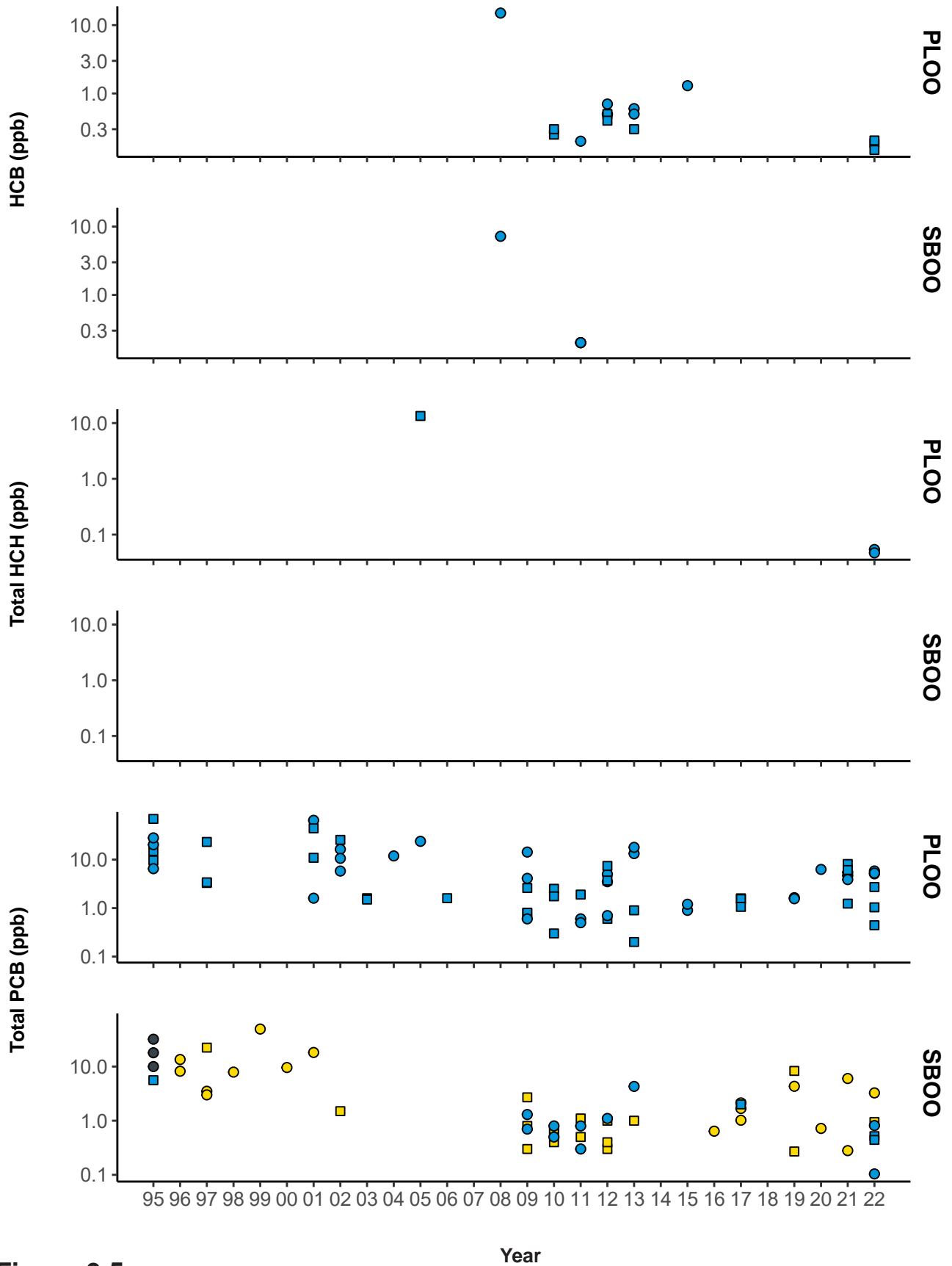


Figure 9.5 continued

Appendices

Appendix A

**Evaluation of Anthropogenic Impacts on the San Diego
Coastal Kelp Forest Ecosystem – Final Project Report**

2019 – 2024

Ed Parnell, PhD

**Scripps Institution of Oceanography, UC San Diego
9500 Gilman Dr., La Jolla, CA 92093-0227**

**Submitted to City of San Diego
Public Utilities Department**

April 1, 2024

Evaluation of Anthropogenic Impacts on the San Diego Coastal Kelp Forest Ecosystem - Final Project Report: 2019 to 2024

Prepared By:

Ed Parnell, PhD^{1*}

April 1, 2024

*Corresponding Author: edparnell@ucsd.edu

¹Scripps Institution of Oceanography, UC San Diego
9500 Gilman Dr, Mail Code 0227, La Jolla, CA 92093-0227

EXECUTIVE SUMMARY

Kelp forests are among the most charismatic marine communities off the southern California coast. They are highly productive, characterized by the rapid growth of their structural species, *Macrocystis pyrifera* (commonly referred to as giant kelp), whose areal rate of primary production can exceed that of tropical rain forests (Towle and Pearse, 1973). Giant kelp forests provide habitat, food and shelter for a host of fishes and invertebrates, and competes with many other algal species. Kelp forests occupy the inner margins of the southern California continental shelf and offshore islands extending to depths as great as thirty meters off the mainland of southern California. Kelp forests also host a range of economically and aesthetically important consumptive and non-consumptive human activities including boating, recreational fishing, spearfishing, SCUBA diving, and the commercial harvest of finfishes, invertebrates, and algae. The kelp forests off Point Loma and La Jolla are among the most important commercial fishing grounds for the red sea urchin (*Mesocentrotus franciscanus*) and spiny lobster (*Panulirus interruptus*) fisheries off California.

Kelp forests off southern California are affected by both natural and human disturbances. The El Niño Southern Oscillation (ENSO) is the primary climate mode that affects kelp abundance, growth, and reproduction along the west coast of the Americas. Positive ENSO's, termed El Niños, are associated with warm water, depressed concentrations of nitrate, the principal nutrient limiting giant kelp, and an altered storm environment off southern California which can produce destructive storm waves. Both phenomenon can severely stress giant kelp and accompanying species of algae. The opposite conditions occur during negative ENSO events known as La Niñas, enhancing both the growth and reproduction of kelps. Together, the two ocean climate states drive the greatest amount of annual variability in surface canopy cover of *M. pyrifera* off southern and Baja California. The periodicity of El Niño is variable, typically occurring at 3-5 year intervals and persisting for <1 year. Kelp forests wax and wane over these cycles, experiencing high mortality during El Niños with varied degrees of recovery afterwards. Recovery rates depend on growth conditions after El Niños ebb.

The kelp forests off San Diego have been studied by researchers at the Scripps Institution of Oceanography (SIO) since the 1950's, and baseline data collection began in the 1970's. All algae and associated animals are currently monitored at twenty permanent study sites. These surveys represent a continuation of ecological studies in the Point Loma and La Jolla kelp forests at some of the same sites established as part of earlier studies conducted in the 1970s and 1980s. These two kelp forests are the largest contiguous kelp forests off the western coast of the United States and are historically one of the most studied kelp forest systems in the world. Additional study sites have been established more recently in both Point Loma and La Jolla, and in kelp forests off northern San Diego County. The main components of the current kelp forest monitoring program include surveys of (1) algal density, growth reproduction, and recruitment, (2) benthic invertebrates, (3) sea urchin demography, (4) ocean temperature, (5) fish and invertebrate censuses at 8 additional reef sites, and (6) benthic light levels.

The kelp forests throughout much of southern California including San Diego County were decimated by a marine heat wave that began in 2014 and persisted through the spring of 2016 due to the combination of two independent but consecutive ocean climatic phenomena. An anomalous warm pool extended across much of the NE Pacific from 2014-2015. This warm pool, unique in the climate record of the NE Pacific, was coined the BLOB and resulted from decreased wind mixing in the NE Pacific. The climatic forcing of the NE Pacific warm pool is different in nature and scale than the ENSO which is caused by anomalous winds along the equatorial Pacific. A strong El Niño occurred during fall of 2015 and the winter of 2016 just as the BLOB was dissipating along the US west coast. Together these consecutive warm events are now referred to as the NE Pacific marine heat wave (MHW) of 2014-15

which was the longest and warmest heat event ever observed in the 115 year record of sea surface temperature at the Scripps Institution of Oceanography (SIO) pier. Cooler conditions returned to the equatorial eastern Pacific and the Southern California Bight by late 2016. The spring upwelling seasons of 2017-2018 brought cool nutrient-laden waters up onto the inner continental shelf and the kelp forests off southern California but was briefly interrupted by a mild El Niño from the fall of 2018 to the summer of 2019. Conditions during the present reporting period (2019-2024) returned to favorable conditions for giant kelp recovery due to persistent La Niña conditions that persisted from 2021 to early 2023. Most recently, a strong El Niño developed beginning in the fall of 2023 and is expected to persist through at least spring of 2024 after which La Niña conditions are predicted to return by summer.

The MHW of 2014-2015 decimated giant kelp (*M. pyrifera*) and had a negative effect on many other species of macroalgae off San Diego. Densities of adult *M. pyrifera* were reduced >90% across our 20 study sites (Fig. 1). Unlike previous warm events attributed to El Niño, the coupled marine heat wave resulted in warming and low nutrient exposure of understory kelp species for prolonged periods of time leading to dramatic reductions of those species in addition to giant kelp. The BLOB persisted longer than a typical El Niño and kelps did not recover after the warm pool dissipated as a result of the stress induced by the following El Niño of 2015-16. Rates of giant kelp recovery between 2017 and 2019 were variable among the study sites and have been depressed since that time. Giant kelp recruitment occurred at many of the sites both after the combined MHW of 2014-16 and the mild El Niño of 2019-2020 but both sets of recruitment cohorts have failed to yield dominant healthy stands of giant kelp. Presently, giant kelp off San Diego is at its lowest historical density (Fig. 1) despite supportive ocean climate conditions over the last three years. The present patchy condition of giant kelp off San Diego can be categorized into four different states. The first includes many of the shallower sites where understory algae that grow close to the bottom have gained a foothold since the MHW. The presence of these kelps can prevent giant kelp from recruiting via competition for space. Category two includes deeper areas of the kelp forest (>16 m) which been affected by low light levels at the sea bottom due to recent extensive phytoplankton blooms. Giant kelp requires adequate light to germinate and produce young plants. Light levels were reduced from 2020 through 2022 and only recently have supported some giant kelp recruitment at these sites. The third category includes sites at mostly intermediate depths where there has been alternation between bouts of moderate giant kelp recruitment and recovery followed by collapse that may be at least partly due to the unprecedented surface warming that has occurred over the last several summers. The fourth category includes sites off North La Jolla and North County, except for Solana Beach, where most algae is now absent, and the areas are becoming dominated by suspension feeding invertebrates including bryozoans and suspension feeders that have negative effects on kelp recruitment. The conditions at these sites will likely continue indefinitely without a large disturbance.

One of the factors that may account for the presently patchy and degraded condition of giant kelp stands off San Diego is the recent extreme (relative to historical records) surface warming during the last four summers. This phenomenon is quite recent occurring only within the last decade. The warming is limited to the upper 3-5 meters of the ocean's surface, and affects much of the southern California coast. Sea surface temperatures have exceeded 28°C during this period, exceeding the previous temperature maximum recorded at the SIO Pier by ~3°C. Summer surface temperature maxima in this record are typically ~23°C. This surface warming has degraded giant kelp canopy tissue which mostly sloughs off and drifts onto nearby beaches. During this period, cooler temperatures have persisted closer to the bottom due to the La Niña conditions, and most giant kelp plants in the initial recovery cohorts of 2017 and 2018 survived and regrew to the surface when the warm pool dissipated by the fall of 2018. This was generally not the case for the post 2018-2019 recruitment.

Diseases in many invertebrates, including sea urchins (echinoids) and predatory seastars (asteroids), are common during MHWs. Mass mortality of red (*Mesocentrotus franciscanus*) and purple sea urchins (*Strongylocentrotus purpuratus*) and seastars in the genus *Pisaster*, began off San Diego in 2014 and persisted through 2017. Sea urchins are primary grazers of most kelp species, and can overgraze giant kelp and associated algal species given the right conditions. They are capable of limiting or even precluding giant kelp recovery. Overgrazed areas, termed urchin barrens, can persist in some areas for decades. The echinoderm epidemic associated with the MHW resulted in the near-disappearance of seastars and the decimation of sea urchins at our study sites and from all San Diego kelp forests generally. Further, little to no recruitment of sea urchins was observed until the fall of 2017 with later episodes occurring after the 2018-19 El Niño. However, there has been no increase in sea urchin densities or evidence of overgrazing despite these pulses of recruitment. This indicates that these cohorts either mostly failed or they remain cryptic and are not actively grazing live plants. These new cohorts of sea urchins may eventually overgraze some areas off San Diego if they emerge from cryptic nursery habitat in high densities and begin to actively forage. Sea urchin overgrazing has been a recurring problem off south Pt. Loma where a unique combination of topography and turbidity emanating from San Diego Bay appear to contribute to a large and resilient sea urchin barren. However, giant kelp recovery has been the strongest within this formerly resilient sea urchin barren, an apparent reversal of the historical spatial pattern of *M. pyrifera* canopy cover. Sea urchin over grazing does not appear to be contributing to the current degraded state of giant kelp off San Diego.

Some invertebrates including predators of sea urchins also collapsed due to disease associated with the 2014-16 MHW. These species include the seastars *Pisaster giganteus* and *Patiria miniata*, which have still not shown any sign of recovery off San Diego. Densities of both species has remained historically low and it is presently unknown whether they will recover to their former densities. Abalone, an important herbivore and the target of a once extensive fishery, depend primarily on giant kelp for food. Abalone once supported a large recreational and commercial fishery off southern California until all harvest was closed in 1996 due to depletion from overfishing and disease mainly associated with warm events. Abalone off San Diego County suffered further mortality during and after the 2014-2016 MHW due to disease and lack of food. Abundances of all abalone species at the study sites off La Jolla and Pt. Loma have since declined to near zero with the exception of pink abalone (*Haliotis corrugata*) which exhibited some recovery at the two shallowest study sites off central Pt. Loma.

Sargassum horneri, an invasive algal species that has overwhelmed giant kelp in some sheltered forests off southern California, was first observed in the kelp forests off San Diego in 2014. By 2018, this species had been observed at 13 of 20 study sites, but has since not spread to the remaining sites. Densities of *S. horneri* at the sites where it has been observed have actually decreased over time with the exception of one study site off northern La Jolla where it covers ~3% of the bottom. Presently, this species does not appear to pose as great a risk to San Diego County kelp forests that it has to more sheltered kelp forests off the California Channel Islands.

The failed recovery of giant kelp at many of our study sites can not be due to any localized effects of treated wastewater discharge by the City of San Diego through the ocean outfalls offshore of Imperial Beach (South Bay Ocean Outfall) or Pt. Loma (Pt. Loma Ocean Outfall). The present patchy nature of giant kelp canopy cover is not related to distance gradients from either outfall. The areas that have exhibited the poorest post-MHW recovery and whose algal communities are the most degraded relative to their historical condition, include northern La Jolla and North County which are the sites furthest from these outfalls.

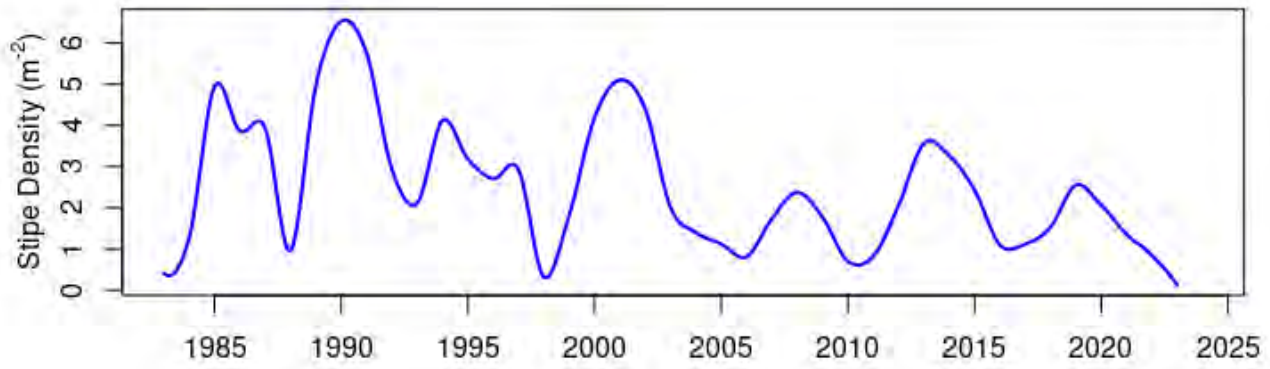


Figure 1. Mean giant kelp (*Macrocystis pyrifera*) stipe densities pooled across all sites over time. Stipe density is a useful proxy for kelp biomass.

INTRODUCTION

Kelp forests are vulnerable to human disturbance mainly due to their proximity to urbanized coasts thereby exposing them to overfishing, polluted surface and groundwater discharge, as well as the discharge of wastewater. Perhaps the largest effect is that due to increased turbidity which limits light penetration for kelps to grow, germinate, and reproduce (Clendenning and North, 1960). Historic reductions in kelp forest canopy off Palos Verdes have been attributed to the combined effects of wastewater disposal and an energetic El Niño in the late 1950's (Grigg, 1978). Nearshore turbidity due to wastewater discharge has since been mitigated by increasing the offshore distances and depths of discharge, and improved outfall design (Roberts, 1991). Beach replenishment can also negatively impact kelp forests via sedimentation and burial. This has been observed at kelp forests off northern San Diego County where replenished sediments erode from beaches and partially bury low relief habitat that is common in those areas.

The Point Loma Ocean Outfall (PLOO) discharges advanced primary treated wastewater through a deep water open ocean outfall. The Outfall was extended and deepened in 1993, and presently discharges treated wastewater ~7.3 km offshore in marine waters ~98 m deep. The PLOO is situated approximately 5 km offshore of the outer edge of the Point Loma kelp forest. Due to its proximity, wastewater discharge through the PLOO presents at least a perceived risk to the health of the nearby kelp forest community off Pt. Loma. Local human risks to kelp forests can magnify risks posed by larger scale natural disturbances by reducing the resilience of kelp forests after episodic natural disturbances.

Kelp forests in southern California are disturbed naturally by ocean climate variability that occurs at interannual (El Niño Southern Oscillation – ENSO; Fig. 2) and decadal (Pacific Decadal Oscillation - PDO) periods. Positive phases of both ocean climate modes are associated with a deepened thermocline limiting nutrient delivery to the inner shelf that is necessary for kelp growth and reproduction. These modes are also associated with increased storm wave energy which can cause giant kelp mortality via plant detachment and abrasion (Seymour et al., 1989). The northeastern Pacific experienced a profound regime shift in the late 1970's in which the main ocean thermocline deepened, resulting in a step reduction in nitrate concentrations along the Southern California Bight (SCB) that persists at present (Parnell et al., 2010 and Fig. 3). Concentrations of nitrate, the main limiting nutrient for kelp growth in southern California switched from being supportive for kelp growth most years prior to the regime shift, with the exception of the most intense El Niños, to being marginal or inadequate most of the time afterward (Parnell et al., 2010). The ecology of giant kelp forests off San Diego has changed fundamentally over the last 50 years due to the increased frequency of natural disturbances resulting in a demographic shift towards younger and smaller *Macrocystis pyrifera* individuals (Parnell et al., 2010) as well as an overall decreased density and post disturbance resilience (see Fig. 1).

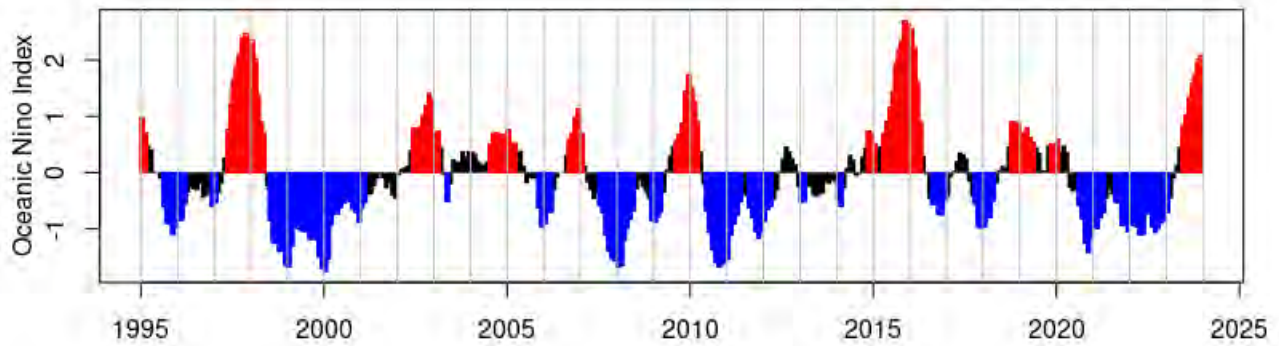


Figure 2. Barplot of the Oceanic Niño Index (ONI) since 1995. Red bars indicate El Niño conditions, blue bars indicate La Niña conditions, and black bars indicate ENSO neutral conditions (data from NOAA, 2024). The ONI index is based on equatorial sea surface temperatures in the Eastern Pacific.

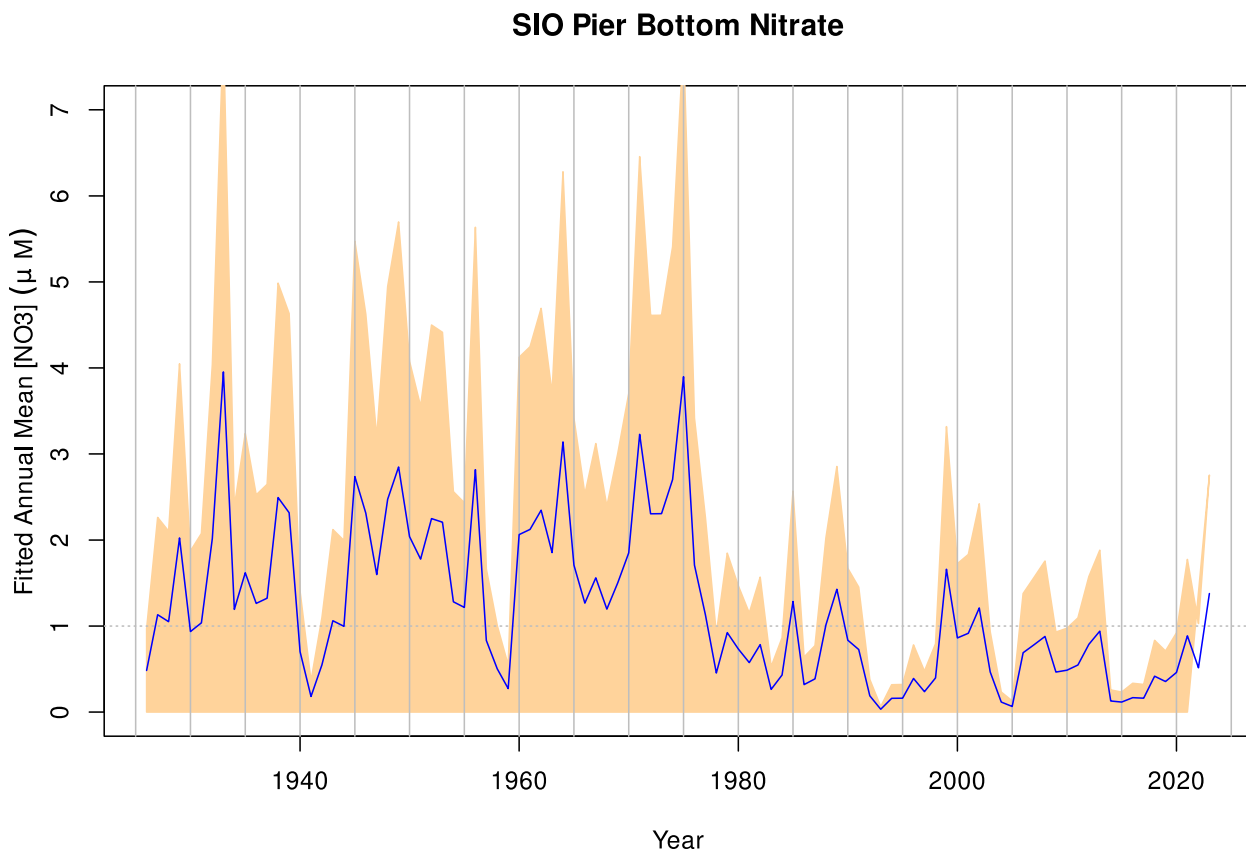


Figure 3. Time series of annual mean nitrate concentrations estimated from daily temperature and salinity sampled at the base of the Scripps Institution of Oceanography Pier (see Parnell et al., 2010 for details). Dotted gray line indicates the minimum nitrate threshold for the growth and reproduction of giant kelp (*M. pyrifera*). Peach area indicates the 95% confidence limits.

Sea urchin overgrazing is another form of natural disturbance within kelp forests (Leighton et al., 1966). Kelps are susceptible to overgrazing when sea urchin densities increase or when sea urchins aggregate into overgrazing fronts. Overgrazing can lead to areas denuded of most or all algae and have been termed barrens. Barrens can be frequent and resilient in some areas including the southern portion of the Pt. Loma kelp forest (Parnell, 2015), or can alternate with forested periods due to external forcing such as reductions in kelp standing stock as a result of El Niño, sea urchin disease epidemics, and indirectly from human activities including the harvest of important sea urchin predators (Steneck et al., 2002). Overfishing of sea urchin predators including spiny lobsters (*Panulirus interruptus*) and sheephead (*Semicossyphus pulcher*) in southern California can lead to outbreaks of sea urchin overgrazing.

A more recent source of disturbance has been the introduction of an invasive alga, *Sargassum horneri*, throughout southern California. This species competes with *Macrocystis pyrifera* for space and light, and is now seasonally dominant in some areas that were previously dominated by *M. pyrifera*. Presently, the most impacted areas include the protected low energy habitats in the lee of islands such as the northern Channel Islands and Santa Catalina Island (Miller et al., 2011). *S. horneri* is now establishing itself in many areas off San Diego County including the kelp forests, bays, and estuaries.

Researchers at the Scripps Institution of Oceanography (SIO) have partnered with the City of San Diego Ocean Monitoring Program to conduct regular surveys of the kelp forests off San Diego County including the kelp forests off Point Loma, La Jolla and North County. These surveys represent a continuation of ecological studies that began at SIO in the Point Loma (PLKF) and La Jolla (LJKF) kelp forests and continue at some of the sites established in the 1970's and 1980's (Dayton and Tegner, 1984). Additional study sites have been established more recently in both kelp forests and in kelp forests off northern San Diego County (North County - NCKF). PLKF and LJKF are the largest contiguous kelp forests off the western United States coast and are historically one of the most studied kelp forest systems in the world.

MATERIALS AND METHODS

Algae, invertebrates and bottom temperatures are monitored at twenty permanently established study sites (Fig. 4). Algae and invertebrates are monitored along four replicate parallel permanent band transects oriented perpendicular to shore (25 x 4 m bands separated 3-5 m apart) except at the DM study site where two sets of band transects are located ~1300 m apart due to the small size and fragmented shape of that forest. The main components of the kelp forest monitoring program include estimation of (1) algal density, growth, reproductive condition and recruitment, (2) invertebrate densities, (3) sea urchin demography (size distributions to monitor for episodic recruitment), and (4) ocean bottom temperature (which is a proxy of ocean nutrient status). The types of data collected and the frequency of collection are listed in Table 1.

Algae

Several life stages of *M. pyrifera* are enumerated to identify recruitment events and follow the fate of recruiting cohorts into adulthood. Survival of recruitment cohorts to adulthood is highly variable and a lack of successful maturation into adulthood indicates changes in the growth environment in the form of stress induced by high temperatures, inadequate nutrient levels, overgrazing by invertebrates, and reduced light. Giant kelp life stages include adults (def., ≥ 4 stipes), pre-adults

(def., plants >1 m tall but with <4 stipes), bifurcates (a late post recruitment stage indicated by the presence of a split in the apical meristem which represents the primary dichotomous branching event), and pre-bifurcates (very early post settlement stage lacking the initial dichotomous split). Stipe numbers are counted and recorded for each adult plant each visit.

Conspicuous macroalgal species/groups are enumerated or percent cover is estimated within 5 x 2 m (10 m²) contiguous quadrats along the band transect lines at all sites. Reproduction and growth of *M. pyrifera*, and the understory kelps *Pterygophora californica* and *Laminaria farlowii*, are measured on permanently tagged plants along the central Pt. Loma study sites.

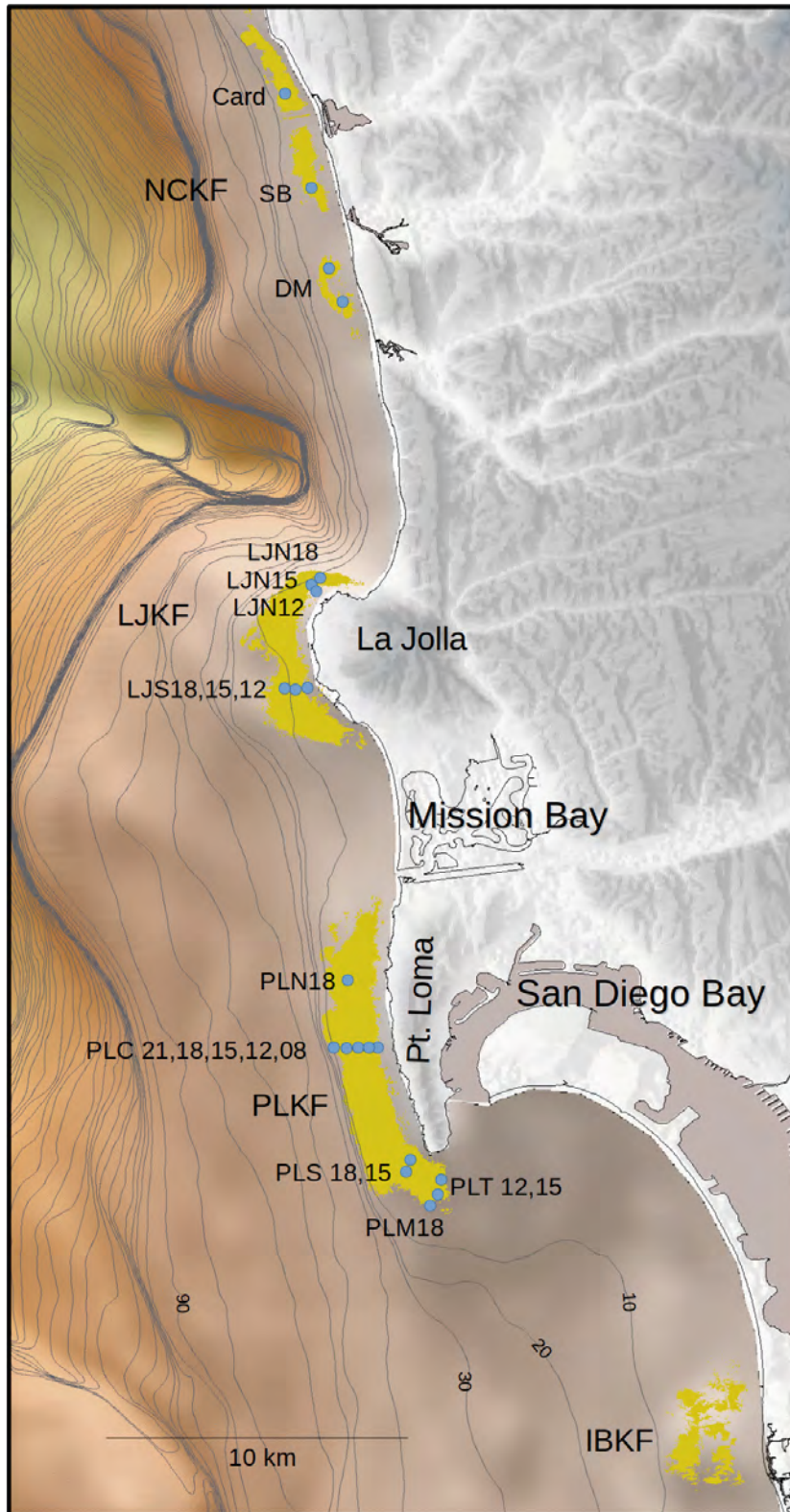


Figure 4. Map of the San Diego inner shelf showing locations of the Point Loma, La Jolla, North County, and Imperial Beach kelp forests (indicated by PLKF, LJKF, NCKF, and IBKF, respectively). Permanent study site locations are indicated by blue circles and corresponding study site names. Depth contour units are meters.

Growth of *M. pyrifera* is monitored by counting the number of stipes on each tagged plant one meter above the substratum. Reproductive state is represented by the size of the sporophyll bundle (germ tissue) at the base of each plant. Sporophyll volume is calculated as a cylinder based on the height and diameter of each bundle. This is an indirect measure of reproductive effort. Reed (1987) has shown that sporophyll biomass is closely related to zoospore production. Reproductive capacity, a derived parameter that represents the relative reproductive potential among plants by coupling sporophyll volume and reproductive state, is calculated as the product of sporophyll volume and squared reproductive state. Reproductive capacity is then standardized by division of each value by the maximal value observed among all sites. Reproductive state for each plant is ranked according to the ordinal scale in Table 2.

Growth of *Pterygophora californica* is determined by the method of DeWreede (1984). A hole (6 mm) is punched into the midrib of the terminal blade ~30 mm from the base of the blade, and another hole is punched monthly at the same location. The distance between the two holes represents the linear growth of each blade. Reproductive effort for *P. californica* is evaluated by a count of the total number of sporophyll blades on each plant and the number with active spore production (def., sori). Growth of *Laminaria farlowii* is determined in a similar manner to *P. californica*. A 13mm diameter hole is punched 100 mm from the base of each blade and is repeated each visit. The distance between the two holes represents the linear growth of each blade. The reproductive status of *L. farlowii* is evaluated as the percent of each blade covered by sori.

The distribution of algal species among all permanent sites was calculated using factor analysis in R (R Core Team, 2018). Factor analysis (Lawley and Maxwell, 1971) was used to reduce the multi-dimensional algal data. This technique facilitates the examination of entire algal communities in two or three dimensions that can then be plotted to assess changes in community composition among study sites and over time. Thirteen algal groups and derived bare space were analyzed among 20 sites. Relative bare space was derived by ranking the sum of rankings for individual algal groups among sampling units. Sampling units (individual 10m² quadrats) with the least amount of total algae (density or percent cover) were ranked highest for bare space.

Invertebrates

All conspicuous sessile and mobile invertebrates are enumerated annually within the 10 m² quadrats during spring. Size frequencies of red (RSU - *Mesocentrotus franciscanus*) and purple (PSU - *Strongylocentrotus purpuratus*) sea urchins are recorded for >100 individuals when possible for each species located near all of the study sites except for the NCKF sites which do not have adequate densities of sea urchins.

Sea urchin recruitment is sampled semi-annually (spring and fall) at all of the Pt. Loma and La Jolla study sites. Sea urchins are exhaustively collected in haphazardly placed 1 m² quadrats in suitable substrate within 50m of each study site. Suitable substrate includes ledges and rocks which can be fully searched for sea urchins as small as 2mm. Sea urchins are measured using calipers and then returned to their place of capture.

Temperature and Sedimentation

Sea bottom temperatures are recorded at 10 min intervals using ONSET Tidbit recorders (accuracy and precision = 0.2°C and 0.3°C (respectively) at the permanent central Pt. Loma study sites

and an additional site located just offshore of PLC21 at a depth of 33 m. Additionally, a water column temperature profile is recorded utilizing a mooring located in south La Jolla at a depth 24 m. Sensors are located at 3 m depth intervals along the mooring.

Sedimentation of the North County kelp forests has been historically episodic. The most noticeable burial appeared to be related to beach sand replenishment activities in the early 2000's when large sections of hard bottom substrate supporting the Solana Beach kelp forest was covered by sediments as they migrated offshore from the beach (Parnell, pers. obs.) . With the establishment of kelp forest study sites in the area, sediment depths are monitored along all of the NCKF sites. Sedimentation is tracked by measuring the height of permanently established spikes at replicate locations within each of those forests.

Study Site	Depth (m)	Year Established	Work Conducted (frequency)
Card	17	2006	ABT(q), Inv(a), BT(10min), Sed(q)
SB	16	2006	ABT(q), Inv(a), BT(10min), Sed(q)
DM	16	2007	ABT(q), Inv(a), BT(10min), Sed(q)
LJN18	18	2004	ABT(q), Inv(a), USF(sa), BT(10 min)
LJN15	15	2004	ABT(q), USF(sa), Inv(a), BT(10 min)
LJN12	12	2004	ABT(q), USF(sa), Inv(a), BT(10 min)
LJS18	18	2004	ABT(q), USF(sa), Inv(a), BT(10 min)
LJS15	15	1992	ABT(q), USF(sa), Inv(a), BT(10 min)
LJS12	12	2004	ABT(q), USF(sa), Inv(a), BT(10 min)
PLN18	18	1983	ABT(q), USF(sa), Inv(a), BT(10 min)
PLC21	21	1995	ABT(q), USF(sa), Inv(a), AR(m), BT(10 min)
PLC18	18	1983	ABT(q), USF(sa), Inv(a), AR(m), BT(10 min)
PLC15	15	1983	ABT(q), USF(sa), Inv(a), AR(m), BT(10 min)
PLC12	12	1983	ABT(q), USF(sa), Inv(a), AR(m), BT(10 min)
PLC08	8	1997	ABT(q), USF(sa), Inv(a), AR(m), BT(10 min)
PLS18	18	1983	ABT(q), USF(sa), Inv(a), BT(10 min)
PLS15	15	1992	ABT(q), USF(sa), Inv(a), BT(10 min)
PLT12	12	1997	ABT(q), USF(sa), Inv(a), BT(10 min)
PLT15	15	1997	ABT(q), USF(sa), Inv(a), BT(10 min)
PLM18	18	1996	ABT(q), USF(sa), Inv(a), BT(10 min)

Table 1. List of study sites including year of establishment and work conducted at each site. ABT = algal band transects, USF = sea urchin size frequency, Inv = Invertebrate censuses, AR = algal reproduction and growth measurements, and BT = bottom temperature. Frequencies are noted in parenthesis: a = annual, sa = semi-annual, q = quarterly, m = monthly.

Reproductive Score	Description
0	No sporophylls present
1	Sporophylls present but no sori (sites of active reproduction) development
2	Sporophylls with sori only at the base of sporophylls
3	Sporophylls with sori over most of the sporophylls surface
4	Sporophylls with sori over all of the sporophylls surface
5	Sporophylls with sori over all of the sporophylls surface releasing zoospore

Table 2. Ordinal ranking criteria for *Macrocystis pyrifera* reproductive state.

Finfishes

Fish surveys were initiated in the fall of 2019 and continue semi-annually (fall/spring) at four sites within the LJKF and four sites within the PLKF (Figs. 5 and 6, respectively). One of the sites off La Jolla ('CGSB') was discontinued in 2021 and was replaced by a site having a reef more similar to the other sites but was previously unknown ('14G'). Sites were chosen based on topographic features that fish are known to prefer and are as similar as possible in reef size and rugosity based on previously collected bathymetric data (Parnell, 2015). Sites were paired within the LJKF where a large marine protected area (MPA, South La Jolla State Marine Reserve) is located in the southern half (Fig. 5). The take of all species is prohibited within the MPA which went into effect in 2012. Study sites within the LJKF and PLKF were paired by depth as best as possible to facilitate comparisons of the fish communities inside and outside the MPA (Table 3). Fish counts are conducted along replicate 30x4 m band transects (up to 3 meters off the bottom) which include an initial swimming count for conspicuous species followed by a thorough search for cryptic species using a dive torch.

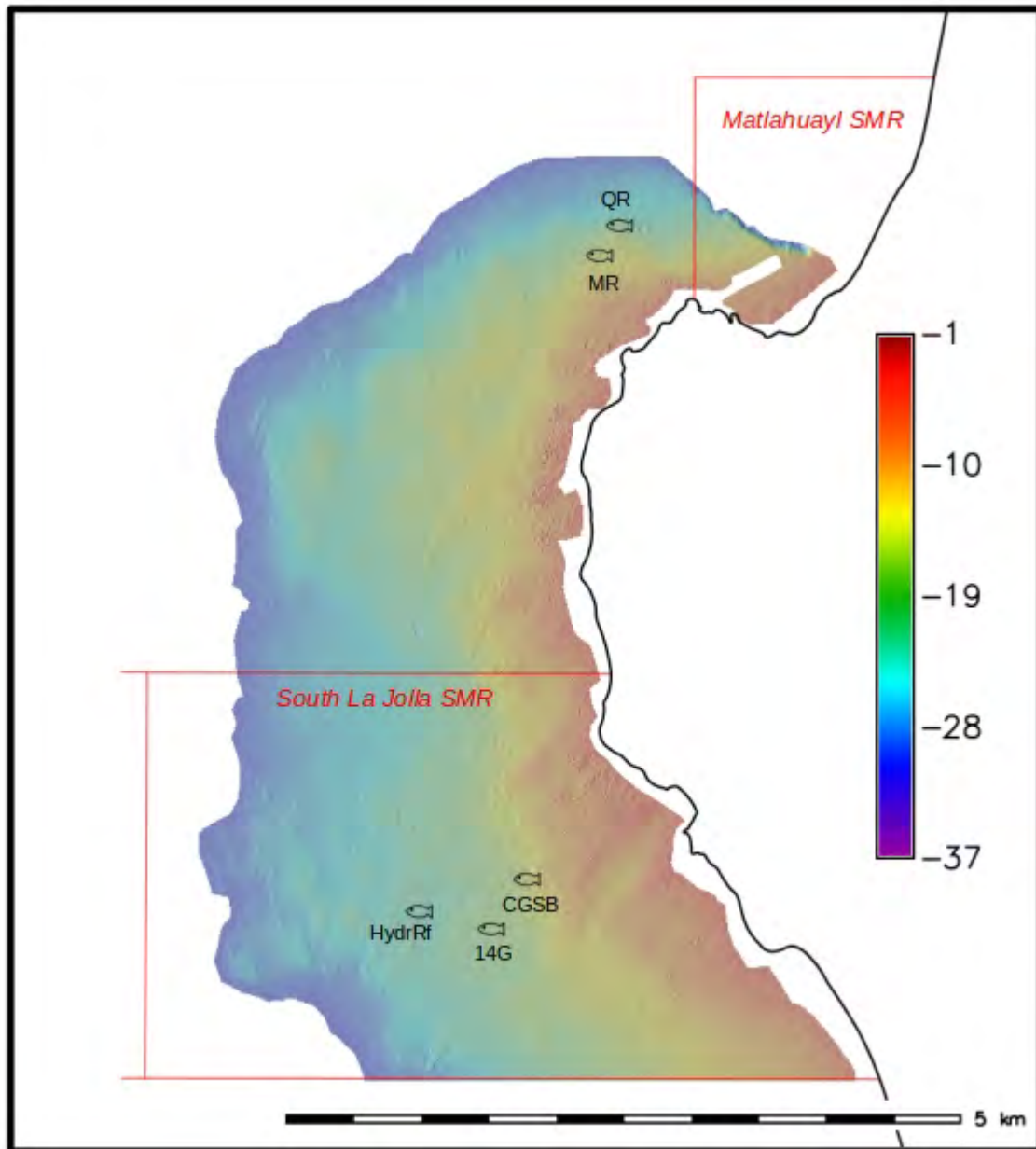


Figure 5. Locations of fish survey study sites within the La Jolla kelp forest. Color legend indicates depth in meters. Note: surveys at ‘CGSB’ were discontinued in 2021 (see text).

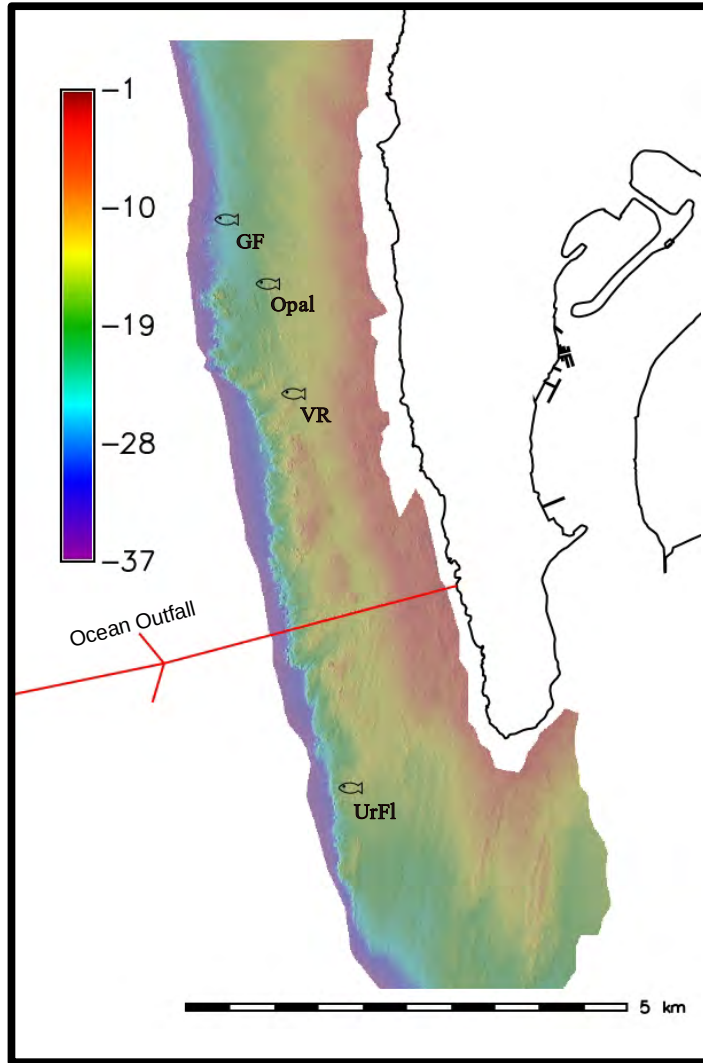


Figure 6. Locations of fish survey study sites within the Pt. Loma kelp forest. Color legend indicates depth in meters. Note: 'UrFL' was replaced by 'VR' in 2020 (see text).

Site	Kelp Forest	Depth (m)	MPA	MPA Pairings	Species Richness
QR	La Jolla	21	No	A	27
HydRf	La Jolla	21	Matlahuayl SMR	A	39
MR	La Jolla	15	No	B	30
14G	La Jolla	17	Matlahuayl SMR	B	38
VR	Pt. Loma	15	No	A	33
Opal	Pt. Loma	15	No	A	37
UrFl	Pt. Loma	16	No	B	
GF	Pt. Loma	21	No	B	33

Table 3. Site details and species richness for fish surveys.

Bottom Light Levels

Marine algae are dependent on ambient light to support photosynthetic production enabling growth, reproduction, and recruitment. The aerial extent of where giant kelp can be found is mainly controlled by the availability of hard substrate at depths where light penetration is adequate for gametogenesis and growth since the plants must all recruit and begin growth at the bottom. Light is attenuated in a logarithmic fashion with ocean depth, and various wavelengths are attenuated differentially. Photosynthesis is facilitated by visible light having wavelengths between 400 and 700 nanometers. Light energy within this bandwidth is generally considered to be of primary importance for photosynthesis and is termed Photosynthetic Active Radiation (PAR). Longer wavelength red light is most rapidly attenuated with depth, while shorter wavelength blue light, most important for gametogenesis in Laminarian kelps including *M. pyrifera* (Lüning and Dring, 1975), penetrates further into the water column. Light availability limits the deepest depths that giant kelp can exist along the mainland shelf of southern California to ~25 m. The clearer offshore waters bathing many of the Channel Islands support kelp stands as deep as ~35 m. The main limiting factor for kelp recruitment at depth is the availability of light for gametogenesis, the lower limit of which has been estimated as a quantum dose of ~0.4 mol of photons m⁻²d⁻¹ (Deysher and Dean, 1984), and ~0.7 mol of photons m⁻²d⁻¹ for early sporophyte growth (Dean and Jacobsen, 1984). As light becomes more limiting with increasing depth, the recovery of giant kelp from disturbances such as a MHW, is increasingly limited due to the abbreviated periods that bottom illumination is adequate for gametogenesis and the growth of the early sporophytes.

Bottom PAR is measured at three depths off central Pt. Loma along a cross-shore transect near the permanent algal study sites but in areas without giant kelp canopy. These areas are dominated by low growing understory algae thus precluding shading by nearby giant kelp canopy. The measurement sites off Pt. Loma are located at 24, 15, and 9 m deep. Submarine light is also measured off southern La Jolla at a depth of 24 m. PME miniPAR loggers equipped with LICOR LI-192 quantum sensors are

used to measure bottom PAR. Sampling was conducted at 1 minute intervals and the sensors were wiped at 4 hour intervals using a PME miniWIPER to keep the sensor surface clear of marine growth.

RESULTS AND DISCUSSION

Ocean Climate

The ENSO index (ONI – Oceanic Niño Index, Fig. 2) is based on equatorial sea surface temperatures in the eastern Pacific Ocean. ENSO warming and cooling of the west coast of the Americas propagates poleward from the tropics, and the extent that individual El Niño or La Niña events propagate to higher latitudes varies greatly. Therefore, while correlated, the magnitude of ENSO events at the equator and temperatures within the SCB can be somewhat decoupled.

The bottom temperature record along the central Pt. Loma study sites (Fig. 7) extends back to 1983 when the strong El Niño of 1982/83 was at its peak. Since then, the largest temperature signals in the time series include the 1997/98 El Niño and the extended warm period of 2014-2016 associated with a large scale anomalous NE Pacific warming event (DiLorenzo and Mantua, 2016) now referred to as the marine heat wave (MHW) of 2015. This was immediately followed by a strong El Niño in 2015/2016 (Figs. 2, 7, and 8). The ONI (Fig. 2) and the Pt. Loma bottom temperature time series (Fig. 7) are highly concordant for the largest ocean climate events including the onset of the coupled MHW/El Niño warm period. A cool period occurred between the fall 2018 and the summer of 2019 followed by slight warming. Most recently conditions have been conducive for kelp growth due to an extended La Niña between 2020 and 2023. However, even though bottom temperatures were cool during this period, there have been increasing episodes of near surface warming during summer when temperatures have exceeded historical levels by as much as 3°C. Surface temperatures during the summer of 2018 during which surface waters (upper 3-5 m) exceeded 27°C and stayed warm through most of the summer. This event was not observed at the bottom at any of the study sites as it was limited to near surface waters, but was evident in the Scripps Pier temperature time series (Fig. 8) and included the warmest temperatures ever observed in the time series. This surface warm event caused significant deterioration of the giant kelp surface canopy which virtually disappeared that summer. However, most plants were still growing and healthy beneath the warm surface layer at the study sites where recovery from the MHW had occurred because bottom temperatures remained relatively cool during the summer of 2018. Surface warming has continued to occur with similar negative effects on the kelp surface canopy during the summers of 2020 to 2023 (Fig. 9, top panel). The recent trend of record and near-record surface temperatures and concomitant near-surface thermocline strengthening poses yet another risk to the health of giant kelp since most canopy biomass is located within the upper 3 meters of the water column. The bottom panel of Figure 9 shows the strength of stratification within the upper 5 meters of the water column. Recent increased near-surface stratification has been attributed to surface warming and exacerbates nutrient limitation as mixing of cooler more nutrient rich waters from below is weakened.

Less pronounced warm periods occurred between the 1997/98 and 2015/16 El Niños. These include the 2005/06, 2009/10, 2018/2019 events when most of the giant kelp canopy disappeared at the surface but plant tissue was still healthy below the thermocline where nutrients were more abundant. Because bottom temperature decreases with depth, nutrient stress during warming events also decreases with depth. This physical forcing is a fundamental mechanism that controls space competition between understory and canopy kelps. Strong El Niños such as the 1997/98 El Niño and the 2014-2016 marine heat wave penetrated to the bottom for extended periods even at the offshore edge of the forest stressing all kelps including understory species. By contrast, milder El Niños do not typically penetrate to the

bottom of the forests for extended periods (e.g., >1 month), and therefore primarily stress the surface canopy kelps (mainly *M. pyrifera*) more than the understory kelps where temperatures are cooler. Repeated cycles of mild to moderate El Niño events over many years in the absence of large storm waves can lead to understory domination at the expense of giant kelp canopy cover.

Bottom temperatures have been cool since the spring of 2018 (<15°C) at all sites except for the shallowest central Pt. Loma sites, leading to recruitment and growth at many of the study sites. Warming occurred during the fall and winter of 2018/19 but temperatures have since cooled with bottom temperatures at study sites deeper than 12 m typically <13°C much of the time. La Niña or near La Niña conditions have dominated the eastern equatorial Pacific since summer of 2020 and southern California by extension. La Niña conditions began to ebb during the late fall of 2022 when ENSO neutral conditions were observed along the equator. El Niño conditions began in the Eastern Pacific tropics in April of 2023 and these conditions persist at present. This latest El Niño has been classified as strong by NOAA and its warming signature in southern California was evident by November of 2023 and is predicted to persist through the spring of 2024 which will likely lead to further loss of giant kelp biomass off San Diego. This is highly likely because giant kelp adult and stipe densities were near or at historic lows for all of the study sites prior to the latest El Niño.

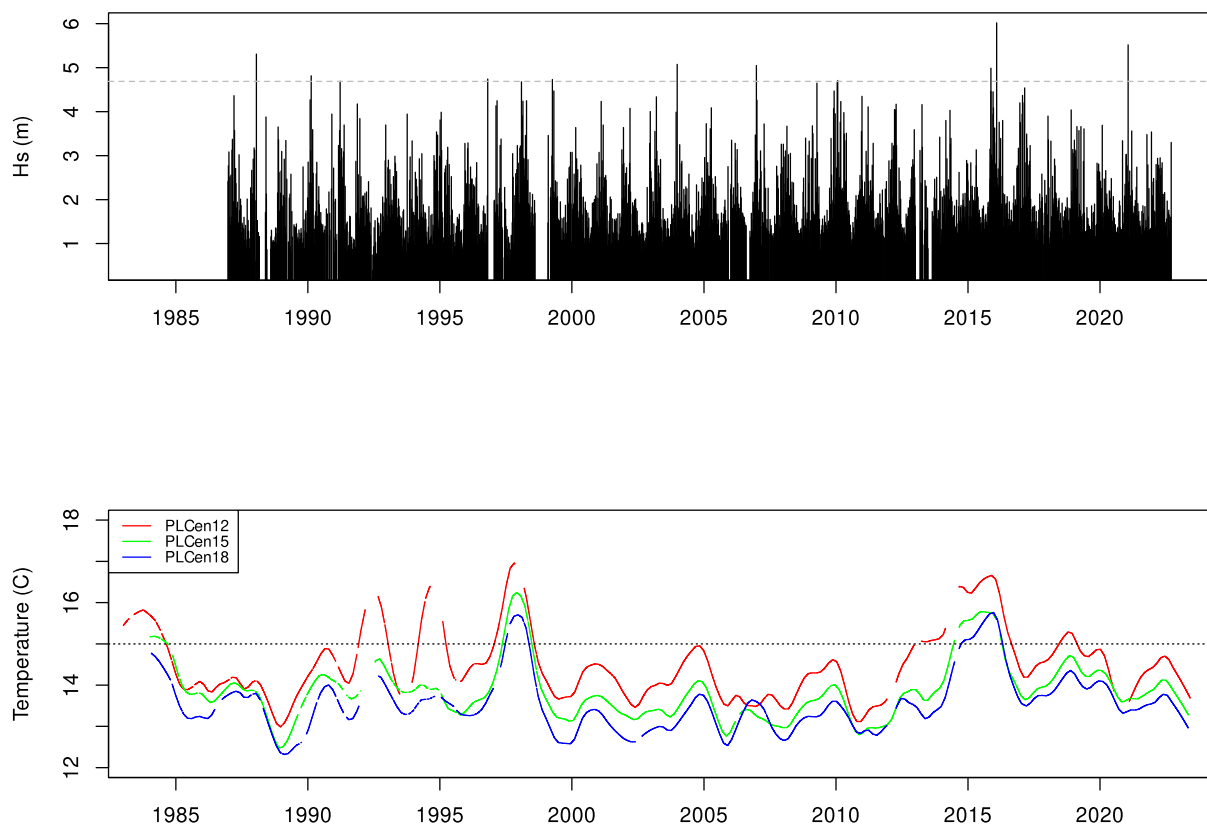


Figure 7. Significant wave height (H_s) offshore of San Diego (top panel), and ocean bottom temperature trends along the central Pt. Loma study sites. Horizontal gray line indicates the temperature above which nitrate concentrations are typically limiting for giant kelp growth.

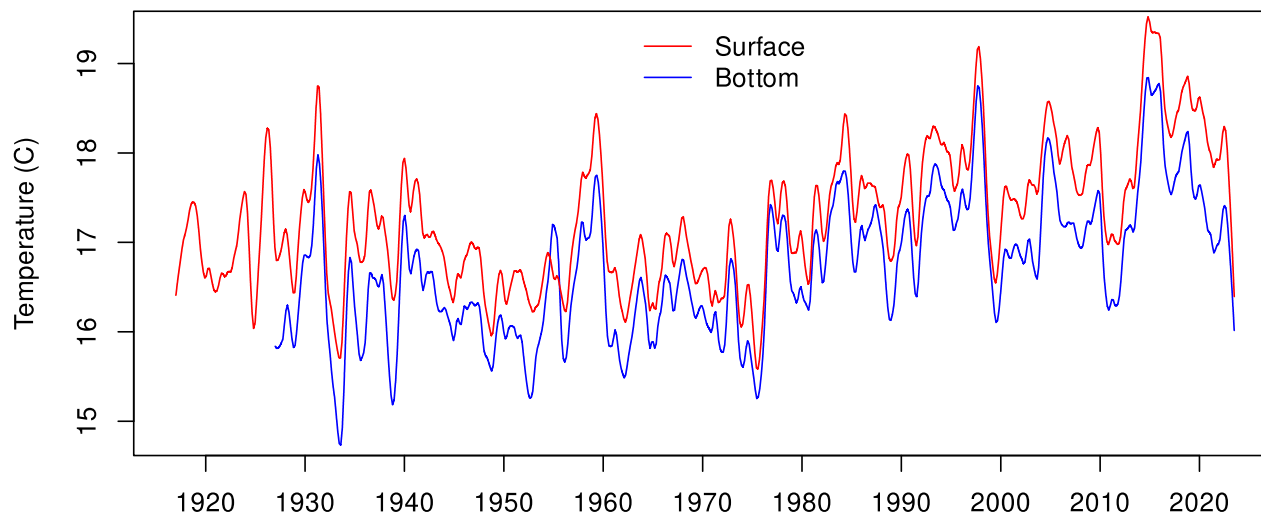


Fig. 8. Trend of surface and bottom (depth=8m) temperatures at the Scripps Institution of Oceanography Pier. Data inclusive through Fall 2021.

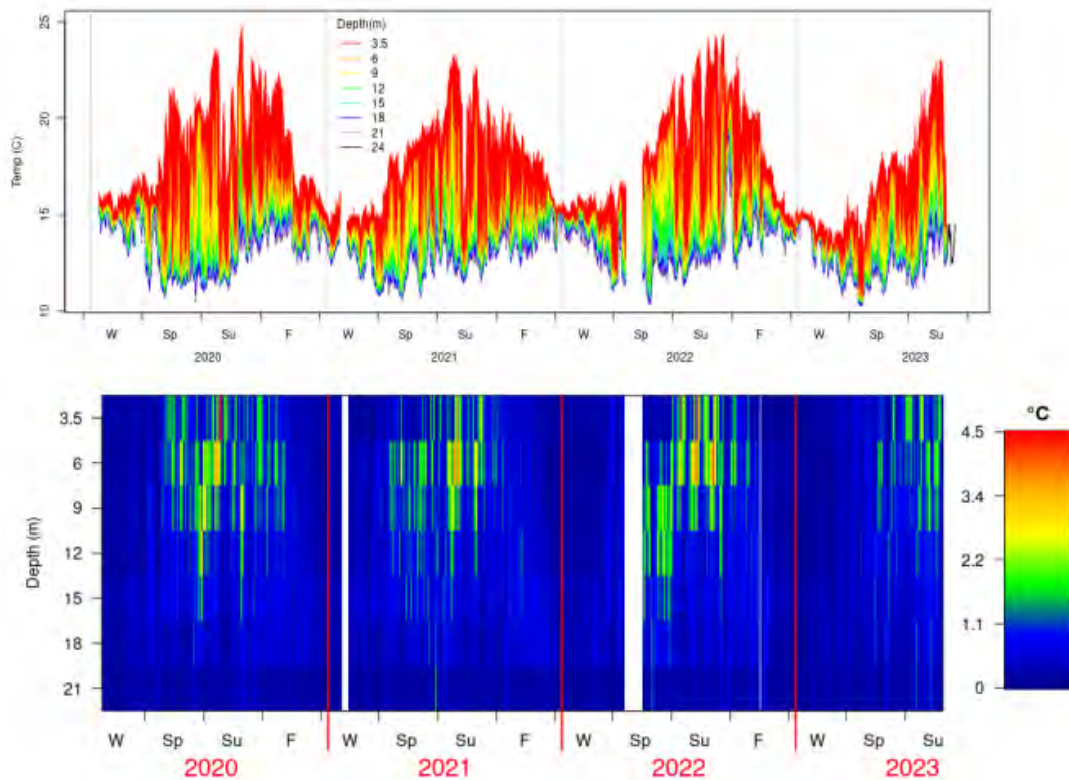


Figure 9. Time series of temperature profiles off south La Jolla (top panel). Bottom panel shows near-surface temperature stratification (temperature difference among thermistors by depth) during spring and summer of 2020 and 2021.

Light

Integrated daily PAR values for the three cross-shore study sites offshore of central Pt. Loma are shown in Fig. 10. Daily PAR levels were typically saturating for giant kelp growth and reproduction at the 9m site except during periods of intense microalgal (phytoplankton) blooms, such as the intense red tide event of spring 2020 when benthic light levels remained near zero for more than a month. This bloom affected the entire coastline of southern California. In contrast, light at the deeper end of the kelp forest at 24 m from 2020 to 2022 was below the gametogenesis and growth thresholds for giant kelp most of the time except for brief periods of increased illumination. Limited benthic light levels at depths >16 m was likely the reason for limited recovery of giant kelp and *Pelagophycus porra* (elk kelp) after the extreme MHW of 2014/15. Benthic light levels at this deeper and all other light meter sites increased for extended periods of time in 2023. Daily PAR values at the 24 m site were saturating for giant kelp growth for much of the summer of 2023.

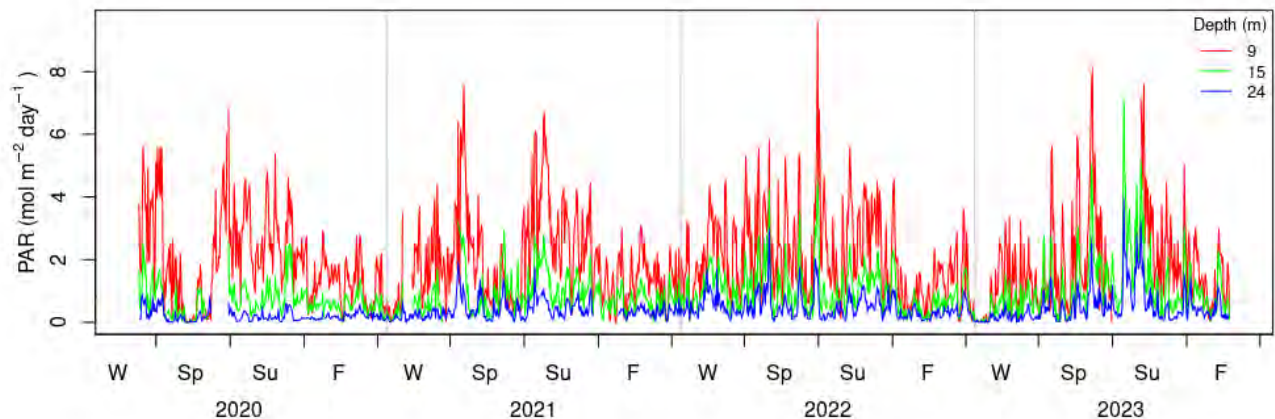


Fig. 10. Daily PAR illuminating the bottom along the central Pt. Loma algal study sites. Horizontal dashed line indicates PAR threshold values for juvenile giant kelp growth (Dean and Jacobsen, 1984).

Giant Kelp Status and Reproduction

The primary pattern of *M. pyrifera* abundance since the 1980's includes rapid declines associated with El Niños and storms (Fig. 11) followed by step increases in plant and stipe density chiefly due to discrete pulses of recruitment after major disturbances. This pattern has been historically reported from aerial photographs and in situ study sites dating back to the 1940s and results from varying levels of recovery. Post-disturbance recovery can also fail due to a lack of reproductive capacity or if a cohort of recruits does not survive to reproductive adulthood or succumbs soon afterward. There are many possible reasons that affect rates of giant kelp recovery that include (1) the magnitude of disturbance leading to kelp mortality, (2) oceanographic conditions and their seasonal timing during the recovery phase, (3) turbidity due to phytoplankton blooms or sediment plumes, (4) space competition with early successional species including *Desmarestia ligulata*, (5) space competition with long-lived understory species, (6) active herbivory, and (7) fouling. Another important factor is the reproductive output of extant adults and their spatial configuration relative to disturbed areas. Presently, there are no nearby sources of giant kelp propagules to support recruitment off northern La Jolla and much of North County.

Adult densities and cohort sizes of *M. pyrifera* off San Diego have decreased since observations began at all long term study sites in the 1980s (Fig. 11 – PLN18, PLC18, PLC15, PLC12, and PLS18) Recent cohorts have become obscured or non-existent despite favorable oceanographic conditions that persisted from 2020 to 2023. The response of giant kelp to disturbance since the 2014/15 MHW appears muted with varying degrees of post-disturbance recovery, resulting in only minor pulses of adult cohort development (Figs. 11-15). Presently, densities of both adults and stipes are at historic lows (Figs. 1, 11, and Table 4) and recruitment has been minimal or non-existent since 2020 (Figs. 12 and 13). The only exceptions are the PLS18 and PLM18 stations in south Pt. Loma. Other southern Pt. Loma stations also experienced some recruitment but only at historically low levels. The reasons for poor kelp performance varied among sites. The most obvious cause was competition for space with understory species at the shallower sites (<15 m) where light is rarely limiting for these species to grow

thus supporting exclusion of *M. pyrifera* recruitment. Deeper sites have likely failed to recover due to low light levels caused by enhanced phytoplankton blooms (Fig. 10). Overgrazing by sea urchins has not been problematic due to their low densities off San Diego since the MHW during which disease decimated their populations.

The 2014-2016 MHW caused massive mortality of giant kelp off San Diego County mainly through a combination of nutrient and temperature stress in addition to storm waves (Fig. 7). Giant kelp surface canopy was nearly entirely lost off most of San Diego, Orange, and Los Angeles counties by 2016. Densities of adult *M. pyrifera* plants (Fig. 11) and stipes (Fig. 14) decreased dramatically at all study sites off San Diego. *M. pyrifera* recruited in some areas of the forests beginning as early as 2016 with subsequent recruitment observed in 2017 and 2018. Low levels of recruitment continued into the spring of 2019 (Figs. 12 and 13). Some of the study site cohorts observed in 2016 partially matured into pre-adults and adults at a subset of the sites but all have since died.

Generally, the status of giant kelp after the last major disturbance can be categorized among the study sites as: (1) recovery to giant kelp dominance, (2) cohort currently in development, (3) recovery followed by collapse, (4) partial recovery followed by collapse, (5) no recovery, and (6) not kelp dominated prior to the latest disturbance nor afterward. These six states are tabulated in Table 4 with regard to the combined warm event of 2019 and the extended period of decreased bottom light of 2020.

Category	Kelp State	# of Study Sites	Study Sites
1	Recovery to dominance	0	
2	Cohort in development after collapse	1	PLS18
3	Recovery followed by collapse	2	PLM18, PLC21 CARD, SB, PLT15, PLS15, PLC18, PLC08, LJS18, LJS15, LJS12, LJN15
4	Partial recovery followed by collapse	10	
5	Kelp abundant prior to disturbance but no recovery	2	PLT12, PLN18 PLC15, PLC12, LJN18,
6	Kelp not abundant prior to disturbance	5	LJN12, DM

Table 4. Recovery states of *M. pyrifera* after the combined disturbances of the 2018/19 warm event and the 2020 phytoplankton bloom which limited light levels to near zero throughout the water column.

Giant kelp stands are presently in a collapsed state where it is absent or nearly so at all but 3 of the 20 sites (PLC08, PLS18, and PLS15). There has essentially been no giant kelp recovery at LJN18 where giant kelp was abundant prior to the MHW and at Del Mar where giant kelp is now completely absent and was sparse prior to the MHW. The reasons for such poor giant kelp performance when growth conditions have been supportive for recovery varies among the study sites, and is not understood at others, particularly LJN18. A combination of competition with understory species, low light conditions, and the lack of nearby reproductive plants all contribute to this pattern of limited giant kelp recovery. An early colonizing post disturbance brown alga, *Desmarestia ligulata*, dominated the

PLT15 and PLM18 study sites until 2019, thus delaying giant kelp recovery via competitive exclusion.

The present poor condition of *M. pyrifera* at most of the study sites is best exemplified in Table 5 which lists the quantiles of stipe sums at each of the sites for the latest sampling bout (Fall, 2023). The site that is currently in the best condition relative to historical data is PLC08 where the quantile for the present stand is ~0.46 representing only 15% of its all time maximum. The next greatest quantiles were observed at PLS18 and PLS15 where stipes counts are <10% of their historical maxima. Presently there are no stipes at half of the study sites which is unprecedented. Table 4 highlights the extremely poor condition of giant kelp off much of San Diego County despite the recent growth conditions that have now been favorable for nearly four years. This may herald the fundamental shift discussed in Parnell et al., (2010) in which the southern limit of *M. pyrifera* shifts northward and kelp forests in southern California begin to mirror algal stands off central Baja California which are typically dominated by understory kelps, particularly *Eisena arborea*. The presently developing El Niño that will likely peak in spring of 2024 will likely further decimate giant kelp. However, this could be buffered by powerful winter storm waves effectively eliminating or significantly reducing understory species followed immediately by the onset of supportive growth conditions such as a La Niña which is now predicted for late summer (NOAA).

Site	Stipes All Time Maximum	Date of Maximum	Stipes Fall 2023	Stipes Quantile 2023	Ratio Max/Fall 2023
PLC08	2454	2018-08-09	363	0.46	0.15
PLS18	2483	1994-06-06	256	0.45	0.10
PLS15	2110	1994-08-25	123	0.27	0.06
LJS15	3341	1994-08-23	49	0.35	0.01
LJS18	2114	2009-08-14	41	0.05	0.02
PLT15	770	1999-10-20	34	0.61	0.04
PLM18	926	2008-12-17	24	0.53	0.03
LJS12	1013	2018-08-07	14	0.04	0.01
PLC18	3336	1990-10-19	9	0.05	0.00
PLC21	3274	2013-05-02	4	0.25	0.00
DM	519	2010-09-03	0	0.48	0.00
PLT12	1952	2008-08-19	0	0.44	0.00
LJN12	607	2014-02-11	0	0.28	0.00
LJN18	2093	2010-08-04	0	0.24	0.00
Card	3341	2014-02-13	0	0.19	0.00
LJN15	2161	2013-11-13	0	0.14	0.00
PLC12	2665	1985-04-11	0	0.13	0.00
SB	2933	2011-11-10	0	0.13	0.00
PLN18	3083	2013-08-15	0	0.10	0.00
PLC15	3819	1989-06-29	0	0.01	0.00

Table 5. Quantiles of giant kelp (*M. pyrifera*) stipe sums observed during the latest sampling bout (Fall, 2023) for all study sites. Date indicates the day that each site maximum was observed. Rows are ordered by decreasing numbers of stipes for Fall, 2023.

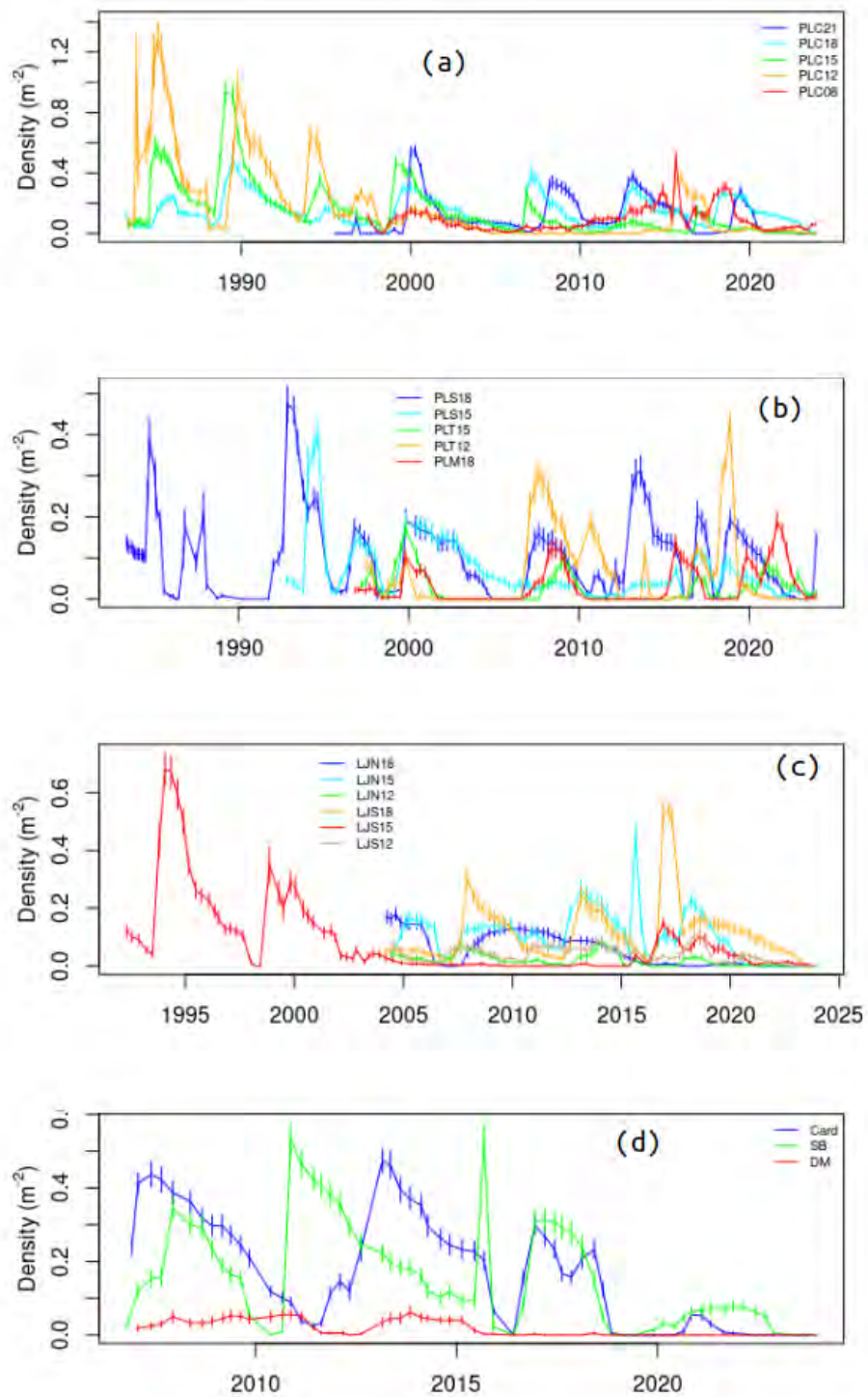


Figure 11. Mean densities of adult *Macrocyctis pyrifera* among study site groups: (a) central Pt. Loma, (b) south Pt. Loma, (c) La Jolla, and (d) North County. Error bars indicate standard errors.

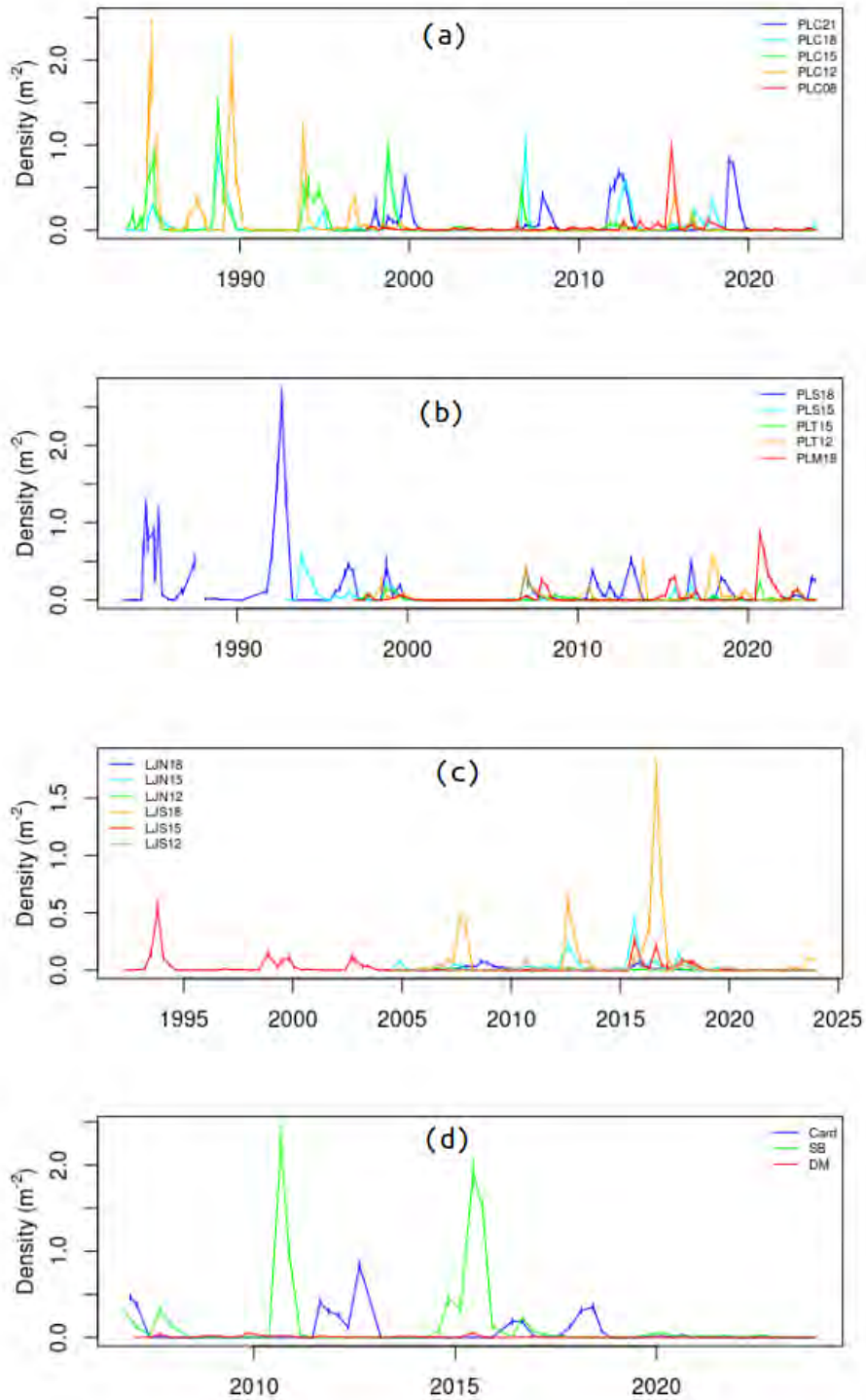


Figure 12. Mean densities of *Macrocyctis pyrifera* pre-adults (<4 stipes): (a) central Pt. Loma, (b) south Pt. Loma, (c) La Jolla, and (d) North County study sites. Error bars indicate standard errors.

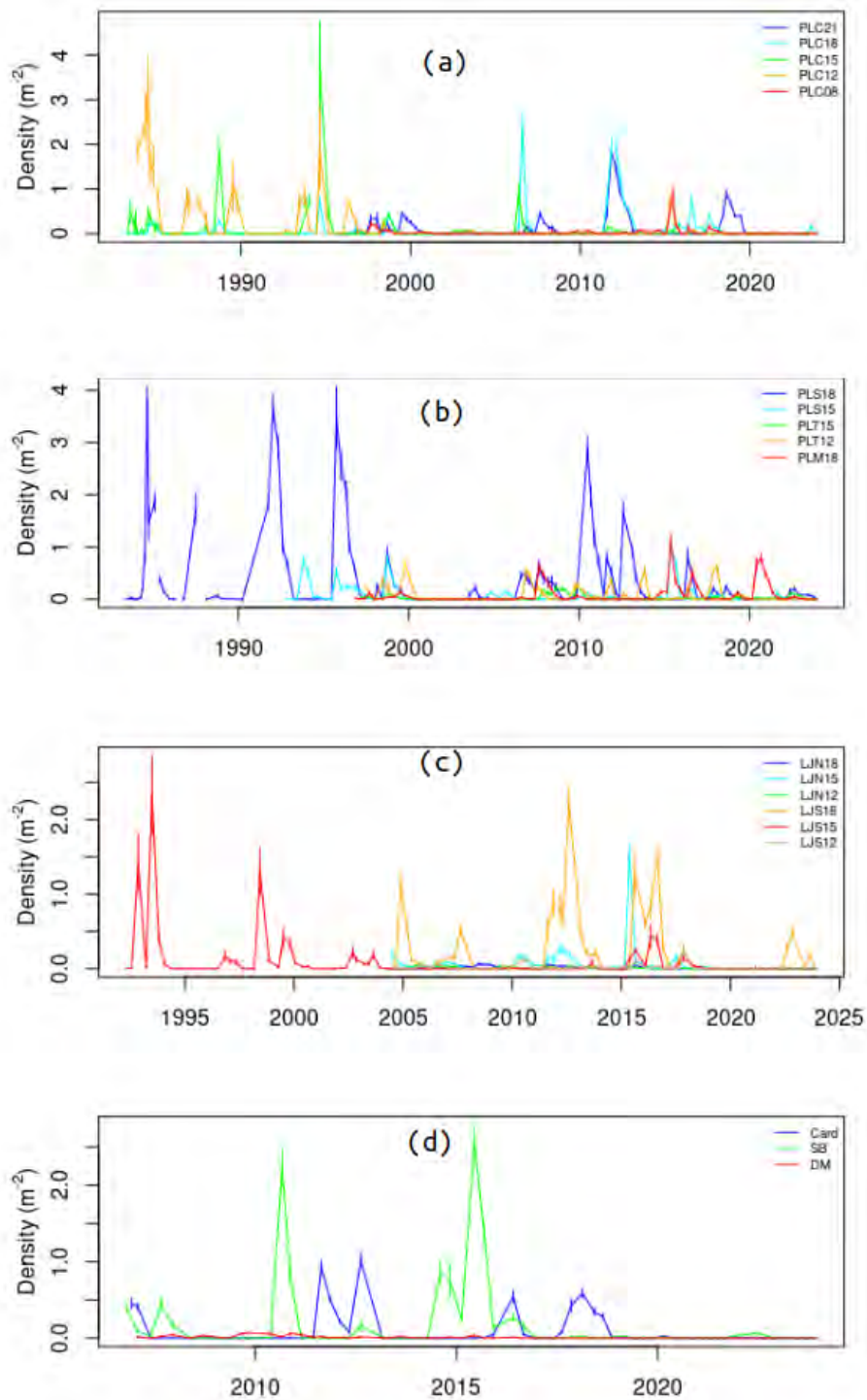


Figure 13. Mean densities of *Macrocystis pyrifera* bifurcates: (a) central Pt. Loma, (b) south Pt. Loma, (c) La Jolla, and (d) North County study sites. Error bars indicate standard errors

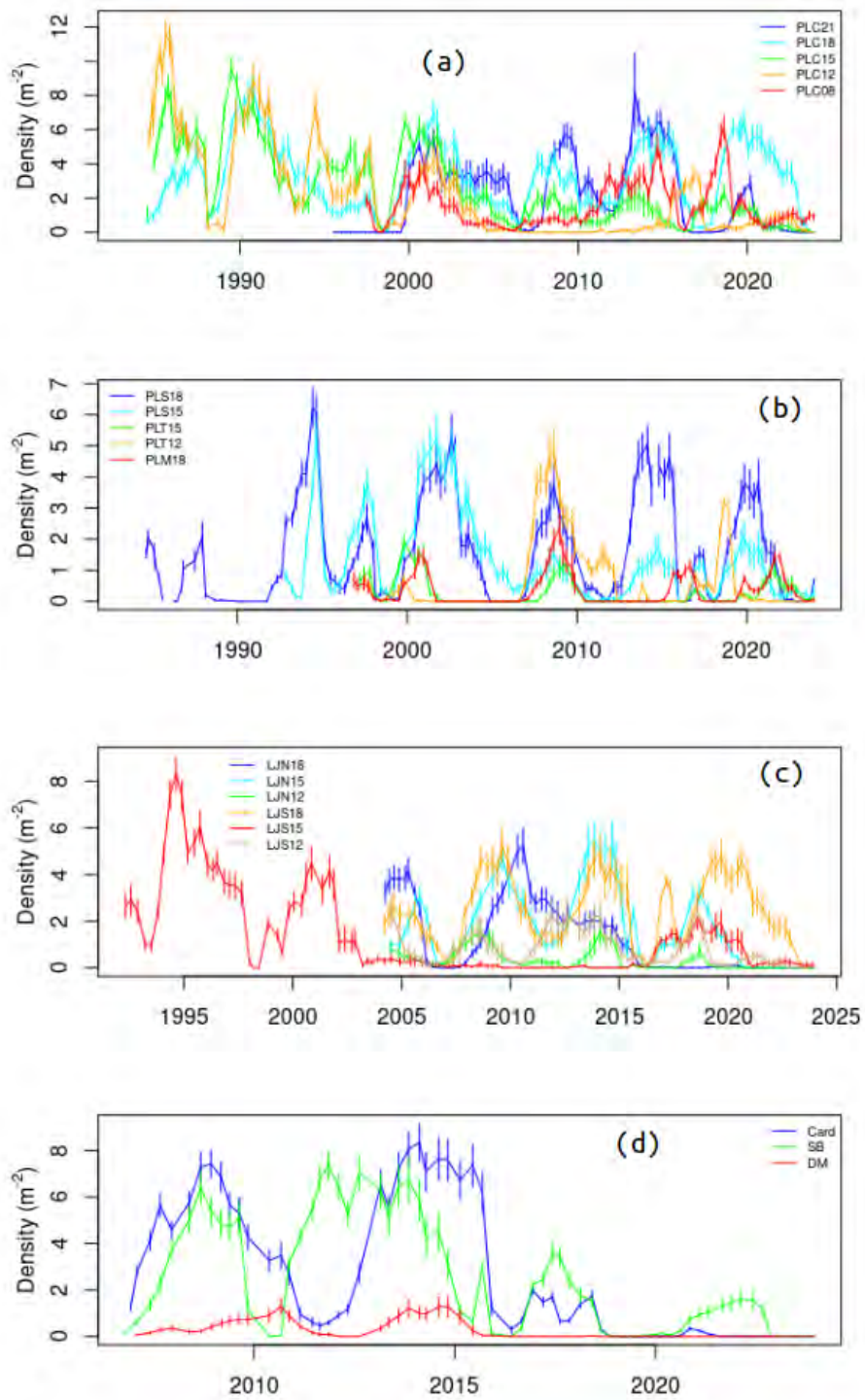


Figure 14. Mean densities of *Macrocyctis pyrifera* stipes: (a) central Pt. Loma, (b) south Pt. Loma, (c) La Jolla, and (d) North County study sites. Error bars indicate standard errors.

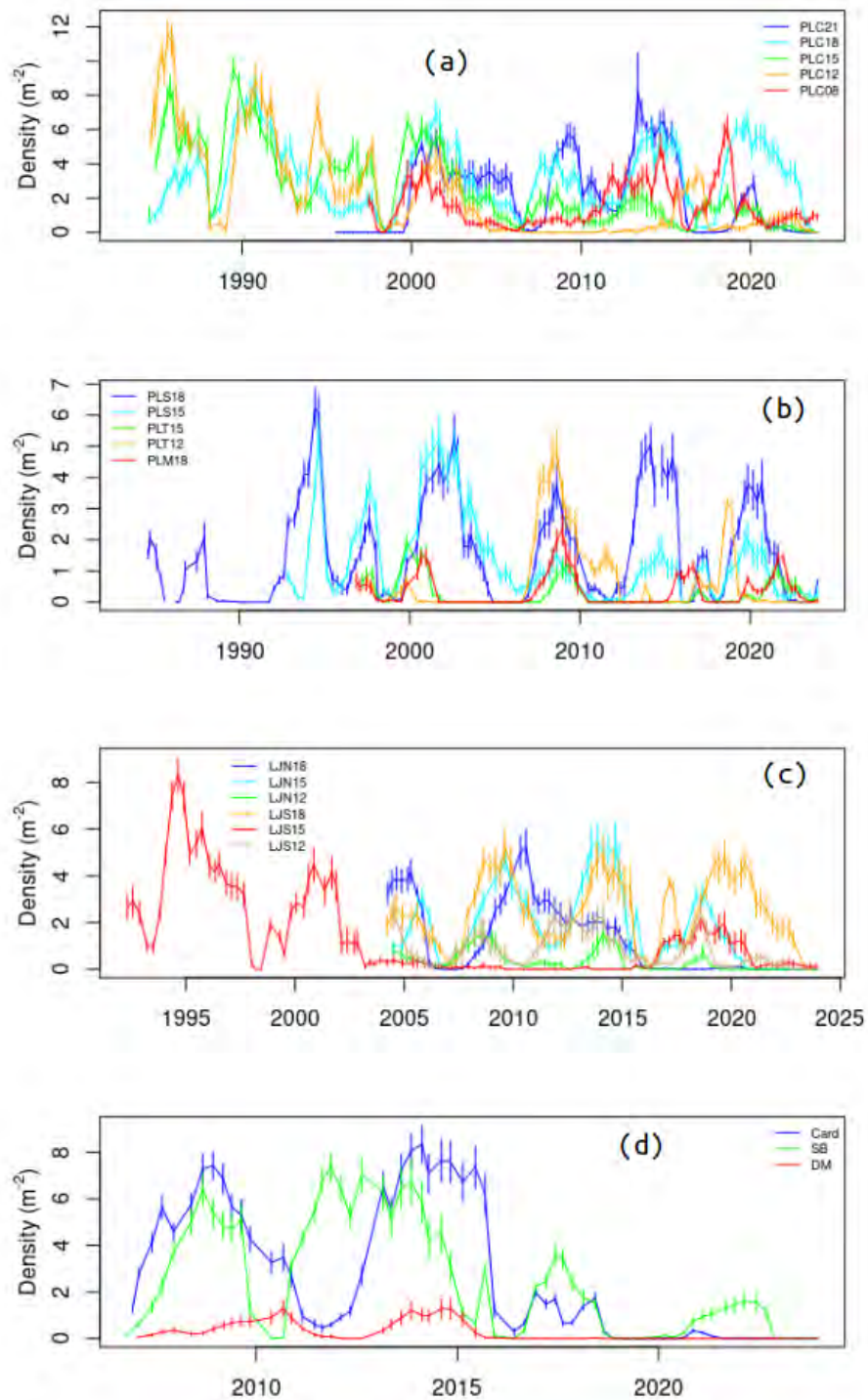


Figure 15. Mean densities of *Macrocyctis pyrifera* (a) adults, (b) pre-adults, (c) pre-bifurcates, and (d) stipes along the 18 m sites off La Jolla and Pt. Loma. Error bars indicate standard errors.

The reproductive condition of giant kelp along the central Pt. Loma study sites was greatly diminished through the MHW. This diminution of reproductive capacity persisted at three of the five central Pt. Loma sites (PLC21, PLC18, and PLC 08 - Fig. 16). Reproductive capacity has since recovered at PLC12 and PLC15. Reproductive capacity at the remaining sites has been at historically low levels dating back to before the 1997/98 El Niño. Sporophyll volumes were greatly reduced by the end of the 2015/16 El Niño and sporophylls were not reproductive at the PLC08 and PLC21 study sites where adult plants were the most abundant. Such greatly diminished reproductive capacity of giant kelp is both an indicator of how stressful the MHW of 2014-2016 was for *M. pyrifera*, but has also likely limited the rate at which giant kelp has been able to recover since that time given the relationship between reproductive capacity as a function of the number of stipes for individual plants (Fig. 16d). Figure 16d indicates that the reproductive output of individual plants relative to their biomass (as estimated by stipe density) has not returned to historical levels and has also likely contributed to the diminished recruitment at these sites. The only study site where reproductive capacity has recovered somewhat is the central Pt. Loma 15 m site (PLC15) where densities of *M. pyrifera* are still low relative to the historical record. Reproductive capacity as a function of stipes (i.e., biomass) has remained diminished during this study period indicating continued reduced reproductive potential that will likely contribute to delayed giant kelp recovery into the future.

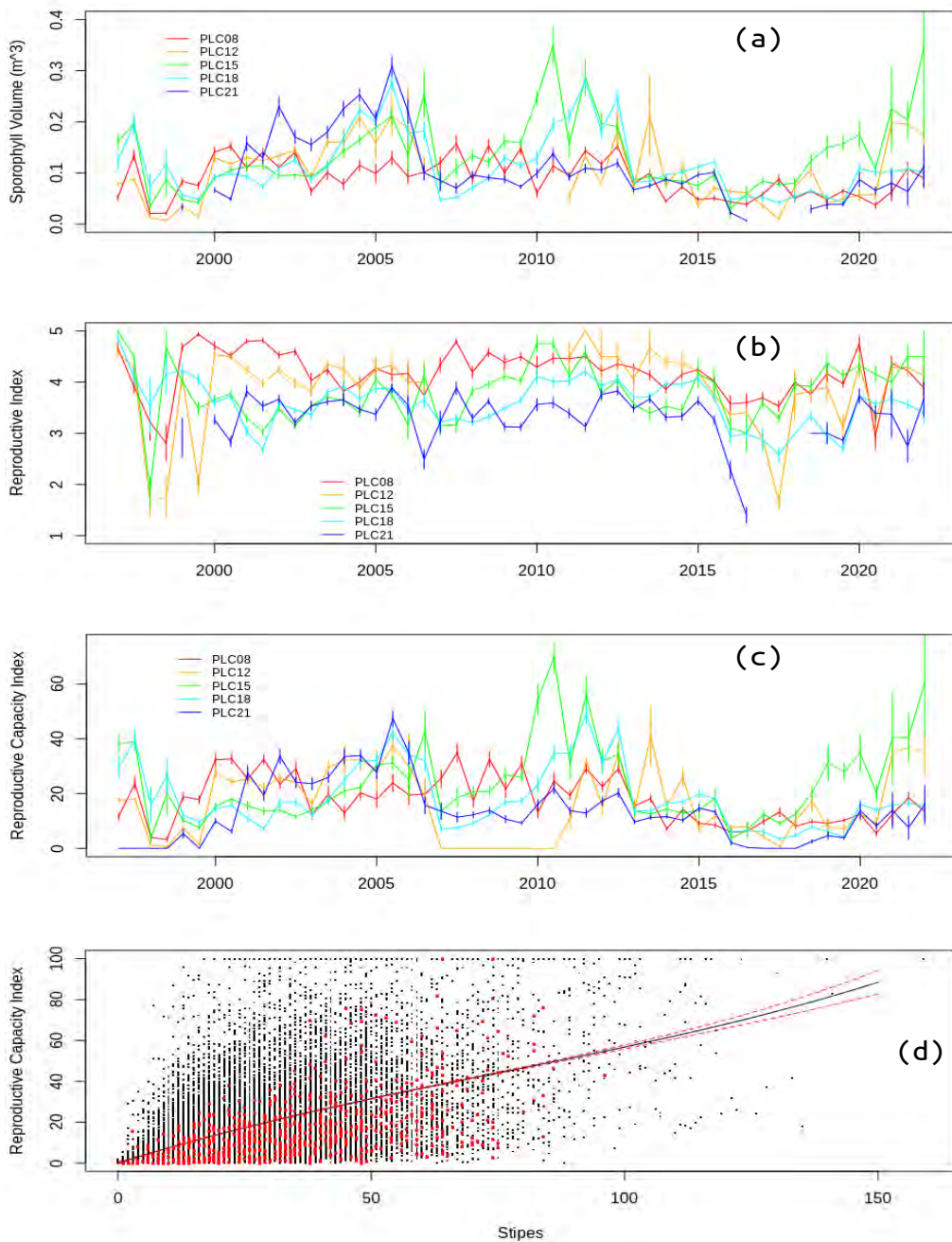


Figure 16. Reproductive states of *Macrocyctis pyrifera* at the central Pt. Loma study sites: (a) sporophyll volume, (b) reproductive index (see Table 2), (c) reproductive capacity (derived index of relative among-site reproductive potential - see Methods). Means are plotted and error bars indicate standard errors. (d) Reproductive capacity of *Macrocyctis pyrifera* as a function of the number of stipes. Fit is a second order polynomial fit and dashed red curves indicate 95% confidence interval. Data are inclusive between 1997-2021. Red points indicate present study period (2020-2021).

Understory Kelp Status and Reproduction

Understory kelps and turf algae grow close to the bottom, and unlike the local canopy forming kelps (*M. pyrifera*, *Egregia menziesii*, and *Pelagophycus porra*), do not have buoyant pneumatocysts to support photosynthetic tissue up in the water column where light is more abundant. Therefore, high densities of canopy forming kelps outcompete understory kelps and turf algae. El Niño events modulate this competition between the two types of canopy guilds. Buoyant, warm and nutrient depleted water is nearest the surface where most of the photosynthetic and nutrient absorbing tissue for giant kelp is distributed. Therefore, giant kelp is disproportionately stressed by El Niños and MHWs. By contrast the understory and turf canopy guilds are exposed to cooler and more nutrient replete waters. As the surface canopy begins to lose tissue and die, the light field for the lower canopy guilds increases leading to rapid growth and reproduction.

Pterygophora californica, a stipitate understory kelp has a central woody stipe that supports photosynthetic blades from below. Stipes can grow up to >2 m in height off the bottom and individuals can persist for decades. The growth form consists of a ribbed terminal blade that grows outward from the end of the stipe. Sporophyll blades grow horizontally outward from the narrowed margins of the stipe. Soral (reproductive) tissue develops on these side branching sporophyll blades. *Laminaria farlowii*, a prostrate understory kelp grows as a long blade along the bottom where it is attached by a small woody stipe and holdfast. Soral tissue develops along the length of the blade. Reproduction and growth is seasonally offset in both species with growth occurring during late spring and summer while reproductive tissue development peaks in winter. *Cystoseira osmundacea* is a low growing fucoid alga in southern California that ranges from the intertidal to shallow subtidal depths and ranges from Oregon to Baja California (Schiel, 1985). Its growth and reproduction is highly seasonal with growth occurring during the spring while reproduction occurs during summer when it can extend to the surface and form a seasonal canopy in shallow depths off central California. Its growth is stunted at deeper depths (>8 m) which includes all sites in this study. It is also known to be able to survive violent storms and thus gains a competitive advantage over giant kelp during such periods.

Pterygophora californica, *Laminaria farlowii*, and *Cystoseira osmundacea* were all profoundly affected by the 2014/15 MHW. Together along with turf species, these species have replaced giant kelp at several sites <18 m deep. Prior to the MHW, *P. californica* stands were relatively dense at the central Pt. Loma and southern La Jolla study sites but then decreased dramatically at all sites by 2016 (Fig. 17). A strong cohort of recruitment was observed at most of these sites shortly afterward leading to a rapid regrowth of young plants. These plants have since been growing and have exhibited self thinning with slow rates of decreasing density. Presently, the greatest densities are located at PLC15, PLT12, LJS15, and are increasing at CARD. Moderate densities exist at the remaining sites except for where it is nearly absent including both North County sites, all north La Jolla sites and PLS18.

Laminaria farlowii abundances also decreased at most sites as a result of the MHW and quickly rebounded within a few years afterward (Fig. 18). Abundances returned to pre-MHW levels within two to three years and still persist at these levels at all of the central Pt. Loma sites except for PLC18. Densities were low at all south Pt. Loma sites prior to the MHW except PLS15 where its abundance has increased and remained high though it is slightly decreasing at present. Abundances at PLT12, PLT15, PLM18 were low prior to the MHW but have since increased. Abundances have been increasing at all North County sites during this study period.

The growth morphology of *Cystoseira osmundacea* is nearly turf-like off southern California including at our study sites where it grows close to the bottom and only extends up to a meter off the

bottom when it is reproductive during summer. The MHW had no negative effects on this species (Fig. 19) as neither the warm water nor high wave events associated with the MHW appeared to affect its density. In fact, densities of *C. osmundacea* have increased since the MHW at most sites and continue to do so with the exception of PLC18, and the southern Pt. Loma sites except for PLT12. Increasing densities have been observed at the North County sites where it had been mainly absent prior to the MHW.

The primary pattern among most of the study sites has been the increase in understory, particularly *L. farlowii* and *C. osmundacea*, which has been facilitated, or has directly contributed to declines in *M. pyrifera* at these sites. The general resistance of understory to heat waves and storm disturbance relative to *M. pyrifera*, and their ability to outcompete giant kelp for space, means that this pattern of understory domination will likely continue well into the future barring the occurrence of a really large storm or strong MHW disturbance.

The complex trajectories of understory species during and after the 2014/15 MHW appear to have switched states. These states can be defined by three canopy/understory modes and are forced by the shading effects of *M. pyrifera* surface canopy. The three modes include (1) lush to moderate surface canopy with less understory, (2) lush understory with reduced surface canopy, and (3) lush to moderate canopy with low fractional cover of understory. A fourth ephemeral mode was also observed during the MHW where both canopy and understory were sparse, forced by the unprecedented duration of nutrient stress. In contrast to previous warming events when the shading effect of giant kelp on understory decreases due to thinning of the surface canopy, warm temperatures during the MHW penetrated to the bottom for an extended period of time (Fig. 7). This resulted in long periods of nutrient stress for these lower canopy species, and delayed their recovery even when bottom light levels increased during periods of low surface canopy. The increased cover of understory and turf species continues at present and is responsible for outcompeting giant kelp at PLN18, PLC15, PLC12, PLC08, LJS15, LJS12, LJN18, LJN15, LJN12, PLS15, PLT15, and PLT12.

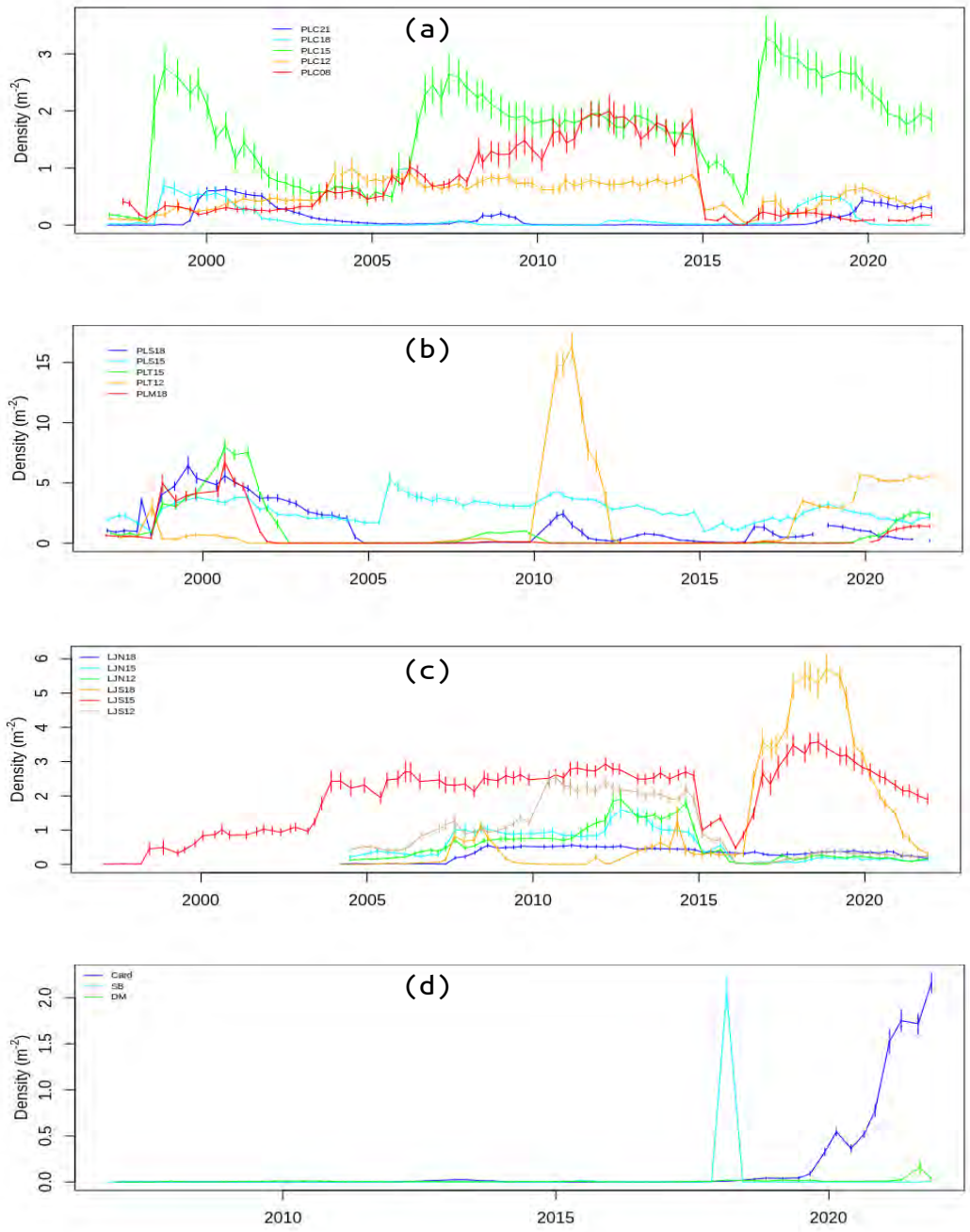


Figure 17. Mean densities of the understory kelp *Pterygophora californica*: (a) central Pt. Loma, (b) south Pt. Loma, (c) La Jolla, and (d) North County study sites. Error bars indicate standard errors.

The growth and reproductive condition of tagged *P. californica* (Figs. 20 and 21) and *L. farlowii* (Figs. 22 and 23) at the central Pt. Loma study sites decreased dramatically during the MHW but have since increased. Growth and reproduction of *P. californica* remained depressed at the deeper central Pt. Loma sites until 2017 and has since decreased at PLC18. Decreased reproductive output by both species can delay understory recovery after El Niño disturbances (Dayton et al., 1984), and may contribute to the persistence of switched canopy/understory patch modes. Such forcing can result in long term dominance over giant kelp that can persist for several years until the occurrence of a new major disturbance. For both species, growth, and reproduction, to a more limited extent, have recovered at all the study sites off central Pt. Loma. Growth and reproduction of *P. californica* was clearly more affected than *L. farlowii* by the marine heat wave of 2014-2016 and has been somewhat slower to recover.

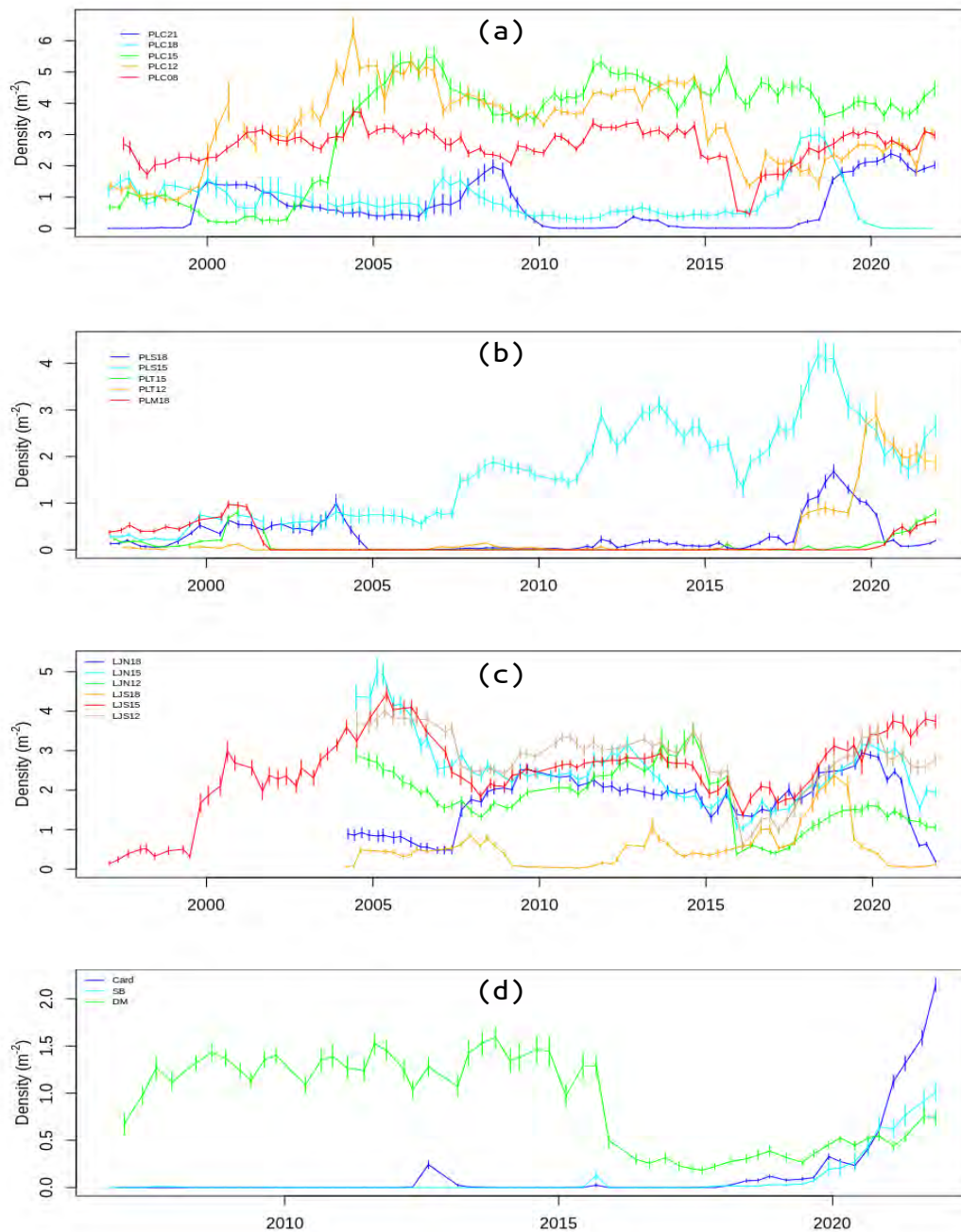


Figure 18. Mean densities of the understory kelp *Laminaria farlowii*: (a) central Pt. Loma, (b) south Pt. Loma, (c) La Jolla, and (d) North County study sites. Error bars indicate standard errors.

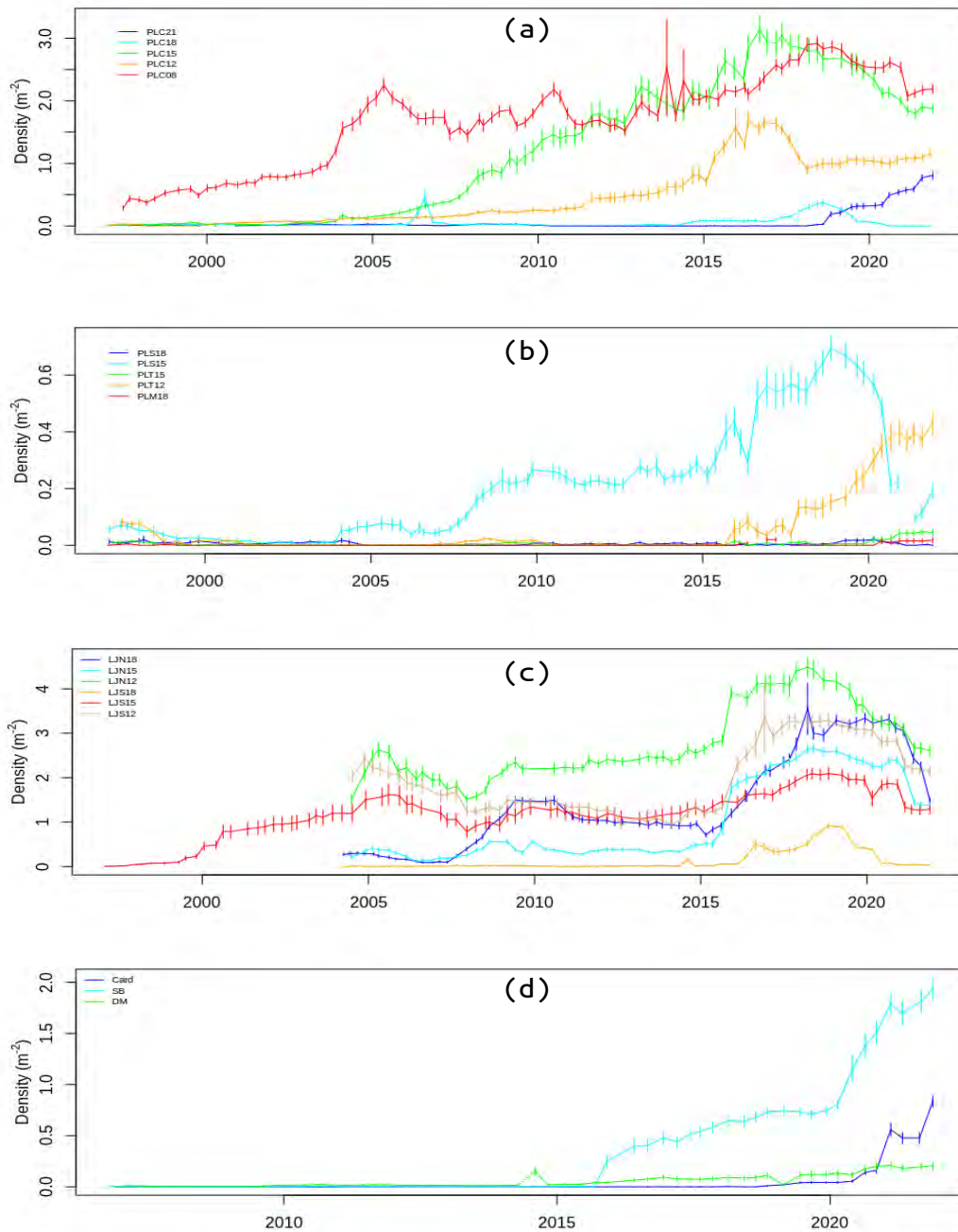


Figure 19. Mean densities of the understory kelp *Cystoseira osmundacea*: (a) central Pt. Loma, (b) south Pt. Loma, (c) La Jolla, and (d) North County study sites. Error bars indicate standard errors.

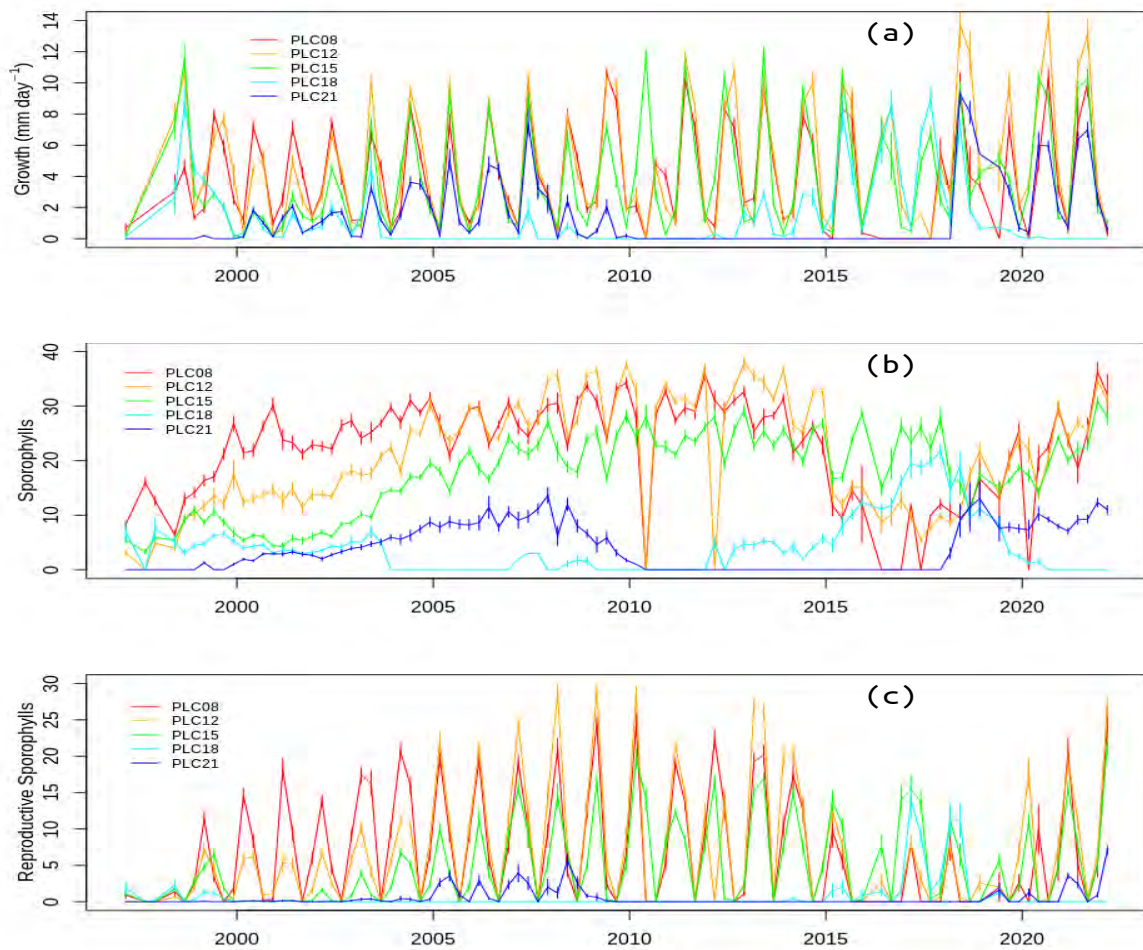


Figure 20. Growth and reproduction of the understory kelp *Pterygophora californica* at the central Pt. Loma study sites: (a) growth, (b) # sporophylls, and (c) # reproductive (sexy) sporophylls. Means are plotted and error bars indicate standard errors.

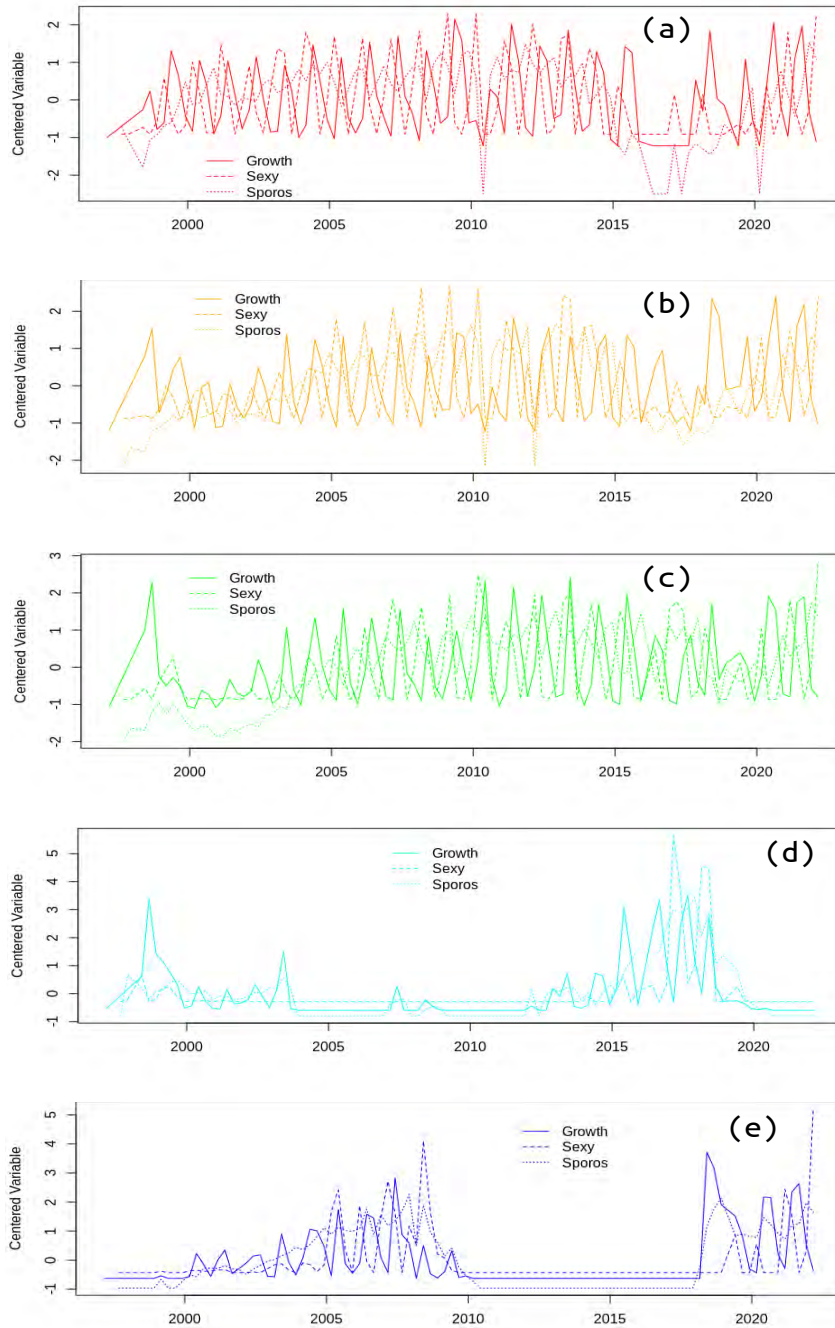


Figure 21. Centered *Pterygophora californica* growth rates, sporophyll, and # of reproductive sporophylls for (a) PLC08, (b) PLC15, (c) PLC18, and (d) PLC21 study sites. Means are plotted and error bars indicate standard errors.

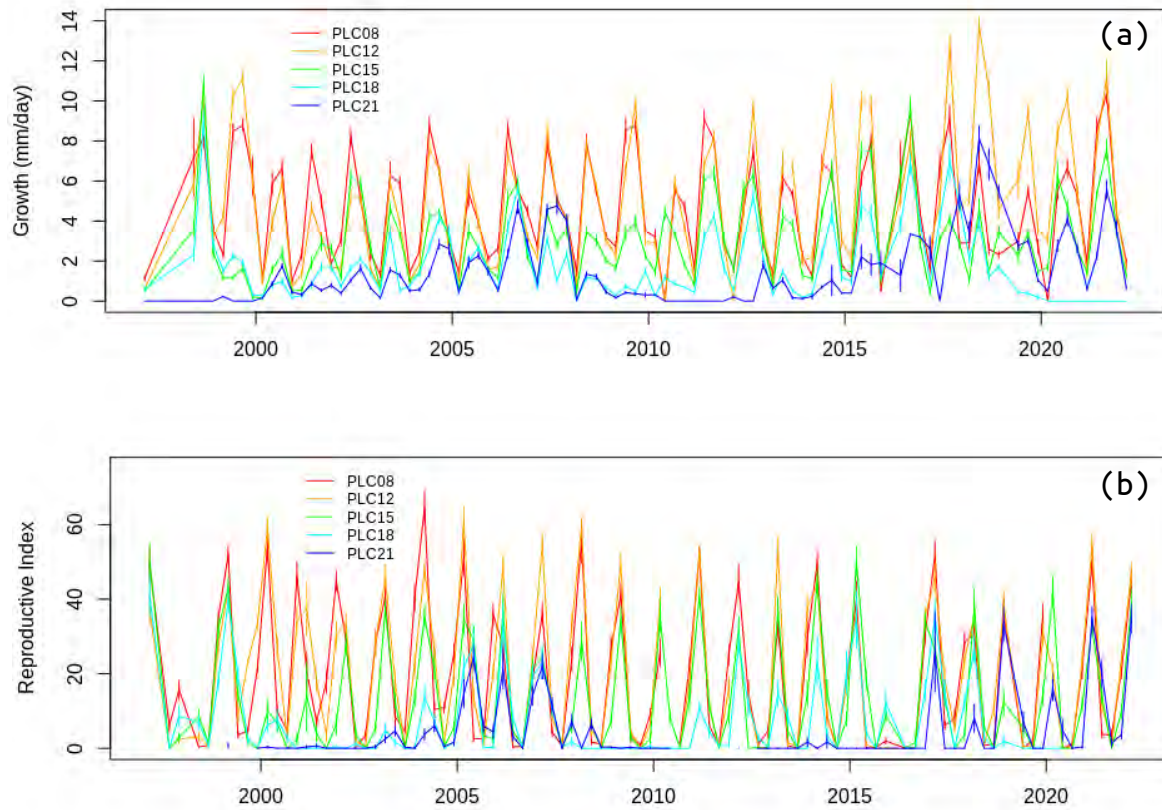


Figure 22. Growth and reproduction of the understory kelp *Laminaria farlowii* at the central Pt. Loma study sites: (a) growth, and (b) % of blade that is sorus (reproductive), Means are plotted and error bars indicate standard errors.

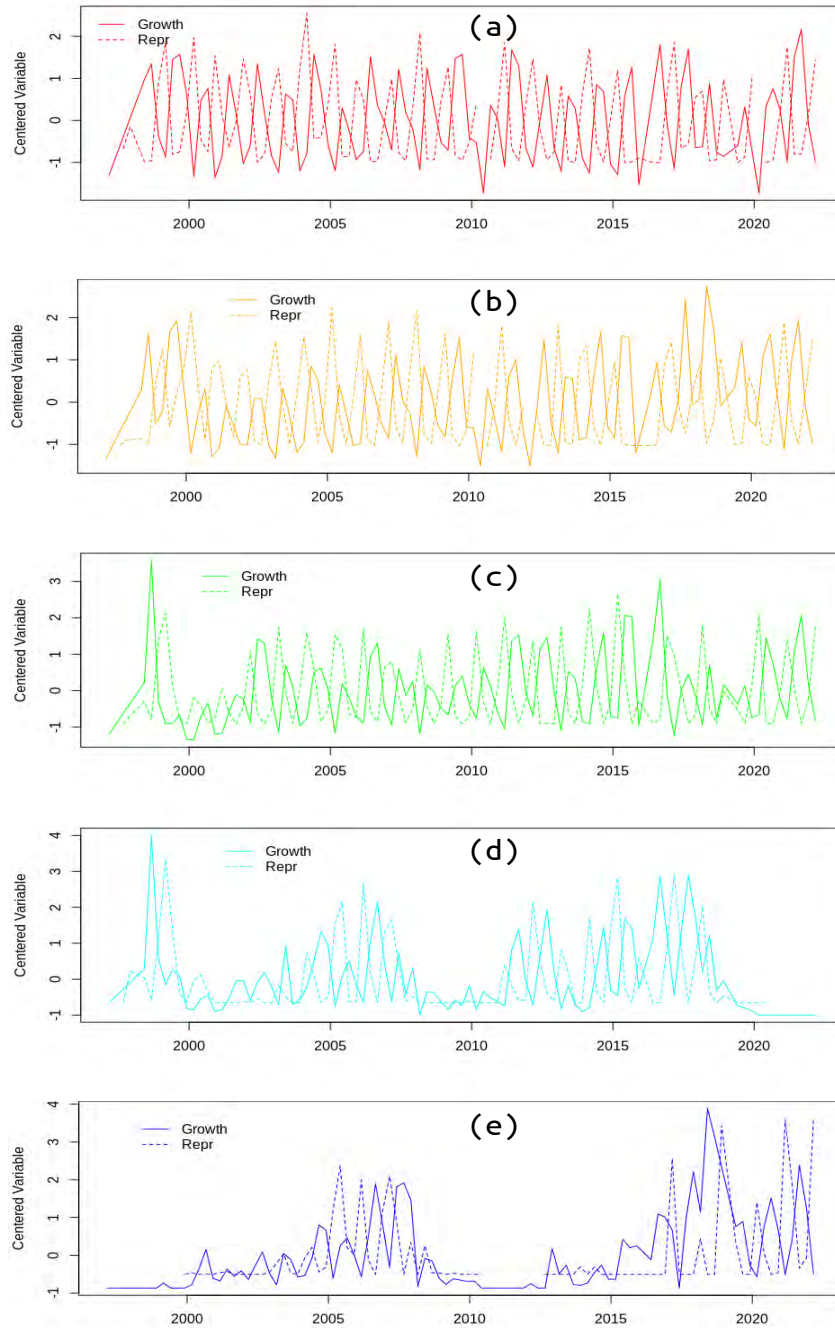


Figure 23. Centered growth and reproduction of the understory kelp *Laminaria farlowii* at the central Pt. Loma study sites. (c) standardized growth and reproduction for the PLC8 and the (d) PLC12 study sites.

Algal Community Analysis

Algal community composition among all of the study sites during the study period are shown in Figures 24-28. These figures were produced using factor analysis to reduce the number of dimensions represented each algal species being tracked over time. All of the algal species and/or groups each represent a single dimension, and factor analysis reduces the number of dimensions to graphically visualize algal community states among sites by year. The most abundant algal species and groups were included in the analysis as well as bare space which was included as a derived ranked variable (see Methods). Here, the first two factors, which account for the greatest amount of variability in the analysis, are plotted against one another. Factor 1 indicates a continuum (from positive to negative) of understory algal composition ranging from fleshy red and articulated coralline algae to the stipitate species, *Eisenia arborea*, and *P. californica*, the prostrate brown alga *L. farlowii*, to the post-disturbance pioneer brown alga *Desmarestia ligulata*, to bare space. This factor captures the depth gradient effect from shallow to deep (positive to negative), representing the gradient in benthic light availability. Shallower sites are typically saturated by adequate light thus facilitating algal domination, whereas deeper sites are light limited thereby reducing algal growth and reproduction, which forces a change from algal domination at shallower depths to domination by encrusting suspension feeders at depth. Factor 2 indicates the condition of *M. pyrifera*, whether sites are dominated by adults and abundant stipes (positive values) or young recruits and pre-adults (values near zero) to a virtual absence of surface canopy (negative values).

A holistic view of macroalgal community composition among the study sites is best envisioned by contrasting the upper left and lower right quadrants of Figs. 24-28. The upper left quadrant indicates *M. pyrifera* domination and sparse understory and turf. The lower right quadrant represents understory and turf domination. A mature giant kelp forested area with heavy canopy will occupy the upper left quadrant whereas an area with patchy or non-existent giant kelp canopy with turf algae will occupy the lower right quadrant. The middle section of each plot represents a mixed stand of *M. pyrifera* with stipitate and laminate kelps and moderate coverage of turf algae. The progression of sites having giant kelp in 2019 after the the first wave of post-MHW recruitment to the diminution of giant kelp at most sites by 2023 is evident in the plots as is the variability among the sites which mirrors the evolving sparse and patchy nature of giant kelp forest condition off San Diego County during this study period.

The algal states of sites PLC18, PLC21, PLN18, PLS18, and LJS18 represented the best condition for giant kelp forests during the study period and generally after the MHW with moderate to moderately high densities of giant kelp over shading understory in 2019 during the first year of this reporting period. Subsequent years showed a progression of *M. pyrifera* loss with one ephemeral episode of growth at PLM18 in 2021. Even this stand began to disappear by the following year. The most consistent site with regard to giant kelp was PLC08 where it is sparse by historical standards (Table 5).

The forcing behind these patterns of algal cover among the sites is not well understood at all study sites. *M. pyrifera* has failed to thrive during the cooler nutritive conditions of the last several years even after initially recovering to some extent at many of the sites where understory kelps have either remained steady or increased since the MHW. These patterns of reduced canopy cannot be attributed to sea urchin overgrazing as both common local species crashed during the MHW and have yet to increase, though some recruitment has recently been observed. But these animals are still small and in low enough density to not yet present a risk of over grazing. The two deeper sites off northern La Jolla are devoid of all giant kelp and look highly disturbed for unknown reasons. Del Mar is also presently highly disturbed with very little macroalgae. These sites are essentially ‘urchin-less barrens’

and have become dominated by suspension feeding invertebrates including bryozoans and gorgonians.

2019

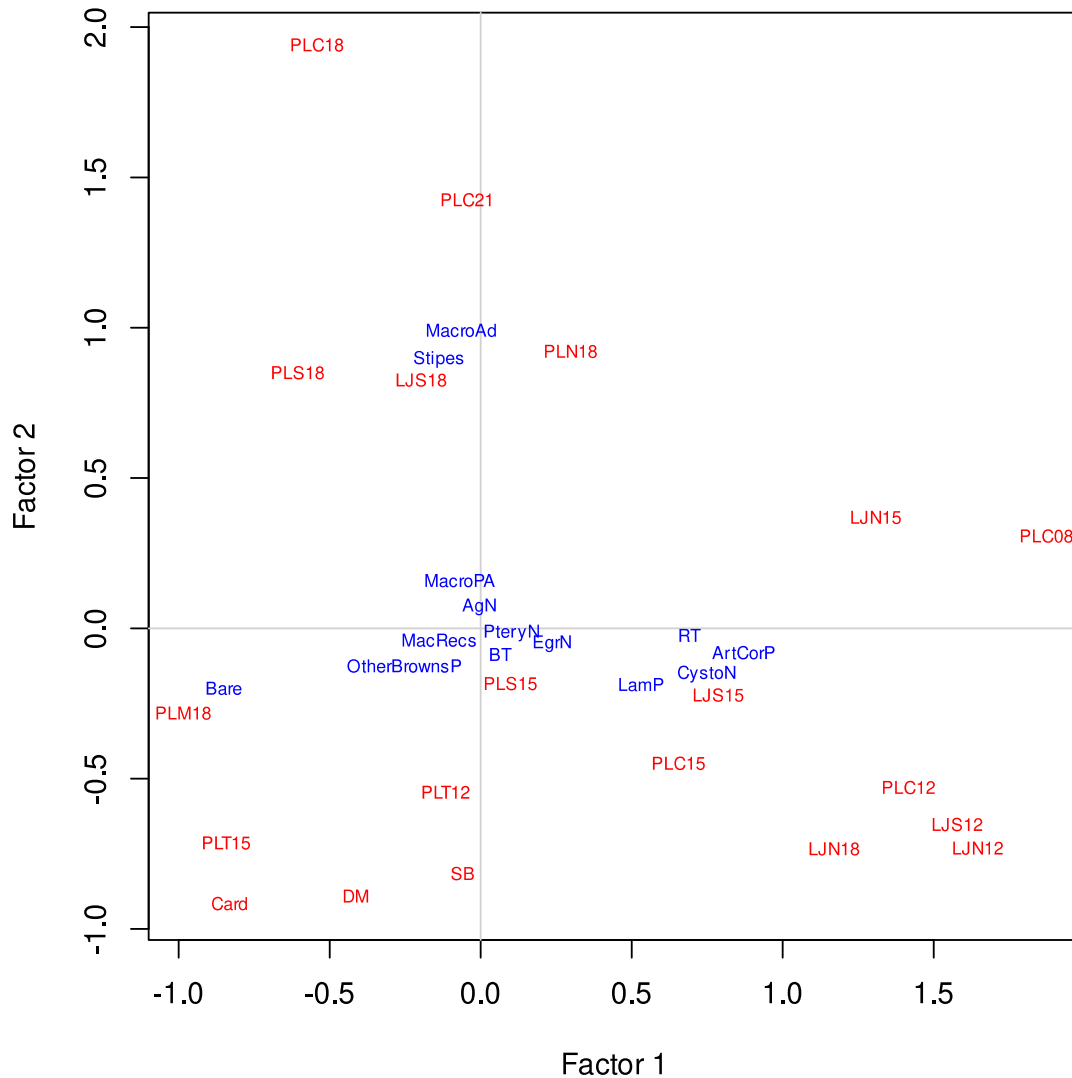


Figure 24. Plot of first two factors resulting from the factor analysis of algal groups among the 20 permanent study sites in 2019. Algal group definitions: Bare = derived bare space, MacRecs = *M. pyrifera* recruit stage (pre-bifurcates + bifurcates), MacroAd = *M. pyrifera* adult density, Stipes = *M. pyrifera* stipe density, MacroPA = *M. pyrifera* pre-adults (<4 stipes), PteryN = *Pteryogophora californica* density, LamP = *Laminaria farlowii* percent cover, EisN = *Eisenia arborea* density, EgrN = *Egria menziesii* density, AgN = *Agarum fimbriatum* density, DesP = *Desmerestia ligulata* percent cover, ArtCorP = articulated coralline algae percent cover, RT = foliose red algal percent cover, BT = brown algal turf percent cover.

2020

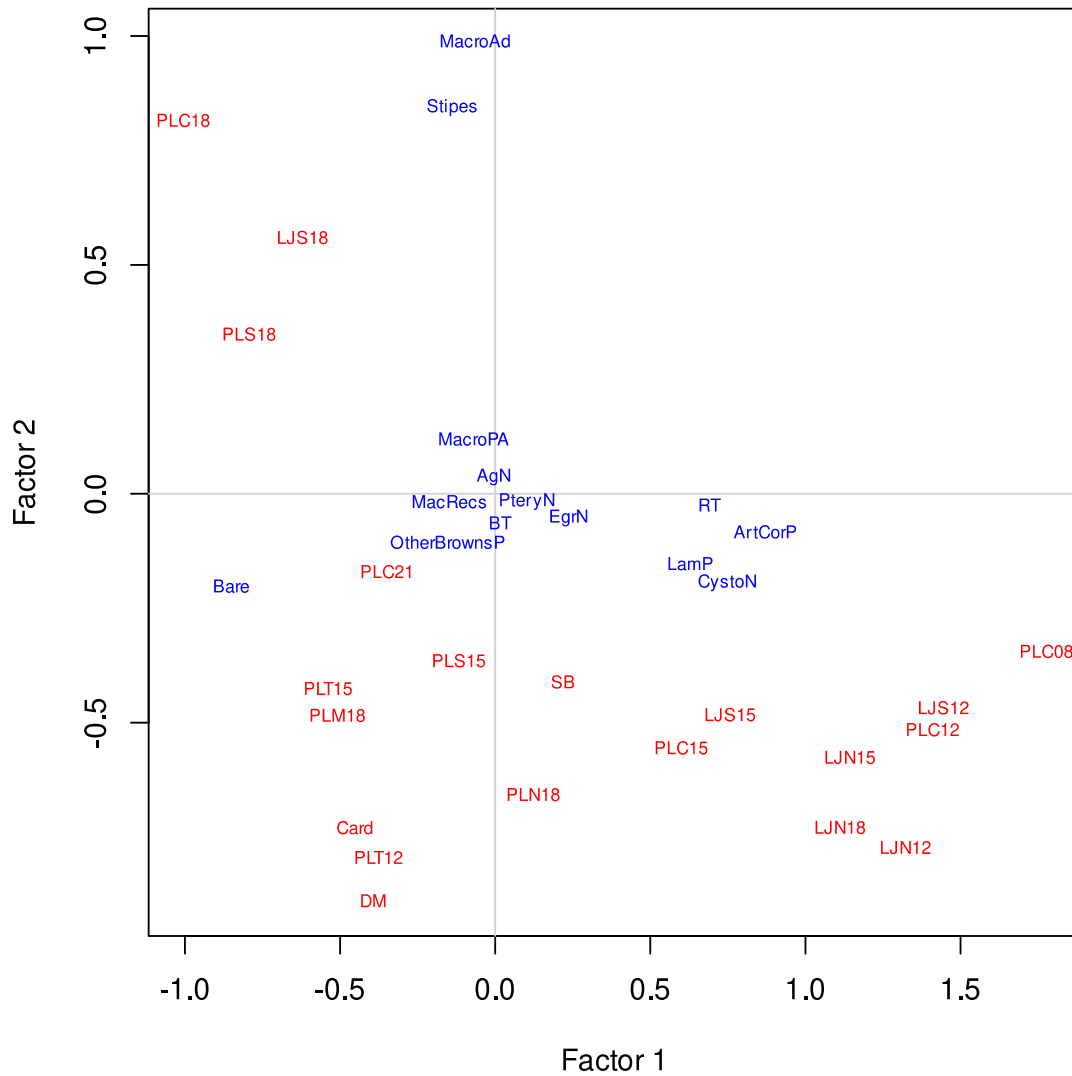


Figure 25. Plot of first two factors resulting from the factor analysis of algal groups among the 20 permanent study sites in 2020. See Figure 24 for description of plot.

2021

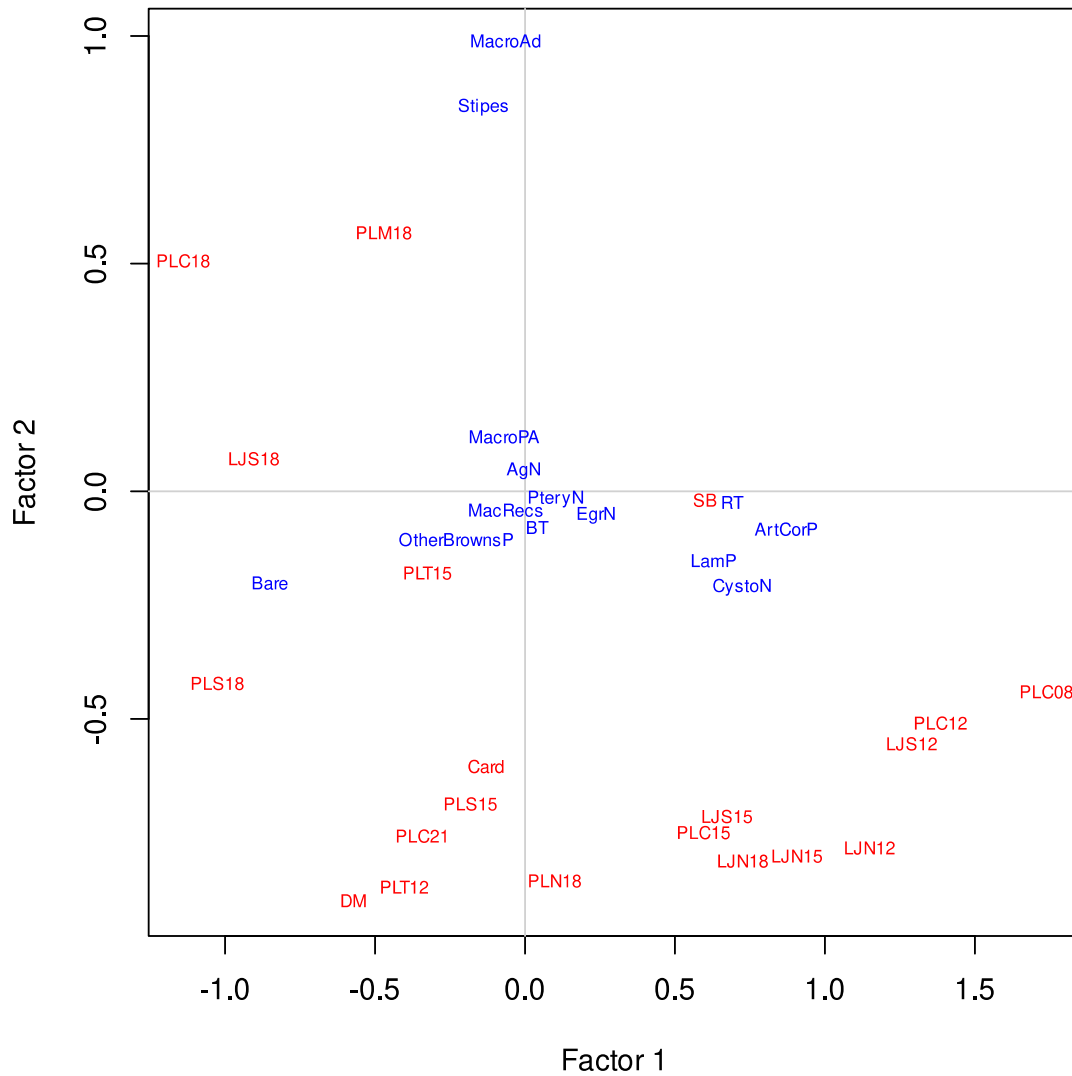


Figure 26. Plot of first two factors resulting from the factor analysis of algal groups among the 20 permanent study sites in 2021. See Figure 24 for description of plot.

2022

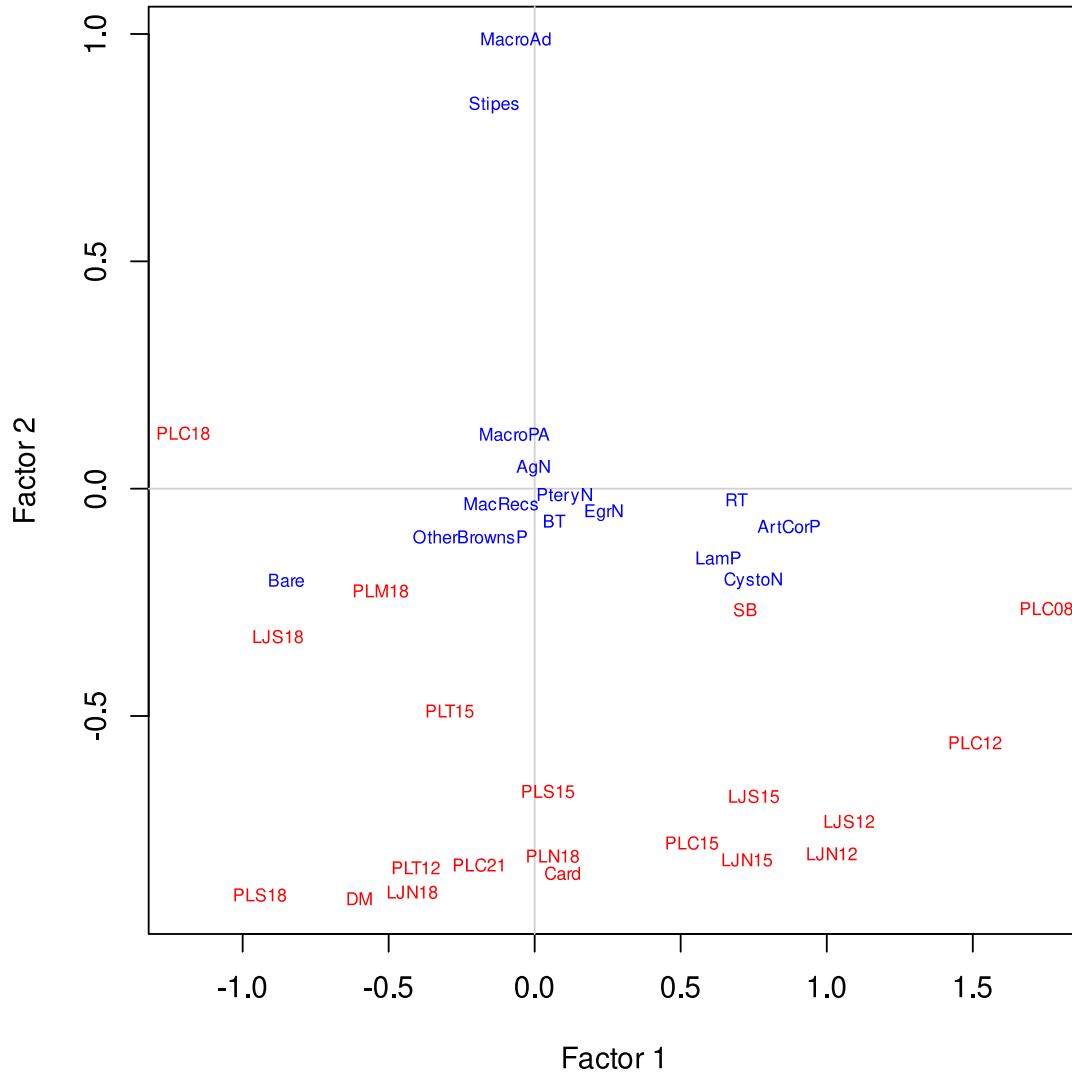


Figure 27. Plot of first two factors resulting from the factor analysis of algal groups among the 20 permanent study sites in 2022. See Figure 24 for description of plot.

2023

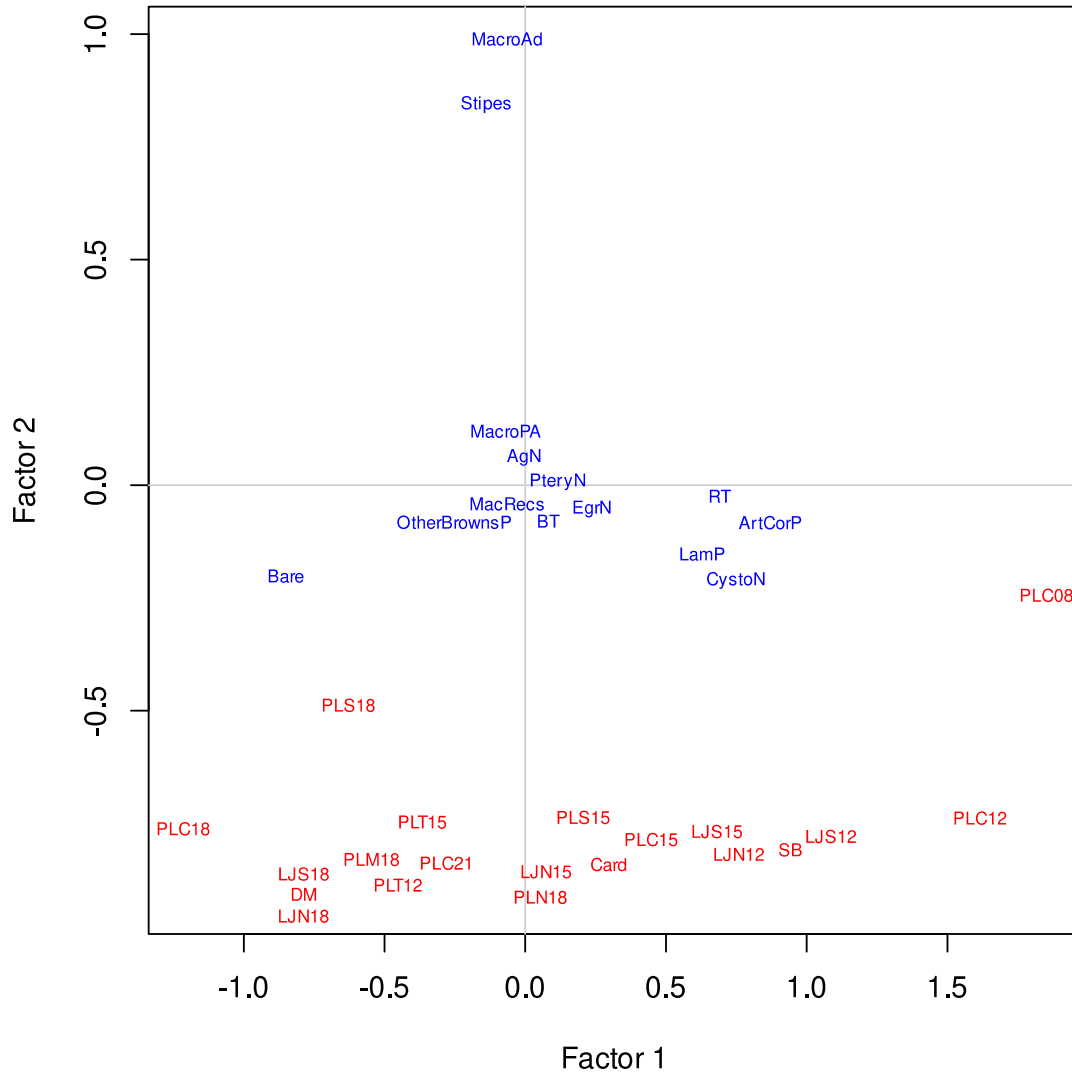


Figure 28. Plot of first two factors resulting from the factor analysis of algal groups among the 20 permanent study sites in 2023. See Figure 24 for description of plot.

Invasive Algal Species

Sargassum horneri is an algal species native to Japanese and Korean coastlines but has invaded southern California within the last couple of decades. *S. horneri* was first reported from Long Beach Harbor in 2006 (Miller et al., 2007) and has gradually spread along the southern California coastal shelf. It was first observed in San Diego County in Mission Bay in 2008. *S. horneri* dominates some areas formerly dominated by *M. pyrifera* including areas off Santa Catalina Island and the Northern Channel Islands off Santa Barbara. *S. horneri* was first observed in the kelp forests off San Diego in early 2014. Since that time, it has spread to 13 of our study sites. Initially, it was only observed near some of the study sites, but has subsequently been observed along the permanent band transects at several sites. Table 6 lists first sightings within the actual band transects, and the relative frequencies among the study sites pooled over time are shown in Figure 29. The greatest percent cover observed

thus far has been at PLC08 (Fig. 30) in the fall of 2017 when mean percent cover exceeded 3.5%. This maximum was followed by a maximum percent cover of ~3% at LJN18 in the fall of 2018 where it has varied in percent cover ever since. However, while *S. horneri* spread relatively quickly to many study sites by 2018, it still has not been observed at seven other sites (Cardiff, Del Mar, PLC15, PLC12, PLS15, PLM18, and PLT15). Rather, it has decreased or disappeared at many of the invaded sites, and presently persists at at very low cover at all sites and disappearing from several others.

However, *S. horneri* clearly poses a risk to *M. pyrifera* and other algal species due to its potentially high seasonal growth rates. It is not implausible for it to take over some areas of San Diego kelp forests especially after a future major disturbance that reduces the densities and cover of native algal species. Presently, it is too sparsely distributed and in low densities to be significantly affecting giant kelp.

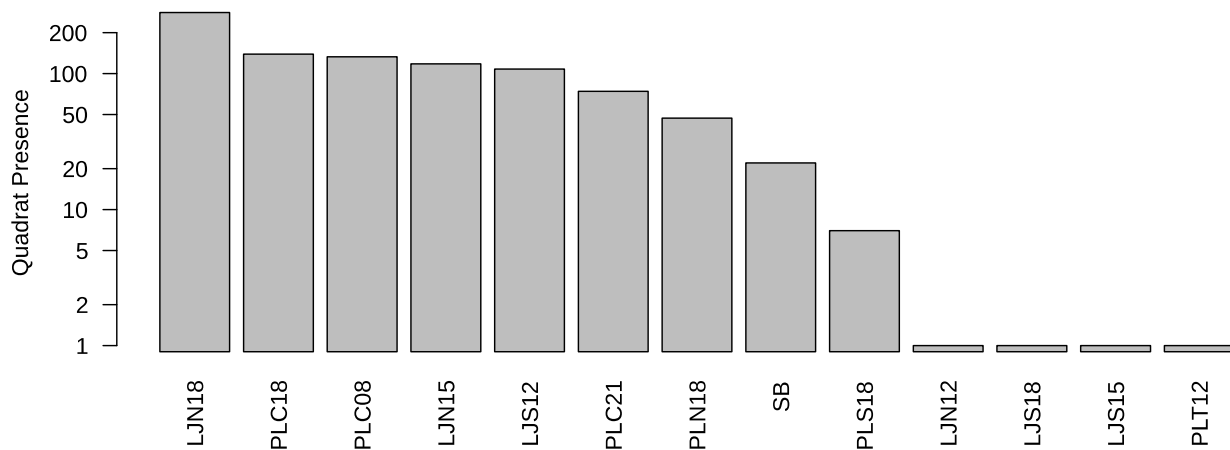


Figure 29. Presence of the invasive alga, *Sargassum horneri*, among the study sites where it has been observed within the permanent band transects. Quadrant presence indicates the total number of 5x2 m quadrats along the transects where it has been observed over time since first sighting at each individual site.

Study Site	Date 1 st Observed
SB	Sept. 9, 2105
PLC18	Oct. 10, 2015
PLN18	Dec. 2, 2015
LJN15	Dec. 3, 2015
LJS12	Feb. 8, 2016
PLC08	Mar. 31, 2016
LJS18	May 3, 2016
LJS15	May 3, 2016
PLT12	May 11, 2016
LJN18	May 19, 2016
PLC21	April 18, 2017
LJN12	Jun. 30, 2017
PLS18	May 30, 2018

Table 6. List of study sites where the invasive alga, *Sargassum horneri*, has been observed within the band transects and the dates it was first observed.

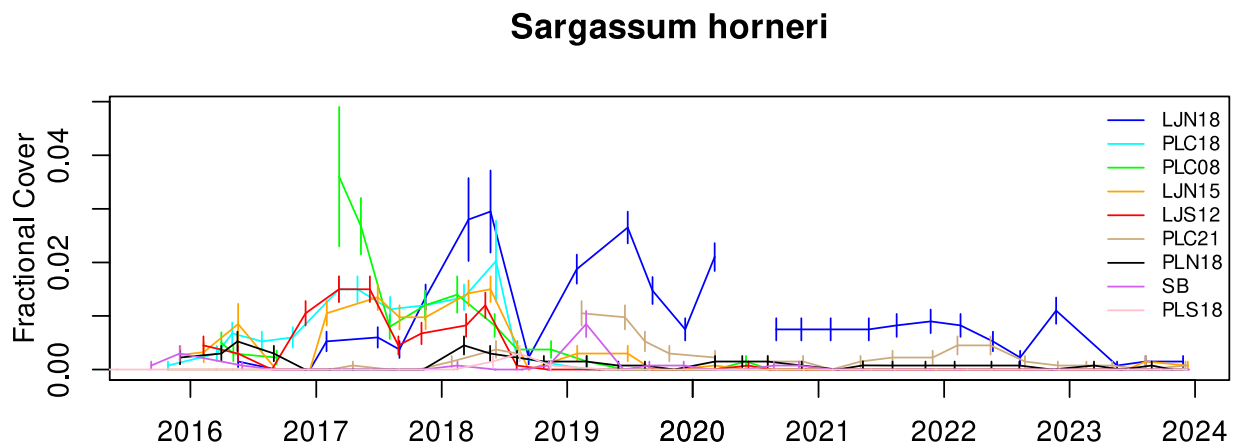


Figure 30. Fractional cover of the invasive alga *Sargassum horneri* over time beginning when it was first observed in the kelp forests off San Diego (see Table 5). Some study sites where *S. horneri* has been observed were omitted because cover values approximate zero.

Invertebrates

Many invertebrate species were negatively impacted by the 2014-2016 MHW. Sea urchins (Echinoids) and seastars (Asteroids) were most affected. Both groups play important functional roles within kelp forest communities. Sea urchins are major grazers of algae capable of overgrazing kelp forests if they become too numerous and mobile. Seastars are important benthic predators and are considered by many as keystone species whose predatory activities can control benthic community structure. Both groups suffered heavy mortality off San Diego during the warm event and remain depressed as of this writing (2022). Decimation of sea urchin populations off San Diego was a direct result of disease mortality and included the 'dark-blotch' disease. Disease epidemics commonly occur in echinoids (sea urchins - Lafferty, 2004) and asteroids ('sea star wasting disease' - Eckert et al., 2000) during periods of warm water stress.

Densities of both red (*Mesocentrotus franciscanus*) and purple (*Strongylocentrotus purpuratus*) sea urchins (RSU and PSU, respectively) either crashed in response to the consecutive warm periods or were already experiencing disease mortality. Time series of sea urchin densities for a subset of the study sites that represent the general population trajectories for these species and where sea urchins have been most numerous historically are shown in Figures 31 and 32. Presently, there are few sea urchins of either species at any of the study sites, especially off south Pt. Loma where sea urchin overgrazing has been historically resilient (Parnell, 2015).

The two major patterns of sea urchin population trends among the sites include (1) dramatically reduced densities at sites where they have spiked in the past and (2) stability at sites where they have typically been observed at low densities. The only exception to this is a the recent modest increase in red sea urchin density at PLN18 in northern Pt. Loma. Red sea urchins at the central Pt. Loma study sites have been relatively stable but at low density. These animals are sparsely distributed in cryptic habitat and have not exhibited overgrazing during the entire time series. By contrast, red and purple sea urchin overgrazing associated with population spikes have been observed at several of the south Pt. Loma study sites. An example for red sea urchins is the dramatic spike beginning in 2012 at PLM18 when giant kelp densities crashed. The sea urchins then emerged into feeding fronts at high densities. The subsequent MHW decimated these feeding fronts mainly through disease, though population diffusion may have also contributed. Purple sea urchins are typically observed at higher densities than reds and have exhibited population spikes along some of the central Pt. Loma study sites. However, their densities at these sites have remained stable and populations continue to remain cryptic over the last two decades and did not succumb in large numbers to the MHW event. That has not been the case in south Pt. Loma where densities have greatly varied and where urchin feeding lines have developed leading to episodic overgrazing fronts that remove young stands of giant kelp.

Sea urchin populations are typically cohort dominated with episodic periods of enhanced larval settlement and juvenile survival. Recruitment of both species was depressed during the MHW (Figs. 33-35), being absent or extremely limited at all study sites until the fall of 2017 when significant recruitment was observed once again. Patterns of recruitment then varied among sites and by species but the general pattern included increased levels of recruitment in 2017-2018 followed by a decrease in 2019-2020 and another increase in recruitment at some of the sites which has persisted to the present. The largest post-MHW pulse of recruitment for both species occurred in 2018 and winter of 2019. This cohort of red and purple sea urchins did not appear to have led to increased adult densities, indicating that their post recruitment survival was been relatively low or they remain cryptic. Probably both factors contribute to this pattern. More recently, during this reporting period, there has continued to be

recruitment of both species at several sites. Red sea urchin recruitment was greatest at PLC21, PLC18, and PLM18. Note, these are the outer areas of the kelp forest which is known to be the major sites of larval arrival to the kelp forest. High recruitment at the shallower sites is mainly due to the fact that very few sea urchins were observed at those sites and most or all were juveniles. Therefore, both red and purple sea urchins were observed to recruit during this study period but at lower levels than the 2018/19 recruitment events and it is highly unlikely that sea urchin overgrazing will occur in the near future in most areas of the LJKF and PLKF.

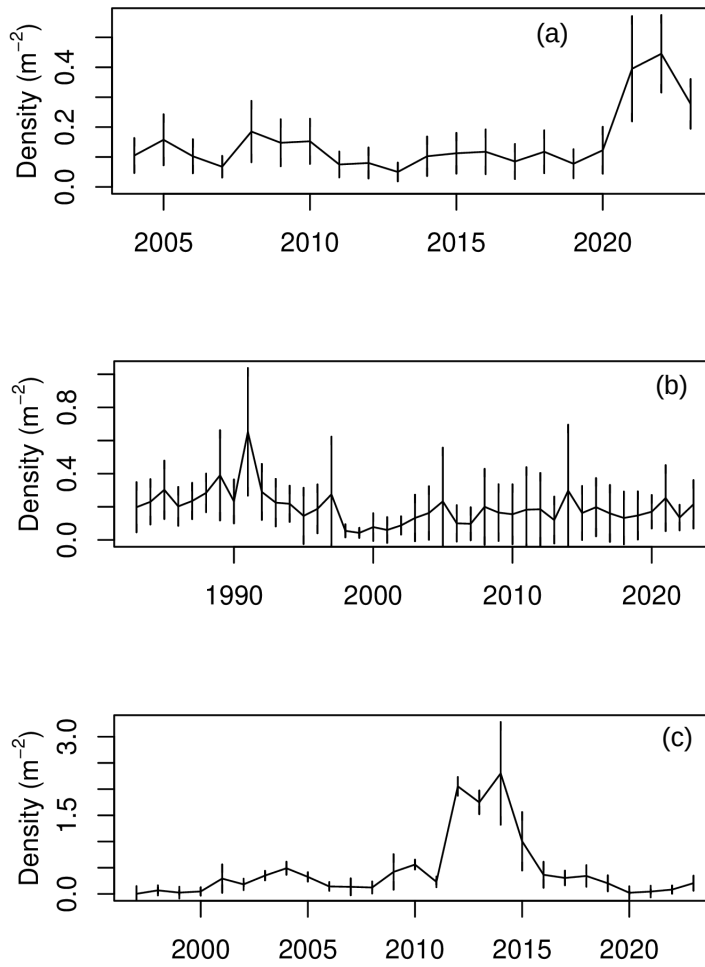


Figure 31. Time series of the red sea urchin (*Mesocentrotus franciscanus*) mean densities at the (a) LJN18, (b) PLC18, and (c) PLM18 study sites. Error bars are standard errors.

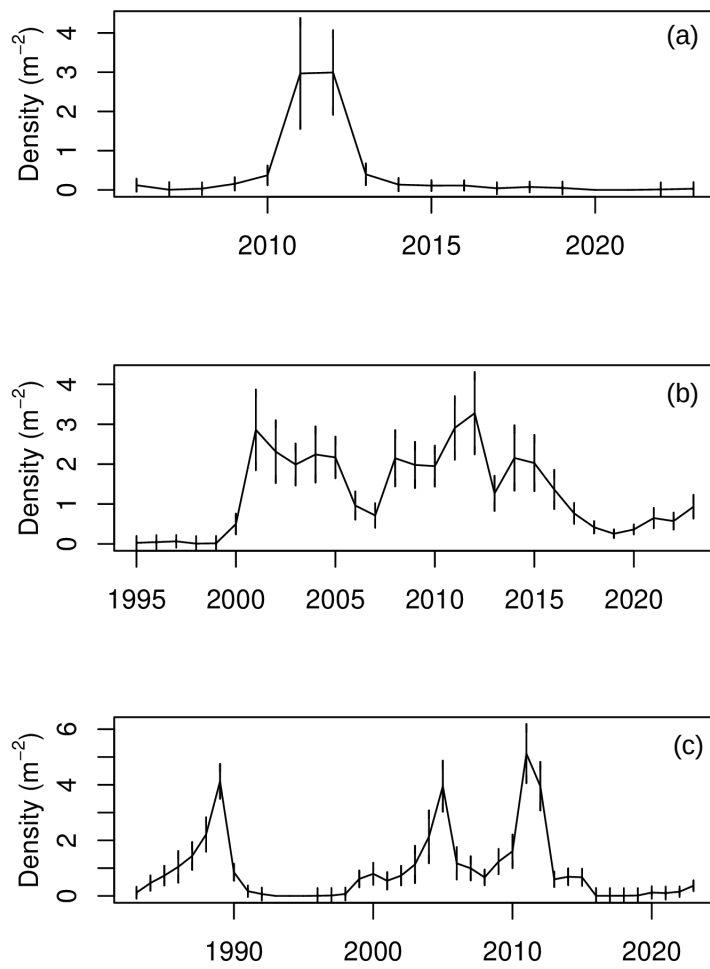


Figure 32. Time series of purple sea urchin (*Strongylocentrotus purpuratus*) mean densities at the (a) Cardiff, (b) PLC21, and (c) PLS18 study sites. Error bars are standard errors.

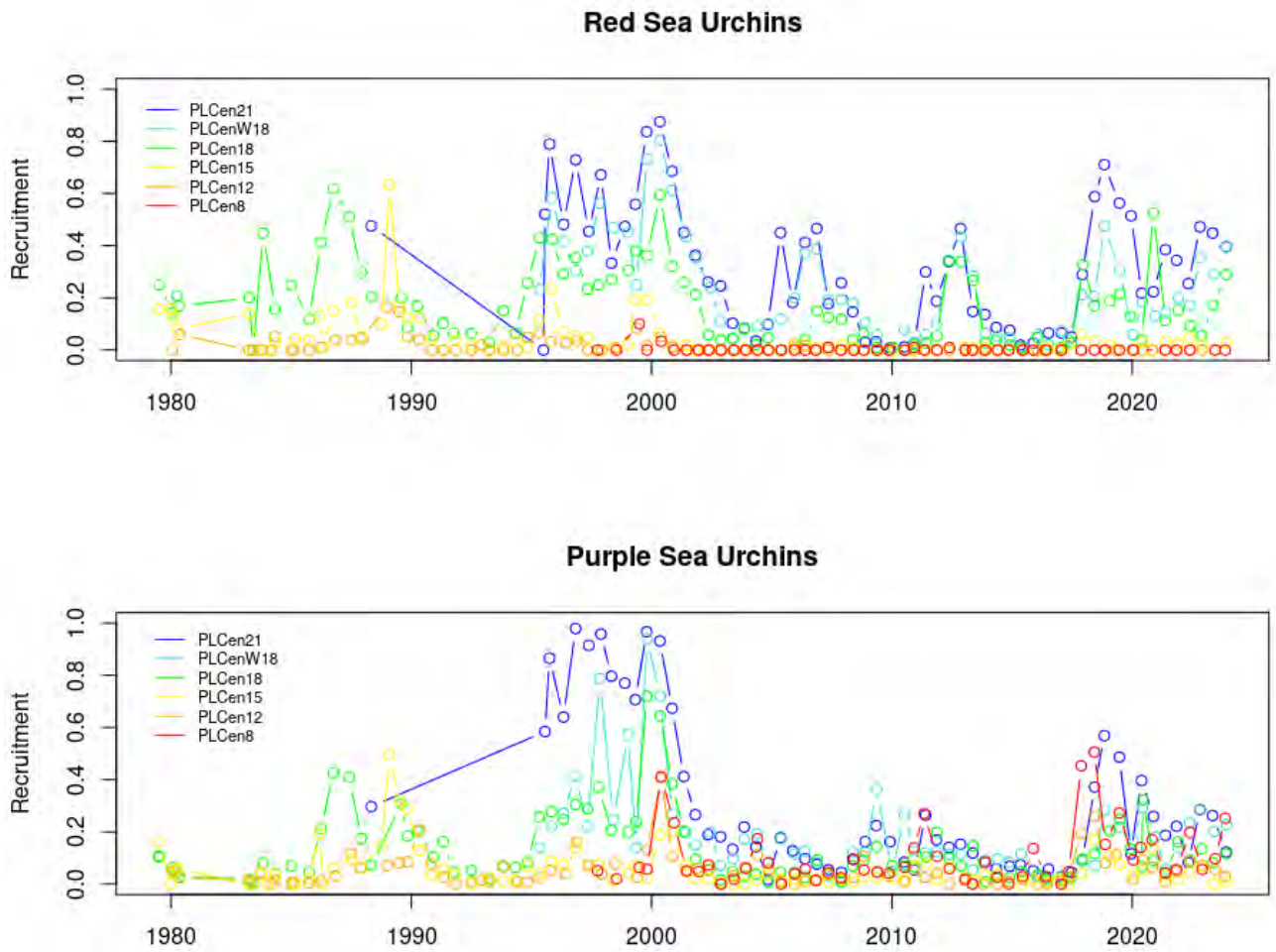


Figure 33. Time series of red (top) and purple (bottom) sea urchin recruitment (fraction of the population considered in the first year class by size - see Methods) at the central Pt. Loma study sites.

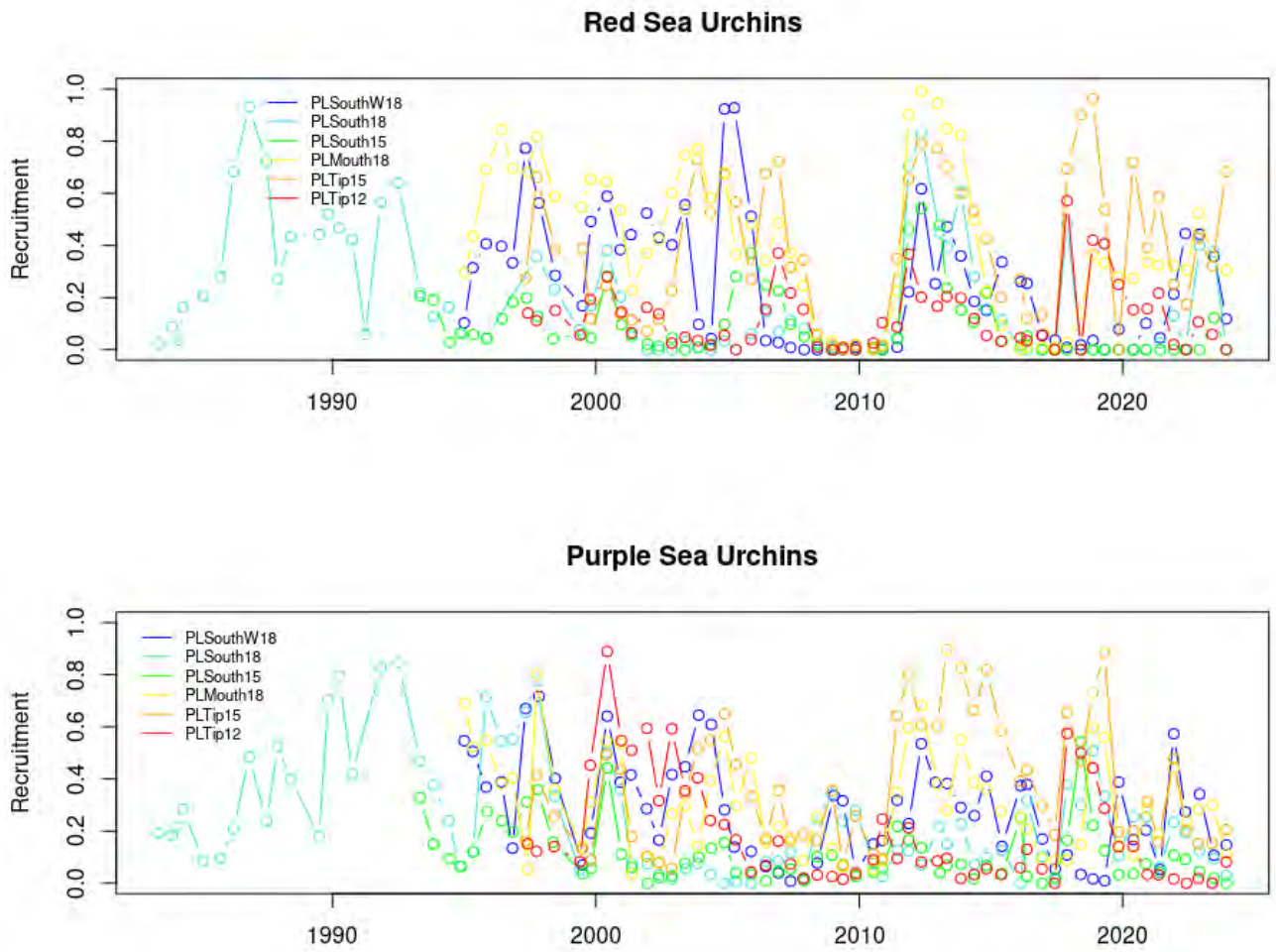


Figure 34. Time series of red (top) and purple (bottom) sea urchin recruitment at the southern Pt. Loma study sites.

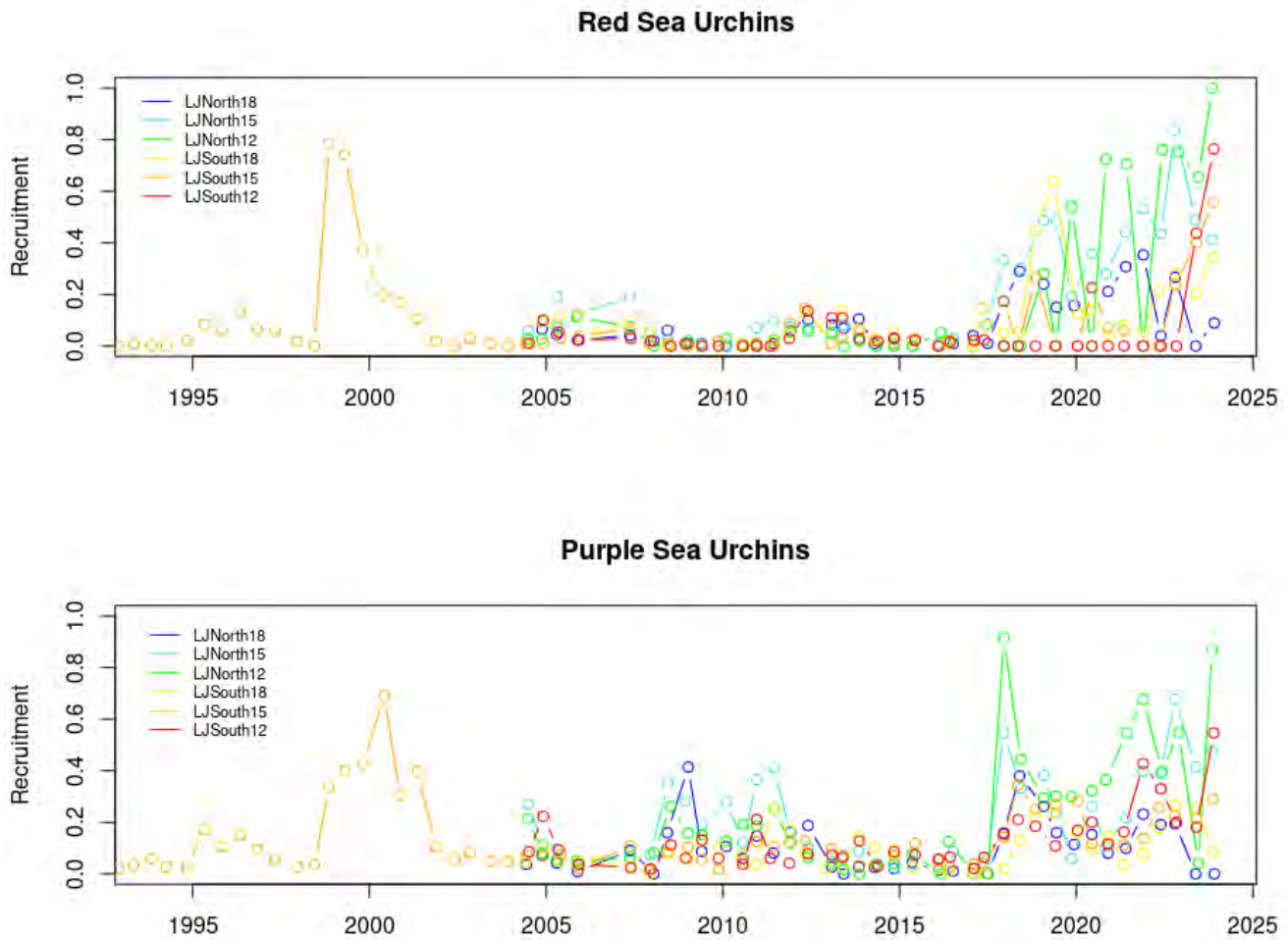


Figure 35. Time series of red (top) and purple (bottom) sea urchin recruitment at the La Jolla study sites.

Diseases and associated die-offs affected many other echinoderm species, mainly asteroids (seastars), throughout the Southern California Bight during the just prior to and during the MHW. Species that suffered the greatest mortality at our study sites included *Pisaster giganteus* (Fig. 36) and *P. brevispinus* where densities were reduced to zero for both species even at sites where they were previously abundant. Disease induced mass mortality events of asteroids and echinoids are commonly followed by recovery at differing rates (Hewson et al., 2014). Juvenile *P. giganteus* were observed recruiting onto giant kelp fronds off Pt. Loma beginning in 2017 continuing into 2018, thus heralding their recovery. However, all species of *Pisaster* are still very uncommon or absent at all of the study sites through the end of 2023. *P. brevispinus* is virtually gone from all the south Pt. Loma study sites where they had been common in the past. Disease has also decimated *Pycnopodia helianthodes*, an important sea urchin predator (Moitza et al., 1979). This species has not been observed anywhere off

San Diego County since 2014 even in areas where they were commonly observed. *P. helianthodes* was in decline even prior to the BLOB event and was listed as a threatened species by IUCN (Gravem et al., 2021).

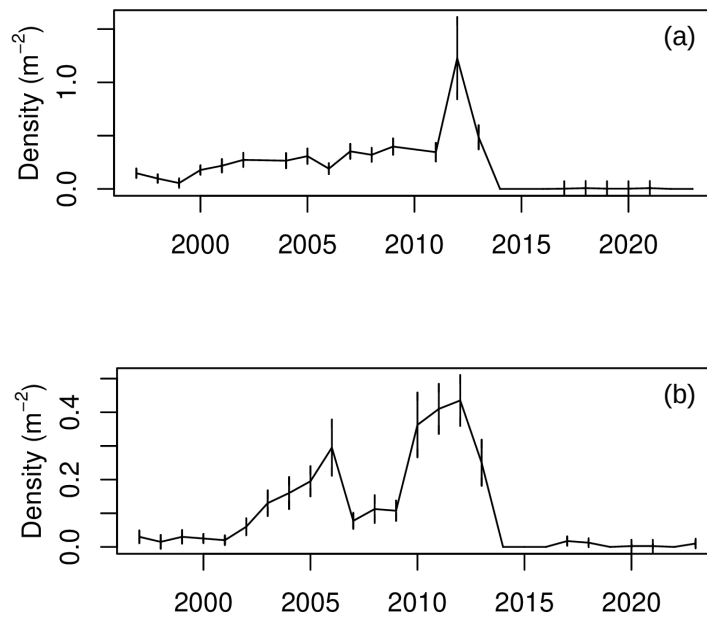


Figure 36. Time series of the seastar *Pisaster giganteus* mean density at the (a) PLT12 and (b) PLM18 study sites. Error bars are standard errors.

Abalones once supported an economically important commercial fishery throughout California until the 1980's. Their primary food in southern California is giant kelp. Therefore, when kelp populations are reduced, abalones become stressed both by the lack of food as well as diseases associated with warm water events (Vilchis et al., 2005). Historically, seven species of abalone have been common off San Diego. Two species, *Haliotis cracherodii* and *H. sorenseni*, are now on the federal endangered species list. Another species, *H. rufescens* has been in decline off southern California since the 1970's, and populations off Pt. Loma crashed in the 1980's (Dayton et al., 1992; Tegner and Dayton, 1987). However, *H. rufescens* persisted in low numbers near PLS18 and LJS18. Those few were lost during the recent prolonged MHW. Presently, there are relatively few *H.*

rufescens throughout San Diego County with the exception of a small population at the extreme western end of the southern Pt. Loma shelf where there has been ephemeral increases in kelp canopy cover since the MHW. However, densities of pink abalone (*H. corrugata*) have increased steadily at PLC08 beginning in the early 2000's (Fig. 37). *H. corrugata* has since increased in density even throughout the warm period reaching peak densities approaching 0.1 m⁻² but have since decreased by ~60% indicating this population is in general decline despite the favorable ocean climate conditions since 2020. For comparison, densities of pink abalone in the early 70's at similar depths off Catalina were >1 m⁻² (Tutschulte, 1976).

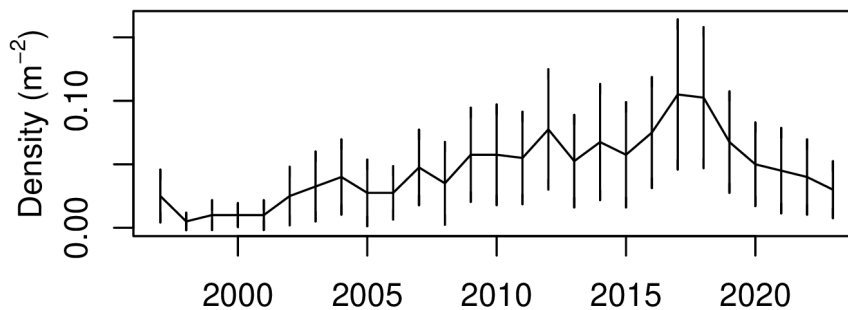


Figure 37. Time series of pink abalone (*Haliotis corrugata*) mean densities at the PLC08 study site. Error bars are standard errors.

North County Sedimentation

The grain size of sediments used for beach replenishment is an important determinant of beach stability. Finer sediments dredged from deeper waters offshore are more rapidly eroded from replenished beaches and are more likely to pose sedimentation risks to nearby kelp forest platforms off North County. The beaches from Carlsbad to Solana Beach were replenished with ~327,000 cubic meters of sand in 2012 using coarser sediments from the San Elijo Lagoon as part of a project to restore the estuary to more marine conditions. Sediments within the NCKF sites have been relatively stable since 2008 indicating that the 2012 replenishment has not been problematic for these kelp forests. Sediment horizons have varied less than 10 cm since 2008 when the sediment time series began. A 50-year replenishment project has recently (2021) been approved for the same area in which sediments will be augmented at 5 to 10 year intervals beginning as soon as 2024. The grain size composition of these sediments is not clearly defined but the sources will be from dredging sediments at deeper depths offshore. Such finer-grained sediments are more susceptible to erosion from beaches than natural sediments. Therefore, potential sediment burial risks to North County kelp forests may be more pronounced than the replenishment of 2012 based on grain sources and proposed replenishment volumes. The initial plan includes replenishing a 2.2 km stretch of Solana Beach with ~535,000 cubic meters of sediment in 2024.

LITERATURE CITED

- Clendenning, K.A. and North, W.J. (1960). Effects of wastes on the giant kelp, *Macrocystis pyrifera*. In *Proceedings of the First International Conference on Waste Disposal in the Marine Environment University of California, Berkeley, July 22-25, 1959* (p. 82). Pergamon.
- Dayton, P. K., and Tegner, M. J. (1984). Catastrophic storms, El Niño, and patch stability in a southern California kelp community. *Science*, 224(4646), 283-285.
- Dayton, P. K., Currie, V., Gerrodette, T., Keller, B. D., Rosenthal, R., and Tresca, D. V. (1984). Patch dynamics and stability of some California kelp communities. *Ecological Monographs*, 54(3), 253-289.
- Dayton, P. K., Tegner, M. J., Parnell, P. E., and Edwards, P. B. (1992). Temporal and spatial patterns of disturbance and recovery in a kelp forest community. *Ecological Monographs*, 62(3), 421-445.
- Dean, T. A., & Jacobsen, F. R. (1984). Growth of juvenile *Macrocystis pyrifera* (Laminariales) in relation to environmental factors. *Marine Biology*, 83(3), 301-311.
- DeWreede, R. E. (1984). "Growth and age class distribution of *Pterygophora californica* (Phaeophyta)." *Marine Ecology Progress Series* 19: 93-100.
- Deysher, L. E., and Dean, T. A. (1984). Critical irradiance levels and the interactive effects of quantum irradiance and dose on gametogenesis in the giant kelp *Macrocystis pyrifera*. *Journal of Phycology*, 20(4), 520-524.
- Di Lorenzo, E., and Mantua, N. (2016). Multi-year persistence of the 2014/15 North Pacific marine heatwave. *Nature Climate Change*, 6(11), 1042-1047.
- Eckert, G. L., Engle, J. M., and Kushner, D. J. (2000). Sea star disease and population declines at the Channel Islands. In *Proceedings of the fifth California Islands symposium* (pp. 390-393).
- Gravem, S.A., Heady, W. N., Saccomanno, V. R., Alvstad, K. F., Gehman, A. L. M., Frierson, T. N. & Hamilton, S.L. 2021. *Pycnopodia helianthoides* (amended version of 2020 assessment). The IUCN Red List of Threatened Species 2021: e.T178290276A197818455. <https://dx.doi.org/10.2305/IUCN.UK.2021-1.RLTS.T178290276A197818455.en>.
- Grigg, R. W. (1978). Long-term changes in rocky bottom communities off Palos Verdes. *Coastal Water Research Project, annual report for the year*, 157-184.
- Hewson, I., Button, J. B., Gudenkauf, B. M., Miner, B., Newton, A. L., Gaydos, J. K., ... and Fradkin, S. (2014). Densovirus associated with sea-star wasting disease and mass mortality. *Proceedings of the National Academy of Sciences*, 111(48), 17278-17283.
- Lafferty, K. D. (2004). Fishing for lobsters indirectly increases epidemics in sea urchins. *Ecological Applications*, 14(5), 1566-1573.
- Lawley, D. N. and Maxwell, A. E. (1971). *Factor Analysis as a Statistical Method*. Second edition. Butterworths.

- Leighton, D. L., Jones, L. G., and North, W. J. (1966). Ecological relationships between giant kelp and sea urchins in southern California. In *Proceedings of the Fifth International Seaweed Symposium, Halifax, August 25–28, 1965* (pp. 141-153).
- Lüning, K., & Dring, M. J. (1975). Reproduction, growth and photosynthesis of gametophytes of *Laminaria saccharina* grown in blue and red light. *Marine Biology*, 29(3), 195-200.
- Miller, K. A., Aguilar-Rosas, L. E., and Pedroche, F. F. (2011). A review of non-native seaweeds from California, USA and Baja California, Mexico. *Hidrobiológica*, 21(3).
- Moitza, D. J., and Phillips, D. W. (1979). Prey defense, predator preference, and nonrandom diet: the interactions between *Pycnopodia helianthoides* and two species of sea urchins. *Marine Biology*, 53(4), 299-304.
- NOAA (2024). ENSO: Recent Evolution, Current Status and Predictions. Update prepared by: Climate Prediction Center/NCEP. Retrieved from NOAA website: https://www.cpc.ncep.noaa.gov/products/analysis_monitoring/laNiña/enso_evolution-status-fcsts-web.pdf
- Parnell, P., Miller, E. F., Cody, C. E. L., Dayton, P. K., Carter, M. L., and Stebbins, T. D. (2010). The response of giant kelp (*Macrocystis pyrifera*) in southern California to low-frequency climate forcing. *Limnology and Oceanography*, 55(6), 2686-2702.
- Parnell, P. E. (2015). The effects of seascape pattern on algal patch structure, sea urchin barrens, and ecological processes. *Journal of experimental marine biology and ecology*, 465, 64-76.
- R Core Team (2022). R: A language and environment for statistical computing. R Foundation for Statistical Computing, Vienna, Austria. URL <https://www.R-project.org/>.
- Reed, D. C. (1987). "Factors affecting the production of sporophylls in the giant kelp *Macrocystis pyrifera*." *Journal of Experimental Marine Biology and Ecology* 113: 61-69.
- Roberts, P. J. (1991). Ocean outfalls. *Critical Reviews in Environmental Science and Technology*, 20(5-6), 311-339.
- Schiel, D.R., 1985. A short-term demographic study of *Cystoseira osmundacea* (Fucales: Cystoseiraceae) in Central California. *Journal of Phycology*, 21(1), pp.99-106.
- Seymour, R. J., Tegner, M. J., Dayton, P. K., and Parnell, P. E. (1989). Storm wave induced mortality of giant kelp, *Macrocystis pyrifera*, in southern California. *Estuarine, Coastal and Shelf Science*, 28(3), 277-292.
- Steneck, R. S., Graham, M. H., Bourque, B. J., Corbett, D., Erlandson, J. M., Estes, J. A., and Tegner, M. J. (2002). Kelp forest ecosystems: biodiversity, stability, resilience and future. *Environmental conservation*, 29(4), 436-459.
- Tegner, M. J., and Dayton, P. K. (1987). El Niño effects on southern California kelp forest communities. In *Advances in Ecological Research* (Vol. 17, pp. 243-279). Academic Press.

- Towle, D. W., and Pearse, J. S. (1973). Production of the giant kelp, *Macrocystis*, estimated by in situ incorporation of ¹⁴C in polyethylene bags. *Limnology and Oceanography*, 18(1), 155-159.
- Tutschulte, T.C. (1976). The comparative ecology of three sympatric abalones. Ph.D thesis, University of California, 335 pp.
- Vilchis, L. I., Tegner, M. J., Moore, J. D., Friedman, C. S., Riser, K. L., Robbins, T. T., and Dayton, P. K. (2005). Ocean warming effects on growth, reproduction, and survivorship of southern California abalone. *Ecological Applications*, 15(2), 469-480.

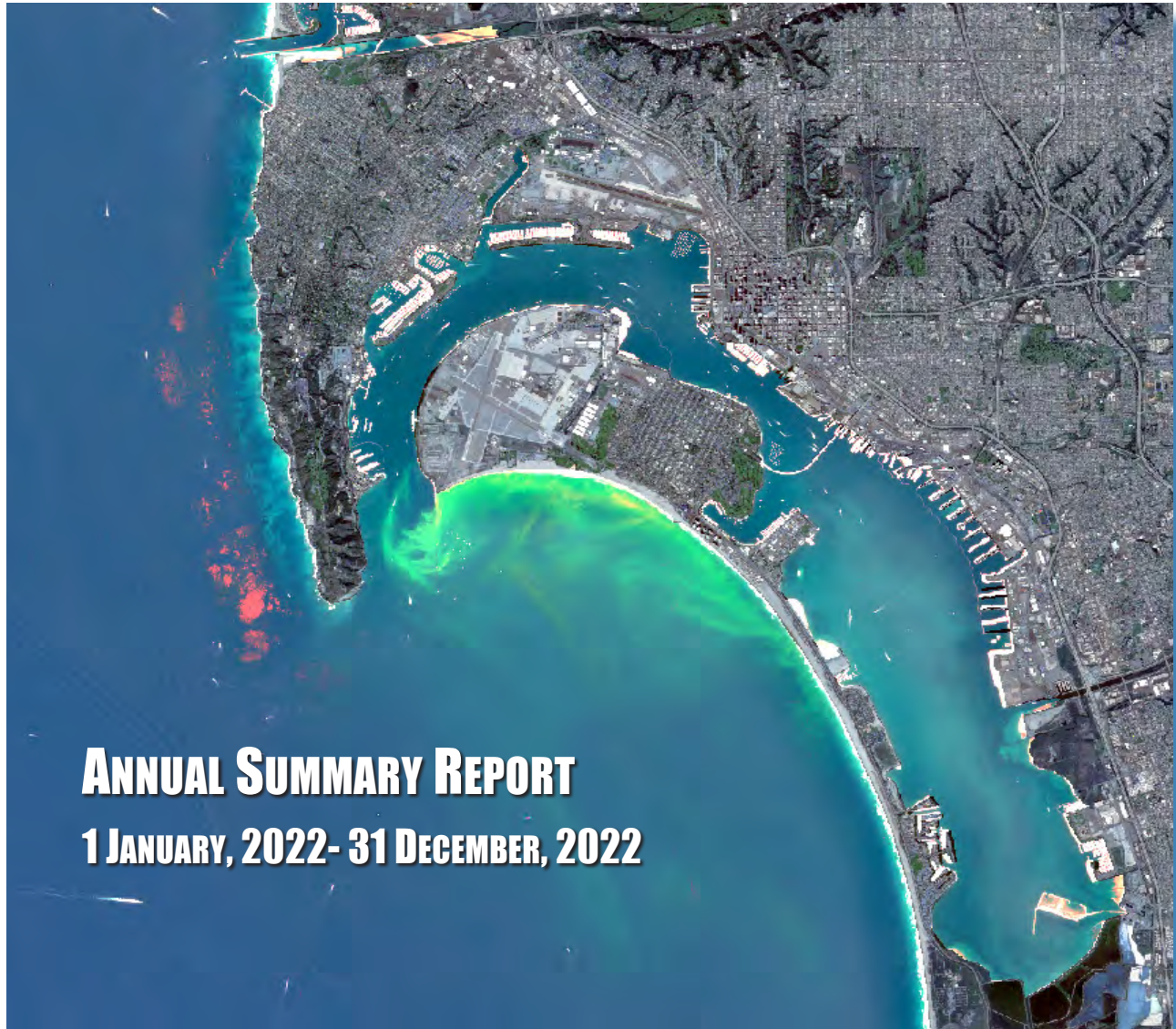
Appendix B
Ocean Imaging Annual Report
2022 – 2023
Mark Hess

Ocean Imaging Corps
13976 West Bowles Avenue, Suite 100, Littleton CO 80127

Submitted to City of San Diego
Public Utilities Department

SATELLITE & AERIAL COASTAL WATER QUALITY MONITORING IN THE SAN DIEGO / TIJUANA REGION

By Mark Hess



All data and imagery contained in this report are strictly subject to Copyright by Ocean Imaging.

No data or imagery contained herein may be copied, digitally reproduced or distributed without written permission by Ocean Imaging Inc.

17 May 2023

Ocean Imaging

13976 West Bowles Avenue, Suite 100, Littleton CO 80127

Phone: 303-948-5272

Fax: 303-948-2549

www.oceani.com

TABLE OF CONTENTS

- 1. INTRODUCTION AND PROJECT HISTORY1
- 2. METHODS AND TECHNOLOGY OVERVIEW 2
 - 2.1 Imaging in the UV-Visible-Near Infrared Spectrum 2
 - 2.2 Imaging in the Thermal Infrared Spectrum..... 2
 - 2.3 Satellites and Sensors Utilized 2
 - 2.4 Data Dissemination and Analysis 7
- 3. HIGHLIGHTS OF 2022 MONITORING..... 8
 - 3.1 Atmospheric and Ocean Conditions 8
 - 3.2 The South Bay Ocean Outfall Region.....16
 - 3.3 The Point Loma Outfall Region..... 24
 - 3.4 Kelp Variability 26
- 4. PRESENT AND FUTURE ENHANCEMENTS OF THE PROJECT28
- 5. REFERENCES 31
- APPENDIX A – HIGH RESOLUTION SATELLITE IMAGERY
SHOWING SBOO-RELATED WASTEWATER PLUME32**

1. INTRODUCTION AND PROJECT HISTORY

In the 1990s, Ocean Imaging Corporation (OI) received multiple research grants from NASA's Commercial Remote Sensing Program for the development and commercialization of remote sensing applications in the coastal zone. As part of these projects, OI developed methods to utilize various types of remotely sensed data for the detection and monitoring of stormwater runoff and wastewater discharges from offshore outfalls. The methodology was initially demonstrated with collaboration of the Orange County Sanitation District in California (Svejkovsky and Haydock, 1998). The NASA-supported research led to a proof-of-concept demonstration project in the San Diego, California region co-funded by the EPA in 2000. Those results led, in 2002, to adding an operational remote sensing-based monitoring component to the San Diego region's established water quality monitoring program. The project continues as a joint effort between the Ocean Monitoring Program of the City of San Diego's Public Utilities Department (SDPUD) and the International Boundary and Water Commission (IBWC).

The first phase of the project was a historical study utilizing several types of satellite data acquired between the early 1980s and 2002. The study established the prevailing near-surface current patterns in the region under various oceanic and atmospheric conditions. The current directions were deduced from patterns of turbidity, ocean temperature and surfactant slicks. In some cases, near-surface current velocity could be computed by tracking recognizable color or thermal features in time-sequential images. The historical study thus established baseline data for the region's current patterns, their persistence, their frequency, and the historical locations, size and dispersion trajectories of various land and offshore discharge sources from Publicly Owned Treatment Works (POTW) (e.g.,

the offshore outfalls, Tijuana River, Punta Bandera Treatment Plant discharge in Mexico, etc.).

The prime objectives of the project have expanded somewhat since its inception. Initially, emphasis was on utilizing the image data to discern and monitor surface and near-surface signatures from the South Bay Ocean Outfall (SBOO) and Point Loma Ocean Outfall (PLOO), separate them from other nearshore point and non-point runoff features, and monitor their locations, extents, and potential impact on the shoreline. Prior to this project, the spatial extents of the plumes could only be estimated from a relatively sparse spatial grid of field samples, which made it difficult to separate, for example, the SBOO near surface plume from the Tijuana River runoff plume. This ambiguity made it difficult, in turn, to objectively evaluate the potential contribution, if any, of the SBOO plume to beach contamination along the nearby shoreline. The satellite and aerial imagery helped directly establish the dispersal trajectories of the SBOO effluent during months when it reaches the near-surface layer and support the claim that it likely never reaches the surf zone.

In October 2002, the operational monitoring phase of the project was initiated using the variety of satellite- and model-derived datasets discussed below. Over the past five to ten years, the project's objectives have broadened from focusing primarily on the outfalls to also provide larger-scale, regional observations of the physical and biological patterns and processes affecting the San Diego County and Tijuana River discharge regions. It is this broader-view perspective that led to the creation of the additional image products from additional sensors for the City.

This report summarizes observations made during the period 1/1/2022 – 12/31/2022.

2. METHODS AND TECHNOLOGY OVERVIEW

OI uses several remote sensing technologies to monitor San Diego's offshore outfalls and shoreline water quality. Their main principle is to reveal light reflectance and heat emission patterns that are characteristic of the different discharges, water masses, plankton blooms and suspended sediment loads. Most often this is due to specific substances contained in the effluent but absent in the surrounding water.

2.1 Imaging in the UV-Visible-Near Infrared Spectrum

This is the most common technique used with satellite and aerial images. Wavelengths (colors) within the range of the human eye are most often used but Ultraviolet (UV) wavelengths are useful for detecting fluorescence from petroleum compounds (oil, diesel, etc.) and near-IR wavelengths can be useful for correcting atmospheric interference from aerosols (e.g., smog and smoke). Near-IR wavelengths are also highly reflected from kelp seaweeds, so such data are particularly useful for delineating the region's kelp beds and monitor their extents through time.

The best detection capabilities are attained when several images in different wavelengths are acquired simultaneously. These "multispectral" data can be digitally processed to enhance features not readily visible in simple color photographs. For example, two such images can be ratioed, thus emphasizing the water features' differences in reflection of the two specific wavelengths. A multi-wavelength image set can also be analyzed with multispectral classification algorithms which separate distinctive features or effluents based on the correlation relationships between the different color signals.

The depth to which the color sensors can penetrate depends on which wavelengths they see, their sensitivity and the general water clarity.

In the San Diego region, green wavelengths tend to reach the deepest and, as elsewhere, UV and near-IR wavelengths penetrate the least. Generally, OI's satellite and aerial sensor data reveal patterns in the upper 1-15 meters.

2.2 Imaging in the Thermal Infrared Spectrum

Some satellite and aerial sensors image heat emanating from the ground and the ocean. They thus reveal patterns and features due to their differences in temperature. Since thermal infrared (TIR) wavelengths are strongly absorbed by water, the images reveal temperature patterns only on the water's surface. Such images can help detect runoff plumes when their temperatures differ from the surrounding ocean water. Runoff from shoreline sources tends to be warmer than the ocean water, although the reverse can be true during the winter. Plumes from offshore outfalls can sometimes also be detected with thermal imaging. Since the effluent contains mostly fresh water, it is less dense than the surrounding salt water and tends to rise towards the surface. How far it rises depends on outfall depth, ocean currents, and stratification conditions. If it makes it all the way to the surface, it is usually cooler than the surrounding sun-warmed surface water. A plume signature detectable in multispectral color imagery but not detectable in simultaneously collected TIR imagery indicates the rising plume has not reached the actual ocean surface and remains submerged.

2.3 Satellites and Sensors Utilized

Until 2010, the project relied heavily on acquisition of multispectral color imagery with OI's DMSC-MKII aerial sensor and TIR imagery from a Jenoptik thermal imager integrated into the system. These aerial image sets were most often collected at 2m resolution. The flights were done on a semi-regular schedule ranging from 1-2 times per month during the summer to once or more per week during the rainy season. The flights were also coordinated

with the City of San Diego's regular offshore field sampling schedule so that the imagery was collected on the same day (usually within 2-3 hours) of the field data collection. Additional flights were done on an on-call basis immediately after major storms or other events such as sewage spills. In late 2010, OI negotiated a special data collection arrangement with Germany's RapidEye Corporation and this project began utilizing their multispectral imagery in lieu of most of the aerial Digital Multispectral Camera (DMSC) image acquisitions. The use of satellite as opposed to aerial data also enables a more regionally contiguous monitoring of events affecting the target areas. In late 2019 the RapidEye satellite constellation was decommissioned by the current operator Planet Labs. Subsequently, OI secured the regular acquisition of SPOT 6 and SPOT 7 satellite imagery covering the same geographical area beginning in 2020. Table 1 lists the properties of the remote sensing image sources routinely used during the project.

Beginning in 2017, OI also began processing and posting imagery from the Sentinel-2A satellite. Sentinel-2A is a satellite operated by the European Space Agency (ESA) and is the spaceborne platform for the Multispectral Instrument (MSI). The Sentinel-2A and 2B MSIs sample 13 spectral bands: four bands at 10 meters, six bands at 20 meters and three bands at 60-meter spatial resolution. The green band focusing in the 560 nm wavelength is ideal for detecting turbidity plumes from the outfalls both at the surface and at depths down to 40 feet depending on ocean conditions. The revisit time of the Sentinel-2A satellite is approximately ten days. A second satellite carrying the MSI sensor, the Sentinel-2B, was launched into orbit by the ESA and provided the first set of data from the MSI sensor as of March 17, 2017. Beginning in 2018, data from Sentinel 2B became a regular addition to the satellite imagery products posted to the OI web portal. On average the Sentinel 2A and 2B imagery processed to highlight anomalous turbidity signals emanating from the PLOO, SBOO, as well as the discharge from the Tijuana River (TJR)

are posted to the OI web portal within 24-36 hours of satellite data acquisition. In some cases, if the data are available to OI earlier, the image products are delivered as quickly as 12 hours post acquisition. During 2022 the Sentinel 2A and 2B satellites provided the most temporally comprehensive set of high-resolution satellite imagery. In total, 117 high resolution satellite images showing the offshore San Diego County region were acquired, processed, and delivered in 2022. This equates to a 13% decrease in satellite data used to document the area when compared to 2021 – most probably due to more instances of total cloud cover over the San Diego region in 2022. Of the 117 total image sets, 81 were from Sentinel 2A or 2B data making up 69% of the high-resolution satellite data processed and posted as part of the project and an increase of 4% over 2021.

In October 2018, OI began using imagery from Sentinel-3A. Shortly thereafter, in December 2018 imagery from Sentinel-3B was incorporated into the mix of observation platforms. Just like Sentinel 2, Sentinel-3A and Sentinel-3B are earth observation satellites developed by the ESA for the Copernicus Program. Sentinel-3A was launched on February 16, 2016, and Sentinel-3B followed on April 25, 2018. The 3A and 3B satellites are identical and deliver products in near-real time. The satellites include four different remote sensing instruments. The Ocean and Land Colour Instrument (OLCI) covers 21 spectral bands (400–1020 nm) with a swath width of 1270 km and a spatial resolution of 300 m. SLSTR covers 9 spectral bands (550–12 000 nm), using a dual-view scan with swath widths of 1420 km (nadir) and 750 km (backwards), at a spatial resolution of 500 m for visible and near-infrared, and 1 km for thermal infrared channels. The Sentinel 3 mission's main objectives are to measure sea surface topography along with the measurement of ocean/land surface temperature and ocean/land surface color. One of the satellites' main secondary missions is to monitor sea-water quality and marine pollution. The instrument on these satellites designed for these purposes is the OLCI. Ocean Imaging creates

Table 1. Satellite sensors utilized in the project and their characteristics.

Sensor	Utilization Period	Resolution (m)	Utilized Wavelength Range
AVHRR	2003 - Present	1100	Channel 4: 10.30 – 11.39 um Channel 5: 11.50 – 12.50 um
MODIS	2003 - Present	250/500/1000	Band 1 (250 m): .620 – .670 um Band 2 (250 m): .841 – .876 um Band 3 (500 m): .459 – .479 um Band 4 (500 m): .545 – .565 um
Landsat TM/ETM+ 4-7	2003 - Present	30 (visible - Near-IR) 60 (Thermal-IR)	Band 1: .450 - .520 um Band 2: .520 - .600 um Band 3: .630 - .690 um Band 4: .760 - .900 um Band 6: 10.40 - 12.50 um (TMS Thermal not used due to noise)
Landsat 8 OLI, TIRS	2013 - Present	30 (visible - Near-IR) 100 (Thermal-IR)	Band 2: .452 - .512 um Band 3: .533 - .590 um Band 4: .636 - .673 um Band 5: .851 - .879 um Band 10: 10.60 - 11.19 um Band 11: 11.50 - 12.51 um
Sentinel 2A/2B	2017 - Present	10 (visible - Near-IR) 60 (Vegetation Red Edge) 60 (UV, SWIR)	Band 1: .443 um Band 2: .490 um Band 3: .560 um Band 4: .665 um Band 5: .705 um Band 6: .740 um Band 7: .783 um Band 8: .842 um Band 8A: .865 um
Sentinel 3A/3B	2018 - Present	300 (all utilized bands)	Band Oa2: .412.5 um Band Oa3: .442.5 um Band Oa4: 490 um Band Oa5: 510 um Band Oa6: .560 um Band Oa7: 620 um Band Oa8: .665 um Band Oa10: .68125 um Band Oa11: .07875 um Band Oa17: .865 um
VIIRS	2019 - Present	750 (all utilized bands)	Band M1: 0.402 - 0.422 um Band M2: 0.436 - 0.454 um Band M3: 0.478 - 0.488 um Band M4: 0.545 - 0.565 um Band M5: 0.662 - 0.682 um Band M6: 0.739 - 0.754 um Band M7: 0.846 - 0.885 um Band M8: 1.23 - 1.25 um Band M9: 1.371 - 1.386 um Band M10: 1.58 - 1.64 um Band M11: 2.23 - 2.28 um Band M12: 3.61 - 3.79 um Band M13: 3.97 - 4.13 um Band M14: 8.4 - 8.7 um Band M15: 10.26 - 11.26 um Band M16: 11.54 - 12.49 um
SPOT 6/7	2019 - Present	6	Band 1: .450 - .745 um Band 2: .450 - .525 um Band 3: .530 - .590 um Band 4: .625 - .695 um Band 5: .760 - .890 um
Sentinel 1A/1B SAR	2021 - Present	5 x 20	C-band operating at a center frequency of 5.405 GHz
Landsat 9 OLI-2, TIRS-2	Late 2021 - Present	30 (visible - Near-IR) 100 (Thermal-IR)	Band 2: .452 - .512 um Band 3: .533 - .590 um Band 4: .636 - .673 um Band 5: .851 - .879 um Band 10: 10.60 - 11.19 um Band 11: 11.50 - 12.51 um

daily products dependent on cloud cover for the entire San Diego/Tijuana region using the OLCI instrument. Between the 3A and 3B satellites this results in better than daily coverage with 3A and 3B data occasionally both being available on the same day. True color, near infrared, products are posted bi-monthly along with the similar resolution MODIS products. Potential future products derived from the Sentinel 3 sensors include total suspended matter, chlorophyll, and sea surface temperature as well as cyanobacteria monitoring. Sentinel 3 carries the only satellite sensor package with the necessary spectral bands, spatial resolution, and coverage for near real-time detection of cyanobacteria. The results of these products may also be compared to the field sampling data in order to assess accuracy.

As stated above, the RapidEye satellite data were discontinued as of late 2019 and replaced by data from the SPOT 6 and SPOT 7 satellites in January of 2020. The two SPOT satellites/sensors are identical in design and function. They both image in spectral bands similar to the RapidEye satellites at a ground sampling distance of 8.8 meters for the multispectral data (see Table 1). The dynamic range of these sensors is 12-bits per pixel. OI uses the blue, green, red, and near-infrared bands from these sensors. Empirically we have found that the SPOT data have a high signal to noise ratio and therefore produce a high-quality product for detecting wastewater surface manifestations and delineating the river run-off plumes. Because of the ability of these sensors to image from off-nadir viewing angles it is also possible to obtain more frequent data. Figure 1 shows a set of images from 11/23/22, 11/24/22, 11/26/22 and 11/29/22 from Landsat 8, SPOT and Sentinel 2 highlighting the ability to obtain high-resolution imagery from multiple satellites on successive days. Note the visible SBOO surface plume on all four days and the TJR discharge moving offshore to the northwest on the 23rd and 24th and then shifting direction and beginning to dissipate by the 29th. 25-hour averaged High Frequency Radar-derived (HF Radar) ocean currents from these days computed

from the period one to two hours of the satellite data acquisition are overlaid on the imagery to help illustrate the shift in surface flow direction.

As detailed in Table 1, to date, this work utilizes 1100 m resolution Advanced Very High Resolution Radiometer (AVHRR)-derived imagery (available multiple times per day), 1000 m resolution chlorophyll and sea surface temperature (SST) Moderate Resolution Imaging Spectroradiometer (MODIS)-derived imagery (available multiple times per day), 500 m resolution MODIS true color imagery (available near-daily), 750 m resolution Visible Infrared Imaging Radiometer Suite (VIIRS) chlorophyll and SST imagery (available multiple times per day), 300 m resolution Sentinel 3 color and thermal imagery (available daily), 30 m & 60 m Landsat 7 ETM+ and Landsat 8 OLI/TIRS and Landsat 9 OLI-2/TIRS-2 color and thermal imagery (each available approximately every 16 days), 10 m resolution Sentinel 2 multispectral imagery (available 2-4 times per week), and 6m resolution Satellite Pour l'Observation de la Terre (SPOT) 6 and SPOT 7 (available approximately every 4-5 days).

Synthetic Aperture Radar (SAR) from the Sentinel 1A and 1B satellites (available every 3-6 days at a spatial resolution of 5m x 20 m) were added to the suite of remote sensing data products in late 2021. SAR can detect surfactant films associated with natural processes (Svejkovsky and Shandley 2001) and plumes containing anthropogenic substances (Svejkovsky and Jones 2001, Gierach et al. 2017, Holt et al. 2017) when optical sensors might be limited by cloud cover or heavy atmospheric haze. The primary purpose of these satellites for this project is to provide another look at the TJR discharge plume to assess its extent and direction of flow. The runoff often contains the natural and anthropogenic surfactants that dampen the SAR signal and therefore make it detectable in the data. In 2022 89 SAR images were acquired and processed for the San Diego region providing an additional source of information even during cloudy conditions. Figure 2

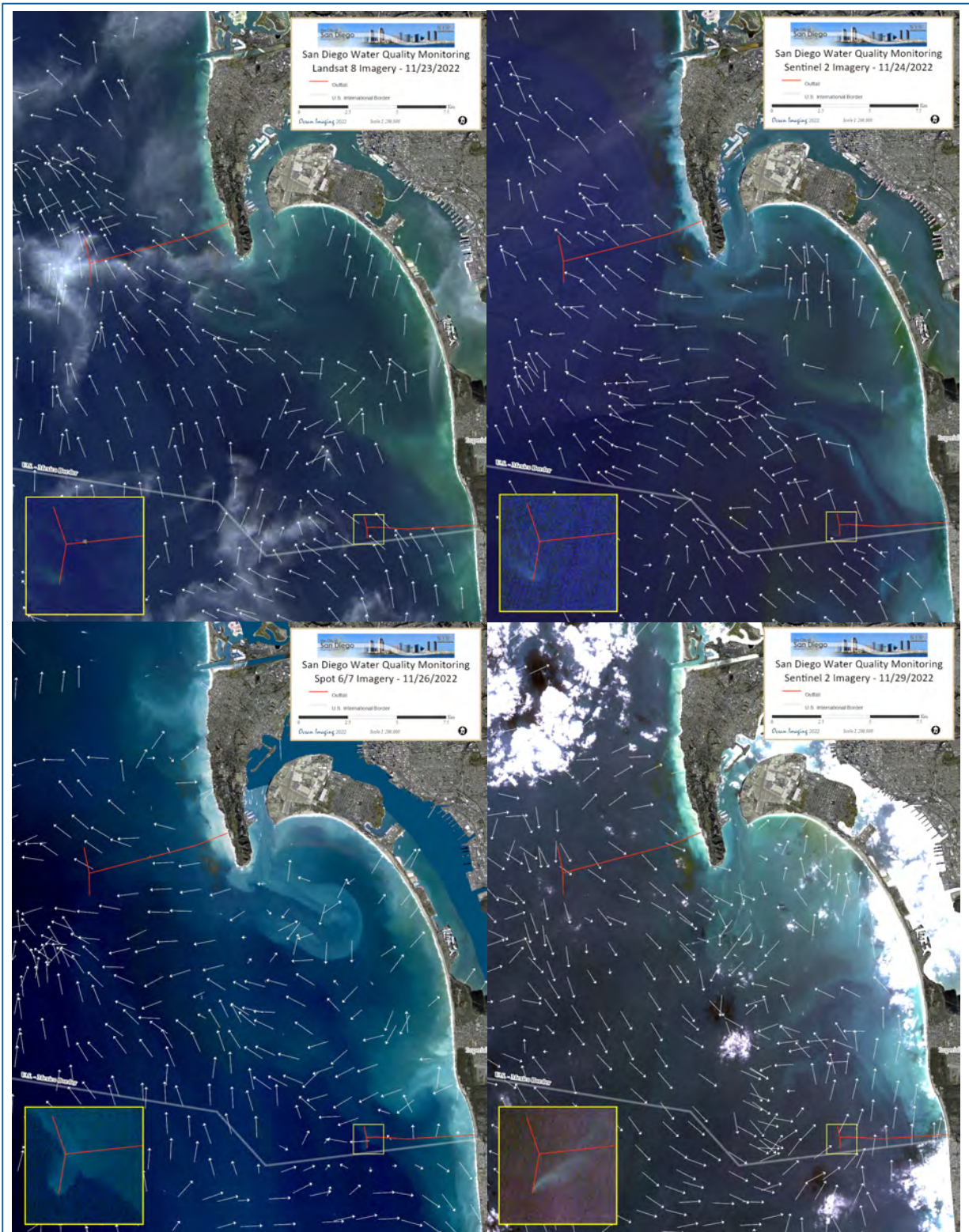


Figure 1. A time series of images from 11/23/22, 11/24/22, 11/26/22 and 11/29/22 from Landsat 8, SPOT and Sentinel 2 monitoring the movement of the TJR discharge plume over the seven-day period as it is pushed to the northwest, shifts direction, and then begins to dissipate. Note the presence of the SBOO outflow surface manifestation through the time series and the relatively fast development and disappearance of a turbidity plume streaming down from the Point Loma area.

shows a sample SAR image from 03/09/22 alongside a Sentinel 2B image highlighting a potential surfactant signature from the TJR discharge.

In 2012, OI added additional broad-scale products to the datasets available to the City and project partners. These include two types of ocean current data: High Frequency Radar-derived surface currents (HF Radar) and Hybrid Coordinate Ocean Model (HYCOM) model-derived surface currents (<http://hycom.org>). The raw data for the HF Radar currents are retrieved from National HF Radar Network via the Scripps Coastal Observing Research and Development Center (CORDC) on an hourly basis and reformatted into ESRI-compatible shapefiles. The hourly products are averages of the previous 25 hours and generated at 1 km and 6 km spatial resolutions. Additional HYCOM model-based products include daily ocean salinity, mixed layer depth, and subsurface temperature at 50, 100, 150 and 200 meters. In 2016 these products were delivered in a Web Map Service (WMS) Representational State Transfer (REST) service format compatible with the City's now retired BioMap server. They are presently being generated and archived in preparation for delivery via a next generation WMS dashboard planned for the future. The existing high resolution (6-30 m)

observation region extends from approximately La Jolla southward to Rosarita Beach, Mexico and out approximately 50 miles. The coarser-scale products (250-1000 m) such as chlorophyll, SST, ocean currents and HYCOM-derived products encompass the entire Southern California Bight (SCB).

2.4 Data Dissemination and Analysis

The satellite data are made available to the SDPUD and other project constituents through a dedicated, password-protected web site. Although it is possible to process most of the data in near-real-time, earlier in the project it was decided that the emphasis of this program is not on providing real-time monitoring support and the extra costs associated with the rapid data turn-around are not warranted. Most satellite data is thus processed and posted within 1-2 days after acquisition. As noted above however, OI has in a number of cases made imagery available to the SDPUD in near-real time (within 12-24 hours) via email when observations appeared to be highly significant to the management of beach closures or other sudden/anomalous events. The website was updated in 2022 to improve it ease of use and presentation of available imagery. Details on the site enhancements follow in section 4 below.

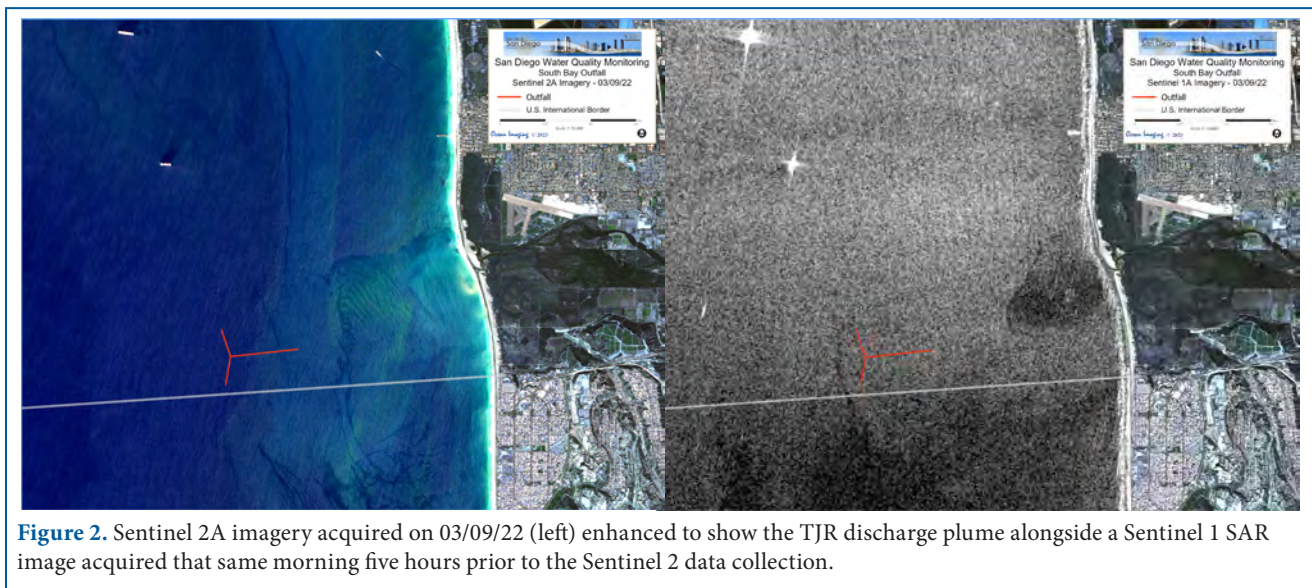


Figure 2. Sentinel 2A imagery acquired on 03/09/22 (left) enhanced to show the TJR discharge plume alongside a Sentinel 1 SAR image acquired that same morning five hours prior to the Sentinel 2 data collection.

3. HIGHLIGHTS OF 2022 MONITORING

3.1 Atmospheric and Ocean Conditions

Coastal and oceanic water quality can often be correlated to rainfall events. Annual recorded precipitation for 2022 was below the previous 10-year average for the region. The San Diego International Airport station (SDIA) measured 5.87 inches of total annual rainfall and the TJR Estuary 5.38 inches, both lower than 2012-2021 averages of 8.13 and 7.61 inches respectively (see Table 2). The monthly rainfall followed normal patterns seasonally, with the winter and spring months matching the expected rainy season and the summer months being dry. Only 0.02 inches of precipitation were recorded between both sites from May through August.

Figure 3 shows cumulative daily precipitation in the Tijuana Estuary. The table to the side of the plot gives the dates for which there was measurable precipitation at that station. As has been noted in the previous reports, the monthly and annual precipitation amounts can differ at times between the two reporting stations. The primary periods of consistent and/or heavy precipitation occurred during the months of February, March, November, and December. All (36 out of 36) significant TJR discharge events observed in the remotely sensed data occurred during the months of January through April and October through December, which is considered to be the Southern California rainy season. Most can be associated with a rainfall event occurring within a few days of the observation (Figure 3).

The coastal turbidity and TJR discharge levels mostly followed the rainfall patterns with water quality levels decreasing one-to-two days following the more significant rain events and water clarity increasing only after a few days of low to zero rainfall. Figure 4 provides an example of heavy coastal turbidity and a large TJR plume observed in the satellite imagery resulting from almost an inch of precipitation rain

between 11/07/22 – 11/09/22 followed by a period of dry and calm conditions and then subsequent improvement of water quality conditions.

As noted above, there was almost no precipitation in the San Diego region during the months of May through the first week of September. River flow rates in cubic feet per second (cfs) measured by the United States Geological Survey (USGS) Fashion Valley gauge correspond well with the rainfall data. In Figure 5 daily SDIA precipitation totals are plotted with the river flow data and monthly precipitation totals are displayed to the right of the plot. The 2022 the river flow rates matched what would be expected given seasonal rainfall patterns.

Despite the dry summer conditions with little coastal runoff measured by the USGS gauge or observed in the satellite data, there were several days during this time period that exhibited strong coastal phytoplankton blooms (Figure 6). This is an indication that the nutrients fueling the blooms likely entered the San Diego region from offshore and/or via upwelling events. Figure 7 shows a summer satellite image with reflectance signatures indicative of a strong red tide event. Also seemingly unrelated to the rainfall and river flow data, November experienced several days late in the month during which the TJR discharge extended far offshore and was documented pushing up past the southern tip of Point Loma - well after the heavy rain event on 11/08/22 (Figure 1 above).

In 2022 the county of San Diego issued 202 posted shoreline and/or rain advisories and 61 beach/shoreline closures. This is a 78.8% and 38.6% increase over the number of advisories and closures as in 2021 (113 and 44 respectively). The longest contiguous 2022 closure lasting the full year and into 2023 was at Border Field State Park along the south end of the Tijuana Slough Shoreline. As is typical for the region, the majority of the closures were in the area between the Tijuana River mouth and Avenida Del Sol at the south end of North Island and the result of contamination from the TJR

Table 2. San Diego and Tijuana Estuary precipitation totals 2012-2022**San Diego International Airport Cumulative Monthly Precipitation in Inches**

	2012	2013	2014	2015	2016	2017	2018	2019	2020	2021	2022
January	0.40	0.70	0.01	0.42	3.21	2.99	1.77	2.42	0.48	1.80	0.16
February	1.19	0.63	1.00	0.28	0.05	1.58	0.35	4.04	0.38	0.10	0.70
March	0.97	1.22	1.28	0.93	0.76	0.08	0.65	1.23	2.15	1.48	1.61
April	0.88	0.01	0.54	0.02	0.55	0.01	0.02	0.10	3.68	0.07	0.02
May	0.02	0.26	--	2.39	0.44	0.87	0.09	0.86	0.02	0.07	0.02
June	--	--	--	0.04	--	0.02	--	0.01	0.14	0.01	--
July	--	0.05	--	1.71	--	--	--	--	--	--	--
August	--	--	0.08	0.01	--	--	0.02	--	--	0.23	--
September	--	--	--	1.24	0.32	0.06	--	0.11	--	0.50	0.65
October	0.70	0.25	--	0.43	0.07	--	0.57	--	0.12	1.01	0.09
November	0.28	1.48	0.37	1.54	0.61	0.02	0.69	2.72	0.14	--	1.07
December	2.19	0.46	4.50	0.88	4.22	--	0.83	4.03	0.60	2.58	1.55
Annual Total	6.63	5.06	7.78	9.89	10.23	5.63	4.99	15.52	7.71	7.85	5.87

Tijuana Estuary Cumulative Monthly Precipitation in Inches

	2012	2013	2014	2015	2016	2017	2018	2019	2020	2021	2022
January	0.70	0.05	0.08	0.32	2.40	3.61	0.82	1.80	0.61	2.21	0.17
February	0.86	--	1.35	0.13	0.02	4.06	0.47	3.62	0.51	0.06	0.58
March	1.21	1.43	0.55	1.01	1.28	0.04	1.17	1.33	2.59	1.12	1.64
April	0.82	0.11	0.35	0.07	1.91	0.01	0.10	0.33	5.52	0.04	0.13
May	--	0.36	--	1.13	0.97	1.07	0.08	0.50	0.02	0.01	--
June	--	--	0.12	--	--	--	--	0.02	0.21	0.06	--
July	--	0.01	0.33	0.39	--	0.01	0.01	--	--	--	--
August	--	--	0.04	--	--	0.02	--	--	--	0.02	--
September	0.02	0.01	--	0.48	0.49	0.03	--	--	--	--	0.48
October	0.50	0.41	--	0.21	--	--	0.13	--	0.04	0.91	0.29
November	--	0.25	0.29	0.61	0.34	0.06	0.82	2.99	0.08	0.02	0.95
December	0.04	0.50	3.09	0.61	4.32	0.09	3.16	3.82	0.60	1.18	1.13
Annual Total	4.15	3.13	6.20	4.94	11.73	8.99	6.76	14.41	10.18	5.63	5.38

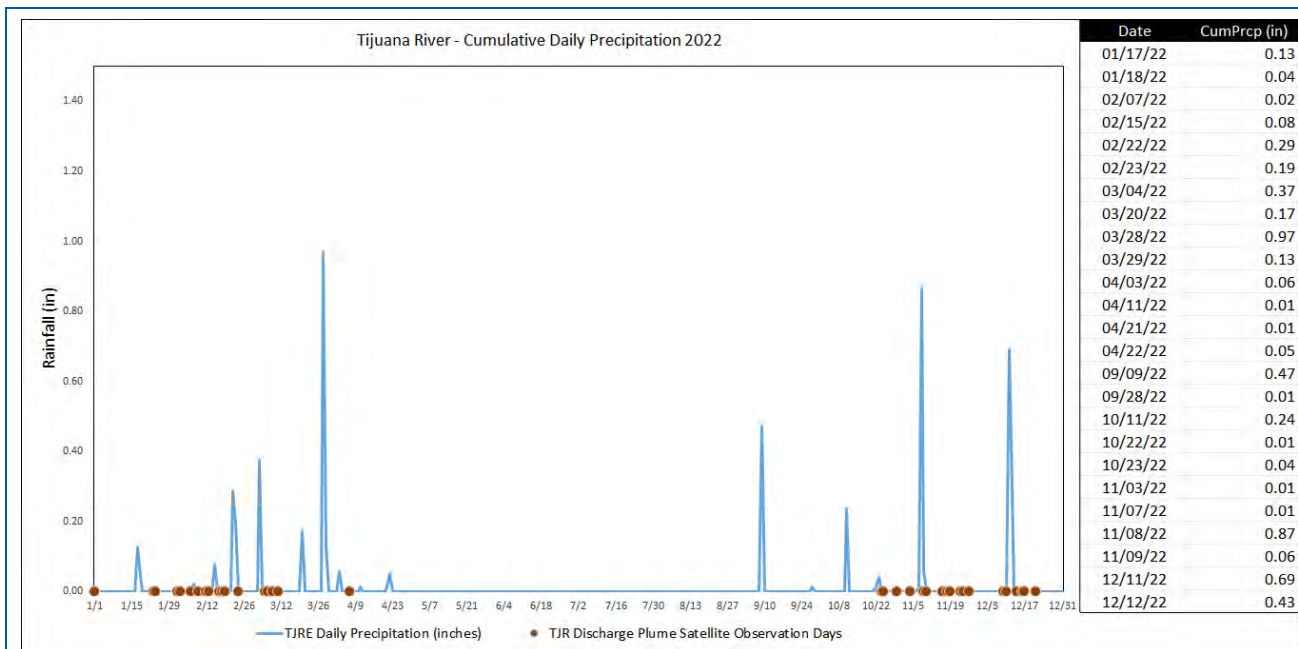


Figure 3. Daily accumulated rainfall in the Tijuana Estuary and days on which significant TJR discharge was observed in the high-resolution satellite imagery, including the Sentinel 1 SAR data.

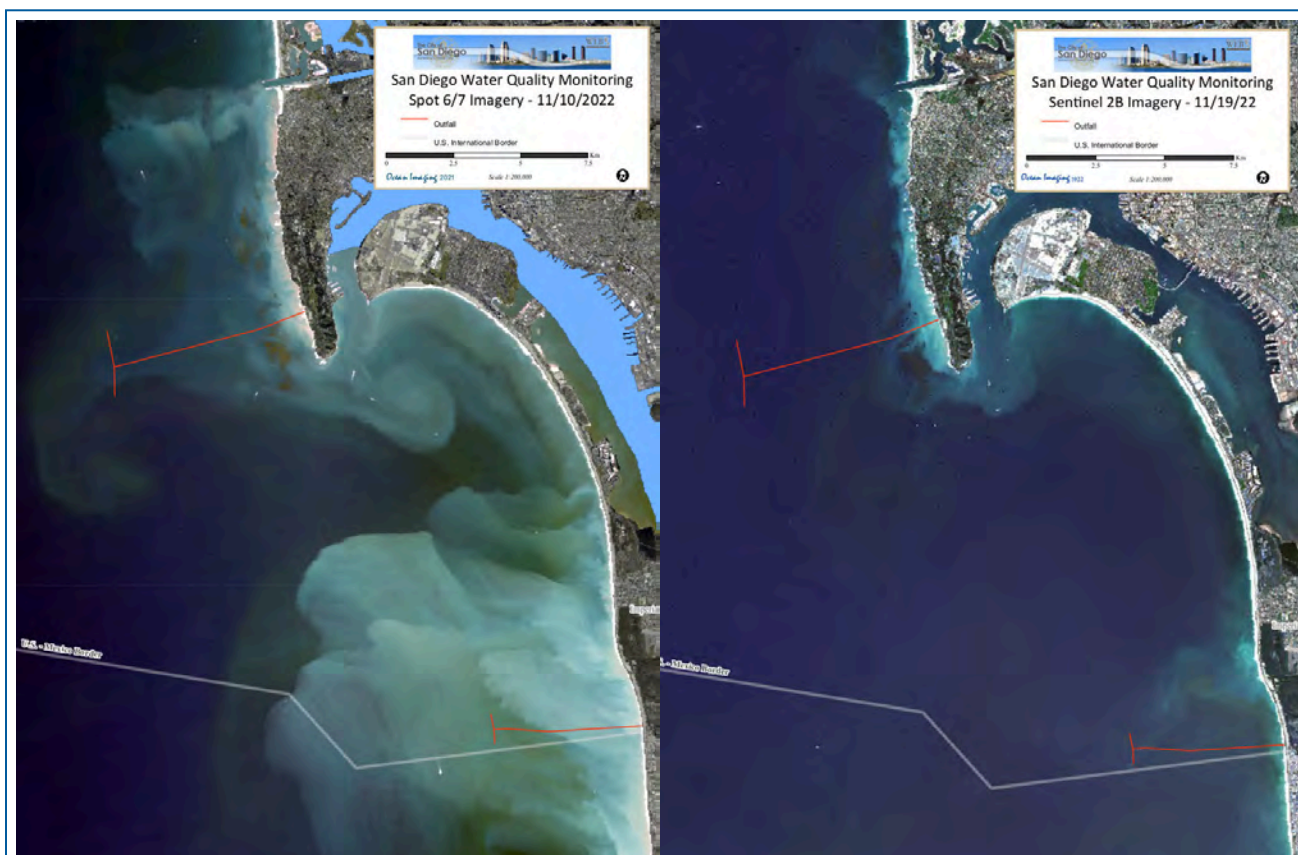


Figure 4. SPOT imagery acquired on 11/10/22 showing heavy coastal turbidity, San Diego River and TJR discharge following 0.94 inches of rainfall measured at the TJR estuary station occurring during the three days prior. A Sentinel 2B image acquired on 11/19/22 shows how the water cleared up during a period of dry and calm conditions after the rain event.

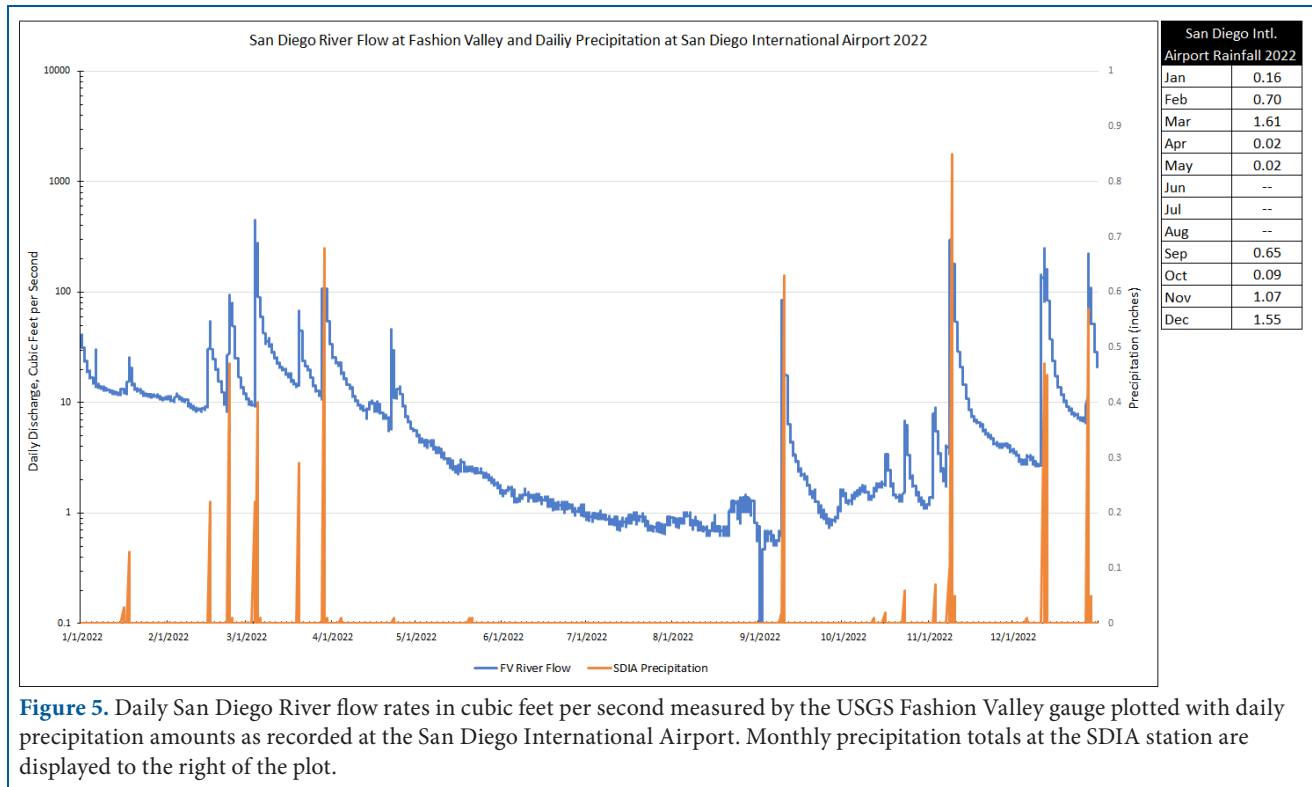


Figure 5. Daily San Diego River flow rates in cubic feet per second measured by the USGS Fashion Valley gauge plotted with daily precipitation amounts as recorded at the San Diego International Airport. Monthly precipitation totals at the SDIA station are displayed to the right of the plot.

runoff. There were nine exceptions when measurements taken from the Avenida Del Sol station warranted the closure of all Coronado City beaches and four sewage spills caused closures in San Diego Bay, at Ocean Beach and the Encina Creek outlet in Carlsbad (Table 3). In some cases, the closures could be attributed to a rain event prior to and/or during the closure period. However, 25 of the 61 closures during 2022 happened between 04/23/22 and 09/08/22 when no rainfall was recorded at the Tijuana Estuary station. As noted above there were strong phytoplankton and red tide blooms during this time which may account for some of the closures. Diatoms (primarily *Pseudo-nitzschia* spp) and dinoflagellates are largely responsible for the local harmful algal blooms and red tides when they occur (Southern California Coastal Water Research Project 2019). Figure 8 shows a strong plankton bloom on 06/14/22 close to the shoreline which was likely a red tide event. Table 3 also shows the date of the high-resolution satellite data in the project’s archive acquired closest in time to the start date of the closure and/or rain advisory. The high-resolution satellite data during the beach closure time periods show high

turbidity and suspended solid and/or high plankton levels along the coastline near the closed regions as well as greater than normal TJR runoff, sometimes being carried north by the ocean currents. Figure 4 (above) and Figure 9 provide examples of the Tijuana River plume extending north corresponding with shoreline closures beginning the day prior or on the same day.

Although discharge from the San Diego River and Mission Bay do not cause the same level of beach contamination issues as the Tijuana River, the runoff from the bay, river, and coastal lagoons did affect nearshore water clarity and quality on several days throughout the year in 2022, directly as a source of suspended sediment and indirectly as a source of high nutrient input, encouraging large scale phytoplankton blooms. While not at the scale or as dramatic as observed in 2020 and 2021, turbidity plumes emanating from the Mission Bay entrance and/or phytoplankton blooms either along the coast or offshore of the area were documented on 57 days in the medium- (MODIS and Sentinel 3) and high-resolution satellite imagery throughout the year. The area surrounding the Point



Figure 6. Sentinel 2A and 2B data from 07/19/22, 08/18/22, 08/28/22 and 09/02/22 highlighting the strong phytoplankton blooms which occurred in the San Diego South Bay region during July, August, and September.

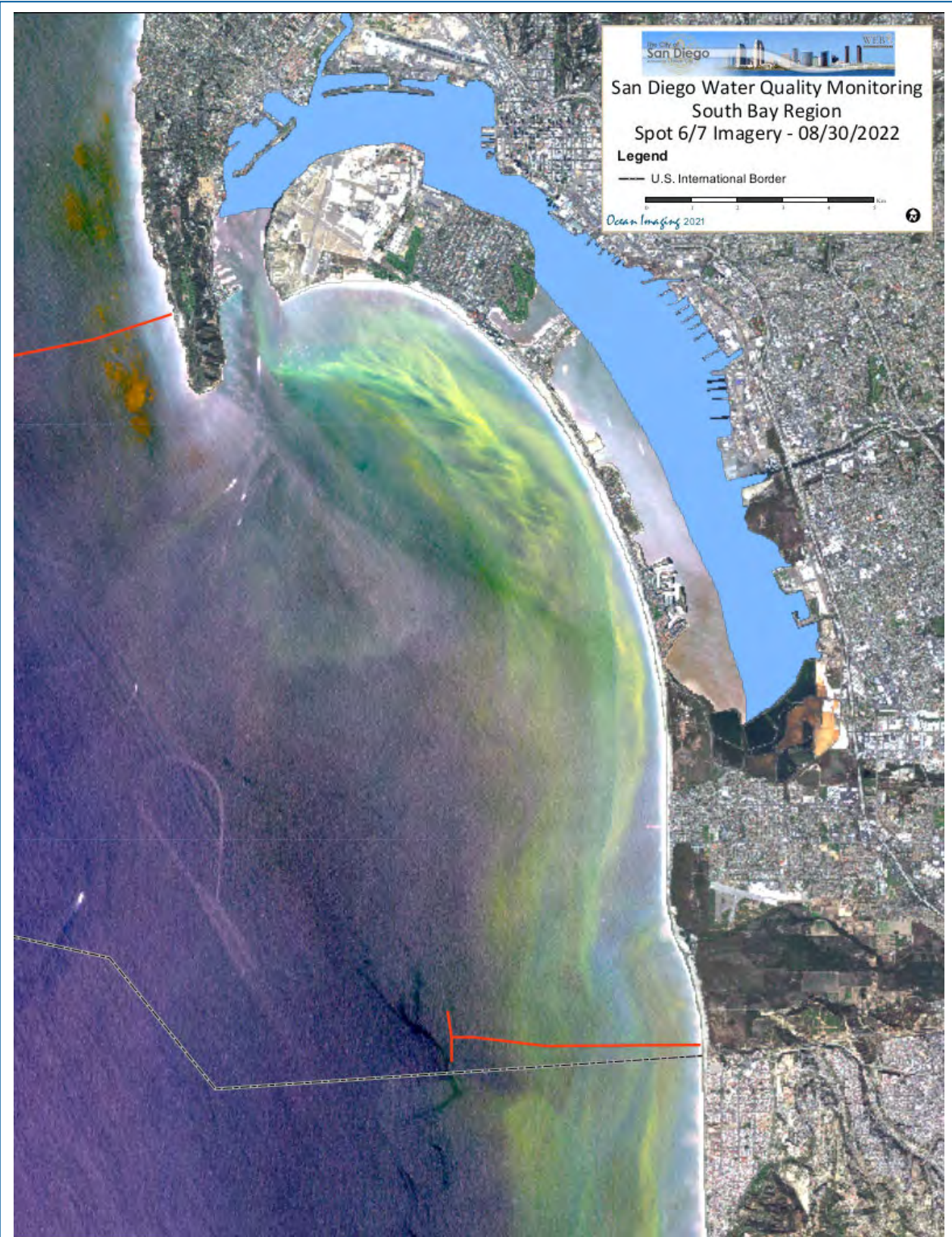


Figure 7. SPOT image acquired on 08/30/22 showing indications of a probable strong red tide event.

Table 3. 2022 County of San Diego shoreline closures and advisories and associated project satellite data (courtesy of the County of San Diego Department of Environmental Health).

Station/Description	Beach Name	Station Name	Type	Cause	Source	Start Date	End Date	Duration (days)	Nearest Rain Date	Time From Rain Event	Satellite Image Data
All_SanDiego_County_Beaches	All_SanDiego_County	All_SanDiego_County_Beaches	Rain			1/1/2022	1/1/2022	1	1/16/2022	15	1/1/22, 1/3/2022
Avd. del Sol	Coronado City beaches	IB-080	Closure	Tijuana River Associated	Sewage/Grease	1/1/2022	1/3/2022	3	1/16/2022	15	1/1/22, 1/3/2022
End of Seacoast Dr	Imperial Beach municipal beach, other	IB-050	Closure	Tijuana River Associated	Sewage/Grease	1/1/2022	1/7/2022	7	1/16/2022	15	1/1/22, 1/3/22, 1/5/22
Border Fence N side	Border Field State Park	IB-010	Closure	Tijuana River Associated	Sewage/Grease	1/1/2022	12/31/2022	365	1/16/2022	15	All
End of Seacoast Dr	Imperial Beach municipal beach, other	IB-050	Closure	Tijuana River Associated	Sewage/Grease	1/9/2022	1/13/2022	5	1/16/2022	7	1/5/2022
End of Seacoast Dr	Imperial Beach municipal beach, other	IB-050	Closure	Tijuana River Associated	Sewage/Grease	1/17/2022	1/22/2022	6	1/17/2022	0	1/19/2022, 1/20/22
All_SanDiego_County_Beaches	All_SanDiego_County	All_SanDiego_County_Beaches	Rain			1/18/2022	1/21/2022	4	1/18/2022	0	1/19/2022, 1/20/22
End of Seacoast Dr	Imperial Beach municipal beach, other	IB-050	Closure	Tijuana River Associated	Sewage/Grease	1/23/2022	1/25/2022	3	1/18/2022	5	1/23/22, 1/24/22
End of Seacoast Dr	Imperial Beach municipal beach, other	IB-050	Closure	Tijuana River Associated	Sewage/Grease	1/27/2022	1/29/2022	3	1/18/2022	9	1/30/2022
End of Seacoast Dr	Imperial Beach municipal beach, other	IB-050	Closure	Tijuana River Associated	Sewage/Grease	1/31/2022	2/7/2022	8	2/15/2022	15	1/30/22, 2/2/22, 2/4/22, 2/7/22
End of Seacoast Dr	Imperial Beach municipal beach, other	IB-050	Closure	Tijuana River Associated	Sewage/Grease	2/18/2022	2/20/2022	3	2/16/2022	2	2/17/22, 2/19/22
All_SanDiego_County_Beaches	All_SanDiego_County	All_SanDiego_County_Beaches	Rain			2/23/2022	2/26/2022	4	2/23/2022	0	2/24/2022
All_SanDiego_County_Beaches	All_SanDiego_County	All_SanDiego_County_Beaches	Rain			3/4/2022	3/7/2022	4	3/4/2022	0	3/4/22, 3/6/22, 3/7/22
Silver Strand N end (ocean)	Silver Strand State Beach	IB-070	Closure	Bacterial Standards Violation	Sewage/Grease	3/4/2022	3/8/2022	5	3/4/2022	0	3/4/22, 3/6/22, 3/7/22, 3/9/22
End of Seacoast Dr	Imperial Beach municipal beach, other	IB-050	Closure	Bacterial Standards Violation	Sewage/Grease	3/4/2022	3/8/2022	5	3/4/2022	0	3/4/22, 3/6/22, 3/7/22, 3/9/22
Silver Strand N end (ocean)	Silver Strand State Beach	IB-070	Closure	Tijuana River Associated	Sewage/Grease	3/11/2022	3/15/2022	5	3/6/2022	5	3/11/22, 3/14/22
End of Seacoast Dr	Imperial Beach municipal beach, other	IB-050	Closure	Tijuana River Associated	Sewage/Grease	3/11/2022	3/15/2022	5	3/6/2022	5	3/11/22, 3/14/22
All_SanDiego_County_Beaches	All_SanDiego_County	All_SanDiego_County_Beaches	Rain			3/20/2022	3/23/2022	4	3/20/2022	0	3/21/22, 3/22/22
All_SanDiego_County_Beaches	All_SanDiego_County	All_SanDiego_County_Beaches	Rain			3/29/2022	4/1/2022	4	3/29/2022	0	3/30/2022
End of Seacoast Dr	Imperial Beach municipal beach, other	IB-050	Closure	Tijuana River Associated	Sewage/Grease	3/29/2022	4/5/2022	8	3/29/2022	0	3/30/2022
End of Seacoast Dr	Imperial Beach municipal beach, other	IB-050	Closure	Tijuana River Associated	Sewage/Grease	4/28/2022	4/30/2022	3	4/23/2022	5	4/28/22, 4/29/22, 4/30/22
End of Seacoast Dr	Imperial Beach municipal beach, other	IB-050	Closure	Tijuana River Associated	Sewage/Grease	5/5/2022	5/16/2022	12	4/23/2022	12	5/5/22, 5/10/22, 5/13/22
Avd. del Sol	Coronado City beaches	IB-080	Closure	Tijuana River Associated	Sewage/Grease	5/10/2022	5/13/2022	4	5/20/2022	10	5/10/22, 5/13/22
Silver Strand N end (ocean)	Silver Strand State Beach	IB-070	Closure	Tijuana River Associated	Sewage/Grease	5/10/2022	5/14/2022	5	5/20/2022	10	5/10/22, 5/13/22
Silver Strand N end (ocean)	Silver Strand State Beach	IB-070	Closure	Tijuana River Associated	Sewage/Grease	5/17/2022	5/28/2022	12	5/20/2022	3	5/18/22, 5/30/22, 6/14/22, 6/24/22
End of Seacoast Dr	Imperial Beach municipal beach, other	IB-050	Closure	Tijuana River Associated	Sewage/Grease	5/17/2022	6/20/2022	35	5/20/2022	3	5/18/22, 5/30/22, 6/14/22
Avd. del Sol	Coronado City beaches	IB-080	Closure	Tijuana River Associated	Sewage/Grease	5/18/2022	5/26/2022	9	5/20/2022	2	5/18/22, 5/30/22, 6/14/22, 6/24/22
Silver Strand N end (ocean)	Silver Strand State Beach	IB-070	Closure	Tijuana River Associated	Sewage/Grease	5/30/2022	6/1/2022	3	5/21/2022	9	5/30/2022
Silver Strand N end (ocean)	Silver Strand State Beach	IB-070	Closure	Tijuana River Associated	Sewage/Grease	6/2/2022	6/8/2022	7	5/21/2022	12	5/30/2022
Avd. del Sol	Coronado City beaches	IB-080	Closure	Tijuana River Associated	Sewage/Grease	6/4/2022	6/6/2022	3	5/21/2022	14	5/30/22, 6/14/22
Silver Strand N end (ocean)	Silver Strand State Beach	IB-070	Closure	Tijuana River Associated	Sewage/Grease	6/10/2022	6/14/2022	5	5/21/2022	20	6/14/2022
Avd. del Sol	Coronado City beaches	IB-080	Closure	Bacterial Standards Violation	Sewage/Grease	6/11/2022	6/14/2022	4	5/21/2022	21	6/14/2022
Silver Strand N end (ocean)	Silver Strand State Beach	IB-070	Closure	Tijuana River Associated	Sewage/Grease	6/15/2022	6/17/2022	3	5/21/2022	25	6/14/2022
Silver Strand N end (ocean)	Silver Strand State Beach	IB-070	Closure	Tijuana River Associated	Sewage/Grease	6/18/2022	6/20/2022	3	5/21/2022	28	6/14/22, 6/24/22
End of Seacoast Dr	Imperial Beach municipal beach, other	IB-050	Closure	Tijuana River Associated	Sewage/Grease	6/24/2022	7/1/2022	8	5/21/2022	34	6/24/22, 6/29/22
Silver Strand N end (ocean)	Silver Strand State Beach	IB-070	Closure	Tijuana River Associated	Sewage/Grease	6/29/2022	7/1/2022	3	5/21/2022	39	6/29/22, 7/2/22
Avd. del Sol	Coronado City beaches	IB-080	Closure	Tijuana River Associated	Sewage/Grease	6/29/2022	7/1/2022	3	5/21/2022	39	6/29/22, 7/2/22
Silver Strand (bayside)	San Diego Bay	EH-090	Closure	Sewage Spill	Sewage/Grease	7/14/2022	7/15/2022	2	5/21/2022	54	7/18/22, 7/19/22
Bayside Park (J Street)	San Diego Bay	EH-120	Closure	Sewage Spill	Sewage/Grease	7/15/2022	7/16/2022	2	5/21/2022	55	7/18/22, 7/19/22
End of Seacoast Dr	Imperial Beach municipal beach, other	IB-050	Closure	Tijuana River Associated	Sewage/Grease	7/18/2022	7/23/2022	6	5/21/2022	58	7/18/22, 7/19/22
End of Seacoast Dr	Imperial Beach municipal beach, other	IB-050	Closure	Tijuana River Associated	Sewage/Grease	7/20/2022	8/8/2022	20	5/21/2022	60	7/19/22, 8/1/22, 8/3/22, 8/8/22
End of Seacoast Dr	Imperial Beach municipal beach, other	IB-050	Closure	Tijuana River Associated	Sewage/Grease	8/2/2022	8/7/2022	6	5/21/2022	73	8/1/22, 8/3/22, 8/8/22
Silver Strand N end (ocean)	Silver Strand State Beach	IB-070	Closure	Tijuana River Associated	Sewage/Grease	8/3/2022	8/6/2022	4	5/21/2022	74	8/3/22, 8/8/22
Avd. del Sol	Coronado City beaches	IB-080	Closure	Tijuana River Associated	Sewage/Grease	8/3/2022	8/6/2022	4	5/21/2022	74	8/3/22, 8/8/22
Silver Strand N end (ocean)	Silver Strand State Beach	IB-070	Closure	Tijuana River Associated	Sewage/Grease	8/8/2022	8/9/2022	2	5/21/2022	79	8/8/22, 8/11/22
Avd. del Sol	Coronado City beaches	IB-080	Closure	Tijuana River Associated	Sewage/Grease	8/10/2022	8/15/2022	6	5/21/2022	81	8/11/22, 8/18/22
Silver Strand N end (ocean)	Silver Strand State Beach	IB-070	Closure	Tijuana River Associated	Sewage/Grease	8/10/2022	8/18/2022	9	5/21/2022	81	8/11/22, 8/18/22
San Diego River outlet	Dog Beach, O.B.	FM-010	Closure	Sewage Spill	Sewage/Grease	9/1/2022	9/4/2022	4	5/21/2022	103	8/30/22, 9/2/22
All_SanDiego_County_Beaches	All_SanDiego_County	All_SanDiego_County_Beaches	Rain			9/9/2022	9/12/2022	4	9/9/2022	0	9/15/2022
Silver Strand N end (ocean)	Silver Strand State Beach	IB-070	Closure	Tijuana River Associated	Sewage/Grease	9/10/2022	9/17/2022	8	9/10/2022	0	9/15/22, 9/16/22
End of Seacoast Dr	Imperial Beach municipal beach, other	IB-050	Closure	Tijuana River Associated	Sewage/Grease	9/10/2022	9/26/2022	17	9/10/2022	0	9/15/22, 9/16/22, 9/20/22, 9/21/22, 9/22/22, 9/25/22, 9/27/22
Avd. del Sol	Coronado City beaches	IB-080	Closure	Tijuana River Associated	Sewage/Grease	9/12/2022	9/16/2022	5	9/10/2022	2	9/15/22, 9/16/22
Silver Strand N end (ocean)	Silver Strand State Beach	IB-070	Closure	Tijuana River Associated	Sewage/Grease	9/24/2022	9/26/2022	3	9/10/2022	14	9/25/22, 9/27/22
Silver Strand N end (ocean)	Silver Strand State Beach	IB-070	Closure	Tijuana River Associated	Sewage/Grease	10/13/2022	10/16/2022	4	10/11/2022	2	10/17/2022
End of Seacoast Dr	Imperial Beach municipal beach, other	IB-050	Closure	Tijuana River Associated	Sewage/Grease	10/13/2022	10/16/2022	4	10/11/2022	2	10/17/2022
End of Seacoast Dr	Imperial Beach municipal beach, other	IB-050	Closure	Tijuana River Associated	Sewage/Grease	10/23/2022	10/25/2022	3	10/23/2022	0	10/24/22, 10/25/22
Silver Strand N end (ocean)	Silver Strand State Beach	IB-070	Closure	Tijuana River Associated	Sewage/Grease	10/24/2022	10/25/2022	2	10/23/2022	1	10/24/22, 10/25/22
San Diego River outlet	Dog Beach, O.B.	FM-010	Closure	Sewage Spill	Sewage/Grease	10/24/2022	10/25/2022	2	10/23/2022	1	10/24/22, 10/25/22
Newport Ave	Ocean Beach	PL-100	Closure	Bacterial Standards Violation	Unknown	10/27/2022	10/28/2022	2	10/23/2022	4	10/27/22, 10/30/22
All_SanDiego_County_Beaches	All_SanDiego_County	All_SanDiego_County_Beaches	Rain			11/8/2022	11/12/2022	5	11/8/2022	0	11/9/22, 11/10/22
Silver Strand N end (ocean)	Silver Strand State Beach	IB-070	Closure	Tijuana River Associated	Sewage/Grease	11/9/2022	11/12/2022	4	11/9/2022	0	11/9/22, 11/10/22
Avd. del Sol	Coronado City beaches	IB-080	Closure	Tijuana River Associated	Sewage/Grease	11/9/2022	11/12/2022	4	11/9/2022	0	11/9/22, 11/10/22
Encina Creek outlet	South Carlsbad State Beach	EN-030	Closure	Sewage Spill	Sewage/Grease	11/9/2022	11/12/2022	4	11/9/2022	0	11/9/22, 11/10/22
End of Seacoast Dr	Imperial Beach municipal beach, other	IB-050	Closure	Tijuana River Associated	Sewage/Grease	11/9/2022	11/18/2022	10	11/9/2022	0	11/9/22, 11/10/22, 11/16/22, 11/18/22
Silver Strand N end (ocean)	Silver Strand State Beach	IB-070	Closure	Tijuana River Associated	Sewage/Grease	11/13/2022	11/14/2022	2	11/10/2022	3	11/10/2022
All_SanDiego_County_Beaches	All_SanDiego_County	All_SanDiego_County_Beaches	Rain			12/12/2022	12/15/2022	4	12/12/2022	0	12/11/22, 12/15/22, 12/16/22
Silver Strand N end (ocean)	Silver Strand State Beach	IB-070	Closure	Tijuana River Associated	Sewage/Grease	12/12/2022	12/25/2022	14	12/12/2022	0	12/11/22, 12/15/22, 12/16/22, 12/19/22, 12/24/22
End of Seacoast Dr	Imperial Beach municipal beach, other	IB-050	Closure	Tijuana River Associated	Sewage/Grease	12/12/2022	12/26/2022	15	12/12/2022	0	12/11/22, 12/15/22, 12/16/22, 12/19/22, 12/24/22
Silver Strand N end (ocean)	Silver Strand State Beach	IB-070	Closure	Tijuana River Associated	Sewage/Grease	12/28/2022	12/31/2022	4	12/28/2022	0	12/24/2022
End of Seacoast Dr	Imperial Beach municipal beach, other	IB-050	Closure	Tijuana River Associated	Sewage/Grease	12/28/2022	12/31/2022	4	12/28/2022	0	12/24/2022
All_SanDiego_County_Beaches	All_SanDiego_County	All_SanDiego_County_Beaches	Rain			12/28/2022	12/31/2022	4	12/28/2022	0	12/24/2022

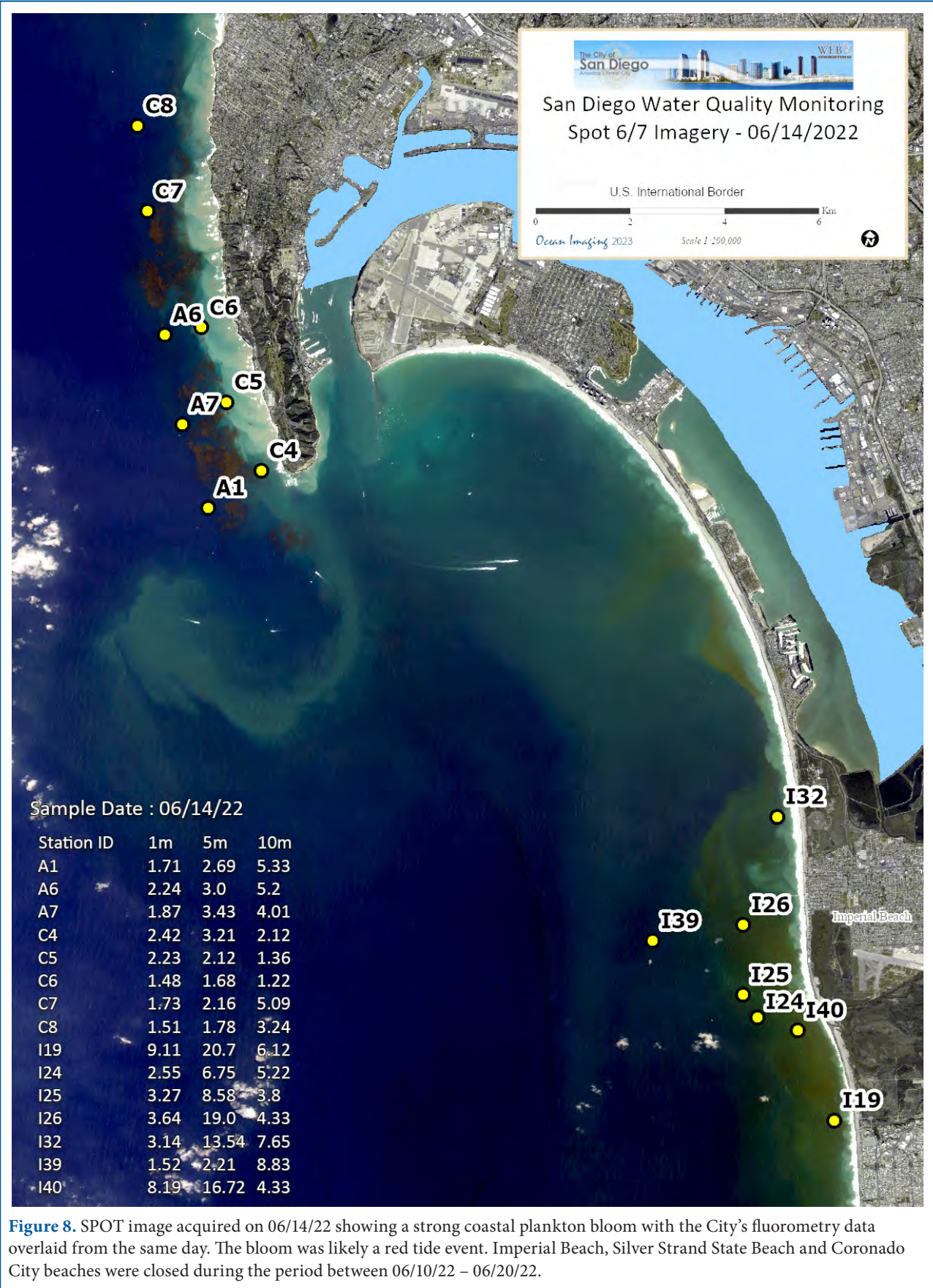


Figure 8. SPOT image acquired on 06/14/22 showing a strong coastal plankton bloom with the City’s fluorometry data overlaid from the same day. The bloom was likely a red tide event. Imperial Beach, Silver Strand State Beach and Coronado City beaches were closed during the period between 06/10/22 – 06/20/22.

Loma kelp bed tended to be more often affected by direct shore runoff and discharges from the San Diego River and Mission Bay during the prevalent southward current regime. Figure 10 provides examples of a few days on which the data revealed heavy discharge, runoff, and plankton blooms in this northern section of the project's area of interest.

The SCB experienced lower overall chlorophyll and plankton in 2022 than in the previous year. The California Current did bring chlorophyll-rich waters deeper into the Southern California region during the early part of the year, especially March through June, however a significant decrease in the SCB-wide levels occurred during the summer months. Figure 11 provides representative MODIS- and VIIRS-derived chlorophyll images for each month of 2022. As is seen in the image data, during the months of July through August, the California Current southeastward push relaxed. However, the coastal San Diego region did experience pulses of phytoplankton blooms throughout the summer and into the fall and winter, but not to the extent of what was observed in 2021. As highlighted in the figures above and in the images with the fluorometry data overlays in Figure 12, there were periods in the spring and summer months that showed periodic heavy plankton blooms, especially in the areas directly west of Point Loma and along the southern shoreline.

The City of San Diego CTD sampling results correlated well with what was observed in the satellite data. Some of the highest chlorophyll levels recorded via CTD (as high as 68.16 $\mu\text{g/L}$ at station I32, 3-meter depth on 06/28/22) occurred between April and June which is later in the season than prior years. Figures 8 (above) and 12 offer examples of the CTD fluorometry data in correlation with the high-resolution satellite imagery on or near the same day as the field samples. While the high-resolution remotely sensed data do not depict quantitative chlorophyll levels, the plankton blooms are self-evident in the imagery and correlate well with the CTD data.

3.2 The South Bay Ocean Outfall Region

The South Bay International Wastewater Treatment Plant (SBIWTP) switched from advanced primary to secondary treatment in January 2011. This change resulted in the reduction of total suspended solids (TSS) concentrations from an average of 60 mg/l for several years prior to the change to the TSS loads reading consistently below 20 mg/L since 2012. Prior to 2011, a distinct effluent signature was regularly detected in multispectral imagery as per the seasonal fluctuation described above. Since then, the effluent signature continues to be observed with multispectral color and thermal imagery during months with weak vertical stratification, however, more intermittently. On occasion the signature is distinctly discernable in thermal images (indicating it has fully reached the ocean surface), but undetectable in the color imagery. We theorize this is due to the reduction in TSS concentrations.

The SBOO wastewater plume generally remains well below the surface between approximately late March and November due to vertical stratification of the water column. During that period, it usually cannot be detected with multispectral aerial and satellite imagery, which penetrate the upper 7 to 15 meters (depending on water clarity), nor can it be detected with thermal IR imaging, which does not penetrate below the surface. Seasonal breakdown of the vertical stratification results in the plume's rise closer to the surface or to actually reach the surface between approximately late November and April when it can often be detected with aerial and satellite imaging. This concept held true in 2022, as the last observation of a SBOO surface plume during the beginning of the year was on 04/23/22 and then was not seen in the image data again until 11/09/22. In total, there were 23 instances during which the SBOO effluent plume was observed in 2022 out of the 117 high resolution satellite scenes acquired and processed. Of the 23, two were instances of the plume observed by different satellites on the same day. This equates to 21 days

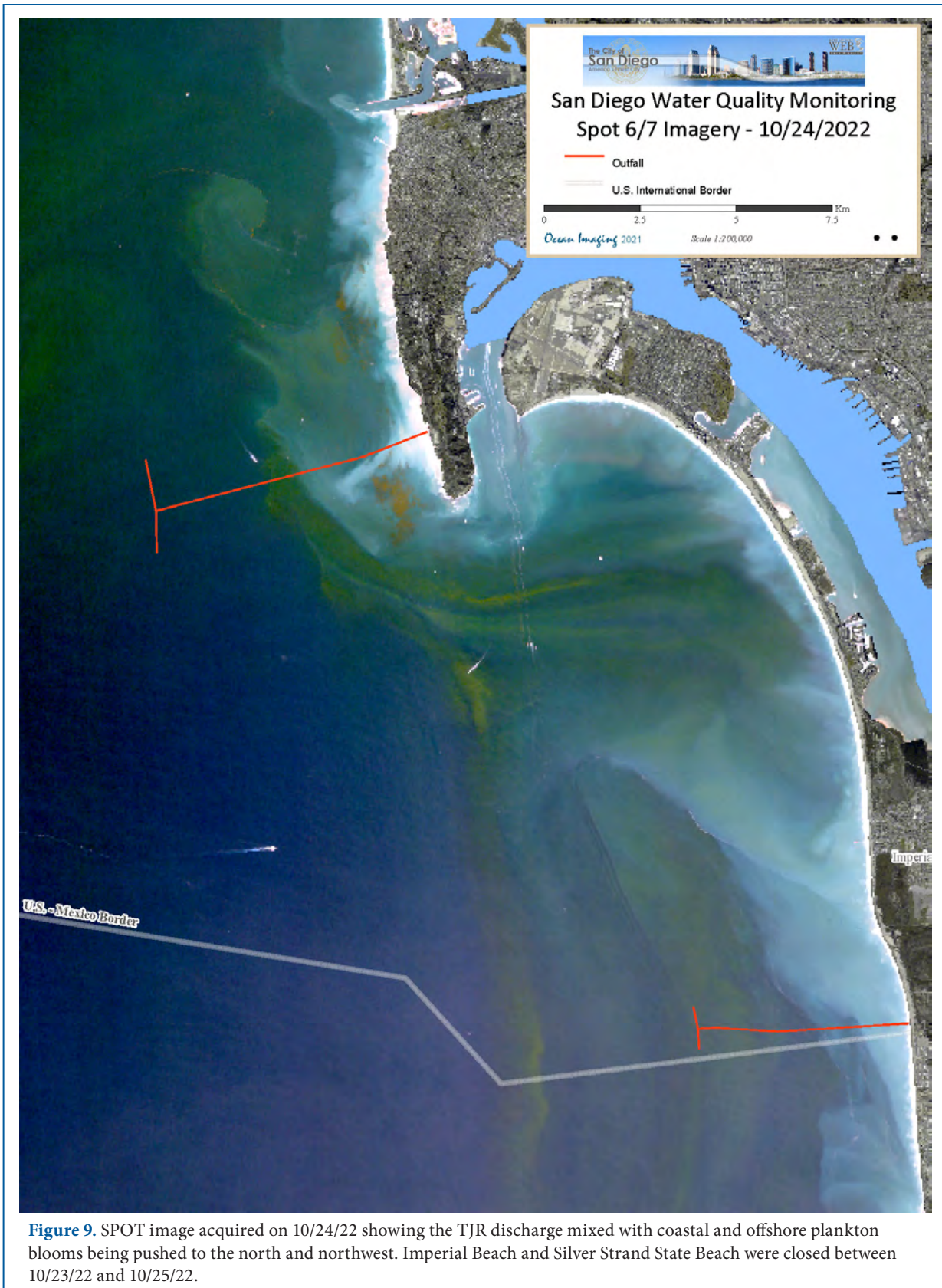


Figure 9. SPOT image acquired on 10/24/22 showing the TJR discharge mixed with coastal and offshore plankton blooms being pushed to the north and northwest. Imperial Beach and Silver Strand State Beach were closed between 10/23/22 and 10/25/22.



Figure 10. Sentinel 3 images (left side) and the higher resolution SPOT and Sentinel 2A images (right side) showing the turbid water flowing out of the Mission Bay entrance and associated plankton blooms on 03/22/22 (top) and 04/25/22 (bottom).

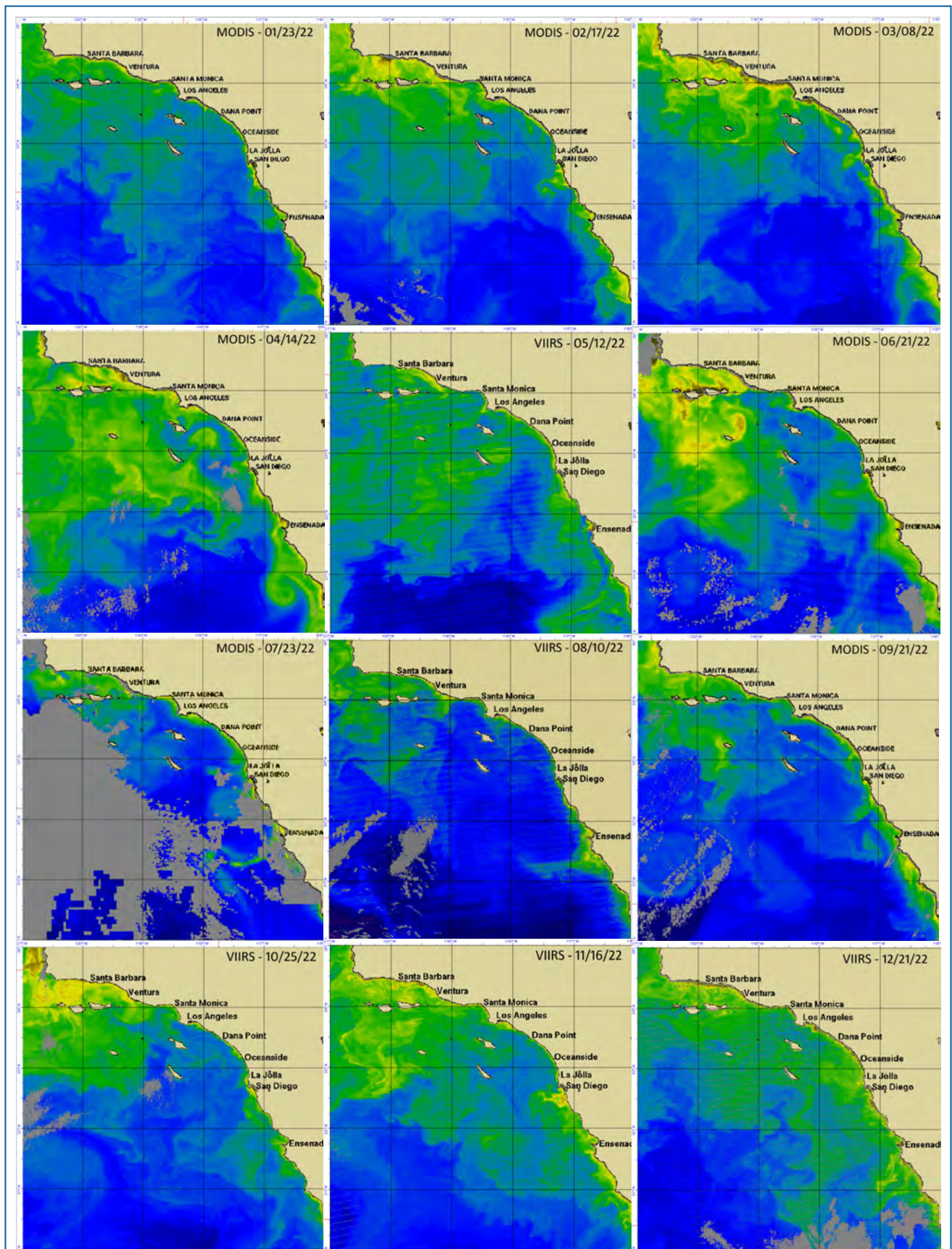


Figure 11. Representative MODIS- and VIIRS-derived chlorophyll images for each month of 2022 in the SCB showing a strong push of chlorophyll-rich California Current water pushing into the bight during the spring months, a relaxation in July, August, and September and then a resurgence of chlorophyll levels beginning in October.

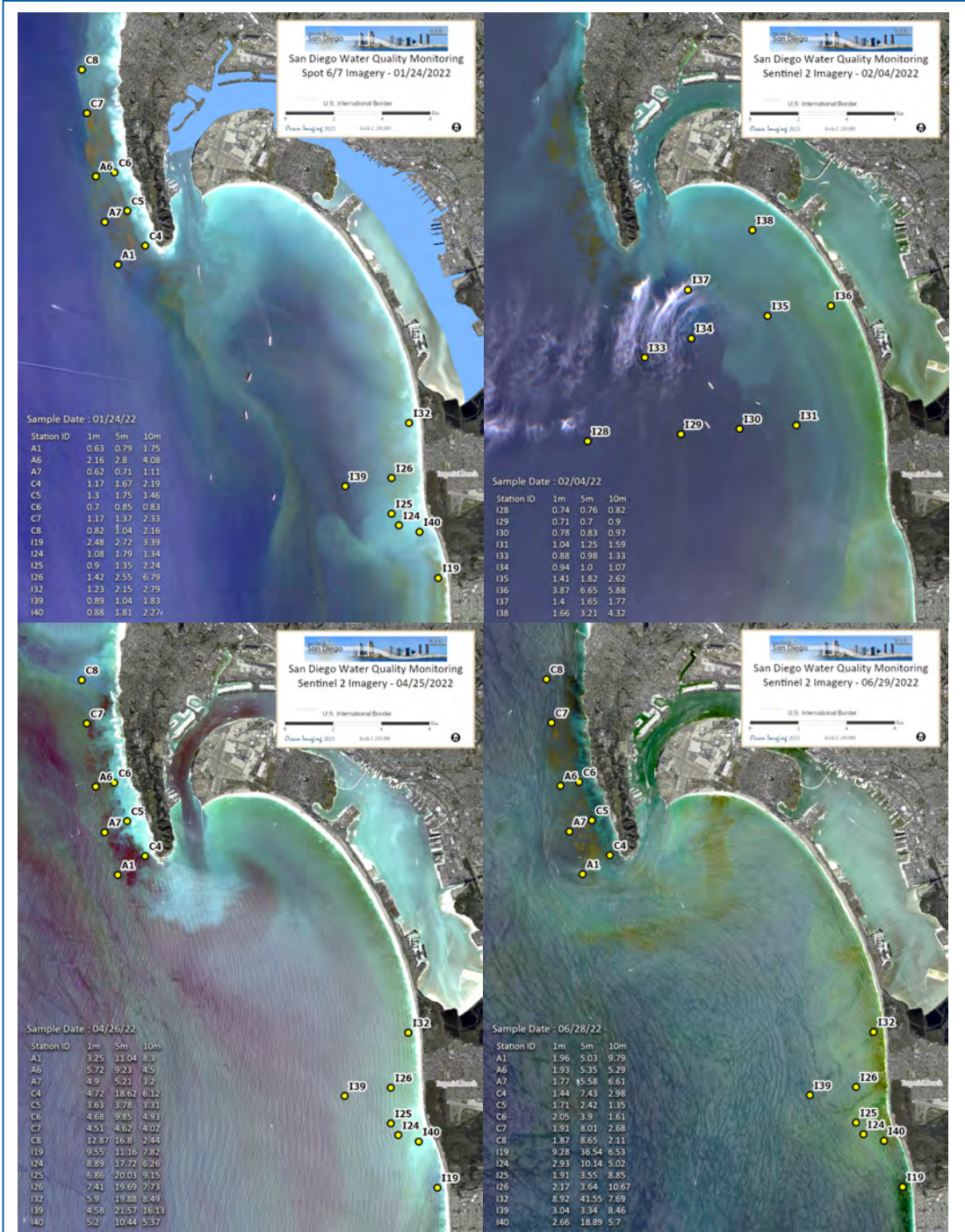


Figure 12. SPOT and Sentinel 2 imagery with CTD sampling data overlaid. SPOT image from 01/24/22 (top left) shows a day exhibiting high turbidity levels mixed with patchy plankton blooms. The Sentinel 2 image data from 02/04/22 (top right) is a day when samples were taken at the sites farther offshore and illustrates a time period when the offshore waters were relatively clear and low in chlorophyll, yet there were relatively strong plankton blooms right along the shoreline. The water column reflectance seen in the imagery from 04/25/22 (bottom left) was obscured somewhat by sun glint, but the green tint of the region-wide high chlorophyll levels is readily apparent and corresponds with the high sample measurements. The Sentinel 2 imagery from 06/29/22 (bottom right) with CTD data from 06/28/22 overlaid provides the most dramatic example of remarkably high chlorophyll measurements matching the green water in the South Bay region – especially along the shoreline.

when the plume was visible in the high-resolution imagery - five more than observed in 2021, but below the average percentage of SBOO plume surface observations per days imaged when compared to the previous 10 years (17.9% vs. 19.4% respectively). Appendix A includes the 2022 SPOT, Sentinel and Landsat imagery on days which the SBOO plume was detected. There were two occurrences when either Sentinel 2A or 2B data were acquired within only a few minutes of SPOT 6/7 data providing a near time-coincident validation of features observed in the imagery.

As has been the case in previous years, there was an occurrence when the SBOO effluent plume appeared in the imagery as a patch of clearer water breaking the more turbid water on the surface. As discussed in prior reports, the clear effluent signal in the imagery is most likely due to the contrast between the higher turbidity coastal surface waters and the 'normal' level of turbidity of the effluent water breaking the surface. It is also possible that the effluent plume became somewhat diluted on its way to the surface if weak vertical stratification did exist, thus slowing down its rise in the water column. Figure 13 provides an example of this situation as well as the satellite's view of a large, discolored discharge plume moving south from the TJR.

The period between 11/19/22 and 12/16/22 exhibited the highest frequency of 2022 SBOO effluent plume observations in the satellite data. As has been documented in previous reports, it is typical to see the highest number of SBOO surface plumes during the November to January timeframe. According to the 2022 IBWC Transboundary Flow Report the documented instances of sewage, solid waste and sediment moving across the U.S.-Mexico border and into the Tijuana Estuary and U.S. coastal waters occurred mainly between 01/07/22 and 03/11/22 and not in the latter part of the year (San Diego Regional Water Quality Control Board 2022). As is typically the case, the relatively frequent effluent surface manifestations that occurred during this time

period were most probably the result of two primary factors: the lack of strong vertical stratification during the winter months and relatively weak subsurface currents over the SBOO which allowed the undispersed effluent to reach the surface.

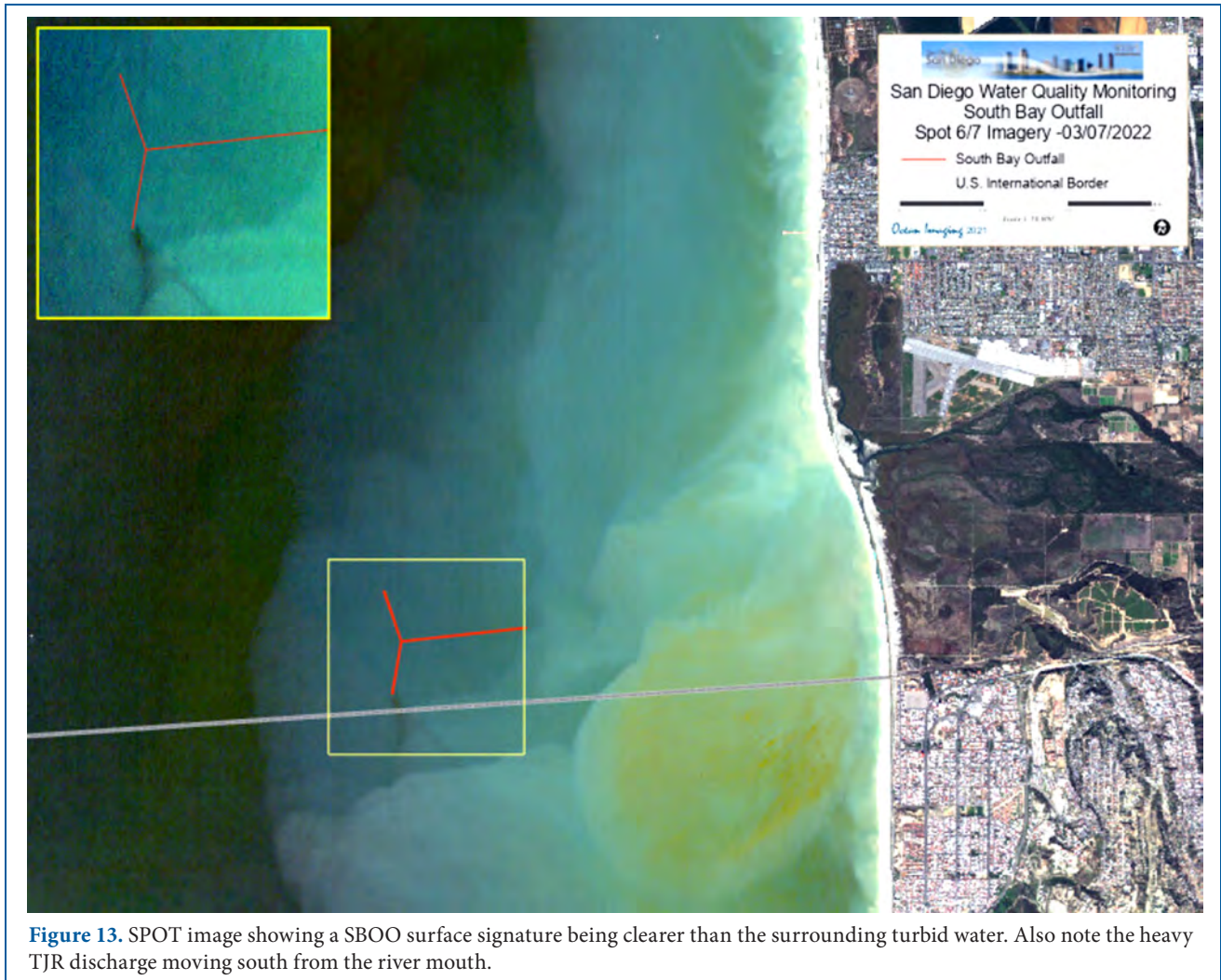
There were several instances during this time period when the SBIWTP took on excess sewage from Tijuana exceeding the maximum capacity (25 MGD) of the SBIWTP. On 07/30/22 Mexico lost pumping capability at their main pumping station and additional flow was diverted to the SBIWTP. This can be seen in Figure 14, which shows the SBIWTP Effluent Flow rate (EFF Flow) and the Effluent Total Suspended Solids (EFF TSS) over the 2022 time period plotted with the dates on which SBOO effluent was observed on the surface of the ocean in the high-resolution satellite imagery. As is also apparent, there were a few spikes in EFF Flow and EFF TSS in the end of February and end of March, both due to rainfall events. Beginning in August the EFF flow averaged higher than the maximum capacity (25 MGD) of the treatment plant through the end of the year due to the loss of pumping capability mentioned above (IBWC monthly NPDES reports). However, no SBOO effluent was observed in the satellite data during the early season flow/TSS spikes or prior to November. There were 12 days on which the SBOO surface plume was evident in the satellite imagery between November 1st and the end of 2022 and 2, 15 and 8 documented days during the same periods of 2021, 2020 and 2019 respectively. This indicates that, while there were a relatively high number of effluent surface observations late in 2022, it cannot be concluded that the additional flow diverted through SBIWTP resulted in the effluent reaching the ocean's surface more often. It should also be noted that the higher flow rate did not result in the effluent breaking through the pycnocline during the months of August through October. This corroborates the belief that the instances of effluent reaching the surface almost always occur because of seasonal changes in ocean conditions when the water

column stratification breaks down and is not directly related to a higher flow rate through the system.

A total of 19 shoreline stations, ranging from Mission Beach to northern Baja (across the US/Mexico border) are sampled weekly by City of San Diego staff to monitor the levels of three types of fecal indicator bacteria (i.e., total coliform, fecal coliform, Enterococcus bacteria) in recreational waters. An additional 15 nearshore (kelp) stations are also sampled weekly to monitor Fecal Indicator Bacteria (FIB) and a range of water quality parameters (i.e., temperature, salinity, dissolved oxygen, pH, transmissivity, Chlorophyll-a, CDOM). Furthermore, 69 offshore stations are sampled quarterly to monitor both water quality conditions and one or more types

of FIB. PLOO stations are located along, or adjacent to, the 18, 60, 80, and 98-m depth contours, and SBOO stations are located along the 9, 19, 28, 38, and 55-m depth contours.

The City Marine Microbiology Laboratory (CMML) follows guidelines issued by the U.S. Environmental Protection Agency (USEPA) Water Quality Office, State Water Resources Control Board (SWRCB) including the 2019 Ocean Plan, the California Department of Public Health (CDPH), and Environmental Laboratory Accreditation Program (ELAP) with respect to sampling and analytical procedures (Bordner, et. al. 1978, American Public Health Association (APHA) 2012, CDPH 2019, USEPA 2014). All bacterial analyses



were initiated within eight hours of sample collection and conformed to standard membrane filtration techniques, for which the laboratory is certified (ELAP Field of Testing 126). FIB densities were determined and validated in accordance with USEPA and APHA guidelines as follows in APHA (2012).

In 2022, the sampling area of the SBOO/Tijuana River outflow region experienced 56 days on which the field sampling showed FIB measurements exceeding the single sample maximum for fecal coliform density for one or more sampling stations as defined by the 2019 California Ocean Plan (the single sample maximum fecal coliform density at a site will not exceed 400 per 100 mL) (SWRCB, 2019). The offshore SBOO region, which includes the stations over the SBOO wye experienced only two days of elevated bacteria levels at depths of six meters or shallower and the nearshore region (referred to as the “kelp” region in previous reports) experienced 21 days on which the bacteria levels were deemed elevated. There were 47 sampling days when at least

one shore station showed elevated levels. The total number of sampling days for all three SBOO areas totaled 96 in 2022 and 122 in 2021. Therefore, in 2022 for the three sampling regions combined, 58.3% of the sampling days resulted in elevated bacteria levels at one station or more, which is less than the 64.7% recorded in 2021 (using the same 2019 California Ocean Plan standards). As has been typical in recent years, the majority of the samples showing elevated levels were recorded at the shore stations. Elevated levels offshore near the SBOO wye are rare. Of the two days when elevated bacteria levels were recorded at an offshore station, both (station I5 and I11) are over five kilometers from the SBOO wye.

The satellite imagery showing substantial discharge from the TJR region often correlate with times when the shoreline and kelp area sampling showed elevated bacteria levels. Heavy and/or persistent rainfall is the most plausible cause for the majority of the elevated bacteria samples and turbid waters seen in the remote sensing data. Figure 15 shows a few examples of the

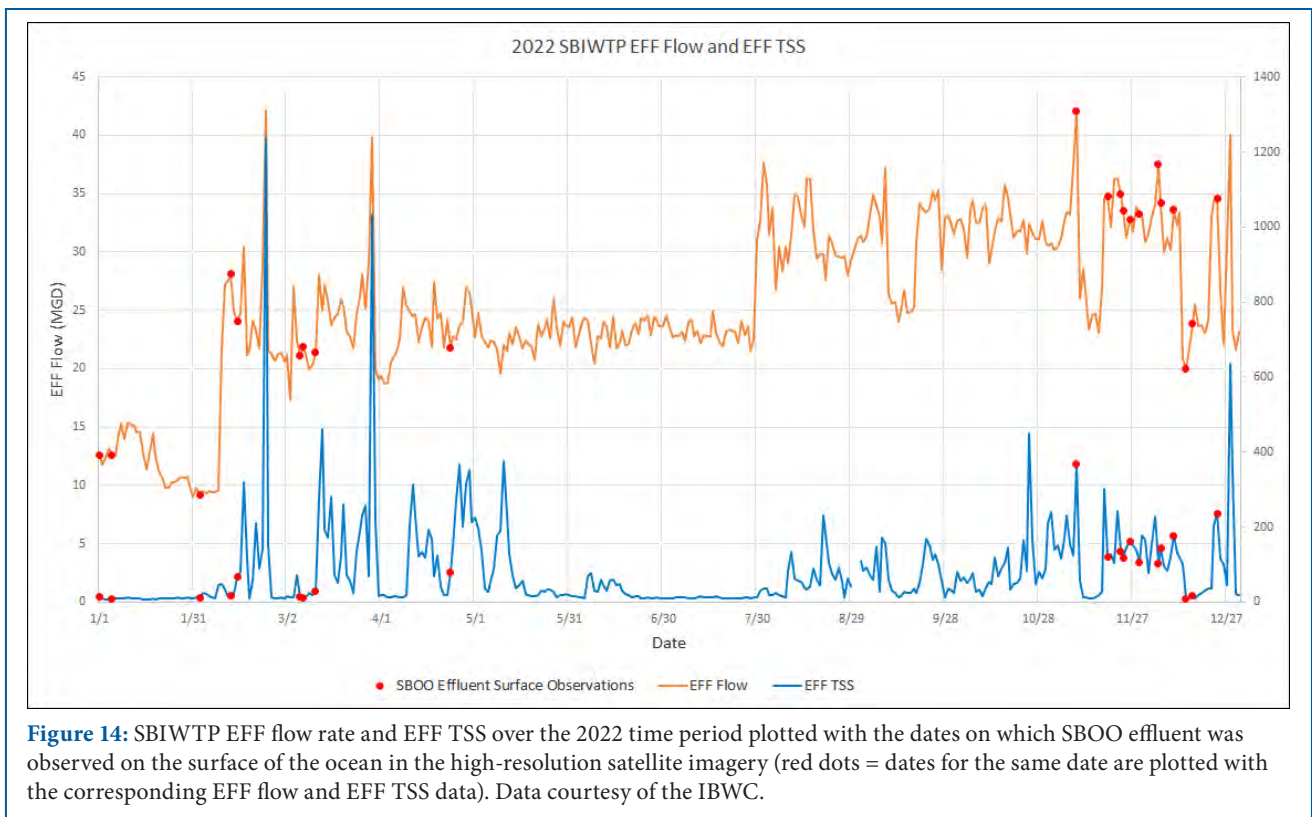


Figure 14: SBIWTP EFF flow rate and EFF TSS over the 2022 time period plotted with the dates on which SBOO effluent was observed on the surface of the ocean in the high-resolution satellite imagery (red dots = dates for the same date are plotted with the corresponding EFF flow and EFF TSS data). Data courtesy of the IBWC.

bacteria sample data overlaid on top of imagery from either the same day or on day after the sampling date. Note the very turbid water emanating from the TJR river and nearby coastline moving to the north on 12/14/22. The southern San Diego beaches were closed from 12/01/22 through the end of the year.

Typically, the best water quality and clarity in the South Bay region is observed from May through August. This was generally true in 2022. Water clarity in the South Bay region was, however, variable during May through August as phytoplankton blooms in the area were prevalent during the summer months.

3.3 The Point Loma Outfall Region

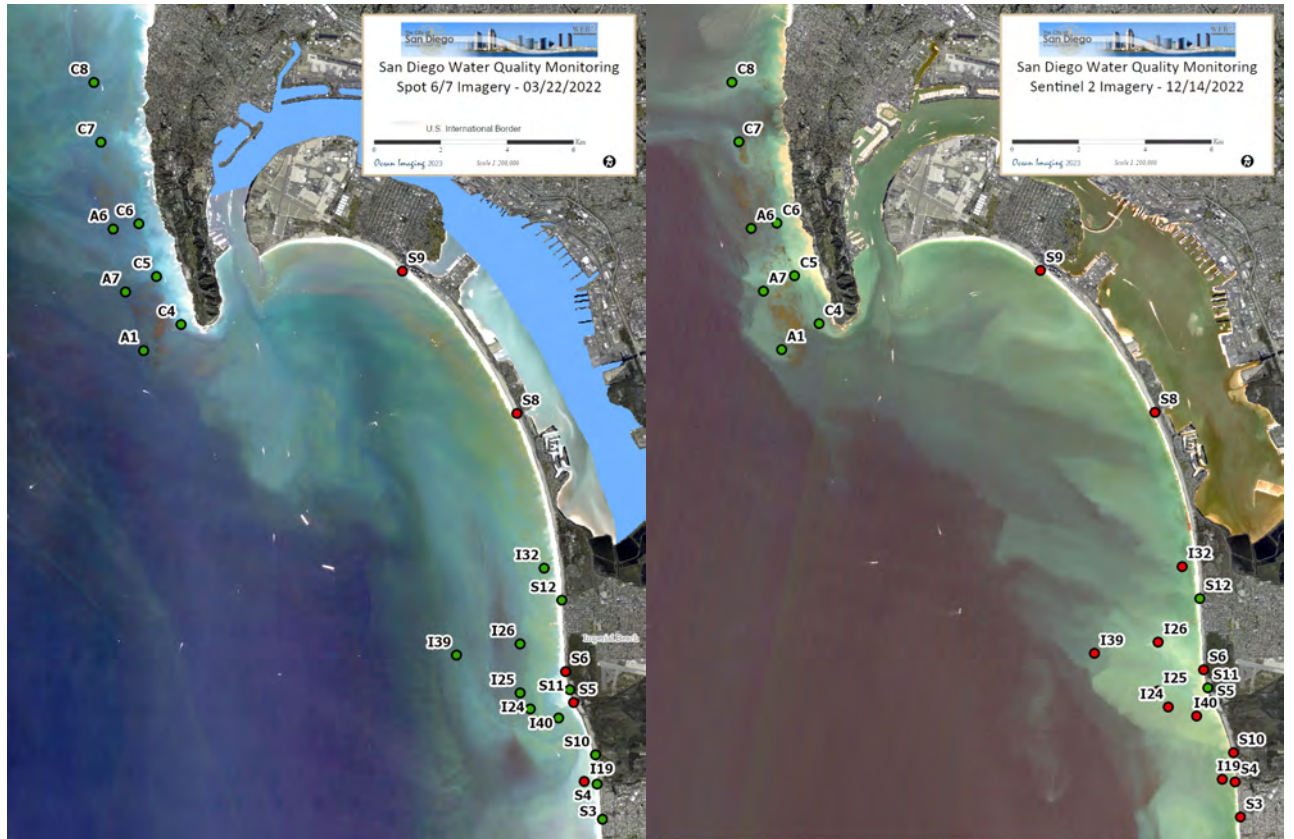
After its seaward extension in 1993, the Point Loma Outfall (PLOO) is one of the deepest and longest wastewater outfalls in the world, discharging at the depth of 320 feet, 4.5 miles offshore. The outfall's plume is generally not observed directly with multispectral color or thermal imagery. It appears to not reach the surface waters, even during the winter months when the water column's vertical stratifications are weakened. We believe that on some occasions we have observed the plume's extents indirectly through an anomalous lateral displacement of thermal or chlorophyll features around the outfall wye. This effect can be explained by the doming up of the discharged effluent and laterally displacing the near-surface waters above it.

In 2022 the Point Loma region was affected by conditions already described for general San Diego County: significant seasonal rainfall during the months of January through March and then again in September through December and almost no rainfall during the months of April through August. Similar to past years, this compromised water clarity is likely a result of runoff from the San Diego River and Mission Bay brought sediment-laden water inside and outside the Point Loma kelp bed after the rain events described above.

The shoreline, kelp and offshore bacterial sampling resulted in a slightly higher number of elevated bacteria measurements than in 2021 as defined by the 2015 California Ocean Plan (Total coliform density will not exceed 10,000 per 100 mL; or Fecal coliform density will not exceed 400 per 100 mL; or Total coliform density will not exceed 1,000 per 100 mL when the ratio of fecal/total coliform exceeds 0.1; or enterococcus density will not exceed 104 per 100 mL) (SWRCB, 2015). Shoreline field sampling yielded 10 days on which one or more stations experienced high bacteria counts. Offshore and kelp station sampling resulted in 8 days and 0 days respectively when stations recorded excessive FIBs. Figure 16 presents an example when three stations in the Point Loma sampling area showed high FIB numbers on 11/15/22. These data are plotted on top of the Sentinel 2 image from 11/16/22. While the imagery from the 16th does not show evidence of any direct correlation to the bacteria samples taken the day before, the image from 11/10/22 does offer an explanation as it documents the substantial discharge from the Mission Bay entrance along with the heavy coastal runoff from there to the south. The Tijuana Estuary station measured 0.94 inches of precipitation between 11/07/22 – 11/09/22 and the SDIA station reported 0.91 inches between 11/08/22 and 11/10/12. An alternate explanation would be that the measurements (all in close proximity to the PLOO wye risers) show high FIB originating from the outfall trapped by a pycnocline barrier at depth so any surface presence would not be visible in the satellite imagery.

3.4 Kelp Variability

One observation provided by the satellite image archive is the continuing variability in the size of the Point Loma kelp bed over time (Figure 17). Table 4 shows the area in km² of three notable kelp beds in the San Diego region over the past 15 years. The September and October dates were chosen to represent the kelp bed canopy coverage for each year since spring and fall are considered to be the



Station	Depth (M)	Entero	Fecal	Total
I19	2	680	12000	16000
	6	66	900	9600
	11	300	2200	16000
S0	NA	12000	6200	16000
S2	NA	12000	12000	16000
S5	NA	120	3400	16000
S6	NA	1400	12000	16000
S8	NA	12000	12000	16000
S9	NA	12000	12000	16000

Station	Depth (M)	Entero	Fecal	Total
I19	2	320	300	1400
	6	280	480	3400
	11	280	140	1600
I24	2	580	740	4400
	6	100	80	840
	11	6800	6400	16000
I25	2	420	680	4400
	6	980	980	5400
	9	880	700	9600
I26	2	200	80	1800
	6	3400	5400	16000
	9	5800	4000	16000
I32	2	240	320	3200
	6	280	300	3200
	9	400	460	3400
I39	2	680	1000	20
	12	160	100	2
	18	200	160	20
I40	2	1000	840	15000
	6	980	800	3000
	9	4800	2800	16000
S0	NA	1400	1400	5800
S2	NA	2600	2200	16000
S3	NA	1400	880	15000
S4	NA	460	940	10000
S5	NA	1600	800	11000
S6	NA	2400	1800	14000
S8	NA	2600	3600	16000
S9	NA	11000	12000	16000
S10	NA	860	760	6600

Figure 15. Sentinel 2 and SPOT data with near-surface bacterial sampling data overlaid from the same day of image acquisition. Stations showing FIB measurements exceeding the single sample maximum as defined by the 2019 California Ocean Plan are shown as red dots. Green dots identify stations at which the FIB levels were in compliance. The tables below each image show the measurement values by depth for each station with elevated bacteria levels. Stations S0 and S2 listed in the table are now shown in the imagery.

time periods when the canopy size is thought to be at or near its peak. The estimated size of the Point Loma bed canopy in the fall of 2022 (4.48 km²) was larger than the average canopy coverage for the 15-year period (4.07 km²). As has been reported in previous years, the satellite data show the bed begin to decrease in size during February of 2016, perhaps due to the storm events taking place during early to mid-January, effects from the 2014-2016 strong El Niño event and/or the Northeast Pacific marine heat wave (Di Lorenzo 2016). Noted in the 2017 and 2018 annual reports, the kelp bed appeared to be coming back in January of 2017, but then decreased in size as the year progressed resulting in much smaller than

average canopy coverage by the end of that year. Using the fall imagery as an indicator for annual health, the bed size appears to be stabilizing since the 2016 and 2017 lows. Contrary to 2018, 2020 and 2021 when the canopy area exhibited significant intra-annual variability, in 2022 the bed size remained somewhat consistent throughout the year. While there were short periods of time in 2022 when the bed's canopy showed a significant decrease in size, overall, the monthly variability in canopy area as judged by visual assessment was relatively stable (Figure 18). On average, the month of September exhibited the largest decrease in canopy coverage – even though September is typically considered to be

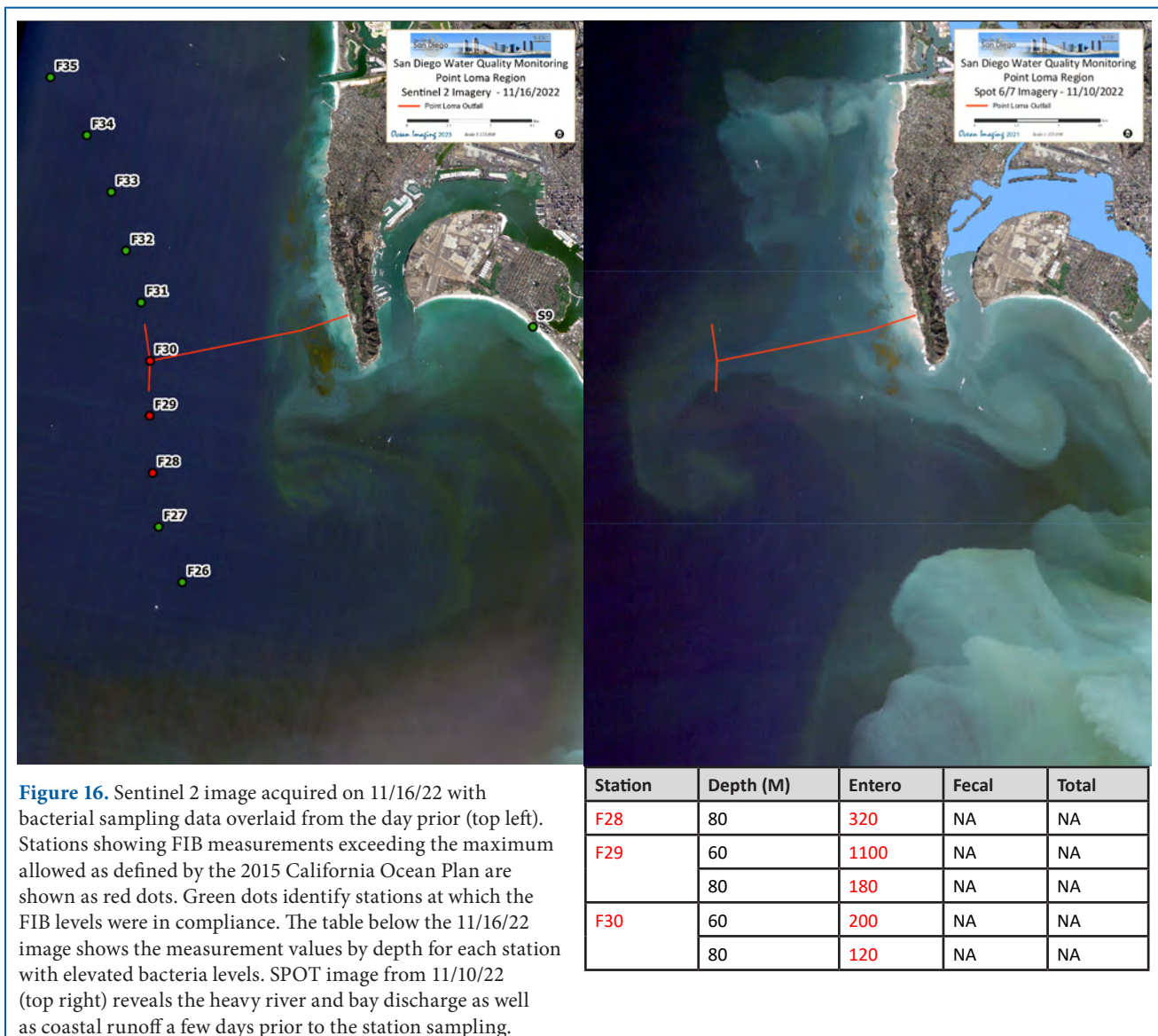


Figure 16. Sentinel 2 image acquired on 11/16/22 with bacterial sampling data overlaid from the day prior (top left). Stations showing FIB measurements exceeding the maximum allowed as defined by the 2015 California Ocean Plan are shown as red dots. Green dots identify stations at which the FIB levels were in compliance. The table below the 11/16/22 image shows the measurement values by depth for each station with elevated bacteria levels. SPOT image from 11/10/22 (top right) reveals the heavy river and bay discharge as well as coastal runoff a few days prior to the station sampling.

a peak growth month. While there were significant differences in tidal heights at the time of each satellite image acquisition, tides cannot be flagged as the primary reason for the difference in canopy coverage observed in the satellite data. There were days when the areal coverage was high, but the tide level was also high and vice versa when the imagery revealed smaller bed size, but the tides were relatively low.

Canopy coverage for each year in Table 4 was computed by first running a Normalized Difference Vegetation Index (NDVI) classification followed by an unsupervised iso cluster unsupervised classification to generate a single exposed kelp class. It is important to point out that the canopy coverages shown in Table 4 may differ slightly from those provided in the Southern California Bight Regional Arial Kelp Survey reports. This is because the canopy



Figure 17. The Point Loma kelp bed as observed in high-resolution satellite imagery for the years 2013-2022 (top to bottom). September and October dates were chosen to represent the kelp bed canopy coverage for each year since that period is when the canopy size is thought to be at or near its peak.

Table 4. Kelp canopy areas of three San Diego kelp beds measured from satellite imagery collected for this project.

Year	Date	Satellite	Kelp (km ²)		
			Point Loma	Imperial Beach	Tijuana
2022	10/20/2022	Sentinel-2B	4.48	0.00	0.00
2021	09/30/2021	Sentinel-2B	3.82	0.00	0.00
2020	09/22/2020	Sentinel-2A	2.93	0.00	0.00
2019	09/18/2019	Sentinel-2A	5.17	0.00	0.00
2018	10/16/2018	Sentinel-2A	2.44	0.00	0.00
2017	10/04/2017	RapidEye	1.05	0.00	0.00
2016	09/08/2016	RapidEye	0.22	0.00	0.00
2015	09/17/2015	Landsat 7	4.11	0.39	0.29
2014	09/14/2014	Landsat 8	5.42	0.59	0.30
2013	09/23/2013	RapidEye	5.89	0.19	0.05
2012	09/15/2012	RapidEye	2.91	0.00	0.00
2011	09/01/2011	RapidEye	1.99	0.00	0.00
2010	09/27/2010	Landsat 7	6.01	0.00	0.00
2009	09/16/2009	Landsat 5	5.96	1.01	0.21
2008	09/05/2008	Landsat 7	8.66	0.82	0.01

* Average surface canopy coverage 2008-2022 = 4.07 km²

areas for the Point Loma bed computed for those reports are averages of four surveys performed throughout the year; while the coverage estimates shown in this report are taken from single satellite images acquired during the fall time period chosen to represent the maximum coverage experienced during that time of year. Tide levels were not a factor in the inter-year comparison as there was little variability in tide level between the years (often approximately two feet or less). However, due to the overflight times of these satellites, the canopy areas could be underrepresented compared to the kelp survey reports because the tide levels at the time of satellite data acquisition could vary significantly from the tides during the aerial surveys. The Imperial Beach and Tijuana beds have not been visible in the satellite data since 2015. It is being documented that kelp forests along the West Coast have been experiencing noteworthy variability in canopy size for the past several years, and thus warrants keeping a close watch on the health of the kelp beds in the San Diego region (Bell, et al. 2020, Schroeder 2019).

4. PRESENT AND FUTURE ENHANCEMENTS OF THE PROJECT

In 2016, OI began to generate the ocean currents and other HYCOM-derived products in a Web Map Service (WMS) Representational State Transfer (REST) service format which is directly compatible with the ESRI WMS the City was working to implement. It was intended that all the OI-delivered data products, including all the satellite imagery would be delivered via OI's ArcGIS Server for easy ingestion into the City's WMS by fall of 2017. While this system has not yet been implemented, OI is in discussion with the City about further developing the project's web server into dashboard style site that incorporates an interactive WMS to better facilitate the delivery of all the existing data products, the HYCOM oceanographic products and any other data sets that the City choose to visualize via the platform. Not only will the server give the user the capability to overlay different data types on top of each other (i.e., ocean currents on top of satellite imagery) it will significantly enhance the information experience providing easy, near real-time access to the many data products delivered as part of this project.

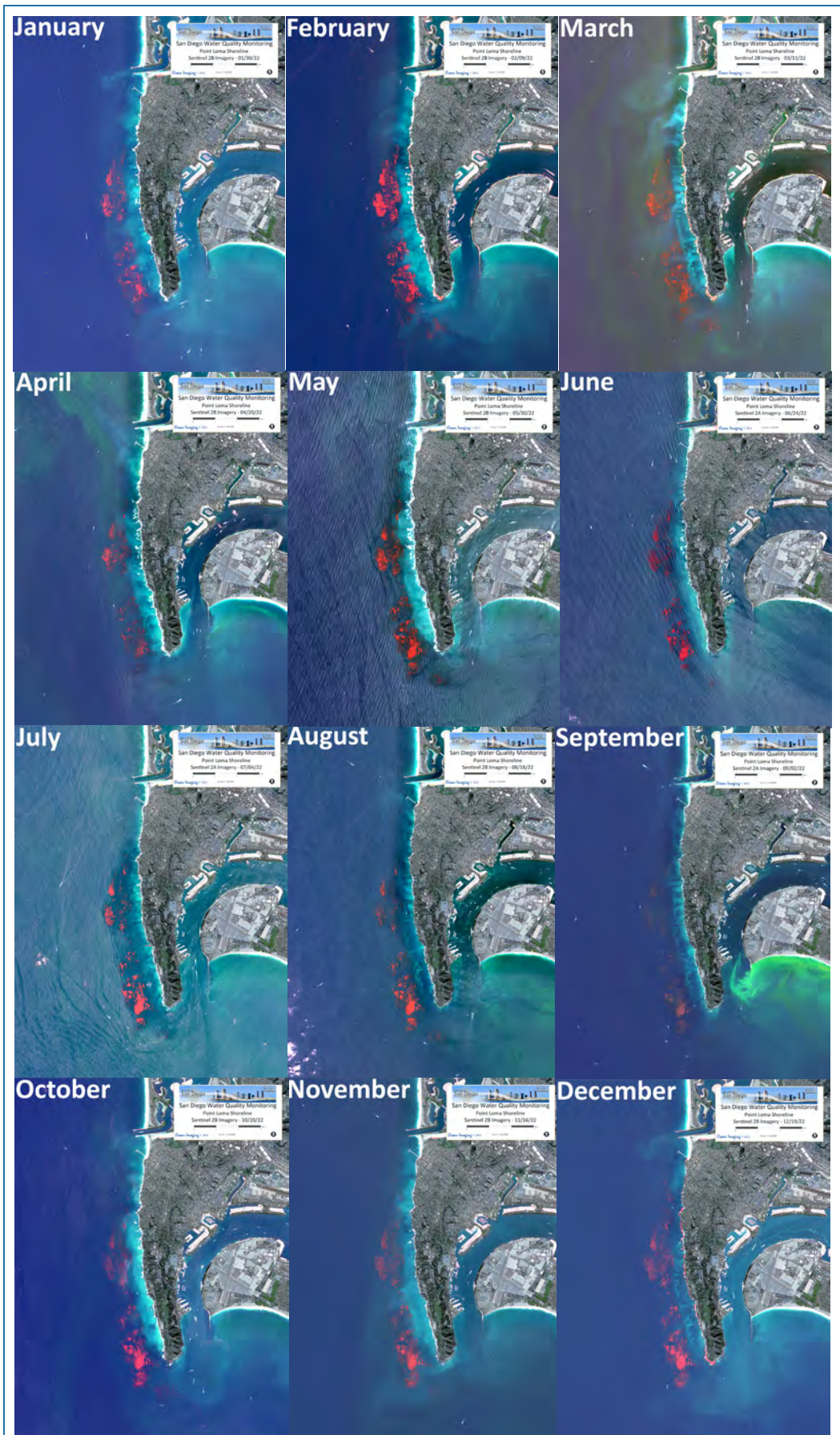


Figure 18. Sentinel 2 satellite imagery documenting the month-to-month variability in the Point Loma kelp bed canopy coverage. The dates were chosen to best represent the maximum-observed canopy coverage for each month.

As part of this process, the historical imagery, data, and reports will remain accessible via the existing web portal. If a more capable web server comes online, OI will progressively work backwards in time to make all historical data available via the City's online WMS, including the archived HYCOM data products.

In the interim this past year, OI updated the project's existing web site to better present the various data products and increase end user interaction. Figures 19a and 19b provide examples of the new look. The upgrades to the site are intended to give the visitor quick, "at a glance" access to thumbnail images for a particular monitoring region from the most recent 10 days in an interactive carousel-style gallery. Clicking on a thumbnail image will open a page with access to the matching month and imaging region. The new site also reduces excessive text links for the older data sets and provides one-click access to the data archive

pages. If implemented, the new, dashboard style site will include some of the aspects of this design but add different data types to the front page 'dashboard' and include the interactive WMS component allowing the overlay and comparative analysis of different oceanographic and biological data types.

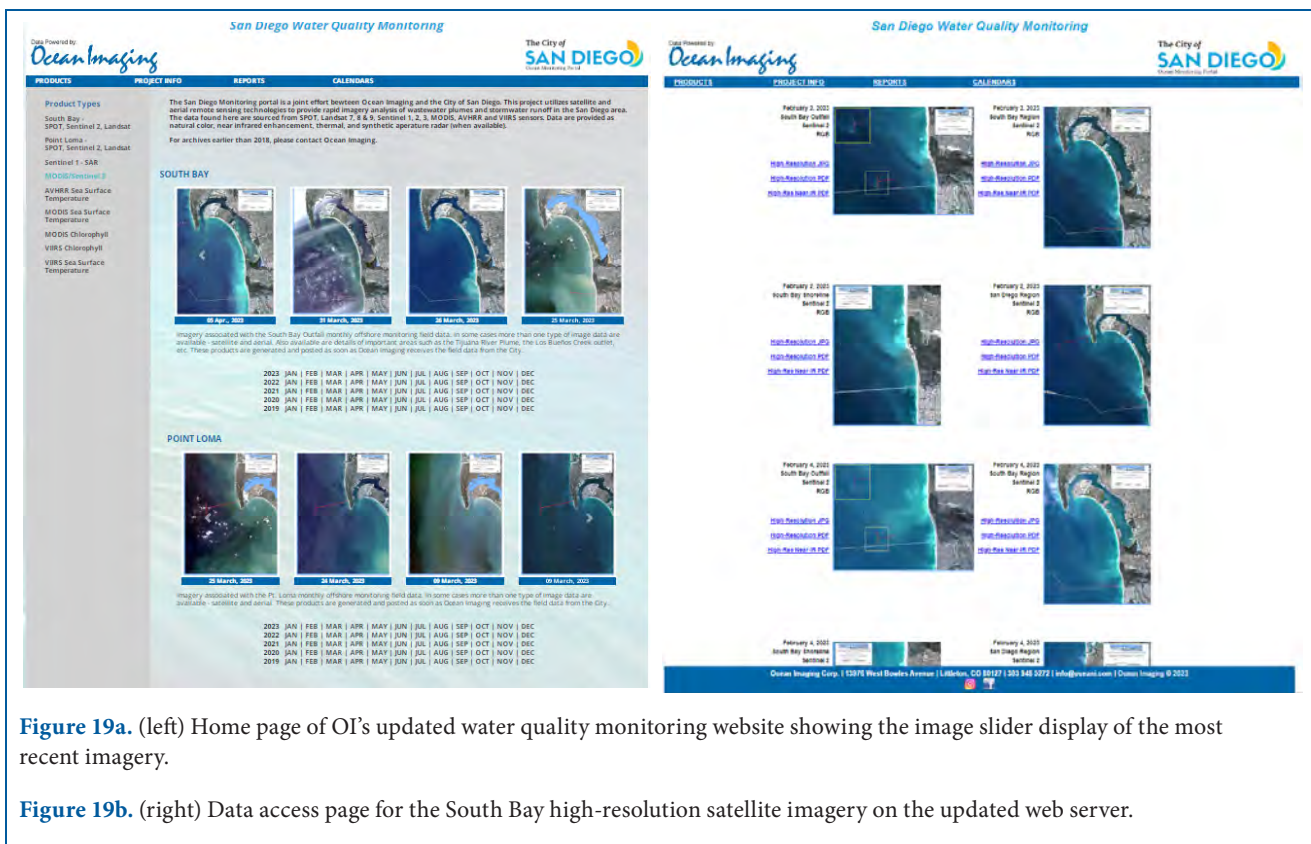


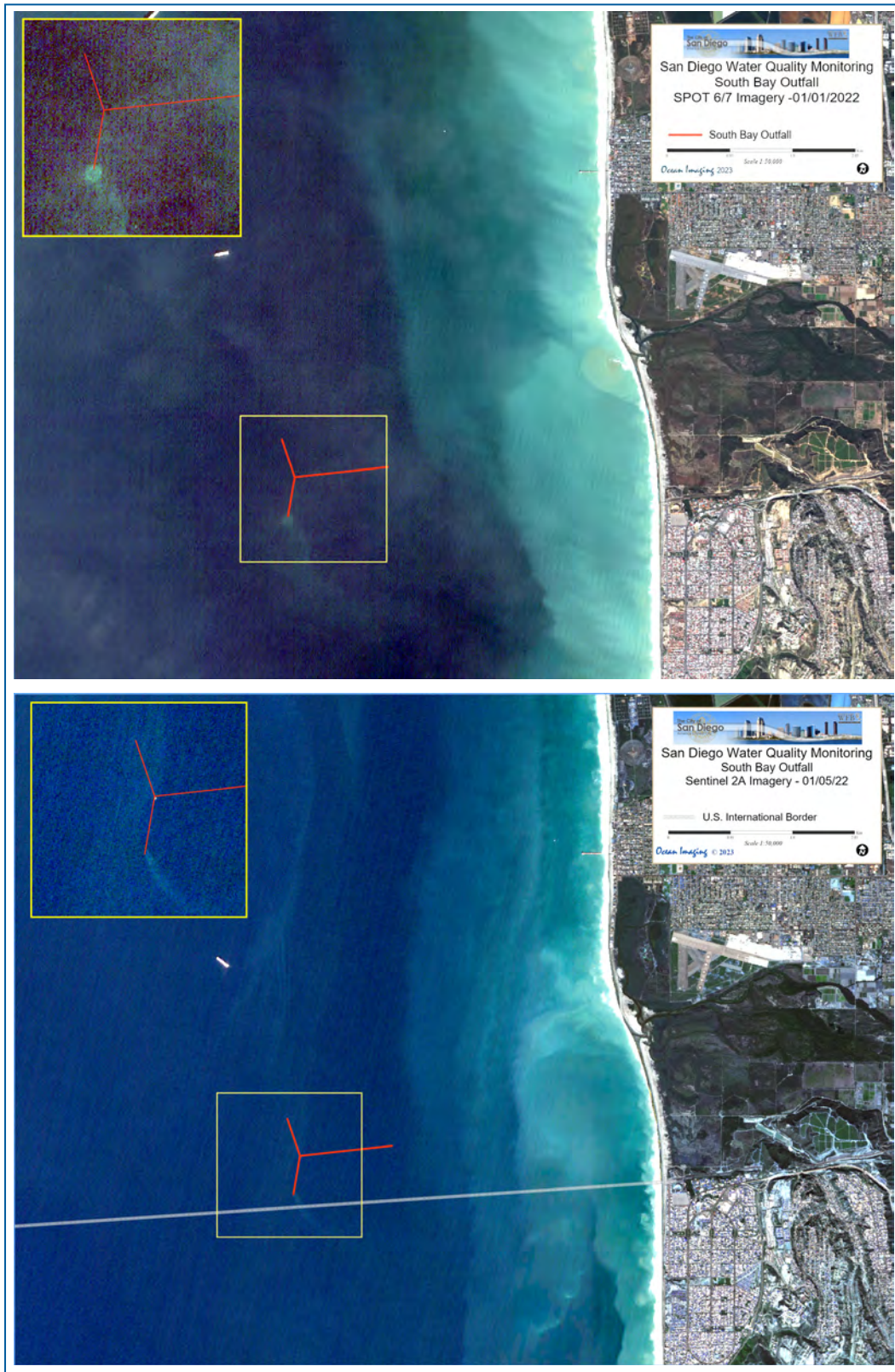
Figure 19a. (left) Home page of OI's updated water quality monitoring website showing the image slider display of the most recent imagery.

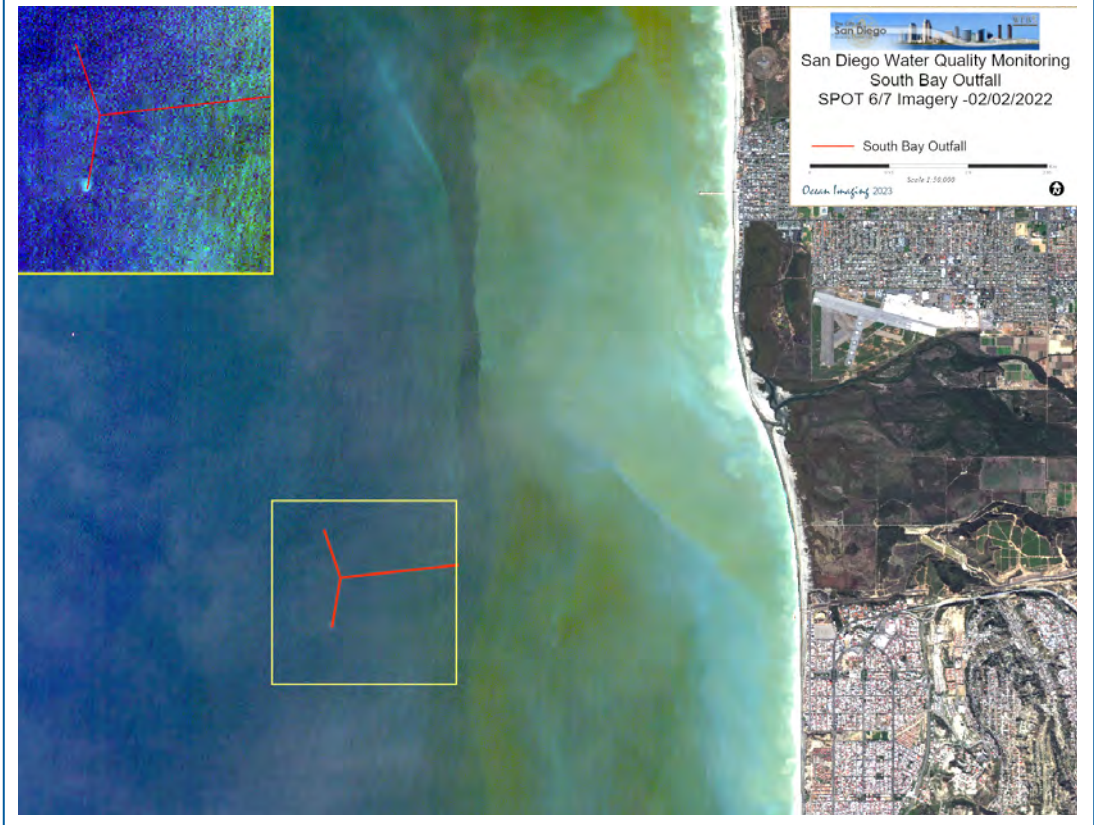
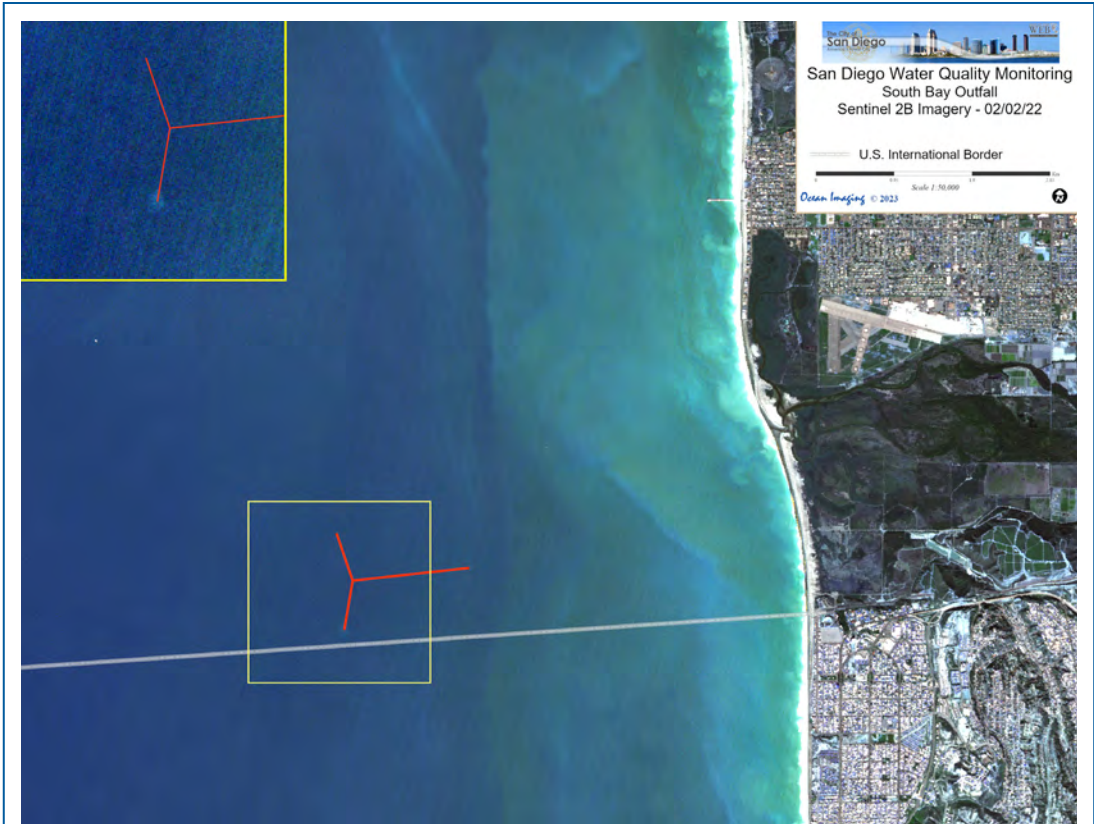
Figure 19b. (right) Data access page for the South Bay high-resolution satellite imagery on the updated web server.

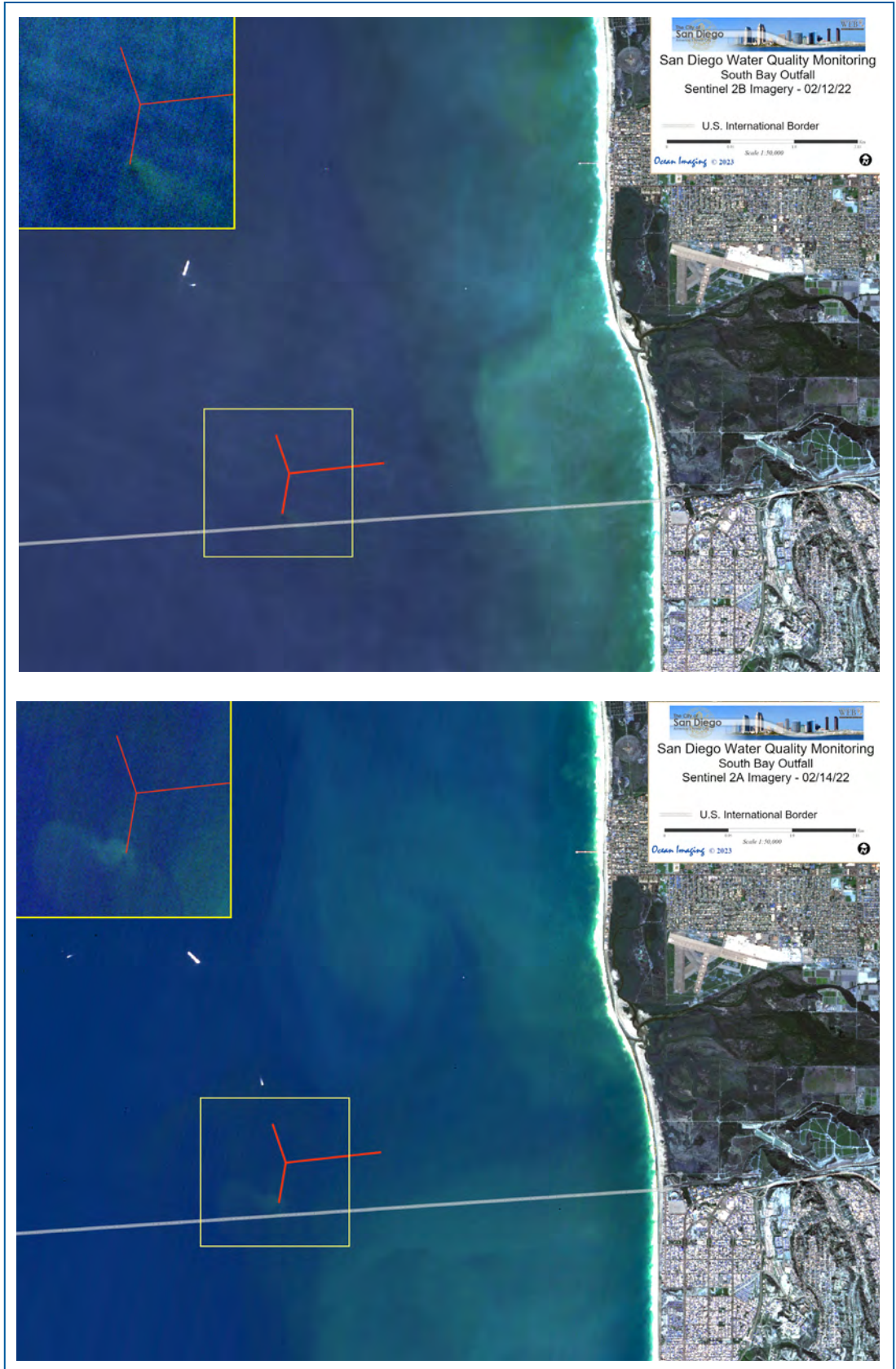
5. REFERENCES

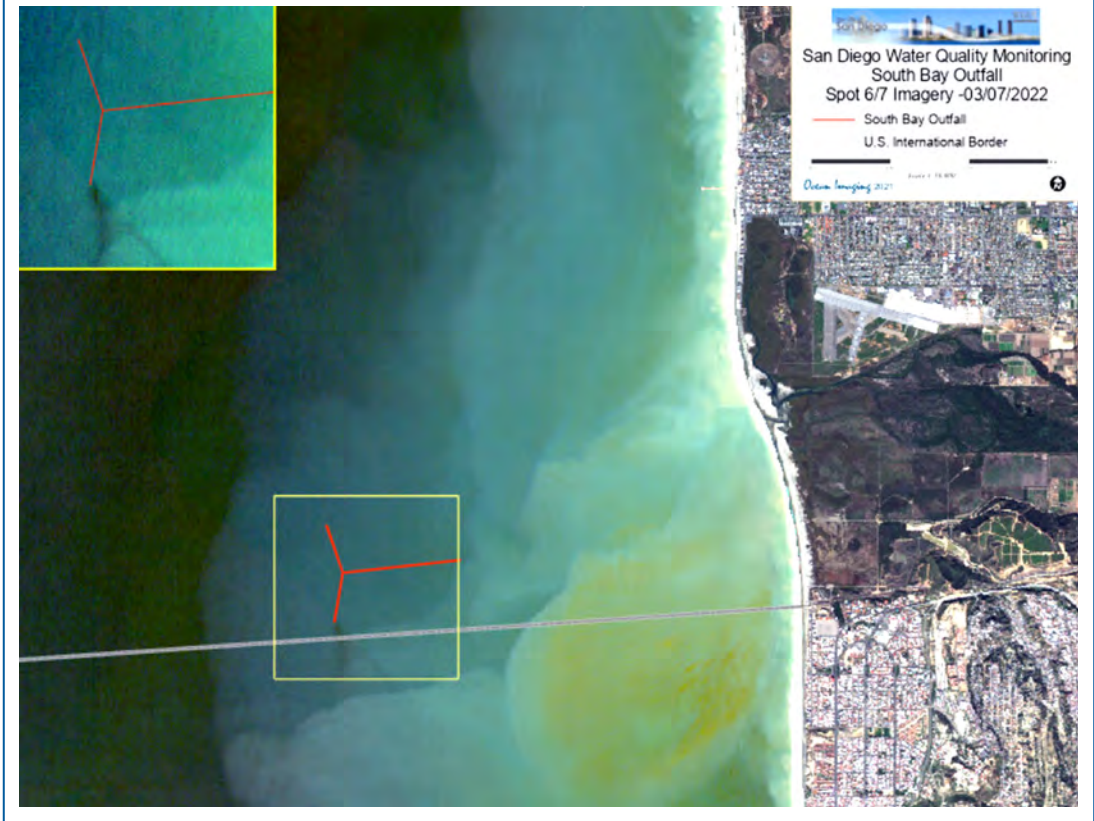
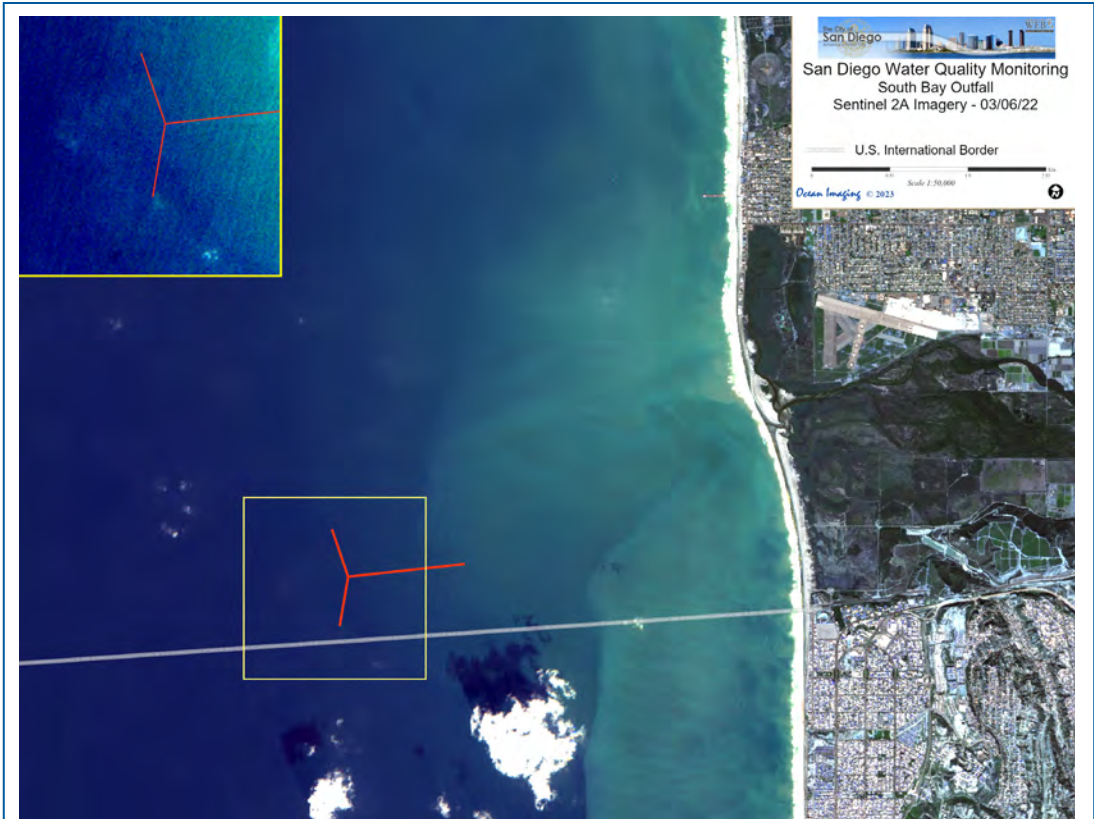
- [APHA] American Public Health Association. (2012). Standard Methods for the Examination of Water and Wastewater, 22nd edition. American Public Health Association, American Water Works Association, and Water Environment Federation.
- Bell, Tom W., et al. “Three Decades of Variability in California’s Giant Kelp Forests from the Landsat Satellites.” *Remote Sensing of Environment*, vol. 238, 2020, p. 110811., doi:10.1016/j.rse.2018.06.039.
- Bordner, R., Winter, J., Scarpino, P., eds. 1978. Microbiological Methods for Monitoring the Environment: Water and Wastes, EPA Research and Development, EPA-600/8-78-017.
- [CDPH] California State Department of Public Health website. (2019). Regulations for Public Beaches and Ocean Water-Contact Sports Areas. Appendix A: Assembly Bill 411, Statutes of 1997, Chapter 765. <https://www.cdph.ca.gov/Programs/CEH/DRSEM/Pages/EMB/RecreationalHealth/Beaches-and-Recreational-Waters.aspx>
- Di Lorenzo, E., Mantua, N. Multi-year persistence of the 2014/15 North Pacific marine heatwave. *Nature Clim Change* 6, 1042–1047 (2016). <https://doi.org/10.1038/nclimate3082>
- Gierach, M. M., Holt, B., Trinh, R., Pan, B.J., Rains, C., 2017. Satellite detection of wastewater diversion plumes in Southern California. *Estuarine, Coastal and Shelf Science*, 186, 171 – 182.
- Schroeder, Sarah B., et al. “Passive Remote Sensing Technology for Mapping Bull Kelp (NEREOCYSTIS Luetkeana): A Review of Techniques and Regional Case Study.” *Global Ecology and Conservation*, vol. 19, 2019, doi:10.1016/j.gecco.2019.e00683.
- San Diego Regional Water Quality Control Board, 2022. “International Boundary and Water Commission Transboundary Flow Reports.” *International Boundary and Water Commission Spill Reports | San Diego Regional Water Quality Control Board*, https://www.waterboards.ca.gov/sandiego/water_issues/programs/tijuana_river_valley_strategy/spill_report.html.
- Southern California Coastal Water Research Project, 10 May 2019, “Harmful Algal Blooms.” <https://www.sccwrp.org/about/research-areas/eutrophication/harmful-algal-blooms/>.
- Svejkovsky, J., Haydock, I., 1998. Satellite remote sensing as part of an ocean outfall environmental monitoring program. In: *Taking a Look at California’s Ocean Resources: An Agenda for the Future*, ASCE, Reston, VA (USA), 2, 1306.
- Svejkovsky, J., Jones, B., 2001. Satellite Imagery Detects Coastal Stormwater and Sewage Runoff. *EOS-Trans. American Geophys. Union*, 82(50).
- Svejkovsky, J., Shandley, J., 2001. Detection of offshore plankton blooms with AVHRR and SAR imagery. *Int. J. of Remote Sensing*, 22 (2&3), 471-485.
- [SWRCB] California State Water Resources Control Board. (2015). California Ocean Plan, Water Quality Control Plan, Ocean Waters of California. California Environmental Protection Agency, Sacramento, CA.
- [SWRCB] California State Water Resources Control Board. (2019). California Ocean Plan, Water Quality Control Plan, Ocean Waters of California. California Environmental Protection Agency, Sacramento, CA.
- [USEPA] United States Environmental Protection Agency. (2014). Method 1600: *Enterococci* in Water by Membrane Filtration Using membrane-*Enterococcus* Indoxyl-β-D-Glucoside Agar (mEI). EPA Document EPA-821-R-14-011. Office of Water (4303T), Washington, DC.

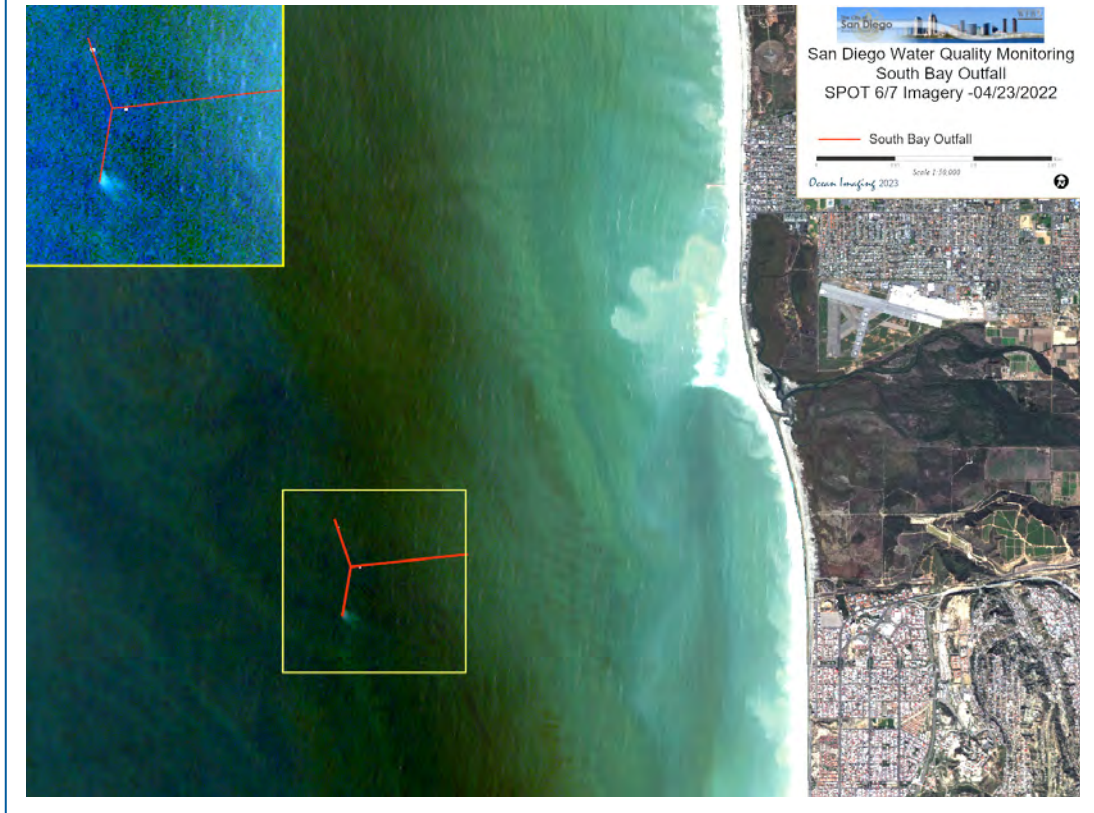
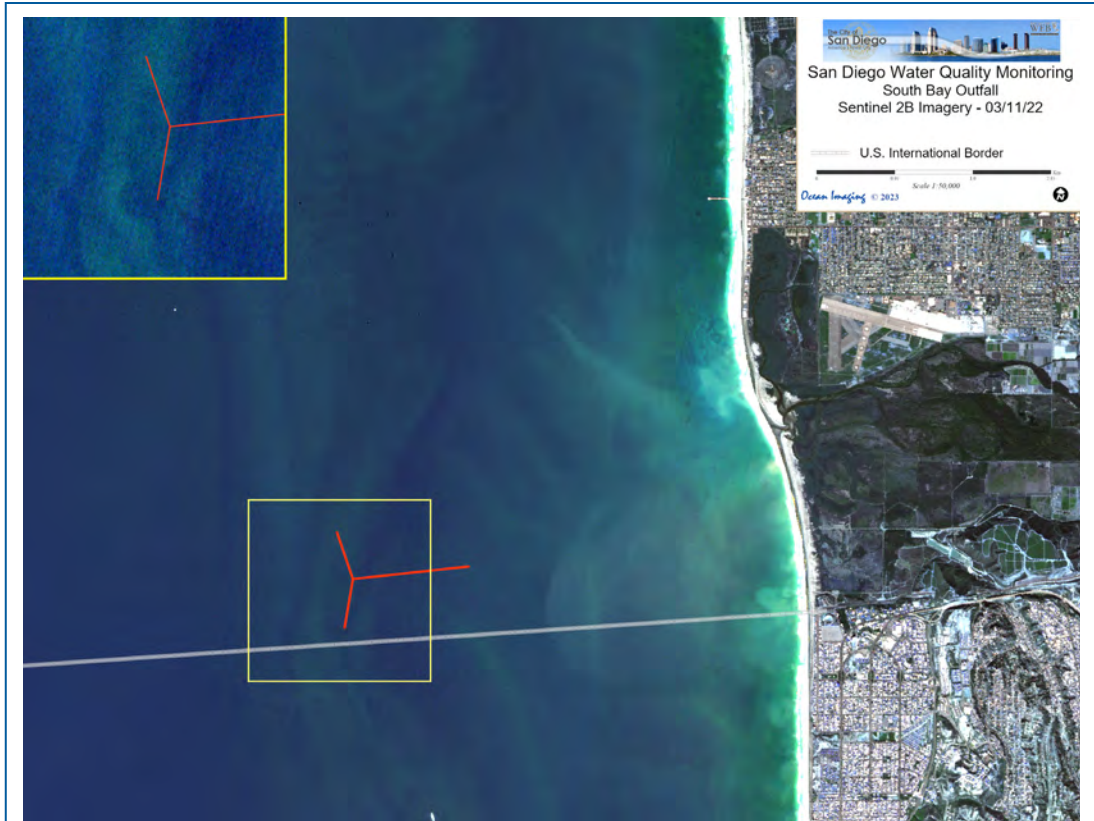
APPENDIX A – HIGH RESOLUTION SATELLITE IMAGERY SHOWING SBOO-RELATED WASTEWATER PLUME

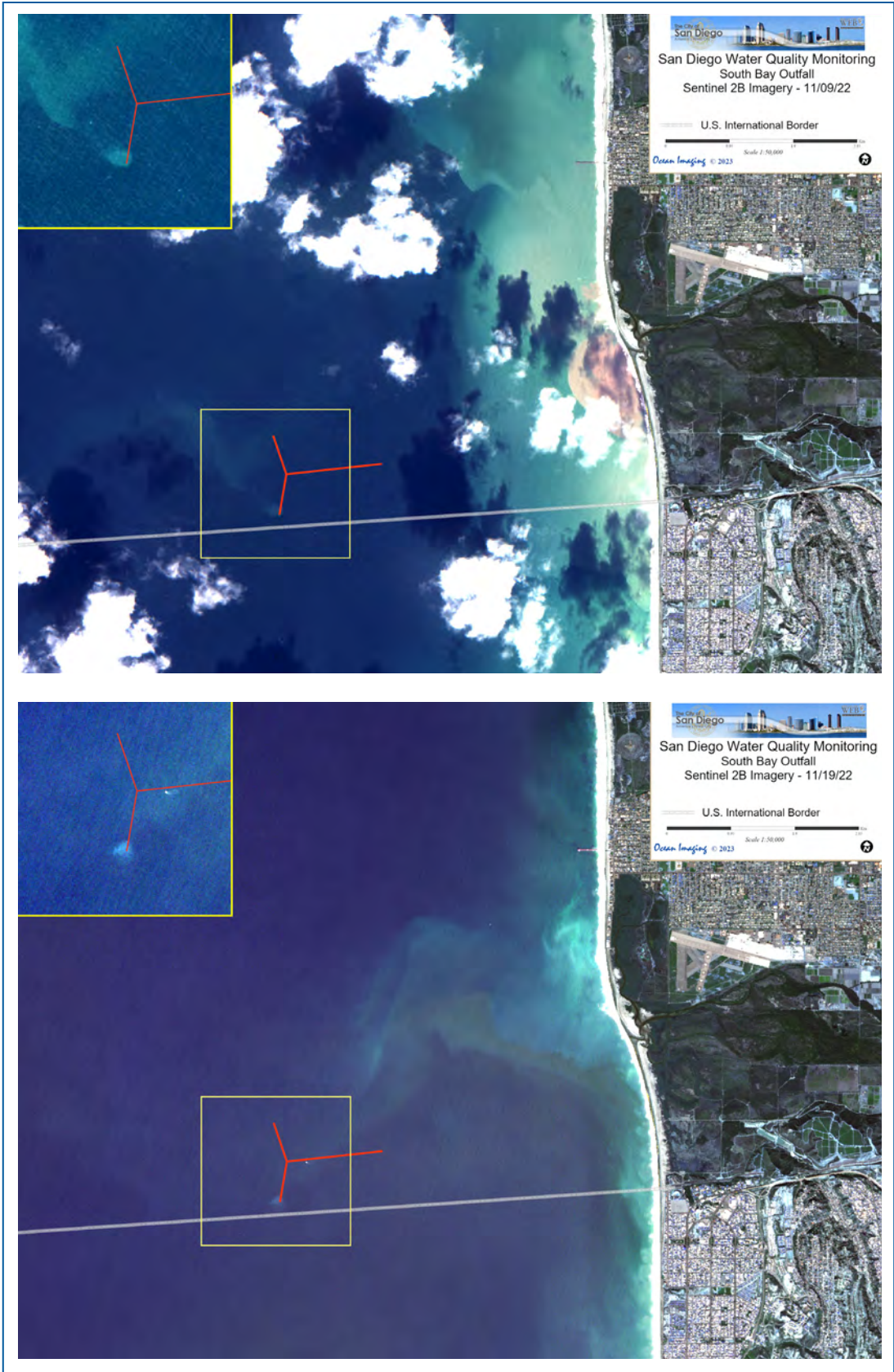


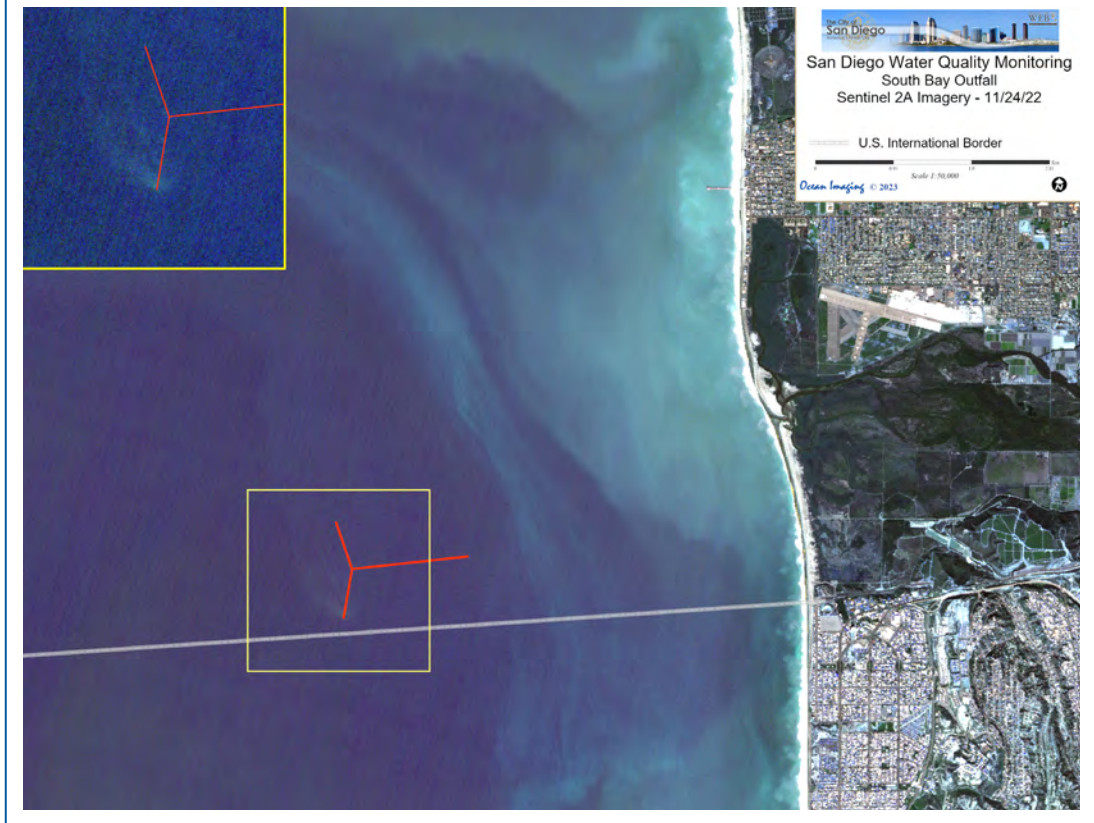
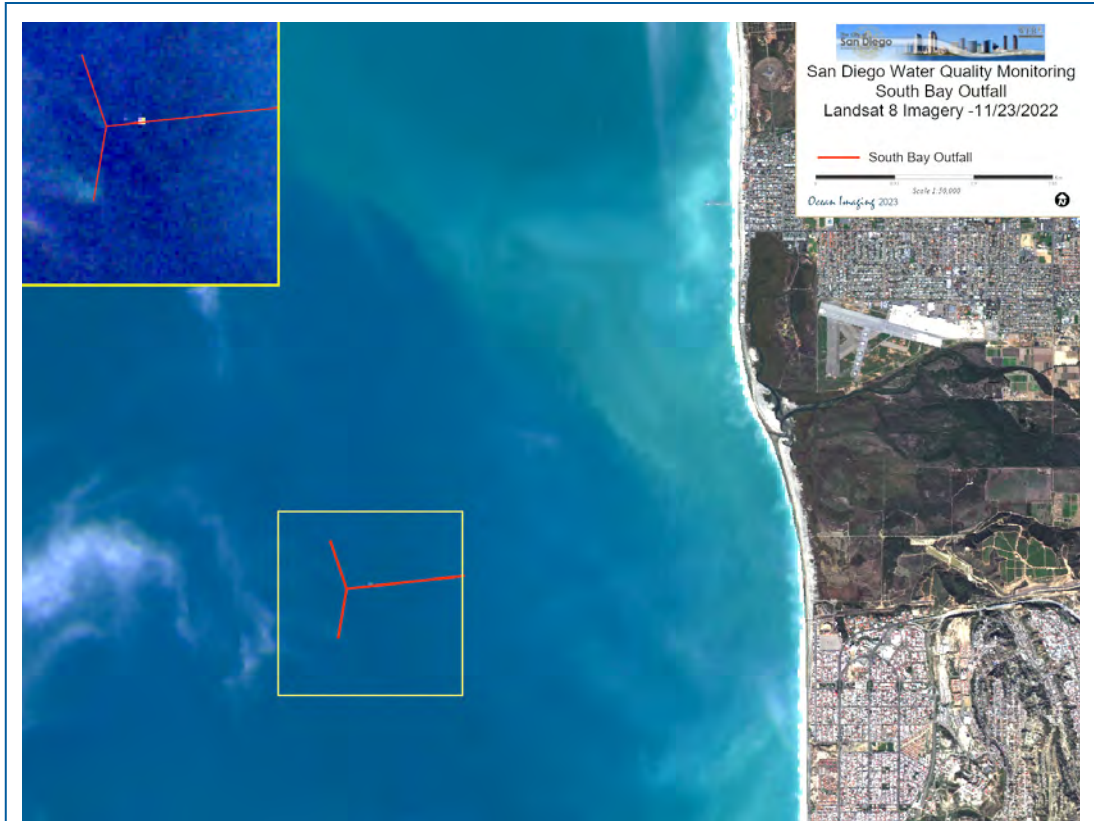


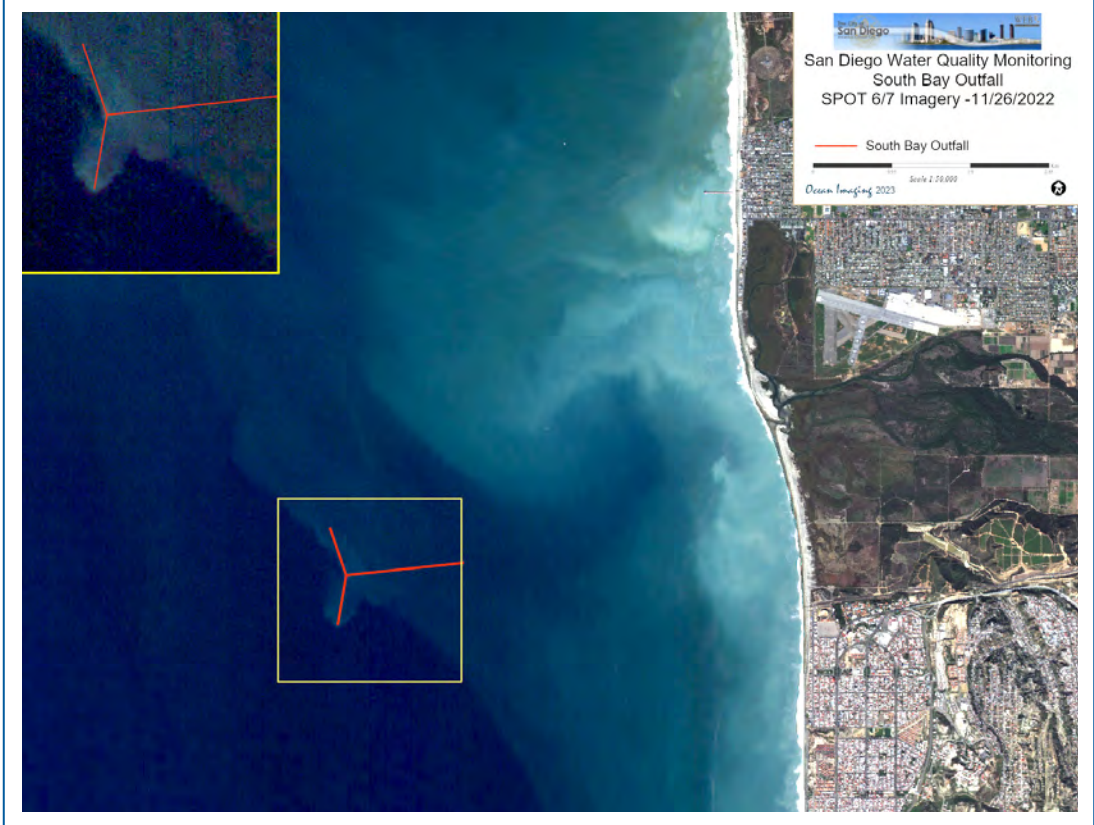
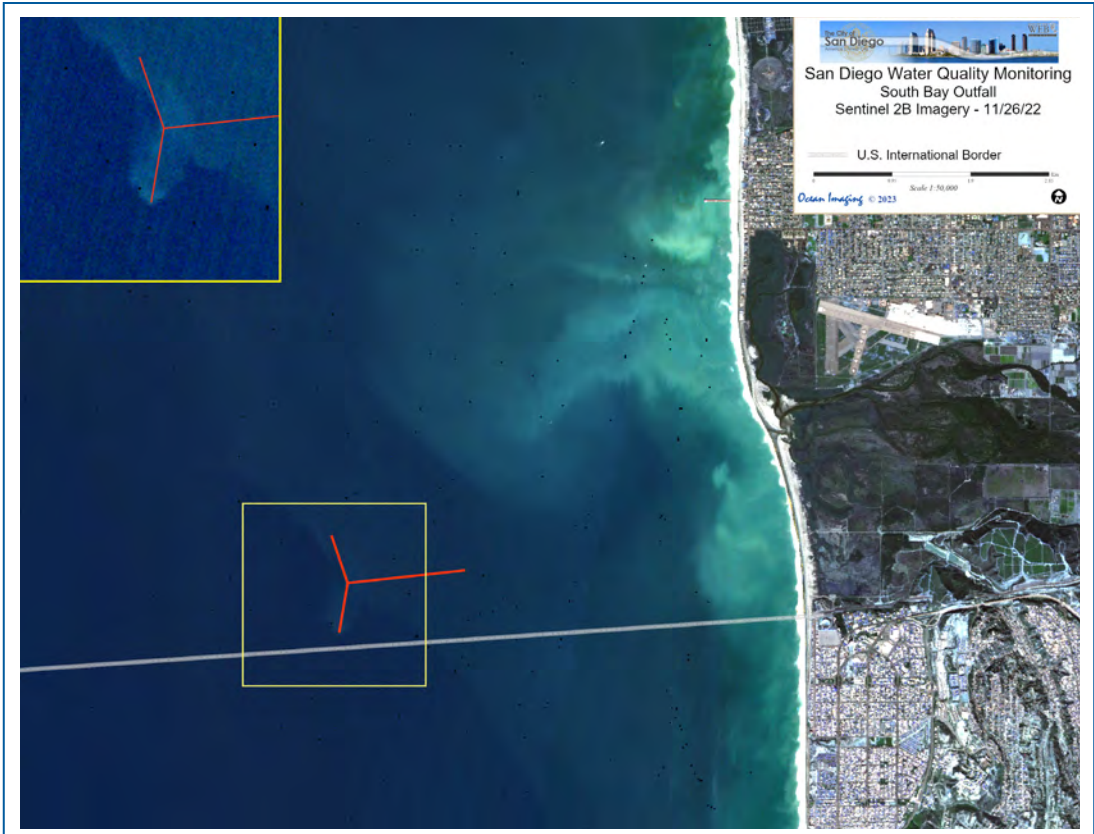


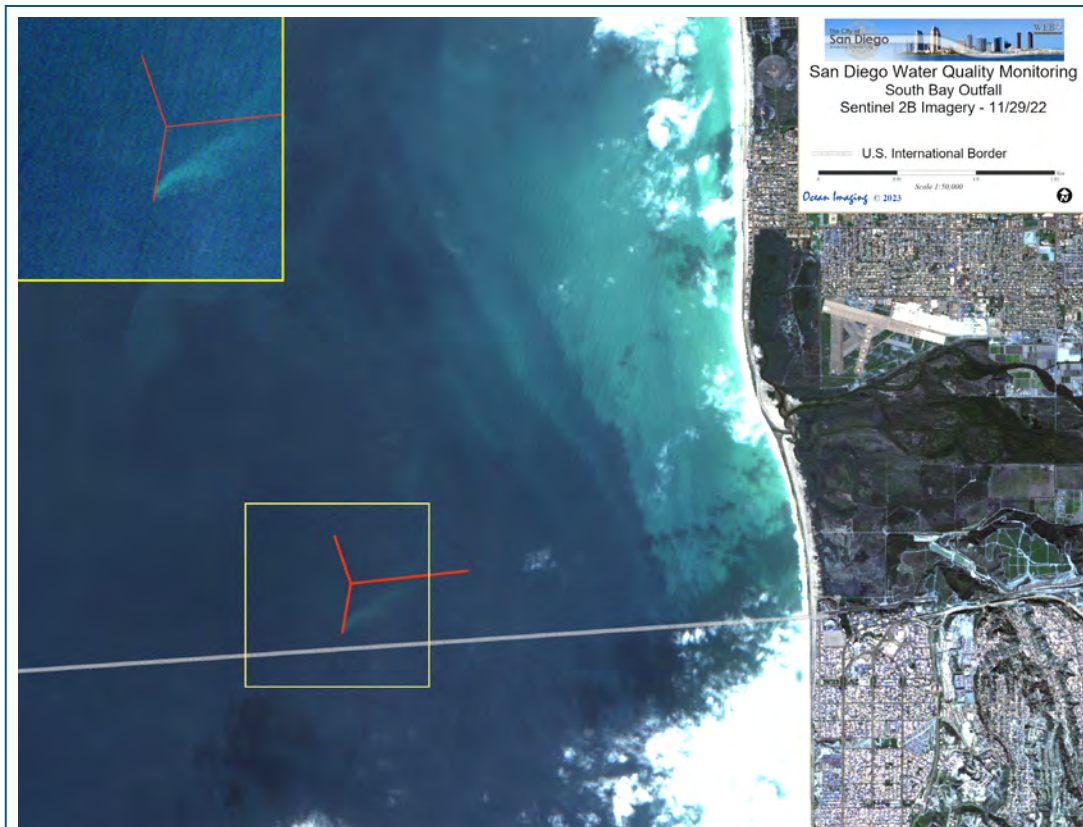


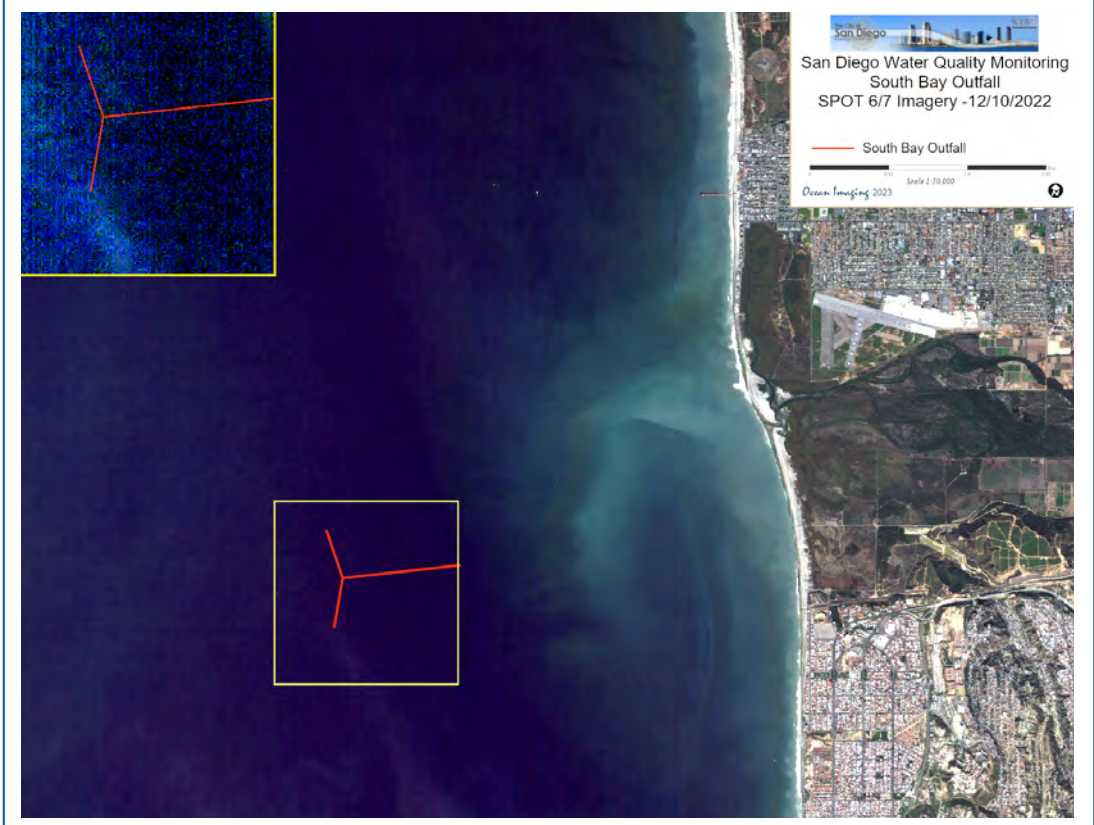
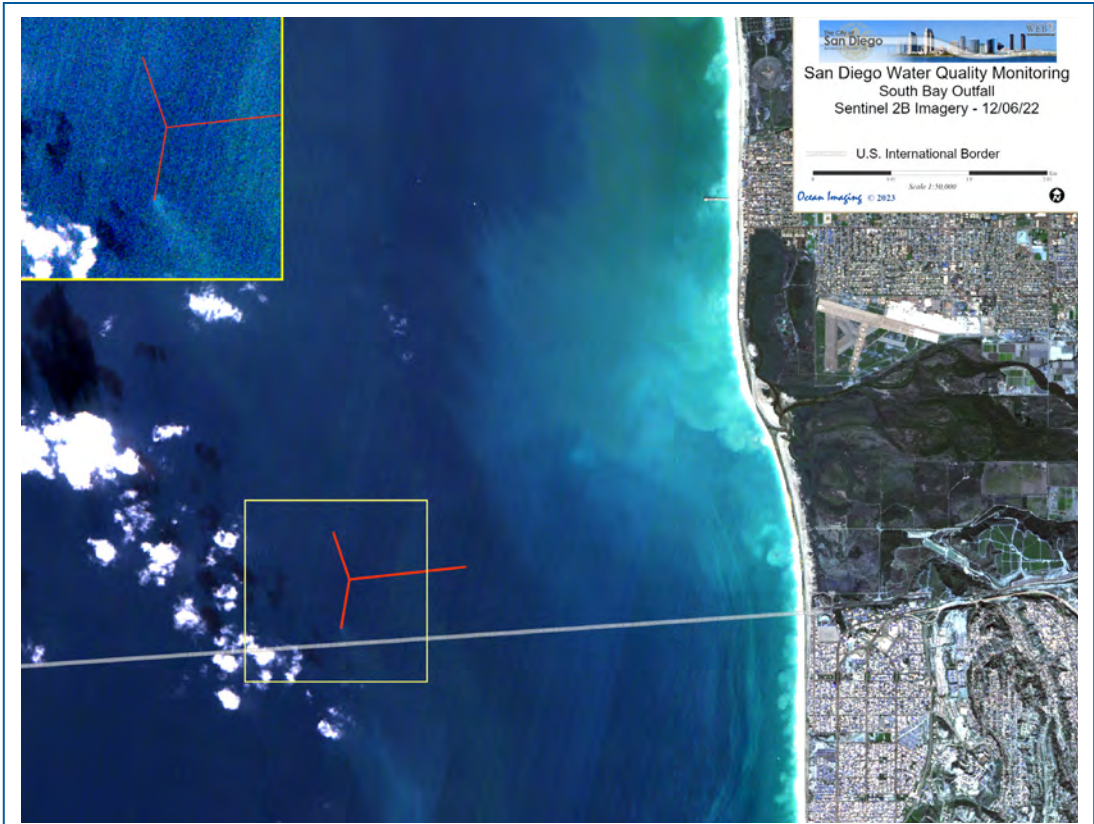


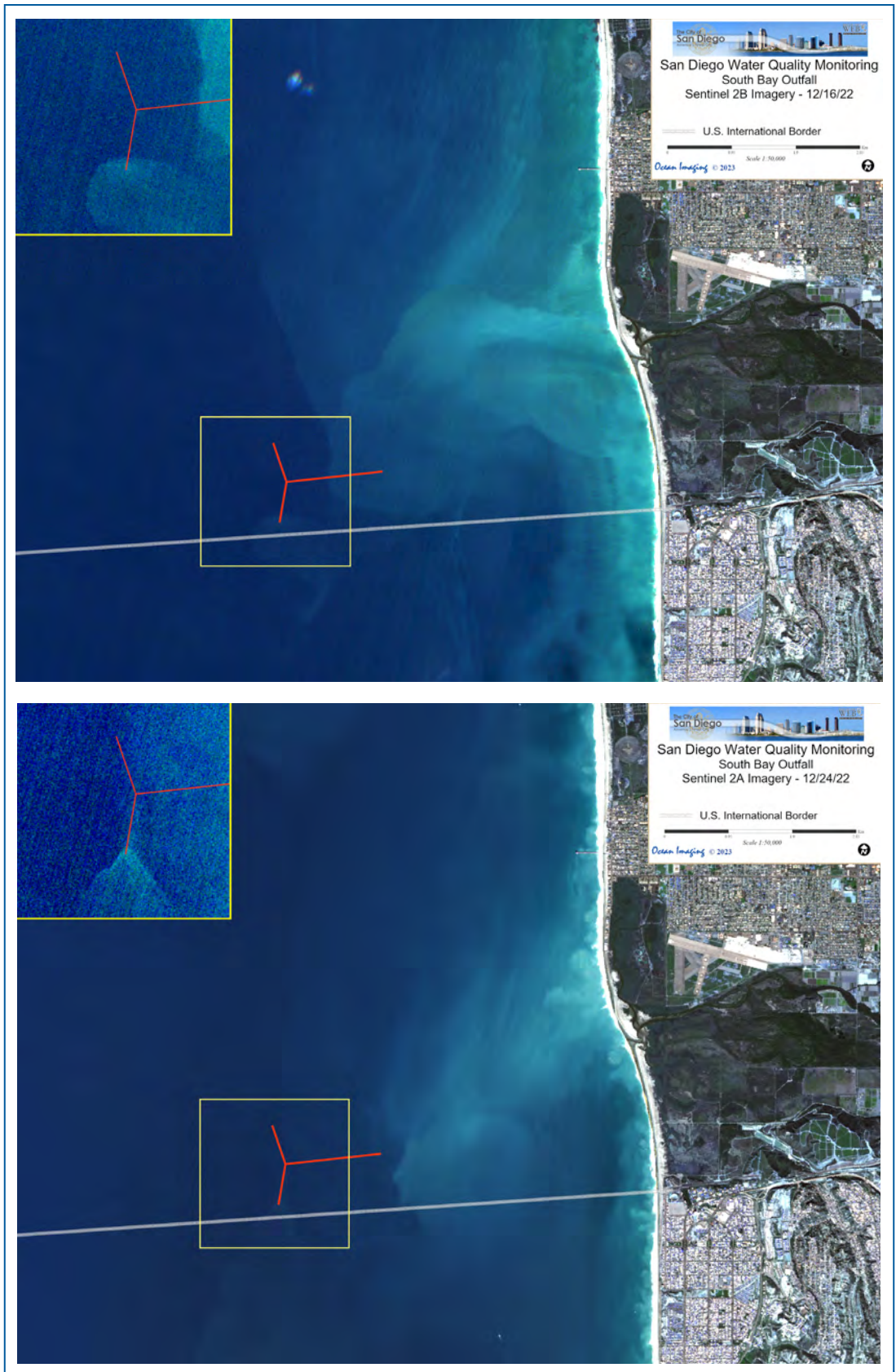






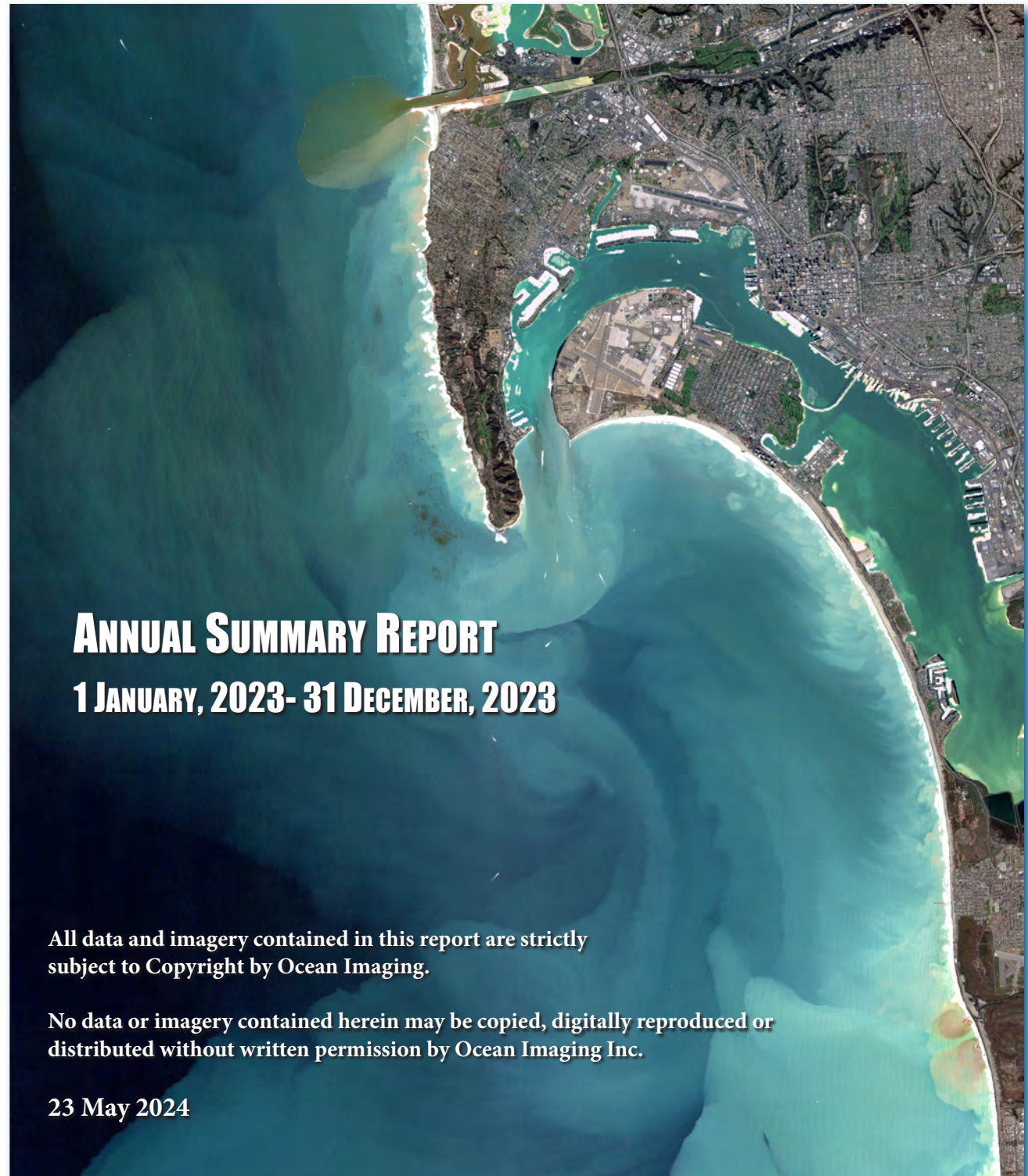






SATELLITE & AERIAL COASTAL WATER QUALITY MONITORING IN THE SAN DIEGO / TIJUANA REGION

By Mark Hess



ANNUAL SUMMARY REPORT 1 JANUARY, 2023- 31 DECEMBER, 2023

All data and imagery contained in this report are strictly subject to Copyright by Ocean Imaging.

No data or imagery contained herein may be copied, digitally reproduced or distributed without written permission by Ocean Imaging Inc.

23 May 2024

Ocean Imaging

TABLE OF CONTENTS

- 1. INTRODUCTION AND PROJECT HISTORY 1
- 2. METHODS AND TECHNOLOGY OVERVIEW 2
 - 2.1 Imaging in the UV-Visible-Near Infrared Spectrum 2
 - 2.2 Imaging in the Thermal Infrared Spectrum 2
 - 2.3 Satellites and Sensors Utilized 2
 - 2.4 Data Dissemination and Analysis 9
- 3. HIGHLIGHTS OF 2023 MONITORING..... 9
 - 3.1 Atmospheric and Ocean Conditions 9
 - 3.2 The South Bay Ocean Outfall Region 23
 - 3.3 The Point Loma Outfall Region 29
 - 3.4 Kelp Variability 31
- 4. PRESENT AND FUTURE ENHANCEMENTS OF THE PROJECT 35
- 5. REFERENCES 36
- APPENDIX A – HIGH RESOLUTION SATELLITE IMAGERY SHOWING SBOO-RELATED WASTEWATER PLUME..... 37**

1. INTRODUCTION AND PROJECT HISTORY

In the 1990s, Ocean Imaging Corporation (OI) received multiple research grants from NASA's Commercial Remote Sensing Program for the development and commercialization of remote sensing applications in the coastal zone. As part of these projects, OI developed methods to utilize various types of remotely sensed data for the detection and monitoring of stormwater runoff and wastewater discharges from offshore outfalls. The methodology was initially demonstrated with collaboration of the Orange County Sanitation District in California (Svejkovsky and Haydock, 1998). The NASA-supported research led to a proof-of-concept demonstration project in the San Diego, California region co-funded by the EPA in 2000. Those results led, in 2002, to adding an operational remote sensing-based monitoring component to the San Diego region's established water quality monitoring program. The project continues as a joint effort between the Ocean Monitoring Program of the City of San Diego's Public Utilities Department (SDPUD) and the International Boundary and Water Commission (IBWC).

The first phase of the project was a historical study utilizing several types of satellite data acquired between the early 1980s and 2002. The study established the prevailing near-surface current patterns in the region under various oceanic and atmospheric conditions. The current directions were deduced from patterns of turbidity, ocean temperature and surfactant slicks. In some cases, near-surface current velocity could be computed by tracking recognizable color or thermal features in time-sequential images. The historical study thus established baseline data for the region's current patterns, their persistence, their frequency, and the historical locations, size and dispersion trajectories of various land and offshore discharge sources from Publicly Owned Treatment Works (POTW) (e.g., the offshore outfalls, Tijuana River, Punta Bandera Treatment Plant discharge in Mexico, etc.).

The prime objectives of the project have expanded somewhat since its inception. Initially, emphasis was on utilizing the image data to discern and monitor surface and near-surface signatures from the South Bay Ocean Outfall (SBOO) and Point Loma Ocean Outfall (PLOO), separate them from other nearshore point and non-point runoff features, and monitor their locations, extents, and potential impact on the shoreline. Prior to this project, the spatial extents of the plumes could only be estimated from a relatively sparse spatial grid of field samples, which made it difficult to separate, for example, the SBOO near surface plume from the Tijuana River runoff plume. This ambiguity made it difficult, in turn, to objectively evaluate the potential contribution, if any, of the SBOO plume to beach contamination along the nearby shoreline. The satellite and aerial imagery helped directly establish the dispersal trajectories of the SBOO effluent during months when it reaches the near-surface layer and support the claim that it likely never reaches the surf zone.

In October 2002, the operational monitoring phase of the project was initiated using the variety of satellite- and model-derived datasets discussed below. Over the past five to ten years, the project's objectives have broadened from focusing primarily on the outfalls to also provide larger-scale, regional observations of the physical and biological patterns and processes affecting the San Diego County and Tijuana River discharge regions. It is this broader-view perspective that led to the creation of supplementary image products from additional sensors and sources for the SDPUD.

This report summarizes observations made during the period 1/1/2023 – 12/31/2023.

2. METHODS AND TECHNOLOGY OVERVIEW

OI uses several remote sensing technologies to monitor San Diego's offshore outfalls and shoreline water quality. Their main principle is to reveal light reflectance and heat emission patterns that are characteristic of the different discharges, water masses, plankton blooms and suspended sediment loads. Most often this is due to specific substances contained in the effluent but absent in the surrounding water.

2.1 Imaging in the UV-Visible-Near Infrared Spectrum

This is the most common technique used with satellite and aerial images. Wavelengths (colors) within the range of the human eye are most often used but ultraviolet (UV) wavelengths are useful for detecting fluorescence from petroleum compounds (oil, diesel, etc.) and near-infrared (near-IR) wavelengths can be useful for correcting atmospheric interference from aerosols (e.g., smog and smoke). Near-IR wavelengths are also highly reflected from kelp seaweeds, so such data are particularly useful for delineating the region's kelp beds and monitoring their extents through time.

The best detection capabilities are attained when several images in different wavelengths are acquired simultaneously. These "multispectral" data can be digitally processed to enhance features not readily visible in simple color photographs. For example, two such images can be ratioed, thus emphasizing the water features' differences in reflection of the two specific wavelengths. A multi-wavelength image set can also be analyzed with multispectral classification algorithms which separate distinctive features or effluents based on the correlation relationships between the different color signals.

The depth to which the color sensors can penetrate depends on which wavelengths they see, their sensitivity and the general water clarity. In the San Diego region, green wavelengths tend to reach the deepest and UV and near-IR wave-lengths penetrate

the least. Generally, OI's satellite and aerial sensor data reveal reflective features in the upper one to fifteen meters of the ocean.

2.2 Imaging in the Thermal Infrared Spectrum

Some satellite and aerial sensors image heat emanating from the ground and the ocean. They thus reveal patterns and features due to their differences in temperature. Since thermal infrared (TIR) wavelengths are strongly absorbed by water, the images reveal temperature patterns only on the water's surface. Such images can help detect runoff plumes when their temperatures differ from the surrounding ocean water. Runoff from shoreline sources tends to be warmer than ocean water, although the reverse can be true during the winter. Plumes from offshore outfalls can sometimes also be detected with thermal imaging. Since the effluent contains mostly fresh water, it is less dense than the surrounding salt water and tends to rise towards the surface. How far it rises depends on outfall depth, ocean currents, and stratification conditions. If it makes it all the way to the surface, it is usually cooler than the surrounding sun-warmed surface water. A plume signature detectable in multispectral color imagery but not detectable in simultaneously collected TIR imagery indicates the rising plume has not reached the actual ocean surface and remains submerged.

2.3 Satellites and Sensors Utilized

Until 2010, the project relied heavily on acquisition of multispectral color imagery with OI's DMSC-MKII aerial sensor and TIR imagery from a Jenoptik thermal imager integrated into the system. These aerial image sets were most often collected at 2m resolution. The flights were done on a semi-regular schedule ranging from one to two times per month during the summer to once or more per week during the rainy season. The flights were also coordinated with the City of San Diego's regular offshore field sampling schedule so that the imagery was collected on the same day (usually within two to three hours) of the field data collection. Additional flights

were performed on an on-call basis immediately after major storms or other events such as sewage spills. In late 2010, OI negotiated a special data collection arrangement with Germany's RapidEye Corporation and this project began utilizing their multispectral imagery in lieu of most of the aerial Digital Multispectral Camera (DMSC) image acquisitions. The use of satellite as opposed to aerial data also enables a more regionally contiguous monitoring of events affecting the target areas. In late 2019 the RapidEye satellite constellation was decommissioned by the current operator Planet Labs. Subsequently, OI secured the regular acquisition of SPOT 6 and SPOT 7 satellite imagery covering the same geographical area beginning in 2020. Tables 1a and 1b list the properties of the remote sensing image sources routinely used during the project.

Beginning in 2017, OI also began processing and posting imagery from the Sentinel-2A satellite. Sentinel-2A is a satellite operated by the European Space Agency (ESA) and is the spaceborne platform for the Multispectral Instrument (MSI). The Sentinel-2A and 2B MSIs sample 13 spectral bands: four bands at 10 meters, six bands at 20 meters and three bands at 60-meter spatial resolution. The green band focusing in the 560 nm wavelength is ideal for detecting turbidity plumes from the outfalls both at the surface and at depths down to 15 meters depending on ocean conditions. The revisit time of the Sentinel-2A satellite is approximately ten days. A second satellite carrying the MSI sensor, the Sentinel-2B, was launched into orbit by the ESA and provided the first set of data from the MSI sensor as of March 17, 2017. Beginning in 2018, data from Sentinel 2B became a regular addition to the satellite imagery products posted to the OI web portal. On average the Sentinel 2A and 2B imagery processed to highlight anomalous turbidity signals emanating from the PLOO, SBOO, as well as the discharge from the Tijuana River (TJR) and San Diego River (SDR) are posted to the OI web portal within 24-36 hours of satellite data acquisition. In some cases, if the data are available to OI earlier, the image products are delivered as quickly as 12 hours post-acquisition. During 2023 the Sentinel 2A and 2B satellites

provided the most temporally comprehensive set of high-resolution satellite imagery. In total, 77 high resolution satellite images showing the offshore San Diego County region were acquired, processed, and delivered in 2023. This equates to a 34% decrease in satellite data used to document the area when compared to 2022 – most probably due to more instances of total cloud cover over the study area. Of the 77 total image sets, 48 were from Sentinel 2A or 2B data making up 62% of the high-resolution satellite data processed and posted as part of the project, a 7% decrease from 2022.

In October 2018, OI began using imagery from Sentinel-3A. Shortly thereafter, in December 2018 imagery from Sentinel-3B was incorporated into the mix of observation platforms. Like Sentinel 2, Sentinel-3A and Sentinel-3B are earth observation satellites developed by the ESA for the Copernicus Program. Sentinel-3A was launched on February 16, 2016, and Sentinel-3B followed on April 25, 2018. The 3A and 3B satellites are identical and deliver products in near-real time. The satellites include four different remote sensing instruments. The Ocean and Land Colour Instrument (OLCI) covers 21 spectral bands (400–1020 nm) with a swath width of 1270 km and a spatial resolution of 300 m. Sea and Land Surface Temperature Instrument covers 9 spectral bands (550–12 000 nm), using a dual-view scan with swath widths of 1420 km (nadir) and 750 km (backwards), at a spatial resolution of 500 m for visible and near-infrared, and 1 km for thermal infrared channels. The Sentinel 3 mission's main objectives are to measure sea surface topography along with the measurement of ocean/land surface temperature and ocean/land surface color. One of the satellites' main secondary missions is to monitor sea-water quality and marine pollution. The instrument on these satellites designed for these purposes is the OLCI. Ocean Imaging creates daily products dependent on cloud cover for the entire San Diego/Tijuana region using the OLCI instrument. Between the 3A and 3B satellites this results in better than daily coverage with 3A and 3B data occasionally both being available on the same day. True color, near infrared, products are

posted bi-monthly along with the similar resolution MODIS products. Possible future products derived from the Sentinel 3 sensors include total suspended matter, chlorophyll, and sea surface temperature as well as cyanobacteria monitoring. Sentinel 3 carries the only satellite sensor package with the necessary spectral bands, spatial resolution, and coverage for near real-time detection of cyanobacteria.

As stated above, the RapidEye satellites were decommissioned in late 2019 and replaced by data from the SPOT 6 and SPOT 7 satellites in January of 2020. The two SPOT satellites/sensors are identical in design and function. They both image in spectral bands similar to the RapidEye satellites at a ground sampling distance of 8.8 meters for the multispectral data (see Tables 1a and 1b). The dynamic range of

these sensors is 12-bits per pixel. OI uses the blue, green, red, and near-infrared bands from these sensors. Empirically we have found that the SPOT data have a high signal to noise ratio and therefore produce a high-quality product for detecting wastewater surface manifestations and delineating the river run-off plumes. In March of 2023, the SPOT 7 satellite stopped functioning, however we continue to receive data from SPOT 6 and are able to acquire roughly two to four clear images per month from this sensor. Figure 1 shows a set of images from 01/18/23, 01/19/23 and 01/20/23 from Landsat 9, SPOT and Sentinel 2 following significant rain events that impacted the region between 01/15/23 and 01/20/23 - highlighting the ability to obtain high-resolution imagery from multiple satellites on the same and successive days. Note the heavy

Table 1a. Satellite sensors utilized in the project and their characteristics.

Sensor	Utilization Period	Resolution (m)	Utilized Wavelength Range
AVHRR	2003 - Present	1100	Channel 4: 10.30 – 11.39 um Channel 5: 11.50 – 12.50 um
MODIS	2003 - Present	250/500/1000	Band 1 (250 m): .620 – .670 um Band 2 (250 m): .841 – .876 um Band 3 (500 m): .459 – .479 um Band 4 (500 m): .545 – .565 um
Landsat TM/ETM+ 4-7	2003 - Present	30 (visible - Near-IR) 60 (Thermal-IR)	Band 1: .450 - .520 um Band 2: .520 - .600 um Band 3: .630 - .690 um Band 4: .760 - .900 um Band 6: 10.40 - 12.50 um (TM5 Thermal not used due to noise)
Landsat 8 OLI, TIRS	2013 - Present	30 (visible - Near-IR) 100 (Thermal-IR)	Band 2: .452 - .512 um Band 3: .533 - .590 um Band 4: .636 - .673 um Band 5: .851 - .879 um Band 10: 10.60 - 11.19 um Band 11: 11.50 - 12.51 um
Sentinel 2A/2B	2017 - Present	10 (visible - Near-IR) 60 (Vegetation Red Edge) 60 (UV, SWIR)	Band 1: .443 um Band 2: .490 um Band 3: .560 um Band 4: .665 um Band 5: .705 um Band 6: .740 um Band 7: .783 um Band 8: .842 um Band 8A: .865 um
Sentinel 3A/3B	2018 - Present	300 (all utilized bands)	Band Oa2: .412.5 um Band Oa3: .442.5 um Band Oa4: .490 um Band Oa5: .510 um Band Oa6: .560 um Band Oa7: .620 um Band Oa8: .665 um Band Oa10: .68125 um Band Oa11: .07875 um Band Oa17: .865 um

discharge from both the TJR and SDR helping to create the turbid offshore waters on the 18th which gradually decreases over the following three-day period. The 25-hour averaged High Frequency Radar-derived (HF Radar) ocean currents computed for a period within one to two hours of the satellite data acquisition have been overlaid on the imagery to help illustrate the surface flow patterns of the various turbidity features. A quick measurement of the movement of ten identifiable turbidity features in the fourteen minutes between the acquisition of the Landsat 9 and Sentinel 2 satellite imagery on the 18th reveals that the water emanating from the river mouths traveled at between roughly 0.4 and 0.5 meters per second (m/s). The offshore currents moved at speeds roughly 0.1 to 0.3 m/s. It should also be noted that the current directions as computed by the feature-tracking method correlate well with the currents derived from the HF Radar system.

As detailed in Tables 1a and 1b, to date, this work utilizes 1100 m resolution Advanced Very High Resolution Radiometer (AVHRR)-derived imagery (available multiple times per day), 1000 m resolution chlorophyll and sea surface temperature (SST) Moderate Resolution Imaging Spectroradiometer (MODIS)-derived imagery (available multiple times per day), 500 m resolution MODIS true color imagery (available near-daily), 750 m resolution Visible Infrared Imaging Radiometer Suite (VIIRS) chlorophyll and SST imagery (available multiple times per day), 300 m resolution Sentinel 3 color and thermal imagery (available daily), 30 m & 60 m Landsat 7 ETM+ and Landsat 8 OLI/TIRS and Landsat 9 OLI-2/TIRS-2 color and thermal imagery (each available approximately every 16 days), 10 m resolution Sentinel 2 multispectral imagery (available 2-4 times per week), and 6m

Table 1b. Satellite sensors utilized in the project and their characteristics.

Sensor	Utilization Period	Resolution (m)	Utilized Wavelength Range
VIIRS	2019 - Present	750 (all utilized bands)	Band M1: 0.402 - 0.422 um Band M2: 0.436 - 0.454 um Band M3: 0.478 - 0.488 um Band M4: 0.545 - 0.565 um Band M5: 0.662 - 0.682 um Band M6: 0.739 - 0.754 um Band M7: 0.846 - 0.885 um Band M8: 1.23 - 1.25 um Band M9: 1.371 - 1.386 um Band M10: 1.58 - 1.64 um Band M11: 2.23 - 2.28 um Band M12: 3.61 - 3.79 um Band M13: 3.97 - 4.13 um Band M14: 8.4 - 8.7 um Band M15: 10.26 - 11.26 um Band M16: 11.54 - 12.49 um
SPOT 6	2019 - Present	6	Band 1: .450 - .745 um Band 2: .450 - .525 um Band 3: .530 - .590 um Band 4: .625 - .695 um Band 5: .760 - .890 um
SPOT 7	2019 - 2023	6	Band 1: .450 - .745 um Band 2: .450 - .525 um Band 3: .530 - .590 um Band 4: .625 - .695 um Band 5: .760 - .890 um
Sentinel 1A SAR	2021 - Present	5 x 20	C-band operating at a center frequency of 5.405 GHz
Landsat 9 OLI-2, TIRS-2	Late 2021 - Present	30 (visible - Near-IR) 100 (Thermal-IR)	Band 2: .452 - .512 um Band 3: .533 - .590 um Band 4: .636 - .673 um Band 5: .851 - .879 um Band 10: 10.60 - 11.19 um Band 11: 11.50 - 12.51 um

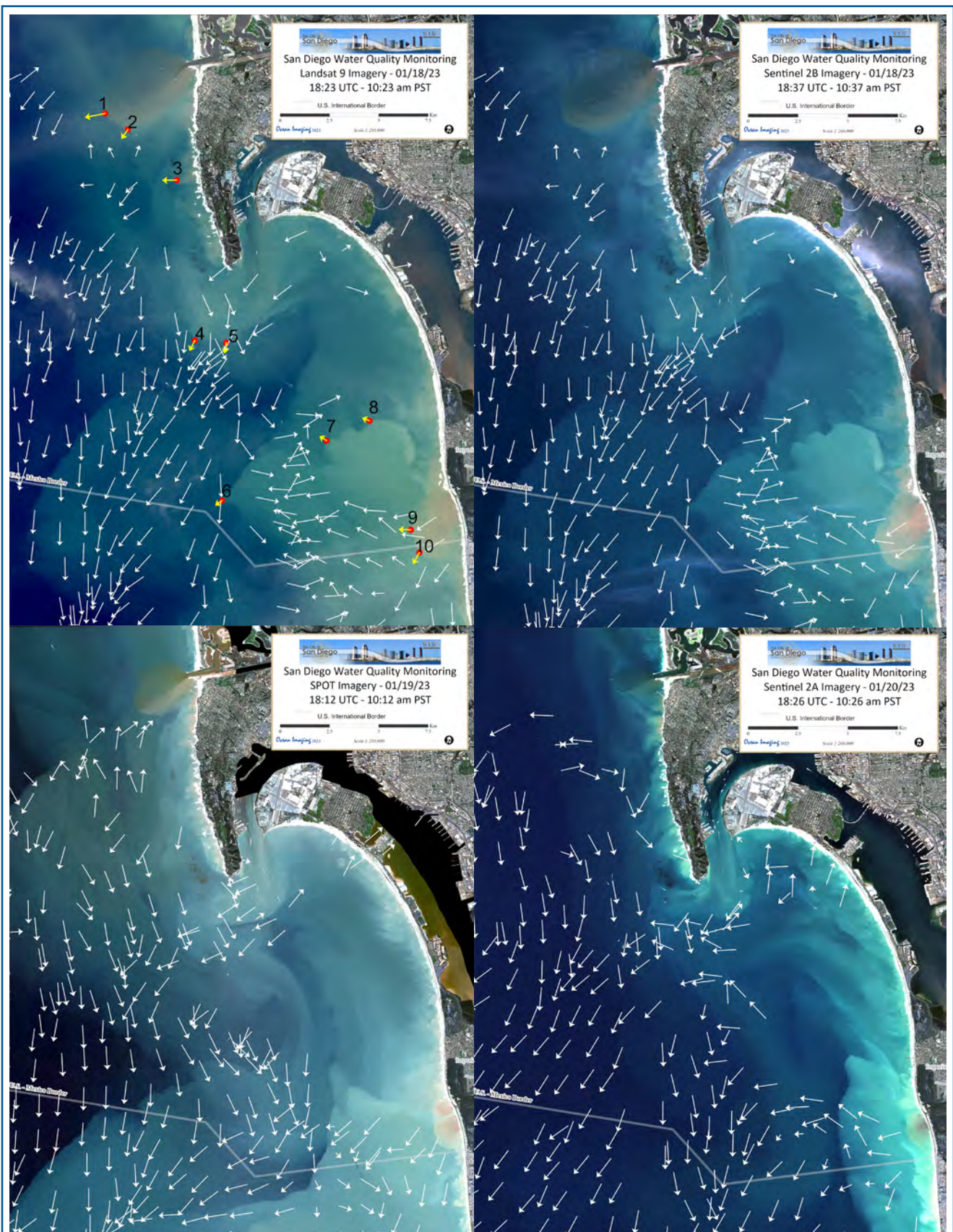


Figure 1. Landsat 9, Sentinel 2, and SPOT 6 high resolution satellite imagery from 01/18/23 to 01/20/23 with HF Radar-derived ocean currents overlaid. The top two scenes were acquired fourteen minutes apart by the Landsat 9 and Sentinel 2 satellite platforms. The top left image shows vectors (yellow) computed by tracking identifiable turbidity features in both 01/18 images and computing the distance between the successive points. By number, the distance each feature moved in the fourteen-minute period between scenes was: 1) 439.1m, 2) 244.6m, 3) 140.7m, 4) 237.9m, 5) 101.2m, 6) 160.0m, 7) 189.6m, 8) 170.5m, 9) 307.1m and 10) 312.1m. Note that most of the vector directions agree with the direction of the currents shown in the HF Radar-derived flow field.

resolution Satellite Pour l'Observation de la Terre (SPOT) 6 (available approximately every 5-7 days).

Synthetic Aperture Radar (SAR) data from the Sentinel 1A satellite (available every 3-6 days at a spatial resolution of 5m x 20 m) were added to the suite of remote sensing products in late 2021. SAR can detect surfactant films associated with natural processes (Svejkovsky and Shandley, 2001) and plumes containing anthropogenic substances (Svejkovsky and Jones, 2001, Gierach et al., 2017) when optical sensors might be limited by cloud cover or heavy atmospheric haze. The primary purpose of these satellites for this project is to provide another look at the TJR discharge plume to assess its offshore extent and direction of flow. The runoff often contains natural and anthropogenic surfactants that dampen the SAR signal and therefore make it detectable in the data. In 2023 88 SAR images were acquired and processed for the San Diego region

providing an additional source of information even during cloudy conditions. Figure 2 shows a sample SAR image from 01/31/23 alongside a SPOT 7 scene from the same day highlighting a probable surfactant signature from the TJR discharge. The satellite data acquisitions were approximately 5.5 hours apart. The TJR discharge plume is clearly identifiable in the SPOT image (right) and, although different in shape and extent due to the time difference of the satellite acquisitions, it corroborates the supposition that the dampened SAR signal (seen in the area outlined by a yellow box in right image) identifies river discharge with a high composition of surfactants. Figure 3 illustrates a situation when on 02/13/23 there was no clear visible satellite data to document the TJR discharge plume, yet the SAR image provides data to show the extent of the plume likely containing surfactant-laden water. A SPOT 6 image acquired two days later offers a clear view of the strong discharge and highly turbid water moving up the

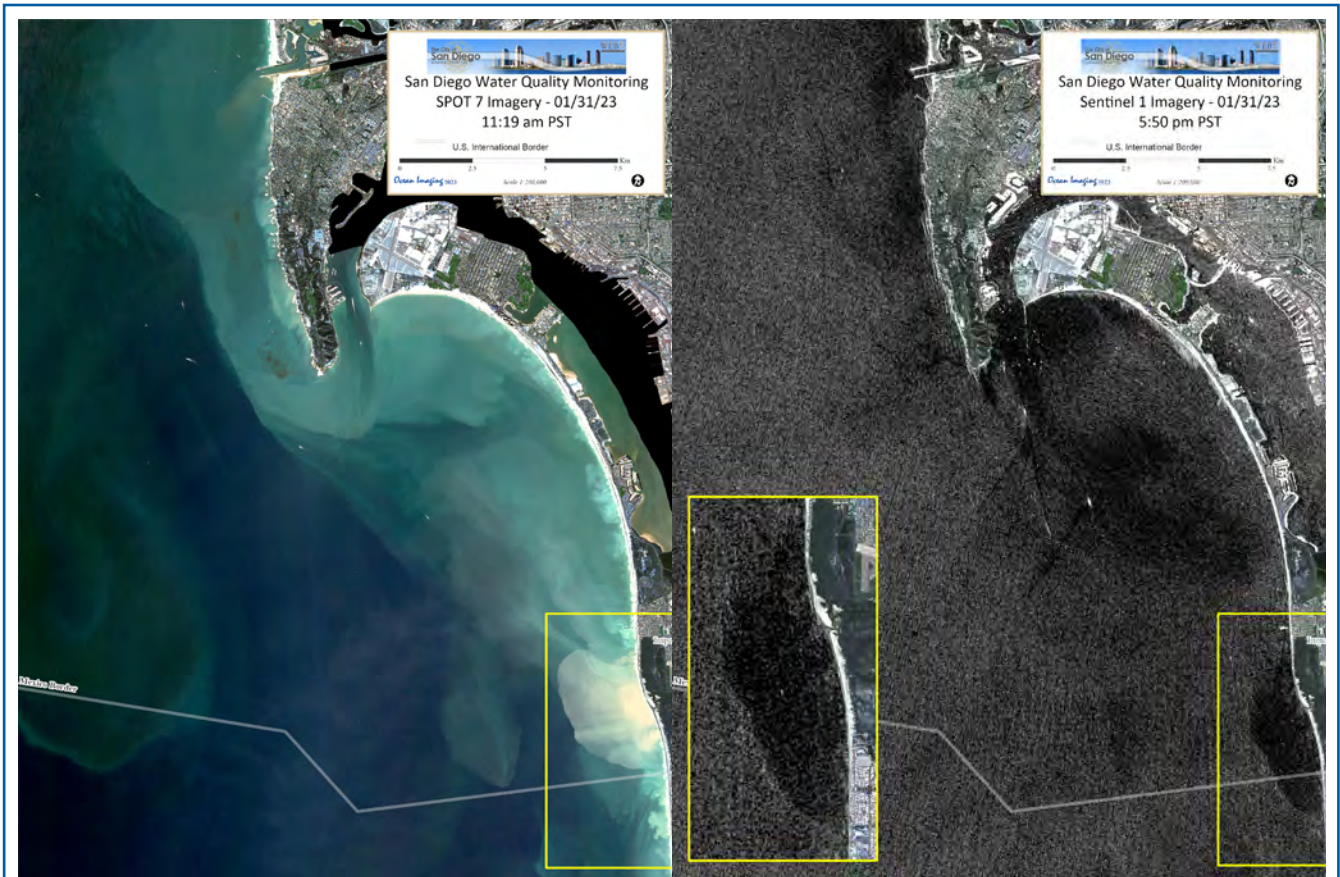
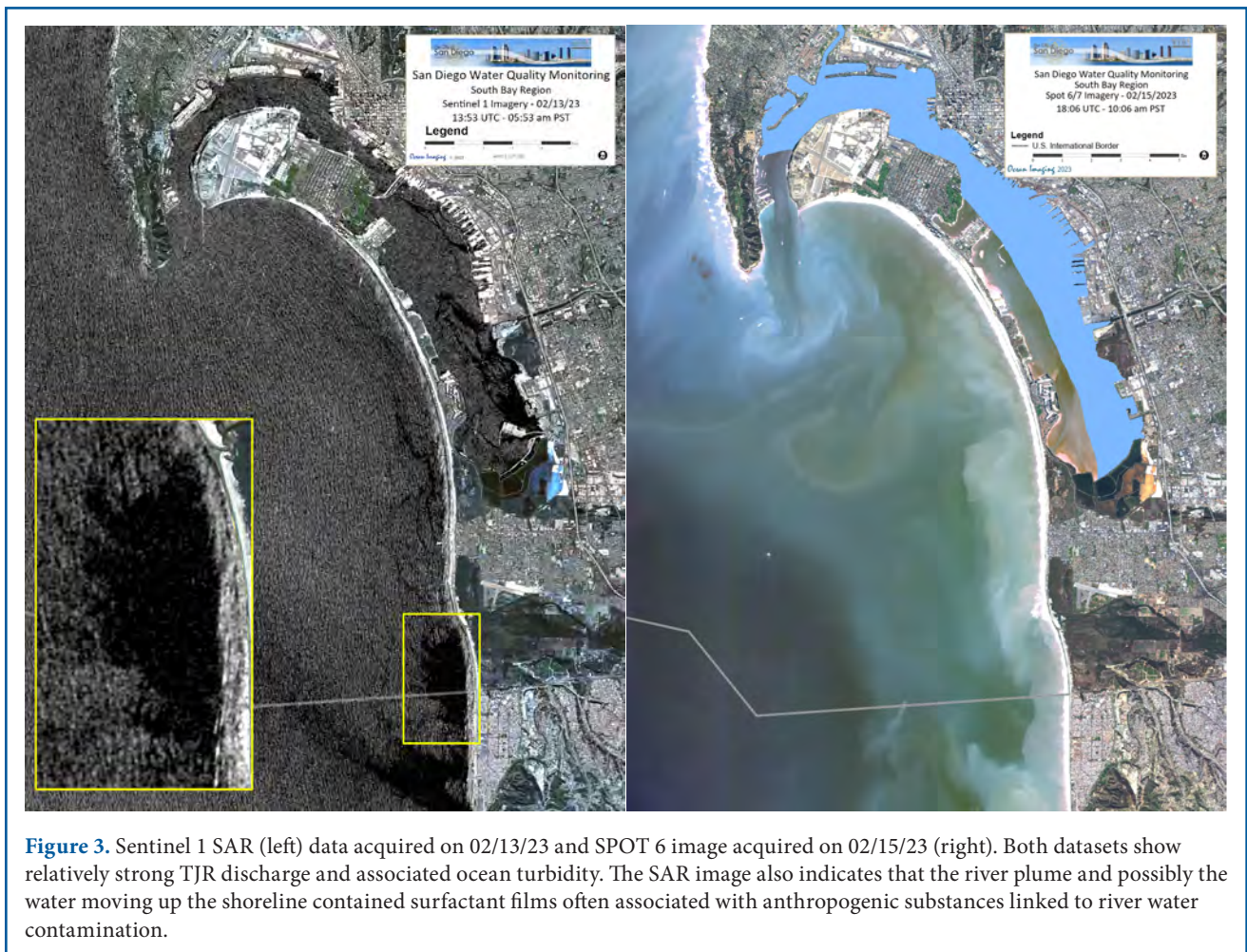


Figure 2. SPOT 7 (left) and Sentinel 1 SAR (right) imagery illustrating the ability of SAR data to help detect and identify areas of TJR discharge containing surface-dampening surfactants.

coastline. The streaky signature in the SAR image north of the river outlet also indicates possible surfactants moving up the coast. Recent attention on the severity of the TJR polluted discharge (Little, 2024) makes monitoring and documenting the TJR discharge plume increasingly important.

In 2012, OI added additional broad-scale products to the datasets available to the SDPUD and project partners. These include two types of ocean current data: High Frequency Radar-derived surface currents (HF Radar) and Hybrid Coordinate Ocean Model (HYCOM) model-derived surface currents (<https://hycom.org>). The raw data for the HF Radar currents are retrieved from National HF Radar Network via the Scripps Coastal Observing Research and Development Center (CORDC) on an hourly basis and reformatted into ESRI-compatible

shapefiles. The hourly products are averages of the previous 25 hours and generated at 1 km and 6 km spatial resolutions. Additional HYCOM model-based products include daily ocean salinity, mixed layer depth, and subsurface temperature at 50, 100, 150 and 200 meters. In 2016 these products were delivered in a Web Map Service (WMS) Representational State Transfer (REST) service format compatible with the City's now retired BioMap server. They are presently being generated and archived in preparation for delivery via a next generation WMS dashboard-style data portal now in development. Details of this project are discussed below. The existing high resolution (6-30 m) observation region extends from approximately La Jolla southward to Rosarito Beach, Mexico and out approximately 50 miles. The coarser-scale products (250-1000 m) such as chlorophyll, SST, ocean



currents and HYCOM-derived products encompass the entire Southern California Bight (SCB).

2.4 Data Dissemination and Analysis

The satellite data are made available to the SDPUD and other project constituents through a dedicated, password-protected web site. Although it is possible to process most of the data in near-real-time, earlier in the project it was decided that the emphasis of this program is not on providing real-time monitoring support and the extra costs associated with the rapid data turn-around are not warranted. Most satellite data are therefore processed and posted within 1-2 days after acquisition. As noted above however, OI has in several cases made imagery available to the SDPUD in near-real time (within 12-24 hours) via email when observations appeared to be highly significant to the management of beach closures or other sudden/anomalous events. The website was updated in 2022 to improve its ease of use and presentation of available imagery.

3. HIGHLIGHTS OF 2023 MONITORING

3.1 Atmospheric and Ocean Conditions

Coastal and oceanic water quality can often be correlated to rainfall events. The annual recorded precipitation for 2023 was well above the previous 10-year average for the region. The San Diego International Airport station (SDIA) measured 14.42 inches of total annual rainfall and the TJR Estuary 12.66 inches, both higher than 2013-2022 averages of 8.05 and 7.73 inches respectively (see Table 2). 2016 was the only comparable year over the twelve-year period. While the monthly rainfall followed normal patterns seasonally, with the winter and spring months for the most part matching the expected rainy season and the summer months being mostly dry, an extreme rain event in mid-January and over twice the normal precipitation during the month of March had a significant impact of the coastal water quality. The May through September summer months were mostly dry except

for Hurricane Hilary which made landfall on San Diego shores on 08/20/23. The SDIA station recorded 1.84 and the Tijuana Estuary station recorded 1.86 inches of precipitation on that day.

Figure 4 shows cumulative daily precipitation in the Tijuana Estuary along with the average daily river discharge at the Tijuana River International Boundary station (TJRIB). The table below the plot gives the dates for which there was measurable precipitation at that station. As has been noted in the previous reports and is evident in Table 2, the monthly and annual precipitation amounts can differ at times between the SDIA and TJR reporting stations. The primary periods of consistent and/or heavy precipitation occurred during the months of January, February, March, November, and December with anomalous 1.84 and 1.89 inches measured at the SDIA and Tijuana Estuary stations in August. We have defined a significant TJR discharge event as when the spectrally distinct “fresh core” of the river discharge plume as defined by Svejksky et al., 2010 is clearly visible in the imagery. The majority (49 out of 50) significant TJR discharge events observed in the remotely sensed data occurred during the months of January through April and October through December, which is during the Southern California rainy season. However, in 2023 only 58% of significant TJR discharge events can be directly correlated to rainfall occurring one to two days prior to the observation. Most of the non-rain related TJR discharge events were observed in October through the first half of December and can in all probability be attributed to the TJR river flow rate largely remaining above 30 cubic feet per second (cfs) during that period. When the increased river discharge levels, higher coastal turbidity and thus lower water quality, did follow the rainfall events, the coastal and offshore conditions typically improved only after one to three days of rainfall totaling less than 0.1 inches. Figures 1, 2, 3 and 5 provide examples of heavy coastal turbidity, extensive SDR and TJR plumes as well as large plankton blooms observed in the satellite imagery resulting from significant precipitation events. On 01/20/23 (Figure 1)

the offshore turbidity visibly decreased following only one day of dryer and calm conditions.

As discussed above, aside from the heavy rainfall associated with Hurricane Hilary in August, there was little measured precipitation in the San Diego region from May through October. River flow rates in cfs measured by the United States Geological Survey (USGS) Fashion Valley gauge generally correspond well with the rainfall data, however, the

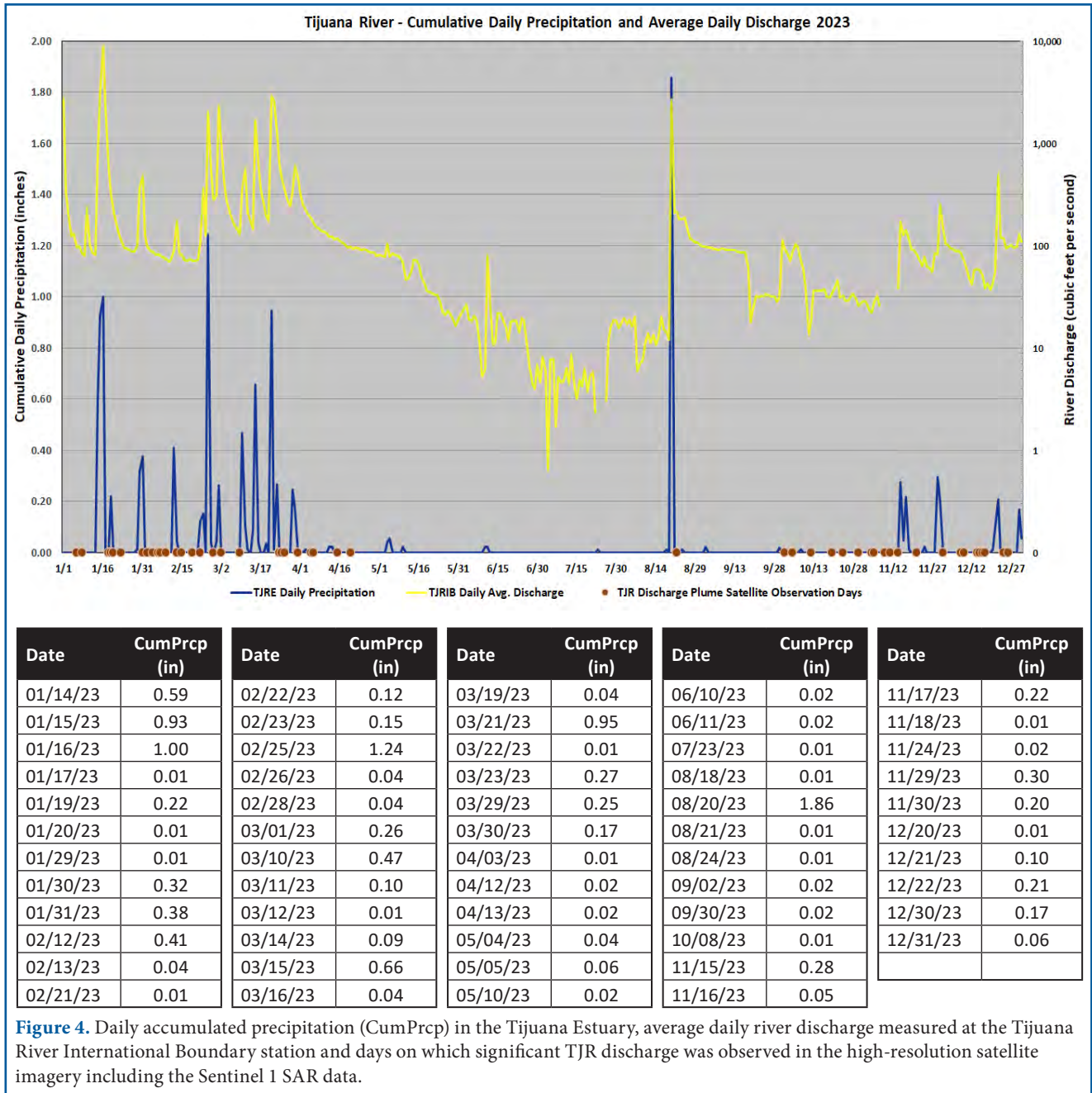
overall flow rate in 2023 was higher when compared to prior years, mostly likely due to heavy rainfall during the first three months of the year (Figure 6). There were also periods in May and October when the discharge rates did not match rainfall recorded at the SDIA. Despite the mostly dry summer conditions, the river flow rates did remain above five cfs for most of the season as documented by both the TJRRIB and USGS gauges. This may explain the days when considerable river discharge

Table 2. San Diego and Tijuana Estuary precipitation totals 2012-2023

San Diego International Airport Cumulative Monthly Precipitation in Inches												
	2012	2013	2014	2015	2016	2017	2018	2019	2020	2021	2022	2023
January	0.40	0.70	0.01	0.42	3.21	2.99	1.77	2.42	0.48	1.80	0.16	5.14
February	1.19	0.63	1.00	0.28	0.05	1.58	0.35	4.04	0.38	0.10	0.70	1.78
March	0.97	1.22	1.28	0.93	0.76	0.08	0.65	1.23	2.15	1.48	1.61	3.97
April	0.88	0.01	0.54	0.02	0.55	0.01	0.02	0.10	3.68	0.07	0.02	0.12
May	0.02	0.26	--	2.39	0.44	0.87	0.09	0.86	0.02	0.07	0.02	0.09
June	--	--	--	0.04	--	0.02	--	0.01	0.14	0.01	--	0.03
July	--	0.05	--	1.71	--	--	--	--	--	--	--	--
August	--	--	0.08	0.01	--	--	0.02	--	--	0.23	--	1.84
September	--	--	--	1.24	0.32	0.06	--	0.11	--	0.50	0.65	0.05
October	0.70	0.25	--	0.43	0.07	--	0.57	--	0.12	1.01	0.09	--
November	0.28	1.48	0.37	1.54	0.61	0.02	0.69	2.72	0.14	--	1.07	0.61
December	2.19	0.46	4.50	0.88	4.22	--	0.83	4.03	0.60	2.58	1.55	0.79
Annual Total	6.63	5.06	7.78	9.89	10.23	5.63	4.99	15.52	7.71	7.85	5.87	14.42
Tijuana Estuary Cumulative Monthly Precipitation in Inches												
	2012	2013	2014	2015	2016	2017	2018	2019	2020	2021	2022	2023
January	0.70	0.05	0.08	0.32	2.40	3.61	0.82	1.80	0.61	2.21	0.17	3.47
February	0.86	--	1.35	0.13	0.02	4.06	0.47	3.62	0.51	0.06	0.58	2.06
March	1.21	1.43	0.55	1.01	1.28	0.04	1.17	1.33	2.59	1.12	1.64	3.32
April	0.82	0.11	0.35	0.07	1.91	0.01	0.10	0.33	5.52	0.04	0.13	0.06
May	--	0.36	--	1.13	0.97	1.07	0.08	0.50	0.02	0.01	--	0.12
June	--	--	0.12	--	--	--	--	0.02	0.21	0.06	--	0.05
July	--	0.01	0.33	0.39	--	0.01	0.01	--	--	--	--	0.01
August	--	--	0.04	--	--	0.02	--	--	--	0.02	--	1.89
September	0.02	0.01	--	0.48	0.49	0.03	--	--	--	--	0.48	0.04
October	0.50	0.41	--	0.21	--	--	0.13	--	0.04	0.91	0.29	0.01
November	--	0.25	0.29	0.61	0.34	0.06	0.82	2.99	0.08	0.02	0.95	1.08
December	0.04	0.50	3.09	0.61	4.32	0.09	3.16	3.82	0.60	1.18	1.13	0.54
Annual Total	4.15	3.13	6.20	4.94	11.73	8.99	6.76	14.41	10.18	5.63	5.38	12.66

and offshore turbidity were observed in the satellite imagery yet there was little to no measurable rainfall from either station within a few days prior to the observations. Figure 7 provides examples of when the satellite data exhibited notable coastal and offshore turbid conditions as well as strong plankton blooms that were unrelated to rainfall.

In 2023 the county of San Diego issued 312 posted shoreline and/or rain advisories and 50 beach/shoreline closures. This is a 54.5% increase in the number of advisories and an 18% decrease in closures compared to 2022 (202 and 61 closures respectively). The longest contiguous 2023 closure lasting the full year and into 2024 was at Border Field State Park along the south end of the Tijuana Slough Shoreline. In fact, this area has been closed for over



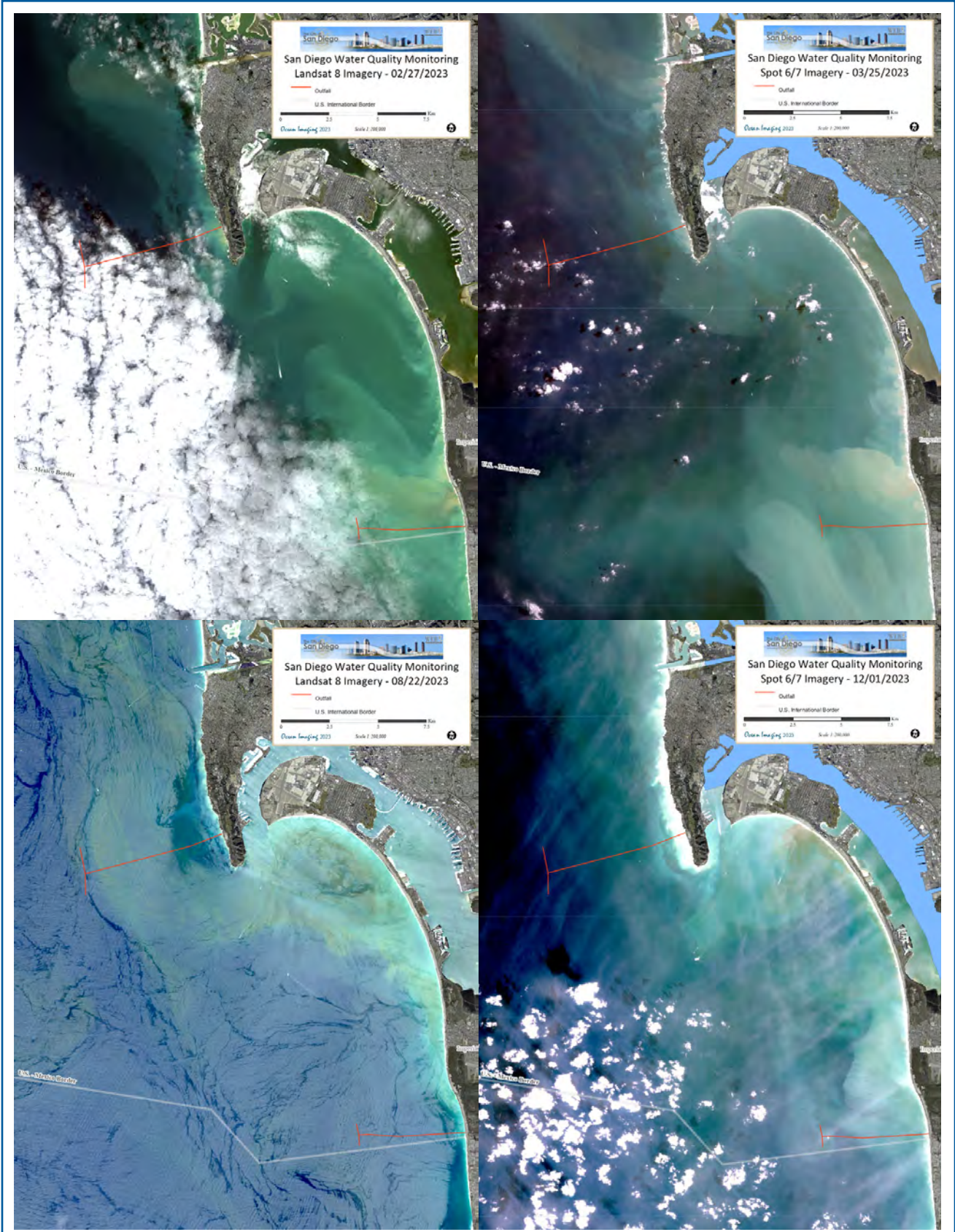


Figure 5. Sample high-resolution imagery from SPOT and Landsat highlighting turbid water, plankton blooms and heavy river runoff immediately following rain events.

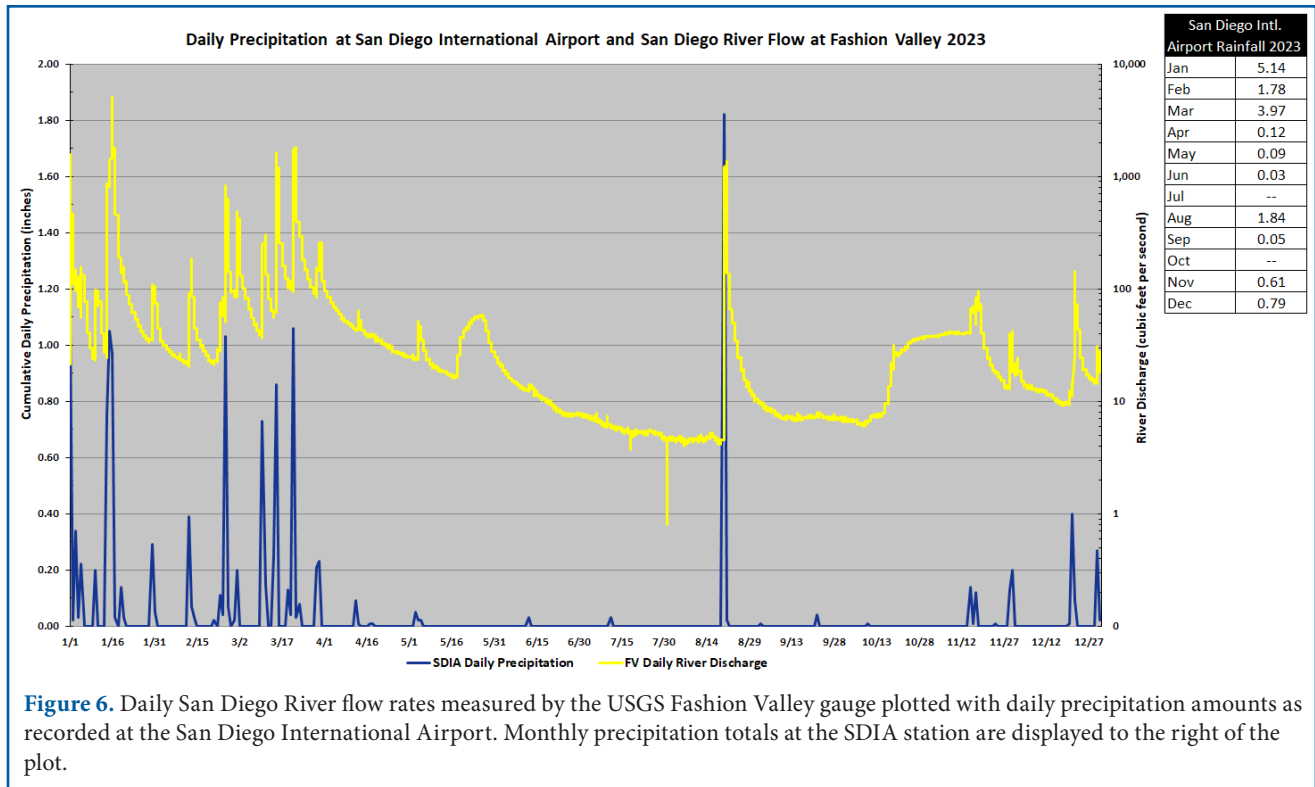


Figure 6. Daily San Diego River flow rates measured by the USGS Fashion Valley gauge plotted with daily precipitation amounts as recorded at the San Diego International Airport. Monthly precipitation totals at the SDIA station are displayed to the right of the plot.

two years. The majority of the closures extended from the Tijuana River mouth all the way past Avenida Del Sol to include most all of the Coronado City beaches. This is farther north than was typical for previous years (Table 3). Most beach closures were associated with contamination from the TJR runoff. Generally, the closures can be attributed to a rain event prior to and/or during the closure period leading to heavy TJR discharge and coastal turbidity as shown in the figures above. However, nine closures were triggered by sewage spills in San Diego Bay, south Carlsbad State Beach, Buccaneer Beach Tecolote Shores, and several locations within Mission Bay. As seen in Table 3 below, most bay closures were associated with sewage spills. Also, 12 of the 50 closures happened between the months of May and October when no rainfall prior to the closure was recorded at the Tijuana Estuary or SDIA stations. Table 3 also shows the date(s) of the high-resolution satellite data in the project's archive acquired closest in time to the start date of the closure and/or rain advisory. The high-resolution satellite data during the beach closure periods regularly show high turbidity and suspended solids and/or high plankton levels along the coastline near the closed regions as

well as greater than normal TJR runoff, sometimes being carried north by the ocean currents. Figure 5 and Figure 8 provide examples of the Tijuana River plume extending north and/or ocean currents pushing the TJR discharge waters north up past Border Field State Park towards the Coronado beaches, corresponding with shoreline closures usually within zero to two days of the image data.

As noted above there were strong phytoplankton and possible harmful algal blooms (HABs) during the spring and late summer to fall of 2023 which may have contributed to decreased offshore water quality. This is seen by dark green and brown to red reflectance in the satellite data caused by phytoplankton containing photosynthetic pigments that vary in color from brown to red and blooms often dominated by the dinoflagellate *L. polyedra* which absorbs light in the ultra violet part of the electromagnetic spectrum (Kahru, et al., 1998, Zheng, et al., 2018). Diatoms (primarily *Pseudo-nitzschia* spp) and dinoflagellates are largely responsible for the local harmful algal blooms (red tides) when they occur (Southern California Coastal Water Research Project, 2019). Figure 9 provides examples of high-

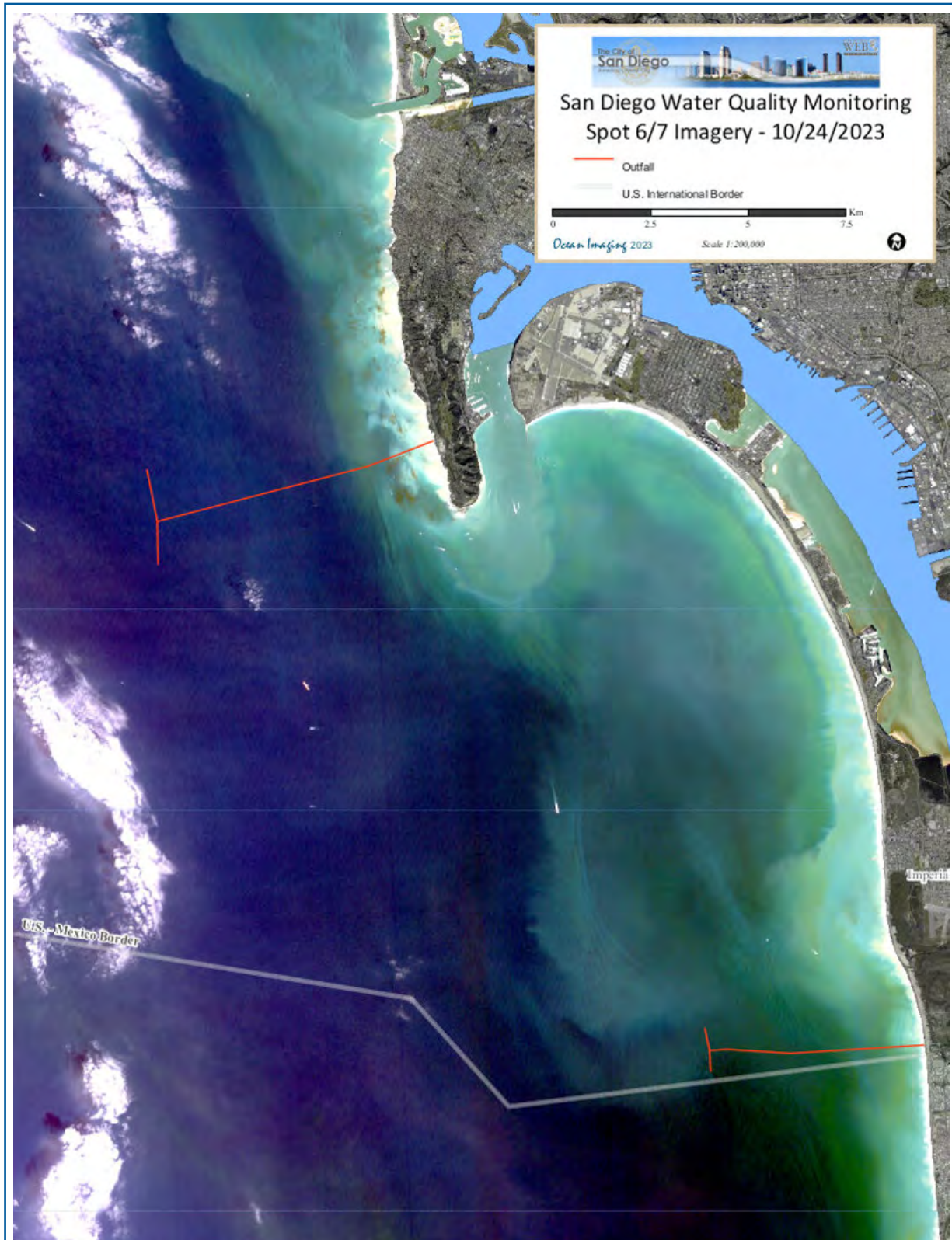






Figure 7. Sample high-resolution SPOT data providing examples of days when the imagery displayed heavier than usual river discharge, coastal and offshore turbidity and plankton blooms that cannot be directly linked to a prior rainfall event. River gauge data do, however, show higher than average flow rates on or near these dates.

Table 3. 2023 County of San Diego shoreline closures, rain advisories and associated project satellite data (Source: California State Water Resources Control Board)  general rain advisory  beach closure associated with the Tijuana River  bay or beach closure due to a sewage spill

 bay or beach closure due to elevated bacteria levels

Station/Description	Beach Name	Station Name	Type	Cause	Source	Start Date	End Date	Duration (days)	Nearest Rain Date	Time From Rain Event	Satellite Image Data
All San Diego County Beaches	All San Diego County	All San Diego County Beaches	Rain			1/2/2023	1/9/2023	9	1/1/2023	0	1/6, 1/8
Silver Strand N end (ocean)	Silver Strand State Beach	IB-070	Closure	Tijuana River Associated	Sewage/Grease	1/1/2023	2/20/2023	51	1/1/2023	0	16 dates
End of Seacoast Dr	Imperial Beach municipal beach, other	IB-050	Closure	Tijuana River Associated	Sewage/Grease	1/1/2023	7/10/2023	191	1/1/2023	0	34 dates
Border Fence N side	Border Field State Park	IB-010	Closure	Tijuana River Associated	Sewage/Grease	1/1/2023	12/31/2023	365	1/1/2023	0	All
Avd. del Sol	Coronado City beaches	IB-080	Closure	Tijuana River Associated	Sewage/Grease	1/2/2023	2/8/2023	38	1/2/2023	0	12 dates
All San Diego County Beaches	All San Diego County	All San Diego County Beaches	Rain			1/10/2023	1/20/2023	11	1/6/2023	4	1/18, 1/19, 1/20
Batiquitos Lagoon outlet	South Carlsbad State Beach	EH-440	Closure	Sewage Spill	Sewage/Grease	1/16/2023	1/21/2023	6	1/16/2023	0	1/18, 1/19, 1/20
Ruocco Park	San Diego Bay	EH-545	Closure	Sewage Spill	Sewage/Grease	1/16/2023	1/23/2023	8	1/16/2023	0	1/18, 1/19, 1/20
All San Diego County Beaches	All San Diego County	All San Diego County Beaches	Rain			1/30/2023	2/2/2023	4	1/30/2023	0	1/31, 2/2
Avd. del Sol	Coronado City beaches	IB-080	Closure	Tijuana River Associated	Sewage/Grease	2/10/2023	2/12/2023	3	2/12/2023	2	2/12
All San Diego County Beaches	All San Diego County	All San Diego County Beaches	Rain			2/11/2023	2/16/2023	4	2/13/2023	0	2/13, 2/15
Silver Strand N end (ocean)	Silver Strand State Beach	IB-070	Closure	Tijuana River Associated	Sewage/Grease	2/22/2023	6/24/2023	123	2/22/2023	0	16 dates
All San Diego County Beaches	All San Diego County	All San Diego County Beaches	Rain			2/23/2023	3/4/2023	10	2/23/2023	0	2/22, 2/27, 3/2
Avd. del Sol	Coronado City beaches	IB-080	Closure	Tijuana River Associated	Sewage/Grease	3/1/2023	4/23/2023	54	3/1/2023	0	11 dates
All San Diego County Beaches	All San Diego County	All San Diego County Beaches	Rain			3/10/2023	3/13/2023	4	3/10/2023	0	--
All San Diego County Beaches	All San Diego County	All San Diego County Beaches	Rain			3/15/2023	3/19/2023	5	3/15/2023	0	--
Batiquitos Lagoon outlet	South Carlsbad State Beach	EH-440	Closure	Sewage Spill	Sewage/Grease	3/15/2023	3/20/2023	6	3/15/2023	0	--
Loma Alta Creek outlet	Buccaneer Beach	OC-022	Closure	Sewage Spill	Sewage/Grease	3/15/2023	3/20/2023	6	3/15/2023	0	--
All San Diego County Beaches	All San Diego County	All San Diego County Beaches	Rain			3/21/2023	3/26/2023	6	3/21/2023	0	3/24, 3/25, 3/26
All San Diego County Beaches	All San Diego County	All San Diego County Beaches	Rain			3/29/2023	4/2/2023	5	3/29/2023	0	3/31
Avd. del Sol	Coronado City beaches	IB-080	Closure	Tijuana River Associated	Sewage/Grease	4/24/2023	5/1/2023	8	4/18/2023	6	--
Enchanted Cove	Mission Bay	MB-015	Closure	Sewage Spill	Sewage/Grease	7/21/2023	7/22/2023	2	6/12/2023	39	--
Fiesta Island East Shore	Mission Bay	MB-045	Closure	Sewage Spill	Sewage/Grease	7/21/2023	7/22/2023	2	6/12/2023	39	--
Leisure Lagoon Point	Mission Bay	MB-046	Closure	Sewage Spill	Sewage/Grease	7/21/2023	7/22/2023	2	6/12/2023	39	--
Tecolote Shores - Pump 58	Mission Bay	MB-047	Closure	Sewage Spill	Sewage/Grease	7/21/2023	7/22/2023	2	6/12/2023	39	--
Tecolote Shores swim area	Tecolote Shores	MB-041	Closure	Sewage Spill	Sewage/Grease	7/21/2023	7/22/2023	2	6/12/2023	39	--
All San Diego County Beaches	All San Diego County	All San Diego County Beaches	Rain			8/20/2023	8/24/2023	5	8/20/2023	0	8/22
Loma Ave (firmly Isabella)	Coronado City beaches	EH-050	Closure	Tijuana River Associated	Sewage/Grease	8/20/2023	8/29/2023	10	8/20/2023	0	8/22, 8/28
Navy Fence (A)	Coronado north beach	EH-060	Closure	Tijuana River Associated	Sewage/Grease	8/20/2023	8/29/2023	10	8/20/2023	0	8/22, 8/28
Avenida Lunar	Coronado City beaches	IB-079	Closure	Tijuana River Associated	Sewage/Grease	8/20/2023	9/21/2023	33	8/20/2023	0	8/22, 8/28, 9/4, 9/7, 9/9, 9/14, 9/20
Silver Strand N end (ocean)	Silver Strand State Beach	IB-070	Closure	Tijuana River Associated	Sewage/Grease	8/20/2023	10/5/2023	47	8/20/2023	0	10 dates
End of Seacoast Dr	Imperial Beach municipal beach, other	IB-050	Closure	Tijuana River Associated	Sewage/Grease	8/20/2023	12/16/2023	119	8/20/2023	0	29 dates
Navy Fence (A)	Coronado north beach	EH-060	Closure	Bacterial Standards	Sewage/Grease	8/31/2023	9/20/2023	21	8/24/2023	7	9/4, 9/7, 9/9, 9/14, 9/20
Loma Ave (firmly Isabella)	Coronado City beaches	EH-050	Closure	Tijuana River Associated	Sewage/Grease	8/31/2023	9/21/2023	22	8/24/2023	7	9/4, 9/7, 9/9, 9/14, 9/20
Avenida Lunar	Coronado City beaches	IB-079	Closure	Tijuana River Associated	Sewage/Grease	9/22/2023	10/2/2023	11	9/3/2023	19	9/25, 10/2
Loma Ave (firmly Isabella)	Coronado City beaches	EH-050	Closure	Tijuana River Associated	Sewage/Grease	9/27/2023	10/2/2023	6	9/3/2023	24	10/2
Navy Fence (A)	Coronado north beach	EH-060	Closure	Tijuana River Associated	Sewage/Grease	9/27/2023	10/2/2023	6	9/2/2023	25	10/2
Campland swimming area	Mission Bay, Campland On The Bay	MB-080	Closure	Bacterial Standards	Unknown	10/2/2023	10/4/2023	3	9/30/2023	2	10/2
Avenida Lunar	Coronado City beaches	IB-079	Closure	Tijuana River Associated	Sewage/Grease	10/3/2023	10/4/2023	2	9/30/2023	3	--
Loma Ave (firmly Isabella)	Coronado City beaches	EH-050	Closure	Tijuana River Associated	Sewage/Grease	10/9/2023	10/13/2023	5	10/8/2023	1	10/10, 10/12
Silver Strand N end (ocean)	Silver Strand State Beach	IB-070	Closure	Tijuana River Associated	Sewage/Grease	10/9/2023	10/24/2023	16	10/8/2023	1	10/10, 10/12, 10/20, 10/24
Navy Fence (A)	Coronado north beach	EH-060	Closure	Tijuana River Associated	Sewage/Grease	10/14/2023	10/16/2023	3	10/11/2023	3	--
Loma Ave (firmly Isabella)	Coronado City beaches	EH-050	Closure	Tijuana River Associated	Sewage/Grease	10/14/2023	10/17/2023	4	10/11/2023	3	--
Silver Strand N end (ocean)	Silver Strand State Beach	IB-070	Closure	Tijuana River Associated	Sewage/Grease	10/26/2023	10/29/2023	4	10/11/2023	15	10/27
Avenida Lunar	Coronado City beaches	IB-079	Closure	Tijuana River Associated	Sewage/Grease	10/28/2023	10/29/2023	2	10/11/2023	17	--
Silver Strand N end (ocean)	Silver Strand State Beach	IB-070	Closure	Tijuana River Associated	Sewage/Grease	10/30/2023	11/14/2023	16	10/11/2023	19	10/30, 11/1, 11/4, 11/5, 11/9, 11/11, 11/14
Avenida Lunar	Coronado City beaches	IB-079	Closure	Tijuana River Associated	Unknown	11/2/2023	11/5/2023	4	10/11/2023	22	11/4, 11/5
Avenida Lunar	Coronado City beaches	IB-079	Closure	Tijuana River Associated	Sewage/Grease	11/9/2023	11/10/2023	2	10/11/2023	29	11/9
Avenida Lunar	Coronado City beaches	IB-079	Closure	Tijuana River Associated	Sewage/Grease	11/12/2023	11/13/2023	2	10/11/2023	32	--
All San Diego County Beaches	All San Diego County	All San Diego County Beaches	Rain			11/16/2023	11/19/2023	4	11/16/2023	0	--
Silver Strand N end (ocean)	Silver Strand State Beach	IB-070	Closure	Tijuana River Associated	Sewage/Grease	11/17/2023	12/16/2023	30	11/17/2023	0	11/21, 12/1, 12/8, 12/9, 12/14, 12/15, 12/16
Navy Fence (A)	Coronado north beach	EH-060	Closure	Tijuana River Associated	Sewage/Grease	11/19/2023	12/3/2023	15	11/18/2023	1	11/21, 12/1
Loma Ave (firmly Isabella)	Coronado City beaches	EH-050	Closure	Tijuana River Associated	Sewage/Grease	11/19/2023	12/6/2023	18	11/18/2023	1	11/21, 12/1
Avenida Lunar	Coronado City beaches	IB-079	Closure	Tijuana River Associated	Sewage/Grease	11/19/2023	12/8/2023	20	11/18/2023	1	11/21, 12/1, 12/8
Navy Fence (A)	Coronado north beach	EH-060	Closure	Tijuana River Associated	Sewage/Grease	12/5/2023	12/6/2023	2	12/1/2023	4	--
Avenida Lunar	Coronado City beaches	IB-079	Closure	Tijuana River Associated	Sewage/Grease	12/9/2023	12/15/2023	7	12/1/2023	8	12/9, 12/14, 12/15
End of Seacoast Dr	Imperial Beach municipal beach, other	IB-050	Closure	Tijuana River Associated	Sewage/Grease	12/18/2023	12/31/2023	14	12/1/2023	17	12/24, 12/26
Avenida Lunar	Coronado City beaches	IB-079	Closure	Tijuana River Associated	Sewage/Grease	12/21/2023	12/31/2023	11	12/21/2023	0	12/24, 12/26
Loma Ave (firmly Isabella)	Coronado City beaches	EH-050	Closure	Tijuana River Associated	Sewage/Grease	12/21/2023	12/31/2023	11	12/21/2023	0	12/24, 12/26
Navy Fence (A)	Coronado north beach	EH-060	Closure	Tijuana River Associated	Sewage/Grease	12/21/2023	12/31/2023	11	12/21/2023	0	12/24, 12/26
Silver Strand N end (ocean)	Silver Strand State Beach	IB-070	Closure	Tijuana River Associated	Sewage/Grease	12/21/2023	12/31/2023	11	12/21/2023	0	12/24, 12/26
All San Diego County Beaches	All San Diego County	All San Diego County Beaches	Rain			12/22/2023	12/25/2023	4	12/22/2023	0	12/24
All San Diego County Beaches	All San Diego County	All San Diego County Beaches	Rain			12/31/2023	12/31/2023	1	12/31/2023	0	--

resolution SPOT data highlighting days when the imagery revealed strong coastal and offshore phytoplankton blooms that cannot be directly linked to a significant (over 0.01 inches) prior rainfall event.

Although discharges from the San Diego River and Mission Bay do not cause the same level of beach contamination issues as the Tijuana River, the runoff from the San Diego River did affect nearshore water clarity and quality on several days

throughout the year in 2023, directly as a source of suspended sediment and indirectly as a source of high nutrient input, encouraging coastal and offshore phytoplankton blooms. While not at the scale or as dramatic as observed in previous years, turbidity plumes emanating from the river entrance and/or phytoplankton blooms either along the coast or offshore of the area were documented on 82 days in the medium-resolution (MODIS and Sentinel 3) and high-resolution satellite imagery

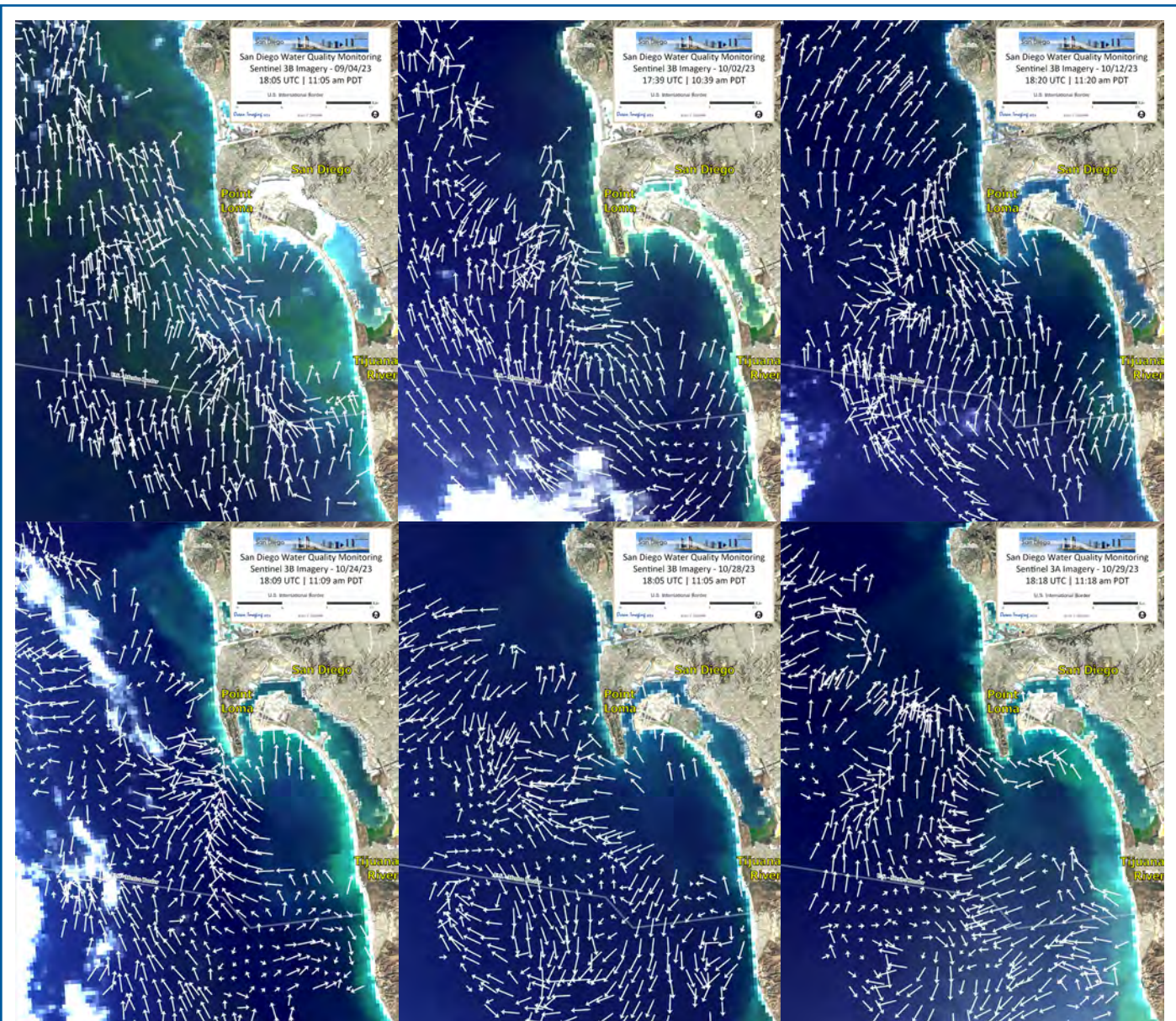


Figure 8. Sentinel 3A & 3B imagery with HF Radar currents overlaid to provide examples of when the Tijuana River plume extended to the north and/or when ocean currents pushed TJR discharge waters north up past Border Field State Park towards the Coronado beaches, corresponding with shoreline closures usually within zero to two days of the image data.

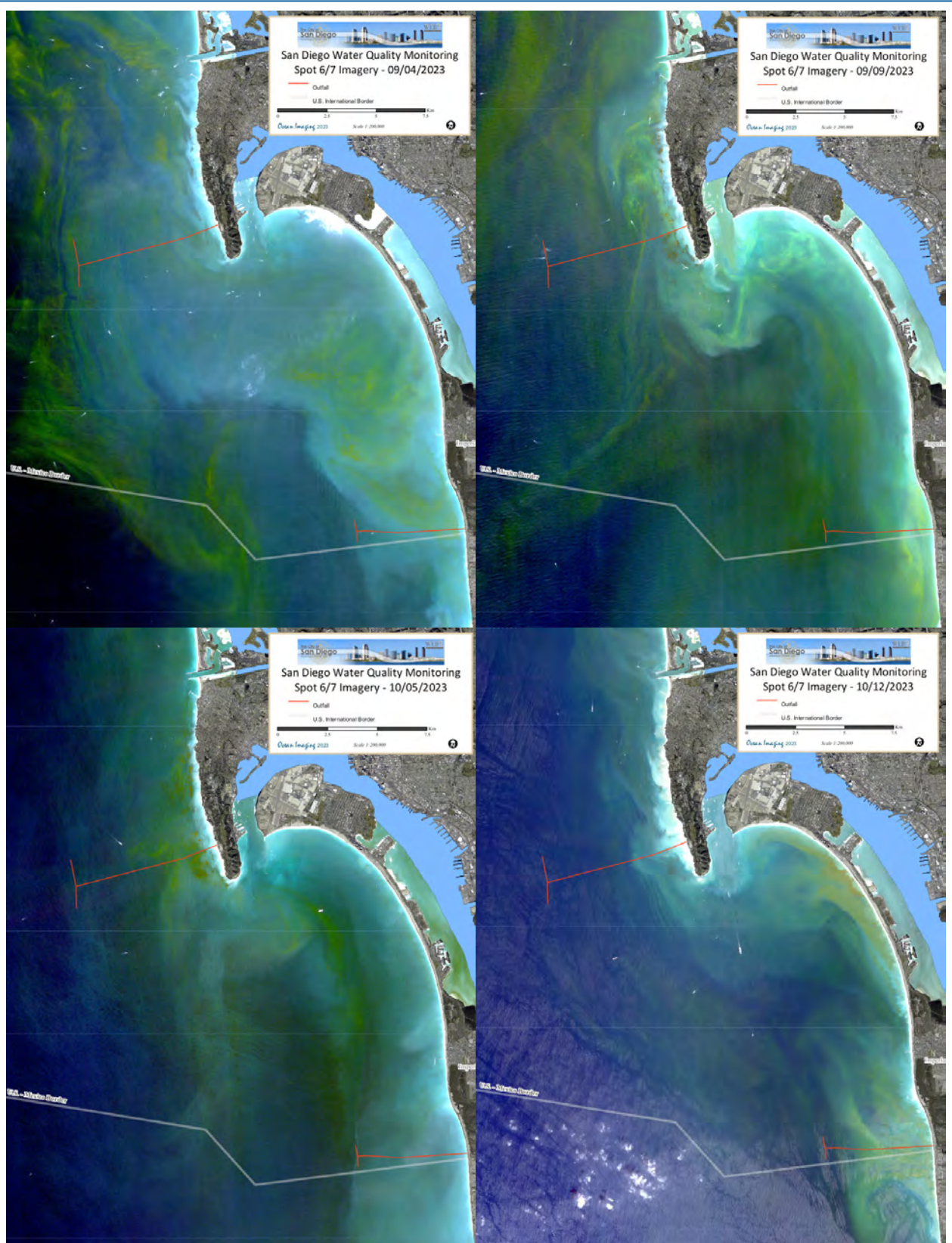


Figure 9. Sample high-resolution SPOT data providing examples of days when the imagery revealed strong coastal and offshore phytoplankton blooms and red tides that cannot be directly linked to a significant (over 0.01 inches) prior rainfall event.

throughout the year. The area surrounding the Point Loma kelp bed tended to be more often affected by direct shore runoff and discharges from the San Diego River and Mission Bay during the prevalent southward current regime. Figure 10 provides examples of days on which the data revealed heavy coastal turbidity and phytoplankton blooms in this northern section of the project's study area.

The SCB experienced lower overall chlorophyll levels throughout 2023 when compared to the previous two years, especially 2021. Chlorophyll levels in the SCB and thus phytoplankton abundance were high during the first four months of the year particularly south of the U.S.-Mexico border during March and April. The heavy rainfall events up through the first part of April introducing nutrients into the ocean system from river discharge and runoff likely contributed to the phytoplankton blooms. A noticeable decrease in offshore chlorophyll levels from June through October is evident in the representative satellite imagery. Figure 11 provides representative MODIS- and VIIRS-derived chlorophyll images for each month of 2023. As is seen in the image data, the California Current relaxed during the summer months and/or was not moving greener/nutrient-rich water into the SCB but appears to gain strength in November and December. Figure 12 shows 300-meter resolution monthly chlorophyll averages for the area offshore of San Diego County and south of the U.S.-Mexico border. These composites were generated from MODIS, VIIRS and OLCI data as part of a SDPUD-funded project to study plankton abundance and extent in the region from 1997 through 2023. The series provides a more coastal, regional perspective of the changes in phytoplankton throughout the year. The data correlate well with the SCB imagery in Figure 11 for the first seven months but show an increase in chlorophyll between August and November along the San Diego coastline down past the Coronado Islands south of the border. This is also evident in the high-resolution images acquired during September and October shown in Figure 9.

The City of San Diego conductivity/temperature/depth (CTD) sampling results correlated well with

the satellite data observations. Some of the highest chlorophyll levels recorded via CTD (as high as 61.17 mg/m³ at station I40, 1-meter depth on 04/18/23) occurred during the month of April. This fits more of the seasonal expectation compared to the post-April blooms in 2022. In fact, 67% of all the fluorometry readings above 10.0 mg/m³ were recorded in the month of April. The imagery in Figures 11 and 12 corroborate these measurements, clearly documenting April as the month exhibiting the highest intensity and spatial extent of phytoplankton blooms in the project's area of interest. Figure 13 offers examples of the CTD fluorometry data in correlation with the high-resolution satellite imagery on or near the same day as the field samples. While the high-resolution remotely sensed data do not depict quantitative chlorophyll levels, the plankton blooms are self-evident in the imagery and correlate well with the CTD data.

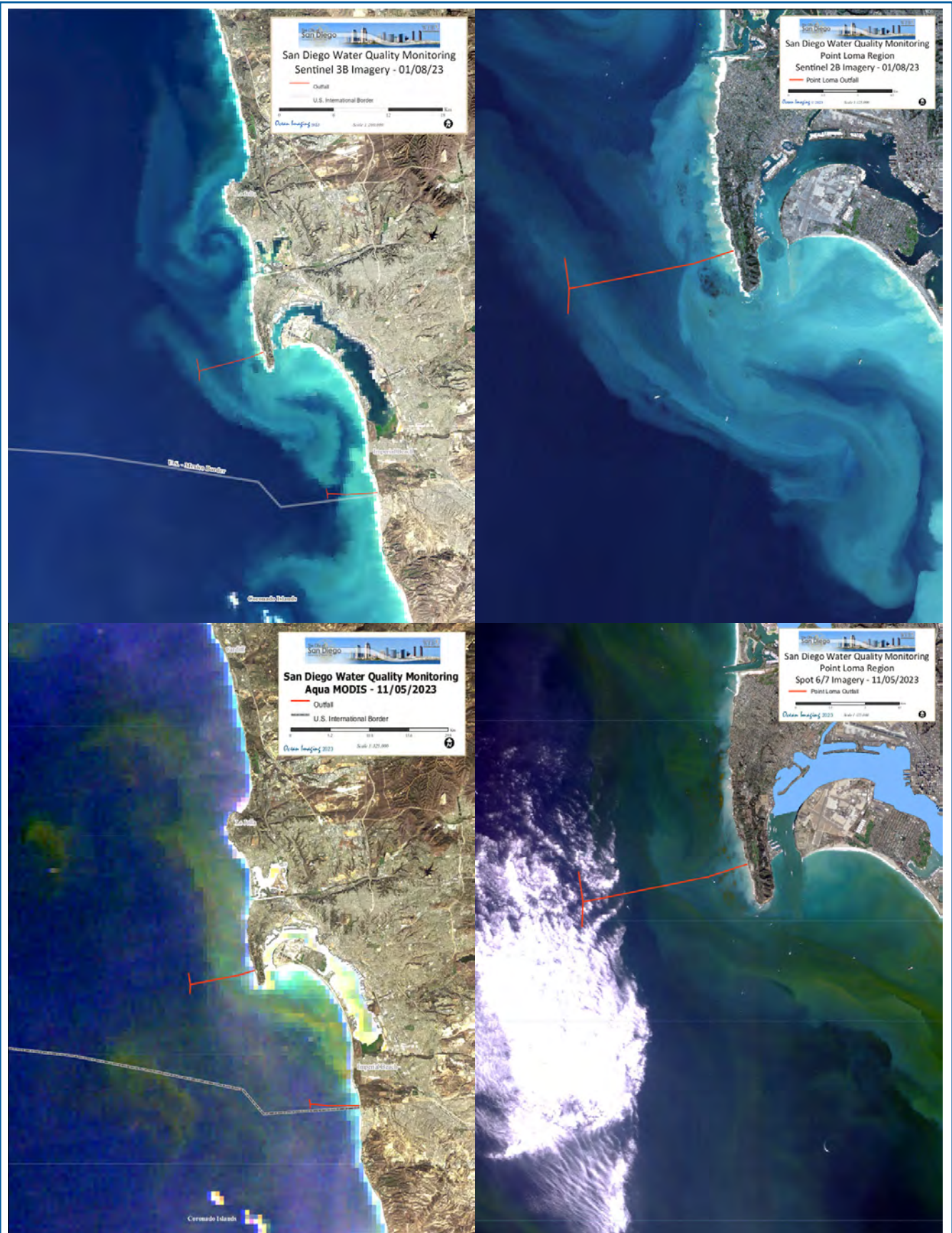


Figure 10. Sentinel 3 images (left side) and the higher resolution SPOT and Sentinel 2A images (right side) showing the turbid water and strong phytoplankton blooms extending from the northern part of this projects focus area all the way down into the South Bay region on 01/08/23 (top) and 11/05/23 (bottom).

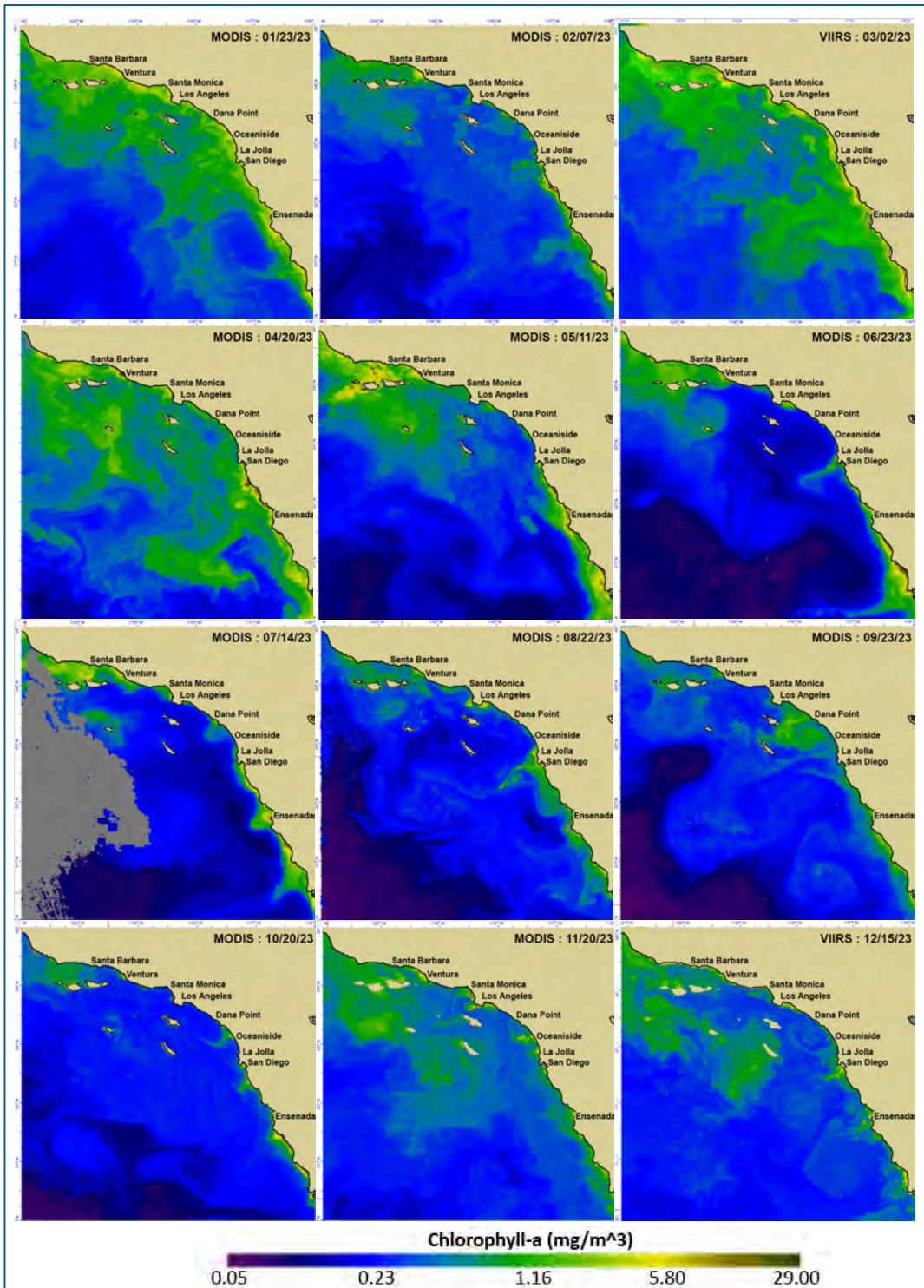


Figure 11. Representative MODIS- and VIIRS-derived chlorophyll images for each month of 2023 showing high levels of chlorophyll-rich water in the SCB during the months of January through April likely due to the heavy rainfall and resulting eutrophication combined with coastal upwelling. SCB-wide levels decreased during the summer months and increased again in November and December, caused by the California Current bringing nutrient-rich water down into the region.

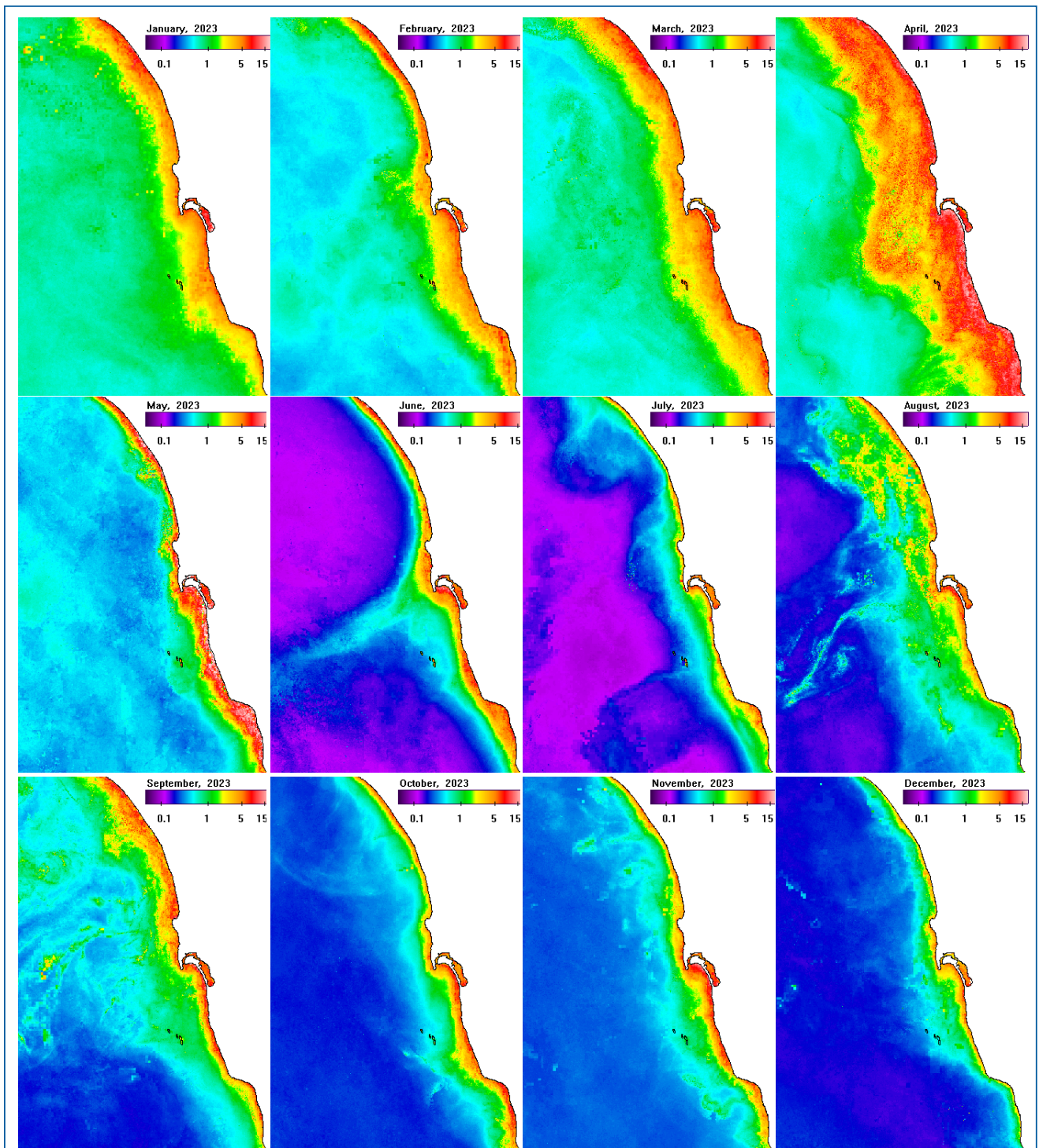


Figure 12. Monthly chlorophyll (mg/m^3) composites of the San Diego County coastal and offshore area derived from 300m and 1km MODIS, VIIRS and OCLI imagery generated by Mati Kahru of Scripps Institution of Oceanography in cooperation with OI as part of a SDPUD-funded project to study a long-term time series of satellite imagery to assess phytoplankton abundance and extent possibly related to increasing eutrophication of the ocean in this region.

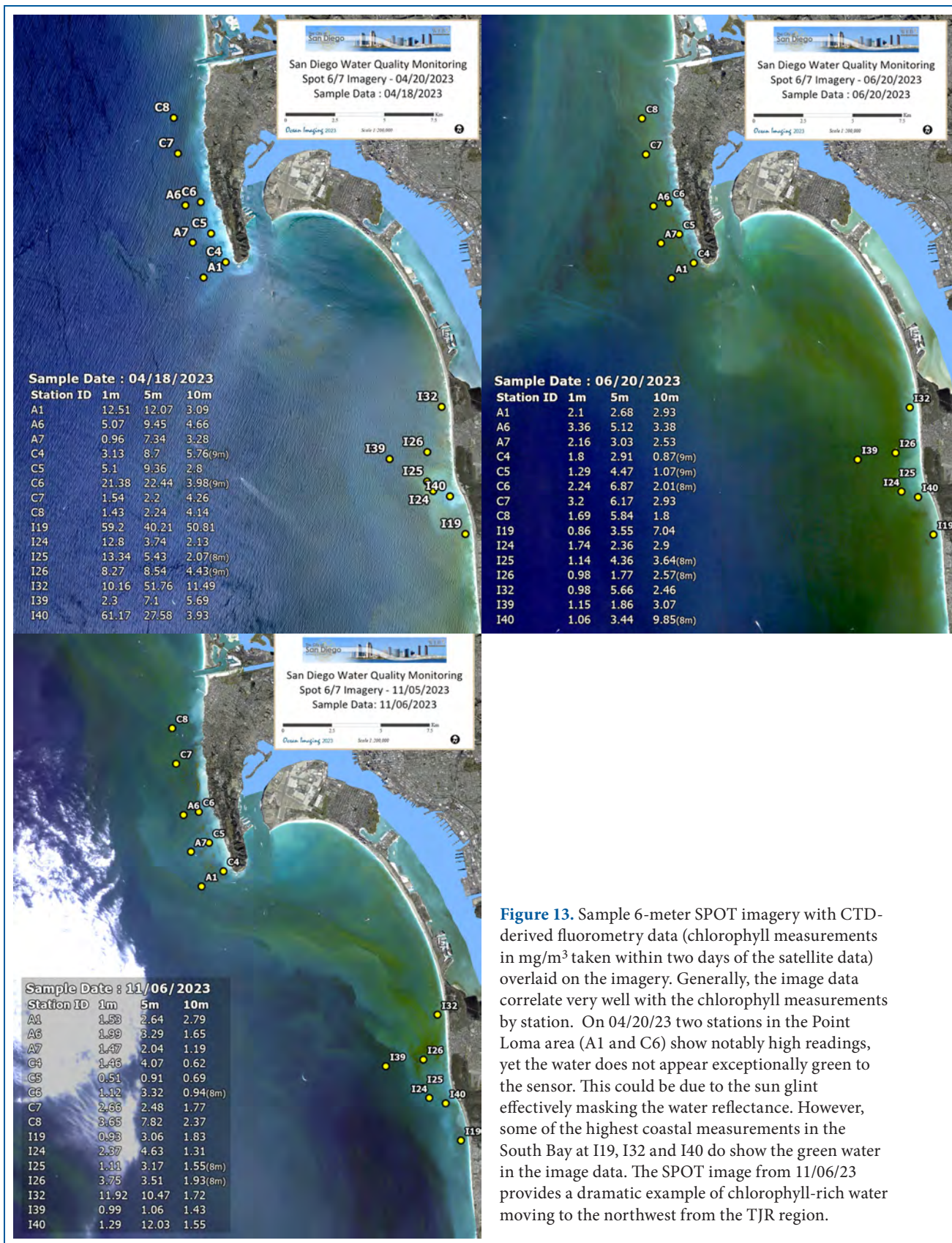


Figure 13. Sample 6-meter SPOT imagery with CTD-derived fluorometry data (chlorophyll measurements in mg/m³ taken within two days of the satellite data) overlaid on the imagery. Generally, the image data correlate very well with the chlorophyll measurements by station. On 04/20/23 two stations in the Point Loma area (A1 and C6) show notably high readings, yet the water does not appear exceptionally green to the sensor. This could be due to the sun glint effectively masking the water reflectance. However, some of the highest coastal measurements in the South Bay at I19, I32 and I40 do show the green water in the image data. The SPOT image from 11/06/23 provides a dramatic example of chlorophyll-rich water moving to the northwest from the TJR region.

3.2 The South Bay Ocean Outfall Region

The South Bay International Wastewater Treatment Plant (SBIWTP) switched from advanced primary to secondary treatment in January 2011. This change resulted in the reduction of total suspended solids (TSS) concentrations from an average of 60 mg/L for several years prior to the change to the TSS loads reading consistently below 20 mg/L since 2012. Prior to 2011, a distinct effluent signature was regularly detected in multispectral imagery as per the seasonal fluctuation described above. Since then, the effluent signature continues to be observed with multispectral color and thermal imagery during months with weak vertical stratification, however, more intermittently. On occasion the signature is distinctly discernable in thermal images (indicating it has fully reached the ocean surface), but undetectable in the color imagery. We theorize this is due to the reduction in TSS concentrations.

The SBOO wastewater plume generally remains well below the surface between approximately late March and November due to vertical stratification of the water column. During that period, it usually cannot be detected with multispectral aerial and satellite imagery, which penetrate the upper 7 to 15 meters (depending on water clarity), nor can it be detected with thermal IR imaging, which does not penetrate below the surface. Seasonal breakdown of the vertical stratification results in the plume's rise closer to the surface or to actually reach the surface between approximately late November and April when it can often be detected with satellite imaging. This concept held true in 2023, as the last observation of a SBOO surface plume during the beginning of the year was on 03/24/23 and then was not seen again in the image data until 10/24/23. In total, there were 22 instances during which the SBOO effluent plume was observed in 2023 out of the 77 high resolution satellite scenes acquired and processed. Of the 22, two were instances of the plume observed by different satellites on the same day. This equates to 20 days when the plume was visible in the high-resolution imagery – only one more than observed in 2022, but above the average

percentage of SBOO plume surface observations per days imaged when compared to the previous 11 years (25.9% vs. 18.6% in 2023). The effluent surface plumes are most often seen moving to the south or as a stagnant body, however there were five days on which the SBOO effluent was observed moving to the north, further into San Diego waters. The 01/31/23 image (Appendix A) provides an example of a large SBOO plume being pushed northward.

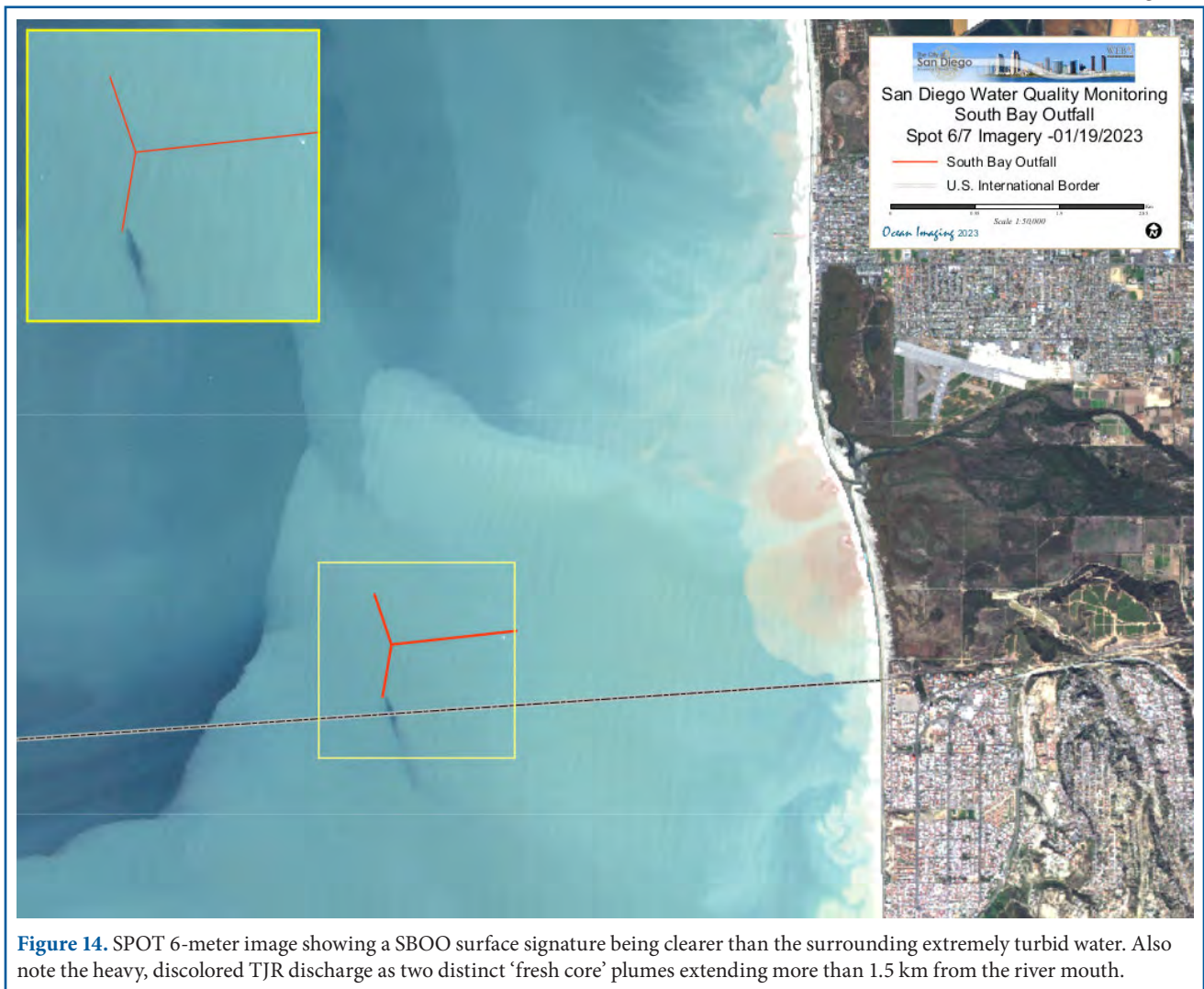
Appendix A includes the 2023 SPOT, Sentinel 2 and Landsat imagery on days which the SBOO plume was detected. There were two occurrences when either Sentinel 2A or 2B data were acquired within minutes of Landsat or SPOT 6/7 data providing a near time-coincident validation of features observed in the imagery.

As has been the case in previous years, there was an occurrence when the SBOO effluent plume appeared in the imagery as a patch of clearer water breaking the more turbid water on the surface. As discussed in prior reports, the clear effluent signal in the imagery is most likely due to the contrast between the higher turbidity coastal surface waters and the 'normal' level of turbidity of the effluent water breaking the surface. It is also possible that the effluent plume became somewhat diluted on its way to the surface if weak vertical stratification did exist, thus slowing down its rise in the water column. Figure 14 provides an example of this situation as well as the satellite's view of two large, discolored discharge plumes flowing from the TJR.

The months of January, February, November, and December exhibited the highest frequency of 2023 SBOO effluent plume observations in the satellite data. As has been documented in previous reports, it is typical to see the highest number of SBOO surface plumes during these months. As is typically the case, the relatively frequent effluent surface manifestations that occurred during this time period were most probably the result of two primary factors: the lack of strong vertical stratification during the winter months and relatively weak subsurface currents over the SBOO which allowed the undispersed effluent to

reach the surface. According to the 2023 IBWC Transboundary Flow Report, there were 25 monthly documented instances of groundwater, urban runoff, storm water, treated sewage wastewater, and untreated sewage wastewater from infrastructure deficiencies and other sources in Mexico coming across the U.S.-Mexico border and into the SBOO pipeline, Tijuana Estuary and U.S. coastal waters. Most of these transboundary flows occurred in the TJR main channel resulting on billions of gallons coming into the U.S. system and waters throughout 2023 (SDRWQCB, 2024). As is discussed above, while the satellite imagery documented many of the related SBOO effluent surface manifestations and pollution discharge from the TJR, several of these instances during the summer months are not seen in the satellite data. This may be because, while many were

documented as caused by rain and weather events, a significant percentage during the months of June through August were considered dry weather flows from numerous sources in Mexico that exceeded the San Diego-Tijuana wastewater system capacity (SDRWQCB, 2024). The relatively lower TJR discharge rate during June and July as seen in Figure 4 above also offers evidence as to why these flows are not observed as expansive, discolored TJR plumes. Figure 15 shows the SBIWTP Effluent Flow rate (EFF Flow) and the Effluent Total Suspended Solids (EFF TSS) over the 2023 period plotted with the dates on which SBOO effluent was observed on the surface of the ocean in the high-resolution satellite imagery. There are a few notable spikes in EFF Flow during January and August, likely due to rainfall events. As can be seen in the trend line, the EFF flow averaged

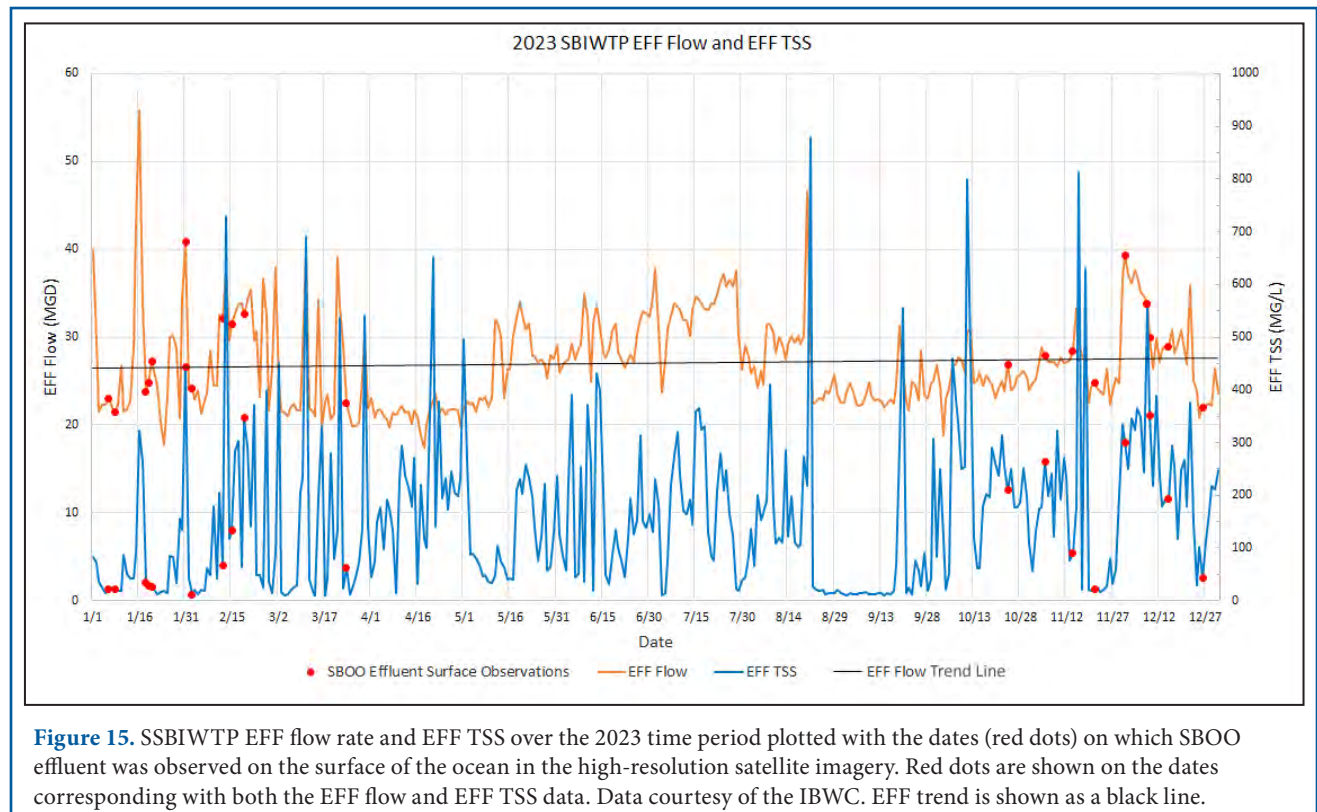


27.04 million gallon per day (MGD) for the year which is higher than the maximum capacity (25 MGD) of the treatment plant. The EFF TSS were highly variable compared to past years, however there is no correlation of the SBOO effluent surface observations to TSS percentage. Of the 20 SBOO effluent observations, 12 occurred when the EFF flow rate exceeded 25 MGD, but it cannot be concluded that the additional flow diverted through SBIWTP resulted in the effluent reaching the ocean's surface more often. It should also be noted that the higher flow rates seen from May through the middle of August did not result in the effluent breaking through the pycnocline during these months. This corroborates the belief that the instances of effluent reaching the surface almost always occur because of seasonal changes in ocean conditions when the water column stratification breaks down and are not always related to a higher flow rate through the system.

A total of 19 shoreline stations, ranging from Mission Beach to northern Baja (across the US/Mexico border) are sampled weekly by City of San Diego staff to monitor the levels of three types of

fecal indicator bacteria (i.e., total coliform, fecal coliform, *Enterococcus* bacteria) in recreational waters. An additional 15 nearshore (kelp) stations are also sampled weekly to monitor Fecal Indicator Bacteria (FIB) and a range of water quality parameters (i.e., temperature, salinity, dissolved oxygen, pH, transmissivity, Chlorophyll-a, colored dissolved organic matter (CDOM)). Furthermore, 69 offshore stations are sampled quarterly to monitor both water quality conditions and one or more types of FIB. PLOO stations are located along, or adjacent to, the 18, 60, 80, and 98-m depth contours, and SBOO stations are located along the 9, 19, 28, 38, and 55-m depth contours.

The City Marine Microbiology Laboratory (CMML) follows guidelines issued by the U.S. Environmental Protection Agency (USEPA) Water Quality Office, State Water Resources Control Board (SWRCB) including the 2019 Ocean Plan, the California Department of Public Health (CDPH), and Environmental Laboratory Accreditation Program (ELAP) with respect to sampling and analytical procedures (Bordner, et. al., 1978,



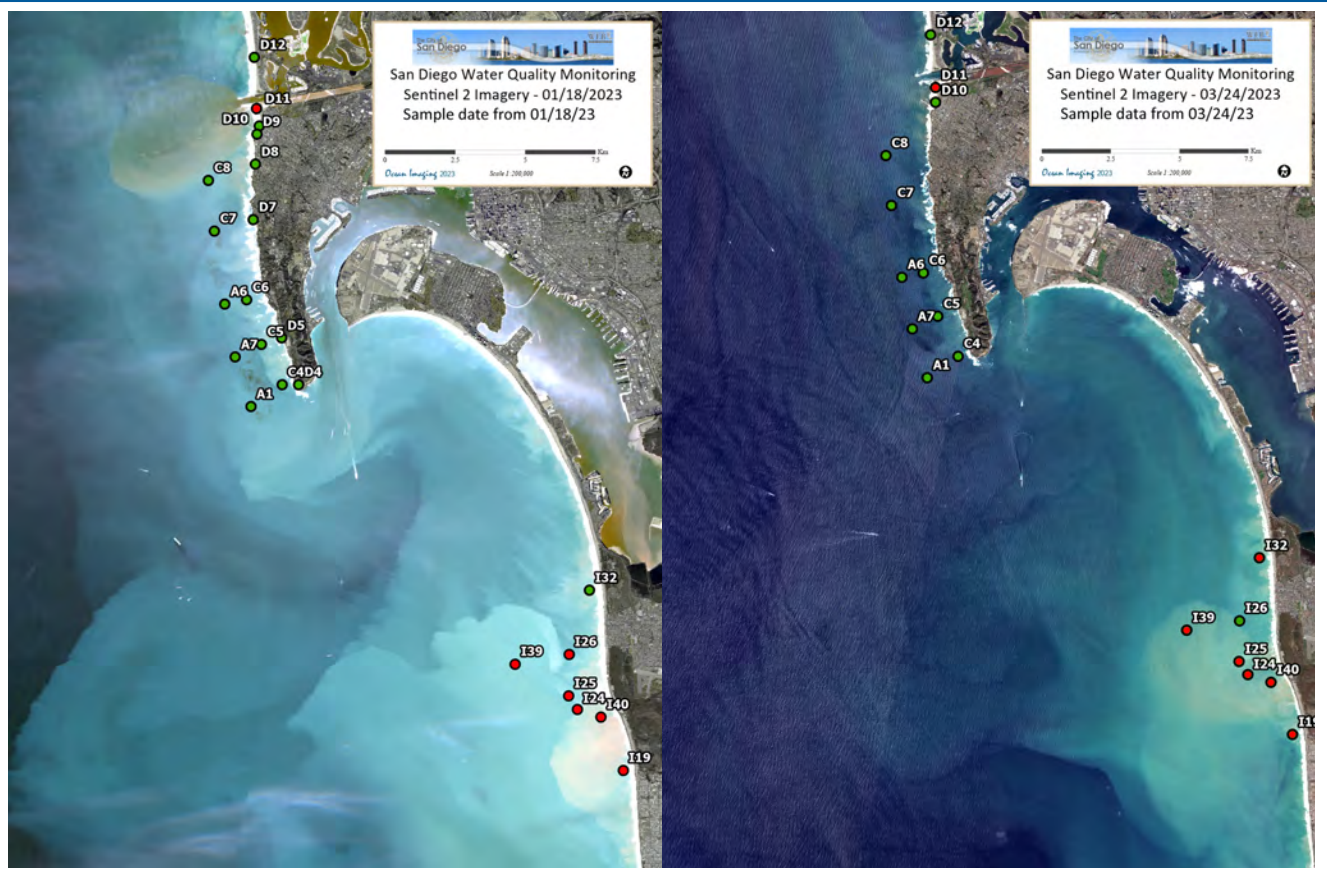
American Public Health Association (APHA), 2012, CDPH, 2019, USEPA, 2014). All bacterial analyses were initiated within eight hours of sample collection and conformed to standard membrane filtration techniques, for which the laboratory is certified (ELAP Field of Testing 126). FIB densities were determined and validated in accordance with USEPA and APHA guidelines as follows in APHA, 2012.

In 2023, the sampling area of the SBOO/Tijuana River outflow region experienced 71 days on which the field sampling showed FIB measurements exceeding the single sample maximum for fecal coliform density for one or more sampling stations as defined by the 2019 California Ocean Plan (the single sample maximum fecal coliform density at a site will not exceed 400 per 100 mL) (SWRCB, 2019). The offshore SBOO region, which includes the stations over the SBOO wye experienced only two days of elevated bacteria levels at depths of six meters or shallower and the nearshore region (referred to as the “kelp” region in previous reports) experienced 32 days on which the bacteria levels were deemed elevated. There were 52 sampling days when at least one shore station showed elevated levels. The total number of sampling days for all three SBOO areas totaled 148 in 2023 and 96 in 2022. Therefore, in 2023 for the three sampling regions combined, 48.0% of the sampling days resulted in elevated bacteria levels at one station or more, which is less than the 58.3% recorded in 2022 (using the same 2019 California Ocean Plan standards). As has been typical in recent years, the majority of the samples showing elevated levels were recorded at the shore stations. Elevated levels offshore near the SBOO wye are rare. Of the two days when elevated bacteria levels were recorded at an offshore station, neither (I11 and I18) were in close proximity to the SBOO wye.

The satellite imagery showing substantial discharge from the TJR region often correlated well with times when the shoreline and kelp area sampling showed elevated bacteria levels. In past years, heavy and/or persistent rainfall was often the most plausible cause for most of the elevated bacteria samples and turbid waters seen in the remote sensing data. However,

given the increasing problems with untreated sewage and other pollutants flowing out of the TJR for much of the year (SDRWQCB, 2024 and Little, 2024), that premise is no longer valid in many cases. Typically, the best water quality and clarity in the South Bay region is observed during the dry season from May through August. This was generally true in terms of water clarity observed in the image data during the summer of 2023, however as noted above, there were several transboundary flow incidents due to ‘dry weather flows from numerous sources in Mexico’ that exceeded the San Diego-Tijuana wastewater system capacity (SDRWQCB, 2024). These breaches to the system undoubtedly contributed to many of the elevated FIB measurements. Figure 16 offers a few examples of the bacteria sample data overlaid on top of imagery acquired on the same day of sampling. Note the very turbid water emanating from the TJR river and trending north in both images. The satellite data were acquired on 01/18/23 and 03/24/23 following heavy, multi-day rain events and SBIWTP EFF flow rates of 55.77 MGD on 01/16/23, 39.11 MGD on 03/21/23 and 33.44 MGD on 03/22/23.

Figure 17 offers an example of a day when, with the exception of phytoplankton blooms, the turbidity levels were low, and the general water clarity was good. The image was taken eight days after Hurricane Hilary moved through the region allowing the ocean conditions time to stabilize. Nutrients in the runoff possibly increased the magnitude and extent of the plankton blooms. Eight sampling stations (three nearshore and five shoreline), however, had fecal coliform densities exceeding the single sample maximum, in all probability the result of the transboundary flow problems. Red dots at SBOO stations indicate fecal coliform densities in exceedance of the fecal coliform SSM (2019 Ocean Plan). Red dots at PLOO stations indicate exceedances of the total coliform, fecal coliform and/or enterococcus SSMs (2015 Ocean Plan). Green dots identify stations at which the FIB levels were in compliance. The table to the left of the image shows the measurement values by depth for each station with elevated bacteria levels.



Station	Depth (M)	Enterococcus	Fecal Coliform	Total Coliform	Station	Depth (M)	Enterococcus	Fecal Coliform	Total Coliform
D11	NA	120	60	800	D11	NA	280	NA	NA
I19	2	3600	4400	16000	I19	2	840	2200	16000
	6	1000	1000	10000		6	860	1200	16000
	11	2600	2200	16000		11	520	1000	11000
I24	2	1600	3400	16000	I24	2	660	3200	16000
	6	2200	1100	8400		6	640	760	6800
	11	2800	1200	8000		11	700	580	7200
I25	2	920	560	7000	I25	2	460	2400	16000
	6	1400	800	6000		6	280	560	8600
	9	3800	880	10000		9	300	900	6200
I25	2	1100	320	5000	I32	2	76	160	2200
	6	760	260	3600		6	62	140	1400
	9	1400	760	9200		9	920	460	8200
I39	2	2400	2200	12000	I39	2	620	3200	16000
	12	560	120	4000		12	2	8	40
	18	1100	220	3000		18	6	2	120
I40	2	7400	10000	16000	I40	2	620	1800	13000
	6	3200	1100	7000		6	740	1200	8000
	9	4400	800	16000		9	1100	1600	16000

Figure 16. Sentinel 2 data with near-surface bacterial sampling data overlaid from the same day of image acquisition. Red dots at SBOO stations indicate fecal coliform densities in exceedance of the fecal coliform SSM (2019 Ocean Plan). Red dots at PLOO stations indicate exceedances of the total coliform, fecal coliform and/or enterococcus SSMs (2015 Ocean Plan). Green dots identify stations at which the FIB levels were in compliance. The tables below each image show the measurement values by depth for each station with stations and elevated bacteria levels in red text.

Station	Depth (M)	Entero	Fecal	Total
I26 (08/28/23)	2	20	80	1000
	6	140	500	16000
	9	80	620	2400
I32 (08/28/23)	2	2	10	60
	6	240	1800	16000
	9	320	2000	16000
I39 (08/28/23)	2	160	520	4000
	12	2	8	20
	18	2	4	38
S0 (08/29/23)	NA	3200	3600	16000
S3 (08/29/23)	NA	24	2000	1600
S5 (08/29/23)	NA	360	800	8400
S11 (08/29/23)	NA	460	740	9400
S12 (08/29/23)	NA	5200	12000	16000

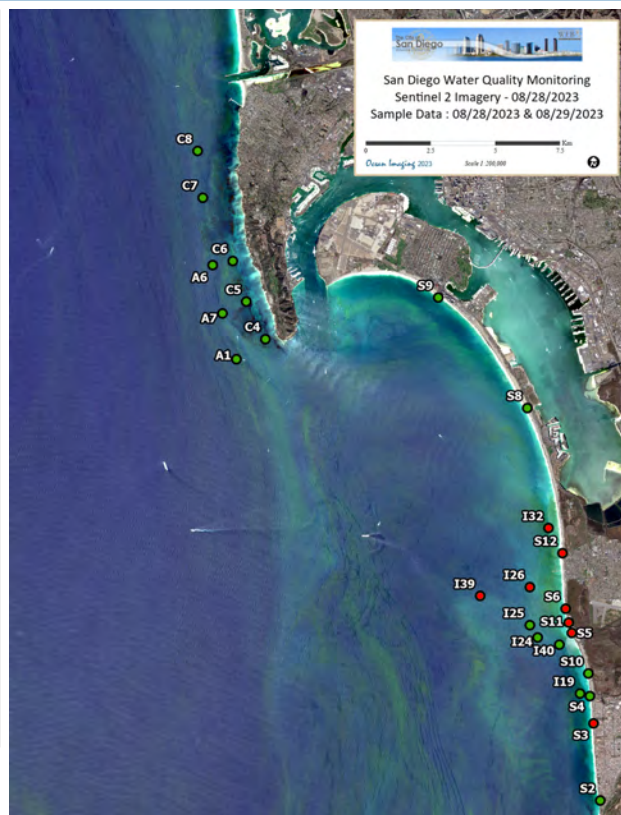


Figure 17. A Sentinel 2 image from 08/28/23 with near-surface bacterial sampling data overlaid from offshore (08/28/23) and shoreline (08/29/23) stations. Phytoplankton blooms are evident, however low turbidity, the lack of a significant TJR discharge plume and lower than average river flow rates on 08/28 and 08/29 (114 and 108 MGD vs. the annual average of 187 MGD) point to other reasons for the high FIB readings that are not readily visible in the imagery.

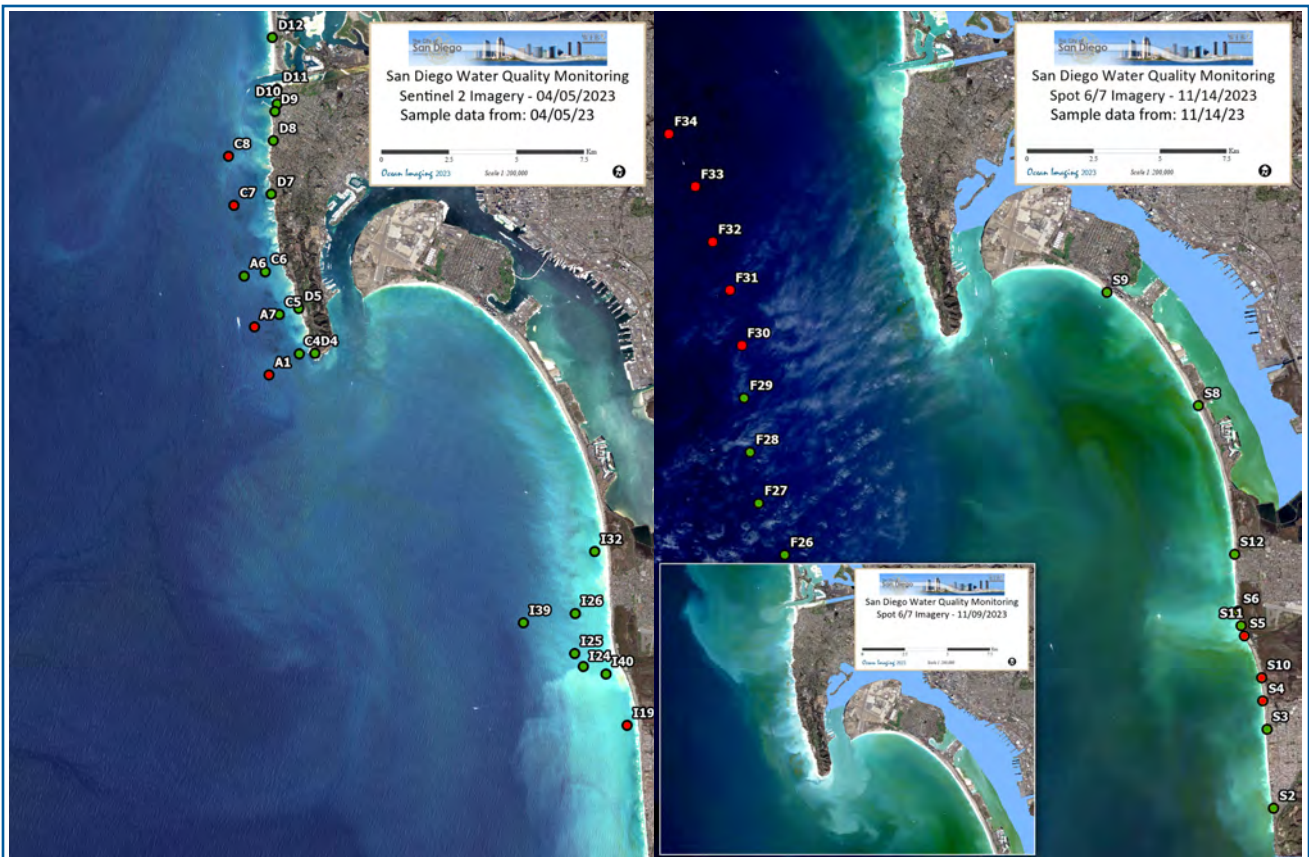
3.3 The Point Loma Outfall Region

After its seaward extension in 1993, the Point Loma Ocean Outfall (PLOO) is one of the deepest and longest wastewater outfalls in the world, discharging at the depth of 320 feet (~97.5 meters), 4.5 miles (7.25 kilometers) offshore. The outfall's plume is generally not observed directly with multispectral color or thermal imagery. It appears to not reach the surface waters, even during the winter months when the water column's vertical stratifications are weakened. We believe that on some occasions we have observed the plume's extents indirectly through an anomalous lateral displacement of thermal or chlorophyll features around the outfall wye. This effect can be explained by the doming up of the discharged effluent and laterally displacing the near-surface waters above it.

In 2023 the Point Loma region was affected by conditions already described for general San Diego County: significant seasonal rainfall during the months of January through March and then again in November through December and almost no rainfall during the months of April through August – apart from Hurricane Hilary in late August. Similar to past years, compromised water clarity was likely a result of runoff from the San Diego River and Mission Bay bringing sediment-laden water inside and outside the Point Loma kelp bed after the rain events described above.

The 2023 Point Loma shoreline, kelp and offshore bacterial sampling resulted in a similar number of elevated bacteria measurements when compared to the previous year as defined by the 2015 California Ocean Plan (Total coliform density will not exceed 10,000 per 100 mL; or Fecal coliform density will not exceed 400 per 100 mL; or Total coliform density will not exceed 1,000 per 100 mL when the ratio of fecal/total coliform exceeds 0.1; or enterococcus density will not exceed 104 per 100 mL) (SWRCB, 2015). Shoreline field sampling yielded 12 days on which one or more stations experienced high bacteria counts. Offshore and kelp station sampling resulted in 7 days and 1 day respectively when stations

recorded excessive FIBs. Figure 18 presents examples when multiple stations in the Point Loma sampling area showed high FIB numbers on 04/05/23 and 11/14/23. The elevated bacteria at PLOO kelp stations on April 5 are possibly related to discharge originating from the San Diego River. There is no evidence of the wastewater plume at the surface in the imagery from November 14. Instead, all bacterial exceedances were found at depths of 80 m or more, indicating that the plume was trapped by the pycnocline barrier and so any surface presence would not be visible in the satellite imagery.



Station	Depth (M)	Entero	Fecal	Total	Station	Depth (M)	Entero	Fecal	Total
A1	1	2	10	110	F30	25	2	NA	NA
	12	60	600	2200		60	2	NA	NA
	18	100	680	5400		80	320	NA	NA
				98		320	NA	NA	
A7	1	2	6	38	F31	1	2	NA	NA
	12	94	360	2200		25	2	NA	NA
	18	110	980	4800		60	2	NA	NA
				80		660	NA	NA	
C7	1	2	2	16	98	460	NA	NA	
	12	18	68	360	F32	1	2	NA	NA
	18	64	500	2200		25	2	NA	NA
				60		2	NA	NA	
				80		620	NA	NA	
C8	1	2	2	4	98	720	NA	NA	
	12	66	400	1400	F33	1	2	NA	NA
	18	78	480	1000		25	2	NA	NA
				60		2	NA	NA	
				80		300	NA	NA	
I19	2	600	3000	16000	98	200	NA	NA	
	6	100	180	4800	F34	1	2	NA	NA
	11	46	50	1200		25	2	NA	NA
						60	2	NA	NA
				80		20	NA	NA	
					98	200	NA	NA	
					S0	NA	5400	6800	16000
					S4	NA	300	640	1200
					S5	NA	400	660	1600
					S10	NA	460	1600	6000

Figure 18. Sentinel 2 and SPOT imagery acquired on 04/05/23 and 11/14/23 respectively with near-surface bacterial sampling data overlaid from the same day. An inset SPOT image from 11/09/23 shows heavy discharge from the San Diego River and Mission Bay along with coastal runoff a few days prior to the 11/14 data. However bacterial exceedances on 11/14 were all at 80 meters or deeper indicating that they were related to the PLOO effluent plume trapped beneath the pycnocline barrier. Stations showing FIB measurements exceeding the single sample maximum as defined by the 2019 California Ocean Plan are shown as red dots for the SBOO region and as defined by the 2015 California Ocean Plan metrics for the PLOO region. The table shows the measurement values by depth for each station that exceeded single sample maximums.

3.4 Kelp Variability

One observation provided by the satellite image archive is the continuing variability in the size of the Point Loma kelp bed over time (Figure 19). Table 4 shows the area in km² of three notable kelp beds in the San Diego region over the past 16 years. The September and October dates were chosen to represent the kelp bed canopy coverage for each year since spring and fall are considered to be the time periods when the canopy size is at or near its peak - with fall being the traditionally preferred time period to map kelp using remote sensing techniques. The estimated size of the Point Loma bed canopy in the fall of 2023 (2.14 km²) was significantly smaller than the average canopy coverage for the prior 15-year period from 2008-2022 (4.07 km²). As has been reported in previous years, the satellite data show the bed begin to decrease in size during February of 2016, perhaps due to the storm events taking place during early to mid-January, effects from the 2014-2016 strong El Niño event and/or the Northeast Pacific marine heat wave (Di Lorenzo, 2016). Noted in the 2017 and 2018 annual reports, the kelp bed looked to be coming back in January of 2017, but then decreased in size as the year progressed resulting in much smaller than average canopy coverage by the end of that year. Using the fall imagery as an indicator for annual health, the bed size appeared to be stabilizing since the 2016 and 2017 lows, however the 2023 computed area shows a considerable decrease in size. Contrary to previous years such as 2018, 2020 and 2021 when the canopy area exhibited significant intra-annual variability, in 2023 the bed size remained consistently depleted throughout the year (Figure 20). While there were significant differences in tidal heights at the time of each satellite image acquisition, tides cannot be flagged as the primary reason for the difference in canopy coverage observed in the satellite data. There were days when the areal coverage was high, but the tide level was also high and vice versa when the imagery revealed smaller bed size, but the tides were relatively low.

Canopy coverage for each year in Table 4 was computed by first running a Normalized Difference Vegetation Index (NDVI) classification followed by a commonly used unsupervised iso cluster classification algorithm (ESRI, 2024). It is important to point out that the canopy coverages shown in Table 4 may differ slightly from those provided in the Southern California Bight Regional Aerial Kelp Survey reports. (<https://www.sandiego.gov/public-utilities/sustainability/ocean-monitoring/reports/kelp-survey-report-archives>). This is because the canopy areas for the Point Loma bed computed for those reports are averages of four surveys performed throughout the year; while the coverage estimates shown in this report are taken from single satellite images acquired during the fall time period chosen to represent the maximum coverage experienced during that time of year. Tide levels were not a factor in the inter-year comparison as there was little variability in tide level between the years (often approximately two feet or less). However, due to the overflight times of these satellites, the canopy areas could be underrepresented compared to the kelp survey reports because the tide levels at the time of satellite data acquisition could vary significantly from the tides during the aerial surveys. The Imperial Beach and Tijuana beds have not been visible in the satellite data since 2015. It is being documented that kelp forests along the West Coast have been experiencing noteworthy variability in canopy size for the past several years, and thus warrants keeping a close watch on the health of the kelp beds in the San Diego region (Bell, et al. 2020, Schroeder 2019).

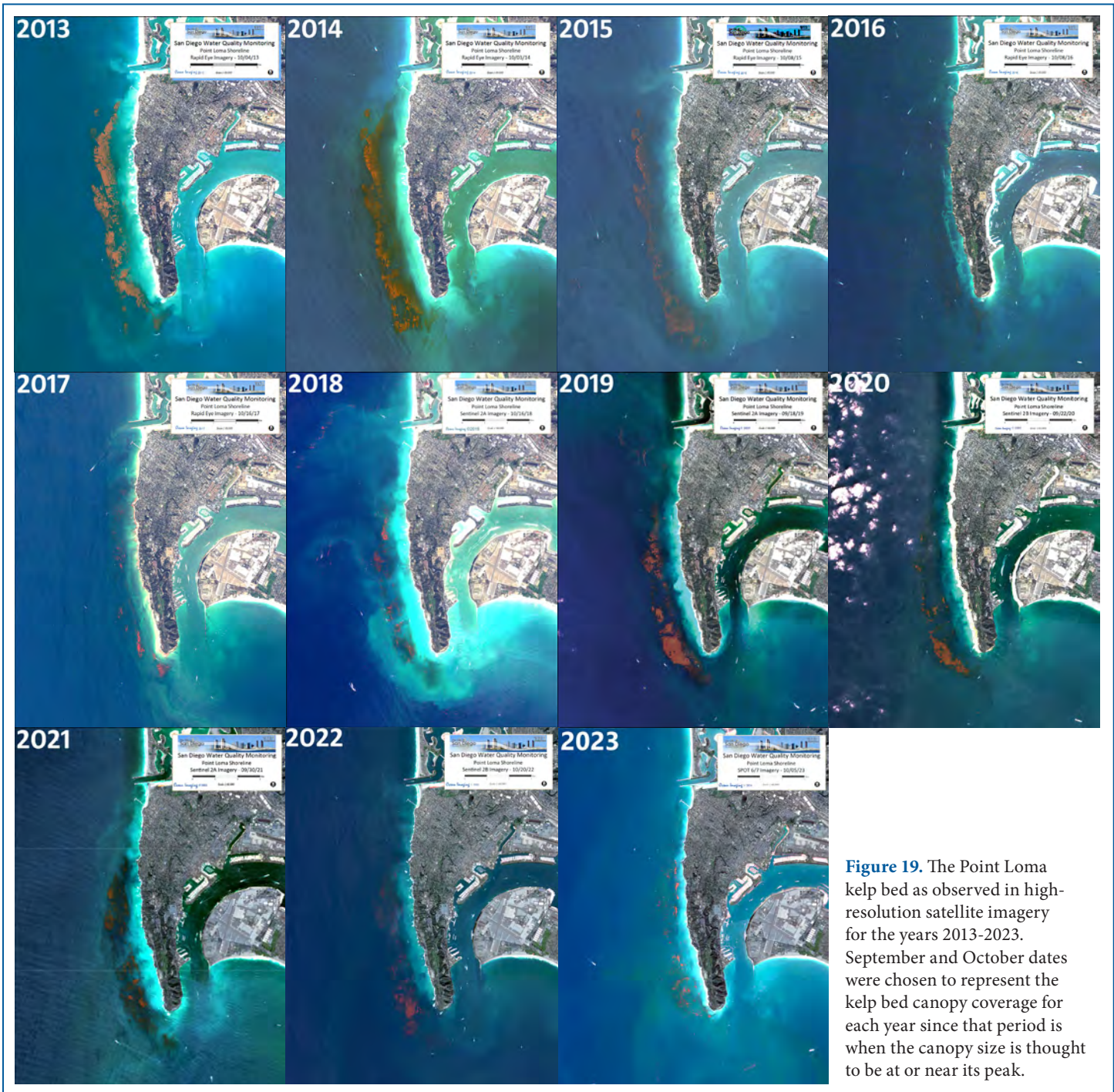


Figure 19. The Point Loma kelp bed as observed in high-resolution satellite imagery for the years 2013-2023. September and October dates were chosen to represent the kelp bed canopy coverage for each year since that period is when the canopy size is thought to be at or near its peak.

Table 4. Kelp canopy areas of three San Diego kelp beds measured from satellite imagery collected for this project.

Year	Date	Satellite	Kelp (km ²)		
			Point Loma	Imperial Beach	Tijuana
2023	10/05/23	SPOT 6/7	2.14	0.00	0.00
2022	10/20/22	Sentinel-2B	4.48	0.00	0.00
2021	09/30/21	Sentinel-2B	3.82	0.00	0.00
2020	09/22/20	Sentinel-2A	2.93	0.00	0.00
2019	09/18/19	Sentinel-2A	5.17	0.00	0.00
2018	10/16/18	Sentinel-2A	2.44	0.00	0.00
2017	10/04/17	RapidEye	1.05	0.00	0.00
2016	09/08/16	RapidEye	0.22	0.00	0.00
2015	09/17/15	Landsat 7	4.11	0.39	0.29
2014	09/14/14	Landsat 8	5.42	0.59	0.30
2013	09/23/13	RapidEye	5.89	0.19	0.05
2012	09/15/12	RapidEye	2.91	0.00	0.00
2011	09/01/11	RapidEye	1.99	0.00	0.00
2010	09/27/10	Landsat 7	6.01	0.00	0.00
2009	09/16/09	Landsat 5	5.96	1.01	0.21
2008	09/05/08	Landsat 7	8.66	0.82	0.01

* Average surface canopy coverage 2008-2022 = 4.07 km²

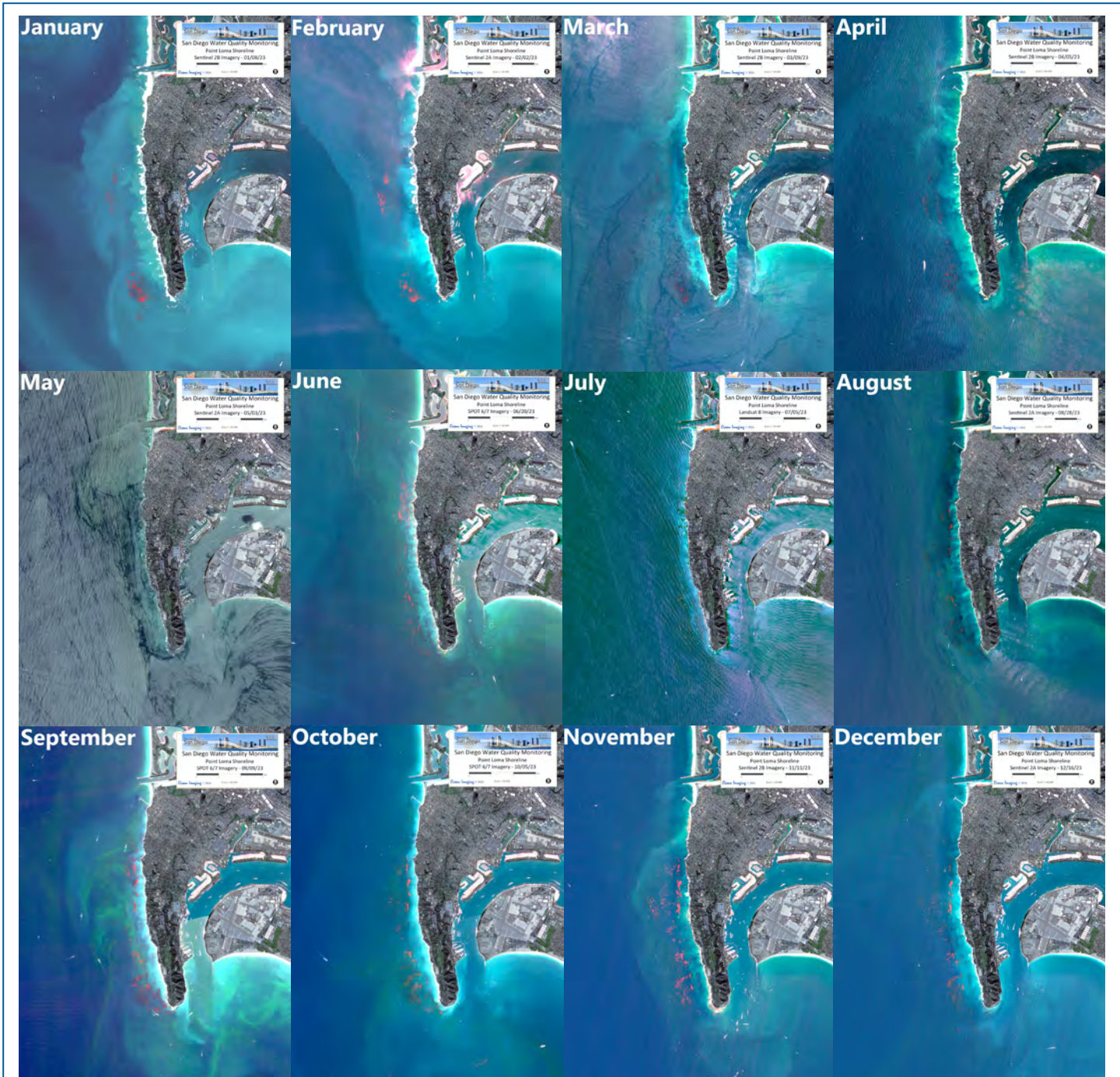


Figure 20. High-resolution satellite imagery documenting the 2023 month-to-month variability in the Point Loma kelp bed canopy coverage. The dates were chosen to best represent the maximum-observed canopy coverage for each month.

4. PRESENT AND FUTURE ENHANCEMENTS OF THE PROJECT

In 2016, OI began to generate ocean currents and other satellite- and model-derived oceanographic data products in a Web Map Service (WMS) Representational State Transfer (REST) format which would have been compatible with a WMS the City was working to implement. It was intended that all the OI-delivered data products, including all the satellite imagery would be delivered via OI's ArcGIS Server for easy ingestion into the City's WMS by fall of 2017. While this system was not implemented, OI is now developing a dashboard-style web portal to fill that purpose. The site will incorporate an interactive WMS to serve as a mechanism to better facilitate the visualization viewing of existing and future satellite image data products as well as any other tabular data sets the City chooses to host on the platform. Not only will the server give the user the capability to overlay different data types on top of each other (i.e., ocean currents on top of satellite imagery) it will significantly enhance the information experience providing fast and easy, near real-time access to the

many data products delivered as part of this project. Initially the site will be password-protected and for internal use only by SDPUD employees and their partners. The server will host present, near real-time imagery and tabular data as well as data from the previous one to two years. Discussions have also begun regarding the development of a public-facing data dashboard hosting most of the same datasets that have been vetted through the City's quality control procedures. As part of this process, the historical imagery, data, and reports will remain accessible via the existing web portal. If a public-facing dashboard style data portal is implemented by the City, OI will progressively work backwards in time to make all historical data available via this platform, including the archived imagery and HYCOM data products. Figure 21 shows a prototype of the dashboard presently in development.

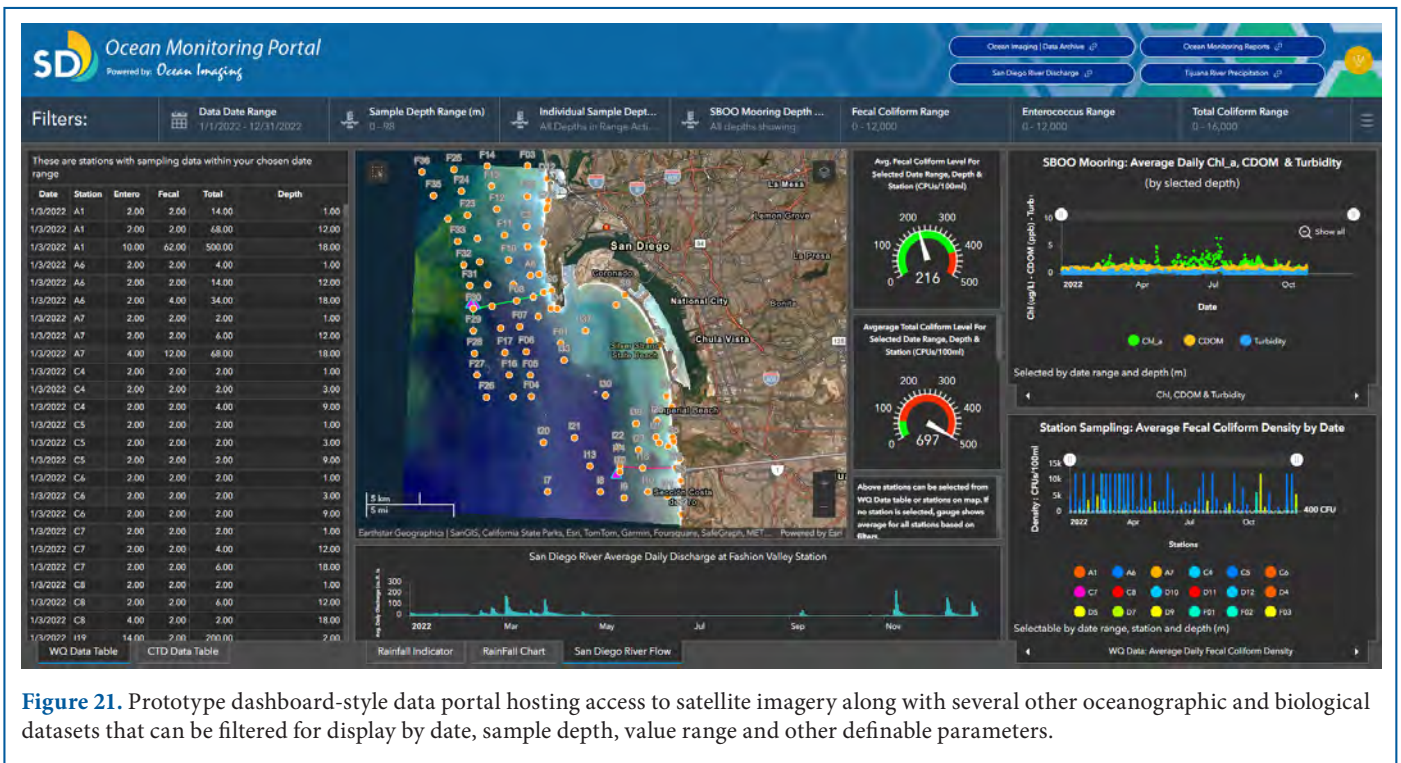
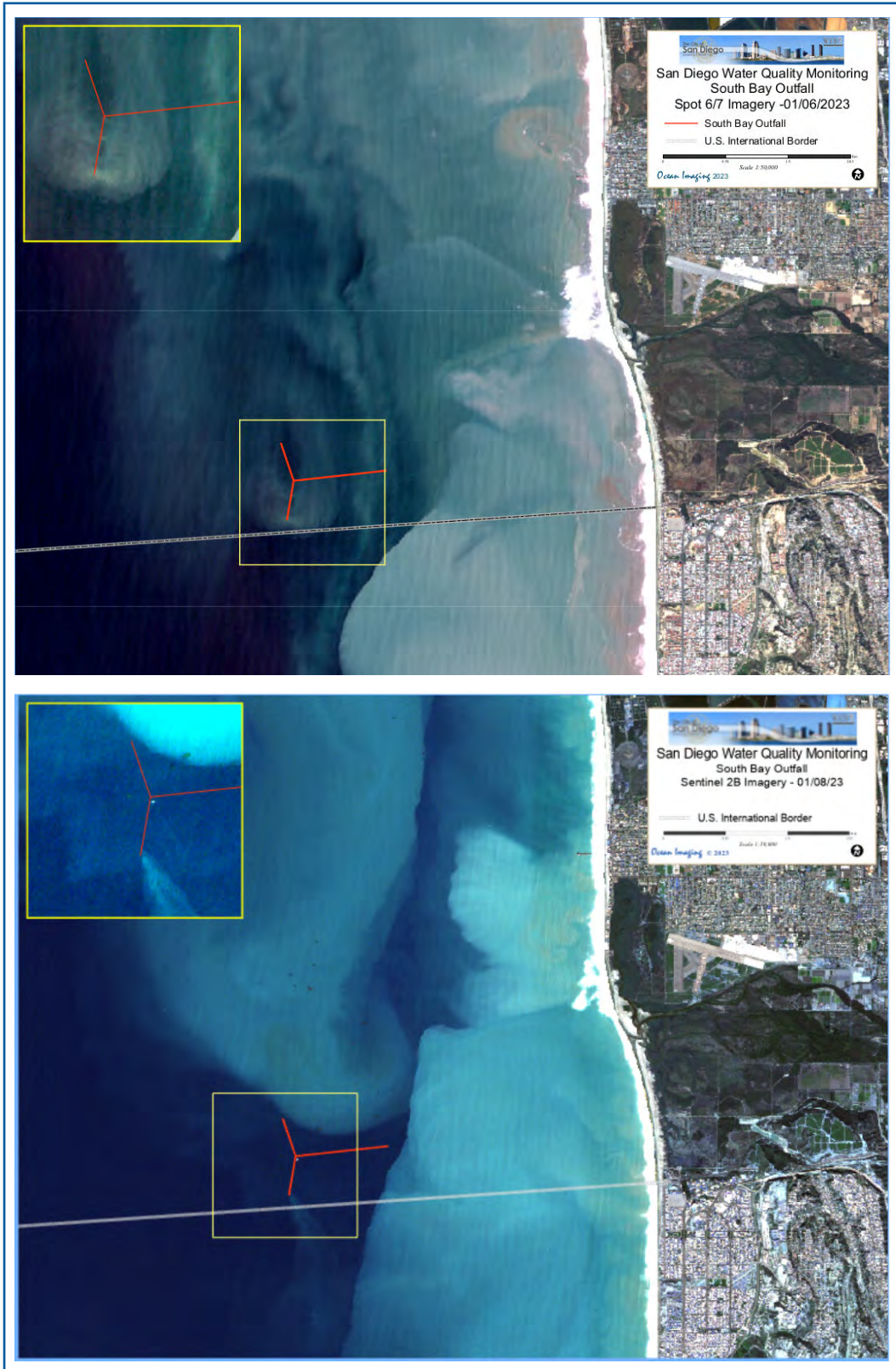


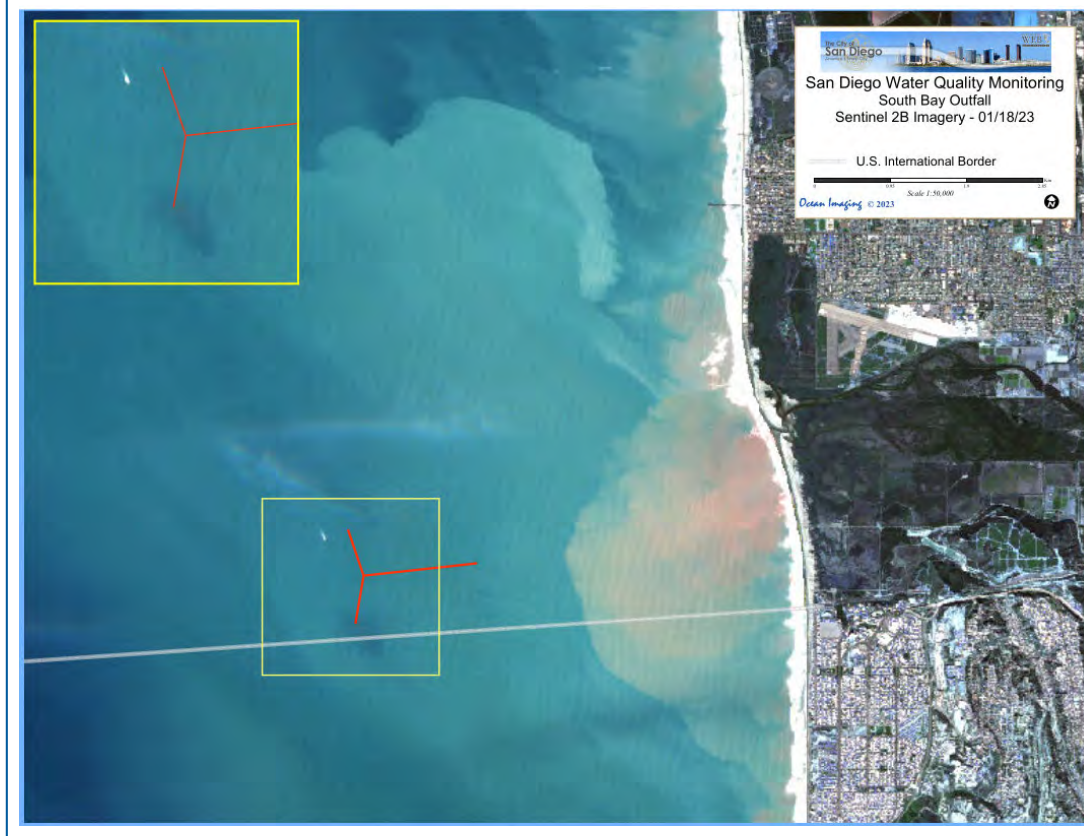
Figure 21. Prototype dashboard-style data portal hosting access to satellite imagery along with several other oceanographic and biological datasets that can be filtered for display by date, sample depth, value range and other definable parameters.

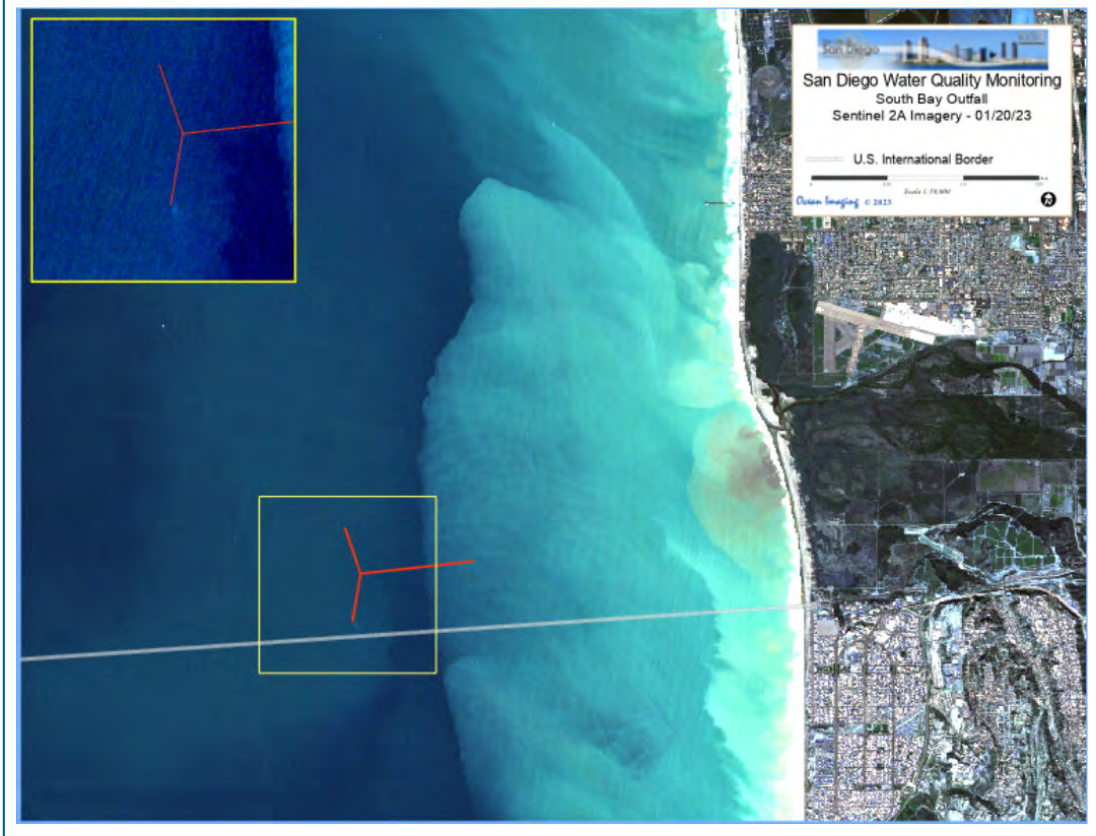
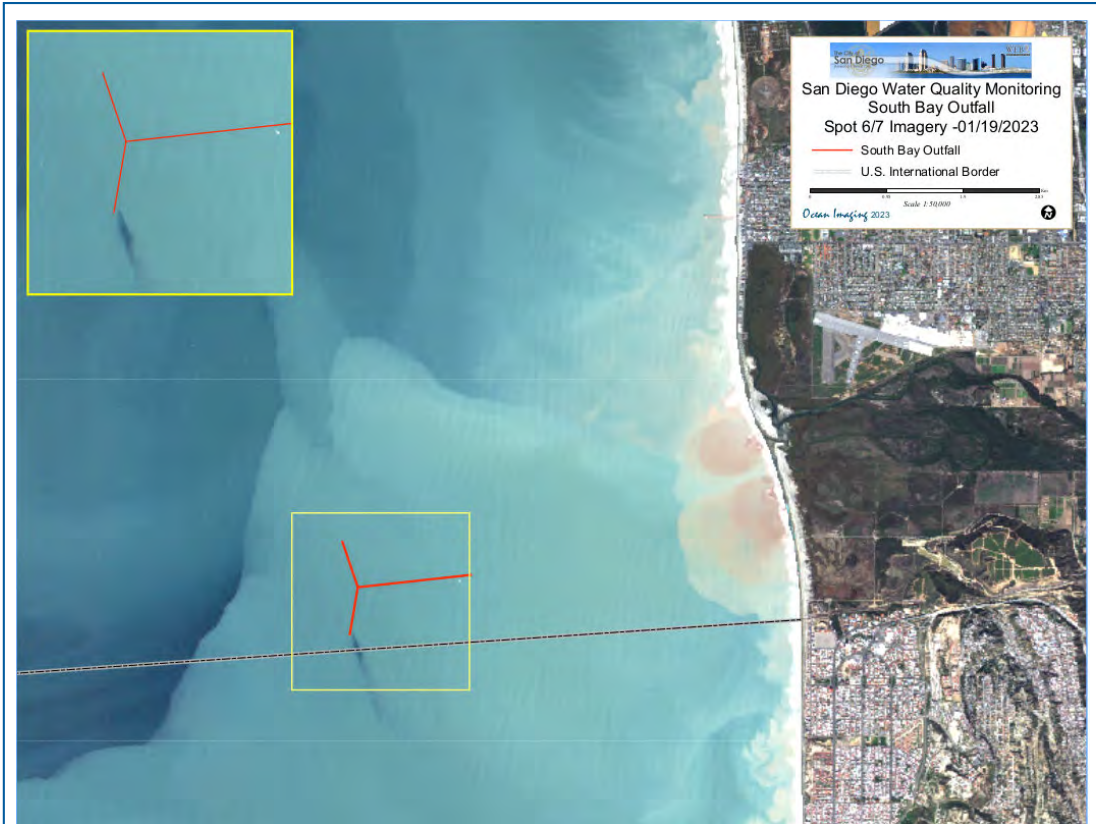
5. REFERENCES

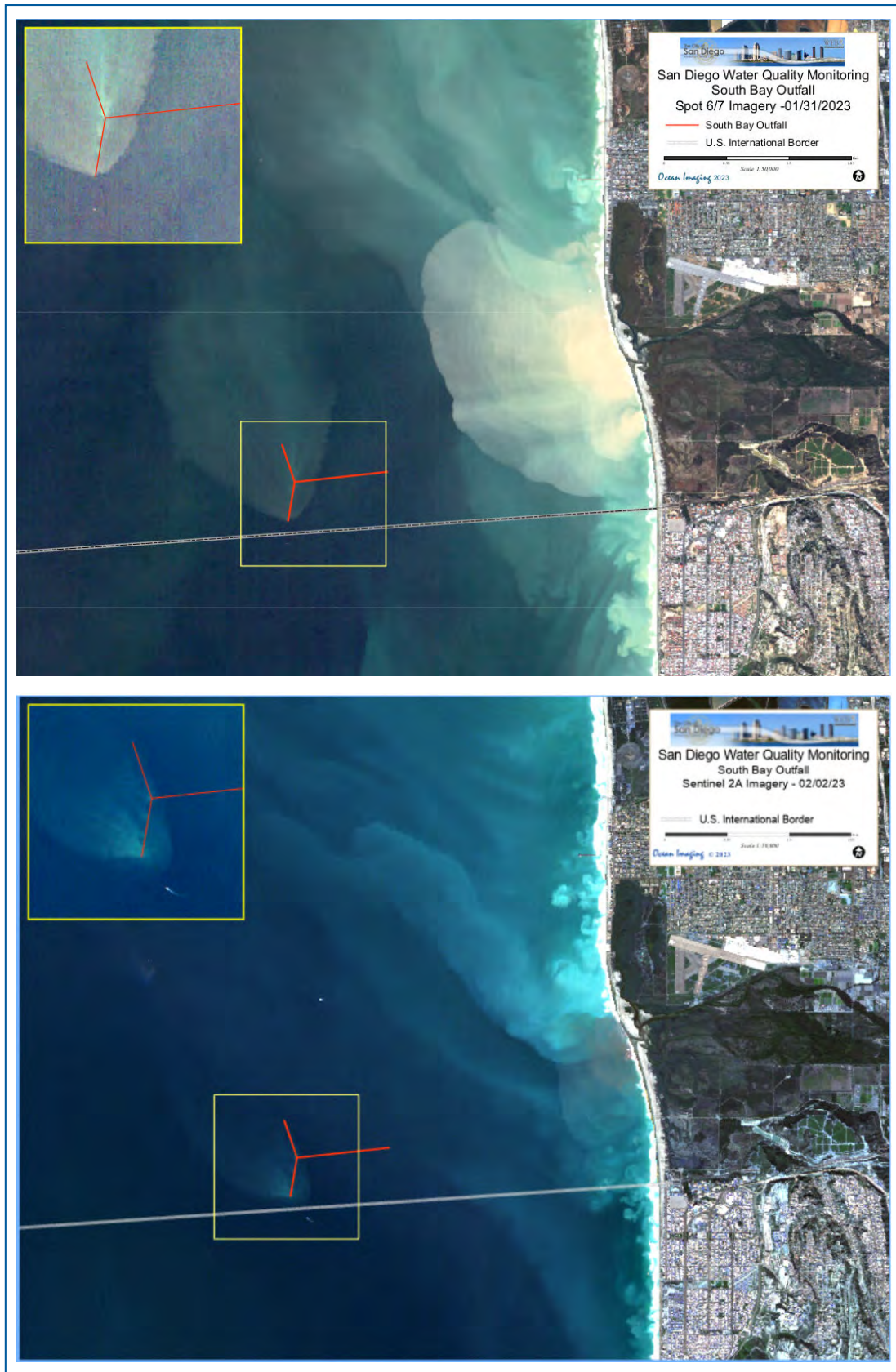
- [APHA] American Public Health Association. (2012). Standard Methods for the Examination of Water and Wastewater, 22nd edition. American Public Health Association, American Water Works Association, and Water Environment Federation.
- Bell, Tom W., et al. “Three Decades of Variability in California’s Giant Kelp Forests from the Landsat Satellites.” *Remote Sensing of Environment*, vol. 238, 2020, p. 110811., doi:10.1016/j.rse.2018.06.039.
- Bordner, R., Winter, J., Scarpino, P., eds., 1978. Microbiological Methods for Monitoring the Environment: Water and Wastes, EPA Research and Development, EPA-600/8-78-017.
- [CDPH] California State Department of Public Health website. (2019). Regulations for Public Beaches and Ocean Water-Contact Sports Areas. Appendix A: Assembly Bill 411, Statutes of 1997, Chapter 765. <https://www.cdph.ca.gov/Programs/CEH/DRSEM/Pages/EMB/RecreationalHealth/Beaches-and-Recreational-Waters.aspx>
- Di Lorenzo, E., Mantua, N. Multi-year persistence of the 2014/15 North Pacific marine heatwave. *Nature Clim Change* 6, 1042–1047 (2016). <https://doi.org/10.1038/nclimate3082>
- [ESRI] “ISO Cluster Unsupervised Classification (Spatial Analyst).” Iso Cluster Unsupervised Classification (Spatial Analyst)-ArcGIS Pro | Documentation, pro.arcgis.com/en/pro-app/latest/tool-reference/spatial-analyst/iso-cluster-unsupervised-classification.htm. Accessed 15 May 2024.
- Gierach, M. M., Holt, B., Trinh, R., Pan, B.J., Rains, C., 2017. Satellite detection of wastewater diversion plumes in Southern California. *Estuarine, Coastal and Shelf Science*, 186, 171 – 182.
- Kahru, Mati, and B. Greg Mitchell. “Spectral reflectance and absorption of a massive red tide off Southern California.” *Journal of Geophysical Research: Oceans*, vol. 103, no. C10, 15 Sept. 1998, pp. 21601–21609, <https://doi.org/10.1029/98jc01945>.
- Little, Joe. “Toxic Tide: The Sewage Crisis at the Border.” NBC 7 San Diego, NBC 7 San Diego, 12 Jan. 2024, <https://www.nbcsandiego.com/news/local/toxic-tide-the-sewage-crisis-at-the-border/3391666/>.
- Schroeder, Sarah B., et al. “Passive Remote Sensing Technology for Mapping Bull Kelp (NEREOCYSTIS Luetkeana): A Review of Techniques and Regional Case Study.” *Global Ecology and Conservation*, vol. 19, 2019, doi:10.1016/j.gecco.2019.e00683.
- [SDRWQCB] San Diego Regional Water Quality Control Board. “San Diego Region - Executive Officer’s Reports.” *Executive Officer’s Report | San Diego Regional Water Quality Control Board*, <https://www.waterboards.ca.gov/sandiego/publications/forms/publications/eoreports.html>. Accessed 26 Mar. 2024.
- Southern California Coastal Water Research Project, 10 May 2019, “Harmful Algal Blooms.” <https://www.sccwrp.org/about/research-areas/eutrophication/harmful-algal-blooms/>.
- [SWRCB] California State Water Resources Control Board. (2015). California Ocean Plan, Water Quality Control Plan, Ocean Waters of California. California Environmental Protection Agency, Sacramento, CA.
- [SWRCB] California State Water Resources Control Board. (2019). California Ocean Plan, Water Quality Control Plan, Ocean Waters of California. California Environmental Protection Agency, Sacramento, CA.
- Svejkovsky, J., Haydock, I., 1998. Satellite remote sensing as part of an ocean outfall environmental monitoring program. In: *Taking a Look at California’s Ocean Resources: An Agenda for the Future*, ASCE, Reston, VA (USA), 2, 1306.
- Svejkovsky, J., Jones, B., 2001. Satellite Imagery Detects Coastal Stormwater and Sewage Runoff. *EOS-Trans. American Geophys. Union*, 82(50).
- Svejkovsky, J., Shandley, J., 2001. Detection of offshore plankton blooms with AVHRR and SAR imagery. *Int. J. of Remote Sensing*, 22 (2&3), 471-485.
- Svejkovsky, J., Nezhlin, N. P., Mustain, N.M. Kum, J. B., 2010. Tracking storm water discharge plumes and water quality of the Tijuana River with multispectral aerial imagery. *Estuarine, Coastal and Shelf Science*. 87(3), 387-398.
- [USEPA] United States Environmental Protection Agency. (2014). Method 1600: *Enterococci* in Water by Membrane Filtration Using membrane-Enterococcus Indoxyl-β-D-Glucoside Agar (mEI). EPA Document EPA-821-R-14-011. Office of Water (4303T), Washington, DC.
- Zheng, Q., Klemas, V.V., Coastal Ocean Environment. *Comprehensive Remote Sensing* Elsevier, Amsterdam (2018), pp. 89-120.

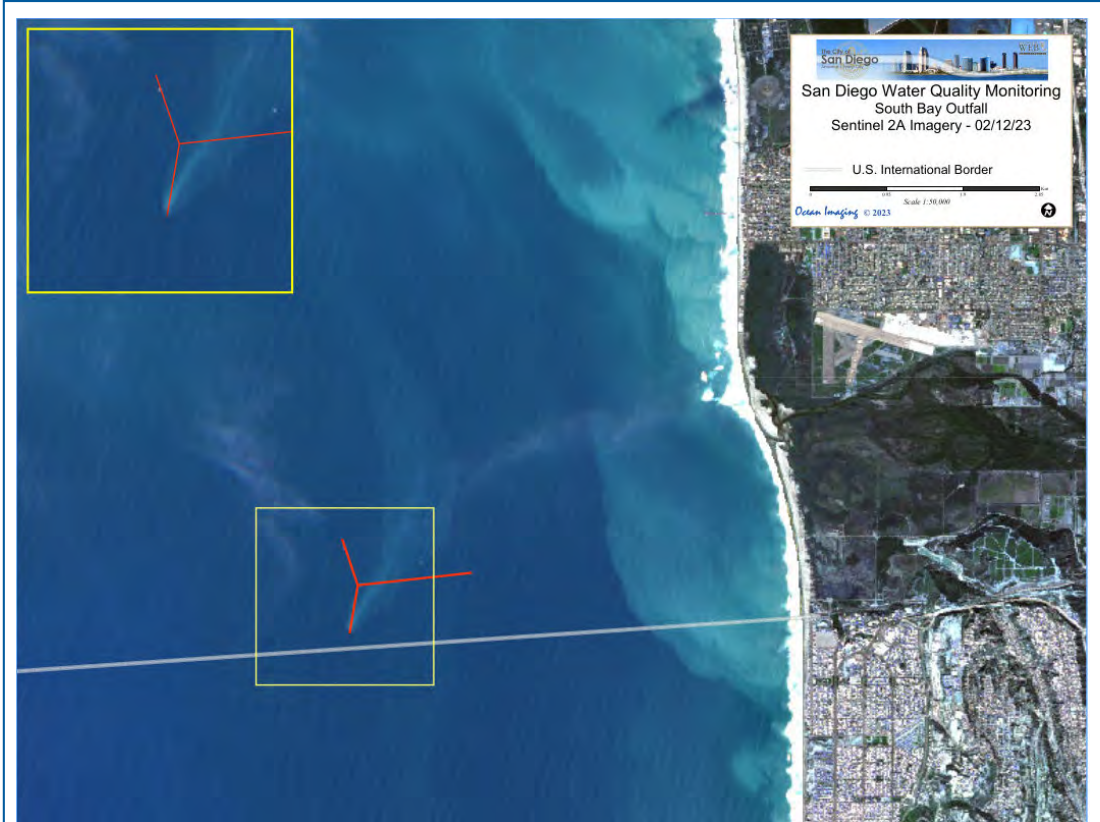
APPENDIX A – HIGH RESOLUTION SATELLITE IMAGERY SHOWING SBOO-RELATED WASTEWATER PLUME

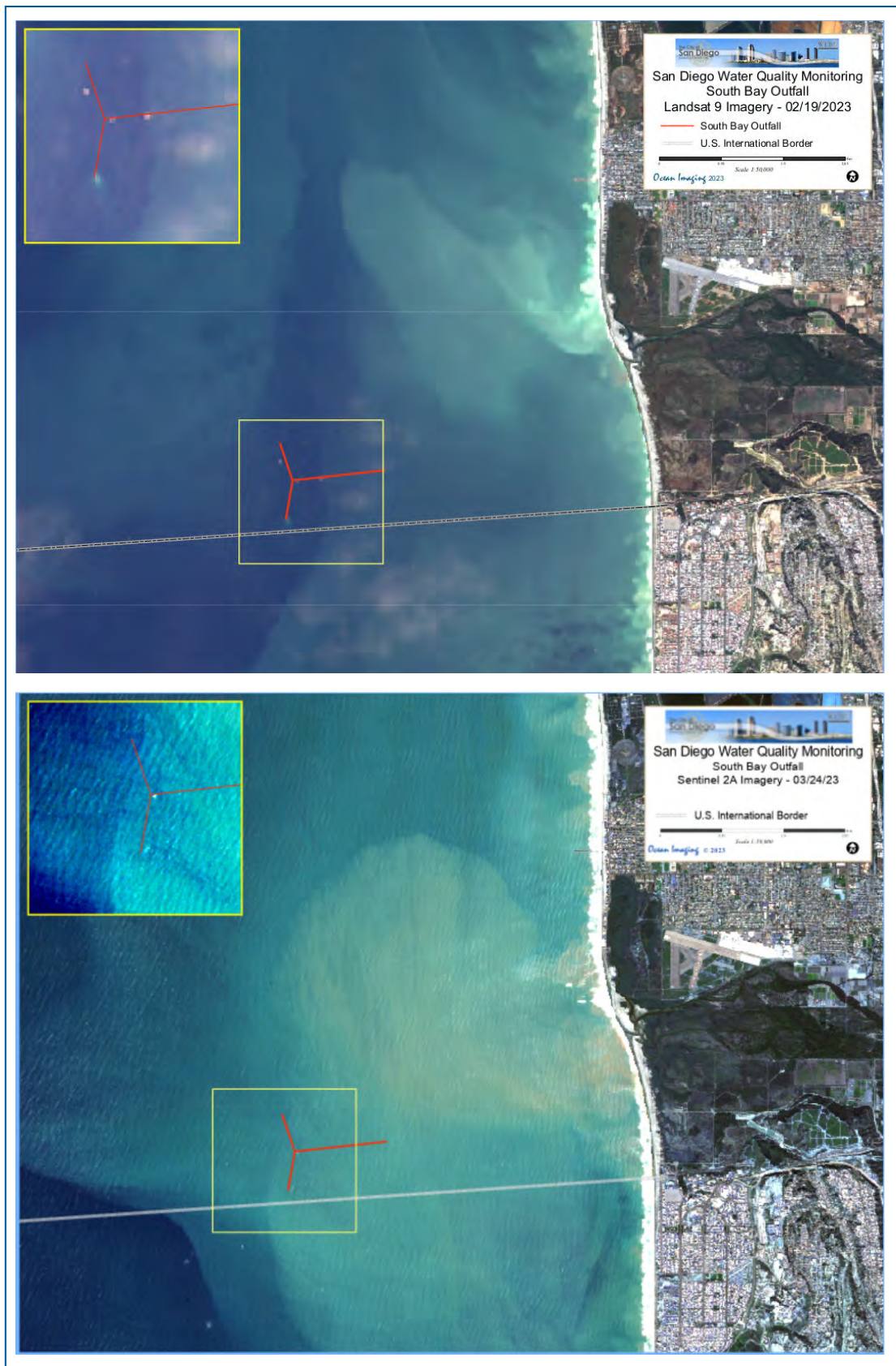


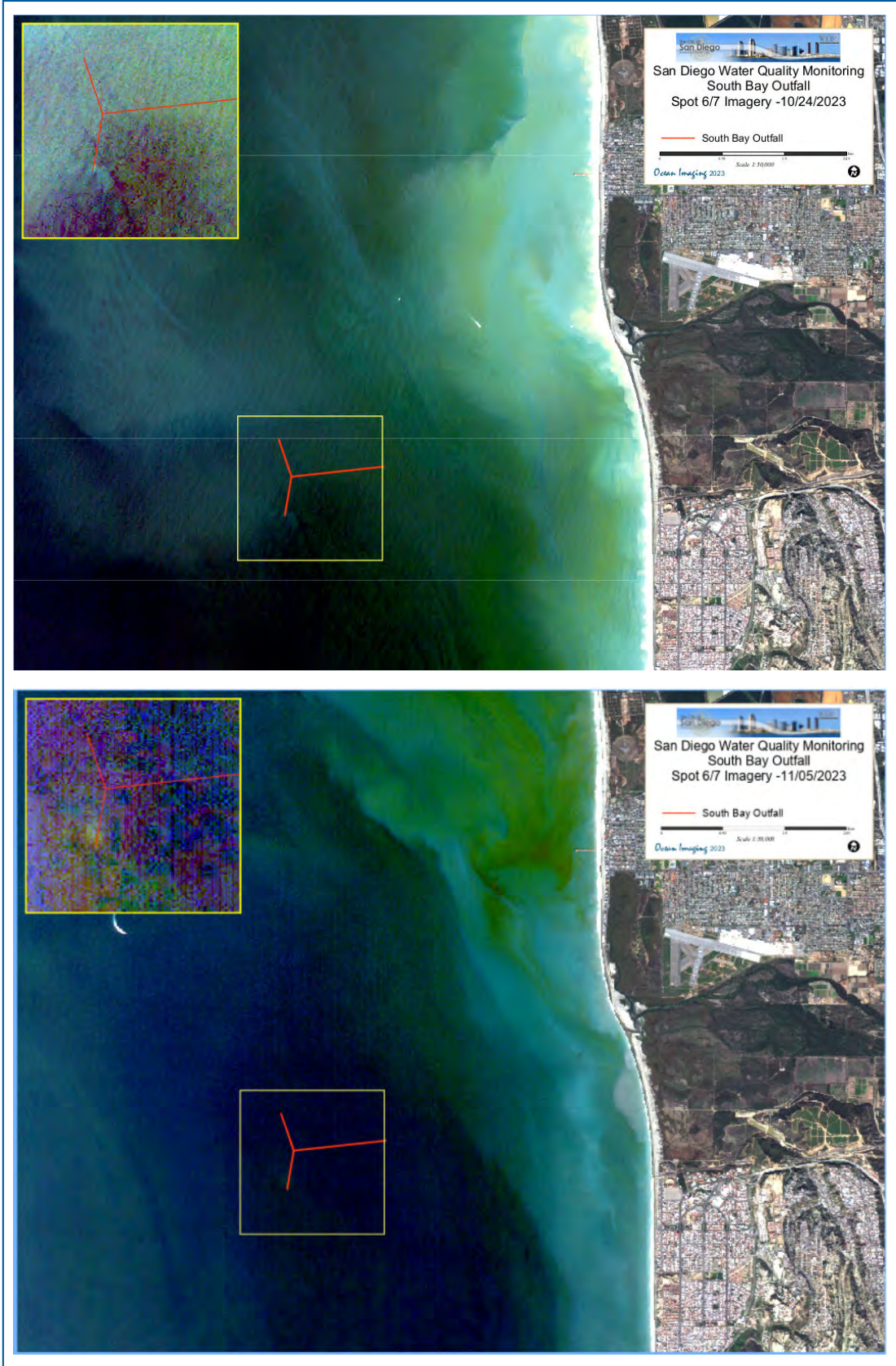


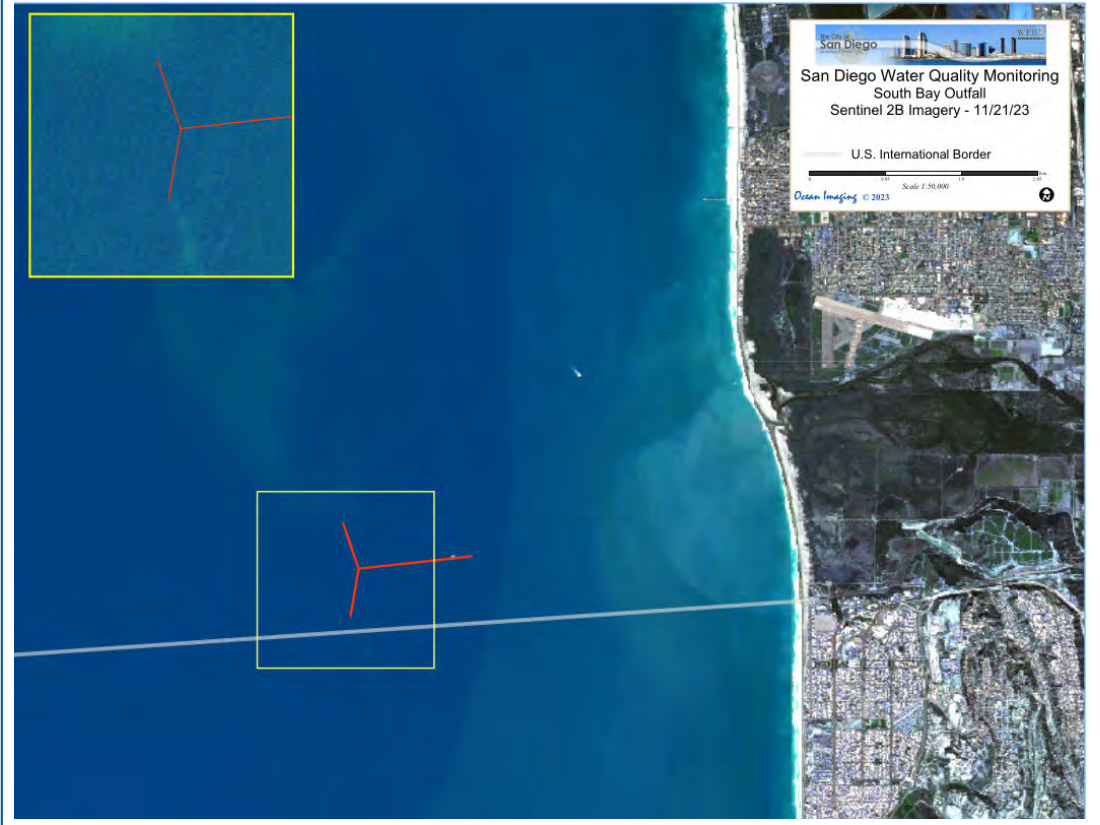
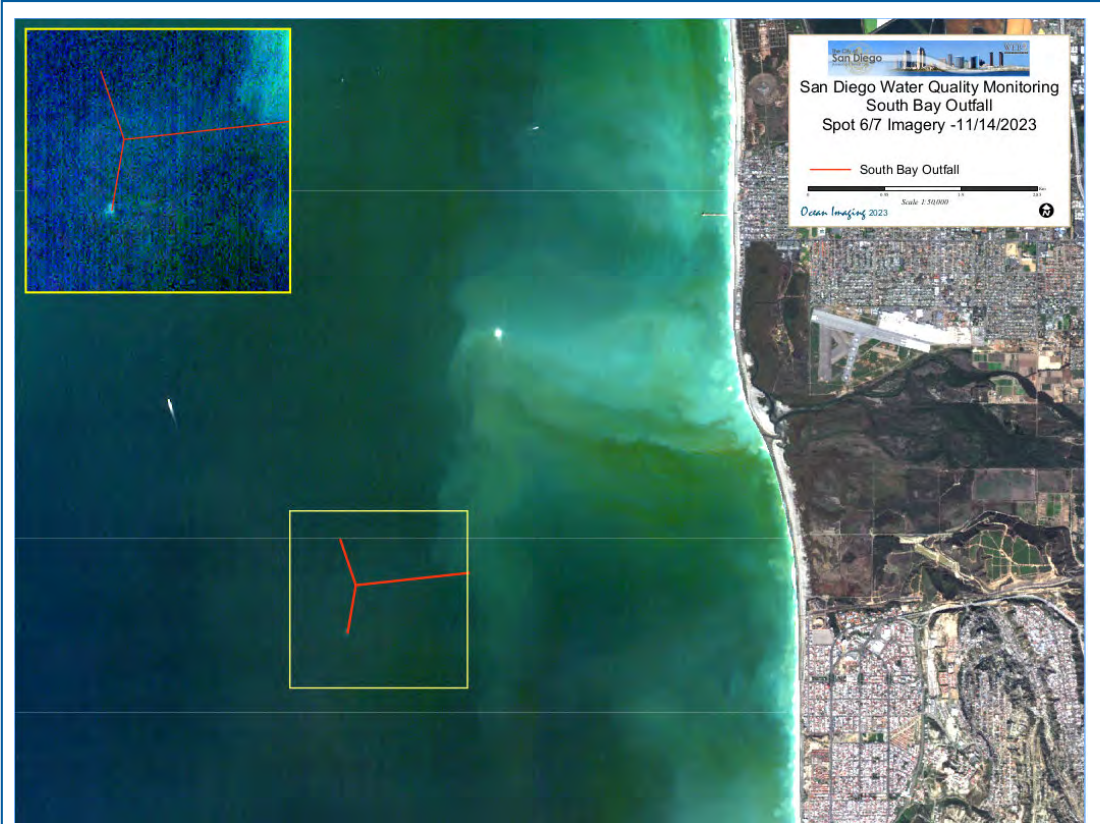


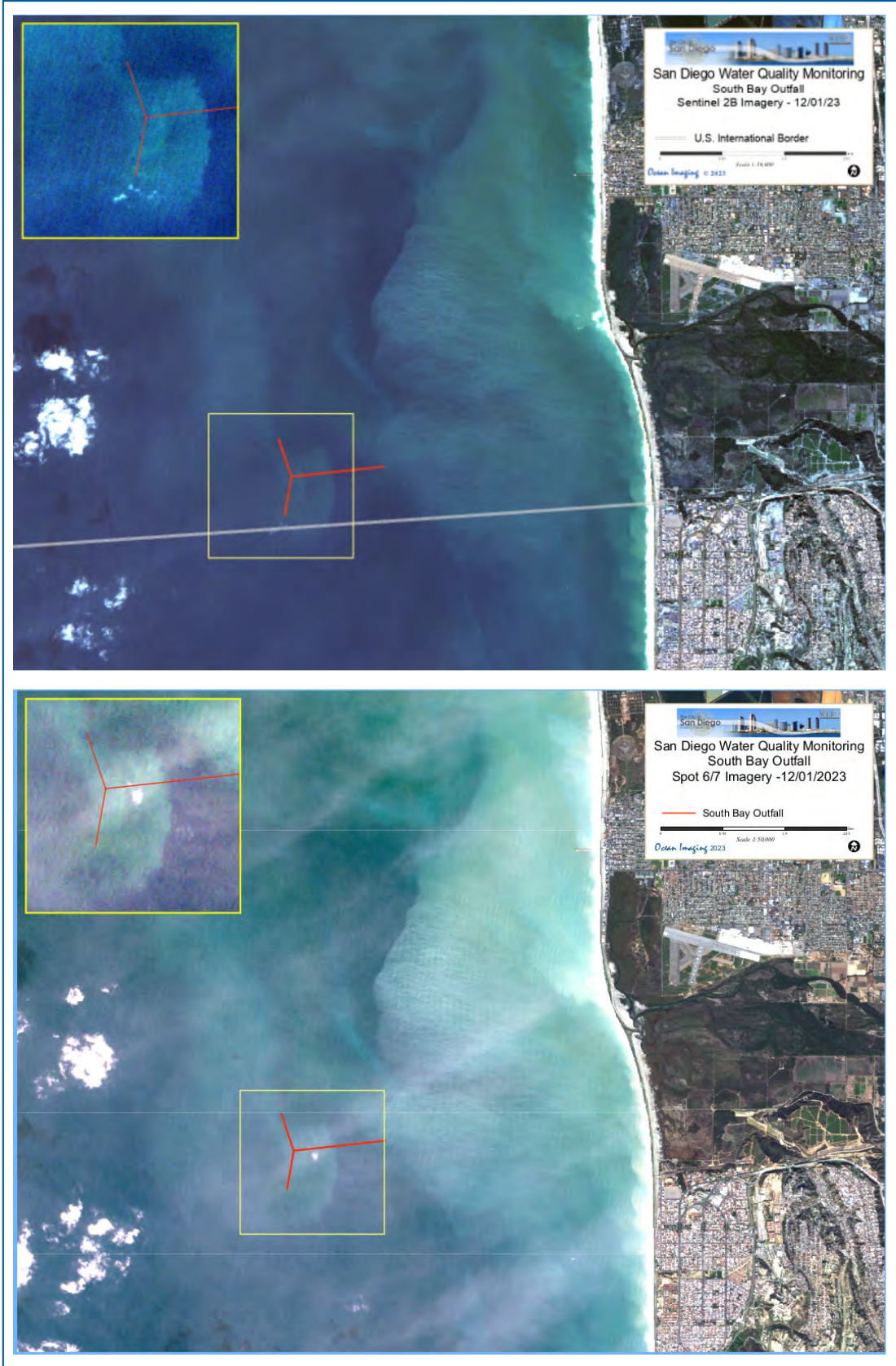


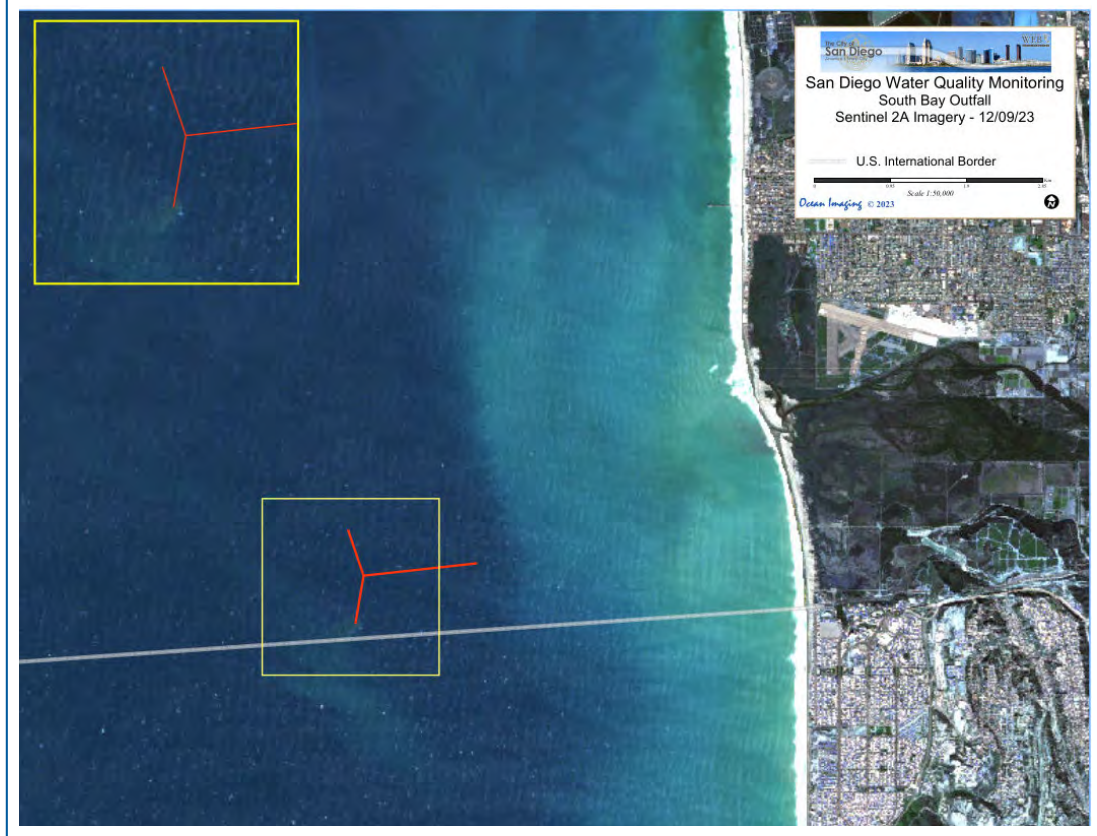


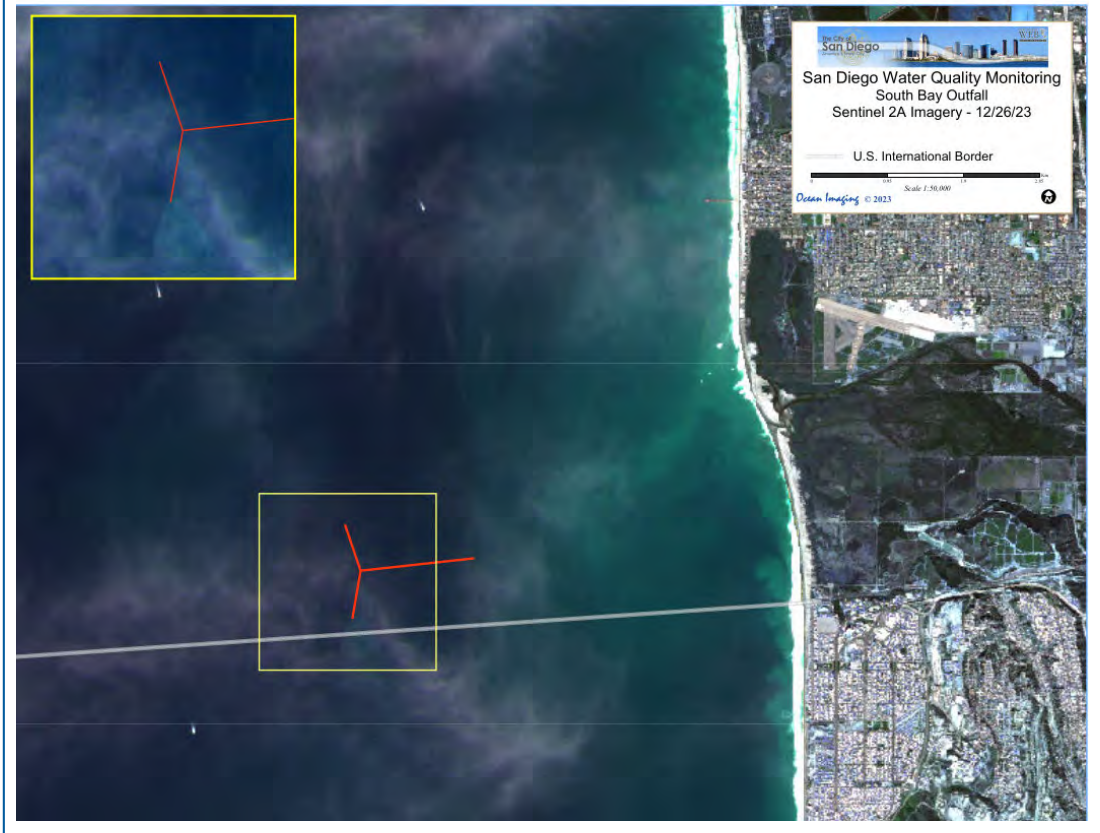
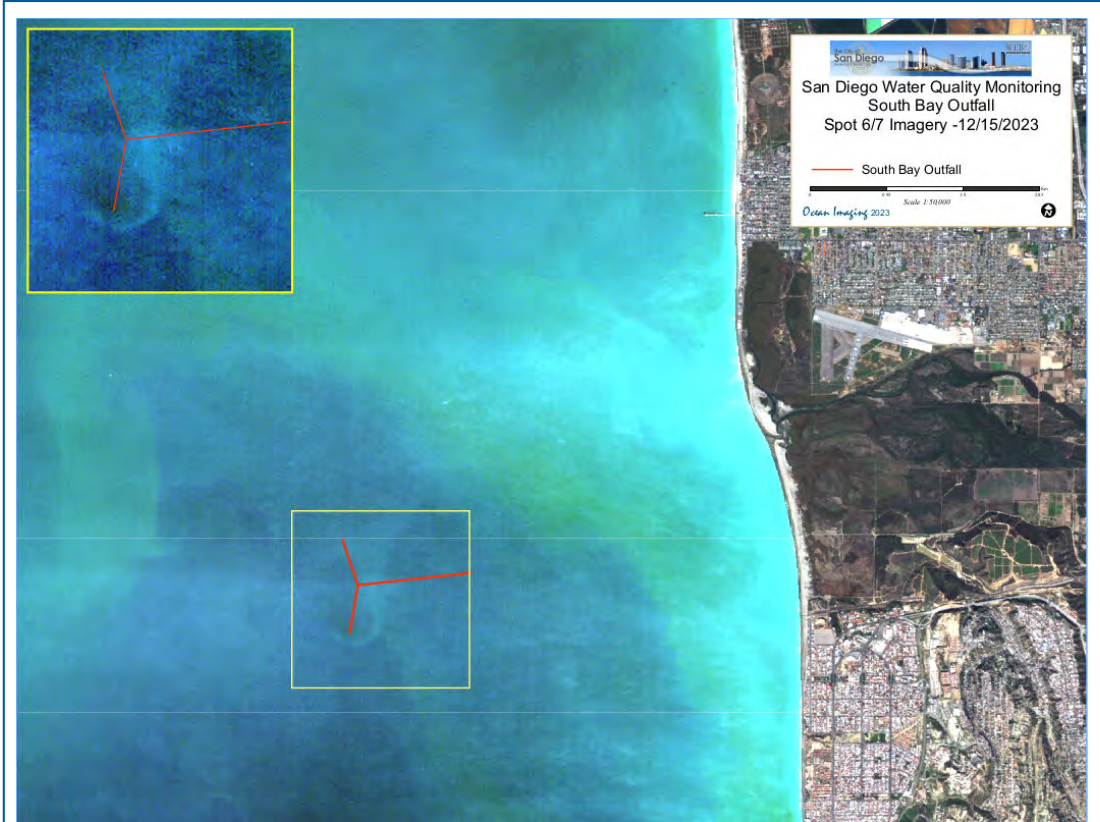












Appendix C

Coastal Oceanographic Conditions

2022 – 2023 Supplemental Analyses

Appendix C.1

Sample dates for quarterly oceanographic surveys conducted during 2022 and 2023. All stations in each station group were sampled on a single day (see Figure 2.1 for stations and locations).

	2022				2023			
	Winter	Spring	Summer	Fall	Winter	Spring	Summer	Fall
<i>PLOO Station Group</i>								
Kelp WQ	Feb-7	May-16	Aug-15	Nov-14	Feb-27	May-22	Aug-23	Nov-13
18 & 60-m WQ	Feb-9	May-19	Aug-17	Nov-17	Mar-2	May-24	Aug-16	Nov-15
80-m WQ	Feb-10	May-20	Aug-18	Nov-18	Mar-3	May-25	Aug-17	Nov-16
98-m WQ	Feb-8	May-18	Aug-16	Nov-15	Feb-28	May-23	Aug-15	Nov-14
<i>SBOO Station Group</i>								
Kelp WQ	Jan-31	May-2	Aug-8	Dec-1	Feb-13	May-15	Aug-7	Nov-6
North WQ	Feb-4	May-5	Aug-10	Nov-29	Feb-9	May-19	Aug-10	Nov-9
Mid WQ	Feb-3	May-4	Aug-9	Nov-30	Feb-8	May-18	Aug-9	Nov-8
South WQ	Feb-1	May-3	Aug-11	Nov-28	Feb-7	May-16	Aug-8	Nov-7

SBOO North (I28–I31, I33–I38); SBOO Mid (I12–I18, I20–I23, I27); SBOO South (I1–I11)

Appendix C.2

Location, depth, and dates for each year-long deployment of the PLOO and SBOO RTOMS. Dates are displayed by deployment, recovery, and period of real-time (RT) data availability. All times are Pacific Standard Time; DD = decimal degrees.

Site	Deployment #	Lat (DD)	Long (DD)	Total Depth (m)	Deployment	RTdata Start	RTdata End	Recovery
PLOO	3	32.66963	-117.32272	95	11/3/2021 9:23	11/3/2021 10:00	11/22/2022 8:20	11/22/2022
	4	32.66953	-117.32404	95	12/8/2022 16:35	12/8/2022 17:00	10/26/2023 7:00	10/26/2023
	5	32.67012	-117.32463	96	12/20/2023 9:32	12/20/2023 9:40	Present	—
SBOO	4	32.53177	-117.18628	31	11/3/2021 12:57	11/3/2021 14:00	11/3/2022 3:00	Lost to Sea
	5	32.53185	-117.18651	31	6/29/2023 11:15	6/29/2023 11:30	Present	—

Appendix C.3

Summary of manual QA/QC review findings, including major sensor problems and data quality issues for the PLOO and SBOO RTOMS. Gaps in data resulted during time periods data were not collected or flagged as bad or suspect.

Parameter	Site	Depths	Time Period	Problem	Action Taken
pH _T	PLOO	75 m	Jan-Nov 2022	SeapHOx pH sensor failed prematurely and began reporting noisy and bad low pH values down to 3.7 pH after two weeks deployed.	Data qualified as bad and not reported
xCO2	PLOO	1 m	Sept-Nov 2022	Solar power system failure due to vessel collision and batteries for operating pCO2 sensor and AIS unit stopped providing sufficient power.	Data qualified as bad and not reported
Nitrate + Nitrite	PLOO	75 m	Apr-Nov 2022	SUNA nitrate sensor instrument failed and reported primarily null values through the end of the deployment.	Sparse reasonable data collected intermittently and reported
Salinity	PLOO	21 m	July-Nov 2022	SBE37IM sensor reported faulty salinity data. The conductivity cell guard had fallen off and cell was damaged.	Data qualified as bad and not reported
DO, pH _T , Salinity, Temperature	PLOO	1 m	Oct-Nov 2022	SeapHOx pH sensor and SBE37-ODO temperature, salinity, oxygen sensor @ 1 m (surface): instruments failed and stopped reporting data.	Data missing for this period
All Parameters	SBOO	All	Nov 2022	Surface buoy broke free during a storm with. Suspected that mooring cable broke between the 10 and 18 m instrument packages.	Recovery attempted but was not possible due to stranding in Mexico
All Parameters	PLOO	All	Jan-Oct 2023	Mooring (below 10m) became fouled in a commercial fishing net and may have caused damage and restricted flushing of sensor flow paths.	Data quality was carefully reviewed for problems due to the nets.
xCO2	PLOO	1 m	Jan-Oct 2023	Loss of solar panels and power to instrument caused lack of data collection.	Data qualified as bad and not reported
DO, pH _T , Salinity	PLOO	75 m	Jan-Oct 2023	Instrument intake was taped over and restricted flow to sensor.	Data qualified as suspect and not reported
All Parameters	SBOO	26 m	July-Dec 2023	Controller stopped working and stopped sending data	Internally recorded data (DO, pH _T , S, T) will be downloaded on recovery but other data (nitrate, chlorophyll, CDOM, turbidity, and BOD) are lost.

Appendix C.3 *continued*

Parameter	Site	Depths	Time Period	Problem	Action Taken
xCO ₂	SBOO	1 m	Nov-Dec 2023	Instrument stopped reporting data, suspected due to failure of solar charging system.	Data are missing for this period.
pH _T	SBOO	1 m	Nov-Dec 2023	SeapHOx pH sensor values dropped low out of range. Values are suspect for remainder of deployment.	Data qualified as suspect and not reported.

Appendix C.4

Location, depth, and dates for each deployment of static moorings located at the PLOO and SBOO. DD = decimal degrees.

Site	Deployment #	Lat (DD)	Long (DD)	Total Depth (m)	Deployment
PLOO	ADCP (#2)	32.6674	117.3270	100	5/19/2023
SBOO	ADCP (#3)	32.5353	117.1980	36	3/19/2023
PLOO	Thermistor (#1) south	32.6640	117.3271	100	9/19/2022
PLOO	Thermistor (#2) north	32.6609	117.3262	100	9/19/2022
SBOO	Thermistor (#6)	32.5303	117.2136	36	3/27/2023

Appendix C.5

Data qualifier definitions for QC data flags. Follows national data standards for summary real-time data flagging (US IOOS 2017), and post-processing data flagging (ARGO 2020).

QC_Flag	Designation	Use
1	Pass/good	For data reviewed both automatically and manually
2	Provisional/unreviewed	For data that is not reviewed or unable to validate; or passed automated test only
3	Suspect/questionable	Failed automated test but not unreasonable (such as climatology test) or manually flagged as possible instrument drift (such as due to biofouling)
4	Bad	Failed automated test (such as out of range test) or manually flagged as clearly bad (such as due to instrument malfunction)
5	Value changed/drift-corrected	Used only in post-processing. Values have been corrected based on new information, such as water sample results to correct for drift or new calibration factors. For data use purposes, this flag can be treated as a "pass." Original data are also retained separately.
9	Missing	Placeholder to show missing real-time data; may be able to be filled in later by downloaded data after mooring recovery

Appendix C.6

Ranges used for automated QC data flagging for each parameter for the gross range test. Values outside of these ranges were assigned a qualifier flag value of 4. Ranges were defined by manufacturers for each sensor configuration.

Parameter	Units	Min	Max
BOD equivalent	mg/L	0	50
CDOM - Eco triplet	ppb	0	375
Chl - Eco triplet	µg/L	0	75
xCO ₂	ppm	0	2000
NO ₃ (Nitrate + Nitrite)	µM	0	3000
NTU (Turbidity)	NTU	0	100
O ₂ (DO)	mg/L	0.1	20
pH (total scale; both internal and external)	pH _T	6.5	9
Sal (Salinity)	PSU	2	42
Temp (Temperature)	°C	-2.5	35

Appendix C.7

Annual ranges used for automated QC data flagging for each parameter, site, and depth for the climatological range test. Temperature, salinity, DO, and pH_T ranges were based on the minimum and maximum values recorded at each site and depth range where the sensors were found to be functional and in reasonable agreement with historical CTD ranges from the City's quarterly surveys. BOD ranges were based on the maximum value observed from all deployments, since that is a new parameter and historical data were not available. CDOM ranges were based on maximum of multiple readings recorded at the PLOO mooring due to proximity to plume. Chlorophyll *a* and turbidity ranges were based on the maximum sensor range for the ECO triplet. Nitrate ranges were based on values observed at both moorings where the sensors were found to be functional, and verified in a reasonable range compared to nearshore data collected by the California Cooperative Oceanic Fisheries Investigations (see: <https://calcofi.org>). Ranges for xCO₂ were based on values observed at both moorings, where the phytoplankton bloom in spring 2020 resulted in lower xCO₂ values than prior years, and comparable to ranges recorded by the closest NOAA/SIO carbon program mooring (CCE2, see: <https://www.pmel.noaa.gov/c02/story/CCE2>).

Parameter	Units	PLOO RTOMS										SBOO RTOMS						Qualifier to assign if outside of site/depth range
		1 m		Mid depths		Bottom depth (>70 m)		1 m		Mid depths		Bottom depth (>25 m)						
		Min	Max	Min	Max	Min	Max	Min	Max	Min	Max	Min	Max	Min	Max			
BOD equivalent	mg/L	NA	NA	0	10	0	10	0	10	NA	NA	0	10	0	10	0	10	3
CDOM-ECO triplet	ppb	0	50	0	50	0	50	0	50	0	50	0	50	0	50	0	50	3
Chl-ECO triplet	µg/L	0	30	0	30	0	30	0	30	0	30	0	30	0	30	0	30	3
xCO ₂	ppm	50	1000	NA	NA	NA	NA	NA	NA	50	1000	NA	NA	NA	NA	NA	NA	3
NO ₃ (Nitrate + Nitrite)	µM	0	39	0	39	0	39	0	39	0	39	0	39	0	39	0	39	3
NTU (Turbidity)	NTU	0	10	0	10	0	10	0	10	0	10	0	10	0	10	0	10	3
O ₂ (DO)	mg/L	5.5	24.0	2.0	9.5	2.0	7.5	2.0	7.5	5.5	24.0	3.0	11.0	2.0	11.0	2.0	11.0	3
pH (total scale; both internal and external)	pH _T	7.6	8.9	7.5	8.1	7.4	8.1	7.6	8.1	7.6	8.7	NA	NA	7.4	8.1	7.4	8.1	3
Sal (Salinity)	PSU	32.0	34.0	32.3	34.0	32.5	34.0	31.0	34.0	31.0	34.0	32.0	34.0	33.0	34.0	33.0	34.0	3
Temp (Temperature)	°C	11.0	26.5	9.0	24.5	9.0	15.0	12.0	26.5	12.0	26.5	10.0	26.0	9.0	19.0	9.0	19.0	3

Appendix C.8

Summary of temperature recorded by the PLOO thermistor array (100 m) at nearest depths to the PLOO RTOMS sensors. These data represent all recovered thermistor strings during the seasons between 2022 to 2023. Data include mean, minimum, and maximum values, sample size (n), and proportion recovered (n_prop) for each depth by season.

Season	6 m	10 m	14 m	18 m	22 m	26 m	30 m	34 m	38 m	42 m	46 m	50 m	54 m	58 m	62 m	66 m	70 m	74 m	78 m	82 m	86 m	90 m	94 m	98 m	
Fall/2023	mean	17.6	17.5	17.4	17.2	16.8	16.5	16.2	16.0	15.6	15.3	15.1	14.9	14.5	14.3	14.2	14.0	13.9	13.7	13.6	13.3	13.2	13.1	12.8	12.7
	min	15.5	15.3	14.8	14.2	14.1	13.7	13.4	13.2	13.0	13.0	12.9	12.6	12.5	12.4	12.3	12.2	12.0	12.1	12.0	11.7	11.5	11.4	11.4	11.2
	max	19.4	19.3	19.1	19.0	18.9	18.6	18.1	18.1	17.9	17.4	17.4	17.3	17.3	17.1	17.0	16.9	16.7	16.6	16.6	16.4	16.3	15.9	15.6	15.4
	n	8727	8727	8727	8727	8727	8727	8727	8727	8727	8727	8727	8727	8727	8727	8727	8727	8727	8727	8727	8727	8727	8727	8727	8727
	n_prop	1	1	1	1	1	1	1	1	1	1	1	1	1	1	1	1	1	1	1	1	1	1	1	1

Appendix C.9

Summary of temperature recorded by the SBOO thermistor array (36 m) at nearest depths to the SBOO RTOMS sensors, during seasons between 2022 to 2023 where RTOMS data were unavailable. These data represent all recovered thermistor strings during the seasons between 2022 to 2023. Data include mean, minimum, and maximum values, sample size (n), and proportion recovered (n_prop) for each depth by season.

Season		6 m	10 m	14 m	18 m	22 m	26 m	30 m	34 m
<i>Fall 2022</i>	mean	16.8	16.2	15.6	14.4	NA	NA	13.7	13.5
	min	13.9	12.9	12.8	12.5	NA	NA	12.3	12.4
	max	21.3	21.1	20.3	18.3	NA	NA	16.9	15.8
	n	13103	13093	13088	13102	NA	NA	13103	13103
	n_prop	0.99	0.99	0.99	0.99	NA	NA	0.99	0.99
<i>Winter 2023</i>	mean	14.0	13.8	13.6	11.3	13.1	11.1	12.7	12.7
	min	11.4	11.2	10.9	10.9	10.6	10.9	10.6	10.6
	max	15.5	15.5	15.5	12.6	15.3	11.4	15.3	15.2
	n	12950	12936	12906	656	12949	656	12950	12950
	n_prop	1	1	1	1		1	1	
<i>Spring 2023</i>	mean	15.1	13.9	12.9	12.2	11.7	11.6	11.4	11.4
	min	11.1	10.9	10.6	10.4	10.2	10.4	10.3	10.3
	max	18.7	18.0	17.6	16.9	14.7	13.3	12.9	12.3
	n	13103	13103	13103	13103	13103	13103	13103	13103
	n_prop	1	1	1	1		1	1	

Appendix C.10

Summary of temperature, salinity, DO, pH (total scale), chlorophyll a, CDOM, turbidity, nitrate + nitrite, BOD, and xCO₂ recorded at various depths by the PLOO RTOMS in 2023. Seasonal summaries from 2022 are available in the interim report by City of San Diego (2023). Data include mean, minimum, and maximum values, sample size (n), and proportion recovered (n_prop) for each depth by season. Sample sizes differed due to variations in sampling interval, deployment date, and data quality (Appendix C.2—C.7); id = insufficient data (see text).

Parameter	Season		1 m	10 m	20 m	30 m	45 m	60 m	75 m	89 m
Temperature (°C)	Winter	mean	14.31	14.11	13.75	13.19	12.23	11.44	10.94	10.75
		min	12.96	12.03	11.15	10.62	10.14	9.78	9.72	9.69
		max	15.78	15.32	15.29	15.26	14.96	14.86	14.08	12.69
		n	11542	11654	11654	11607	11666	11664	11598	11869
		n_prop	0.89	0.9	0.9	0.9	0.9	0.9	0.89	0.92
	Spring	mean	16.29	14.51	12.34	11.51	10.85	10.43	10.23	10.14
		min	12.13	10.45	10.22	9.91	9.79	9.72	9.7	9.61
		max	19.03	18.08	17.4	14.18	12.67	11.44	10.9	10.65
		n	12059	12126	12121	12081	12120	12148	12072	12256
		n_prop	0.92	0.93	0.92	0.92	0.92	0.93	0.92	0.94
	Summer	mean	20.66	17.41	14.67	13.41	12.39	11.76	11.39	11.23
		min	15.02	11.81	11.19	10.64	10.25	10.09	10.01	9.89
		max	23.67	22.38	19.52	16.09	14.73	14.14	13.78	13.59
		n	11723	13145	13145	13097	13133	13140	13077	13247
		n_prop	0.88	0.99	0.99	0.99	0.99	0.99	0.99	1
	Fall	mean	—	17.17	15.65	—	14.24	13.62	—	12.48
		min	—	14.4	13.28	—	12.23	11.77	—	11.39
		max	—	20.66	18.75	—	17.39	17.14	—	16.06
		n	id	5252	5257	id	5257	5257	id	5253
		n_prop	0.39	0.4	0.4	0.39	0.4	0.4	0.33	0.4
Salinity (psu)	Winter	mean	33.27	33.3	33.38	33.44	33.55	33.6	—	33.68
		min	32.34	32.88	33.1	33.13	33.11	33.17	—	33.26
		max	33.47	33.51	33.78	33.91	34.01	33.95	—	33.93
		n	11546	11660	11658	11613	11670	11669	id	11875
		n_prop	0.89	0.9	0.9	0.9	0.9	0.9	0	0.92
	Spring	mean	33.44	33.5	33.57	33.61	33.66	33.43	—	33.52
		min	32.92	33.01	33.16	33.29	33.27	32.91	—	33.14
		max	33.65	33.92	34	34.05	34.06	33.98	—	33.94
		n	12053	12124	12119	12081	12120	12146	id	12256
		n_prop	0.92	0.93	0.92	0.92	0.92	0.93	0	0.94

Appendix C.10 *continued*

Parameter	Season		1 m	10 m	20 m	30 m	45 m	60 m	75 m	89 m
Salinity (cont.)	<i>Summer</i>	mean	33.28	33.45	33.33	33.33	33.3	33.2	—	32.95
		min	32.83	33.22	32.91	32.95	32.94	32.74	—	32.59
		max	33.45	33.65	33.69	33.7	33.74	33.44	—	33.32
		n	11723	6578	13139	13095	13132	13140	id	13245
		n_prop	0.88	0.5	0.99	0.99	0.99	0.99	0	1
	<i>Fall</i>	mean	—	—	33.23	—	33.19	33.2	—	32.97
		min	—	—	32.89	—	32.93	32.97	—	32.61
		max	—	—	33.42	—	33.45	33.43	—	33.55
		n	id	id	5250	id	5251	5251	id	5246
		n_prop	0.39	0.12	0.4	0.39	0.4	0.4	0.06	0.4
DO (mg/L)	<i>Winter</i>	mean	8.37	—	—	6.6	—	—	—	3.37
		min	5.54	—	—	3.12	—	—	—	2.06
		max	10.52	—	—	9.14	—	—	—	6.08
		n	11642	—	—	11710	—	—	id	11842
		n_prop	0.9	—	—	0.9	—	—	0	0.91
	<i>Spring</i>	mean	8.74	—	—	5.25	—	—	—	3.02
		min	5.52	—	—	2.37	—	—	—	1.79
		max	13.43	—	—	9.15	—	—	—	4.72
		n	12159	—	—	12181	—	—	id	12250
		n_prop	0.93	—	—	0.93	—	—	0	0.93
	<i>Summer</i>	mean	8.25	—	—	7.63	—	—	—	4.48
		min	7.22	—	—	4.74	—	—	—	2.71
		max	13.44	—	—	9.23	—	—	—	6.78
		n	11833	—	—	13215	—	—	id	13246
		n_prop	0.89	—	—	1	—	—	0	1
<i>Fall</i>	mean	—	—	—	—	—	—	—	4.73	
	min	—	—	—	—	—	—	—	2.58	
	max	—	—	—	—	—	—	—	7.56	
	n	id	—	—	id	—	—	id	5246	
	n_prop	0.39	—	—	0.39	—	—	0.06	0.4	
pH_T (pH Total scale)	<i>Winter</i>	mean	8.06	—	—	7.94	—	—	—	—
		min	7.84	—	—	7.69	—	—	—	—
		max	8.19	—	—	8.1	—	—	—	—
		n	11651	—	—	11720	—	—	id	—
		n_prop	0.9	—	—	0.9	—	—	—	—

Appendix C.10 *continued*

Parameter	Season		1 m	10 m	20 m	30 m	45 m	60 m	75 m	89 m
pH_T (cont.)	<i>Spring</i>	mean	8.1	—	—	7.83	—	—	—	—
		min	7.82	—	—	7.63	—	—	—	—
		max	8.42	—	—	8.08	—	—	—	—
		n	12153	—	—	12180	—	—	id	—
		n_prop	0.93	—	—	0.93	—	—	0	—
	<i>Summer</i>	mean	8.08	—	—	7.99	—	—	—	—
		min	7.98	—	—	7.77	—	—	—	—
		max	8.31	—	—	8.09	—	—	—	—
		n	11833	—	—	13213	—	—	id	—
		n_prop	0.89	—	—	1	—	—	0	—
	<i>Fall</i>	mean	8.06	—	—	8.01	—	—	—	—
		min	8.01	—	—	7.91	—	—	—	—
		max	8.15	—	—	8.06	—	—	—	—
		n	5279	—	—	5266	—	—	id	—
		n_prop	0.4	—	—	0.4	—	—	0	—
Chlorophyll a (µg/L)	<i>Winter</i>	mean	—	—	—	0.77	—	—	0.06	—
		min	—	—	—	0.12	—	—	0.01	—
		max	—	—	—	4.38	—	—	1.05	—
		n	id	—	—	7442	—	—	11519	—
		n_prop	0.38	—	—	0.57	—	—	0.89	—
	<i>Spring</i>	mean	0.81	—	—	0.96	—	—	0.08	—
		min	0.02	—	—	0.06	—	—	0.01	—
		max	14.35	—	—	5	—	—	1.3	—
		n	11605	—	—	11126	—	—	12007	—
		n_prop	0.89	—	—	0.85	—	—	0.92	—
	<i>Summer</i>	mean	—	—	—	—	—	—	0.13	—
		min	—	—	—	—	—	—	0.02	—
		max	—	—	—	—	—	—	1.09	—
		n	id	—	—	id	—	—	13050	—
		n_prop	0.09	—	—	0.07	—	—	0.99	—
<i>Fall</i>	mean	—	—	—	—	—	—	—	—	
	min	—	—	—	—	—	—	—	—	
	max	—	—	—	—	—	—	—	—	
	n	id	—	—	id	—	—	id	—	
	n_prop	0.06	—	—	0.12	—	—	0.39	—	

Appendix C.10 *continued*

Parameter	Season		1 m	10 m	20 m	30 m	45 m	60 m	75 m	89 m
CDOM (ppb)	<i>Winter</i>	mean	—	—	—	0.75	—	—	0.32	—
		min	—	—	—	0.35	—	—	0	—
		max	—	—	—	4.95	—	—	3.58	—
		n	id	—	—	6689	—	—	11519	—
		n_prop	0.08	—	—	0.52	—	—	0.89	—
	<i>Spring</i>	mean	—	—	—	—	—	—	0.24	—
		min	—	—	—	—	—	—	0	—
		max	—	—	—	—	—	—	1.01	—
		n	id	—	—	id	—	—	12007	—
		n_prop	0	—	—	0	—	—	0.92	—
	<i>Summer</i>	mean	—	—	—	—	—	—	0.19	—
		min	—	—	—	—	—	—	0	—
		max	—	—	—	—	—	—	1.83	—
		n	id	—	—	id	—	—	10748	—
		n_prop	0	—	—	0	—	—	0.81	—
<i>Fall</i>	n	id	—	—	id	—	—	id	—	
	n_prop	0.06	—	—	0.12	—	—	0.12	—	
Turbidity (NTU)	<i>Winter</i>	mean	—	—	—	0.28	—	—	0.22	—
		min	—	—	—	0.05	—	—	0.04	—
		max	—	—	—	2	—	—	1.86	—
		n	id	—	—	7419	—	—	11518	—
		n_prop	0.08	—	—	0.57	—	—	0.89	—
	<i>Spring</i>	mean	0.26	—	—	—	—	—	0.18	—
		min	0.02	—	—	—	—	—	0.03	—
		max	1.98	—	—	—	—	—	1.73	—
		n	10594	—	—	id	—	—	12007	—
		n_prop	0.81	—	—	0	—	—	0.92	—
	<i>Summer</i>	mean	—	—	—	—	—	—	0.2	—
		min	—	—	—	—	—	—	0.03	—
		max	—	—	—	—	—	—	1.95	—
		n	id	—	—	id	—	—	8265	—
		n_prop	0.1	—	—	0	—	—	0.62	—
<i>Fall</i>	n	id	—	—	id	—	—	id	—	
	n_prop	0.06	—	—	0.12	—	—	0.12	—	

Appendix C.10 *continued*

Parameter	Season		1 m	10 m	20 m	30 m	45 m	60 m	75 m	89 m
Nitrate + nitrite (µM)	<i>Winter</i>	mean	—	—	—	9.93	—	—	—	21.63
		min	—	—	—	1.25	—	—	—	10.66
		max	—	—	—	24.2	—	—	—	29.31
		n	—	—	—	1893	—	—	—	1896
		n_prop	—	—	—	0.88	—	—	—	0.88
	<i>Spring</i>	mean	—	—	—	17.27	—	—	—	20.3
		min	—	—	—	3.12	—	—	—	5.51
		max	—	—	—	26.93	—	—	—	30.55
		n	—	—	—	1996	—	—	—	1701
		n_prop	—	—	—	0.91	—	—	—	0.78
	<i>Summer</i>	mean	—	—	—	5.08	—	—	—	—
		min	—	—	—	0.23	—	—	—	—
		max	—	—	—	20.16	—	—	—	—
		n	—	—	—	2164	—	—	—	id
		n_prop	—	—	—	0.98	—	—	—	0.3
	<i>Fall</i>	mean	—	—	—	—	—	—	—	—
		min	—	—	—	—	—	—	—	—
		max	—	—	—	—	—	—	—	—
n		—	—	—	id	—	—	—	id	
n_prop		—	—	—	0.27	—	—	—	0.39	
BOD (mg/L)	<i>Winter</i>	mean	—	—	—	0.05	—	—	—	—
		min	—	—	—	0	—	—	—	—
		max	—	—	—	0.73	—	—	—	—
		n	—	—	—	11168	—	—	id	—
		n_prop	—	—	—	0.86	—	—	0.34	—
	<i>Spring</i>	mean	—	—	—	0.05	—	—	—	—
		min	—	—	—	0	—	—	—	—
		max	—	—	—	0.82	—	—	—	—
		n	—	—	—	11819	—	—	id	—
		n_prop	—	—	—	0.9	—	—	0	—

Appendix C.10 *continued*

Parameter	Season		1 m	10 m	20 m	30 m	45 m	60 m	75 m	89 m
BOD (cont.)	<i>Summer</i>	mean	—	—	—	0.16	—	—	—	—
		min	—	—	—	0.02	—	—	—	—
		max	—	—	—	0.83	—	—	—	—
	<i>Fall</i>	n	—	—	—	13108	—	—	id	—
		n_prop	—	—	—	0.99	—	—	0	—
		n	—	—	—	id	—	—	id	—
xCO2 (ppm)	<i>Winter</i>	n	id	—	—	—	—	—	—	—
		n_prop	0.06	—	—	—	—	—	—	—
	<i>Spring</i>	n	id	—	—	—	—	—	—	—
		n_prop	0	—	—	—	—	—	—	—
	<i>Summer</i>	n	id	—	—	—	—	—	—	—
		n_prop	0	—	—	—	—	—	—	—
	<i>Fall</i>	n	id	—	—	—	—	—	—	—
		n_prop	0.13	—	—	—	—	—	—	—

Appendix C.11

Summary of temperature, salinity, DO, pH (total scale), chlorophyll a, CDOM, turbidity, nitrate + nitrite, BOD, and xCO₂ recorded at various depths by the SBOO RTOMS in 2023. Seasonal summaries from 2022 are available in the interim report by City of San Diego (2023). Data include mean, minimum, and maximum values, sample size (n), and proportion recovered (n_prop) for each depth by season. Sample sizes differed due to variations in sampling interval, deployment date, and data quality (Appendix C.2 to C.7); id = insufficient data (see text).

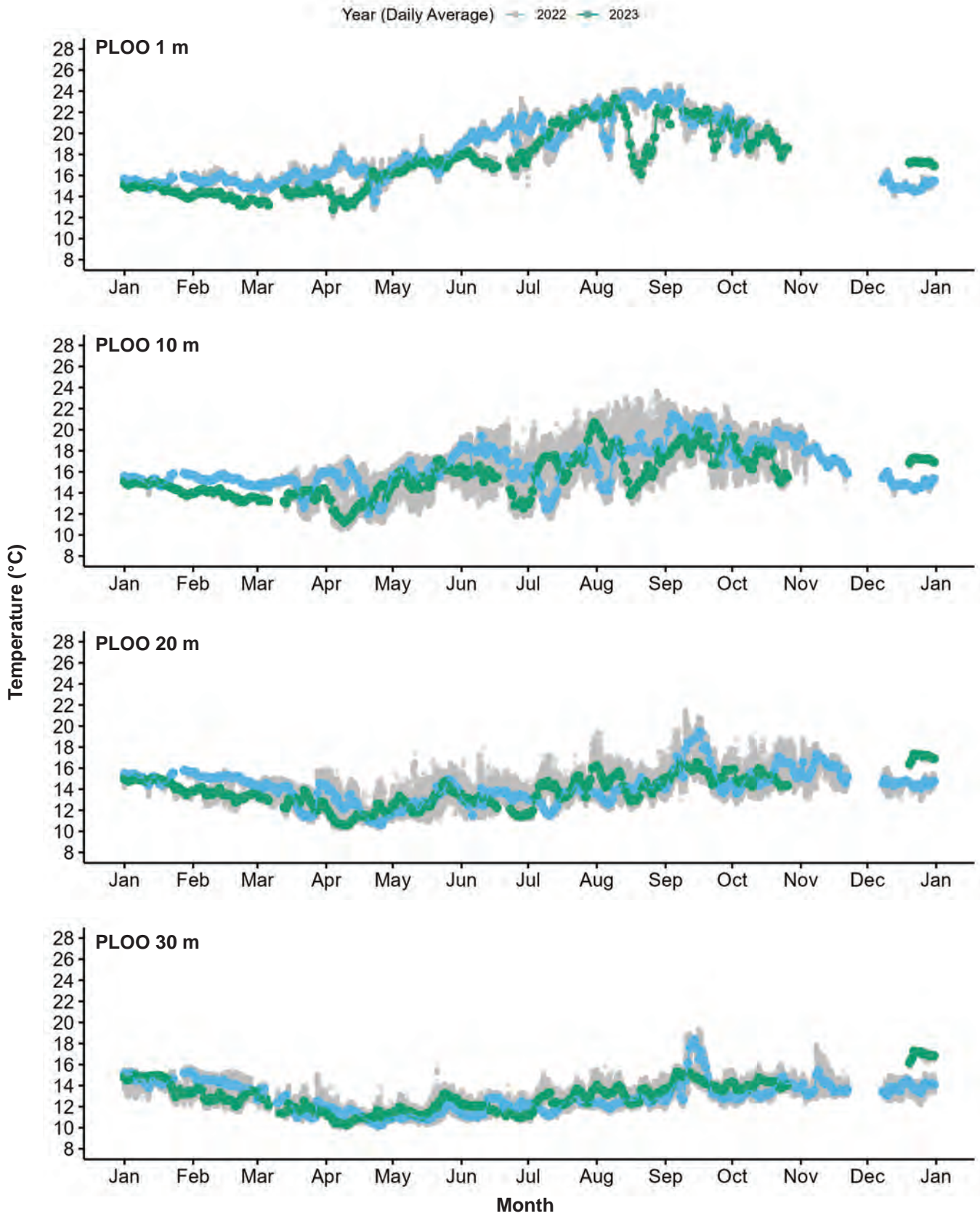
Parameter	Season		1 m	10 m	18 m	26 m	
Temperature (°C)	<i>Spring</i>	n	id	id	id	id	
		n_prop	0.02	0.02	0.02	0.02	
	<i>Summer</i>	mean	19.5	15.85	14.27	—	
		min	14.95	11.66	11.22	—	
		max	22.99	22.16	20.31	—	
		n	13165	13242	13176	id	
		n_prop	0.99	1	0.99	0.3	
	<i>Fall</i>	mean	17.37	16.46	15.73	—	
		min	14.98	13.99	13.71	—	
		max	20.72	20.66	18.74	—	
		n	13099	13199	13109	id	
		n_prop	0.99	1	0.99	0	
	Salinity (psu)	<i>Spring</i>	n	id	id	id	id
			n_prop	0.02	0.02	0.02	0.02
<i>Summer</i>		mean	33.32	33.26	33.25	—	
		min	32.06	32.87	32.7	—	
		max	33.52	33.53	33.52	—	
		n	13165	13241	13175	id	
		n_prop	0.99	1	0.99	0.3	
<i>Fall</i>		mean	33.18	33.17	33.19	—	
		min	32.44	32.72	32.78	—	
		max	33.42	33.36	33.38	—	
		n	13077	13191	13101	id	
		n_prop	0.99	1	0.99	0	
DO (mg/L)		<i>Spring</i>	n	id	—	id	id
			n_prop	0.02	—	0.02	0.02
	<i>Summer</i>	mean	8.93	—	8.27	—	
		min	7.54	—	5.67	—	
		max	14.13	—	10.31	—	
		n	13236	—	13247	id	
		n_prop	1	—	1	0.3	

Appendix C.11 *continued*

Parameter	Season		1 m	10 m	18 m	26 m
DO (cont.)	<i>Fall</i>	mean	8.18	—	7.82	—
		min	7.04	—	6.17	—
		max	10.98	—	8.89	—
		n	13199	—	13210	id
		n_prop	1	—	1	0
pHT (pH Total scale)	<i>Spring</i>	n	id	—	—	id
		n_prop	0.02	—	—	0.02
	<i>Summer</i>	mean	8.08	—	—	—
		min	7.98	—	—	—
		max	8.35	—	—	—
		n	13242	—	—	id
		n_prop	1	—	—	0.3
	<i>Fall</i>	mean	8.05	—	—	—
		min	7.93	—	—	—
		max	8.22	—	—	—
		n	7842	—	—	id
		n_prop	0.59	—	—	0
	Chlorophyll a (µg/L)	<i>Spring</i>	n	id	—	—
n_prop			0.01	—	—	0.02
<i>Summer</i>		n	id	—	—	id
		n_prop	0.33	—	—	0.03
<i>Fall</i>		n	id	—	—	id
	n_prop	0.33	—	—	0	
CDOM (ppb)	<i>Spring</i>	n	id	—	id	id
		n_prop	0.01	—	0.02	0.02
	<i>Summer</i>	mean	—	—	3.84	—
		min	—	—	2	—
		max	—	—	6	—
		n	id	—	12890	id
		n_prop	0.32	—	0.97	0.03
	<i>Fall</i>	mean	—	—	3.56	—
		min	—	—	2	—
		max	—	—	6	—
		n	id	—	12347	id
		n_prop	0.15	—	0.93	0
	Turbidity (NTU)	<i>Spring</i>	n	id	—	id
n_prop			0.01	—	0.02	0.02

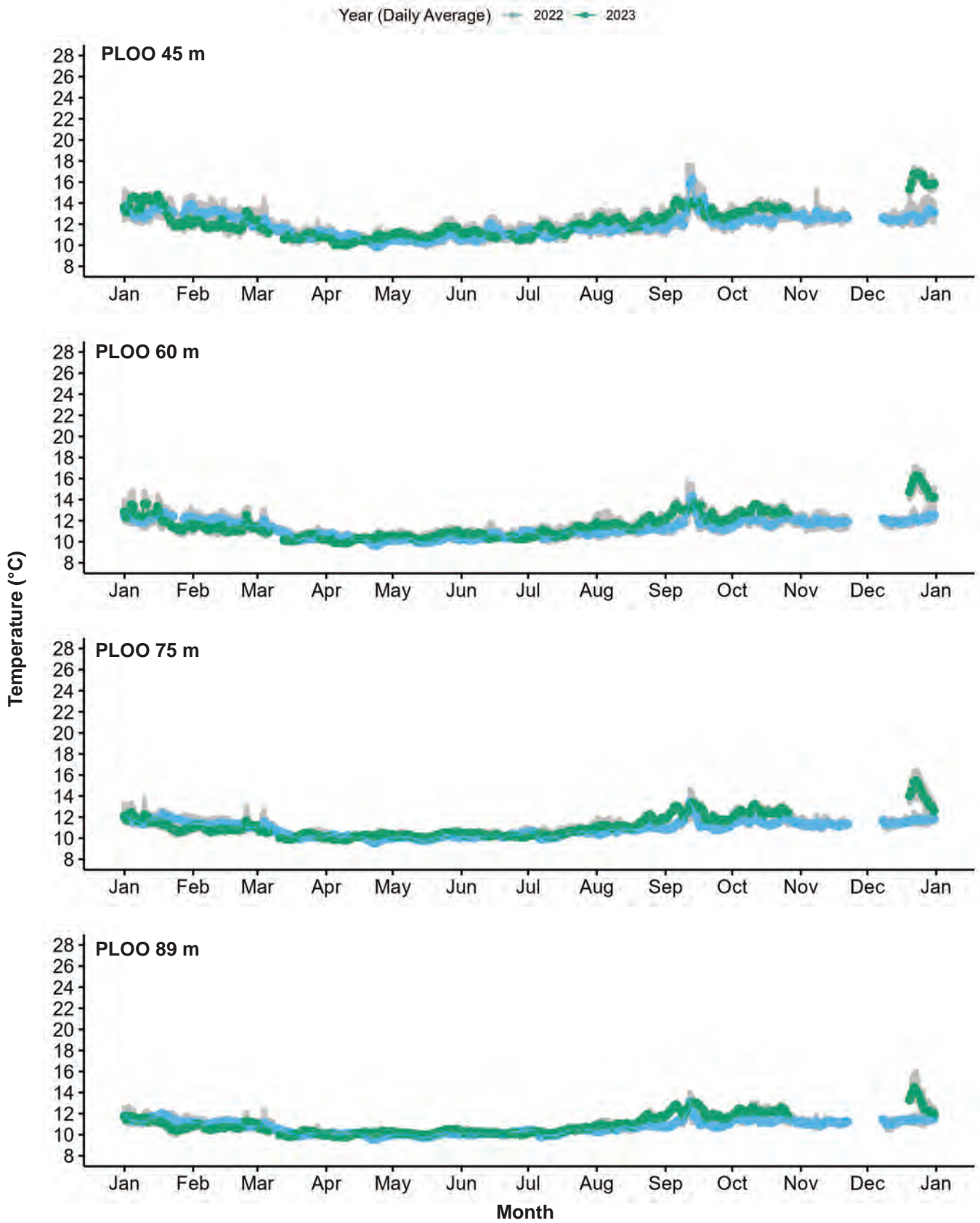
Appendix C.11 *continued*

Parameter	Season		1 m	10 m	18 m	26 m
Turbidity (<i>cont.</i>)	<i>Summer</i>	mean	—	—	0.19	—
		min	—	—	0.05	—
		max	—	—	1.9	—
		n	id	—	13164	id
		n_prop	0.3	—	0.99	0.03
	<i>Fall</i>	mean	—	—	0.23	—
		min	—	—	0.05	—
		max	—	—	1.84	—
		n	id	—	12579	id
		n_prop	0.15	—	0.95	0
Nitrate + nitrite (µM)	<i>Spring</i>	n	id	—	—	id
		n_prop	0.02	—	—	0.02
	<i>Summer</i>	mean	1.08	—	—	—
		min	0	—	—	—
		max	2.76	—	—	—
		n	1783	—	—	id
		n_prop	0.81	—	—	0.3
	<i>Fall</i>	mean	1.77	—	—	—
		min	0	—	—	—
		max	3.19	—	—	—
n		1576	—	—	id	
n_prop		0.71	—	—	0	
BOD (mg/L)	<i>Spring</i>	n	—	—	—	id
		n_prop	—	—	—	0.01
	<i>Summer</i>	n	—	—	—	id
		n_prop	—	—	—	0.09
	<i>Fall</i>	n	—	—	—	id
		n_prop	—	—	—	0
xCO ₂ (ppm)	<i>Spring</i>	n	id	—	—	—
		n_prop	0.02	—	—	—
	<i>Summer</i>	mean	323.57	—	—	—
		min	152.36	—	—	—
		max	441.94	—	—	—
		n	2208	—	—	—
		n_prop	1	—	—	—
	<i>Fall</i>	n	id	—	—	—
		n_prop	0.37	—	—	—

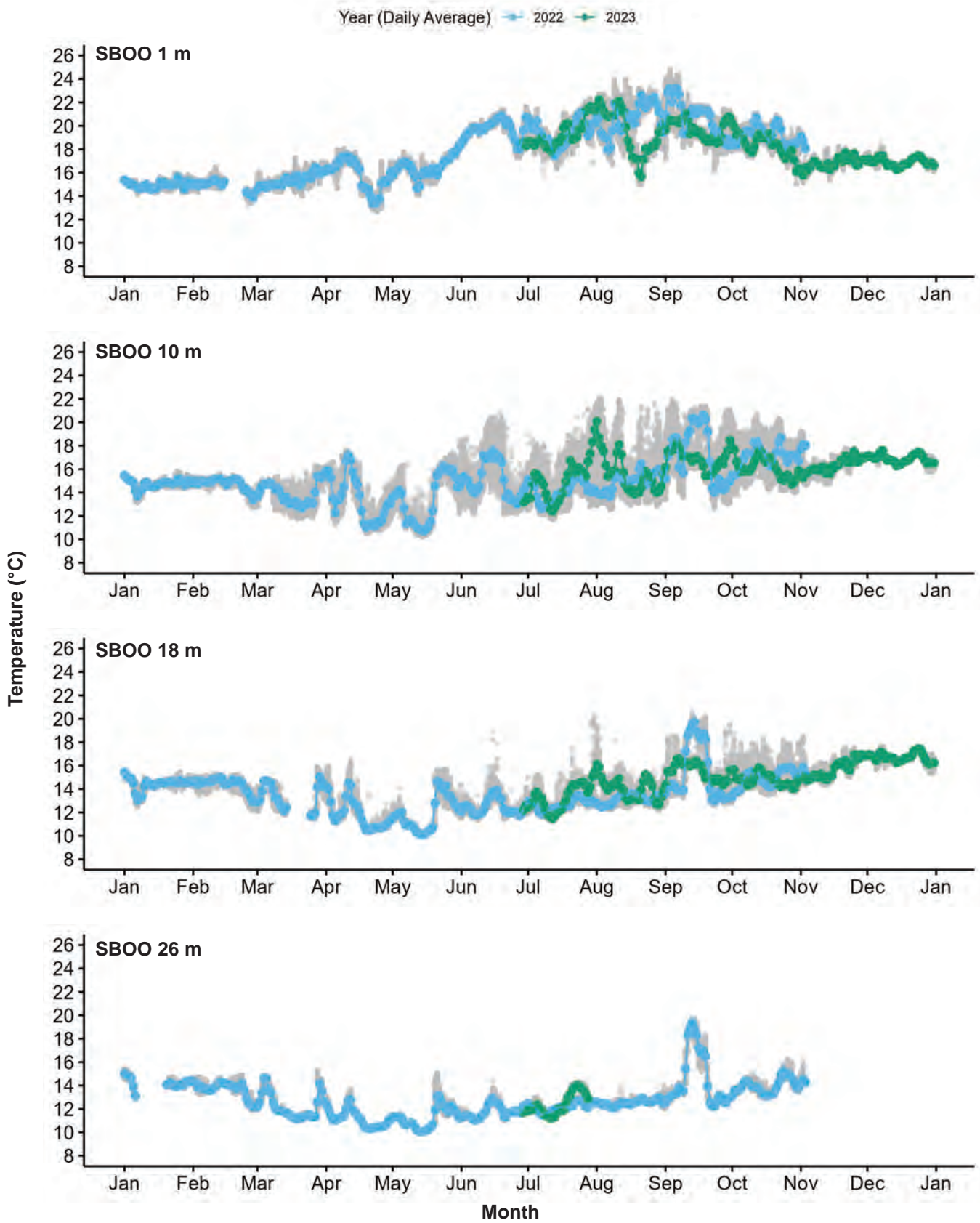


Appendix C.12

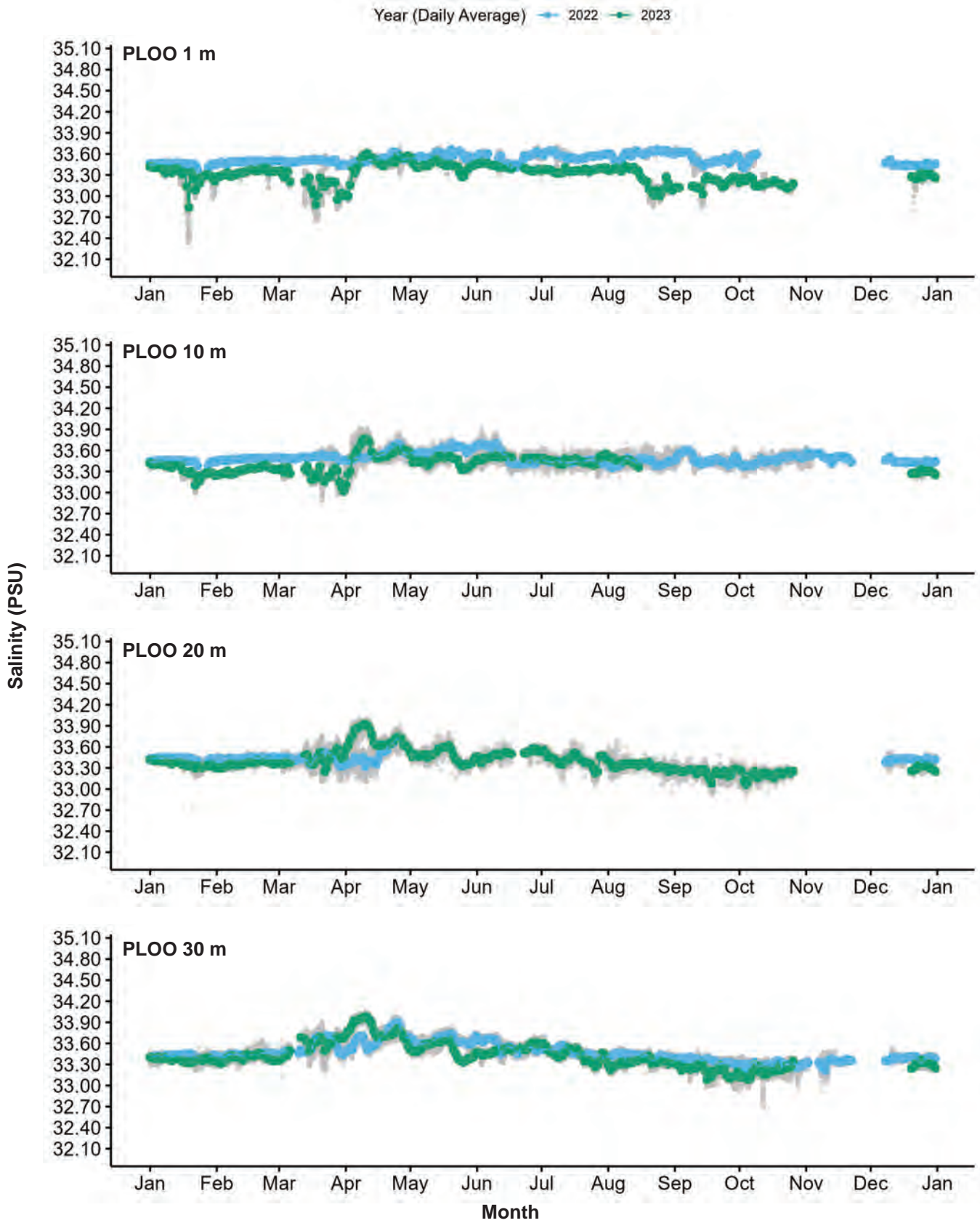
Temperature, salinity, DO, pH (total scale), chlorophyll a, CDOM, turbidity, nitrate + nitrite, BOD, and xCO₂ recorded at various depths by the PLOO and SBOO RTOMS during 2022 and 2023. Grey points represent raw data while green and blue points represent daily averaged data.



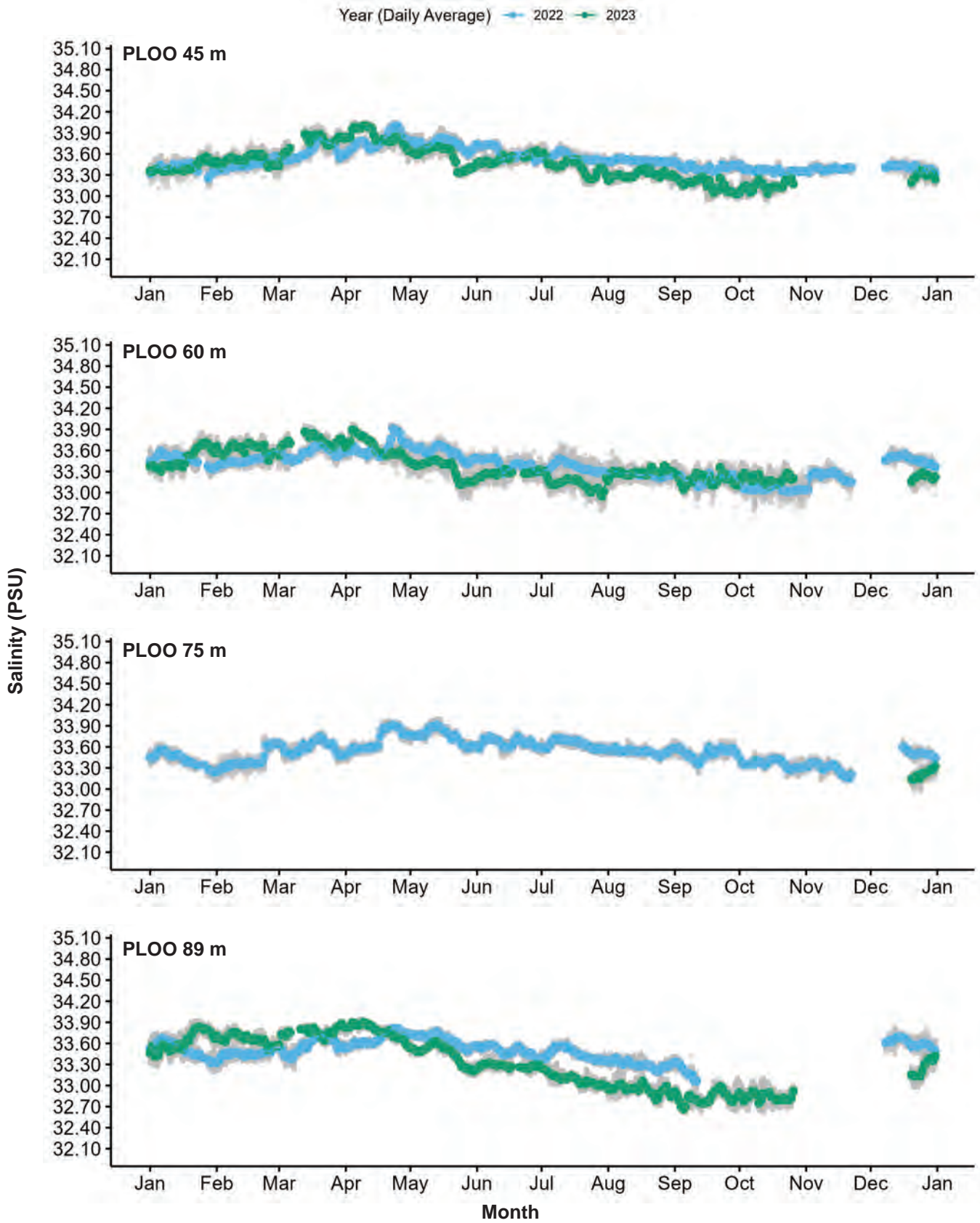
Appendix C.12 *continued*



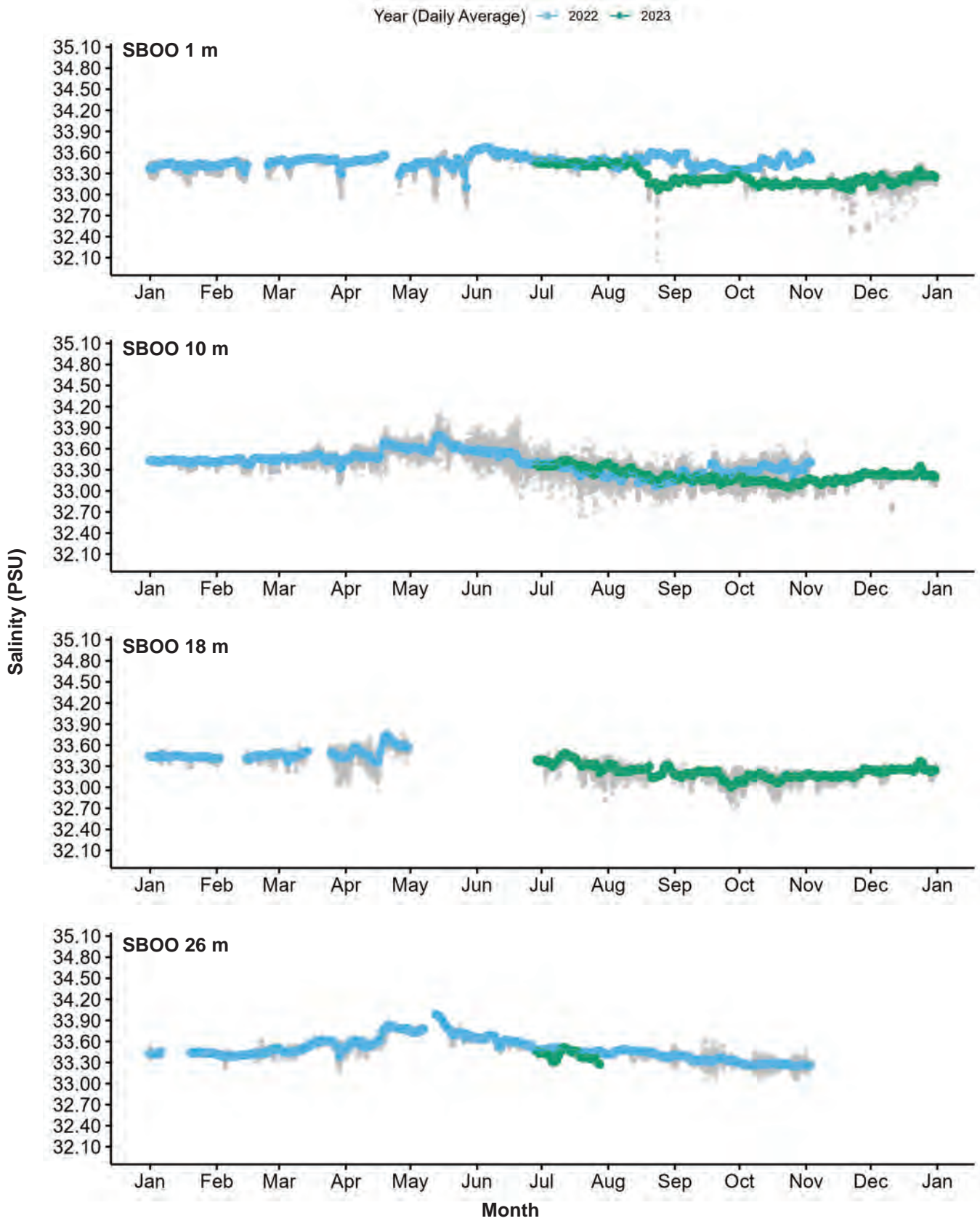
Appendix C.12 *continued*



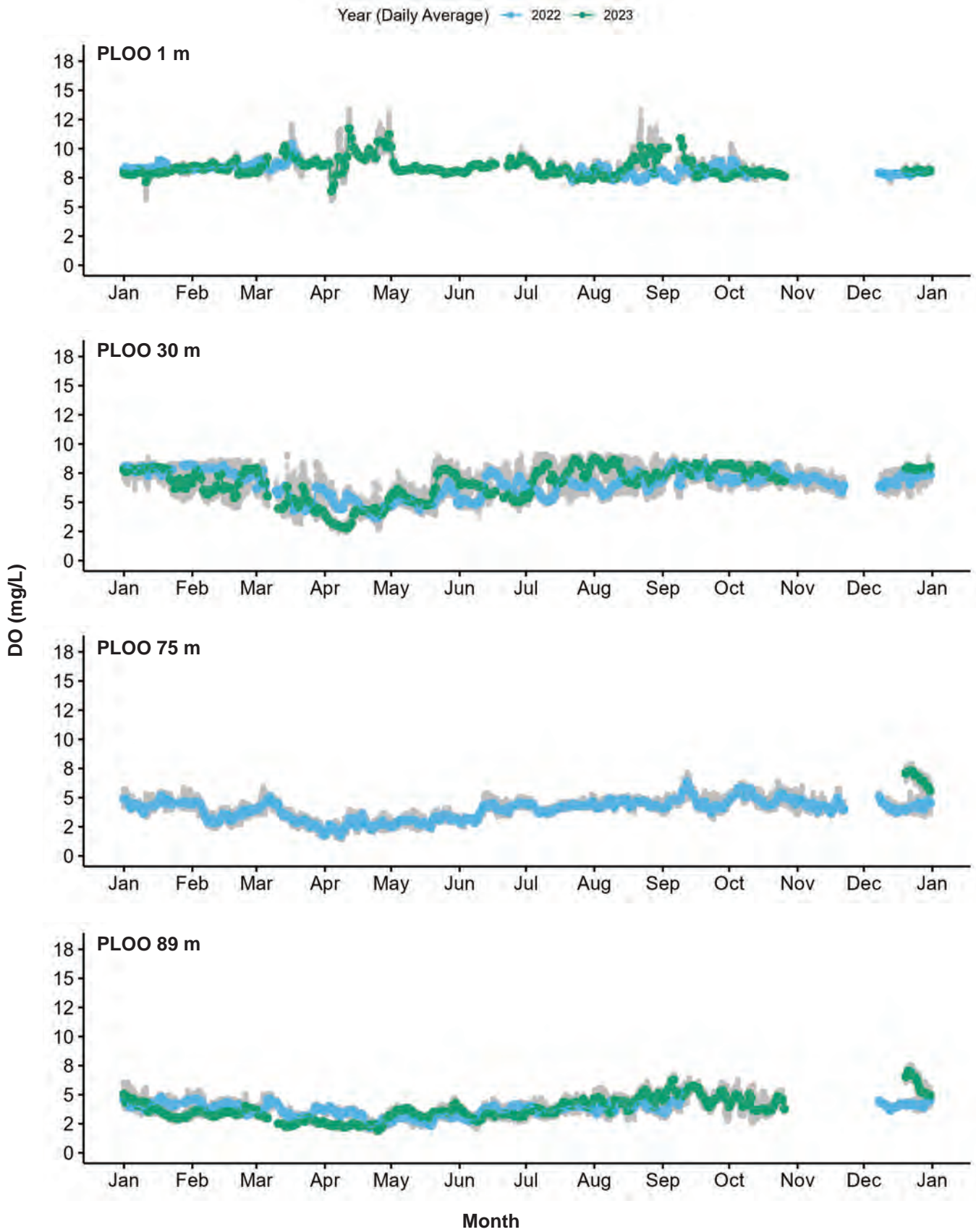
Appendix C.12 *continued*



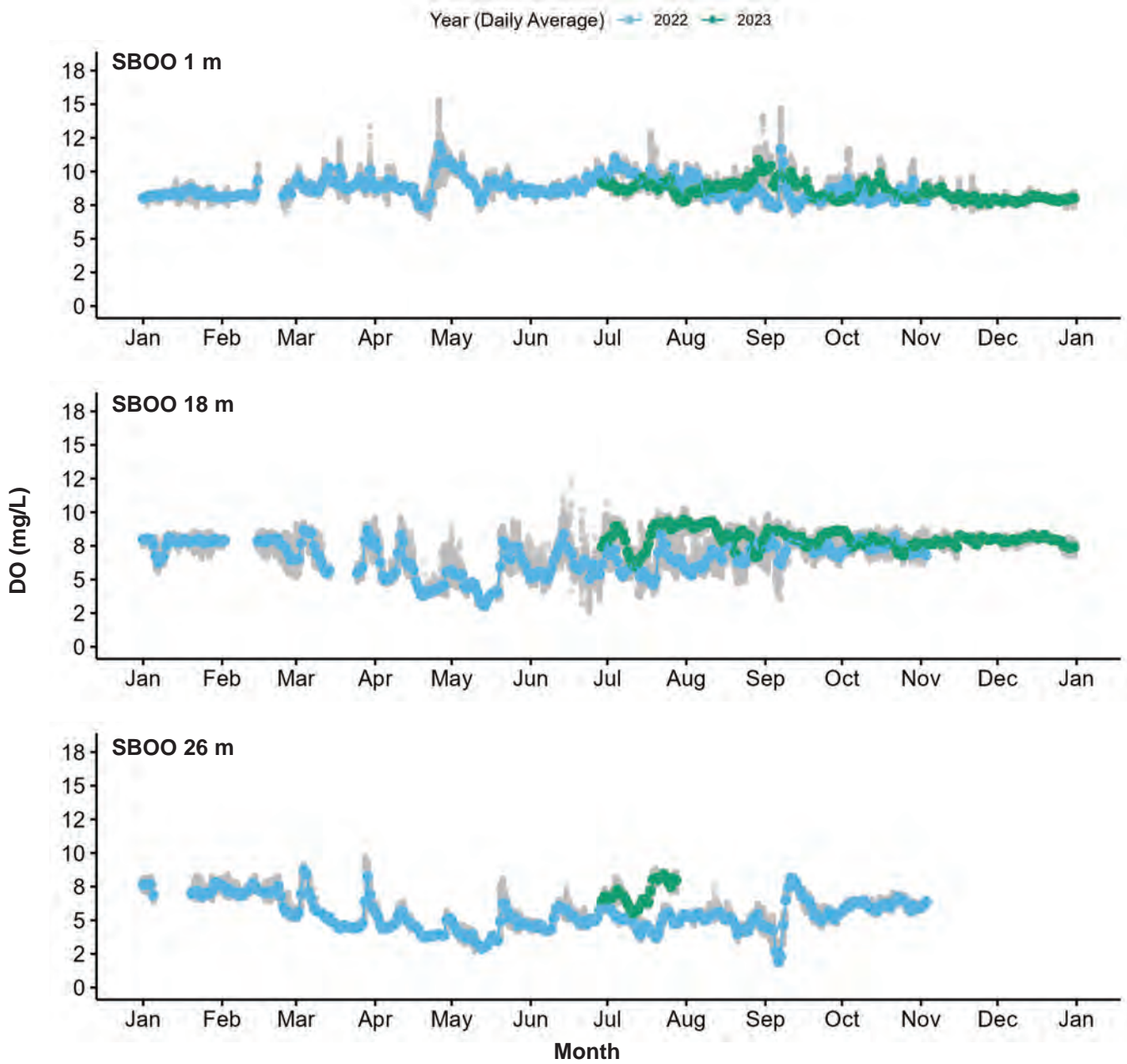
Appendix C.12 *continued*



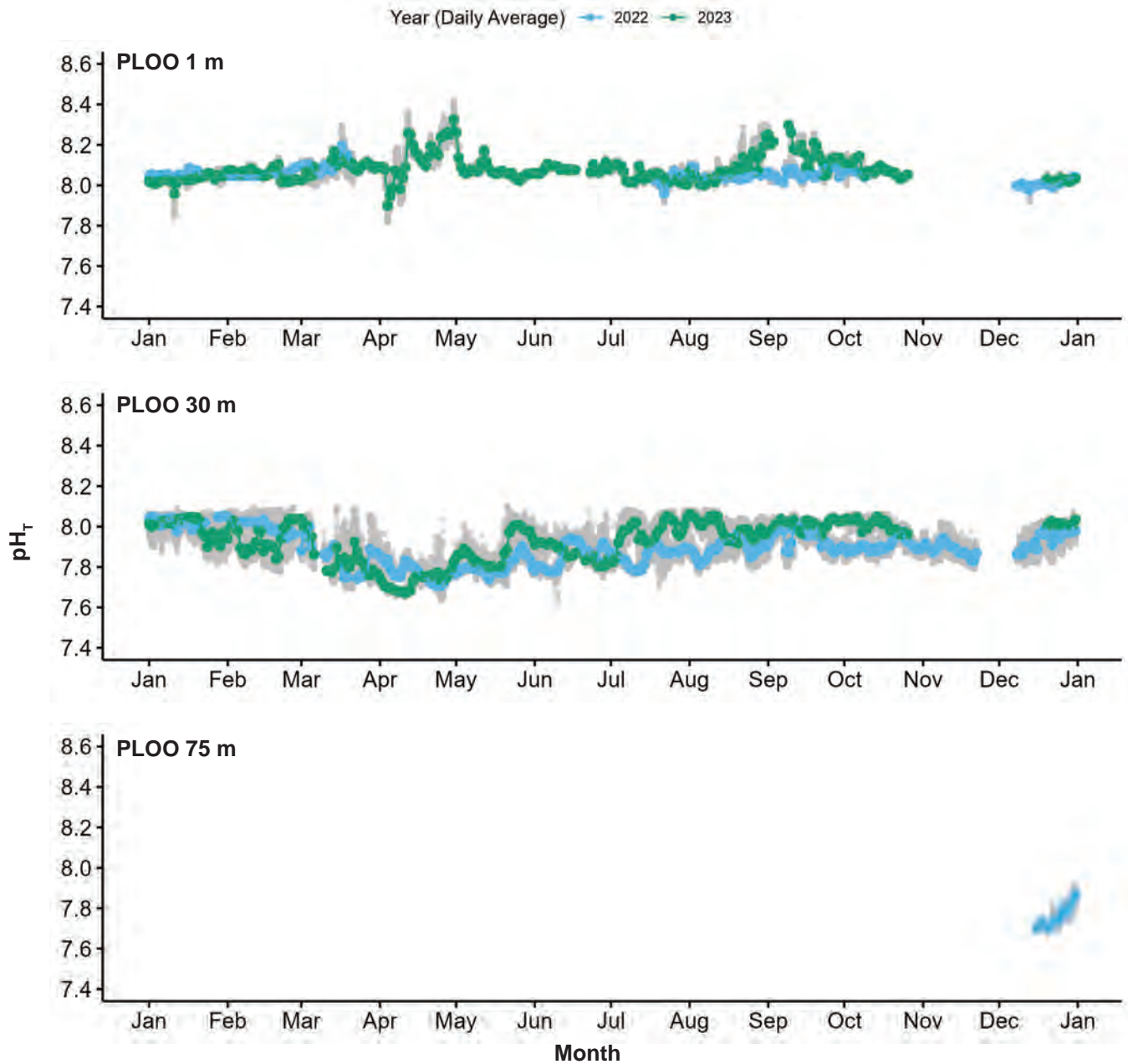
Appendix C.12 *continued*



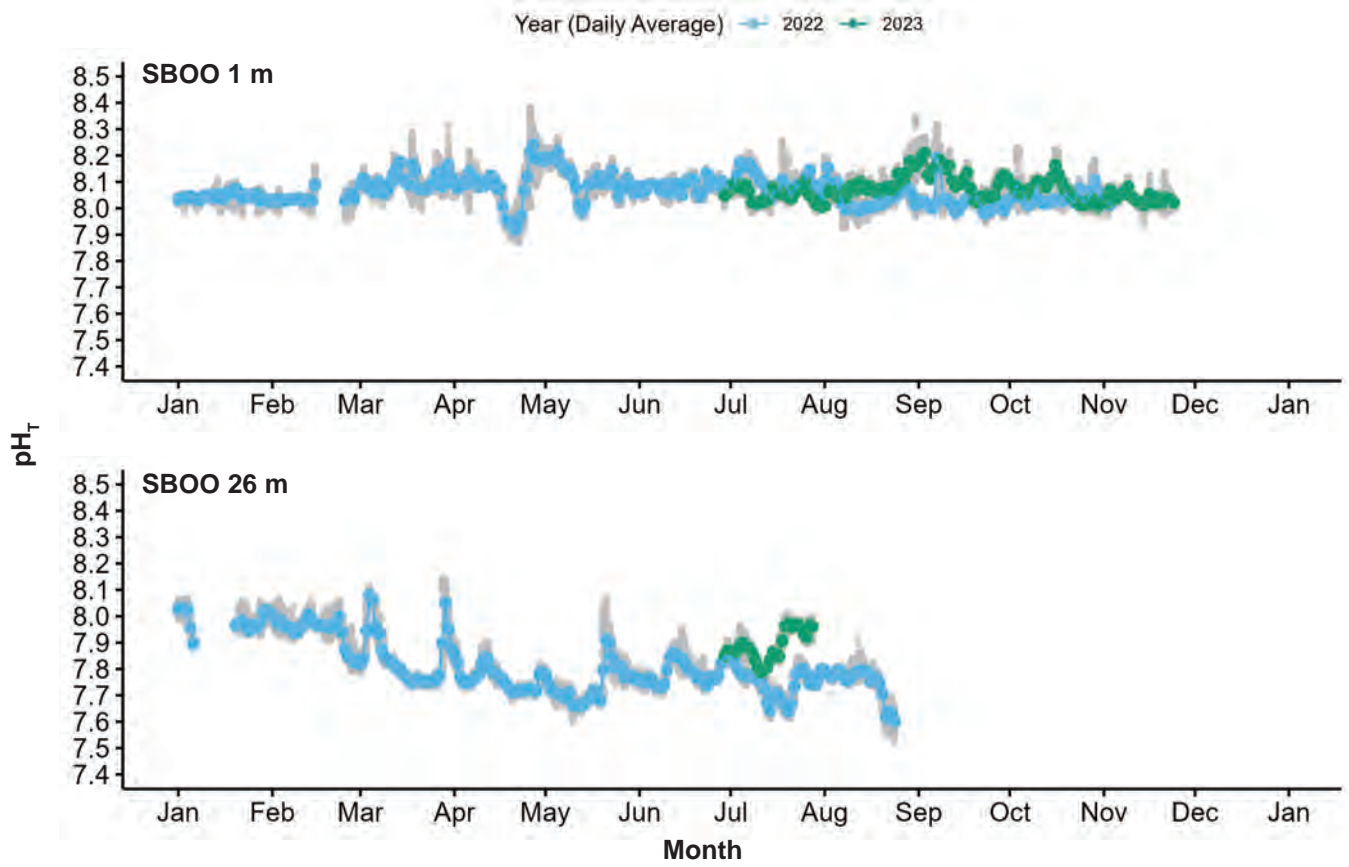
Appendix C.12 *continued*



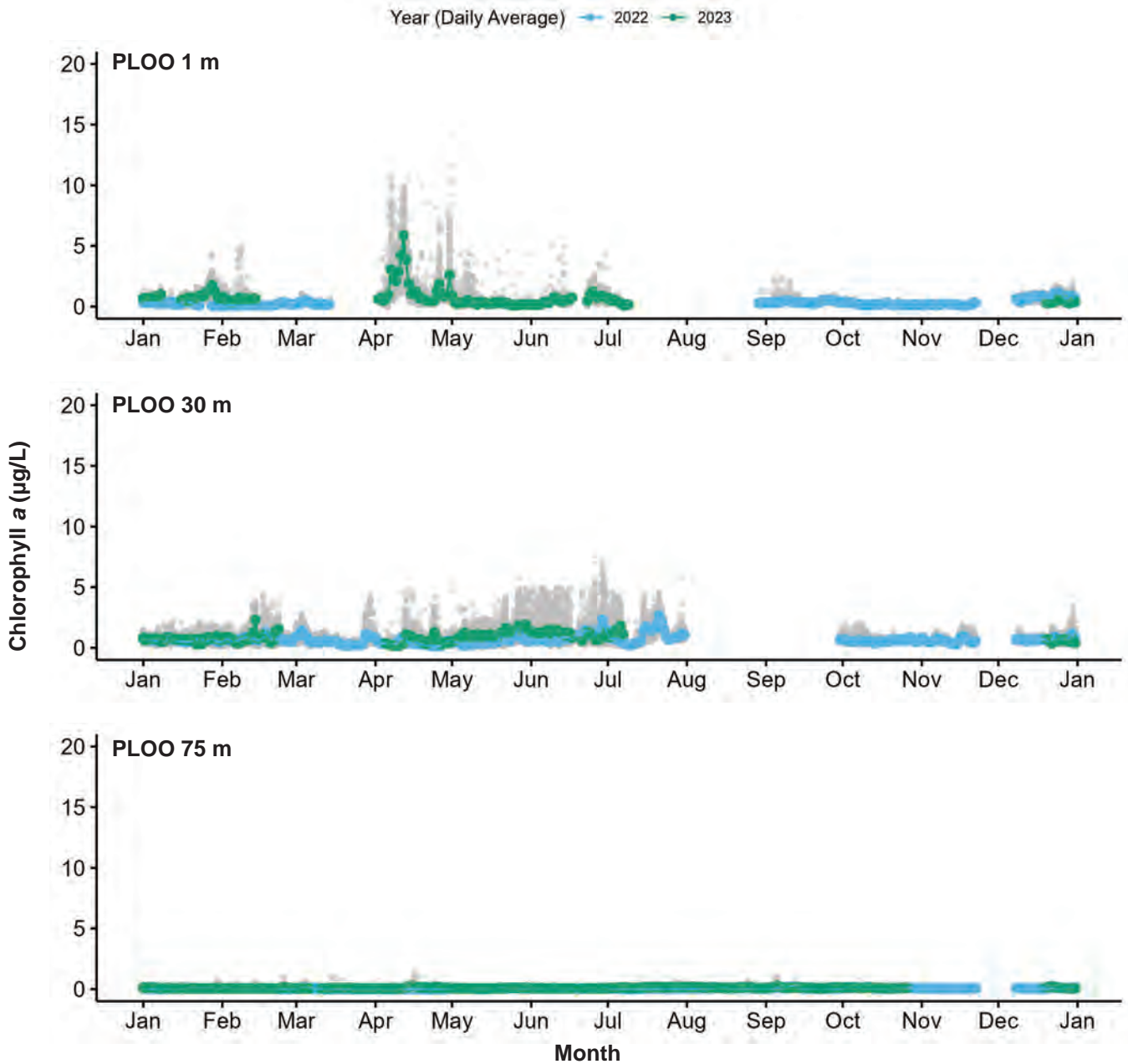
Appendix C.12 *continued*



Appendix C.12 *continued*

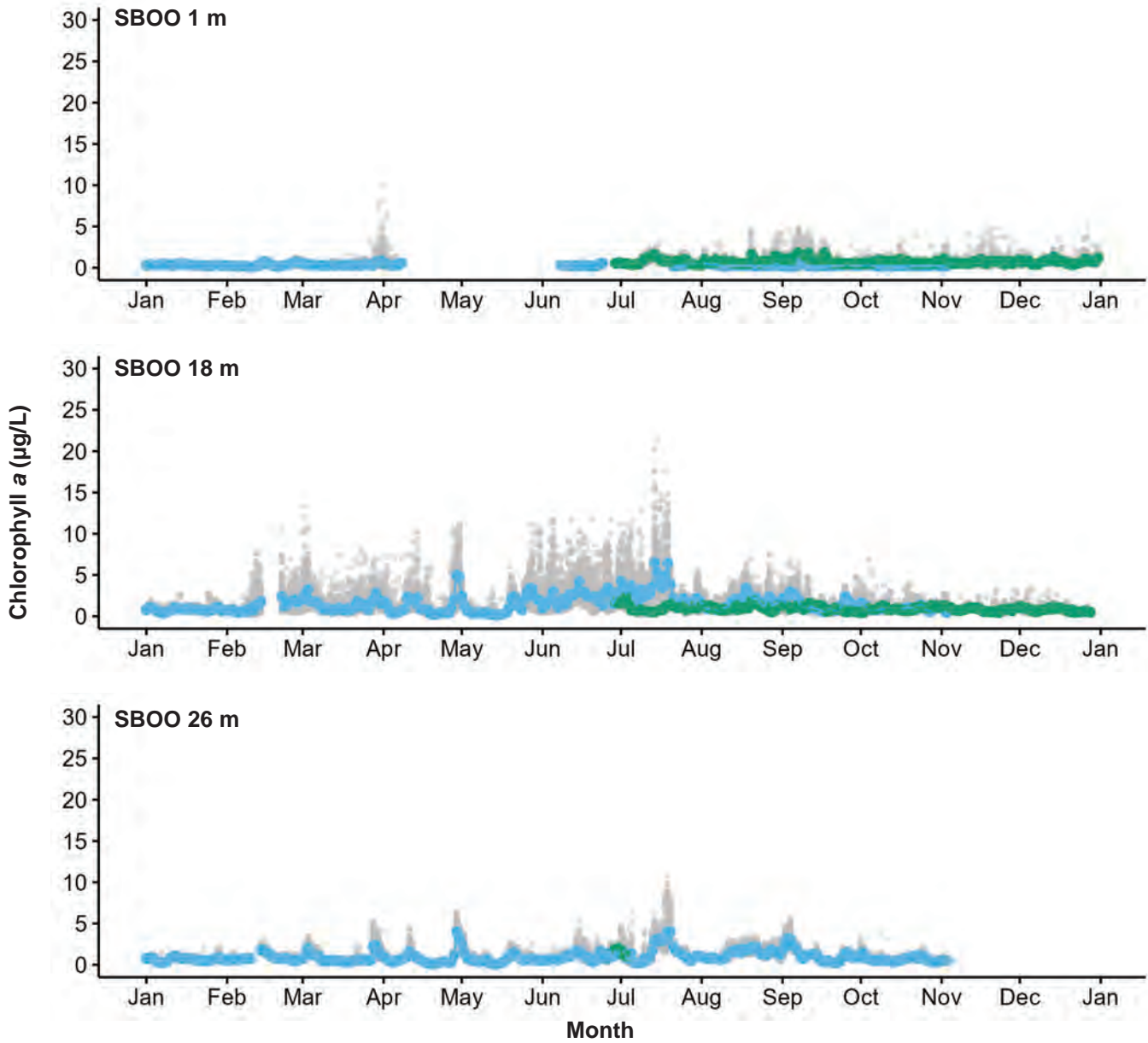


Appendix C.12 *continued*

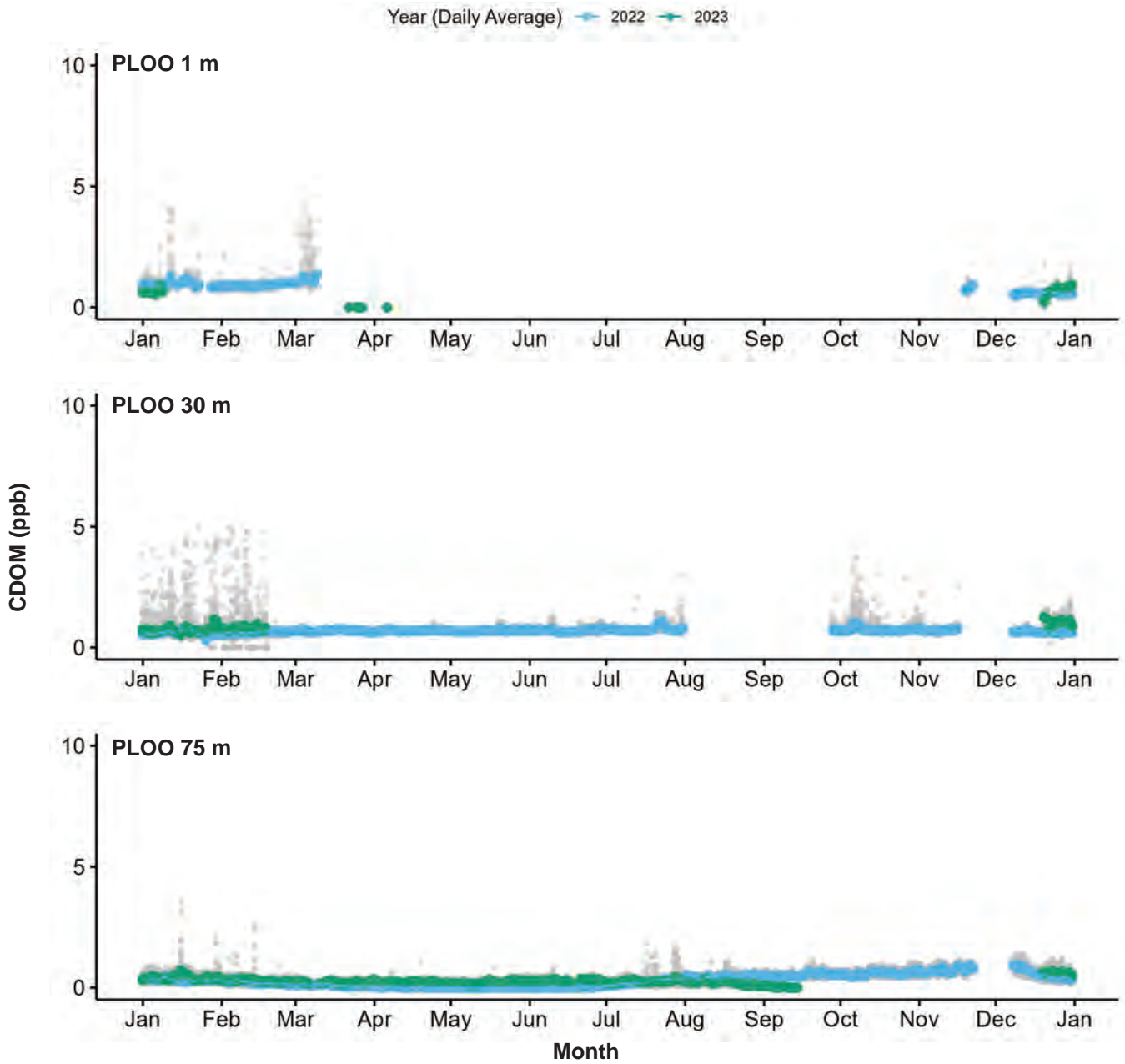


Appendix C.12 *continued*

Year (Daily Average) — 2022 — 2023

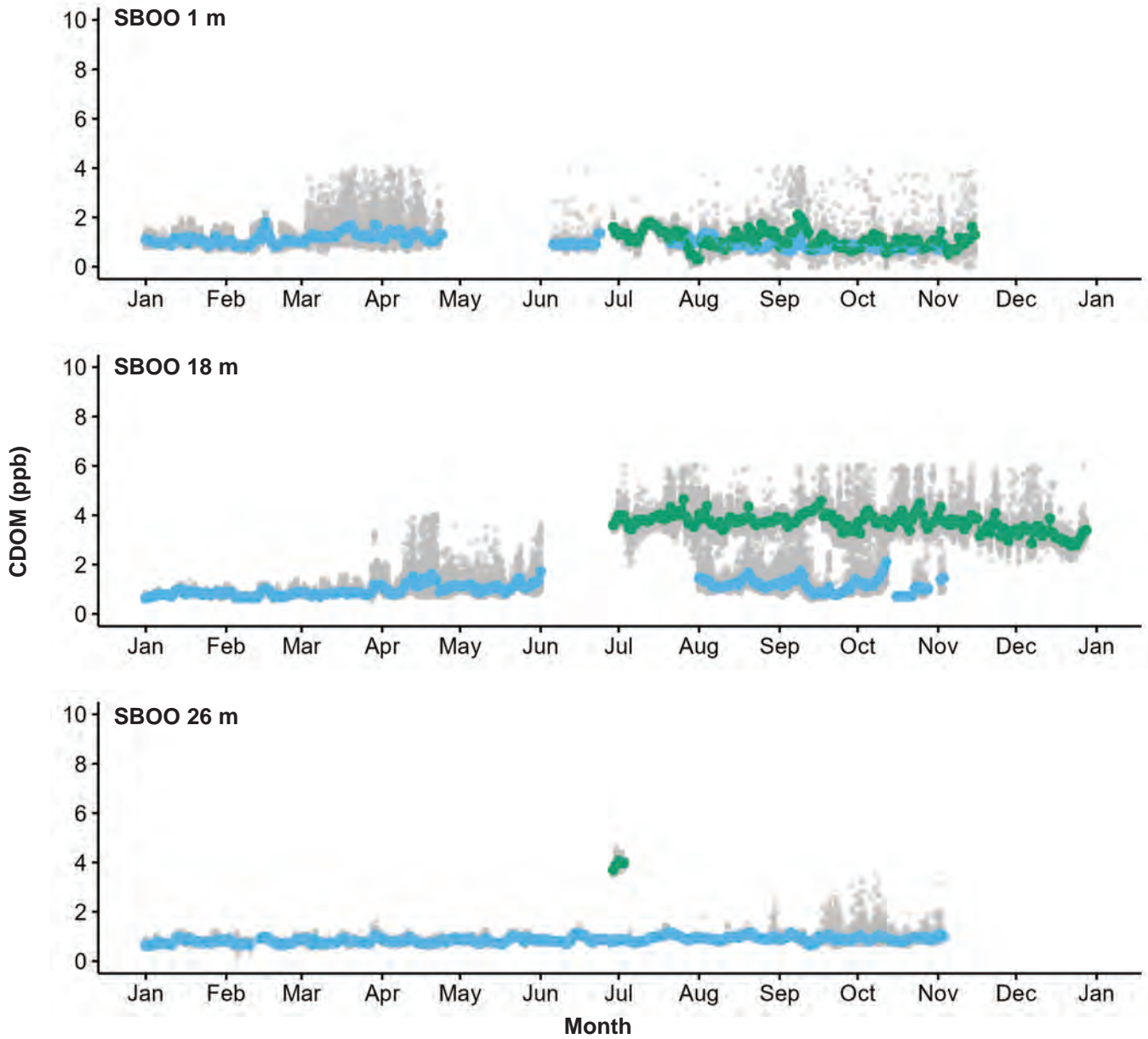


Appendix C.12 *continued*

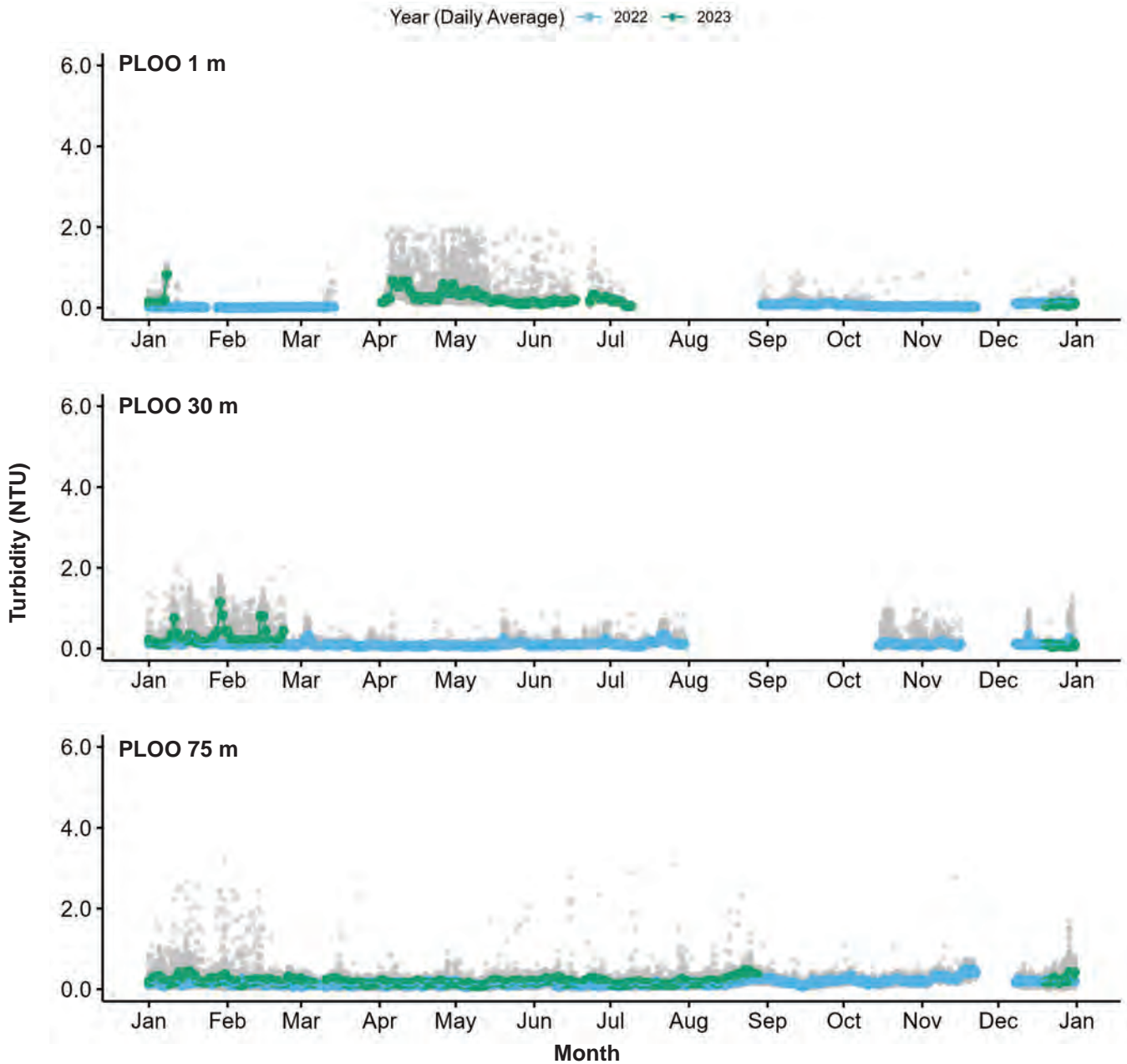


Appendix C.12 *continued*

Year (Daily Average) — 2022 — 2023

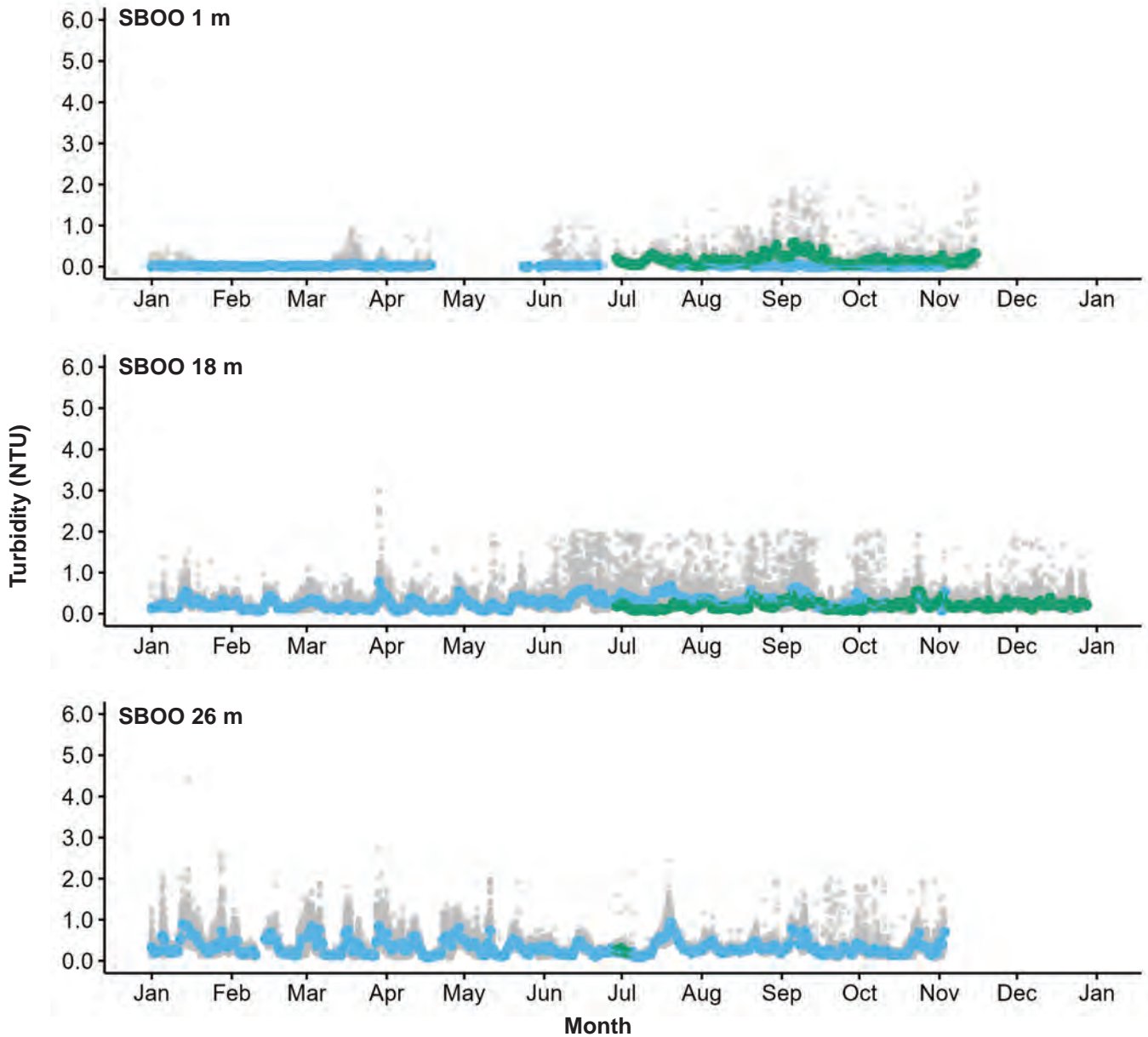


Appendix C.12 *continued*

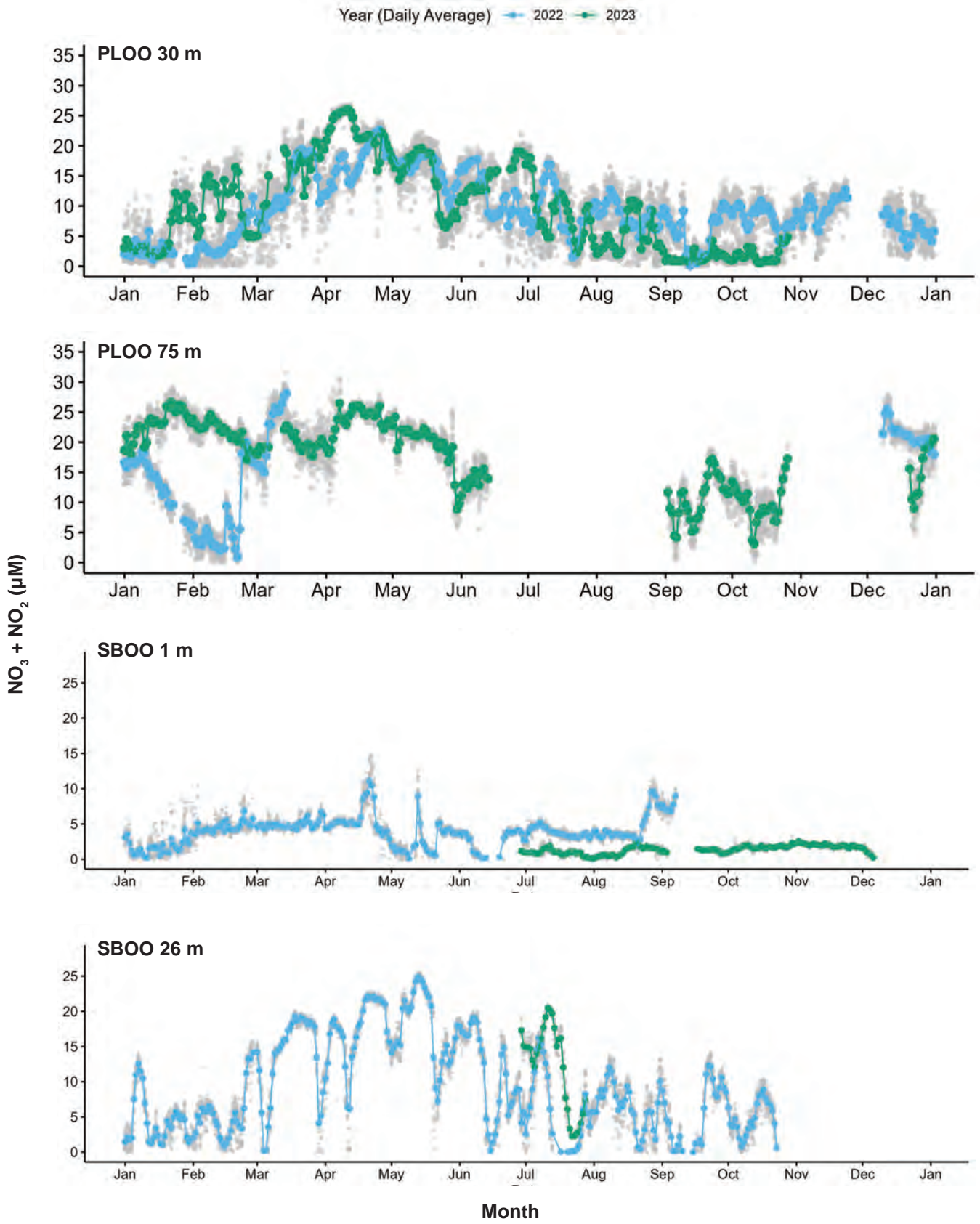


Appendix C.12 *continued*

Year (Daily Average) 2022 2023

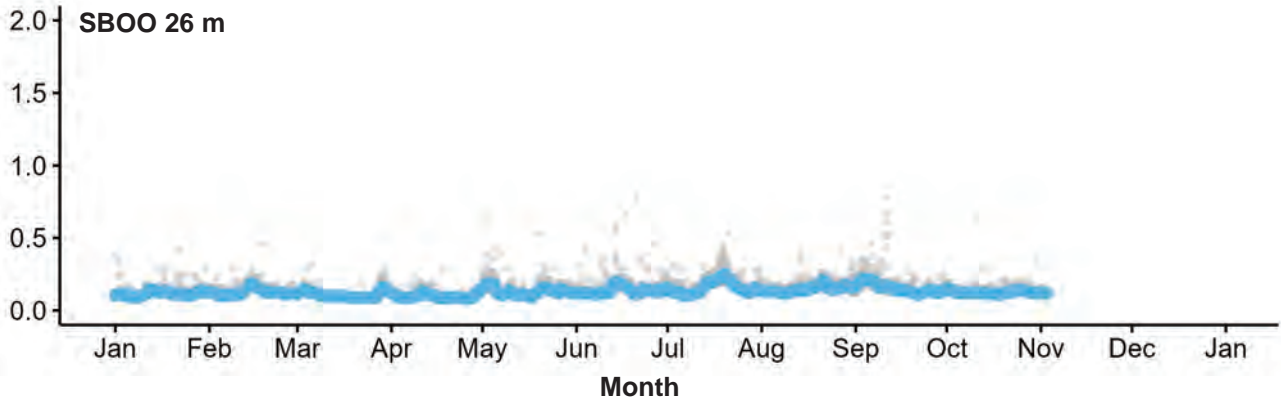
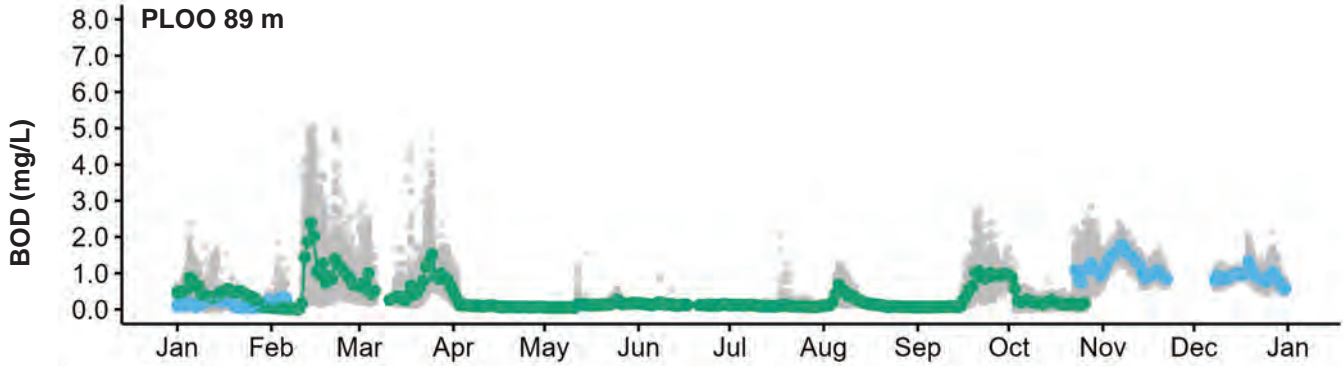
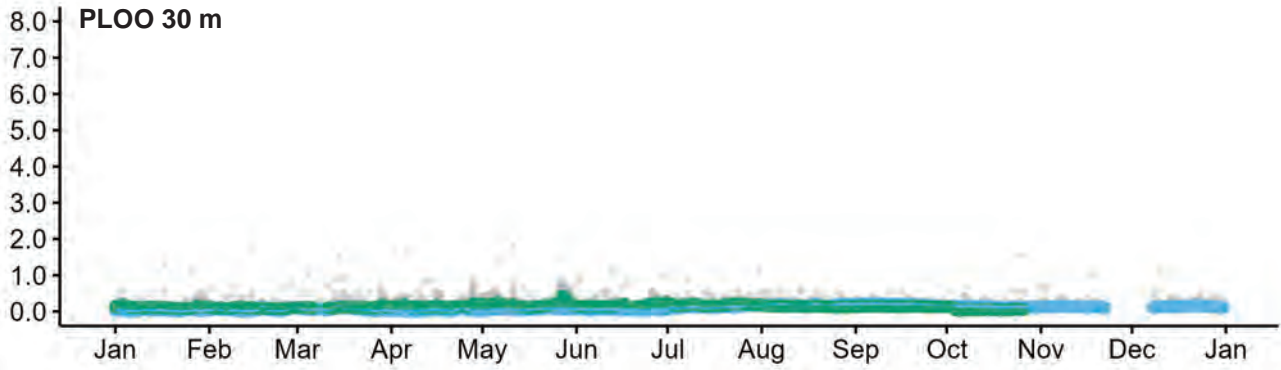


Appendix C.12 *continued*

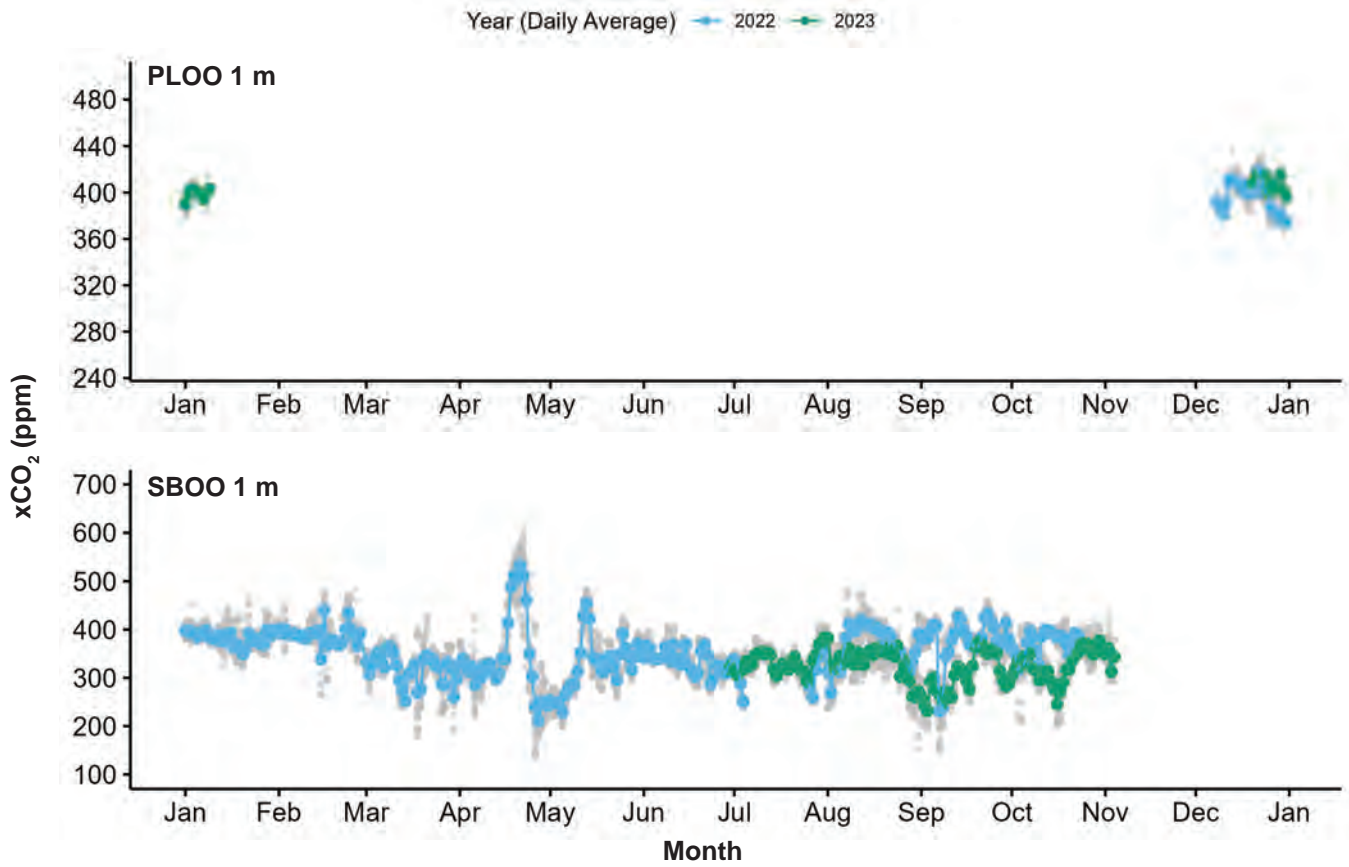


Appendix C.12 *continued*

Year (Daily Average) 2022 2023



Appendix C.12 *continued*

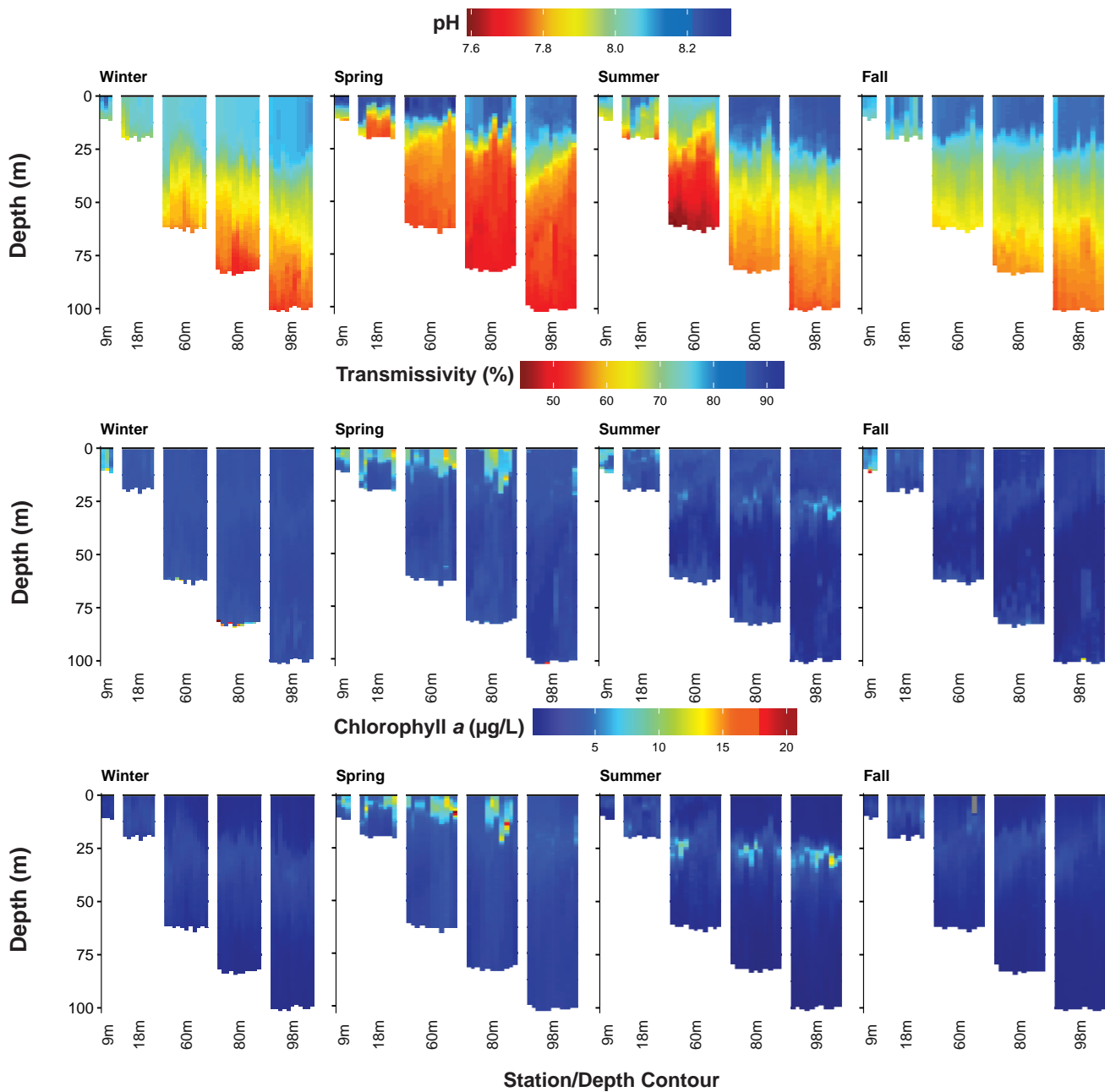


Appendix C.12 *continued*

Appendix C.13

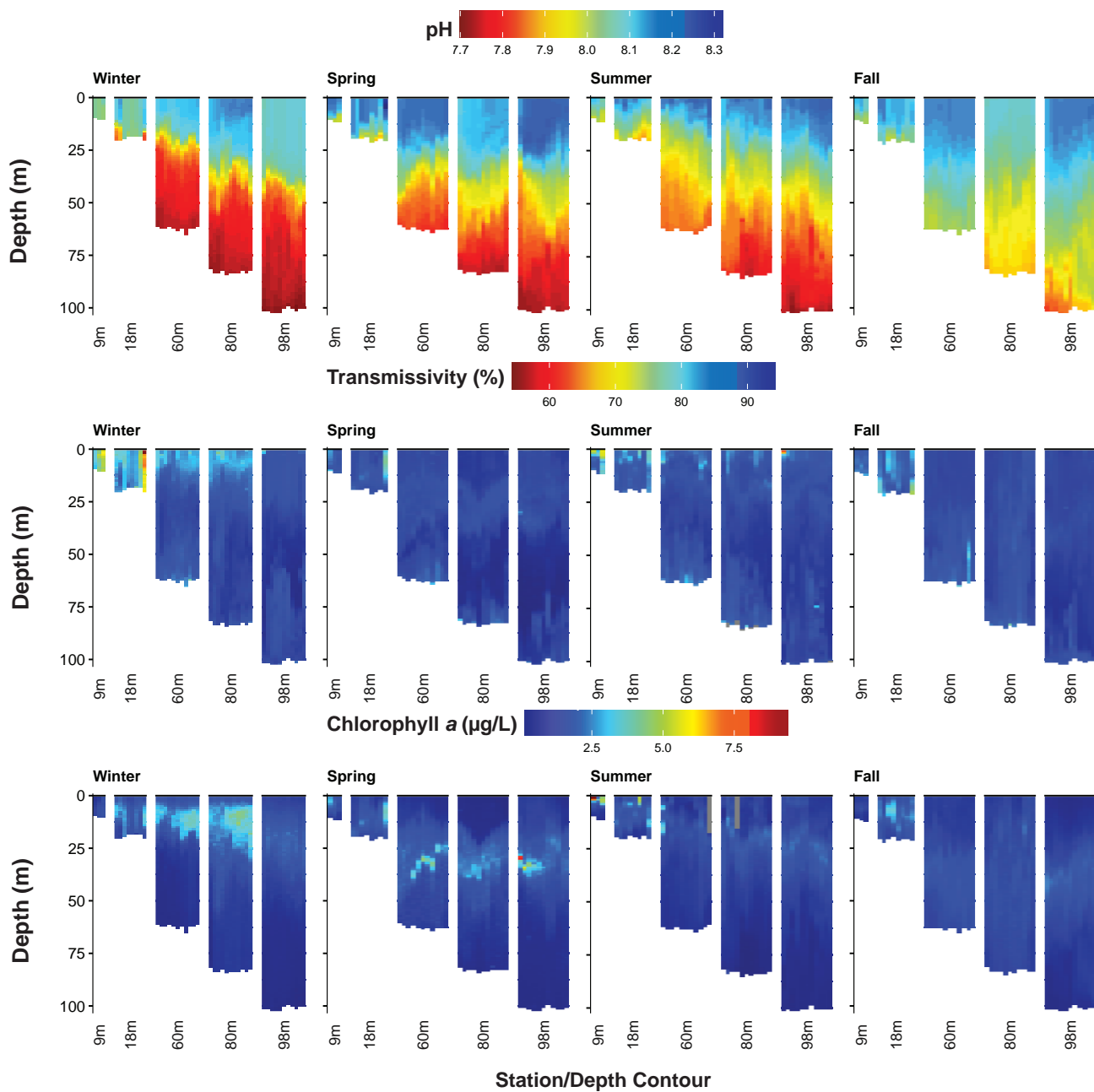
Summary of seasonal buoyancy frequency in the PLOO and SBOO regions during 2022 and 2023. Depth refers to the depth of maximum buoyancy frequency. Max BF refers to the maximum buoyancy frequency, measured in cycles per second. For each quarter: n=11 (PLOO), n=13 (SBOO).

	2022		2023	
	Depth (m)	Max BF (s ⁻¹)	Depth (m)	Max BF (s ⁻¹)
<i>PLOO Region</i>				
Winter	37	5.33	40	7.12
Spring	11	8.68	20	8.92
Summer	5	16.93	6	16.77
Fall	26	8.99.	29	6.34
<i>SBOO Region</i>				
Winter	28	5.29	13	8.03
Spring	11	10.88	7	9.44
Summer	3	14.22	7	12.56
Fall	20	3.89	15	5.68



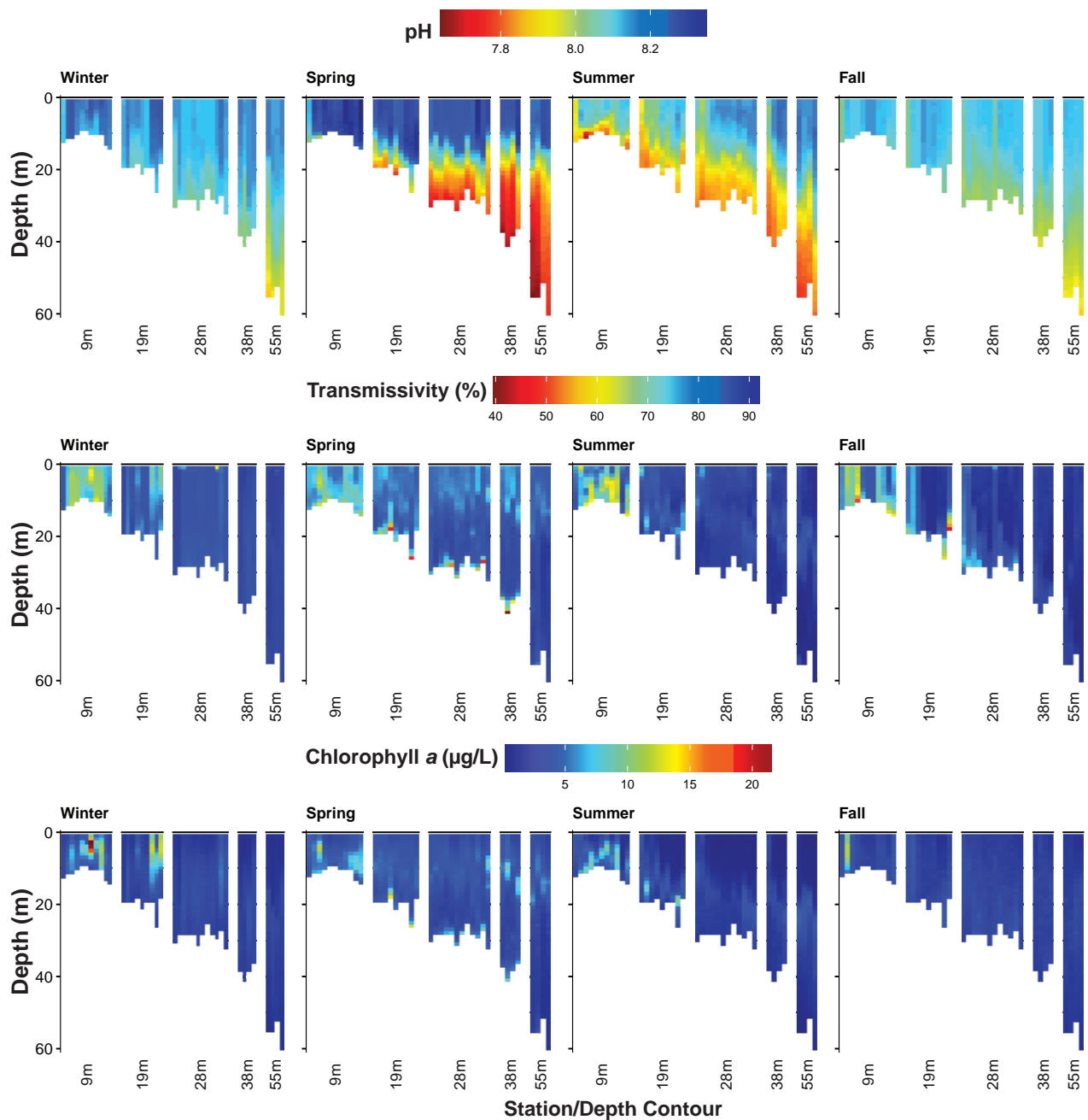
Appendix C.14

Values of pH, transmissivity, and chlorophyll a recorded in the PLOO region during 2022. Data are 1-m binned values per depth for each station and were collected over 4–5 days during each quarterly survey. Stations are depicted from north to south along each depth contour.



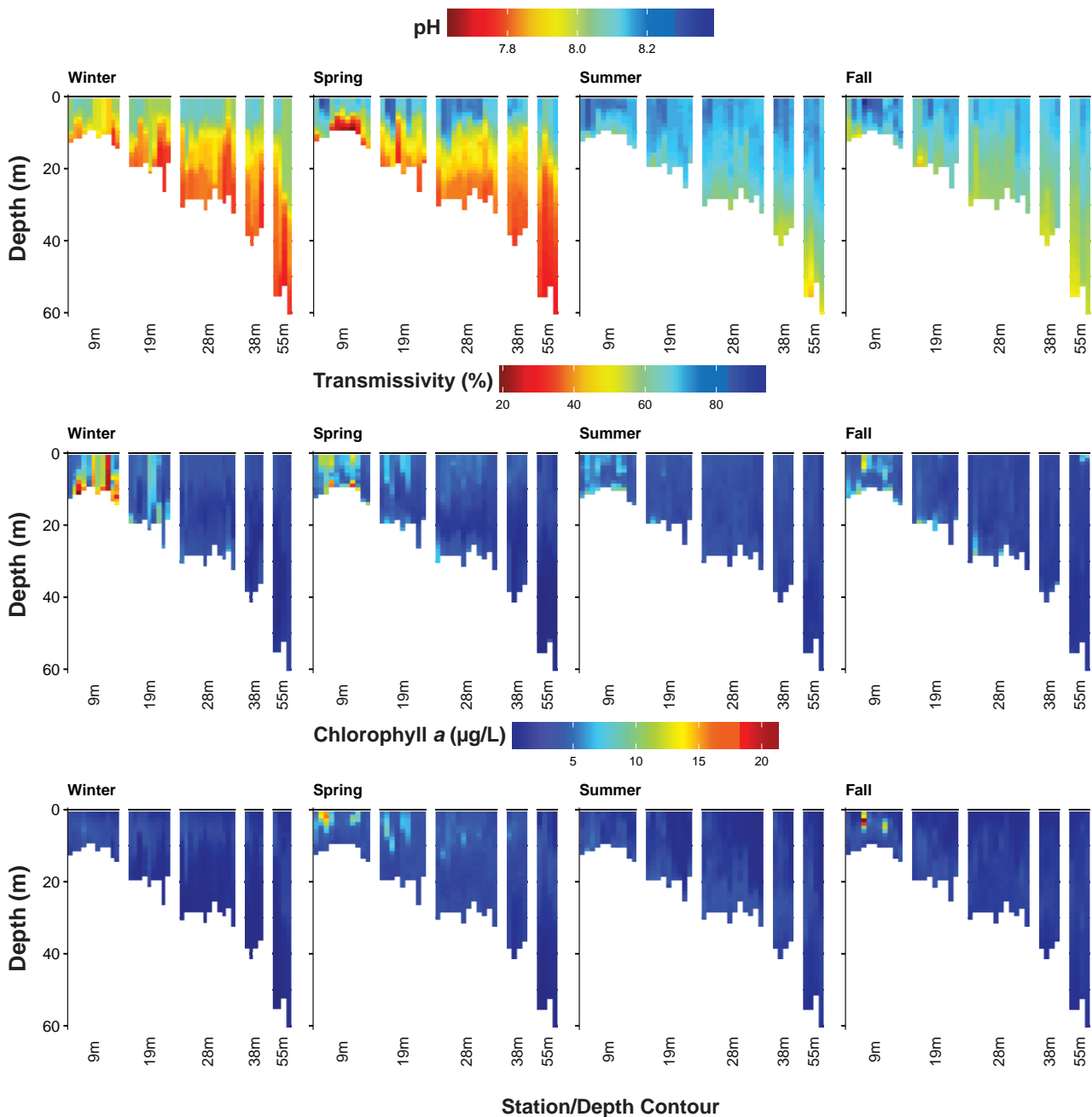
Appendix C.15

Values of pH, transmissivity, and chlorophyll a recorded in the PLOO region during 2023. Data are 1-m binned values per depth for each station and were collected over 4–5 days during each quarterly survey. Stations are depicted from north to south along each depth contour.



Appendix C.16

Values of pH, transmissivity, and chlorophyll *a* recorded in the SBOO region during 2022. Data are 1-m binned values per depth for each station and were collected over 4–5 days during each quarterly survey. Stations are depicted from north to south along each depth contour.



Appendix C.17

Values of pH, transmissivity, and chlorophyll a recorded in the SBOO region during 2023. Data are 1-m binned values per depth for each station and were collected over 4–5 days during each quarterly survey. Stations are depicted from north to south along each depth contour.

Appendix C.18

Summary of current velocity magnitude and direction from the PLOO RTOMS ADCP during 2022 and 2023. Data are presented by depth bin as seasonal recovered observations (n), minimum (min), maximum (max), and means with 95% confidence intervals (CI). Proportion of recovered observations (n_prop) differed due to variations in data quality (see text). Minimum and maximum angles of velocity are not shown due to the circular nature of the measurement.

Season	Depth (m)	n	n_prop	Magnitude (mm/s)				Angle	
				Min	Max	Mean	95% CI	Mean	95% CI
<i>Winter</i>	3	23499	1	1	498	155	1	163	73
	4	23498	1	1	510	155	1	161	72
	5	23498	1	0	507	159	1	162	73
	6	23498	1	2	521	161	1	162	74
	7	23499	1	1	514	162	1	162	74
	8	23497	1	2	529	158	1	163	74
	9	23497	1	2	534	156	1	161	74
	10	23498	1	6	542	162	1	162	74
	11	23498	1	1	539	165	1	162	75
	12	23496	1	2	527	166	1	162	75
	13	23497	1	1	526	165	1	162	75
	14	23495	1	2	533	163	1	162	75
	15	23495	1	5	516	164	1	161	75
	16	23494	1	2	513	164	1	161	75
	17	23494	1	6	513	163	1	161	75
	18	23495	1	1	505	163	1	160	75
	19	23494	1	4	495	162	1	160	75
	20	23496	1	0	488	162	1	158	75
	21	23494	1	5	475	160	1	158	75
	22	23496	1	5	470	159	1	158	75
	23	23493	1	0	462	157	1	157	75
	24	23495	1	3	460	155	1	156	75
	25	23490	1	2	441	152	1	156	76
	26	23491	1	3	424	142	1	163	75
	27	23488	1	0	404	136	1	162	76
	28	23490	1	1	408	143	1	152	76
	29	23489	1	6	391	142	1	150	76
	30	23492	1	2	396	140	1	149	77
	31	23489	1	1	406	138	1	149	77
	32	23488	1	6	401	136	1	148	77
	33	23487	1	4	398	134	1	147	77
	34	23490	1	4	402	132	1	146	77
	35	23490	1	2	397	129	1	144	77
	36	23489	1	4	390	126	1	142	77

Appendix C.18 *continued*

Season	Depth (m)	n	n_prop	Magnitude (mm/s)				Angle	
				Min	Max	Mean	95% CI	Mean	95% CI
37	23488	1	1	1	385	123	1	140	77
38	23490	1	1	0	378	121	1	140	77
39	23489	1	1	1	375	118	1	139	77
40	23486	1	1	0	356	115	1	138	77
41	23486	1	1	1	351	111	1	137	77
42	23487	1	1	1	360	110	1	133	77
43	23485	1	1	0	365	109	1	132	77
44	23486	1	1	0	361	108	1	132	77
45	23488	1	1	1	362	106	1	129	77
46	23487	1	1	1	366	104	1	127	76
47	23482	1	1	3	359	102	1	126	77
48	23486	1	1	1	339	101	1	123	76
49	23484	1	1	3	338	99	1	120	76
50	23483	1	1	0	315	97	1	117	76
51	23477	1	1	4	315	95	1	112	76
52	23483	1	1	3	297	93	1	109	75
53	23482	1	1	3	290	92	1	106	75
54	23486	1	1	1	276	90	1	103	75
55	23479	1	1	1	264	88	1	99	74
56	23484	1	1	0	258	88	1	97	75
57	23475	1	1	1	254	88	1	95	74
58	23474	1	1	4	254	87	1	92	74
59	23478	1	1	0	247	85	1	91	73
60	23471	1	1	1	241	85	1	89	73
61	23469	1	1	0	246	84	1	89	73
62	23473	1	1	1	240	83	1	86	73
63	23467	1	1	8	234	82	1	84	72
64	23470	1	1	6	226	81	1	83	72
65	23463	1	1	1	217	80	1	82	72
66	23469	1	1	2	211	78	1	81	71
67	23469	1	1	0	197	76	1	80	70
68	23466	1	1	1	190	74	0	78	72
69	23466	1	1	2	177	72	0	76	71
70	23465	1	1	4	173	72	0	74	70
71	23469	1	1	5	175	76	0	78	69
72	23462	1	1	0	173	77	0	80	70
73	23445	1	1	5	163	76	0	80	69

Appendix C.18 *continued*

Season	Depth (m)	n	n_prop	Magnitude (mm/s)				Angle	
				Min	Max	Mean	95% CI	Mean	95% CI
	74	23444	1	0	162	74	0	81	69
	75	23427	1	1	166	73	0	81	69
	76	23408	1	1	165	72	0	83	69
	77	23401	1	0	161	71	0	82	68
	78	23379	0.99	1	160	69	0	82	68
	79	23363	0.99	1	157	67	0	83	69
	80	23371	0.99	0	152	65	0	80	68
	81	23376	0.99	1	152	64	0	82	70
	82	23383	1	0	150	61	0	78	67
	83	23384	1	0	139	61	0	79	67
	84	23386	1	1	141	59	0	89	68
	85	23378	0.99	0	172	58	0	87	69
	86	23348	0.99	1	152	56	0	51	68
	87	23336	0.99	1	164	55	0	317	64
	88	23364	0.99	0	143	51	0	309	65
	89	23431	1	1	147	42	0	290	63
	90	23454	1	0	139	34	0	628	56
	91	23462	1	0	88	24	0	585	54
	92	23462	1	0	69	16	0	168	48
<i>Spring</i>	3	24940	1	4	568	157	1	171	70
	4	24939	1	2	681	172	2	167	67
	5	24940	1	1	699	182	2	167	67
	6	24940	1	6	689	182	2	167	68
	7	24938	1	0	678	178	2	167	69
	8	24936	1	1	624	173	2	168	71
	9	24937	1	1	618	173	1	168	71
	10	24939	1	1	584	172	1	168	72
	11	24936	1	3	537	170	1	169	73
	12	24934	1	2	515	166	1	168	73
	13	24937	1	0	501	161	1	168	73
	14	24938	1	1	484	157	1	168	74
	15	24936	1	0	480	153	1	167	74
	16	24935	1	1	454	150	1	166	74
	17	24934	1	1	440	147	1	166	74
	18	24934	1	1	442	144	1	163	74
	19	24935	1	1	438	142	1	163	74
	20	24935	1	1	414	139	1	161	74

Appendix C.18 *continued*

Season	Depth (m)	n	n_prop	Magnitude (mm/s)				Angle	
				Min	Max	Mean	95% CI	Mean	95% CI
21	24933	1	1	3	406	137	1	160	74
22	24933	1	1	1	398	135	1	159	75
23	24934	1	1	1	382	132	1	159	75
24	24933	1	1	1	374	129	1	158	75
25	24934	1	1	0	350	126	1	157	76
26	24931	1	1	1	313	118	1	163	76
27	24934	1	1	0	322	111	1	164	77
28	24931	1	1	1	363	118	1	150	75
29	24933	1	1	1	353	120	1	148	75
30	24936	1	1	2	343	117	1	149	75
31	24929	1	1	1	334	115	1	148	76
32	24931	1	1	0	329	113	1	147	76
33	24932	1	1	2	322	111	1	144	76
34	24932	1	1	4	326	109	1	142	76
35	24931	1	1	5	312	107	1	141	76
36	24934	1	1	1	315	106	1	139	75
37	24933	1	1	3	308	104	1	135	76
38	24934	1	1	0	304	102	1	134	76
39	24933	1	1	1	296	100	1	131	76
40	24933	1	1	0	296	99	1	127	75
41	24932	1	1	3	291	98	1	122	74
42	24933	1	1	3	289	97	1	118	75
43	24933	1	1	2	283	95	1	115	75
44	24934	1	1	2	284	94	1	114	76
45	24931	1	1	4	269	94	1	109	76
46	24934	1	1	0	270	92	1	106	76
47	24933	1	1	0	270	91	1	100	75
48	24933	1	1	5	266	90	1	98	75
49	24932	1	1	1	262	89	1	95	75
50	24931	1	1	1	256	89	1	92	73
51	24931	1	1	3	253	87	1	88	74
52	24932	1	1	2	254	88	1	90	72
53	24934	1	1	0	240	86	1	86	73
54	24930	1	1	0	238	84	1	82	74
55	24932	1	1	2	228	83	1	80	74
56	24929	1	1	1	223	83	1	80	72
57	24932	1	1	0	228	83	1	80	73

Appendix C.18 *continued*

Season	Depth (m)	n	n_prop	Magnitude (mm/s)				Angle	
				Min	Max	Mean	95% CI	Mean	95% CI
	58	24929	1	3	229	84	1	80	72
	59	24930	1	5	228	82	1	79	73
	60	24929	1	9	224	81	1	80	72
	61	24929	1	12	224	81	0	80	72
	62	24928	1	4	220	80	0	79	72
	63	24927	1	0	218	81	0	80	72
	64	24927	1	1	207	79	0	79	71
	65	24928	1	4	196	78	0	79	71
	66	24930	1	0	192	76	0	80	71
	67	24924	1	3	181	75	0	79	72
	68	24925	1	4	173	73	0	78	71
	69	24927	1	5	187	70	0	76	71
	70	24924	1	2	177	69	0	74	70
	71	24928	1	1	206	73	0	80	70
	72	24918	1	1	213	76	0	86	69
	73	24916	1	0	203	75	0	86	69
	74	24922	1	0	205	72	0	85	70
	75	24922	1	1	190	71	0	85	71
	76	24917	1	0	193	69	0	86	71
	77	24915	1	2	176	68	0	84	72
	78	24910	1	1	182	66	0	85	72
	79	24902	1	2	187	65	0	83	72
	80	24911	1	0	185	64	0	85	71
	81	24905	1	0	177	62	0	78	72
	82	24900	1	0	193	60	0	78	72
	83	24907	1	1	178	60	0	65	73
	84	24905	1	0	180	59	0	67	73
	85	24887	1	0	172	57	0	40	73
	86	24877	1	1	175	57	0	318	73
	87	24853	1	0	153	54	0	314	73
	88	24805	0.99	0	138	48	0	294	74
	89	24783	0.99	1	131	42	0	304	70
	90	24876	1	0	121	34	0	290	66
	91	24913	1	0	79	26	0	276	53
	92	24916	1	0	98	22	0	621	38
<i>Summer</i>	3	26368	1	1	464	147	1	165	69
	4	26368	1	0	531	163	1	162	69

Appendix C.18 *continued*

Season	Depth (m)	n	n_prop	Magnitude (mm/s)				Angle	
				Min	Max	Mean	95% CI	Mean	95% CI
	5	26368	1	0	462	167	1	158	69
	6	26367	1	0	466	161	1	154	68
	7	26367	1	1	478	162	1	153	69
	8	26368	1	1	472	160	1	153	69
	9	26367	1	0	489	157	1	152	69
	10	26365	1	0	500	153	1	151	70
	11	26366	1	1	520	150	1	148	70
	12	26366	1	1	531	147	1	146	71
	13	26364	1	0	548	142	1	143	71
	14	26365	1	0	553	138	1	141	71
	15	26364	1	1	561	135	1	138	72
	16	26365	1	0	566	134	1	133	72
	17	26364	1	0	576	131	1	130	72
	18	26366	1	0	577	129	1	125	72
	19	26362	1	0	583	128	1	120	73
	20	26363	1	2	592	126	1	114	73
	21	26362	1	1	592	124	1	109	73
	22	26364	1	4	592	122	1	102	73
	23	26363	1	0	598	120	1	94	73
	24	26363	1	0	602	119	1	88	73
	25	26363	1	2	605	118	1	83	74
	26	26363	1	0	580	115	1	72	74
	27	26362	1	0	572	108	1	57	74
	28	26364	1	0	575	110	1	63	75
	29	26362	1	1	568	114	1	65	75
	30	26362	1	1	559	113	1	60	76
	31	26361	1	1	558	112	1	59	76
	32	26361	1	2	546	112	1	56	76
	33	26360	1	0	540	112	1	55	76
	34	26361	1	2	529	111	1	53	76
	35	26363	1	1	522	111	1	53	77
	36	26360	1	1	518	110	1	52	76
	37	26360	1	0	503	110	1	52	76
	38	26363	1	1	495	109	1	52	76
	39	26358	1	0	481	110	1	50	76
	40	26354	1	1	473	109	1	48	75
	41	26357	1	1	466	108	1	49	75

Appendix C.18 *continued*

Season	Depth (m)	n	n_prop	Magnitude (mm/s)				Angle	
				Min	Max	Mean	95% CI	Mean	95% CI
	42	26357	1	1	456	108	1	50	75
	43	26355	1	1	435	108	1	50	75
	44	26356	1	1	427	108	1	50	75
	45	26354	1	3	422	108	1	50	74
	46	26358	1	1	418	107	1	49	75
	47	26359	1	1	411	106	1	49	75
	48	26355	1	4	413	106	1	47	75
	49	26355	1	1	418	106	1	48	75
	50	26356	1	3	421	106	1	49	75
	51	26354	1	1	415	105	1	48	75
	52	26354	1	2	414	104	1	48	76
	53	26357	1	1	414	104	1	47	76
	54	26351	1	0	415	103	1	48	76
	55	26354	1	2	416	102	1	46	76
	56	26355	1	3	418	101	1	48	76
	57	26353	1	6	413	101	1	49	77
	58	26353	1	1	412	100	1	49	77
	59	26353	1	0	409	99	1	49	77
	60	26355	1	4	407	98	1	49	78
	61	26355	1	0	405	97	1	49	78
	62	26352	1	4	412	96	1	49	79
	63	26352	1	2	410	96	1	50	78
	64	26356	1	1	405	95	1	50	79
	65	26352	1	1	403	95	1	50	79
	66	26351	1	4	396	95	1	51	79
	67	26349	1	1	396	93	1	52	78
	68	26351	1	4	392	92	1	51	78
	69	26352	1	3	387	91	1	50	78
	70	26349	1	1	380	89	1	49	78
	71	26351	1	0	385	89	1	51	78
	72	26351	1	3	386	90	1	54	78
	73	26350	1	3	374	91	1	57	78
	74	26346	1	1	371	90	1	58	78
	75	26352	1	5	374	89	1	56	78
	76	26347	1	3	372	88	1	55	78
	77	26346	1	4	370	87	1	56	77
	78	26341	1	3	371	86	1	55	77

Appendix C.18 *continued*

Season	Depth (m)	n	n_prop	Magnitude (mm/s)				Angle	
				Min	Max	Mean	95% CI	Mean	95% CI
	79	26344	1	4	372	86	1	53	77
	80	26341	1	3	369	85	1	50	77
	81	26346	1	1	357	83	1	45	76
	82	26336	1	2	360	82	1	42	77
	83	26327	1	4	354	81	1	31	76
	84	26308	1	1	357	81	1	23	76
	85	26283	1	0	351	79	1	7	76
	86	26240	1	1	346	78	1	344	76
	87	26191	0.99	1	343	75	1	326	76
	88	26108	0.99	1	330	73	1	317	76
	89	26005	0.99	0	304	67	1	304	75
	90	25982	0.99	0	250	58	1	300	74
	91	26082	0.99	1	171	45	0	299	73
	92	26305	1	0	96	30	0	286	64
<i>Fall</i>	3	16022	1	0	253	86	1	543	70
	4	16019	1	0	261	86	1	175	72
	5	16001	1	1	249	92	1	171	72
	6	15992	1	1	239	94	1	171	73
	7	15991	1	5	240	96	1	170	74
	8	15992	1	1	242	96	1	168	74
	9	15992	1	1	229	96	1	167	76
	10	15994	1	3	227	95	1	165	76
	11	15991	1	1	231	95	1	161	76
	12	15992	1	1	242	95	1	155	76
	13	15992	1	0	245	94	1	153	75
	14	15992	1	1	235	94	1	145	76
	15	15992	1	0	238	93	1	134	76
	16	15991	1	0	239	92	1	124	76
	17	15990	1	0	247	91	1	105	77
	18	15988	1	2	246	92	1	90	77
	19	15989	1	0	241	90	1	87	77
	20	15989	1	0	240	90	1	76	76
	21	15989	1	0	240	89	1	67	75
	22	15987	1	0	225	88	1	60	76
	23	15992	1	4	238	91	1	58	76
	24	15988	1	1	235	90	1	49	76
	25	15989	1	1	235	88	1	43	76

Appendix C.18 *continued*

Season	Depth (m)	n	n_prop	Magnitude (mm/s)				Angle	
				Min	Max	Mean	95% CI	Mean	95% CI
26	15989	1	1	1	220	82	1	15	74
27	15990	1	1	0	227	77	1	3	74
28	15987	1	1	1	236	85	1	37	76
29	15990	1	1	0	232	88	1	34	76
30	15993	1	1	1	240	87	1	32	76
31	15989	1	2	2	238	87	1	30	76
32	15989	1	1	1	237	87	1	30	77
33	15988	1	1	1	238	87	1	30	76
34	15992	1	0	0	235	86	1	29	76
35	15990	1	1	1	245	86	1	29	75
36	15987	1	0	0	238	86	1	33	75
37	15990	1	2	2	228	84	1	33	75
38	15993	1	0	0	232	84	1	34	74
39	15988	1	1	1	229	84	1	34	74
40	15990	1	3	3	236	84	1	34	74
41	15986	1	2	2	231	83	1	36	74
42	15988	1	3	3	238	82	1	37	74
43	15988	1	2	2	239	82	1	38	74
44	15988	1	0	0	245	82	1	41	73
45	15986	1	1	1	246	81	1	38	74
46	15988	1	1	1	242	81	1	39	74
47	15986	1	1	1	246	81	1	40	74
48	15987	1	1	1	249	81	1	41	75
49	15986	1	1	1	245	81	1	42	74
50	15987	1	1	1	244	80	1	39	74
51	15981	1	0	0	254	80	1	41	74
52	15982	1	1	1	251	80	1	40	73
53	15986	1	2	2	261	80	1	43	73
54	15983	1	1	1	260	79	1	43	74
55	15983	1	2	2	259	79	1	41	73
56	15979	1	2	2	253	78	1	44	73
57	15982	1	0	0	258	78	1	48	73
58	15983	1	1	1	269	78	1	51	73
59	15990	1	1	1	267	77	1	50	73
60	15984	1	2	2	259	78	1	54	72
61	15981	1	4	4	259	76	1	55	73
62	15985	1	2	2	260	76	1	56	72

Appendix C.18 *continued*

Season	Depth (m)	n	n_prop	Magnitude (mm/s)				Angle	
				Min	Max	Mean	95% CI	Mean	95% CI
63	15983	1	1	0	252	74	1	59	72
64	15984	1	1	2	254	73	1	62	72
65	15982	1	1	2	241	72	1	64	73
66	15979	1	1	1	238	71	1	67	72
67	15976	1	1	0	233	69	1	66	72
68	15981	1	1	3	224	68	1	68	71
69	15974	1	1	2	204	65	1	68	71
70	15977	1	1	3	192	64	1	72	71
71	15978	1	1	2	183	63	1	72	71
72	15974	1	1	4	186	64	1	77	71
73	15974	1	1	0	195	62	1	79	70
74	15970	1	1	2	199	61	1	79	70
75	15972	1	1	2	194	60	1	82	70
76	15977	1	1	1	188	59	1	83	69
77	15977	1	1	1	193	57	1	86	69
78	15972	1	1	3	191	55	1	89	69
79	15966	1	1	1	196	55	1	90	69
80	15966	1	1	1	194	53	1	92	70
81	15958	0.99	0.99	0	194	51	1	93	69
82	15948	0.99	0.99	1	190	50	0	99	69
83	15939	0.99	0.99	1	196	50	0	102	69
84	15911	0.99	0.99	1	183	48	0	104	68
85	15867	0.99	0.99	0	186	47	1	125	67
86	15835	0.99	0.99	0	177	46	0	175	66
87	15776	0.98	0.98	1	180	45	0	576	68
88	15713	0.98	0.98	0	179	42	0	596	65
89	15676	0.98	0.98	0	171	37	0	607	66
90	15793	0.98	0.98	0	137	30	0	616	65
91	15863	0.99	0.99	0	84	21	0	608	59
92	15961	1	1	0	62	16	0	549	40

Appendix C.19

Summary of current velocity magnitude and direction from the SBOO RTOMS ADCP during 2022 and 2023. Data are presented by depth bin as seasonal recovered observations (n), minimum (min), maximum (max), and means with 95% confidence intervals (CI). Proportion of recovered observations (n_prop) differed due to variations in data quality (see text). Minimum and maximum angles of velocity are not shown due to the circular nature of the measurement.

Season	Depth (m)	n	n_prop	Magnitude (mm/s)				Angle		
				Min	Max	Mean	95% CI	Mean	95% CI	
<i>Winter</i>	3	12445	1	3	297	112	1	178	74	
	4	12445	1	1	308	116	1	174	75	
	5	12446	1	1	304	114	1	173	75	
	6	12445	1	5	300	113	1	172	75	
	7	12446	1	5	309	113	1	169	75	
	8	12445	1	0	316	110	1	166	75	
	9	12444	1	4	295	101	1	169	74	
	10	12445	1	4	302	102	1	162	75	
	11	12446	1	4	305	101	1	159	75	
	12	12446	1	0	294	99	1	157	75	
	13	12445	1	2	289	97	1	155	76	
	14	12446	1	1	278	94	1	153	76	
	15	12446	1	2	265	91	1	149	76	
	16	12444	1	6	253	86	1	148	75	
	17	12444	1	2	238	84	1	146	76	
	18	12446	1	5	260	86	1	143	77	
	19	12445	1	5	263	88	1	139	78	
	20	12445	1	8	259	86	1	138	78	
	21	12445	1	3	249	83	1	134	78	
	22	12444	1	5	224	75	1	133	79	
	23	12445	1	0	182	64	1	134	76	
	24	12445	1	0	203	61	1	144	76	
	25	12443	1	1	215	62	1	131	76	
	26	12446	1	2	200	57	1	124	75	
	27	12443	1	1	190	51	1	106	72	
	<i>Spring</i>	3	13314	1	1	336	80	1	164	70
		4	13313	1	1	350	85	1	159	72
5		13314	1	1	335	84	1	156	73	
6		13313	1	2	317	82	1	151	74	
7		13312	1	4	316	80	1	146	75	
8		13312	1	0	293	77	1	140	75	
9		13312	1	1	230	71	1	136	75	
10		13313	1	3	246	70	1	117	77	
11		13312	1	1	253	70	1	109	76	
12		13312	1	0	247	70	1	86	75	
13		13312	1	4	241	70	1	71	74	

Appendix C.19 *continued*

Season	Depth (m)	n	n_prop	Magnitude (mm/s)				Angle	
				Min	Max	Mean	95% CI	Mean	95% CI
	14	13311	1	2	236	71	1	61	74
	15	13312	1	1	216	70	1	46	75
	16	13311	1	3	203	68	1	30	75
	17	13311	1	1	198	68	1	25	76
	18	13309	1	1	207	70	1	39	77
	19	13310	1	1	196	72	1	48	76
	20	13309	1	1	189	73	1	50	76
	21	13311	1	0	185	73	1	48	76
	22	13308	1	1	172	69	1	39	77
	23	13310	1	1	155	62	1	16	75
	24	13310	1	4	160	63	1	6	74
	25	13310	1	3	155	64	1	29	77
	26	13309	1	9	148	63	1	35	75
	27	13311	1	11	132	57	0	29	75
<i>Summer</i>	3	26469	1	2	410	86	1	166	66
	4	26469	1	4	468	104	1	149	63
	5	26468	1	1	439	106	1	148	66
	6	26467	1	0	400	102	1	148	70
	7	26468	1	0	376	100	1	146	72
	8	26466	1	0	363	96	1	142	72
	9	26467	1	2	368	86	1	143	72
	10	26468	1	1	371	84	1	136	74
	11	26467	1	0	379	88	1	121	74
	12	26467	1	0	381	86	1	102	74
	13	26467	1	3	383	84	1	74	75
	14	26465	1	0	377	83	1	55	76
	15	26464	1	0	373	83	1	44	77
	16	26467	1	1	376	81	1	35	77
	17	26467	1	1	373	79	1	30	77
	18	26465	1	1	363	78	1	36	77
	19	26464	1	1	366	83	1	38	77
	20	26463	1	0	348	84	1	37	77
	21	26464	1	0	344	83	1	36	77
	22	26465	1	3	341	80	1	29	76
	23	26464	1	0	324	74	1	16	75
	24	26464	1	0	313	69	1	8	74
	25	26466	1	1	303	68	1	21	75
	26	26465	1	1	289	67	1	23	73
	27	26464	1	1	265	61	0	15	72

Appendix C.19 *continued*

Season	Depth (m)	n	n_prop	Magnitude (mm/s)				Angle	
				Min	Max	Mean	95% CI	Mean	95% CI
<i>Fall</i>	3	18056	1	2	220	73	1	168	71
	4	18030	1	1	327	93	1	143	72
	5	18025	1	1	300	93	1	134	73
	6	18026	1	0	269	91	1	126	73
	7	18026	1	3	247	90	1	121	74
	8	18025	1	1	245	87	1	109	75
	9	18027	1	0	228	80	1	97	74
	10	18025	1	0	237	80	1	78	75
	11	18024	1	1	233	82	1	72	76
	12	18024	1	1	236	81	1	58	76
	13	18024	1	0	233	81	1	49	77
	14	18025	1	1	233	82	1	45	77
	15	18024	1	0	230	82	1	39	77
	16	18024	1	1	225	82	1	33	77
	17	18024	1	5	229	79	1	25	77
	18	18024	1	1	223	75	1	18	78
	19	18022	1	1	231	80	1	29	78
	20	18022	1	2	237	81	1	27	78
	21	18023	1	2	232	79	1	23	77
	22	18021	1	1	219	76	1	18	78
	23	18025	1	1	198	71	1	1	77
	24	18022	1	0	179	64	1	346	76
	25	18022	1	1	190	62	1	2	77
	26	18021	1	2	198	64	1	9	75
	27	18021	1	1	180	58	1	4	74

Appendix C.20

Summary of current velocity magnitude and direction from the PLOO static ADCP during 2022 and 2023. Data are presented by depth bin as seasonal recovered observations (n), minimum (min), maximum (max), and means with 95% confidence intervals (CI). Proportion of recovered observations (n_prop) differed due to variations in data quality (see text). Minimum and maximum angles of velocity are not shown due to the circular nature of the measurement.

Season	Depth (m)	n	n_prop	Magnitude (mm/s)				Angle	
				Min	Max	Mean	95% CI	Mean	95% CI
<i>Winter</i>	9	4083	0.96	2	412	145	2	138	66
	13	4164	0.97	3	620	174	4	165	69
	17	4235	0.99	3	569	168	4	165	69
	21	4268	1	3	522	161	3	163	69
	25	4275	1	2	526	154	3	161	69
	29	4275	1	2	476	143	3	159	69
	33	4275	1	3	446	133	3	156	70
	37	4275	1	1	404	123	3	153	70
	41	4275	1	1	379	113	2	150	71
	45	4275	1	1	366	104	2	144	71
	49	4275	1	2	350	97	2	133	71
	53	4275	1	2	305	90	2	111	69
	57	4275	1	1	274	84	2	71	68
	61	4275	1	0	253	78	2	26	66
	65	4275	1	1	215	73	1	1	65
	69	4275	1	1	210	69	1	352	64
	73	4275	1	1	206	66	1	352	63
	77	4275	1	0	191	64	1	0	64
	81	4275	1	2	178	61	1	18	66
	85	4275	1	1	169	59	1	44	68
89	4275	1	1	160	58	1	74	68	
93	4274	1	0	149	53	1	102	65	
<i>Spring</i>	9	3131	0.95	1	454	151	3	166	66
	13	3223	0.98	0	480	151	4	171	68
	17	3261	0.99	2	479	137	3	168	68
	21	3281	1	2	428	126	3	164	68
	25	3281	1	4	358	117	3	162	69
	29	3281	1	3	308	109	2	161	70
	33	3281	1	1	283	102	2	155	69
	37	3281	1	1	267	95	2	142	68
	41	3281	1	1	249	89	2	115	68
	45	3281	1	1	234	84	2	70	68
	49	3281	1	0	226	80	2	21	67
	53	3281	1	2	214	76	2	353	66
	57	3281	1	0	198	72	2	338	65
	61	3281	1	1	191	69	1	331	64
65	3281	1	2	187	66	1	328	63	

Appendix C.20 *continued*

Season	Depth (m)	n	n_prop	Magnitude (mm/s)				Angle	
				Min	Max	Mean	95% CI	Mean	95% CI
<i>Summer</i>	69	3281	1	2	180	63	1	331	64
	73	3281	1	1	175	60	1	339	65
	77	3281	1	1	176	58	1	356	68
	81	3281	1	1	172	57	1	23	71
	85	3281	1	1	164	57	1	52	73
	89	3281	1	4	154	56	1	76	74
	93	3281	1	2	134	49	1	95	74
	9	3637	0.83	4	481	144	3	140	66
	13	4146	0.95	0	601	140	3	147	67
	17	4319	0.99	1	610	127	3	136	67
	21	4358	1	3	600	119	3	108	68
	25	4369	1	2	589	113	3	60	69
	29	4370	1	2	572	110	3	36	70
	33	4370	1	2	554	109	2	28	71
	37	4370	1	2	537	107	2	25	71
	41	4370	1	4	512	107	2	24	71
	45	4370	1	2	482	106	2	23	71
	49	4370	1	3	456	104	2	20	71
	53	4370	1	1	435	102	2	16	71
	<i>Fall</i>	57	4370	1	2	409	99	2	9
61		4370	1	1	380	97	2	0	72
65		4370	1	1	364	95	2	352	72
69		4370	1	2	352	94	2	347	72
73		4370	1	1	335	92	2	345	73
77		4370	1	1	339	90	2	349	74
81		4370	1	1	327	88	2	357	75
85		4370	1	1	320	85	2	14	76
89		4370	1	2	304	80	2	43	76
93		4370	1	1	257	69	2	89	75
9		3478	0.95	2	294	98	2	106	64
13		3570	0.98	1	304	98	2	126	66
17		3617	0.99	1	304	94	2	48	64
21		3642	1	2	304	92	2	22	65
25		3651	1	1	297	88	2	10	66
29		3653	1	1	283	85	2	4	66
33		3654	1	1	269	83	2	4	67
37		3654	1	1	283	82	2	6	67
41		3654	1	1	293	80	2	8	67
45		3654	1	2	284	78	2	9	67
49	3654	1	2	268	77	2	9	68	
53	3654	1	1	263	75	2	8	68	

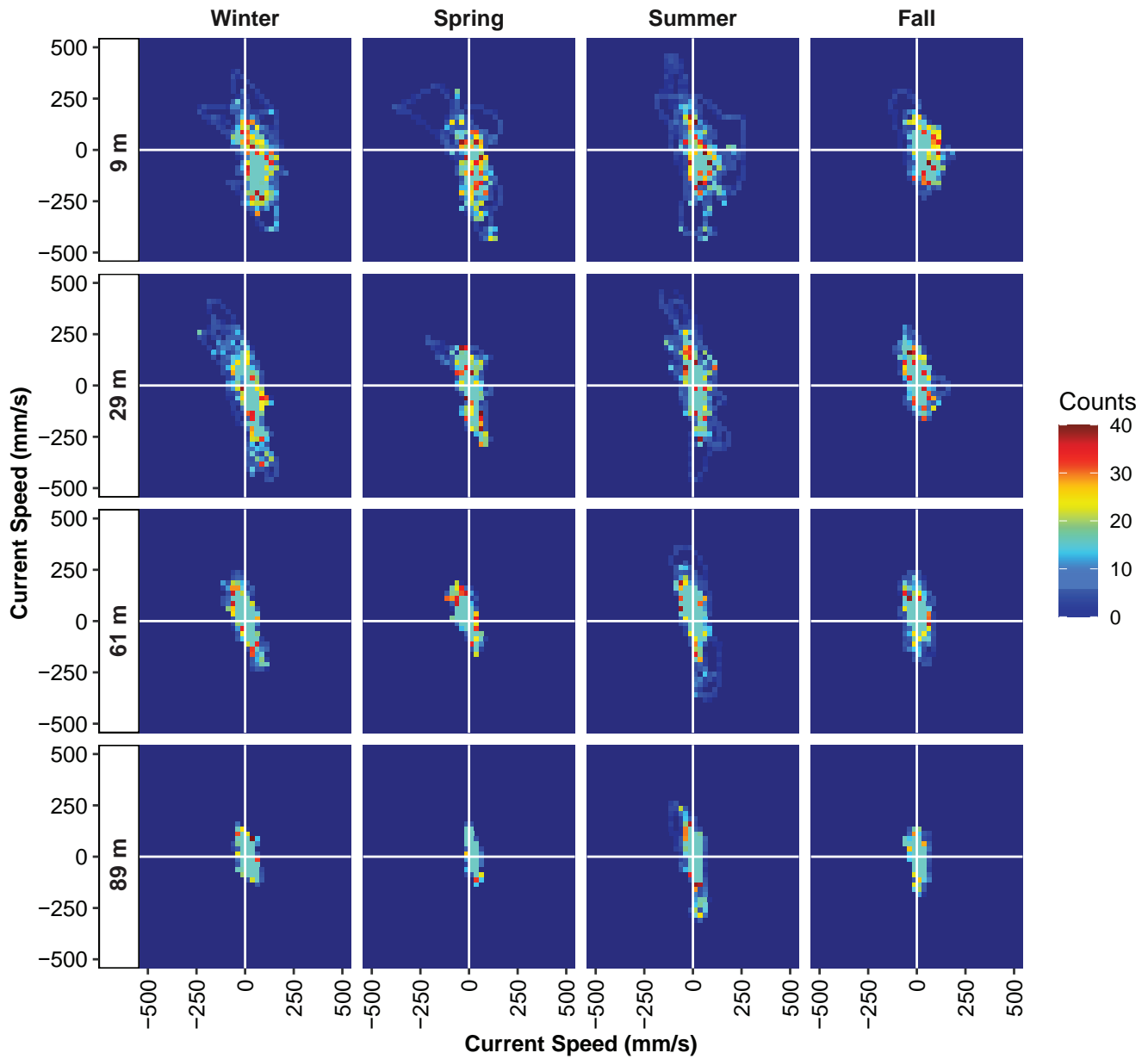
Appendix C.20 *continued*

Season	Depth (m)	n	n_prop	Magnitude (mm/s)				Angle	
				Min	Max	Mean	95% CI	Mean	95% CI
	57	3654	1	1	256	73	2	5	67
	61	3654	1	0	242	71	1	1	67
	65	3654	1	3	227	68	1	354	66
	69	3654	1	1	212	66	1	349	65
	73	3654	1	0	198	64	1	347	65
	77	3654	1	1	185	60	1	352	67
	81	3654	1	1	181	57	1	5	69
	85	3654	1	2	184	54	1	33	71
	89	3654	1	0	179	52	1	91	70
	93	3654	1	0	163	48	1	141	66

Appendix C.21

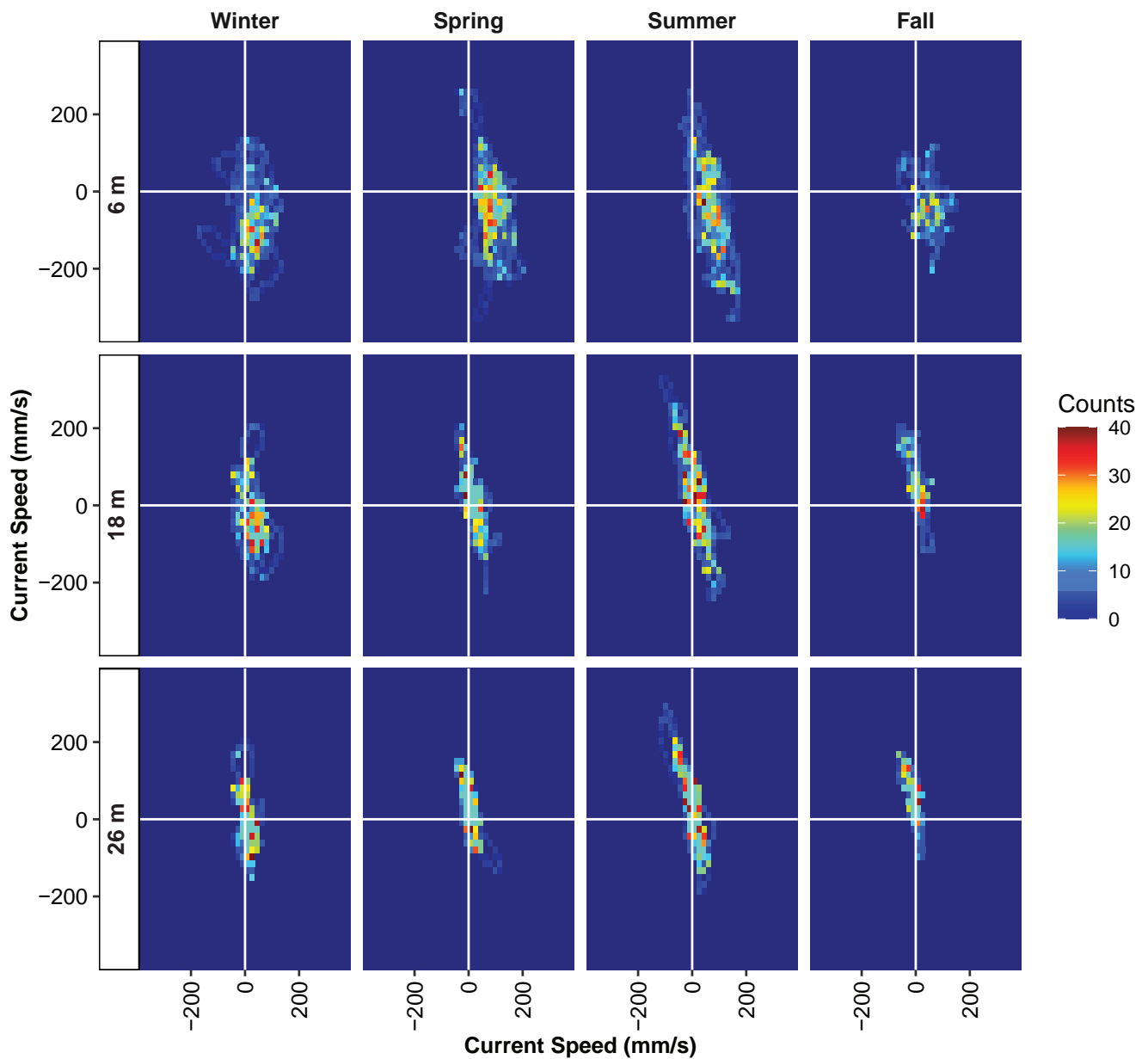
Summary of current velocity magnitude and direction from the SBOO static ADCP during 2022 and 2023. Data are presented by depth bin as seasonal recovered observations (n), minimum (min), maximum (max), and means with 95% confidence intervals (CI). Proportion of recovered observations (n_prop) differed due to variations in data quality (see text). Minimum and maximum angles of velocity are not shown due to the circular nature of the measurement.

Season	Depth (m)	n	n_prop	Magnitude (mm/s)				Angle	
				Min	Max	Mean	95% CI	Mean	95% CI
<i>Winter</i>	6	1553	1	3	275	114	3	157	61
	10	1559	1	1	251	97	3	163	69
	14	1559	1	1	237	91	2	148	68
	18	1559	1	3	214	85	2	133	67
	22	1559	1	1	203	76	2	126	69
	26	1559	1	1	196	60	2	128	72
	30	1559	1	1	158	45	2	620	70
<i>Spring</i>	6	2183	1	29	380	133	2	120	67
	10	2184	1	5	339	75	2	125	65
	14	2184	1	0	283	67	2	85	66
	18	2184	1	0	233	58	2	46	69
	22	2184	1	1	195	54	2	22	70
	26	2184	1	0	167	50	1	8	69
	30	2184	1	2	137	43	1	356	67
<i>Summer</i>	6	2202	1	3	420	135	3	128	70
	10	2207	1	3	383	123	4	123	71
	14	2207	1	1	406	113	3	77	70
	18	2208	1	2	388	101	3	26	69
	22	2208	1	3	350	92	3	6	69
	26	2208	1	2	305	83	2	359	70
	30	2208	1	1	250	68	2	355	69
<i>Fall</i>	6	944	0.99	2	209	90	3	131	56
	10	949	1	1	178	65	3	42	65
	14	949	1	9	194	67	3	20	68
	18	950	1	5	207	73	3	5	68
	22	950	1	3	204	74	3	355	69
	26	950	1	2	184	67	3	348	70
	30	950	1	2	155	53	2	344	69



Appendix C.22

Frequency distribution (counts) by season of current speed (mm/s) and direction from 2022 and 2023 at the PLOO static ADCP location at representative depth bins. On the x-axis, positive values indicate an eastward direction while negative values indicate a westward direction. On the y-axis, positive values indicate a northward direction while negative values indicate a southward direction.



Appendix C.23

Frequency distribution (counts) by season of current speed (mm/s) and direction from 2022 and 2023 at the SBOO static ADCP location at representative depth bins. On the x-axis, positive values indicate an eastward direction while negative values indicate a westward direction. On the y-axis, positive values indicate a northward direction while negative values indicate a southward direction.

Appendix D

Water Quality: 2015 California Ocean Plan Objectives for the Point Loma Ocean Outfall

2022 – 2023 Supplemental Analyses

Appendix D. Water Quality: 2015 California Ocean Plan Objectives for the Point Loma Ocean Outfall

INTRODUCTION

NB: This appendix presents data analysis to meet the 2015 Ocean Plan water quality bacterial objectives as required by the National Pollutant Discharge Elimination System (NPDES) permit for the Point Loma Wastewater Treatment Plant (NPDES No. CA0107409; Order No. R9-2017-0007). However, additional analyses using current 2019 Ocean Plan Objectives are presented in Chapter 3.

The City of San Diego conducts extensive monitoring along the shoreline (beaches), nearshore (e.g., kelp forests), and other offshore coastal waters surrounding the Point Loma Ocean Outfall (PLOO) to characterize regional water quality conditions and to identify possible impacts of wastewater discharge, or other contaminant sources, on the marine environment. Densities of fecal indicator bacteria (FIB), including total coliforms, fecal coliforms and *Enterococcus*, are measured and evaluated in context with various oceanographic parameters (see Chapter 2) to provide information about the movement and dispersion of wastewater discharged into the Pacific Ocean through the PLOO. Evaluation of these data may also help to identify other sources of bacterial contamination off San Diego. In addition, the City's water quality monitoring efforts are designed to assess compliance with the bacterial water contact standards and other physical and chemical water quality objectives specified in the California Ocean Plan (Ocean Plan) that are intended to help protect the beneficial uses of State ocean waters (herein utilizing 2015 objectives: see SWRCB 2015).

Multiple sources of bacterial contamination exist in the Point Loma region, and being able to separate any impact that may be associated with wastewater discharge from other point, or non-point, sources of contamination is often challenging. Examples include outflows from the San Diego River and San Diego Bay. Likewise, storm water discharges and terrestrial runoff from local watersheds during storms, or other wet weather events, can also flush sediments and contaminants into nearshore coastal waters (Noble et al. 2003, Reeves et al. 2004, Sercu et al. 2009, Griffith et al. 2010). Moreover, decaying kelp and seagrass (beach wrack), sediments and sludge accumulating in storm drains, and sandy beach sediments themselves can serve as reservoirs for bacteria until release into coastal waters by returning tides, rain events, or other disturbances (Gruber et al. 2005, Martin and Gruber 2005, Noble et al. 2006, Yamahara et al. 2007, Phillips et al. 2011). Further, the presence of shore birds and their droppings has been associated with high bacterial counts that may impact nearshore water quality (Grant et al. 2001, Griffith et al. 2010).

This appendix presents an analysis and assessment of bacterial distribution patterns, during 2022 and 2023, at more than 50 permanent water quality monitoring stations surrounding the PLOO. The primary goals are to: (1) document overall water quality conditions off of the San Diego, Point Loma region; and (2) assess compliance with the 2015 Ocean Plan water contact standards.

MATERIALS AND METHODS

Field Sampling

Shore stations

Seawater samples were collected weekly at 8 shoreline stations to monitor concentrations of FIB in waters adjacent to public beaches (Appendix D.1). All of these stations are in California State waters and are therefore subject to Ocean Plan water contact standards (Appendix D.2) (SWRCB 2015). PLOO shoreline stations (D4, D5, D7, D8-A/D8-B, D9, D10, D11, D12) are located from Mission Beach southward to the tip of Point Loma.

Seawater samples were collected from the surf zone at each of the above stations in sterile 250mL bottles, after which they were transported on blue ice to the City's Marine Microbiology Laboratory and analyzed to determine concentrations of three types of FIB (i.e., total coliform, fecal coliform, *Enterococcus* bacteria). In addition, weather conditions and visual observations of water color and clarity, surf height, and human or animal activity were recorded at the time of sample collection. Wind speed and direction were measured using a hand-held anemometer with a compass. These observations were previously reported in monthly receiving waters monitoring reports submitted to the San Diego Regional Water Quality Control Board (SDRWQCB) (see City of San Diego 2022–2023). These reports are available online (City of San Diego 2024a).

Kelp and offshore stations

Eight stations located in relatively shallow waters within or near the Point Loma kelp beds (i.e., referred to as “kelp” stations herein) were monitored weekly to assess water quality conditions and Ocean Plan compliance in nearshore areas used for recreational activities such as SCUBA diving, surfing, fishing, and kayaking (Appendix D.1). These included stations C4, C5, and C6 located along the 9m depth contour near the inner edge of the Point Loma kelp forest, and stations A1, A6, A7, C7, and C8 located along the 18m depth contour near the outer edge of the Point Loma kelp forest.

An additional 36 offshore stations were sampled quarterly over consecutive days in winter (February or March), spring (May), summer (August), and fall (November) to monitor water quality conditions. PLOO stations are designated F1–F36 and are located along or adjacent to the 18, 60, 80, and 98m depth contours. Seawater samples for FIB were collected at all of these stations (see below). Additionally, 15 of the PLOO stations (F01–F03, F06–F14, F18–F20) are located within State jurisdictional waters (i.e., within 3 nautical miles of shore) and therefore subject to the Ocean Plan compliance standards.

Seawater samples for FIB analyses were collected from 3 to 5 discrete depths at the kelp and offshore stations as indicated in Appendix D.3. These samples were typically collected using a rosette sampler fitted with Niskin bottles surrounding a central Conductivity, Temperature, and Depth (CTD) instrument, although replacement samples due to misfires or other causes may have been collected from a separate follow-up cast using stand-alone Van Dorn bottles if necessary. All weekly kelp/nearshore samples were analyzed for all three types of FIB, while the quarterly offshore samples were only analyzed for *Enterococcus* per permit requirements. All samples were refrigerated at sea and then transported on blue ice to the City's Marine Microbiology Laboratory for processing and analysis. Oceanographic data were collected simultaneously with the water samples at each station (see Chapter 2). Visual observations of weather, sea conditions, and human or animal activity were also recorded at the time of sampling. These latter observations were also reported

previously in monthly receiving waters monitoring reports submitted to the SDRWQCB (see City of San Diego 2022–2023). These reports are available online (City of San Diego 2024a).

Laboratory Analyses

The City Marine Microbiology Laboratory follows guidelines issued by the U.S. Environmental Protection Agency (USEPA) Water Quality Office, State Water Resources Control Board (SWRCB) including the 2015 Ocean Plan, the California Department of Public Health (CDPH), and Environmental Laboratory Accreditation Program (ELAP) with respect to sampling and analytical procedures (Bordner et al. 1978, APHA 2012, USEPA 2014). All bacterial analyses were initiated within eight hours of sample collection and conformed to standard membrane filtration techniques, for which the laboratory is certified (ELAP Field of Testing 126).

FIB densities were determined and validated in accordance with USEPA and APHA guidelines (Bordner et al. 1978, APHA 2012, USEPA 2014). Plates with FIB densities above or below the ideal counting range were given greater than ($>$), greater than or equal to (\geq), less than ($<$), or estimated (e) qualifiers. However, all qualifiers were dropped, and densities were treated as discrete values, when determining compliance with Ocean Plan standards.

Quality assurance tests were performed routinely on bacterial samples to ensure that analyses and sampling variability did not exceed acceptable limits. Laboratory and field duplicate bacteriological samples were processed according to method requirements to measure analyst precision and variability between samples, respectively. Results of these procedures were reported under separate cover (City of San Diego 2023a, 2024b).

Data Analyses

Bacteriology

Compliance with Ocean Plan water contact standards was summarized as the number of times per sampling period that each shore, kelp, and offshore station within State waters exceeded geometric mean or single sample maximum (SSM) standards for total coliforms, fecal coliforms, and *Enterococcus* (Appendix D.2) (SWRCB 2015). Compliance calculations were limited to shore, kelp and offshore stations located within State waters. For shore stations, these calculations included resamples; no resamples are required to be collected at kelp or other offshore stations. To assess temporal and spatial trends, data were summarized as the number of samples in which FIB concentrations exceeded SSM benchmark levels. These calculations were performed for all shore, kelp and offshore stations located within and outside of State waters, but excluded resamples at shore stations.

Bacterial densities were compared to rainfall data from Lindbergh Field, San Diego, CA (NOAA 2022). Satellite images of the San Diego coastal region were provided by Ocean Imaging of Solana Beach, California and used to aid in the analysis and interpretation of water quality data (see Appendix C). All analyses were performed using R (R Core Team 2019) and various functions within the `gtools`, `Hmisc`, `psych`, `reshape2`, `RODBC`, `tidyverse`, `ggpubr`, `quantreg`, and `openxlsx` packages (Wickham 2007, 2017, Harrell et al. 2015, Warnes et al. 2015, Revelle 2015, Ripley and Lapsley 2017, Kassambara 2019, Koenker 2019, Schauburger and Walker 2019). All raw data for the 2022–2023 sampling period have been submitted to either the Regional Water Quality Control Board or the California Environmental Data Exchange Network (CEDEN) and may be accessed upon request.

RESULTS AND DISCUSSION

Bacteriological Compliance and Distribution

Shore stations

Overall compliance with the Ocean Plan water contact standards specified in Appendix D.2 was high at the PLOO shore stations in 2022–2023. Seawater samples collected from the eight PLOO shore stations were 100% compliant with the fecal coliform geometric mean standards, while compliance with the 30 day *Enterococcus* geometric mean standard was 98% and >99% with the total coliform standard (Appendix D.4A). Compliance with the SSM standards at these sites was 100% for total coliforms, >99% for fecal coliforms, 97% for *Enterococcus*, and >99% for the fecal:total coliform ratio (FTR) (Appendix D.4B). Overall, of the 832 sea water samples collected at the PLOO shore stations in 2022–2023 (not including resamples), 3.6% (n = 30) had elevated FIB. A majority of the shore samples with elevated FIB (83%) were collected during the wet seasons when rainfall totaled 18.44 inches over both years (Appendix D.5). This general relationship between rainfall and elevated bacterial levels at shore stations has been evident since water quality monitoring began.

Kelp bed stations

Overall compliance with Ocean Plan water contact standards was also high at the eight PLOO kelp stations in 2022–2023. Seawater samples from these stations were 100% compliant with each of the geometric mean standards and $\geq 99\%$ compliant with the SSM standards for total coliform, fecal coliform, *Enterococcus*, and the FTR criterion (Appendix D.6). Of the 2496 samples collected at the PLOO kelp stations in 2022–2023, only 8 samples had elevated FIB and each of those occurred in the wet season (Appendix D.7).

Offshore stations

Water quality was high at all non-kelp offshore stations that were sampled quarterly in the PLOO region in 2022–2023. Of the 1128 samples collected at these stations over the past two years, only about 5% (n = 61) had elevated FIB, with approximately 52% occurring in the wet season (Appendix D.8). All most all of the offshore samples with elevated FIB (n = 61) in 2022–2023 occurred at stations located along the 80 or 98m depth contours, and 21% were from stations F29, F30 and F31 located within 1000 m of the PLOO discharge site (i.e., nearfield stations). These results suggest that the PLOO wastewater plume continues to be restricted to relatively deep, offshore waters throughout the year. Additionally, there were no signs of wastewater at any of the 36 offshore PLOO stations based on visual observations of the surface. This conclusion is consistent with historical remote sensing observations that have provided no evidence of the PLOO plume reaching surface waters (see Appendix B: Svejksky and Hess 2022).

The above findings are consistent with historical ocean monitoring results, which revealed that < 4% of samples collected at depths of ≤ 25 m from the PLOO 98m (i.e., discharge depth) stations had elevated levels of *Enterococcus* during the pre-chlorination years (1993–2008). This percentage dropped to <1% at these depths following the initiation of partial chlorination at the Point Loma Wastewater Treatment Plant (PLWTP) in 2008 (City of San Diego 2009) and was zero during the current reporting period (Appendix D.9A). Overall, detection of elevated *Enterococcus* has been significantly more likely at the three nearfield stations (F29, F30, F31) than at any other 98m site (14% versus 5%, respectively; n = 7220, $\chi^2 = 198.03$, $p < 0.0001$). The addition of chlorination significantly decreased the number of samples with elevated *Enterococcus* at these three stations (i.e., 17% before versus 11% after, n = 2321, $\chi^2 = 17.8$, $p < 0.0001$), and the other 98m stations (6.2% before versus 3% after; n = 4899, $\chi^2 = 22.0$, $p < 0.0001$) (Appendix D.4B).

SUMMARY

Overall compliance with Ocean Plan water contact standards was over 99%. As is typical, reduced compliance at shore and kelp stations tended to occur during the wet season. The reduced compliance at shore and kelp stations in 2022 and 2023 was likely driven by heavy rainfall over the report period which was nearly double the volume of the preceding report period and included Hurricane Hilary, which hit San Diego in August of 2023 and was a rare dry-season heavy rain event. Compliance with 2015 Ocean Plan water contact standards at offshore stations was not reduced compared to the previous report period and, as expected, offshore stations in the PLOO region did not show an impact on compliance with increased rain fall, likely due to the distance of these stations from land based runoff. In addition, there was no evidence that wastewater discharged into the ocean reached nearshore waters. Historically, elevated FIB along the shore, or at the kelp bed stations, has typically been associated with storm activity (rain), heavy recreational use, the presence of seabirds, and decaying kelp or surfgrass (e.g., City of San Diego 2022). Exceptions to the above patterns have occurred over the years due to specific events. For example, the elevated bacteria that occurred at the PLOO shore and kelp stations during a few months in 1992 followed a catastrophic rupture of the outfall that occurred within the Point Loma kelp forest (Tegner et al. 1995).

The above results are also consistent with observations from remote sensing studies (i.e., satellite imagery) over several years that show a lack of shoreward transport of wastewater plumes from the PLOO (see Appendix B: Svejksky and Hess 2022), and with previous studies that have indicated the PLOO wastefield typically remains submerged in deep offshore waters (Rogowski et al. 2012a,b, 2013). The approximately 98m depth of the PLOO discharge site is likely an important factor that inhibits the wastewater plume from reaching surface waters. Wastewater released into these deep, cold and dense waters does not appear to mix with the upper 25 m of the water column (Rogowski et al. 2012a,b, 2013).

LITERATURE CITED

- [APHA] American Public Health Association. (2012). Standard Methods for the Examination of Water and Wastewater, 22nd edition. E.W. Rice, R. Baird, A. Eaton and L. Clesceri (eds.). American Public Health Association, American Water Works Association, and Water Pollution Control Federation.
- Bordner, R., J. Winter, and P. Scarpino, eds. (1978). Microbiological Methods for Monitoring the Environment: Water and Wastes, EPA Research and Development, EPA-600/8-78-017.
- City of San Diego. (2009). Annual Receiving Waters Monitoring Report for the Point Loma Ocean Outfall, 2008. City of San Diego Ocean Monitoring Program, Metropolitan Wastewater Department, Environmental Monitoring and Technical Services Division, San Diego, CA.
- City of San Diego. (2022–2023). Monthly Receiving Waters Monitoring Reports for the Point Loma Ocean Outfall (Point Loma Wastewater Treatment Plant), January 2022–December 2023. City of San Diego Ocean Monitoring Program, Public Utilities Department, Environmental Monitoring and Technical Services Division, San Diego, CA.
- City of San Diego. (2022). Biennial Receiving Waters Monitoring and Assessment Report for the Point Loma and South Bay Ocean Outfalls, 2020-2021. City of San Diego Ocean Monitoring Program, Public Utilities Department, Environmental Monitoring and Technical Services Division, San Diego, CA.

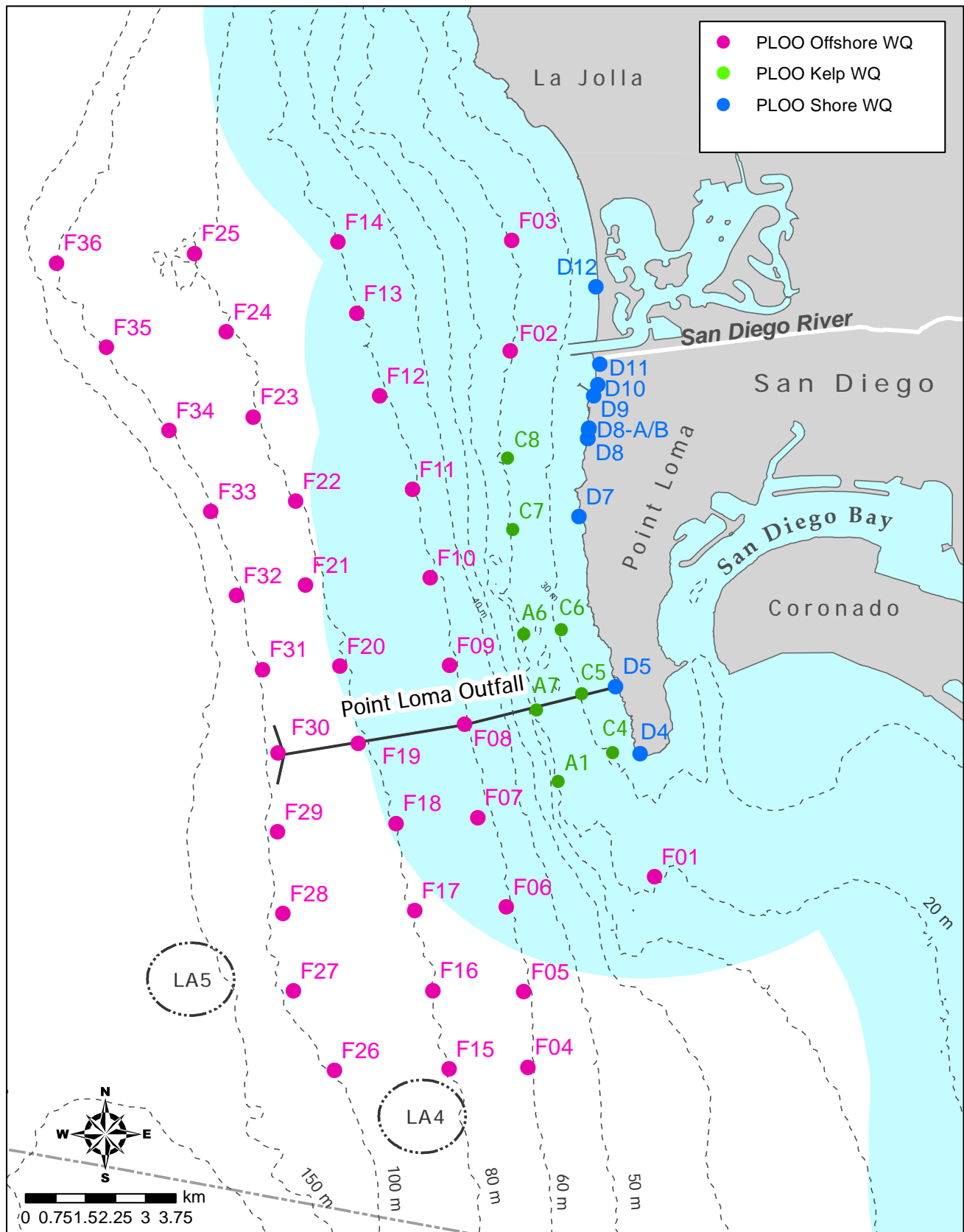
- City of San Diego. (2023a). Annual Receiving Waters Monitoring and Toxicity Testing Quality Assurance Report, 2020. City of San Diego Ocean Monitoring Program, Public Utilities Department, Environmental Monitoring and Technical Services Division, San Diego, CA.
- City of San Diego. (2024a). Ocean Monitoring Reports. <https://www.sandiego.gov/public-utilities/sustainability/ocean-monitoring/reports>
- City of San Diego. (2024b). Annual Receiving Waters Monitoring and Toxicity Testing Quality Assurance Report, 2021. City of San Diego Ocean Monitoring Program, Public Utilities Department, Environmental Monitoring and Technical Services Division, San Diego, CA.
- Grant, S.B., B.F. Sanders, A. Boehm, J. Redman, R. Kim, A. Chu, M. Gouldin, C. McGee, N. Gardiner, B. Jones, J. Svejksky, and G. Leipzig. (2001). Generation of enterococci bacteria in a coastal saltwater marsh and its impact on surf zone water quality. *Environmental Science Technology*, 35: 2407–2416.
- Griffith, J., K.C. Schiff, G. Lyon, and J. Fuhrman. (2010). Microbiological water quality at non-human influenced reference beaches in southern California during wet weather. *Marine Pollution Bulletin*, 60: 500–508.
- Gruber, S., L. Aumand, and A. Martin. (2005). Sediments as a reservoir of indicator bacteria in a coastal embayment: Mission Bay, California, Technical paper 0506. Weston Solutions, Inc. Presented at StormCon 2005. Orlando, FL, USA. July 2005.
- Harrell, F.E. Jr, C. Dupont and many others. (2015). Hmisc: Harrell Miscellaneous. R package version 3.17-0. <http://CRAN.R-project.org/package=Hmisc>.
- Kassambara, A. (2019). ggpubr: 'ggplot2' Based Publication Ready Plots. R package version 0.2.4. <https://CRAN.R-project.org/package=ggpubr>.
- Koenker, R. (2019). quantreg: Quantile Regression. R package version 5.52. <https://CRAN.R-project.org/package=quantreg>.
- Martin, A., and S. Gruber. (2005). Amplification of indicator bacteria in organic debris on southern California beaches. Technical Paper 0507. Weston Solutions, Inc. Presented at StormCon 2005. Orlando, FL, USA. July 2005.
- [NOAA] National Oceanic and Atmospheric Administration. (2022). National Climatic Data Center. <https://www.ncdc.noaa.gov/cdo-web/search>
- Noble, R.T., D.F. Moore, M.K. Leecaster, C.D. McGee, and S.B. Weisberg. (2003). Comparison of total coliform, fecal coliform, and *Enterococcus* bacterial indicator response for ocean recreational water quality testing. *Water Research*, 37: 1637–1643.
- Noble, M.A., J.P. Xu, G.L. Robertson, and K.L. Rosenfeld. (2006). Distribution and sources of surfzone bacteria at Huntington Beach before and after disinfection of an ocean outfall—A frequency-domain analysis. *Marine Environmental Research*, 61: 494–510.

- Phillips, C.P., H.M. Solo-Gabriele, A.J. Reneiers, J.D. Wang, R.T. Kiger, and N. Abdel-Mottaleb. (2011). Pore water transport of enterococci out of beach sediments. *Marine Pollution Bulletin*, 62: 2293–2298.
- R Core Team. (2019). R: A language and environment for statistical computing. R Foundation for Statistical Computing, Vienna, Austria. URL <https://www.R-project.org/>.
- Reeves, R.L., S.B. Grant, R.D. Mrse, C.M. Copil Oancea, B.F. Sanders, and A.B. Boehm. (2004). Scaling and management of fecal indicator bacteria in runoff from a coastal urban watershed in southern California. *Environmental Science and Technology*, 38: 2637–2648.
- Revelle, W. (2015). *psych: Procedures for Personality and Psychological Research*, Northwestern University, Evanston, Illinois, USA, <http://CRAN.R-project.org/package=psych> version 1.5.8.
- Ripley, B. and M. Lapsley. (2017). RODBC: ODBC Database Access. R package version 1.3-12. <http://CRAN.R-project.org/package=RODBC>.
- Rogowski, P., E. Terrill, M. Otero, L. Hazard, S.Y. Kim, P.E. Parnell, and P. Dayton. (2012a). Final Report: Point Loma Ocean Outfall Plume Behavior Study. Prepared for City of San Diego Public Utilities Department by Scripps Institution of Oceanography, University of California, San Diego, CA.
- Rogowski, P., E. Terrill, M. Otero, L. Hazard, and W. Middleton. (2012b). Mapping ocean outfall plumes and their mixing using Autonomous Underwater Vehicles. *Journal of Geophysical Research*, 117: C07016.
- Rogowski, P., E. Terrill, M. Otero, L. Hazard, and W. Middleton. (2013). Ocean outfall plume characterization using an Autonomous Underwater Vehicle. *Water Science & Technology*, 67: 925–933.
- Schauberger, P and A. Walker (2019). openxlsx: Read, Write and Edit xlsx Files. R package version 4.1.4. <https://CRAN.R-project.org/package=openxlsx>.
- Sercu, B., L.C. Van de Werfhorst, J. Murray, and P.A. Holden. (2009). Storm drains are sources of human fecal pollution during dry weather in three urban southern California watersheds. *Environmental Science and Technology*, 43: 293–298.
- Svejkovsky, J. and Hess, M. (2022). *Satellite & Aerial Coastal Water Quality Monitoring in the San Diego/Tijuana Region: Five Year Summary Report: 1 January 2017 – 31 December 2021*. Littleton, CO.
- [SWRCB] California State Water Resources Control Board. (2015). *California Ocean Plan, Water Quality Control Plan, Ocean Waters of California*. California Environmental Protection Agency, Sacramento, CA.
- Tegner, M.J., P.K. Dayton, P.B. Edwards, K.L. Riser, D.B. Chadwick, T.A. Dean, and L. Deysher. (1995). Effects of a large sewage spill on a kelp forest community: Catastrophe or disturbance? *Marine Environmental Research*, 40: 181–224.

- [USEPA] United States Environmental Protection Agency. (2014). Method 1600: Enterococci in Water by Membrane Filtration Using membrane-Enterococcus Indoxyl- β -D-Glucoside Agar (mEI). EPA Document EPA-821-R-14-011. Office of Water (4303T), Washington, DC.
- Warnes, G., B. Bolker, and T. Lumley. (2015). gtools: Various R Programming Tools. R package version 3.5.0. <http://CRAN.R-project.org/package=gtools>.
- Wickham, H. (2007). Reshaping Data with the reshape Package. *Journal of Statistical Software*, 21(12), 1-20. URL <http://www.jstatsoft.org/v21/i12/>.
- Wickham, H. (2017). tidyverse: Easily Install and Load the 'Tidyverse'. R package version 1.2.1. <https://CRAN.R-project.org/package=tidyverse>.
- Yamahara, K.M., B.A. Layton, A.E. Santoro, and A.B. Boehm. (2007). Beach sands along the California coast are diffuse sources of fecal bacteria to coastal waters. *Environmental Science and Technology*, 41: 4515–4521.

APPENDIX D

FIGURES & TABLES



Appendix D.1

Water quality (WQ) monitoring station locations sampled around the PLOO as part of the City of San Diego's Ocean Monitoring Program. Light blue shading represents State jurisdictional waters.

Appendix D.2

Water quality objectives for water contact areas, California Ocean Plan (SWRCB 2015).

A. Bacterial Characteristics – Water Contact Standards; CFU = colony forming units.

(a) 30-day Geometric Mean – The following standards are based on the geometric mean of the five most recent samples from each site:

- 1) Total coliform density shall not exceed 1000 CFU/100 mL
- 2) Fecal coliform density shall not exceed 200 CFU/100 mL
- 3) Enterococcus density shall not exceed 35 CFU/100 mL

(b) Single Sample Maximum:

- 1) Total coliform density shall not exceed 10,000 CFU/100 mL
- 2) Fecal coliform density shall not exceed 400 CFU/100 mL
- 3) Enterococcus density shall not exceed 104 CFU/100 mL
- 4) Total coliform density shall not exceed 1000 CFU/100 mL when the fecal coliform:total coliform ratio exceeds 0.1

B. Physical Characteristics

- (a) Floating particulates and oil and grease shall not be visible.
- (b) The discharge of waste shall not cause aesthetically undesirable discoloration of the ocean surface.
- (c) Natural light shall not be significantly reduced at any point outside of the initial dilution zone as the result of the discharge of waste.

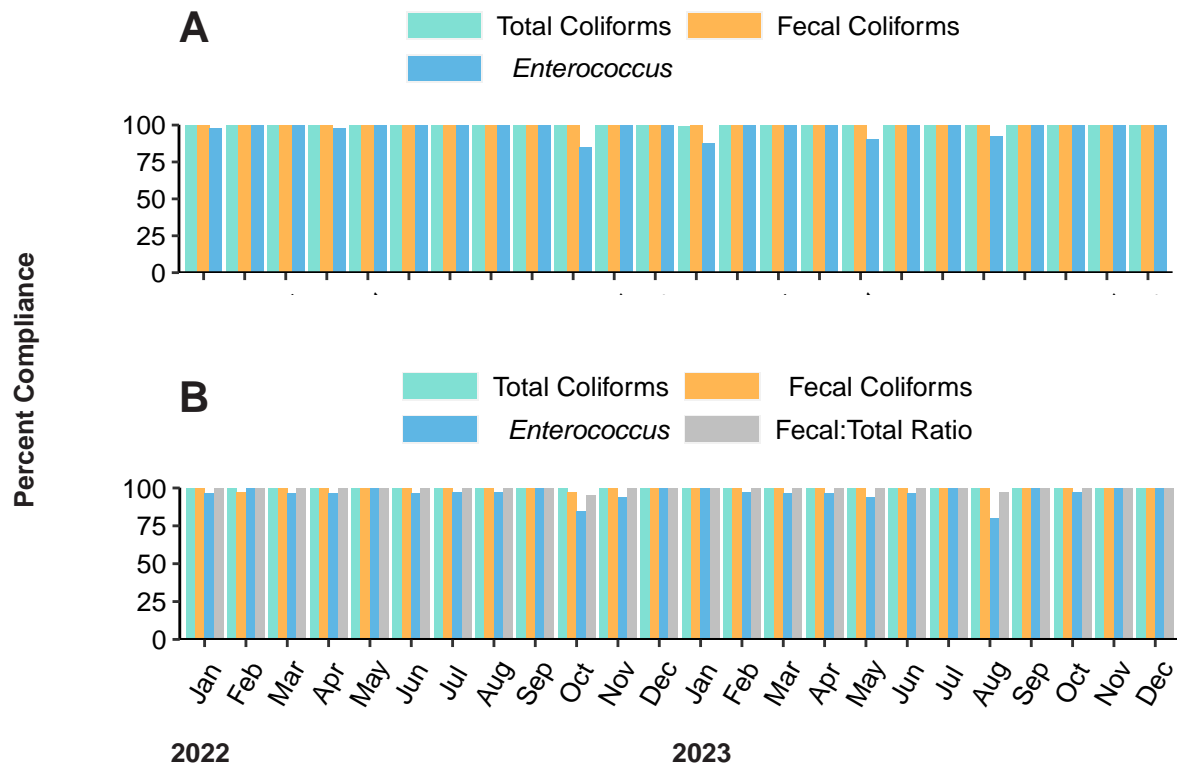
C. Chemical Characteristics

- (a) The dissolved oxygen concentration shall not at any time be depressed more than 10 percent from what occurs naturally, as a result of the discharge of oxygen demanding waste materials.
- (b) The pH shall not be changed at any time more than 0.2 units from that which occurs naturally.

Appendix D.3

Depths from which seawater samples are collected for bacteriological analysis from kelp and offshore stations.

Station	PLOO Sample Depth (m)								
Contour	1	3	9	12	18	25	60	80	98
<i>Kelp Bed</i>									
9-m	x	x	x						
18-m	x			x	x				
<i>Offshore</i>									
18-m	x			x	x				
60-m	x					x	x		
80-m	x					x	x	x	
98-m	x					x	x	x	x



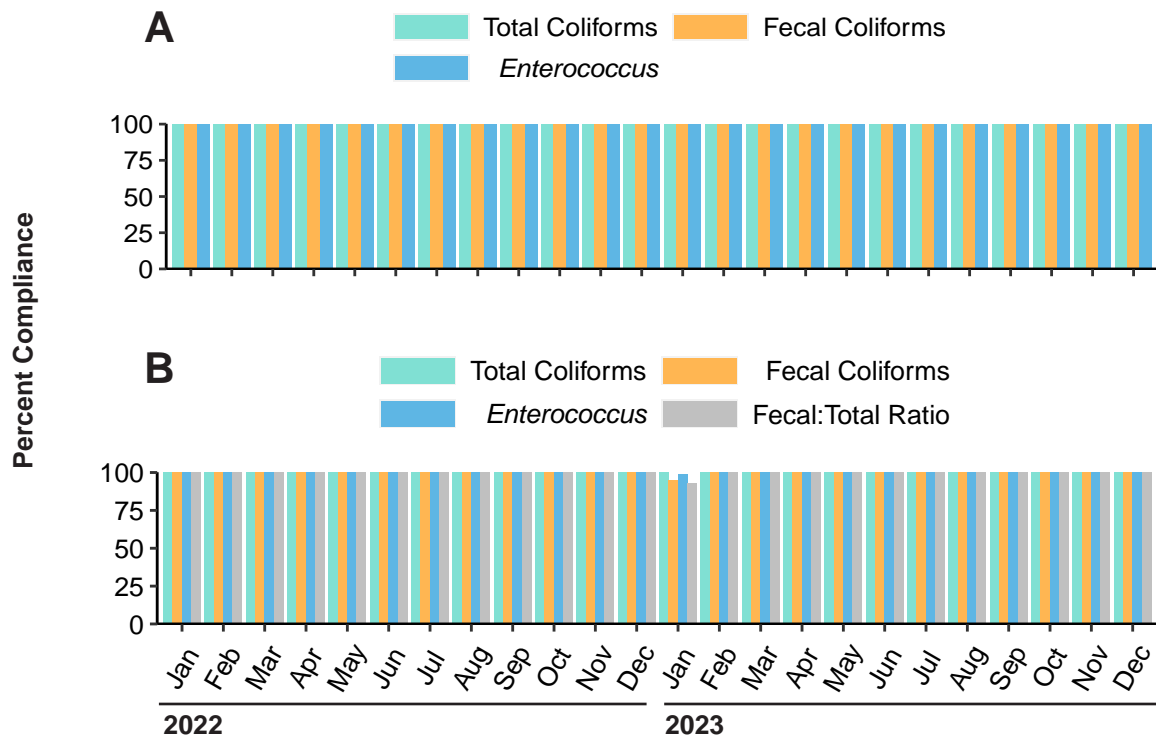
Appendix D.4

Compliance rates for (A) geometric mean and (B) single sample maximum water contact standards at PLOO shore stations during 2022 and 2023.

Appendix D.5

Number of samples with elevated FIB (eFIB) densities collected from PLOO shore stations during wet and dry seasons, and percent occurring in wet season (%wet), during 2022 and 2023. Stations are listed north to south from top to bottom.

	Seasons		% Wet
	Wet	Dry	
PLOO			
D10	4	1	80
D11	8	2	80
D12	1	0	100
D5	3	0	100
D7	2	1	67
D8-B	9	1	90
D9	2	0	100
Total eFIB	29	5	85
Total Analyses	1,920	1,408	58



Appendix D.6

Compliance rates for (A) geometric mean and (B) single sample maximum water contact standards at PLOO kelp stations during 2022 and 2023.

Appendix D.7

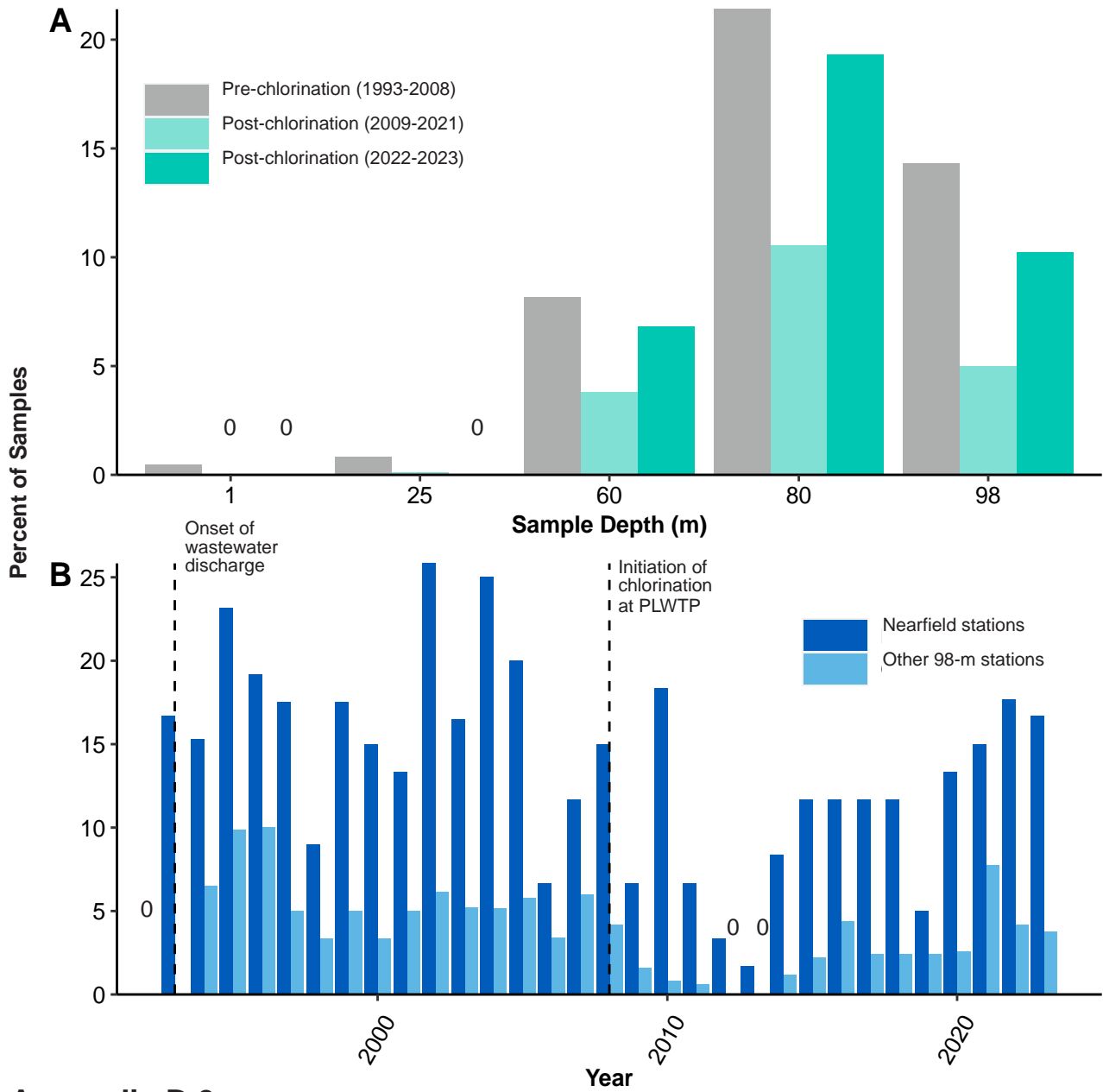
Number of samples with elevated FIB (eFIB) densities collected at PLOO kelp stations during wet and dry seasons, and percent occurring in wet season (%wet), during 2022 and 2023. Within each contour stations are listed from north to south. Stations not listed had no samples with elevated FIB concentrations during this time period.

	Seasons		% Wet
	Wet	Dry	
PLOO			
<i>18-m Depth Contour</i>			
A1	4	0	100
A6	1	0	100
A7	4	0	100
C7	2	0	100
C8	2	0	100
Total eFIB	13	0	100
Total Analyses	5,760	4,224	58

Appendix D.8

Number of samples with elevated FIB (eFIB) densities collected at PLOO offshore stations during wet and dry seasons, and percent occurring in wet season (%wet), during 2022 and 2023. Within each contour stations are listed from north to south. Stations not listed had no samples with elevated FIB concentrations during this time period.

	Seasons		% Wet
	Wet	Dry	
PLOO			
<i>80-m Depth Contour</i>			
F25	0	1	0
F23	1	2	33
F22	1	2	33
F21	2	3	40
F20	1	3	25
F19	3	1	75
F17	0	1	0
<i>100-m Depth Contour</i>			
F36	1	0	100
F35	2	0	100
F34	1	0	100
F33	3	0	100
F32	4	1	80
F31	3	0	100
F30	5	8	38
F29	2	3	40
F28	2	1	67
F27	0	2	0
F26	1	1	50
Total eFIB	32	29	52
Total Analyses	564	564	50



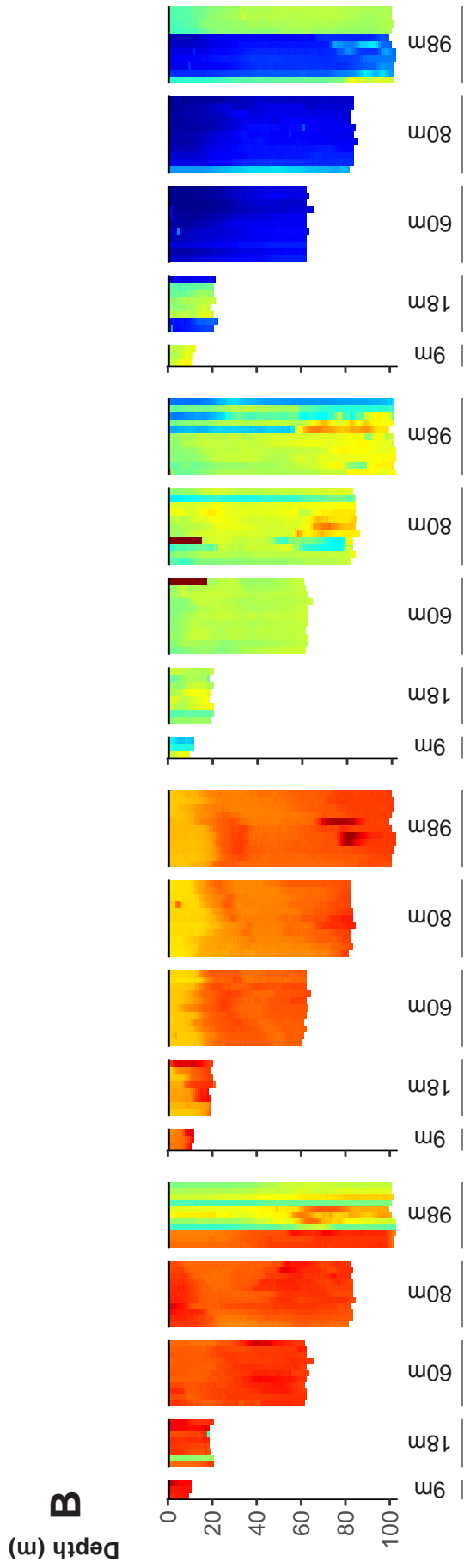
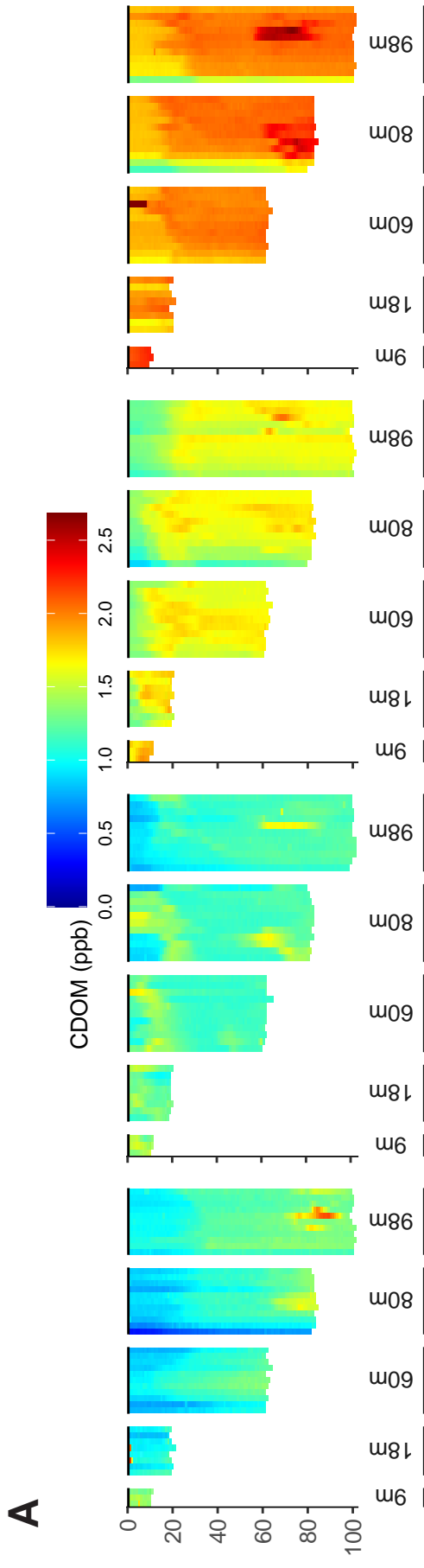
Appendix D.9

Percent of samples collected from PLOO 98-m offshore stations with elevated FIB. Samples from 2022 and 2023 are compared to those collected from 1993 through 2022 by (A) sampling depth and (B) year.

Appendix E

Plume Dispersion

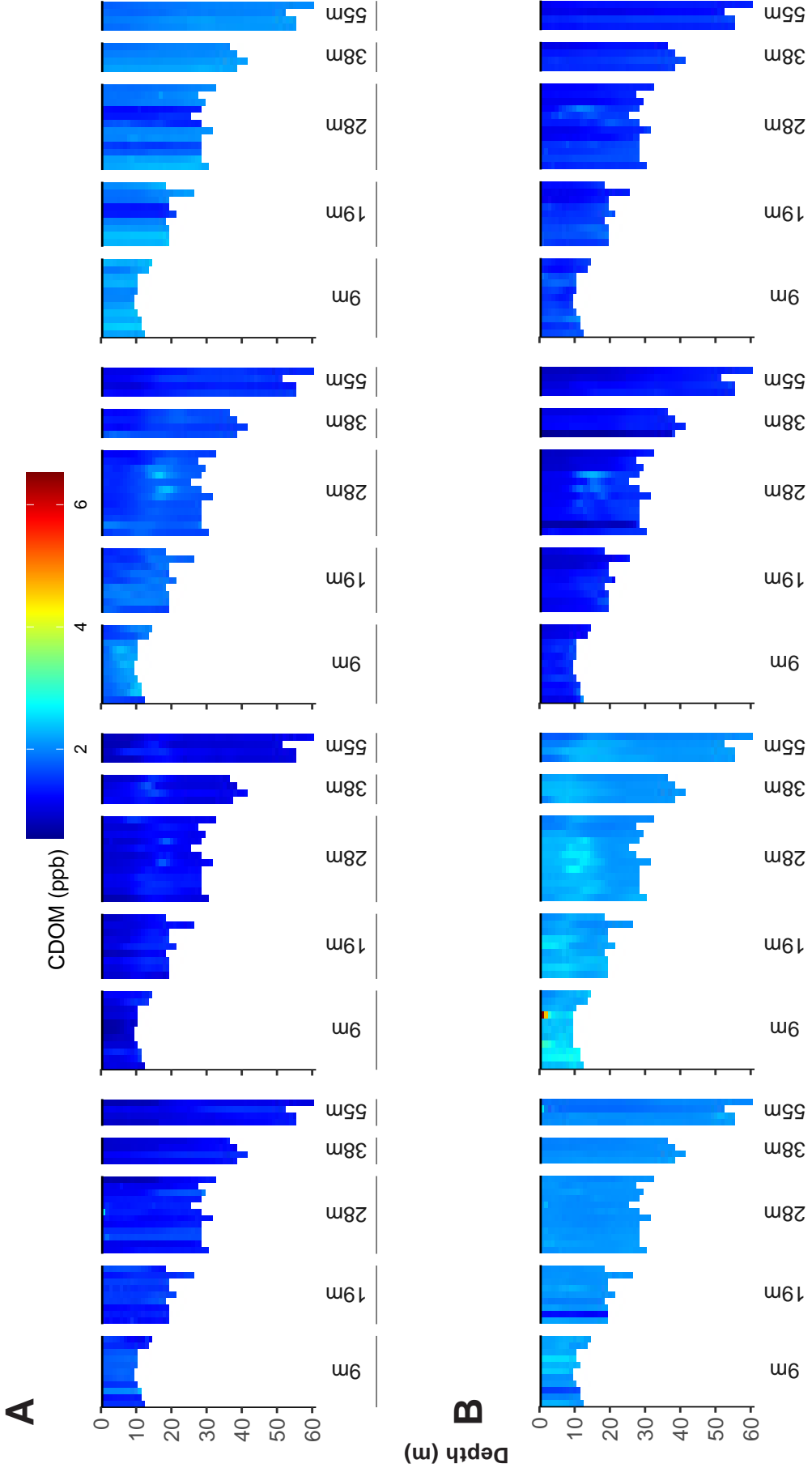
2022 – 2023 Supplemental Analyses



Contour

Appendix E.1

Concentrations of CDOM recorded in the PLOO region during (A) 2022 and (B) 2023. Data are 1-m binned values per depth for each station during each quarterly survey. Stations depicted from north to south along each depth contour. See Chapter 2 for additional sampling details.



Contour

Appendix E.2

Concentrations of CDOM recorded in the SBOO region during (A) 2022 and (B) 2023. Data are 1-m binned values per depth for each station during each quarterly survey. Stations depicted from north to south along each depth contour. See Chapter 2 for additional sampling details.

Appendix E.3

Summary of oceanographic data within potential detected plume at PLOO offshore stations and corresponding reference values during 2022 and 2023. Plume depth is the minimum depth at which CDOM exceeds the 95th percentile while plume width is the number of meters across which that exceedance occurs. Out-of-range values are in **bold**. DO = dissolved oxygen (mg/L); XMS = transmissivity (%); SD = standard deviation; CI = confidence interval.

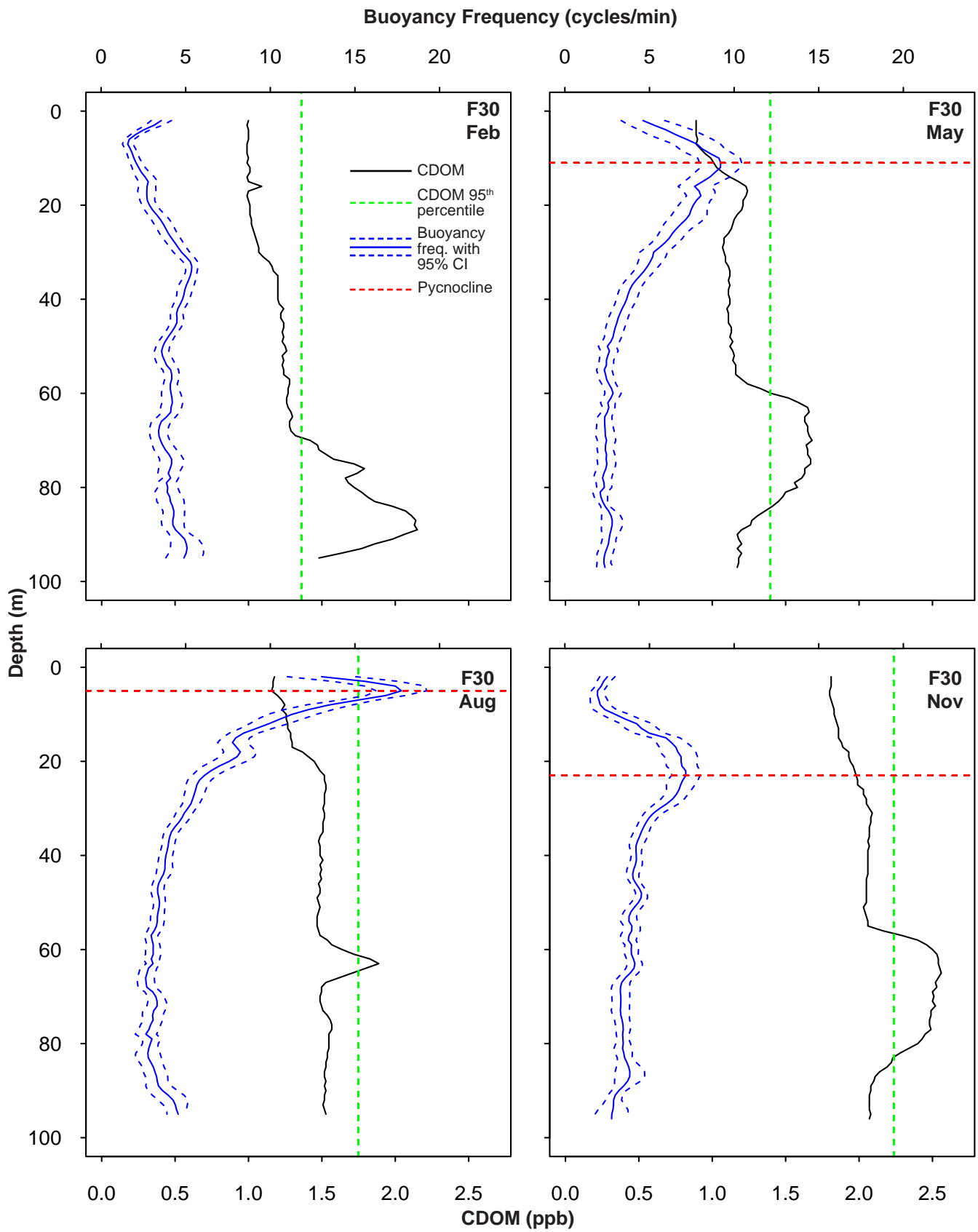
Station	Date	Potential Plume						Reference			
		Width (m)	Depth (m)	Mean DO	Mean pH	Mean XMS	DO (Mean-SD)	pH (Mean)	XMS (Mean -95% CI)	XMS (Mean -95% CI)	
F26	08-Feb-22	21	74	4.2	7.8	88	4.4	7.8	7.8	87	
F28	08-Feb-22	2	82	4.7	7.8	88	4.4	7.8	7.8	89	
F29	08-Feb-22	9	81	4.1	7.8	86	4.3	7.8	7.8	89	
F30	08-Feb-22	26	70	4.2	7.8	87	4.6	7.8	7.8	86	
F31	08-Feb-22	4	72	4.7	7.8	89	4.9	7.8	7.8	86	
F32	08-Feb-22	15	75	4.2	7.8	88	4.5	7.8	7.8	86	
F35	08-Feb-22	3	80	4.5	7.8	87	4.5	7.8	7.8	85	
F19 ^a	10-Feb-22	10	71	4.3	7.7	87	4.8	7.8	7.8	85	
F20 ^a	10-Feb-22	16	65	4.2	7.7	87	4.9	7.8	7.8	85	
F21	10-Feb-22	13	67	4.1	7.7	87	4.8	7.8	7.8	85	
F30	18-May-22	25	60	3.0	7.7	85	3.3	7.7	7.7	90	
F21	20-May-22	3	62	3.4	7.7	87	3.4	7.7	7.7	90	
F22	20-May-22	16	55	3.1	7.7	87	3.5	7.7	7.7	90	
F23	20-May-22	13	58	3.1	7.7	87	3.4	7.7	7.7	90	
F24	20-May-22	8	68	3.0	7.7	87	3.3	7.7	7.7	90	
F25	20-May-22	7	72	3.0	7.7	87	3.2	7.7	7.7	90	
F27	16-Aug-22	13	59	4.6	7.8	91	4.5	7.8	7.8	90	
F28	16-Aug-22	13	64	4.4	7.8	90	4.4	7.8	7.8	90	
F30	16-Aug-22	3	62	4.5	7.8	89	4.5	7.8	7.8	91	
F17	18-Aug-22	16	52	4.5	7.8	92	4.6	7.8	7.8	91	
F18 ^a	18-Aug-22	4	64	4.4	7.8	91	4.5	7.8	7.8	90	
F20 ^a	18-Aug-22	8	65	4.2	7.8	90	4.4	7.8	7.8	90	
F28	15-Nov-22	3	78	4.0	7.8	91	4.0	7.8	7.8	91	
F29	15-Nov-22	23	58	3.9	7.8	89	4.4	7.8	7.8	92	
F30	15-Nov-22	26	57	4.0	7.8	90	4.4	7.8	7.8	92	
F19 ^a	18-Nov-22	11	62	4.3	7.8	91	4.5	7.8	7.8	93	
F20 ^a	18-Nov-22	6	62	4.4	7.8	91	4.5	7.8	7.8	93	
F21	18-Nov-22	14	68	4.0	7.8	90	4.2	7.8	7.8	92	
F22	18-Nov-22	9	65	4.1	7.8	90	4.2	7.8	7.8	92	

^aStation located within State jurisdictional waters

Appendix E.3 *continued*

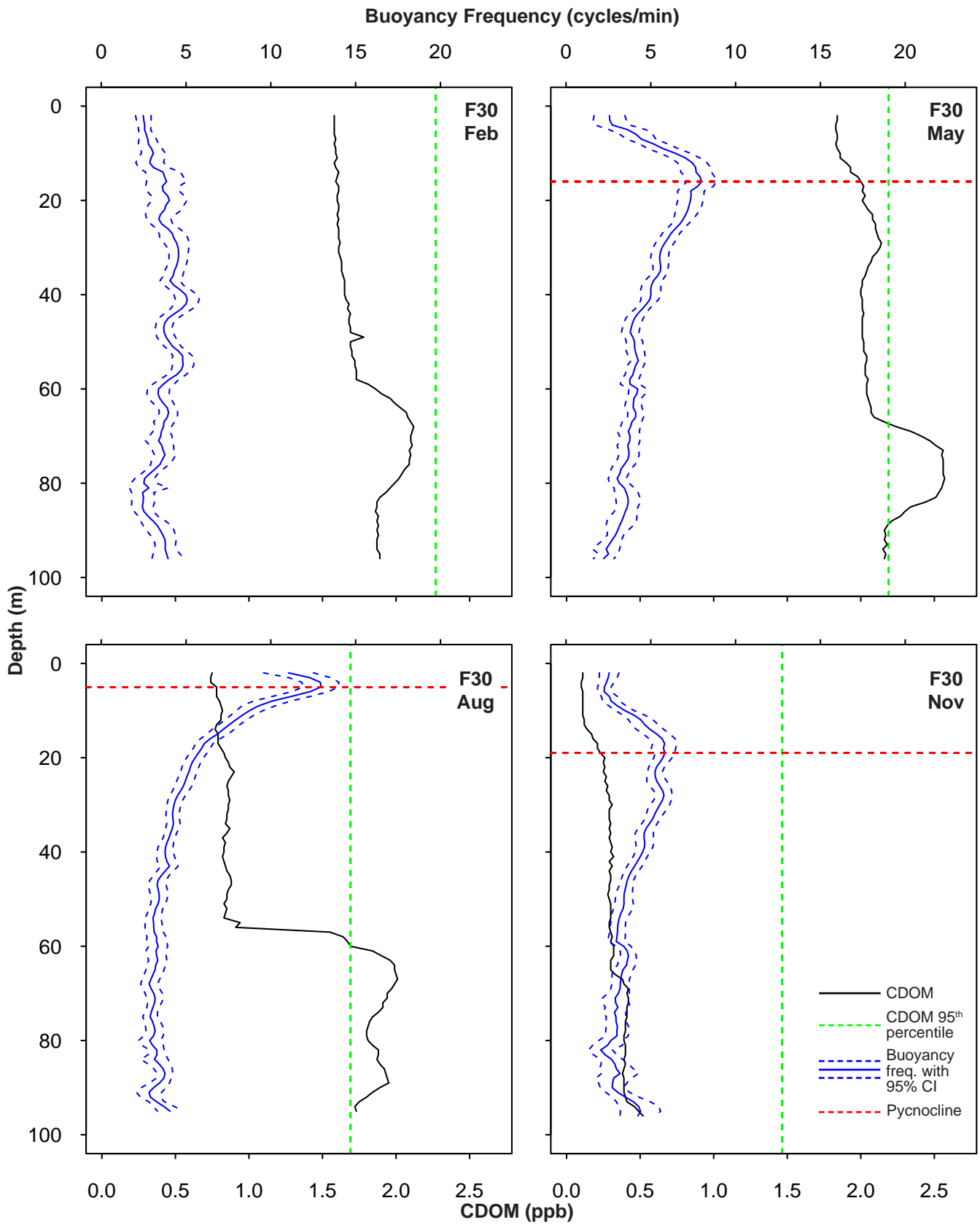
Station	Date	Potential Plume					Reference				
		Width (m)	Depth (m)	Mean DO	Mean pH	Mean XMS	DO (Mean-SD)	pH (Mean)	XMS (Mean -95% CI)		
F23	18-Nov-22	6	70	4.1	7.8	90	4.3	7.8	7.8	92	
F34	28-Feb-23	8	69	4.0	7.8	90	3.7	7.8	7.8	89	
F04	02-Mar-23	32	36	3.9	7.8	91	5.4	7.9	7.9	92	
F10 ^a	02-Mar-23	19	38	4.0	7.8	89	5.1	7.9	7.9	92	
F11 ^a	02-Mar-23	8	44	3.9	7.8	90	4.9	7.9	7.9	92	
F12 ^a	02-Mar-23	4	47	3.8	7.8	90	4.8	7.8	7.8	92	
F15	03-Mar-23	6	53	4.1	7.8	92	4.2	7.8	7.8	91	
F16	03-Mar-23	10	50	4.0	7.8	92	4.4	7.8	7.8	92	
F17	03-Mar-23	1	75	3.5	7.8	91	3.7	7.8	7.8	90	
F30	23-May-23	21	68	3.9	7.8	90	4.2	7.8	7.8	90	
F31	23-May-23	4	77	4.1	7.8	93	4.0	7.8	7.8	88	
F32	23-May-23	22	77	3.7	7.8	91	4.0	7.8	7.8	88	
F33	23-May-23	14	77	3.7	7.8	92	4.0	7.8	7.8	88	
F20a	25-May-23	7	74	4.1	7.7	91	4.0	7.8	7.8	89	
F21	25-May-23	11	71	4.4	7.8	93	4.1	7.8	7.8	90	
F29	15-Aug-23	14	66	5.0	7.8	90	5.1	7.9	7.9	89	
F30	15-Aug-23	35	61	4.8	7.8	90	4.9	7.8	7.8	88	
F18 ^a	17-Aug-23	10	69	4.3	7.8	88	4.8	7.8	7.8	88	
F19 ^a	17-Aug-23	18	64	4.3	7.8	91	4.9	7.8	7.8	89	
F20 ^a	17-Aug-23	17	64	4.3	7.8	90	4.9	7.8	7.8	88	
F21	17-Aug-23	21	57	4.5	7.8	91	5.1	7.9	7.9	88	
F26	14-Nov-23	35	47	6.4	8.0	92	6.7	8.0	8.0	89	
F27	14-Nov-23	33	34	6.6	8.0	92	6.9	8.0	8.0	90	
F36	14-Nov-23	17	81	5.5	7.9	92	5.3	7.9	7.9	89	

^aStation located within State jurisdictional waters



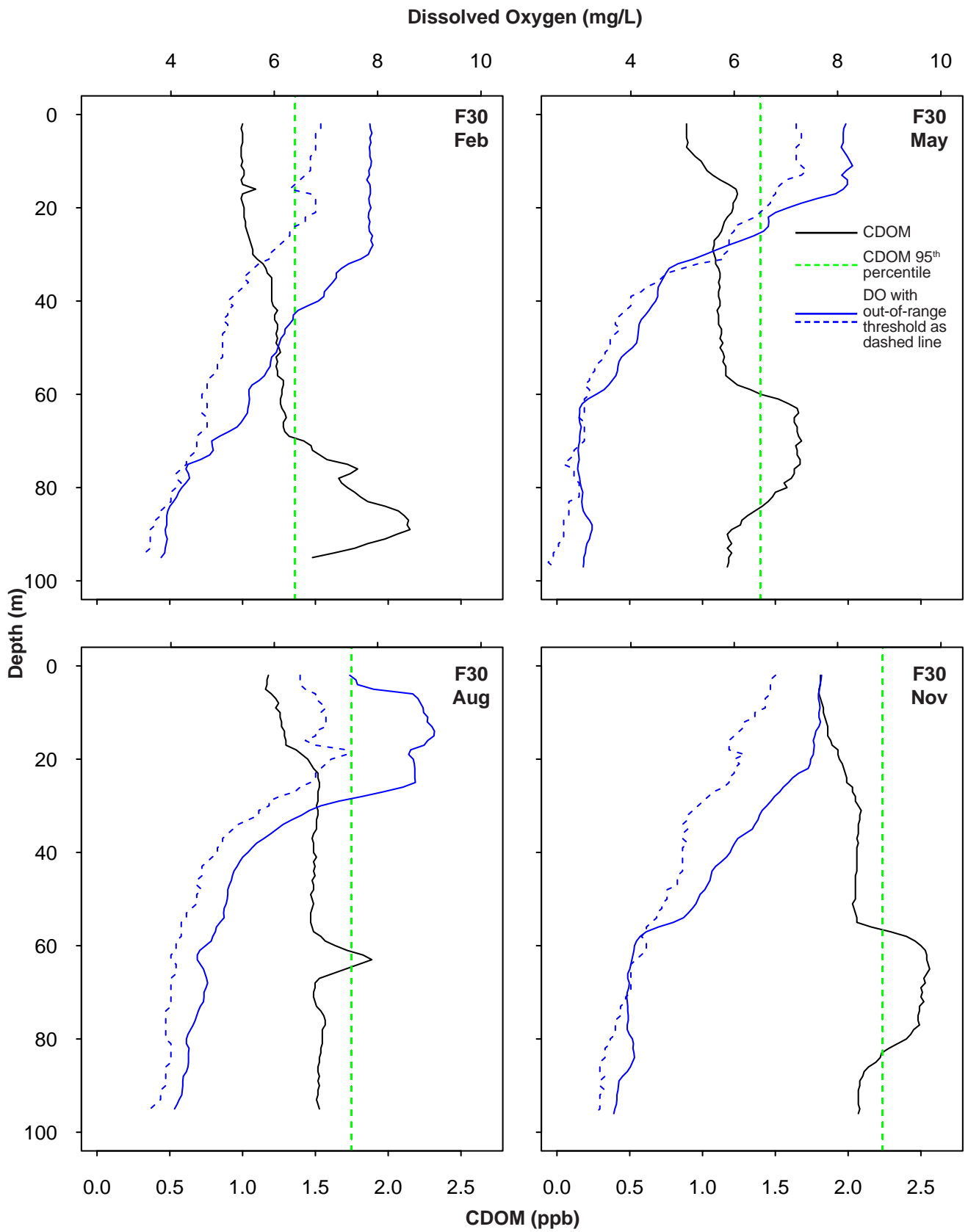
Appendix E.4

Representative vertical profiles of CDOM and buoyancy frequency from PLOO nearfield station F30 during 2022.



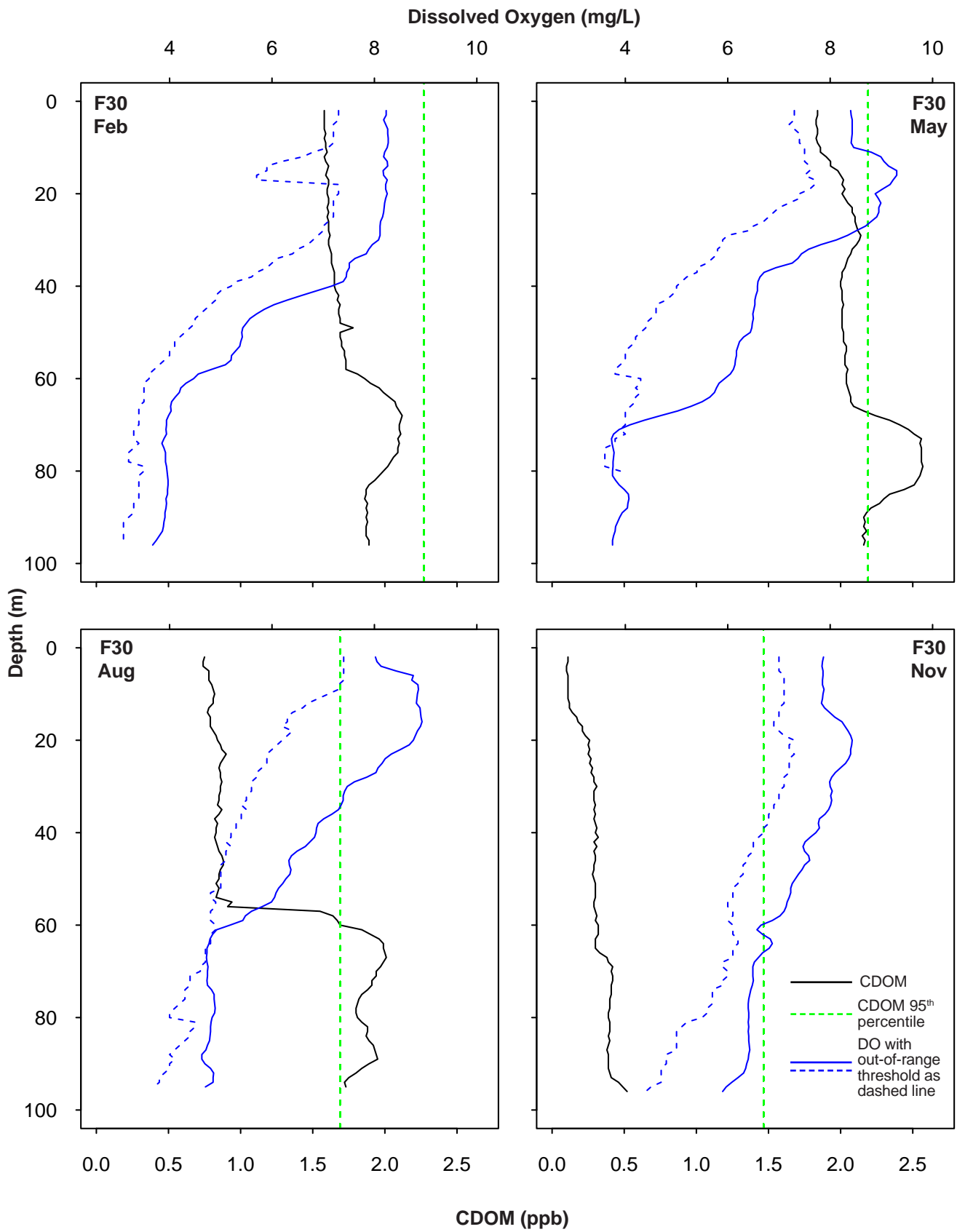
Appendix E.5

Representative vertical profiles of CDOM and buoyancy frequency from PLOO nearfield station F30 during 2023.



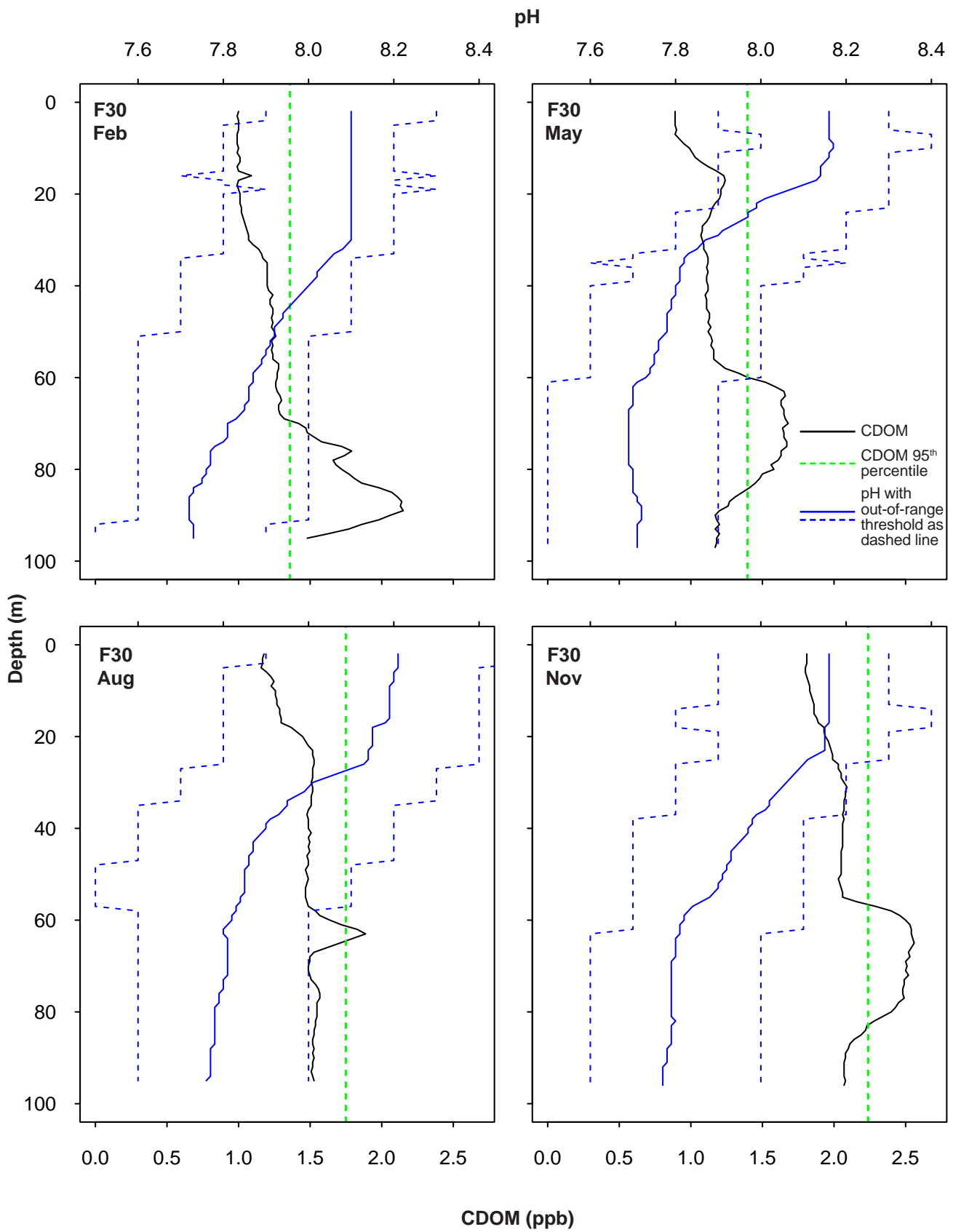
Appendix E.6

Representative vertical profiles of CDOM and DO from PLOO nearfield station F30 during 2022.



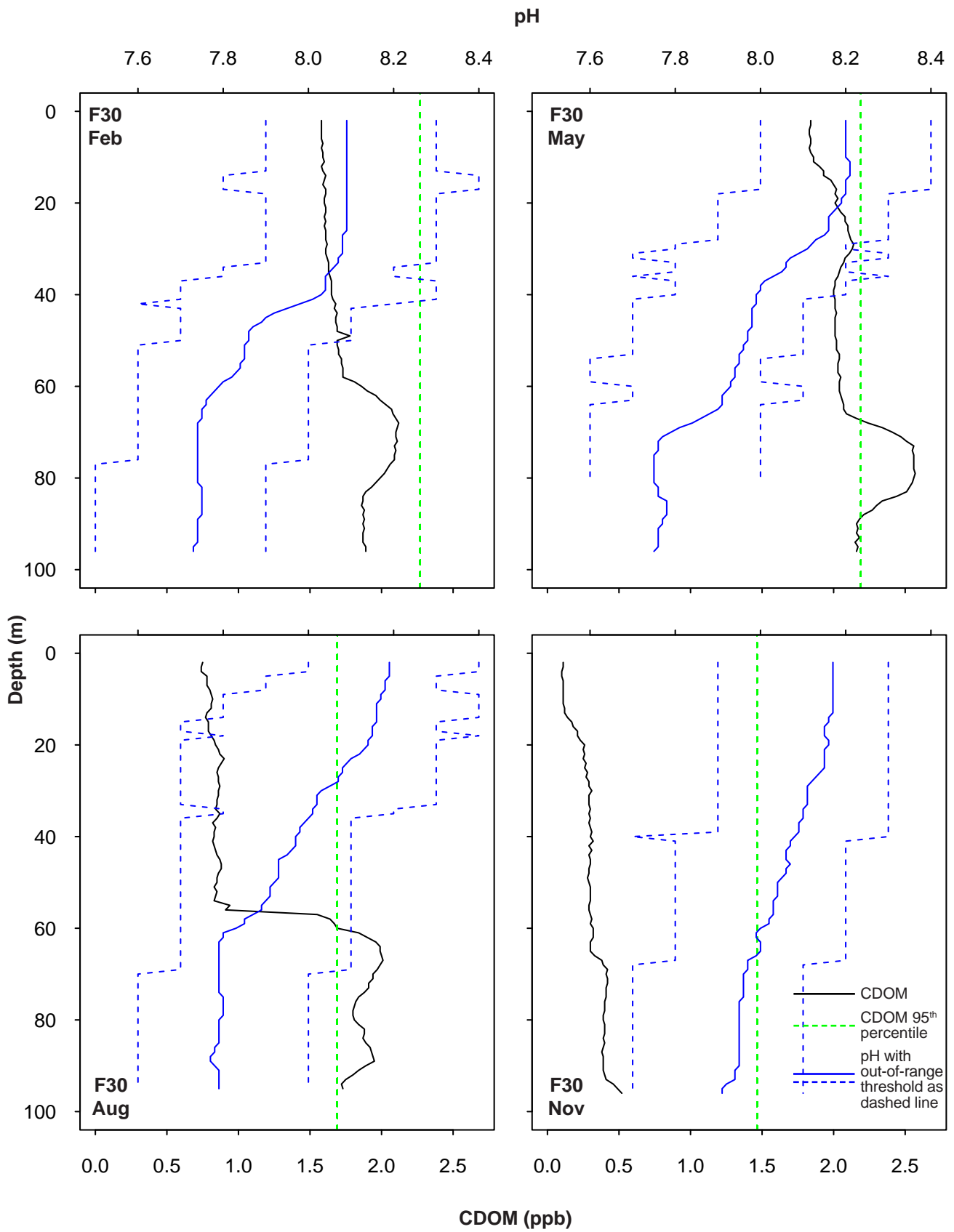
Appendix E.7

Representative vertical profiles of CDOM and DO from PLOO nearfield station F30 during 2023.



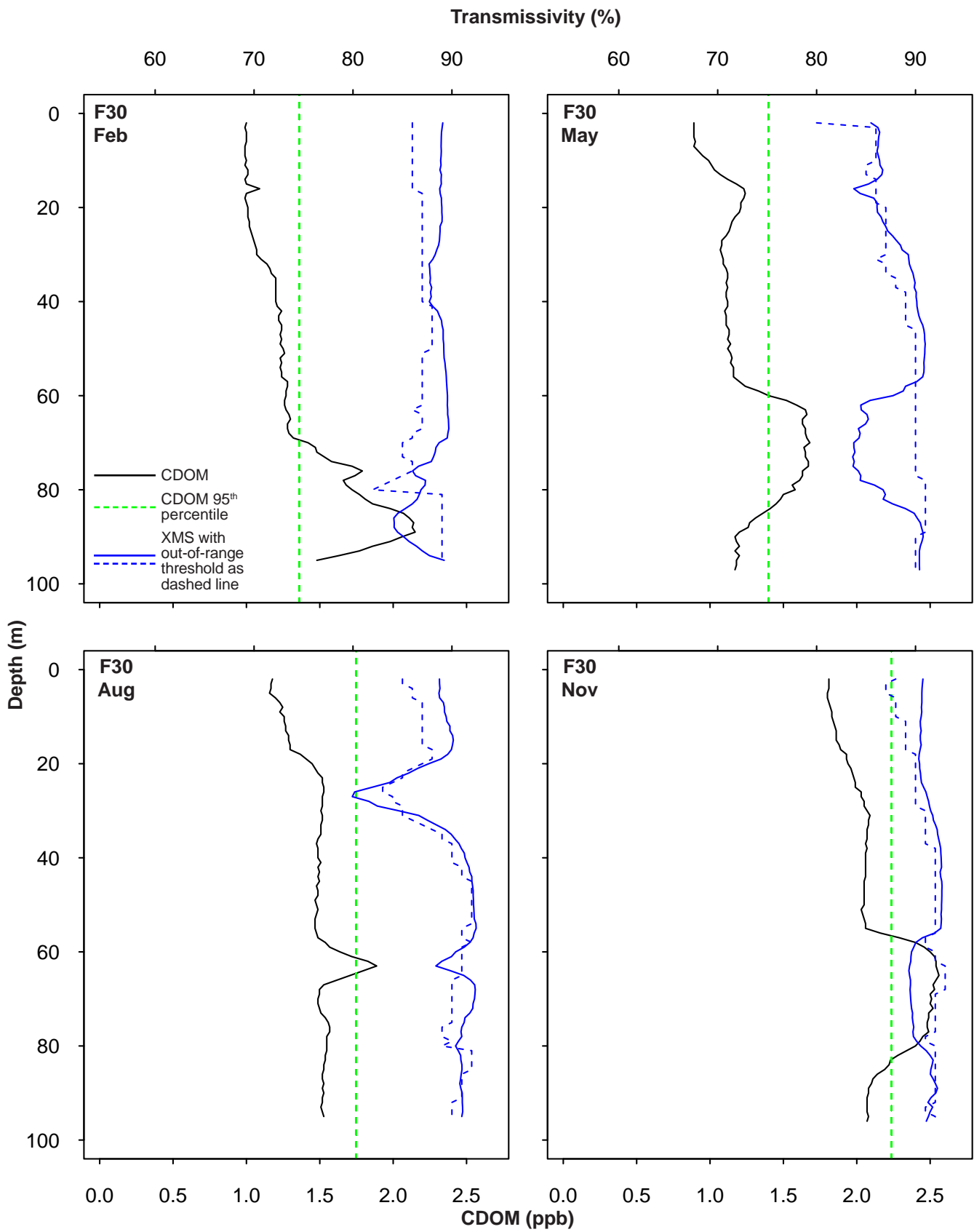
Appendix E.8

Representative vertical profiles of CDOM and pH from PLOO nearfield station F30 during 2022.



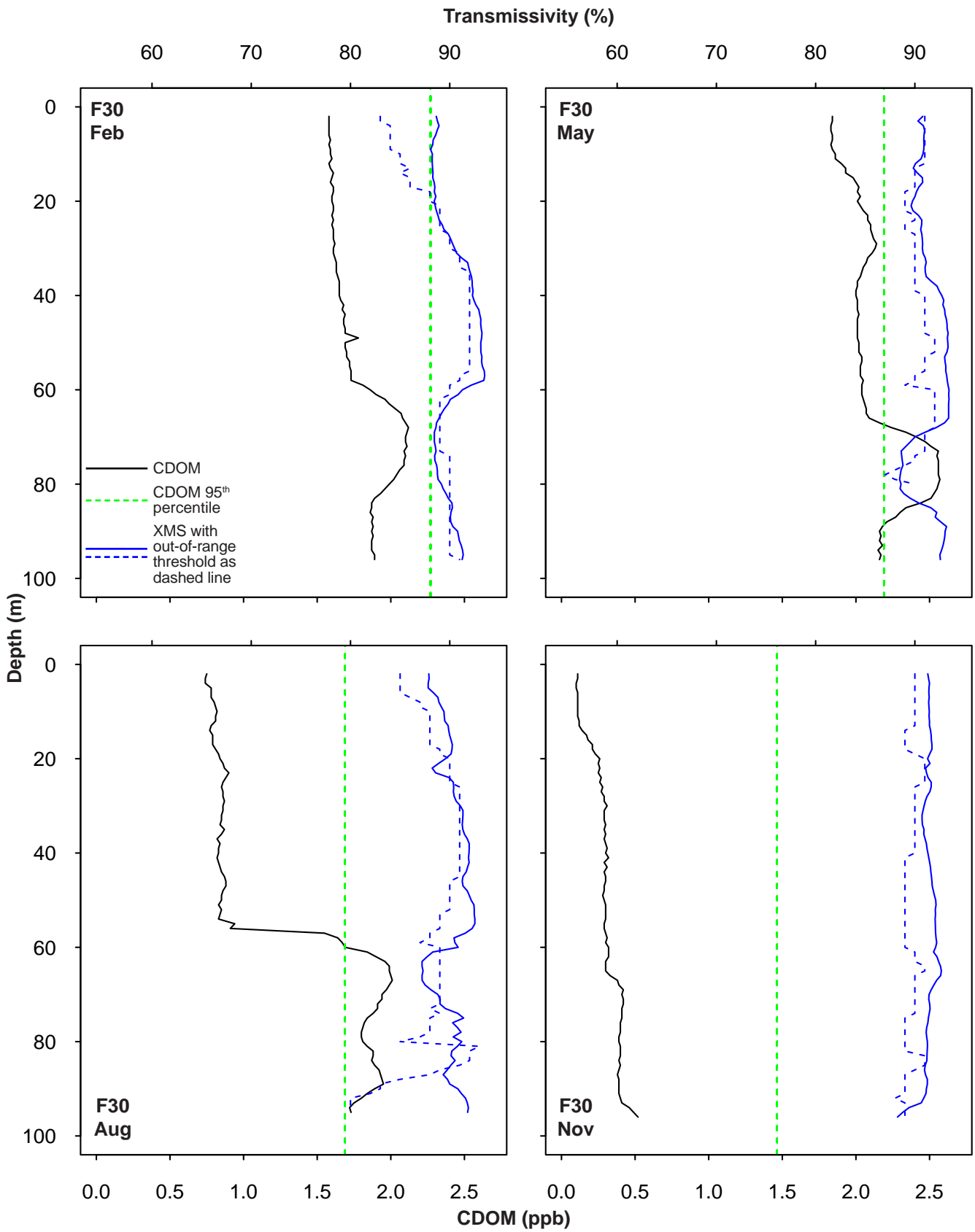
Appendix E.9

Representative vertical profiles of CDOM and pH from PLOO nearfield station F30 during 2023.



Appendix E.10

Representative vertical profiles of CDOM and transmissivity (XMS) from PLOO nearfield station F30 during 2022.



Appendix E.11

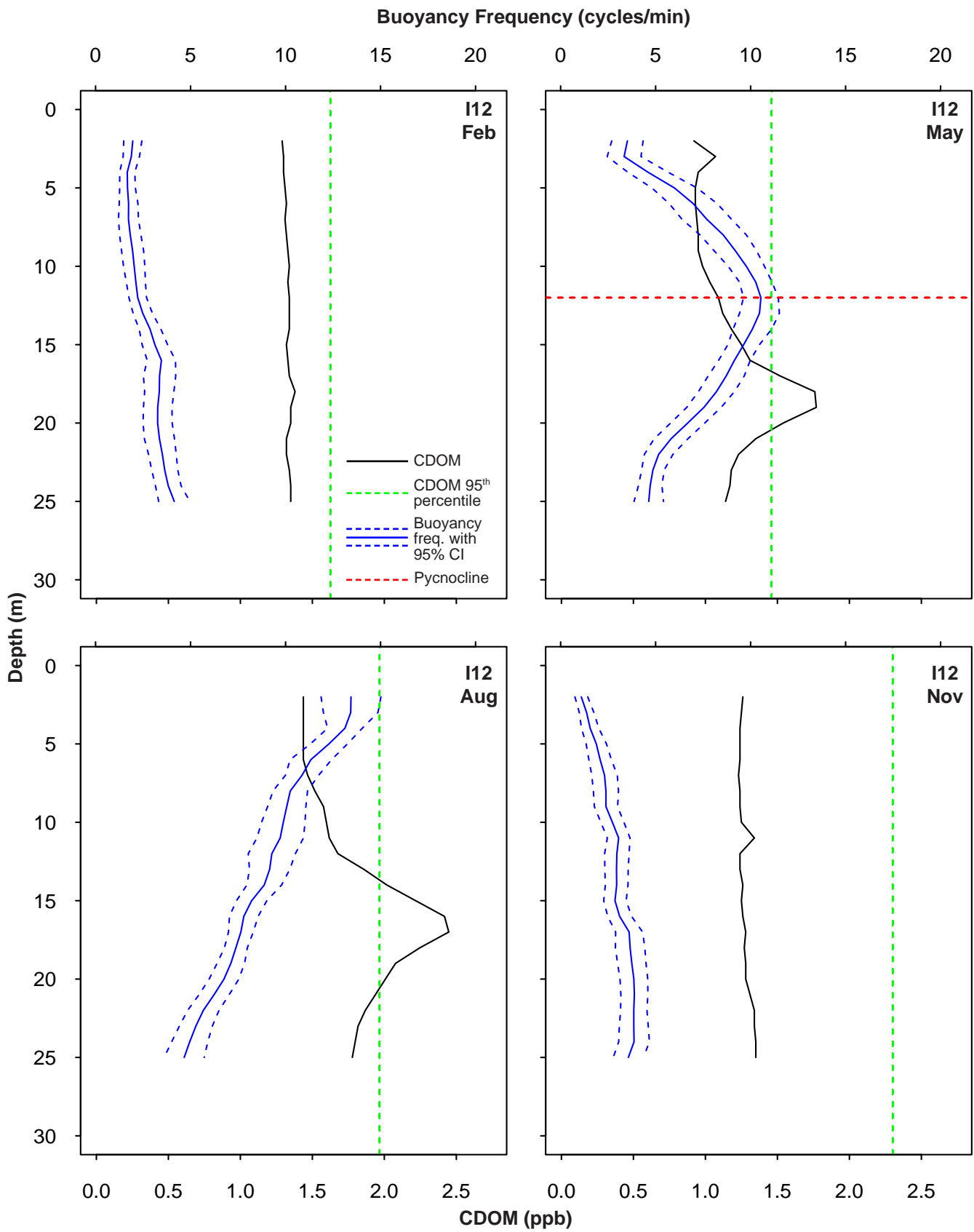
Representative vertical profiles of CDOM and transmissivity (XMS) from PLOO nearfield station F30 during 2023.

Appendix E.12

Summary of oceanographic data within potential detected plume at SBOO offshore stations and corresponding reference values during 2022 and 2023. Plume depth is the minimum depth at which CDOM exceeds the 95th percentile while plume width is the number of meters across which that exceedance occurs. Out-of-range values are in **bold**. DO = dissolved oxygen (mg/L); XMS = transmissivity (%); SD = standard deviation; CI = confidence interval.

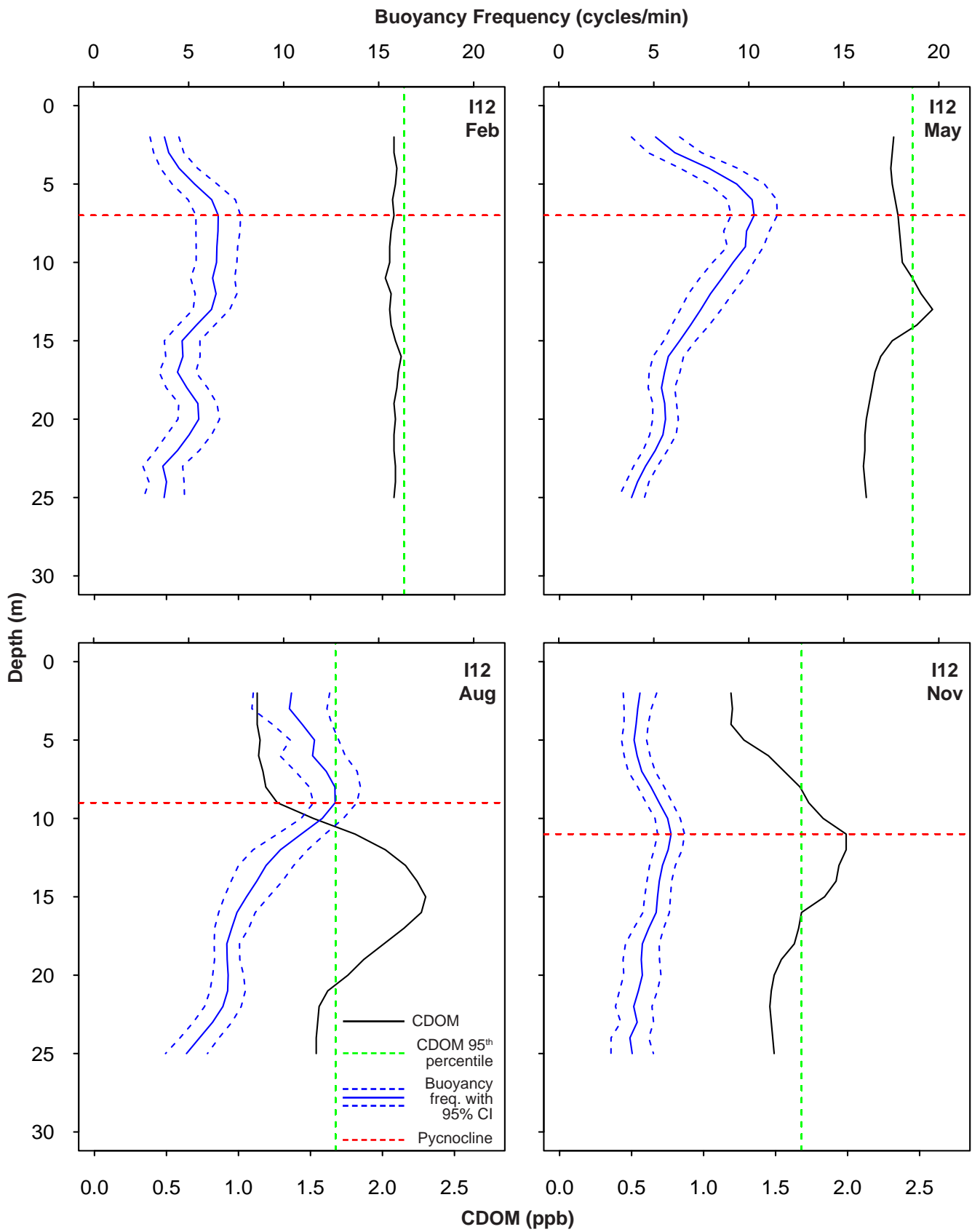
Station	Date	Potential Plume						Reference			
		Width (m)	Depth (m)	Mean DO	Mean pH	Mean XMS	DO (Mean-SD)	pH (Mean)	XMS (Mean-95% CI)	XMS (Mean-95% CI)	
I9	01-Feb-22	7	20	7.2	8.1	83	6.8	8.1	8.1	85	
I23 ^a	03-Feb-22	4	15	6.9	8.1	79	7.2	8.1	8.1	85	
I27 ^a	03-Feb-22	9	17	7.4	8.1	84	6.9	8.1	8.1	85	
I12 ^a	04-May-22	4	17	4.9	8.0	81	4.9	8.0	8.0	84	
I13	04-May-22	2	13	5.1	7.9	83	7.3	8.2	8.2	80	
I15	04-May-22	3	17	5.1	8.0	83	5.0	8.0	8.0	84	
I21	04-May-22	4	14	6.4	8.0	84	6.2	8.1	8.1	82	
I12 ^a	09-Aug-22	7	14	6.1	8.0	88	6.4	8.1	8.1	87	
I15	09-Aug-22	3	16	6.0	7.9	89	6.5	8.1	8.1	87	
I16 ^a	09-Aug-22	6	16	5.7	7.9	89	6.1	8.0	8.0	87	
I31 ^a	10-Aug-22	2	7	6.8	8.0	85	7.2	8.1	8.1	88	
I9	11-Aug-22	5	14	7.2	8.0	86	6.5	8.1	8.1	87	
I9	07-Feb-23	3	9	6.8	7.9	84	5.9	8.0	8.0	85	
I18 ^a	08-Feb-23	7	8	6.6	7.9	70	5.6	7.9	7.9	86	
I12 ^a	18-May-23	3	12	5.7	7.9	88	5.3	7.9	7.9	87	
I14 ^a	18-May-23	5	8	6.0	7.9	83	5.7	8.0	8.0	86	
I15	18-May-23	4	11	5.7	7.9	85	5.4	8.0	8.0	87	
I16 ^a	18-May-23	7	8	6.2	8.0	84	5.6	8.0	8.0	87	
I17 ^a	18-May-23	2	9	6.2	8.0	84	5.8	8.0	8.0	86	
I12 ^a	09-Aug-23	10	11	8.1	8.1	87	8.7	8.2	8.2	86	
I15	09-Aug-23	1	18	9.0	8.1	86	8.9	8.2	8.2	87	
I16 ^a	09-Aug-23	8	11	8.6	8.1	85	8.7	8.2	8.2	86	
I17 ^a	09-Aug-23	3	15	8.8	8.1	86	8.8	8.2	8.2	86	
I12 ^a	08-Nov-23	4	12	7.9	8.0	85	8.1	8.1	8.1	88	
I16 ^a	08-Nov-23	4	19	7.9	8.0	87	7.8	8.1	8.1	89	
I17 ^a	08-Nov-23	2	14	7.8	8.0	88	8.0	8.1	8.1	88	

^aStation located within State jurisdictional waters



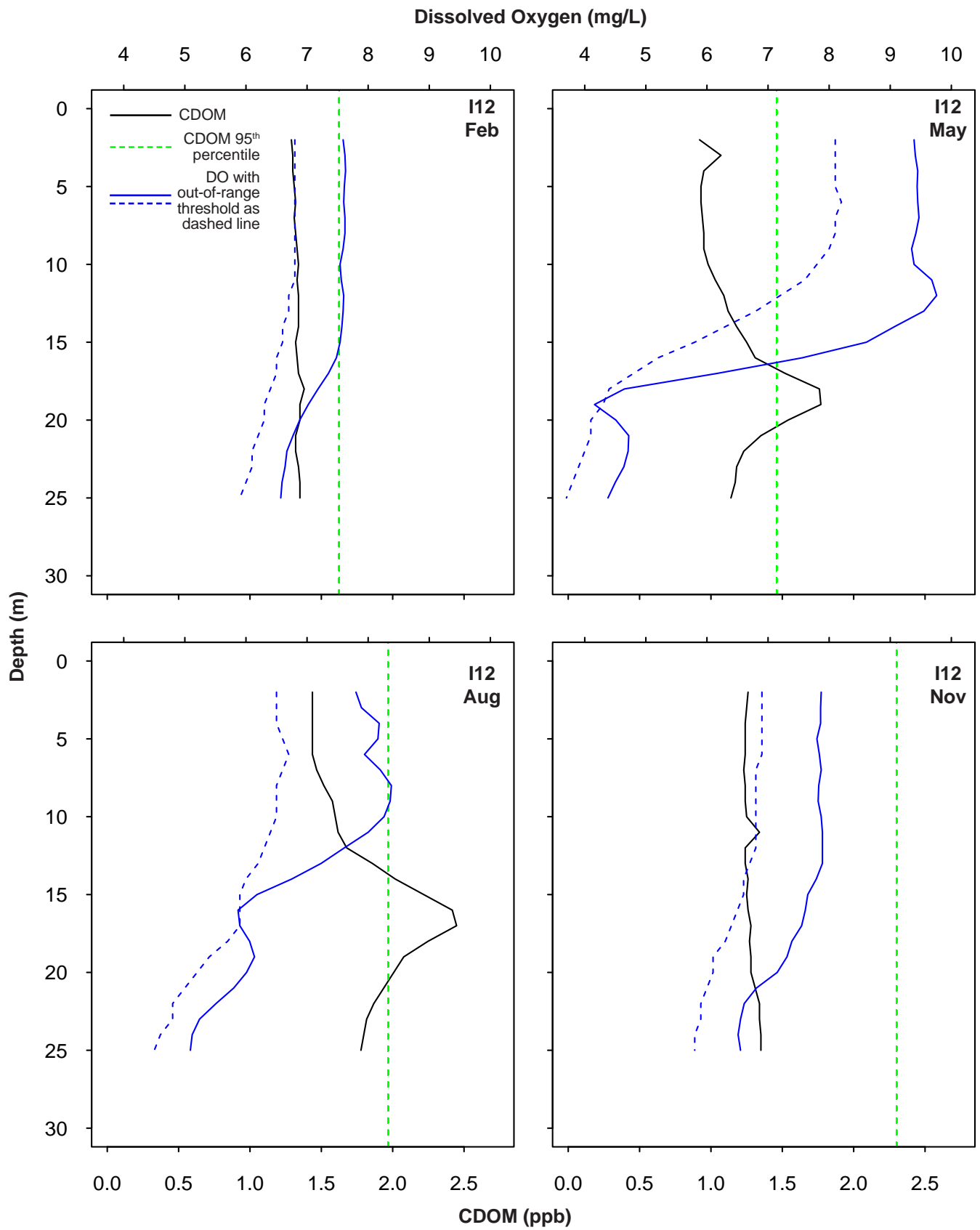
Appendix E.13

Representative vertical profiles of CDOM and buoyancy frequency from SBOO nearfield station I12 during 2022.



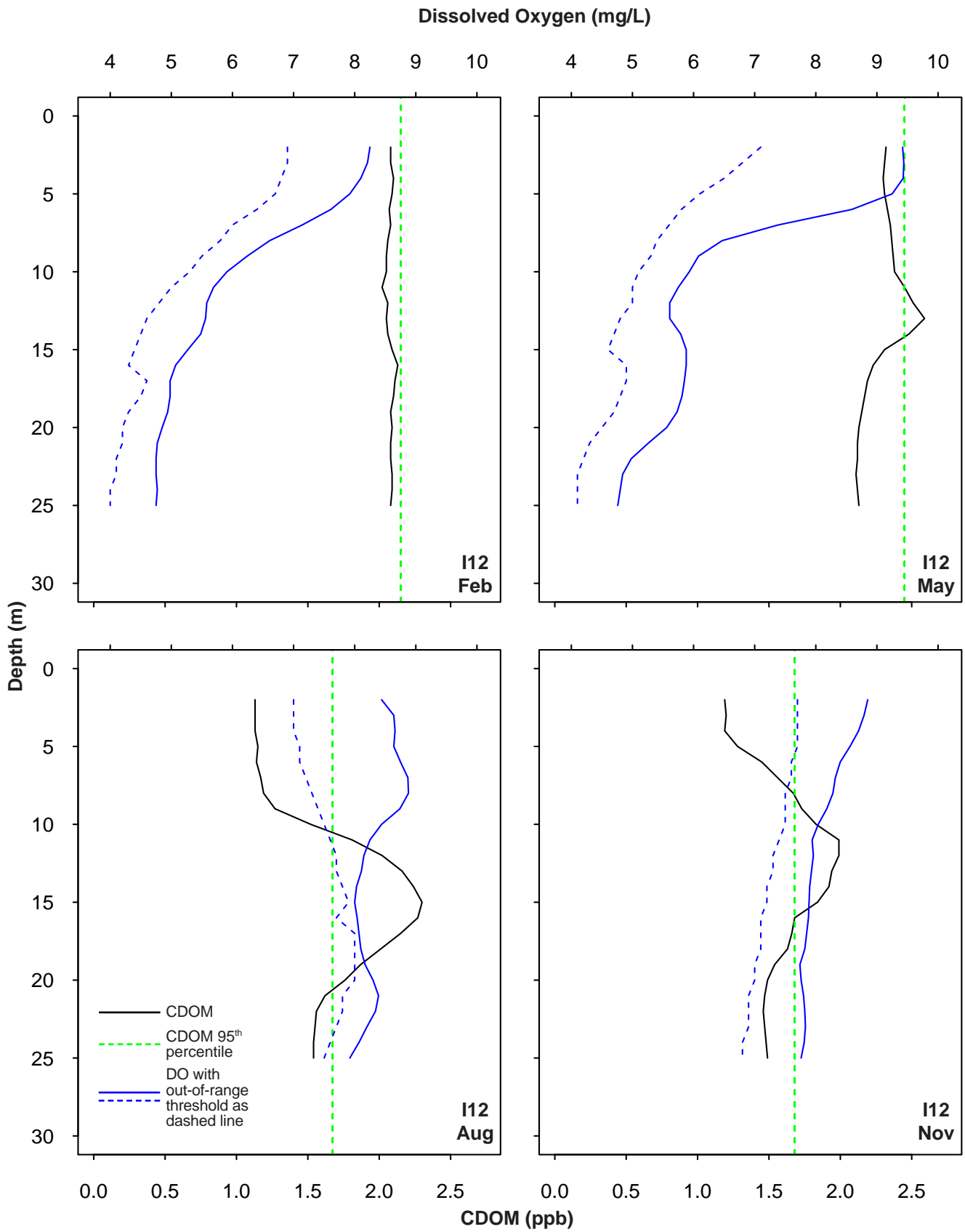
Appendix E.14

Representative vertical profiles of CDOM and buoyancy frequency from SBOO nearfield station I12 during 2023.



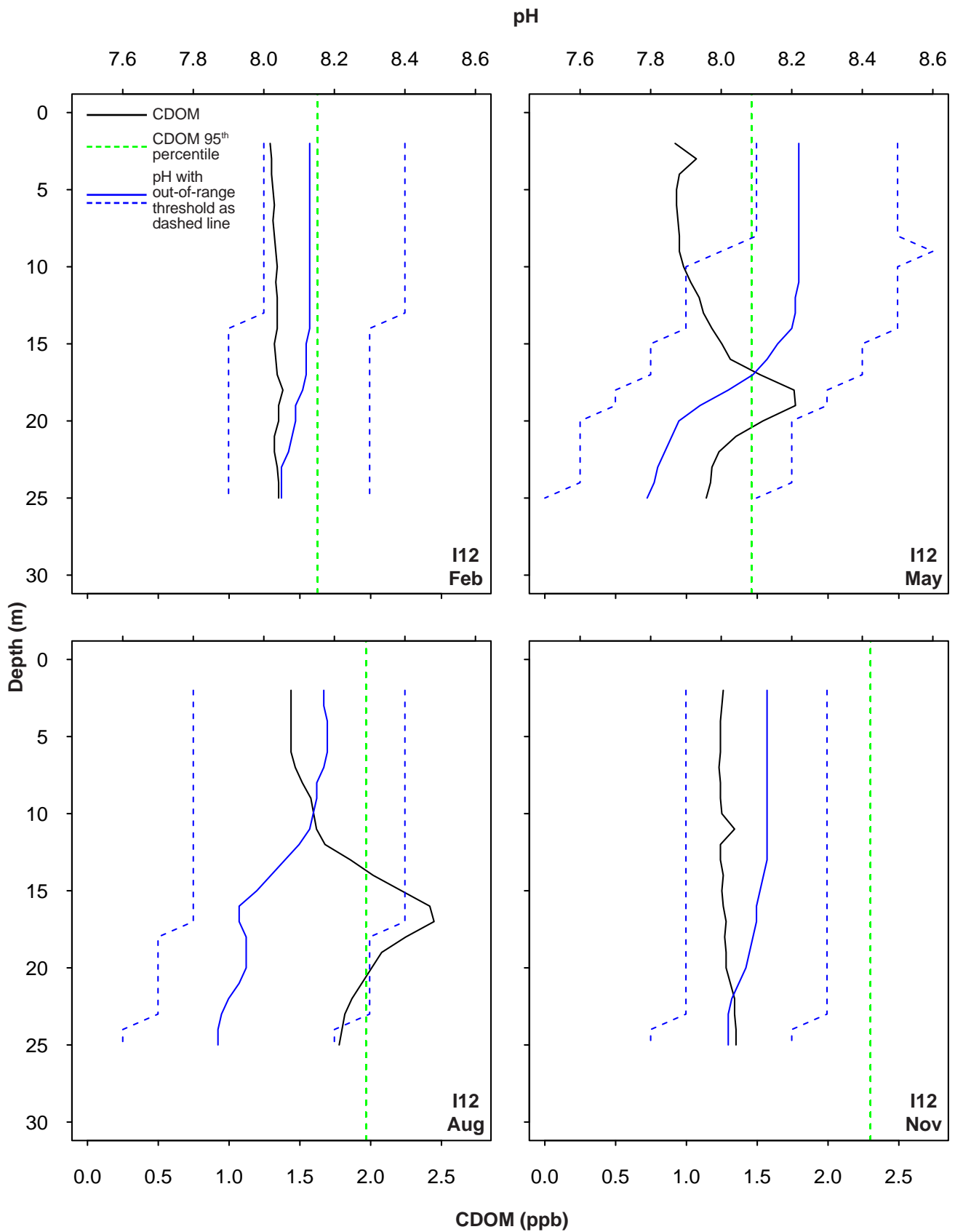
Appendix E.15

Representative vertical profiles of CDOM and DO from SBOO nearfield station I12 during 2022.



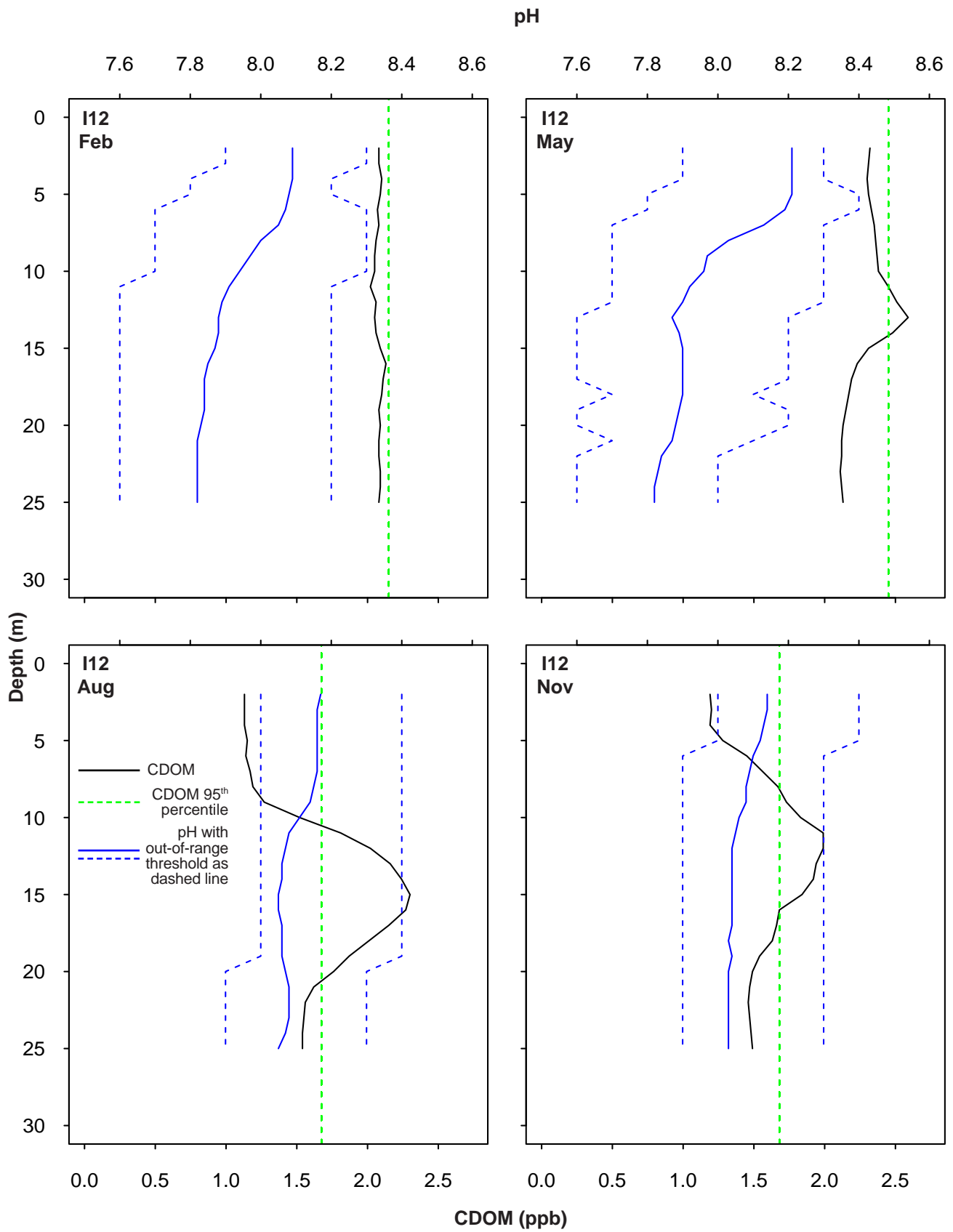
Appendix E.16

Representative vertical profiles of CDOM and DO from SBOO nearfield station I12 during 2023.



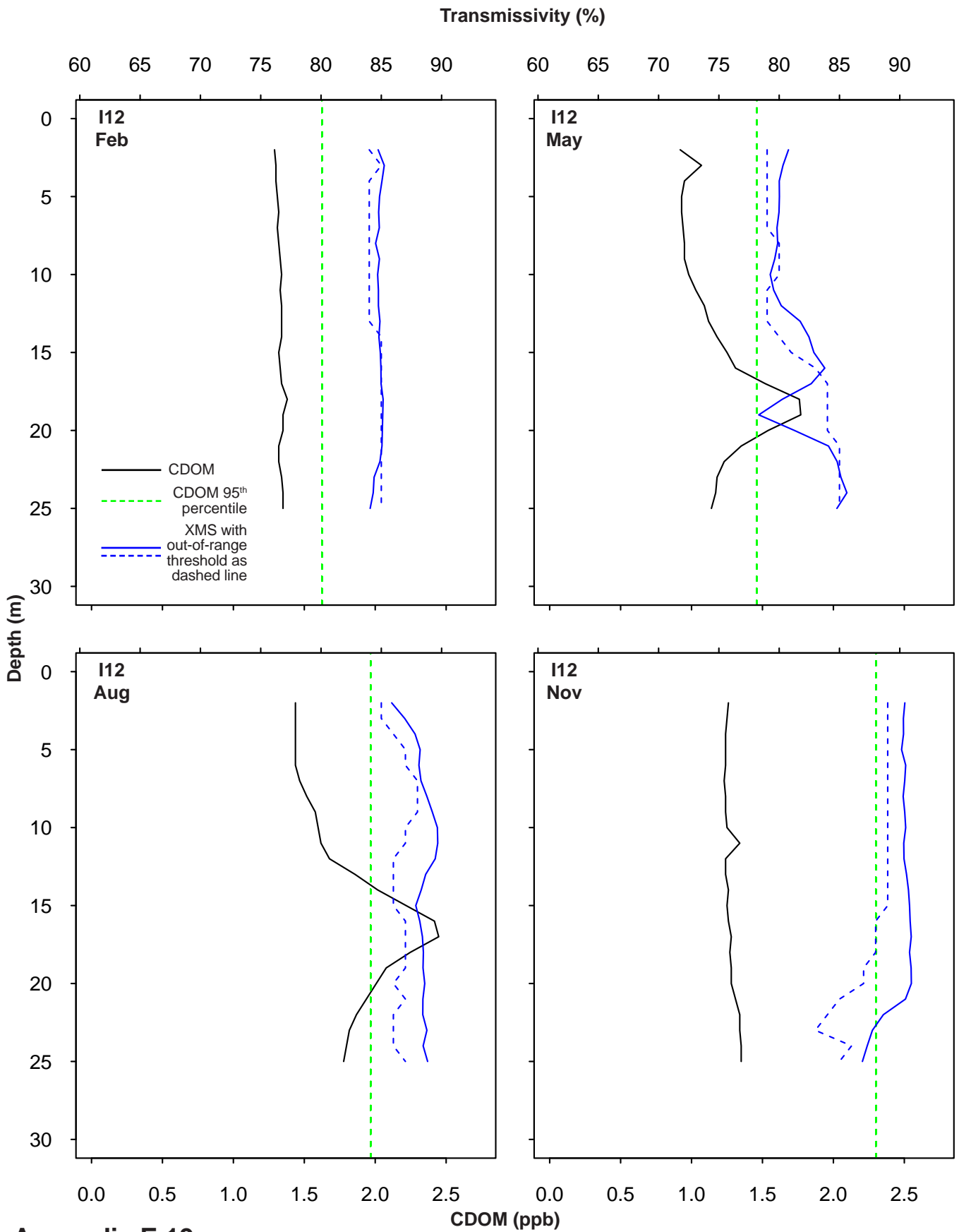
Appendix E.17

Representative vertical profiles of CDOM and pH from SBOO nearfield station I12 during 2022.



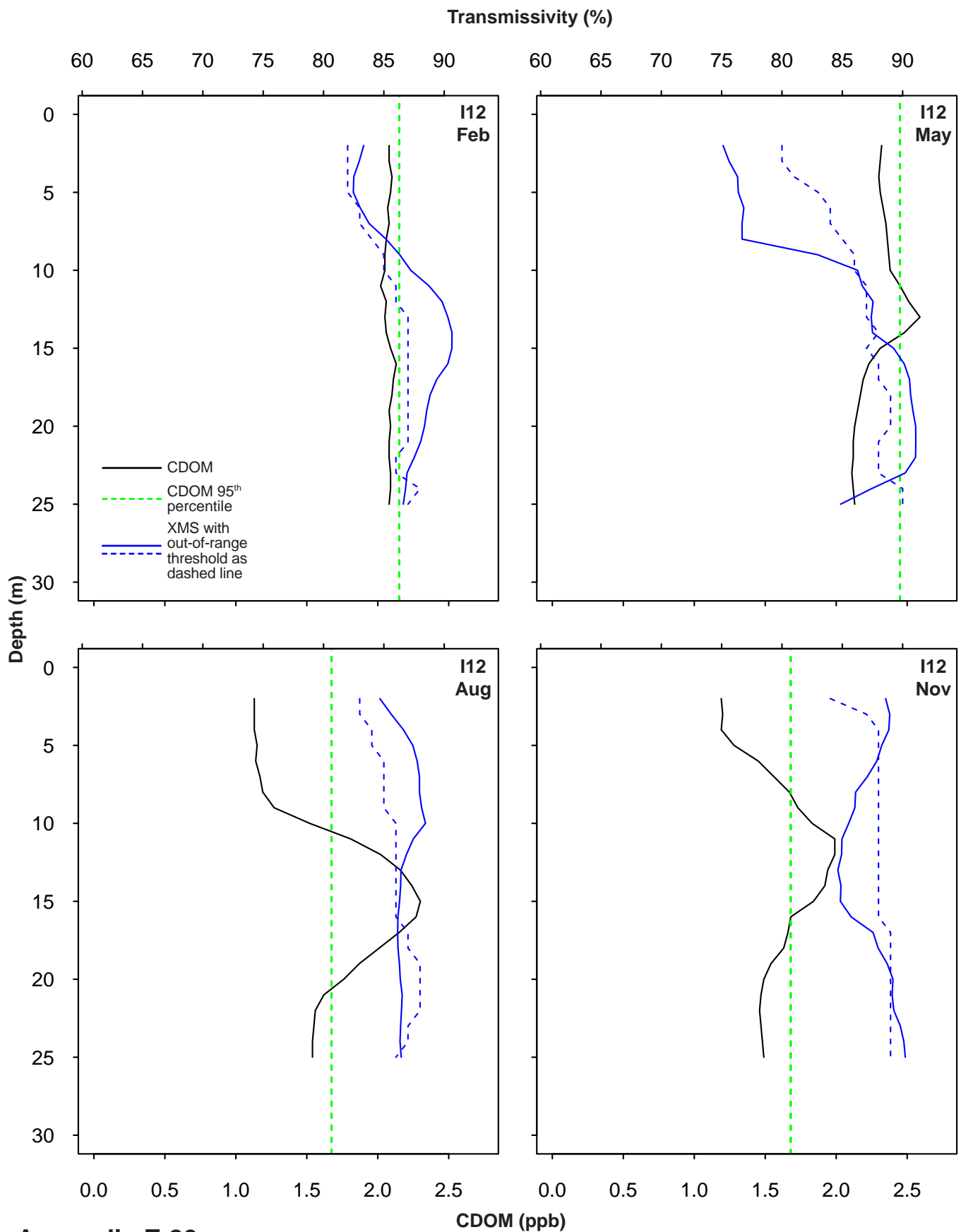
Appendix E.18

Representative vertical profiles of CDOM and pH from SBOO nearfield station I12 during 2023.



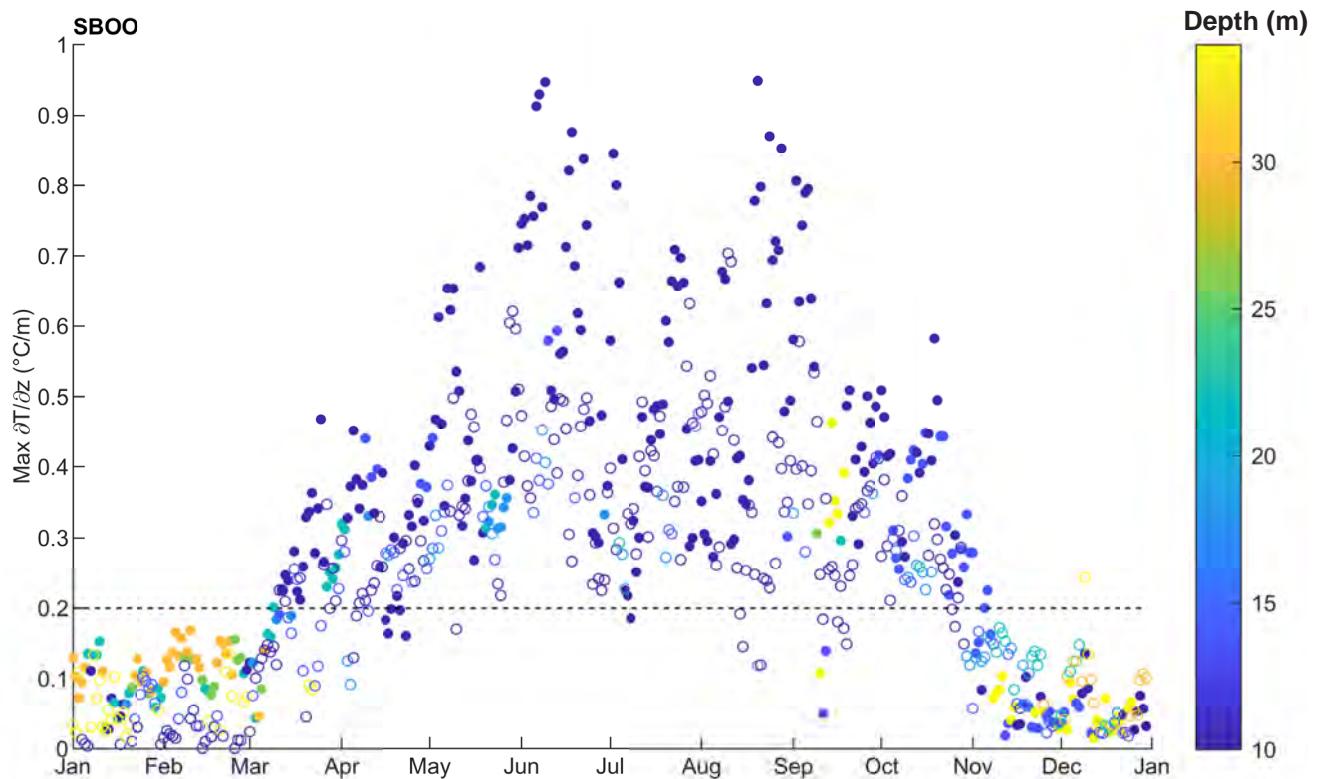
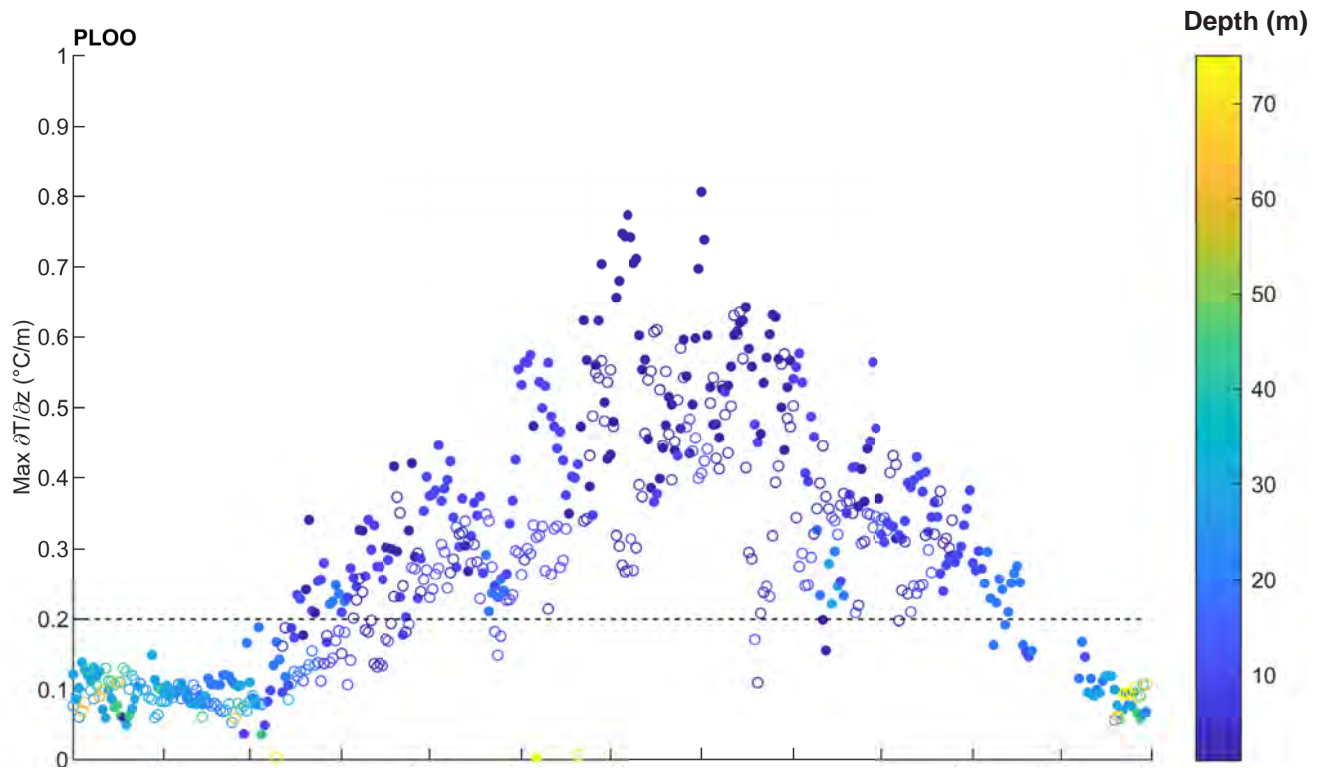
Appendix E.19

Representative vertical profiles of CDOM and transmissivity (XMS) from SBOO nearfield station I12 during 2022.



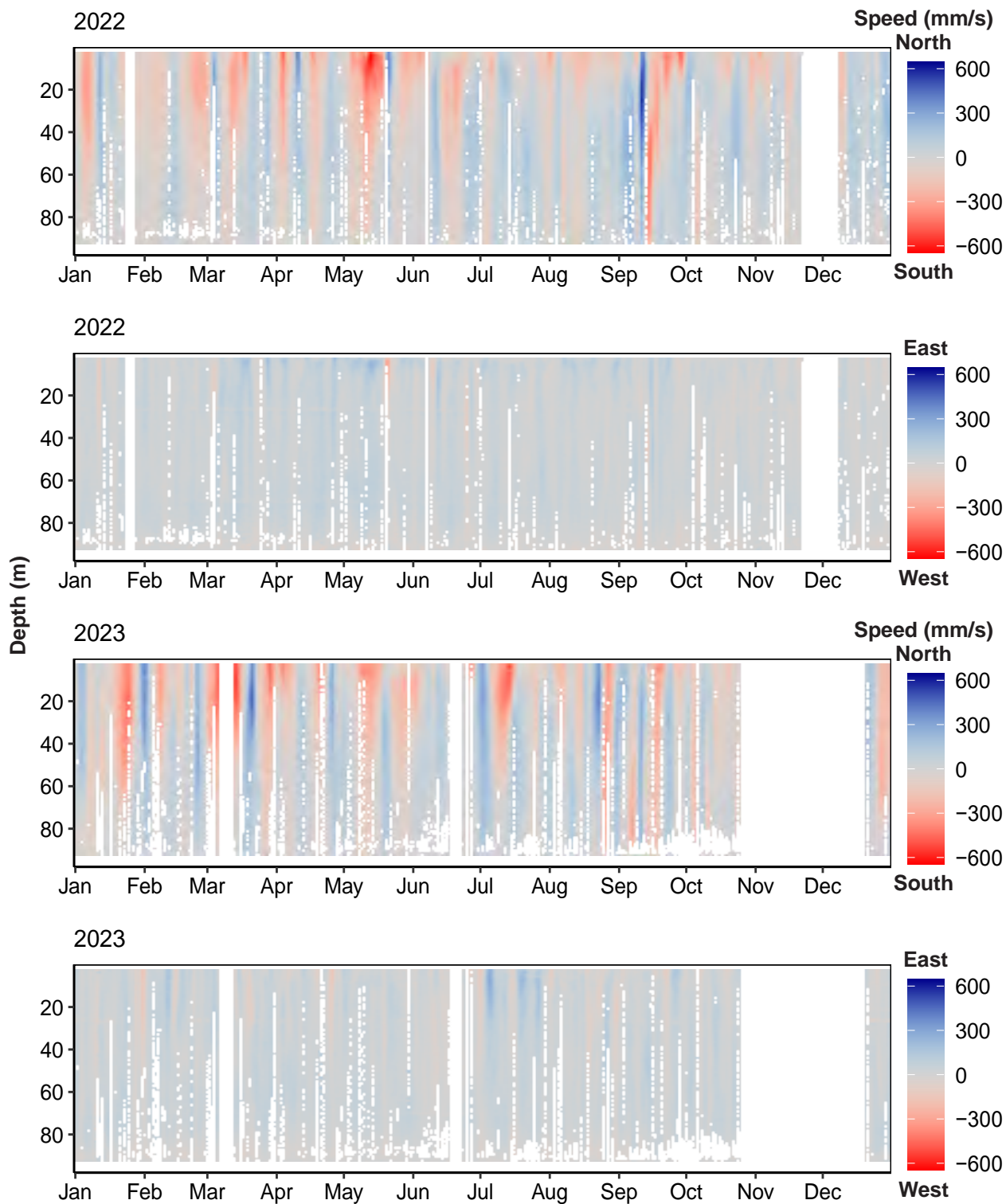
Appendix E.20

Representative vertical profiles of CDOM and transmissivity (XMS) from SBOO nearfield station I12 during 2023.



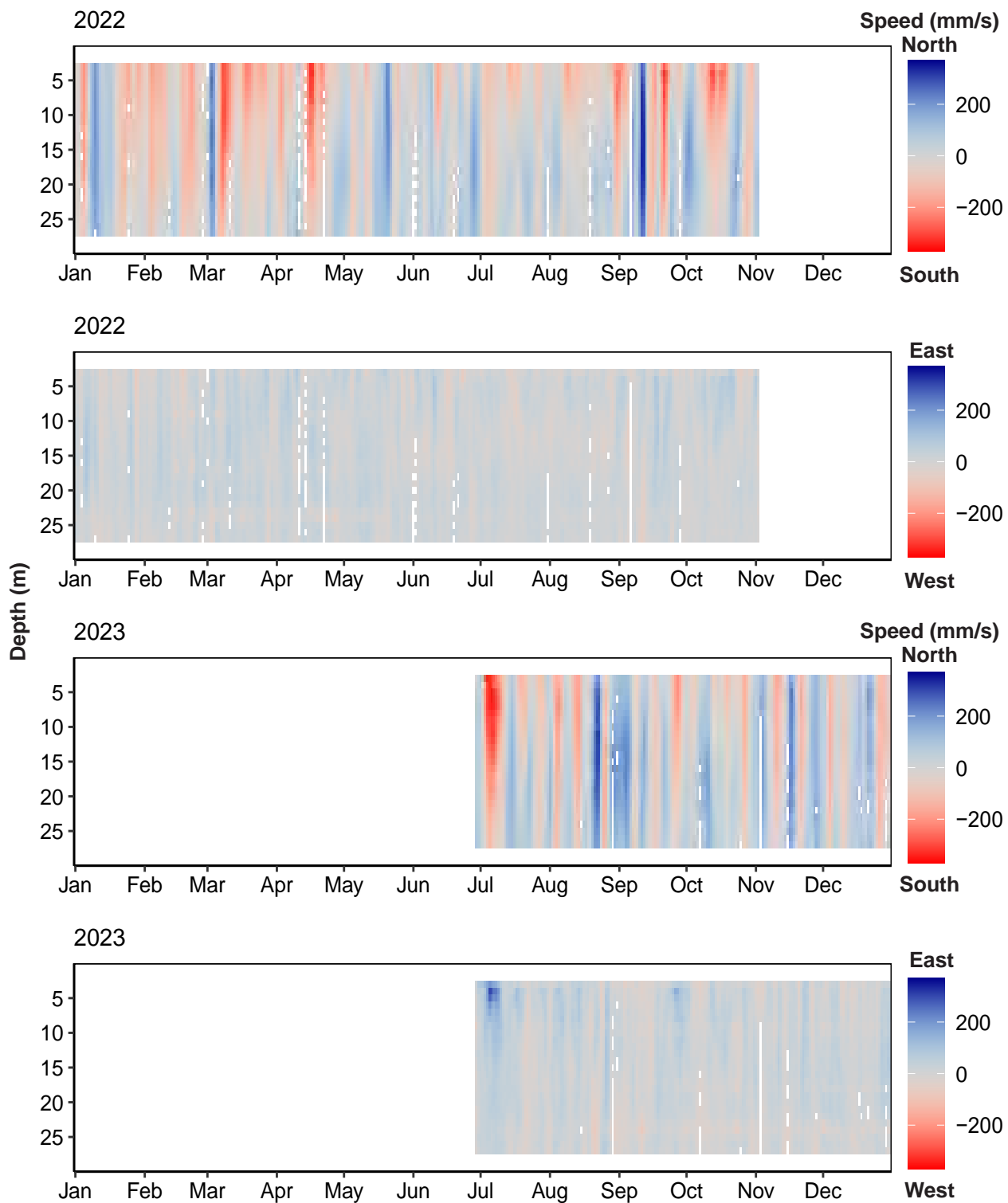
Appendix E.21

Maximum daily averaged thermal gradients ($\delta T/\delta z$) by depth of occurrence collected by RTOMS near PLOO (95 m) and thermistor arrays near SBOO (36 m) in 2022 (filled circles) and 2023 (open circles). Dashed line indicates moderate relative stratification ($0.2^{\circ}\text{C}/\text{m}$), with values below line showing more weakly stratified conditions. Thermistor arrays used instead of RTOMS near SBOO due to data availability (see text).



Appendix E.22

North-south and east-west daily averaged current speeds (tides removed) from the PLOO RTOMS in 2022 and 2023. White areas indicate loss of data due to instrumentation issues or failure to meet data quality criteria (see text).



Appendix E.23

North-south and east-west daily averaged current speeds (tides removed) from the SBOO RTOMS in 2022 and 2023. White areas indicate loss of data due to instrumentation issues or failure to meet data quality criteria (see text).

Appendix F
Sediment Quality
2022 – 2023
Raw Data Tables & Supplemental Analyses

Appendix F.1

Constituents and method detection limits (MDL) used for the analysis of sediments during 2022 and 2023. MDLs are summarized as minimum, and maximum values over the two years, abbreviations are in parentheses.

Parameter	MDL		Parameter	MDL	
	Min	Max		Min	Max
Organic Indicators					
BOD (ppm)	2	2	Sulfides (ppm)	2.2	2.2
TN (% wt.)	0.004	0.022	TVS (% wt.)	0.11	0.11
TOC (% wt.)	0.054	0.134			
Metals (ppm)					
Aluminum (Al)	0.282	1.84	Lead (Pb)	0.053	0.143
Antimony (Sb)	0.163	0.385	Manganese (Mn)	0.01	0.151
Arsenic (As)	0.151	0.237	Mercury (Hg)	0.001	0.004
Barium (Ba)	0.033	0.49	Nickel (Ni)	0.056	0.1
Beryllium (Be)	0.001	0.01	Selenium (Se)	0.213	0.44
Cadmium (Cd)	0.014	0.078	Silver (Ag)	0.023	0.133
Chromium (Cr)	0.029	0.106	Thallium (Tl)	0.122	0.261
Copper (Cu)	0.047	1.19	Tin (Sn)	0.054	0.088
Iron (Fe)	1.88	1.97	Zinc (Zn)	0.19	0.402
Chlorinated Pesticides (ppt)					
<i>Chlordanes</i>					
Alpha (cis) Chlordane [A(c)C]	46	93	Heptachlor epoxide (HeptEpox)	35	149
Cis Nonachlor (cNon)	44	88.9	Methoxychlor (Methoxy)	423	855
Gamma (trans) Chlordane [G(t)C]	30.1	115	Oxychlordane (Oxychlor)	66.2	134
Heptachlor (Hept)	79.3	160	Trans Nonachlor (tNon)	60.8	121
<i>Dichlorodiphenyltrichloroethane (DDT)</i>					
o,p-DDD	73.5	149	p,p-DDE	52.6	106
o,p-DDE	49	99.1	p,p-DDMU	35.5	71.7
o,p-DDT	29.2	59	p,p-DDT	57	115
p,p-DDD	32.3	65.3			
<i>Endrin</i>					
Endrin	92.3	187	Endrin aldehyde (EndAld)	314	635
<i>Endosulfan</i>					
Alpha-Endosulfan	59.2	120	Endosulfan sulfate	110	222
Beta-Endosulfan	580	1170			
<i>Hexachlorocyclohexane (HCH)</i>					
HCH, Alpha isomer	24.4	49.3	HCH, Delta isomer	42.1	94.7
HCH, Beta isomer	76	154	HCH, Gamma isomer	65.9	133
<i>Miscellaneous Pesticides</i>					
Aldrin	32	141	Hexachlorobenzene (HCB)	123	246
Dieldrin	57.1	205	Mirex	26.4	53.4

Appendix F.1 *continued*

Parameter	MDL		Parameter	MDL	
	Min	Max		Min	Max
Polychlorinated Biphenyl Congeners (PCBs) (ppt)					
PCB 8	42	88.1	PCB 126	53.7	109
PCB 18	52.2	106	PCB 128	41	82.9
PCB 28	23.6	47.8	PCB 138	46.6	94.3
PCB 37	59.7	121	PCB 149	64.3	130
PCB 44	43.8	88.5	PCB 151	36	72.8
PCB 49	59.8	121	PCB 153/168	160	323
PCB 52	63.3	128	PCB 156	59.3	120
PCB 66	49.9	101	PCB 157	65.5	132
PCB 70	54.1	109	PCB 158	65.5	132
PCB 74	50.4	102	PCB 167	40.9	82.7
PCB 77	25.8	52.1	PCB 169	39.7	80.3
PCB 81	28.4	57.5	PCB 170	33.3	67.4
PCB 87	52.1	105	PCB 177	21.7	43.3
PCB 99	41.3	83.6	PCB 180	36.1	73
PCB 101	38.2	77.3	PCB 183	24.5	49.5
PCB 105	81.5	165	PCB 187	30.5	61.6
PCB 110	32.6	65.9	PCB 189	60.7	123
PCB 114	47.8	96.7	PCB 194	46.3	93.7
PCB 118	49.9	101	PCB 195	19	2802
PCB 119	60.1	121	PCB 201	40.6	82.1
PCB 123	51.5	104	PCB 206	80.5	163
Polycyclic Aromatic Hydrocarbons (PAHs) (ppb)					
1-methylnaphthalene	4.94	12	Benzo[G,H,I]perylene	4.15	20.6
1-methylphenanthrene	4.44	12.2	Benzo[K]fluoranthene	5.8	14.3
2-methylnaphthalene	4.01	12.9	Biphenyl	3.4	11.1
2,3,5-trimethylnaphthalene	7.26	14.7	Chrysene	3.56	9.72
2,6-dimethylnaphthalene	3.64	12.5	Dibenzo(A,H)anthracene	3.24	20.1
3,4-benzo(B)fluoranthene	3.05	7.94	Fluoranthene	5.82	13.7
Acenaphthene	3.85	11.9	Fluorene	3.46	12.1
Acenaphthylene	4.44	14.9	Indeno(1,2,3-CD)pyrene	3.47	15.7
Anthracene	3.77	15	Naphthalene	3.75	15.7
Benzo[A]anthracene	1.63	12.6	Perylene	6.51	13.6
Benzo[A]pyrene	3.93	8.83	Phenanthrene	3.21	14
Benzo[e]pyrene	2.91	11.3	Pyrene	2.74	11.3

Appendix F.1 *continued*

Parameter	MDL		Parameter	MDL	
	Min	Max		Min	Max
Polybrominated Diphenyl Ethers (PBDEs) (ppt)					
BDE-17	65.1	132	BDE-100	39	78.9
BDE-28	52.2	106	BDE-138	31.8	64.4
BDE-47	25.8	91.2	BDE-153	39.4	79.7
BDE-49	37.8	76.5	BDE-154	37.6	109
BDE-66	42.8	86.6	BDE-183	67	136
BDE-85	15.2	84.7	BDE-190	33	66.8
BDE-99	45.7	92.5			

Appendix F.2

Concentrations of organic loading indicators detected in sediments from PLOO stations sampled during winter and summer 2022 and 2023. See Appendix F.1 for MDLs; ND=not detected; NR=not reportable. Only primary core stations sampled during summer 2023 due to resource exchange for Bight'23 (see text).

2022	Winter					Summer				
	BOD ^b (ppm)	Sulfides (ppm)	TN (% wt)	TOC (% wt)	TVS (% wt)	BOD (ppm)	Sulfides (ppm)	TN (% wt)	TOC (% wt)	TVS (% wt)
<i>88-m Depth Contour</i>										
B11	—	3.13	0.086	2.22	3.4	—	11.1	0.071	2.59	3.2
B8	—	ND	0.077	0.770	2.8	—	10.4	0.076	0.795	2.8
E19	—	ND	0.053	0.522	2.1	—	3.51	0.051	0.481	2.2
E7	—	ND	0.053	0.464	1.9	—	ND	0.043	0.450	2.1
E1	—	ND	0.058	0.547	1.8	—	27.9	0.052	0.514	2.1
<i>98-m Depth Contour</i>										
B12	NR	2.52	0.070	3.12	3.0	431	10.9	0.057	2.52	2.5
B9	NR	ND	0.062	0.786	2.8	442	17.6	0.065	0.771	3.1
E26	NR	5.98	0.051	0.519	2.0	324	11.3	0.052	0.475	2.1
E25	NR	ND	0.046	0.434	1.9	321	5.66	0.047	0.415	2.2
E23	NR	4.42	0.046	0.451	1.9	413	9.45	0.056	0.503	2.2
E20	NR	7.36	0.046	0.432	1.8	295	19.1	0.049	0.427	1.7
E17 ^a	NR	ND	0.065	0.566	1.6	347	50.6	0.042	0.374	1.8
E14 ^a	NR	70.1	0.042	0.385	3.2	660	30.7	0.050	0.538	1.6
E11 ^a	NR	ND	0.040	0.371	1.6	412	18.5	0.038	0.434	1.8
E8	NR	ND	0.048	0.468	1.9	304	22.4	0.048	0.472	1.9
E5	NR	ND	0.041	0.396	1.8	376	16.1	0.054	0.535	2.2
E2	NR	ND	0.055	0.645	2.4	297	7.69	0.057	0.666	2.3
<i>116-m Depth Contour</i>										
B10	—	14.1	0.047	0.994	2.2	—	5.68	0.045	0.702	2.2
E21	—	9.84	0.039	0.359	1.6	—	ND	0.039	0.339	1.7
E15 ^a	—	10.5	0.042	0.429	1.7	—	ND	0.035	0.357	1.6
E9	—	ND	0.052	1.20	2.2	—	26.8	0.030	0.866	2.0
E3	—	ND	0.048	0.503	1.4	—	16.2	0.042	0.477	1.4
Detection Rate (%)	NR	41	100	100	100	100	86	100	100	100

^aNear-ZID station

^bBOD only sampled at PLOO primary core stations

Appendix F.2 *continued*

2023	Winter					Summer				
	BOD ^b (ppm)	Sulfides (ppm)	TN (% wt)	TOC (% wt)	TVS (% wt)	BOD (ppm)	Sulfides (ppm)	TN (% wt)	TOC (% wt)	TVS (% wt)
<i>88-m Depth Contour</i>										
B11	—	ND	0.066	1.71	3.1	—	—	—	—	—
B8	—	2.64	0.070	0.724	2.5	—	—	—	—	—
E19	—	11.6	0.056	0.534	2.4	—	—	—	—	—
E7	—	6.22	0.054	0.558	2.2	—	—	—	—	—
E1	—	ND	0.054	0.534	1.8	—	—	—	—	—
<i>98-m Depth Contour</i>										
B12	215	ND	0.048	2.98	2.7	283	ND	0.050	2.81	NR
B9	245	2.74	0.052	0.723	2.5	290	ND	0.056	0.719	NR
E26	319	3.19	0.044	0.502	2.1	355	11.2	0.055	0.599	NR
E25	245	3.12	0.038	0.441	1.9	213	ND	0.029	0.436	NR
E23	436	ND	0.042	0.492	1.9	235	4.02	0.032	0.456	NR
E20	329	7.32	0.046	0.478	1.8	203	13.8	0.031	0.370	NR
E17 ^a	357	34.8	0.040	0.384	1.7	245	34.9	0.033	0.405	NR
E14 ^a	377	2.84	0.028	0.285	1.5	250	8.58	0.028	0.307	NR
E11 ^a	466	7.72	0.034	0.466		262	17.1	0.034	0.441	NR
E8	301	5.76	0.033	0.476	1.8	186	ND	0.040	0.469	NR
E5	293	2.99	0.037	0.470		202	14.9	0.040	0.535	NR
E2	346	3.27	0.054	0.710	2.5	204	3.34	0.041	0.649	NR
<i>116-m Depth Contour</i>										
B10	—	ND	0.037	1.04	2.3	—	—	—	—	—
E21	—	ND	0.047	0.466	1.9	—	—	—	—	—
E15 ^a	—	10.4	0.042	0.475	1.9	—	9.02	0.035	0.449	NR
E9	—	ND	0.063	1.32	2.2	—	—	—	—	—
E3	—	16.1	0.044	0.490	1.4	—	—	—	—	—
Detection Rate (%)	100	68	100	100	100	100	69	100	100	NR

^aNear-ZID station

^bBOD only sampled at PLOO primary core stations

Appendix F.3

Concentrations of organic indicators detected in sediments from SBOO stations sampled during winter and summer 2022 and 2023. See Appendix F.1 for MDLs; ND=not detected; NR=not reportable. Only primary core stations sampled during summer 2023 due to resource exchange for Bight'23 (see text).

2022	Winter				Summer			
	Sulfides (ppm)	TN (% wt)	TOC (% wt)	TVS (% wt)	Sulfides (ppm)	TN (% wt)	TOC (% wt)	TVS (% wt)
<i>19-m Stations</i>								
I35	39.5	0.033	0.235	1.3	NR	0.029	0.206	1.3
I34	ND	ND	ND	0.3	NR	ND	ND	0.4
I31	ND	ND	ND	0.6	NR	0.020	0.105	0.8
I23	ND	0.037	4.03	0.8	NR	0.030	1.82	0.9
I18	ND	ND	0.134	0.6	NR	0.022	0.125	0.9
I10	ND	ND	ND	0.7	ND	0.022	ND	0.9
I4	ND	ND	ND	0.2	ND	ND	0.219	0.4
<i>28-m Stations</i>								
I33	ND	ND	0.221	1.4	NR	0.031	0.290	1.4
I30	ND	0.030	0.210	0.9	NR	0.026	0.177	1.3
I27	7.85	ND	0.201	0.9	NR	0.023	0.143	1.1
I22	2.27	ND	0.198	0.8	NR	0.030	0.200	1.0
I14 ^a	7.15	ND	0.193	0.9	NR	0.029	0.183	1.1
I16 ^a	ND	ND	0.134	0.6	NR	ND	ND	0.6
I15	ND	ND	ND	0.2	NR	0.020	0.087	0.5
I12 ^a	ND	0.048	ND	0.6	NR	0.016	0.058	0.65
I9	8.78	ND	0.150	1.1	2.77	0.029	0.201	1.3
I6	ND	ND	ND	0.4	ND	ND	ND	0.4
I2	ND	ND	ND	0.2	ND	ND	ND	0.5
I3	ND	ND	ND	0.3	ND	0.025	ND	0.4
<i>38-m Stations</i>								
I29	ND	0.034	0.324	1.4	NR	ND	ND	1.8
I21	ND	ND	ND	0.5	NR	ND	ND	0.6
I13	ND	ND	ND	0.5	ND	ND	ND	0.4
I8	ND	ND	ND	0.3	4.77	ND	ND	0.5
<i>55-m Stations</i>								
I28	15.4	0.074	0.926	1.8	NR	0.071	0.792	1.5
I20	ND	ND	ND	0.5	NR	0.026	0.163	0.6
I7	ND	ND	ND	0.4	ND	0.024	0.137	0.2
I1	3.25	0.028	0.184	0.95	ND	0.029	0.187	1.1
Detection Rate (%)	26	26	48	100	20	67	63	100

^aNear-ZID station

Appendix F.3 *continued*

2023	Winter				Summer			
	Sulfides (ppm)	TN (% wt)	TOC (% wt)	TVS (% wt)	Sulfides (ppm)	TN (% wt)	TOC (% wt)	TVS (% wt)
<i>19-m Stations</i>								
I35	9.91	0.031	0.233	1.3	—	—	—	—
I34	ND	ND	ND	0.3	—	—	—	—
I31	ND	ND	0.071	0.5	—	—	—	—
I23	ND	ND	0.095	0.8	—	—	—	—
I18	ND	ND	0.094	0.8	—	—	—	—
I10	ND	ND	0.073	0.7	—	—	—	—
I4	ND	0.021	0.115	0.4	—	—	—	—
<i>28-m Stations</i>								
I33	16.0	0.024	0.335	1.5	8.50	0.033	0.345	NR
I30	ND	0.030	0.127	1.0	15.5	0.022	0.197	NR
I27	ND	0.028	0.122	0.8	14.7	0.021	0.193	NR
I22	ND	0.031	0.186	0.9	ND	0.020	0.172	NR
I14 ^a	ND	0.030	0.156	0.9	2.67	0.024	0.194	NR
I16 ^a	ND	ND	0.076	0.6	ND	0.017	0.101	NR
I15	ND	0.028	0.144	0.6	ND	0.024	0.178	NR
I12 ^a	ND	ND	ND	0.5	11.4	0.023	0.172	NR
I9	ND	0.022	0.133	1.2	ND	0.017	0.189	NR
I6	ND	0.019	0.095	0.4	ND	0.018	0.145	NR
I2	ND	ND	ND	0.4	ND	0.014	0.098	NR
I3	ND	ND	ND	0.4	ND	0.013	0.082	NR
<i>38-m Stations</i>								
I29	6.38	0.051	0.440	1.6	—	—	—	—
I21	ND	0.025	0.127	0.52	—	—	—	—
I13	ND	ND	0.087	0.4	—	—	—	—
I8	ND	0.021	0.092	0.4	—	—	—	—
<i>55-m Stations</i>								
I28	ND	0.066	0.830	1.5	—	—	—	—
I20	3.42	0.025	0.192	0.4	—	—	—	—
I7	ND	ND	ND	0.3	—	—	—	—
I1	ND	0.033	0.192	1.0	—	—	—	—
Detection Rate (%)	15	59	81	100	20	67	63	NR

^aNear-ZID station

Appendix F.4

Concentrations of trace metals (ppm) detected in sediments from PLOO stations sampled during winter and summer 2022 and 2023. See Appendix F.1 for MDLs and translation of periodic table symbols; DR = detection rate; DNQ = do not quantify; ND = not detected; NR = not reportable; NA = not analyzed. Only primary core stations sampled during summer 2023 due to resource exchange for Bight'23 (see text).

Winter 2022	Al	Sb	As	Ba	Be	Cd	Cr	Cu	Fe	Pb	Mn	Hg	Ni	Se	Ag	Ti	Sn	Zn
<i>88-m Depth Contour</i>																		
B11	7850	1.03 DNQ	3.69	33.5	0.156	ND	18.9	9.01	15600	3.69	119	0.025 DNQ	5.49	ND	ND	ND	0.831	37.0
B8	9830	1.36 DNQ	2.44	40.8	0.214	ND	19.1	7.61	13000	4.17	107	0.033	6.86	ND	ND	ND	1.03	31.3
E19	8350	1.43 DNQ	2.68	39.2	0.186	ND	16.8	7.00	11600	3.32	101	0.022 DNQ	6.65	ND	ND	ND	1.00	30.4
E7	7260	1.18 DNQ	2.86	31.5	0.168	ND	14.9	6.55	10100	3.53	87.3	0.026 DNQ	5.57	ND	ND	ND	0.751	24.0
E1	7430	1.15 DNQ	2.72	34.0	0.157	ND	14.3	7.31	9430	4.25	84.2	0.035	4.96	ND	ND	ND	0.895	25.7
<i>98-m Depth Contour</i>																		
B12	6190	0.981 DNQ	5.07	20.5	0.197	ND	23.4	7.17	20300	3.06	60.9	0.018 DNQ	3.60	ND	ND	ND	0.725	37.5
B9	8310	1.52	2.52	46.6	0.240	ND	20.7	6.58	14900	3.76	104	0.025 DNQ	6.20	ND	ND	ND	1.02	36.9
E26	7550	1.07 DNQ	2.87	32.8	0.168	ND	15.2	6.09	10400	3.15	91.9	0.022 DNQ	5.87	ND	ND	ND	0.779	27.7
E25	6580	1.13 DNQ	2.32	27.8	0.150	ND	13.7	6.24	9200	3.10	82.1	0.018 DNQ	4.84	ND	ND	ND	0.726	25.2
E23	7060	1.18 DNQ	2.64	30.7	0.157	ND	14.5	5.96	9800	3.31	85.0	0.028 DNQ	5.39	ND	ND	ND	0.745	26.7
E20	6350	1.16 DNQ	2.15	26.9	0.144	ND	13.4	5.43	8800	2.92	78.4	0.021 DNQ	4.88	ND	ND	ND	0.746	24.2
E17 ^a	5770	0.903 DNQ	2.44	21.9	0.143	ND	12.5	5.38	8480	2.57	69.2	0.015 DNQ	4.54	ND	ND	ND	0.581	20.1
E14 ^a	4700	0.732 DNQ	2.90	17.7	0.125	0.101 DNQ	11.8	6.88	7550	2.20	60.6	0.014 DNQ	4.24	ND	ND	ND	0.595	19.6
E11 ^a	5370	0.793 DNQ	2.25	19.2	0.134	ND	11.7	4.80	7790	2.29	66.3	0.014 DNQ	4.09	ND	ND	ND	0.564	18.8
E8	5980	0.995 DNQ	2.33	23.8	0.153	ND	13.0	5.32	8750	2.70	71.4	0.019 DNQ	4.46	ND	ND	ND	0.696	20.4
E5	6390	0.947 DNQ	2.60	26.6	0.153	ND	12.9	5.61	9240	2.85	76.6	0.019 DNQ	4.57	ND	ND	ND	0.671	21.2
E2	8690	1.53	2.60	39.4	0.203	ND	16.4	8.33	12500	3.74	98.8	0.032	5.56	ND	ND	ND	0.969	29.2
<i>116-m Depth Contour</i>																		
B10	6140	1.18 DNQ	2.82	22.6	0.171	ND	16.9	5.35	12000	2.79	70.0	0.017 DNQ	4.08	ND	ND	ND	0.612	28.8
E21	5730	0.93 DNQ	2.11	23.0	0.132	ND	12.5	4.83	8060	2.81	70.6	0.021 DNQ	4.49	ND	ND	ND	0.642	21.8
E15 ^a	5490	1.06 DNQ	2.22	19.3	0.144	ND	12.8	5.00	8260	2.62	65.2	0.016 DNQ	4.22	ND	ND	ND	0.461	19.1
E9	5800	1.15 DNQ	2.82	21.8	0.164	ND	15.6	9.12	10600	3.11	64.5	0.023 DNQ	4.25	ND	ND	ND	0.528	27.7
E3	6180	1.12 DNQ	1.81	35.0	0.117	ND	11.0	7.13	9120	4.14	72.5	0.035	2.85	ND	ND	ND	0.804	25.1
DR (%)	100	100	100	100	100	5	100	100	100	100	100	100	100	0	0	0	100	100

^a Near-ZID station

Appendix F.4 continued

Summer 2022	AI	Sb	As	Ba	Be	Cd	Cr	Cu	Fe	Pb	Mn	Hg	Ni	Se	Ag	Ti	Sn	Zn	
<i>88-m Depth Contour</i>																			
B11	8700	1.73	3.65	32.6	0.245	ND	21.1	15.0	17600	3.65	116	0.023	5.85	ND	ND	ND	0.744	36.5	
B8	10900	1.24 DNQ	3.10	46.4	0.239	ND	20.7	8.52	14200	4.45	114	0.036	8.20	ND	ND	ND	0.998	35.7	
E19	9090	0.998 DNQ	3.44	40.2	0.193	ND	17.2	7.62	11800	3.75	96.9	0.028	6.76	ND	ND	ND	0.929	30.6	
E7	8290	0.931 DNQ	2.84	36.1	0.176	ND	15.8	7.54	10900	3.65	88.6	0.028	6.26	ND	ND	ND	0.950	28.1	
E1	8370	0.822 DNQ	2.72	39.4	0.177	ND	15.4	8.86	11100	4.83	87.8	0.048	5.85	ND	ND	ND	1.23	29.4	
<i>98-m Depth Contour</i>																			
B12	6080	0.889 DNQ	5.32	21.0	0.268	ND	24.8	6.77	19400	2.72	60.6	0.016	4.42	ND	ND	ND	0.429	35.3	
B9	9740	2.13	3.93	42.6	0.362	ND	27.1	6.57	22500	4.08	105	0.026	5.97	ND	ND	ND	0.688	38.0	
E26	7310	0.504 DNQ	1.99	33.0	0.168	ND	14.8	6.51	9990	3.09	84.6	0.022	5.90	ND	ND	ND	0.628	26.1	
E25	6950	0.568 DNQ	2.65	26.8	0.141	ND	12.7	5.23	9070	2.59	75.9	0.020	4.95	ND	ND	ND	0.483	23.0	
E23	7210	0.566 DNQ	2.92	31.6	0.165	ND	14.7	6.75	10100	3.13	81.5	0.026	5.75	ND	ND	ND	0.685	26.0	
E20	6200	0.433 DNQ	1.90	27.2	0.143	ND	13.3	6.13	8730	2.81	72.4	0.022	4.99	ND	ND	ND	0.593	23.7	
E17 ^a	5790	0.566 DNQ	2.12	25.5	0.136	ND	12.5	5.74	8090	2.38	68.0	0.017	4.71	ND	ND	ND	0.580	22.4	
E14 ^a	4760	0.408 DNQ	1.88	17.5	0.104	0.087 DNQ	9.67	4.68	6470	1.89	56.0	0.013 DNQ	3.57	ND	ND	ND	0.421	17.6	
E11 ^a	4970	0.540 DNQ	2.24	19.4	0.126	ND	11.3	5.16	7690	2.18	57.9	0.015 DNQ	3.90	ND	ND	ND	0.435	19.2	
E8	6590	0.522 DNQ	2.75	25.3	0.141	ND	12.3	5.40	8910	2.93	70.8	0.022	4.52	ND	ND	ND	0.591	22.5	
E5	7420	0.695 DNQ	2.72	28.9	0.151	ND	13.4	6.50	9780	3.12	76.8	0.022	5.11	ND	ND	ND	0.676	24.5	
E2	8710	0.714 DNQ	2.28	44.5	0.190	ND	16.0	9.44	12400	3.49	91.9	0.034	5.75	ND	ND	ND	0.875	31.4	
<i>116-m Depth Contour</i>																			
B10	6460	1.34 DNQ	1.98	23.0	0.172	ND	15.8	13.1	10700	2.50	73.4	0.017	4.42	ND	ND	ND	0.536	25.3	
E21	5750	0.713 DNQ	2.22	23.0	0.136	ND	12.2	5.04	8070	2.71	63.8	0.017	4.63	ND	ND	ND	0.588	21.1	
E15 ^a	5510	0.653 DNQ	2.45	20.8	0.133	ND	11.9	4.58	7930	2.34	62.2	0.016	4.24	ND	ND	ND	0.485	19.8	
E9	6210	0.912 DNQ	3.26	21.2	0.166	ND	15.6	8.30	11200	2.49	61.0	0.018	4.68	ND	ND	ND	0.598	25.8	
E3	6440	0.696 DNQ	2.45	45.4	0.129	ND	11.5	12.3	9720	5.44	78.5	0.029	3.45	ND	ND	ND	0.640	36.9	
DR (%)	100	100	100	100	100	5	100	100	100	100	100	100	100	0	0	0	100	100	

^aNear-ZID station

Appendix F.4 continued

Winter 2023	AI	Sb	As	Ba	Be	Cd	Cr	Cu	Fe	Pb	Mn	Hg	Ni	Se	Ag	Ti	Sn	Zn
<i>88-m Depth Contour</i>																		
B11	7560	0.444 DNQ	3.37	31.7	0.224	ND	18.9	8.90	16300	3.67	149	0.024	5.46	0.444 DNQ	ND	ND	0.517	31.9
B8	9330	ND	2.44	44.8	0.208	ND	18.0	8.27	13100	3.65	110	0.024	7.34	ND	ND	ND	0.522	29.4
E19	8440	ND	2.80	38.4	0.179	0.086 DNQ	16.7	8.45	12000	4.05	98.0	0.027	6.57	ND	ND	ND	0.569	28.0
E7	7470	ND	2.52	33.9	0.160	ND	14.8	7.84	10500	3.69	87.3	0.041	5.95	ND	ND	ND	0.603	24.4
E1	6300	ND	2.22	30.0	0.142	ND	13.1	7.54	9470	4.20	75.2	0.033	4.85	ND	ND	ND	0.440	23.4
<i>98-m Depth Contour</i>																		
B12	5760	0.736 DNQ	4.51	20.3	0.230	ND	21.9	7.68	18400	2.65	54.4	0.016	3.76	ND	ND	ND	0.531	32.4
B9	7510	ND	3.11	34.0	0.222	ND	19.0	6.89	13900	3.64	87.9	0.023	5.78	ND	ND	ND	0.616	30.9
E26	7240	ND	2.09	31.9	0.163	ND	14.4	6.59	10000	3.11	85.4	0.019	5.73	ND	ND	ND	0.318	23.5
E25	6170	ND	2.40	26.0	0.144	ND	12.8	5.54	8980	2.78	74.0	0.019	4.72	ND	ND	ND	0.306	20.8
E23	6960	ND	2.16	33.1	0.152	ND	13.8	6.51	9700	2.37	81.1	0.015	5.57	ND	ND	ND	0.279	22.8
E20	6060	ND	1.85	26.6	0.139	0.080 DNQ	12.7	5.84	8590	2.77	72.2	0.016	4.76	ND	ND	ND	0.303	20.6
E17 ^a	6010	ND	2.47	25.5	0.138	0.120 DNQ	12.6	6.46	8490	2.58	69.6	0.022	4.96	ND	ND	ND	0.500	22.0
E14 ^a	4220	ND	2.02	16.2	0.105	0.110 DNQ	9.91	5.26	6410	1.94	52.3	0.010 DNQ	3.62	ND	ND	ND	0.398	17.0
E11 ^a	5490	ND	2.99	21.6	0.133	0.088 DNQ	11.8	5.97	8360	2.38	63.2	0.018	4.19	ND	ND	ND	0.505	20.2
E8	6420	ND	1.90	27.7	0.149	ND	13.0	6.35	9180	2.71	74.2	0.018	4.73	ND	ND	ND	0.295	21.5
E5	6380	ND	2.20	30.2	0.146	ND	12.9	6.34	9330	2.85	73.4	0.019	4.67	ND	ND	ND	0.308	20.9
E2	8470	ND	2.61	45.6	0.186	ND	16.4	10.2	12500	4.01	98.4	0.039	5.80	ND	ND	ND	0.446	29.7
<i>116-m Depth Contour</i>																		
B10	5640	ND	1.99	21.7	0.171	ND	15.6	5.57	11500	2.63	67.2	0.013 DNQ	3.82	ND	ND	ND	0.273	23.4
E21	5790	ND	2.06	22.3	0.133	0.091 DNQ	12.7	6.17	8750	3.07	67.2	0.017	5.43	ND	ND	ND	0.445	20.0
E15 ^a	4930	ND	1.95	17.1	0.123	ND	11.8	5.33	7910	2.65	56.3	0.015	3.99	ND	ND	ND	0.294	18.2
E9	5410	ND	3.27	19.1	0.140	ND	14.8	8.77	10600	2.73	56.5	0.015	4.16	ND	ND	ND	0.283	22.9
E3	5280	ND	2.11	33.6	0.102	ND	9.44	18.8	8950	4.29	80.0	0.031	3.03	ND	ND	ND	0.288	26.4
DR (%)	100	9	100	100	100	27	100	100	100	100	100	100	100	5	0	0	100	100

^aNear-ZID station

Appendix F.4 continued

Summer 2023	Al	Sb	As	Ba	Be	Cd	Cr	Cu	Fe	Pb	Mn	Hg	Ni	Se	Ag	Ti	Sn	Zn
<i>88-m Depth Contour</i>																		
B11	—	—	—	—	—	—	—	—	—	—	—	—	—	—	—	—	—	—
B8	—	—	—	—	—	—	—	—	—	—	—	—	—	—	—	—	—	—
E19	—	—	—	—	—	—	—	—	—	—	—	—	—	—	—	—	—	—
E7	—	—	—	—	—	—	—	—	—	—	—	—	—	—	—	—	—	—
E1	—	—	—	—	—	—	—	—	—	—	—	—	—	—	—	—	—	—
<i>98-m Depth Contour</i>																		
B12	5970	1.14	5.84	16.3	0.281	0.064 DNQ	23.9	4.24	18400	2.90	53.6	0.009 DNQ	5.19	0.519 DNQ	ND	NA	0.483	30.9
B9	8380	1.05	4.30	39.5	0.331	0.041 DNQ	24.9	6.24	19500	4.02	93.5	0.022	7.29	0.542 DNQ	ND	NA	0.777	36.4
E26	7750	0.462 DNQ	3.14	32.3	0.170	0.088 DNQ	15.7	6.88	10400	3.18	85.3	0.024	7.09	0.519 DNQ	ND	NA	0.791	25.3
E25	6000	0.392 DNQ	2.76	24.3	0.138	0.068 DNQ	12.6	5.04	8490	2.69	68.5	0.020	5.36	0.335 DNQ	ND	NA	0.578	19.9
E23	7090	0.508 DNQ	2.70	29.0	0.154	0.094	14.4	6.18	9540	2.96	79.2	0.023	6.28	0.327 DNQ	ND	NA	0.727	23.1
E20	5950	0.378 DNQ	2.40	23.6	0.133	0.09 DNQ	12.6	5.42	8170	2.75	67.2	0.022	5.31	0.382 DNQ	ND	NA	0.631	19.6
E17 ^a	5640	0.487 DNQ	2.50	21.6	0.129	0.104	12.2	5.52	7950	2.39	64.5	0.019	5.10	0.392 DNQ	ND	NA	0.631	19.6
E14 ^a	4420	0.438 DNQ	2.05	15.8	0.109	0.122	10.5	4.98	6430	2.02	52.9	0.014	4.34	0.310 DNQ	ND	NA	0.560	16.9
E11 ^a	5630	0.405 DNQ	2.32	20.4	0.134	0.097	12.0	5.21	7850	2.30	62.0	0.015	4.88	0.332 DNQ	ND	NA	0.591	19.4
E8	5950	0.516 DNQ	2.54	23.5	0.140	0.064 DNQ	12.5	5.34	8450	2.45	67.5	0.020	5.15	0.441 DNQ	ND	NA	0.622	20.9
E5	6140	0.574 DNQ	2.60	25.0	0.145	0.079 DNQ	12.7	5.70	8710	2.60	66.8	0.022	5.24	0.370 DNQ	ND	NA	0.638	20.8
E2	8100	0.655 DNQ	3.04	38.2	0.168	0.064 DNQ	15.4	9.39	11700	4.13	86.9	0.045	6.27	0.374 DNQ	ND	NA	0.906	27.5
<i>116-m Depth Contour</i>																		
B10	—	—	—	—	—	—	—	—	—	—	—	—	—	—	—	—	—	—
E21	—	—	—	—	—	—	—	—	—	—	—	—	—	—	—	—	—	—
E15 ^a	5300	0.498 DNQ	2.33	19.7	0.132	0.080 DNQ	12.2	4.89	7700	2.46	57.9	0.057	4.72	0.315 DNQ	ND	NA	0.534	18.5
E9	—	—	—	—	—	—	—	—	—	—	—	—	—	—	—	—	—	—
E3	—	—	—	—	—	—	—	—	—	—	—	—	—	—	—	—	—	—
DR (%)	100	100	100	100	100	100	100	100	100	100	100	100	100	100	0	NA	100	100

^a Near-ZID station

Appendix F.5

Concentrations of trace metals (ppm) detected in sediments from SBOO stations sampled during winter and summer 2022 and 2023. See Appendix F.1 for MDLs and translation of periodic table symbols; DR = detection rate; ND = not detected; NR = not reportable; NA = not analyzed. Only primary core stations sampled during summer 2023 due to resource exchange for Bight'23 (see text).

Winter 2022	Al	Sb	As	Ba	Be	Cd	Cr	Cu	Fe	Pb	Mn	Hg	Ni	Se	Ag	Ti	Sn	Zn
<i>19-m Stations</i>																		
I35	7220	1.23 DNQ	1.77	34.5	0.131	ND	12.7	4.42	8670	2.57	91.0	0.017 DNQ	3.33	ND	ND	ND	0.638	24.0
I34	1770	ND	1.47	7.99	0.031	ND	3.67	ND	2980	1.26	29.8	0.004 DNQ	0.476	ND	ND	ND	0.259	6.07
I31	3210	0.462 DNQ	1.25	14.1	0.058	ND	7.14	1.22 DNQ	3740	1.13	51.4	0.002 DNQ	1.11	ND	ND	ND	0.227	8.00
I23	1230	ND	2.58	6.43	ND	ND	3.80	3.66 DNQ	2300	1.17	19.0	0.002 DNQ	0.497	ND	ND	ND	0.309	5.27
I18	4450	1.02 DNQ	1.28	33.6	0.082	ND	11.1	2.00 DNQ	6330	1.23	74.0	0.002 DNQ	1.63	ND	ND	ND	ND	11.7
I10	4800	0.906 DNQ	1.31	28.4	0.084	ND	9.67	2.12 DNQ	5840	1.19	67.4	0.002 DNQ	1.77	ND	ND	ND	ND	12.5
I4	628	ND	1.37	1.37 DNQ	0.023 DNQ	ND	3.42	ND	1270	0.879	11.2	ND	0.322 DNQ	ND	ND	ND	0.143 DNQ	2.59
<i>28-m Stations</i>																		
I33	4220	0.688 DNQ	2.14	19.4	0.077	ND	8.22	3.01 DNQ	5430	2.52	71.5	0.013 DNQ	1.86	ND	ND	ND	0.545	15.1
I30	5820	0.874 DNQ	2.20	25.8	0.102	ND	10.5	2.95 DNQ	5710	1.63	61.2	0.005 DNQ	2.64	ND	ND	ND	0.348	16.3
I27	5830	0.665 DNQ	1.01	27.7	0.100	ND	10.3	2.62 DNQ	5980	1.47	63.3	0.004 DNQ	2.42	ND	ND	ND	0.435	15.3
I22	4520	0.628 DNQ	0.864	18.9	0.082	ND	9.04	2.10 DNQ	4790	1.27	54.2	0.004 DNQ	2.07	ND	ND	ND	0.361	11.5
I14 ^a	5720	0.864 DNQ	1.20	32.1	0.104	ND	10.4	2.86 DNQ	5870	1.37	69.7	0.004 DNQ	2.69	ND	ND	ND	0.464	16.9
I16 ^a	3720	0.748 DNQ	1.45	18.6	0.076	ND	7.74	2.05 DNQ	4560	1.08	52.2	0.003 DNQ	1.46	ND	ND	ND	0.290	12.2
I15	1570	0.500 DNQ	1.74	4.26	0.053	ND	7.44	ND	3610	1.36	20.3	ND	0.447	ND	ND	ND	ND	6.01
I12 ^a	2530	0.579 DNQ	1.64	11.3	0.062	ND	6.67	ND	3690	1.02	33.8	0.003 DNQ	0.83	ND	ND	ND	0.197 DNQ	9.73
I9	7290	0.995 DNQ	1.26	41.3	0.125	ND	12.5	3.75 DNQ	8050	1.32	83.5	0.006 DNQ	3.66	ND	ND	ND	ND	20.7
I6	810	0.473 DNQ	4.34	1.53 DNQ	0.036	ND	7.72	ND	3470	1.42	7.52	ND	0.149 DNQ	ND	ND	ND	ND	3.06
I2	989	ND	0.592	2.04	0.022 DNQ	ND	5.16	ND	1190	0.769	7.64	0.002 DNQ	0.517	ND	ND	ND	ND	2.19
I3	893	0.440 DNQ	1.03	1.54 DNQ	0.026 DNQ	ND	6.02	ND	1220	1.02	8.15	ND	0.503	ND	ND	ND	ND	2.37
<i>38-m Stations</i>																		
I29	5560	0.654 DNQ	2.40	24.3	0.111	ND	11.1	3.43 DNQ	7110	2.11	60.9	0.012 DNQ	3.03	ND	ND	ND	0.472	15.7
I21	1070	0.651 DNQ	8.22	2.01	0.066	ND	11.5	ND	7640	2.87	13.0	0.002 DNQ	ND	ND	ND	ND	0.179 DNQ	6.04
I13	989	0.603 DNQ	7.19	2.12	0.052	ND	9.21	ND	5770	2.13	13.4	ND	ND	ND	ND	ND	ND	4.74
I8	1370	0.569 DNQ	2.12	3.32	0.049	ND	6.71	ND	3270	1.02	14.9	0.002 DNQ	0.412	ND	ND	ND	ND	5.90
<i>55-m Stations</i>																		
I28	4600	1.01 DNQ	2.04	18.6	0.100	ND	8.63	3.69 DNQ	6130	2.31	47.6	0.022 DNQ	3.69	ND	ND	ND	0.524	14.3
I20	1260	0.496 DNQ	2.73	3.35	0.058	ND	5.05	ND	4910	1.53	17.1	0.002 DNQ	0.257 DNQ	ND	ND	ND	ND	5.72
I7	1160	0.747 DNQ	6.59	2.41	0.053	ND	8.54	ND	6610	2.22	17.5	ND	ND	ND	ND	ND	ND	5.37
I1	2710	0.587 DNQ	0.997	9.59	0.064	ND	7.28	1.61 DNQ	3820	1.44	42.4	0.006 DNQ	2.35	ND	ND	ND	ND	8.11
DR (%)	100	85	100	100	96	0	100	56	100	100	100	78	89	0	0	0	56	100

^a Near-ZID station

Appendix F.5 continued

Summer 2022	Al	Sb	As	Ba	Be	Cd	Cr	Cu	Fe	Pb	Mn	Hg	Ni	Se	Ag	Ti	Sn	Zn
<i>19-m Stations</i>																		
I35	5220	ND	2.35	30.0	0.103	ND	10.6	3.31 DNQ	7050	2.51	71.5	0.014 DNQ	2.80	ND	ND	ND	0.460	18.8
I34	1590	ND	1.77	7.66	0.033	ND	3.68	ND	2990	1.50	26.3	0.005 DNQ	0.598	ND	ND	ND	0.157 DNQ	6.06
I31	3880	0.65 DNQ	1.15	16.1	0.096	ND	7.03	1.33 DNQ	3870	1.03	56.8	0.016 DNQ	1.25	ND	ND	ND	0.312	8.82
I23	1090	ND	2.94	5.41	0.018 DNQ	ND	4.19	3.15 DNQ	2620	1.28	18.2	ND	0.581	ND	ND	ND	ND	4.88
I18	4970	1.18 DNQ	0.852	39.2	0.137	ND	10.5	2.05 DNQ	6500	1.16	82.9	ND	1.78	ND	ND	ND	0.379	12.8
I10	4720	0.401 DNQ	1.34	25.2	0.091	ND	9.97	2.77 DNQ	5960	1.13	63.5	0.003 DNQ	2.29	ND	ND	ND	0.261	13.5
I4	758	ND	0.964	2.38	0.029 DNQ	ND	4.09	ND	1480	0.928	8.34	ND	0.561	ND	ND	ND	0.097 DNQ	2.56
<i>28-m Stations</i>																		
I33	3890	0.485 DNQ	2.39	16.5	0.081	ND	8.23	3.70 DNQ	6140	2.50	64.3	0.013 DNQ	1.92	ND	ND	ND	0.467	15.1
I30	5840	0.515 DNQ	1.74	31.8	0.102	ND	11.0	3.88 DNQ	6480	1.80	62.8	0.007 DNQ	3.00	ND	ND	ND	0.289	18.1
I27	6340	1.06 DNQ	1.32	29.7	0.145	ND	10.3	2.86 DNQ	6120	1.40	69.9	0.004 DNQ	2.66	ND	ND	ND	0.372	16.3
I22	4260	0.427 DNQ	1.68	22.7	0.084	ND	9.19	2.35 DNQ	5130	1.50	51.2	0.004 DNQ	2.41	ND	ND	ND	0.278	12.7
I14 ^a	6850	1.16 DNQ	1.75	35.6	0.155	ND	10.4	3.01 DNQ	6900	1.31	79.6	0.004 DNQ	2.91	ND	ND	ND	0.425	17.5
I16 ^a	1860	ND	1.48	7.03	0.049	ND	5.91	ND	3240	1.36	29.9	0.003 DNQ	0.823	ND	ND	ND	0.180 DNQ	17.6
I15	1690	0.461 DNQ	2.53	4.76	0.071	ND	7.15	ND	3660	1.37	21.0	ND	0.438	ND	ND	ND	0.124 DNQ	6.58
I12 ^a	1690	0.399 DNQ	1.77	5.43	0.060	ND	5.10	ND	2890	1.06	20.6	ND	0.449	ND	ND	ND	ND	5.87
I9	7510	0.696 DNQ	1.58	46.2	0.141	ND	13.3	4.57 DNQ	8500	1.25	86.1	0.004 DNQ	4.39	ND	ND	ND	0.364	23.2
I6	1060	ND	4.63	2.75	0.044	ND	7.87	ND	3940	1.60	12.5	ND	0.503	ND	ND	ND	0.150 DNQ	3.86
I2	1040	ND	0.814	2.36	0.024 DNQ	ND	5.27	ND	1250	0.865	8.54	0.003 DNQ	0.617	ND	ND	ND	ND	2.50
I3	748	ND	0.917	1.39 DNQ	0.024 DNQ	ND	5.74	ND	1160	0.937	5.97	ND	0.513	ND	ND	ND	0.089 DNQ	1.87
<i>38-m Stations</i>																		
I29	6160	0.500 DNQ	2.73	31.8	0.129	ND	12.8	4.53	8160	2.67	69.4	0.015	4.14	ND	ND	ND	0.552	19.9
I21	1090	0.847 DNQ	9.81	2.21	0.110	ND	10.8	ND	7840	2.79	13.3	ND	ND	ND	ND	ND	0.200 DNQ	5.79
I13	899	0.438 DNQ	7.18	2.92	0.051	ND	8.47	ND	5610	2.08	13.4	0.003 DNQ	0.445	ND	ND	ND	0.106 DNQ	5.10
I8	1720	0.478 DNQ	2.30	4.66	0.061	ND	9.18	ND	4130	1.26	20.1	0.002 DNQ	0.912	ND	ND	ND	0.105 DNQ	7.65
<i>55-m Stations</i>																		
I28	4440	0.598 DNQ	2.18	17.6	0.125	ND	8.37	3.61 DNQ	5650	2.01	46.9	0.022	3.40	ND	ND	ND	0.344	13.0
I20	1910	0.576 DNQ	2.84	3.95	0.059	ND	4.95	ND	4640	1.54	18.0	0.002 DNQ	0.411	ND	ND	ND	0.123 DNQ	6.08
I7	1070	0.512 DNQ	4.59	2.48	0.056	ND	7.87	ND	5700	1.83	15.7	ND	0.548	ND	ND	ND	0.132 DNQ	5.47
I1	3340	0.667 DNQ	1.44	10.9	0.096	0.088 DNQ	7.26	1.83 DNQ	4180	1.53	46.8	0.006 DNQ	2.63	ND	ND	ND	0.250	9.02
DR (%)	100	70	100	100	100	4	100	52	100	100	100	67	96	0	0	0	89	100

^aNear-ZID station

Appendix F.5 *continued*

Winter 2023	Al	Sb	As	Ba	Be	Cd	Cr	Cu	Fe	Pb	Mn	Hg	Ni	Se	Ag	Ti	Sn	Zn
<i>19-m Stations</i>																		
I35	5980	ND	1.77	29.7	0.109	ND	11.2	4.78	7990	2.82	80.6	0.014	DNQ	3.16	ND	ND	0.218	19.7
I34	1320	ND	1.21	4.10	0.028	DNQ	3.54	ND	3020	1.53	27.3	NR	0.387	DNQ	ND	ND	0.263	4.78
I31	2960	ND	1.00	18.0	0.052	ND	6.62	1.55	3290	1.08	45.8	NR	1.10	ND	ND	ND	0.255	7.29
I23	3150	ND	1.28	19.7	ND	ND	7.63	2.18	4280	1.27	54.0	NR	1.32	DNQ	ND	ND	0.331	9.12
I18	4450	ND	1.36	27.8	ND	ND	10.5	2.53	6290	1.38	70.2	NR	2.34	DNQ	ND	ND	0.401	14.3
I10	4380	ND	1.30	23.9	0.077	ND	9.14	2.56	5440	1.45	59.2	NR	2.14	ND	ND	ND	0.339	11.8
I4	1990	ND	1.26	9.31	0.046	ND	6.26	1.70	3120	1.39	32.2	NR	1.76	ND	ND	0.103	DNQ	6.46
<i>28-m Stations</i>																		
I33	3410	ND	1.38	13.6	0.067	ND	7.20	3.58	5760	2.58	61.6	0.01	DNQ	1.53	ND	ND	0.244	13.2
I30	5050	ND	1.76	25.0	0.087	ND	9.49	2.92	5400	1.62	53.2	NR	2.33	ND	ND	ND	0.310	14.0
I27	5350	ND	1.39	27.5	0.091	ND	9.54	3.02	5600	1.40	59.0	NR	2.41	ND	ND	ND	0.390	15.1
I22	4830	ND	1.55	26.3	ND	ND	10.3	2.83	6110	1.54	64.3	NR	2.70	DNQ	ND	ND	0.367	16.2
I14 ^a	4560	ND	1.29	25.3	ND	ND	9.33	2.86	5460	1.38	60.8	NR	2.42	DNQ	ND	ND	0.352	14.4
I16 ^a	2980	ND	1.19	12.8	ND	ND	7.31	1.39	4210	1.18	44.7	NR	1.29	DNQ	ND	ND	0.204	9.19
I15	2510	ND	1.81	11.9	ND	ND	9.13	1.33	4680	1.46	35.0	NR	1.37	DNQ	ND	ND	0.205	9.81
I12 ^a	1750	ND	1.69	7.29	ND	ND	6.09	ND	3290	1.11	25.9	NR	0.637	DNQ	ND	ND	0.134	8.19
I9	6310	ND	1.43	35.4	0.110	ND	11.3	3.88	7000	1.13	73.1	NR	3.25	ND	ND	ND	0.129	18.0
I6	1140	ND	4.82	4.09	0.040	ND	7.93	ND	4030	1.56	13.5	NR	0.356	DNQ	ND	ND	ND	4.11
I2	976	ND	0.469	1.84	0.021	DNQ	5.09	ND	1210	0.812	10.7	NR	0.574	ND	ND	ND	0.111	2.30
I3	713	ND	0.793	1.39	0.020	DNQ	5.32	ND	1200	0.931	7.09	NR	0.456	ND	ND	ND	ND	1.83
<i>38-m Stations</i>																		
I29	5960	ND	2.01	31.7	0.118	ND	11.9	4.82	7460	2.45	68.9	NR	3.91	ND	ND	ND	0.571	18.4
I21	1100	0.490	6.68	2.25	ND	ND	11.6	ND	7180	2.73	14.3	NR	0.220	DNQ	ND	ND	0.174	6.60
I13	811	ND	6.16	1.71	ND	ND	9.47	ND	5580	2.24	13.8	NR	0.201	DNQ	ND	ND	0.096	7.21
I8	1670	ND	2.18	4.29	0.053	ND	8.96	ND	3880	1.25	20.7	NR	0.802	ND	ND	ND	ND	6.73
<i>55-m Stations</i>																		
I28	3180	ND	2.02	13.1	0.081	ND	6.33	3.14	4950	1.93	35.4	NR	4.87	ND	ND	ND	0.334	10.4
I20	1400	ND	2.91	3.88	ND	ND	5.57	ND	4740	1.74	18.6	NR	0.831	DNQ	ND	ND	0.230	7.01
I7	1020	0.461	5.62	2.33	0.052	ND	9.03	ND	6680	2.08	18.8	NR	0.166	DNQ	ND	ND	ND	5.44
I1	2500	ND	0.784	10.2	0.058	ND	6.71	1.75	3470	1.50	37.7	NR	2.28	ND	ND	ND	0.257	7.26
DR (%)	100	7	100	100	63	0	100	63	100	100	100	100	100	0	0	0	85	100

^a Near-ZID station

Appendix F.5 *continued*

Summer 2023	Al	Sb	As	Ba	Be	Cd	Cr	Cu	Fe	Pb	Mn	Hg	Ni	Se	Ag	Ti	Sn	Zn
<i>19-m Stations</i>																		
I35	—	—	—	—	—	—	—	—	—	—	—	—	—	—	—	—	—	—
I34	—	—	—	—	—	—	—	—	—	—	—	—	—	—	—	—	—	—
I31	—	—	—	—	—	—	—	—	—	—	—	—	—	—	—	—	—	—
I23	—	—	—	—	—	—	—	—	—	—	—	—	—	—	—	—	—	—
I18	—	—	—	—	—	—	—	—	—	—	—	—	—	—	—	—	—	—
I10	—	—	—	—	—	—	—	—	—	—	—	—	—	—	—	—	—	—
I4	—	—	—	—	—	—	—	—	—	—	—	—	—	—	—	—	—	—
<i>28-m Stations</i>																		
I33	3690	0.492 DNQ	1.90	16.3	0.056	0.036 DNQ	7.74	2.83	5450	2.35	58.8	0.014	2.19	ND	ND	NA	0.526	13.2
I30	5440	0.522 DNQ	1.47	27.7	0.062	0.034 DNQ	10.4	3.06	5810	1.64	58.1	0.006 DNQ	3.13	ND	ND	NA	0.393 DNQ	15.4
I27	5100	0.453 DNQ	1.74	26.8	0.059	0.029 DNQ	9.61	2.84	5650	1.53	56.2	ND	2.98	0.247 DNQ	ND	NA	0.406 DNQ	14.1
I22	4290	0.408 DNQ	1.19	25.7	0.052	0.028 DNQ	8.99	2.46	4740	1.88	51.2	ND	2.81	ND	ND	NA	0.464 DNQ	11.6
I14 ^a	5430	0.435 DNQ	1.43	30.9	0.063	0.033 DNQ	10.0	3.23	6000	1.40	62.9	0.005 DNQ	3.43	ND	ND	NA	0.464 DNQ	15.6
I16 ^a	1910	0.262 DNQ	1.53	6.67	0.037 DNQ	ND	5.77	0.891	3400	1.21	26.6	ND	1.14	ND	ND	NA	0.185 DNQ	7.49
I15	1730	0.292 DNQ	1.86	6.52	0.041 DNQ	ND	7.78	0.773	3650	1.42	22.3	ND	1.15	ND	ND	NA	0.195 DNQ	6.70
I12 ^a	2890	0.380 DNQ	1.63	15.5	0.043 DNQ	ND	7.24	1.48	4390	1.23	39.1	ND	1.63	ND	ND	NA	0.253 DNQ	10.3
I9	7030	0.397 DNQ	1.59	39.5	0.106	0.055 DNQ	12.3	4.12	7670	1.43	78.2	0.004 DNQ	4.32	0.225 DNQ	ND	NA	0.484 DNQ	20.5
I6	906	0.385 DNQ	5.54	2.22	0.033 DNQ	0.031 DNQ	7.85	0.447 DNQ	3900	1.59	8.85	ND	0.638	ND	ND	NA	0.097 DNQ	3.45
I2	920	0.178 DNQ	0.880 DNQ	1.99	0.016 DNQ	ND	5.24	0.368 DNQ	1140	0.764	7.63	ND	0.690	ND	ND	NA	0.076 DNQ	2.25
I3	665	0.216 DNQ	1.23	1.41	0.018 DNQ	ND	5.32	0.307 DNQ	1340	0.815	5.57	ND	0.632	ND	ND	NA	0.110 DNQ	2.04
<i>38-m Stations</i>																		
I29	—	—	—	—	—	—	—	—	—	—	—	—	—	—	—	—	—	—
I21	—	—	—	—	—	—	—	—	—	—	—	—	—	—	—	—	—	—
I13	—	—	—	—	—	—	—	—	—	—	—	—	—	—	—	—	—	—
I8	—	—	—	—	—	—	—	—	—	—	—	—	—	—	—	—	—	—
<i>55-m Stations</i>																		
I28	—	—	—	—	—	—	—	—	—	—	—	—	—	—	—	—	—	—
I20	—	—	—	—	—	—	—	—	—	—	—	—	—	—	—	—	—	—
I7	—	—	—	—	—	—	—	—	—	—	—	—	—	—	—	—	—	—
I1	—	—	—	—	—	—	—	—	—	—	—	—	—	—	—	—	—	—
DR (%)	100	7	100	100	63	0	100	63	100	100	100	100	100	0	0	0	85	100

^a Near-ZID station

Appendix F.6

Concentrations of pesticides (ppt) detected in sediments from PLOO stations sampled during winter and summer 2022 and 2023. See Appendix F.1 for MDLs and abbreviations; DR = detection rate; DNQ = do not quantify; ND = not detected; NR = not reportable. Only primary core stations sampled during summer 2023 due to resource exchange for Bight'23 (see text).

Winter 2022	Chlordane										DDT							
	A(c)C	cNon	G(t)C	Hept	Hept	Hept	Epox	Methoxy	Oxychlor	tNon	o,p-DDD	o,p-DDE	o,p-DDT	p,p-DDMU	p,p-DDD	p,p-DDE	p,p-DDT	
<i>88-m Depth Contour</i>																		
B11	ND	ND	ND	ND	ND	ND	ND	ND	ND	ND	ND	ND	ND	ND	ND	408	ND	ND
B8	ND	ND	ND	ND	ND	ND	ND	ND	ND	ND	ND	ND	ND	50.0 DNQ	49.5 DNQ	636	ND	110
E19	ND	ND	41.0 DNQ	ND	ND	ND	ND	ND	ND	ND	ND	ND	ND	ND	ND	316	ND	ND
E7	ND	ND	ND	ND	ND	ND	ND	ND	ND	ND	ND	ND	ND	ND	46.6 DNQ	384	ND	ND
E1	ND	ND	ND	ND	ND	ND	ND	ND	ND	ND	ND	ND	ND	47.2 DNQ	72.9 DNQ	492	ND	ND
<i>98-m Depth Contour</i>																		
B12	ND	ND	ND	ND	ND	ND	ND	ND	ND	ND	ND	ND	ND	ND	ND	325	ND	ND
B9	ND	ND	ND	ND	ND	ND	ND	ND	ND	ND	ND	ND	ND	ND	53.2 DNQ	484	ND	ND
E26	ND	ND	ND	ND	ND	ND	ND	ND	ND	ND	ND	ND	ND	ND	ND	323	ND	ND
E25	ND	ND	ND	ND	ND	ND	ND	ND	ND	ND	ND	ND	ND	ND	ND	210	ND	ND
E23	ND	ND	ND	ND	ND	ND	ND	ND	ND	ND	ND	ND	ND	ND	ND	275	ND	ND
E20	ND	ND	ND	ND	ND	ND	ND	ND	ND	ND	ND	ND	ND	ND	ND	237	ND	ND
E17 ^a	ND	ND	ND	ND	ND	ND	ND	ND	ND	ND	ND	ND	ND	ND	ND	196	ND	ND
E14 ^a	ND	ND	ND	ND	ND	ND	ND	ND	ND	ND	ND	ND	ND	ND	ND	163	ND	ND
E11 ^a	ND	ND	51.6 DNQ	ND	ND	ND	ND	ND	ND	ND	ND	ND	ND	ND	47.5 DNQ	195	ND	ND
E8	ND	ND	ND	ND	ND	ND	ND	ND	ND	ND	ND	ND	ND	ND	ND	255	ND	ND
E5	ND	ND	ND	ND	ND	ND	ND	ND	ND	ND	ND	ND	ND	ND	ND	267	ND	ND
E2	ND	ND	ND	ND	ND	ND	ND	ND	ND	ND	ND	ND	ND	ND	54.5 DNQ	347	ND	ND
<i>116-m Depth Contour</i>																		
B10	ND	ND	ND	ND	ND	ND	ND	ND	ND	ND	ND	ND	ND	ND	ND	325	ND	ND
E21	ND	ND	ND	ND	ND	ND	ND	ND	ND	ND	ND	ND	ND	ND	ND	220	ND	ND
E15 ^a	ND	ND	ND	ND	ND	ND	ND	ND	ND	ND	ND	ND	ND	ND	ND	277	ND	ND
E9	ND	ND	ND	ND	ND	ND	ND	ND	ND	ND	ND	ND	ND	ND	ND	255	ND	ND
E3	ND	ND	ND	ND	ND	ND	ND	ND	ND	ND	ND	ND	ND	81.6 DNQ	212	ND	ND	ND
DR (%)	0	0	9	0	0	0	0	0	0	0	0	0	0	9	32	100	5	5

^a Near-ZID station

Appendix F.6 continued

Winter	HCH			Gamma	Delta	Aldrin	Dieldrin	Endosulfan		Endrin	EndAld	HCB	Mirex
	2022	Alpha	Beta					Alpha	Beta				
<i>88-m Depth Contour</i>													
B11	ND	ND	ND	ND	ND	ND	ND	ND	ND	ND	ND	ND	ND
B8	ND	ND	ND	ND	ND	ND	ND	ND	ND	ND	ND	ND	ND
E19	39.9	DNQ	131	ND	ND	ND	ND	ND	ND	ND	ND	ND	ND
E7	ND	ND	ND	ND	ND	ND	ND	ND	ND	ND	ND	ND	ND
E1	ND	ND	ND	ND	ND	ND	ND	ND	ND	ND	ND	ND	ND
<i>98-m Depth Contour</i>													
B12	ND	ND	ND	ND	ND	ND	ND	ND	ND	ND	ND	ND	ND
B9	ND	ND	ND	ND	ND	ND	ND	ND	ND	ND	ND	ND	ND
E26	ND	ND	ND	ND	ND	ND	ND	ND	ND	ND	ND	ND	ND
E25	ND	ND	ND	ND	ND	ND	ND	ND	ND	ND	ND	ND	ND
E23	ND	ND	ND	ND	ND	ND	ND	ND	ND	ND	ND	ND	ND
E20	ND	ND	ND	ND	ND	ND	ND	ND	ND	ND	ND	ND	ND
E17 ^a	ND	ND	ND	ND	ND	ND	ND	ND	ND	ND	ND	ND	ND
E14 ^a	ND	ND	ND	ND	ND	ND	ND	ND	ND	ND	ND	ND	ND
E11 ^a	ND	ND	ND	ND	ND	ND	ND	ND	ND	ND	ND	ND	ND
E8	ND	ND	ND	ND	ND	ND	ND	ND	ND	ND	ND	ND	ND
E5	ND	ND	ND	ND	ND	ND	ND	ND	ND	ND	ND	ND	ND
E2	ND	ND	ND	ND	ND	ND	ND	ND	ND	ND	ND	ND	ND
<i>116-m Depth Contour</i>													
B10	ND	ND	ND	ND	ND	ND	ND	ND	ND	ND	ND	ND	ND
E21	ND	ND	ND	ND	ND	ND	ND	ND	ND	ND	ND	ND	ND
E15 ^a	77.2	DNQ	97.7	ND	ND	ND	ND	ND	ND	ND	ND	ND	ND
E9	ND	ND	ND	ND	ND	ND	ND	ND	ND	ND	ND	ND	ND
E3	ND	ND	ND	ND	ND	ND	ND	ND	ND	ND	ND	ND	ND
DR (%)	9	0	0	9	0	0	0	0	0	0	0	0	0

^aNear-ZID station

Appendix F.6 *continued*

Summer 2022	Chlordane										DDT				
	A(c)C	cNon	G(t)C	Hept HeptEpoX	Methoxy Oxychlor	tNon	o,p-DDD	o,p-DDE	o,p-DDT	p,p-DDMU	p,p-DDD	p,p-DDE	p,p-DDT		
<i>88-m Depth Contour</i>															
B11	ND	ND	ND	ND	ND	ND	ND	ND	59.8 DNQ	ND	49.4 DNQ	654	98.9		
B8	ND	ND	ND	ND	ND	ND	ND	ND	ND	ND	49.0 DNQ	563	83.1 DNQ		
E19	ND	ND	ND	ND	ND	ND	ND	ND	ND	ND	ND	286	ND		
E7	ND	ND	ND	ND	ND	ND	ND	ND	ND	ND	ND	288	ND		
E1	ND	ND	ND	ND	ND	ND	ND	ND	ND	ND	82.1 DNQ	432	ND		
<i>98-m Depth Contour</i>															
B12	ND	ND	ND	ND	ND	ND	ND	ND	ND	ND	ND	242	ND		
B9	ND	ND	ND	ND	ND	ND	ND	ND	ND	ND	91.4 DNQ	669	ND		
E26	ND	ND	ND	ND	ND	ND	ND	ND	ND	ND	78.8 DNQ	470	ND		
E25	ND	ND	ND	ND	ND	ND	ND	ND	ND	ND	ND	265	ND		
E23	ND	ND	ND	ND	ND	ND	ND	ND	ND	ND	ND	338	ND		
E20	ND	ND	ND	ND	ND	ND	ND	ND	ND	ND	ND	163	ND		
E17 ^a	ND	ND	ND	ND	ND	ND	ND	ND	ND	ND	57.9 DNQ	172	ND		
E14 ^a	ND	ND	ND	ND	ND	ND	ND	ND	ND	ND	ND	101	ND		
E11 ^a	ND	ND	ND	ND	ND	ND	ND	ND	ND	ND	ND	120	ND		
E8	ND	ND	ND	ND	ND	ND	ND	ND	ND	ND	45.0 DNQ	177	ND		
E5	ND	ND	ND	ND	ND	ND	ND	ND	ND	ND	51.5 DNQ	223	ND		
E2	ND	ND	ND	ND	ND	ND	ND	ND	ND	ND	85.4 DNQ	338	ND		
<i>116-m Depth Contour</i>															
B10	ND	ND	ND	ND	ND	ND	ND	ND	ND	ND	ND	367	ND		
E21	ND	ND	ND	ND	ND	ND	ND	ND	ND	ND	ND	159	ND		
E15 ^a	ND	ND	ND	ND	ND	ND	ND	ND	ND	ND	ND	122	ND		
E9	ND	ND	ND	ND	ND	ND	ND	ND	ND	ND	ND	156	ND		
E3	218	80.8 DNQ	235	ND	ND	116	ND	ND	ND	ND	129	223	ND		
DR (%)	5	5	5	0	0	5	0	0	5	0	45	100	9		

^a Near-ZID station

Appendix F.6 *continued*

Summer 2022	HCH			Endosulfan							Mirex		
	Alpha	Beta	Gamma	Aldrin	Dieldrin	Alpha	Beta	Sulfate	Endrin	EndAld		HCB	
<i>88-m Depth Contour</i>													
B11	ND	ND	ND	ND	ND	ND	ND	ND	ND	ND	ND	ND	ND
B8	ND	ND	ND	ND	ND	ND	ND	ND	ND	ND	ND	ND	ND
E19	ND	ND	ND	ND	ND	ND	ND	ND	ND	ND	ND	ND	ND
E7	ND	ND	ND	ND	ND	ND	ND	ND	ND	ND	ND	ND	ND
E1	ND	ND	ND	ND	ND	ND	ND	ND	ND	ND	ND	ND	ND
<i>98-m Depth Contour</i>													
B12	ND	ND	ND	ND	ND	ND	ND	ND	ND	ND	ND	ND	ND
B9	ND	ND	ND	ND	ND	ND	ND	ND	ND	ND	ND	ND	ND
E26	54 DNQ			ND	ND	ND	ND	ND	ND	ND	ND	ND	ND
E25	ND	ND	ND	ND	ND	ND	ND	ND	ND	ND	ND	ND	ND
E23	ND	ND	ND	ND	ND	ND	ND	ND	ND	ND	ND	ND	ND
E20	ND	ND	ND	ND	ND	ND	ND	ND	ND	ND	ND	ND	ND
E17 ^a	ND	ND	ND	ND	ND	ND	ND	ND	ND	ND	ND	ND	ND
E14 ^a	ND	ND	ND	ND	ND	ND	ND	ND	ND	ND	ND	ND	ND
E11 ^a	ND	ND	ND	ND	ND	ND	ND	ND	ND	ND	ND	ND	ND
E8	ND	ND	ND	ND	ND	ND	ND	ND	ND	ND	ND	ND	ND
E5	ND	ND	ND	ND	ND	ND	ND	ND	ND	ND	ND	ND	ND
E2	ND	ND	ND	ND	ND	ND	ND	ND	ND	ND	ND	ND	ND
<i>116-m Depth Contour</i>													
B10	ND	ND	ND	ND	ND	ND	ND	ND	ND	ND	ND	ND	ND
E21	ND	ND	ND	ND	ND	ND	ND	ND	ND	ND	ND	ND	ND
E15 ^a	ND	ND	ND	ND	ND	ND	ND	ND	ND	ND	ND	ND	ND
E9	ND	ND	ND	ND	ND	ND	ND	ND	ND	ND	ND	ND	ND
E3	ND	ND	ND	ND	ND	ND	ND	ND	ND	ND	ND	ND	ND
DR (%)	5	0	0	0	0	0	0	0	0	0	0	0	0

^aNear-ZID station

Appendix F.6 *continued*

Winter	Chlordane										DDT					
	2023	A(c)C	cNon	G(t)C	Hept	HeptEpo	Methoxy	Oxychlor	tNon	o,p-DDD	o,p-DDE	o,p-DDT	p,p-DDMU	p,p-DDD	p,p-DDE	p,p-DDT
<i>88-m Depth Contour</i>																
B11	ND	ND	ND	ND	ND	ND	ND	ND	ND	ND	ND	ND	ND	ND	200	ND
B8	ND	ND	ND	ND	ND	ND	ND	ND	ND	ND	ND	ND	52.9 DNQ	ND	360	ND
E19	ND	ND	ND	ND	ND	ND	ND	ND	ND	ND	ND	ND	55.8 DNQ	ND	246	ND
E7	ND	ND	ND	ND	ND	ND	ND	ND	ND	ND	ND	ND	62.2 DNQ	ND	315	ND
E1	ND	ND	ND	ND	ND	ND	ND	ND	ND	ND	ND	ND	ND	193	ND	ND
<i>98-m Depth Contour</i>																
B12	ND	ND	ND	ND	ND	ND	ND	ND	ND	ND	ND	ND	ND	ND	248	ND
B9	ND	ND	ND	ND	ND	ND	ND	ND	ND	ND	ND	ND	46.1 DNQ	ND	373	ND
E26	ND	ND	ND	ND	ND	ND	ND	ND	ND	ND	ND	ND	ND	182	ND	ND
E25	ND	ND	ND	ND	ND	ND	ND	ND	ND	ND	ND	ND	ND	149	ND	ND
E23	ND	ND	ND	ND	ND	ND	ND	ND	ND	ND	ND	ND	ND	186	ND	ND
E20	ND	ND	ND	ND	ND	ND	ND	ND	ND	ND	35.9 DNQ	ND	45.6 DNQ	248	133	ND
E17 ^a	ND	ND	ND	ND	ND	ND	ND	ND	ND	ND	ND	ND	ND	159	ND	ND
E14 ^a	ND	ND	ND	ND	ND	ND	ND	ND	ND	ND	ND	ND	ND	114	ND	ND
E11 ^a	ND	ND	ND	ND	ND	ND	ND	ND	ND	ND	ND	ND	ND	163	ND	ND
E8	ND	ND	ND	ND	ND	ND	ND	ND	ND	ND	ND	ND	ND	111	ND	ND
E5	ND	ND	ND	ND	ND	ND	ND	ND	ND	ND	ND	ND	ND	148	ND	ND
E2	ND	ND	ND	ND	ND	ND	ND	ND	ND	ND	ND	ND	44.2 DNQ	322	ND	ND
<i>116-m Depth Contour</i>																
B10	ND	ND	ND	ND	ND	ND	ND	ND	ND	ND	ND	ND	ND	ND	122	ND
E21	ND	ND	ND	ND	ND	ND	ND	ND	ND	ND	ND	ND	ND	134	ND	ND
E15 ^a	ND	ND	ND	ND	ND	ND	ND	ND	ND	ND	ND	ND	ND	142	ND	ND
E9	ND	ND	ND	ND	ND	ND	ND	ND	ND	ND	ND	ND	ND	157	ND	ND
E3	ND	ND	ND	ND	ND	ND	ND	ND	ND	ND	ND	ND	124	113	ND	ND
DR (%)	0	0	0	0	0	0	0	0	0	0	5	0	32	100	5	5

^a Near-ZID station

Appendix F.6 continued

Winter 2023	HCH			Endosulfan			Aldrin	Dieldrin	Alpha	Beta	Sulfate	Endrin	EndAld	HCB	Mirex
	Alpha	Beta	Delta	Gamma	Delta	Gamma									
<i>88-m Depth Contour</i>															
B11	ND	ND	ND	ND	ND	ND	ND	ND	ND	ND	ND	ND	ND	ND	ND
B8	ND	ND	ND	ND	ND	ND	ND	ND	ND	ND	ND	ND	ND	ND	ND
E19	ND	ND	ND	ND	ND	ND	ND	ND	ND	ND	ND	ND	ND	ND	ND
E7	ND	ND	ND	ND	ND	ND	ND	ND	ND	ND	ND	ND	ND	ND	ND
E1	ND	ND	ND	ND	ND	ND	ND	ND	ND	ND	ND	ND	ND	ND	ND
<i>98-m Depth Contour</i>															
B12	ND	ND	ND	ND	ND	ND	ND	ND	ND	ND	ND	ND	ND	ND	ND
B9	ND	ND	ND	ND	ND	ND	ND	ND	ND	ND	ND	ND	ND	ND	ND
E26	ND	ND	ND	ND	ND	ND	ND	ND	ND	ND	ND	ND	ND	ND	ND
E25	ND	ND	ND	ND	ND	ND	ND	ND	ND	ND	ND	ND	ND	ND	ND
E23	ND	ND	ND	ND	ND	ND	ND	ND	ND	ND	ND	ND	ND	ND	ND
E20	ND	ND	ND	ND	ND	ND	ND	ND	ND	ND	ND	ND	ND	ND	ND
E17 ^a	ND	ND	ND	ND	ND	ND	ND	ND	ND	ND	ND	ND	ND	ND	ND
E14 ^a	ND	ND	ND	ND	ND	ND	ND	ND	ND	ND	ND	ND	ND	ND	ND
E11 ^a	ND	ND	ND	ND	ND	ND	ND	ND	ND	ND	ND	ND	ND	ND	ND
E8	ND	ND	ND	ND	ND	ND	ND	ND	ND	ND	ND	ND	ND	ND	ND
E5	ND	ND	ND	ND	ND	ND	ND	ND	ND	ND	ND	ND	ND	ND	ND
E2	ND	ND	ND	ND	ND	ND	ND	ND	ND	ND	ND	ND	ND	ND	ND
<i>116-m Depth Contour</i>															
B10	ND	ND	ND	ND	ND	ND	ND	ND	ND	ND	ND	ND	ND	ND	ND
E21	ND	ND	ND	ND	ND	ND	ND	ND	ND	ND	ND	ND	ND	ND	ND
E15 ^a	ND	ND	ND	ND	ND	ND	ND	ND	ND	ND	ND	ND	ND	ND	ND
E9	ND	ND	ND	ND	ND	ND	ND	ND	ND	ND	ND	ND	ND	ND	ND
E3	ND	ND	ND	ND	ND	ND	ND	ND	ND	ND	ND	ND	ND	ND	ND
DR (%)	0	0	0	0	0	0	0	0	0	0	0	0	0	0	0

^aNear-ZID station

Appendix F.6 *continued*

Summer	Chlordane										DDT					
	2023	A(c)C	cNon	G(t)C	Hept	HeptEpo	Methoxy	Oxychlor	tNon	o,p-DDD	o,p-DDE	o,p-DDT	p,p-DDMU	p,p-DDD	p,p-DDE	p,p-DDT
<i>88-m Depth Contour</i>																
B11	—	—	—	—	—	—	—	—	—	—	—	—	—	—	—	—
B8	—	—	—	—	—	—	—	—	—	—	—	—	—	—	—	—
E19	—	—	—	—	—	—	—	—	—	—	—	—	—	—	—	—
E7	—	—	—	—	—	—	—	—	—	—	—	—	—	—	—	—
E1	—	—	—	—	—	—	—	—	—	—	—	—	—	—	—	—
<i>98-m Depth Contour</i>																
B12	NR	NR	NR	NR	NR	NR	NR	NR	NR	NR	NR	NR	NR	NR	NR	NR
B9	NR	NR	NR	NR	NR	NR	NR	NR	NR	NR	NR	NR	NR	NR	NR	NR
E26	NR	NR	NR	NR	NR	NR	NR	NR	NR	NR	NR	NR	NR	NR	NR	NR
E25	NR	NR	NR	NR	NR	NR	NR	NR	NR	NR	NR	NR	NR	NR	NR	NR
E23	NR	NR	NR	NR	NR	NR	NR	NR	NR	NR	NR	NR	NR	NR	NR	NR
E20	NR	NR	NR	NR	NR	NR	NR	NR	NR	NR	NR	NR	NR	NR	NR	NR
E17 ^a	NR	NR	NR	NR	NR	NR	NR	NR	NR	NR	NR	NR	NR	NR	NR	NR
E14 ^a	NR	NR	NR	NR	NR	NR	NR	NR	NR	NR	NR	NR	NR	NR	NR	NR
E11 ^a	NR	NR	NR	NR	NR	NR	NR	NR	NR	NR	NR	NR	NR	NR	NR	NR
E8	NR	NR	NR	NR	NR	NR	NR	NR	NR	NR	NR	NR	NR	NR	NR	NR
E5	NR	NR	NR	NR	NR	NR	NR	NR	NR	NR	NR	NR	NR	NR	NR	NR
E2	NR	NR	NR	NR	NR	NR	NR	NR	NR	NR	NR	NR	NR	NR	NR	NR
<i>116-m Depth Contour</i>																
B10	—	—	—	—	—	—	—	—	—	—	—	—	—	—	—	—
E21	—	—	—	—	—	—	—	—	—	—	—	—	—	—	—	—
E15 ^a	NR	NR	NR	NR	NR	NR	NR	NR	NR	NR	NR	NR	NR	NR	NR	NR
E9	—	—	—	—	—	—	—	—	—	—	—	—	—	—	—	—
E3	—	—	—	—	—	—	—	—	—	—	—	—	—	—	—	—
DR (%)	NR	NR	NR	NR	NR	NR	NR	NR	NR	NR	NR	NR	NR	NR	NR	NR

^a Near-ZID station

Appendix F.6 continued

Summer 2023	HCH				Endosulfan				Mirex				
	Alpha	Beta	Delta	Gamma	Aldrin	Dieldrin	Alpha	Beta		Sulfate	Endrin	EndAld	HCB
<i>88-m Depth Contour</i>													
B11	—	—	—	—	—	—	—	—	—	—	—	—	—
B8	—	—	—	—	—	—	—	—	—	—	—	—	—
E19	—	—	—	—	—	—	—	—	—	—	—	—	—
E7	—	—	—	—	—	—	—	—	—	—	—	—	—
E1	—	—	—	—	—	—	—	—	—	—	—	—	—
<i>98-m Depth Contour</i>													
B12	NR	NR	NR	NR	NR	NR	NR	NR	NR	NR	NR	NR	NR
B9	NR	NR	NR	NR	NR	NR	NR	NR	NR	NR	NR	NR	NR
E26	NR	NR	NR	NR	NR	NR	NR	NR	NR	NR	NR	NR	NR
E25	NR	NR	NR	NR	NR	NR	NR	NR	NR	NR	NR	NR	NR
E23	NR	NR	NR	NR	NR	NR	NR	NR	NR	NR	NR	NR	NR
E20	NR	NR	NR	NR	NR	NR	NR	NR	NR	NR	NR	NR	NR
E17 ^a	NR	NR	NR	NR	NR	NR	NR	NR	NR	NR	NR	NR	NR
E14 ^a	NR	NR	NR	NR	NR	NR	NR	NR	NR	NR	NR	NR	NR
E11 ^a	NR	NR	NR	NR	NR	NR	NR	NR	NR	NR	NR	NR	NR
E8	NR	NR	NR	NR	NR	NR	NR	NR	NR	NR	NR	NR	NR
E5	NR	NR	NR	NR	NR	NR	NR	NR	NR	NR	NR	NR	NR
E2	NR	NR	NR	NR	NR	NR	NR	NR	NR	NR	NR	NR	NR
<i>116-m Depth Contour</i>													
B10	—	—	—	—	—	—	—	—	—	—	—	—	—
E21	—	—	—	—	—	—	—	—	—	—	—	—	—
E15 ^a	NR	NR	NR	NR	NR	NR	NR	NR	NR	NR	NR	NR	NR
E9	—	—	—	—	—	—	—	—	—	—	—	—	—
E3	—	—	—	—	—	—	—	—	—	—	—	—	—
DR (%)	NR	NR	NR	NR	NR	NR	NR	NR	NR	NR	NR	NR	NR

^aNear-ZID station

Appendix F.7

Concentrations of pesticides (ppt) detected in sediments from SBOO stations sampled during 2022 and 2023. See Appendix F.1 for MDLs and abbreviations; DR = detection rate; DNQ = do not quantify; ND = not detected; NR = not reportable. Only primary core stations sampled during summer 2023 due to resource exchange for Bight'23 (see text).

Winter 2022	Chlordane							DDT								
	A(c)C	cNon	G(t)C	Hept	HeptEpo	Methoxy	Oxychlor	tNon	o,p-DDD	o,p-DDE	o,p-DDT	p,p-DDMU	p,p-DDD	p,p-DDE	p,p-DDT	
<i>19-m Stations</i>																
I35	ND	ND	ND	ND	ND	ND	ND	ND	ND	ND	ND	ND	ND	94.5	ND	ND
I34	ND	ND	ND	ND	ND	ND	ND	ND	ND	ND	ND	ND	ND	ND	ND	ND
I31	ND	ND	ND	ND	ND	ND	ND	ND	ND	ND	ND	ND	ND	ND	ND	ND
I23	ND	ND	ND	ND	ND	ND	ND	ND	ND	ND	ND	ND	ND	ND	ND	ND
I18	ND	ND	ND	ND	ND	ND	ND	ND	ND	ND	ND	ND	ND	ND	ND	ND
I10	ND	ND	ND	ND	ND	ND	ND	ND	ND	ND	ND	ND	ND	ND	ND	ND
I4	ND	ND	ND	ND	ND	ND	ND	ND	ND	ND	ND	ND	ND	ND	ND	ND
<i>28-m Stations</i>																
I33	ND	ND	ND	ND	ND	ND	ND	ND	ND	ND	ND	ND	40.9 DNQ	99.8	ND	ND
I30	ND	ND	ND	ND	ND	ND	ND	ND	ND	ND	ND	ND	ND	ND	ND	ND
I27	ND	ND	ND	ND	ND	ND	ND	ND	ND	ND	ND	ND	ND	ND	ND	ND
I22	ND	ND	ND	ND	ND	ND	ND	ND	ND	ND	ND	ND	ND	105	ND	ND
I14 ^a	ND	ND	ND	ND	ND	ND	ND	ND	ND	ND	ND	ND	ND	71.5 DNQ	ND	ND
I16 ^a	ND	ND	ND	ND	ND	ND	ND	ND	ND	ND	ND	ND	ND	ND	ND	ND
I15	ND	ND	ND	ND	ND	ND	ND	ND	ND	ND	ND	ND	ND	ND	ND	ND
I12 ^a	ND	ND	ND	ND	ND	ND	ND	ND	ND	ND	ND	ND	ND	ND	ND	ND
I9	ND	ND	ND	ND	ND	ND	ND	ND	ND	ND	ND	ND	ND	ND	ND	ND
I6	ND	ND	ND	ND	ND	ND	ND	ND	ND	ND	ND	ND	ND	ND	ND	ND
I2	ND	ND	ND	ND	ND	ND	ND	ND	ND	ND	ND	ND	ND	ND	ND	ND
I3	ND	ND	ND	ND	ND	ND	ND	ND	ND	ND	ND	ND	ND	ND	ND	ND
<i>38-m Stations</i>																
I29	ND	ND	ND	ND	ND	ND	ND	ND	ND	ND	ND	ND	42.8 DNQ	428	ND	ND
I21	ND	ND	ND	ND	ND	ND	ND	ND	ND	ND	ND	ND	ND	ND	ND	ND
I13	ND	ND	ND	ND	ND	ND	ND	ND	ND	ND	ND	ND	ND	ND	ND	ND
I8	ND	ND	ND	ND	ND	ND	ND	ND	ND	ND	ND	ND	ND	ND	ND	ND
<i>55-m Stations</i>																
I28	ND	ND	ND	ND	ND	ND	ND	ND	ND	ND	ND	ND	43.6 DNQ	610	ND	108
I20	ND	ND	ND	ND	ND	ND	ND	ND	ND	ND	ND	ND	ND	ND	ND	ND
I7	ND	ND	ND	ND	ND	ND	ND	ND	ND	ND	ND	ND	ND	ND	ND	ND
I1	ND	ND	ND	ND	ND	ND	ND	ND	ND	ND	ND	ND	ND	ND	ND	ND
DR (%)	0	0	0	0	0	0	0	0	0	0	0	0	11	22	4	4

^aNear-ZID station

Appendix F.7 *continued*

Winter 2022	HCH				Endosulfan				Mirex					
	Alpha	Beta	Delta	Gamma	Aldrin	Dieldrin	Alpha	Beta		Sulfate	Endrin	EndAld	HCB	
<i>19-m Stations</i>														
I35	ND	ND	ND	ND	ND	ND	ND	ND	ND	ND	ND	ND	ND	ND
I34	ND	ND	ND	ND	ND	ND	ND	ND	ND	ND	ND	ND	ND	ND
I31	ND	ND	ND	ND	ND	ND	ND	ND	ND	ND	ND	ND	ND	ND
I23	ND	ND	ND	ND	ND	ND	ND	ND	ND	ND	ND	ND	ND	ND
I18	ND	ND	ND	ND	ND	ND	ND	ND	ND	ND	ND	ND	ND	ND
I10	ND	ND	ND	ND	ND	ND	ND	ND	ND	ND	ND	ND	ND	ND
I4	ND	ND	ND	ND	ND	ND	ND	ND	ND	ND	ND	ND	ND	ND
<i>28-m Stations</i>														
I33	32.2 DNQ	ND	ND	ND	ND	ND	ND	ND	ND	ND	ND	ND	ND	50.4 DNQ
I30	ND	ND	ND	ND	ND	ND	ND	ND	ND	ND	ND	ND	ND	ND
I27	ND	ND	ND	ND	ND	ND	ND	ND	ND	ND	ND	ND	196	ND
I22	ND	ND	ND	ND	ND	ND	ND	ND	ND	ND	ND	ND	ND	ND
I14 ^a	ND	ND	ND	ND	ND	ND	ND	ND	ND	ND	ND	ND	ND	ND
I16 ^a	ND	ND	ND	ND	ND	ND	ND	ND	ND	ND	ND	ND	ND	ND
I15	ND	ND	ND	ND	ND	ND	ND	ND	ND	ND	ND	ND	ND	ND
I12 ^a	ND	ND	ND	ND	ND	ND	ND	ND	ND	ND	ND	ND	ND	ND
I9	ND	ND	ND	ND	ND	ND	ND	ND	ND	ND	ND	ND	ND	ND
I6	ND	ND	ND	ND	ND	ND	ND	ND	ND	ND	ND	ND	ND	ND
I2	ND	ND	ND	ND	ND	ND	ND	ND	ND	ND	ND	ND	ND	ND
I3	ND	ND	ND	ND	ND	ND	ND	ND	ND	ND	ND	ND	ND	ND
<i>38-m Stations</i>														
I29	ND	ND	ND	ND	ND	ND	ND	ND	ND	ND	ND	ND	ND	ND
I21	ND	ND	ND	ND	ND	ND	ND	ND	ND	ND	ND	ND	ND	ND
I13	ND	ND	ND	ND	ND	ND	ND	ND	ND	ND	ND	ND	ND	ND
I8	ND	ND	ND	ND	ND	ND	ND	ND	ND	ND	ND	ND	ND	ND
<i>55-m Stations</i>														
I28	ND	ND	ND	ND	ND	ND	ND	ND	ND	ND	ND	ND	ND	ND
I20	ND	ND	ND	ND	ND	ND	ND	ND	ND	ND	ND	ND	ND	ND
I7	ND	ND	ND	ND	ND	ND	ND	ND	ND	ND	ND	ND	ND	ND
I1	ND	ND	ND	ND	ND	ND	ND	ND	ND	ND	ND	ND	ND	ND
DR (%)	4	0	0	0	0	0	0	0	0	0	0	0	4	4

^a Near-ZID station

Appendix F.7 *continued*

Summer 2022	Chlordane										DDT				
	A(c)C	cNon	G(t)C	Hept	HeptEpo	Methoxy	Oxychlor	tNon	o,p-DDD	o,p-DDE	o,p-DDT	p,p-DDMU	p,p-DDD	p,p-DDE	p,p-DDT
<i>19-m Stations</i>															
I35	ND	ND	ND	ND	ND	ND	ND	ND	ND	ND	ND	ND	ND	74.3 DNQ	ND
I34	ND	ND	ND	ND	ND	ND	ND	ND	ND	ND	ND	ND	ND	ND	ND
I31	ND	ND	ND	ND	ND	ND	ND	ND	ND	ND	ND	ND	ND	ND	ND
I23	ND	ND	ND	ND	ND	ND	ND	ND	ND	ND	ND	ND	ND	ND	ND
I18	ND	ND	ND	ND	ND	ND	ND	ND	ND	ND	ND	ND	ND	ND	ND
I10	ND	ND	ND	ND	ND	ND	ND	ND	ND	ND	ND	ND	ND	ND	ND
I4	ND	ND	ND	ND	ND	ND	ND	ND	ND	ND	ND	ND	ND	ND	ND
<i>28-m Stations</i>															
I33	ND	ND	ND	ND	ND	ND	ND	ND	ND	ND	ND	ND	ND	ND	ND
I30	ND	ND	ND	ND	ND	ND	ND	ND	ND	ND	ND	ND	ND	123	ND
I27	ND	ND	ND	ND	ND	ND	ND	ND	ND	ND	ND	ND	ND	ND	ND
I22	ND	ND	ND	ND	ND	ND	ND	ND	ND	ND	ND	ND	ND	ND	ND
I14 ^a	ND	ND	ND	ND	ND	ND	ND	ND	ND	ND	ND	ND	ND	ND	ND
I16 ^a	ND	ND	ND	ND	ND	ND	ND	ND	ND	ND	ND	ND	ND	ND	ND
I15	ND	ND	ND	ND	ND	ND	ND	ND	ND	ND	ND	ND	ND	ND	ND
I12 ^a	ND	ND	ND	ND	ND	ND	ND	ND	ND	ND	ND	ND	ND	ND	ND
I9	ND	ND	ND	ND	ND	ND	ND	ND	ND	ND	ND	ND	ND	ND	ND
I6	ND	ND	ND	ND	ND	ND	ND	ND	ND	ND	ND	ND	ND	ND	ND
I2	ND	ND	ND	ND	ND	ND	ND	ND	ND	ND	ND	ND	ND	ND	ND
I3	ND	ND	ND	ND	ND	ND	ND	ND	ND	34.1 DNQ	ND	ND	ND	ND	ND
<i>38-m Stations</i>															
I29	ND	ND	ND	ND	ND	ND	ND	ND	ND	ND	69.7 DNQ	84.2 DNQ	816	ND	ND
I21	ND	ND	ND	ND	ND	ND	ND	ND	ND	ND	ND	ND	ND	ND	ND
I13	ND	ND	ND	ND	ND	ND	ND	ND	ND	ND	ND	ND	ND	ND	ND
I8	ND	ND	ND	ND	ND	ND	ND	ND	ND	ND	ND	ND	ND	ND	ND
<i>55-m Stations</i>															
I28	ND	ND	ND	ND	ND	ND	ND	ND	ND	ND	ND	54.6 DNQ	663	ND	ND
I20	ND	ND	ND	ND	ND	ND	ND	ND	ND	ND	ND	ND	ND	ND	ND
I7	ND	ND	ND	ND	ND	ND	ND	ND	ND	ND	ND	ND	ND	ND	ND
I1	ND	ND	ND	ND	ND	ND	ND	ND	ND	ND	ND	ND	81.8 DNQ	ND	ND
DR (%)	0	0	0	0	0	0	0	0	0	0	4	4	7	19	0

^a Near-ZID station

Appendix F.7 *continued*

Summer 2022	HCH				Endosulfan				Mirex					
	Alpha	Beta	Delta	Gamma	Aldrin	Dieldrin	Alpha	Beta		Sulfate	Endrin	EndAld	HCB	
<i>19-m Stations</i>														
I35	ND	ND	ND	ND	ND	ND	ND	ND	ND	ND	ND	ND	ND	ND
I34	ND	ND	ND	ND	ND	ND	ND	ND	ND	ND	ND	ND	ND	ND
I31	ND	ND	ND	ND	ND	ND	ND	ND	ND	ND	ND	ND	ND	ND
I23	ND	ND	ND	ND	ND	ND	ND	ND	ND	ND	ND	ND	ND	ND
I18	ND	ND	ND	ND	ND	ND	ND	ND	ND	ND	ND	ND	ND	ND
I10	ND	ND	ND	ND	ND	ND	ND	ND	ND	ND	ND	ND	ND	ND
I4	ND	ND	ND	ND	ND	ND	ND	ND	ND	ND	ND	ND	ND	ND
<i>28-m Stations</i>														
I33	ND	ND	ND	ND	ND	ND	ND	ND	ND	ND	ND	ND	ND	ND
I30	ND	ND	ND	ND	ND	ND	ND	ND	ND	ND	ND	ND	ND	ND
I27	ND	ND	ND	ND	ND	ND	ND	ND	ND	ND	ND	ND	ND	ND
I22	ND	ND	ND	ND	ND	ND	ND	ND	ND	ND	ND	ND	ND	ND
I14 ^a	ND	ND	ND	ND	ND	ND	ND	ND	ND	ND	ND	ND	ND	ND
I16 ^a	ND	ND	ND	ND	ND	ND	ND	ND	ND	ND	ND	ND	ND	ND
I15	ND	ND	ND	ND	ND	ND	ND	ND	ND	ND	ND	ND	ND	ND
I12 ^a	ND	ND	ND	ND	ND	ND	ND	ND	ND	ND	ND	ND	ND	ND
I9	ND	ND	ND	ND	ND	ND	ND	ND	ND	ND	ND	ND	ND	ND
I6	ND	ND	ND	ND	ND	ND	ND	ND	ND	ND	ND	ND	ND	ND
I2	ND	ND	ND	ND	ND	ND	ND	ND	ND	ND	ND	ND	ND	ND
I3	ND	ND	ND	ND	ND	ND	ND	ND	ND	ND	ND	ND	ND	ND
<i>38-m Stations</i>														
I29	ND	ND	ND	ND	ND	ND	ND	ND	ND	ND	ND	ND	ND	ND
I21	ND	ND	ND	ND	ND	ND	ND	ND	ND	ND	ND	ND	ND	ND
I13	ND	ND	ND	ND	ND	ND	ND	ND	ND	ND	ND	ND	ND	ND
I8	ND	ND	ND	ND	ND	ND	ND	ND	ND	ND	ND	ND	ND	ND
<i>55-m Stations</i>														
I28	ND	ND	ND	ND	ND	ND	ND	ND	ND	ND	ND	ND	ND	ND
I20	ND	ND	ND	ND	ND	ND	ND	ND	ND	ND	ND	ND	ND	ND
I7	ND	ND	ND	ND	ND	ND	ND	ND	ND	ND	ND	ND	ND	ND
I1	ND	ND	ND	ND	ND	ND	ND	ND	ND	ND	ND	ND	ND	ND
DR (%)	0	0	0	0	0	0	0	0	0	0	0	0	0	4

^a Near-ZID station

Appendix F.7 *continued*

Winter 2023	Chlordane							DDT							
	A(c)C	cNon	G(t)C	Hept	HeptEpo	Methoxy	Oxychlor	tNon	o,p-DDD	o,p-DDE	o,p-DDT	p,p-DDMU	p,p-DDD	p,p-DDE	p,p-DDT
<i>19-m Stations</i>															
I35	ND	ND	ND	ND	ND	ND	ND	ND	ND	ND	ND	ND	ND	ND	ND
I34	ND	ND	ND	ND	ND	ND	ND	ND	ND	ND	ND	ND	ND	ND	ND
I31	ND	ND	ND	ND	ND	ND	ND	ND	ND	ND	ND	ND	ND	ND	ND
I23	ND	ND	ND	ND	ND	ND	ND	ND	ND	ND	ND	ND	ND	ND	ND
I18	ND	ND	ND	ND	ND	ND	ND	ND	ND	ND	ND	ND	64.9 DNQ	ND	ND
I10	ND	ND	ND	ND	ND	ND	ND	ND	ND	ND	ND	ND	ND	ND	ND
I4	ND	ND	ND	ND	ND	ND	ND	ND	ND	ND	ND	ND	ND	ND	ND
<i>28-m Stations</i>															
I33	ND	ND	ND	ND	ND	ND	ND	ND	ND	ND	ND	ND	ND	ND	ND
I30	ND	ND	ND	ND	ND	ND	ND	ND	ND	ND	ND	ND	ND	ND	ND
I27	ND	ND	ND	ND	ND	ND	ND	ND	ND	ND	ND	ND	ND	ND	ND
I22	ND	ND	ND	ND	ND	ND	ND	ND	ND	ND	ND	ND	ND	ND	ND
I14 ^a	ND	ND	ND	ND	ND	ND	ND	ND	ND	ND	ND	ND	ND	90.8	ND
I16 ^a	ND	ND	ND	ND	ND	ND	ND	ND	ND	ND	ND	ND	ND	ND	ND
I15	ND	ND	ND	ND	ND	ND	ND	ND	ND	ND	ND	ND	ND	ND	ND
I12 ^a	ND	ND	ND	ND	ND	ND	ND	ND	ND	ND	ND	ND	ND	ND	ND
I9	ND	ND	ND	ND	ND	ND	ND	ND	ND	ND	ND	ND	ND	ND	ND
I6	ND	ND	ND	ND	ND	ND	ND	ND	ND	ND	ND	ND	ND	ND	ND
I2	ND	ND	ND	ND	ND	ND	ND	ND	ND	ND	ND	ND	ND	ND	ND
I3	ND	ND	ND	ND	ND	ND	ND	ND	ND	ND	ND	ND	ND	ND	ND
<i>38-m Stations</i>															
I29	ND	ND	ND	ND	ND	ND	ND	ND	ND	83.5 DNQ	50.2 DNQ	179	620	413	ND
I21	ND	ND	ND	ND	ND	ND	ND	ND	ND	ND	ND	ND	ND	ND	ND
I13	ND	ND	ND	ND	ND	ND	ND	ND	ND	ND	ND	ND	ND	ND	ND
I8	ND	ND	ND	ND	ND	ND	ND	ND	ND	ND	ND	ND	ND	ND	ND
<i>55-m Stations</i>															
I28	ND	ND	ND	ND	ND	ND	ND	ND	ND	ND	ND	38.3 DNQ	371	73.0 DNQ	ND
I20	ND	ND	ND	ND	ND	ND	ND	ND	ND	ND	ND	ND	ND	ND	ND
I7	ND	ND	ND	ND	ND	ND	ND	ND	ND	ND	ND	ND	ND	ND	ND
I1	ND	ND	ND	ND	ND	ND	ND	ND	ND	ND	ND	ND	ND	ND	ND
DR (%)	0	0	0	0	0	0	0	0	0	0	4	4	7	15	7

^a Near-ZID station

Appendix F.7 *continued*

Winter 2023	HCH				Endosulfan				EndAld	HCB	Mirex	
	Alpha	Beta	Delta	Gamma	Aldrin	Dieldrin	Alpha	Beta				Sulfate
<i>19-m Stations</i>												
I35	ND	ND	ND	ND	ND	ND	ND	ND	ND	ND	ND	ND
I34	ND	ND	ND	ND	ND	ND	ND	ND	ND	ND	ND	ND
I31	ND	ND	ND	ND	ND	ND	ND	ND	ND	ND	ND	ND
I23	ND	ND	ND	ND	ND	ND	ND	ND	ND	ND	ND	ND
I18	ND	ND	ND	ND	ND	ND	ND	ND	ND	ND	ND	ND
I10	ND	ND	ND	ND	ND	ND	ND	ND	ND	ND	ND	ND
I4	ND	ND	ND	ND	ND	ND	ND	ND	ND	ND	ND	ND
<i>28-m Stations</i>												
I33	ND	ND	ND	ND	ND	ND	ND	ND	ND	ND	ND	ND
I30	ND	ND	ND	ND	ND	ND	ND	ND	ND	ND	ND	ND
I27	ND	ND	ND	ND	ND	ND	ND	ND	ND	ND	ND	ND
I22	ND	ND	ND	ND	ND	ND	ND	ND	ND	ND	ND	ND
I14 ^a	ND	ND	ND	ND	ND	ND	ND	ND	ND	ND	ND	ND
I16 ^a	ND	ND	ND	ND	ND	ND	ND	ND	ND	ND	ND	ND
I15	ND	ND	ND	ND	ND	ND	ND	ND	ND	ND	ND	ND
I12 ^a	ND	ND	ND	ND	ND	ND	ND	ND	ND	ND	ND	ND
I9	ND	ND	ND	ND	ND	ND	ND	ND	ND	ND	ND	ND
I6	ND	ND	ND	ND	ND	ND	ND	ND	ND	ND	ND	ND
I2	ND	ND	ND	ND	ND	ND	ND	ND	ND	ND	ND	ND
I3	ND	ND	ND	ND	ND	ND	ND	ND	ND	ND	ND	ND
<i>38-m Stations</i>												
I29	ND	ND	ND	ND	ND	ND	ND	ND	ND	ND	ND	ND
I21	ND	ND	ND	ND	ND	ND	ND	ND	ND	ND	ND	ND
I13	ND	ND	ND	ND	ND	ND	ND	ND	ND	ND	ND	ND
I8	ND	ND	ND	ND	ND	ND	ND	ND	ND	ND	ND	ND
<i>55-m Stations</i>												
I28	ND	ND	ND	ND	ND	ND	ND	ND	ND	ND	ND	ND
I20	ND	ND	ND	ND	ND	ND	ND	ND	ND	ND	ND	ND
I7	ND	ND	ND	ND	ND	ND	ND	ND	ND	ND	ND	ND
I1	ND	ND	ND	ND	ND	ND	ND	ND	ND	ND	ND	ND
DR (%)	0	0	0	0	0	0	0	0	0	0	0	0

^a Near-ZID station

Appendix F.7 *continued*

Summer 2023	Chlordane							DDT							
	A(c)C	cNon	G(t)C	Hept	HeptEpo	Methoxy	Oxychlor	tNon	o,p-DDD	o,p-DDE	o,p-DDT	p,p-DDMU	p,p-DDD	p,p-DDE	p,p-DDT
<i>19-m Stations</i>															
I35	—	—	—	—	—	—	—	—	—	—	—	—	—	—	—
I34	—	—	—	—	—	—	—	—	—	—	—	—	—	—	—
I31	—	—	—	—	—	—	—	—	—	—	—	—	—	—	—
I23	—	—	—	—	—	—	—	—	—	—	—	—	—	—	—
I18	—	—	—	—	—	—	—	—	—	—	—	—	—	—	—
I10	—	—	—	—	—	—	—	—	—	—	—	—	—	—	—
I4	—	—	—	—	—	—	—	—	—	—	—	—	—	—	—
<i>28-m Stations</i>															
I33	NR	NR	NR	NR	NR	NR	NR	NR	NR	NR	NR	NR	NR	NR	NR
I30	NR	NR	NR	NR	NR	NR	NR	NR	NR	NR	NR	NR	NR	NR	NR
I27	NR	NR	NR	NR	NR	NR	NR	NR	NR	NR	NR	NR	NR	NR	NR
I22	NR	NR	NR	NR	NR	NR	NR	NR	NR	NR	NR	NR	NR	NR	NR
I14 ^a	NR	NR	NR	NR	NR	NR	NR	NR	NR	NR	NR	NR	NR	NR	NR
I16 ^a	NR	NR	NR	NR	NR	NR	NR	NR	NR	NR	NR	NR	NR	NR	NR
I15	NR	NR	NR	NR	NR	NR	NR	NR	NR	NR	NR	NR	NR	NR	NR
I12 ^a	NR	NR	NR	NR	NR	NR	NR	NR	NR	NR	NR	NR	NR	NR	NR
I9	NR	NR	NR	NR	NR	NR	NR	NR	NR	NR	NR	NR	NR	NR	NR
I6	NR	NR	NR	NR	NR	NR	NR	NR	NR	NR	NR	NR	NR	NR	NR
I2	NR	NR	NR	NR	NR	NR	NR	NR	NR	NR	NR	NR	NR	NR	NR
I3	NR	NR	NR	NR	NR	NR	NR	NR	NR	NR	NR	NR	NR	NR	NR
<i>38-m Stations</i>															
I29	—	—	—	—	—	—	—	—	—	—	—	—	—	—	—
I21	—	—	—	—	—	—	—	—	—	—	—	—	—	—	—
I13	—	—	—	—	—	—	—	—	—	—	—	—	—	—	—
I8	—	—	—	—	—	—	—	—	—	—	—	—	—	—	—
<i>55-m Stations</i>															
I28	—	—	—	—	—	—	—	—	—	—	—	—	—	—	—
I20	—	—	—	—	—	—	—	—	—	—	—	—	—	—	—
I7	—	—	—	—	—	—	—	—	—	—	—	—	—	—	—
I1	—	—	—	—	—	—	—	—	—	—	—	—	—	—	—
DR (%)	NR	NR	NR	NR	NR	NR	NR	NR	NR	NR	NR	NR	NR	NR	NR

^a Near-ZID station

Appendix F.7 *continued*

Summer 2023	HCH										Mirex		
	Alpha	Beta	Delta	Gamma	Aldrin	Dieldrin	Alpha	Beta	Sulfate	Endrin		EndAld	HCB
<i>19-m Stations</i>													
I35	—	—	—	—	—	—	—	—	—	—	—	—	—
I34	—	—	—	—	—	—	—	—	—	—	—	—	—
I31	—	—	—	—	—	—	—	—	—	—	—	—	—
I23	—	—	—	—	—	—	—	—	—	—	—	—	—
I18	—	—	—	—	—	—	—	—	—	—	—	—	—
I10	—	—	—	—	—	—	—	—	—	—	—	—	—
I4	—	—	—	—	—	—	—	—	—	—	—	—	—
<i>28-m Stations</i>													
I33	NR	NR	NR	NR	NR	NR	NR	NR	NR	NR	NR	NR	NR
I30	NR	NR	NR	NR	NR	NR	NR	NR	NR	NR	NR	NR	NR
I27	NR	NR	NR	NR	NR	NR	NR	NR	NR	NR	NR	NR	NR
I22	NR	NR	NR	NR	NR	NR	NR	NR	NR	NR	NR	NR	NR
I14 ^a	NR	NR	NR	NR	NR	NR	NR	NR	NR	NR	NR	NR	NR
I16 ^a	NR	NR	NR	NR	NR	NR	NR	NR	NR	NR	NR	NR	NR
I15	NR	NR	NR	NR	NR	NR	NR	NR	NR	NR	NR	NR	NR
I12 ^a	NR	NR	NR	NR	NR	NR	NR	NR	NR	NR	NR	NR	NR
I9	NR	NR	NR	NR	NR	NR	NR	NR	NR	NR	NR	NR	NR
I6	NR	NR	NR	NR	NR	NR	NR	NR	NR	NR	NR	NR	NR
I2	NR	NR	NR	NR	NR	NR	NR	NR	NR	NR	NR	NR	NR
I3	NR	NR	NR	NR	NR	NR	NR	NR	NR	NR	NR	NR	NR
<i>38-m Stations</i>													
I29	—	—	—	—	—	—	—	—	—	—	—	—	—
I21	—	—	—	—	—	—	—	—	—	—	—	—	—
I13	—	—	—	—	—	—	—	—	—	—	—	—	—
I8	—	—	—	—	—	—	—	—	—	—	—	—	—
<i>55-m Stations</i>													
I28	—	—	—	—	—	—	—	—	—	—	—	—	—
I20	—	—	—	—	—	—	—	—	—	—	—	—	—
I7	—	—	—	—	—	—	—	—	—	—	—	—	—
I1	—	—	—	—	—	—	—	—	—	—	—	—	—
DR (%)	NR	NR	NR	NR	NR	NR	NR	NR	NR	NR	NR	NR	NR

^a Near-ZID station

Appendix F.8

Concentrations of PCBs (ppt) detected in sediments from PLOO stations sampled during 2022 and 2023. See Appendix F.1 for MDLs; DR = detection rate; DNQ = do not quantify; ND = not detected; NR = not reportable. Only primary core stations sampled during summer 2023 due to resource exchange for Bight'23 (see text).

	Winter																					
	PCB Congener																					
	2022	8	18	28	37	44	49	52	66	70	74	77	81	87	99	101	105	110	114	118	119	
<i>88-m Depth Contour</i>																						
B11	ND	ND	ND	ND	ND	ND	ND	ND	ND	ND	ND	ND	ND	ND	ND	ND	ND	ND	ND	ND	ND	ND
B8	ND	ND	ND	ND	ND	ND	ND	ND	ND	ND	ND	ND	ND	ND	ND	110	ND	110	ND	ND	ND	ND
E19	ND	ND	ND	ND	ND	ND	ND	ND	ND	ND	ND	ND	ND	ND	ND	ND	ND	ND	ND	ND	ND	ND
E7	ND	ND	ND	ND	ND	ND	ND	ND	ND	ND	ND	ND	ND	ND	ND	ND	ND	50.5 DNQ	ND	ND	ND	ND
E1	ND	ND	ND	ND	ND	ND	ND	ND	ND	ND	ND	ND	ND	ND	94.0	130	ND	140	ND	ND	140	ND
<i>98-m Depth Contour</i>																						
B12	ND	ND	ND	ND	ND	ND	ND	ND	ND	ND	ND	71.8 DNQ	57.7 DNQ	ND	ND	ND	ND	ND	ND	ND	72.7 DNQ	ND
B9	ND	ND	ND	ND	ND	ND	ND	ND	ND	ND	ND	ND	ND	ND	ND	ND	ND	50.6 DNQ	ND	ND	ND	ND
E26	ND	ND	ND	ND	ND	ND	ND	ND	ND	ND	ND	ND	ND	ND	ND	ND	ND	ND	ND	ND	ND	ND
E25	ND	ND	ND	ND	ND	ND	ND	ND	ND	ND	ND	ND	ND	ND	ND	ND	ND	ND	ND	ND	ND	ND
E23	ND	ND	ND	ND	ND	ND	ND	ND	ND	ND	ND	ND	ND	ND	ND	55.8 DNQ	ND	71.1 DNQ	ND	ND	66.1 DNQ	ND
E20	ND	ND	ND	ND	ND	ND	ND	ND	ND	ND	ND	ND	ND	ND	ND	ND	ND	ND	ND	ND	ND	ND
E17 ^a	ND	ND	ND	ND	ND	ND	ND	ND	ND	ND	ND	ND	ND	ND	ND	ND	ND	ND	ND	ND	ND	ND
E14 ^a	ND	ND	ND	ND	ND	ND	ND	ND	ND	ND	ND	ND	ND	ND	ND	ND	ND	ND	ND	ND	ND	ND
E11 ^a	ND	ND	ND	ND	ND	ND	ND	ND	ND	ND	ND	ND	ND	ND	ND	ND	ND	ND	ND	ND	ND	ND
E8	ND	ND	ND	ND	ND	ND	ND	ND	ND	ND	ND	ND	ND	ND	ND	50.3 DNQ	ND	ND	ND	ND	ND	ND
E5	ND	ND	ND	ND	ND	ND	ND	ND	ND	ND	ND	ND	ND	ND	ND	59.1 DNQ	ND	53.7 DNQ	ND	ND	ND	ND
E2	ND	ND	ND	ND	ND	ND	ND	ND	ND	ND	ND	ND	ND	ND	89	110	ND	130	ND	ND	120	ND
<i>116-m Depth Contour</i>																						
B10	ND	ND	ND	ND	ND	ND	ND	ND	ND	ND	ND	ND	ND	ND	ND	ND	ND	ND	ND	ND	ND	ND
E21	ND	ND	ND	ND	ND	ND	ND	ND	ND	ND	ND	ND	ND	ND	ND	52.5 DNQ	ND	69.0 DNQ	ND	ND	ND	ND
E15 ^a	ND	ND	ND	ND	ND	ND	ND	ND	ND	ND	ND	ND	ND	ND	ND	ND	ND	43.4 DNQ	ND	ND	ND	ND
E9	ND	ND	ND	ND	ND	ND	ND	ND	ND	ND	ND	ND	ND	ND	ND	62.5 DNQ	ND	53.2 DNQ	ND	ND	ND	ND
E3	ND	70.6 DNQ	62.6 DNQ	ND	ND	180	470	520	540	680	280	ND	ND	1600	3000	4700	2400	3900	170	7300	340	
DR (%)	0	5	5	5	0	5	5	5	5	5	5	5	5	5	14	41	5	50	5	5	23	5

^a Near-ZID station

Appendix F.8 *continued*

		PCB Congener																						
Winter	2022	123	126	128	138	149	151	153/168	156	157	158	167	169	170	177	180	183	187	189	194	195	201	206	
<i>88-m Depth Contour</i>																								
B11	ND	ND	ND	ND	ND	ND	ND	ND	ND	ND	ND	ND	ND	ND	ND	ND	ND	ND	ND	ND	ND	ND	ND	ND
B8	ND	ND	ND	ND	230	260	86.0 DNQ	480	ND	ND	ND	ND	ND	120	82.8 DNQ	310	73.8 DNQ	160	ND	81.7 DNQ	ND	ND	ND	ND
E19	ND	ND	ND	ND	ND	ND	ND	ND	ND	ND	ND	ND	ND	ND	ND	ND	ND	ND	ND	ND	ND	ND	ND	ND
E7	ND	ND	ND	ND	ND	ND	ND	ND	ND	ND	ND	ND	ND	ND	ND	ND	ND	ND	ND	ND	ND	ND	ND	ND
E1	ND	ND	ND	ND	ND	150	ND	240	ND	ND	ND	ND	ND	45.7 DNQ	35.3 DNQ	110	76.4 DNQ	ND	ND	ND	ND	ND	ND	ND
<i>98-m Depth Contour</i>																								
B12	ND	ND	ND	ND	ND	ND	ND	ND	ND	ND	ND	ND	ND	ND	ND	ND	ND	ND	ND	ND	ND	ND	ND	ND
B9	ND	ND	ND	ND	92.3 DNQ	ND	ND	ND	ND	ND	ND	ND	ND	80.3 DNQ	46.5 DNQ	190	ND	85.5 DNQ	ND	160	44.1 DNQ	ND	ND	110
E26	ND	ND	ND	ND	63.2 DNQ	ND	ND	ND	ND	ND	ND	ND	ND	ND	ND	ND	ND	ND	ND	ND	ND	ND	ND	ND
E25	ND	ND	ND	ND	ND	ND	ND	ND	ND	ND	ND	ND	ND	ND	ND	ND	ND	ND	ND	ND	ND	ND	ND	ND
E23	ND	ND	ND	ND	70.2 DNQ	ND	ND	ND	ND	ND	ND	ND	ND	ND	ND	ND	ND	ND	ND	ND	ND	ND	ND	ND
E20	ND	ND	ND	ND	ND	ND	ND	ND	ND	ND	ND	ND	ND	ND	ND	ND	ND	ND	ND	ND	ND	ND	ND	ND
E17 ^a	ND	ND	ND	ND	ND	ND	ND	ND	ND	ND	ND	ND	ND	ND	ND	ND	ND	ND	ND	ND	ND	ND	ND	ND
E14 ^a	ND	ND	ND	ND	ND	ND	ND	ND	ND	ND	ND	ND	ND	ND	ND	ND	ND	ND	ND	ND	ND	ND	ND	ND
E11 ^a	ND	ND	ND	ND	ND	ND	ND	ND	ND	ND	ND	ND	ND	ND	ND	ND	ND	ND	ND	ND	ND	ND	ND	ND
E8	ND	ND	ND	ND	ND	ND	ND	ND	ND	ND	ND	ND	ND	ND	ND	ND	ND	ND	ND	ND	ND	ND	ND	ND
E5	ND	ND	ND	ND	ND	ND	ND	ND	ND	ND	ND	ND	ND	64.0 DNQ	ND	110	ND	ND	ND	ND	ND	ND	ND	ND
E2	ND	ND	ND	ND	ND	110	ND	ND	ND	ND	ND	ND	ND	ND	ND	ND	ND	58.9 DNQ	ND	ND	ND	ND	ND	ND
<i>116-m Depth Contour</i>																								
B10	ND	ND	ND	ND	ND	ND	ND	ND	ND	ND	ND	ND	ND	ND	ND	ND	ND	ND	ND	ND	ND	ND	ND	ND
E21	ND	ND	ND	ND	ND	ND	ND	ND	ND	ND	ND	ND	ND	ND	ND	ND	ND	ND	ND	ND	ND	ND	ND	ND
E15 ^a	ND	ND	ND	ND	ND	ND	ND	ND	ND	ND	ND	ND	ND	ND	ND	ND	ND	ND	ND	ND	ND	ND	ND	ND
E9	ND	ND	ND	ND	77.8 DNQ	ND	ND	ND	ND	ND	ND	ND	ND	ND	ND	ND	ND	ND	ND	ND	ND	ND	ND	ND
E3	560	ND	1600	5500	3100	730	7500	1100	220	810	330	ND	680	280	1000	260	480	ND	150	59.0	ND	150	ND	110
DR (%)	5	0	0	5	27	18	9	14	5	5	5	5	0	23	18	23	9	23	0	14	9	0	0	9

^aNear-ZID station

Appendix F.8 continued

Summer 2022	PCB Congener																				
	8	18	28	37	44	49	52	66	70	74	77	81	87	99	101	105	110	114	118	119	
<i>88-m Depth Contour</i>																					
B11	ND	ND	ND	ND	ND	ND	ND	ND	ND	ND	ND	ND	ND	ND	ND	ND	ND	ND	ND	ND	ND
B8	ND	ND	ND	ND	ND	ND	ND	ND	ND	ND	ND	ND	ND	71.6 DNQ	110	ND	120	ND	150	ND	ND
E19	ND	ND	ND	ND	ND	ND	ND	ND	ND	ND	ND	ND	ND	ND	ND	ND	ND	ND	ND	ND	ND
E7	ND	ND	ND	ND	ND	ND	ND	ND	ND	ND	ND	ND	ND	ND	ND	ND	ND	ND	ND	ND	ND
E1	ND	ND	32.8 DNQ	ND	68.2 DNQ	83.5 DNQ	130	78.0 DNQ	95.0	ND	ND	ND	110	150	270	110	250	ND	250	ND	ND
<i>98-m Depth Contour</i>																					
B12	ND	ND	ND	ND	ND	ND	ND	ND	ND	ND	ND	ND	ND	ND	ND	ND	ND	ND	ND	ND	ND
B9	ND	ND	ND	ND	ND	ND	ND	ND	ND	ND	ND	ND	ND	ND	ND	ND	54.0 DNQ	ND	ND	ND	ND
E26	ND	ND	ND	ND	ND	ND	ND	ND	ND	ND	ND	ND	ND	ND	49.9 DNQ	ND	50.4 DNQ	ND	66.0 DNQ	ND	ND
E25	ND	ND	ND	ND	ND	ND	ND	ND	ND	ND	ND	ND	ND	ND	ND	ND	ND	ND	ND	ND	ND
E23	ND	ND	ND	ND	ND	ND	ND	ND	ND	ND	ND	ND	ND	ND	ND	ND	ND	ND	ND	ND	ND
E20	ND	ND	ND	ND	ND	ND	ND	ND	ND	ND	ND	ND	ND	ND	ND	ND	ND	ND	ND	ND	ND
E17 ^a	ND	ND	ND	ND	ND	ND	ND	ND	ND	ND	ND	ND	ND	ND	ND	ND	ND	ND	ND	ND	ND
E14 ^a	ND	ND	ND	ND	ND	ND	ND	ND	ND	ND	ND	ND	ND	ND	ND	ND	ND	ND	ND	ND	ND
E11 ^a	ND	ND	ND	ND	ND	ND	ND	ND	ND	ND	ND	ND	ND	ND	ND	ND	ND	ND	ND	ND	ND
E8	ND	ND	ND	ND	ND	ND	ND	ND	ND	ND	ND	ND	ND	ND	ND	ND	ND	ND	ND	ND	ND
E5	ND	ND	ND	ND	ND	ND	ND	ND	ND	ND	ND	ND	ND	ND	56.5 DNQ	ND	52.5 DNQ	ND	ND	ND	ND
E2	ND	ND	ND	ND	140	81.7 DNQ	260	110	190	69.4 DNQ	ND	ND	210	210	450	180	480	ND	400	ND	ND
<i>116-m Depth Contour</i>																					
B10	ND	ND	ND	ND	ND	ND	ND	ND	ND	ND	ND	ND	ND	ND	ND	ND	ND	ND	ND	ND	ND
E21	ND	ND	ND	ND	ND	ND	ND	ND	ND	ND	ND	ND	ND	ND	ND	ND	ND	ND	ND	ND	ND
E15 ^a	ND	ND	ND	ND	ND	ND	ND	ND	ND	ND	ND	ND	ND	ND	ND	ND	ND	ND	ND	ND	ND
E9	ND	ND	ND	ND	ND	ND	ND	ND	ND	ND	ND	ND	ND	ND	ND	ND	ND	ND	ND	ND	ND
E3	ND	81.5 DNQ	88.0	ND	190	170	350	140	220	75.0 DNQ	ND	ND	250	220	540	190	550	ND	450	ND	ND
DR (%)	0	5	9	0	14	14	14	14	14	9	0	0	14	18	27	14	32	0	23	0	0

^aNear-ZID station

Appendix F.8 *continued*

		PCB Congener																						
Summer	2022	123	126	128	138	149	151	153/168	156	157	158	167	169	170	177	180	183	187	189	194	195	201	206	
<i>88-m Depth Contour</i>																								
B11	ND	ND	ND	ND	72.7 DNQ	ND	ND	ND	ND	ND	ND	ND	ND	ND	ND	ND	ND	48.9 DNQ	ND	ND	ND	ND	ND	
B8	ND	ND	ND	ND	140	110	ND	ND	ND	ND	ND	ND	ND	ND	ND	57.1 DNQ	ND	ND	ND	ND	ND	ND	ND	
E19	ND	ND	ND	ND	ND	ND	ND	ND	ND	ND	ND	ND	ND	ND	ND	ND	ND	ND	ND	ND	ND	ND	ND	
E7	ND	ND	ND	ND	ND	ND	ND	ND	ND	ND	ND	ND	ND	ND	ND	ND	ND	ND	ND	ND	ND	ND	ND	
E1	ND	ND	76.7 DNQ	230	300	64.3 DNQ	410	ND	ND	ND	ND	ND	ND	83.6 DNQ	52.8 DNQ	160	44.2 DNQ	120	ND	ND	ND	ND	ND	
<i>98-m Depth Contour</i>																								
B12	ND	ND	ND	ND	ND	ND	ND	ND	ND	ND	ND	ND	ND	ND	ND	ND	ND	ND	ND	ND	ND	ND	ND	ND
B9	ND	ND	ND	ND	ND	ND	ND	ND	ND	ND	ND	ND	ND	ND	ND	ND	ND	ND	ND	ND	ND	ND	ND	ND
E26	ND	ND	ND	ND	72.8 DNQ	ND	ND	ND	ND	ND	ND	ND	ND	ND	ND	52.9 DNQ	ND	48.7 DNQ	ND	ND	ND	ND	ND	ND
E25	ND	ND	ND	ND	ND	ND	ND	ND	ND	ND	ND	ND	ND	ND	ND	ND	ND	ND	ND	ND	ND	ND	ND	ND
E23	ND	ND	ND	ND	ND	ND	ND	ND	ND	ND	ND	ND	ND	ND	ND	ND	ND	ND	ND	ND	ND	ND	ND	ND
E20	ND	ND	ND	ND	ND	ND	ND	ND	ND	ND	ND	ND	ND	ND	ND	ND	ND	ND	ND	ND	ND	ND	ND	ND
E17 ^a	ND	ND	ND	ND	ND	ND	ND	ND	ND	ND	ND	ND	ND	ND	ND	ND	ND	ND	ND	ND	ND	ND	ND	ND
E14 ^a	ND	ND	ND	ND	ND	ND	ND	ND	ND	ND	ND	ND	ND	ND	ND	ND	ND	ND	ND	ND	ND	ND	ND	ND
E11 ^a	ND	ND	ND	ND	ND	ND	ND	ND	ND	ND	ND	ND	ND	ND	ND	ND	ND	ND	ND	ND	ND	ND	ND	ND
E8	ND	ND	ND	ND	ND	ND	ND	ND	ND	ND	ND	ND	ND	ND	ND	ND	ND	ND	ND	ND	ND	ND	ND	ND
E5	ND	ND	ND	ND	67.8 DNQ	ND	ND	ND	ND	ND	ND	ND	ND	ND	ND	ND	ND	ND	ND	ND	ND	ND	ND	ND
E2	ND	ND	110	290	300	58.3 DNQ	450	ND	ND	ND	ND	ND	ND	75.2 DNQ	40.0 DNQ	110	34.4 DNQ	82.7 DNQ	ND	ND	ND	ND	ND	ND
<i>116-m Depth Contour</i>																								
B10	ND	ND	ND	ND	ND	ND	ND	ND	ND	ND	ND	ND	ND	ND	ND	ND	ND	ND	ND	ND	ND	ND	ND	ND
E21	ND	ND	ND	ND	ND	ND	ND	ND	ND	ND	ND	ND	ND	ND	ND	ND	ND	ND	ND	ND	ND	ND	ND	ND
E15 ^a	ND	ND	ND	ND	ND	ND	ND	ND	ND	ND	ND	ND	ND	ND	ND	ND	ND	ND	ND	ND	ND	ND	ND	ND
E9	ND	ND	ND	ND	ND	ND	ND	ND	ND	ND	ND	ND	ND	ND	ND	ND	ND	ND	ND	ND	ND	ND	ND	ND
E3	ND	ND	130	380	370	92.0	620	ND	ND	ND	ND	ND	ND	85.0	56.9 DNQ	160	46.7 DNQ	110	ND	ND	ND	ND	ND	ND
DR (%)	0	0	14	32	18	14	14	0	0	0	0	0	0	14	14	23	14	23	0	0	0	0	0	0

^aNear-ZID station

Appendix F.8 *continued*

	PCB Congener																					
	2023	8	18	28	37	44	49	52	66	70	74	77	81	87	99	101	105	110	114	118	119	
<i>88-m Depth Contour</i>																						
B11	ND	ND	ND	ND	ND	ND	ND	ND	ND	ND	ND	ND	ND	ND	ND	ND	ND	ND	ND	ND	ND	ND
B8	ND	ND	ND	ND	ND	ND	ND	ND	ND	ND	ND	ND	ND	ND	ND	100	ND	110	ND	100	ND	ND
E19	ND	ND	ND	ND	ND	ND	ND	ND	ND	ND	ND	ND	ND	ND	ND	ND	ND	ND	ND	ND	ND	ND
E7	ND	ND	ND	ND	ND	ND	ND	ND	ND	ND	ND	ND	ND	ND	ND	ND	ND	ND	ND	ND	ND	ND
E1	ND	ND	ND	ND	ND	ND	ND	ND	ND	ND	ND	ND	ND	ND	58.1 DNQ	110	ND	110	ND	100	ND	ND
<i>98-m Depth Contour</i>																						
B12	ND	ND	ND	ND	ND	ND	ND	ND	ND	ND	ND	ND	ND	ND	ND	ND	ND	ND	ND	ND	ND	ND
B9	ND	ND	ND	ND	ND	ND	ND	ND	ND	ND	ND	ND	ND	ND	ND	110	ND	120	ND	99	ND	ND
E26	ND	ND	ND	ND	ND	ND	ND	ND	ND	ND	ND	ND	ND	ND	ND	ND	ND	ND	ND	ND	ND	ND
E25	ND	ND	ND	ND	ND	ND	ND	ND	ND	ND	ND	ND	ND	ND	ND	ND	ND	ND	ND	ND	ND	ND
E23	ND	ND	ND	ND	ND	ND	ND	ND	ND	ND	ND	ND	ND	ND	ND	ND	ND	37.3 DNQ	ND	ND	ND	ND
E20	ND	ND	ND	ND	ND	ND	ND	ND	ND	ND	ND	ND	ND	ND	ND	ND	ND	ND	ND	ND	ND	ND
E17 ^a	ND	ND	ND	ND	ND	ND	ND	ND	ND	ND	ND	ND	ND	ND	ND	ND	ND	ND	ND	ND	ND	ND
E14 ^a	ND	ND	ND	ND	ND	ND	ND	ND	ND	ND	ND	ND	ND	ND	ND	ND	ND	ND	ND	ND	ND	ND
E11 ^a	ND	ND	ND	ND	ND	ND	ND	ND	ND	ND	ND	ND	ND	ND	ND	ND	ND	ND	ND	ND	ND	ND
E8	ND	ND	ND	ND	ND	ND	ND	ND	ND	ND	ND	ND	ND	ND	ND	ND	ND	ND	ND	ND	ND	ND
E5	ND	ND	ND	ND	ND	ND	ND	ND	ND	ND	ND	ND	ND	ND	ND	54.3 DNQ	ND	55.9 DNQ	ND	ND	ND	ND
E2	ND	ND	ND	ND	ND	ND	ND	ND	ND	ND	ND	ND	ND	ND	88.2 DNQ	130	ND	140	ND	130	ND	ND
<i>116-m Depth Contour</i>																						
B10	ND	ND	ND	ND	ND	ND	ND	ND	ND	ND	ND	ND	ND	ND	ND	ND	ND	ND	ND	ND	ND	ND
E21	ND	ND	ND	ND	ND	68.7 DNQ	ND	170	ND	110	ND	ND	ND	180	140	370	140	390	ND	330	ND	ND
E15 ^a	ND	ND	ND	ND	ND	ND	ND	ND	ND	ND	ND	ND	ND	ND	ND	ND	ND	ND	ND	ND	ND	ND
E9	ND	ND	ND	ND	ND	ND	ND	ND	ND	ND	ND	ND	ND	ND	ND	68.8 DNQ	ND	68.1 DNQ	ND	66.4 DNQ	ND	ND
E3	ND	ND	37.8 DNQ	ND	ND	170	110	390	120	270	74.3 DNQ	ND	ND	420	310	860	330	930	ND	760	ND	ND
DR (%)	0	0	0	5	0	9	5	9	5	9	5	0	0	9	18	36	9	41	0	32	0	0

^aNear-ZID station

Appendix F.8 *continued*

		PCB Congener																						
		2023	123	126	128	138	149	151	153/168	156	157	158	167	169	170	177	180	183	187	189	194	195	201	206
<i>88-m Depth Contour</i>																								
B11	ND	ND	ND	ND	ND	ND	ND	ND	ND	ND	ND	ND	ND	ND	ND	ND	ND	ND	ND	ND	ND	ND	ND	ND
B8	ND	ND	ND	100	ND	ND	ND	ND	ND	ND	ND	ND	ND	ND	ND	ND	ND	ND	ND	ND	ND	ND	ND	ND
E19	ND	ND	ND	ND	ND	ND	ND	ND	ND	ND	ND	ND	ND	ND	ND	ND	ND	ND	ND	ND	ND	ND	ND	ND
E7	ND	ND	ND	ND	ND	ND	ND	ND	ND	ND	ND	ND	ND	ND	ND	ND	ND	ND	ND	ND	ND	ND	ND	230
E1	ND	ND	ND	110	99	ND	ND	ND	ND	ND	ND	ND	ND	ND	ND	51.4 DNQ	ND	39.0 DNQ	ND	ND	ND	ND	ND	ND
<i>98-m Depth Contour</i>																								
B12	ND	ND	ND	ND	ND	ND	ND	ND	ND	ND	ND	ND	ND	ND	ND	ND	ND	ND	ND	ND	ND	ND	ND	ND
B9	ND	ND	ND	84	ND	ND	ND	ND	ND	ND	ND	ND	ND	ND	ND	ND	ND	ND	ND	ND	ND	ND	ND	ND
E26	ND	ND	ND	ND	ND	ND	ND	ND	ND	ND	ND	ND	ND	ND	ND	ND	ND	ND	ND	ND	ND	ND	ND	ND
E25	ND	ND	ND	ND	ND	ND	ND	ND	ND	ND	ND	ND	ND	ND	ND	ND	ND	ND	ND	ND	ND	ND	ND	ND
E23	ND	ND	ND	ND	ND	ND	ND	ND	ND	ND	ND	ND	ND	ND	ND	ND	ND	ND	ND	ND	ND	ND	ND	ND
E20	ND	ND	ND	ND	ND	ND	ND	ND	ND	ND	ND	ND	ND	ND	ND	ND	ND	ND	ND	ND	ND	ND	ND	ND
E17 ^a	ND	ND	ND	ND	ND	ND	ND	ND	ND	ND	ND	ND	ND	ND	ND	ND	ND	ND	ND	ND	ND	ND	ND	ND
E14 ^a	ND	ND	ND	ND	ND	ND	ND	ND	ND	ND	ND	ND	ND	ND	ND	ND	ND	ND	ND	ND	ND	ND	ND	ND
E11 ^a	ND	ND	ND	ND	ND	ND	ND	ND	ND	ND	ND	ND	ND	ND	ND	ND	ND	ND	ND	ND	ND	ND	ND	ND
E8	ND	ND	ND	ND	ND	ND	ND	ND	ND	ND	ND	ND	ND	ND	ND	ND	ND	ND	ND	ND	ND	ND	ND	ND
E5	ND	ND	ND	ND	ND	ND	ND	ND	ND	ND	ND	ND	ND	ND	ND	ND	ND	ND	ND	ND	ND	ND	ND	ND
E2	ND	ND	55.6 DNQ	160	150	ND	ND	ND	ND	ND	ND	ND	ND	ND	ND	29.4 DNQ	87.7 DNQ	69.8 DNQ	ND	ND	ND	ND	ND	ND
<i>116-m Depth Contour</i>																								
B10	ND	ND	ND	ND	ND	ND	ND	ND	ND	ND	ND	ND	ND	ND	ND	ND	ND	ND	ND	ND	ND	ND	ND	ND
E21	ND	ND	93.0	290	210	ND	410	ND	ND	ND	ND	47.4 DNQ	ND	ND	ND	89	ND	45.8 DNQ	ND	ND	ND	ND	ND	ND
E15 ^a	ND	ND	ND	ND	ND	ND	ND	ND	ND	ND	ND	ND	ND	ND	ND	ND	ND	ND	ND	ND	ND	ND	ND	ND
E9	ND	ND	ND	81.2 DNQ	ND	ND	ND	ND	ND	ND	ND	ND	ND	ND	ND	ND	ND	ND	ND	ND	ND	ND	ND	ND
E3	ND	ND	250	750	570	110	760	120	52.0 DNQ	120	5	130	62.7 DNQ	170	50.5 DNQ	84.0	ND	ND	ND	ND	ND	ND	ND	ND
DR (%)	0	0	14	32	18	5	9	5	5	5	0	14	9	18	5	18	5	18	0	0	0	0	0	5

^a Near-ZID station

Appendix F.8 *continued*

Summer	PCB Congener																					
	2023	8	18	28	37	44	49	52	66	70	74	77	81	87	99	101	105	110	114	118	119	
<i>88-m Depth Contour</i>																						
B11	—	—	—	—	—	—	—	—	—	—	—	—	—	—	—	—	—	—	—	—	—	—
B8	—	—	—	—	—	—	—	—	—	—	—	—	—	—	—	—	—	—	—	—	—	—
E19	—	—	—	—	—	—	—	—	—	—	—	—	—	—	—	—	—	—	—	—	—	—
E7	—	—	—	—	—	—	—	—	—	—	—	—	—	—	—	—	—	—	—	—	—	—
E1	—	—	—	—	—	—	—	—	—	—	—	—	—	—	—	—	—	—	—	—	—	—
<i>98-m Depth Contour</i>																						
B12	NR	NR	NR	NR	NR	NR	NR	NR	NR	NR	NR	NR	NR	NR	NR	NR	NR	NR	NR	NR	NR	NR
B9	NR	NR	NR	NR	NR	NR	NR	NR	NR	NR	NR	NR	NR	NR	NR	NR	NR	NR	NR	NR	NR	NR
E26	NR	NR	NR	NR	NR	NR	NR	NR	NR	NR	NR	NR	NR	NR	NR	NR	NR	NR	NR	NR	NR	NR
E25	NR	NR	NR	NR	NR	NR	NR	NR	NR	NR	NR	NR	NR	NR	NR	NR	NR	NR	NR	NR	NR	NR
E23	NR	NR	NR	NR	NR	NR	NR	NR	NR	NR	NR	NR	NR	NR	NR	NR	NR	NR	NR	NR	NR	NR
E20	NR	NR	NR	NR	NR	NR	NR	NR	NR	NR	NR	NR	NR	NR	NR	NR	NR	NR	NR	NR	NR	NR
E17 ^a	NR	NR	NR	NR	NR	NR	NR	NR	NR	NR	NR	NR	NR	NR	NR	NR	NR	NR	NR	NR	NR	NR
E14 ^a	NR	NR	NR	NR	NR	NR	NR	NR	NR	NR	NR	NR	NR	NR	NR	NR	NR	NR	NR	NR	NR	NR
E11 ^a	NR	NR	NR	NR	NR	NR	NR	NR	NR	NR	NR	NR	NR	NR	NR	NR	NR	NR	NR	NR	NR	NR
E8	NR	NR	NR	NR	NR	NR	NR	NR	NR	NR	NR	NR	NR	NR	NR	NR	NR	NR	NR	NR	NR	NR
E5	NR	NR	NR	NR	NR	NR	NR	NR	NR	NR	NR	NR	NR	NR	NR	NR	NR	NR	NR	NR	NR	NR
E2	NR	NR	NR	NR	NR	NR	NR	NR	NR	NR	NR	NR	NR	NR	NR	NR	NR	NR	NR	NR	NR	NR
<i>116-m Depth Contour</i>																						
B10	—	—	—	—	—	—	—	—	—	—	—	—	—	—	—	—	—	—	—	—	—	—
E21	—	—	—	—	—	—	—	—	—	—	—	—	—	—	—	—	—	—	—	—	—	—
E15 ^a	NR	NR	NR	NR	NR	NR	NR	NR	NR	NR	NR	NR	NR	NR	NR	NR	NR	NR	NR	NR	NR	NR
E9	—	—	—	—	—	—	—	—	—	—	—	—	—	—	—	—	—	—	—	—	—	—
E3	—	—	—	—	—	—	—	—	—	—	—	—	—	—	—	—	—	—	—	—	—	—
DR (%)	NR	NR	NR	NR	NR	NR	NR	NR	NR	NR	NR	NR	NR	NR	NR	NR	NR	NR	NR	NR	NR	NR

^a Near-ZID station

Appendix F.8 *continued*

Summer	PCB Congener																							
	2023	123	126	128	138	149	151	153/168	156	157	158	167	169	170	177	180	183	187	189	194	195	201	206	
<i>88-m Depth Contour</i>																								
B11	—	—	—	—	—	—	—	—	—	—	—	—	—	—	—	—	—	—	—	—	—	—	—	—
B8	—	—	—	—	—	—	—	—	—	—	—	—	—	—	—	—	—	—	—	—	—	—	—	—
E19	—	—	—	—	—	—	—	—	—	—	—	—	—	—	—	—	—	—	—	—	—	—	—	—
E7	—	—	—	—	—	—	—	—	—	—	—	—	—	—	—	—	—	—	—	—	—	—	—	—
E1	—	—	—	—	—	—	—	—	—	—	—	—	—	—	—	—	—	—	—	—	—	—	—	—
<i>98-m Depth Contour</i>																								
B12	NR	NR	NR	NR	NR	NR	NR	NR	NR	NR	NR	NR	NR	NR	NR	NR	NR	NR	NR	NR	NR	NR	NR	NR
B9	NR	NR	NR	NR	NR	NR	NR	NR	NR	NR	NR	NR	NR	NR	NR	NR	NR	NR	NR	NR	NR	NR	NR	NR
E26	NR	NR	NR	NR	NR	NR	NR	NR	NR	NR	NR	NR	NR	NR	NR	NR	NR	NR	NR	NR	NR	NR	NR	NR
E25	NR	NR	NR	NR	NR	NR	NR	NR	NR	NR	NR	NR	NR	NR	NR	NR	NR	NR	NR	NR	NR	NR	NR	NR
E23	NR	NR	NR	NR	NR	NR	NR	NR	NR	NR	NR	NR	NR	NR	NR	NR	NR	NR	NR	NR	NR	NR	NR	NR
E20	NR	NR	NR	NR	NR	NR	NR	NR	NR	NR	NR	NR	NR	NR	NR	NR	NR	NR	NR	NR	NR	NR	NR	NR
E17 ^a	NR	NR	NR	NR	NR	NR	NR	NR	NR	NR	NR	NR	NR	NR	NR	NR	NR	NR	NR	NR	NR	NR	NR	NR
E14 ^a	NR	NR	NR	NR	NR	NR	NR	NR	NR	NR	NR	NR	NR	NR	NR	NR	NR	NR	NR	NR	NR	NR	NR	NR
E11 ^a	NR	NR	NR	NR	NR	NR	NR	NR	NR	NR	NR	NR	NR	NR	NR	NR	NR	NR	NR	NR	NR	NR	NR	NR
E8	NR	NR	NR	NR	NR	NR	NR	NR	NR	NR	NR	NR	NR	NR	NR	NR	NR	NR	NR	NR	NR	NR	NR	NR
E5	NR	NR	NR	NR	NR	NR	NR	NR	NR	NR	NR	NR	NR	NR	NR	NR	NR	NR	NR	NR	NR	NR	NR	NR
E2	NR	NR	NR	NR	NR	NR	NR	NR	NR	NR	NR	NR	NR	NR	NR	NR	NR	NR	NR	NR	NR	NR	NR	NR
<i>116-m Depth Contour</i>																								
B10	—	—	—	—	—	—	—	—	—	—	—	—	—	—	—	—	—	—	—	—	—	—	—	—
E21	—	—	—	—	—	—	—	—	—	—	—	—	—	—	—	—	—	—	—	—	—	—	—	—
E15 ^a	NR	NR	NR	NR	NR	NR	NR	NR	NR	NR	NR	NR	NR	NR	NR	NR	NR	NR	NR	NR	NR	NR	NR	NR
E9	—	—	—	—	—	—	—	—	—	—	—	—	—	—	—	—	—	—	—	—	—	—	—	—
E3	—	—	—	—	—	—	—	—	—	—	—	—	—	—	—	—	—	—	—	—	—	—	—	—
DR (%)	NR	NR	NR	NR	NR	NR	NR	NR	NR	NR	NR	NR	NR	NR	NR	NR	NR	NR	NR	NR	NR	NR	NR	NR

^aNear-ZID station

Appendix F.9

Concentrations of PCBs (ppt) detected in sediments from SBOO stations sampled during 2022 and 2023. See Appendix F.1 for MDLs; DR=detection rate; DNQ = do not quantify; ND = not detected; NR = not reportable. Only primary core stations sampled during summer 2023 due to resource exchange for Bight'23 (see text).

	PCB Congener																				
	8	18	28	37	44	49	52	66	70	74	77	81	87	99	101	105	110	114	118	119	
Winter 2022																					
<i>19-m Stations</i>																					
I35	ND	ND	ND	ND	ND	ND	ND	ND	ND	ND	ND	ND	ND	ND	ND	ND	ND	ND	ND	ND	ND
I34	ND	ND	ND	ND	ND	ND	ND	ND	ND	ND	ND	ND	ND	ND	ND	ND	ND	ND	ND	ND	ND
I31	ND	ND	ND	ND	ND	ND	ND	ND	ND	ND	ND	ND	ND	ND	ND	ND	ND	ND	ND	ND	ND
I23	ND	ND	ND	ND	ND	ND	ND	ND	ND	ND	ND	ND	ND	ND	ND	ND	ND	ND	ND	ND	ND
I18	ND	ND	ND	ND	ND	ND	ND	ND	ND	ND	ND	ND	ND	ND	ND	ND	ND	ND	ND	ND	ND
I10	ND	ND	ND	ND	ND	ND	ND	ND	ND	ND	ND	ND	ND	ND	ND	ND	ND	ND	ND	ND	ND
I4	ND	ND	ND	ND	ND	ND	ND	ND	ND	ND	ND	ND	ND	ND	ND	ND	ND	ND	ND	ND	ND
<i>28-m Stations</i>																					
I33	ND	ND	ND	ND	ND	ND	ND	ND	ND	ND	ND	ND	ND	ND	ND	ND	ND	ND	ND	ND	ND
I30	ND	ND	ND	ND	ND	ND	ND	ND	ND	ND	ND	ND	ND	ND	ND	ND	ND	ND	ND	ND	ND
I27	ND	ND	ND	ND	ND	ND	ND	ND	ND	ND	ND	ND	ND	ND	ND	ND	ND	ND	ND	ND	ND
I22	ND	ND	ND	ND	ND	ND	ND	ND	ND	ND	ND	ND	ND	ND	ND	ND	ND	ND	ND	ND	ND
I14 ^a	ND	ND	ND	ND	ND	ND	ND	ND	ND	ND	ND	ND	ND	ND	ND	ND	ND	ND	ND	ND	ND
I16 ^a	ND	ND	ND	ND	ND	ND	ND	ND	ND	ND	ND	ND	ND	ND	ND	ND	ND	ND	ND	ND	ND
I15	ND	ND	ND	ND	ND	ND	ND	ND	ND	ND	ND	ND	ND	ND	ND	ND	ND	ND	ND	ND	ND
I12 ^a	ND	ND	ND	ND	ND	ND	ND	ND	ND	ND	ND	ND	ND	ND	ND	ND	ND	ND	ND	ND	ND
I9	ND	ND	ND	ND	ND	ND	ND	ND	ND	ND	ND	ND	ND	ND	ND	ND	ND	ND	ND	ND	ND
I6	ND	ND	ND	ND	ND	ND	ND	ND	ND	ND	ND	ND	ND	ND	ND	ND	ND	ND	ND	ND	ND
I2	ND	ND	ND	ND	ND	ND	ND	ND	ND	ND	ND	ND	ND	ND	ND	ND	ND	ND	ND	ND	ND
I3	ND	ND	ND	ND	ND	ND	ND	ND	ND	ND	ND	ND	ND	ND	ND	ND	ND	ND	ND	ND	ND
<i>38-m Stations</i>																					
I29	ND	ND	ND	ND	ND	ND	ND	ND	ND	ND	ND	ND	ND	ND	ND	ND	ND	ND	ND	ND	ND
I21	ND	ND	ND	ND	ND	ND	ND	ND	ND	ND	ND	ND	ND	ND	ND	ND	ND	ND	ND	ND	ND
I13	ND	ND	ND	ND	ND	ND	ND	ND	ND	ND	ND	ND	ND	ND	ND	ND	ND	ND	ND	ND	ND
I8	ND	ND	ND	ND	ND	ND	ND	ND	ND	ND	ND	ND	ND	ND	ND	ND	ND	ND	ND	ND	ND
<i>55-m Stations</i>																					
I28	ND	ND	ND	ND	ND	ND	ND	ND	ND	ND	ND	ND	ND	65.6 DNQ	73.5 DNQ	ND	66.0 DNQ	ND	93.0	ND	ND
I20	ND	ND	ND	ND	ND	ND	ND	ND	ND	ND	ND	ND	ND	ND	ND	ND	ND	ND	ND	ND	ND
I7	ND	ND	ND	ND	ND	ND	ND	ND	ND	ND	ND	ND	ND	ND	ND	ND	ND	ND	ND	ND	ND
I1	ND	ND	ND	ND	ND	ND	ND	ND	ND	ND	ND	ND	ND	ND	ND	ND	ND	ND	ND	ND	ND
DR (%)	0	0	0	0	0	0	0	0	0	0	0	0	0	4	4	0	4	0	4	0	0

^aNear-ZID station

Appendix F.9 *continued*

		PCB Congener																			
Winter 2022	123	126	128	138	149	151 ^{153/168}	156	157	158	167	169	170	177	180	183	187	189	194	195	201	206
<i>19-m Stations</i>																					
I35	ND	ND	ND	ND	ND	ND	ND	ND	ND	ND	ND	ND	ND	ND	ND	ND	ND	ND	ND	ND	ND
I34	ND	ND	ND	ND	ND	ND	ND	ND	ND	ND	ND	ND	ND	ND	ND	ND	ND	ND	ND	ND	ND
I31	ND	ND	ND	ND	ND	ND	ND	ND	ND	ND	ND	ND	ND	ND	ND	ND	ND	ND	ND	ND	ND
I23	ND	ND	ND	ND	ND	ND	ND	ND	ND	ND	ND	ND	ND	ND	ND	ND	ND	ND	ND	ND	ND
I18	ND	ND	ND	ND	ND	ND	ND	ND	ND	ND	ND	ND	ND	ND	ND	ND	ND	ND	ND	ND	ND
I10	ND	ND	ND	ND	ND	ND	ND	ND	ND	ND	ND	ND	ND	ND	ND	ND	ND	ND	ND	ND	ND
I4	ND	ND	ND	ND	ND	ND	ND	ND	ND	ND	ND	ND	ND	ND	ND	ND	ND	ND	ND	ND	ND
<i>28-m Stations</i>																					
I33	ND	ND	ND	ND	ND	ND	ND	ND	ND	ND	ND	ND	ND	ND	ND	ND	ND	ND	ND	ND	ND
I30	ND	ND	ND	ND	ND	ND	ND	ND	ND	ND	ND	ND	ND	ND	ND	ND	ND	ND	ND	ND	ND
I27	ND	ND	ND	ND	ND	ND	ND	ND	ND	ND	ND	ND	ND	ND	ND	ND	ND	ND	ND	ND	ND
I22	ND	ND	ND	ND	ND	ND	ND	ND	ND	ND	ND	ND	ND	ND	ND	ND	ND	ND	ND	ND	ND
I14 ^a	ND	ND	ND	ND	ND	ND	ND	ND	ND	ND	ND	ND	ND	ND	ND	ND	ND	ND	ND	ND	ND
I16 ^a	ND	ND	ND	ND	ND	ND	ND	ND	ND	ND	ND	ND	ND	ND	ND	ND	ND	ND	ND	ND	ND
I15	ND	ND	ND	ND	ND	ND	ND	ND	ND	ND	ND	ND	ND	ND	ND	ND	ND	ND	ND	ND	ND
I12 ^a	ND	ND	ND	ND	ND	ND	ND	ND	ND	ND	ND	ND	ND	ND	ND	ND	ND	ND	ND	ND	ND
I9	ND	ND	ND	ND	ND	ND	ND	ND	ND	ND	ND	ND	ND	ND	ND	ND	ND	ND	ND	ND	ND
I6	ND	ND	ND	ND	ND	ND	ND	ND	ND	ND	ND	ND	ND	ND	ND	ND	ND	ND	ND	ND	ND
I2	ND	ND	ND	ND	ND	ND	ND	ND	ND	ND	ND	ND	ND	ND	ND	ND	ND	ND	ND	ND	ND
I3	ND	ND	ND	ND	ND	ND	ND	ND	ND	ND	ND	ND	ND	ND	ND	ND	ND	ND	ND	ND	ND
<i>38-m Stations</i>																					
I29	ND	ND	ND	ND	ND	ND	ND	ND	ND	ND	ND	ND	ND	ND	ND	ND	ND	ND	ND	ND	ND
I21	ND	ND	ND	ND	ND	ND	ND	ND	ND	ND	ND	ND	ND	ND	ND	ND	ND	ND	ND	ND	ND
I13	ND	ND	ND	ND	ND	ND	ND	ND	ND	ND	ND	ND	ND	ND	ND	ND	ND	ND	ND	ND	ND
I8	ND	ND	ND	ND	ND	ND	ND	ND	ND	ND	ND	ND	ND	ND	ND	ND	ND	ND	ND	ND	ND
<i>55-m Stations</i>																					
I28	ND	ND	ND	100	88.6 DNQ	ND	ND	ND	ND	ND	ND	ND	ND	ND	ND	51.5 DNQ	ND	ND	ND	ND	ND
I20	ND	ND	ND	ND	ND	ND	ND	ND	ND	ND	ND	ND	ND	ND	ND	ND	ND	ND	ND	ND	ND
I7	ND	ND	ND	ND	ND	ND	ND	ND	ND	ND	ND	ND	ND	ND	ND	ND	ND	ND	ND	ND	ND
I1	ND	ND	ND	ND	ND	ND	ND	ND	ND	ND	ND	ND	ND	ND	ND	ND	ND	ND	ND	ND	ND
DR (%)	0	0	0	4	4	0	0	0	0	0	0	0	0	0	0	4	0	0	0	0	0

^aNear-ZID station

Appendix F.9 *continued*

Summer 2022	PCB Congener																				
	8	18	28	37	44	49	52	66	70	74	77	81	87	99	101	105	110	114	118	119	
<i>19-m Stations</i>																					
I35	ND	ND	ND	ND	ND	ND	ND	ND	ND	ND	ND	ND	ND	ND	66.4 DNQ	ND	71.4 DNQ	ND	ND	ND	
I34	ND	ND	ND	ND	ND	ND	ND	ND	ND	ND	ND	ND	ND	ND	ND	ND	ND	ND	ND	ND	
I31	ND	ND	ND	ND	ND	ND	ND	ND	ND	ND	ND	ND	ND	ND	ND	ND	ND	ND	ND	ND	
I23	ND	ND	ND	ND	ND	ND	ND	ND	ND	ND	ND	ND	ND	ND	ND	ND	ND	ND	ND	ND	
I18	ND	ND	ND	ND	ND	ND	ND	ND	ND	ND	ND	ND	ND	ND	ND	ND	ND	ND	ND	ND	
I10	ND	ND	ND	ND	ND	ND	ND	ND	ND	ND	ND	ND	ND	ND	ND	ND	ND	ND	ND	ND	
I4	ND	ND	ND	ND	ND	ND	ND	ND	ND	ND	ND	ND	ND	ND	ND	ND	ND	ND	ND	ND	
<i>28-m Stations</i>																					
I33	ND	ND	ND	ND	ND	ND	ND	ND	ND	ND	ND	ND	ND	ND	ND	ND	ND	ND	ND	ND	
I30	ND	ND	ND	ND	ND	ND	ND	ND	ND	ND	ND	ND	ND	ND	ND	ND	ND	ND	ND	ND	
I27	ND	ND	ND	ND	ND	ND	ND	ND	ND	ND	ND	ND	ND	ND	ND	ND	ND	ND	ND	ND	
I22	ND	ND	ND	ND	ND	ND	ND	ND	ND	ND	ND	ND	ND	ND	ND	ND	ND	ND	ND	ND	
I14 ^a	ND	ND	ND	ND	ND	ND	ND	ND	ND	ND	ND	ND	ND	ND	ND	ND	ND	ND	ND	ND	
I16 ^a	ND	ND	ND	ND	ND	ND	ND	ND	ND	ND	ND	ND	ND	ND	ND	ND	ND	ND	ND	ND	
I15	ND	ND	ND	ND	ND	ND	ND	ND	ND	ND	ND	ND	ND	ND	ND	ND	ND	ND	ND	ND	
I12 ^a	ND	ND	ND	ND	ND	ND	ND	ND	ND	ND	ND	ND	ND	ND	ND	ND	ND	ND	ND	ND	
I9	ND	ND	ND	ND	ND	ND	ND	ND	ND	ND	ND	ND	ND	ND	ND	ND	ND	ND	ND	ND	
I6	ND	ND	ND	ND	ND	ND	ND	ND	ND	ND	ND	ND	ND	ND	ND	ND	ND	ND	ND	ND	
I2	ND	ND	28.9 DNQ	ND	ND	ND	ND	ND	ND	ND	ND	ND	ND	ND	ND	ND	ND	ND	ND	ND	
I3	ND	ND	ND	ND	ND	ND	ND	ND	ND	ND	32.4 DNQ	ND	ND	ND	ND	ND	ND	ND	ND	ND	
<i>38-m Stations</i>																					
I29	ND	ND	ND	ND	ND	ND	ND	ND	ND	ND	ND	ND	ND	ND	ND	ND	ND	ND	ND	ND	
I21	ND	ND	ND	ND	ND	ND	ND	ND	ND	ND	ND	ND	ND	ND	ND	ND	ND	ND	ND	ND	
I13	ND	ND	ND	ND	ND	ND	ND	ND	ND	ND	ND	ND	ND	ND	ND	ND	ND	ND	ND	ND	
I8	ND	ND	ND	ND	ND	ND	ND	ND	ND	ND	ND	ND	ND	ND	ND	ND	ND	ND	ND	ND	
<i>55-m Stations</i>																					
I28	ND	ND	ND	ND	ND	ND	ND	ND	ND	ND	ND	ND	ND	68.4 DNQ	76.5 DNQ	ND	59.0 DNQ	ND	81.6 DNQ	ND	
I20	ND	ND	ND	ND	ND	ND	ND	ND	ND	ND	ND	ND	ND	ND	ND	ND	ND	ND	ND	ND	
I7	ND	ND	ND	ND	ND	ND	ND	ND	ND	ND	ND	ND	ND	ND	ND	ND	ND	ND	ND	ND	
I1	ND	ND	ND	ND	ND	ND	ND	ND	ND	ND	ND	ND	ND	ND	ND	ND	ND	ND	ND	ND	
DR (%)	0	0	4	0	0	0	0	0	0	0	4	0	0	4	7	0	7	0	4	0	

^a Near-ZID station

Appendix F.9 *continued*

		PCB Congener																				
Summer 2022	123	126	128	138	149	151	153/168	156	157	158	167	169	170	177	180	183	187	189	194	195	201	206
<i>19-m Stations</i>																						
I35	ND	ND	ND	ND	ND	ND	ND	ND	ND	ND	ND	ND	ND	ND	ND	ND	ND	ND	ND	ND	ND	ND
I34	ND	ND	ND	ND	ND	ND	ND	ND	ND	ND	ND	ND	ND	ND	ND	ND	ND	ND	ND	ND	ND	ND
I31	ND	ND	ND	ND	ND	ND	ND	ND	ND	ND	ND	ND	ND	ND	ND	ND	ND	ND	ND	ND	ND	ND
I23	ND	ND	ND	ND	ND	ND	ND	ND	ND	ND	ND	ND	ND	ND	ND	ND	ND	ND	ND	ND	ND	ND
I18	ND	ND	ND	ND	ND	ND	ND	ND	ND	ND	ND	ND	ND	ND	ND	ND	ND	ND	ND	ND	ND	ND
I10	ND	ND	ND	ND	ND	ND	ND	ND	ND	ND	ND	ND	ND	ND	ND	ND	ND	ND	ND	ND	ND	ND
I4	ND	ND	ND	ND	ND	ND	ND	ND	ND	ND	ND	ND	ND	ND	ND	ND	ND	ND	ND	ND	ND	ND
<i>28-m Stations</i>																						
I33	ND	ND	ND	ND	ND	ND	ND	ND	ND	ND	ND	ND	ND	ND	ND	ND	ND	ND	ND	ND	ND	ND
I30	ND	ND	ND	ND	ND	ND	ND	ND	ND	ND	ND	ND	ND	ND	ND	ND	ND	ND	ND	ND	ND	ND
I27	ND	ND	ND	ND	ND	ND	ND	ND	ND	ND	ND	ND	ND	ND	ND	ND	ND	ND	ND	ND	ND	ND
I22	ND	ND	ND	ND	ND	ND	ND	ND	ND	ND	ND	ND	ND	ND	ND	ND	ND	ND	ND	ND	ND	ND
I14 ^a	ND	ND	ND	ND	ND	ND	ND	ND	ND	ND	ND	ND	ND	ND	ND	ND	ND	ND	ND	ND	ND	ND
I16 ^a	ND	ND	ND	ND	ND	ND	ND	ND	ND	ND	ND	ND	ND	ND	ND	ND	ND	ND	ND	ND	ND	ND
I15	ND	ND	ND	ND	ND	ND	ND	ND	ND	ND	ND	ND	ND	ND	ND	ND	ND	ND	ND	ND	ND	ND
I12 ^a	ND	ND	ND	ND	ND	ND	ND	ND	ND	ND	ND	ND	ND	ND	ND	ND	ND	ND	ND	ND	ND	ND
I9	ND	ND	ND	ND	ND	ND	ND	ND	ND	ND	ND	58.2 DNQ	46.0 DNQ	ND	ND	ND	ND	ND	ND	ND	ND	ND
I6	ND	ND	ND	ND	ND	ND	ND	ND	ND	ND	ND	ND	ND	ND	ND	ND	ND	ND	ND	ND	ND	ND
I2	ND	ND	ND	ND	ND	ND	ND	ND	ND	ND	ND	ND	ND	ND	ND	ND	ND	ND	ND	ND	ND	ND
I3	ND	ND	ND	ND	ND	ND	ND	ND	ND	ND	ND	48.4 DNQ	39.0 DNQ	32.9 DNQ	ND	30.2 DNQ	ND	ND	ND	ND	ND	ND
<i>38-m Stations</i>																						
I29	ND	ND	ND	ND	ND	ND	ND	ND	ND	ND	ND	ND	ND	ND	ND	ND	ND	ND	ND	ND	ND	ND
I21	ND	ND	ND	ND	ND	ND	ND	ND	ND	ND	ND	ND	ND	ND	ND	ND	ND	ND	ND	ND	ND	ND
I13	ND	ND	ND	ND	ND	ND	ND	ND	ND	ND	ND	ND	ND	ND	ND	ND	ND	ND	ND	ND	ND	ND
I8	ND	ND	ND	ND	ND	ND	ND	ND	ND	ND	ND	69.8 DNQ	55.4 DNQ	33.4 DNQ	52.9 DNQ	ND	ND	80.5 DNQ	69.7 DNQ	ND	ND	ND
<i>55-m Stations</i>																						
I28	ND	ND	ND	88.0	93.0	ND	ND	ND	ND	ND	ND	ND	ND	ND	45.1 DNQ	ND	46.3 DNQ	ND	ND	ND	ND	ND
I20	ND	ND	ND	ND	ND	ND	ND	ND	ND	ND	ND	ND	ND	ND	ND	ND	ND	ND	ND	ND	ND	ND
I7	ND	ND	ND	ND	ND	ND	ND	ND	ND	ND	ND	ND	ND	ND	ND	ND	ND	ND	ND	ND	ND	ND
I1	ND	ND	ND	ND	ND	ND	ND	ND	ND	ND	ND	ND	ND	ND	ND	ND	ND	ND	ND	ND	ND	ND
DR (%)	0	0	0	4	4	0	0	0	0	0	0	11	11	7	7	4	4	4	4	0	0	0

^aNear-ZID station

Appendix F.9 *continued*

	PCB Congener																				
	8	18	28	37	44	49	52	66	70	74	77	81	87	99	101	105	110	114	118	119	
Winter 2023																					
<i>19-m Stations</i>																					
I35	ND	ND	ND	ND	ND	ND	ND	ND	ND	ND	ND	ND	ND	ND	ND	ND	ND	ND	ND	ND	ND
I34	ND	ND	ND	ND	ND	ND	ND	ND	ND	ND	ND	ND	ND	ND	ND	ND	ND	ND	ND	ND	ND
I31	ND	ND	ND	ND	ND	ND	ND	ND	ND	ND	ND	ND	ND	ND	ND	ND	ND	ND	ND	ND	ND
I23	ND	ND	ND	ND	ND	ND	ND	ND	ND	ND	ND	ND	ND	ND	ND	ND	ND	ND	ND	ND	ND
I18	ND	ND	ND	ND	ND	ND	ND	ND	ND	ND	ND	ND	ND	ND	ND	ND	ND	ND	ND	ND	ND
I10	ND	ND	ND	ND	ND	ND	ND	ND	ND	ND	ND	ND	ND	ND	ND	ND	ND	ND	ND	ND	ND
I4	ND	ND	ND	ND	ND	ND	ND	ND	ND	ND	ND	ND	ND	ND	ND	ND	ND	ND	ND	ND	ND
<i>28-m Stations</i>																					
I33	ND	ND	ND	ND	ND	ND	ND	ND	ND	ND	ND	ND	ND	ND	ND	ND	ND	ND	ND	ND	ND
I30	ND	ND	ND	ND	ND	ND	ND	ND	ND	ND	ND	ND	ND	ND	ND	ND	ND	ND	ND	ND	ND
I27	ND	ND	ND	ND	ND	ND	ND	ND	ND	ND	ND	ND	ND	ND	ND	ND	ND	ND	ND	ND	ND
I22	ND	ND	ND	ND	ND	ND	ND	ND	ND	ND	ND	ND	ND	ND	ND	ND	ND	ND	ND	ND	ND
I14 ^a	ND	ND	ND	ND	ND	ND	ND	ND	ND	ND	ND	ND	ND	ND	ND	ND	ND	ND	ND	ND	ND
I16 ^a	ND	ND	ND	ND	ND	ND	ND	ND	ND	ND	ND	ND	ND	ND	ND	ND	ND	ND	ND	ND	ND
I15	ND	ND	ND	ND	ND	ND	ND	ND	ND	ND	ND	ND	ND	ND	ND	ND	ND	ND	ND	ND	ND
I12 ^a	ND	ND	ND	ND	ND	ND	ND	ND	ND	ND	ND	ND	ND	ND	ND	ND	ND	ND	ND	ND	ND
I9	ND	ND	ND	ND	ND	ND	ND	ND	ND	ND	ND	ND	ND	ND	ND	ND	ND	ND	ND	ND	ND
I6	ND	ND	ND	ND	ND	ND	ND	ND	ND	ND	ND	ND	ND	ND	ND	ND	ND	ND	ND	ND	ND
I2	ND	ND	ND	ND	ND	ND	ND	ND	ND	ND	ND	ND	ND	ND	ND	ND	ND	ND	ND	ND	ND
I3	ND	ND	ND	ND	ND	ND	ND	ND	ND	ND	ND	ND	ND	ND	ND	ND	ND	ND	ND	ND	ND
<i>38-m Stations</i>																					
I29	ND	ND	ND	ND	ND	ND	ND	ND	ND	ND	ND	ND	ND	ND	ND	ND	ND	ND	ND	ND	ND
I21	ND	ND	ND	ND	ND	ND	ND	ND	ND	ND	ND	ND	ND	ND	ND	ND	ND	ND	ND	ND	ND
I13	ND	ND	ND	ND	ND	ND	ND	ND	ND	ND	ND	ND	ND	ND	ND	ND	ND	ND	ND	ND	ND
I8	ND	ND	ND	ND	ND	ND	ND	ND	ND	ND	ND	ND	ND	ND	ND	ND	ND	ND	ND	ND	ND
<i>55-m Stations</i>																					
I28	ND	ND	ND	ND	ND	ND	ND	ND	ND	ND	ND	ND	ND	ND	ND	ND	42.7 DNQ	ND	ND	ND	ND
I20	ND	ND	ND	ND	ND	ND	ND	ND	ND	ND	ND	ND	ND	ND	ND	ND	ND	ND	ND	ND	ND
I7	ND	ND	ND	ND	ND	ND	ND	ND	ND	ND	ND	ND	ND	ND	ND	ND	ND	ND	ND	ND	ND
I1	ND	ND	ND	ND	ND	ND	ND	ND	ND	ND	ND	ND	ND	ND	ND	ND	ND	ND	ND	ND	ND
DR (%)	0	0	0	0	0	0	0	0	0	0	0	0	0	0	4	0	4	0	0	0	0

^aNear-ZID station

Appendix F.9 *continued*

		PCB Congener																				
Winter 2023	123	126	128	138	149	151	153/168	156	157	158	167	169	170	177	180	183	187	189	194	195	201	206
<i>19-m Stations</i>																						
I35	ND	ND	ND	ND	ND	ND	ND	ND	ND	ND	ND	ND	ND	ND	ND	ND	ND	ND	ND	ND	ND	ND
I34	ND	ND	ND	ND	ND	ND	ND	ND	ND	ND	ND	ND	ND	ND	ND	ND	ND	ND	ND	ND	ND	ND
I31	ND	ND	ND	ND	ND	ND	ND	ND	ND	ND	ND	ND	ND	ND	ND	ND	ND	ND	ND	ND	ND	ND
I23	ND	ND	ND	ND	ND	ND	ND	ND	ND	ND	ND	ND	ND	ND	ND	ND	ND	ND	ND	ND	ND	ND
I18	ND	ND	ND	ND	ND	ND	ND	ND	ND	ND	ND	ND	ND	ND	ND	ND	ND	ND	ND	ND	ND	ND
I10	ND	ND	ND	ND	ND	ND	ND	ND	ND	ND	ND	ND	ND	ND	ND	ND	ND	ND	ND	ND	ND	ND
I4	ND	ND	ND	ND	ND	ND	ND	ND	ND	ND	ND	ND	ND	ND	ND	ND	ND	ND	ND	ND	ND	ND
<i>28-m Stations</i>																						
I33	ND	ND	ND	ND	ND	ND	ND	ND	ND	ND	ND	ND	ND	ND	ND	ND	ND	ND	ND	ND	ND	ND
I30	ND	ND	ND	ND	ND	ND	ND	ND	ND	ND	ND	ND	ND	ND	ND	ND	ND	ND	ND	ND	ND	ND
I27	ND	ND	ND	ND	ND	ND	ND	ND	ND	ND	ND	ND	ND	ND	ND	ND	ND	ND	ND	ND	ND	ND
I22	ND	ND	ND	ND	ND	ND	ND	ND	ND	ND	ND	ND	ND	ND	ND	ND	ND	ND	ND	ND	ND	ND
I14 ^a	ND	ND	ND	ND	ND	ND	ND	ND	ND	ND	ND	ND	ND	ND	ND	ND	ND	ND	ND	ND	ND	ND
I16 ^a	ND	ND	ND	ND	ND	ND	ND	ND	ND	ND	ND	ND	ND	ND	ND	ND	ND	ND	ND	ND	ND	ND
I15	ND	ND	ND	ND	ND	ND	ND	ND	ND	ND	ND	ND	ND	ND	ND	ND	ND	ND	ND	ND	ND	ND
I12 ^a	ND	ND	ND	75.8 DNQ	96.0	ND	ND	ND	ND	ND	ND	ND	64.0 DNQ	32.1 DNQ	120	ND	52.0 DNQ	ND	ND	ND	ND	ND
I9	ND	ND	ND	ND	ND	ND	ND	ND	ND	ND	ND	ND	ND	ND	ND	ND	ND	ND	ND	ND	ND	ND
I6	ND	ND	ND	ND	ND	ND	ND	ND	ND	ND	ND	ND	ND	ND	ND	ND	ND	ND	ND	ND	ND	ND
I2	ND	ND	ND	ND	ND	ND	ND	ND	ND	ND	ND	ND	ND	ND	ND	ND	ND	ND	ND	ND	ND	ND
I3	ND	ND	ND	ND	ND	ND	ND	ND	ND	ND	ND	ND	ND	ND	ND	ND	ND	ND	ND	ND	ND	ND
<i>38-m Stations</i>																						
I29	ND	ND	ND	ND	ND	ND	ND	ND	ND	ND	ND	ND	ND	ND	ND	ND	ND	ND	ND	ND	ND	ND
I21	ND	ND	ND	ND	ND	ND	ND	ND	ND	ND	ND	ND	ND	ND	ND	ND	ND	ND	ND	ND	ND	ND
I13	ND	ND	ND	ND	ND	ND	ND	ND	ND	ND	ND	ND	ND	ND	ND	ND	ND	ND	ND	ND	ND	ND
I8	ND	ND	ND	ND	ND	ND	ND	ND	ND	ND	ND	ND	ND	ND	ND	ND	ND	ND	ND	ND	ND	ND
<i>55-m Stations</i>																						
I28	ND	ND	ND	64.4 DNQ	ND	ND	ND	ND	ND	ND	ND	ND	ND	ND	ND	ND	ND	ND	ND	ND	ND	ND
I20	ND	ND	ND	ND	ND	ND	ND	ND	ND	ND	ND	ND	ND	ND	ND	ND	ND	ND	ND	ND	ND	ND
I7	ND	ND	ND	ND	ND	ND	ND	ND	ND	ND	ND	ND	ND	ND	ND	ND	ND	ND	ND	ND	ND	ND
I1	ND	ND	ND	ND	ND	ND	ND	ND	ND	ND	ND	ND	ND	ND	ND	ND	ND	ND	ND	ND	ND	ND
DR (%)	0	0	0	7	4	0	0	0	0	0	0	0	4	4	4	0	4	0	0	0	0	0

^aNear-ZID station

Appendix F.9 *continued*

	PCB Congener																				
	8	18	28	37	44	49	52	66	70	74	77	81	87	99	101	105	110	114	118	119	
Summer 2023																					
<i>19-m Stations</i>																					
I35	—	—	—	—	—	—	—	—	—	—	—	—	—	—	—	—	—	—	—	—	—
I34	—	—	—	—	—	—	—	—	—	—	—	—	—	—	—	—	—	—	—	—	—
I31	—	—	—	—	—	—	—	—	—	—	—	—	—	—	—	—	—	—	—	—	—
I23	—	—	—	—	—	—	—	—	—	—	—	—	—	—	—	—	—	—	—	—	—
I18	—	—	—	—	—	—	—	—	—	—	—	—	—	—	—	—	—	—	—	—	—
I10	—	—	—	—	—	—	—	—	—	—	—	—	—	—	—	—	—	—	—	—	—
I4	—	—	—	—	—	—	—	—	—	—	—	—	—	—	—	—	—	—	—	—	—
<i>28-m Stations</i>																					
I33	NR	NR	NR	NR	NR	NR	NR	NR	NR	NR	NR	NR	NR	NR	NR	NR	NR	NR	NR	NR	NR
I30	NR	NR	NR	NR	NR	NR	NR	NR	NR	NR	NR	NR	NR	NR	NR	NR	NR	NR	NR	NR	NR
I27	NR	NR	NR	NR	NR	NR	NR	NR	NR	NR	NR	NR	NR	NR	NR	NR	NR	NR	NR	NR	NR
I22	NR	NR	NR	NR	NR	NR	NR	NR	NR	NR	NR	NR	NR	NR	NR	NR	NR	NR	NR	NR	NR
I14 ^a	NR	NR	NR	NR	NR	NR	NR	NR	NR	NR	NR	NR	NR	NR	NR	NR	NR	NR	NR	NR	NR
I16 ^a	NR	NR	NR	NR	NR	NR	NR	NR	NR	NR	NR	NR	NR	NR	NR	NR	NR	NR	NR	NR	NR
I15	NR	NR	NR	NR	NR	NR	NR	NR	NR	NR	NR	NR	NR	NR	NR	NR	NR	NR	NR	NR	NR
I12 ^a	NR	NR	NR	NR	NR	NR	NR	NR	NR	NR	NR	NR	NR	NR	NR	NR	NR	NR	NR	NR	NR
I9	NR	NR	NR	NR	NR	NR	NR	NR	NR	NR	NR	NR	NR	NR	NR	NR	NR	NR	NR	NR	NR
I6	NR	NR	NR	NR	NR	NR	NR	NR	NR	NR	NR	NR	NR	NR	NR	NR	NR	NR	NR	NR	NR
I2	NR	NR	NR	NR	NR	NR	NR	NR	NR	NR	NR	NR	NR	NR	NR	NR	NR	NR	NR	NR	NR
I3	NR	NR	NR	NR	NR	NR	NR	NR	NR	NR	NR	NR	NR	NR	NR	NR	NR	NR	NR	NR	NR
<i>38-m Stations</i>																					
I29	—	—	—	—	—	—	—	—	—	—	—	—	—	—	—	—	—	—	—	—	—
I21	—	—	—	—	—	—	—	—	—	—	—	—	—	—	—	—	—	—	—	—	—
I13	—	—	—	—	—	—	—	—	—	—	—	—	—	—	—	—	—	—	—	—	—
I8	—	—	—	—	—	—	—	—	—	—	—	—	—	—	—	—	—	—	—	—	—
<i>55-m Stations</i>																					
I28	—	—	—	—	—	—	—	—	—	—	—	—	—	—	—	—	—	—	—	—	—
I20	—	—	—	—	—	—	—	—	—	—	—	—	—	—	—	—	—	—	—	—	—
I7	—	—	—	—	—	—	—	—	—	—	—	—	—	—	—	—	—	—	—	—	—
I1	—	—	—	—	—	—	—	—	—	—	—	—	—	—	—	—	—	—	—	—	—
DR (%)	NR	NR	NR	NR	NR	NR	NR	NR	NR	NR	NR	NR	NR	NR	NR	NR	NR	NR	NR	NR	NR

^a Near-ZID station

Appendix F.9 *continued*

		PCB Congener																				
Summer 2023	123	126	128	138	149	151	153/168	156	157	158	167	169	170	177	180	183	187	189	194	195	201	206
<i>19-m Stations</i>																						
I35	-	-	-	-	-	-	-	-	-	-	-	-	-	-	-	-	-	-	-	-	-	-
I34	-	-	-	-	-	-	-	-	-	-	-	-	-	-	-	-	-	-	-	-	-	-
I31	-	-	-	-	-	-	-	-	-	-	-	-	-	-	-	-	-	-	-	-	-	-
I23	-	-	-	-	-	-	-	-	-	-	-	-	-	-	-	-	-	-	-	-	-	-
I18	-	-	-	-	-	-	-	-	-	-	-	-	-	-	-	-	-	-	-	-	-	-
I10	-	-	-	-	-	-	-	-	-	-	-	-	-	-	-	-	-	-	-	-	-	-
I4	-	-	-	-	-	-	-	-	-	-	-	-	-	-	-	-	-	-	-	-	-	-
<i>28-m Stations</i>																						
I33	NR	NR	NR	NR	NR	NR	NR	NR	NR	NR	NR	NR	NR	NR	NR	NR	NR	NR	NR	NR	NR	NR
I30	NR	NR	NR	NR	NR	NR	NR	NR	NR	NR	NR	NR	NR	NR	NR	NR	NR	NR	NR	NR	NR	NR
I27	NR	NR	NR	NR	NR	NR	NR	NR	NR	NR	NR	NR	NR	NR	NR	NR	NR	NR	NR	NR	NR	NR
I22	NR	NR	NR	NR	NR	NR	NR	NR	NR	NR	NR	NR	NR	NR	NR	NR	NR	NR	NR	NR	NR	NR
I14 ^a	NR	NR	NR	NR	NR	NR	NR	NR	NR	NR	NR	NR	NR	NR	NR	NR	NR	NR	NR	NR	NR	NR
I16 ^a	NR	NR	NR	NR	NR	NR	NR	NR	NR	NR	NR	NR	NR	NR	NR	NR	NR	NR	NR	NR	NR	NR
I15	NR	NR	NR	NR	NR	NR	NR	NR	NR	NR	NR	NR	NR	NR	NR	NR	NR	NR	NR	NR	NR	NR
I12 ^a	NR	NR	NR	NR	NR	NR	NR	NR	NR	NR	NR	NR	NR	NR	NR	NR	NR	NR	NR	NR	NR	NR
I9	NR	NR	NR	NR	NR	NR	NR	NR	NR	NR	NR	NR	NR	NR	NR	NR	NR	NR	NR	NR	NR	NR
I6	NR	NR	NR	NR	NR	NR	NR	NR	NR	NR	NR	NR	NR	NR	NR	NR	NR	NR	NR	NR	NR	NR
I2	NR	NR	NR	NR	NR	NR	NR	NR	NR	NR	NR	NR	NR	NR	NR	NR	NR	NR	NR	NR	NR	NR
I3	NR	NR	NR	NR	NR	NR	NR	NR	NR	NR	NR	NR	NR	NR	NR	NR	NR	NR	NR	NR	NR	NR
<i>38-m Stations</i>																						
I29	-	-	-	-	-	-	-	-	-	-	-	-	-	-	-	-	-	-	-	-	-	-
I21	-	-	-	-	-	-	-	-	-	-	-	-	-	-	-	-	-	-	-	-	-	-
I13	-	-	-	-	-	-	-	-	-	-	-	-	-	-	-	-	-	-	-	-	-	-
I8	-	-	-	-	-	-	-	-	-	-	-	-	-	-	-	-	-	-	-	-	-	-
<i>55-m Stations</i>																						
I28	-	-	-	-	-	-	-	-	-	-	-	-	-	-	-	-	-	-	-	-	-	-
I20	-	-	-	-	-	-	-	-	-	-	-	-	-	-	-	-	-	-	-	-	-	-
I7	-	-	-	-	-	-	-	-	-	-	-	-	-	-	-	-	-	-	-	-	-	-
I1	-	-	-	-	-	-	-	-	-	-	-	-	-	-	-	-	-	-	-	-	-	-
DR (%)	NR	NR	NR	NR	NR	NR	NR	NR	NR	NR	NR	NR	NR	NR	NR	NR	NR	NR	NR	NR	NR	NR

^aNear-ZID station

Appendix F.10

Concentrations of PAHs (ppb) detected in sediments from PLOO stations sampled during 2022 and 2023. See Appendix F.1 for MDLs; DR =detection rate; DNQ = do not quantify; ND= not detected; NR= not reportable. Only primary core stations sampled during summer 2023 due to resource exchange for Bight'23 (see text).

Winter 2022	1-methyl naphthalene	1-methyl phenanthrene	2-methyl naphthalene	2,3,5-trimethyl naphthalene	2,6-dimethyl naphthalene	3,4-benzo(B) fluoranthene	Acenaphthene	Acenaphthylene	Anthracene	Benzo[A] anthracene	Benzo[A] pyrene
<i>88-m Depth Contour</i>											
B11	ND	ND	ND	ND	ND	ND	ND	ND	ND	ND	ND
B8	ND	ND	ND	ND	9.28	ND	ND	ND	ND	ND	ND
E19	ND	ND	ND	ND	ND	ND	ND	ND	ND	ND	ND
E7	ND	8.71	11.1	ND	12.8	ND	ND	ND	ND	ND	ND
E1	ND	ND	ND	ND	ND	ND	ND	ND	ND	ND	ND
<i>98-m Depth Contour</i>											
B12	ND	ND	ND	ND	ND	ND	ND	ND	ND	ND	ND
B9	ND	ND	ND	ND	ND	ND	ND	ND	ND	ND	ND
E26	ND	ND	ND	ND	ND	ND	ND	ND	ND	ND	ND
E25	ND	ND	ND	ND	ND	ND	ND	ND	ND	ND	ND
E23	ND	ND	ND	ND	ND	ND	ND	ND	ND	ND	ND
E20	ND	ND	ND	ND	ND	ND	ND	ND	ND	ND	ND
E17 ^a	ND	ND	ND	ND	ND	ND	ND	ND	ND	ND	ND
E14 ^a	ND	ND	ND	ND	ND	ND	ND	ND	ND	ND	ND
E11 ^a	ND	ND	ND	ND	ND	ND	ND	ND	ND	ND	ND
E8	ND	ND	ND	ND	ND	ND	ND	ND	ND	ND	ND
E5	ND	ND	ND	ND	ND	ND	ND	ND	ND	ND	ND
E2	ND	ND	ND	ND	ND	23.4	ND	ND	ND	ND	ND
<i>116-m Depth Contour</i>											
B10	ND	ND	ND	ND	ND	ND	ND	ND	ND	ND	ND
E21	ND	ND	ND	ND	ND	ND	ND	ND	ND	ND	ND
E15 ^a	ND	ND	ND	ND	ND	ND	ND	ND	ND	ND	ND
E9	ND	ND	ND	ND	ND	ND	ND	ND	ND	ND	ND
E3	ND	ND	ND	ND	ND	ND	ND	ND	ND	ND	ND
DR (%)	0	5	5	0	9	5	0	0	0	0	0

^a Near-ZID station

Appendix F.10 *continued*

Winter 2022	Benzo[e] pyrene	Benzo[G,H,I] perylene	Benzo[K] fluoranthene	Biphenyl	Chrysene	Dibenzo(A,H) anthracene	Fluoranthene	Fluorene	Indeno(1,2,3-CD) pyrene	Naphthalene	Perylene	Phenanthrene	Pyrene
<i>88-m Depth Contour</i>													
B11	ND	ND	ND	ND	ND	ND	ND	ND	ND	ND	ND	ND	11.2
B8	ND	ND	ND	ND	ND	ND	10.2	ND	ND	ND	ND	ND	9.68
E19	ND	ND	ND	ND	ND	ND	ND	ND	ND	ND	ND	ND	ND
E7	ND	ND	ND	9.87	ND	ND	ND	ND	ND	13.5	ND	ND	ND
E1	ND	ND	ND	ND	ND	ND	ND	ND	ND	ND	ND	ND	9.35
<i>98-m Depth Contour</i>													
B12	ND	ND	ND	ND	ND	ND	ND	ND	ND	ND	ND	ND	ND
B9	ND	ND	ND	ND	ND	ND	ND	ND	ND	ND	ND	ND	ND
E26	ND	ND	ND	ND	ND	ND	ND	ND	ND	ND	ND	ND	ND
E25	ND	ND	ND	ND	ND	ND	ND	ND	ND	ND	ND	ND	ND
E23	ND	ND	ND	ND	ND	ND	ND	ND	ND	ND	ND	ND	ND
E20	ND	ND	ND	ND	ND	ND	ND	ND	ND	ND	ND	ND	ND
E17 ^a	ND	ND	ND	ND	ND	ND	ND	ND	ND	ND	ND	ND	ND
E14 ^a	ND	ND	ND	ND	ND	ND	ND	ND	ND	ND	ND	ND	ND
E11 ^a	ND	ND	ND	ND	ND	ND	ND	ND	ND	ND	ND	ND	ND
E8	ND	ND	ND	ND	ND	ND	ND	ND	ND	ND	ND	ND	ND
E5	ND	ND	ND	ND	ND	ND	ND	ND	ND	ND	ND	ND	ND
E2	ND	15.1	ND	ND	15.2	ND	11.2	ND	13.0	ND	ND	ND	15.2
<i>116-m Depth Contour</i>													
B10	ND	ND	ND	ND	ND	ND	ND	ND	ND	ND	ND	ND	ND
E21	ND	ND	ND	ND	ND	ND	ND	ND	ND	ND	ND	ND	ND
E15 ^a	ND	ND	ND	ND	ND	ND	ND	ND	ND	ND	ND	ND	ND
E9	ND	ND	ND	ND	ND	ND	ND	ND	ND	ND	ND	ND	ND
E3	ND	ND	ND	ND	ND	ND	ND	ND	ND	ND	ND	ND	9.11
DR (%)	0	5	0	5	5	0	9	0	5	5	0	0	23

^aNear-ZID station

Appendix F.10 *continued*

Summer 2022	1-methyl naphthalene	1-methyl phenanthrene	2-methyl naphthalene	2,3,5-trimethyl naphthalene	2,6-dimethyl naphthalene	3,4-benzo(B) fluoranthene	Acenaphthene	Acenaphthylene	Anthracene	Benzo[A] anthracene	Benzo[A] pyrene
<i>88-m Depth Contour</i>											
B11	ND	ND	ND	ND	ND	ND	ND	ND	ND	ND	ND
B8	ND	ND	ND	ND	ND	ND	ND	ND	ND	ND	ND
E19	ND	ND	ND	ND	9.80	ND	ND	ND	ND	ND	ND
E7	ND	ND	ND	ND	8.58	ND	ND	ND	ND	ND	ND
E1	ND	ND	ND	ND	ND	ND	ND	ND	ND	ND	ND
<i>98-m Depth Contour</i>											
B12	ND	ND	ND	ND	ND	ND	ND	ND	ND	ND	ND
B9	ND	ND	ND	ND	ND	ND	ND	ND	ND	ND	ND
E26	ND	ND	ND	ND	ND	ND	ND	ND	ND	ND	ND
E25	ND	ND	ND	ND	ND	ND	ND	ND	ND	ND	ND
E23	ND	ND	ND	ND	ND	ND	ND	ND	ND	ND	ND
E20	ND	ND	ND	ND	ND	ND	ND	ND	ND	ND	ND
E17 ^a	ND	ND	ND	ND	ND	ND	ND	ND	ND	ND	ND
E14 ^a	ND	ND	ND	ND	ND	ND	ND	ND	ND	ND	ND
E11 ^a	ND	ND	ND	ND	ND	ND	ND	ND	ND	ND	ND
E8	ND	ND	ND	ND	ND	ND	ND	ND	ND	ND	ND
E5	ND	ND	ND	ND	ND	ND	ND	ND	ND	ND	ND
E2	ND	ND	ND	ND	ND	ND	ND	ND	ND	ND	ND
<i>116-m Depth Contour</i>											
B10	ND	ND	ND	ND	ND	ND	ND	ND	ND	ND	ND
E21	ND	ND	ND	ND	ND	ND	ND	ND	ND	ND	ND
E15 ^a	ND	ND	ND	ND	ND	ND	ND	ND	ND	ND	ND
E9	ND	ND	ND	ND	ND	ND	ND	ND	ND	ND	ND
E3	ND	ND	ND	ND	ND	ND	ND	ND	ND	ND	ND
DR (%)	0	0	0	0	9	0	0	0	0	0	0

^a Near-ZID station

Appendix F.10 *continued*

Summer 2022	Benzo[e]pyrene	Benzo[G,H,I]perylene	Benzo[K]fluoranthene	Biphenyl	Chrysene	Dibenzo(A,H)anthracene	Fluoranthene	Fluorene	Indeno(1,2,3-CD)pyrene	Naphthalene	Perylene	Phenanthrene	Pyrene
<i>88-m Depth Contour</i>													
B11	ND	ND	ND	9.27	ND	ND	ND	ND	ND	ND	ND	ND	ND
B8	ND	ND	ND	8.98	ND	ND	ND	ND	ND	ND	ND	ND	ND
E19	ND	ND	ND	ND	ND	ND	ND	ND	ND	ND	ND	ND	ND
E7	ND	ND	ND	7.76	ND	ND	ND	ND	ND	ND	ND	ND	ND
E1	ND	ND	ND	ND	11.2	ND	10.1	ND	ND	ND	ND	ND	10.8
<i>98-m Depth Contour</i>													
B12	ND	ND	ND	ND	ND	ND	ND	ND	ND	ND	ND	ND	ND
B9	ND	ND	ND	ND	ND	ND	ND	ND	ND	ND	ND	ND	ND
E26	ND	ND	ND	NR	ND	ND	ND	ND	ND	ND	ND	ND	ND
E25	ND	ND	ND	ND	ND	ND	ND	ND	ND	ND	ND	ND	ND
E23	ND	ND	ND	NR	ND	ND	ND	ND	ND	ND	ND	ND	ND
E20	ND	ND	ND	ND	ND	ND	ND	ND	ND	ND	ND	ND	ND
E17 ^a	ND	ND	ND	NR	ND	ND	ND	ND	ND	ND	ND	ND	ND
E14 ^a	ND	ND	ND	ND	ND	ND	ND	ND	ND	ND	ND	ND	ND
E11 ^a	ND	ND	ND	ND	ND	ND	ND	ND	ND	ND	ND	ND	ND
E8	ND	ND	ND	ND	ND	ND	ND	ND	ND	ND	ND	ND	ND
E5	ND	ND	ND	NR	ND	ND	ND	ND	ND	ND	ND	ND	ND
E2	ND	ND	ND	NR	ND	ND	ND	ND	ND	ND	ND	ND	8.89
<i>116-m Depth Contour</i>													
B10	ND	ND	ND	8.45	ND	ND	ND	ND	ND	ND	ND	ND	ND
E21	ND	ND	ND	ND	ND	ND	ND	ND	ND	ND	ND	ND	ND
E15 ^a	ND	ND	ND	ND	ND	ND	ND	ND	ND	ND	ND	ND	ND
E9	ND	ND	ND	ND	ND	ND	ND	ND	ND	ND	ND	ND	ND
E3	ND	ND	ND	ND	10.8	ND	14.1	ND	ND	ND	ND	9.31	19.1
DR (%)	0	0	0	24	9	0	9	0	0	0	0	5	14

^aNear-ZID station

Appendix F.10 *continued*

Winter 2023	1-methyl naphthalene	1-methyl phenanthrene	2-methyl naphthalene	2,3,5-trimethyl naphthalene	2,6-dimethyl naphthalene	3,4-benzo(B) fluoranthene	Acenaphthene	Acenaphthylene	Anthracene	Benzo[A] anthracene	Benzo[A] pyrene
<i>88-m Depth Contour</i>											
B11	ND	ND	ND	ND	ND	ND	ND	ND	ND	ND	ND
B8	ND	ND	ND	ND	ND	ND	ND	ND	ND	ND	ND
E19	ND	ND	ND	ND	11.9	ND	ND	ND	ND	ND	ND
E7	ND	ND	ND	ND	8.98	ND	ND	ND	ND	ND	ND
E1	ND	ND	ND	ND	ND	ND	ND	ND	ND	ND	ND
<i>98-m Depth Contour</i>											
B12	ND	ND	ND	ND	ND	ND	ND	ND	ND	ND	ND
B9	ND	ND	ND	ND	8.61	ND	ND	ND	ND	ND	ND
E26	ND	ND	ND	ND	ND	ND	ND	ND	ND	ND	ND
E25	ND	ND	ND	ND	ND	ND	ND	ND	ND	ND	ND
E23	ND	ND	ND	ND	4.89 DNQ	ND	ND	ND	ND	ND	ND
E20	ND	ND	ND	ND	11.9	ND	ND	ND	ND	ND	ND
E17 ^a	ND	ND	ND	ND	16.9	ND	ND	ND	ND	ND	ND
E14 ^a	ND	ND	ND	ND	10.1	ND	ND	ND	ND	ND	ND
E11 ^a	ND	ND	ND	ND	6.42 DNQ	ND	ND	ND	ND	ND	ND
E8	ND	ND	ND	ND	ND	ND	ND	ND	ND	ND	ND
E5	ND	ND	ND	ND	6.18 DNQ	ND	ND	ND	ND	ND	ND
E2	ND	ND	ND	ND	6.42 DNQ	32.4	ND	7.57	ND	ND	27.2
<i>116-m Depth Contour</i>											
B10	ND	ND	ND	ND	12.4	ND	ND	ND	ND	ND	ND
E21	ND	ND	ND	ND	8.36	ND	ND	ND	ND	ND	ND
E15 ^a	ND	ND	ND	ND	5.23 DNQ	ND	ND	ND	ND	ND	ND
E9	ND	ND	ND	ND	ND	ND	ND	ND	ND	ND	ND
E3	ND	ND	ND	ND	ND	37.8	ND	ND	ND	32.8	28.0
DR (%)	0	0	0	0	59	9	0	0	5	5	9

^a Near-ZID station

Appendix F.10 *continued*

Winter 2023	Benzo[e] pyrene	Benzo[G,H,I] perylene	Benzo[K] fluoranthene	Biphenyl	Chrysene	Dibenzo(A,H) anthracene	Fluoranthene	Fluorene	Indeno(1,2,3-CD) pyrene	Naphthalene	Perylene	Phenanthrene	Pyrene
<i>88-m Depth Contour</i>													
B11	ND	ND	ND	ND	ND	ND	ND	ND	ND	ND	ND	ND	ND
B8	ND	ND	ND	ND	ND	ND	ND	ND	ND	ND	ND	ND	ND
E19	ND	ND	ND	ND	ND	ND	ND	ND	ND	ND	ND	ND	ND
E7	ND	ND	ND	ND	ND	ND	ND	ND	ND	ND	ND	ND	6.46 DNQ
E1	4.54 DNQ	ND	ND	ND	ND	ND	ND	ND	ND	ND	ND	ND	ND
<i>98-m Depth Contour</i>													
B12	ND	ND	ND	ND	ND	ND	ND	ND	ND	ND	ND	ND	ND
B9	ND	ND	ND	6.93 DNQ	ND	ND	ND	ND	ND	ND	ND	ND	ND
E26	ND	ND	ND	ND	ND	ND	ND	ND	ND	ND	ND	ND	ND
E25	ND	ND	ND	ND	ND	ND	ND	ND	ND	ND	ND	ND	ND
E23	ND	ND	ND	ND	ND	ND	ND	ND	ND	ND	ND	ND	ND
E20	ND	ND	ND	ND	ND	ND	ND	ND	ND	ND	ND	ND	ND
E17 ^a	ND	ND	ND	ND	ND	ND	ND	ND	ND	ND	ND	ND	ND
E14 ^a	ND	ND	ND	ND	ND	ND	ND	ND	ND	ND	ND	ND	ND
E11 ^a	ND	ND	ND	ND	ND	ND	ND	ND	ND	ND	ND	ND	ND
E8	ND	ND	ND	ND	ND	ND	ND	ND	ND	ND	ND	ND	ND
E5	ND	ND	ND	ND	ND	ND	ND	ND	ND	ND	ND	ND	ND
E2	15.5	14.4	15.2	ND	34.7	5.72 DNQ	46.4	ND	13.1	ND	ND	7.61	53.7
<i>116-m Depth Contour</i>													
B10	ND	ND	ND	ND	ND	ND	ND	ND	ND	ND	ND	ND	ND
E21	ND	ND	ND	ND	ND	ND	ND	ND	ND	ND	ND	ND	ND
E15 ^a	ND	ND	ND	ND	ND	ND	ND	ND	ND	ND	ND	ND	ND
E9	ND	ND	ND	ND	ND	ND	ND	ND	ND	ND	ND	ND	ND
E3	18.6	17.1	16.5	ND	24.3	ND	42.1	ND	14.3	ND	ND	8.23	41.1
DR (%)	14	9	9	5	9	5	9	0	9	0	0	9	14

^aNear-ZID station

Appendix F.10 *continued*

Summer 2023	1-methyl naphthalene	1-methyl phenanthrene	2-methyl naphthalene	2,3,5-trimethyl naphthalene	2,6-dimethyl naphthalene	3,4-benzo(B) fluoranthene	Acenaphthene	Acenaphthylene	Anthracene	Benzo[A] anthracene	Benzo[A] pyrene
<i>88-m Depth Contour</i>											
B11	—	—	—	—	—	—	—	—	—	—	—
B8	—	—	—	—	—	—	—	—	—	—	—
E19	—	—	—	—	—	—	—	—	—	—	—
E7	—	—	—	—	—	—	—	—	—	—	—
E1	—	—	—	—	—	—	—	—	—	—	—
<i>98-m Depth Contour</i>											
B12	ND	ND	ND	ND	ND	ND	ND	ND	ND	ND	ND
B9	ND	ND	ND	ND	ND	ND	ND	ND	ND	ND	ND
E26	ND	ND	ND	ND	5.36 DNQ	ND	ND	ND	ND	ND	ND
E25	ND	ND	ND	ND	ND	ND	ND	ND	ND	ND	ND
E23	ND	ND	ND	ND	5.26 DNQ	ND	ND	ND	ND	ND	ND
E20	ND	ND	ND	ND	ND	ND	ND	ND	ND	ND	ND
E17 ^a	ND	ND	ND	ND	4.97 DNQ	ND	ND	ND	ND	ND	ND
E14 ^a	ND	ND	ND	ND	ND	ND	ND	ND	ND	ND	ND
E11 ^a	ND	ND	ND	ND	ND	ND	ND	ND	ND	ND	ND
E8	ND	ND	ND	ND	5.06 DNQ	ND	ND	ND	ND	ND	ND
E5	ND	ND	ND	ND	4.92 DNQ	ND	ND	ND	ND	ND	ND
E2	ND	ND	ND	ND	ND	43.2	ND	ND	4.86 DNQ	ND	33.8
<i>116-m Depth Contour</i>											
B10	—	—	—	—	—	—	—	—	—	—	—
E21	—	—	—	—	—	—	—	—	—	—	—
E15 ^a	ND	ND	ND	ND	ND	ND	ND	ND	ND	ND	ND
E9	—	—	—	—	—	—	—	—	—	—	—
E3	—	—	—	—	—	—	—	—	—	—	—
DR (%)	0	0	0	0	38	8	0	0	8	0	8

^a Near-ZID station

Appendix F.10 *continued*

Summer 2023	Benzo[e]pyrene	Benzo[G,H,I]perylene	Benzo[K]fluoranthene	Biphenyl	Chrysene	Dibenzo(A,H)anthracene	Fluoranthene	Fluorene	Indeno(1,2,3-CD)pyrene	Naphthalene	Perylene	Phenanthrene	Pyrene
<i>88-m Depth Contour</i>													
B11	—	—	—	—	—	—	—	—	—	—	—	—	—
B8	—	—	—	—	—	—	—	—	—	—	—	—	—
E19	—	—	—	—	—	—	—	—	—	—	—	—	—
E7	—	—	—	—	—	—	—	—	—	—	—	—	—
E1	—	—	—	—	—	—	—	—	—	—	—	—	—
<i>98-m Depth Contour</i>													
B12	ND	ND	ND	NR	ND	ND	ND	ND	ND	ND	ND	ND	ND
B9	ND	ND	ND	ND	ND	ND	ND	ND	ND	ND	ND	ND	ND
E26	ND	ND	ND	NR	ND	ND	ND	ND	ND	ND	ND	ND	ND
E25	ND	ND	ND	NR	ND	ND	ND	ND	ND	ND	ND	ND	ND
E23	ND	ND	ND	NR	ND	ND	ND	ND	ND	ND	ND	ND	ND
E20	ND	ND	ND	NR	ND	ND	ND	ND	ND	ND	ND	ND	ND
E17 ^a	ND	ND	ND	NR	ND	ND	ND	ND	ND	ND	ND	ND	ND
E14 ^a	ND	ND	ND	NR	ND	ND	ND	ND	ND	ND	ND	ND	ND
E11 ^a	ND	ND	ND	ND	ND	ND	ND	ND	ND	ND	ND	ND	ND
E8	ND	ND	ND	NR	ND	ND	ND	ND	ND	ND	ND	ND	ND
E5	ND	ND	ND	NR	ND	ND	ND	ND	ND	ND	ND	ND	ND
E2	23.9	23.6	22.5	NR	35.5	10.9 DNQ	69.0	ND	22.8	ND	ND	46.8	66.0
<i>116-m Depth Contour</i>													
B10	—	—	—	—	—	—	—	—	—	—	—	—	—
E21	—	—	—	—	—	—	—	—	—	—	—	—	—
E15 ^a	ND	ND	ND	ND	ND	ND	ND	ND	ND	ND	ND	ND	ND
E9	—	—	—	—	—	—	—	—	—	—	—	—	—
E3	—	—	—	—	—	—	—	—	—	—	—	—	—
DR (%)	8	8	8	0	8	8	8	0	8	0	0	8	8

^aNear-ZID station

Appendix F.11

Concentrations of PAHs (ppb) detected in sediments from SBOO stations sampled during 2022 and 2023. See Appendix F.1 for MDLs; DR = detection rate; DNQ = do not quantify; ND = not detected; NR = not reportable. Only primary core stations sampled during summer 2023 due to resource exchange for Bight'23 (see text).

Winter 2022	1-methyl naphthalene	1-methyl phenanthrene	2-methyl naphthalene	2,3,5-trimethyl naphthalene	2,6-dimethyl naphthalene	3,4-benzo(B) fluoranthene	Acenaphthene	Acenaphthylene	Anthracene	Benzo[A] anthracene	Benzo[A] pyrene
<i>19-m Stations</i>											
I35	ND	ND	ND	ND	ND	ND	ND	ND	ND	ND	ND
I34	ND	ND	ND	ND	ND	ND	ND	ND	ND	ND	ND
I31	ND	ND	ND	ND	ND	ND	ND	ND	ND	ND	ND
I23	ND	ND	ND	ND	ND	ND	ND	ND	ND	ND	ND
I18	ND	ND	ND	ND	ND	ND	ND	ND	ND	ND	ND
I10	ND	ND	ND	ND	ND	ND	ND	ND	ND	ND	ND
I4	ND	ND	ND	ND	ND	ND	ND	ND	ND	ND	ND
<i>28-m Stations</i>											
I33	ND	ND	ND	ND	ND	ND	ND	ND	ND	ND	ND
I30	ND	ND	ND	ND	ND	ND	ND	ND	ND	ND	ND
I27	ND	ND	ND	10.1	ND	ND	ND	ND	ND	ND	ND
I22	ND	ND	ND	ND	ND	ND	ND	ND	ND	ND	ND
I14 ^a	ND	ND	ND	ND	ND	ND	ND	ND	ND	ND	ND
I16 ^a	ND	ND	ND	ND	ND	ND	ND	ND	ND	ND	ND
I15	ND	ND	ND	ND	ND	ND	ND	ND	ND	ND	ND
I12 ^a	ND	ND	ND	ND	ND	ND	ND	ND	ND	ND	ND
I9	ND	ND	ND	ND	ND	ND	ND	ND	ND	ND	ND
I6	ND	ND	ND	ND	ND	ND	ND	ND	ND	ND	ND
I2	ND	ND	ND	ND	ND	ND	ND	ND	ND	ND	ND
I3	ND	ND	ND	ND	ND	ND	ND	ND	ND	ND	ND
<i>38-m Stations</i>											
I29	ND	ND	ND	ND	ND	ND	ND	ND	ND	ND	ND
I21	ND	ND	ND	ND	ND	ND	ND	ND	ND	ND	ND
I13	ND	ND	ND	ND	ND	ND	ND	ND	ND	ND	ND
I8	ND	ND	ND	ND	ND	ND	ND	ND	ND	ND	ND
<i>55-m Stations</i>											
I28	ND	ND	ND	10.4	ND	ND	ND	ND	ND	ND	ND
I20	ND	ND	ND	ND	ND	ND	ND	ND	ND	ND	ND
I7	ND	ND	ND	ND	ND	ND	ND	ND	ND	ND	ND
I1	ND	ND	ND	ND	ND	ND	ND	ND	ND	ND	ND
DR (%)	0	0	0	0	7	0	0	0	0	0	0

^a Near-ZID station

Appendix F.11 *continued*

Winter 2022	Benzo[e]pyrene	Benzo[g,h,i]perylene	Benzo[k]fluoranthene	Biphenyl	Chrysene	Dibenzo(a,h)anthracene	Fluoranthene	Fluorene	Indeno(1,2,3-cd)pyrene	Naphthalene	Perylene	Phenanthrene	Pyrene
<i>19-m Stations</i>													
I35	ND	ND	ND	ND	ND	ND	ND	ND	ND	ND	ND	ND	ND
I34	ND	ND	ND	ND	ND	ND	ND	ND	ND	ND	ND	ND	ND
I31	ND	ND	ND	ND	ND	ND	ND	ND	ND	ND	ND	ND	ND
I23	ND	ND	ND	ND	ND	ND	ND	ND	ND	ND	ND	ND	ND
I18	ND	ND	ND	NR	ND	ND	ND	ND	ND	ND	ND	ND	ND
I10	ND	ND	ND	ND	ND	ND	ND	ND	ND	ND	ND	ND	ND
I4	ND	ND	ND	ND	ND	ND	ND	ND	ND	ND	ND	ND	ND
<i>28-m Stations</i>													
I33	ND	ND	ND	ND	ND	ND	ND	ND	ND	ND	ND	ND	ND
I30	ND	ND	ND	ND	ND	ND	ND	ND	ND	ND	ND	ND	ND
I27	ND	ND	ND	NR	ND	ND	ND	ND	ND	ND	ND	ND	ND
I22	ND	ND	ND	ND	ND	ND	ND	ND	ND	ND	ND	ND	ND
I14 ^a	ND	ND	ND	NR	ND	ND	ND	ND	ND	ND	ND	ND	ND
I16 ^a	ND	ND	ND	ND	ND	ND	ND	ND	ND	ND	ND	ND	ND
I15	ND	ND	ND	NR	ND	ND	ND	ND	ND	ND	ND	ND	ND
I12 ^a	ND	ND	ND	ND	ND	ND	ND	ND	ND	ND	ND	ND	ND
I9	ND	ND	ND	ND	ND	ND	ND	ND	ND	ND	ND	ND	ND
I6	ND	ND	ND	ND	ND	ND	ND	ND	ND	ND	ND	ND	ND
I2	ND	ND	ND	ND	ND	ND	ND	ND	ND	ND	ND	ND	ND
I3	ND	ND	ND	ND	ND	ND	ND	ND	ND	ND	ND	ND	ND
<i>38-m Stations</i>													
I29	ND	ND	ND	ND	ND	ND	ND	ND	ND	ND	ND	ND	ND
I21	ND	ND	ND	ND	ND	ND	ND	ND	ND	ND	ND	ND	ND
I13	ND	ND	ND	ND	ND	ND	ND	ND	ND	ND	ND	ND	ND
I8	ND	ND	ND	ND	ND	ND	ND	ND	ND	ND	ND	ND	ND
<i>55-m Stations</i>													
I28	ND	ND	ND	ND	ND	ND	ND	ND	ND	ND	ND	ND	ND
I20	ND	ND	ND	ND	ND	ND	ND	ND	ND	ND	ND	ND	ND
I7	ND	ND	ND	ND	ND	ND	ND	ND	ND	ND	ND	ND	ND
I1	ND	ND	ND	ND	ND	ND	ND	ND	ND	ND	ND	ND	ND
DR (%)	0	0	0	0	0	0	0	0	0	0	0	0	0

^aNear-ZID station

Appendix F.11 *continued*

Summer 2022	1-methyl naphthalene	1-methyl phenanthrene	2-methyl naphthalene	2,3,5-trimethyl naphthalene	2,6-dimethyl naphthalene	3,4-benzo(B) fluoranthene	Acenaphthene	Acenaphthylene	Anthracene	Benzo(A) anthracene	Benzo(A) pyrene
<i>19-m Stations</i>											
I35	ND	ND	ND	ND	10.8	ND	ND	ND	ND	ND	ND
I34	ND	ND	ND	ND	ND	ND	ND	ND	ND	ND	ND
I31	ND	ND	ND	ND	ND	ND	ND	ND	ND	ND	ND
I23	ND	ND	ND	ND	ND	ND	ND	ND	ND	ND	ND
I18	ND	ND	ND	ND	ND	ND	ND	ND	ND	ND	ND
I10	ND	ND	ND	ND	ND	ND	ND	ND	ND	ND	ND
I4	ND	ND	ND	ND	ND	ND	ND	ND	ND	ND	ND
<i>28-m Stations</i>											
I33	ND	ND	ND	ND	ND	ND	ND	ND	ND	ND	ND
I30	ND	ND	ND	ND	16.5	ND	ND	ND	ND	ND	ND
I27	ND	ND	ND	ND	ND	ND	ND	ND	ND	ND	ND
I22	ND	ND	ND	ND	8.26	ND	ND	ND	ND	ND	ND
I14 ^a	ND	8.12	9.97	ND	11.4	ND	ND	ND	ND	ND	ND
I16 ^a	ND	ND	ND	ND	ND	ND	ND	ND	ND	ND	ND
I15	ND	ND	ND	ND	ND	ND	ND	ND	ND	ND	ND
I12 ^a	ND	ND	ND	ND	ND	ND	ND	ND	ND	ND	ND
I9	ND	ND	ND	ND	8.56	ND	ND	ND	ND	ND	ND
I6	ND	ND	ND	ND	ND	ND	ND	ND	ND	ND	ND
I2	ND	ND	ND	ND	ND	ND	ND	ND	ND	ND	ND
I3	ND	ND	ND	ND	ND	ND	ND	ND	ND	ND	ND
<i>38-m Stations</i>											
I29	ND	ND	ND	ND	10.8	ND	ND	ND	ND	ND	ND
I21	ND	ND	ND	ND	ND	ND	ND	ND	ND	ND	ND
I13	ND	ND	ND	ND	ND	ND	ND	ND	ND	ND	ND
I8	ND	ND	ND	ND	ND	ND	ND	ND	ND	ND	ND
<i>55-m Stations</i>											
I28	ND	ND	ND	ND	8.02	ND	ND	ND	ND	ND	ND
I20	ND	ND	ND	ND	ND	ND	ND	ND	ND	ND	ND
I7	ND	ND	ND	ND	ND	ND	ND	ND	ND	ND	ND
I1	ND	ND	ND	ND	ND	ND	ND	ND	ND	ND	ND
DR (%)	0	4	4	0	26	0	0	0	0	0	0

^a Near-ZID station

Appendix F.11 *continued*

Summer 2022	Benzo[e] pyrene	Benzo[G,H,I] perylene	Benzo[K] fluoranthene	Biphenyl	Chrysene	Dibenzo(A,H) anthracene	Fluoranthene	Fluorene	Indeno(1,2,3-CD) pyrene	Naphthalene	Perylene	Phenanthrene	Pyrene
<i>19-m Stations</i>													
I35	ND	ND	ND	7.67	ND	ND	ND	ND	ND	ND	ND	ND	ND
I34	ND	ND	ND	ND	ND	ND	ND	ND	ND	ND	ND	ND	ND
I31	ND	ND	ND	ND	ND	ND	ND	ND	ND	ND	ND	ND	ND
I23	ND	ND	ND	ND	ND	ND	ND	ND	ND	ND	ND	ND	ND
I18	ND	ND	ND	ND	ND	ND	ND	ND	ND	ND	ND	ND	ND
I10	ND	ND	ND	ND	ND	ND	ND	ND	ND	ND	ND	ND	ND
I4	ND	ND	ND	ND	ND	ND	ND	ND	ND	ND	ND	ND	ND
<i>28-m Stations</i>													
I33	ND	ND	ND	ND	ND	ND	ND	ND	ND	ND	ND	ND	ND
I30	ND	ND	ND	7.29	ND	ND	ND	ND	ND	ND	ND	ND	ND
I27	ND	ND	ND	ND	ND	ND	ND	ND	ND	ND	ND	ND	ND
I22	ND	ND	ND	ND	ND	ND	ND	ND	ND	ND	ND	ND	ND
I14 ^a	ND	ND	ND	ND	ND	ND	ND	ND	14.8	ND	ND	ND	ND
I16 ^a	ND	ND	ND	ND	ND	ND	ND	ND	ND	ND	ND	ND	ND
I15	ND	ND	ND	ND	ND	ND	ND	ND	ND	ND	ND	ND	ND
I12 ^a	ND	ND	ND	ND	ND	ND	ND	ND	ND	ND	ND	ND	ND
I9	ND	ND	ND	ND	ND	ND	ND	ND	ND	ND	ND	ND	ND
I6	ND	ND	ND	ND	ND	ND	ND	ND	ND	ND	ND	ND	ND
I2	ND	ND	ND	ND	ND	ND	ND	ND	ND	ND	ND	ND	ND
I3	ND	ND	ND	ND	ND	ND	ND	ND	ND	ND	ND	ND	ND
<i>38-m Stations</i>													
I29	ND	ND	ND	ND	ND	ND	ND	ND	ND	ND	ND	ND	9.62
I21	ND	ND	ND	ND	11	ND	ND	ND	ND	ND	ND	ND	ND
I13	ND	ND	ND	ND	ND	ND	ND	ND	ND	ND	ND	ND	ND
I8	ND	ND	ND	ND	ND	ND	ND	ND	ND	ND	ND	ND	ND
<i>55-m Stations</i>													
I28	ND	ND	ND	ND	ND	ND	ND	ND	ND	ND	ND	ND	ND
I20	ND	ND	ND	ND	ND	ND	ND	ND	ND	ND	ND	ND	ND
I7	ND	ND	ND	ND	ND	ND	ND	ND	ND	ND	ND	ND	ND
I1	ND	ND	ND	ND	ND	ND	ND	ND	ND	ND	ND	ND	ND
DR (%)	0	0	0	7	4	0	0	0	0	4	0	0	4

^aNear-ZID station

Appendix F.11 *continued*

Winter 2023	1-methyl naphthalene	1-methyl phenanthrene	2-methyl naphthalene	2,3,5-trimethyl naphthalene	2,6-dimethyl naphthalene	3,4-benzo(B) fluoranthene	Acenaphthene	Acenaphthylene	Anthracene	Benzo(A) anthracene	Benzo(A) pyrene
<i>19-m Stations</i>											
I35	ND	ND	ND	ND	ND	ND	ND	ND	ND	ND	ND
I34	ND	ND	ND	ND	ND	ND	ND	ND	ND	ND	ND
I31	ND	ND	ND	ND	ND	ND	ND	ND	ND	ND	ND
I23	ND	ND	ND	ND	ND	ND	ND	ND	ND	ND	ND
I18	ND	ND	ND	ND	ND	ND	ND	ND	ND	ND	ND
I10	ND	ND	ND	ND	ND	ND	ND	ND	ND	ND	ND
I4	ND	ND	ND	ND	ND	ND	ND	ND	ND	ND	ND
<i>28-m Stations</i>											
I33	ND	ND	ND	ND	5.87 DNQ	ND	ND	ND	ND	ND	ND
I30	ND	ND	ND	ND	ND	ND	ND	ND	ND	ND	ND
I27	ND	ND	ND	ND	ND	ND	ND	ND	ND	ND	ND
I22	ND	ND	ND	ND	ND	ND	ND	ND	ND	ND	ND
I14 ^a	ND	ND	ND	ND	ND	ND	ND	ND	ND	ND	ND
I16 ^a	ND	ND	ND	ND	ND	ND	ND	ND	ND	ND	ND
I15	ND	ND	ND	ND	ND	ND	ND	ND	ND	ND	ND
I12 ^a	ND	ND	ND	ND	ND	ND	ND	ND	ND	ND	ND
I9	ND	ND	ND	ND	5.67 DNQ	ND	ND	ND	ND	ND	ND
I6	ND	ND	ND	ND	ND	ND	ND	ND	ND	ND	ND
I2	ND	ND	ND	ND	ND	ND	ND	ND	ND	ND	ND
I3	ND	ND	ND	ND	ND	ND	ND	ND	ND	ND	ND
<i>38-m Stations</i>											
I29	ND	ND	ND	ND	7.62	ND	ND	ND	ND	ND	ND
I21	ND	ND	ND	ND	ND	ND	ND	ND	ND	ND	ND
I13	ND	ND	ND	ND	ND	ND	ND	ND	ND	ND	ND
I8	ND	ND	ND	ND	ND	ND	ND	ND	ND	ND	ND
<i>55-m Stations</i>											
I28	ND	ND	ND	ND	5.43 DNQ	ND	ND	ND	ND	ND	ND
I20	ND	ND	ND	ND	ND	ND	ND	ND	ND	ND	ND
I7	ND	ND	ND	ND	ND	ND	ND	ND	ND	ND	ND
I1	ND	ND	ND	ND	ND	ND	ND	ND	ND	ND	ND
DR (%)	0	0	0	0	15	0	0	0	0	0	0

^a Near-ZID station

Appendix F.11 *continued*

Winter 2023	Benzo[e] pyrene	Benzo[G,H,I] perylene	Benzo[K] fluoranthene	Biphenyl	Chrysene	Dibenzo(A,H) anthracene	Fluoranthene	Fluorene	Indeno(1,2,3-CD) pyrene	Naphthalene	Perylene	Phenanthrene	Pyrene
<i>19-m Stations</i>													
I35	ND	ND	ND	ND	ND	ND	ND	ND	ND	ND	ND	ND	ND
I34	ND	ND	ND	ND	ND	ND	ND	ND	ND	ND	ND	ND	ND
I31	ND	ND	ND	ND	ND	ND	ND	ND	ND	ND	ND	ND	ND
I23	ND	ND	ND	ND	ND	ND	ND	ND	ND	ND	ND	ND	ND
I18	ND	ND	ND	ND	ND	ND	ND	ND	ND	ND	ND	ND	ND
I10	ND	ND	ND	ND	ND	ND	ND	ND	ND	ND	ND	ND	ND
I4	ND	ND	ND	ND	ND	ND	ND	ND	ND	ND	ND	ND	ND
<i>28-m Stations</i>													
I33	ND	ND	ND	5.37 DNQ	ND	ND	ND	ND	ND	ND	ND	ND	ND
I30	ND	ND	ND	ND	ND	ND	ND	ND	ND	ND	ND	ND	ND
I27	ND	ND	ND	ND	ND	ND	ND	ND	ND	ND	ND	ND	ND
I22	ND	ND	ND	ND	ND	ND	ND	ND	ND	ND	ND	ND	ND
I14 ^a	ND	ND	ND	ND	ND	ND	ND	ND	ND	ND	ND	ND	ND
I16 ^a	ND	ND	ND	ND	ND	ND	ND	ND	ND	ND	ND	ND	ND
I15	ND	ND	ND	ND	ND	ND	ND	ND	ND	ND	ND	ND	ND
I12 ^a	ND	ND	ND	ND	ND	ND	ND	ND	ND	ND	ND	ND	ND
I9	ND	ND	ND	ND	ND	ND	ND	ND	ND	ND	ND	ND	ND
I6	ND	ND	ND	ND	ND	ND	ND	ND	ND	ND	ND	ND	ND
I2	ND	ND	ND	ND	ND	ND	ND	ND	ND	ND	ND	ND	ND
I3	ND	ND	ND	ND	ND	ND	ND	ND	ND	ND	ND	ND	ND
<i>38-m Stations</i>													
I29	ND	ND	ND	ND	ND	ND	ND	ND	ND	ND	ND	ND	ND
I21	ND	ND	ND	ND	ND	ND	ND	ND	ND	ND	ND	ND	ND
I13	ND	ND	ND	ND	ND	ND	ND	ND	ND	ND	ND	ND	ND
I8	ND	ND	ND	ND	ND	ND	ND	ND	ND	ND	ND	ND	ND
<i>55-m Stations</i>													
I28	ND	ND	ND	ND	ND	ND	ND	ND	ND	ND	ND	ND	ND
I20	ND	ND	ND	ND	ND	ND	ND	ND	ND	ND	ND	ND	ND
I7	ND	ND	ND	ND	ND	ND	ND	ND	ND	ND	ND	ND	ND
I1	ND	ND	ND	NR	ND	ND	ND	ND	ND	ND	ND	ND	ND
DR (%)	0	0	0	4	0	0	0	0	0	0	0	0	0

^aNear-ZID station

Appendix F.11 *continued*

Summer 2023	1-methyl naphthalene	1-methyl phenanthrene	2-methyl naphthalene	2,3,5-trimethyl naphthalene	2,6-dimethyl naphthalene	3,4-benzo(B) fluoranthene	Acenaphthene	Acenaphthylene	Anthracene	Benzo[A] anthracene	Benzo[A] pyrene
<i>19-m Stations</i>											
I35	—	—	—	—	—	—	—	—	—	—	—
I34	—	—	—	—	—	—	—	—	—	—	—
I31	—	—	—	—	—	—	—	—	—	—	—
I23	—	—	—	—	—	—	—	—	—	—	—
I18	—	—	—	—	—	—	—	—	—	—	—
I10	—	—	—	—	—	—	—	—	—	—	—
I4	—	—	—	—	—	—	—	—	—	—	—
<i>28-m Stations</i>											
I33	ND	ND	ND	ND	4.69	ND	ND	ND	ND	ND	ND
I30	ND	ND	ND	ND	ND	ND	ND	ND	ND	ND	ND
I27	ND	ND	ND	ND	4.84 DNQ	ND	ND	ND	ND	ND	ND
I22	ND	ND	ND	ND	5.07 DNQ	ND	ND	ND	ND	ND	ND
I14 ^a	ND	ND	ND	ND	ND	ND	ND	ND	ND	ND	ND
I16 ^a	ND	ND	ND	ND	ND	ND	ND	ND	ND	ND	ND
I15	ND	ND	ND	ND	4.29 DNQ	ND	ND	ND	ND	ND	ND
I12 ^a	ND	ND	ND	ND	ND	ND	ND	ND	ND	ND	ND
I9	ND	ND	ND	ND	8.37 DNQ	ND	ND	ND	ND	ND	ND
I6	ND	ND	ND	ND	ND	ND	ND	ND	ND	ND	ND
I2	ND	ND	ND	ND	ND	ND	ND	ND	ND	ND	ND
I3	ND	ND	ND	ND	ND	ND	ND	ND	ND	ND	ND
<i>38-m Stations</i>											
I29	—	—	—	—	—	—	—	—	—	—	—
I21	—	—	—	—	—	—	—	—	—	—	—
I13	—	—	—	—	—	—	—	—	—	—	—
I8	—	—	—	—	—	—	—	—	—	—	—
<i>55-m Stations</i>											
I28	—	—	—	—	—	—	—	—	—	—	—
I20	—	—	—	—	—	—	—	—	—	—	—
I7	—	—	—	—	—	—	—	—	—	—	—
I1	—	—	—	—	—	—	—	—	—	—	—
DR (%)	0	0	0	0	42	0	0	0	0	0	0

^a Near-ZID station

Appendix F.11 continued

Summer 2023	Benzo[e] pyrene	Benzo[G,H,I] perylene	Benzo[K] fluoranthene	Biphenyl	Chrysene	Dibenzo(A,H) anthracene	Fluoranthene	Fluorene	Indeno(1,2,3-CD) pyrene	Naphthalene	Perylene	Phenanthrene	Pyrene
<i>19-m Stations</i>													
I35	—	—	—	—	—	—	—	—	—	—	—	—	—
I34	—	—	—	—	—	—	—	—	—	—	—	—	—
I31	—	—	—	—	—	—	—	—	—	—	—	—	—
I23	—	—	—	—	—	—	—	—	—	—	—	—	—
I18	—	—	—	—	—	—	—	—	—	—	—	—	—
I10	—	—	—	—	—	—	—	—	—	—	—	—	—
I4	—	—	—	—	—	—	—	—	—	—	—	—	—
<i>28-m Stations</i>													
I33	ND	ND	ND	NR	ND	ND	ND	ND	ND	ND	ND	ND	ND
I30	ND	ND	ND	NR	ND	ND	ND	ND	ND	ND	ND	ND	ND
I27	ND	ND	ND	NR	ND	ND	ND	ND	ND	ND	ND	ND	ND
I22	ND	ND	ND	NR	ND	ND	ND	ND	ND	ND	ND	ND	ND
I14 ^a	ND	ND	ND	NR	ND	ND	ND	ND	ND	ND	ND	ND	ND
I16 ^a	ND	ND	ND	NR	ND	ND	ND	ND	ND	ND	ND	ND	ND
I15	ND	ND	ND	ND	ND	ND	ND	ND	ND	ND	ND	ND	ND
I12 ^a	ND	ND	ND	NR	ND	ND	ND	ND	ND	ND	ND	ND	ND
I9	ND	ND	ND	NR	ND	ND	ND	ND	ND	ND	ND	ND	ND
I6	ND	ND	ND	NR	ND	ND	ND	ND	ND	ND	ND	ND	ND
I2	ND	ND	ND	NR	ND	ND	ND	ND	ND	ND	ND	ND	ND
I3	ND	ND	ND	NR	ND	ND	ND	ND	ND	ND	ND	ND	ND
<i>38-m Stations</i>													
I29	—	—	—	—	—	—	—	—	—	—	—	—	—
I21	—	—	—	—	—	—	—	—	—	—	—	—	—
I13	—	—	—	—	—	—	—	—	—	—	—	—	—
I8	—	—	—	—	—	—	—	—	—	—	—	—	—
<i>55-m Stations</i>													
I28	—	—	—	—	—	—	—	—	—	—	—	—	—
I20	—	—	—	—	—	—	—	—	—	—	—	—	—
I7	—	—	—	—	—	—	—	—	—	—	—	—	—
I1	—	—	—	—	—	—	—	—	—	—	—	—	—
DR (%)	0	0	0	0	0	0	0	0	0	0	0	0	0

^aNear-ZID station

Appendix F.12

Concentrations of PBDEs (ppt) detected in sediments from PLOO stations sampled during 2022 and 2023. See Appendix F.1 for MDLs; DR = detection rate; DNQ = do not quantify; ND = not detected; NR = not reportable. Only primary core stations sampled during summer 2023 due to resource exchange for Bight'23 (see text).

Winter 2022	BDE-17	BDE-28	BDE-47	BDE-49	BDE-66	BDE-85	BDE-99	BDE-100	BDE-138	BDE-153	BDE-154	BDE-183	BDE-190
<i>88-m Depth Contour</i>													
B11	ND	ND	NR	ND	ND	ND	87.8 DNQ	ND	ND	ND	ND	ND	ND
B8	ND	ND	NR	ND	ND	ND	78.1 DNQ	ND	ND	ND	ND	ND	ND
E19	ND	ND	NR	ND	ND	ND	123	ND	ND	ND	ND	ND	ND
E7	ND	ND	NR	ND	ND	ND	66.7 DNQ	ND	ND	ND	ND	ND	ND
E1	ND	ND	NR	ND	ND	ND	60.7 DNQ	ND	ND	ND	ND	ND	ND
<i>98-m Depth Contour</i>													
B12	ND	ND	NR	ND	ND	ND	ND	ND	ND	ND	ND	ND	ND
B9	ND	ND	NR	ND	ND	ND	ND	ND	ND	ND	ND	ND	ND
E26	ND	ND	NR	ND	ND	ND	ND	ND	ND	ND	ND	ND	ND
E25	ND	ND	NR	ND	ND	ND	62.6 DNQ	ND	ND	ND	ND	ND	ND
E23	ND	ND	NR	ND	ND	ND	72.0 DNQ	ND	ND	ND	ND	ND	ND
E20	ND	ND	NR	ND	ND	ND	81.3 DNQ	ND	ND	ND	ND	ND	ND
E17 ^a	ND	ND	172	ND	ND	ND	115	ND	ND	ND	ND	ND	ND
E14 ^a	ND	ND	309	ND	ND	ND	227	87.0 DNQ	ND	ND	ND	ND	ND
E11 ^a	ND	ND	130	ND	ND	ND	91.2	ND	ND	ND	ND	ND	ND
E8	ND	ND	NR	ND	ND	ND	74.1 DNQ	ND	ND	ND	ND	ND	ND
E5	ND	ND	NR	ND	ND	ND	ND	ND	ND	ND	ND	ND	ND
E2	ND	ND	NR	ND	ND	ND	ND	ND	ND	ND	ND	ND	ND
<i>116-m Depth Contour</i>													
B10	ND	ND	NR	ND	ND	ND	ND	ND	ND	ND	ND	ND	ND
E21	ND	ND	NR	ND	ND	ND	74.1 DNQ	ND	ND	ND	ND	ND	ND
E15 ^a	ND	ND	153	ND	ND	ND	126	55.8 DNQ	ND	ND	ND	ND	ND
E9	ND	ND	NR	ND	ND	ND	ND	ND	ND	ND	ND	ND	ND
E3	ND	ND	NR	ND	ND	ND	ND	ND	ND	ND	ND	ND	ND
DR (%)	0	0	100	0	0	0	64	9	0	0	0	0	0

^a Near-ZID station

Appendix F.12 continued

Summer 2022	BDE-17	BDE-28	BDE-47	BDE-49	BDE-66	BDE-85	BDE-99	BDE-100	BDE-138	BDE-154	BDE-183	BDE-190
<i>88-m Depth Contour</i>												
B11	ND	ND	NR	ND	ND	ND	ND	ND	ND	ND	ND	ND
B8	ND	ND	119	ND	ND	ND	94.9 DNQ	ND	ND	ND	ND	ND
E19	ND	ND	NR	ND	ND	ND	92.2 DNQ	ND	ND	ND	ND	ND
E7	ND	ND	NR	ND	ND	ND	94.2 DNQ	ND	ND	ND	ND	ND
E1	ND	ND	NR	ND	ND	ND	90.4 DNQ	ND	ND	ND	ND	ND
<i>98-m Depth Contour</i>												
B12	ND	ND	ND	ND	ND	ND	ND	ND	ND	ND	ND	ND
B9	ND	ND	NR	ND	ND	ND	69.9 DNQ	ND	ND	ND	ND	ND
E26	ND	ND	134	ND	ND	ND	93.4	ND	ND	ND	ND	ND
E25	ND	ND	NR	ND	ND	ND	70.3 DNQ	ND	ND	ND	ND	ND
E23	ND	ND	NR	ND	ND	ND	93.2 DNQ	ND	ND	ND	ND	ND
E20	ND	ND	NR	ND	ND	ND	ND	ND	ND	ND	ND	ND
E17 ^a	ND	ND	133	ND	ND	ND	107	ND	ND	ND	ND	ND
E14 ^a	ND	ND	148	ND	ND	ND	107	ND	ND	ND	ND	ND
E11 ^a	ND	ND	NR	ND	ND	ND	67.4 DNQ	ND	ND	ND	ND	ND
E8	ND	ND	NR	ND	ND	ND	77.4 DNQ	ND	ND	ND	ND	ND
E5	ND	ND	NR	ND	ND	ND	66.1 DNQ	ND	ND	ND	ND	ND
E2	ND	ND	NR	ND	ND	ND	ND	ND	ND	ND	ND	ND
<i>116-m Depth Contour</i>												
B10	ND	ND	NR	ND	ND	ND	ND	ND	ND	ND	ND	ND
E21	ND	ND	NR	ND	ND	ND	NR	ND	ND	ND	ND	ND
E15 ^a	ND	ND	NR	ND	ND	ND	ND	ND	ND	ND	ND	ND
E9	ND	ND	NR	ND	ND	ND	ND	ND	ND	ND	ND	ND
E3	ND	ND	NR	ND	ND	ND	ND	ND	ND	ND	ND	ND
DR (%)	0	0	80	0	0	0	62	0	0	0	0	0

^a Near-ZID station

Appendix F.12 continued

Winter 2023	BDE-17	BDE-28	BDE-47	BDE-49	BDE-66	BDE-85	BDE-99	BDE-100	BDE-138	BDE-153	BDE-154	BDE-183	BDE-190
<i>88-m Depth Contour</i>													
B11	ND	ND	ND	ND	ND	ND	ND	ND	ND	ND	ND	ND	ND
B8	ND	ND	ND	ND	ND	ND	72.5 DNQ	ND	ND	ND	ND	ND	ND
E19	ND	ND	96	ND	ND	ND	105	ND	ND	ND	ND	ND	ND
E7	ND	ND	92.9	ND	ND	ND	79.4 DNQ	ND	ND	ND	ND	ND	ND
E1	ND	ND	ND	ND	ND	ND	ND	ND	ND	ND	ND	ND	ND
<i>98-m Depth Contour</i>													
B12	ND	ND	ND	ND	ND	ND	ND	ND	ND	ND	ND	ND	ND
B9	ND	ND	ND	ND	ND	ND	76.6 DNQ	ND	ND	ND	ND	ND	ND
E26	ND	ND	ND	ND	ND	ND	ND	ND	ND	ND	ND	ND	ND
E25	ND	ND	ND	ND	ND	ND	ND	ND	ND	ND	ND	ND	ND
E23	ND	ND	75.1 DNQ	ND	ND	ND	82.0	ND	ND	ND	ND	ND	ND
E20	ND	ND	79.5 DNQ	ND	ND	ND	83.9 DNQ	ND	ND	ND	ND	ND	ND
E17 ^a	ND	ND	140	ND	ND	ND	141	51.9 DNQ	ND	ND	ND	ND	ND
E14 ^a	ND	ND	216	ND	ND	ND	229	73.6 DNQ	ND	ND	ND	ND	ND
E11 ^a	ND	ND	119	ND	ND	ND	123	ND	ND	ND	ND	ND	ND
E8	ND	ND	ND	ND	ND	ND	ND	ND	ND	ND	ND	ND	ND
E5	ND	ND	ND	ND	ND	ND	ND	ND	ND	ND	ND	ND	ND
E2	ND	ND	ND	ND	ND	ND	71.3 DNQ	ND	ND	ND	ND	ND	ND
<i>116-m Depth Contour</i>													
B10	ND	ND	ND	ND	ND	ND	57.8 DNQ	ND	ND	ND	ND	ND	ND
E21	ND	ND	ND	ND	ND	ND	63.3 DNQ	ND	ND	ND	ND	ND	ND
E15 ^a	ND	ND	ND	ND	ND	ND	78.1 DNQ	ND	ND	ND	ND	ND	ND
E9	ND	ND	ND	ND	ND	ND	ND	ND	ND	ND	ND	ND	ND
E3	ND	ND	ND	ND	ND	ND	ND	ND	ND	ND	ND	ND	ND
DR (%)	0	0	32	0	0	0	59	9	0	0	0	0	0

^a Near-ZID station

Appendix F.12 continued

Summer 2023	BDE-17	BDE-28	BDE-47	BDE-49	BDE-66	BDE-85	BDE-99	BDE-100	BDE-138	BDE-154	BDE-183	BDE-190
<i>88-m Depth Contour</i>												
B11	—	—	—	—	—	—	—	—	—	—	—	—
B8	—	—	—	—	—	—	—	—	—	—	—	—
E19	—	—	—	—	—	—	—	—	—	—	—	—
E7	—	—	—	—	—	—	—	—	—	—	—	—
E1	—	—	—	—	—	—	—	—	—	—	—	—
<i>98-m Depth Contour</i>												
B12	ND	ND	ND	ND	ND	ND	ND	ND	ND	ND	ND	ND
B9	ND	ND	ND	ND	ND	ND	60.9 DNQ	ND	ND	ND	ND	ND
E26	ND	ND	ND	ND	ND	ND	88.6 DNQ	ND	ND	ND	ND	ND
E25	ND	ND	86.4 DNQ	ND	ND	ND	80.6 DNQ	ND	ND	ND	ND	ND
E23	ND	ND	97.7	ND	ND	ND	89.2	ND	ND	ND	ND	ND
E20	ND	ND	88.9	ND	ND	ND	90.9	ND	ND	ND	ND	ND
E17 ^a	ND	ND	174	ND	ND	ND	154	57.8 DNQ	ND	ND	ND	ND
E14 ^a	ND	ND	200	57.5 DNQ	ND	ND	198	73.8 DNQ	ND	ND	ND	ND
E11 ^a	ND	ND	134	ND	ND	ND	130	ND	ND	ND	ND	ND
E8	ND	ND	81.2 DNQ	ND	ND	ND	69.5 DNQ	ND	ND	ND	ND	ND
E5	ND	ND	87.5	ND	ND	ND	83.4 DNQ	ND	ND	ND	ND	ND
E2	ND	ND	88.2	ND	ND	ND	88.5	ND	ND	ND	ND	ND
<i>116-m Depth Contour</i>												
B10	—	—	—	—	—	—	—	—	—	—	—	—
E21	—	—	—	—	—	—	—	—	—	—	—	—
E15 ^a	ND	ND	83.2 DNQ	ND	ND	ND	71.6 DNQ	ND	ND	ND	ND	ND
E9	—	—	—	—	—	—	—	—	—	—	—	—
E3	—	—	—	—	—	—	—	—	—	—	—	—
DR (%)	0	0	77	8	0	0	92	15	0	0	0	0

^a Near-ZID station

Appendix F.13

Concentrations of PBDEs (ppt) detected in sediments from SBOO stations sampled during 2022 and 2023. See Appendix F.1 for MDLs; DR=detection rate; DNQ = do not quantify; ND=not detected; NR=not reportable. Only primary core stations sampled during summer 2023 due to resource exchange for Bight'23 (see text).

Winter 2022	BDE-17	BDE-28	BDE-47	BDE-49	BDE-66	BDE-85	BDE-99	BDE-100	BDE-138	BDE-153	BDE-154	BDE-183	BDE-190
<i>19-m Stations</i>													
I35	ND	ND	NR	ND	ND	ND	ND	ND	ND	ND	ND	ND	ND
I34	ND	ND	ND	ND	ND	ND	ND	ND	ND	ND	ND	ND	ND
I31	ND	ND	NR	ND	ND	ND	ND	ND	ND	ND	ND	ND	ND
I23	ND	ND	ND	ND	ND	ND	ND	ND	ND	ND	ND	ND	ND
I18	ND	ND	NR	ND	ND	ND	ND	ND	ND	ND	ND	ND	ND
I10	ND	ND	ND	ND	ND	ND	ND	ND	ND	ND	ND	ND	ND
I4	ND	ND	NR	ND	ND	ND	ND	ND	ND	ND	ND	ND	ND
<i>28-m Stations</i>													
I33	ND	ND	ND	ND	ND	ND	ND	ND	ND	ND	ND	ND	ND
I30	ND	ND	NR	ND	ND	ND	67.3 DNQ	ND	ND	ND	ND	ND	ND
I27	ND	ND	NR	ND	ND	ND	ND	ND	ND	ND	ND	ND	ND
I22	ND	ND	NR	ND	ND	ND	ND	ND	ND	ND	ND	ND	ND
I14 ^a	ND	ND	NR	ND	ND	ND	ND	ND	ND	ND	ND	ND	ND
I16 ^a	ND	ND	ND	ND	ND	ND	ND	ND	ND	ND	ND	ND	ND
I15	ND	ND	ND	ND	ND	ND	ND	ND	ND	ND	ND	ND	ND
I12 ^a	ND	ND	NR	ND	ND	ND	ND	ND	ND	ND	ND	ND	ND
I9	ND	ND	NR	ND	ND	ND	ND	ND	ND	ND	ND	ND	ND
I6	ND	ND	NR	ND	ND	ND	ND	ND	ND	ND	ND	ND	ND
I2	ND	ND	NR	ND	ND	ND	ND	ND	ND	ND	ND	ND	ND
I3	ND	ND	ND	ND	ND	ND	ND	ND	ND	ND	ND	ND	ND
<i>38-m Stations</i>													
I29	ND	ND	NR	ND	ND	ND	ND	ND	ND	ND	ND	ND	ND
I21	ND	ND	ND	ND	ND	ND	ND	ND	ND	ND	ND	ND	ND
I13	ND	ND	ND	ND	ND	ND	ND	ND	ND	ND	ND	ND	ND
I8	ND	ND	ND	ND	ND	ND	ND	ND	ND	ND	ND	ND	ND
<i>55-m Stations</i>													
I28	ND	ND	NR	ND	ND	ND	ND	ND	ND	ND	ND	ND	ND
I20	ND	ND	ND	ND	ND	ND	ND	ND	ND	ND	ND	ND	ND
I7	ND	ND	ND	ND	ND	ND	ND	ND	ND	ND	ND	ND	ND
I1	ND	ND	NR	ND	ND	ND	ND	ND	ND	ND	ND	ND	ND
DR (%)	0	0	0	0	0	0	4	0	0	0	0	0	0

^aNear-ZID station

Appendix F.13 *continued*

Summer 2022	BDE-17	BDE-28	BDE-47	BDE-49	BDE-66	BDE-85	BDE-99	BDE-100	BDE-138	BDE-153	BDE-154	BDE-183	BDE-190
<i>19-m Stations</i>													
I35	ND	ND	NR	ND	ND	ND	ND	ND	ND	ND	ND	ND	ND
I34	ND	ND	NR	ND	ND	ND	ND	ND	ND	ND	ND	ND	ND
I31	ND	ND	NR	ND	ND	ND	ND	ND	ND	ND	ND	ND	ND
I23	ND	ND	NR	ND	ND	ND	ND	ND	ND	ND	ND	ND	ND
I18	ND	ND	NR	ND	ND	ND	ND	ND	ND	ND	ND	ND	ND
I10	ND	ND	NR	ND	ND	ND	ND	ND	ND	ND	ND	ND	ND
I4	ND	ND	NR	ND	ND	ND	ND	ND	ND	ND	ND	ND	ND
<i>28-m Stations</i>													
I33	ND	ND	NR	ND	ND	ND	ND	ND	ND	ND	ND	ND	ND
I30	ND	ND	NR	ND	ND	ND	ND	ND	ND	ND	ND	ND	ND
I27	ND	ND	NR	ND	ND	ND	ND	ND	ND	ND	ND	ND	ND
I22	ND	ND	NR	ND	ND	ND	ND	ND	ND	ND	ND	ND	ND
I14 ^a	ND	ND	NR	ND	ND	ND	ND	ND	ND	ND	ND	ND	ND
I16 ^a	ND	ND	ND	ND	ND	ND	ND	ND	ND	ND	ND	ND	ND
I15	ND	ND	ND	ND	ND	ND	ND	ND	ND	ND	ND	ND	ND
I12 ^a	ND	ND	ND	ND	ND	ND	ND	ND	ND	ND	ND	ND	ND
I9	ND	ND	NR	ND	ND	ND	ND	ND	ND	ND	ND	ND	ND
I6	ND	ND	ND	ND	ND	ND	ND	ND	ND	ND	ND	ND	ND
I2	ND	ND	ND	ND	ND	ND	ND	ND	ND	ND	ND	ND	ND
I3	ND	ND	NR	ND	ND	29.9 DNQ	ND	ND	ND	ND	ND	ND	ND
<i>38-m Stations</i>													
I29	ND	ND	NR	ND	ND	ND	ND	ND	ND	ND	ND	ND	ND
I21	ND	ND	NR	ND	ND	ND	ND	ND	ND	ND	ND	ND	ND
I13	ND	ND	ND	ND	ND	ND	ND	ND	ND	ND	ND	ND	ND
I8	ND	ND	ND	ND	ND	ND	ND	ND	ND	ND	ND	ND	ND
<i>55-m Stations</i>													
I28	ND	ND	NR	ND	ND	ND	ND	ND	ND	ND	ND	ND	ND
I20	ND	ND	NR	ND	ND	ND	ND	ND	ND	ND	ND	ND	ND
I7	ND	ND	ND	ND	ND	ND	ND	ND	ND	ND	ND	ND	ND
I1	ND	ND	NR	ND	ND	ND	ND	ND	ND	ND	ND	ND	ND
DR (%)	0	0	0	0	0	4	0	0	0	0	0	0	0

^a Near-ZID station

Appendix F.13 *continued*

Winter 2023	BDE-17	BDE-28	BDE-47	BDE-49	BDE-66	BDE-85	BDE-99	BDE-100	BDE-138	BDE-153	BDE-154	BDE-183	BDE-190
<i>19-m Stations</i>													
I35	ND	ND	ND	ND	ND	ND	ND	ND	ND	ND	ND	ND	ND
I34	ND	ND	ND	ND	ND	ND	ND	ND	ND	ND	ND	ND	ND
I31	ND	ND	ND	ND	ND	ND	ND	ND	ND	ND	ND	ND	ND
I23	ND	ND	ND	ND	ND	ND	ND	ND	ND	ND	ND	ND	ND
I18	ND	ND	ND	ND	ND	ND	ND	ND	ND	ND	ND	ND	ND
I10	ND	ND	ND	ND	ND	50.9 DNQ	ND	ND	ND	ND	ND	ND	ND
I4	ND	ND	ND	ND	ND	ND	ND	ND	ND	ND	ND	ND	ND
<i>28-m Stations</i>													
I33	ND	ND	ND	ND	ND	ND	ND	ND	ND	ND	ND	ND	ND
I30	ND	ND	ND	ND	ND	ND	ND	ND	ND	ND	ND	ND	ND
I27	ND	ND	ND	ND	ND	ND	ND	ND	ND	ND	ND	ND	ND
I22	ND	ND	ND	ND	ND	72.8 DNQ	ND	ND	ND	ND	ND	ND	ND
I14 ^a	ND	ND	ND	ND	ND	ND	NR	ND	ND	ND	ND	ND	ND
I16 ^a	ND	ND	ND	ND	ND	76.2 DNQ	ND	ND	ND	ND	ND	ND	ND
I15	ND	ND	ND	ND	ND	ND	ND	ND	ND	ND	ND	ND	ND
I12 ^a	ND	ND	ND	ND	ND	ND	ND	ND	ND	ND	ND	ND	ND
I9	ND	ND	ND	ND	ND	ND	ND	ND	ND	ND	ND	ND	ND
I6	ND	ND	ND	ND	ND	ND	ND	ND	ND	ND	ND	ND	ND
I2	ND	ND	ND	ND	ND	ND	ND	ND	ND	ND	ND	ND	ND
I3	ND	ND	ND	ND	ND	ND	ND	ND	ND	ND	ND	ND	ND
<i>38-m Stations</i>													
I29	ND	ND	NR	ND	ND	ND	142	ND	ND	ND	ND	ND	ND
I21	ND	ND	ND	ND	ND	ND	ND	ND	ND	ND	ND	ND	ND
I13	ND	ND	ND	ND	ND	ND	ND	ND	ND	ND	ND	ND	ND
I8	ND	ND	ND	ND	ND	ND	ND	ND	ND	ND	ND	ND	ND
<i>55-m Stations</i>													
I28	ND	ND	ND	ND	ND	ND	81.4 DNQ	ND	ND	ND	ND	ND	ND
I20	ND	ND	ND	ND	ND	ND	ND	ND	ND	ND	ND	ND	ND
I7	ND	ND	ND	ND	ND	ND	ND	ND	ND	ND	ND	ND	ND
I1	ND	ND	ND	ND	ND	ND	ND	ND	ND	ND	ND	ND	ND
DR (%)	0	0	0	0	0	0	19	0	0	0	0	0	0

^a Near-ZID station

Appendix F.13 *continued*

Summer 2023	BDE-17	BDE-28	BDE-47	BDE-49	BDE-66	BDE-85	BDE-99	BDE-100	BDE-138	BDE-153	BDE-154	BDE-183	BDE-190
<i>19-m Stations</i>													
I35	—	—	—	—	—	—	—	—	—	—	—	—	—
I34	—	—	—	—	—	—	—	—	—	—	—	—	—
I31	—	—	—	—	—	—	—	—	—	—	—	—	—
I23	—	—	—	—	—	—	—	—	—	—	—	—	—
I18	—	—	—	—	—	—	—	—	—	—	—	—	—
I10	—	—	—	—	—	—	—	—	—	—	—	—	—
I4	—	—	—	—	—	—	—	—	—	—	—	—	—
<i>28-m Stations</i>													
I33	ND	ND	ND	ND	ND	ND	ND	ND	ND	ND	ND	ND	ND
I30	ND	ND	ND	ND	ND	ND	ND	ND	ND	ND	ND	ND	ND
I27	ND	ND	ND	ND	ND	ND	ND	ND	ND	ND	ND	ND	ND
I22	ND	ND	ND	ND	ND	67.7 DNQ	ND	ND	ND	ND	ND	ND	ND
I14 ^a	ND	ND	ND	ND	ND	66.3 DNQ	ND	ND	ND	ND	ND	ND	ND
I16 ^a	ND	ND	ND	ND	ND	ND	ND	ND	ND	ND	ND	ND	ND
I15	ND	ND	ND	ND	ND	ND	ND	ND	ND	ND	ND	ND	ND
I12 ^a	ND	ND	ND	ND	ND	73.4 DNQ	ND	ND	ND	ND	ND	ND	ND
I9	ND	ND	ND	ND	ND	ND	ND	ND	ND	ND	ND	ND	ND
I6	ND	ND	ND	ND	ND	ND	ND	ND	ND	ND	ND	ND	ND
I2	ND	ND	ND	ND	ND	ND	ND	ND	ND	ND	ND	ND	ND
I3	ND	ND	ND	ND	ND	ND	ND	ND	ND	ND	ND	ND	ND
<i>38-m Stations</i>													
I29	—	—	—	—	—	—	—	—	—	—	—	—	—
I21	—	—	—	—	—	—	—	—	—	—	—	—	—
I13	—	—	—	—	—	—	—	—	—	—	—	—	—
I8	—	—	—	—	—	—	—	—	—	—	—	—	—
<i>55-m Stations</i>													
I28	—	—	—	—	—	—	—	—	—	—	—	—	—
I20	—	—	—	—	—	—	—	—	—	—	—	—	—
I7	—	—	—	—	—	—	—	—	—	—	—	—	—
I1	—	—	—	—	—	—	—	—	—	—	—	—	—
DR (%)	0	0	0	0	0	0	25	0	0	0	0	0	0

^a Near-ZID station

Appendix F.14

Particle size classification schemes (based on Folk 1980) used in the analysis of sediments during 2022 and 2023. Included is a subset of the Wentworth scale presented as “phi” categories with corresponding Horiba channels, sieve sizes, and size fractions.

Wentworth Scale					
Phi size	Horiba^a		Sieve Size	Sub-Fraction	Fraction
	Min μm	Max μm			
-1	—	—	SIEVE_2000	Granules	Coarse Particles
0	1100	2000	SIEVE_1000	Very coarse sand	Coarse Particles
1	590	1000	SIEVE_500	Coarse sand	Med-Coarse Sands
2	300	500	SIEVE_250	Medium sand	Med-Coarse Sands
3	149	250	SIEVE_125	Fine sand	Fine Sands
4	64	125	SIEVE_75	Very fine sand	Fine Sands
4	64	125	SIEVE_63	Very fine sand	Fine Sands
5	32	62.5	SIEVE_0 ^b	Coarse silt	Fine Particles ^c
6	16	31	—	Medium silt	Fine Particles ^c
7	8	15.6	—	Fine silt	Fine Particles ^c
8	4	7.8	—	Very fine silt	Fine Particles ^c
9	\leq	3.9	—	Clay	Fine Particles ^c

^aValues correspond to Horiba channels; particles > 2000 μm measured by sieve

^bSIEVE_0=sum of all silt and clay, which cannot be distinguished for samples processed by nested sieves

^cFine particles also referred to as percent fines

Appendix F.15

Summary of visual observations for each PLOO and SBOO station sampled during 2022–2023. Visual observations are from sieved “grunge” (i.e., particles retained on 1-mm mesh screen and preserved with infauna for benthic community analysis).

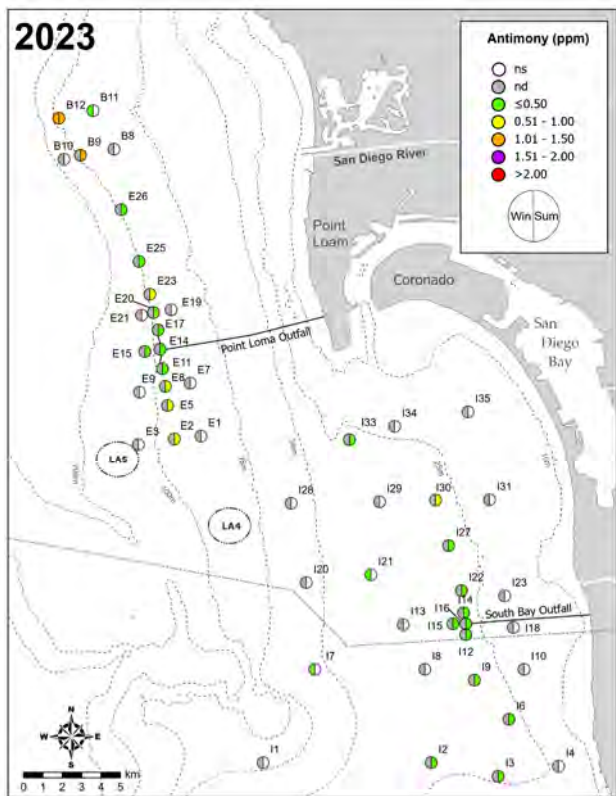
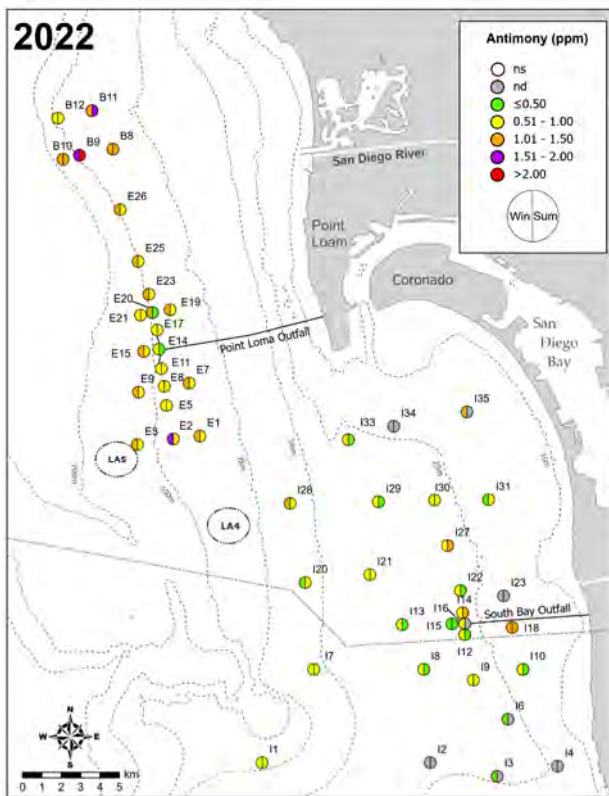
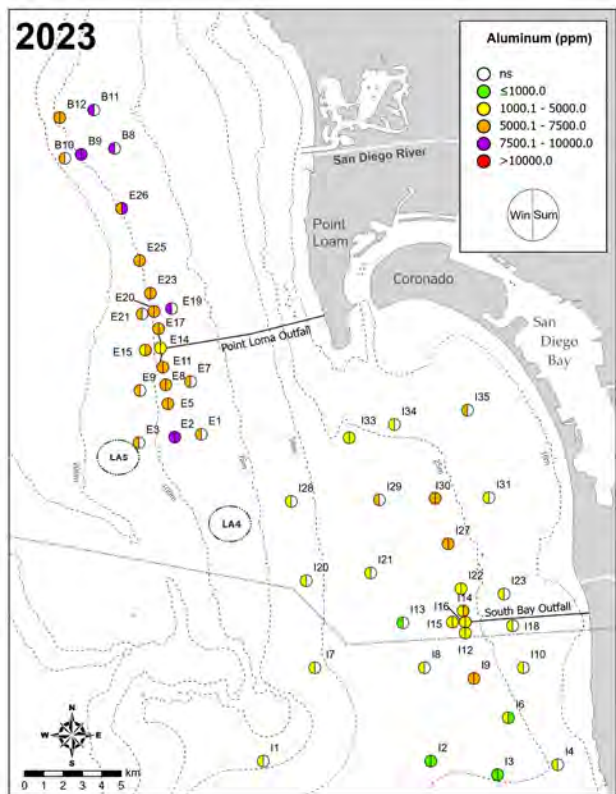
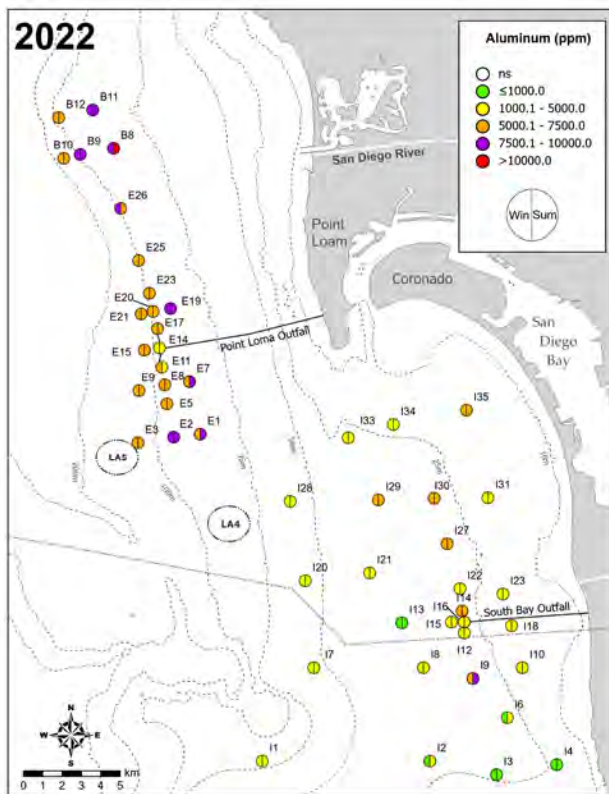
PLOO	Winter 2022		Summer 2022		Winter 2023		Summer 2023	
	Station	Observations	Station	Observations	Station	Observations	Station	Observations
88-m Stations	B11	coarse sand; shell hash		gravel; shell hash		coarse sand; pea gravel		—
	B8	—		—		—		—
	E19	—		—		—		—
	E7	—		—		—		—
	E1	large cobble; shell hash		shell hash		shell hash; pea gravel		—
	B12	gravel; shell hash		gravel; shell hash		shell hash; pea gravel		pea gravel; shell hash
	B9	pea gravel; organic debris		pea gravel		—		pea gravel
98-m Stations	E26	—		—		shell hash		shell hash; organic debris
	E25	—		shell hash; organic debris		—		shell hash
	E23	shell hash		shell hash; organic debris		—		shell hash; organic debris
	E20	shell hash		—		—		organic debris
	E17 ^a	—		worm tubes		organic debris		organic debris
	E14 ^a	gravel; shell hash		coarse black sand; shell hash; organic debris		shell hash; pea gravel; organic debris		pea gravel; shell hash; organic debris
	E11 ^a	—		—		—		shell hash; organic debris
	E8	coarse sand; shell hash		—		—		shell hash; organic debris
	E5	shell hash; organic debris		shell hash; organic debris		—		shell hash; organic debris
	E2	cobble, shell hash		gravel; cobble; shell hash		shell hash; pea gravel		gravel; cobble; shell hash
116-m Stations	B10	shell hash; organic debris		—		shell hash; organic debris		—
	E21	—		—		—		—
	E15 ^a	gravel; shell hash; organic debris		—		coarse sand		pea gravel; shell hash; organic debris
E9	coarse black sand; shell hash		coarse black sand; shell hash		shell hash; pea gravel		—	
	E3	gravel; shell hash		coarse sand		coarse sand; pea gravel		—

^a Near-ZID station

Appendix F.15 *continued*

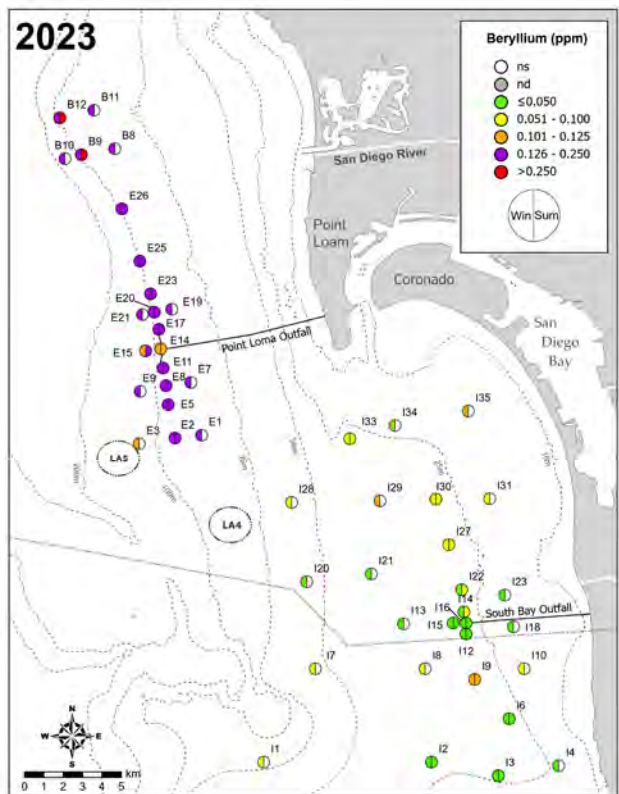
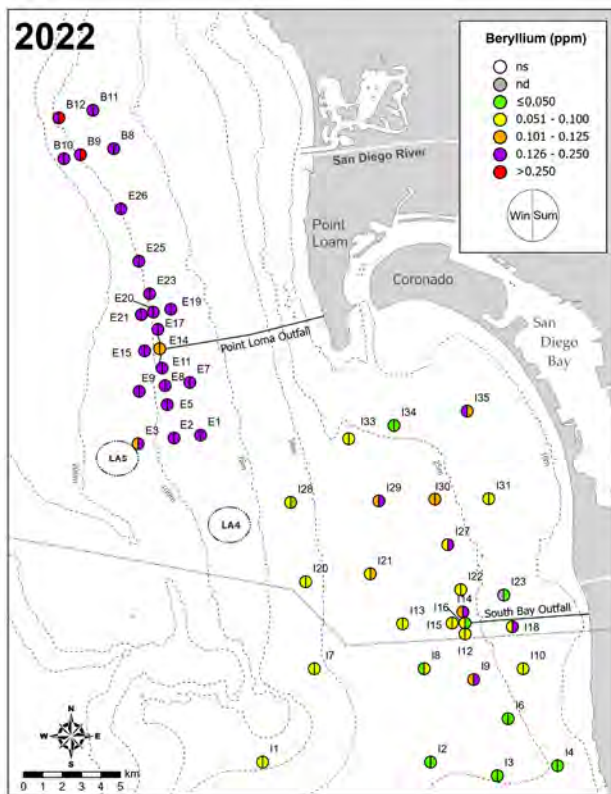
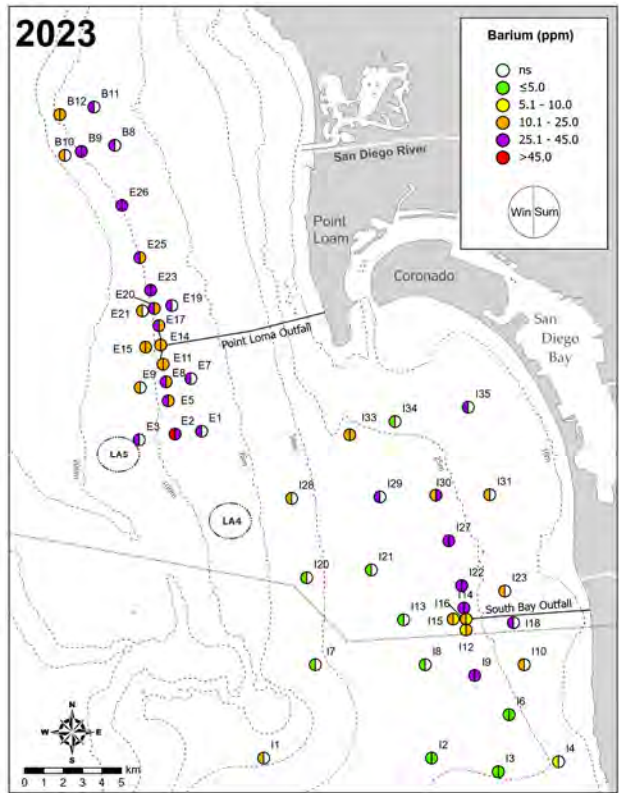
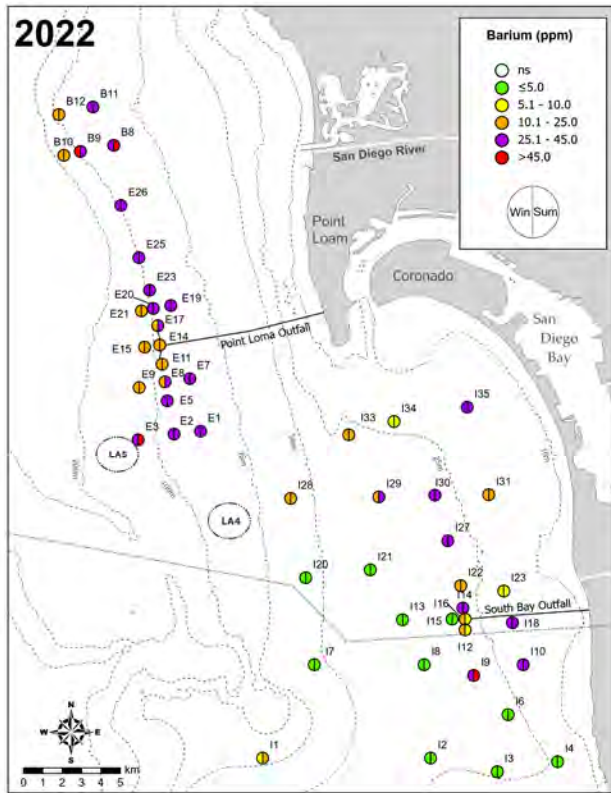
	Winter 2022	Summer 2022	Winter 2023	Summer 2023
SBOO				
<i>19-m Stations</i>				
135	—	—	organic debris	—
134	—	—	shell hash; coarse sand	—
131	—	—	—	—
123	coarse sand; shell hash	coarse sand; shell hash	shell hash; pea gravel	—
118	—	—	—	—
110	—	—	—	—
14	shell hash; cobble	—	shell hash; pea gravel	—
<i>28-m Stations</i>				
133	—	—	coarse sand; pea gravel; organic debris	organic debris
130	—	—	—	organic debris
127	—	—	—	—
122	—	—	—	organic debris
114 ^a	—	—	—	—
116 ^a	—	—	—	shell hash; coarse sand
115 ^a	—	—	—	—
112 ^a	shell hash	shell hash	—	—
19	—	—	—	—
16	shell hash	—	shell hash; coarse sand	shell hash; coarse sand
12	—	—	—	—
13	—	—	—	—
<i>38-m Stations</i>				
129	—	—	—	—
121	—	—	—	—
113	—	shell hash	shell hash; coarse sand	—
18	coarse sand; shell hash	—	—	—
<i>55-m Stations</i>				
128	coarse black sand; shell hash; organic debris	shell hash; gravel; shell hash	coarse sand; pea gravel; organic debris	—
120	red relict sand	red relict sand; shell hash	coarse sand	—
17	red relict sand	red relict sand	red relict sand	—
11	—	—	—	—

^a Near-ZID station

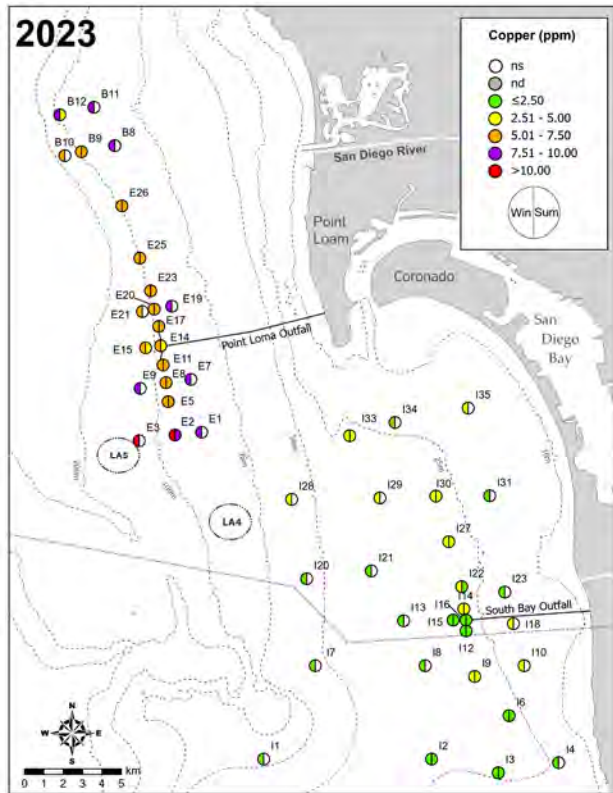
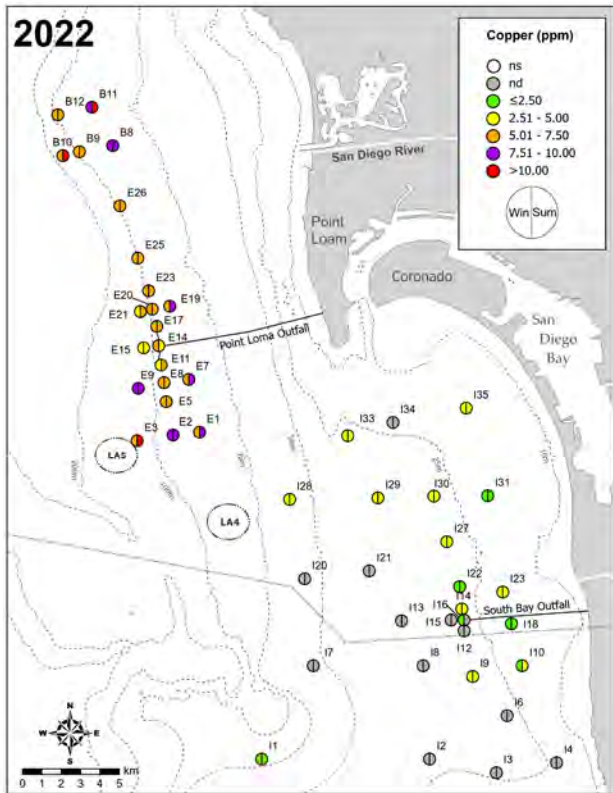
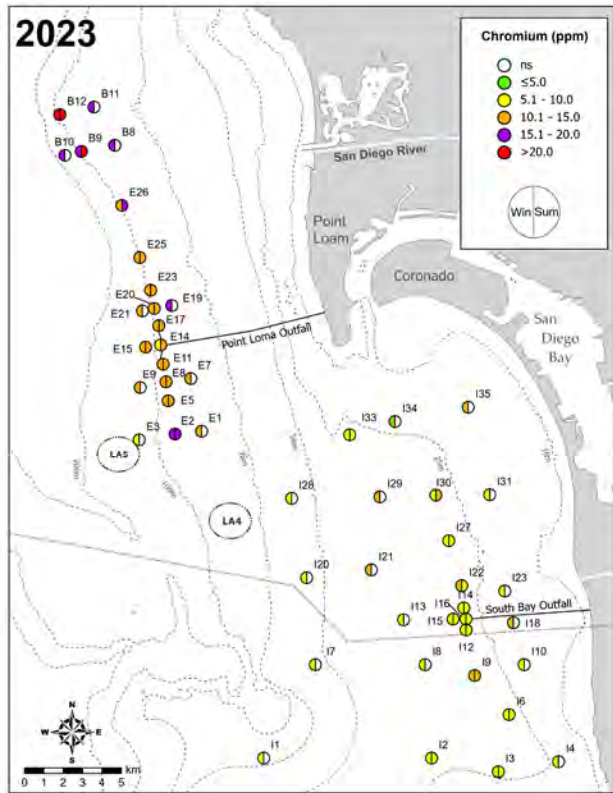
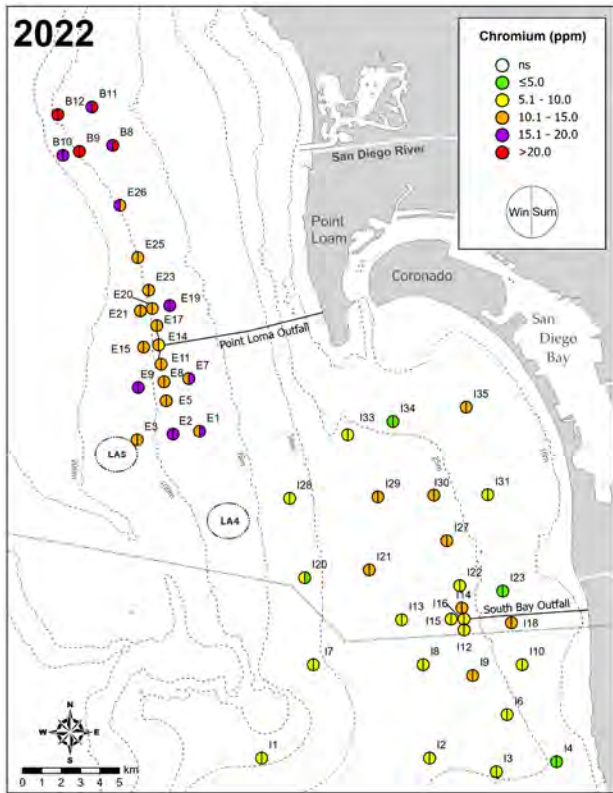


Appendix F.16

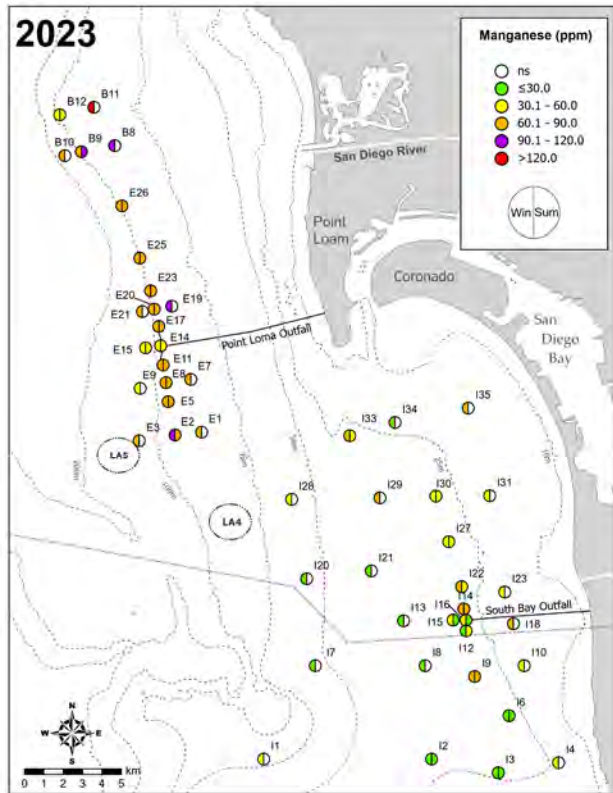
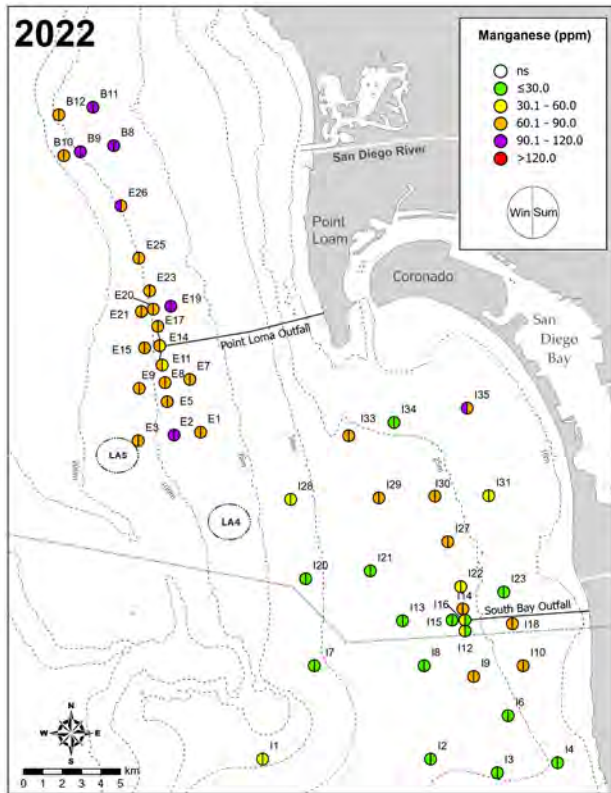
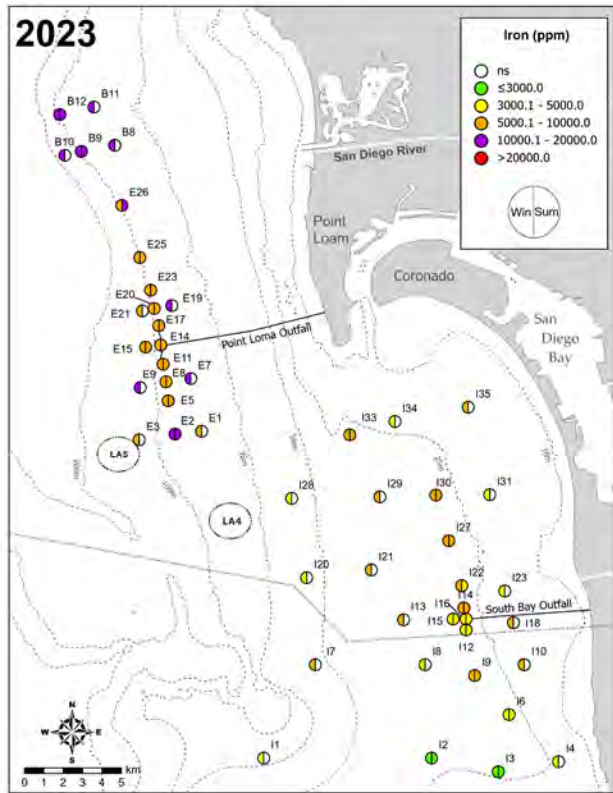
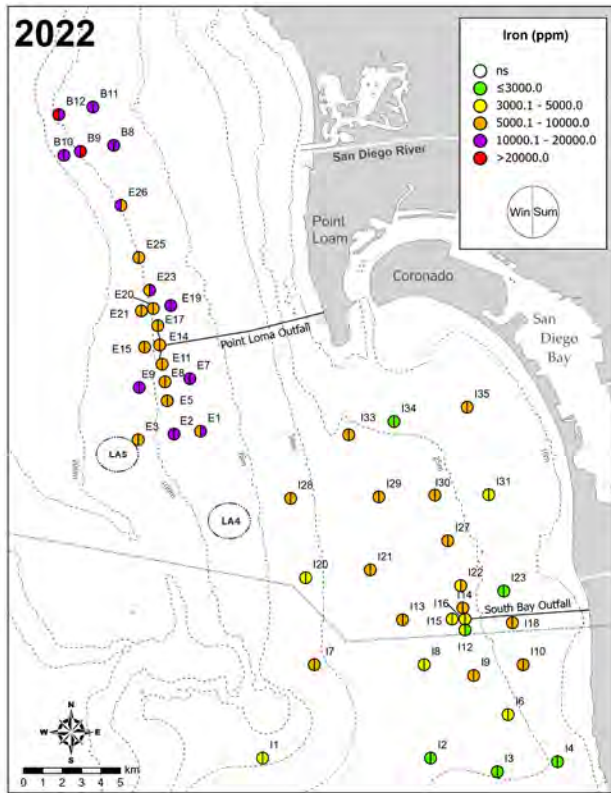
Distribution of select metals (ppm) in sediments from the PLOO and SBOO regions during winter and summer surveys of 2022 and 2023; ns = not sampled (or not reportable, see text); nd = not detected.



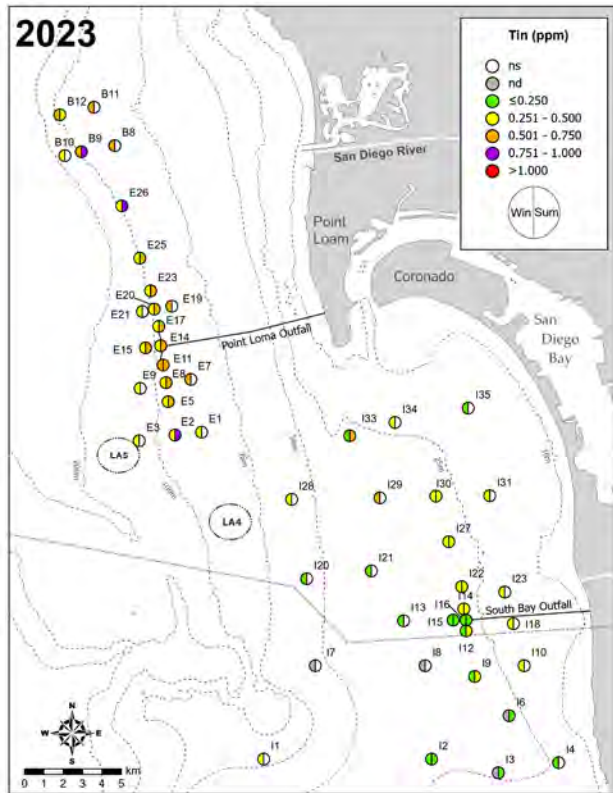
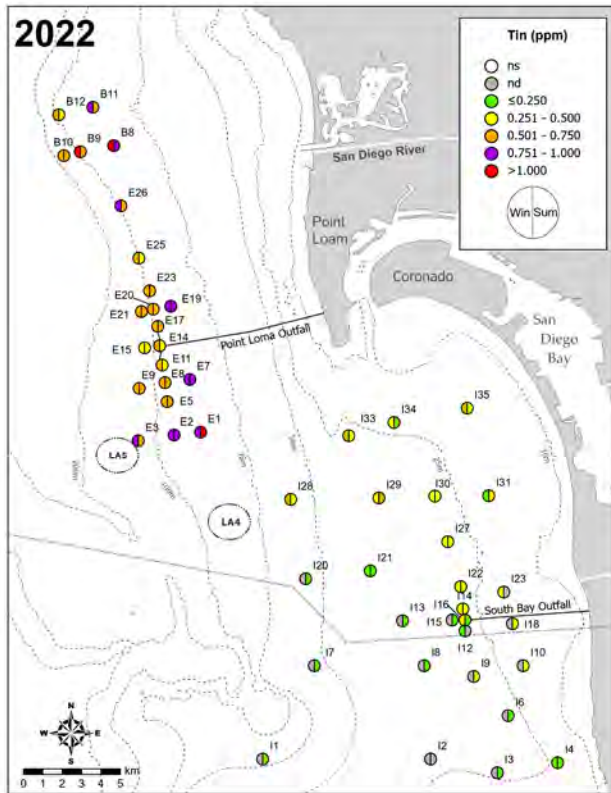
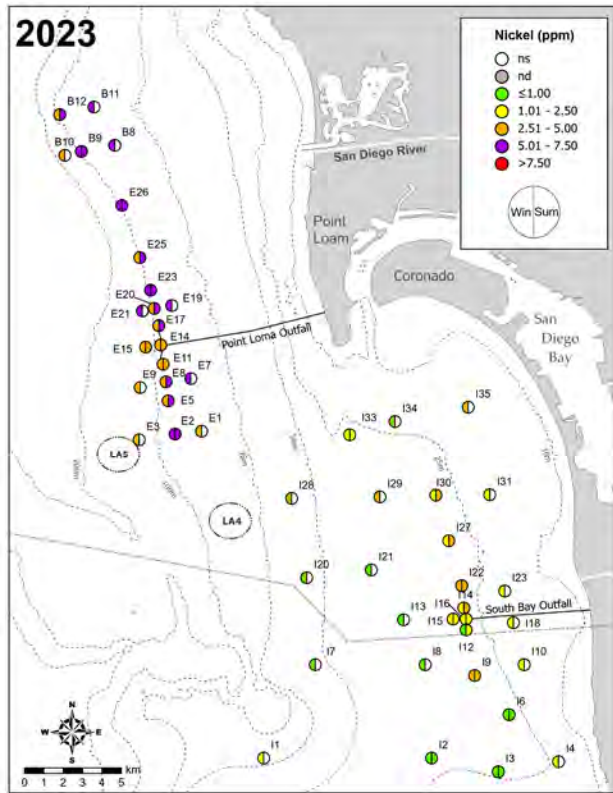
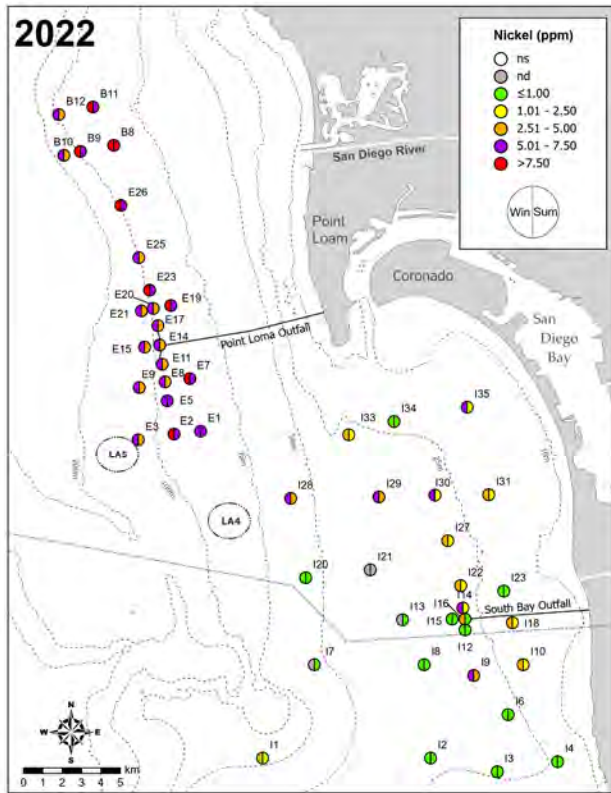
Appendix F.16 *continued*



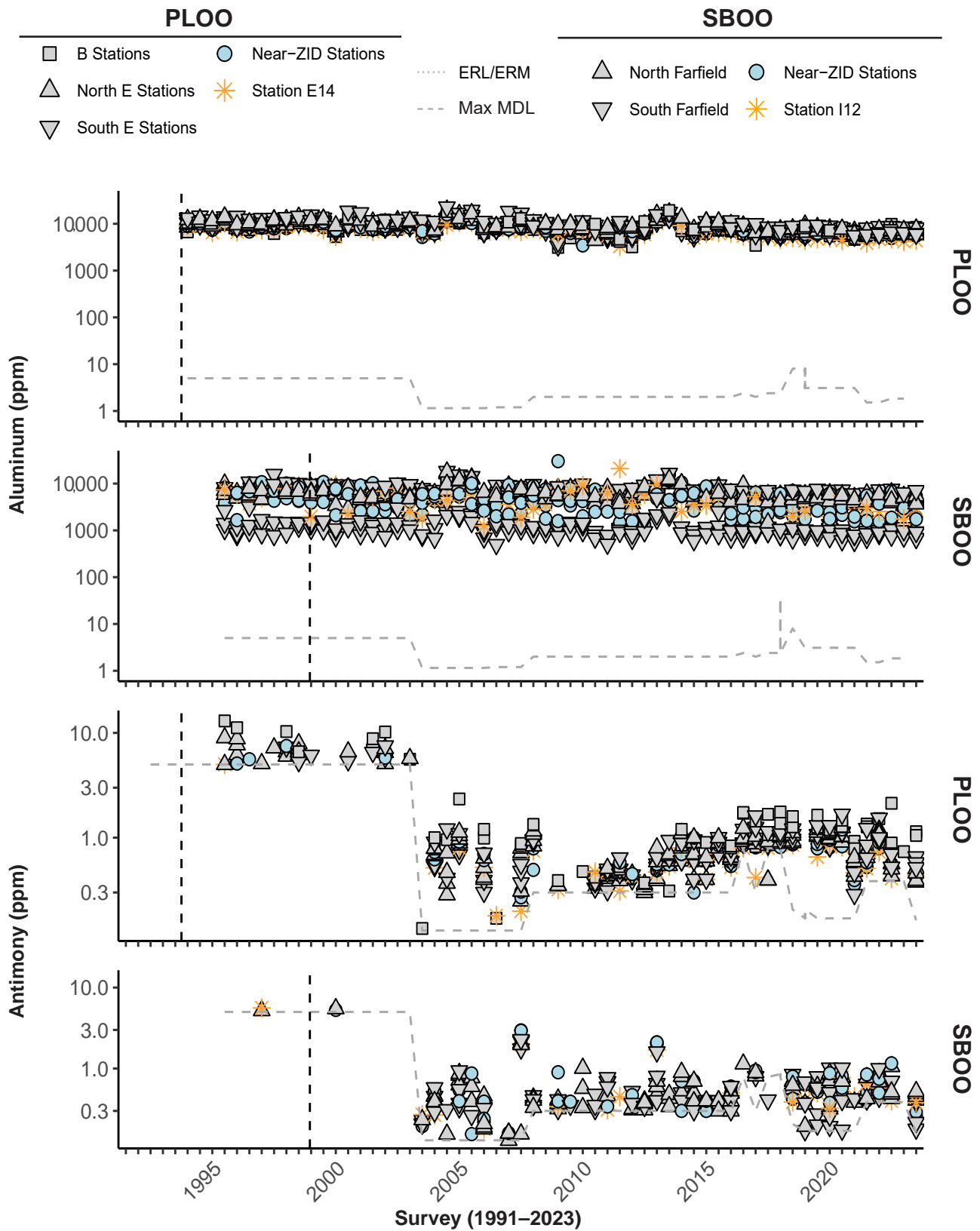
Appendix F.16 *continued*



Appendix F.16 *continued*

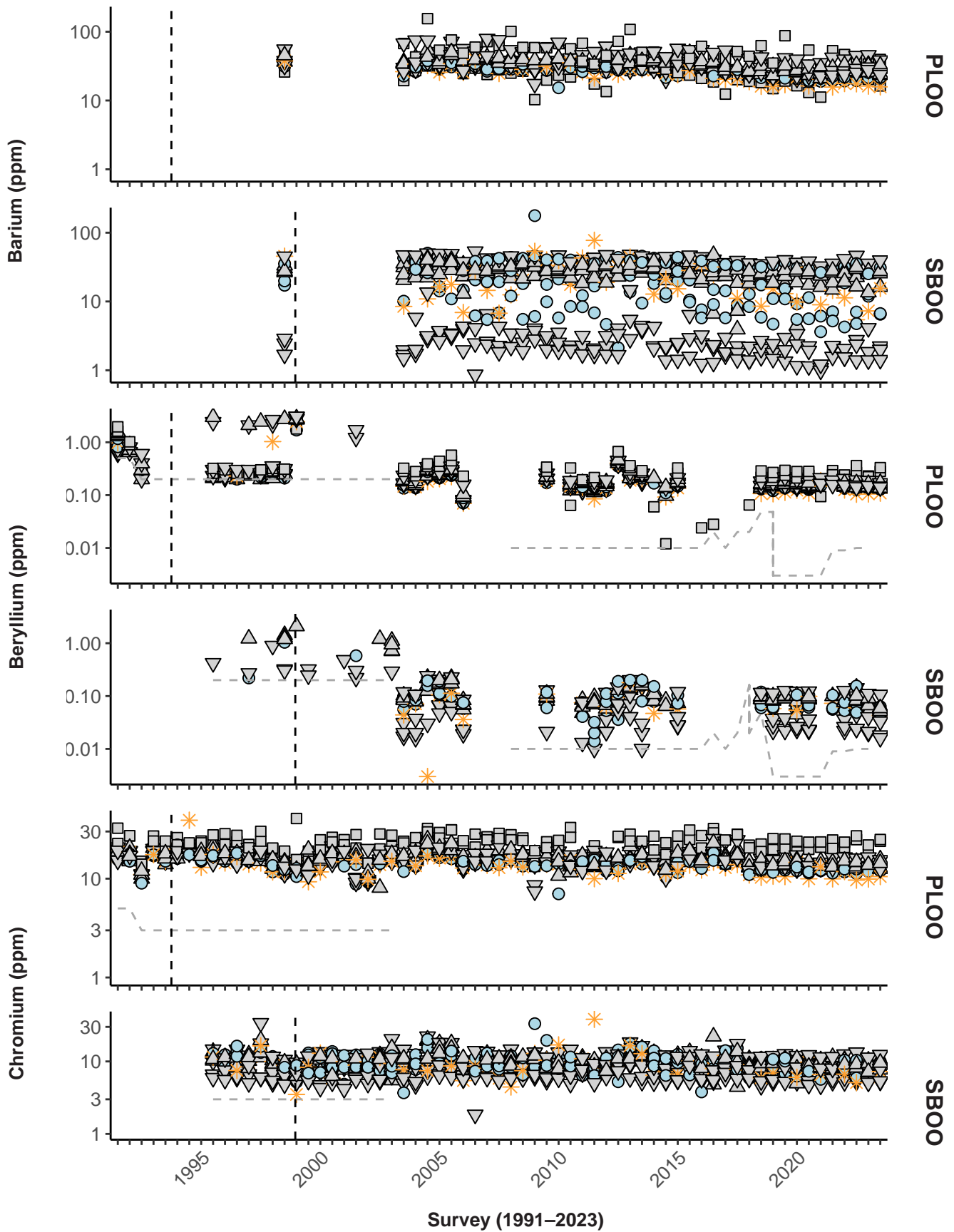


Appendix F.16 *continued*

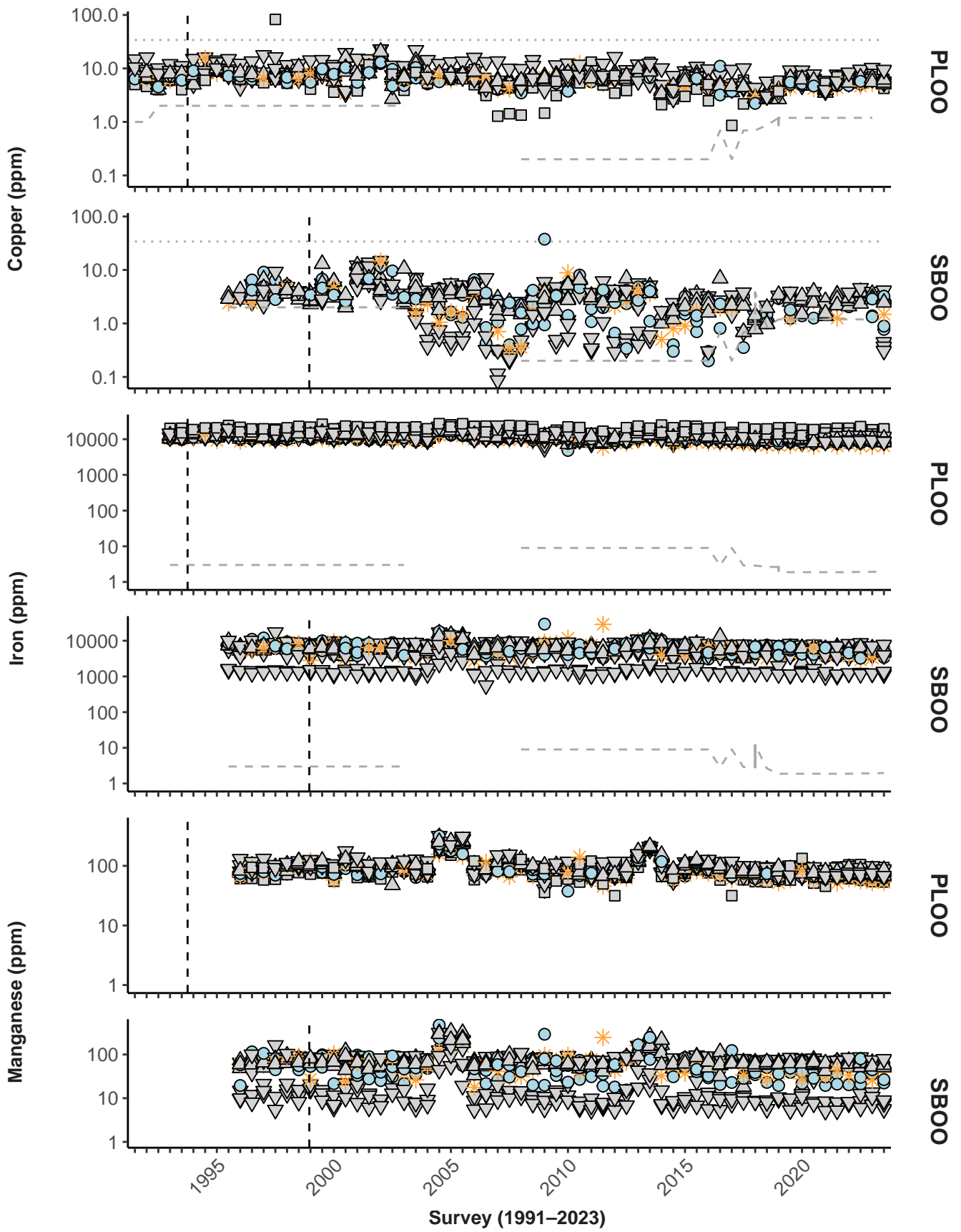


Appendix F.17

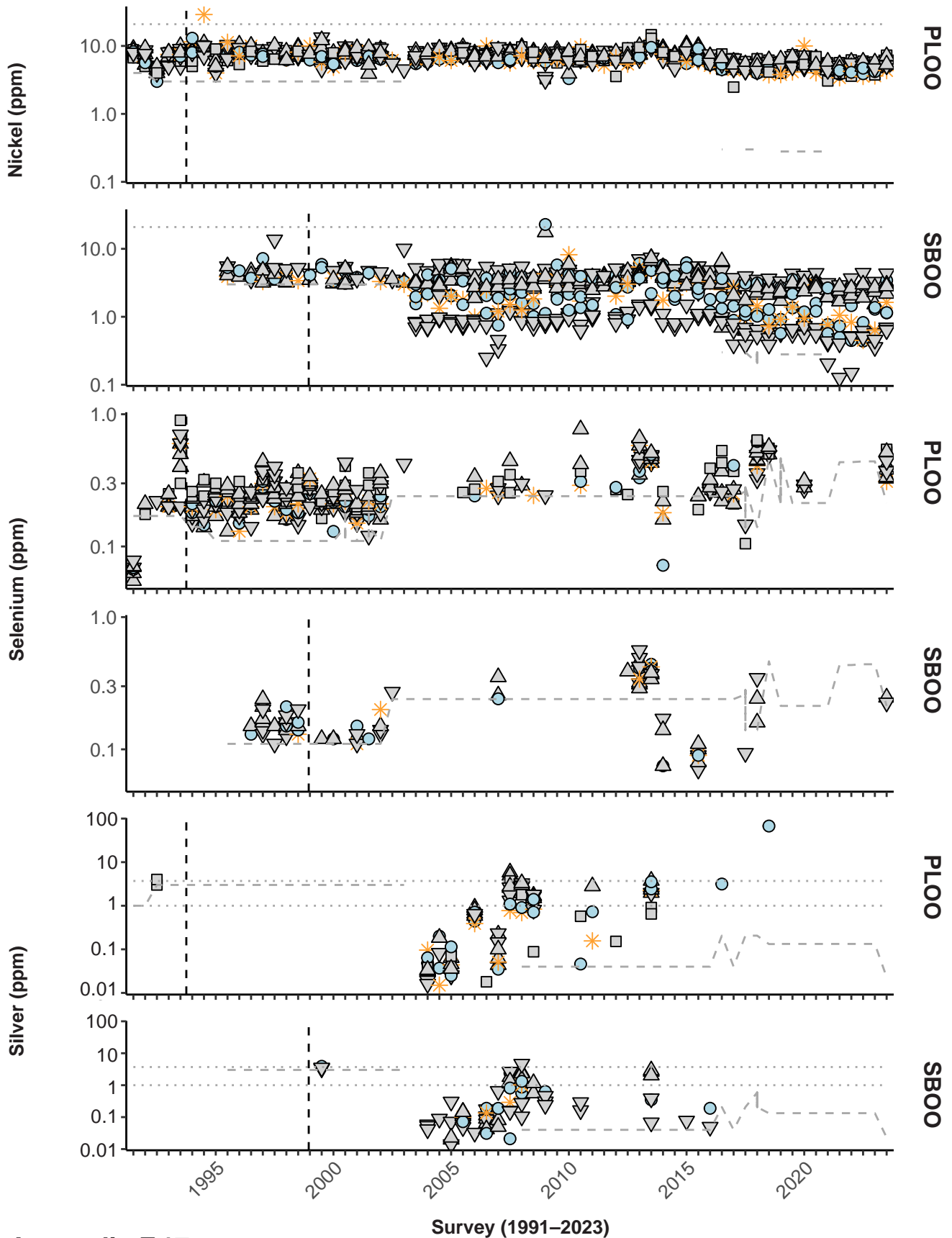
Concentrations of select metals in sediments sampled during winter and summer surveys at PLOO primary core stations from 1991 through 2023 and at SBOO primary core stations from 1995 through 2023. Data represent detected values from each station, $n \leq 12$ samples per survey. Vertical dashed lines indicate onset of discharge from the PLOO or SBOO. Thresholds included (ERLs, ERMs) when relevant (see Table 5.3), along with the maximum MDL per survey.



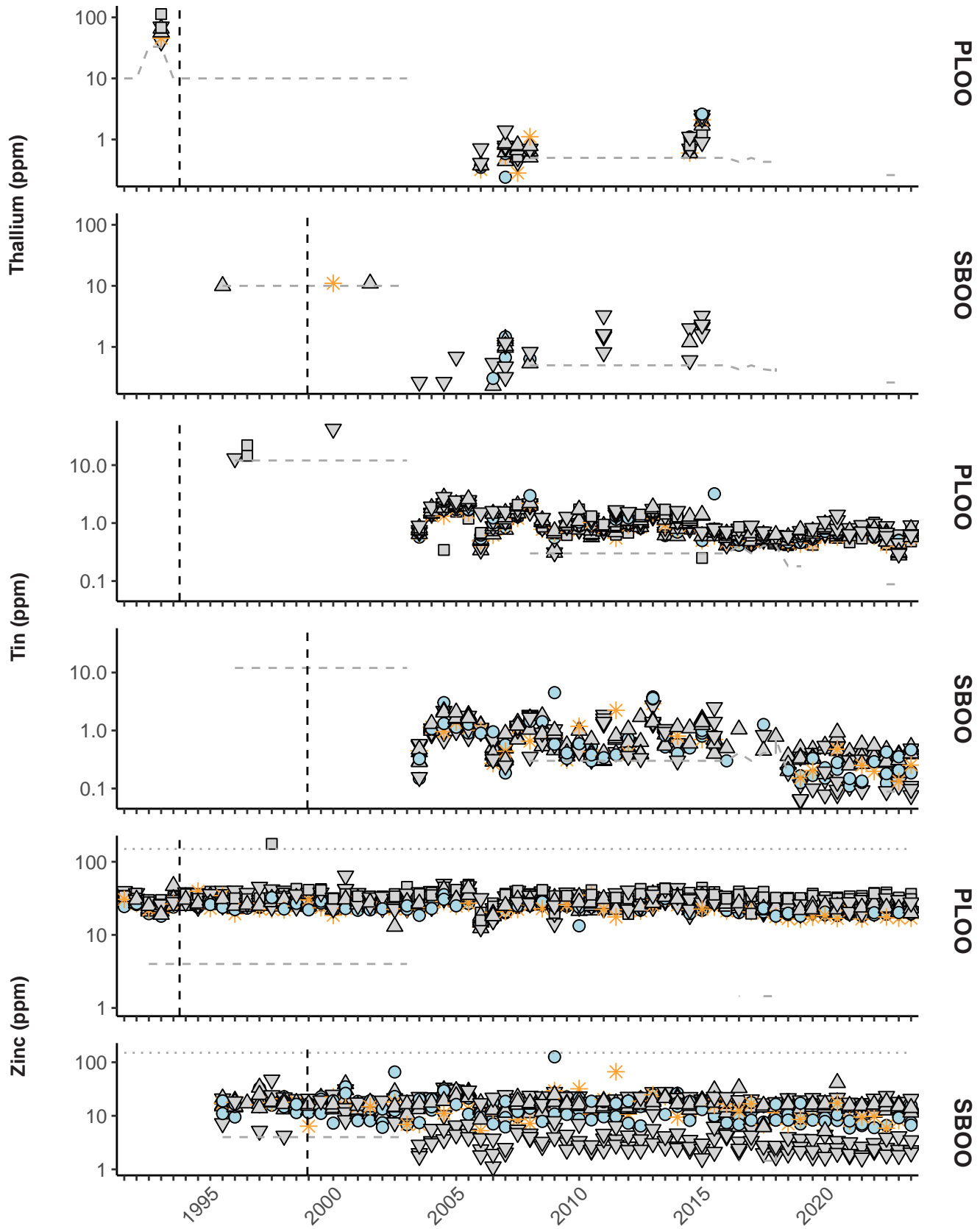
Appendix F.17 *continued*



Appendix F.17 *continued*



Appendix F.17 *continued*



Survey (1991–2023)

Appendix G

Macrobenthic Communities

2022 – 2023 Supplemental Analyses

Appendix G.1

Macrofaunal community parameters by grab for PLOO benthic stations sampled during 2023. SR=species richness; Abun=abundance; H'=Shannon diversity index; J'=Pielou's evenness; Dom=Swartz dominance; BRI=Benthic Response Index. ns=Not Sampled

Depth	Contour	Station	Survey	SR	Abun	H'	J'	Dom	BRI
88-m	B11	winter	117	300	4.3	0.90	49	8	
		summer	ns	ns	ns	ns	ns	ns	
	B8	winter	58	158	3.7	0.91	25	6	
		summer	ns	ns	ns	ns	ns	ns	
	E19	winter	93	319	4.0	0.89	34	8	
		summer	ns	ns	ns	ns	ns	ns	
	E7	winter	111	391	4.1	0.86	36	11	
		summer	ns	ns	ns	ns	ns	ns	
	E1	winter	76	216	3.8	0.87	30	5	
		summer	ns	ns	ns	ns	ns	ns	
	98-m	B12	winter	100	228	4.1	0.89	44	8
			summer	90	249	4.1	0.91	37	13
		B9	winter	102	233	4.2	0.91	46	10
			summer	90	299	4.1	0.91	36	12
E26		winter	74	213	3.9	0.91	30	5	
		summer	115	368	4.2	0.88	42	11	
E25		winter	90	270	4.1	0.90	36	9	
		summer	105	340	4.2	0.89	36	7	
E23		winter	80	305	3.9	0.88	30	4	
		summer	105	411	4.1	0.89	38	10	
E20		winter	64	227	3.8	0.91	27	10	
		summer	85	267	4.0	0.91	34	11	
E17 ^a		winter	83	349	3.7	0.84	22	17	
		summer	85	248	4.0	0.91	36	16	
E14 ^a		winter	68	218	3.6	0.86	25	23	
		summer	74	295	3.7	0.86	24	23	
E11 ^a		winter	66	234	3.7	0.88	23	12	
		summer	97	394	4.1	0.89	34	14	
E8		winter	78	255	3.9	0.88	29	13	
		summer	87	280	4.0	0.89	35	10	
E5		winter	85	263	4.0	0.91	33	11	
		summer	106	373	4.2	0.89	38	12	
E2		winter	108	313	4.3	0.91	44	8	
		summer	115	342	4.3	0.90	45	12	

^aNear-ZID station

Appendix G.1 *continued*

Depth Contour	Station	Survey	SR	Abun	H'	J'	Dom	BRI
116-m	B10	winter	84	227	4.0	0.90	36	17
		summer	ns	ns	ns	ns	ns	ns
	E21	winter	92	314	4.1	0.91	35	7
		summer	ns	ns	ns	ns	ns	ns
	E15 ^a	winter	49	121	3.6	0.92	22	8
		summer	112	456	4.0	0.86	36	11
	E9	winter	127	324	4.5	0.92	52	10
		summer	ns	ns	ns	ns	ns	ns
	E3	winter	92	238	4.2	0.92	41	8
		summer	ns	ns	ns	ns	ns	ns

^a Near-ZID station

Appendix G.2

Macrofaunal community parameters by grab for SBOO benthic stations sampled during 2023. SR = species richness; Abun = abundance; H' = Shannon diversity index; J' = Pielou's evenness; Dom = Swartz dominance; BRI = Benthic Response Index. ns = Not Sampled

Depth	Contour	Station	Survey	SR	Abun	H'	J'	Dom	BRI
19-m	I35	winter	65	174	3.8	0.91	27	26	
		summer	ns	ns	ns	ns	ns	ns	
	I34	winter	39	171	2.8	0.76	10	6	
		summer	ns	ns	ns	ns	ns	ns	
	I31	winter	47	97	3.5	0.92	23	18	
		summer	ns	ns	ns	ns	ns	ns	
	I23	winter	44	74	3.5	0.91	26	18	
		summer	ns	ns	ns	ns	ns	ns	
	I18	winter	52	135	3.6	0.91	21	18	
		summer	ns	ns	ns	ns	ns	ns	
	I10	winter	58	127	3.8	0.93	28	12	
		summer	ns	ns	ns	ns	ns	ns	
	I4	winter	16	163	1.2	0.43	2	-7	
		summer	ns	ns	ns	ns	ns	ns	
	28-m	I33	winter	88	247	4.0	0.88	35	23
			summer	110	358	3.9	0.84	37	21
		I30	winter	81	241	3.7	0.84	28	25
			summer	89	386	3.4	0.75	23	26
I27		winter	56	165	3.4	0.84	22	23	
		summer	96	316	3.8	0.83	33	25	
I22		winter	48	127	3.4	0.88	19	24	
		summer	77	308	3.6	0.82	27	23	
I14 ^a		winter	49	135	3.5	0.90	20	19	
		summer	63	206	3.7	0.89	24	21	
I16 ^a		winter	59	207	3.5	0.86	21	21	
		summer	68	710	2.3	0.55	7	19	
I15 ^a		winter	68	228	3.8	0.90	27	24	
		summer	64	418	2.6	0.62	12	19	
I12 ^a		winter	44	93	3.2	0.85	21	20	
		summer	54	554	2.1	0.54	5	23	
I9		winter	70	224	3.7	0.88	28	27	
		summer	86	278	3.8	0.86	27	27	
I6		winter	50	171	3.1	0.79	14	13	
		summer	44	205	2.6	0.69	10	9	
I2	winter	35	132	3.0	0.83	13	10		
	summer	46	200	2.8	0.72	12	17		
I3	winter	25	114	2.5	0.78	8	9		
	summer	38	238	2.3	0.62	6	7		

^aNear-ZID station

Appendix G.2 *continued*

Depth Contour	Station	Survey	SR	Abun	H'	J'	Dom	BRI
38-m	I29	winter	137	583	4.3	0.88	44	15
		summer	ns	ns	ns	ns	ns	ns
	I21	winter	49	164	3.3	0.86	19	2
		summer	ns	ns	ns	ns	ns	ns
	I13	winter	49	136	3.4	0.86	21	8
		summer	ns	ns	ns	ns	ns	ns
	I8	winter	43	179	3.1	0.83	13	20
		summer	ns	ns	ns	ns	ns	ns
55-m	I28	winter	149	718	4.0	0.81	37	13
		summer	ns	ns	ns	ns	ns	ns
	I20	winter	98	428	3.9	0.84	32	15
		summer	ns	ns	ns	ns	ns	ns
	I7	winter	57	215	3.5	0.87	19	11
		summer	ns	ns	ns	ns	ns	ns
	I1	winter	113	459	4.1	0.87	37	11
		summer	ns	ns	ns	ns	ns	ns

Appendix G.3

Summary taxonomic listing of benthic infauna taxa identified from PLOO stations during 2023. Data are total number of individuals (n). Taxonomic arrangement follows SCAMIT (2021).

Phylum	Class	Family	Taxon	n					
Cnidaria	Anthozoa	Virgulariidae	<i>Acanthoptilum</i> sp	2					
			<i>Virgularia agassizii</i>	1					
		Edwardsiidae	<i>Edwardsia olguini</i>	7					
			<i>Scolanthus triangulus</i>	11					
			Halcampidae	<i>Halcompa decemtentaculata</i>	2				
				<i>Halianthella</i> sp A	2				
		Platyhelminthes Nemertea	Rhabditophora	Faubelidae	<i>Diplandros singularis</i>	1			
						3			
			Palaeonemertea				2		
						Carinomidae	<i>Carinoma mutabilis</i>	7	
Tubulanidae	<i>Tubulanus cingulatus</i>						6		
	<i>Tubulanus polymorphus</i>					12			
	Tubulanidae sp B					1			
Pilidiophora							Tubulanidae sp D	1	
							Heteronemertea	5	
							Lineidae	<i>Cerebratulus marginatus</i>	2
								<i>Siphonenteron bilineatum</i>	49
								Lineidae sp SD1	3
			Heteronemertea sp SD2	79					
			Hoplonemertea					6	
Emplectonematidae	<i>Cryptonemertes actinophila</i>					2			
	<i>Paranemertes californica</i>					12			
Neesidae	<i>Prosorhochmus albidus</i>					2			
Prosorhochmidae	<i>Amphiporus californicus</i>					1			
Amphiporidae	<i>Tetrastemma candidum</i>					2			
Tetrastemmatidae	<i>Chaetoderma marinellii</i>	4							
Mollusca	Caudofoveata	Chaetodermatidae				<i>Chaetoderma pacificum</i>	1		
			<i>Falcidens longus</i>	1					
			Gastropoda			<i>Minolia peramabilis</i>	8		
						<i>Lirobittium rugatum</i> Cmplx	2		
						<i>Caecum crebricinctum</i>	1		
	<i>Melanella rosa</i>	1							
	<i>Polygireulima rutila</i>	1							
	Mangeliidae	<i>Kurtzia arteaga</i>				1			
		<i>Kurtzina beta</i>				35			
		Pseudomelatomidae	<i>Megasurcula carpenteriana</i>	1					
			<i>Acteon traskii</i>	2					
		Acteonidae	<i>Rictaxis punctocaelatus</i>	2					
	Aplustridae			<i>Parvaplustrum cadieni</i>	2				
				Pyramidellidae	<i>Odostomia</i> sp	5			
					<i>Turbonilla</i> sp	1			
					<i>Turbonilla santarosana</i>	1			
					<i>Turbonilla</i> sp A	2			

Appendix G.3 *continued*

Phylum	Class	Family	Taxon	n
		Rhizoridae	<i>Volvulella californica</i>	10
			<i>Volvulella cylindrica</i>	7
			<i>Volvulella panamica</i>	2
		Tornatinidae	<i>Acteocina cerealis</i>	3
		Philinidae	<i>Philine auriformis</i>	9
		Aglajidae	<i>Aglaja ocelligera</i>	2
		Cylichnidae	<i>Cylichna diegensis</i>	12
	Bivalvia			4
		Nuculidae	<i>Acila castrensis</i>	1
			<i>Ennucula tenuis</i>	17
		Solemyidae	<i>Petrasma pervernicosa</i>	17
		Nuculanidae	<i>Nuculana hamata</i>	2
			<i>Saccula</i> sp A	61
		Mytilidae	<i>Crenella decussata</i>	1
			<i>Amygdalum pallidulum</i>	4
		Pectinidae	<i>Delectopecten vancouverensis</i>	1
		Carditidae	<i>Coanicardita ventricosa</i>	2
		Lucinidae	<i>Lucinoma annulatum</i>	10
			<i>Parvilucina tenuisculpta</i>	47
		Thyasiridae	<i>Adontorhina cyclia</i>	7
			<i>Axinopsida serricata</i>	63
			<i>Thyasira flexuosa</i>	3
		Lasaeidae	<i>Kurtiella tumida</i>	6
			<i>Kurtiella</i> sp D	24
		Cardiidae	<i>Keenaea centifilosa</i>	12
		Tellinidae	<i>Tellina cadieni</i>	80
			<i>Tellina carpenteri</i>	35
			<i>Macoma</i> sp	1
			<i>Macoma yoldiformis</i>	1
		Petricolidae	<i>Cooperella subdiaphana</i>	1
		Lyonsiidae	<i>Lyonsia californica</i>	1
		Periplomatidae	<i>Periploma</i> sp	1
		Cuspidariidae	<i>Cuspidaria parapodema</i>	7
		Verticordiidae	<i>Trigonulina novemcostatus</i>	1
	Scaphopoda			1
		Gadilidae	<i>Polyschides quadrifissatus</i>	35
		uncertain	<i>Compressidens stearnsii</i>	7
Sipuncula	Sipunculidea	Golfingiidae	<i>Thysanocardia nigra</i>	3
		Phascolionidae	<i>Phascolion</i> sp A	20
Annelida	Polychaeta		<i>Echiura</i>	1
		Amphinomidae	<i>Chloeia pinnata</i>	139
		Eunicidae		2
			<i>Leodice americana</i>	1
		Lumbrineridae		1
			<i>Eranno bicirrata</i>	1
			<i>Eranno lagunae</i>	9
			<i>Lumbrineris</i> sp	3
			<i>Lumbrineris cruzensis</i>	123
			<i>Lumbrineris latreilli</i>	31

Appendix G.3 *continued*

Phylum	Class	Family	Taxon	n
			<i>Lumbrineris ligulata</i>	5
			<i>Lumbrineris limicola</i>	2
			<i>Scoletoma</i> sp	1
			<i>Scoletoma tetraura</i> Cmplx	14
			<i>Lumbrineris</i> sp Group I	44
		Oeononidae	<i>Drilonereis</i> sp	5
			<i>Drilonereis falcata</i>	13
			<i>Drilonereis</i> sp A	1
			<i>Notocirrus californiensis</i>	2
		Onuphidae		20
			<i>Nothria occidentalis</i>	9
			<i>Mooreonuphis</i> sp	2
			<i>Mooreonuphis segmentispadix</i>	2
			<i>Onuphis iridescens</i>	2
			<i>Onuphis</i> sp A	11
			<i>Paradiopatra parva</i>	262
		Acoetidae	<i>Acoetes pacifica</i>	3
		Polynoidae	<i>Lepidasthenia longicirrata</i>	1
			<i>Malmgreniella baschi</i>	4
			<i>Malmgreniella sanpedroensis</i>	7
			<i>Malmgreniella scriptoria</i>	1
			<i>Malmgreniella</i> sp A	46
			<i>Subadyte mexicana</i>	2
			<i>Tenonia priops</i>	1
		Sigalionidae	<i>Sigalion spinosus</i>	39
			<i>Sthenelais tertiaglabra</i>	2
			<i>Sthenelais verruculosa</i>	1
			<i>Pholoe glabra</i>	89
			<i>Sthenelanella uniformis</i>	30
		Glyceridae	<i>Glycera americana</i>	4
			<i>Glycera nana</i>	79
			<i>Glycera oxycephala</i>	1
		Goniadidae	<i>Glycinde armigera</i>	46
			<i>Goniada brunnea</i>	1
			<i>Goniada maculata</i>	26
		Hesionidae	<i>Podarkeopsis glabrus</i>	6
		Nereididae	<i>Gymnonereis crosslandi</i>	1
			<i>Nereis</i> sp A	8
		Syllidae	<i>Eusyllis blomstrandii</i> Cmplx	1
			<i>Paraehlersia articulata</i>	5
			<i>Exogone lourei</i>	16
			<i>Megasyllis nipponica</i>	1
			<i>Syllis gracilis</i> Cmplx	1
			<i>Syllis heterochaeta</i>	6
			<i>Syllis</i> sp SD2	1
		Nephtyidae	<i>Aglaophamus verrilli</i>	6
			<i>Bipalponephtys cornuta</i>	6
			<i>Nephtys caecoides</i>	10
			<i>Nephtys ferruginea</i>	19

Appendix G.3 *continued*

Phylum	Class	Family	Taxon	n
			<i>Nephtys simoni</i>	2
			<i>Nephtys</i> sp SD2	1
		Phyllodoceidae	<i>Eteone pigmentata</i>	3
			<i>Eulalia levicornuta</i> Cmplx	2
			<i>Eumida longicornuta</i>	1
			<i>Mystides</i> sp	1
			<i>Sige</i> sp A	6
			<i>Nereiphylla</i> sp 2	5
			<i>Paranaitis polynoides</i>	2
			<i>Phyllodoce groenlandica</i>	4
			<i>Phyllodoce hartmanae</i>	16
			<i>Phyllodoce longipes</i>	5
			<i>Phyllodoce pettiboneae</i>	1
		Oweniidae	<i>Galathowenia pygidialis</i>	10
			<i>Myriochele gracilis</i>	60
			<i>Myriochele olgae</i>	3
			<i>Myriochele striolata</i>	6
		Sabellidae	<i>Acromegalomma pigmentum</i>	1
			<i>Acromegalomma splendidum</i>	4
			<i>Dialychnone albocincta</i>	10
			<i>Dialychnone trilineata</i>	114
			<i>Euchone arenae</i>	2
			<i>Euchone hancocki</i>	8
			<i>Euchone incolor</i>	80
			<i>Euchone</i> sp A	9
			<i>Jasmineira</i> sp B	20
			<i>Myxicola</i> sp	6
			<i>Paradialychnone ecaudata</i>	1
			<i>Paradialychnone harrisae</i>	4
			<i>Paradialychnone paramollis</i>	1
			<i>Potamethus</i> sp A	4
		Longosomatidae	<i>Heterospio catalinensis</i>	2
		Magelonidae	<i>Magelona berkeleyi</i>	5
			<i>Magelona hartmanae</i>	2
			<i>Magelona</i> sp B	2
		Spionidae	<i>Dipolydora socialis</i>	2
			<i>Laonice cirrata</i>	24
			<i>Laonice nuchala</i>	12
			<i>Microspio pigmentata</i>	21
			<i>Paraprionospio alata</i>	65
			<i>Prionospio dubia</i>	267
			<i>Prionospio jubata</i>	354
			<i>Prionospio lighti</i>	4
			<i>Prionospio pygmaeus</i>	3
			<i>Spio filicornis</i>	11
			<i>Spiophanes berkeleyorum</i>	37
			<i>Spiophanes duplex</i>	296
			<i>Spiophanes kimballi</i>	230
			<i>Spiophanes norrisi</i>	5

Appendix G.3 *continued*

Phylum	Class	Family	Taxon	n
			<i>Spiophanes wigleyi</i>	2
		Cirratulidae		1
			<i>Aphelochaeta</i> sp	1
			<i>Aphelochaeta glandaria</i> Cmplx	53
			<i>Aphelochaeta monilaris</i>	22
			<i>Aphelochaeta phillipsi</i>	14
			<i>Aphelochaeta tigrina</i>	7
			<i>Aphelochaeta williamsae</i>	3
			<i>Aphelochaeta</i> sp D	23
			<i>Aphelochaeta</i> sp E	3
			<i>Chaetozone</i> sp	2
			<i>Chaetozone corona</i>	1
			<i>Chaetozone hartmanae</i>	45
			<i>Chaetozone</i> sp SD5	2
			<i>Chaetozone</i> sp SD7	4
			<i>Kirkegaardia cryptica</i>	3
			<i>Kirkegaardia sibilina</i>	38
			<i>Kirkegaardia tessellata</i>	9
			<i>Kirkegaardia</i> sp SD9	3
		Flabelligeridae	<i>Bradabyssa pilosa</i>	1
			<i>Pherusa neopapillata</i>	2
			<i>Trophoniella harrisae</i>	1
		Sternaspidae	<i>Sternaspis affinis</i>	46
		Ampharetidae		7
			<i>Amage anops</i>	7
			<i>Amage scutata</i>	14
			<i>Ampharete finmarchica</i>	14
			<i>Ampharete labrops</i>	2
			<i>Ampharete lineata</i>	4
			<i>Ampharete manriquei</i>	6
			<i>Amphicteis scaphobranchiata</i>	11
			<i>Amphisamytha bioculata</i>	1
			<i>Anobothrus gracilis</i>	45
			<i>Eclysippe trilobata</i>	203
			<i>Lysippe</i> sp A	27
			<i>Lysippe</i> sp B	45
			<i>Samytha californiensis</i>	7
			<i>Sosane occidentalis</i>	21
			<i>Ampharetidae</i> sp SD1	5
			<i>Melinna oculata</i>	7
		Pectinariidae	<i>Pectinaria californiensis</i>	84
		Terebellidae		1
			<i>Amaeana occidentalis</i>	4
			<i>Polycirrus</i> sp	41
			<i>Polycirrus californicus</i>	47
			<i>Polycirrus</i> sp I	1
			<i>Polycirrus</i> sp A	72
			<i>Polycirrus</i> sp OC1	57
			<i>Artacama coniferi</i>	1

Appendix G.3 *continued*

Phylum	Class	Family	Taxon	n
			<i>Lanassa venusta venusta</i>	108
			<i>Phisidia sanctaemariae</i>	62
			<i>Pista</i> sp	1
			<i>Pista brevibranchiata</i>	4
			<i>Pista estevanica</i>	80
			<i>Pista pacifica</i>	2
			<i>Pista wui</i>	9
			<i>Proclea</i> sp A	65
			<i>Scionella japonica</i>	1
			<i>Streblosoma</i> sp B	3
			<i>Thelepus hamatus</i>	1
		Trichobranchidae	<i>Terebellides californica</i>	62
			<i>Terebellides</i> sp Type C	2
			<i>Trichobranchus hancocki</i>	1
		Chaetopteridae	<i>Chaetopterus variopedatus</i> Cmplx	1
			<i>Phyllochaetopterus limicolus</i>	7
			<i>Spiochaetopterus costarum</i> Cmplx	24
		Capitellidae		7
			<i>Capitella teleta</i>	42
			<i>Decamastus gracilis</i>	25
			<i>Mediomastus</i>	450
			<i>Notomastus hemipodus</i>	13
			<i>Notomastus latericeus</i>	3
		Cossuridae	<i>Cossura candida</i>	4
		Maldanidae		45
			<i>Isocirrus longiceps</i>	1
			Euclymeninae	18
			<i>Petaloclymene pacifica</i>	51
			<i>Praxillella gracilis</i>	2
			<i>Praxillella pacifica</i>	166
			Euclymeninae sp A	287
			<i>Clymenura gracilis</i>	92
			<i>Maldane sarsi</i>	29
			<i>Notoproctus pacificus</i>	2
			<i>Rhodine bitorquata</i>	103
		Opheliidae	<i>Ophelina acuminata</i>	1
		Orbiniidae	<i>Scoloplos acmeceps</i>	1
			<i>Scoloplos armiger</i> Cmplx	391
		Paraonidae		1
			<i>Aricidea (Acmira) catherinae</i>	50
			<i>Aricidea (Acmira) horikoshii</i>	1
			<i>Aricidea (Acmira) lopezi</i>	18
			<i>Aricidea (Acmira) rubra</i>	2
			<i>Aricidea (Acmira) simplex</i>	67
			<i>Aricidea (Acmira) sp</i>	2
			<i>Aricidea (Aricidea) wassi</i>	1
			<i>Aricidea (Strelzovia) antennata</i>	53
			<i>Aricidea (Strelzovia) hartleyi</i>	3
			<i>Aricidea (Strelzovia) sp A</i>	9

Appendix G.3 *continued*

Phylum	Class	Family	Taxon	n		
Arthropoda	Ostracoda		<i>Levinsenia gracilis</i>	7		
			<i>Levinsenia kirbyae</i>	8		
			<i>Paradoneis spinifera</i>	1		
		Scalibregmatidae	<i>Scalibregma californicum</i>	11		
		Travisiidae	<i>Travisia brevis</i>	48		
		Cypridinidae	<i>Vargula tsujii</i>	1		
		Cylindroleberididae	<i>Xenoleberis californica</i>	24		
		Philomedidae	<i>Euphilomedes carcharodonta</i>	302		
			<i>Euphilomedes producta</i>	352		
			<i>Scleroconcha trituberculata</i>	7		
		Malacostraca	Rutidermatidae	<i>Rutiderma lomae</i>	1	
			Mysidae		1	
					<i>Mysidella americana</i>	2
					<i>Inusitatomysis insolita</i>	1
			--	Amphipoda	2	
	Caprellidae		<i>Caprella mendax</i>	2		
			<i>Mayerella banksia</i>	7		
	Photidae		<i>Photis</i> sp	6		
			<i>Photis bifurcata</i>	1		
			<i>Photis californica</i>	13		
			<i>Photis lacia</i>	31		
			<i>Photis parvidons</i>	2		
			<i>Photis</i> sp OC1	1		
			<i>Photis</i> sp SD10	7		
			Aoridae	<i>Aoroides</i> sp	7	
		<i>Aoroides inermis</i>		3		
		<i>Aoroides</i> sp A		1		
	Corophiidae	<i>Protomedeia articulata</i> Cmplx	5			
	Oedicerotidae	<i>Americhelidium shoemakeri</i>	9			
		<i>Americhelidium</i> sp SD4	1			
		<i>Bathymedon pumilus</i>	34			
		<i>Deflexilodes similis</i>	14			
		<i>Monoculodes emarginatus</i>	41			
		<i>Westwoodilla tone</i>	9			
		Eusiridae	<i>Rhachotropis</i> sp A	4		
			<i>Rhachotropis</i> sp SD1	1		
		Liljeborgiidae	<i>Listriella eriopisa</i>	1		
			<i>Listriella goleta</i>	5		
	Stenothoidae	<i>Stenula modosa</i>	1			
	Pardaliscidae	<i>Halicoides synopiae</i>	37			
<i>Nicippe tumida</i>		7				
Ampeliscidae	<i>Ampelisca</i> sp	7				
	<i>Ampelisca brevisimulata</i>	31				
	<i>Ampelisca cf brevisimulata</i>	6				
	<i>Ampelisca careyi</i>	87				
	<i>Ampelisca cristata cristata</i>	3				
	<i>Ampelisca cristata microdentata</i>	2				
	<i>Ampelisca hancocki</i>	56				

Appendix G.3 *continued*

Phylum	Class	Family	Taxon	n
			<i>Ampelisca indentata</i>	2
			<i>Ampelisca pacifica</i>	21
			<i>Ampelisca pugetica</i>	36
			<i>Ampelisca romigi</i>	1
			<i>Byblis mills</i>	10
		Argissidae	<i>Argissa hamatipes</i>	3
		Urothoidae	<i>Urothoe elegans</i> Cmplx	10
		Phoxocephalidae		1
			<i>Foxiphalus</i> sp	1
			<i>Foxiphalus obtusidens</i>	4
			<i>Foxiphalus similis</i>	1
			<i>Rhepoxynius</i> sp	4
			<i>Rhepoxynius bicuspidatus</i>	121
			<i>Rhepoxynius menziesi</i>	60
			<i>Rhepoxynius stenodes</i>	1
			<i>Rhepoxynius variatus</i>	2
			<i>Eyakia robusta</i>	3
			<i>Heterophoxus</i> sp	1
			<i>Heterophoxus oculatus</i>	6
		Lysianassidae	<i>Aruga oculata</i>	8
		Opisidae	<i>Opisa tridentata</i>	1
		Uristidae	<i>Anonyx lilljeborgi</i>	8
		Tryphosidae	<i>Hippomedon</i> sp A	1
			<i>Orchomenella decipiens</i>	1
		Acidostomatidae	<i>Acidostoma hancocki</i>	2
		Pakynidae	<i>Pachynus barnardi</i>	1
			<i>Prachynella lodo</i>	1
		Gnathiidae	<i>Caecognathia crenulatifrons</i>	81
		Anthuridae	<i>Haliophasma geminata</i>	15
		Arcturidae	<i>Idarcturus allelomorphus</i>	1
		Serolidae	<i>Heteroserolis carinata</i>	1
		--	Tanaidacea	6
		Akanthophoreidae	<i>Chauliopeleona dentata</i>	13
		Anarthruridae	<i>Siphonolabrum californiensis</i>	3
		Leptocheliidae	<i>Chondrochelia dubia</i> Cmplx	89
		Tanaellidae	<i>Araphura</i> sp	2
			<i>Araphura breviarua</i>	35
			<i>Araphura cuspirostris</i>	1
			<i>Tanaella propinquus</i>	18
		Typhlotanaidae	<i>Typhlotanais williamsae</i>	7
		Pseudotanaidae	<i>Pseudotanais californiensis</i>	2
		Tanaopsidae	<i>Tanaopsis cadieni</i>	21
		Nannastacidae	<i>Campylaspis canaliculata</i>	1
			<i>Procampylaspis caenosa</i>	6
		Diastylidae	<i>Diastylis californica</i>	2
			<i>Diastylis crenellata</i>	23
		Crangonidae	<i>Crangon</i> sp	1
		--	Paguroidea	1
		Pinnotheridae	<i>Pinnixa longipes</i>	1

Appendix G.3 *continued*

Phylum	Class	Family	Taxon	n
			<i>Pinnixa occidentalis</i> Cmplx	6
Nematoda				16
Echinodermata	Asteroidea			29
		Astropectinidae	<i>Astropecten</i> sp	7
			<i>Astropecten californicus</i>	5
	Ophiuroidea			35
		Ophiuridae	<i>Ophiura luetkenii</i>	10
		Amphiuridae		143
			<i>Amphichondrius granulatus</i>	30
			<i>Amphiodia</i> sp	130
			<i>Amphiodia digitata</i>	31
			<i>Amphiodia urtica</i>	447
			<i>Amphipholis</i> sp	1
			<i>Amphipholis squamata</i>	4
			<i>Amphiura arcystata</i>	2
			<i>Dougaloplus amphacanthus</i>	9
			<i>Dougaloplus</i> sp A	1
	Echinoidea	Toxopneustidae	<i>Lytechinus pictus</i>	3
		Brissidae	<i>Brissopsis pacifica</i>	2
		Spatangidae	<i>Spatangus californicus</i>	1
	Holothuroidea	Synaptidae	<i>Leptosynapta</i> sp	57
		Chiridotidae	<i>Chiridota</i> sp	29
		Molpadiidae	<i>Molpadia intermedia</i>	1
Phoronida		Phoronidae		5
			<i>Phoronis</i> sp	11
			<i>Phoronis</i> sp SD1	3
Brachiopoda	Lingulata	Lingulidae	<i>Glottidia albida</i>	1
Chordata	Enteropneusta			1
	Enteropneusta	Ptychoderidae	<i>Balanoglossus</i> sp	3
		Harrimaniidae	<i>Saccoglossus</i> sp	1
			<i>Stereobalanus</i> sp	4
	Ascidiacea	Molgulidae	<i>Eugyra arenosa californica</i>	1
			<i>Molgula</i> sp	1
			<i>Molgula napiformis</i>	2

Appendix G.4

Summary taxonomic listing of benthic infauna taxa identified from SBOO stations during 2023. Data are total number of individuals (n). Taxonomic arrangement follows SCAMIT (2021).

Phylum	Class	Family	Taxon	n	
Cnidaria	Hydrozoa	Corymorphidae	<i>Corymorpha bigelowi</i>	2	
			<i>Euphysa</i> sp A	3	
	Anthozoa	Virgulariidae		1	
			<i>Stylatula</i> sp	1	
			<i>Stylatula</i> sp A	25	
			--	Ceriantharia	2
			Arachnactidae	<i>Arachnanthus</i> sp A	1
			--	Actiniaria	2
			Edwardsiidae		28
			<i>Edwardsia juliae</i>	78	
			<i>Edwardsia olguini</i>	3	
			<i>Scolanthus triangulus</i>	12	
			Halcampidae	<i>Halcampa decemtentaculata</i>	15
				<i>Pentactinia californica</i>	1
	Isanthidae	<i>Zaolutus actius</i>	8		
	Limnactiniidae	Limnactiniidae sp A	2		
	Platyhelminthes	Rhabditophora	Stylochidae	<i>Stylochus exiguus</i>	5
			Cryptocelidae	<i>Cryptocelis occidentalis</i>	2
			--	Rhabditophora sp A	2
--			Rhabditophora sp C	1	
				13	
Nemertea	Palaeonemertea			4	
		Cephalotrichidae	<i>Cephalothrix</i> sp	5	
		Carinomidae	<i>Carinoma mutabilis</i>	30	
		Tubulanidae		13	
			<i>Tubulanus cingulatus</i>	4	
			<i>Tubulanus polymorphus</i>	60	
			<i>Tubulanus</i> sp A	1	
			Tubulanidae sp B	3	
		Pilidiophora	Heteronemertea	2	
				25	
		<i>Cerebratulus californiensis</i>	3		
		<i>Cerebratulus marginatus</i>	3		
		<i>Maculaura alaskensis</i> Cmplx	3		
		<i>Siphonenteron bilineatum</i>	16		
		Lineidae sp SD1	12		
		Heteronemertea sp SD2	43		
			12		
	Hoplonemertea	Hoplonemertea	Emplectonematidae	<i>Cryptonemertes actinophila</i>	12
			Neesidae	<i>Paranemertes californica</i>	11
			Prosorhochmidae	<i>Prosorhochmus albidus</i>	21
Oerstediiidae			<i>Oerstedtia dorsalis</i> Cmplx	26	
Amphiporidae			<i>Amphiporus californicus</i>	2	
			<i>Amphiporus flavescens</i>	4	
Tetrastemmatidae			<i>Tetrastemma candidum</i>	24	
uncertain			<i>Quasitetrastemma nigrifrons</i>	7	
--			Hoplonemertea sp A	1	

Appendix G.4 *continued*

Phylum	Class	Family	Taxon	n	
Mollusca	Caudofoveata	--	Hoplonemertea sp D	2	
		Chaetodermatidae	<i>Chaetoderma marinellii</i>	3	
			<i>Falcidens longus</i>	2	
	Gastropoda				1
		Trochidae	<i>Halistylus pupoideus</i>	1	
		Cerithiidae	<i>Lirobittium rugatum</i> Cmplx	2	
		Calyptraeidae	<i>Calyptraea fastigiata</i>	8	
		Naticidae	<i>Glossaulax reclusiana</i>	1	
		Rissoidae	<i>Alvania compacta</i>	1	
		Eulimidae	<i>Balcis oldroydae</i>	7	
			<i>Polygireulima rutila</i>	10	
		Epitoniidae	<i>Epitonium bellastriatum</i>	1	
			<i>Opalia spongiosa</i>	2	
		Columbellidae	<i>Amphissa undata</i>	3	
			<i>Mitrella gausapata</i>	1	
		Olividae	<i>Callianax alectona</i>	81	
		Mangeliidae	<i>Kurtzia arteaga</i>	6	
			<i>Kurtziella plumbea</i>	8	
			<i>Kurtzina beta</i>	6	
		Terebridae	<i>Neoterebra hemphilli</i>	1	
		Acteonidae	<i>Rictaxis punctocaelatus</i>	27	
		Arminidae	<i>Armina californica</i>	1	
		--	Aeolidioidea	1	
		Pleurobranchidae	<i>Pleurobranchaea californica</i>	1	
		Pyramidellidae	<i>Odostomia</i> sp	1	
			<i>Turbonilla chocolata</i>	1	
			<i>Turbonilla santarosana</i>	9	
		--	Cephalaspidea	1	
		Rhizoridae	<i>Volvulella</i> sp	1	
			<i>Volvulella californica</i>	1	
		Tornatinidae	<i>Acteocina cerealis</i>	1	
		Philineae	<i>Philine auriformis</i>	14	
		Aglajidae	<i>Aglaja ocelligera</i>	2	
		Cylichnidae	<i>Cylichna diegensis</i>	5	
		--	Bullomorpha sp A	1	
		Bivalvia			
	Solemyidae		<i>Petrasma pervernicosa</i>	4	
	Nuculanidae		<i>Nuculana hamata</i>	2	
			<i>Saccella taphria</i>	12	
	Mytilidae		<i>Crenella decussata</i>	17	
			<i>Solamen columbianum</i>	1	
Modiolinae			32		
	<i>Modiolatus neglectus</i>		1		
Pectinidae	<i>Leptopecten latiauratus</i>		11		
Carditidae	<i>Scalaricarditinae</i>		1		
Lucinidae	<i>Lucinoma annulatum</i>		4		
	<i>Parvilucina tenuisculpta</i>		10		
Thyasiridae	<i>Axinopsida serricata</i>		3		

Appendix G.4 *continued*

Phylum	Class	Family	Taxon	n
		Lasaeidae	<i>Kurtiella grippi</i>	2
			<i>Kurtiella tumida</i>	13
		Cardiidae	<i>Keenaea centifilosa</i>	5
		Tellinidae	<i>Tellina</i> sp	1
			<i>Tellina bodegensis</i>	12
			<i>Tellina cadieni</i>	5
			<i>Tellina carpenteri</i>	2
			<i>Tellina meropsis</i>	1
			<i>Tellina modesta</i>	89
			<i>Macoma</i> sp	2
			<i>Macoma yoldiformis</i>	11
			<i>Psammotreta obesa</i>	1
		Solecurtidae	<i>Solecurtus guaymasensis</i>	1
		Solenidae	<i>Solen sicarius</i>	2
		Pharidae	<i>Ensis myrae</i>	4
			<i>Siliqua lucida</i>	1
		Veneridae	<i>Compsomyax subdiaphana</i>	4
		Petricolidae	<i>Cooperella subdiaphana</i>	14
		Mactridae	<i>Simomactra falcata</i>	21
		Pandoridae	<i>Pandora bilirata</i>	1
		Lyonsiidae		5
			<i>Entodesma navicula</i>	3
			<i>Lyonsia californica</i>	2
		--	Thracioidea	3
		Thraciidae	<i>Cyathodonta pedroana</i>	1
		Periplomatidae	<i>Periploma</i> sp	1
		Cuspidariidae	<i>Cardiomya pectinata</i>	1
			<i>Cuspidaria parapodema</i>	1
	Scaphopoda			4
		Dentaliidae	<i>Dentalium vallicolens</i>	4
		Gadilidae	<i>Polyschides quadrifissatus</i>	28
			<i>Gadila aberrans</i>	76
		uncertain	<i>Compressidens stearnsii</i>	1
Sipuncula				4
	Sipunculidea	Golfingiidae	<i>Thysanocardia nigra</i>	3
		Phascolionidae	<i>Phascolion</i> sp A	3
	Phascolosomatidea	Phascolosomatidae	<i>Apionsoma misakianum</i>	8
Annelida	Polychaeta	Dorvilleidae	<i>Parougia caeca</i>	1
			<i>Pettiboneia sanmatiensis</i>	1
			<i>Protodorvillea gracilis</i>	189
		Eunicidae		1
			<i>Leodice americana</i>	3
			<i>Paucibranchia disjuncta</i>	2
		Lumbrineridae		1
			<i>Eranno bicirrata</i>	1
			<i>Eranno lagunae</i>	1
			<i>Lumbrinerides platypygos</i>	36
			<i>Lumbrineris</i> sp	1

Appendix G.4 *continued*

Phylum	Class	Family	Taxon	n
			<i>Lumbrineris cruzensis</i>	20
			<i>Lumbrineris japonica</i>	2
			<i>Lumbrineris latreilli</i>	46
			<i>Lumbrineris ligulata</i>	36
			<i>Lumbrineris limicola</i>	3
			<i>Scoletoma</i> sp	4
			<i>Scoletoma tetraura</i> Cmplx	3
			<i>Lumbrineris</i> sp Group I	6
		Oeonidae	<i>Drilonereis</i> sp	1
			<i>Drilonereis falcata</i>	6
			<i>Notocirrus californiensis</i>	1
		Onuphidae		10
			<i>Diopatra</i> sp	7
			<i>Diopatra ornata</i>	10
			<i>Diopatra splendidissima</i>	1
			<i>Diopatra tridentata</i>	7
			<i>Mooreonuphis</i> sp	16
			<i>Mooreonuphis nebulosa</i>	18
			<i>Mooreonuphis</i> sp SD1	21
			<i>Mooreonuphis</i> sp SD2	9
			<i>Onuphis</i> sp	6
			<i>Onuphis eremita parva</i>	1
			<i>Onuphis iridescens</i>	2
			<i>Onuphis</i> sp A	53
			<i>Paradiopatra parva</i>	33
			<i>Rhamphobrachium longisetosum</i>	4
		Aphroditidae	<i>Aphrodita</i> sp	5
		Polynoidae	<i>Lepidasthenia longicirrata</i>	1
			<i>Lepidonotus spiculus</i>	1
			<i>Malmgreniella macginitiei</i>	5
			<i>Malmgreniella sanpedroensis</i>	1
			<i>Malmgreniella</i> sp A	4
			<i>Tenonia priops</i>	11
		Sigalionidae	<i>Sigalion spinosus</i>	98
			<i>Sthenelais tertagliabra</i>	5
			<i>Sthenelais verruculosa</i>	3
			<i>Pholoe glabra</i>	3
			<i>Pisione</i> sp	3
			<i>Sthenelanella uniformis</i>	73
		Glyceridae	<i>Glycera americana</i>	1
			<i>Glycera macrobranchia</i>	1
			<i>Glycera nana</i>	20
			<i>Glycera oxycephala</i>	125
		Goniadidae	<i>Glycinde armigera</i>	197
			<i>Goniada acicula</i>	1
			<i>Goniada brunnea</i>	1
			<i>Goniada maculata</i>	20
		Hesionidae	<i>Oxydromus pugettensis</i>	2

Appendix G.4 *continued*

Phylum	Class	Family	Taxon	n
			<i>Podarkeopsis glabrus</i>	3
			<i>Micropodarke dubia</i>	7
		Nereididae		1
			<i>Gymnonereis crosslandi</i>	1
			<i>Nereis latescens</i>	2
			<i>Nereis</i> sp A	46
			<i>Platynereis bicanaliculata</i>	33
		Syllidae	<i>Syllides mikeli</i>	3
			<i>Epigamia-Myrianida</i> Cmplx	1
			<i>Eusyllis habeii</i>	19
			<i>Eusyllis longicirrata</i>	15
			<i>Eusyllis transecta</i>	7
			<i>Eusyllis</i> sp SD2	3
			<i>Odontosyllis phosphorea</i>	10
			<i>Paraehlersia articulata</i>	2
			<i>Exogone</i> sp	1
			<i>Exogone dwisula</i>	108
			<i>Exogone lourei</i>	29
			<i>Parexogone breviseta</i>	7
			<i>Sphaerosyllis californiensis</i>	3
			<i>Syllis gracilis</i> Cmplx	1
			<i>Syllis heterochaeta</i>	74
			<i>Syllis</i> sp SD1	15
			<i>Syllis</i> sp SD2	9
		Nephtyidae	<i>Bipalponephtys cornuta</i>	1
			<i>Nephtys caecoides</i>	21
			<i>Nephtys ferruginea</i>	3
			<i>Nephtys simoni</i>	11
			<i>Nephtys</i> sp SD2	17
		Sphaerodoridae	<i>Sphaerephesia biserialis</i>	1
		Phyllodoceidae		2
			<i>Eteone</i> sp	1
			<i>Eteone brigitteae</i>	1
			<i>Eteone leptotes</i>	1
			<i>Eteone pigmentata</i>	3
			<i>Eulalia levicornuta</i> Cmplx	2
			<i>Eumida</i> sp	1
			<i>Eumida longicornuta</i>	39
			<i>Sige</i> sp A	7
			<i>Clavadoce</i> sp	2
			<i>Nereiphylla</i> sp 2	3
			<i>Nereiphylla</i> sp SD1	3
			<i>Paranaitis polynoides</i>	1
			<i>Phyllodoce cuspidata</i>	2
			<i>Phyllodoce hartmanae</i>	60
			<i>Phyllodoce longipes</i>	19
			<i>Phyllodoce pettiboneae</i>	4
		Fabriciidae	<i>Pseudofabriciola californica</i>	5

Appendix G.4 *continued*

Phylum	Class	Family	Taxon	n
		Oweniidae	<i>Galathowenia pygidialis</i>	4
			<i>Myriochele gracilis</i>	8
			<i>Myriochele striolata</i>	1
			<i>Owenia collaris</i>	15
		Sabellidae		3
			<i>Acromegalomma pigmentum</i>	8
			<i>Acromegalomma splendidum</i>	5
			<i>Dialychone albocincta</i>	5
			<i>Dialychone trilineata</i>	1
			<i>Dialychone veleronis</i>	48
			<i>Euchone arenae</i>	5
			<i>Euchone hancocki</i>	3
			<i>Euchone incolor</i>	21
			<i>Euchone</i> sp A	2
			<i>Jasmineira</i> sp B	82
			<i>Paradialychone bimaculata</i>	3
			<i>Paradialychone ecaudata</i>	3
			<i>Paradialychone harrisae</i>	11
			<i>Paradialychone paramollis</i>	11
		Apistobranchidae	<i>Apistobranchus ornatus</i>	1
		Magelonidae	<i>Magelona hartmanae</i>	5
		Poecilochaetidae	<i>Poecilochaetus johnsoni</i>	3
		Spionidae	<i>Dipolydora socialis</i>	12
			<i>Dispio</i> sp SD2	4
			<i>Dispio</i> sp SD1	10
			<i>Laonice cirrata</i>	11
			<i>Laonice nuchala</i>	6
			<i>Malacoceros indicus</i>	14
			<i>Microspio pigmentata</i>	2
			<i>Paraprionospio alata</i>	69
			<i>Polydora</i> sp	1
			<i>Polydora biocpipitalis</i>	2
			<i>Polydora cirrosa</i>	9
			<i>Polydora cornuta</i>	8
			<i>Prionospio dubia</i>	10
			<i>Prionospio jubata</i>	46
			<i>Prionospio lighti</i>	3
			<i>Prionospio pygmaeus</i>	17
			<i>Spio maculata</i>	58
			<i>Spiophanes berkeleyorum</i>	64
			<i>Spiophanes duplex</i>	157
			<i>Spiophanes kimballi</i>	4
			<i>Spiophanes norrisi</i>	1574
		Acrocirridae	<i>Macrochaeta</i> sp A	4
		Cirratulidae	<i>Aphelochaeta glandaria</i> Cmplx	6
			<i>Aphelochaeta monilaris</i>	6
			<i>Aphelochaeta petersenae</i>	2
			<i>Aphelochaeta phillipsi</i>	1

Appendix G.4 *continued*

Phylum	Class	Family	Taxon	n
			<i>Aphelochaeta williamsae</i>	6
			<i>Aphelochaeta</i> sp D	33
			<i>Chaetozone</i> sp	2
			<i>Chaetozone armata</i>	3
			<i>Chaetozone columbiana</i>	5
			<i>Chaetozone corona</i>	5
			<i>Chaetozone hartmanae</i>	4
			<i>Chaetozone hedgpethi</i>	1
			<i>Chaetozone lunula</i>	26
			<i>Chaetozone</i> sp SD2	10
			<i>Chaetozone</i> sp SD4	1
			<i>Chaetozone</i> sp SD5	16
			<i>Chaetozone</i> sp SD7	5
			<i>Kirkegaardia cryptica</i>	8
			<i>Kirkegaardia sibilina</i>	339
			<i>Kirkegaardia tessellata</i>	25
		Flabelligeridae	<i>Bradabyssa pilosa</i>	1
			<i>Flabelligera</i> sp SD1	3
			<i>Lamispina schmidtii</i>	1
			<i>Pherusa neopapillata</i>	6
			<i>Therochaeta</i> sp	7
		Sternaspidae	<i>Sternaspis affinis</i>	2
		Ampharetidae		7
			<i>Amage scutata</i>	7
			<i>Ampharete</i> sp	4
			<i>Ampharete acutifrons</i>	1
			<i>Ampharete labrops</i>	99
			<i>Ampharete lineata</i>	1
			<i>Ampharete manriquei</i>	103
			<i>Amphicteis scaphobranchiata</i>	31
			<i>Anobothrus gracilis</i>	8
			<i>Eclysippe trilobata</i>	5
			<i>Lysippe</i> sp A	18
			<i>Lysippe</i> sp B	9
			<i>Phyllocomus</i> sp A	8
			<i>Ampharetidae</i> sp SD1	1
			<i>Melinna oculata</i>	29
		Pectinariidae	<i>Pectinaria californiensis</i>	12
		Terebellidae		1
			<i>Amaeana occidentalis</i>	59
			<i>Polycirrus</i> sp	10
			<i>Polycirrus californicus</i>	17
			<i>Polycirrus</i> sp I	1
			<i>Polycirrus</i> sp A	62
			<i>Polycirrus</i> sp OC1	2
			<i>Polycirrus</i> sp SD3	1
			Terebellinae	2
			<i>Artacama coniferi</i>	1

Appendix G.4 *continued*

Phylum	Class	Family	Taxon	n
			<i>Eupolymnia heterobranchia</i>	3
			<i>Lanassa venusta venusta</i>	37
			<i>Phisidia sanctaemariae</i>	11
			<i>Pista</i> sp	2
			<i>Pista brevibranchiata</i>	4
			<i>Pista elongata</i>	2
			<i>Pista estevanica</i>	22
			<i>Pista wui</i>	466
			<i>Proclea</i> sp A	35
			<i>Streblosoma</i>	1
			<i>Streblosoma</i> sp B	7
			<i>Streblosoma</i> sp C	51
			<i>Thelepus hamatus</i>	1
		Trichobranchidae	<i>Terebellides</i> sp	1
			<i>Terebellides californica</i>	5
			<i>Terebellides</i> sp Type D	2
			<i>Trichobranchus hancocki</i>	11
		Chaetopteridae	<i>Phyllochaetopterus</i> sp	1
			<i>Phyllochaetopterus prolifica</i>	1
			<i>Spiochaetopterus costarum</i> Cmplx	22
		Capitellidae	<i>Capitella teleta</i>	3
			<i>Mediomastus</i> sp	119
			<i>Notomastus</i> sp	5
			<i>Notomastus hemipodus</i>	11
			<i>Notomastus latericeus</i>	39
		Cossuridae	<i>Cossura candida</i>	1
			<i>Cossura</i> sp A	2
		Maldanidae		22
			<i>Isocirrus longiceps</i>	1
			Euclymeninae	2
			<i>Axiothella</i>	1
			<i>Clymenella complanata</i>	1
			<i>Clymenella</i> sp A	1
			<i>Clymenella</i> sp SD1	1
			<i>Petaloclymene pacifica</i>	27
			<i>Praxillella pacifica</i>	21
			Euclymeninae sp A	77
			<i>Clymenura gracilis</i>	1
			<i>Maldane sarsi</i>	6
			<i>Metasychis disparidentatus</i>	12
			<i>Rhodine bitorquata</i>	3
		Opheliidae	<i>Ophelia pulchella</i>	36
			<i>Armandia brevis</i>	3
			<i>Ophelina</i> sp SD3	1
		Orbiniidae	<i>Leitoscoloplos pugettensis</i>	3
			<i>Naineris</i> sp	1
			<i>Naineris uncinata</i>	4
			<i>Scoloplos acmeceps</i>	22

Appendix G.4 *continued*

Phylum	Class	Family	Taxon	n	
Arthropoda	Pycnogonida	Paraonidae	<i>Scoloplos armiger</i> Cmplx	70	
			<i>Aricidea (Acmira) catherinae</i>	3	
			<i>Aricidea (Acmira) horikoshii</i>	1	
			<i>Aricidea (Acmira) lopezi</i>	1	
			<i>Aricidea (Acmira) simplex</i>	11	
			<i>Aricidea (Aricidea) wassi</i>	2	
			<i>Aricidea (Strelzovia) hartleyi</i>	1	
			<i>Levinsenia kirbyae</i>	2	
			<i>Paradoneis</i> sp SD1	19	
			<i>Scalibregma californicum</i>	7	
	Ostracoda	Cylindroleberididae	<i>Prototrygaeus jordanae</i>	5	
			<i>Anoplodactylus erectus</i>	1	
	Malacostraca	Philomedidae	<i>Leuroleberis sharpei</i>	3	
			<i>Xenoleberis californica</i>	1	
		Sarsiellidae	<i>Euphilomedes carcharodonta</i>	169	
			<i>Eusarsiella thominx</i>	1	
		Mysididae	Nebaliidae	<i>Nebalia daytoni</i>	10
				<i>Nebalia pugettensis</i> Cmplx	3
					1
				<i>Neomysis kadiakensis</i>	6
				<i>Pacifacanthomysis nephrophthalma</i>	1
				<i>Metamysidopsis elongata</i>	3
	<i>Mysidopsis intii</i>			5	
	--			Amphipoda	1
	Caprellidae				1
				<i>Caprella mendax</i>	12
		<i>Hemiproto</i> sp A	6		
	Ischyroceridae		<i>Erichthonius brasiliensis</i>	5	
			<i>Microjassa litotes</i>	1	
			<i>Notopoma</i> sp A	15	
			<i>Amphideutopus oculatus</i>	14	
	Photidae	Kamakidae	<i>Ampelisciphotis podophthalma</i>	12	
			<i>Gammaropsis thompsoni</i>	3	
			<i>Photis</i> sp	58	
			<i>Photis bifurcata</i>	4	
			<i>Photis brevipes</i>	37	
			<i>Photis californica</i>	93	
			<i>Photis lacia</i>	11	
			<i>Photis macinerneyi</i>	3	
			<i>Photis parvidons</i>	2	
<i>Photis</i> sp C			1		
Aoridae	Photidae	<i>Photis</i> sp OC1	25		
		<i>Photis</i> sp SD10	3		
		<i>Aoroides</i> sp	2		
		<i>Aoroides</i> sp A	9		
		Unciolidae		<i>Rudilemboides</i> sp	1
				<i>Rudilemboides stenopropodus</i>	1
				<i>Rudilemboides</i> sp A	6

Appendix G.4 *continued*

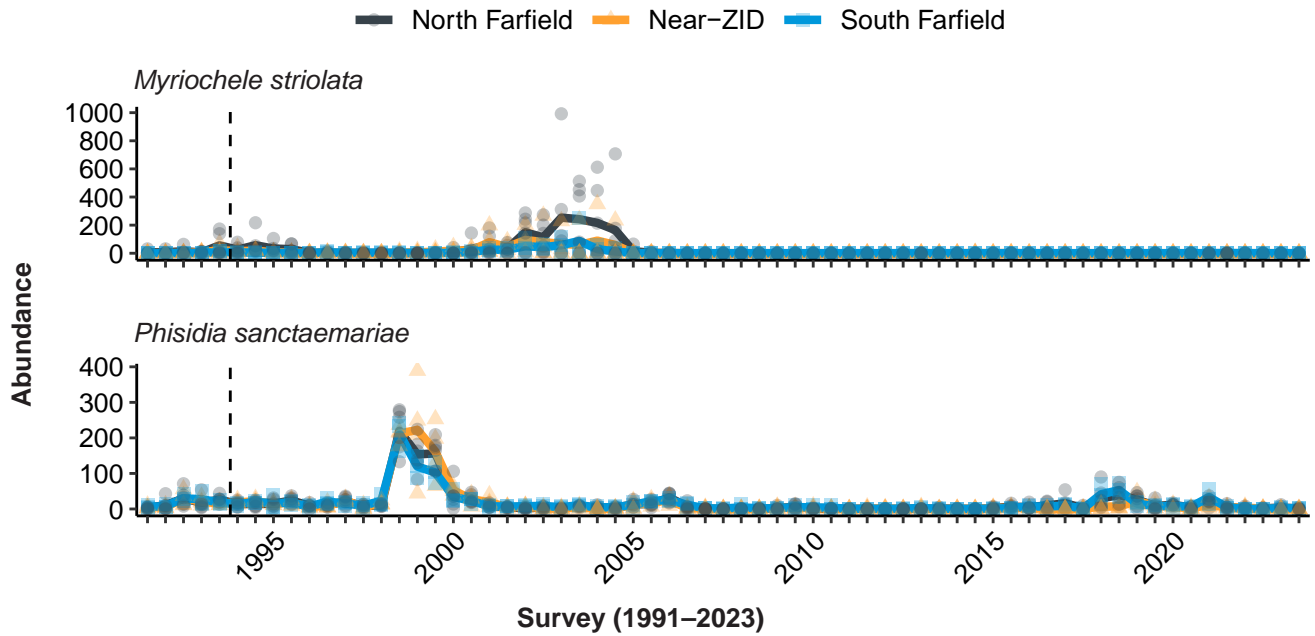
Phylum	Class	Family	Taxon	n
		Corophiidae	<i>Laticorophium baconi</i>	27
		Hornelliidae	<i>Hornellia occidentalis</i>	2
		Megalurotidae	<i>Gibberosus myersi</i>	12
			<i>Megalurotidae</i> sp A	3
		Oedicerotidae		1
			<i>Americhelidium</i> sp	1
			<i>Americhelidium shoemakeri</i>	15
			<i>Americhelidium</i> sp SD1	15
			<i>Americhelidium</i> sp SD4	2
			<i>Bathymedon pumilus</i>	1
			<i>Hartmanodes hartmanae</i>	5
			<i>Hartmanodes</i> sp SD1	2
			<i>Westwoodilla tone</i>	12
		Liljeborgiidae	<i>Listriella eriopisa</i>	1
			<i>Listriella goleta</i>	4
			<i>Listriella melanica</i>	1
		Pleustidae	<i>Pleusymtes subglaber</i>	1
		Stenothoidae	<i>Metopa dawsoni</i>	5
		Melphidippidae	<i>Melphisana bola</i> Cmplx	3
		Pardaliscidae	<i>Halicoides synopiae</i>	2
		Ampeliscidae	<i>Ampelisca</i> sp	11
			<i>Ampelisca agassizi</i>	15
			<i>Ampelisca brachycladus</i>	8
			<i>Ampelisca brevisimulata</i>	128
			<i>Ampelisca cf brevisimulata</i>	12
			<i>Ampelisca careyi</i>	48
			<i>Ampelisca cristata cristata</i>	101
			<i>Ampelisca cristata microdentata</i>	83
			<i>Ampelisca indentata</i>	3
			<i>Ampelisca milleri</i>	3
			<i>Ampelisca pugetica</i>	25
			<i>Byblis millsii</i>	16
		Synopiidae	<i>Metatiron tropakis</i>	7
			<i>Tiron biocellata</i>	3
		Argissidae	<i>Argissa hamatipes</i>	7
		Phoxocephalidae		5
			<i>Foxiphalus obtusidens</i>	59
			<i>Rhepoxynius</i> sp	3
			<i>Rhepoxynius daboius</i>	4
			<i>Rhepoxynius fatigans</i>	4
			<i>Rhepoxynius heterocuspoidatus</i>	77
			<i>Rhepoxynius lucubrans</i>	15
			<i>Rhepoxynius menziesi</i>	89
			<i>Rhepoxynius stenodes</i>	46
			<i>Rhepoxynius variatus</i>	4
		Lysianassidae	<i>Aruga oculata</i>	1
		Uristidae	<i>Anonyx lilljeborgi</i>	3
		Tryphosidae	<i>Hippomedon zetesimus</i>	15

Appendix G.4 *continued*

Phylum	Class	Family	Taxon	n
			<i>Hippomedon</i> sp A	1
			<i>Lepidepecreum gurjanovae</i>	4
			<i>Lepidepecreum serraculum</i>	1
			<i>Orchomenella pacifica</i>	1
			<i>Orchomenella pinguis</i>	1
			Tryphosinae incertae sedis <i>ental-</i> <i>ladurus</i>	13
		Acidostomatidae	<i>Acidostoma hancocki</i>	3
		Pakynidae	<i>Pachynus barnardi</i>	1
			<i>Prachynella lodo</i>	2
		Cirolanidae	<i>Eurydice caudata</i>	18
		Gnathiidae	<i>Caecognathia crenulatifrons</i>	29
			<i>Caecognathia</i> sp SD1	1
		Anthuridae	<i>Haliophasma geminata</i>	17
		Arcturidae	<i>Neastacilla californica</i>	3
		Idoteidae	<i>Edotia sublittoralis</i>	29
			<i>Synidotea magnifica</i>	5
		Serolidae	<i>Heteroserolis carinata</i>	10
		--	Tanaidacea	1
		Akanthophoreidae	<i>Chauliopeleona dentata</i>	3
		Leptocheliidae	<i>Chondrochelia dubia</i> Cmplx	241
		Tanaellidae	<i>Araphura breviarua</i>	2
			<i>Tanaella propinquus</i>	1
		Typhlotanaiidae	<i>Typhlotanais williamsae</i>	1
		Bodotriidae	<i>Cyclaspis nubila</i>	15
		Nannastacidae	<i>Campylaspis canaliculata</i>	5
			<i>Campylaspis rubromaculata</i>	2
			<i>Procampylaspis caenosa</i>	1
		Lampropidae	<i>Hemilamprops californicus</i>	28
			<i>Mesolamprops bispinosus</i>	2
		Diastylidae	<i>Anchicolurus occidentalis</i>	13
			<i>Diastylis californica</i>	10
			<i>Oxyurostylis pacifica</i>	7
		Crangonidae		1
			<i>Crangon</i> sp	7
			<i>Mesocrangon munitella</i>	1
		--	Paguroidea	1
		Albuneidae	<i>Lepidopa californica</i>	13
		Cyclodorippidae	<i>Deilocerus planus</i>	1
		--	Majoidea	1
		Inachidae	<i>Erileptus spinosus</i>	2
		Inachoididae	<i>Pyromaia tuberculata</i>	2
		Parthenopidae	<i>Latulambrus occidentalis</i>	1
		Cancriidae		2
			<i>Metacarcinus gracilis</i>	1
			<i>Romaleon jordani</i>	1
		Pinnotheridae	<i>Pinnixa</i> sp	2
			<i>Pinnixa franciscana</i>	1
			<i>Pinnixa longipes</i>	4

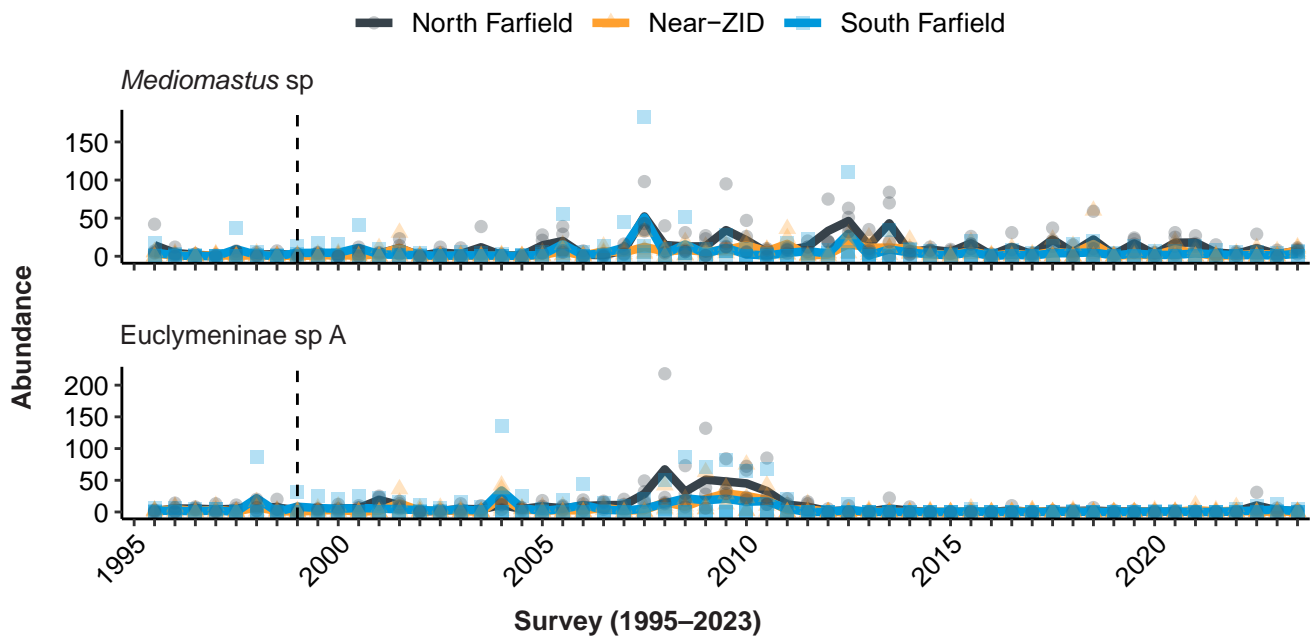
Appendix G.4 *continued*

Phylum	Class	Family	Taxon	n
	Hexanauplia	Balanidae	<i>Balanus</i> sp	2
Nematoda				155
Echinodermata	Asteroidea	Astropectinidae	<i>Astropecten</i> sp	1
		Astropectinidae	<i>Astropecten californicus</i>	17
	Ophiuroidea	Ophiroscolecidae	<i>Ophiuroconis bispinosa</i>	108
		Ophiopsilidae	<i>Ophiopsila californica</i>	1
		Amphiuridae		46
			<i>Amphiodia</i> sp	11
			<i>Amphiodia digitata</i>	3
			<i>Amphiodia urtica</i>	10
			<i>Amphipholis</i> sp	7
			<i>Amphipholis squamata</i>	2
			<i>Dougaloplus</i> sp A	2
			<i>Ophiothrix spiculata</i>	5
	Echinoidea	Ophiotrichidae	<i>Ophiothrix spiculata</i>	5
		Toxopneustidae	<i>Lytechinus pictus</i>	7
		Dendrasteridae	<i>Dendraster</i> sp	11
			<i>Dendraster terminalis</i>	73
		Loveniidae	<i>Lovenia cordiformis</i>	6
	Holothuroidea		Dendrochirotida	1
		Synaptidae	<i>Leptosynapta</i> sp	5
Phoronida		Phoronidae		5
			<i>Phoronis</i> sp	19
			<i>Phoronis</i> sp SD1	9
			<i>Phoronopsis</i> sp	3
Brachiopoda	Lingulata	Lingulidae	<i>Glottidia albida</i>	18
Chordata	Enteropneusta			1
		Ptychoderidae	<i>Balanoglossus</i> sp	2
		Harrimaniidae	<i>Saccoglossus</i> sp	1
	Ascidiacea	Styelidae	<i>Cnemidocarpa rhizopus</i>	9
		Molgulidae	<i>Molgula pugetiensis</i>	1
	Leptocardii	Branchiostomatidae	<i>Branchiostoma californiense</i>	4
		Ptychoderidae	<i>Balanoglossus</i> sp	8
		Harrimaniidae	<i>Saccoglossus</i> sp	1
			<i>Stereobalanus</i> sp	1
	Ascidiacea	Agneziidae	<i>Agnezia septentrionalis</i>	1
		Styelidae	<i>Cnemidocarpa rhizopus</i>	19
		Molgulidae	<i>Molgula regularis</i>	1
	Leptocardii	Branchiostomatidae	<i>Branchiostoma californiense</i>	16



Appendix G.5

Two of the five historically most abundant species recorded from 1991 through 2023 at PLOO north farfield, near-ZID, and south farfield primary core stations. The other historically dominant taxa, *Amphiodia urtica*, *Spiophanes duplex*, and *Proclea* sp A, are shown in Figures 6.4 and 6.5. For each station group, mean abundance per survey is shown by the solid line ($n \leq 8$) while abundance per station is shown by the symbols. Dashed lines indicate onset of wastewater discharge.



Appendix G.6

Two of the five historically most abundant species recorded from 1995 through 2023 at SBOO north farfield, near-ZID, and south farfield primary core stations. The other historically dominant taxa, *Spiophanes norrisi*, *Spiophanes duplex*, and *Kirkegaardia siblina*, are shown in Figure 6.6. For each station group, mean abundance per survey is shown by the solid line ($n \leq 8$) while abundance per station is shown by the symbols. Dashed lines indicate onset of wastewater discharge.

Appendix H

San Diego Regional Benthic Condition Assessment

2022 – 2023

Raw Data Tables & Supplemental Analyses

Appendix H.1

Summary of visual observations for each regional station sampled during summer 2022. Visual observations are from sieved “grunge” (i.e., particles retained on 1-mm mesh screen and preserved with infauna for benthic community analysis).

	Station	Depth (m)	Vis Obs
Inner Shelf	9309	8	—
	9322	8	shell hash
	9301	16	—
	9318	17	—
	9326	18	—
	9341	18	—
	9317	19	red relict sand; shell hash
	9311	23	—
	9304	25	—
	9342	30	shell hash
Mid Shelf	9313	32	organic debris
	9348	35	—
	9302	36	gravel; shell hash; organic debris
	9308	46	coarse sand; shell hash; organic debris
	9336	63	—
	9324	66	—
	9347	69	—
	9306	76	shell hash; organic debris
	9327	78	—
	9320	81	—
	9329	81	—
	9305	87	shell hash
	9338	92	coarse sand; shell hash
	9330	99	—
9328	103	coarse sand; shell hash; organic debris	
Outer Shelf	9335	123	cobble; shell hash
	9314	126	shell hash; organic debris
	9303	129	coralline debris; shell hash
	9340	133	coarse sand; shell hash; organic debris
	9312	137	cobble; shell hash
	9307	173	coarse sand
	9351	179	—
	9310	189	worm tubes; coarse sand; shell hash
	9323	199	worm tubes
Upper Slope	9316	236	worm tubes
	9331	237	cobble; shell hash
	9321	249	—
	9315	321	gravel; shell hash
	9332	422	—
	9325	453	—

Appendix H.2

Concentrations of organic indicators detected in sediments from the San Diego regional benthic stations sampled during summer 2022. See Appendix F.1 for MDLs; DR=detection rate; DNQ = do not quantify; ND=not detected; NR=not reportable.

	Station	Depth (m)	Sulfides (ppm)	TN (% wt)	TOC (% wt)	TVS (% wt)
Inner Shelf	9309	8	NR	0.017	0.076	0.8
	9322	8	2.40	ND	0.069	0.7
	9301	16	3.59	0.021	0.148	0.9
	9318	17	NR	0.021	0.102	0.5
	9326	18	ND	ND	0.100	0.9
	9341	18	7.38	0.030	0.194	1.1
	9317	19	ND	0.025	0.600	0.75
	9311	23	NR	0.030	0.202	1.0
	9304	25	NR	0.022	0.129	0.9
	9342	30	ND	0.025	0.329	1.1
Mid Shelf	9313	32	NR	0.034	0.262	1.4
	9348	35	6.68	0.030	0.331	1.6
	9302	36	ND	0.038	1.22	2.9
	9308	46	NR	0.053	0.495	1.7
	9336	63	NR	0.046	0.490	1.9
	9324	66	ND	0.061	0.733	2.9
	9347	69	2.63	0.031	0.229	1.1
	9306	76	NR	0.072	0.795	2.9
	9327	78	6.11	0.072	0.671	2.85
	9320	81	2.53	0.060	0.673	2.8
	9329	81	ND	0.073	0.660	2.2
	9305	87	19.4	0.035	0.455	1.8
	9338	92	5.51	0.042	0.469	1.7
	9330	99	NR	0.056	0.573	2.8
9328	103	NR	0.051	0.599	2.4	
Outer Shelf	9335	123	NR	0.059	1.45	7.9
	9314	126	5.52	0.052	1.65	2.7
	9303	129	NR	0.088	6.17	4.1
	9340	133	3.93	0.033	0.568	1.9
	9312	137	ND	0.028	0.525	1.68
	9307	173	2.51	0.060	0.925	4.2
	9351	179	2.67	0.033	0.516	2.1
	9310	189	ND	0.056	0.970	2.9
	9323	199	NR	0.083	1.09	4.0
Upper Slope	9316	236	4.53	0.131	2.59	6.7
	9331	237	33.2	0.130	1.82	2.5
	9321	249	20.9	0.166	2.44	6.6
	9315	321	ND	0.086	2.00	3.6
	9332	422	12.5	0.223	2.69	5.2
	9325	453	34.3	0.187	2.54	8.1
	DR (%)		67	95	100	100

Appendix H.3

Concentrations of metals (ppm) detected in sediments from the San Diego regional benthic stations sampled during summer 2022. See Appendix F.1 for MDLs and translation of periodic table symbols; DR=detection rate; DNQ = do not quantify; ND=not detected; NR = not reportable.

	Station	Depth (m)	Al	Sb	As	Ba	Be	Cd	Cr	Cu	Fe
Inner Shelf	9309	8	4270	0.986 DNQ	1.41	32.6	0.062	ND	7.63	10.0	6300
	9322	8	2560	ND	1.64	15.2	0.045	ND	5.12	8.88	4260
	9301	16	7080	1.24 DNQ	1.88	27.7	0.103	ND	10.7	3.01 DNQ	6550
	9318	17	2540	ND	1.47	10.3	0.048	ND	5.87	1.19 DNQ	3640
	9326	18	2870	1.15 DNQ	1.79	17.8	0.038	ND	6.82	1.99 DNQ	5400
	9341	18	4190	ND	1.68	18.0	0.074	ND	8.65	10.2	4480
	9317	19	1190	ND	4.82	8.20	0.017 DNQ	ND	2.84	11.6	3510
	9311	23	4770	0.472 DNQ	1.67	20.6	0.093	ND	9.56	2.37 DNQ	5080
	9304	25	5230	0.936 DNQ	1.47	24.2	0.122	ND	8.72	2.22 DNQ	5160
	9342	30	2960	0.443 DNQ	1.47	9.22	0.037	ND	6.63	2.35 DNQ	4320
Mid Shelf	9313	32	4820	0.572 DNQ	1.86	24.9	0.094	ND	9.68	3.42 DNQ	6290
	9348	35	8720	1.32 DNQ	2.26	40.3	0.139	ND	13.3	5.02	8800
	9302	36	11,500	1.50	3.12	47.6	0.213	0.079 DNQ	15.9	9.00	11,500
	9308	46	6490	1.18 DNQ	2.37	27.0	0.126	ND	12.6	13.6	8020
	9336	63	7410	1.35 DNQ	2.95	39.9	0.151	ND	14.3	12.7	10,200
	9324	66	13,000	2.06	3.42	53.7	0.232	0.087 DNQ	20.5	9.55	14,000
	9347	69	3980	0.754 DNQ	1.60	10.3	0.078	ND	7.14	2.60 DNQ	4540
	9306	76	10,700	1.91	3.44	50.8	0.212	ND	19.9	19.5	13,200
	9327	78	10,200	0.819 DNQ	3.51	49.0	0.226	ND	20.1	8.37	13,700
	9320	81	11,700	1.10 DNQ	3.91	52.1	0.237	ND	21.4	9.81	14,600
	9329	81	10,600	0.850 DNQ	3.70	43.6	0.206	ND	18.4	8.08	13,100
	9305	87	5460	1.35 DNQ	2.71	28.6	0.120	ND	14.1	16.9	7790
	9338	92	6940	0.898 DNQ	3.58	35.8	0.172	0.099 DNQ	14.3	12.6	10,700
	9330	99	8350	0.631 DNQ	2.42	32.7	0.173	ND	15.0	6.36	10,600
9328	103	7490	1.50	2.81	29.2	0.166	ND	15.1	14.3	10,200	
Outer Shelf	9335	123	4540	0.498 DNQ	2.74	17.1	0.124	ND	10.8	4.27	8160
	9314	126	7740	1.17 DNQ	3.49	33.5	0.223	ND	18.1	12.5	16,200
	9303	129	6830	1.33 DNQ	3.47	23.6	0.249	ND	22.4	16.2	19,400
	9340	133	6700	0.815 DNQ	3.19	35.4	0.186	0.135 DNQ	15.4	12.5	11,100
	9312	137	7600	0.743 DNQ	2.30	39.5	0.149	ND	12.0	17.7	10,200
	9307	173	13,800	1.10 DNQ	3.40	73.2	0.263	ND	22.6	28.9	17,500
	9351	179	6290	0.745 DNQ	2.60	24.9	0.161	0.240 DNQ	14.3	5.05	9230
	9310	189	14,600	1.19 DNQ	3.15	73.5	0.295	ND	26.1	30.3	17,800
	9323	199	12,300	0.902 DNQ	3.02	49.8	0.244	0.147 DNQ	22.3	11.6	14,200
Upper Slope	9316	236	15,700	2.17	3.55	62.4	0.305	0.152 DNQ	29.1	17.6	16,700
	9331	237	12,900	1.07 DNQ	3.48	53.9	0.271	0.195 DNQ	25.0	13.2	15,500
	9321	249	15,400	1.25 DNQ	3.05	66.7	0.312	0.134 DNQ	29.5	16.0	17,000
	9315	321	8550	1.90	4.62	41.0	0.300	ND	27.5	8.46	14,800
	9332	422	17,500	2.61	3.47	97.2	0.381	0.383	37.0	27.1	19,100
	9325	453	16,500	1.58	3.05	105	0.373	0.409	35.7	18.8	18,600
DR (%)			100	90	100	100	100	27.5	100	100	100

Appendix H.3 *continued*

	Station	Depth (m)	Pb	Mn	Hg	Ni	Se	Ag	Ti	Sn	Zn
Inner Shelf	9309	8	1.15	67.4	0.004 DNQ	1.83	ND	ND	ND	0.345	17.0
	9322	8	0.605	50.3	0.002 DNQ	1.39	ND	ND	ND	0.094 DNQ	10.4
	9301	16	1.85	79.1	0.004 DNQ	2.55	ND	ND	0.341 DNQ	0.471	15.5
	9318	17	1.63	40.3	0.006 DNQ	1.12	ND	ND	ND	0.190 DNQ	9.14
	9326	18	1.42	103	ND	0.621	ND	ND	ND	0.454	9.54
	9341	18	1.30	54.6	0.006 DNQ	2.36	ND	ND	ND	0.220	12.8
	9317	19	3.09	56.6	0.007 DNQ	0.852	ND	ND	ND	0.161 DNQ	9.21
	9311	23	1.60	53.2	0.007 DNQ	2.43	ND	ND	ND	0.309	13.1
	9304	25	1.19	58.6	0.004 DNQ	1.97	ND	ND	ND	0.350	12.7
	9342	30	2.11	40.6	0.006 DNQ	1.17	ND	ND	ND	0.321	9.64
Mid Shelf	9313	32	2.54	68.5	0.027	2.57	ND	ND	ND	0.557	18.3
	9348	35	2.20	88.2	0.009 DNQ	4.08	ND	ND	ND	0.490	22.4
	9302	36	4.61	97.8	0.021	6.21	ND	ND	ND	0.763	32.2
	9308	46	3.19	76.1	0.024	4.49	ND	ND	ND	0.852	21.4
	9336	63	2.75	96.8	0.015 DNQ	4.67	ND	ND	ND	0.500	25.1
	9324	66	4.49	132	0.037	7.46	ND	ND	ND	1.22	36.1
	9347	69	2.17	44.7	0.011 DNQ	2.65	ND	ND	ND	0.343	10.0
	9306	76	7.73	114	0.065	8.05	ND	ND	ND	1.19	39.1
	9327	78	4.70	112	0.042	7.72	ND	ND	ND	1.01	35.1
	9320	81	4.95	134	0.041	8.58	ND	ND	ND	1.15	36.4
	9329	81	4.05	109	0.031	7.30	ND	ND	ND	0.955	33.2
	9305	87	6.78	70.9	0.062	4.46	ND	ND	ND	0.847	33.9
	9338	92	3.16	92.2	0.015	5.08	ND	ND	ND	0.590	25.9
	9330	99	2.91	89.1	0.023	6.15	ND	ND	ND	0.682	26.7
	9328	103	2.84	81.9	0.022	5.69	ND	ND	ND	0.595	25.5
Outer Shelf	9335	123	1.80	52.3	0.015 DNQ	3.18	ND	ND	ND	0.269	18.8
	9314	126	5.78	71.3	0.038	4.58	ND	ND	ND	0.839	41.6
	9303	129	2.46	46.2	0.019	6.10	0.454 DNQ	ND	ND	0.689	34.6
	9340	133	3.14	85.6	0.016	5.60	ND	ND	ND	0.496	25.0
	9312	137	3.19	90.2	0.035	4.21	ND	ND	ND	0.577	26.4
	9307	173	5.92	147	0.086	9.07	ND	ND	ND	1.23	46.1
	9351	179	3.10	70.4	0.018	5.22	ND	ND	ND	0.511	24.5
	9310	189	7.55	147	0.113	11.0	ND	ND	ND	1.47	50.6
	9323	199	4.30	116	0.045	10.7	ND	ND	ND	0.948	39.2
	Upper Slope	9316	236	5.10	130	0.066	15.1	0.553 DNQ	ND	ND	1.37
9331		237	4.61	118	0.053	11.0	ND	ND	ND	1.03	43.9
9321		249	4.84	137	0.062	15.5	ND	ND	ND	1.21	49.1
9315		321	3.21	53.6	0.025	6.72	ND	ND	ND	0.604	26.3
9332		422	5.17	159	0.061	18.9	0.633 DNQ	ND	ND	1.20	59.6
9325		453	5.84	146	0.064	19.2	ND	ND	ND	1.37	61.4
DR (%)			100	100	97.5	100	7.5	0	2.5	100	100

Appendix H.4

Concentrations of pesticides (ppt) detected in sediments from the San Diego regional benthic stations sampled during summer 2022. See Appendix F.1 for MDLs and abbreviations; DR=detection rate; DNQ = do not quantify; ND=not detected; NR=not reportable.

		Chlordane								
Station	Depth (m)	A(c)C	cNon	G(t)C	Hept	HeptEpox	Methoxy	Oxychlor	tNon	
Inner Shelf	9309	8	ND	ND	ND	ND	ND	ND	ND	ND
	9322	8	ND	ND	ND	ND	ND	ND	ND	ND
	9301	16	ND	ND	ND	ND	ND	ND	ND	ND
	9318	17	ND	ND	ND	ND	ND	ND	ND	ND
	9326	18	ND	ND	ND	ND	ND	ND	ND	ND
	9341	18	ND	ND	ND	ND	ND	ND	ND	ND
	9317	19	ND	ND	ND	ND	ND	ND	ND	ND
	9311	23	ND	ND	ND	ND	ND	ND	ND	ND
	9304	25	ND	ND	ND	ND	ND	ND	ND	ND
9342	30	ND	ND	ND	ND	ND	ND	ND	ND	
Mid Shelf	9313	32	ND	ND	ND	ND	ND	ND	ND	ND
	9348	35	ND	ND	ND	ND	ND	ND	ND	ND
	9302	36	ND	ND	ND	ND	ND	ND	ND	ND
	9308	46	ND	ND	ND	ND	ND	ND	ND	ND
	9336	63	ND	ND	ND	ND	ND	ND	ND	ND
	9324	66	ND	ND	ND	ND	ND	ND	ND	ND
	9347	69	ND	ND	ND	ND	ND	ND	ND	ND
	9306	76	ND	ND	ND	ND	ND	ND	ND	ND
	9327	78	ND	ND	ND	ND	ND	ND	ND	ND
	9320	81	ND	ND	ND	ND	ND	ND	ND	ND
	9329	81	ND	ND	ND	ND	ND	ND	ND	ND
	9305	87	ND	ND	ND	ND	ND	ND	ND	ND
9338	92	ND	ND	ND	ND	ND	ND	ND	ND	
9330	99	ND	ND	ND	ND	ND	ND	ND	ND	
9328	103	ND	ND	ND	ND	ND	ND	ND	ND	
Outer Shelf	9335	123	ND	ND	ND	ND	ND	ND	ND	ND
	9314	126	ND	ND	ND	ND	ND	ND	ND	ND
	9303	129	ND	ND	ND	ND	ND	ND	ND	ND
	9340	133	ND	ND	ND	ND	ND	ND	ND	ND
	9312	137	ND	ND	ND	ND	ND	ND	ND	ND
	9307	173	ND	ND	ND	ND	ND	ND	ND	ND
	9351	179	ND	ND	ND	ND	ND	ND	ND	ND
	9310	189	78.4 DNQ	ND	91.9 DNQ	ND	ND	ND	ND	ND
	9323	199	ND	ND	ND	ND	ND	ND	ND	ND
Upper Slope	9316	236	ND	ND	ND	ND	ND	ND	ND	ND
	9331	237	ND	ND	ND	ND	ND	ND	ND	ND
	9321	249	ND	ND	ND	ND	ND	ND	ND	ND
	9315	321	ND	ND	ND	ND	ND	ND	ND	ND
	9332	422	ND	ND	ND	ND	ND	ND	ND	ND
	9325	453	ND	ND	ND	ND	ND	ND	ND	ND
DR (%)		2.5	0	2.5	0	0	0	0	0	

Appendix H.4 *continued*

	Station	Depth (m)	DDT							
			o,p-DDD	o,p-DDE	o,p-DDT	p,p-DDMU	p,p-DDD	p,p-DDE		
Inner Shelf	9309	8	ND	ND	ND	ND	ND	ND	ND	ND
	9322	8	ND	ND	ND	ND	ND	ND	ND	ND
	9301	16	ND	ND	ND	ND	ND	ND	ND	ND
	9318	17	ND	ND	ND	ND	ND	ND	ND	ND
	9326	18	ND	ND	ND	ND	ND	ND	ND	ND
	9341	18	ND	ND	ND	ND	ND	ND	ND	ND
	9317	19	ND	ND	ND	ND	ND	ND	ND	ND
	9311	23	ND	ND	ND	ND	ND	ND	ND	ND
	9304	25	ND	ND	ND	ND	ND	69.5 DNQ	ND	ND
	9342	30	ND	ND	ND	ND	ND	ND	ND	ND
Mid Shelf	9313	32	ND	ND	ND	ND	ND	ND	ND	ND
	9348	35	ND	ND	ND	76.0 DNQ	145	947	96.1	
	9302	36	298	208	179	774	521	7430	526	
	9308	46	ND	ND	ND	ND	56.5 DNQ	283	ND	
	9336	63	ND	ND	ND	ND	ND	180	ND	
	9324	66	ND	ND	ND	ND	58.9 DNQ	379	ND	
	9347	69	ND	ND	ND	ND	ND	189	ND	
	9306	76	160	ND	237	111	618	2470	1000	
	9327	78	ND	ND	ND	ND	66.6 DNQ	540	86.1 DNQ	
	9320	81	ND	ND	ND	ND	45.2 DNQ	441	ND	
	9329	81	ND	ND	ND	ND	77.2 DNQ	472	ND	
	9305	87	ND	ND	ND	46.3 DNQ	323	529	4670	
	9338	92	ND	ND	ND	ND	ND	212	ND	
9330	99	ND	ND	ND	ND	ND	540	ND		
9328	103	ND	ND	ND	ND	ND	309	ND		
Outer Shelf	9335	123	ND	ND	ND	ND	ND	410	ND	
	9314	126	ND	ND	ND	ND	105	317	ND	
	9303	129	ND	ND	ND	ND	ND	464	ND	
	9340	133	ND	ND	ND	ND	40.7 DNQ	192	92.9	
	9312	137	ND	ND	ND	ND	ND	201	ND	
	9307	173	ND	ND	100 DNQ	ND	162	572	545	
	9351	179	ND	ND	ND	ND	ND	233	ND	
	9310	189	ND	ND	ND	ND	392	442	ND	
9323	199	ND	ND	ND	ND	62.0 DNQ	718	ND		
Upper Slope	9316	236	ND	ND	48.6 DNQ	68.9 DNQ	106 DNQ	1180	124	
	9331	237	ND	ND	ND	ND	71.0 DNQ	832	116	
	9321	249	ND	100 DNQ	ND	95.8 DNQ	191	1570	116 DNQ	
	9315	321	ND	ND	ND	ND	47.6 DNQ	458	ND	
	9332	422	ND	118	ND	77.3 DNQ	102	1360	107	
	9325	453	ND	255	ND	185	185	2590	128 DNQ	
DR (%)			5	10	10	20	50	75	30	

Appendix H.4 *continued*

	Station	Depth (m)	HCH				Endosulfan		
			Alpha	Beta	Delta	Gamma	Alpha	Beta	Sulfate
Inner Shelf	9309	8	ND	ND	ND	ND	ND	ND	ND
	9322	8	ND	ND	ND	ND	ND	ND	ND
	9301	16	ND	ND	ND	ND	ND	ND	ND
	9318	17	ND	ND	ND	ND	ND	ND	ND
	9326	18	ND	ND	ND	ND	ND	ND	ND
	9341	18	ND	ND	ND	ND	ND	ND	ND
	9317	19	ND	ND	ND	ND	ND	ND	ND
	9311	23	ND	ND	ND	ND	ND	ND	ND
	9304	25	ND	ND	ND	ND	ND	ND	ND
	9342	30	ND	ND	ND	ND	ND	ND	ND
Mid Shelf	9313	32	ND	ND	ND	ND	ND	ND	ND
	9348	35	ND	ND	ND	ND	ND	ND	ND
	9302	36	ND	ND	ND	ND	ND	ND	ND
	9308	46	ND	ND	ND	ND	ND	ND	ND
	9336	63	ND	ND	ND	ND	ND	ND	ND
	9324	66	ND	ND	ND	ND	ND	ND	ND
	9347	69	ND	ND	ND	ND	ND	ND	ND
	9306	76	ND	ND	ND	ND	ND	ND	ND
	9327	78	ND	ND	ND	ND	ND	ND	ND
	9320	81	ND	ND	ND	ND	ND	ND	ND
9329	81	ND	ND	ND	ND	ND	ND	ND	
9305	87	ND	ND	ND	ND	ND	ND	ND	
9338	92	ND	ND	ND	ND	ND	ND	ND	
9330	99	ND	ND	ND	ND	ND	ND	ND	
9328	103	ND	ND	ND	ND	ND	ND	ND	
Outer Shelf	9335	123	ND	ND	ND	ND	ND	ND	ND
	9314	126	ND	ND	ND	ND	ND	ND	ND
	9303	129	ND	ND	ND	ND	ND	ND	ND
	9340	133	ND	ND	ND	ND	ND	ND	ND
	9312	137	ND	ND	ND	ND	ND	ND	ND
	9307	173	ND	ND	ND	ND	ND	ND	ND
	9351	179	ND	ND	ND	ND	ND	ND	ND
	9310	189	ND	ND	ND	ND	ND	ND	ND
9323	199	ND	ND	ND	ND	ND	ND	ND	
Upper Slope	9316	236	ND	ND	ND	ND	ND	ND	ND
	9331	237	ND	ND	ND	ND	ND	ND	ND
	9321	249	ND	ND	ND	ND	ND	ND	ND
	9315	321	ND	ND	ND	ND	ND	ND	ND
	9332	422	ND	ND	ND	ND	ND	ND	ND
9325	453	ND	ND	ND	ND	ND	ND	ND	
DR (%)			0	0	0	0	0	0	0

Appendix H.4 *continued*

	Station	Depth (m)	Aldrin	Dieldrin	Endrin	EndAld	HCB	Mirex
Inner Shelf	9309	8	ND	ND	ND	ND	ND	ND
	9322	8	ND	ND	ND	ND	ND	ND
	9301	16	ND	ND	ND	ND	ND	ND
	9318	17	ND	ND	ND	ND	ND	ND
	9326	18	ND	ND	ND	ND	ND	ND
	9341	18	ND	ND	ND	ND	ND	ND
	9317	19	ND	ND	ND	ND	ND	ND
	9311	23	ND	ND	ND	ND	ND	ND
	9304	25	ND	ND	ND	ND	ND	ND
	9342	30	ND	ND	ND	ND	ND	ND
Mid Shelf	9313	32	ND	ND	ND	ND	ND	ND
	9348	35	ND	ND	ND	ND	ND	ND
	9302	36	ND	ND	ND	ND	ND	ND
	9308	46	ND	ND	ND	ND	ND	ND
	9336	63	ND	ND	ND	ND	ND	ND
	9324	66	ND	ND	ND	ND	ND	ND
	9347	69	ND	ND	ND	ND	ND	ND
	9306	76	ND	ND	ND	ND	ND	ND
	9327	78	ND	ND	ND	ND	ND	ND
	9320	81	ND	ND	ND	ND	ND	ND
	9329	81	ND	ND	ND	ND	ND	ND
	9305	87	ND	ND	ND	ND	173	169
	9338	92	ND	ND	ND	ND	ND	ND
	9330	99	ND	ND	ND	ND	ND	ND
9328	103	ND	ND	ND	ND	ND	ND	
Outer Shelf	9335	123	ND	ND	ND	ND	ND	ND
	9314	126	ND	ND	ND	ND	ND	ND
	9303	129	ND	ND	ND	ND	ND	ND
	9340	133	ND	ND	ND	ND	ND	ND
	9312	137	ND	ND	ND	ND	ND	ND
	9307	173	ND	ND	ND	ND	ND	ND
	9351	179	ND	ND	ND	ND	ND	ND
	9310	189	ND	ND	ND	ND	ND	ND
	9323	199	ND	ND	ND	ND	ND	ND
Upper Slope	9316	236	ND	ND	ND	ND	ND	ND
	9331	237	ND	ND	ND	ND	ND	ND
	9321	249	ND	ND	ND	ND	ND	ND
	9315	321	ND	ND	ND	ND	ND	ND
	9332	422	ND	ND	ND	ND	ND	ND
	9325	453	ND	ND	ND	ND	ND	ND
DR (%)			0	0	0	0	2.5	2.5

Appendix H.5

Concentrations of PCBs (ppt) detected in sediments from the San Diego regional benthic stations sampled during summer 2022. See Appendix F.1 for MDLs; DR = detection rate; DNQ = do not quantify; ND = not detected; NR = not reportable.

	Station	Depth (m)	PCB									
			8	18	28	37	44	49	52	66	70	74
Inner Shelf	9309	8	ND	ND	ND	ND	ND	ND	ND	ND	ND	ND
	9322	8	ND	ND	ND	ND	ND	ND	ND	ND	ND	ND
	9301	16	ND	ND	ND	ND	ND	ND	ND	ND	ND	ND
	9318	17	ND	ND	ND	ND	ND	ND	ND	ND	ND	ND
	9326	18	ND	ND	ND	ND	ND	ND	ND	ND	ND	ND
	9341	18	ND	ND	ND	ND	ND	ND	ND	ND	ND	ND
	9317	19	ND	ND	ND	ND	ND	ND	ND	ND	ND	ND
	9311	23	ND	ND	ND	ND	ND	ND	ND	ND	ND	ND
	9304	25	ND	ND	ND	ND	ND	ND	ND	ND	ND	ND
	9342	30	ND	ND	ND	ND	ND	ND	ND	ND	ND	ND
Mid Shelf	9313	32	ND	ND	ND	ND	ND	ND	ND	ND	ND	ND
	9348	35	ND	ND	ND	ND	ND	ND	96.0	ND	ND	ND
	9302	36	ND	ND	ND	ND	ND	ND	ND	ND	ND	ND
	9308	46	ND	ND	ND	ND	ND	ND	ND	ND	ND	ND
	9336	63	ND	ND	ND	ND	ND	ND	ND	ND	ND	ND
	9324	66	ND	ND	52.0 DNQ	ND	68.0 DNQ	ND	140	ND	91.0 DNQ	ND
	9347	69	ND	ND	ND	ND	ND	ND	ND	ND	ND	ND
	9306	76	ND	ND	61.6 DNQ	ND	180	320	440	240	270	ND
	9327	78	ND	ND	ND	ND	ND	ND	ND	ND	ND	ND
	9320	81	ND	ND	ND	ND	ND	ND	ND	ND	ND	ND
9329	81	ND	ND	ND	ND	ND	ND	ND	ND	ND	ND	
9305	87	ND	ND	ND	ND	ND	ND	ND	ND	ND	ND	
9338	92	ND	ND	ND	ND	ND	ND	ND	ND	ND	ND	
9330	99	ND	ND	ND	ND	ND	ND	ND	ND	ND	ND	
9328	103	ND	ND	ND	ND	ND	ND	ND	ND	ND	ND	
Outer Shelf	9335	123	ND	ND	ND	ND	ND	ND	ND	ND	ND	ND
	9314	126	ND	ND	ND	ND	59.6 DNQ	84.1 DNQ	130	72.9 DNQ	84.6 DNQ	ND
	9303	129	ND	ND	ND	ND	ND	ND	ND	ND	ND	ND
	9340	133	ND	ND	ND	ND	ND	ND	ND	ND	ND	ND
	9312	137	ND	ND	ND	ND	75.4 DNQ	ND	180	62.9 DNQ	110	ND
	9307	173	ND	ND	44.0 DNQ	ND	240	170	580	190	360	102 DNQ
	9351	179	ND	ND	ND	ND	ND	ND	ND	ND	ND	ND
	9310	189	ND	ND	45.8 DNQ	ND	200	190	480	180	310	140
	9323	199	ND	ND	ND	ND	72.7 DNQ	ND	160	ND	99.6 DNQ	ND
Upper Slope	9316	236	ND	ND	ND	ND	ND	ND	ND	ND	ND	ND
	9331	237	ND	ND	ND	ND	ND	ND	ND	ND	ND	ND
	9321	249	ND	ND	ND	ND	ND	ND	ND	ND	ND	ND
	9315	321	ND	ND	ND	ND	ND	ND	ND	ND	ND	ND
	9332	422	ND	ND	ND	ND	ND	ND	ND	ND	ND	ND
	9325	453	ND	ND	ND	ND	ND	ND	ND	ND	ND	ND
DR (%)			0	0	10	0	17.5	10	20	12.5	17.5	5

Appendix H.5 *continued*

		PCB										
Station	Depth (m)	77	81	87	99	101	105	110	114	118	119	
Inner Shelf	9309	8	ND	ND	ND	ND	ND	ND	ND	ND	ND	
	9322	8	ND	ND	ND	ND	ND	ND	ND	ND	ND	
	9301	16	ND	ND	ND	ND	ND	ND	ND	ND	ND	
	9318	17	ND	ND	ND	ND	ND	ND	ND	ND	ND	
	9326	18	ND	ND	ND	ND	ND	ND	ND	ND	ND	
	9341	18	ND	ND	ND	ND	ND	ND	ND	ND	ND	
	9317	19	ND	ND	ND	ND	ND	ND	ND	ND	ND	
	9311	23	ND	ND	ND	ND	ND	ND	ND	ND	ND	
	9304	25	ND	ND	ND	ND	ND	ND	ND	ND	ND	
	9342	30	ND	ND	ND	ND	ND	ND	ND	ND	ND	
Mid Shelf	9313	32	ND	ND	ND	ND	ND	ND	ND	ND	ND	
	9348	35	ND	ND 86.4 DNQ	78.7 DNQ	180	ND	170	ND	180	ND	
	9302	36	ND	ND	ND 66.0 DNQ	110	ND	89.4 DNQ	ND	76.5 DNQ	ND	
	9308	46	ND	ND	ND	ND 57.6 DNQ	ND	53.5 DNQ	ND	ND	ND	
	9336	63	ND	ND	ND	ND	ND	ND	ND	ND	ND	
	9324	66	ND	ND 100 DNQ	110 DNQ	220	ND	220	ND	210	ND	
	9347	69	ND	ND	ND	ND	ND	ND	ND	ND	ND	
	9306	76	ND	ND	320	600	1000	320	1100	ND	960 94.9 DNQ	
	9327	78	ND	ND	ND	ND	ND	ND	54.0 DNQ	ND	73.0 DNQ	
	9320	81	ND	ND	ND	ND	ND 53.6 DNQ	ND	53.0 DNQ	ND	ND	
	9329	81	ND	ND	ND	ND	ND	ND	53.4 DNQ	ND	65.9 DNQ	
	9305	87	ND	ND 68.2 DNQ	180	250	ND	230	ND	220	ND	
	9338	92	ND	ND	ND	ND	ND	ND	ND	ND	ND	
	9330	99	ND	ND	ND 70.0 DNQ	100	ND	120	ND	120	ND	
9328	103	ND	ND	ND	ND	ND	ND	ND	ND	ND		
Outer Shelf	9335	123	ND	ND	ND	ND	ND	ND	ND	ND	ND	
	9314	126	ND	ND	120	180	320	120	310	ND	310	
	9303	129	ND	ND	ND	ND	ND	ND	ND	ND	ND	
	9340	133	ND	ND	ND	ND	ND	ND	ND	ND	ND	
	9312	137	ND	ND	170	170	390	130	390	ND	340	
	9307	173	ND	ND	520	530	1200	410	1200	ND	1100	
	9351	179	ND	ND	ND	ND	ND	ND	ND	ND	ND	
	9310	189	ND	ND	410	470	970	370	970	ND	1000	
	9323	199	ND	ND	140	150	310	120	340	ND	270	
Upper Slope	9316	236	ND	ND	ND 86.2 DNQ	108 DNQ	ND	120	ND	150	ND	
	9331	237	ND	ND	ND	ND 60.8 DNQ	ND	63.7 DNQ	ND	73.9 DNQ	ND	
	9321	249	ND	ND	ND 88.2 DNQ	120	ND	120	ND	150	ND	
	9315	321	ND	ND	ND	ND	ND	47.1 DNQ	ND	ND	ND	
	9332	422	ND	ND	ND	ND 57.8 DNQ	ND	61.1 DNQ	ND	ND	ND	
	9325	453	ND	ND	ND	ND 95.1 DNQ	ND	87.0 DNQ	ND	ND	ND	
DR (%)		0	0	22.5	32.5	45	15	52.5	0	40	2.5	

Appendix H.5 *continued*

	Station	Depth (m)	PCB											
			123	126	128	138	149	151	153/168	156	157	158	167	
Inner Shelf	9309	8	ND	ND	ND	ND	ND	ND	ND	ND	ND	ND	ND	ND
	9322	8	ND	ND	ND	ND	ND	ND	ND	ND	ND	ND	ND	ND
	9301	16	ND	ND	ND	ND	ND	ND	ND	ND	ND	ND	ND	ND
	9318	17	ND	ND	ND	ND	ND	ND	ND	ND	ND	ND	ND	ND
	9326	18	ND	ND	ND	ND	ND	ND	ND	ND	ND	ND	ND	ND
	9341	18	ND	ND	ND	ND	ND	ND	ND	ND	ND	ND	ND	ND
	9317	19	ND	ND	ND	ND	ND	ND	ND	ND	ND	ND	ND	ND
	9311	23	ND	ND	ND	ND	ND	ND	ND	ND	ND	ND	ND	ND
	9304	25	ND	ND	ND	ND	ND	ND	ND	ND	ND	ND	ND	ND
	9342	30	ND	ND	ND	ND	ND	ND	ND	ND	ND	ND	ND	ND
Mid Shelf	9313	32	ND	ND	ND	ND	ND	ND	ND	ND	ND	ND	ND	ND
	9348	35	ND	ND	ND	160	110	ND	ND	ND	ND	ND	ND	ND
	9302	36	ND	ND	ND	140	210	62.1 DNQ	320	ND	ND	ND	ND	ND
	9308	46	ND	ND	ND	67.1 DNQ	ND	ND	ND	ND	ND	ND	ND	ND
	9336	63	ND	ND	ND	ND	ND	ND	ND	ND	ND	ND	ND	ND
	9324	66	ND	ND	66.0 DNQ	210	160	ND	ND	ND	ND	ND	ND	ND
	9347	69	ND	ND	ND	ND	ND	ND	ND	ND	ND	ND	ND	ND
	9306	76	91.3 DNQ	ND	310	840	1000	210	1400	160	ND	130	59.6 DNQ	ND
	9327	78	ND	ND	ND	75.0 DNQ	ND	ND	ND	ND	ND	ND	ND	ND
	9320	81	ND	ND	ND	76.8 DNQ	ND	ND	ND	ND	ND	ND	ND	ND
	9329	81	ND	ND	ND	65.2 DNQ	ND	ND	ND	ND	ND	ND	ND	ND
	9305	87	ND	ND	84.0 DNQ	250	370	100	610	ND	ND	ND	ND	ND
	9338	92	ND	ND	ND	ND	ND	ND	ND	ND	ND	ND	ND	ND
	9330	99	ND	ND	ND	120	ND	ND	ND	ND	ND	ND	ND	ND
9328	103	ND	ND	ND	ND	ND	ND	ND	ND	ND	ND	ND	ND	
Outer Shelf	9335	123	ND	ND	ND	ND	ND	ND	ND	ND	ND	ND	ND	ND
	9314	126	ND	ND	110	300	310	72.3 DNQ	600	ND	ND	ND	ND	ND
	9303	129	ND	ND	ND	ND	ND	ND	ND	ND	ND	ND	ND	ND
	9340	133	ND	ND	ND	ND	ND	ND	ND	ND	ND	ND	ND	ND
	9312	137	ND	ND	95.0	300	330	59.3 DNQ	400	ND	ND	ND	ND	ND
	9307	173	95.4 DNQ	ND	320	1000	960	200	1300	150	ND	140	ND	ND
	9351	179	ND	ND	ND	ND	ND	ND	ND	ND	ND	ND	ND	ND
	9310	189	79.5 DNQ	ND	260	970	780	160	1000	140	ND	120	ND	ND
	9323	199	ND	ND	96.6 DNQ	240	220	ND	340	ND	ND	ND	ND	ND
Upper Slope	9316	236	ND	ND	ND	180	160	ND	320	ND	ND	ND	ND	ND
	9331	237	ND	ND	ND	100	ND	ND	ND	ND	ND	ND	ND	ND
	9321	249	ND	ND	ND	170	150	ND	330	ND	ND	ND	ND	ND
	9315	321	ND	ND	ND	81.2 DNQ	ND	ND	ND	ND	ND	ND	ND	ND
	9332	422	ND	ND	ND	80.3 DNQ	ND	ND	ND	ND	ND	ND	ND	ND
	9325	453	ND	ND	ND	113 DNQ	ND	ND	ND	ND	ND	ND	ND	ND
DR (%)			7.5	0	20	52.5	30	17.5	25	7.5	0	7.5	2.5	

Appendix H.5 *continued*

	Station	Depth (m)	PCB										
			169	170	177	180	183	187	189	194	195	201	206
Inner Shelf	9309	8	ND	ND	ND	ND	ND	ND	ND	ND	ND	ND	ND
	9322	8	ND	ND	ND	ND	ND	ND	ND	ND	ND	ND	ND
	9301	16	ND	ND	ND	ND	ND	ND	ND	ND	ND	ND	ND
	9318	17	ND	ND	ND	ND	ND	ND	ND	ND	ND	ND	ND
	9326	18	ND	ND	ND	ND	ND	ND	ND	ND	ND	ND	ND
	9341	18	ND	ND	ND	ND	ND	ND	ND	ND	ND	ND	ND
	9317	19	ND	ND	ND	ND	ND	ND	ND	ND	ND	ND	ND
	9311	23	ND	ND	ND	ND	ND	ND	ND	ND	ND	ND	ND
	9304	25	ND	ND	ND	ND	ND	ND	ND	ND	ND	ND	ND
	9342	30	ND	ND	ND	ND	ND	ND	ND	ND	ND	ND	ND
Mid Shelf	9313	32	ND	ND	ND	ND	ND	ND	ND	ND	ND	ND	ND
	9348	35	ND	ND	ND	ND	ND	ND	ND	ND	ND	ND	ND
	9302	36	ND	92.9 DNQ	58.9 DNQ	190	55.4 DNQ	130	ND	ND	ND	ND	ND
	9308	46	ND	ND	ND	ND	ND	ND	ND	ND	ND	ND	ND
	9336	63	ND	ND	ND	ND	ND	ND	ND	ND	ND	ND	ND
	9324	66	ND	ND	ND	62.0 DNQ	ND	46.0 DNQ	ND	ND	ND	ND	ND
	9347	69	ND	ND	ND	ND	ND	ND	ND	ND	ND	ND	ND
	9306	76	ND	220	150	450	120	290	ND	120	ND	ND	NR
	9327	78	ND	ND	ND	60.0 DNQ	ND	52.0 DNQ	ND	ND	ND	ND	ND
	9320	81	ND	ND	ND	55.1 DNQ	ND	44.6 DNQ	ND	ND	ND	ND	ND
	9329	81	ND	ND	ND	48.9 DNQ	ND	43.3 DNQ	ND	ND	ND	ND	ND
	9305	87	ND	110	80.6 DNQ	250	75.6 DNQ	240	ND	110	ND	ND	NR
	9338	92	ND	ND	ND	ND	ND	ND	ND	ND	ND	ND	ND
	9330	99	ND	ND	ND	ND	ND	ND	ND	ND	ND	ND	ND
9328	103	ND	ND	ND	ND	ND	ND	ND	ND	ND	ND	ND	
Outer Shelf	9335	123	ND	ND	ND	ND	ND	ND	ND	ND	ND	ND	ND
	9314	126	ND	68.6 DNQ	61.3 DNQ	120	32.5 DNQ	140	ND	ND	ND	ND	ND
	9303	129	ND	ND	ND	ND	ND	ND	ND	ND	ND	ND	ND
	9340	133	ND	ND	ND	ND	ND	ND	ND	ND	ND	ND	ND
	9312	137	ND	49.6 DNQ	34.7 DNQ	88.3 DNQ	ND	74.6 DNQ	ND	ND	ND	ND	ND
	9307	173	ND	190	130	370	90.0 DNQ	290	ND	140	ND	ND	NR
	9351	179	ND	ND	ND	ND	ND	ND	ND	ND	ND	ND	ND
	9310	189	ND	170	86.5 DNQ	260	65.4 DNQ	200	ND	100	ND	ND	NR
	9323	199	ND	55.4 DNQ	36.9 DNQ	75.8 DNQ	ND	71.6 DNQ	ND	ND	ND	ND	ND
Upper Slope	9316	236	ND	59.9 DNQ	56.3 DNQ	150	ND	140	ND	95.6 DNQ	ND	ND	NR
	9331	237	ND	ND	29 DNQ	74.0 DNQ	ND	75.0 DNQ	ND	63.1 DNQ	ND	ND	ND
	9321	249	ND	ND	49 DNQ	88.1 DNQ	ND	104 DNQ	ND	ND	ND	ND	ND
	9315	321	ND	ND	ND	ND	ND	ND	ND	ND	ND	ND	ND
	9332	422	ND	ND	ND	ND	ND	45.4 DNQ	ND	ND	ND	ND	ND
	9325	453	ND	ND	ND	ND	ND	70.4 DNQ	ND	ND	ND	ND	ND
DR (%)			0	22.5	27.5	37.5	15	42.5	0	15	0	0	0

Appendix H.6

Concentrations of PAHs (ppb) detected in sediments from the San Diego regional benthic stations sampled during summer 2022. See Appendix F.1 for MDLs; DR=detection rate; DNQ = do not quantify; ND=not detected; NR=not reportable.

	Station	Depth (m)	1-methyl naphthalene	1-methyl phenanthrene	2-methyl naphthalene	2,3,5-trimethyl naphthalene	2,6-dimethyl naphthalene	3,4-benzo(B) fluoranthene	Acenaphthene	Acenaphthylene
Inner Shelf	9309	8	ND	ND	ND	ND	ND	ND	ND	ND
	9322	8	ND	ND	ND	ND	ND	ND	ND	ND
	9301	16	ND	ND	ND	ND	ND	ND	ND	ND
	9318	17	ND	ND	ND	ND	ND	ND	ND	ND
	9326	18	ND	ND	ND	ND	ND	ND	ND	ND
	9341	18	ND	ND	ND	ND	11.4	ND	ND	ND
	9317	19	ND	ND	ND	ND	ND	ND	ND	ND
	9311	23	ND	ND	ND	ND	12.5	ND	ND	ND
	9304	25	ND	ND	ND	ND	ND	ND	ND	ND
	9342	30	ND	ND	ND	ND	ND	ND	ND	ND
Mid Shelf	9313	32	ND	ND	ND	ND	ND	ND	ND	ND
	9348	35	ND	ND	ND	ND	ND	ND	ND	ND
	9302	36	ND	ND	ND	ND	ND	ND	ND	ND
	9308	46	ND	ND	ND	ND	11.9	ND	ND	ND
	9336	63	ND	ND	ND	ND	ND	ND	ND	ND
	9324	66	ND	ND	ND	ND	ND	ND	ND	ND
	9347	69	ND	ND	ND	ND	ND	ND	ND	ND
	9306	76	ND	ND	ND	ND	ND	ND	ND	ND
	9327	78	ND	ND	ND	ND	ND	ND	ND	ND
	9320	81	ND	ND	ND	ND	ND	ND	ND	ND
	9329	81	ND	ND	ND	ND	ND	ND	ND	ND
	9305	87	ND	ND	ND	ND	ND	ND	ND	ND
	9338	92	ND	ND	ND	ND	ND	ND	ND	ND
	9330	99	ND	ND	ND	ND	ND	ND	ND	ND
9328	103	ND	ND	ND	ND	ND	ND	ND	ND	
Outer Shelf	9335	123	ND	ND	ND	ND	ND	ND	ND	ND
	9314	126	ND	ND	ND	ND	ND	ND	ND	ND
	9303	129	ND	ND	ND	ND	ND	ND	ND	ND
	9340	133	ND	ND	ND	ND	ND	ND	ND	ND
	9312	137	ND	ND	ND	ND	ND	ND	ND	ND
	9307	173	ND	ND	ND	ND	ND	ND	ND	ND
	9351	179	ND	ND	ND	ND	ND	ND	ND	ND
	9310	189	ND	ND	ND	ND	ND	ND	ND	ND
	9323	199	ND	ND	ND	ND	ND	ND	ND	ND
Upper Slope	9316	236	ND	ND	ND	ND	ND	ND	ND	ND
	9331	237	ND	ND	ND	ND	ND	ND	ND	ND
	9321	249	ND	ND	ND	ND	11.2	ND	ND	ND
	9315	321	ND	ND	ND	ND	ND	ND	ND	ND
	9332	422	ND	ND	ND	ND	ND	ND	ND	ND
	9325	453	ND	ND	ND	ND	ND	ND	ND	ND
DR (%)			0	0	0	0	10	0	0	0

Appendix H.6 *continued*

	Station	Depth (m)	Anthracene	Benzo[A] anthracene	Benzo[A] pyrene	Benzo[e] pyrene	Benzo[G,H,I] perylene	Benzo[K] fluoranthene	Biphenyl	Chrysene
Inner Shelf	9309	8	ND	ND	ND	ND	ND	ND	7.36	ND
	9322	8	ND	ND	ND	ND	ND	ND	ND	ND
	9301	16	ND	ND	ND	ND	ND	ND	ND	ND
	9318	17	ND	ND	ND	ND	ND	ND	7.12	ND
	9326	18	ND	ND	ND	ND	ND	ND	ND	ND
	9341	18	ND	ND	ND	ND	ND	ND	9.46	ND
	9317	19	ND	ND	ND	ND	ND	ND	ND	ND
	9311	23	ND	ND	ND	ND	ND	ND	11.4	ND
	9304	25	ND	ND	ND	ND	ND	ND	ND	ND
	9342	30	ND	ND	ND	ND	ND	ND	ND	ND
Mid Shelf	9313	32	ND	ND	ND	ND	ND	ND	7.71	ND
	9348	35	ND	ND	ND	ND	ND	ND	8.22	ND
	9302	36	ND	ND	ND	ND	ND	ND	ND	ND
	9308	46	ND	ND	ND	ND	ND	ND	8.50	ND
	9336	63	ND	ND	ND	ND	ND	ND	8.20	ND
	9324	66	ND	ND	ND	ND	ND	ND	ND	ND
	9347	69	ND	ND	ND	ND	ND	ND	6.82	ND
	9306	76	ND	40.0	79.1	41.2	35.7	32.2	9.83	59.1
	9327	78	ND	ND	ND	ND	ND	ND	7.77	ND
	9320	81	ND	ND	ND	ND	ND	ND	ND	ND
	9329	81	ND	ND	ND	ND	ND	ND	ND	ND
	9305	87	18.4	108	113	73.9	64.5	63.9	ND	143
	9338	92	ND	ND	ND	ND	ND	ND	ND	ND
	9330	99	ND	ND	ND	ND	ND	ND	ND	ND
9328	103	ND	ND	ND	ND	ND	ND	7.40	ND	
Outer Shelf	9335	123	ND	ND	ND	ND	ND	ND	ND	ND
	9314	126	ND	ND	25.7	ND	14.7	ND	ND	16.5
	9303	129	ND	ND	ND	ND	ND	ND	ND	ND
	9340	133	ND	ND	ND	ND	ND	ND	ND	ND
	9312	137	ND	ND	38.3	20.7	13.3	24.8	ND	21.3
	9307	173	13.4	ND	48.3	31.6	29.7	28.2	ND	36.6
	9351	179	ND	ND	ND	ND	ND	ND	ND	ND
	9310	189	ND	ND	37.1	26.5	25.9	25.5	ND	28.2
	9323	199	ND	ND	ND	ND	ND	ND	9.61	ND
Upper Slope	9316	236	ND	ND	ND	ND	ND	ND	ND	ND
	9331	237	ND	ND	ND	ND	ND	ND	ND	ND
	9321	249	ND	ND	ND	ND	ND	ND	ND	ND
	9315	321	ND	ND	ND	ND	ND	ND	ND	ND
	9332	422	ND	ND	ND	ND	ND	ND	ND	ND
	9325	453	ND	ND	ND	ND	ND	ND	ND	ND
DR (%)			5	5	15	12.5	15	12.5	32.5	15

Appendix H.6 *continued*

	Station	Depth (m)	Dibenzo(A,H) anthracene	Fluoranthene	Fluorene	Indeno(1,2,3-CD) pyrene	Naphthalene	Perylene	Phenanthrene	Pyrene
Inner Shelf	9309	8	ND	ND	ND	ND	ND	ND	ND	ND
	9322	8	ND	ND	ND	ND	ND	ND	ND	ND
	9301	16	ND	ND	ND	ND	ND	ND	ND	ND
	9318	17	ND	ND	ND	ND	ND	ND	ND	ND
	9326	18	ND	ND	ND	ND	ND	ND	ND	ND
	9341	18	ND	ND	ND	ND	ND	ND	ND	ND
	9317	19	ND	ND	ND	ND	ND	ND	ND	ND
	9311	23	ND	ND	ND	ND	ND	ND	ND	ND
	9304	25	ND	ND	ND	ND	ND	ND	ND	ND
	9342	30	ND	ND	ND	ND	ND	ND	ND	ND
Mid Shelf	9313	32	ND	ND	ND	ND	ND	ND	ND	ND
	9348	35	ND	ND	ND	ND	ND	ND	ND	ND
	9302	36	ND	ND	ND	ND	ND	ND	ND	ND
	9308	46	ND	ND	ND	ND	ND	ND	ND	ND
	9336	63	ND	ND	ND	ND	ND	ND	ND	ND
	9324	66	ND	ND	ND	ND	ND	ND	ND	ND
	9347	69	ND	ND	ND	ND	ND	ND	ND	ND
	9306	76	ND	26.0	ND	30.1	ND	13.7	ND	28.2
	9327	78	ND	ND	ND	ND	ND	ND	ND	ND
	9320	81	ND	ND	ND	ND	ND	ND	ND	ND
	9329	81	ND	ND	ND	ND	ND	ND	ND	ND
	9305	87	13.9 DNQ	161	ND	51.5 DNQ	ND	28.4	25.8	131
	9338	92	ND	ND	ND	ND	ND	ND	ND	ND
	9330	99	ND	ND	ND	ND	ND	ND	ND	ND
9328	103	ND	ND	ND	ND	ND	ND	ND	ND	
Outer Shelf	9335	123	ND	ND	ND	ND	ND	ND	ND	ND
	9314	126	ND	10.3	ND	12.1	ND	ND	ND	12.9
	9303	129	ND	ND	ND	ND	ND	ND	ND	ND
	9340	133	ND	ND	ND	ND	ND	ND	ND	ND
	9312	137	ND	ND	ND	12.0	ND	ND	ND	10.2
	9307	173	ND	26.8	ND	22.5 DNQ	12.6	ND	11.0	28.3
	9351	179	ND	ND	ND	ND	ND	ND	ND	ND
	9310	189	ND	25.4	ND	20.4 DNQ	ND	ND	ND	29.4
	9323	199	ND	ND	ND	ND	ND	ND	ND	ND
Upper Slope	9316	236	ND	ND	ND	ND	ND	ND	ND	ND
	9331	237	ND	ND	ND	ND	ND	ND	ND	ND
	9321	249	ND	ND	ND	ND	ND	ND	ND	10.8
	9315	321	ND	ND	ND	ND	ND	ND	ND	ND
	9332	422	ND	ND	ND	ND	ND	ND	ND	ND
	9325	453	ND	ND	ND	ND	ND	ND	ND	ND
DR (%)			2.5	12.5	0	15	2.5	5	5	17.5

Appendix H.7

Concentrations of PBDEs (ppt) detected in sediments from the San Diego regional benthic stations sampled during summer 2022. See Appendix F.1 for MDLs; DR=detection rate; DNQ = do not quantify; ND=not detected; NR = not reportable.

	Station	Depth (m)	BDE-17	BDE-28	BDE-47	BDE-49	BDE-66	BDE-85	BDE-99
Inner Shelf	9309	8	ND	ND	ND	ND	ND	ND	ND
	9322	8	ND	ND	ND	ND	ND	ND	ND
	9301	16	ND	ND	NR	ND	ND	ND	ND
	9318	17	ND	ND	ND	ND	ND	ND	ND
	9326	18	ND	ND	ND	ND	ND	ND	ND
	9341	18	ND	ND	ND	ND	ND	ND	ND
	9317	19	ND	ND	ND	ND	ND	ND	ND
	9311	23	ND	ND	NR	ND	ND	ND	ND
	9304	25	ND	ND	NR	ND	ND	ND	ND
	9342	30	ND	ND	ND	ND	ND	ND	ND
Mid Shelf	9313	32	ND	ND	NR	ND	ND	ND	ND
	9348	35	ND	ND	ND	ND	ND	ND	ND
	9302	36	ND	ND	NR	ND	ND	ND	ND
	9308	46	ND	ND	NR	ND	ND	ND	ND
	9336	63	ND	ND	NR	ND	ND	ND	ND
	9324	66	ND	ND	NR	ND	ND	ND	ND
	9347	69	ND	ND	ND	ND	ND	ND	ND
	9306	76	ND	ND	126	ND	ND	ND	70.6 DNQ
	9327	78	ND	ND	138	ND	ND	ND	105
	9320	81	ND	ND	134	ND	ND	ND	110
	9329	81	ND	ND	136	ND	ND	ND	105
	9305	87	ND	ND	NR	ND	ND	ND	75.7 DNQ
	9338	92	ND	ND	ND	ND	ND	ND	ND
	9330	99	ND	ND	NR	ND	ND	ND	65.9 DNQ
9328	103	ND	ND	143	ND	ND	ND	115	
Outer Shelf	9335	123	ND	ND	NR	ND	ND	ND	ND
	9314	126	ND	ND	NR	ND	ND	ND	ND
	9303	129	ND	ND	NR	ND	ND	ND	ND
	9340	133	ND	ND	ND	ND	ND	ND	ND
	9312	137	ND	ND	NR	ND	ND	ND	ND
	9307	173	ND	ND	NR	ND	ND	ND	ND
	9351	179	ND	ND	ND	ND	ND	ND	ND
	9310	189	ND	ND	NR	ND	ND	ND	ND
	9323	199	ND	ND	NR	ND	ND	ND	ND
Upper Slope	9316	236	ND	ND	ND	ND	ND	ND	ND
	9331	237	ND	ND	NR	ND	ND	ND	ND
	9321	249	ND	ND	NR	ND	ND	ND	ND
	9315	321	ND	ND	NR	ND	ND	ND	ND
	9332	422	ND	ND	ND	ND	ND	ND	ND
	9325	453	ND	ND	ND	ND	ND	ND	ND
DR (%)			0	0	25	0	0	0	17.5

Appendix H.7 *continued*

	Station	Depth (m)	BDE-100	BDE-138	BDE-153	BDE-154	BDE-183	BDE-190
Inner Shelf	9309	8	ND	ND	ND	ND	ND	ND
	9322	8	ND	ND	ND	ND	ND	ND
	9301	16	ND	ND	ND	ND	ND	ND
	9318	17	ND	ND	ND	ND	ND	ND
	9326	18	ND	ND	ND	ND	ND	ND
	9341	18	ND	ND	ND	ND	ND	ND
	9317	19	ND	ND	ND	ND	ND	ND
	9311	23	ND	ND	ND	ND	ND	ND
	9304	25	ND	ND	ND	ND	ND	ND
	9342	30	ND	ND	ND	ND	ND	ND
Mid Shelf	9313	32	ND	ND	ND	ND	ND	ND
	9348	35	ND	ND	ND	ND	ND	ND
	9302	36	ND	ND	ND	ND	ND	ND
	9308	46	ND	ND	ND	ND	ND	ND
	9336	63	ND	ND	ND	ND	ND	ND
	9324	66	ND	ND	ND	ND	ND	ND
	9347	69	ND	ND	ND	ND	ND	ND
	9306	76	ND	ND	ND	ND	ND	ND
	9327	78	ND	ND	ND	ND	ND	ND
	9320	81	ND	ND	ND	ND	ND	ND
	9329	81	52.5 DNQ	ND	ND	ND	ND	ND
	9305	87	ND	ND	ND	ND	ND	ND
	9338	92	ND	ND	ND	ND	ND	ND
	9330	99	ND	ND	ND	ND	ND	ND
9328	103	ND	ND	ND	ND	ND	ND	
Outer Shelf	9335	123	ND	ND	ND	ND	ND	ND
	9314	126	ND	ND	ND	ND	ND	ND
	9303	129	ND	ND	ND	ND	ND	ND
	9340	133	ND	ND	ND	ND	ND	ND
	9312	137	ND	ND	ND	ND	ND	ND
	9307	173	ND	ND	ND	ND	ND	ND
	9351	179	ND	ND	ND	ND	ND	ND
	9310	189	ND	ND	ND	ND	ND	ND
	9323	199	ND	ND	ND	ND	ND	ND
Upper Slope	9316	236	ND	ND	ND	ND	ND	ND
	9331	237	ND	ND	ND	ND	ND	ND
	9321	249	ND	ND	ND	ND	ND	ND
	9315	321	ND	ND	ND	ND	ND	ND
	9332	422	ND	ND	ND	ND	ND	ND
	9325	453	ND	ND	ND	ND	ND	ND
DR (%)			2.5	0	0	0	0	0

Appendix H.8

Summary taxonomic listing of benthic infauna taxa identified from regional stations during 2022. Data are total number of individuals (n). Taxonomic arrangement follows SCAMIT (2021).-- indicates taxon is not within previous family.

Phylum	Class	Family	Taxon	n			
Cnidaria	Hydrozoa	Corymorphidae	<i>Corymorpha bigelowi</i>	1			
			<i>Euphysa</i> sp	4			
	Anthozoa	Plexauridae	<i>Thesea</i> sp B	1			
			<i>Virgularia</i> sp	1			
			--	Ceriantharia	1		
			Arachnactidae	<i>Arachnanthus</i> sp A	2		
			--	Actiniaria	3		
			Edwardsiidae		12		
			<i>Edwardsia juliae</i>	4			
			<i>Edwardsia olguini</i>	9			
			<i>Edwardsia</i> sp SD1	5			
			<i>Scolanthus triangulus</i>	17			
	Anthozoa	Halcampidae	<i>Halcompa decemtentaculata</i>	4			
			<i>Halianthella</i> sp A	3			
			<i>Pentactinia californica</i>	3			
			Isanthidae	<i>Zaolutus actius</i>	2		
			Limnactiniidae	Limnactiniidae sp A	2		
			Platyhelminthes	Rhabditophora	--	Polycladida	1
					Stylochidae	<i>Stylochus exiguus</i>	2
					Plehnidae	<i>Diplehnia caeca</i>	3
Stylochoplanidae					<i>Armatoplana reishi</i>	1	
Euryleptidae					<i>Acerotisa langi</i>	1	
<i>Eurylepta</i> sp	1						
--	<i>Rhabdocoela</i> sp A	1					
Nemertea	Palaeonemertea	Cephalotrichidae			<i>Cephalothrix</i> sp	2	
		Carinomidae			<i>Carinoma mutabilis</i>	28	
		Tubulanidae				2	
		Tubulanidae sp B	1				
		Tubulanidae sp D	1				
		<i>Tubulanus cingulatus</i>	6				
		<i>Tubulanus polymorphus</i>	42				
		--	<i>Palaeonemertea</i> sp	7			
		Pilidiophora	Lineidae	<i>Cerebratulus</i> sp	2		
				<i>Cerebratulus californiensis</i>	2		
Lineidae sp SD1	10						
<i>Macaulaura alaskensis</i> Cmplx	1						
<i>Siphonenteron bilineatum</i>	42						
<i>Zygeupolia rubens</i>	6						
--	Heteronemertea sp SD2			102			
Heteronemertea	1						
Hoplonemertea	Emplectonematidae				1		
				Neesidae	<i>Paranemertes californica</i>	7	
		Oerstedidae	<i>Oerstedtia dorsalis</i> Cmplx	1			
		Amphiporidae	<i>Amphiporus californicus</i>	1			
		<i>Amphiporus flavescens</i>	1				

Appendix H.8 *continued*

Phylum	Class	Family	Taxon	n			
		Tetrastemmatidae	<i>Tetrastemma candidum</i>	4			
		Zygonemertidae	<i>Zygonemertes virescens</i>	1			
		--	<i>QuasitetraSTEMMA nigrifrons</i>	2			
			HoplonemerteA sp D	1			
			HoplonemerteA	12			
Mollusca	Caudofoveata	Chaetodermatidae	<i>Chaetoderma marinellii</i>	2			
			<i>Chaetoderma pacificum</i>	8			
			<i>Falcidens hartmanae</i>	3			
			<i>Falcidens longus</i>	9			
				Limifossoridae	<i>Limifossor fratula</i>	3	
			Polyplacophora	Leptochitonidae	<i>Leptochiton rugatus</i>	6	
							2
			Gastropoda		Fissurellidae	<i>Puncturella cooperi</i>	2
					Trochidae	<i>Halistylus pupoideus</i>	5
					Calyptraeidae		1
	<i>Calyptraea fastigiata</i>	1					
	<i>Glossaulax reclusiana</i>	1					
	Naticidae	<i>Caecum crebricinctum</i>			5		
	Caecidae				2		
	Eulimidae	<i>Balcis oldroydae</i>			3		
		<i>Haliella abyssicola</i>			1		
		<i>Polygireulima rutila</i>			1		
	Epitoniidae	<i>Epitonium bellastriatum</i>			3		
	Nassariidae	<i>Caesia perpinguis</i>			1		
	Olividae	<i>Callianax alectona</i>			113		
	Borsoniidae	<i>Ophiodermella inermis</i>			1		
	Mangeliidae				1		
		<i>Kurtzia arteaga</i>			4		
		<i>Kurtziella plumbea</i>			6		
		<i>Kurtzina beta</i>			9		
		Pseudomelatomidae			<i>Pseudotaranis strongi</i>	1	
		Arminidae			<i>Armina californica</i>	1	
		Aeolidiidae	<i>Cerberilla mosslandica</i>	2			
		Pleurobranchidae	<i>Pleurobranchaea californica</i>	1			
		Pyramidellidae	<i>Odostomia</i> sp	3			
			<i>Turbonilla</i> sp	1			
	<i>Turbonilla santarosana</i>		4				
	<i>Turbonilla</i> sp A		2				
<i>Turbonilla</i> sp SD5	1						
<i>Turbonilla</i> sp SD9	1						
Rhizoridae	<i>Volvulella californica</i>		2				
	<i>Volvulella cylindrica</i>	12					
	<i>Volvulella panamica</i>	4					
Philinidae	<i>Philine auriformis</i>	22					
	<i>Philine ornatissima</i>	1					
Aglajidae	<i>Aglaja ocelligera</i>	6					
Gastropteridae	<i>Gastropteron pacificum</i>	6					
Cylichnidae	<i>Cylichna diegensis</i>	7					
--		<i>Bullomorpha</i> sp A	1				

Appendix H.8 *continued*

Phylum	Class	Family	Taxon	n
	Bivalvia			8
		Nuculidae	<i>Ennucula tenuis</i>	11
		Solemyidae	<i>Petrasma pervernicosa</i>	3
		Nuculanidae	<i>Nuculana hamata</i>	3
			<i>Propeleda conceptionis</i>	1
			<i>Propeleda</i> sp B	1
			<i>Saccella</i> sp A	24
			<i>Saccella taphria</i>	30
		Yoldiidae	<i>Yoldiella nana</i>	3
		Mytilidae		1
			<i>Amygdalum pallidulum</i>	11
			<i>Crenella decussata</i>	2
			Modiolinae	1
			<i>Solamen columbianum</i>	1
		Limidae	<i>Limaria hemphilli</i>	1
		Pectinidae		1
			<i>Delectopecten vancouverensis</i>	1
			<i>Leptopecten latiauratus</i>	14
		Lucinidae	<i>Lucinisca nuttalli</i>	1
			<i>Lucinoma annulatum</i>	7
			<i>Parvilucina tenuisculpta</i>	79
		Thyasiridae	<i>Adontorhina cyclia</i>	9
			<i>Axinopsida serricata</i>	126
			<i>Thyasira flexuosa</i>	10
		Lasaeidae		1
			<i>Kurtiella tumida</i>	10
			<i>Neaeromya compressa</i>	2
		Cardiidae	<i>Keenaea centifilosa</i>	8
		Tellinidae		2
			<i>Macoma</i> sp	1
			<i>Macoma carlottensis</i>	1
			<i>Macoma yoldiformis</i>	76
			<i>Tellina</i> sp	2
			<i>Tellina bodegensis</i>	4
			<i>Tellina cadieni</i>	98
			<i>Tellina carpenteri</i>	33
			<i>Tellina idae</i>	1
			<i>Tellina modesta</i>	94
		Solenidae	<i>Solen sicarius</i>	10
		Pharidae	<i>Ensis myrae</i>	5
			<i>Siliqua lucida</i>	12
		Veneridae	Venerinae	10
			<i>Compsomyax subdiaphana</i>	5
		Petricolidae	<i>Cooperella subdiaphana</i>	247
		Mactridae	<i>Simomactra falcata</i>	9
		Myidae	<i>Sphenia luticola</i>	2
		Corbulidae	<i>Caryocorbula porcella</i>	2
		Spheniopsidae	<i>Grippina californica</i>	1
		Lyonsiidae		5

Appendix H.8 *continued*

Phylum	Class	Family	Taxon	n
			<i>Entodesma navicula</i>	2
			<i>Lyonsia californica</i>	6
		--	Thracioidea	4
		Periplomatidae	<i>Periploma</i> sp	1
		Cuspidariidae	<i>Cuspidaria parapodema</i>	11
	Scaphopoda			2
		Rhabdidae	<i>Rhabdus rectius</i>	6
		Gadilidae	<i>Cadulus californicus</i>	3
			<i>Gadila aberrans</i>	60
			<i>Polyschides quadrifissatus</i>	20
		--	<i>Compressidens stearnsii</i>	5
Sipuncula				8
	Sipunculidea	Golfingiidae	<i>Nephasoma diaphanes</i>	6
			<i>Thysanocardia nigra</i>	5
		Phascolionidae	<i>Phascolion</i> sp A	37
		Sipunculidae	<i>Siphonosoma ingens</i>	1
	Phascolosomatidea	Phascolosomatidae	<i>Apionsoma misakianum</i>	23
Annelida	Polychaeta	Amphinomidae	<i>Chloeia pinnata</i>	38
		Dorvilleidae	<i>Pettiboneia sanmatiensis</i>	1
			<i>Protodorvillea gracilis</i>	14
		Eunicidae	<i>Leodice americana</i>	4
			<i>Paucibranchia disjuncta</i>	6
		Lumbrineridae	<i>Eranno bicirrata</i>	3
			<i>Eranno lagunae</i>	2
			Lumbrineridae Group III	10
			<i>Lumbrinerides platypygos</i>	6
			<i>Lumbrineriopsis</i> sp SD1	1
			<i>Lumbrineris</i> sp	4
			<i>Lumbrineris cruzensis</i>	41
			<i>Lumbrineris index</i>	1
			<i>Lumbrineris japonica</i>	4
			<i>Lumbrineris latreilli</i>	39
			<i>Lumbrineris ligulata</i>	19
			<i>Lumbrineris limicola</i>	3
			<i>Lumbrineris</i> sp Group I	36
			<i>Scoletoma tetraura</i> Cmplx	32
		Oeonidae	<i>Drilonereis falcata</i>	6
			<i>Drilonereis</i> sp A	2
			<i>Drilonereis</i> sp	3
			<i>Notocirrus californiensis</i>	1
		Onuphidae		5
			<i>Diopatra ornata</i>	27
			<i>Diopatra tridentata</i>	35
			<i>Diopatra</i> sp	22
			<i>Mooreonuphis exigua</i>	7
			<i>Mooreonuphis nebulosa</i>	23
			<i>Mooreonuphis segmentispadix</i>	3
			<i>Mooreonuphis</i> sp SD1	3
			<i>Mooreonuphis</i> sp	2

Appendix H.8 *continued*

Phylum	Class	Family	Taxon	n
			<i>Nothria occidentalis</i>	5
			<i>Nothria</i> sp	4
			<i>Onuphis affinis</i>	1
			<i>Onuphis iridescens</i>	13
			<i>Onuphis</i> sp A	31
			<i>Onuphis</i> sp	2
			<i>Paradiopatra parva</i>	374
			<i>Rhamphobranchium longisetosum</i>	4
		Aphroditidae	<i>Aphrodita</i> sp	7
		Polynoidae		1
			<i>Hesperonoe laevis</i>	1
			<i>Lepidasthenia berkeleyae</i>	1
			<i>Lepidonotus spiculus</i>	1
			<i>Malmgreniella baschi</i>	1
			<i>Malmgreniella liei</i>	1
			<i>Malmgreniella macginitiei</i>	2
			<i>Malmgreniella sanpedroensis</i>	4
			<i>Malmgreniella scriptoria</i>	4
			<i>Malmgreniella</i> sp A	15
			<i>Malmgreniella</i> sp	1
			<i>Subadyte mexicana</i>	8
			<i>Tenonia priops</i>	14
		Sigalionidae	<i>Pholoe glabra</i>	43
			<i>Pholoides asperus</i>	31
			<i>Pisione</i> sp	4
			<i>Sigalion spinosus</i>	61
			<i>Sthenelais tertiaglabra</i>	12
			<i>Sthenelais verruculosa</i>	8
			<i>Sthenelanella uniformis</i>	91
		Glyceridae	<i>Glycera americana</i>	7
			<i>Glycera macrobranchia</i>	1
			<i>Glycera nana</i>	50
			<i>Glycera oxycephala</i>	2
			<i>Glycera tessellata</i>	2
			<i>Hemipodia borealis</i>	6
		Goniadidae	<i>Glycinde armigera</i>	113
			<i>Goniada brunnea</i>	3
			<i>Goniada littorea</i>	16
			<i>Goniada maculata</i>	40
		Hesionidae	<i>Gyptis brunnea</i>	2
			<i>Oxydromus pugettensis</i>	3
			<i>Podarkeopsis glabrus</i>	9
		Microphthalmidae	<i>Microphthalmus hystrix</i>	1
		Nereididae	<i>Ceratocephale hartmanae</i>	1
			<i>Ceratocephale loveni</i>	1
			<i>Nereis</i> sp A	19
			<i>Nicon moniloceras</i>	2
			<i>Platynereis bicanaliculata</i>	24
		Pilargidae	<i>Hermundura fauveli</i>	1

Appendix H.8 *continued*

Phylum	Class	Family	Taxon	n
			<i>Sigambra setosa</i>	3
		Syllidae	<i>Epigamia-Myrianida</i> Cmplx	1
			<i>Eusyllis</i> sp SD2	1
			<i>Eusyllis transecta</i>	6
			<i>Exogone dwisula</i>	4
			<i>Exogone lourei</i>	42
			<i>Odontosyllis phosphorea</i>	12
			<i>Paraehlersia articulata</i>	1
			<i>Parexogone acutipalpa</i>	9
			<i>Proceraea</i> sp	2
			<i>Salvatoria californiensis</i>	2
			<i>Sphaerosyllis californiensis</i>	4
			<i>Streptosyllis latipalpa</i>	1
			<i>Syllides mikeli</i>	1
			<i>Syllides</i> sp SD1	4
			<i>Syllis farallonensis</i>	1
			<i>Syllis heterochaeta</i>	69
			<i>Syllis hyperioni</i>	7
			<i>Syllis</i> sp SD2	1
		Nephtyidae	<i>Aglaophamus verrilli</i>	1
			<i>Bipalponephtys cornuta</i>	8
			<i>Nephtys caecoides</i>	21
			<i>Nephtys ferruginea</i>	9
			<i>Nephtys simoni</i>	7
			<i>Nephtys</i> sp	1
		Phyllodoceidae	<i>Eteone leptotes</i>	1
			<i>Eteone pigmentata</i>	11
			<i>Eulalia levicornuta</i> Cmplx	4
			<i>Eulalia</i> sp SD3	1
			<i>Eumida longicornuta</i>	10
			<i>Nereiphylla ferruginea</i> Cmplx	1
			<i>Nereiphylla</i> sp SD1	2
			<i>Phyllodoce hartmanae</i>	61
			<i>Phyllodoce longipes</i>	30
			<i>Phyllodoce pettiboneae</i>	10
			<i>Sige</i> sp A	13
		Fabriciidae	<i>Pseudofabriciola californica</i>	22
		Oweniidae	<i>Galathowenia pygidialis</i>	5
			<i>Myriochele gracilis</i>	19
			<i>Myriochele striolata</i>	5
			<i>Myriowenia californiensis</i>	1
			<i>Owenia collaris</i>	6
		Sabellariidae	<i>Neosabellaria cementarium</i>	1
		Sabellidae		1
			<i>Acromegalomma pigmentum</i>	10
			<i>Acromegalomma splendidum</i>	1
			<i>Chone</i> sp SD3	3
			<i>Dialychone albocincta</i>	11
			<i>Dialychone trilineata</i>	19

Appendix H.8 *continued*

Phylum	Class	Family	Taxon	n
			<i>Dialychone veleronis</i>	12
			<i>Euchone arenae</i>	1
			<i>Euchone hancocki</i>	2
			<i>Euchone incolor</i>	29
			<i>Euchone</i> sp A	3
			<i>Jasmineira</i> sp B	27
			<i>Myxicola</i> sp	2
			<i>Paradialychone bimaculata</i>	4
			<i>Paradialychone ecaudata</i>	3
			<i>Paradialychone harrisae</i>	12
			<i>Paradialychone paramollis</i>	4
			<i>Potamethus</i> sp A	5
		Serpulidae		2
		Longosomatidae	<i>Heterospio catalinensis</i>	1
		Magelonidae	<i>Magelona berkeleyi</i>	5
			<i>Magelona hartmanae</i>	1
			<i>Magelona pitelkai</i>	1
			<i>Magelona</i> sp A	2
			<i>Magelona</i> sp B	3
		Poecilochaetidae	<i>Poecilochaetus johnsoni</i>	3
			<i>Poecilochaetus</i> sp	1
		Spionidae		1
			<i>Dipolydora socialis</i>	11
			<i>Dipolydora</i> sp	4
			<i>Dispio</i> sp SD1	2
			<i>Dispio</i> sp SD2	1
			<i>Laonice cirrata</i>	24
			<i>Laonice nuchala</i>	42
			<i>Microspio pigmentata</i>	14
			<i>Microspio</i> sp	3
			<i>Paraprionospio alata</i>	191
			<i>Polydora cirrosa</i>	46
			<i>Polydora cornuta</i>	1
			<i>Polydora narica</i>	2
			<i>Prionospio</i> cf <i>lobulata</i>	1
			<i>Prionospio dubia</i>	198
			<i>Prionospio ehlersi</i>	13
			<i>Prionospio jubata</i>	260
			<i>Prionospio lighti</i>	8
			<i>Prionospio pygmaeus</i>	245
			<i>Scolelepis (Scolelepis) bullibranchia</i>	1
			<i>Scolelepis (Scolelepis) squamata</i>	1
			<i>Spio filicornis</i>	2
			<i>Spiophanes berkeleyorum</i>	61
			<i>Spiophanes duplex</i>	700
			<i>Spiophanes kimballi</i>	369
			<i>Spiophanes norrisi</i>	268
			<i>Spiophanes wigleyi</i>	3
		Cirratulidae	<i>Aphelochaeta glandaria</i> Cmplx	49

Appendix H.8 *continued*

Phylum	Class	Family	Taxon	n
			<i>Aphelochaeta monilaris</i>	30
			<i>Aphelochaeta petersenae</i>	5
			<i>Aphelochaeta phillipsi</i>	30
			<i>Aphelochaeta</i> sp B	1
			<i>Aphelochaeta</i> sp D	26
			<i>Aphelochaeta</i> sp E	2
			<i>Aphelochaeta</i> sp	1
			<i>Aphelochaeta tigrina</i>	13
			<i>Aphelochaeta williamsae</i>	17
			<i>Chaetozone armata</i>	1
			<i>Chaetozone columbiana</i>	1
			<i>Chaetozone commonalis</i>	2
			<i>Chaetozone corona</i>	1
			<i>Chaetozone hartmanae</i>	16
			<i>Chaetozone lunula</i>	1
			<i>Chaetozone setosa</i> Cmplx	1
			<i>Chaetozone</i> sp A	2
			<i>Chaetozone</i> sp SD2	2
			<i>Chaetozone</i> sp SD5	10
			<i>Chaetozone</i> sp SD7	1
			<i>Chaetozone</i> sp	1
			<i>Kirkegaardia cryptica</i>	46
			<i>Kirkegaardia serratiseta</i>	2
			<i>Kirkegaardia sibilina</i>	90
			<i>Kirkegaardia</i> sp SD9	10
			<i>Kirkegaardia tessellata</i>	18
		Fauveliopsidae	<i>Fauveliopsis armata</i>	1
			<i>Fauveliopsis glabra</i>	2
			<i>Fauveliopsis magna</i>	8
			<i>Fauveliopsis</i> sp SD1	6
		Flabelligeridae	<i>Bradabyssa pilosa</i>	3
			<i>Bradabyssa pluribranchiata</i>	3
			<i>Pherusa neopapillata</i>	8
			<i>Trophoniella</i> sp	1
		Sternaspidae	<i>Sternaspis affinis</i>	45
		Ampharetidae		17
			<i>Amage anops</i>	4
			<i>Amage scutata</i>	7
			<i>Ampharete</i> sp	1
			<i>Ampharete finmarchica</i>	13
			<i>Ampharete labrops</i>	53
			<i>Ampharete manriquei</i>	50
			Ampharetidae sp SD1	1
			<i>Amphicteis mucronata</i>	3
			<i>Amphicteis scaphobranchiata</i>	11
			<i>Amphisamytha bioculata</i>	8
			<i>Anobothrus gracilis</i>	17
			<i>Eclysippe trilobata</i>	112
			<i>Lysippe</i> sp A	28

Appendix H.8 *continued*

Phylum	Class	Family	Taxon	n
			<i>Lysippe</i> sp B	27
			<i>Melinna heterodonta</i>	8
			<i>Melinna oculata</i>	19
			<i>Phyllocomus hiltoni</i>	2
			<i>Phyllocomus</i> sp A	1
			<i>Samytha californiensis</i>	5
			<i>Sosane occidentalis</i>	12
		Pectinariidae	<i>Pectinaria californiensis</i>	25
		Terebellidae		1
			<i>Amaeana occidentalis</i>	10
			<i>Artacama coniferi</i>	1
			<i>Lanassa venusta venusta</i>	13
			<i>Phisidia sanctaemariae</i>	26
			<i>Pista brevibranchiata</i>	1
			<i>Pista estevanica</i>	29
			<i>Pista moorei</i>	1
			<i>Pista pacifica</i>	5
			<i>Pista wui</i>	12
			<i>Pista</i> sp	4
			<i>Polycirrus californicus</i>	4
			<i>Polycirrus</i> sp A	31
			<i>Polycirrus</i> sp OC1	9
			<i>Polycirrus</i> sp SD1	5
			<i>Polycirrus</i> sp	19
			<i>Proclea</i> sp A	15
			<i>Streblosoma crassibranchia</i>	22
			<i>Streblosoma</i> sp B	2
			<i>Streblosoma</i> sp C	6
			<i>Streblosoma</i> sp	2
		Trichobranchidae	<i>Terebellides</i> sp	1
			<i>Terebellides californica</i>	15
			<i>Terebellides</i> sp Type D	1
			<i>Trichobranchus hancocki</i>	4
		Chaetopteridae	<i>Phyllochaetopterus limicolus</i>	386
			<i>Spiochaetopterus costarum</i> Cmplx	79
		Capitellidae	<i>Capitella teleta</i>	14
			<i>Decamastus gracilis</i>	10
			<i>Mediomastus acutus</i>	3
			<i>Mediomastus</i> sp	268
			<i>Notomastus hemipodus</i>	15
			<i>Notomastus latericeus</i>	2
		Cossuridae	<i>Cossura candida</i>	17
			<i>Cossura</i> sp A	5
		Maldanidae		58
			<i>Clymenella complanata</i>	2
			<i>Clymenella</i> sp A	1
			<i>Clymenura gracilis</i>	26
			Euclymeninae	2
			Euclymeninae sp A	186

Appendix H.8 *continued*

Phylum	Class	Family	Taxon	n	
			<i>Isocirrus longiceps</i>	1	
			<i>Maldane sarsi</i>	74	
			<i>Metasychis disparidentatus</i>	14	
			<i>Petaloclymene pacifica</i>	91	
			<i>Praxillella pacifica</i>	67	
			<i>Praxillura maculata</i>	6	
			<i>Rhodine bitorquata</i>	37	
		Opheliidae	<i>Armandia brevis</i>	8	
			<i>Ophelina pallida</i>	1	
			<i>Ophelina</i> sp SD1	1	
		Orbiniidae	<i>Leitoscoloplos pugettensis</i>	8	
			<i>Leitoscoloplos</i> sp A	1	
			<i>Scoloplos armiger</i> Cmplx	116	
			<i>Scoloplos</i> sp	1	
		Paraonidae	<i>Aricidea (Acmira) catherinae</i>	44	
			<i>Aricidea (Acmira) cerrutii</i>	1	
			<i>Aricidea (Acmira) horikoshii</i>	1	
			<i>Aricidea (Acmira) lopezi</i>	4	
			<i>Aricidea (Acmira) simplex</i>	10	
			<i>Aricidea (Aedicira) pacifica</i>	1	
			<i>Aricidea (Aricidea) wassi</i>	1	
			<i>Aricidea (Strelzovia) antennata</i>	12	
			<i>Aricidea (Strelzovia) hartleyi</i>	12	
			<i>Aricidea (Strelzovia)</i> sp A	7	
			<i>Aricidea (Strelzovia)</i> sp SD1	1	
			<i>Cirrophorus branchiatus</i>	2	
			<i>Cirrophorus furcatus</i>	3	
			<i>Levinsenia gracilis</i>	24	
			<i>Levinsenia kirbyae</i>	6	
			<i>Levinsenia oculata</i>	1	
			<i>Paradoneis lyra</i>	1	
			<i>Paradoneis</i> sp SD1	93	
		Scalibregmatidae	<i>Scalibregma californicum</i>	32	
		Travisiidae	<i>Travisia brevis</i>	85	
			<i>Travisia pupa</i>	1	
			Oligochaeta	2	
Arthropoda	Clitellata				
	Pycnogonida	Ammotheidae		1	
		Phoxichilidiidae	<i>Anoplodactylus erectus</i>	6	
			<i>Bathyleberis</i> cf <i>garthi</i>	1	
			<i>Leuroleberis sharpei</i>	3	
			<i>Xenoleberis californica</i>	6	
			<i>Euphilomedes carcharodonta</i>	14	
			<i>Euphilomedes producta</i>	33	
			<i>Scleroconcha trituberculata</i>	2	
			Sarsiellidae	<i>Eusarsiella thominx</i>	2
			Rutidermatidae	<i>Rutiderma lomae</i>	2
		Malacostraca	Nebaliidae	<i>Nebalia pugettensis</i> Cmplx	1
			Mysidae	<i>Neomysis kadiakensis</i>	4
			<i>Pacifacanthomysis nephrophthalma</i>	2	

Appendix H.8 *continued*

Phylum	Class	Family	Taxon	n
		Caprellidae	<i>Caprella mendax</i>	8
			<i>Mayerella banksia</i>	8
		Ischyroceridae	<i>Erichthonius brasiliensis</i>	1
			<i>Notopoma</i> sp A	6
		Kamakidae	<i>Amphideutopus oculatus</i>	10
		Photidae	<i>Ampelisciphotis podophthalma</i>	19
			<i>Gammaropsis thompsoni</i>	4
			<i>Photis brevipes</i>	23
			<i>Photis californica</i>	29
			<i>Photis lacia</i>	5
			<i>Photis parvidons</i>	1
			<i>Photis</i> sp OC1	21
			<i>Photis</i> sp	35
		Aoridae		1
			<i>Aoroides inermis</i>	1
			<i>Aoroides intermedia</i>	1
			<i>Aoroides</i> sp A	20
			<i>Aoroides</i> sp	2
		Unciolidae	<i>Rudilemboides</i> sp A	1
			<i>Rudilemboides stenopropodus</i>	4
		Corophiidae	<i>Laticorophium baconi</i>	1
			<i>Protomedeia articulata</i> Cmplx	8
		Maeridae	<i>Maera jerrica</i>	7
		Hornelliidae	<i>Hornellia occidentalis</i>	1
		Megaluropidae	<i>Gibberosus myersi</i>	4
			<i>Megaluropidae</i> sp A	2
		Oedicerotidae	<i>Americhelidium shoemakeri</i>	11
			<i>Americhelidium</i> sp SD4	1
			<i>Bathymedon pumilus</i>	29
			<i>Deflexilodes similis</i>	9
			<i>Hartmanodes hartmanae</i>	8
			<i>Hartmanodes</i> sp SD1	3
			<i>Monoculodes emarginatus</i>	12
			<i>Monoculodes perditus</i>	1
			<i>Westwoodilla tone</i>	12
		Eusiridae	<i>Rhachotropis</i> sp A	1
		Liljeborgiidae	<i>Listriella eriopisa</i>	2
			<i>Listriella goleta</i>	3
			<i>Listriella melanica</i>	1
			<i>Listriella</i> sp	1
		Pleustidae	<i>Pleusymtes subglaber</i>	1
		Pardaliscidae	<i>Halicoides synopiae</i>	20
			<i>Nicippe tumida</i>	4
		Ampeliscidae	<i>Ampelisca agassizi</i>	6
			<i>Ampelisca brachycladus</i>	10
			<i>Ampelisca brevisimulata</i>	52
			<i>Ampelisca careyi</i>	56
			<i>Ampelisca</i> cf <i>brevisimulata</i>	1
			<i>Ampelisca cristata cristata</i>	12

Appendix H.8 *continued*

Phylum	Class	Family	Taxon	n
			<i>Ampelisca cristata microdentata</i>	26
			<i>Ampelisca hancocki</i>	8
			<i>Ampelisca indentata</i>	4
			<i>Ampelisca milleri</i>	1
			<i>Ampelisca pacifica</i>	27
			<i>Ampelisca pugetica</i>	33
			<i>Ampelisca romigi</i>	5
			<i>Ampelisca unsocalae</i>	7
			<i>Ampelisca</i> sp	12
			<i>Byblis millsii</i>	7
		Synopiidae	<i>Bruzelia tuberculata</i>	3
			<i>Garosyrrhoë bigarra</i>	1
			<i>Metatiron tropakis</i>	6
			<i>Tiron biocellata</i>	4
		Argissidae	<i>Argissa hamatipes</i>	1
		Urothoidae	<i>Urothoe elegans</i> Cmplx	1
		Phoxocephalidae	<i>Eyakia robusta</i>	3
			<i>Foxiphalus obtusidens</i>	17
			<i>Heterophoxus ellisi</i>	7
			<i>Heterophoxus oculatus</i>	12
			<i>Rhepoxynius bicuspidatus</i>	58
			<i>Rhepoxynius heterocuspoidatus</i>	12
			<i>Rhepoxynius menziesi</i>	47
			<i>Rhepoxynius stenodes</i>	23
			<i>Rhepoxynius variatus</i>	4
		Lysianassidae	<i>Aruga holmesii</i>	2
			<i>Aruga oculata</i>	6
		Opisidae	<i>Opisa tridentata</i>	1
		Uristidae	<i>Anonyx lilljeborgii</i>	9
		Tryphosidae	<i>Hippomedon</i> sp A	8
			<i>Hippomedon zetesimus</i>	5
			<i>Lepidepcreum serraculum</i>	1
		Acidostomatidae	<i>Acidostoma hancocki</i>	4
		Pakynidae	<i>Prachynella lodo</i>	2
		Gnathiidae	<i>Caecognathia crenulatifrons</i>	47
		Anthuridae	<i>Haliophasma geminata</i>	12
		Arcturidae	<i>Neastacilla californica</i>	3
		Idoteidae	<i>Edotia</i> sp B	3
			<i>Edotia sublittoralis</i>	3
		Ancinidae	<i>Ancinus granulatus</i>	4
		Sphaeromatidae	<i>Dynamenella</i> sp	2
		Serolidae	<i>Heteroserolis carinata</i>	1
		Joeropsididae	<i>Joeropsis dubia</i>	2
		Munnopsidae	<i>Ilyarachna acarina</i>	2
		Akanthophoreidae	<i>Akanthophoreus phillipsi</i>	1
			<i>Chaulioleona dentata</i>	5
		Anarthruridae	Anarthruridae sp 3	1
			<i>Siphonolabrum californiense</i>	1
		Leptocheliidae	<i>Chondrochelia dubia</i> Cmplx	70

Appendix H.8 *continued*

Phylum	Class	Family	Taxon	n
		Tanaellidae	<i>Araphura breviarua</i>	11
			<i>Araphura cuspirostris</i>	1
			<i>Tanaella propinquus</i>	5
		Typhlotanaiidae	<i>Typhlotanais crassus</i>	1
			<i>Typhlotanais williamsae</i>	1
		Tanaopsidae	<i>Tanaopsis cadieni</i>	22
		Leuconidae	<i>Eudorella pacifica</i>	2
			<i>Leucon declivis</i>	1
		Nannastacidae	<i>Campylaspis canaliculata</i>	1
			<i>Procampylaspis caenosa</i>	2
		Lampropidae	<i>Hemilamprops californicus</i>	24
			<i>Mesolamprops bispinosus</i>	19
		Diastylidae	<i>Anchicolurus occidentalis</i>	5
			<i>Diastylis californica</i>	6
			<i>Diastylis crenellata</i>	2
			<i>Diastylis pellucida</i>	2
			<i>Diastylis sentosa</i>	1
			<i>Diastylopsis tenuis</i>	1
			<i>Leptostylis abditis</i>	1
			<i>Oxyurostylis pacifica</i>	5
		Callianassidae	<i>Neotrypaea</i> sp	1
		Axiidae	<i>Calocarides</i> sp	1
		Inachoididae	<i>Pyromaia tuberculata</i>	1
		Cancridae	<i>Metacarcinus gracilis</i>	1
			<i>Romaleon jordani</i>	1
		Pinnotheridae	<i>Pinnixa occidentalis</i> Cmplx	5
			<i>Pinnixa</i> sp	1
Nematoda				78
Echinodermata	Asteroidea			49
		Luidiidae	<i>Luidia asthenosoma</i>	1
		Astropectinidae	<i>Astropecten californicus</i>	9
			<i>Astropecten</i> sp	8
	Ophiuroidea			16
		Ophiuridae	<i>Ophiura luetkenii</i>	18
		Ophioscolecidae	<i>Ophiuroconis bispinosa</i>	18
		Amphiuridae		135
			<i>Amphichondrius granulatus</i>	13
			<i>Amphiodia digitata</i>	45
			<i>Amphiodia urtica</i>	348
			<i>Amphiodia</i> sp	112
			<i>Amphioplus strongyloplax</i>	2
			<i>Amphioplus</i> sp	4
			<i>Amphipholis pugetana</i>	1
			<i>Amphipholis squamata</i>	22
			<i>Amphiura arcystata</i>	4
			<i>Dougaloplus amphacanthus</i>	13
			<i>Dougaloplus</i> sp	2
	Echinoidea			5
		Toxopneustidae	<i>Lytechinus pictus</i>	6

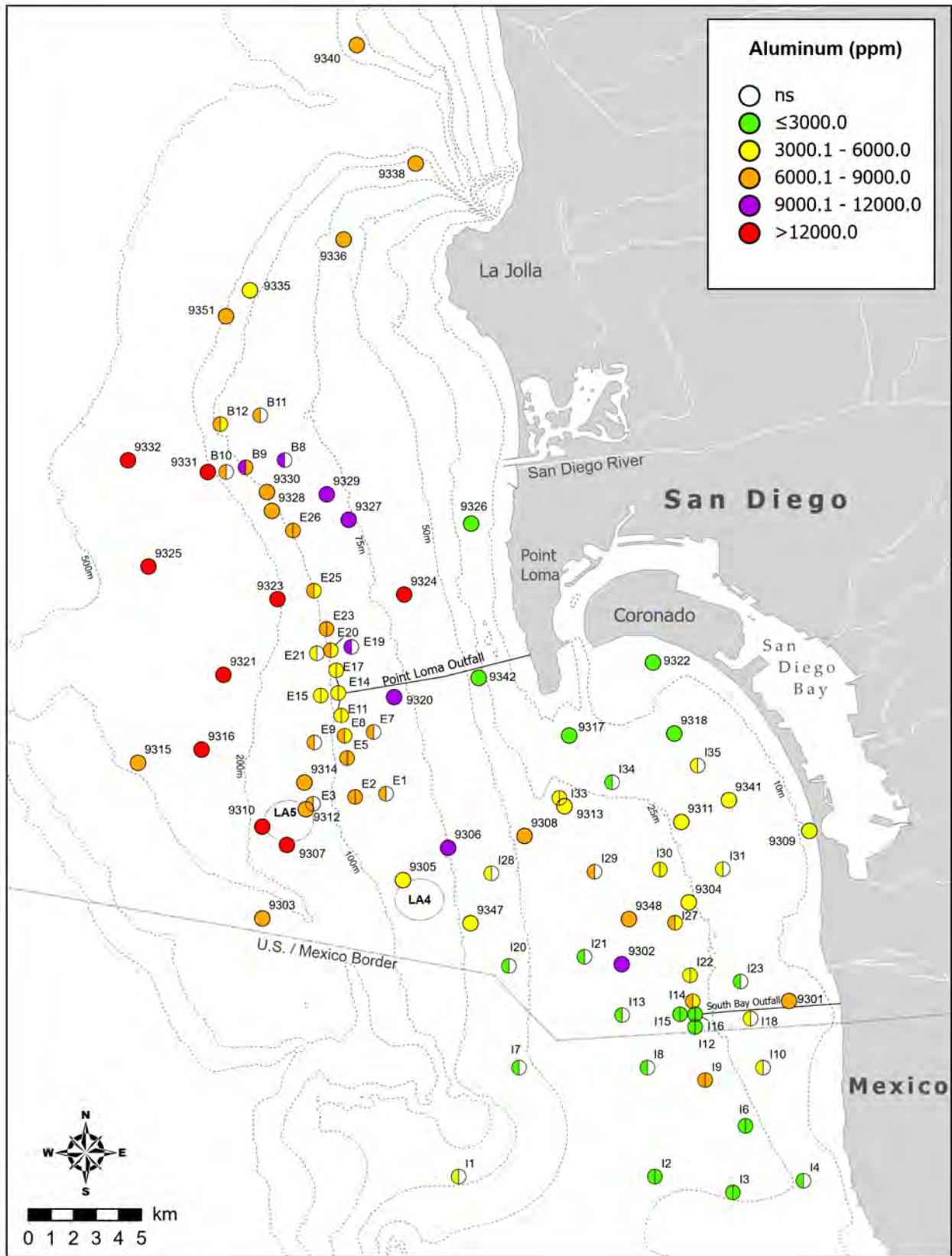
Appendix H.8 *continued*

Phylum	Class	Family	Taxon	n
Phoronida	Holothuroidea	Strongylocentrotidae	<i>Strongylocentrotus fragilis</i>	2
		Dendrasteridae	<i>Dendraster excentricus</i>	16
			<i>Dendraster terminalis</i>	15
		Schizasteridae	<i>Brisaster</i> sp	2
		Brissidae	<i>Brissopsis pacifica</i>	12
		Spatangidae	<i>Spatangus californicus</i>	1
			Dendrochirotida	1
		Synaptidae	<i>Leptosynapta</i> sp	17
		Chiridotidae	<i>Chiridota</i> sp	19
		Phoronidae		16
			<i>Phoronis</i> sp SD1	7
			<i>Phoronis</i> sp	14
			<i>Phoronopsis</i> sp	2
Brachiopoda	Lingulata	Lingulidae	<i>Glottidia albida</i>	29
Chordata	Enteropneusta			4
		Ptychoderidae	<i>Balanoglossus</i> sp	1
		Spengeliidae	<i>Schizocardium</i> sp	1
		Harrimaniidae	<i>Saccoglossus</i> sp	2
			<i>Stereobalanus</i> sp	25
	Asciacea	Agneziidae	<i>Agnezia septentrionalis</i>	1
		Styelidae	<i>Cnemidocarpa rhizopus</i>	10
		Molgulidae		1
			<i>Molgula pugetiensis</i>	1
	Leptocardii	Branchiostomatidae	<i>Branchiostoma californiense</i>	1

Appendix H.9

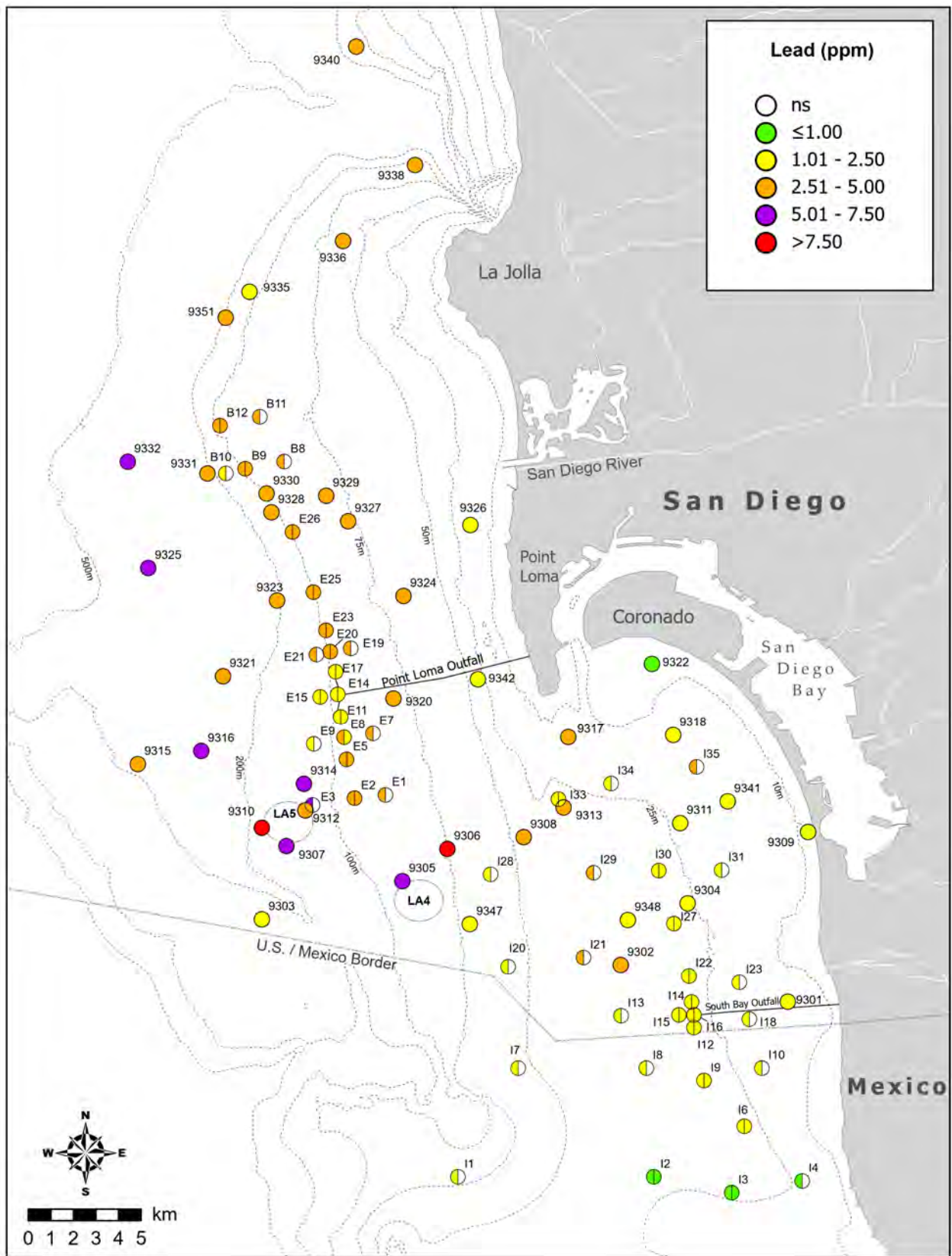
Results of Spearman Rank correlation analyses of various sediment parameters from San Diego regional and core benthic stations sampled during summer 2022 and 2023. Data include the correlation coefficient (r_s) for all parameters with detection rates $\geq 50\%$ (see Table 7.1). Correlation coefficients $r_s \geq 0.70$ are highlighted.

	Depth	Fines	Sul	TN	TOC	TVS	Al	Sb	As	Ba	Be	Cr	Cu	Fe	Pb	Mn	Hg	Ni	Sn	Zn
Fines	0.71																			
Sul	0.35	0.35																		
TN	0.86	0.69	0.37																	
TOC	0.60	0.41	0.23	0.69																
TVS	0.78	0.65	0.32	0.82	0.69															
Al	0.72	0.82	0.25	0.81	0.50	0.77														
Sb	0.57	0.59	0.11	0.65	0.52	0.59	0.75													
As	0.28	0.16	-0.04	0.23	0.34	0.22	0.19	0.31												
Ba	0.71	0.74	0.25	0.78	0.42	0.72	0.95	0.70	0.12											
Be	0.77	0.79	0.25	0.80	0.65	0.79	0.89	0.78	0.40	0.82										
Cr	0.82	0.76	0.25	0.85	0.68	0.81	0.90	0.78	0.42	0.84	0.97									
Cu	0.66	0.70	0.18	0.67	0.54	0.63	0.78	0.63	0.22	0.78	0.70	0.72								
Fe	0.69	0.75	0.22	0.73	0.42	0.75	0.84	0.75	0.48	0.76	0.96	0.95	0.72							
Pb	0.61	0.73	0.22	0.63	0.42	0.60	0.78	0.63	0.41	0.74	0.75	0.76	0.80	0.76						
Mn	0.58	0.78	0.23	0.69	0.36	0.66	0.94	0.70	0.12	0.93	0.80	0.79	0.77	0.77	0.75					
Hg	0.69	0.73	0.25	0.68	0.41	0.67	0.81	0.55	0.22	0.77	0.73	0.74	0.84	0.70	0.89	0.76				
Ni	0.86	0.80	0.33	0.91	0.58	0.84	0.94	0.66	0.22	0.90	0.87	0.91	0.76	0.80	0.75	0.84	0.81			
Sn	0.66	0.81	0.29	0.73	0.45	0.70	0.92	0.67	0.23	0.86	0.82	0.83	0.77	0.80	0.88	0.89	0.88	0.88		
Zn	0.76	0.83	0.33	0.82	0.61	0.79	0.94	0.73	0.29	0.90	0.92	0.93	0.83	0.92	0.86	0.89	0.84	0.91	0.91	
tDDT	0.26	0.35	0.11	0.33	0.26	0.38	0.44	0.43	0.12	0.42	0.37	0.37	0.40	0.33	0.55	0.37	0.43	0.41	0.42	0.44

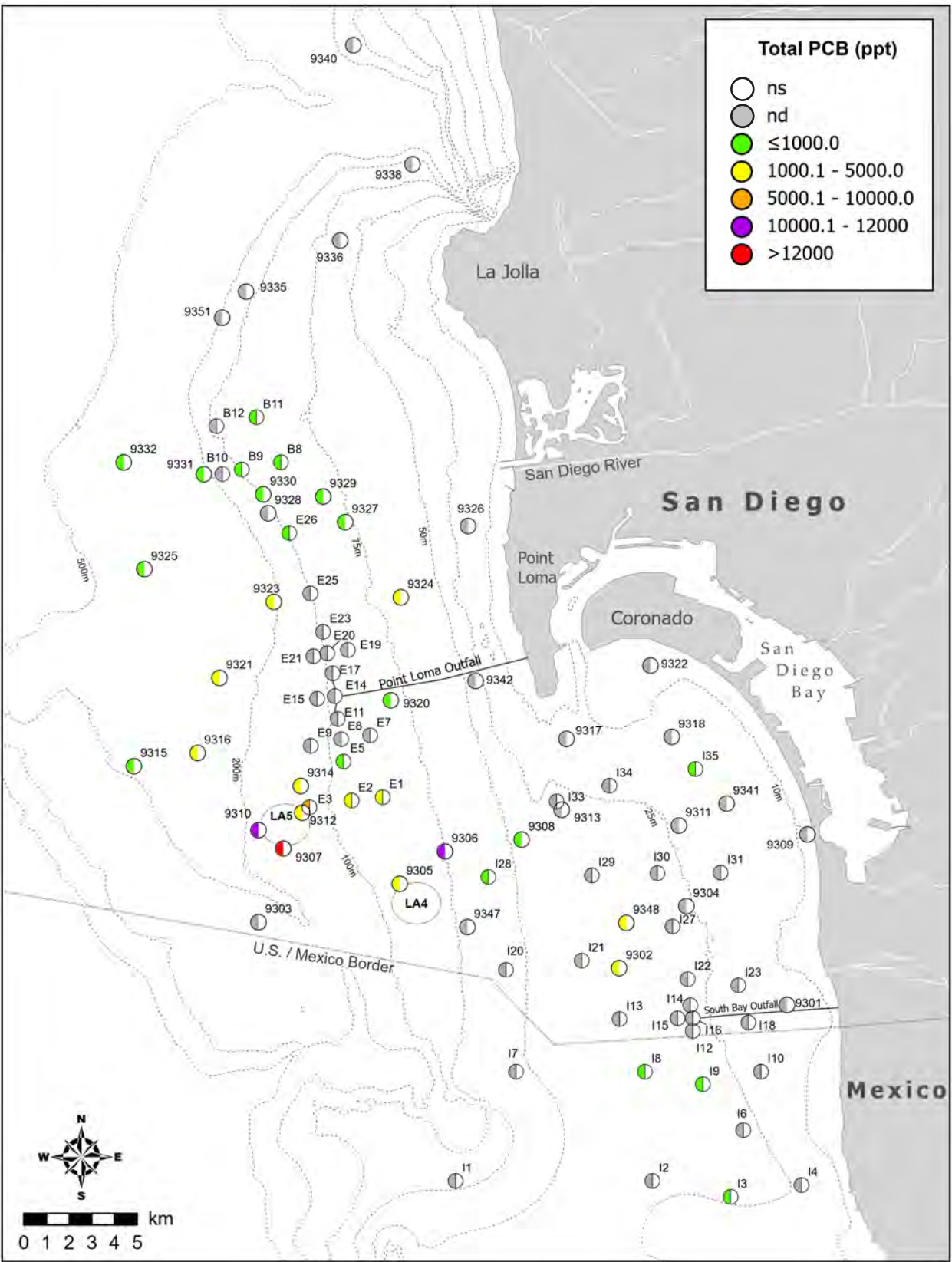


Appendix H.10

Distribution of select metals (ppm) and Total PCBs (ppt) in sediments from San Diego regional and core benthic stations sampled during summer 2022 and 2023; ns = not sampled (or not reportable, see text); nd = not detected.



Appendix H.10 *continued*

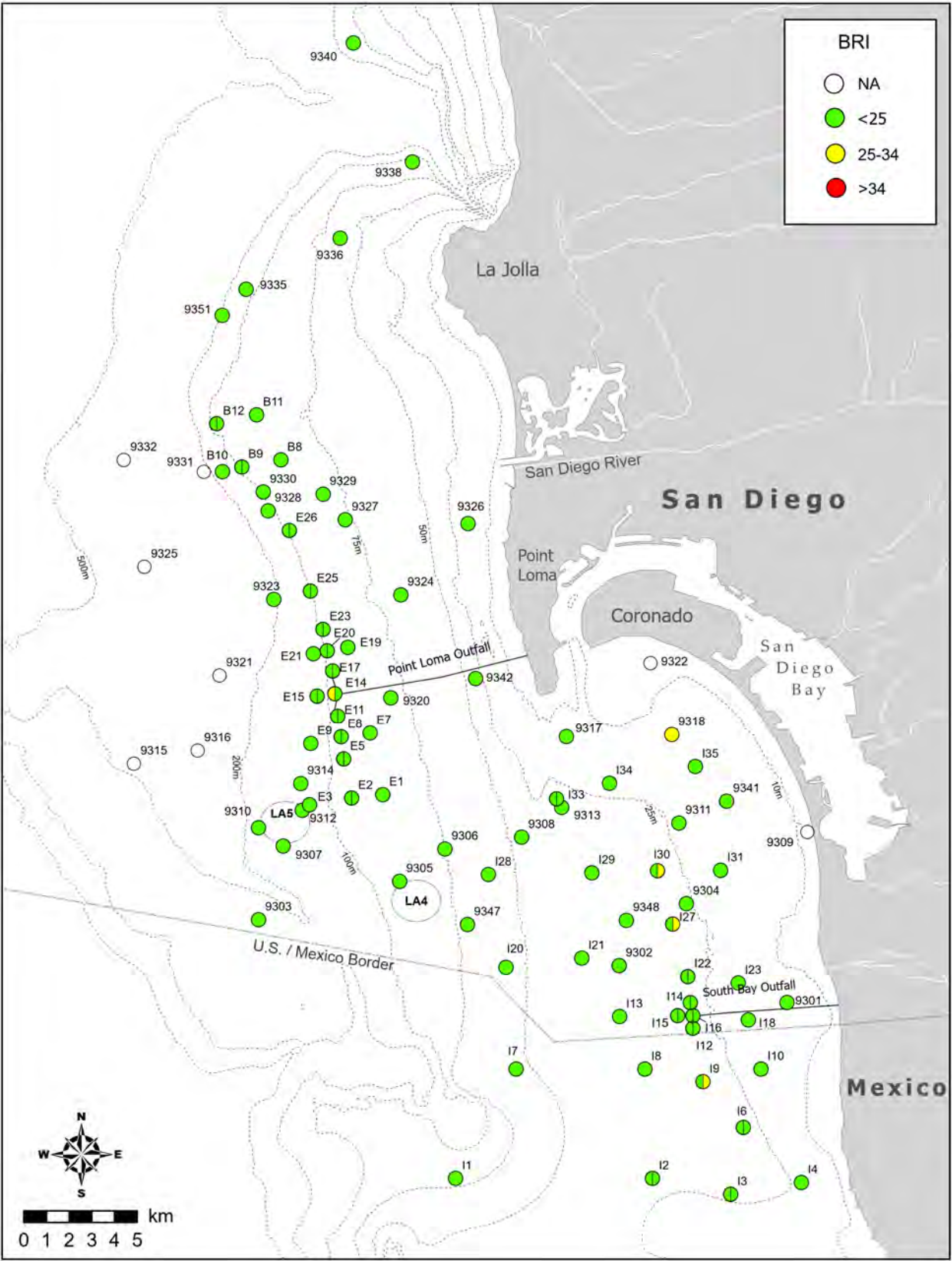


Appendix H.10 *continued*

Appendix H.11

Bioassay results (10-day amphipod survival tests) for sediment toxicity testing conducted for San Diego regional benthic stations sampled during summer 2022. Percent fines = percentage of silt + clay combined. Test results (% Survival) are expressed as mean percent survival \pm 1 standard deviation.

	Site/Sample	Depth Stratum	Station Depth (m)	Percent Fines	Sample Date	Test Initiation	% Survival (Mean \pm SD)
Summer 2022	Lab Control	—	—	—	—	26 Jul 2022	98 \pm 2.7
	9301	Inner Shelf	16	33.8	19 Jul 2022	26 Jul 2022	95 \pm 5.0
	9302	Mid Shelf	36	52.9	19 Jul 2022	26 Jul 2022	97 \pm 4.5
	9305	Mid Shelf	87	66.5	19 Jul 2022	26 Jul 2022	98 \pm 4.5
	9312	Outer Shelf	137	61.1	19 Jul 2022	26 Jul 2022	99 \pm 2.2
	9317	Inner Shelf	19	3.4	18 Jul 2022	26 Jul 2022	96 \pm 5.5
	9320	Mid Shelf	81	63.6	18 Jul 2022	26 Jul 2022	97 \pm 2.7
	9327	Mid Shelf	78	70.6	18 Jul 2022	26 Jul 2022	96 \pm 4.2
	9340	Outer Shelf	133	61.8	18 Jul 2022	26 Jul 2022	96 \pm 4.2



Appendix H.12

Distribution of BRI values from San Diego regional and core benthic stations sampled during summer 2022 (left side of circle, where applicable) and 2023 (right side of circle, where applicable); NA= not applicable.

Appendix H.13

Particle size summary for each macrofauna cluster group A–G (defined in Figure 7.5). Data are presented as means (ranges) calculated over all grabs within a cluster group. VF = very fine; F = fine; M = medium; C = coarse; VC = very coarse.

Cluster		Particle Size (%)						
Group	n	Fines	VFSand	FSand	MSand	CSand	VCSand	Granules
A	2	33.9 (9.1-58.8)	15.7 (13.3-18.0)	32.4 (13.4-51.3)	16.5 (13.0-19.9)	1.6 (1.5-1.7)	0 —	0 —
B	2	23.4 (13.0-33.8)	29.0 (17.5-40.4)	33.5 (13.8-53.1)	8.9 (2.5-15.3)	2.4 (1.1-3.8)	2.6 (0-5.3)	0.4 (0.4-0.4)
C	23	11.1 (0-85.9)	4.0 (0-19.9)	11.0 (0.8-33.0)	35.5 (6.2-55.5)	32.4 (8.6-71.0)	8.2 (0-26.8)	2.4 (0-12.4)
D	1	85.2	10.0	4.4	0.2	0	0	0
E	82	47.5 (10.5-92.3)	34.9 (11.5-65.5)	13.0 (3.2-36.6)	2.0 (0.1-37.2)	2.1 (0-57.6)	1.3 (0-34.1)	0.7 (0-10.8)
F	2	85.2 (84.1-86.4)	11.9 (11.8-11.9)	2.8 (2.5-3.2)	0.1 (0.1-0.1)	0 —	0 —	0 —
G	2	77.2 (74.9-79.5)	17.8 (17.5-18.1)	4.7 (3.9-5.4)	0.3 (0.1-0.5)	0 —	0 —	0 —

Appendix H.14

Mean abundance of the characteristic species found in each macrofauna cluster group A–G (defined in Figure 7.6). Highlighted values indicate the top most characteristic species according to SIMPER analysis.

Taxa	Cluster Group						
	A	B	C	D ^a	E	F	G
<i>Prionospio pygmaeus</i>	24	15	1	0	3	0	0
<i>Dendraster excentricus</i>	8	0	0	0	0	0	0
<i>Rhepoxynius menziesi</i>	8	0	2	0	2	0	0
<i>Carinoma mutabilis</i>	6	3	<1	0	<1	0	0
Lineidae	4	0	2	1	2	0	0
<i>Spiophanes norrisi</i>	2	6	104	0	11	0	0
<i>Spiophanes duplex</i>	1	45	2	0	19	0	0
<i>Pista wui</i>	0	0	19	1	<1	0	0
<i>Jasmineira</i> sp B	0	0	8	1	<1	0	0
Amphiuridae	0	0	3	6	4	0	<1
<i>Ampharete labrops</i>	0	7	2	0	1	0	0
<i>Mediomastus</i> spp	0	6	1	2	14	0	0
<i>Spiochaetopterus costarum</i> Cmplx	0	0	<1	1	<1	0	29
<i>Paradiopatra parva</i>	0	0	<1	0	10	0	0
<i>Amphiodia urtica</i>	0	0	<1	0	10	0	0
<i>Paraprionospio alata</i>	0	<1	<1	2	4	2	21
<i>Spiophanes kimballi</i>	0	0	<1	0	9	0	6
<i>Eclysippe trilobata</i>	0	0	<1	4	4	1	0
<i>Phyllochaetopterus limicolus</i>	0	0	0	0	4	0	32
<i>Maldane sarsi</i>	0	0	0	3	1	8	1
<i>Amphiodia digitata</i>	0	0	0	22	<1	0	0
<i>Polydora cirrosa</i>	0	23	0	0	<1	0	0
<i>Prionospio ehlersi</i>	0	0	0	0	<1	5	<1
<i>Goniada littorea</i>	0	8	0	0	0	0	0
<i>Ampelisca unsocalae</i>	0	0	0	6	0	0	<1
<i>Fauveliopsis magna</i>	0	0	0	5	0	2	0

^a SIMPER analyses not conducted on cluster groups that contain only one grab. For these groups, highlight indicates five most abundant taxa.

Appendix I

Demersal Fishes and Megabenthic Invertebrates

2022 – 2023 Supplemental Analyses

Appendix I.1

Taxonomic listing of demersal fish species collected at PLOO trawl stations during 2022 and 2023. Data are reported as total number of fish (n), biomass (BM, wet weight, kg), minimum, maximum, and mean length (standard length, cm unless otherwise noted). Taxonomic arrangement follows Eschmeyer and Herald (1998) and Page et al. (2013).

Taxonomic Classification	Common Name	n	Length (cm)			
			Bm	Min	Max	Mean
RAJIFORMES						
Rajidae	<i>Bathyraja interrupta</i>	2	0.2	20	23	22
	<i>Raja inornata</i>	6	3.6	19	54	37
	<i>Raja rhina</i>	1	1.2	—	—	55
CLUPEIFORMES						
Engraulidae	<i>Engraulis mordax</i>	9	0.1	6	13	10
ARGENTINIFORMES						
Argentinidae	<i>Argentina sialis</i>	13	0.7	6	12	8
AULOPIFORMES						
Synodontidae	<i>Synodus lucioceps</i>	9	0.6	14	25	21
GADIFORMES						
Merlucciidae	<i>Merluccius productus</i>	13	1.2	14	26	23
BATRACHOIDIFORMES						
Batrachoididae	<i>Porichthys notatus</i>	24	1.1	6	18	12
SCORPAENIFORMES						
Scorpaenidae	<i>Scorpaena guttata</i>	38	8.9	13	22	18
Sebastidae	<i>Sebastes auriculatus</i>	3	0.3	15	22	19
	<i>Sebastes elongatus</i>	14	0.6	5	10	7
	<i>Sebastes eos</i>	3	0.2	10	15	12
	<i>Sebastes goodei</i>	8	0.4	12	16	13
	<i>Sebastes levis</i>	1	0.1	—	—	9
	<i>Sebastes miniatus</i>	1	0.2	—	—	17
	<i>Sebastes rosenblatti</i>	4	0.4	5	10	8
	<i>Sebastes rubrivinctus</i>	3	0.2	7	9	8
	<i>Sebastes saxicola</i>	385	4.4	6	14	8
	<i>Sebastes semicinctus</i>	799	20.7	7	16	11
	<i>Sebastes sp</i>	38	1.1	3	11	6
Hexagrammidae	<i>Zaniolepis frenata</i>	338	4.7	7	18	11
	<i>Zaniolepis latipinnis</i>	362	5.6	6	16	12
Cottidae	<i>Chitonotus pugetensis</i>	27	0.5	5	11	8
	<i>Icelinus quadriseriatus</i>	210	1	3	8	6
	<i>Icelinus tenuis</i>	2	0.1	10	10	10
Agonidae	<i>Xeneretmus latifrons</i>	2	0.1	12	13	12

^a measured as total length (cm)

Appendix I.1 *continued*

Taxonomic Classification	Common Name	n	Length (cm)				
			Bm	Min	Max	Mean	
PERCIFORMES							
Sciaenidae	<i>Genyonemus lineatus</i>	White Croaker	1	0.1	—	—	17
Embiotocidae	<i>Cymatogaster aggregata</i>	Shiner Perch	2	0.1	10	11	10
	<i>Zalemnius rosaceus</i>	Pink Seaperch	408	5.3	3	14	9
Zoarcidae	<i>Lycodes pacificus</i>	Blackbelly Eelpout	11	0.5	13	23	18
Uranoscopidae	<i>Kathetostoma averruncus</i>	Smooth Stargazer	1	0.1	—	—	10
PLEURONECTIFORMES							
Paralichthyidae	<i>Citharichthys sordidus</i>	Pacific Sanddab	5533	82.1	4	26	9
	<i>Citharichthys xanthostigma</i>	Longfin Sanddab	701	23.9	5	21	12
	<i>Hippoglossina stomata</i>	Bigmouth Sole	94	6	10	24	16
	<i>Paralichthys californicus</i>	California Halibut	1	2.7	—	—	67
Pleuronectidae	<i>Glyptocephalus zachirus</i>	Rex Sole	8	0.4	11	16	14
	<i>Lyopsetta exilis</i>	Slender Sole	21	0.3	6	14	11
	<i>Microstomus pacificus</i>	Dover Sole	882	25.8	5	21	13
	<i>Parophrys vetulus</i>	English Sole	209	16.1	11	25	17
	<i>Pleuronichthys verticalis</i>	Hornyhead Turbot	36	2	9	20	14
Cynoglossidae	<i>Symphurus atricaudus</i>	California Tonguefish	86	1.7	9	17	14
	<i>Parophrys vetulus</i>	English Sole	306	18.6	8	23	15
	<i>Pleuronichthys decurrens</i>	Curlfin Sole	3	0.2	11	16	14
	<i>Pleuronichthys verticalis</i>	Hornyhead Turbot	79	3.1	10	19	13
Cynoglossidae	<i>Symphurus atricaudus</i>	California Tonguefish	68	2	9	16	13

Appendix I.2

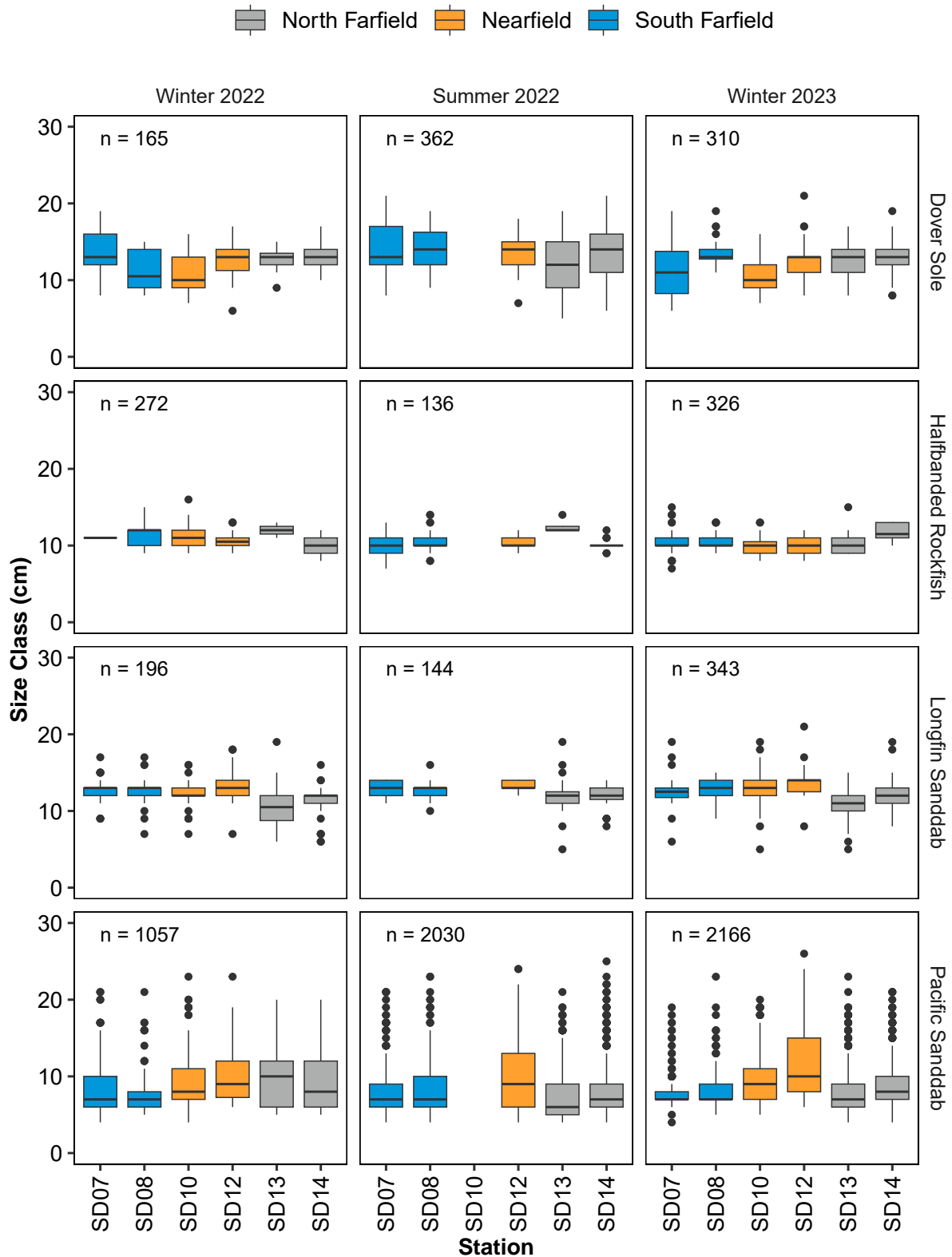
Taxonomic listing of demersal fish species collected at SBOO trawl stations during 2022 and 2023. Data are reported as total number of fish (n), biomass (BM, wet weight, kg), minimum, maximum, and mean length (standard length, cm unless otherwise noted). Taxonomic arrangement follows Eschmeyer and Herald (1998) and Page et al. (2013).

Taxonomic Classification		Common Name	n	Bm	Length (cm)		
					Min	Max	Mean
RAJIFORMES							
Rhinobatidae	<i>Rhinobatos productus</i>	Shovelnose Guitarfish ^a	4	1.7	32	55	42
Rajidae	<i>Raja inornata</i>	California Skate ^a	4	2.2	32	49	40
	<i>Raja rhina</i>	Longnose Skate ^a	2	1.9	36	37	36
MYLIOBATIFORMES							
Urolophidae	<i>Urobatis halleri</i>	Round Stingray	4	1.7	28	39	31
CLUPEIFORMES							
Engraulidae	<i>Engraulis mordax</i>	Northern Anchovy	231	1.7	8	12	10
Clupeidae	<i>Sardinops sagax</i>	Pacific Sardine	5	0.1	9	11	10
AULOPIIFORMES							
Synodontidae	<i>Synodus lucioceps</i>	California Lizardfish	255	4.8	4	26	13
OPHIDIIFORMES							
Ophidiidae	<i>Chilara taylori</i>	Spotted Cusk-eel	1	0.1	—	—	12
BATRACHOIDIFORMES							
Batrachoididae	<i>Porichthys myriaster</i>	Specklefin Midshipman	26	1.3	7	36	12
	<i>Porichthys notatus</i>	Plainfin Midshipman	6	0.6	4	7	6
GASTEROSTEIFORMES							
Syngnathidae	<i>Syngnathus californiensis</i>	Kelp Pipefish	5	0.3	16	23	19
	<i>Syngnathus exilis</i>	Barcheek Pipefish	18	0.6	13	23	19
	<i>Syngnathus</i> sp	Pipefish Unidentified	16	0.5	14	21	17
SCORPAENIFORMES							
Scorpaenidae	<i>Scorpaena guttata</i>	California Scorpionfish	4	1.1	17	24	20
Sebastidae	<i>Sebastes</i> sp	Rockfish Unidentified	6	0.5	2	4	3
Hexagrammidae	<i>Zaniolepis latipinnis</i>	Longspine Combfish	28	0.8	12	15	13
Cottidae	<i>Chitonotus pugetensis</i>	Roughback Sculpin	81	1.9	3	12	7
	<i>Icelinus quadriseriatus</i>	Yellowchin Sculpin	89	0.6	3	8	6
Agonidae	<i>Odontopyxis trispinosa</i>	Pygmy Poacher	2	0.2	6	7	6
PERCIFORMES							
Malacanthidae	<i>Caulolatilus princeps</i>	Ocean Whitefish	5	0.4	4	6	5
Bramidae	<i>Brama japonica</i>	Pacific Pomfret	57	1.1	9	11	10
Sciaenidae	<i>Genyonemus lineatus</i>	White Croaker	341	12.4	10	19	14
	<i>Seriphus politus</i>	Queenfish	4	0.5	12	15	14
Embiotocidae	<i>Cymatogaster aggregata</i>	Shiner Perch	35	0.7	9	11	10
Clinidae	<i>Heterostichus rostratus</i>	Giant Kelpfish	1	0.1	—	—	12
Stromateidae	<i>Pepilus simillimus</i>	Pacific Pompano	19	0.3	10	13	11

^a measured as total length (cm)

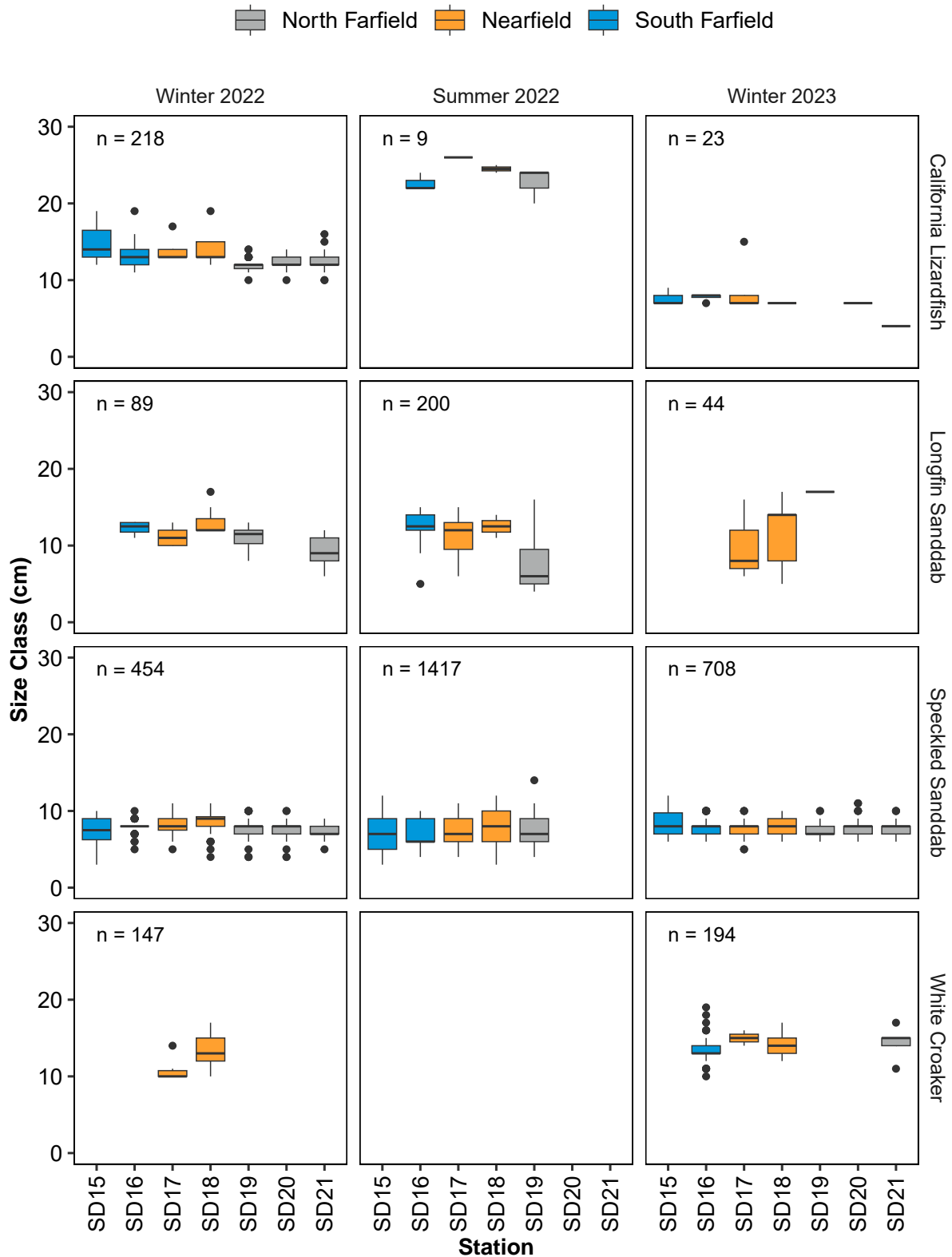
Appendix I.2 *continued*

Taxonomic Classification	Common Name	n	Length (cm)				
			Bm	Min	Max	Mean	
PLEURONECTIFORMES							
Paralichthyidae	<i>Citharichthys sordidus</i>	Pacific Sanddab	144	0.6	3	10	5
	<i>Citharichthys stigmaeus</i>	Speckled Sanddab	3263	23.3	3	14	8
	<i>Citharichthys xanthostigma</i>	Longfin Sanddab	656	11.1	4	17	9
	<i>Hippoglossina stomata</i>	Bigmouth Sole	5	1.5	20	38	25
	<i>Paralichthys californicus</i>	California Halibut	27	17.4	17	66	30
	<i>Xystreurus liolepis</i>	Fantail Sole	12	2.7	7	26	20
Pleuronectidae	<i>Parophrys vetulus</i>	English Sole	54	6.9	11	31	18
	<i>Pleuronichthys decurrens</i>	Curlfin Sole	1	0.1	—	—	15
	<i>Pleuronichthys ritteri</i>	Spotted Turbot	13	1.6	14	21	17
	<i>Pleuronichthys verticalis</i>	Hornyhead Turbot	69	4.5	4	22	12
Cynoglossidae	<i>Symphurus atricaudus</i>	California Tonguefish	159	2.1	7	16	11



Appendix I.3

Summary of fish lengths by survey and station for the four most abundant species collected in the PLOO region during 2022 and 2023. Data are median, upper and lower quartiles, 1.5 times the interquartile range (whiskers), and outliers (open circles). No trawls were conducted during the summer of 2023 due to Bight'23 resource exchange (see text).



Appendix I.4

Summary of fish lengths by survey and station for the four most abundant species collected in the SBOO region during 2022 and 2023. Data are median, upper and lower quartiles, 1.5 times the interquartile range (whiskers), and outliers (open circles). No trawls were conducted during the summer of 2023 due to Bight'23 resource exchange (see text).

Appendix I.5

Summary of demersal fish abnormalities and parasites at PLOO and SBOO trawl stations during 2022 and 2023.

Region	Year	Survey	Station	Species	AbnormalitiesParasite	n
PLOO	2022	Winter	SD7	Pacific Sanddab	<i>Phrioxocephalus cininnatus</i>	1
			SD10	Dover Sole	Lesion	1
			SD10	Pacific Sanddab	<i>Phrioxocephalus cininnatus</i>	3
			SD13	Pacific Sanddab	<i>Phrioxocephalus cininnatus</i>	1
			SD14	Pacific Sanddab	<i>Phrioxocephalus cininnatus</i>	6
		Summer	SD8	Pacific Sanddab	<i>Phrioxocephalus cininnatus</i>	1
			SD12	Pacific Sanddab	<i>Phrioxocephalus cininnatus</i>	1
			SD13	Longfin Sanddab	<i>Phrioxocephalus cininnatus</i>	1
			SD13	Pacific Sanddab	<i>Phrioxocephalus cininnatus</i>	1
	Fall	SD10	Pacific Sanddab	<i>Phrioxocephalus cininnatus</i>	2	
	2023	Winter	SD7	Pacific Sanddab	<i>Phrioxocephalus cininnatus</i>	4
			SD8	Pacific Sanddab	<i>Phrioxocephalus cininnatus</i>	3
			SD10	Pacific Sanddab	<i>Phrioxocephalus cininnatus</i>	6
			SD12	Dover Sole	Tumor	1
			SD12	Pacific Sanddab	<i>Phrioxocephalus cininnatus</i>	10
SD13			Dover Sole	Tumor	1	
SD13			Pacific Sanddab	<i>Phrioxocephalus cininnatus</i>	15	
SD14	Pacific Sanddab	<i>Phrioxocephalus cininnatus</i>	8			
SBOO	2022	Winter	SD20	Speckled Sanddab	<i>Elthusa vulgaris</i>	1
		Summer	SD16	Hornyhead Turbot	Leech	1
			SD16	Speckled Sanddab	<i>Phrioxocephalus cininnatus</i>	1
	2023	Winter	SD16	Hornyhead Turbot	<i>Elthusa vulgaris</i>	1
			SD17	Speckled Sanddab	<i>Elthusa vulgaris</i>	1

Appendix I.6

Description of PLOO demersal fish cluster groups defined in Figure 8.6. Data are mean abundance of the characteristic species. Highlighted/bold values indicate the most characteristic species according to SIMPER analysis.

Species	Cluster Group						
	A ^a	B ^a	C ^a	D	E	F	G
Pacific Sanddab	23	75	110	89	220	48	71
California Lizardfish	0	0	0	126	9	0	<1
Plainfin Midshipman	0	116	4	1	9	2	3
Halfbanded Rockfish	16	0	60	10	26	0	2
Dover Sole	0	36	1	8	28	6	9
Longspine Combfish	0	7	2	8	18	2	1
Squarespot Rockfish	0	0	23	1	<1	0	<1
Shortspine Combfish	0	0	3	7	7	0	3
Longfin Sanddab	1	0	0	0	5	1	6
Greenblotched Rockfish	0	0	8	<1	<1	2	<1
Gulf Sanddab	1	5	0	0	<1	1	<1
Vermilion Rockfish	0	0	6	0	<1	0	0
California Tonguefish	0	0	1	<1	1	0	3
Greenstriped Rockfish	0	0	0	<1	1	1	<1
Greenspotted Rockfish	1	0	1	0	<1	0	<1

^a SIMPER analysis only conducted on cluster groups that contain more than one haul. For these groups, shading indicates five most abundant species.

Appendix I.7

Description of SBOO demersal fish cluster groups defined in Figure 8.7. Data are mean abundance of the characteristic species. Highlighted/bold values indicate the most characteristic species according to SIMPER analysis.

Species	Cluster Group					
	A ^a	B	C	D	E	F
Speckled Sanddab	7	74	260	225	130	32
California Lizardfish	1	3	4	188	36	19
Longfin Sanddab	5	1	22	5	32	13
Yellowchin Sculpin	0	<1	7	9	22	1
Pacific Sanddab	4	<1	17	7	<1	<1
Hornyhead Turbot	0	3	5	7	4	4
California Tonguefish	2	<1	3	7	6	3
Roughback Sculpin	0	<1	5	4	6	<1
English Sole	0	<1	1	3	3	4
White Croaker	0	0	0	<1	0	5

^aSIMPER analysis only conducted on cluster groups that contain more than one haul. For these groups, shading indicates five most abundant species.

Appendix I.8

Taxonomic listing of megabenthic invertebrate taxa collected at all PLOO trawl stations during 2022 and 2023. Data are total number of individuals (n). Taxonomic arrangement follows SCAMIT (2018). -- indicates taxon is not within previous family.

Taxonomic Classification				n
SILICEA	Hexactinellida	Rossellidae	<i>Aphorme horrida</i>	2
	Demospongiae	Suberitidae	<i>Suberites latus</i>	2
CNIDARIA	Anthozoa	Plexauridae	<i>Thesea</i> sp B	2
		Virgulariidae	<i>Acanthoptilum</i> sp	4
		Metridiidae	<i>Metridium farcimen</i>	2
MOLLUSCA	Gastropoda	Calliostomatidae	<i>Calliostoma turbinum</i>	2
		Naticidae		1
		Cancellariidae	<i>Cancellaria cooperii</i>	1
			<i>Cancellaria crawfordiana</i>	1
		Pseudomelatomidae	<i>Antiplanes catalinae</i>	2
			<i>Megasurcula carpenteriana</i>	2
		Discodorididae	<i>Platydorid macfarlandi</i>	1
	Pleurobranchidae	<i>Pleurobranchaea californica</i>	25	
	Philinidae	<i>Philina auriformis</i>	3	
	Cephalopoda	Sepiolidae	<i>Rossia pacifica</i>	4
		Octopodidae	<i>Octopus rubescens</i>	28
	<i>Octopus veligero</i>		5	
ARTHROPODA	Malacostraca	Sicyoniidae	<i>Sicyonia ingentis</i>	139
		Pandalidae	<i>Pandalus danae</i>	1
		Crangonidae	<i>Neocrangon zacaе</i>	2
		Diogenidae	<i>Paguristes bakeri</i>	5
			<i>Paguristes turgidus</i>	2
		Calappidae	<i>Platymera gaudichaudii</i>	11
		Epialtidae	<i>Loxorhynchus crispatus</i>	1
ECHINODERMATA	Crinoidea	Antedonidae	<i>Florometra serratissima</i>	1
	Asteroidea	Luidiidae	<i>Luidia asthenosoma</i>	28
			<i>Luidia foliolata</i>	70
			<i>Astropecten californicus</i>	75
	Ophiuroidea	Ophiuridae	<i>Ophiura luetkenii</i>	26
		Ophiopholidae	<i>Ophiopholis bakeri</i>	1
		Ophiotrichidae	<i>Ophiothrix spiculata</i>	3
	Echinoidea	Toxopneustidae	<i>Lytechinus pictus</i>	11365
		Strongylocentrotidae	<i>Strongylocentrotus fragilis</i>	4190
		Spatangidae	<i>Spatangus californicus</i>	3
Holothuroidea	Stichopodidae	<i>Apostichopus californicus</i>	11	

Appendix I.9

Taxonomic listing of megabenthic invertebrate taxa collected at all SBOO trawl stations during 2022 and 2023. Data are total number of individuals (n). Taxonomic arrangement follows SCAMIT (2018).

Taxonomic Classification				n
CNIDARIA	Anthozoa	Plexauridae	<i>Thesea</i> sp B	1
		Virgulariidae	<i>Acanthoptilum</i> sp	1
			<i>Stylatula elongata</i>	7
MOLLUSCA	Polyplacophora	Ischnochitonidae	<i>Lepidozona scrobiculata</i>	1
	Gastropoda	Calliostomatidae	<i>Calliostoma gloriosum</i>	1
		Turbinidae	<i>Megastrea turbanica</i>	1
			<i>Megastrea undosa</i>	1
		Velutinidae	<i>Lamellaria diegoensis</i>	2
		Naticidae	<i>Glossaulax reclusiana</i>	2
			<i>Neverita draconis</i>	1
		Bursidae	<i>Crossata ventricosa</i>	4
		Epitoniidae	<i>Epitonium bellastratum</i>	1
		Buccinidae	<i>Kelletia kelletii</i>	7
			<i>Pteropurpura festiva</i>	1
		Muricidae	<i>Pteropurpura vokesae</i>	1
			<i>Burchia semiinflata</i>	6
		Pseudomelatomidae	<i>Megasurcula carpenteriana</i>	1
			<i>Acanthodoris brunnea</i>	3
		Onchidorididae	<i>Acanthodoris rhodoceras</i>	2
			<i>Flabellinopsis iodinea</i>	1
		Flabellinopsidae	<i>Pleurobranchaea californica</i>	10
		Pleurobranchidae	<i>Philine auriformis</i>	280
Philinidae	<i>Octopus rubescens</i>	3		
Cephalopoda	Octopodidae	<i>Hemisquilla californiensis</i>	11	
	Malacostraca	Penaeidae	<i>Farfantepenaeus californiensis</i>	2
Sicyoniidae		<i>Sicyonia penicillata</i>	126	
Thoridae		<i>Eualus subtilis</i>	4	
		<i>Heptacarpus palpator</i>	3	
Heptacarpidae		<i>Heptacarpus stimpsoni</i>	10	
		<i>Crangon alba</i>	23	
Crangonidae		<i>Crangon nigromaculata</i>	360	
		Palinuridae	<i>Panulirus interruptus</i>	2
Diogenidae		<i>Paguristes bakeri</i>	1	
Paguridae		<i>Pagurus spilocarpus</i>	11	
Calappidae		<i>Platymera gaudichaudii</i>	8	
Leucosiidae		<i>Randallia ornata</i>	1	
Epiplatidae		<i>Pugettia dalli</i>	2	
		<i>Loxorhynchus grandis</i>	5	
Inachidae		<i>Ericerodes hemphillii</i>	8	
Inachoididae		<i>Pyromaia tuberculata</i>	26	

Appendix I.9 *continued*

Taxonomic Classification			n	
		Parthenopidae	<i>Latulambrus occidentalis</i>	8
		Cancriidae		1
			<i>Metacarcinus anthonyi</i>	1
			<i>Metacarcinus gracilis</i>	10
			<i>Romaleon jordani</i>	1
		Portunidae	<i>Portunus xantusii</i>	25
ECHINODERMATA	Asteroidea	Luidiidae	<i>Luidia armata</i>	32
			<i>Luidia asthenosoma</i>	1
		Astropectinidae	<i>Astropecten californicus</i>	520
	Ophiuroidea	Ophiuridae	<i>Ophiura luetkenii</i>	1
		Ophiotrichidae	<i>Ophiothrix spiculata</i>	51
	Echinoidea	Toxopneustidae	<i>Lytechinus pictus</i>	44
		Strongylocentrotidae	<i>Mesocentrotus franciscanus</i>	1
		Dendrasteridae	<i>Dendraster terminalis</i>	89
		Loveniidae	<i>Lovenia cordiformis</i>	32

Appendix I.10

Description of PLOO megabenthic invertebrate cluster groups defined in Figure 8.11. Data are mean abundance of the characteristic species. Highlighted/bold values indicate the most characteristic species according to SIMPER analysis.

Species	Cluster Group						
	A	B	C	D	E ^a	F	G
<i>Pleuroncodes planipes</i>	3	7514	0	2	0	2	<1
<i>Ophiura luetkenii</i>	0	0	0	2	2640	47	15
<i>Lytechinus pictus</i>	1	124	12	10	102	2151	228
<i>Strongylocentrotus fragilis</i>	51	26	0	6	442	4	120
<i>Acanthoptilum</i> sp	0	0	0	121	0	41	33
<i>Sicyonia ingentis</i>	53	71	<1	9	0	6	4
<i>Luidia foliolata</i>	<1	0	3	0	11	4	5
<i>Astropecten ornatissimus</i>	0	0	0	0	5	<1	<1

^aSIMPER analysis only conducted on cluster groups that contain more than one haul. For these groups, shading indicates five most abundant species.

Appendix I.11

Description of SBOO megabenthic invertebrate cluster groups defined in Figure 8.12. Data are mean abundance of the characteristic species. Highlighted/bold values indicate the most characteristic species according to SIMPER analysis.

Species	Cluster Group				
	A ^a	B	C ^a	D	E
<i>Lytechinus pictus</i>	0	<1	951	7	2
<i>Ophiura luetkenii</i>	72	<1	0	<1	0
<i>Astropecten californicus</i>	0	2	6	33	0
<i>Sicyonia penicillata</i>	0	8	0	<1	0
<i>Ophiothrix spiculata</i>	3	<1	4	<1	0
<i>Pyromaia tuberculata</i>	1	<1	4	<1	<1
<i>Dendraster terminalis</i>	3	2	0	1	<1
<i>Octopus rubescens</i>	1	2	0	<1	<1
<i>Crangon alba</i>	2	0	1	<1	0
<i>Kelletia kelletii</i>	0	1	0	<1	<1
<i>Crangon nigromaculata</i>	0	<1	1	<1	<1
<i>Pisaster brevispinus</i>	0	0	2	<1	0
<i>Philine auriformis</i>	0	<1	0	2	<1
<i>Latulambrus occidentalis</i>	0	<1	0	2	<1
<i>Crossata ventricosa</i>	0	<1	0	<1	1
<i>Platymera gaudichaudii</i>	0	<1	0	<1	<1
<i>Acanthodoris brunnea</i>	0	<1	0	<1	0
<i>Luidia armata</i>	0	0	0	<1	0
<i>Metacarcinus gracilis</i>	0	<1	0	<1	0

^aSIMPER analysis only conducted on cluster groups that contain more than one haul. For these groups, shading indicates five most abundant species.

Appendix J

Contaminants in Marine Fishes

2022 – 2023

Raw Data Tables & Supplemental Analyses

Appendix J.1

Lengths and weights of fishes used for each composite (Comp) tissue sample from PLOO trawl and rig fishing zones during 2022. Data are summarized as number of individuals (n), minimum, maximum, and mean values.

Zone	Comp	Species	n	Length (cm)			Weight (g)		
				Min	Max	Mean	Min	Max	Mean
RF1	1	Vermilion Rockfish	3	18	29	22	164	765	375
RF1	2	Vermilion Rockfish	3	23	28	25	439	683	521
RF1	3	Vermilion Rockfish	3	21	31	27	269	930	655
RF2	1	Squarespot Rockfish	3	18	22	20	102	249	162
RF2	2	Starry Rockfish	3	19	26	22	142	506	310
RF2	3	Mixed Rockfish	3	18	32	24	156	1057	490
TZ1	1	Pacific Sanddab	7	16	22	19	67	163	102
TZ1	2	Pacific Sanddab	7	15	24	17	44	236	85
TZ1	3	Pacific Sanddab	8	16	51	22	48	98	72
TZ2	1	Pacific Sanddab	5	18	24	20	98	202	133
TZ2	2	Pacific Sanddab	4	17	20	19	88	145	120
TZ2	3	Pacific Sanddab	7	16	20	18	69	138	95
TZ3	1	Pacific Sanddab	6	13	22	18	30	178	99
TZ3	2	Pacific Sanddab	5	16	21	18	64	194	105
TZ3	3	Pacific Sanddab	6	14	23	20	43	185	124
TZ4	1	Pacific Sanddab	7	14	169	38	41	131	75
TZ4	2	Pacific Sanddab	6	15	24	19	57	242	113
TZ4	3	Pacific Sanddab	4	18	24	21	103	248	174

Appendix J.2

Lengths and weights of fishes used for each composite (Comp) tissue sample from SBOO trawl and rig fishing zones during 2022. Data are summarized as number of individuals (n), minimum, maximum, and mean values.

Zone	Comp	Species	n	Length (cm)			Weight (g)		
				Min	Max	Mean	Min	Max	Mean
RF3	1	Brown Rockfish	3	24	26	25	349	470	428
RF3	2	California Scorpionfish	3	22	24	23	389	461	416
RF3	3	Mixed Rockfish	3	23	25	24	392	465	425
RF4	1	California Scorpionfish	3	21	28	25	329	618	478
RF4	2	Gopher Rockfish	3	21	23	22	290	410	352
RF4	3	Mixed Rockfish	3	21	23	22	269	418	340
TZ5	1	Longfin Sanddab	13	12	15	14	35	67	49
TZ5	2	Longfin Sanddab	13	13	16	14	38	71	51
TZ5	3	Hornyhead Turbot	7	17	19	18	126	224	161
TZ6	1	Longfin Sanddab	10	14	16	15	48	74	60
TZ6	2	Longfin Sanddab	11	13	14	14	36	66	50
TZ6	3	Longfin Sanddab	11	13	16	15	40	63	55
TZ7	1	Longfin Sanddab	10	13	19	15	42	117	62
TZ7	2	Longfin Sanddab	14	12	14	13	31	47	40
TZ7	3	Hornyhead Turbot	7	16	20	18	106	211	159
TZ8	1	Longfin Sanddab	12	13	15	13	34	64	46
TZ8	2	California Scorpionfish	3	16	22	19	123	305	238
TZ8	3	Hornyhead Turbot	10	12	19	14	44	163	82
TZ9	1	Hornyhead Turbot	10	12	18	14	38	146	68
TZ9	2	Spotted Turbot	8	12	16	14	46	131	74
TZ9	3	Fantail Sole	3	14	17	16	61	99	80

Appendix J.3

Constituents and method detection limits (MDL) used for the analysis of liver and muscle tissues of fishes collected during 2022.

Parameter	MDL		Parameter	MDL	
	Liver	Muscle		Liver	Muscle
Metals (ppm)					
Aluminum (Al)	6.448-6.650	2.168-3.022	Lead (Pb)	0.257-0.265	0.087-0.121
Antimony (Sb)	0.527-0.543	0.177-0.247	Manganese (Mn)	0.302-0.311	0.102-0.142
Arsenic (As)	0.813-0.838	0.274-0.382	Mercury (Hg)	0.003-0.007	0.001-0.002
Barium (Ba)	0.543-0.560	0.183-0.255	Nickel (Ni)	0.102-0.105	0.034-0.048
Beryllium (Be)	0.045-0.046	0.015-0.021	Selenium (Se)	0.564-0.963	0.315-0.439
Cadmium (Cd)	0.055-0.057	0.019-0.026	Silver (Ag)	0.216-0.222	0.073-0.101
Chromium (Cr)	0.181-0.187	0.061-0.085	Thallium (Tl)	0.939-0.968	0.316-0.440
Copper (Cu)	0.254-0.262	0.086-0.119	Tin (Sn)	3.250-3.350	1.099-1.532
Iron (Fe)	3.030-3.130	1.010-1.408	Zinc (Zn)	0.512-0.527	0.173-0.242
Chlorinated Pesticides (ppb)					
<i>Hexachlorocyclohexane (HCH)</i>					
HCH, Alpha isomer	0.457-0.595	0.049-0.060	HCH, Delta isomer	0.660-0.859	0.070-0.086
HCH, Beta isomer	0.318-0.414	0.042-0.051	HCH, Gamma isomer	0.634-0.825	0.067-0.083
<i>Total Chlordane</i>					
Alpha (cis) chlordane [A(c)C]	0.856-1.120	0.091-0.112	Heptachlor epoxide [HeptEpoX]	0.58-0.756	0.062-0.076
Cis nonachlor [cNon]	0.670-0.873	0.071-0.087	Methoxychlor [Methoxy]	3.980-5.190	0.422-0.519
Gamma (trans) chlordane [G(t)C]	0.722-0.941	0.077-0.094	Oxychlordane [Oxychlor]	0.714-0.930	0.076-0.093
Heptachlor [Hept]	0.718-0.936	0.076-0.094	Trans nonachlor [tNon]	0.948-1.230	0.100-0.123
<i>Total Dichlorodiphenyltrichloroethane (DDT)</i>					
o,p-DDD	0.910-1.180	0.096-0.118	p,p-DDD	2.690-3.500	0.285-0.350
o,p-DDE	0.406-0.529	0.043-0.053	p,p-DDE	0.401-0.523	0.043-0.052
o,p-DDT	0.423-0.552	0.045-0.055	p,p-DDT	0.571-0.744	0.061-0.074
p,-p-DDMU	0.511-0.666	0.054-0.067			
<i>Miscellaneous Pesticides</i>					
Aldrin	1.030-1.340	0.109-0.134	Endrin	0.482-0.627	0.051-0.063
AlphaEndosulfan	0.657-0.855	0.07-0.086	Endrin aldehyde [EndAld]	1.320-1.720	0.140-0.172
BetaEndosulfan	2.490-3.250	0.264-0.325	Hexachlorobenzene (HCB)	0.643-0.837	0.068-0.084
Dieldrin	0.803-1.050	0.085-0.105	Mirex	0.709-0.924	0.075-0.092
EndosulfanSulfate	1.220-1.580	0.129-0.158			

Appendix J.3 *continued*

Parameter	MDL		Parameter	MDL	
	Liver	Muscle		Liver	Muscle
Polychlorinated Biphenyls Congeners (PCBs) (ppb)					
PCB 8	0.636-0.828	0.067-0.083	PCB 126	0.739-0.963	0.078-0.096
PCB 18	0.396-0.516	0.042-0.052	PCB 128	0.626-0.815	0.066-0.082
PCB 28	0.520-0.677	0.055-0.068	PCB 138	0.682-0.888	0.072-0.089
PCB 37	0.362-0.472	0.038-0.047	PCB 149	0.755-0.984	0.080-0.098
PCB 44	0.376-0.490	0.040-0.049	PCB 151	0.635-0.827	0.067-0.083
PCB 49	0.718-0.936	0.076-0.094	PCB 153/168	0.533-0.694	0.057-0.069
PCB 52	0.423-0.552	0.045-0.055	PCB 156	1.210-1.570	0.128-0.157
PCB 66	0.645-0.840	0.068-0.084	PCB 157	0.600-0.782	0.064-0.078
PCB 70	0.744-0.970	0.079-0.097	PCB 158	0.749-0.976	0.079-0.098
PCB 74	0.670-0.873	0.071-0.087	PCB 167	0.735-0.957	0.078-0.096
PCB 77	0.560-0.730	0.059-0.073	PCB 169	0.955-1.240	0.101-0.124
PCB 81	0.871-1.140	0.092-0.113	PCB 170	0.521-0.678	0.055-0.068
PCB 87	0.795-1.040	0.084-0.104	PCB 177	1.090-1.420	0.116-0.142
PCB 99	0.366-0.477	0.039-0.048	PCB 180	0.695-0.905	0.074-0.091
PCB 101	0.386-0.503	0.041-0.050	PCB 183	0.925-1.20	0.098-0.120
PCB 105	0.621-0.809	0.066-0.081	PCB 187	0.750-0.977	0.080-0.098
PCB 110	0.489-0.637	0.052-0.064	PCB 189	0.636-0.828	0.067-0.083
PCB 114	1.200-1.560	0.127-0.156	PCB 194	0.482-0.627	0.051-0.063
PCB 118	0.519-0.676	0.055-0.068	PCB 195	0.925-1.20	0.098-0.120
PCB 119	0.750-0.977	0.080-0.098	PCB 201	1.020-1.320	0.108-0.132
PCB 123	0.668-0.870	0.071-0.087	PCB 206	0.984-1.250	0.103-0.126
Polycyclic Aromatic Hydrocarbons (PAHs) (ppb)					
1-methylnaphthalene	125-148	126-149	Benzo[G,H,I]perylene	108-128	109-126
1-methylphenanthrene	86.6-102	87.3-103	Benzo[K]fluoranthene	152-179	153-177
2-methylnaphthalene	84.9-100	85.6-101	Biphenyl	123-145	124-143
2,3,5-trimethylnaphthalene	137-161	138-163	Chrysene	113-134	114-132
2,6-dimethylnaphthalene	102-120	103-121	Dibenzo(A,H)anthracene	95.8-113	96.6-114
3,4-benzo(B)fluoranthene	108-127	108-125	Fluoranthene	128-150	129-152
Acenaphthene	110-130	111-131	Fluorene	112-132	113-133
Acenaphthylene	109-129	110-130	Indeno(1,2,3-CD)pyrene	94.1-111	94.9-110
Anthracene	118-139	119-140	Naphthalene	63.9-75.2	64.4-76
Benzo[A]anthracene	89.9-106	90.7-105	Perylene	120-142	121-143
Benzo[A]pyrene	125-148	126-146	Phenanthrene	109-129	110-127
Benzo[e]pyrene	134-158	136-157	Pyrene	126-149	127-147
Polybrominated Diphenyl Ethers (PBDEs)					
BDE-17	0.417-0.544	0.044-0.054	BDE-100	0.902-1.170	0.096-0.117
BDE-28	0.702-0.915	0.075-0.092	BDE-138	2.450-3.200	0.260-0.320
BDE-47	2.140-2.790	0.227-0.279	BDE-153	1.910-2.490	0.203-0.249
BDE-49	1.380-1.790	0.146-0.179	BDE-154	0.910-1.180	0.096-0.118
BDE-66	0.772-1.010	0.082-0.101	BDE-183	4.060-5.290	0.430-0.529
BDE-85	1.830-2.390	0.194-0.239	BDE-190	4.520-5.880	0.479-0.588
BDE-99	1.470-1.910	0.156-0.191			

Appendix J.4

Concentrations of metals (ppm) detected in liver tissues of fishes collected from PLOO and SBOO trawl zones during 2022. See Appendix J.3 for MDLs and abbreviations; DNQ = do not quantify; ND = not detected; NR = not reportable.

Zone	Comp	Species	Al	Sb	As	Ba	Be	Cd	Cr	Cu	Fe
TZ1	1	Pacific Sanddab	ND	ND	3.82	ND	ND	3.44	ND	5.17	107
	2	Pacific Sanddab	ND	ND	2.61	ND	ND	3.38	ND	3.17	101
	3	Pacific Sanddab	ND	ND	2.06	ND	ND	2.40	ND	4.20	76.5
TZ2	1	Pacific Sanddab	ND	ND	3.05	ND	ND	3.20	ND	5.01	76.0
	2	Pacific Sanddab	ND	ND	2.74	ND	ND	2.50	0.199 DNQ	5.16	94.9
	3	Pacific Sanddab	ND	ND	2.99	ND	ND	2.91	ND	5.06	74.0
TZ3	1	Pacific Sanddab	ND	ND	3.17	ND	ND	3.30	ND	4.42	111
	2	Pacific Sanddab	ND	ND	2.66	ND	ND	1.98	ND	4.47	98.1
	3	Pacific Sanddab	ND	ND	3.53	ND	ND	4.17	ND	5.16	87.5
TZ4	1	Pacific Sanddab	ND	ND	3.29	ND	ND	3.07	ND	4.46	99.9
	2	Pacific Sanddab	ND	ND	3.04	ND	ND	4.36	ND	4.41	92.9
	3	Pacific Sanddab	ND	ND	3.46	ND	ND	5.11	ND	3.91	88.5
TZ5	1	Longfin Sanddab	ND	ND	4.51	ND	ND	1.56	ND	6.27	87.4
	2	Longfin Sanddab	ND	ND	5.93	ND	ND	2.05	ND	5.67	116
	3	Hornyhead Turbot	ND	ND	6.91	ND	ND	5.31	ND	9.56	50.8
TZ6	1	Longfin Sanddab	ND	ND	7.55	ND	ND	1.85	ND	9.01	113
	2	Longfin Sanddab	ND	ND	5.44	ND	ND	1.25	ND	6.67	105
	3	Longfin Sanddab	ND	ND	4.70	ND	ND	1.83	ND	7.06	112
TZ7	1	Longfin Sanddab	ND	ND	6.33	ND	ND	1.44	ND	6.21	86.5
	2	Longfin Sanddab	ND	ND	4.16	ND	ND	1.03	ND	5.96	83.5
	3	Hornyhead Turbot	ND	ND	5.88	ND	ND	4.43	ND	16.3	43.7
TZ8	1	Longfin Sanddab	ND	ND	4.98	ND	ND	1.55	ND	6.30	92.3
	2	CA Scorpionfish	ND	ND	1.26 DNQ	ND	ND	4.29	ND	12.8	66.8
	3	Hornyhead Turbot	ND	ND	4.63	ND	ND	3.70	ND	9.34	46.1
TZ9	1	Hornyhead Turbot	ND	ND	4.74	ND	ND	4.29	0.439 DNQ	8.03	64.3
	2	Spotted Turbot	ND	ND	8.20	ND	ND	0.577	ND	8.85	120
	3	No sample	—	—	—	—	—	—	—	—	—

Appendix J.4 continued

Zone	Comp	Species	Pb	Mn	Hg	Ni	Se	Ag	Tl	Sn	Zn
TZ1	1	Pacific Sanddab	ND	1.1	0.151	ND	1.65 DNQ	ND	1.35 DNQ	ND	22.3
	2	Pacific Sanddab	ND	0.659 DNQ	0.099	ND	1.56 DNQ	ND	1.20 DNQ	ND	21.0
	3	Pacific Sanddab	ND	0.520 DNQ	0.114	ND	1.27 DNQ	ND	1.17 DNQ	ND	17.8
TZ2	1	Pacific Sanddab	ND	1.06	0.093	ND	1.28 DNQ	ND	ND	ND	24.2
	2	Pacific Sanddab	ND	1.10	0.082	ND	1.33 DNQ	ND	ND	ND	23.9
	3	Pacific Sanddab	ND	1.03	0.084	ND	1.26 DNQ	ND	ND	ND	26.9
TZ3	1	Pacific Sanddab	ND	0.968	0.147	ND	1.64 DNQ	ND	ND	ND	22.6
	2	Pacific Sanddab	ND	0.874 DNQ	0.098	ND	1.43 DNQ	ND	ND	ND	21.1
	3	Pacific Sanddab	ND	0.959	0.084	ND	1.39 DNQ	ND	ND	ND	25.1
TZ4	1	Pacific Sanddab	ND	0.802 DNQ	0.080	ND	1.49 DNQ	ND	ND	ND	22.7
	2	Pacific Sanddab	ND	1.06	0.199	ND	1.76 DNQ	ND	ND	ND	24.8
	3	Pacific Sanddab	ND	1.33	0.111	ND	1.58 DNQ	ND	ND	ND	25.5
TZ5	1	Longfin Sanddab	ND	0.708 DNQ	0.028	ND	1.40 DNQ	ND	ND	ND	20.7
	2	Longfin Sanddab	ND	0.749 DNQ	0.038	ND	1.70 DNQ	ND	ND	ND	22.1
	3	Hornyhead Turbot	ND	0.916 DNQ	0.086	ND	1.23 DNQ	0.235 DNQ	ND	ND	67.9
TZ6	1	Longfin Sanddab	ND	0.631 DNQ	0.052	ND	1.80 DNQ	ND	1.79 DNQ	ND	24.9
	2	Longfin Sanddab	ND	0.637 DNQ	0.041	ND	1.77 DNQ	ND	1.55 DNQ	ND	21.7
	3	Longfin Sanddab	ND	0.554 DNQ	0.045	ND	1.91 DNQ	ND	1.85 DNQ	ND	19.5
TZ7	1	Longfin Sanddab	ND	0.754 DNQ	0.057	ND	1.60 DNQ	ND	0.988 DNQ	ND	21.1
	2	Longfin Sanddab	ND	0.538 DNQ	0.041	ND	1.64 DNQ	ND	2.11 DNQ	ND	18.4
	3	Hornyhead Turbot	ND	0.899 DNQ	0.101	ND	1.14 DNQ	ND	ND	ND	73.3
TZ8	1	Longfin Sanddab	ND	0.651 DNQ	0.029	ND	1.59 DNQ	ND	ND	ND	19.5
	2	CA Scorpionfish	ND	0.568 DNQ	0.208	ND	1.22 DNQ	ND	ND	ND	83.8
	3	Hornyhead Turbot	ND	0.896 DNQ	0.081	ND	1.37 DNQ	ND	ND	ND	52.2
TZ9	1	Hornyhead Turbot	ND	1.21	0.059	ND	1.44 DNQ	ND	ND	ND	54.2
	2	Spotted Turbot	0.49 DNQ	1.25	0.040	ND	1.96 DNQ	ND	ND	ND	46.2
	3	No sample	—	—	—	—	—	—	—	—	—

Appendix J.5

Concentrations of pesticides (ppb) and lipids (% weight) detected in liver tissues of fishes collected from PLOO and SBOO trawl zones during 2022. See Appendix J.3 for MDLs and abbreviations; DNQ=do not quantify; ND=not detected; NR=not reportable.

Zone	Comp	Species	Chlordane							
			A(c)C	cNon	G(t)C	Hept	HeptEpo	Methoxy	Oxychlor	tNon
TZ1	1	Pacific Sanddab	2.05 DNQ	0.904 DNQ	ND	ND	ND	ND	ND	2.01 DNQ
	2	Pacific Sanddab	2.80 DNQ	ND	ND	ND	ND	ND	ND	3.12
	3	Pacific Sanddab	3.36	1.68 DNQ	ND	ND	ND	ND	ND	3.76
TZ2	1	Pacific Sanddab	1.48 DNQ	ND	ND	ND	ND	ND	ND	1.35 DNQ
	2	Pacific Sanddab	2.01 DNQ	ND	ND	ND	ND	ND	ND	1.93 DNQ
	3	Pacific Sanddab	ND	ND	ND	ND	ND	ND	ND	1.65 DNQ
TZ3	1	Pacific Sanddab	2.00 DNQ	1.12 DNQ	ND	ND	ND	ND	ND	2.63 DNQ
	2	Pacific Sanddab	2.27 DNQ	ND	ND	ND	ND	ND	ND	2.46 DNQ
	3	Pacific Sanddab	1.81 DNQ	ND	ND	ND	ND	ND	ND	1.66 DNQ
TZ4	1	Pacific Sanddab	2.08 DNQ	0.910 DNQ	ND	ND	ND	ND	ND	2.33 DNQ
	2	Pacific Sanddab	1.49 DNQ	ND	ND	ND	ND	ND	ND	1.78 DNQ
	3	Pacific Sanddab	1.55 DNQ	ND	ND	ND	ND	ND	ND	1.50 DNQ
TZ5	1	Longfin Sanddab	1.75 DNQ	1.05 DNQ	ND	ND	ND	ND	ND	2.42 DNQ
	2	Longfin Sanddab	1.86 DNQ	1.15 DNQ	ND	ND	ND	ND	ND	2.71
	3	Hornyhead Turbot	ND	ND	ND	ND	ND	ND	ND	ND
TZ6	1	Longfin Sanddab	ND	ND	ND	ND	ND	ND	ND	2.36 DNQ
	2	Longfin Sanddab	ND	0.829 DNQ	ND	ND	ND	ND	ND	1.62 DNQ
	3	Longfin Sanddab	ND	ND	ND	ND	ND	ND	ND	1.91 DNQ
TZ7	1	Longfin Sanddab	1.24 DNQ	ND	ND	ND	ND	ND	ND	1.87 DNQ
	2	Longfin Sanddab	1.17 DNQ	ND	ND	ND	ND	ND	ND	2.20 DNQ
	3	Hornyhead Turbot	ND	ND	ND	ND	ND	ND	ND	ND
TZ8	1	Longfin Sanddab	ND	ND	ND	ND	ND	ND	ND	1.36 DNQ
	2	California Scorpionfish	ND	0.779 DNQ	ND	ND	ND	ND	ND	2.54 DNQ
	3	Hornyhead Turbot	ND	ND	ND	ND	ND	ND	ND	ND
TZ9	1	Hornyhead Turbot	ND	ND	ND	ND	ND	ND	ND	ND
	2	Spotted Turbot	ND	ND	ND	ND	ND	ND	ND	ND
	3	Fantail Sole	ND	ND	ND	ND	ND	ND	ND	ND

Appendix J.5 *continued*

Zone	Comp	Species	DDT						Endosulfan			
			o,p-DDD	o,p-DDE	o,p-DDT	p,p-DDMU	p,p-DDD	p,p-DDE	p,p-DDT	Alpha	Beta	Sulfate
TZ1	1	Pacific Sanddab	ND	1.01 DNQ	ND	4.50	ND	80.6	1.31 DNQ	ND	ND	ND
	2	Pacific Sanddab	ND	1.75 DNQ	ND	5.34	ND	91.8	1.52 DNQ	ND	ND	ND
	3	Pacific Sanddab	ND	1.89 DNQ	0.727 DNQ	7.96	ND	137	2.40 DNQ	ND	ND	ND
TZ2	1	Pacific Sanddab	ND	0.572 DNQ	ND	3.42	ND	66.1	1.13 DNQ	ND	ND	ND
	2	Pacific Sanddab	ND	1.22 DNQ	ND	5.58	ND	79.3	1.37 DNQ	ND	ND	ND
	3	Pacific Sanddab	ND	0.771 DNQ	ND	4.42	ND	76.5	1.19 DNQ	ND	ND	ND
TZ3	1	Pacific Sanddab	ND	0.901 DNQ	ND	5.04	ND	90.6	1.48 DNQ	ND	ND	ND
	2	Pacific Sanddab	ND	1.06 DNQ	ND	5.37	ND	107	1.34 DNQ	ND	ND	ND
	3	Pacific Sanddab	ND	ND	ND	5.52	ND	84.3	1.18 DNQ	ND	ND	ND
TZ4	1	Pacific Sanddab	ND	1.85 DNQ	ND	6.35	ND	92.1	1.23 DNQ	ND	ND	ND
	2	Pacific Sanddab	ND	0.729 DNQ	ND	4.94	ND	88.7	1.60 DNQ	ND	ND	ND
	3	Pacific Sanddab	ND	0.853 DNQ	ND	4.19	ND	67.7	1.54 DNQ	ND	ND	ND
TZ5	1	Longfin Sanddab	ND	2.80 DNQ	ND	7.09	ND	196	2.38 DNQ	ND	ND	ND
	2	Longfin Sanddab	ND	2.52 DNQ	ND	7.33	ND	196	2.47 DNQ	ND	ND	ND
	3	Hornyhead Turbot	ND	ND	1.29 DNQ	18.4	ND	18.4	ND	ND	ND	ND
TZ6	1	Longfin Sanddab	ND	2.60 DNQ	ND	8.75	ND	179	2.55 DNQ	ND	ND	ND
	2	Longfin Sanddab	ND	2.02 DNQ	ND	6.13	ND	159	2.39 DNQ	ND	ND	ND
	3	Longfin Sanddab	ND	2.02 DNQ	ND	5.19	ND	222	1.64 DNQ	ND	ND	ND
TZ7	1	Longfin Sanddab	ND	1.79 DNQ	ND	5.35	ND	136	1.70 DNQ	ND	ND	ND
	2	Longfin Sanddab	ND	1.91 DNQ	ND	4.89	ND	137	1.50 DNQ	ND	ND	ND
	3	Hornyhead Turbot	ND	ND	ND	ND	ND	14.9	ND	ND	ND	ND
TZ8	1	Longfin Sanddab	ND	1.32 DNQ	ND	3.14	ND	90.0	1.44 DNQ	ND	ND	ND
	2	CA Scorpionfish	ND	ND	1.70 DNQ	181	ND	181	0.611 DNQ	ND	ND	ND
	3	Hornyhead Turbot	ND	ND	0.668 DNQ	15.5	ND	15.5	ND	ND	ND	ND
TZ9	1	Hornyhead Turbot	ND	ND	ND	ND	ND	12.4	ND	ND	ND	ND
	2	Spotted Turbot	ND	ND	ND	ND	ND	3.87	ND	ND	ND	ND
	3	Fantail Sole	ND	ND	ND	ND	ND	6.22	ND	ND	ND	ND

Appendix J.5 *continued*

Zone	Comp	Species	HCH						EndAld	HCB	Mirex	Lipids
			Alpha	Beta	Delta	Gamma	Aldrin	Dieldrin				
TZ1	1	Pacific Sanddab	ND	1.46 DNQ	ND	ND	ND	ND	ND	ND	ND	28.1
	2	Pacific Sanddab	ND	2.47 DNQ	ND	ND	ND	ND	ND	ND	ND	30.6
	3	Pacific Sanddab	ND	2.25 DNQ	ND	ND	ND	ND	ND	ND	ND	39.2
TZ2	1	Pacific Sanddab	ND	1.35 DNQ	ND	ND	ND	ND	ND	ND	ND	25.4
	2	Pacific Sanddab	ND	2.51 DNQ	ND	ND	ND	ND	ND	ND	ND	38.3
	3	Pacific Sanddab	ND	1.74 DNQ	ND	ND	ND	ND	ND	3.30 DNQ	ND	31.3
TZ3	1	Pacific Sanddab	ND	1.77 DNQ	ND	ND	ND	ND	ND	ND	ND	37.0
	2	Pacific Sanddab	ND	1.69 DNQ	ND	ND	ND	6.9	ND	ND	ND	38.0
	3	Pacific Sanddab	ND	1.79 DNQ	ND	ND	ND	ND	ND	5.11	ND	42.0
TZ4	1	Pacific Sanddab	ND	2.08 DNQ	ND	ND	ND	ND	ND	ND	ND	47.4
	2	Pacific Sanddab	ND	1.76 DNQ	ND	ND	ND	ND	ND	4.37	ND	38.3
	3	Pacific Sanddab	ND	1.33 DNQ	ND	ND	ND	ND	ND	2.93 DNQ	ND	32.8
TZ5	1	Longfin Sanddab	ND	1.61 DNQ	ND	ND	ND	ND	ND	ND	ND	45.8
	2	Longfin Sanddab	ND	1.62 DNQ	ND	ND	ND	ND	ND	2.82	ND	45.5
	3	Hornyhead Turbot	ND	ND	ND	ND	ND	ND	ND	ND	ND	8.57
TZ6	1	Longfin Sanddab	ND	1.55 DNQ	ND	ND	ND	ND	ND	ND	ND	42.3
	2	Longfin Sanddab	ND	1.58 DNQ	ND	ND	ND	ND	ND	1.86 DNQ	ND	47.2
	3	Longfin Sanddab	ND	1.60 DNQ	ND	ND	ND	ND	ND	1.68 DNQ	ND	46.6
TZ7	1	Longfin Sanddab	ND	1.51 DNQ	ND	ND	ND	ND	ND	ND	ND	45.6
	2	Longfin Sanddab	ND	1.52 DNQ	ND	ND	ND	ND	ND	2.38 DNQ	ND	38.0
	3	Hornyhead Turbot	ND	ND	ND	ND	ND	ND	ND	ND	ND	7.31
TZ8	1	Longfin Sanddab	ND	1.4 DNQ	ND	ND	ND	ND	ND	ND	ND	45.0
	2	CA Scorpionfish	ND	0.67 DNQ	ND	ND	ND	ND	ND	0.863 DNQ	ND	17.7
	3	Hornyhead Turbot	ND	ND	ND	ND	ND	ND	ND	ND	ND	7.42
TZ9	1	Hornyhead Turbot	ND	ND	ND	ND	ND	ND	ND	ND	ND	5.82
	2	Spotted Turbot	ND	ND	ND	ND	ND	ND	ND	ND	ND	2.24
	3	Fantail Sole	ND	ND	ND	ND	ND	ND	ND	ND	ND	NS

Appendix J.6

Concentrations of PCBs (ppb) detected in liver tissues of fishes collected from PLOO and SBOO trawl zones during 2022. See Appendix J.3 for MDLs; DNQ=do not quantify; ND = not detected; NR = not reportable.

		PCB Congener										
Zone	Comp	Species	8	18	28	37	44	49	52	66	70	74
TZ1	1	Pacific Sanddab	ND	ND	0.629 DNQ	ND	1.43 DNQ	3.38	8.06	3.32	4.31	1.80 DNQ
	2	Pacific Sanddab	ND	ND	0.693 DNQ	ND	0.647 DNQ	1.66 DNQ	2.26 DNQ	1.75 DNQ	1.37 DNQ	0.786 DNQ
	3	Pacific Sanddab	ND	ND	1.09 DNQ	ND	1.05 DNQ	2.94	3.67	2.91	2.22 DNQ	1.47 DNQ
TZ2	1	Pacific Sanddab	ND	ND	ND	ND	ND	0.843 DNQ	1.13 DNQ	0.928 DNQ	0.778 DNQ	ND
	2	Pacific Sanddab	ND	ND	ND	ND	0.461 DNQ	1.14 DNQ	1.43 DNQ	1.22 DNQ	0.951 DNQ	ND
	3	Pacific Sanddab	ND	ND	ND	ND	ND	ND	1.16 DNQ	1.03 DNQ	ND	ND
TZ3	1	Pacific Sanddab	ND	ND	1.05 DNQ	ND	1.15 DNQ	3.91	5.10	3.35	2.71 DNQ	1.66 DNQ
	2	Pacific Sanddab	ND	ND	0.863 DNQ	ND	0.928 DNQ	2.94	3.87	2.70	2.16 DNQ	1.40 DNQ
	3	Pacific Sanddab	ND	ND	0.958 DNQ	ND	1.11 DNQ	3.39	4.14	2.92 DNQ	2.30 DNQ	1.30 DNQ
TZ4	1	Pacific Sanddab	ND	ND	0.604 DNQ	ND	0.649 DNQ	1.58 DNQ	2.01 DNQ	1.53 DNQ	1.17 DNQ	0.753 DNQ
	2	Pacific Sanddab	ND	ND	ND	ND	0.423 DNQ	1.24 DNQ	1.62 DNQ	1.24 DNQ	0.954 DNQ	ND
	3	Pacific Sanddab	ND	ND	ND	ND	ND	1.03 DNQ	1.48 DNQ	1.07 DNQ	0.907 DNQ	ND
TZ5	1	Longfin Sanddab	ND	ND	ND	ND	ND	ND	1.33 DNQ	1.55 DNQ	ND	0.835 DNQ
	2	Longfin Sanddab	ND	ND	0.637 DNQ	ND	ND	0.848 DNQ	1.53 DNQ	1.78 DNQ	0.784 DNQ	0.925 DNQ
	3	Hornyhead Turbot	ND	ND	ND	ND	ND	ND	ND	ND	ND	ND
TZ6	1	Longfin Sanddab	ND	ND	ND	ND	ND	ND	1.28 DNQ	1.65 DNQ	ND	ND
	2	Longfin Sanddab	ND	ND	ND	ND	ND	ND	1.09 DNQ	1.34 DNQ	ND	ND
	3	Longfin Sanddab	ND	ND	ND	ND	ND	ND	0.745 DNQ	1.08 DNQ	ND	ND
TZ7	1	Longfin Sanddab	ND	ND	1.05 DNQ	ND	ND	1.42 DNQ	1.80 DNQ	2.50 DNQ	1.06 DNQ	1.11 DNQ
	2	Longfin Sanddab	ND	ND	1.43 DNQ	ND	ND	1.43 DNQ	1.85 DNQ	2.91	1.07 DNQ	1.19 DNQ
	3	Hornyhead Turbot	ND	ND	ND	ND	ND	ND	ND	ND	ND	ND
TZ8	1	Longfin Sanddab	ND	ND	ND	ND	ND	ND	0.614 DNQ	ND	ND	ND
	2	CA Scorpionfish	ND	ND	ND	ND	ND	ND	0.953 DNQ	1.04 DNQ	ND	ND
	3	Hornyhead Turbot	ND	ND	ND	ND	ND	ND	ND	ND	ND	ND
TZ9	1	Hornyhead Turbot	ND	ND	ND	ND	ND	ND	ND	ND	ND	ND
	2	Spotted Turbot	ND	ND	ND	ND	ND	ND	ND	ND	ND	ND
	3	Fantail Sole	ND	ND	ND	ND	ND	ND	ND	ND	ND	ND

Appendix J.6 *continued*

		PCB Congener										
Zone	Comp Species	77	81	87	99	101	105	110	114	118	119	
TZ1	1 Pacific Sanddab	ND	ND	7.14	16.2	19.3	9.55	18.2	ND	26.2	0.944 DNQ	
	2 Pacific Sanddab	ND	ND	1.15 DNQ	8.38	5.34	2.63 DNQ	4.08	ND	10.0	ND	
	3 Pacific Sanddab	ND	ND	1.99 DNQ	13.2	8.87	5.20	8.12	ND	16.9	ND	
TZ2	1 Pacific Sanddab	ND	ND	ND	4.19	2.67	1.38 DNQ	ND	ND	4.99	ND	
	2 Pacific Sanddab	ND	ND	ND	5.10	3.50	1.52 DNQ	2.77 DNQ	ND	5.47	ND	
	3 Pacific Sanddab	ND	ND	ND	4.27	2.67 DNQ	1.49 DNQ	2.04 DNQ	ND	5.55	ND	
TZ3	1 Pacific Sanddab	ND	ND	2.68 DNQ	17.7	11.6	6.35	10.5	ND	25.2	1.03 DNQ	
	2 Pacific Sanddab	ND	ND	1.91 DNQ	13.1	9.44	5.28	8.04	ND	17.8	ND	
	3 Pacific Sanddab	ND	ND	1.95 DNQ	11.5	10.4	3.38	6.76	ND	13.7	ND	
TZ4	1 Pacific Sanddab	ND	ND	1.29 DNQ	7.17	6.31	2.11 DNQ	4.57	ND	8.62	ND	
	2 Pacific Sanddab	ND	ND	0.889 DNQ	5.79	4.20	1.82 DNQ	2.89	ND	6.89	ND	
	3 Pacific Sanddab	ND	ND	ND	5.45	3.56	2.06 DNQ	2.69 DNQ	ND	7.78	ND	
TZ5	1 Longfin Sanddab	ND	ND	ND	7.94	4.13	3.01	1.68 DNQ	ND	9.95	ND	
	2 Longfin Sanddab	ND	ND	ND	8.40	4.48	2.74	1.78 DNQ	ND	10.9	ND	
	3 Hornyhead Turbot	ND	ND	ND	1.62 DNQ	0.860 DNQ	ND	ND	ND	0.869 DNQ	ND	
TZ6	1 Longfin Sanddab	ND	ND	ND	8.99	4.33	2.33 DNQ	2.22 DNQ	ND	11.3	ND	
	2 Longfin Sanddab	ND	ND	ND	5.97	3.52	1.87 DNQ	1.60 DNQ	ND	7.65	ND	
	3 Longfin Sanddab	ND	ND	ND	6.47	2.75 DNQ	2.12 DNQ	1.16 DNQ	ND	8.52	ND	
TZ7	1 Longfin Sanddab	ND	ND	ND	10.7	5.73	3.51	2.78 DNQ	ND	12.8	ND	
	2 Longfin Sanddab	ND	ND	ND	12.5	6.31	3.42	2.92	ND	14.3	ND	
	3 Hornyhead Turbot	ND	ND	ND	1.67 DNQ	1.44 DNQ	ND	ND	ND	1.74 DNQ	ND	
TZ8	1 Longfin Sanddab	ND	ND	ND	3.49	1.85 DNQ	1.54 DNQ	0.774 DNQ	ND	4.71	ND	
	2 CA Scorpionfish	ND	ND	1.00 DNQ	5.38	5.38	2.57 DNQ	2.37 DNQ	ND	9.38	ND	
	3 Hornyhead Turbot	ND	ND	ND	0.652 DNQ	0.553 DNQ	ND	ND	ND	ND	ND	
TZ9	1 Hornyhead Turbot	ND	ND	ND	0.477 DNQ	ND	ND	ND	ND	ND	ND	
	2 Spotted Turbot	ND	ND	ND	1.75 DNQ	2.35 DNQ	ND	0.614 DNQ	ND	3.38	ND	
	3 Fantail Sole	ND	ND	ND	ND	ND	ND	ND	ND	ND	ND	

Appendix J.6 *continued*

PCB Congener

Zone	Comp Species	123	126	128	138	149	151	153/168	156	157	158
TZ1	1 Pacific Sanddab	2.15 DNQ	ND	6.46	27.3	7.14	3.09	41.5	2.64 DNQ	0.690 DNQ	1.74 DNQ
	2 Pacific Sanddab	0.938 DNQ	ND	3.60	14.9	3.67	2.11 DNQ	32.9	1.70 DNQ	ND	1.33 DNQ
	3 Pacific Sanddab	1.67 DNQ	ND	6.06	23.4	5.90	3.06	59.4	2.80	0.669 DNQ	2.12 DNQ
TZ2	1 Pacific Sanddab	ND	ND	1.68 DNQ	6.54	2.01 DNQ	1.05 DNQ	14.3	ND	ND	ND
	2 Pacific Sanddab	ND	ND	2.02 DNQ	7.55	2.62 DNQ	1.03 DNQ	19.3	ND	ND	ND
	3 Pacific Sanddab	ND	ND	1.70 DNQ	6.36	2.63 DNQ	0.932 DNQ	17.0	ND	ND	ND
TZ3	1 Pacific Sanddab	2.42 DNQ	ND	7.00	29.7	5.67	3.87	29.5	3.48	0.841 DNQ	2.75 DNQ
	2 Pacific Sanddab	1.67 DNQ	ND	5.61	21.9	6.72	3.54	52.8	2.54 DNQ	ND	2.38 DNQ
	3 Pacific Sanddab	1.51 DNQ	ND	3.49	18.1	6.68	2.81 DNQ	43.1	1.90 DNQ	ND	1.60 DNQ
TZ4	1 Pacific Sanddab	0.877 DNQ	ND	3.99	20.9	19.6	6.45	51.6	2.38 DNQ	ND	2.57
	2 Pacific Sanddab	0.676 DNQ	ND	2.24 DNQ	11.4	2.47 DNQ	1.35 DNQ	25.9	ND	ND	0.831 DNQ
	3 Longfin Sanddab	0.802 DNQ	ND	2.01 DNQ	9.64	2.12 DNQ	1.44 DNQ	18.4	ND	ND	ND
TZ5	1 Longfin Sanddab	1.16 DNQ	ND	3.21	17.4	3.03	2.02 DNQ	40.0	1.55 DNQ	ND	0.921 DNQ
	2 Hornyhead Turbot	1.17 DNQ	ND	3.17	17.2	3.09	2.17 DNQ	41.9	1.46 DNQ	ND	1.01 DNQ
	3 Spotted Turbot	ND	ND	ND	1.38 DNQ	ND	ND	3.35 DNQ	ND	ND	ND
TZ6	1 Longfin Sanddab	1.24 DNQ	ND	3.17 DNQ	19.9	3.92	2.35 DNQ	36.5	ND	ND	ND
	2 Longfin Sanddab	1.01 DNQ	ND	2.27 DNQ	12.1	4.00	1.81 DNQ	25.7	ND	ND	ND
	3 Longfin Sanddab	0.854 DNQ	ND	2.47 DNQ	15.0	3.26	1.88 DNQ	31.8	ND	ND	ND
TZ7	1 Longfin Sanddab	1.61 DNQ	ND	3.63	19.5	5.89	2.53 DNQ	39.6	1.65 DNQ	ND	1.15 DNQ
	2 Longfin Sanddab	1.61 DNQ	ND	4.15	19.6	7.03	2.64	44.0	1.75 DNQ	ND	1.26 DNQ
	3 Longfin Sanddab	ND	ND	ND	2.72 DNQ	1.25 DNQ	ND	6.29	ND	ND	ND
TZ8	1 Hornyhead Turbot	ND	ND	1.40 DNQ	7.37	2.11 DNQ	1.03 DNQ	15.9	ND	ND	ND
	2 CA Scorpionfish	ND	ND	ND	1.06 DNQ	ND	ND	2.53 DNQ	ND	ND	ND
	3 Longfin Sanddab	1.11 DNQ	ND	2.93	14.2	3.69	1.77 DNQ	29.1	1.31 DNQ	ND	0.974 DNQ
TZ9	1 Hornyhead Turbot	ND	ND	ND	0.999 DNQ	ND	ND	2.11 DNQ	ND	ND	ND
	2 Spotted Turbot	ND	ND	ND	3.31	1.13 DNQ	ND	7.91	ND	ND	ND
	3 Fantail Sole	ND	ND	ND	ND	ND	ND	1.25 DNQ	ND	ND	ND

Appendix J.6 *continued*

		PCB Congener													
Zone	Comp Species	167	169	170	177	180	183	187	189	194	195	201	206		
TZ1	1 Pacific Sanddab	1.46 DNQ	ND	4.93	2.13 DNQ	12.9	3.81	11.2	ND	4.38	1.37	ND	NR		
	2 Pacific Sanddab	1.02 DNQ	ND	4.79	1.84 DNQ	14.2	3.94	11.3	ND	4.51	1.49	ND	NR		
	3 Pacific Sanddab	1.69 DNQ	ND	7.63	2.86	20.5	6.02	17.2	ND	7.25	2.37 DNQ	ND	NR		
TZ2	1 Pacific Sanddab	ND	ND	2.26 DNQ	ND	5.23	1.64 DNQ	5.26	ND	1.98 DNQ	ND	ND	NR		
	2 Pacific Sanddab	ND	ND	2.83 DNQ	ND	9.18	2.21 DNQ	6.34	ND	2.75 DNQ	ND	ND	NR		
	3 Pacific Sanddab	ND	ND	2.13 DNQ	ND	5.14	1.76 DNQ	5.29	ND	2.01 DNQ	ND	ND	NR		
TZ3	1 Pacific Sanddab	2.10 DNQ	ND	7.28	3.11	19.9	6.36	18.7	ND	6.67	2.15 DNQ	ND	4.71		
	2 Pacific Sanddab	1.54 DNQ	ND	6.40	3.15	16.0	5.02	16.3	ND	5.55	1.73 DNQ	ND	NR		
	3 Pacific Sanddab	1.24 DNQ	ND	4.49	2.50 DNQ	11.9	3.88	11.5	ND	3.76	1.32 DNQ	ND	NR		
TZ4	1 Pacific Sanddab	1.25 DNQ	ND	15.3	8.50	38.2	9.79	23.6	ND	9.53	4.00	1.15 DNQ	NR		
	2 Pacific Sanddab	ND	ND	2.78	1.16 DNQ	7.69	2.26 DNQ	6.90	ND	2.61	ND	ND	NR		
	3 Pacific Sanddab	ND	ND	2.02 DNQ	ND	6.03	1.92 DNQ	6.49	ND	2.00 DNQ	ND	ND	NR		
TZ5	1 Longfin Sanddab	0.99 DNQ	ND	3.89	2.72 DNQ	9.38	3.56	15.3	ND	3.36	1.24 DNQ	ND	NR		
	2 Longfin Sanddab	1.04 DNQ	ND	3.70	2.63	8.02	2.97	14.1	ND	2.94	1.18 DNQ	ND	NR		
	3 Hornyhead Turbot	ND	ND	ND	ND	0.807 DNQ	ND	1.01 DNQ	ND	ND	ND	ND	NR		
TZ6	1 Longfin Sanddab	ND	ND	3.71 DNQ	2.37 DNQ	7.90	2.83 DNQ	13.6	ND	3.41 DNQ	ND	ND	2.27 DNQ		
	2 Longfin Sanddab	ND	ND	2.41 DNQ	1.92 DNQ	4.78	1.75 DNQ	9.84	ND	1.87 DNQ	ND	ND	1.96 DNQ		
	3 Longfin Sanddab	ND	ND	3.22	1.94 DNQ	7.29	2.36 DNQ	12.1	ND	2.43 DNQ	ND	ND	2.22 DNQ		
TZ7	1 Longfin Sanddab	1.13 DNQ	ND	3.94	2.56 DNQ	8.52	2.88 DNQ	13.9	ND	3.23	ND	ND	2.67 DNQ		
	2 Longfin Sanddab	1.28 DNQ	ND	4.20	3.07	8.42	2.78	15.2	ND	2.99	1.17 DNQ	ND	2.64		
	3 Hornyhead Turbot	ND	ND	0.704 DNQ	ND	1.64 DNQ	ND	1.99 DNQ	ND	0.776 DNQ	ND	ND	1.10 DNQ		
TZ8	1 Longfin Sanddab	ND	ND	1.54 DNQ	ND	2.97 DNQ	ND	6.00	ND	1.01 DNQ	ND	ND	1.40 DNQ		
	2 CA Scorpionfish	0.877 DNQ	ND	3.50	2.50 DNQ	8.02	2.41 DNQ	10.3	ND	2.75	ND	ND	2.13 DNQ		
	3 Hornyhead Turbot	ND	ND	ND	ND	ND	ND	0.902 DNQ	ND	ND	ND	ND	ND		
TZ9	1 Hornyhead Turbot	ND	ND	ND	ND	ND	ND	ND	ND	ND	ND	ND	ND		
	2 Spotted Turbot	ND	ND	0.659 DNQ	ND	1.48 DNQ	ND	1.71 DNQ	ND	ND	ND	ND	1.22 DNQ		
	3 Fantail Sole	ND	ND	ND	ND	ND	ND	ND	ND	ND	ND	ND	ND		

Appendix J.7

Concentrations of PAHs (ppb) detected in liver tissues of fishes collected from PLOO and SBOO trawl zones during 2022. See Appendix J.3 for MDLs; DNQ=do not quantify; ND = not detected; NR = not reportable.

Zone	Comp	Species	1-methyl naphthalene	1-methyl phenanthrene	2-methyl naphthalene	2,3,5-trimethyl naphthalene	2,6-dimethyl naphthalene	3,4-benzo(B) fluoranthene	Acenaphthene	Acenaphthylene	Anthracene	Benzo[A] anthracene	Benzo[A] pyrene
TZ1	1	Pacific Sanddab	ND	ND	ND	ND	ND	ND	ND	ND	ND	ND	ND
	2	Pacific Sanddab	NR	NR	NR	NR	NR	NR	NR	NR	NR	NR	NR
	3	Pacific Sanddab	ND	ND	ND	ND	ND	ND	ND	ND	ND	ND	ND
TZ2	1	Pacific Sanddab	NR	NR	NR	NR	NR	NR	NR	NR	NR	NR	NR
	2	Pacific Sanddab	NR	NR	NR	NR	NR	NR	NR	NR	NR	NR	NR
	3	Pacific Sanddab	ND	ND	ND	ND	ND	ND	ND	ND	ND	ND	ND
TZ3	1	Pacific Sanddab	NR	NR	NR	NR	NR	NR	NR	NR	NR	NR	NR
	2	Pacific Sanddab	NR	NR	NR	NR	NR	NR	NR	NR	NR	NR	NR
	3	Pacific Sanddab	ND	ND	ND	ND	ND	ND	ND	ND	ND	ND	ND
TZ4	1	Pacific Sanddab	NR	NR	NR	NR	NR	NR	NR	NR	NR	NR	NR
	2	Pacific Sanddab	ND	ND	ND	ND	ND	ND	ND	ND	ND	ND	ND
	3	Pacific Sanddab	ND	ND	ND	ND	ND	ND	ND	ND	ND	ND	ND
TZ5	1	Longfin Sanddab	NR	NR	NR	NR	NR	NR	NR	NR	NR	NR	NR
	2	Longfin Sanddab	ND	ND	ND	ND	ND	ND	ND	ND	ND	ND	ND
	3	Hornyhead Turbot	ND	ND	ND	ND	ND	ND	ND	ND	ND	ND	ND
TZ6	1	Longfin Sanddab	ND	ND	ND	ND	ND	ND	ND	ND	ND	ND	ND
	2	Longfin Sanddab	ND	ND	ND	ND	ND	ND	ND	ND	ND	ND	ND
	3	Longfin Sanddab	ND	ND	ND	ND	ND	ND	ND	ND	ND	ND	ND
TZ7	1	Longfin Sanddab	ND	ND	ND	ND	ND	ND	ND	ND	ND	ND	ND
	2	Longfin Sanddab	ND	ND	ND	ND	ND	ND	ND	ND	ND	ND	ND
	3	Hornyhead Turbot	ND	ND	ND	ND	ND	ND	ND	ND	ND	ND	ND
TZ8	1	Longfin Sanddab	NR	NR	NR	NR	NR	NR	NR	NR	NR	NR	NR
	2	CA Scorpionfish	NR	NR	NR	NR	NR	NR	NR	NR	NR	NR	NR
	3	Hornyhead Turbot	NR	NR	NR	NR	NR	NR	NR	NR	NR	NR	NR
TZ9	1	Hornyhead Turbot	NR	NR	NR	NR	NR	NR	NR	NR	NR	NR	NR
	2	Spotted Turbot	NR	NR	NR	NR	NR	NR	NR	NR	NR	NR	NR
	3	Fantail Sole	NR	NR	NR	NR	NR	NR	NR	NR	NR	NR	NR

Appendix J.7 *continued*

Zone	Comp	Species	Benzo[e]pyrene	Benzo[a,H,I]perylene	Benzo[k]fluoranthene	Biphenyl	Chrysene	Dibenzo[A,H]anthracene	Fluoranthene	Fluorene	Indeno[1,2,3-cd]pyrene	Naphthalene	Perylene	Phenanthrene	Pyrene
TZ1	1	Pacific Sanddab	ND	ND	ND	ND	ND	ND	ND	ND	ND	ND	ND	ND	ND
	2	Pacific Sanddab	NR	NR	NR	NR	NR	NR	NR	NR	NR	NR	NR	NR	NR
	3	Pacific Sanddab	ND	ND	ND	ND	ND	ND	ND	ND	ND	ND	ND	ND	ND
TZ2	1	Pacific Sanddab	NR	NR	NR	NR	NR	NR	NR	NR	NR	NR	NR	NR	NR
	2	Pacific Sanddab	NR	NR	NR	NR	NR	NR	NR	NR	NR	NR	NR	NR	NR
	3	Pacific Sanddab	ND	ND	ND	ND	ND	ND	ND	ND	ND	ND	ND	ND	ND
TZ3	1	Pacific Sanddab	NR	NR	NR	NR	NR	NR	NR	NR	NR	NR	NR	NR	NR
	2	Pacific Sanddab	NR	NR	NR	NR	NR	NR	NR	NR	NR	NR	NR	NR	NR
	3	Pacific Sanddab	ND	ND	ND	ND	ND	ND	ND	ND	ND	ND	ND	ND	ND
TZ4	1	Pacific Sanddab	NR	NR	NR	NR	NR	NR	NR	NR	NR	NR	NR	NR	NR
	2	Pacific Sanddab	ND	ND	ND	ND	ND	ND	ND	ND	ND	ND	ND	ND	ND
	3	Pacific Sanddab	ND	ND	ND	ND	ND	ND	ND	ND	ND	96 DNQ	ND	ND	ND
TZ5	1	Longfin Sanddab	NR	NR	NR	NR	NR	NR	NR	NR	NR	NR	NR	NR	NR
	2	Longfin Sanddab	ND	ND	ND	ND	ND	ND	ND	ND	ND	ND	ND	ND	ND
	3	Hornyhead Turbot	ND	ND	ND	ND	ND	ND	ND	ND	ND	ND	ND	ND	ND
TZ6	1	Longfin Sanddab	ND	ND	ND	ND	ND	ND	ND	ND	ND	ND	ND	ND	ND
	2	Longfin Sanddab	ND	ND	ND	ND	ND	ND	ND	ND	ND	ND	ND	ND	ND
	3	Longfin Sanddab	ND	ND	ND	ND	ND	ND	ND	ND	ND	ND	ND	ND	ND
TZ7	1	Longfin Sanddab	ND	ND	ND	ND	ND	ND	ND	ND	ND	ND	ND	ND	ND
	2	Longfin Sanddab	ND	ND	ND	ND	ND	ND	ND	ND	ND	ND	ND	ND	ND
	3	Hornyhead Turbot	ND	ND	ND	ND	ND	ND	ND	ND	ND	ND	ND	ND	ND
TZ8	1	Longfin Sanddab	NR	NR	NR	NR	NR	NR	NR	NR	NR	NR	NR	NR	NR
	2	CA Scorpionfish	NR	NR	NR	NR	NR	NR	NR	NR	NR	NR	NR	NR	NR
	3	Hornyhead Turbot	NR	NR	NR	NR	NR	NR	NR	NR	NR	NR	NR	NR	NR
TZ9	1	Hornyhead Turbot	NR	NR	NR	NR	NR	NR	NR	NR	NR	NR	NR	NR	NR
	2	Spotted Turbot	NR	NR	NR	NR	NR	NR	NR	NR	NR	NR	NR	NR	NR
	3	Fantail Sole	NR	NR	NR	NR	NR	NR	NR	NR	NR	NR	NR	NR	NR

Appendix J.8

Concentrations of PBDEs (ppb) detected in liver tissues of fishes collected from PLOO and SBOO trawl zones during 2022. See Appendix J.3 for MDLs; DNQ=do not quantify; ND= not detected; NR = not reportable.

		PBDE												
Zone	Comp Species	17	28	47	49	66	85	99	100	138	153	154	183	190
PLOO	TZ1	1	Pacific Sanddab	ND	0.777 DNQ	22.6	ND	ND	ND	6.20	ND	1.63 DNQ	ND	ND
		2	Pacific Sanddab	ND	1.26 DNQ	27.5	1.72 DNQ	ND	7.77	ND	ND	2.13 DNQ	ND	ND
		3	Pacific Sanddab	ND	0.778 DNQ	24.2	1.87 DNQ	ND	7.09	ND	ND	1.89 DNQ	ND	ND
		1	Pacific Sanddab	ND	ND	17.5	ND	ND	4.93	ND	ND	1.76 DNQ	ND	ND
		2	Pacific Sanddab	ND	ND	25.3	1.76 DNQ	ND	5.63	ND	ND	1.91 DNQ	ND	ND
		3	Pacific Sanddab	ND	ND	17.8	ND	ND	4.34	ND	ND	1.54 DNQ	ND	ND
		1	Pacific Sanddab	ND	ND	18.6	ND	ND	6.37	ND	ND	1.77 DNQ	ND	ND
		2	Pacific Sanddab	ND	1.19 DNQ	36.9	2.46 DNQ	ND	8.65	ND	ND	2.57 DNQ	ND	ND
		3	Pacific Sanddab	ND	1.06 DNQ	21.4	ND	ND	5.76	ND	ND	1.79 DNQ	ND	ND
SBOO	TZ4	1	Pacific Sanddab	ND	0.822 DNQ	19.5	1.53 DNQ	ND	5.54	ND	ND	1.64 DNQ	ND	ND
		2	Pacific Sanddab	ND	ND	11.2	ND	ND	3.09	ND	ND	ND	ND	ND
		3	Pacific Sanddab	ND	ND	12.6	ND	ND	3.23	ND	ND	ND	ND	ND
		1	Longfin Sanddab	ND	ND	52.7	2.95	ND	NR	29.3	ND	4.93	10.2	ND
		2	Longfin Sanddab	ND	ND	59.4	3.80	ND	NR	33.5	ND	5.50	10.4	ND
		3	Hornyhead Turbot	ND	ND	20.7	2.09 DNQ	ND	13.9	5.67	ND	3.06	3.32	ND
		1	Longfin Sanddab	ND	ND	35.0	2.93 DNQ	ND	ND	18.3	ND	ND	5.74	ND
		2	Longfin Sanddab	ND	ND	43.2	3.76	ND	3.32	22.9	ND	3.46	7.23	ND
		3	Longfin Sanddab	ND	ND	30.6	2.08 DNQ	ND	ND	19.4	ND	ND	5.79	ND
	1	Longfin Sanddab	ND	ND	20.8	2.47 DNQ	ND	ND	10.4	ND	ND	3.25	ND	
	2	Longfin Sanddab	ND	ND	18.7	2.48 DNQ	ND	2.52 DNQ	10.6	ND	ND	3.77	ND	
	3	Hornyhead Turbot	ND	ND	10.9	ND	ND	4.77	3.42	ND	ND	1.50 DNQ	ND	
	1	Longfin Sanddab	ND	ND	36.5	3.11	ND	2.48 DNQ	19.6	ND	3.13	5.69	ND	
	2	CA Scorpionfish	ND	ND	63.0	1.86 DNQ	ND	ND	14.1	ND	ND	5.14	ND	
	3	Hornyhead Turbot	ND	ND	20.4	1.88 DNQ	ND	17.8	7.07	ND	2.30 DNQ	3.49	ND	
	1	Hornyhead Turbot	ND	ND	18.9	2.34 DNQ	ND	13.3	7.17	ND	ND	2.66 DNQ	ND	
	2	Spotted Turbot	ND	ND	ND	ND	ND	ND	ND	ND	ND	ND	ND	
	3	Fantail Sole	ND	ND	NR	ND	ND	ND	ND	ND	ND	ND	ND	

Appendix J.9

Concentrations of metals (ppm) detected in muscle tissues of fishes collected from PLOO and SBOO rig fishing zones during 2022. See Appendix J.3 for MDLs and abbreviations; DNGQ = do not quantify; ND = not detected; NR = not reportable.

Zone	Comp	Species	Al	Sb	As	Ba	Be	Cd	Cr	Cu	Fe
PLOO	RF1	Vermilion Rockfish	ND	ND	1.60	ND	ND	0.022 DNGQ	0.158 DNGQ	0.433	6.11
	RF1	Vermilion Rockfish	ND	ND	2.92	ND	ND	0.033 DNGQ	0.102 DNGQ	0.429	ND
	RF1	Vermilion Rockfish	ND	ND	3.44	ND	ND	0.044 DNGQ	0.130 DNGQ	0.314	1.57 DNGQ
SBOO	RF2	Squarespot Rockfish	ND	ND	1.36	ND	ND	0.028 DNGQ	0.386	0.327	3.32 DNGQ
	RF2	Starry Rockfish	ND	ND	1.57	ND	ND	0.023 DNGQ	0.119 DNGQ	0.263	ND
	RF2	Mixed Rockfish	ND	ND	1.99	ND	ND	0.029 DNGQ	0.089 DNGQ	0.374	1.14 DNGQ
SBOO	RF3	Brown Rockfish	ND	ND	1.19	ND	ND	0.024 DNGQ	0.100 DNGQ	0.329	4.48
	RF3	CA Scorpionfish	ND	ND	2.39	ND	ND	0.037 DNGQ	0.114 DNGQ	0.338	2.81 DNGQ
	RF3	Mixed Rockfish	ND	ND	3.88	ND	ND	0.060 DNGQ	0.159 DNGQ	0.305	7.52
SBOO	RF4	CA Scorpionfish	ND	ND	2.03	ND	ND	0.034 DNGQ	0.121 DNGQ	0.368	5.12
	RF4	Gopher Rockfish	ND	ND	2.73	ND	ND	0.043 DNGQ	0.114 DNGQ	0.258	3.71 DNGQ
	RF4	Mixed Rockfish	ND	ND	1.40	ND	ND	0.025 DNGQ	0.195 DNGQ	0.249	20.8

Appendix J.9 continued

Zone	Comp	Species	Pb	Mn	Hg	Ni	Se	Ag	Tl	Sn	Zn
RF1	1	Vermilion Rockfish	ND	0.135 DNQ	0.052	ND	0.463 DNQ	ND	0.386 DNQ	ND	4.32
RF1	2	Vermilion Rockfish	ND	ND	0.093	ND	0.657 DNQ	ND	ND	ND	3.64
RF1	3	Vermilion Rockfish	ND	ND	NA	0.056 DNQ	0.799 DNQ	ND	ND	ND	4.31
RF2	1	Squarespot Rockfish	ND	ND	0.111	0.259	0.753 DNQ	ND	0.368 DNQ	ND	3.32
RF2	2	Starry Rockfish	ND	ND	0.224	0.038 DNQ	0.689 DNQ	ND	0.358 DNQ	ND	3.14
RF2	3	Mixed Rockfish	ND	ND	0.149	ND	0.674 DNQ	ND	ND	ND	3.61
RF3	1	Brown Rockfish	ND	0.119 DNQ	0.073	ND	0.683 DNQ	ND	0.385 DNQ	ND	3.75
RF3	2	CA Scorpionfish	ND	ND	0.104	ND	0.500 DNQ	ND	0.351 DNQ	ND	3.69
RF3	3	Mixed Rockfish	ND	ND	0.084	ND	1.22	ND	0.522 DNQ	1.31	4.54
RF4	1	CA Scorpionfish	ND	ND	0.113	ND	0.587 DNQ	ND	0.367 DNQ	ND	4.68
RF4	2	Gopher Rockfish	ND	ND	0.205	ND	0.721 DNQ	ND	0.340 DNQ	ND	3.68
RF4	3	Mixed Rockfish	ND	0.127 DNQ	0.230	0.098	0.667 DNQ	ND	0.375 DNQ	ND	4.19

Appendix J.10

Concentrations of pesticides (ppb) and lipids (% weight) detected in muscle tissues of fishes collected from PLOO and SBOO rig fishing zones during 2022. See Appendix J.3 for MDLs and abbreviations; DNQ=do not quantify; ND=not detected; NR=not reportable; NS=not sampled.

Zone	Comp	Species	Chlordane									
			A(c)C	cNon	G(t)C	Hept	HeptEpoX	Methoxy	Oxychlor	tNon		
PLOO	RF1	1	Vermilion Rockfish	ND	ND	ND	ND	ND	ND	ND	ND	ND
	RF1	2	Vermilion Rockfish	ND	ND	ND	ND	ND	ND	ND	ND	0.167 DNQ
	RF1	3	Vermilion Rockfish	ND	ND	ND	ND	ND	ND	ND	ND	ND
	RF2	1	Squarespot Rockfish	ND	ND	ND	ND	ND	ND	ND	ND	ND
	RF2	2	Starry Rockfish	ND	ND	ND	ND	ND	ND	ND	ND	ND
	RF2	3	Mixed Rockfish	ND	ND	ND	ND	ND	ND	ND	ND	ND
SBOO	RF3	1	Brown Rockfish	ND	ND	ND	ND	ND	ND	ND	ND	ND
	RF3	2	CA Scorpionfish	ND	ND	ND	ND	ND	ND	ND	ND	ND
	RF3	3	Mixed Rockfish	ND	ND	ND	ND	ND	ND	ND	ND	ND
	RF4	1	CA Scorpionfish	ND	ND	ND	ND	ND	ND	ND	ND	ND
	RF4	2	Gopher Rockfish	ND	ND	ND	ND	ND	ND	ND	ND	ND
	RF4	3	Mixed Rockfish	ND	ND	ND	ND	ND	ND	ND	ND	ND

Appendix J.10 *continued*

Zone	Comp Species	DDT										Endosulfan		
		o,p-DDD	o,p-DDE	o,p-DDT	p,-p-DDMU	p,p-DDD	p,p-DDE	p,p-DDT	Alpha	Beta	Sulfate			
PO	RF1 1	ND	0.142 DNQ	ND	0.715	ND	5.57	ND	ND	ND	ND	ND	ND	
	RF1 2	ND	0.071 DNQ	ND	0.363	ND	5.21	0.092 DNQ	ND	ND	ND	ND	ND	
	RF1 3	ND	0.076 DNQ	ND	0.366	ND	4.42	ND	ND	ND	ND	ND	ND	
P	RF2 1	ND	ND	ND	0.125 DNQ	ND	1.95	ND	ND	ND	ND	ND	ND	
	RF2 2	ND	ND	ND	0.131 DNQ	ND	4.92	0.086 DNQ	ND	ND	ND	ND	ND	
	RF2 3	ND	ND	ND	0.074 DNQ	ND	2.52	ND	ND	ND	ND	ND	ND	
SBO	RF3 1	ND	ND	ND	ND	ND	1.58	ND	ND	ND	ND	ND	ND	
	RF3 2	ND	ND	ND	0.119 DNQ	ND	4.25	ND	ND	ND	ND	ND	ND	
	RF3 3	ND	ND	ND	ND	ND	0.494	ND	ND	ND	ND	ND	ND	
RF4	RF4 1	ND	ND	ND	ND	ND	1.55	ND	ND	ND	ND	ND	ND	
	RF4 2	ND	ND	ND	ND	ND	0.922	ND	ND	ND	ND	ND	ND	
	RF4 3	ND	ND	ND	ND	ND	0.555	ND	ND	ND	ND	ND	ND	

Appendix J.10 *continued*

Zone	Comp	Species	HCH							Mirex	Lipids		
			Alpha	Beta	Delta	Gamma	Aldrin	Dieldrin	Endrin			EndAld	HCB
P O	RF1	1	Vermilion Rockfish	ND	0.054 DNQ	ND	ND	ND	ND	ND	ND	ND	1.63
	RF1	2	Vermilion Rockfish	ND	0.047 DNQ	ND	ND	ND	ND	ND	ND	ND	1.34
	RF1	3	Vermilion Rockfish	ND	ND	ND	ND	ND	ND	ND	ND	ND	1.10
P O	RF2	1	Squarespot Rockfish	ND	ND	ND	ND	ND	ND	ND	ND	ND	1.16
	RF2	2	Starry Rockfish	ND	ND	ND	ND	ND	ND	ND	ND	ND	0.797
	RF2	3	Mixed Rockfish	ND	ND	ND	ND	ND	ND	ND	ND	ND	0.835
S B O	RF3	1	Brown Rockfish	ND	ND	ND	ND	ND	ND	ND	ND	ND	0.935
	RF3	2	CA Scorpionfish	ND	ND	ND	ND	ND	ND	ND	ND	ND	1.15
	RF3	3	Mixed Rockfish	ND	ND	ND	ND	ND	ND	ND	ND	ND	0.618
S B O	RF4	1	CA Scorpionfish	ND	ND	ND	ND	ND	ND	ND	ND	ND	0.495
	RF4	2	Gopher Rockfish	ND	ND	ND	ND	ND	ND	ND	ND	ND	2.45
	RF4	3	Mixed Rockfish	ND	ND	ND	ND	ND	ND	ND	ND	ND	0.729

Appendix J.11

Concentrations of PCBs (ppb) detected in muscle tissues of fishes collected from PLOO and SBOO rig fishing zones during 2022. See Appendix J.3 for MDLs; DNQ=do not quantify; ND = not detected; NR = not reportable.

		PCB Congener											
Zone	Comp	Species	8	18	28	37	44	49	52	66	70	74	
PLOO	RF1	1	Vermilion Rockfish	ND	ND	ND	ND	0.089 DNQ	0.127 DNQ	0.088 DNQ	ND	ND	
	RF1	2	Vermilion Rockfish	ND	ND	ND	ND	ND	0.076 DNQ	ND	ND	ND	
	RF1	3	Vermilion Rockfish	ND	ND	ND	ND	ND	0.090 DNQ	ND	ND	ND	
PLOO	RF2	1	Squarespot Rockfish	ND	ND	ND	ND	ND	ND	ND	ND	ND	
	RF2	2	Starry Rockfish	ND	ND	ND	ND	ND	0.059 DNQ	ND	ND	ND	
	RF2	3	Mixed Rockfish	ND	ND	ND	ND	ND	ND	ND	ND	ND	
SBOO	RF3	1	Brown Rockfish	ND	ND	ND	ND	ND	ND	ND	ND	ND	
	RF3	2	CA Scorpionfish	ND	ND	ND	ND	ND	0.117 DNQ	ND	ND	ND	
	RF3	3	Mixed Rockfish	ND	ND	ND	ND	ND	ND	ND	ND	ND	
SBOO	RF4	1	CA Scorpionfish	ND	ND	ND	ND	ND	ND	ND	ND	ND	
	RF4	2	Gopher Rockfish	ND	ND	ND	ND	ND	ND	ND	ND	ND	
	RF4	3	Mixed Rockfish	ND	ND	ND	ND	ND	ND	ND	ND	ND	

Appendix J.11 *continued*

		PCB Congener											
Zone	Comp	Species	77	81	87	99	101	105	110	114	118	119	
POL	RF1	1	Vermilion Rockfish	ND	ND	0.152 DNQ	0.152 DNQ	0.495	0.196 DNQ	ND	0.604	ND	
	RF1	2	Vermilion Rockfish	ND	ND	ND	0.278	0.111 DNQ	0.344	ND	0.569	ND	
	RF1	3	Vermilion Rockfish	ND	ND	0.114 DNQ	0.337	0.191 DNQ	0.159 DNQ	ND	0.650	ND	
	RF2	1	Squarespot Rockfish	ND	ND	ND	0.092 DNQ	ND	ND	ND	ND	ND	
	RF2	2	Starry Rockfish	ND	ND	ND	0.283 DNQ	ND	0.122 DNQ	ND	0.276 DNQ	ND	
	RF2	3	Mixed Rockfish	ND	ND	ND	0.111 DNQ	ND	ND	ND	0.143 DNQ	ND	
	RF3	1	Brown Rockfish	ND	ND	ND	0.112 DNQ	ND	ND	ND	0.114 DNQ	ND	
	RF3	2	CA Scorpionfish	ND	ND	ND	0.300 DNQ	0.081 DNQ	0.101 DNQ	ND	0.362	ND	
	RF3	3	Mixed Rockfish	ND	ND	ND	ND	ND	ND	ND	ND	ND	
SBO	RF4	1	CA Scorpionfish	ND	ND	ND	0.066 DNQ	ND	ND	ND	0.125 DNQ	ND	
	RF4	2	Gopher Rockfish	ND	ND	ND	0.058 DNQ	ND	ND	ND	0.061 DNQ	ND	
	RF4	3	Mixed Rockfish	ND	ND	ND	ND	ND	ND	ND	0.068 DNQ	ND	

Appendix J.11 *continued*

PCB Congener

Zone	Comp	Species	123	126	128	138	149	151	153/168	156	157	158
PO	RF1	1 Vermilion Rockfish	ND	ND	0.167 DNQ	0.642	0.283 DNQ	0.080 DNQ	0.925	ND	ND	ND
	RF1	2 Vermilion Rockfish	ND	ND	0.122 DNQ	0.707	0.250 DNQ	0.082 DNQ	1.68	ND	ND	ND
	RF1	3 Vermilion Rockfish	ND	ND	0.173 DNQ	0.687	0.225 DNQ	ND	1.24	ND	ND	ND
	RF2	1 Squarespot Rockfish	ND	ND	ND	ND	ND	ND	0.284 DNQ	ND	ND	ND
	RF2	2 Starry Rockfish	ND	ND	ND	0.373	0.198 DNQ	ND	0.739	ND	ND	ND
	RF2	3 Mixed Rockfish	ND	ND	0.169 DNQ	ND	ND	ND	0.404 DNQ	ND	ND	ND
	RF3	1 Brown Rockfish	ND	ND	0.16 DNQ	ND	ND	ND	0.340 DNQ	ND	ND	ND
	RF3	2 CA Scorpionfish	ND	ND	ND	0.441	ND	ND	0.922	ND	ND	ND
	RF3	3 Mixed Rockfish	ND	ND	ND	ND	ND	ND	0.104 DNQ	ND	ND	ND
SBO	RF4	1 CA Scorpionfish	ND	ND	0.159 DNQ	ND	ND	ND	0.408 DNQ	ND	ND	ND
	RF4	2 Gopher Rockfish	ND	ND	0.096 DNQ	ND	ND	ND	0.227 DNQ	ND	ND	ND
	RF4	3 Mixed Rockfish	ND	ND	0.106 DNQ	ND	ND	ND	0.268 DNQ	ND	ND	ND

Appendix J.11 *continued*

		PCB Congener												
Zone	Comp	Species	167	169	170	180	183	187	189	194	195	201	206	
PO	RF1	1 Vermilion Rockfish	ND	ND	0.108 DNQ	0.214 DNQ	ND	0.213 DNQ	ND	ND	ND	ND	ND	
	RF1	2 Vermilion Rockfish	ND	ND	0.186 DNQ	0.425	0.145 DNQ	0.402	ND	0.139 DNQ	ND	ND	0.145 DNQ	
	RF1	3 Vermilion Rockfish	ND	ND	0.153 DNQ	0.318 DNQ	ND	0.294 DNQ	ND	0.112 DNQ	ND	ND	ND	
PO	RF2	1 Squarespot Rockfish	ND	ND	ND	ND	ND	ND	ND	ND	ND	ND	ND	
	RF2	2 Starry Rockfish	ND	ND	0.070 DNQ	0.191 DNQ	ND	0.208 DNQ	ND	ND	ND	ND	ND	
	RF2	3 Mixed Rockfish	ND	ND	ND	ND	ND	0.106 DNQ	ND	ND	ND	ND	ND	
SBO	RF3	1 Brown Rockfish	ND	ND	ND	ND	ND	ND	ND	ND	ND	ND	ND	
	RF3	2 CA Scorpionfish	ND	ND	0.092 DNQ	0.230 DNQ	ND	0.263 DNQ	ND	0.077 DNQ	ND	ND	ND	
	RF3	3 Mixed Rockfish	ND	ND	ND	ND	ND	ND	ND	ND	ND	ND	ND	
SBO	RF4	1 CA Scorpionfish	ND	ND	ND	0.091 DNQ	ND	ND	ND	ND	ND	ND	ND	
	RF4	2 Gopher Rockfish	ND	ND	ND	ND	ND	ND	ND	ND	ND	ND	ND	
	RF4	3 Mixed Rockfish	ND	ND	ND	ND	ND	ND	ND	ND	ND	ND	ND	

Appendix J.12

Concentrations of PAHs (ppb) detected in muscle tissues of fishes collected from PLOO and SBOO rig fishing zones during 2022. See Appendix J.3 for MDLs; DNQ=do not quantify; ND = not detected; NR = not reportable.

Zone	Comp	Species	1-methyl naphthalene	1-methyl phenanthrene	2-methyl naphthalene	2,3,5-trimethyl naphthalene	2,6-dimethyl naphthalene	3,4-benzo(B) fluoranthene	Acenaphthene	Acenaphthylene	Anthracene	Benzo(A) anthracene	Benzo(A) pyrene
PLOO	RF1	1	Vermillion Rockfish	ND	ND	ND	ND	ND	ND	ND	ND	ND	ND
	RF1	2	Vermillion Rockfish	ND	ND	ND	ND	ND	ND	ND	ND	ND	ND
	RF1	3	Vermillion Rockfish	ND	ND	ND	ND	ND	ND	ND	ND	ND	ND
	RF2	1	Squarespot Rockfish	ND	ND	ND	ND	ND	ND	ND	ND	ND	ND
	RF2	2	Starry Rockfish	ND	ND	ND	ND	ND	ND	ND	ND	ND	ND
	RF2	3	Mixed Rockfish	ND	ND	ND	ND	ND	ND	ND	ND	ND	ND
SBOO	RF3	1	Brown Rockfish	ND	ND	ND	ND	ND	ND	ND	ND	ND	ND
	RF3	2	CA Scorpionfish	ND	ND	ND	ND	ND	ND	ND	ND	ND	ND
	RF3	3	Mixed Rockfish	ND	ND	ND	ND	ND	ND	ND	ND	ND	ND
	RF4	1	CA Scorpionfish	NR	NR	NR	NR	NR	NR	NR	NR	NR	NR
	RF4	2	Gopher Rockfish	NR	NR	NR	NR	NR	NR	NR	NR	NR	NR
	RF4	3	Mixed Rockfish	NR	NR	NR	NR	NR	NR	NR	NR	NR	NR

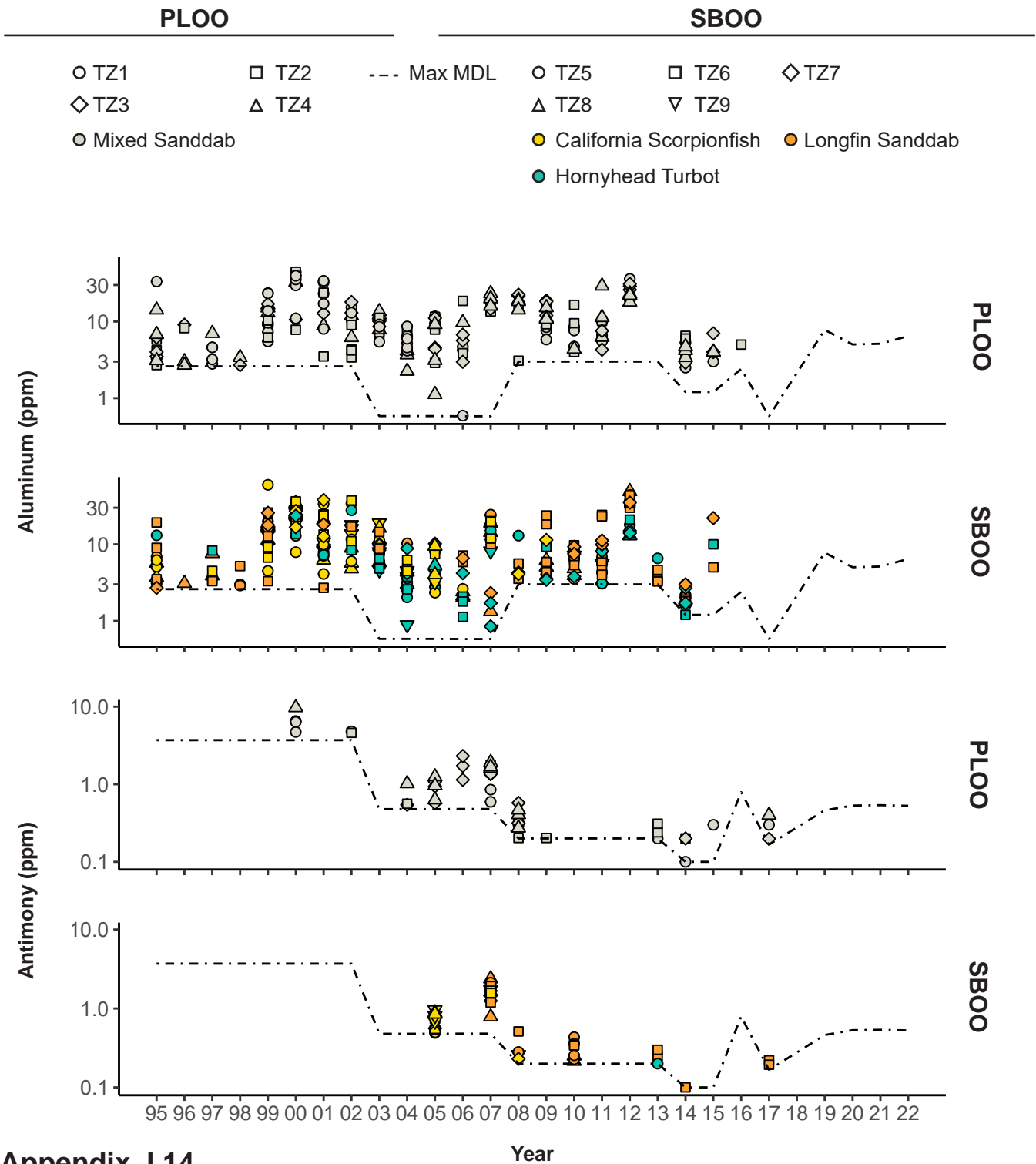
Appendix J.12 *continued*

Zone	Comp	Species	Benzo[e]pyrene	Benzo[G,H,I]perylene	Benzo[K]fluoranthene	Biphenyl	Chrysene	Dibenzo(A,H)anthracene	Fluoranthene	Fluorene	Indeno(1,2,3-CD)pyrene	Naphthalene	Perylene	Phenanthrene	Pyrene
FO	RF1	Vermilion Rockfish	ND	ND	ND	ND	ND	ND	ND	ND	ND	96.5	ND	ND	ND
	RF1	Vermilion Rockfish	ND	ND	ND	ND	ND	ND	ND	ND	ND	ND	ND	ND	ND
	RF1	Vermilion Rockfish	ND	ND	ND	ND	ND	ND	ND	ND	ND	ND	ND	ND	ND
FO	RF2	Squarespot Rockfish	ND	ND	ND	ND	ND	ND	ND	ND	ND	ND	ND	ND	ND
	RF2	Starry Rockfish	ND	ND	ND	ND	ND	ND	ND	ND	ND	ND	ND	ND	ND
	RF2	Mixed Rockfish	ND	ND	ND	ND	ND	ND	ND	ND	ND	ND	ND	ND	ND
SBO	RF3	Brown Rockfish	ND	ND	ND	ND	ND	ND	ND	ND	ND	ND	ND	ND	ND
	RF3	CA Scorpionfish	ND	ND	ND	ND	ND	ND	ND	ND	ND	ND	ND	ND	ND
	RF3	Mixed Rockfish	ND	ND	ND	ND	ND	ND	ND	ND	ND	ND	ND	ND	ND
SBO	RF4	CA Scorpionfish	NR	NR	NR	NR	NR	NR	NR	NR	NR	NR	NR	NR	NR
	RF4	Gopher Rockfish	NR	NR	NR	NR	NR	NR	NR	NR	NR	NR	NR	NR	NR
	RF4	Mixed Rockfish	NR	NR	NR	NR	NR	NR	NR	NR	NR	NR	NR	NR	NR

Appendix J.13

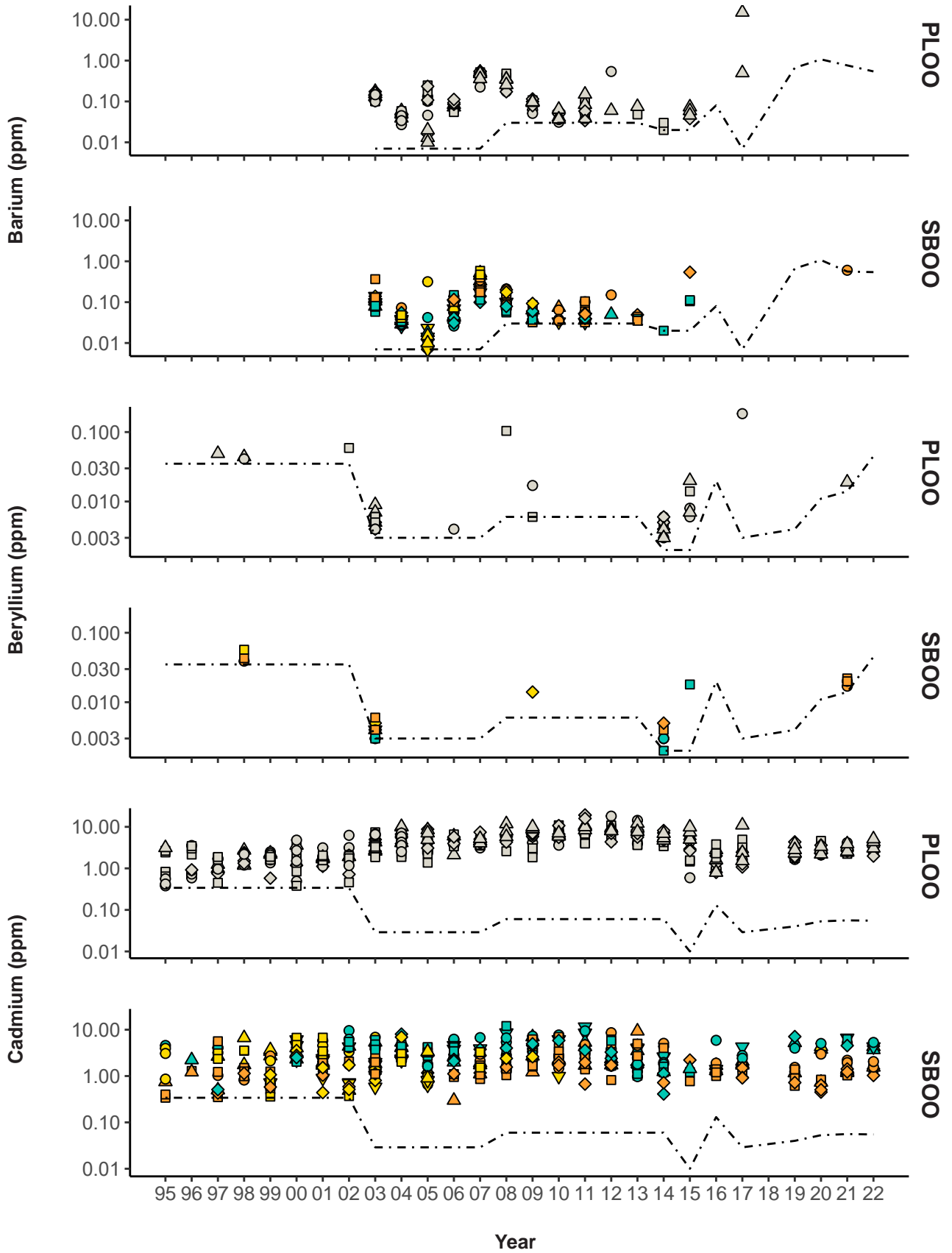
Concentrations of PBDEs (ppb) detected in muscle tissues of fishes collected from PLOO and SBOO rig fishing zones during 2022. See Appendix J.3 for MDLs; DNQ=do not quantify; ND = not detected; NR = not reportable.

Zone	Comp	Species	PBDE															
			17	28	47	49	66	85	99	100	138	153	154	183	190			
PLOO	RF1	1	Vermilion Rockfish	ND	ND	1.27	ND	ND	ND	ND	ND	ND	0.245 DNQ	ND	ND	ND	ND	ND
	RF1	2	Vermilion Rockfish	ND	ND	1.76	ND	ND	ND	ND	ND	0.429	0.104 DNQ	ND	ND	ND	ND	ND
	RF1	3	Vermilion Rockfish	ND	ND	1.25	ND	ND	ND	ND	ND	0.262 DNQ	ND	ND	ND	ND	ND	ND
	RF2	1	Squarespot Rockfish	ND	ND	0.472	ND	ND	ND	ND	ND	ND	ND	ND	ND	ND	ND	ND
	RF2	2	Starry Rockfish	ND	ND	1.05	ND	ND	ND	ND	ND	0.270 DNQ	ND	ND	ND	ND	ND	ND
	RF2	3	Mixed Rockfish	ND	ND	0.687	ND	ND	ND	ND	ND	0.148 DNQ	ND	ND	ND	ND	ND	ND
				ND	ND	1.76	ND	ND	ND	ND	ND	0.327	ND	ND	ND	ND	ND	ND
				ND	ND	2.52	ND	ND	ND	ND	ND	0.477	0.123 DNQ	ND	ND	ND	ND	ND
				ND	ND	1.47	ND	ND	ND	ND	ND	0.162 DNQ	ND	ND	ND	ND	ND	ND
SBOO	RF3	1	Brown Rockfish	ND	ND	0.377	ND	ND	ND	ND	ND	ND	ND	ND	ND	ND	ND	ND
	RF3	2	CA Scorpionfish	ND	ND	0.311	ND	ND	ND	ND	ND	ND	ND	ND	ND	ND	ND	ND
	RF3	3	Mixed Rockfish	ND	ND	ND	ND	ND	ND	ND	ND	ND	ND	ND	ND	ND	ND	ND
	RF4	1	CA Scorpionfish	ND	ND	35.0	2.93 DNQ	ND	ND	ND	ND	18.3	5.74	ND	ND	ND	ND	ND
	RF4	2	Gopher Rockfish	ND	ND	43.2	3.76	ND	ND	ND	3.32	22.9	7.23	3.46	ND	ND	ND	ND
	RF4	3	Mixed Rockfish	ND	ND	30.6	2.08 DNQ	ND	ND	ND	ND	19.4	5.79	ND	ND	ND	ND	ND

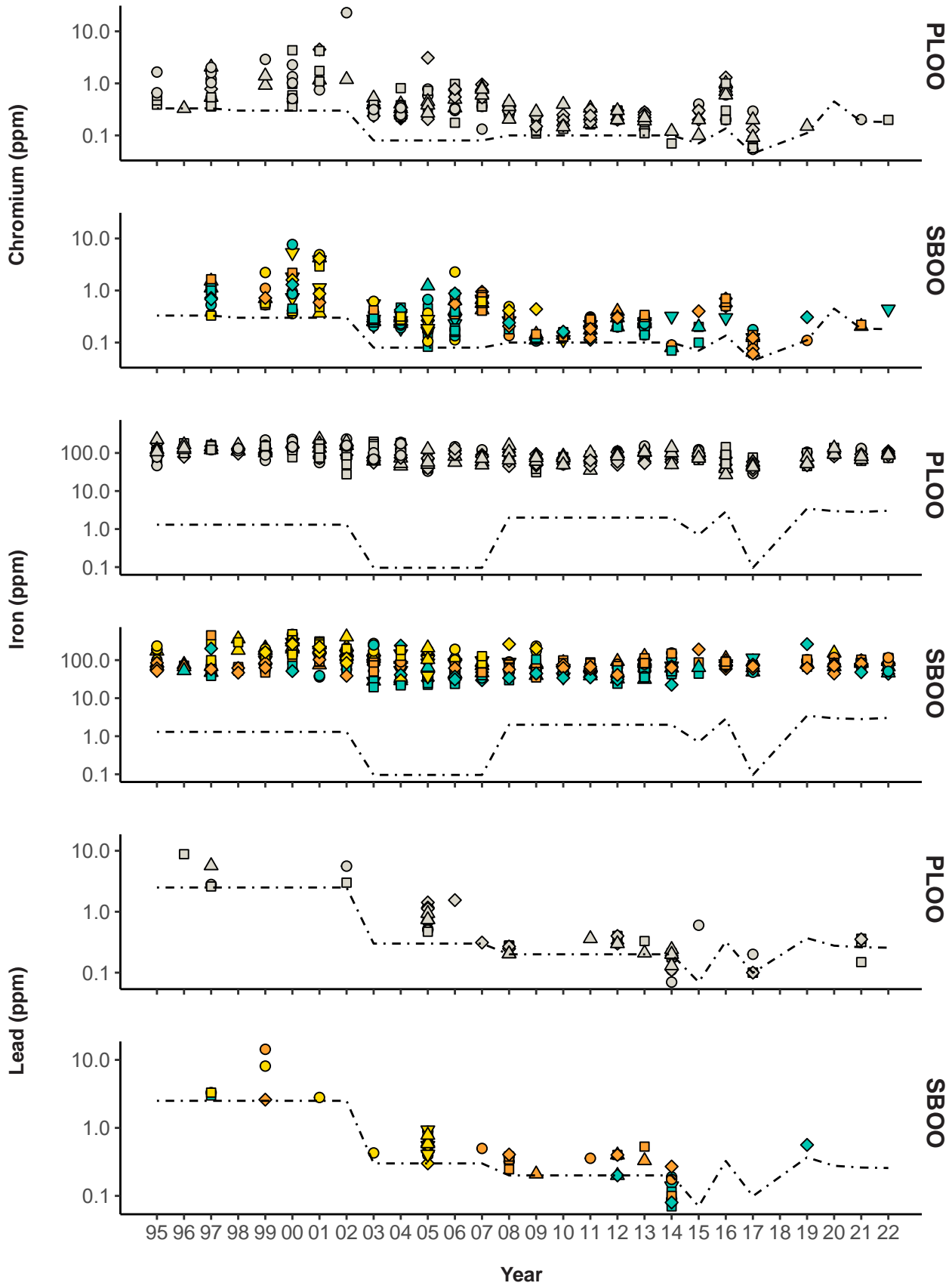


Appendix J.14

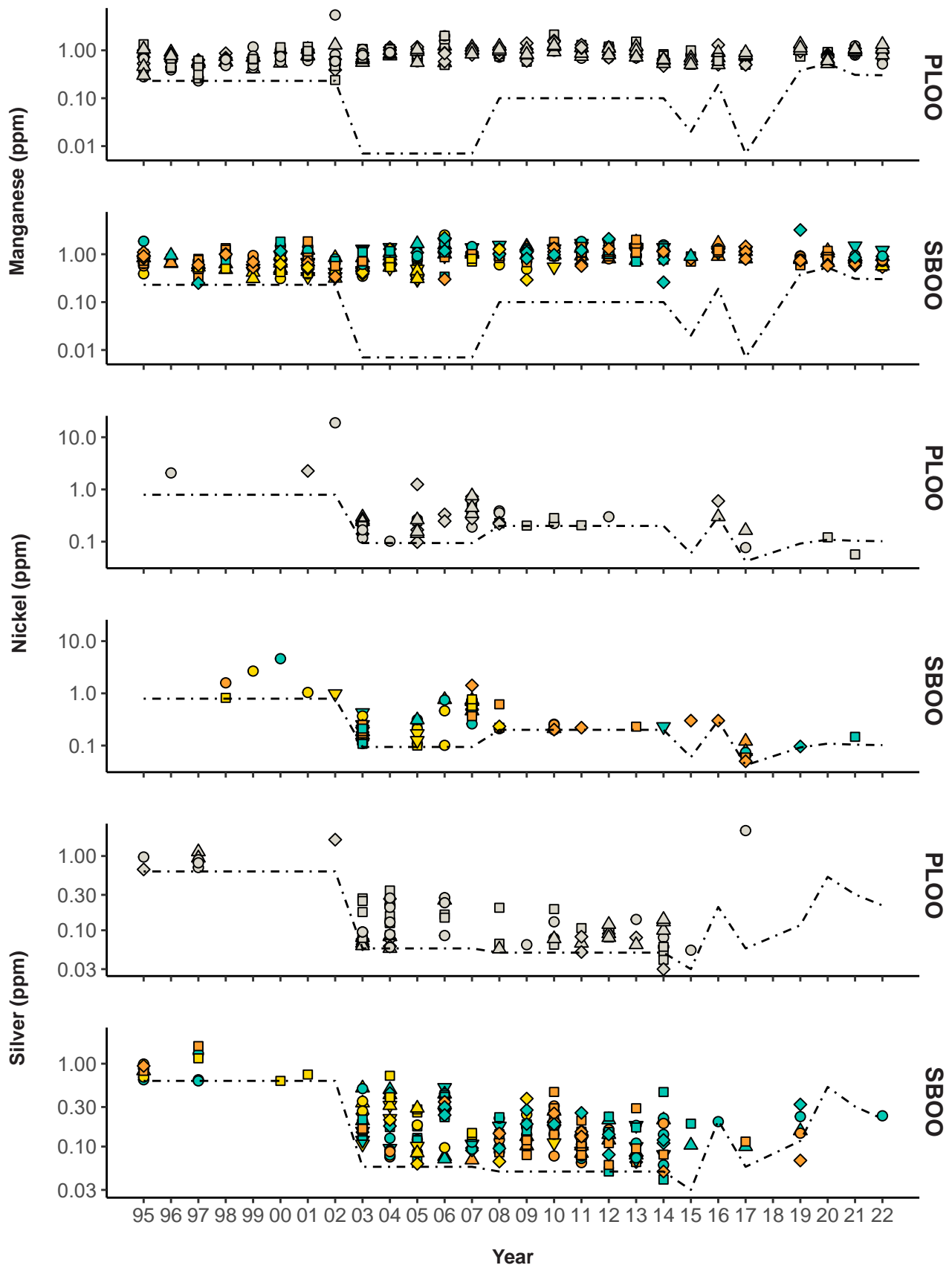
Concentrations of select metals in liver tissues of fishes collected from PLOO and SBOO trawl zones from 1995 through 2022. Zones TZ1 and TZ5 are considered nearfield. No samples were collected in 2018 and 2023 as described in text.



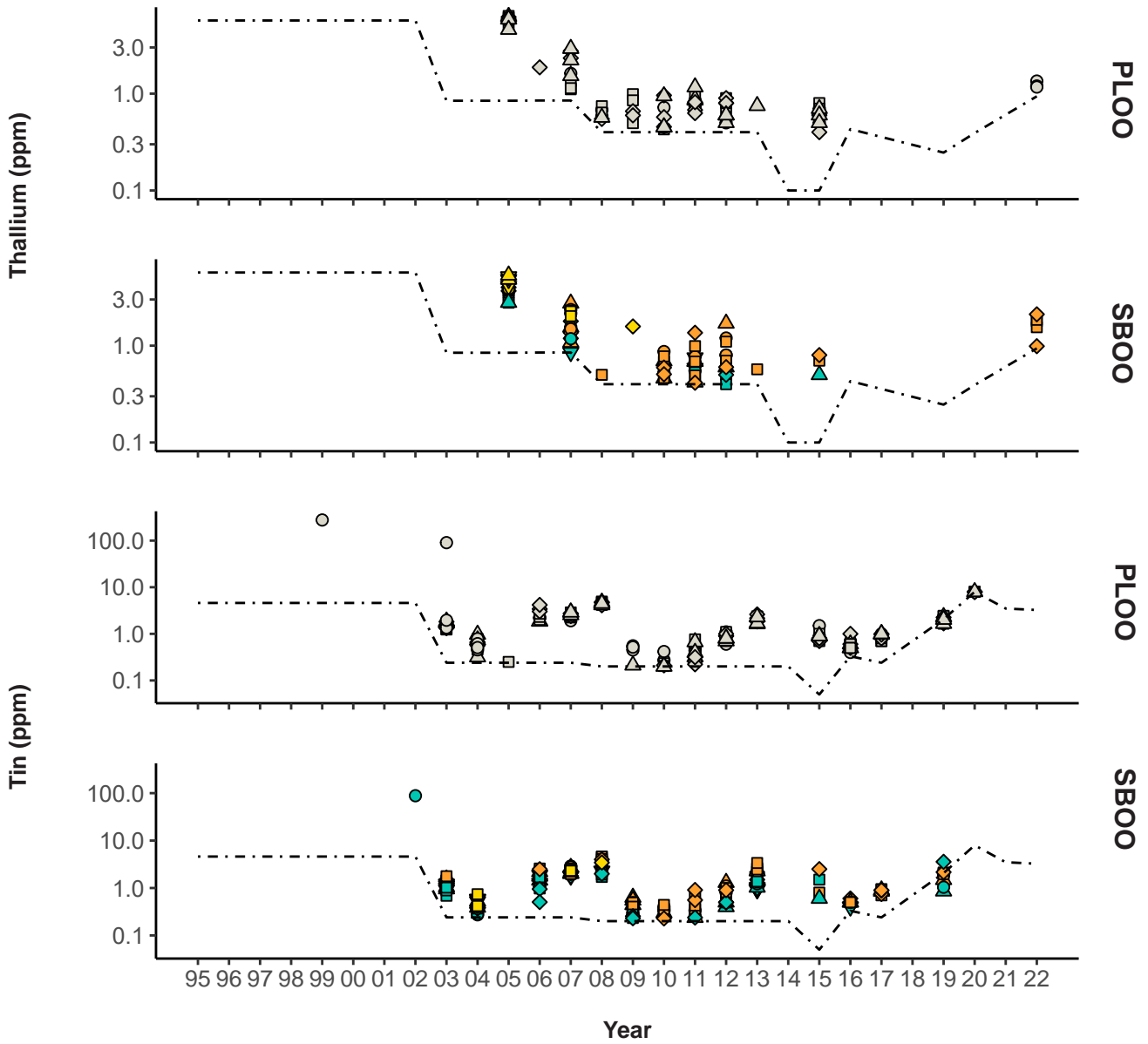
Appendix J.14 *continued*



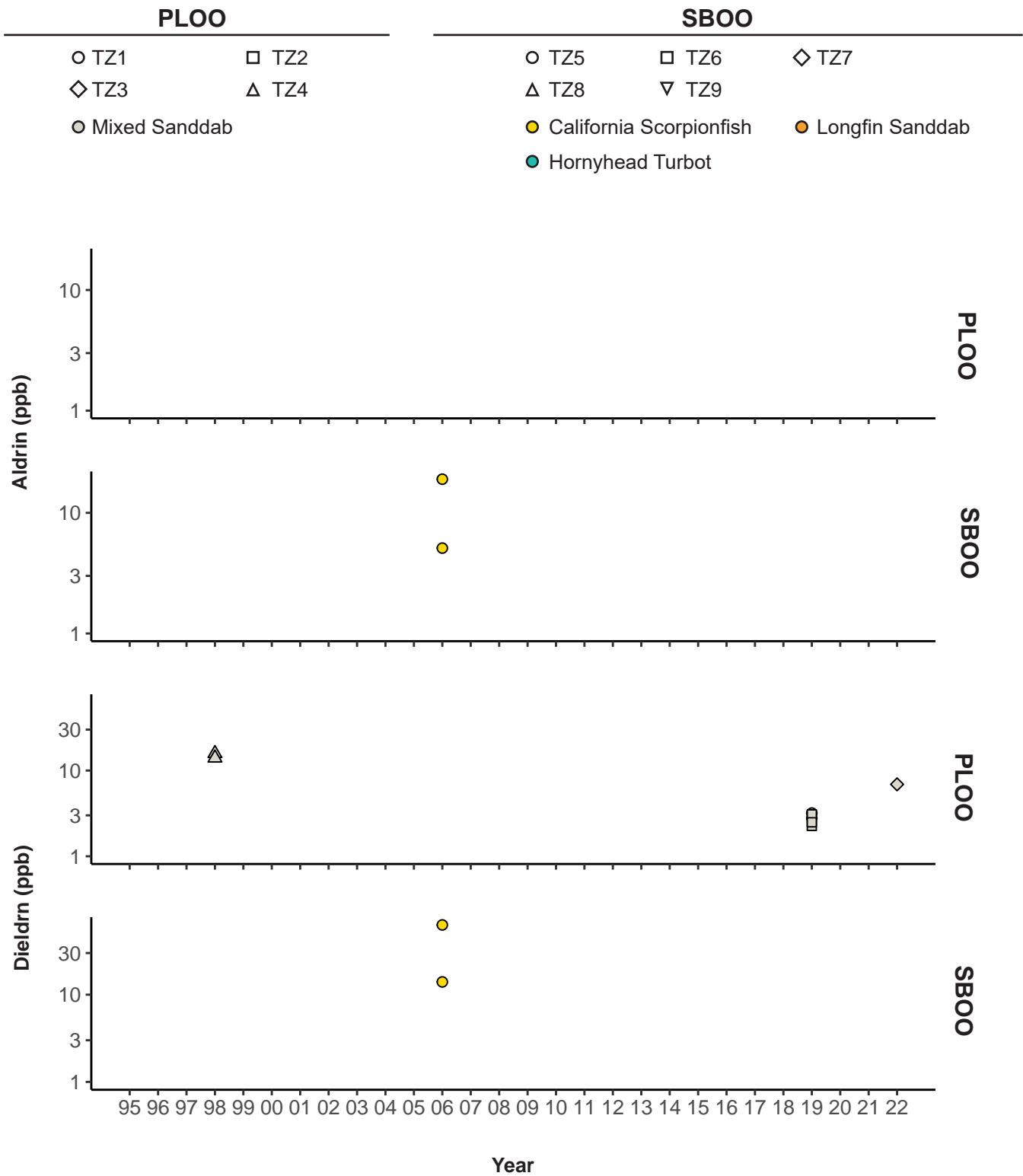
Appendix J.14 *continued*



Appendix J.14 *continued*

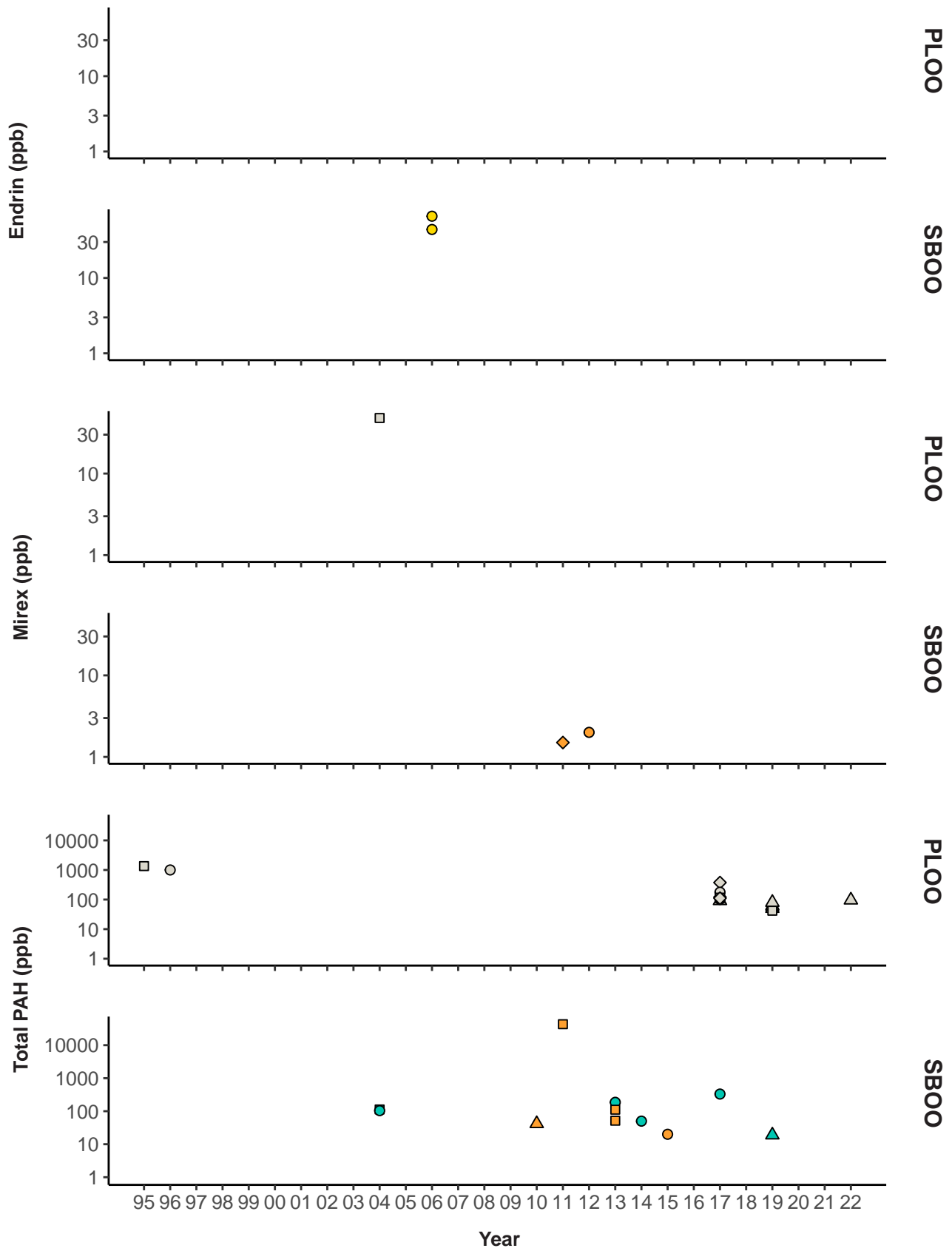


Appendix J.14 *continued*

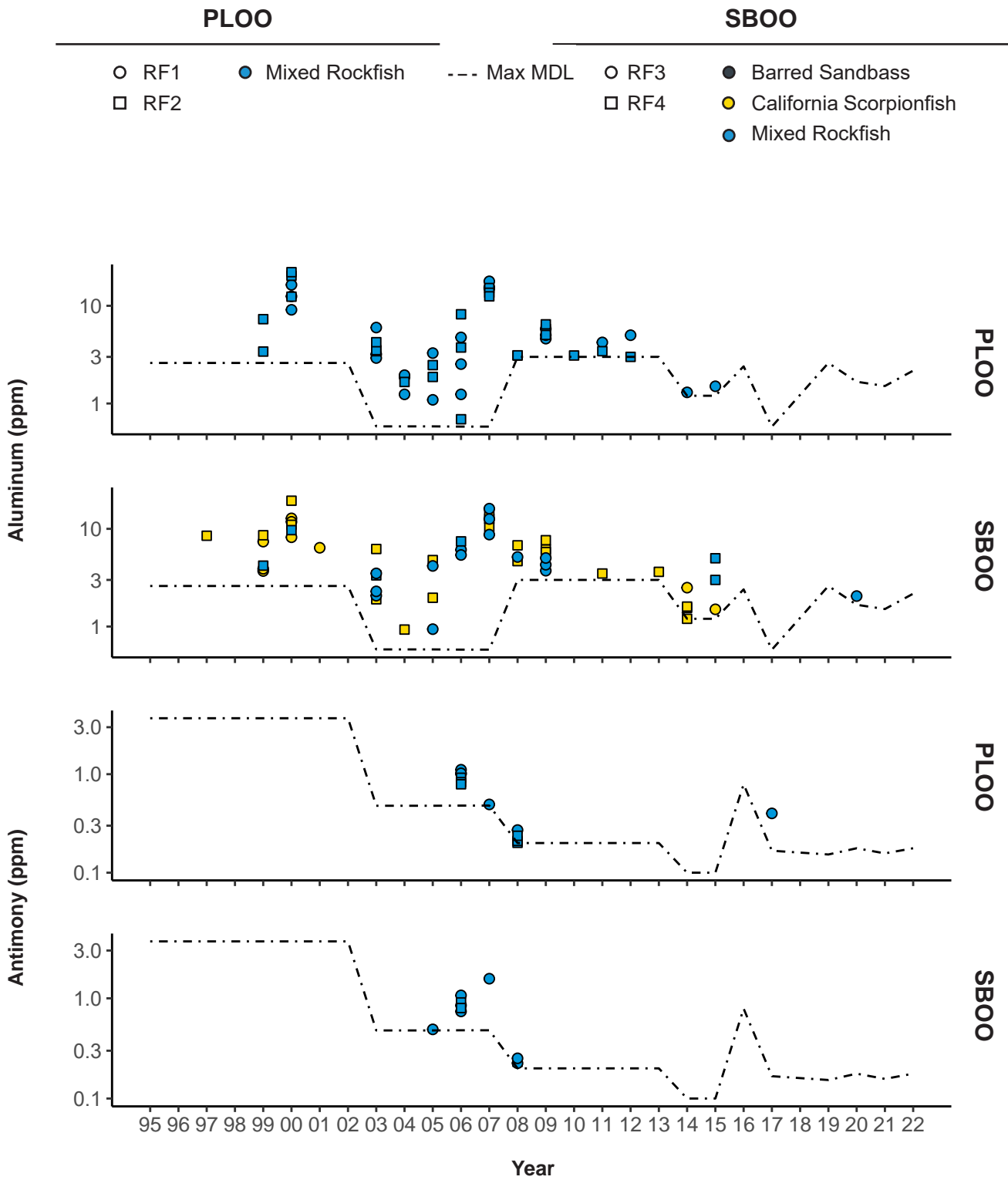


Appendix J.15

Concentrations of pesticides and total PAH in liver tissues of fishes collected from PLOO and SBOO trawl zones from 1995 through 2022. Zones TZ1 and TZ5 are considered nearfield. No samples were collected in 2018 and 2023 as described in text.

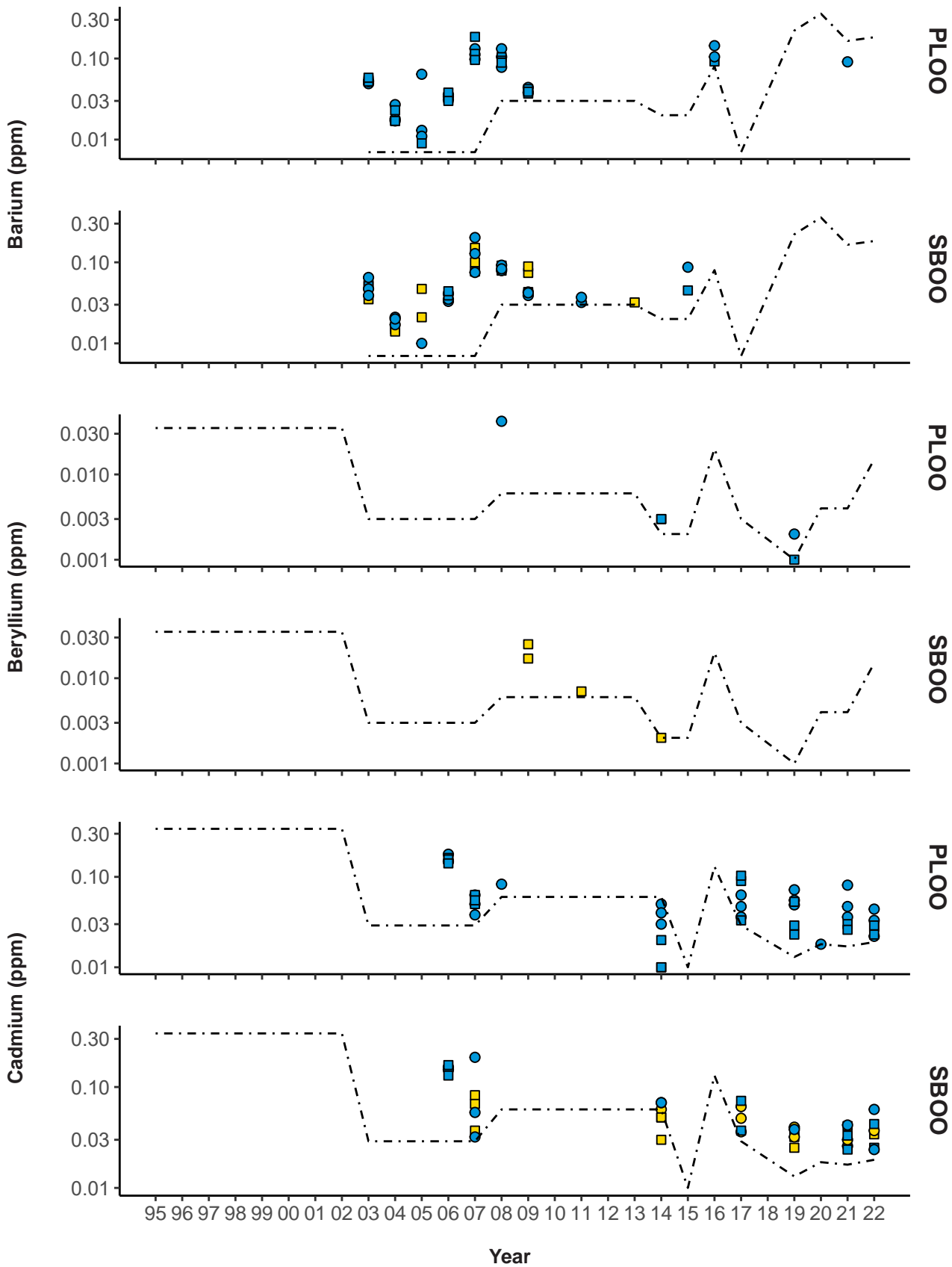


Appendix J.15 *continued*

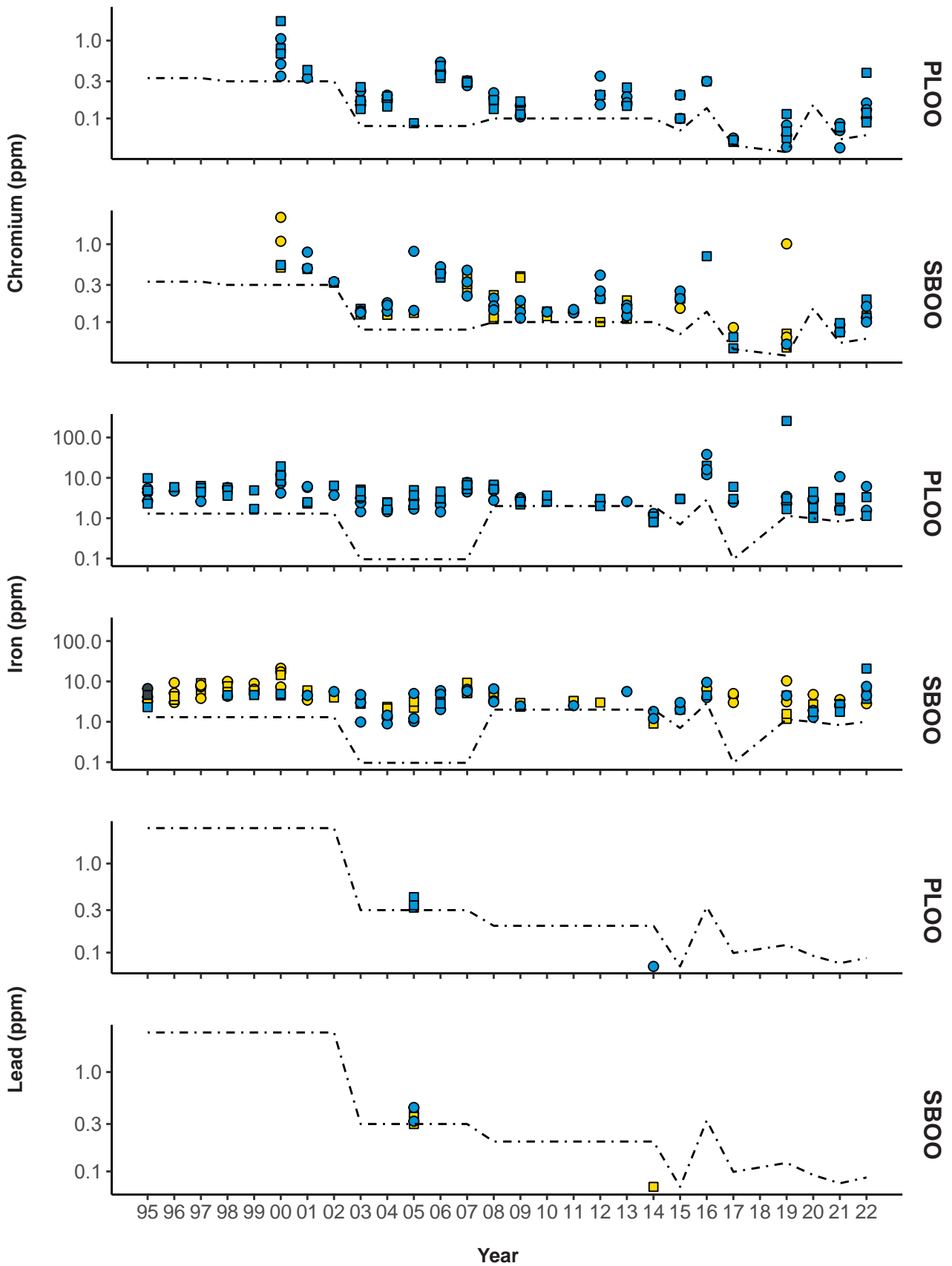


Appendix J.16

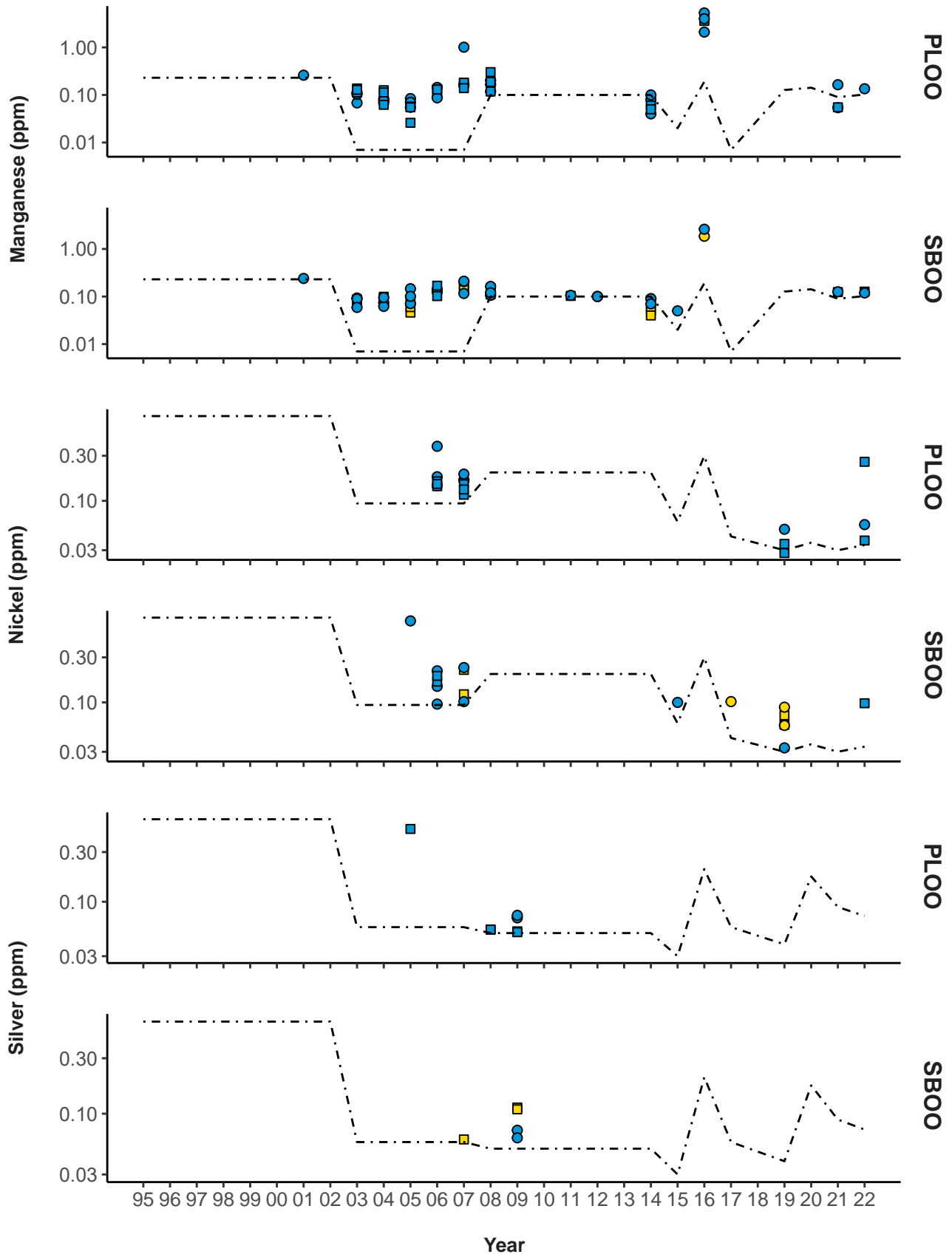
Concentrations of select metals in muscle tissues of fishes collected from PLOO and SBOO rig fishing zones from 1995 through 2022. Zones RF1 and RF3 are considered nearfield. No samples were collected in 2018 and 2023 as described in text.



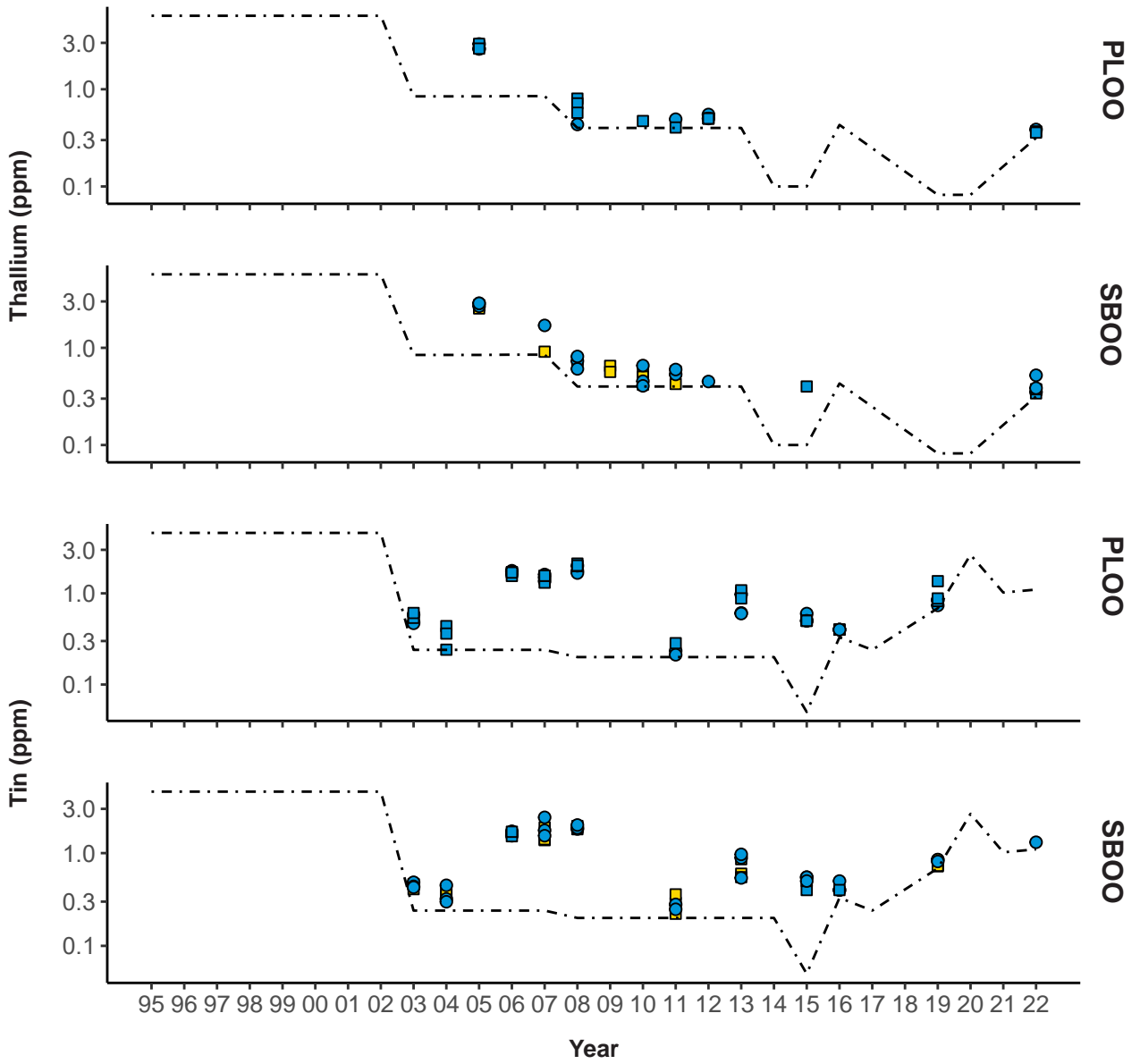
Appendix J.16 *continued*



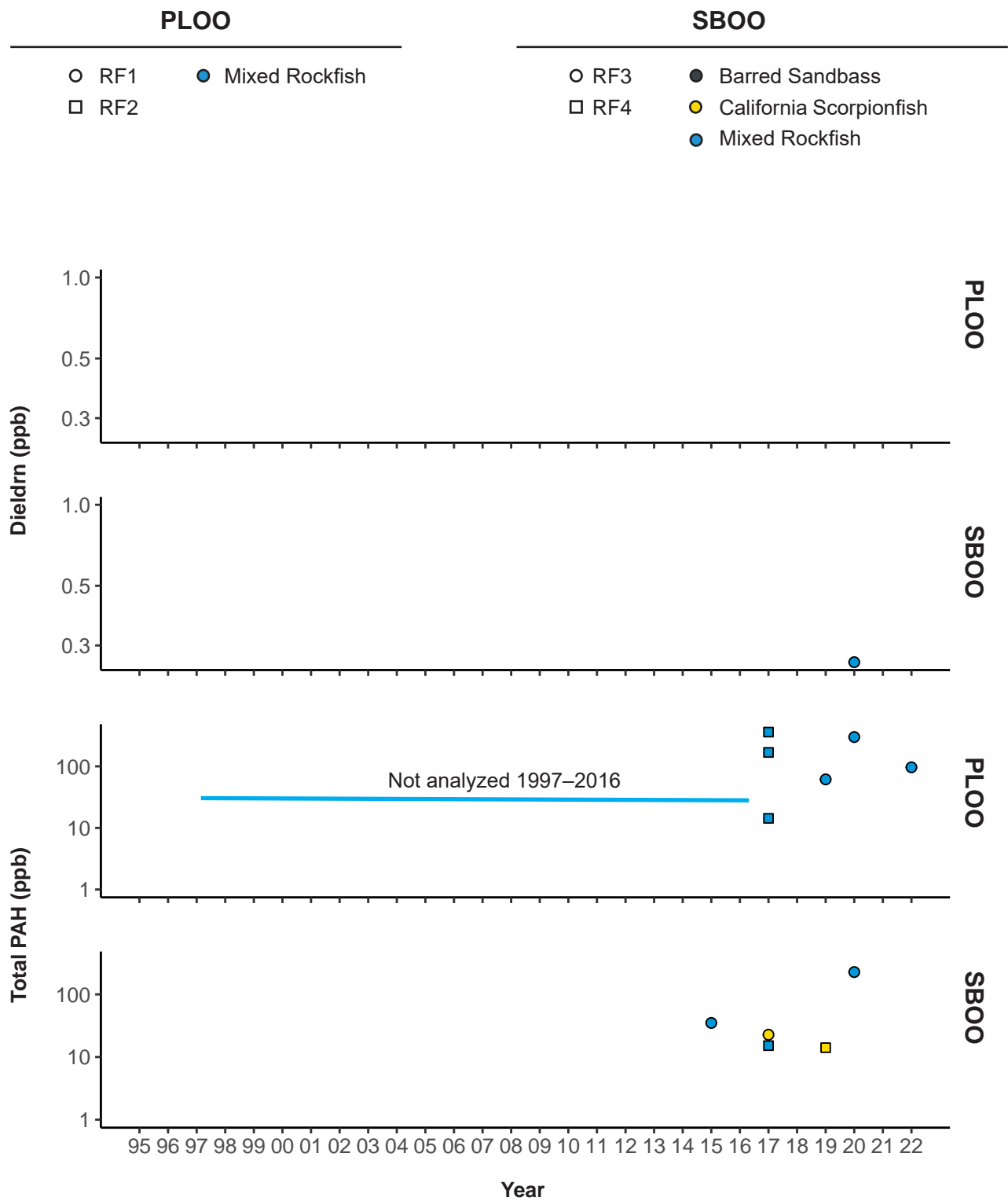
Appendix J.16 *continued*



Appendix J.16 *continued*



Appendix J.16 *continued*



Appendix J.17

Concentrations of dieldrin and total PAH in muscle tissues of fishes collected from PLOO and SBOO rig fishing zones from 1995 through 2022. Analysis of Total PAH was not a permit requirement from 1997–2016. Zones RF1 and RF3 are considered nearfield. No samples were collected in 2018 and 2023 as described in text.